THE

LONDON, EDINBURGH, and DUBLIN

PHILOSOPHICAL MAGAZINE

AND

JOURNAL OF SCIENCE.

" Nec aranearum sane textus ideo melior quia ex se fila gignunt, nec noster vilior quia ex alienis libamus ut apes." Just. Lips. *Polit.* lib. i. cap. 1. Not.

VOL. XIII.—SEVENTH SERIES.

JANUARY—JUNE 1932.

"Meditationis est perscrutari occulta; contemplationis est admirari perspicua .... Admiratio generat quæstionem, quæstio investigationem, investigatio inventionem."—*Hugo de S. Victore.*

———

———"Cur spirent venti, cur terra dehiscat,
Cur mare turgescat, pelago cur tantus amaror,
Cur caput obscura Phœbus ferrugine condat,
Quid toties diros cogat flagrare cometas,
Quid pariat nubes, veniant cur fulmina cœlo,
Quo micet igne Iris, superos quis conciat orbes
Tam vario motu."

J. B. Pinelli ad Mazonium.

ALERE FLAMMAM.

CONTENTS OF VOL. XIII.

(SEVENTH SERIES).

NUMBER LXXXII.—JANUARY 1932.

NUMBER LXXXIII.—FEBRUARY.

NUMBER LXXXV.—MARCH.

PLATES.

ERRATA.

Page 1159, line 18, *for* The noted pore volume,
read The total pore volume.

Page 1168, line 20, *for* amount of sulphuric acid,
read amount of sulphur dioxide.

In the paper on " Activities and the Standard State " all the terms in curved brackets on pp. 288-290 should be differentials; thus equation (13) should read :

$$\left(\frac{\delta \ln \alpha}{\delta T}\right)_{p, N} = -\frac{H}{RT^2}.$$

I. *The Charge carried by Atoms of Radium* D *emitted by α-ray Recoil from a Source of Radium* C *on a Metallic Surface, and its Relations with the Surface Forces.- By* J. D. McGEE, *M.Sc., Exhibition of* 1851 *Scholar of Sydney University, Clare College, Cambridge* *.

Introduction.

WHEN an α-particle is emitted by a radioactive nucleus the residual atom recoils with a momentum equal and opposite to that of the α-particle. Its velocity is about 4×10^7 cm. per sec., and it travels a distance of about ·12 mm. in air at atmospheric pressure. Since by the emission of the α-particle the charge of the nucleus is reduced by two units the residual atom will have two superfluous electrons in its outer structure. If these are retained by the new atom it will appear initially with a double negative charge, but they can only be bound to the atom with a negligible energy, and will most probably be dislodged very easily.

An α-particle in escaping from an atom passes right through the extranuclear electrons with which it may experience collisions and so ionize the atom. It is known that an α-particle in passing through a gas produces intense ionization along its path, somewhat less than half of which is due to the expulsion of electrons from gas atoms by the

---

α-particle *. It seems reasonable to suppose that the deeper an α-particle penetrates into the structure of an atom the greater the probability of ionization taking place. On this assumption it can easily be shown that an α-particle must pass within an average distance of 2×10^{-9} cm. of the nucleus of an atom of air in order to ionize it—that is, it must penetrate well into the structure of the atom.

A case analogous to the expulsion of an α-particle by a radioactive atom is that in which the nucleus of a gas atom is involved in a " head-on " collision with an α-particle. In the latter case the α-particle must pass into and out of the atom, whereas in the former it passes out only ; but the disturbance produced in each case must be of the same order of magnitude and very similar in nature. It seems highly probable that an atom involved in such a " head-on " collision would lose one if not more electrons and a similar result is to be expected from the emission of an α-particle by a radioactive atom. Some evidence on this point has been obtained by Blackett from photographs of forked α-particle tracks in an expansion chamber †. These represent very close collisions between the α-particle and the gas atom, and the recoil range and initial energy of the latter can be determined. From a consideration of the relative ranges for the same initial energy of such recoil atoms in air, hydrogen, helium, and argon their average charge can be estimated, and is found to be between two and three positive units for the heavier gases.

The initial charge carried by recoil atoms can only be investigated when they are observed under such conditions that they cannot interact with surfaces or other atoms before their charge is determined. Until the recent experiments of Mund, Capron, and Jodogne ‡ the charge on recoil atoms had only been observed after they had escaped from a metal surface on which the parent substance was deposited. In their experiments, however, they appear to have successfully determined the charge carried by radium A recoil atoms in such a way that the effect of interaction with other atoms has been eliminated. They conclude that the radium A recoil atoms carry an initial average charge of two positive units.

In their experiments radon was admitted for a short time (about one minute) into a glass vessel at a pressure of ·001 mm. The glass vessel contained two parallel metal

---

* *Cf.* Rutherford, Chadwick, and Ellis, ' Radiations from Radioactive Substances,' pp. 143 *et seq.*

† *Loc. cit.* p. 252.

‡ *Bulletin de la Soc. d. Chim. d. Belgique*, no. 1, Jan. 1931.

plates, 1 cm. apart, between which a field of 3200 volts per cm. could be maintained. This field was sufficient to collect an appreciable excess of the recoil atoms on one or other of the plates if they were initially charged, and the pressure was such that not more than 10 per cent. of the recoil atoms made collisions with other atoms before reaching the collecting plates.

They found that the cathode received a larger number of recoil atoms than the anode. Since the mass and initial velocity of the recoil atoms are known, and their distribution in space between the electrodes is uniform, the fraction captured by each electrode can be calculated for any assumed value of their initial charge. They found that the observed distribution of activity between the two plates corresponded to that calculated on the assumption that the initial charge on the recoil atoms was $+2\cdot0e$.

This result is of considerable interest, since it shows that the escaping α-particle leaves the radium A recoil atom doubly ionized. In the passage of α-particles through gases doubly ionized atoms are only found in the case of helium *, and then only at the end of the range of the particle. But it is to be noted that collisions of an α-particle in a gas which can be compared with the case of the escape of an α-particle from a nucleus are so rare that, even if they did produce double ionization, their effect would not usually be detected. This conclusion is, however, in good agreement with Blackett's observation that atoms recoiling after a close collision with an α-particle carry two or three unit positive charges.

In radioactive experiments it is customary to use sources in which the active matter is deposited on a metal surface, and it is of considerable importance to know the behaviour of recoil atoms emitted from such a source. The charge carried by the recoil atoms will still be dependent to some extent on its initial state, but it will be subjected to the further influences of the surface forces and any collisions it may make with other atoms before escaping from the surface. In sources prepared in the usual way by exposing a metal surface at a negative potential in radon it is very probable that some of the active matter is embedded in the metal surface. Hence some of the recoil atoms from such a source must make collisions with atoms of the metal. Again, part of the active matter which is deposited on the surface may exist in the form of aggregates or it may be covered by a

---

* T. R. Wilkins, Phys. Rev. xix. p. 210 (1922).

layer of adsorbed gas. In either case the escaping recoil atoms would interact with other atoms. Finally, the charges carried by recoil atoms of the same type may be different when they escape from the clean surfaces of different metals, since the work-functions vary considerably.

The charge carried by a recoil atom escaping from a source deposited on a metal surface and recoiling *in vacuo* was first investigated by Makower [*] and his collaborators by bending a beam of α-rays and recoil atoms in a magnetic field. They concluded that the momentum of the recoil atoms was closely equal to that of the α-particles, and that each carried one positive unit of charge. The same result was obtained for radium B atoms recoiling from radium A and radium D atoms from radium C, except that in the latter case the average momentum of the recoil atoms appeared slightly smaller than that of the α-particles. This was attributed to some of the radium C being slightly embedded in the metal surface in the preparation of the source.

A more direct method of measuring the charge on radium D recoil atoms from a source of radium C has been used by L. Wertenstein [†]. He collected a beam of rays from a radium C source in a Faraday cylinder, and measured the charge received by it per unit time (a) when α-, β-, and recoil rays were received by the cylinder, (b) when the recoil atoms had been stopped by a very thin screen of aluminium, and (c) when both α-rays and recoil atoms were cut out of the beam by a screen of greater stopping power. Now $(b-c)$ gives the charge received by the Faraday cylinder from a certain number of α-particles, and $(a-b)$ gives the charge contributed by the same number of recoil atoms, provided the efficiency of recoil is 100 per cent. Then $\left(\dfrac{a-b}{b-c}\right) \times 2e$ gives the charge on the recoil atoms. Wertenstein found the recoil atoms to be neutral when the pressure in his apparatus was ·0005 mm. of mercury, determined by a Knudsen absolute pressure gauge, but they became positive when a pressure of ·0025 mm. of gas was admitted. He therefore concluded that the recoil atoms were always neutral initially, and became positively charged only after collisions with other atoms. The distance travelled by the recoil atoms in his experiments was short, about 1·5 cm., so that the chance of a collision with a gas molecule at the

[*] Phil. Mag. xx. p. 815 (1910); xx. p. 882 (1910); xxix. p. 253 (1915); xxx. p. 811 (1915).

[†] *C. R. de la Soc. d. Varsovie*, viii. p. 327 (1915).

pressure at which he worked (·0005 mm.) was too small to influence his results.

Neither in Wertenstein's experiments nor in those by Makower and his collaborators were any precautions taken to eliminate the effects on the charge of the recoil atoms of the various factors which have been mentioned above. It is with the separate effects of these factors and the determination of the charge carried by recoil atoms subject only to the electrical forces of the surface from which they come that the experiments to be described are chiefly concerned.

Discussion of the Conditions necessary for the Experiment.

In order to approximate to the ideal conditions of recoil the disintegrating atoms must be deposited *on* the surface and not *in* the metal, as appears to be the case with sources of radium C prepared by recoil in radon, and the surface must be free from adsorbed layers of gases and vapours. Under these conditions it seems reasonable to suppose that a recoil atom which is shot out perpendicular to the surface will be influenced only by the surface forces of the metal.

The experiments by Barton[*] and Philipp and Donat[†] have shown that it is possible to obtain up to 20 per cent. efficiency for β-ray recoil when the source is prepared *in vacuo* by distillation and kept *in vacuo* during the experiment. Barton also found that efficiency of β-ray recoil of the same order could be obtained by depositing the source on platinum by electrolysis and afterwards heating it up to 400° or 500° C. for a few seconds in a good vacuum to remove adsorbed vapours and gas from the surface.

Since the β-ray recoil atoms in general have energies of less than 0·5 electron-volts and the α-ray recoil atoms have energies of 10^5 electron-volts, the surface conditions which give a good efficiency of β-ray recoil should be almost perfect for α-ray recoil.

The recoil must take place in a sufficiently high vacuum to ensure that only a very small percentage of the recoil atoms make collisions with gas molecules during their passage from the source to the Faraday cylinder.

The Faraday cylinder itself must be an efficient collector of the rays.

Description of Apparatus.

In order to repeat Wertenstein's experiments with the suggested improvements the apparatus shown in fig. 1 was
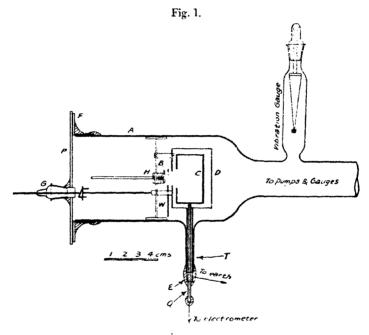
[*] Phil. Mag. i. p. 835 (1926).
[†] *Zeit. f. Phys.* xlv. p. 512 (1927); also lix. p. 6 (1930).

constructed. Modifications that were made will be described at the various stages in the work at which they were found necessary.

The apparatus consisted of a glass cylinder A, 6·3 cm. in diameter, closed at one end by a brass plate P, which was ground to fit a brass flange F, which in turn was waxed on to the glass cylinder. The Faraday cylinder C was insulated from the screening cylinder D by quartz rods. The lead from the Faraday cylinder to the electrometer was taken out

Fig. 1.

through the tube T from which it was insulated by a quartz tube Q, which was screened by a surrounding brass tube E. The joints were made air-tight with sealing-wax. The metal disk B, on which the source was deposited, was fixed in front of the opening in the screening cylinder D, and between the two was the wheel W carrying three circular "windows," *a*, *b*, and *c*, slightly greater in diameter than the opening in the cylinder D. This wheel could be rotated by rotating the stopper in the ground-glass joint G. This was cemented through the brass plate P with sealing-wax.

Of the three windows in the wheel W, (*a*) was open, (*b*) was covered by a thin collodion film of stopping power

for α-rays equivalent to 2 to 3 mm. of air, this being sufficient to stop the recoil atoms, but not to absorb the α- or β-rays appreciably. The third window (c) was covered by a sheet of mica of 8 cm. stopping power for α-particles, which was sufficient to stop all the α-rays from radium C, but did not stop more than a small percentage of the β-rays.

The end of the screening cylinder D which faced the source was lined with lead sheet of 1 mm. thickness, so as to limit the beam of rays received by the Faraday cylinder quite definitely. The Faraday cylinder itself was made of brass and lined with lead sheet 1 mm. thick to prevent fast β-rays which enter it from penetrating its walls and escaping.

The lead lining was used for a further reason. Recent experiments by Philipp and Donat * and L. Wertenstein † have shown that the temperature of the collecting cylinder and the metal from which it is made influence very greatly the number of β-ray recoil atoms that are collected. While this effect cannot be expected to apply to α-ray recoil atoms, since they penetrate deeply into the collecting surface, there is no definite evidence on the matter. The Faraday cylinder was therefore lined with lead, an isotope of the atoms of radium D which were to be collected.

A magnetic field of strength about 2000 gauss was applied perpendicular to the plane of the diagram. This was necessary to prevent secondary β-rays (δ-rays) which are produced at the source or screens in large numbers from reaching the Faraday cylinder. Similarly δ-rays produced inside the Faraday cylinder are prevented from getting out of it.

The current received by the Faraday cylinder was measured by a Dolezalek electrometer and Townsend induction balance. The electrometer and condenser were situated 2 metres from the source, to reduce ionization due to γ-rays as much as possible. Also the lead from the Faraday cylinder to the electrometer was taken through a brass tube, which was roughly evacuated in order to reduce electrical leaks caused by γ-ray ionization to a negligible amount.

The apparatus was exhausted by a mercury diffusion pump backed by a Fleuss pump, and the pressure could be reduced from atmospheric to ·0002 mm. in less than five minutes. A liquid-air trap between the pumps and gauges and the main recoil chamber removed mercury and other heavy vapours.

* *Zeit. f. Phys.* lix. p. 6 (1930).
† *C. R.* clxxxviii. pp. 1045, 1429.

The pressure was ordinarily measured by a MacLeod gauge, which always registered less than ·0001 mm. during a run; but to make quite certain that no vapours were present which would not be measured by the MacLeod gauge a quartz fibre vibration gauge was also used (see fig. 1). With this gauge a pressure of ·0002 mm. of any gas or vapour could be detected easily, and during a run it always showed less than this pressure.

Experimental Method.

The source to be examined was screwed into position, as shown in fig. 1, in front of the Faraday cylinder. The apparatus was then closed and exhausted, and when the pressure was sufficiently low observations were commenced. From the time the source was ready until observations began was about 10 minutes.

Observations were made of the charge received by the Faraday cylinder in unit time, with the windows (a), (b), and (c) successively rotated in front of the source. Each observation lasted from 20 to 60 seconds, and over such an interval of time, short compared with the life of the source, the strength of the latter may be considered constant. The mean time of each observation was noted, and the charge received per unit time by the cylinder was plotted against the time the source had been decaying. The smooth curves through the points corresponding to each of the windows (a), (b), and (c) are marked with these letters in the diagrams.

With window (a) in front of the source all particles with sufficient energy to pass through the magnetic field were received by the Faraday cylinder. With window (b) in front of the source the recoil atoms will be stopped by the collodion screen and only α- and β-rays received by the cylinder, while with window (c) only β-rays can reach it.

The difference of the ordinates of curves (a) and (b) gives the charge received by the Faraday cylinder per second due to recoil atoms, while the difference of curves (b) and (c) gives that due to α-particles. For every α-particle, of charge $+2e$, reaching the Faraday cylinder a recoil atom of unknown charge is also received, assuming the efficiency of recoil to be 100 per cent. This assumption should not be more than 20 per cent. from the truth provided the source is clean. Hence the average charge " Q " carried by a recoil atom can be compared with the charge on an α-particle.

It is to be noticed that, though the magnetic field employed (2000 gauss) was sufficient to prevent δ-rays or any β-particles

with energies under 10^4 electron-volts from reaching the Faraday cylinder, it is not strong enough to remove heavy ions of only a few volts energy from the beam of rays. The presence of such ions in considerable numbers was not suspected until later in the research, when special arrangements had to be made to remove them from the beam.

In these experiments it is not necessary to know the strength of the sources accurately, or in the case of a radium $(B+C)$ source to know the relative amounts of radium B and radium C present, since the results depend only upon the differences in the ordinates of the curves. Nevertheless the source was always measured roughly at the beginning of a run, and the charge received by the Faraday cylinder compared with what would be expected from the strength of the source and the solid angle subtended at it by the opening in the Faraday cylinder. The agreement was satisfactory considering the approximate nature of the calculations.

Experimental Results.

The first experiments were made using sources prepared by exposing nickel disks in radon at a negative potential. Before use the disks were washed in methylated spirit and heated in a fairly good vacuum. The recoil atoms from these sources always appeared positively charged, and although Q was always constant throughout a run using one particular source it varied considerably for different sources.

As this method is open to the objection that the radium C may be partially buried in the metal surface, the well-known method due to von Lerch of depositing radium C on a nickel surface from a HCl solution was tried. In this way sources were obtained on a very clean polished nickel surface.

Most of the sources prepared in this way gave small positive values for Q, but for some it was almost zero and for a few it had a negative value. Most of the values found were fractional ($e.g., +0\cdot 3e$) and lay between $-1\cdot 0e$ and $+1\cdot 0e$. Also the charge on the recoil atoms appeared to increase, changing from negative to positive, when gas was admitted to the apparatus at such a pressure that the recoil atoms made collisions with gas atoms on their way to the Faraday cylinder. Thus curve "a" rose considerably, but curves "b" and "c" were unaffected when $\cdot 01$ mm. of air was admitted to the chamber.

Efforts were next directed towards preparing the sources as cleanly as possible and under identical conditions each

time. These conditions seemed to be satisfied by the method of electrolysing radium C on to platinum from a solution of radium B + C in HCl[*]. The sources prepared in this way were even more inconsistent in their behaviour, the value of Q varying from $-1.25e$ to $+4.0e$ for different sources. In searching for the cause of the inconsistency in the results it was found that if a source on a nickel surface which was giving recoil atoms of apparent positive charge was removed from the apparatus and heated in air so as to oxidise the surface slightly and then returned to the apparatus the charge was invariably decreased, frequently becoming negative. In one instance Q dropped from $+2.0e$ to $-1.0e$, and was quite steady at that value until gas was admitted, when it increased with increasing pressure to about its original value. This effect will be discussed later.

These preliminary experiments led to the conclusion that the charge carried by a recoil atom was very strongly influenced by some factor which was not controlled in these experiments. After a search for the cause of the inconsistency of the results, it was traced to the presence of ions, both positive and negative, in the beam of rays collected by the Faraday cylinder. It was found that the positive charge received by the Faraday cylinder was greatly increased by raising the potential of the source to a few volts positive when the open window was in front of the opening in the Faraday cylinder. Also curve "a" dropped far below curve "b" when the source was kept at a negative potential of a few volts. Curves "b" and "c" were quite unaffected by alterations in the potential of the source, which is to be expected, since the ions have not sufficient energy to pass through even the thin collodion window.
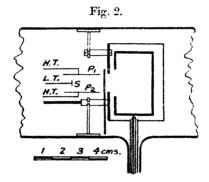
The origin of these ions will be discussed later, but it is sufficient to say here that they cannot be produced by collisions of the recoil atoms with atoms of residual gas, since the pressure was always kept below 10^{-4} mm., and not more than 1 per cent. of the recoil atoms can then make collisions in their path to the Faraday cylinder.

In order to remove these ions from the beam of rays the apparatus was remodelled as shown in fig. 2. The source S was fixed between two parallel horizontal nickel plates P_1 and P_2, 1 cm. apart, between which a strong electric field could be maintained. The radium C was deposited on a thin oil (3 mm. × 10 mm.) of nickel or platinum, and was held in position by heavy copper leads, which also served to carry a

current to heat the foil electrically. These current leads, as well as the high-tension leads to the parallel plates, were sealed in through the brass plate P (fig. 1). The position of the foil on which the source was deposited could be varied, but in the first experiments it was about 1·5 cm. from the end of the plates and 2·5 cm. from the opening in the Faraday cylinder. With these dimensions an ion will be captured by the plates when its energy, expressed in electron-volts, is approximately equal to the voltage between the plates. By moving the foil farther away from the Faraday cylinder ions of higher energy could be removed from the beam of rays.

By passing a current of about 6 amp. through the foil it could be raised to a red heat. Barton * has shown that raising a platinum foil on which radium C was deposited to

Fig. 2.

a visible red heat for a few seconds increased the efficiency of β-ray recoil. This increase is probably due to the removal of surface layers of adsorbed gases and vapours which impede the low energy β-ray recoil atoms. Hence in these experiments it seemed probable that such partial outgassing would decrease the chance of a recoil atom making a collision with an atom of adsorbed gas before it left the surface. The sources cannot be outgassed thoroughly, since radium C in the metallic state begins to volatilize at temperatures below 400° C.† When the radium C is in the form of an oxide it does not begin to volatilize until it is raised to about 700° C. In these experiments the radium C was apparently almost all in the metallic state, as considerable losses of the source were noticed when it was kept at a temperature judged by eye as about 550° C. for more than a few seconds.

* *Loc. cit.*
† St. Meyer u. E. Schweidler, ' Radioactivität,' p. 424.

The sources were prepared by electrolysis in the same way as described in the earlier experiments, and the surfaces of the foils always appeared quite clean after preparation. The source was kept in distilled water until it was quickly dried on filter-paper and introduced into the apparatus.

Each source was first examined cold, with and without a field between the parallel plates. Without the electric field the values found for the charge on the recoil atoms were quite as erratic as in the earlier experiments, but the application of a field of about 200 volts per cm. between the parallel plates immediately showed that Q had a positive
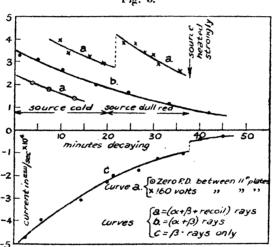
Fig. 3.

value of approximately 0·5e, which increased after heating the source to 1·0e.

The results of observations made with a radium C source deposited on a platinum foil are shown in fig. 3, the source being 14 mm. from the end of the parallel plates. During the first 20 minutes of the run observations were made without a field between the parallel plates (points shown thus ☉) and with a field of 160 volts/cm. between them (points thus ×), when the open window " a " was in front of the source. These points were found to lie on curves respectively below and above curve " b," corresponding in the former case to a negative value of Q and in the latter to a positive value of about +0·4e. As is to be expected, curves " b " and " c " are quite unaffected by this field. After observations had

been continued for 20 minutes the platinum foil was brought
to a barely visible red heat by passing an electric current
through it, and observations continued. The curve "*a*" has
now risen much above curve "*b*," and the value of Q deduced
from it is about $+1\cdot2\,e$. The distance between curves "*b*"
and "*c*" falls off exponentially, with the half-value period
of 19·5 minutes of radium C, within experimental error.
The curve "*a*" also decays according to the same law.

After observations had been in progress for 38 minutes
the source was heated to a bright red heat for 15 seconds
and then cooled again. It was then found that all the curves
had been considerably changed, due no doubt to loss and
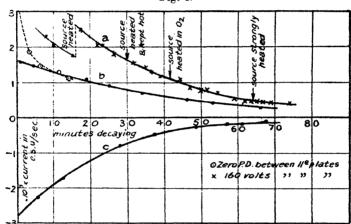
Fig. 4.

redistribution of the radium C, which would be volatilized at
that temperature *in vacuo.*

In fig. 4 are shown the curves obtained with a similar
radium C source on platinum. The general behaviour is
much as before, except that the apparent value of Q without
the field and from the cold source is almost zero. With
160 volts between the parallel plates it is found to be $+0\cdot5\,e$,
and finally, after heating the source to a dull red glow for a
few seconds and cooling again, it becomes very closely equal
to $+1\cdot0\,e$. This value is not affected when the source is raised
to a dull red heat (after 30 minutes decay), and kept constant
at that temperature for 12 minutes. A pressure of 5 mm. of
oxygen was then admitted, and the platinum foil raised to a
bright red heat in it for half a minute and cooled. On
pumping out the gas the value of Q was found to be

unchanged, and could not be changed by subsequent heating. Also no signs of volatilization were noticeable, the curves all maintaining their exponential form. This agrees with the view * that radium C oxide is less volatile than the element in the metallic state. It also indicates that the charge on the recoil atoms does not depend on whether the parent atom is a pure metal or an oxide.

In several runs, particularly when the source was only 1 cm. from the end of the parallel plates, and small fields, of the order of 200 volts, were applied between them, the value of Q found differed by as much as 40 per cent. from one positive unit. If, as should be the case, the efficiency of
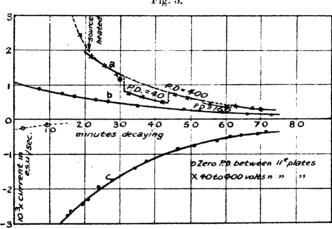
Fig. 5.

recoil is nearly 100 per cent., the value of Q would be expected to be integral ; but if high energy ions are present the variation of Q from unity may be due to those ions which have sufficient energy, to avoid capture in the electric field and enter the Faraday cylinder.

The results shown in figs. 5 and 6 show that this is the case. In fig. 5 the curves show the result when the source is only 1 cm. from the end of the parallel plates and voltages of 40, 160, and 400 are applied between them. The observed points on curve " a " for each particular P.D. between the parallel plates are consistent amongst themselves and lie nicely on exponential decay curves, but increasing P.D. gives increasing values of Q.
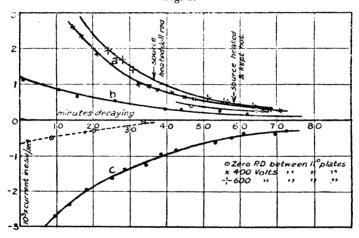
* Meyer u. Schweidler, ' Radioactivität,' p. 424.

Similarly for fig. 6, where the source is 14 mm. from the
end of the parallel plates, there is a large increase in the
value of Q when the P.D. is raised from 0 to 400 volts, and
when it is raised to 600 volts Q becomes very closely equal
to unity.　Further increases in the distance of the source
from the ends of the parallel plates up to 2 cm. and increases
in the P.D. between them up to 800 volts gave no values of
Q which were greater than + 1·0 *e* by more than the experi-
mental error.

Thus, we have

	From fig. 5.			From fig. 6.		
P.D. in volts ...	40	160	400	0	400	600
Q	·35*e*	·55*e*	·75*e*	·20*e*	·70*e*	1·0*e*

Fig. 6.
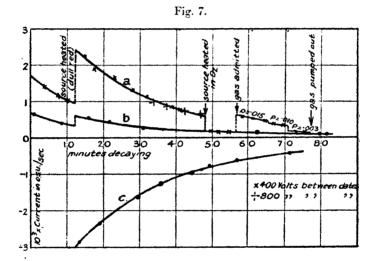
It is therefore concluded that the real value of the charge
on a recoil atom coming from such a partially outgassed
platinum surface *in vacuo* is one positive unit of electricity.
The beam of recoil atoms is accompanied, however, by a
stream of ions, both positive and negative, of which a number,
comparable with the number of recoil atoms, have energies
of the order of 1000 electron volts.

By applying a small positive accelerating potential to the
source the apparent value of Q can be increased to five or
ten times the true value if the source has not been baked out,
and the order of double the true value after baking out.
Similarly for a negative accelerating potential.　This obser-
vation shows that the ions must be produced mainly in the

layer of adsorbed gas on the surface of the metal, which is
at least partially removed by the heating *in vacuo*.

It is to be noticed in figs. 5 and 6 that, although Q appears
negative in the early part of the run, when there is no field
between the parallel plates, the value of Q found with a field
of 400 volts between the plates is at first quite large, but
drops quickly in a smooth curve to the value found after
outgassing.   In fact, the heating of the source has no effect.
This is probably due to the fact that in these cases the
platinum foil had been cleaned by heating strongly *in vacuo*
before the radium C was deposited on it.   In this way the

Fig. 7.

foil could be obtained in a much cleaner condition than by
the normal methods of cleaning, with the result that it
cleaned up of its own accord when subsequently placed in a
vacuum.

It was mentioned, in describing the earlier experiments,
that recoil atoms coming from a source on a slightly oxidized
nickel surface appeared to have negative charges.   This effect
seemed so definite that it was investigated again after the
method of removing the ions had been developed, and it was
found to be partially true.   In fig. 7 are shown the results
obtained using a radium C source on a very clean nickel
foil.   The source was 2 cm. from the end of the parallel
plates, and it is not surprising that there is no increase in the
value of Q when the voltage between them is raised from
400 to 800 volts.   The first part of the run is quite similar

to the runs already described using platinum foils, but after 48 minutes the foil was heated strongly in a few millimetres pressure of air, so that its surface became coated with a thin oxide film. As shown in the figure the curve "*a*" then drops and coincides with curve "*b*." This may be due either to the recoil atoms under these circumstances leaving the surface with no charge, or they may not leave the surface at all because of the oxidation. The latter hypothesis is shown to be untrue by the observation that when a small pressure of air of ·015 mm. was admitted to the apparatus the curve "*a*" immediately rose again as shown in fig. 7, giving an apparent value of $Q = +1\cdot85e$. As the gas was then pumped out in several stages, the curve fell in steps as the pressure decreased, until when the original pressure of ·001 mm. was attained Q again appeared to be zero. This rise in the curve "*a*" can only be due to positive charges produced when the recoil atoms collide with air atoms, and hence is strong evidence that the recoil atoms do leave the oxidized nickel foil. They must therefore be neutral in high vacuum when they originate at such a source. In no case did the recoil atoms appear to carry negative charges, as was found in the earlier experiments.

The fact that no similar effect was found when the source was heated on a platinum foil shows that it is due to oxidation of the metal surface itself rather than to oxidation of the radium C.

Discussion

It has been shown that the average charge carried by a recoil atom of radium D originating from a source of radium C on a clean nickel or platinum surface is, in a good vacuum, one positive unit.

This conclusion is in agreement with the findings of Makower *, but not with the results of Wertenstein's † experiments. It seems possible that the high speed ions observed in these experiments were also present in those of Wertenstein, and, by chance, in such numbers as to give an apparent zero value for the charge on the recoil atoms.

The value found for Q of $+1\cdot0e$ is only a statistical average, and it must be borne in mind that a certain percentage of doubly charged and neutral recoil atoms may be present in the beam, though the close approximation of the value found to unity indicates that that is the normal charge of a recoil atom under the circumstances of these experiments.

---

* *Loc. cit.*   † *Loc. cit.*

The experiments of Mund, Capron, and Jodogne* cannot be directly compared with those described here, since they investigated the charge on recoil atoms of radium A originating from radon, and these belong to different groups in the periodic table from the elements radium D and radium C respectively. Nevertheless their conclusion that the radium A atom is doubly ionized at the moment of its formation can be shown to be consistent with the present observation that a radium D recoil atom leaves a clean metal surface in a singly ionized state by considering the effect of the work function of the surface on the charge.

When the recoil atoms originated from a slightly oxidized nickel surface they were found to be neutral (see fig. 7). Such an effect would be expected if the work function of the surface was lowered by oxidation. The effect on the work function of a nickel surface of a layer of oxygen is not known, but it seems probable that the work function will be raised, as is the case with most metals. However, Oliphant † found that a gas-covered nickel surface, when bombarded by positive ions, emitted electrons much more freely than a surface which had been outgassed, and it was found in the writer's experiments that the proportion of negative ions escaping from a surface due to the action of the recoil atoms was greatly increased when it was slightly oxidized. These facts indicate that the recoil atoms, if positively charged initially, have a better chance of becoming neutral when they originate from an oxidized nickel surface, though the effect cannot be attributed solely to the influence of the work function.

If the radium D recoil atoms are really doubly ionized at the instant of their formation from radium C, as seems to be the case in the formation of radium A from radon, it seems certain that only a negligible percentage of them would escape from the surface without first extracting one electron from it, and so reducing their charge to one positive unit. The double ionization potential of radium D would probably be of the order of 15 to 20 volts, while the work function of a nickel or platinum surface is about 5 volts. Hence the chance of a doubly ionized recoil atom capturing one electron would be very great. If, however, it extracted one electron from the surface its electron affinity would be immediately lowered to about the same as that of the surface, and the probability of complete neutralization would be small.

* *Loc. cit.*
† Proc. Roy. Soc. A, cxxvii. p. 373 (1930).

Hence it appears that if the recoil atoms were initially doubly or singly charged in these experiments they would have left the surface of a clean metal with an average charge of one positive unit. The fact that they leave an oxidized nickel surface with no charge is also in agreement with one other experiment on an analogous problem.

One of the chief difficulties encountered in these experiments arose from the fact that large numbers of high energy ions, both positive and negative, are given off from the surface on which the active matter was deposited. These ions travel out from the surface of the source with sufficient energy to pass through the magnetic field (2000 gauss) and enter the Faraday cylinder. In the absence of the collodion window the charge received by the Faraday cylinder was greatly increased or decreased by the application of a small accelerating potential of two volts positive or negative respectively. From consideration of the energy required by an ion in order to pass through the magnetic field it was concluded that the greater number of these ions were oxygen or nitrogen ions with less than ten electron-volts energy. They were removed from the beam of rays by the application of a transverse electric field, and from the magnitude of the field required to finally eliminate their effects it was concluded that a considerable fraction of them must have energies as high as 500 electron-volts, and some even as high as 1000 electron-volts. Negative ions seemed to predominate in numbers at the higher energies.

These ions must be produced at the surface of the source by the action of the recoil atoms. There is definite evidence that they are not produced by the α-rays, since if this were the case we would expect similar ions to be liberated from the collodion window (*b*) on the side facing the Faraday cylinder from which the α-rays emerge. These ions would enter the Faraday cylinder and produce irregularities similar to those observed when no screen was placed in the path of the rays. No such irregularities were observed. Further, it is theoretically impossible for an α-particle to communicate such a large amount of energy to an atom except in very close collisions with the nucleus, which are so rare that they can be neglected in these experiments. Also, in the experiments to determine the number of α-rays emitted by radium * by collecting the α-rays in a Faraday cylinder and measuring the total charge received, the source is always covered by a thin screen sufficient to stop the recoil atoms. If charged

* Braddick and Cave, Proc. Roy. Soc. A cxxi. 1928, pp. 367 etc.

ions were set free from this screen by the α-particles, results entirely in disagreement with those of the many other methods, which could not be affected by such ions, would be expected. No such disagreement has been found.

There are two possible modes of production of the high speed ions. They may be produced by the action of the recoil atoms, which are shot into the metal surface with great energy, the process being analogous to the " sputtering " which takes place when a surface is bombarded with canal rays. It is difficult, however, to see how such sputtered particles could receive such large energies, for under ordinary conditions they are found to have energies of the order of one electron-volt. It seems much more probable that the ions are produced by the recoil atoms as they pass through the layer of adsorbed gas which certainly exists on the surface of the source before it is heated. It is to be expected that a recoil atom in passing through these adsorbed atoms would produce considerable ionization, and that in a few "head-on" collisions a large amount of energy would be transferred to the ions. This hypothesis is supported by the fact that the number of ions produced is greatly reduced by heating the source to about 500° C., which is sufficient to drive off most of the adsorbed gas. That some remain after heating is not surprising, since in no case was the heating sufficient to drive off the last monomolecular layer of oxygen which is known to persist on metal surfaces until the temperature is raised to 800° C. or more. It was not feasible to raise the temperature of the source sufficiently high to drive off the adsorbed gas completely on account of the volatilization of the radium C, which became serious at temperatures much over 500° C.

If a recoil atom of radium D, which has an initial energy of 1.46×10^5 electron-volts, makes an elastic collision with a light gas atom (*e.g.*, H_2, O_2, N_2), the latter will recoil with an energy depending on the angle θ that the direction of its path makes with the original direction of flight of the recoil atom. The energies for different values of θ in the cases of hydrogen and oxygen are shown in the following table :—

θ gas.	0°.	45°.	60°.	80°.
Hydrogen	2.800	1,400	700	—
Oxygen	45,000	22,500	11,200	1,350

From the tabulated figures it appears that if the ions observed are really oxygen ions they must be ejected at a large angle (greater than 80°) with the direction of motion of the recoil atom. Even allowing for a large dissipation of energy in the collision, the energy of a recoiling oxygen ion for which $\theta < 60°$ would still be far too great for it to be captured by the transverse electric field employed in these experiments. The calculated values for the energies of the recoiling hydrogen ions are more of the right order of magnitude to agree with the experimental results, but it is found that most of the high speed ions are negatively charged, and this seems definitely to exclude the possibility that they are hydrogen ions.

The most probable explanation that can be advanced for the origin of these ions is that they are produced by recoil atoms travelling nearly parallel with the surface of the source, and that they leave the surface in directions making angles of between about 10° and zero with the normal to the surface. The ions of higher energy which would make greater angles with the normal could not enter the Faraday cylinder. It is known that a recoil atom in passing through a gas travels in a practically straight path. Hence in most collisions the recoil atom suffers only a very small deflexion and the struck gas atom recoils in a direction making an angle of nearly 90° with its path. The relative number of gas ions whose paths make a small angle with the direction of motion of the recoil atom must be small, decreasing rapidly as the angle decreases from 90° to zero. These considerations account for the large number of low-energy ions observed, and also for the absence of very high-energy ions corresponding to "head-on" collisions with recoil atoms. If many such ions were produced by the recoil atoms which travel normal to the surface of the source they could not be stopped by the transverse electric field, and would enter the Faraday cylinder. Hence saturation of the ion current between the parallel plates could not be obtained at a potential difference of about 600 volts, as was observed.

Some knowledge of the behaviour of recoil atoms which escape from a surface which has not been outgassed can be obtained from these experiments, and it is of considerable importance since sources are seldom outgassed in radioactive experiments.

In figs. 3 and 4 it will be seen that the value of Q before outgassing was about $+0.5 e$. The same value for Q was found in almost all runs before outgassing, with the exception of those in which the foil had been thoroughly outgassed

in vacuo previous to the deposition of the radium C on it. The results then obtained are shown in figs. 5 and 6. It is improbable that the adsorbed layer of gas would decrease the efficiency of recoil by more than about 20 per cent. Hence the decrease in the charge received by the Faraday cylinder may be explained by assuming either that only 50 per cent. of the recoil atoms leave the surface charged or that negative ions are produced with sufficient energy to avoid capture in the transverse electric field. Since the recoil atoms must make many collisions in passing through this layer of adsorbed gas it is to be expected that they would emerge with a charge of at least $+2 \cdot 0 e$. This expectation is based on the apparent increase of Q to several positive units when sufficient gas is admitted to the apparatus, the increase being proportional to the pressure. However, it is clear that a recoil atom would propel some of the gas atoms with which it collides in a direction making small angles with its own direction of flight. Most of these atoms would probably be ionized in the collision, and thus the increase in the charge received by the Faraday cylinder may be due to positive gas ions which are driven into it by the recoil atoms which themselves do not lose more than one or two electrons.

The apparent small value of Q before the source is out-gassed may now be explained by supposing a process of capture and loss of electrons by the recoil atoms to take place in their passage through the gas layer, the net result of which is that only half of them emerge positively charged, the rest being neutral. An analogous process is known to occur in the passage of an α-particle through a gas, becoming very marked towards the end of its range, where its velocity is small. A similar effect also occurs during the passage of a positive ion through the gas in a discharge-tube. This explanation, however, does not seem to agree with the results obtained by Briggs[*] and Dee[†], who found by different methods that 80 per cent. of recoil atoms still carried one unit positive charge at the end of their recoil path in air.

A more probable explanation seems to be that the recoil atoms in passing out through the layer of adsorbed gas are able to make a considerable number of "head-on" or very close collisions with atoms of gas when travelling in a direction nearly normal to the surface. The ions so formed would have sufficient energy to avoid capture by the trans-verse electric field and enter the Faraday cylinder, thus masking the true charge of the recoil atoms. Also it was

* Briggs, Phil. Mag. xli. p. 357 (1921).
† Dee, Proc. Roy. Soc. no. 116, p. 664 (1927).

found that negatively charged ions predominated in numbers amongst those of large energy, so we might reasonably expect those which are not captured to be mainly negative, which is in accord with the results found.

In the experiments, the results of which are shown in figs. 5 and 6, the value of Q is initially very large, and falls off rapidly to the normal value of $+1\cdot0\,e$, so that the heating has then no further effect. This is probably due to the very clean outgassed metal surface losing the layers of adsorbed gas much more rapidly *in vacuo* than a roughly cleaned foil. However, it is rather surprising that such a big difference in behaviour should exist.

In conclusion, it may be said that the value of the charge carried by recoil atoms of radium D determined in these experiments is probably the true value under the circumstances in which the atoms were investigated. It cannot, however, be regarded as giving the initial charge on the recoil atoms before they have interacted with a surface, since they originate from a surface. When allowance is made for the probable effect of the surface forces on the charge the results are shown to be in fair agreement with those of Mund, Capron, and Jodogne, in whose experiments this effect was avoided.

Summary.

The charge carried by α-ray recoil atoms of radium D escaping from a source of radium C has been investigated, and found to be one positive unit when the source is deposited on a clean nickel or platinum surface.

Evidence has been obtained that the charge carried by a recoil atom is influenced by interaction with the surface from which it escapes, and this theory has been extended to correlate the results of other observers with those obtained in these experiments.

The cause of earlier conflicting results has been traced to the presence of high-energy ions. A method of removing these from the beam has been developed, and a possible mechanism for their production suggested. The small average value of the apparent charge carried by recoil atoms before the source was outgassed is also explained by the presence of ions.

II. *Third-Order Terms in the Theory of the Stark Effect.* By M. A. EL-SHERBINI, *B.Sc., The Faculty of Science, The Egyptian University, Cairo* *.

§ 1. *Introductory.*

THE effect of an electric field on the emission of spectral lines was first examined by J. Stark † in 1913. A first-order theory was given on the old quantum dynamics by K. Schwarzschild ‡ and P. Epstein § independently in 1916. The second-order terms, based on the old quantum theory, were worked out by P. Epstein ‖ and A. M Mosharrafa ¶ independently. On the new wave mechanics Schrödinger ** has worked out first-order terms, and Epstein †† has obtained both first- and second-order terms. The second order terms have also been worked out simultaneously by Wentzel and Waller ‡‡, without using Schrödinger's perturbation theory.

The aim of this paper is to obtain third-order terms on the new theory. Although the effect of these terms is of little or no experimental significance at present, yet the work may be said to be of some theoretical interest ; for each of the two previous approximations is characterized by the appearance of a new mode of vibration corresponding to the loss of a degree of degeneracy. When it comes to the third-order approximation, however, the system being already non-degenerate, no new frequency should appear. We find this is actually the case (see equation (19) below).

Another point of some theoretical interest is that the third-, like the first-order terms, affect the spectral lines symmetrically. This is due to the appearance of the factor $(m-n)$ in the expression for the increment of energy (see equation (21) below), which results in the occurrence of a negative value for the energy increment (and therefore for the line displacement) corresponding and numerically equal to every positive value.

---

* Communicated by Prof. A. M. Mosharrafa, Ph.D., D.Sc.
† *Berliner Sitzungsber.* Nov. 1913 ; *Ann. d. Phys.* xliii. pp. 965 and 983 (1914).
‡ "Zur Quantentheorie," *Berliner Sitzungsber.*, April 1916.
§ "Zur Theorie des Starkeffektes," *Ann. d. Phys.* l. p. 498 (1916).
‖ *Ann. d. Phys.* li. p. 184 (1916).
¶ *Phil. Mag.*, Aug. 1922 and Nov. 1923.
** *Ann. d. Phys.* (4) lxxx. (1926).
†† *Phys. Rev.* Oct. 1926.
‡‡ G. Wentzel, *Zeit. f. Phys.* xxxviii. p. 518 (1927) ; J. Waller, *ibid.* p. 635.

§ 2. *Previous Work.*

The starting point is Schrödinger's equation

$$\frac{\partial^2\psi}{\partial x^2} + \frac{\partial^2\psi}{\partial y^2} + \frac{\partial^2\psi}{\partial z^2} + \frac{2\mu}{k^2}(E-U)\psi = 0, \quad . \quad (1)$$

where μ and e are the mass and charge of an electron,

$$\left.\begin{array}{l} k = \dfrac{h}{2\pi}, \quad E = \text{the total energy}, \\[2mm] U = \text{potential energy} = \dfrac{-Ze^2}{r} + eDz \end{array}\right\} \quad . \quad . \quad (2)$$

$+Ze =$ the charge on the nucleus, and $D =$ the strength of the field.

Let the z-axis be in the direction of the field and use parabolic coordinates

$$\left.\begin{array}{lll} x = \sqrt{\xi\eta}\cos\phi, & y = \sqrt{\xi\eta}\sin\phi, & z = \dfrac{\xi-\eta}{2}, \\[2mm] 0 \le \xi \le \infty, & 0 \le \eta \le \infty, & 0 \le \phi \le 2\pi. \end{array}\right\} \quad (3)$$

Equation (1) then becomes

$$\frac{\partial}{\partial\xi}\left(\xi\frac{\partial\psi}{\partial\xi}\right) + \frac{\partial}{\partial\eta}\left(\eta\frac{\partial\psi}{\partial\eta}\right) + \frac{1}{4}\left(\frac{1}{\xi}+\frac{1}{\eta}\right)\frac{\partial^2\psi}{\partial\phi^2} + \frac{\mu}{2k^2}$$

$$\left[E(\xi+\eta) + 2Ze^2 - \frac{eD(\xi^2-\eta^2)}{2}\right]\psi = 0 . \quad . \quad . \quad (4)$$

Make the substitution

$$\psi = M(\xi)N(\eta)\,{\cos\atop\sin}(s-1)\phi.$$

We get for the functions M, N the two ordinary differential equations

$$\left.\begin{array}{l} \dfrac{d^2M}{d\xi^2} + \dfrac{1}{\xi}\dfrac{dM}{d\xi} + \left(\dfrac{\mu E}{2k^2} + \dfrac{A}{\xi} - \dfrac{(s-1)^2}{4\xi^2} - \dfrac{\mu eD}{4k^2}\xi\right)M = 0, \\[3mm] \dfrac{d^2N}{d\eta^2} + \dfrac{1}{\eta}\dfrac{dN}{d\eta} + \left(\dfrac{\mu E}{2k^2} + \dfrac{A'}{\eta} - \dfrac{(s-1)^2}{4\eta^2} + \dfrac{\mu eD}{4k^2}\eta\right)N = 0. \end{array}\right\}$$

$$. \quad . \quad . \quad (5)$$

where

$$A + A' = \frac{\mu Ze^2}{k^2}.$$

Simplify the equations by substituting

$$M = \xi^{(s-1)/2} e^{\alpha\xi} X(\xi), \qquad N = \eta^{(s-1)/2} e^{\alpha\eta} Y(\eta),$$

$$\alpha = \sqrt{-\frac{\mu E}{2k^2}}. \qquad \ldots \ldots (6)$$

Equations (5) are reduced to

$$\left. \begin{aligned} &\frac{d^2 X}{d\xi^2} + \left(2\alpha + \frac{s}{\xi}\right)\frac{dX}{d\xi} + \left[\frac{A+s\alpha}{\xi} - \frac{\mu e D}{4k^2}\xi\right]X = 0, \\ &\frac{d^2 Y}{d\eta^2} + \left(2\alpha + \frac{s}{\eta}\right)\frac{dY}{d\eta} + \left[\frac{A'+s\alpha}{\eta} + \frac{\mu e D}{4k^2}\eta\right]Y = 0. \end{aligned} \right\} \quad (7)$$

Let $A_0 + s\alpha_0 = -2\alpha_0 m, \qquad A_0' + s\alpha_0 = -2\alpha_0 n;$. (8)

$$\therefore \qquad \alpha_0 = -\frac{\mu Z e^2}{2k^2(m+n+s)} \qquad \ldots \ldots (9)$$

and

$$E_0 = -\frac{2k^2}{\mu}\alpha_0^2 = -\frac{\mu Z^2 e^4}{2k^2(m+n+s)^2}. \qquad \ldots (10)$$

§ 3. *Third-Order Terms.*

We solve by the method of successive approximation. We set

$$\left. \begin{aligned} &\alpha = \alpha_0 + D\alpha_1 + D^2\alpha_2 + D^3\alpha_3 + \ldots, \\ &A = A_0 + DA_1 + D^2A_2 + D^3A_3 + \ldots, \\ &A' = A_0' - DA_1 - D^2A_2 - D^3A_3 - \ldots, \\ &X = X_0 + DX_1 + D^2X_2 + D^3X_3 + \ldots, \\ &Y = Y_0 + DY_1 + D^2Y_2 + D^3Y_3 + \ldots, \\ &E = E_0 + \Delta_1 E + \Delta_2 E + \Delta_3 E + \ldots. \end{aligned} \right\} \quad (11)$$

Substitute in equation (7), we get for X,

$$\frac{d^2 X_0}{d\xi^2} + \left(2\alpha_0 + \frac{s}{\xi}\right)\frac{dX_0}{d\xi} - \frac{2\alpha_0 m}{\xi}X_0 = 0, \qquad \ldots \ldots (12)$$

$$\frac{d^2 X_1}{d\xi^2} + \left(2\alpha_0 + \frac{s}{\xi}\right)\frac{dX_1}{d\xi} - \frac{2\alpha_0 m}{\xi}X_1$$

$$= -2\alpha_1\frac{dX_0}{d\xi} - \frac{A_1 + s\alpha_1}{\xi}X_0 + \frac{\mu e}{4k^2}\xi X_0, \qquad \ldots \ldots (13)$$

$$\frac{d^2X_2}{d\xi^2} + \left(2\alpha_0 + \frac{s}{\xi}\right)\frac{dX_2}{d\xi} - \frac{2\alpha_0 m}{\xi}X_2$$

$$= -2\alpha_1\frac{dX_1}{d\xi} - \frac{A_1 + s\alpha_1}{\xi}X_1 + \frac{\mu e}{4k^2}\xi X_1$$

$$-2\alpha_2\frac{dX_0}{d\xi} - \frac{A_2 + s\alpha_2}{\xi}X_0, \quad . \quad (14)$$

$$\frac{d^2X_3}{d\xi^2} + \left(2\alpha_0 + \frac{s}{\xi}\right)\frac{dX_3}{d\xi} - \frac{2\alpha_0 m}{\xi}X_3$$

$$= -2\alpha_1\frac{dX_2}{d\xi} - \frac{A_1 + s\alpha_1}{\xi}X_2 + \frac{\mu e}{4k^2}\xi X_2$$

$$-2\alpha_2\frac{dX_1}{d\xi} - \frac{A_2 + s\alpha_2}{\xi}X_1 - 2\alpha_3\frac{dX_0}{d\xi} - \frac{A_3 + s\alpha_3}{\xi}X_0, \quad (15)$$

with four corresponding equations for Y.

I have evaluated X_2 from equation (14) as a sum of functions of the form $CX_0(m', s)$, and X_1 has already been expressed by Epstein [*] in the same form. Therefore equation (15) can be reduced to the form

$$\frac{d^2u}{d\xi} + \left(2\alpha_0 + \frac{s}{\xi}\right)\frac{du}{d\xi} - \frac{2\alpha_0 m}{\xi}u = \frac{CX_0(m', s)}{\xi}, \quad . \quad (16)$$

whose solution [†] is

$$u = \frac{C}{2\alpha_0(m' - m)}X_0(m', s). \quad . \quad . \quad . \quad (17)$$

This solution satisfies all the requirement of finiteness when $m' \neq m$. So the condition which we have to impose on the third-order terms in equation (15) is that the sum of the coefficients of $X_0(m, s)$ must vanish.

Proceeding in this manner I have obtained [‡]

$$(2m + s)\alpha_3 + A_3$$

$$= -\frac{20\mu^2 e^2\alpha_1}{64 \times 32k^4\alpha_0^6}(s + 2m)(34m^2 + 34sm + 4s^2 + 9s + 5)$$

$$+ \frac{12\mu e\alpha_1^2}{64k^2\alpha_0^4}(6m^2 + 6ms + s^2 + s)$$

$$- \frac{\mu e\alpha_2}{8k^2\alpha_0^3}(6m^2 + 6ms + s^2 + s)$$

---

[*] Phys. Rev. xxviii. no. 4, October 1926, p. 700, equation (28).
[†] *Ibid.* p. 700, equation (26).
[‡] The full details are somewhat cumbersome and have been omitted here for brevity.

$$+ \frac{8\mu^3 e^3}{32 \times 32 \times 64 k^6 \alpha_0{}^8} (750 m^4 + 1500 m^3 s + 996 m^2 s^2$$
$$+ 258 m^2 s + 330 m^2 + 246 m s^3 + 258 m s^2$$
$$+ 330 m s + 16 s^4 + 59 s^3 + 73 s^2 + 30 s), \quad . \quad . \quad . \quad (18)$$

and a corresponding condition (obtained from the equations for Y), which may be derived from (18) by interchanging m and n and reversing the signs of A_3 and μ respectively. From these two conditions we obtain by addition and substitution for α_1 and α_2 in terms of m, n, and s (see Epstein's paper quoted above, equations (29) and (30), pages 701 and 702),

$$\alpha_3 = \frac{3\mu^3 e^3 (m-n)}{128 \times 64 k^6 \alpha_0{}^8}$$
$$\{3(m+n+s)^2 + 10(m-n)^2 + 10 s^2 - 20 s + 20\}, \quad (19)$$

or since

$$\Delta_3 \mathrm{E} = -\frac{2k^2}{\mu} (\alpha_0 \alpha_3 + 2\alpha_1 \alpha_2) \mathrm{D}^3, \quad . \quad . \quad . \quad (20)$$

we finally have

$$\Delta_3 \mathrm{E} = -\frac{3\mu^2 e^3 \mathrm{D}^3 (m-n)}{64 \times 64 k^4 \alpha_0{}^7}$$
$$\{20(m+n+s)^2 - 11(m-n)^2 + s^2 - 2 s + 30\}$$
$$= \frac{3 \mathrm{D}^3}{32 \mu^5 Z^7 \times e^{11}} \times \left(\frac{h}{2\pi}\right)^{10} (m-n)(m+n+s)^7$$
$$\{20(m+n+s)^2 - 11(m-n)^2 + s^2 - 2 s + 30\}. \quad (21)$$

My thanks are due to Prof. A. M. Mosharrafa, under whose direction the above work was done.

III. *The Existence of the J-Phenomena.* By IVOR BACK-HURST, *M.Sc., Physics Department, National Physical Laboratory, Teddington, Middlesex* *.

INTRODUCTION.

IN association with the scattering of X-rays, phenomena have been observed which were at first [8, 9] attributed to the excitation of " J " characteristic radiation of an irradiated atom, but were later [11, 12] thought to be

due to the occurrence of a "J-transformation" of the scattered radiation during its passage through an absorbing medium. It has been supposed [20] that the appearance or non-appearance of these phenomena was determined by some unknown factor, since apparently similar experimental conditions prevailed in either case. For some years experiments on "J-transformations" have, from time to time, been described [11] to [30], although in the same period a number of investigators have reported failure to find any evidence for such phenomena [31] to [44]. In 1929, Barkla and Sen Gupta [29] described an experiment in which heterogeneous radiation from a Coolidge tube was scattered at 90° by a slab of paraffin wax placed at 45° to the incident radiation. One ionization chamber S was placed to receive the scattered beam and another T to receive the transmitted beam. Sheets of aluminium of total thickness x were placed in the path of the scattered beam, and a number of sheets of the same total thickness were placed in the path of the transmitted beam. The ratio of the ionization current measured by S to that measured by T was plotted for different values of x. The discontinuous nature of the curve obtained was said to be due to sudden changes of intensity of the partially absorbed scattered beam. The changes were of the order of 7 per cent., and were supposed to be due to "J-transformations."

The extent to which it is justifiable to regard such a curve as discontinuous would naturally depend on the amount of fluctuation due to experimental error. Unsteadiness of the X-ray source would normally be thought the chief cause of error, but Barkla, to whom we owe the conception of J-phenomena, has emphasised the importance of maintaining steady conditions of X-ray intensity in order to obtain the phenomena. On this account it seemed improbable that the changes of intensity of 7 per cent., referred to above, could be accounted for in this way. Barkla has, however, suggested the desirability of investigating these phenomena with the aid of a "constant potential" high tension generator, and an attempt to do this is described below.

Apparatus.

The "constant potential" high tension plant used had full wave rectification, and has been described by E. Bell [1].

It was supplied with alternating current from a rotary converter driven by accumulators. The input voltage to the converter was maintained within a range of ± 0.2 per cent. of its mean value by means of a potentiometer arrangement P_1 (fig. 1) and a hand operated rheostat R_l in the supply circuit. The current supplied to the converter was held within ± 0.5 per cent. of its mean value by means of another potentiometer arrangement P_2 (fig. 1) and a hand operated rheostat in the circuit supplying current to the filament of the X-ray tube. All the potentiometer resistances were eureka and, with the exception of the slide wires S, variable only in fixed steps. No sliding contacts were used ; the contacts on the slide wires were screwed, and all
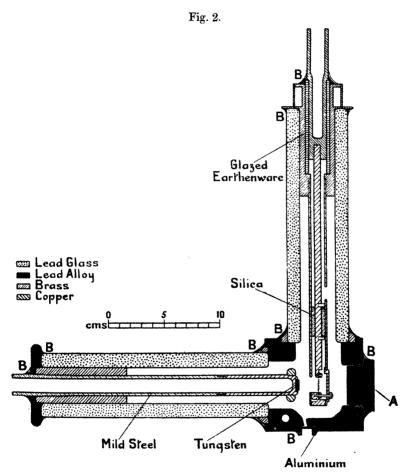
Fig. 1.

other contacts were screwed or soldered. The cadmium cell balance was checked at frequent intervals r with the aid of a microammeter (M), one division deflection of which corresponded to a change of potentiometer battery voltage of 0.03 per cent. The galvanometers employed in the voltage and current measuring potentiometers had time periods of 2 and 0.5 seconds respectively, and were not far from aperiodic under the conditions obtaining. A change of 1 per cent. in the voltage or current produced a deflexion of 11 or 6 divisions respectively in the corresponding galvanometers G_1 and G_2.

A rheostat was included in the circuit between converter and high tension transformer, but this was used only when putting the plant into operation, and was brought to zero resistance when taking readings in order that current fluctuations should affect the high tension voltage as little as possible. Change of voltage was effected

by an auto-transformer. The high tension voltage was continuously indicated by an attracted disk electrometer, the calibration of which was verified by comparison with a 10 cm. sphere spark gap. The mid-point of the secondary winding of the high tension transformer was earthed,

Fig. 2.

Glazed Earthenware

Lead Glass
Lead Alloy
Brass
Copper

Silica

0   5   10
cms

B
B
B
B
B
B
B

A

Mild Steel   Tungsten   B

Aluminium

and for part of the investigation sufficient voltage was obtained by arranging the constant potential plant so that one output lead was earthed. When this was done the potentiometer P_2 was used to measure the high tension current directly, instead of the converter current as shown in the diagram.

The X-ray tube (fig. 2) was constructed specially for
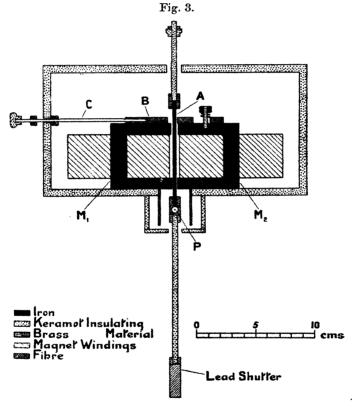
research on X-ray scattering. The objects aimed at in particular were (*a*) high power for continuous operation, (*b*) exceptionally high X-ray protection, and, (*c*) the facilitation of large angle scattering measurements. The importance of (*a*) and (*b*) is considerable, since the intensity of scattered radiation is in general only a small fraction of that of the primary beam. The main features of the X-ray tube are as follows.

The anticathode stem and cathode are contained in lead glass tubes emerging at right angles from a lead alloy box of minimum wall thickness 1 cm. and at earth potential. The tungsten anticathode is situated in the lead alloy box 4 cm. from an aluminium window. The glass tubes have a lead equivalent of 3 mm., but since the radiation from the anticathode is everywhere incident obliquely on the glass the minimum effective stopping power is equivalent to 5 mm. of lead. A spectrometer may be brought close to the aluminium window, and undue restriction of the maximum scattering angle measurable is avoided.

The anticathode is cooled by a forced circulation of oil, which passes through ebonite tubes to a water cooler at earth potential. Thermo-syphon water cooling is used for the cathode, and the lead alloy box is water cooled from the main. Removal of the plug A permits the replacement of a filament to be effected without difficulty. A vacuum is maintained by means of oil diffusion pumps. It was found that for outputs exceeding 1·3 kilowatts the lead glass surrounding the anticathode stem became too much heated. The capacity of the X-ray tube was, however, found ample for the purpose of the investigation.

The X-ray tube was continuously in operation, while readings were being taken, X-ray exposure times of multiples of half a minute being obtained by means of a specially constructed exposure meter (fig. 3). The meter was controlled by a master clock and in order to maintain the accuracy of the meter as high as that of the clock it was arranged to operate without the aid of a mechanical relay. Some form of relay action had to be introduced, however, as the electrical pulse available from the clock circuit was of too low power and short duration to actuate with sufficient speed and certainty a lead shutter of the requisite dimensions. In the arrangement adopted, a lead shutter 3 mm. thick is

connected by a keramot rod, pivoted at the centre of gravity, to an iron strip A lying between the poles of two electromagnets. The main windings of the magnets are connected in series and included in a Laboratory clock circuit. A rotary switch short-circuits either or both of these windings. Auxiliary windings on the two magnets are supplied with unequal continuous currents

Fig. 3.

Iron
Keramot Insulating
Brass Material
Magnet Windings
Fibre

Lead Shutter

through a change over switch. The iron strip A is pushed clear of the pole-face of the weaker magnet, say M_2, by the slotted fibre bar B, the auxiliary currents being adjusted so that the resultant magnetic force on A is just sufficient to hold it in contact with B under the obtaining conditions of vibration.

During a half-minute interval between consecutive current pulses from the master clock the rotary switch is set to allow the following impulse to increase the pull

of M_1 and thereby supply a " trigger " action resulting in the movement of the lead shutter out of the path of the X-ray beam.

Succeeding current pulses produce no effect on the meter until the currents through the auxiliary windings are interchanged, and the rotary switch and fibre bar actuated, allowing the following impulse to terminate the exposure. The auxiliary currents are necessary to prevent the iron strip A rebounding from the magnet pole-faces and also serve to accelerate greatly the motion of the shutter. The above device was found completely

TABLE I.

Stopwatch observations.		Calculated equal time intervals.		Differences.
Mins.	Secs.	Mins.	Secs.	Secs.
0	5·82	0	5·820	0
0	35·79	0	35·788	— 0·002
1	5·76	1	5·756	— 0·004
1	35·72	1	35·724	0·004
2	5·69	2	5·692	0·002
2	35·66	2	35·660	0·000
3	5·60	3	5·628	0·028
3	35·58	3	35·596	0·016
4	5·55	4	5·564	0·014
4	35·53	4	35·532	0·002
5	5·49	5	5·500	0·010
5	35·47	5	35·468	— 0·002
6	5·46	6	5·436	— 0·024
6	35·42	6	35·404	— 0·016
7	5·37	7	5·372	0·002
7	35·34	7	35·340	0

reliable and enabled exposures of half-a-minute to be automatically timed to within 0·1 per cent. The accuracy of the meter was checked by observing stopwatch readings without stopping the watch while listening to the " ticks " made by the meter as the iron strip A hit the magnet polefaces. Some readings obtained are shown in Table I. ; the bulk of the error indicated is clearly observational, and not due to the meter, but the maximum total error is within the estimate given above.

The X-ray intensity-time product was measured by means of an air-filled ionization chamber and Compton electrometer. In order to have a short time period and stable zero, the electrometer was used with a short

quartz fibre and adjusted to a low sensitivity (1000 mm. per metre per volt). It was used as a null instrument, the insulated system being coupled through a small air-condenser to a potentiometer constructed to read to thousandths of its full range. The values of the condenser and potentiometer current were adjusted so that one small potentiometer unit corresponded approximately to 1 mm. per metre deflexion of the electrometer needle.

Method of Experiment and Results.

When an attempt was made to repeat the experiment described by Barkla and Sen Gupta it was found that the arrangements described above secured sufficient constancy of X-ray intensity to render unnecessary comparison with the transmitted beam. The experiment consisted, therefore, in measuring the absorption in aluminium of the beam scattered at 90°. The scattering material used was a slab of paraffin wax placed so that a normal to the face of the slab was the external bisector of the angle of scattering. An area approximately 2 mm. wide and 2 cm. high of the face of the slab was irradiated, the angular divergence of the incident beam in the plane of the scattering angle being about 1° 4′. In the same plane the angular divergence of the scattered beam received by the ionization chamber was 1° 48′. The solid angle subtended at any point in the aluminium absorber by the effective aperture of the ionization chamber was less than 0·0027 of 4π, so that the absorption measured was the total absorption, *i. e.*, only a negligible fraction of the radiation scattered by the aluminium absorber could enter the ionization chamber.

High tension voltages were chosen to obtain radiation of the right " hardness," as measured by a " half-value " thickness of aluminium, to cover the region in which the J-phenomena have been found. In particular J-discontinuities have been stated to occur [24] for values of μ/ρ in aluminium of 3·76, 3·24, 2·44, 1·94, 1·40, 0·73, 0·47 corresponding to half-value thicknesses of 0·683, 0·792, 1·051, 1·322, 1·833, 3·52, 5·46 mm. respectively. The first six of these positions are marked on the curves shown in figs. 4 and 5. For curve (1) the X-ray tube window was a sheet of aluminium 0·03 mm. thick, while for the other curves it was 0·5 mm. thick. The curves

have been scaled to make the average gradient of each somewhere near 45° in order to make as marked as possible any deviations of the experimental points. In order that the extent of fluctuations due to experimental error may better be gauged, the observations from which curve (3) of fig. 5 is deduced are given in Table II. in the order in which they were obtained. The other curves
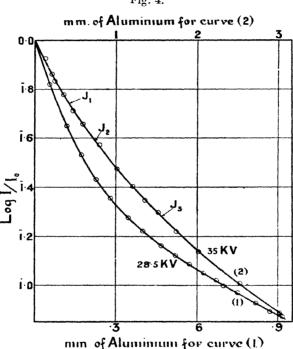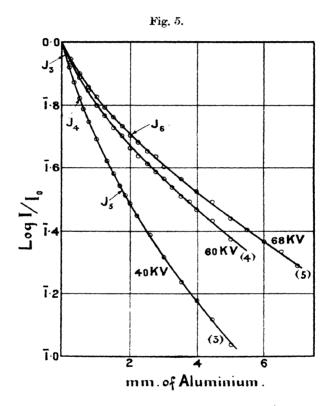
Fig. 4.

were deduced from similar sets of readings, each point being calculated from the average of two, or sometimes three, consecutive potentiometer readings.

Log (I/I_0), instead of I/I_0, has been plotted in order that the distance of a point from the curve, when measured along the ordinate, should be directly proportional to the percentage error in the ratio I/I_0. From measurements made in this way on large scale graphs, an analysis is given in Table III. of the extent of the departure of the

experimental points from a smooth curve drawn so that $f''(x)$ is always positive. The result is evidently consistent with the assumption that absorption of a heterogeneous beam is determined by the intensity distribution over its constituent wave-lengths in the manner given by the equation $I = \int I_\lambda e^{-\mu_\lambda \lambda^r} d\lambda$ where $I_\lambda\, d\lambda$ is the initial intensity

Fig. 5.

associated with the wave-length range $d\lambda$ at the wave-length λ, μ_λ is the corresponding absorption coefficient and I is the total intensity of the transmitted radiation. This is mentioned as the validity of the above assumption appears to have been questioned [11, 23].

It will be noticed that the average percentage error shown in Table III. is several times the estimated error in the constancy of the supply current and voltage. Although this is partly due to the fact that a perfectly

constant input to a high tension plant would not necessarily mean a perfectly constant output, it is mainly due to the proportionality factor existing between change of high tension voltage and change of intensity of the scattered radiation. Thus $\Delta I/I = k \cdot \Delta V/V$ where k is always greater than unity and becomes greater the higher the

TABLE II.

Values for curve (3) of fig. 5.

MM. of Aluminium.	Potentiometer Readings.	A Averages.	B Inter-polated values for 0 mm.	log (A/B) =log (I/I_0).
0	966·5, 972	969·2	—	—
2·009	298, 297	297·5	968·6	$\bar{1}$·4874
3·017	200, 200	200	968·0	$\bar{1}$·3152
4·000	145, 145·5	145·2	967·4	$\bar{1}$·1764
0	968·5, 965	966·8	—	—
0·207	804, 805·5	804·8	966·9	$\bar{1}$·9203
0·351	721, 721	721	,,	$\bar{1}$·8726
0·514	642, 640	641	,,	$\bar{1}$·8215
0·636	595, 594	594·5	,,	$\bar{1}$·7888
0·797	542, 541	541·5	,,	$\bar{1}$·7482
1·008	475, 477	476	,,	$\bar{1}$·6922
1·337	405, 406·5	405·8	,,	$\bar{1}$·6229
0	967, 967	967	—	—
1·522	368, 368	368	967·1	$\bar{1}$·5804
1·705	339, 339	339	967·3	$\bar{1}$·5446
1·868	314·5, 315	314·7	967·4	$\bar{1}$·5124
2·216	273, 270, 271	271·1	967·6	$\bar{1}$·4473
2·600	236, 235·5	235·7	967·7	$\bar{1}$·3867
3·531	165, 168, 168	167	967·9	$\bar{1}$·2369
0	969, 967	968	—	—
4·470	126, 126·5	126·7	966	$\bar{1}$·1163
5·010	104, 106	105	964	$\bar{1}$·0371
2·009	297, 296	296·5	962	$\bar{1}$·4889
0	961, 959	960	—	—

absorption of the scattered beam. The value of k under various conditions was determined by changing the high tension voltage about 2 per cent. In Table IV. are given values of k corresponding to conditions of "hardness" and absorption under which the J-phenomena have mostly been found. A 1 per cent. change in supply current was found to produce a 1 per cent. change, or less, in the intensity of the scattered beam for any of the high tension voltages employed.

Taking the factor k into account, the percentage errors shown in Table III. correspond to the estimated variation in voltage and current. For example, the

TABLE III.

Point number on curve.	Percentage departure from curve of the ratio I/I_0. Curve Number.				
	1	2	3 ·	4	5
1	0·0	1·2	0·0	0·2	0·0
2	0·0	0·7	0·0	0·2	0·2
3	0·0	0·2	—0·1	0·5	—0·5
4	0·0	—0·2	0·0	—0·5	0·7
5	0·0	0·0	0·0	0·4	0·9
6	0·0	0·5	—0·6	0·3	0·3
7	0·0	0·5	0·4	1·6	0·4
8	0·0	—0·9	0·0	—0·9	—0·5
9	0·0	0·7	0·3	—0·5	—0·9
10	0·2	0·0	—0·2	0·3	0·0
11	—0·3	0·2	0·4	—0·9	1·2
12	0·8	—0·5	—0·9	0·5	—1·5
13	—0·7	—1·2	0·6	0·2	0·0
14	0·3	0·6	—0·5	—0·6	0·1
15	0·0	—0·9	—0·6	0·9	1·6
16	—0·6	—	0·8	—0·5	0·8
17	0·8	—	1·1	1·2	0·4
18	—	—	—1·9	—1·4	0·0
19	—	—	—	—	1·4
20	—	—	—	—	—1·0

TABLE IV.

Kilovoltage.	MM. of Aluminium.	K=percentage intensity increase for 1 per cent. increase in kilovoltage.
36	0	3·04
	0·348	5·1
	0·815	5·9
43	0	1·7
	1·522	3·4
	3·017	4·9
54	4·001	4·9
	6·018	5·5

maximum error of —1·9 per cent. (Point no. 18 of Curve 3) occurs when the ratio I/I_0 is approximately 0·1, and a unit of the electrometer potentiometer is therefore 1 per cent. of I/I_0. Actually, however, the reading was

estimated to 0·5 per cent. of I/I_0. The factor k was over 6, so that an effective voltage variation of (1·9–0·5)/6 or 0·23 per cent. would account for this discrepancy without considering effects due to current supply variation or variations occurring in the high tension plant. Clearly, therefore, there is no room for the supposition that J-discontinuities of a magnitude approaching 7 per cent. exist under the conditions obtaining in these experiments.

Critical Summary and Discussion of Evidence for J-Phenomena.

Prior to about 1923, the theory of the existence of J-phenomena depended on experiments of a different character from those considered above. To make the position clear, these early experiments are briefly summarized and criticised below.

(1) Barkla [6, 8] found that the ratio of absorption in iron to absorption in aluminium, when plotted against wavelength, gave a curve showing a sharp change in slope at $\lambda = 0·5$ Å.U. and concluded that this was occasioned by a selective J-absorption in aluminium.

(2) Williams [3] found that the curve obtained by plotting absorption in aluminium against absorption in copper showed a discontinuity at $\lambda = 0·49$ Å.U. and attributed it to J-absorption in aluminium.

Richtmyer [34] in 1921 found these results could not be confirmed and Duane and Shimizu [31] had previously shown that no characteristic radiation of aluminium existed in this region of wave-length.

(3) Barkla and Miss White [7] measured the absorption in aluminium, paper, water, paraffin wax, and copper, of filtered primary rays. Curves of relative absorption, obtained by plotting for different " effective " wavelengths the mass absorption coefficients of the first four materials against the mass absorption coefficient of copper, showed discontinuities thought to indicate J selective absorption.

As pointed out by Richtmyer [35], the data for these curves showed discontinuities at points other than those cited as positions of J-absorption edges, and the experimental accuracy was clearly insufficient to warrant the conclusions drawn.

(4) Owen [2] noticed a small subsidiary minimum in the spectral intensity curve of radiation from a palladium

anticathode and suggested that it might possibly be occasioned by a selective Jβ absorption in the silicon of the carborundum analysing crystal.

Siegbahn and Wingardh [32] pointed out that the minimum could have been occasioned by selective K-absorption in the palladium anticathode.

(5) Dauvillier [4] obtained spectral intensity curves of primary rays. When aluminium filters were used he detected an irregularity at 0·358 Å.U. which he attributed to J-absorption in aluminium. Richtmyer [35] suggested this might be due to K-absorption of the iodine in the ionization chamber. As Dauvillier remarked at the time, however, this irregularity was practically within the limits of experimental error.

Dauvillier also noticed a small peak in the tungsten spectrum which he attributed to J-absorption in the bromine of the ionization chamber, but, as Richtmyer pointed out, this was presumably the Kα peak of tungsten.

(6) Crowther [5] measured the absorption of rays scattered from aluminium placed in the path of a heterogeneous beam. He found the scattered rays more heterogeneous than the primary, comprising longer wave-lengths than the latter, and attributed this to J characteristic radiation from the aluminium scatterer. Alternatively, he considered it possible that the primary radiation might suffer a slight increase in wave-length in the process of scattering. Numerous experiments by Compton and others have shown the latter hypothesis to be the correct one.

As far as the writer is aware, no evidence for J-phenomena in addition to the above has at any time been brought forward except by Barkla and his co-workers [9–29], who have carried out experiments in which the essential feature has been the detection of " J-transformation " discontinuities in curves showing the relative intensities of transmitted and scattered rays after partial absorption by various equal thicknesses of some material. Some slight irregularities in early spectroscopic data have been considered by Khastgir and Watson [13, 14] to support the " J-transformation " theory, but, as pointed out by Siegbahn [39] and by Nipper [40], later spectroscopic measurements with improved apparatus have not shown these irregularities.

The position is, therefore, that all the early results thought to show J-phenomena can either be attributed to experimental error or else explained in terms of phenomena, the existence of which has been well confirmed. The hypothesis of J-phenomena must therefore depend entirely on the validity of the later results [9-29] concerning " J-transformations " of scattered radiation, in which the discontinuities have been stated to be 7·5 or 10 per cent., and which have been performed with a knowledge of criticisms passed on the earlier work and of the failure of a number of investigators to obtain corroborant results. Summaries of the published accounts of experiments on " J-transformations " have been given by Gaertner [42] and by Alexander [44]. These investigators and also Dunbar [38, 43] and Worsnop [41] have endeavoured without success to obtain J-phenomena. Gaertner comments on the lack of information concerning arrangements made to secure accuracy in the J-experiments. Dunbar concludes that J-irregularities may have been due to varying amounts of soft radiation reaching the measuring electroscopes, and considers that the method of experiment was unsuitable to distinguish between the effects of classical and modified scattering. Worsnop remarks that some unknown condition must be necessary for the occurrence of J-phenomena. Alexander concludes that the factors necessary for such are restricted to very special experimental conditions. A brief account of J-phenomena is given by Barkla in the International Critical Tables, and reference to later unpublished work has recently been made by him [30].

The conclusion reached by the writer is that " J-transformations " have mainly been due to the following causes :—

(1) Fluctuations, both irregular and periodic, in the voltage-time curve of the high tension generator.

(2) Change of wave-length in the process of scattering, taking into account the effect of twice sc⁻ ered radiation.

(3) A systematic tendency on the part of thɛ ti-gators concerned to overestimate the sensitivity and accuracy of the balance method of measurement they used.

(4) The vitiation of results by entry into the ionization chambers of " stray " scattered radiation from surrounding objects.

The object of the balance method used throughout in the J-experiments has been to minimise error due to fluctuations of intensity of the beam incident on the scattering material. The intensity ratio of scattered to transmitted radiation can, however, remain constant only if the intensity of the incident beam varies in such a manner as to maintain unchanged the relative intensities of its component wave-lengths. Otherwise, variation in the intensity ratio must necessarily occur, since the scattering coefficient is not independent of wave-length, and a considerable variation must result from the dependence on wave-length of the proportion of modified to unmodified scattering. A change in the high tension voltage-time curve will therefore, in general, alter the intensity ratio, although the peak voltage may remain unchanged. The latter case may be regarded as a change in the peak voltage of part of the X-ray beam, and this change will be magnified by different amounts in its effect on the intensities of the partially absorbed transmitted and scattered beams, since the k factors for these beams will not be the same. In this connexon it may be observed that

(*a*) by gradually changing the frequency of interruption of the primary current to the induction coil the J-discontinuities could be made to become less sharp and finally disappear [23];

(*b*) when a high tension transformer was used, together with a Coolidge tube, the J-discontinuities were found to be under " perfect control" [24];

(*c*) the condition for and character of J-discontinuities has been considered to be dependent on some unknown factor in the method of excitation of the X-rays [23, 28].

It is impossible to believe that the Compton effect can have failed to be present to an observable extent in most of the J-experiments of which there are published accounts. The intensity ratio of scattered to primary rays in these experiments was almost always found to decrease with increasing absorption of each beam by equal thicknesses of material, the decrease occurring either

evenly or in steps. Since the ratio was found to be con-
stant between adjacent steps it was deduced that the
Compton effect was not operative. On the other hand,
no evidence was produced that the accuracy of any of these
experiments was sufficiently high to show with certainty
the change of ratio to be expected from the Compton
effect in the interval between consecutive steps. In some
J-experiments [21] in which the range of wave-length was
stated to be from 0·3 to 0·6 Å.U. it was calculated that the
Compton effect should have produced a total change
in absorption coefficient of from 12 to 20 per cent., of
which one-tenth could easily be measured. The con-
clusion reached was that there was no evidence at all
of the existence of the Compton effect.

In actual fact it can be shown that with scattering
materials of very low atomic weight such as those used in
the J-experiments and with incident radiation of wave-
length in the neighbourhood of 0·3 Å.U. the observed
change of absorption coefficient is greater than that
calculated by means of the equation $\lambda' - \lambda = 0·024\,(1 - \cos\phi)$
even if it be assumed that the whole of the scattered
radiation is modified. By altering the size of the scatterer
it may be proved that a large part, if not quite all, of this
extra change in absorption is due to the effect of radiation
twice scattered and modified in the scatterer. Using
a crystal selected incident beam, the writer has measured
the intensity of the scattered beam (*a*) without an absorbing
screen, (*b*) with an absorbing screen in the incident beam
(*c*) with the same absorbing screen in the scattered beam.
Values found for a scattering angle of 90° with paraffin
wax as scattering material and an absorbing screen of
copper 0·210 ∓0·005 mm. thick are shown in Table V.

The calculated increase in absorption coefficient is
obtained using the equation $\mu = 3·34 + 1{,}340\lambda^3$ (sufficiently
exact in the neighbourhood of 0·3 Å.U.) to calculate
λ from μ and then using the derived expression

$$(\mu' - \mu)/\mu = \left(1 - \frac{3·34}{\mu}\right)\left\{\left(\frac{\lambda'}{\lambda}\right)^3 - 1\right\}$$

Similar results have also been obtained with beryllium
or water as scattering materials, the range of scattering
angle investigated being from 20° to 120° *. It should

* It is hoped to publish later a full account of scattering experiments
with a crystal selected incident beam.

be mentioned that the cross-section of the incident beam at the surface of the paraffin slab was 0·5 mm. by 16 mm., the angular divergence being 11 minutes of arc. The cross-section, at the slab, of the scattered beam reaching the ionisation chamber was 5 mm. by 16 mm. For scattered beams of larger cross-section the increase in absorption coefficient becomes greater.

The effect of heterogeneity of beam is to make the apparent change of wave-length, as deduced from the absorption coefficients, somewhat less than the true value. In the J-experiments [21], however, in which it was

TABLE V.

Scatterer.		Intensity Readings.	Interpolated value for (a)	Intensity Ratio.	Linear Absorption Coefficient (μ).	Experimental increase in μ.	Calculated increase in μ.
Paraffin wax cylinder	a	708·5					
Diameter 3 mm...	b	278·5	708·3	2·543	44·4		
Height 25 mm. ..	c	224·5	708·1	3·154	54·7	23·1%	22·9%
	a	708					
Paraffin wax slab	a	991					
	b	391	990·3	2·533	44·3		
Thickness 15 mm.	c	297	989·7	3·332	57·3	29·5%	
	a	989					

concluded that the Compton effect did not exist, the main factor in reducing the apparent change of wavelength would be the proportion present of unmodified long wave-lengths, the existence of which would render any calculation of wave-length change from absorption measurements quite valueless. It appears impossible to escape the conclusion that the sensitivity of J-experiments of this type, in the estimation of change of quality of scattered radiation, has been considerably overestimated by the investigators concerned.

Other results found in connexion with J-experiments seem to be capable of easy explanation. In particular, it has been stated that radiation scattered from thin

sheets of material, *e. g.*, paper, was found to be unmodified, while that scattered from thick sheets was modified [28]. In the latter case, since in general, large angle cones of radiation have apparently been used, a large proportion of twice scattered and modified radiation would enter the ionization chamber, and the apparent change in absorption coefficient would be considerably greater than in the former case, in which the intensity of the scattered radiation would necessarily be less and the consequent reduced accuracy of the experiment probably insufficient to show definitely the smaller amount of modification actually present.

An alteration of the absorption of one X-ray beam in a sheet of material, due to the transmission through the sheet, in another direction, of a second X-ray beam has been found in some of the J-experiments, *e. g.* [29]. Some time ago the writer endeavoured to find some trace of such an effect without success. Pseudo effects of this character were, however, very easily obtained due to " stray " scattered radiation, the reduction of which to completely negligible proportions was found to require care.

It has been argued that, since some of the J-experiments showed J-phenomena while other apparently similar experiments did not, no negative result could be regarded as disproving the existence of the phenomena. On the other hand, whether this argument may be valid or not, a careful experimental investigation, together with a perusal of the literature, leads inevitably to the conclusion that up to the present time no experimental work has been reported that does, in fact, constitute any real evidence for the existence of J-phenomena, and there seems to be no reason of any kind why the existence of such phenomena need be postulated.

In conclusion I desire to express my thanks to Dr. G. W. C. Kaye, O.B.E., the Superintendent of the Physics Department, for his interest in this investigation, and to acknowledge efficient assistance rendered by Mr. P. R. Pallister, B.Sc. in the experimental work. The X-ray tube and X-ray exposure meter described were made by Mr. W. G. H. Turl in the Instrument Workshop of the Laboratory, the high lead content glass tubes having been specially manufactured due to the courtesy of Messrs. Philips of Holland.

Summary.

A full-wave rectification "constant potential" high tension generator has been employed in an attempt to obtain evidence of the existence of J-phenomena. The X-ray tube, of which a description is given, was specially designed for use in intensity measurements of scattered X-rays and adapted for excitation by a "mid-point earthed" high tension generator. Potentiometers were used in the control of supply voltage and current, and intensity measurements were made by means of a potentiometer coupled through a condenser to the insulated system of the ionization chamber and Compton electrometer. X-ray exposures were automatically timed by means of a simple type of exposure meter, operated without mechanical relay by a master clock.

With these arrangements, sufficiently accurate absorption curves of radiation scattered from paraffin wax at 90° were obtained, without recourse being necessary to the custom, in J-experiments, of making comparison measurements of the transmitted beam. No indication of J-phenomena was found, but the intensity of the scattered beam was found to be highly sensitive to change of high tension voltage. Values of the proportionality factor for small percentage changes were determined for conditions of hardness and absorption under which the J-phenomena have been stated to occur.

A short critical discussion of the literature is given, together with a bibliography. In particular, comment is made on the alleged non-appearance of the Compton effect in some of the J-experiments, and some results obtained with a crystal selected incident beam are given to show that the actual change of absorption is greater than the theoretical value on account of the effect of twice scattered radiation. It is considered that in all the reported accounts of J-transformations the investigators concerned have overestimated the accuracy of their experiments. Probable causes of error are enumerated, the chief being fluctuation of the time voltage curve of the high tension plant.

It is concluded that so far there has been no real experimental evidence whatever for J-phenomena, and that there seems to be no reason why the existence of such should be postulated.

References.

(1) Bell, Brit. Journ. of Rad. ii. p. 156 (1929).

EVIDENCE FOR J-PHENOMENA.

(2) Owen, Proc. Roy. Soc. A. xciv. p. 339 (1918).
(3) Williams, Proc. Roy. Soc. A. xciv. p. 567 (1918).
(4) Dauvillier, *Ann. de Phys.* xiii. p. 49 (1920).
(5) Crowther, Phil. Mag. xlii. p. 719 (1921).
(6) Barkla, Proc. Roy. Soc. A. xcii. p. 501 (1916).
(7) Barkla and Miss White, Phil. Mag. xxxiv. p. 270 (1917).
(8) Barkla, Phil. Trans. of the Roy. Soc. A. ccxvii. p. 315 (1918).
(9) Barkla, 'Nature,' cxii. p. 723 (1923).
(10) Barkla and Miss Sale, Phil. Mag. xlv. p. 737 (1923).
(11) Barkla, 'Nature,' cxiv. p. 753 (1924).
(12) Watson, Proc. Roy. Soc. of Edinburgh. xlv. p. 48 (1924-5).
(13) Khastgir and Watson, 'Nature,' cxv. p. 604 (1925).
(14) Khastgir and Watson, 'Nature,' cxvi. p. 47 (1925).
(15) Barkla and Miss Mackenzie, 'Nature,' cxvi. p. 942 (1925).
(16) Barkla and Khastgir, Phil. Mag. xlix. p. 251 (1925).
(17) Barkla, Phil. Mag. xlix. p. 1033 (1925).
(18) Barkla and Khastgir, Phil. Mag. l. p. 1115 (1925).
(19) Barkla and Khastgir, 'Nature,' cxvii. p. 228 (1926).
(20) Barkla, 'Nature,' cxvii. p. 448 (1926).
(21) Barkla and Miss Mackenzie, Phil. Mag. i. p. 542 (1926).
(22) Barkla and Khastgir, Phil. Mag. ii. p. 642 (1926).
(23) Barkla and Miss Mackenzie, Phil. Mag. ii. p. 1116 (1926).
(24) Barkla and Watson, Phil. Mag. ii. 1122 (1926).
(25) Barkla, 'Nature,' cxix. p. 778 (1927).
(26) Barkla and Khastgir, Phil. Mag. iv. p. 735 (1927).
(27) Watson, Phil. Mag. v. p. 1146 (1928).
(28) Barkla, Phil. Mag. v. p. 1164 (1928).
(29) Barkla and Sen Gupta, Phil. Mag. vii. p. 737 (1929).
(30) Barkla, 'International Critical Tables,' vi. p. 1 (1929) and 'Nature,' cxxvii. p. 877 (1931).

EVIDENCE AGAINST J-PHENOMENA.

(31) Duane and Shimizu, Phys. Rev. xiv. p. 389 (1919).
(32) Siegbahn and Wingardh, *Phys. Zeit.* xxi. p 83 (1920).
(33) Richtmyer and Grant, Phys. Rev. xv. p. 547 (1920).
(34) Richtmyer, Phys. Rev. xvii. p. 434 (1921).
(35) Richtmyer, Phys. Rev. xviii. p. 13 (1921).
(36) Richtmyer, Phys. Rev. xix. p. 418 (1922).
(37) Compton, 'Nature,' cxiii. p. 160 (1924).
(38) Dunbar, Phil. Mag. xlix. p. 210 (1925).
(39) Siegbahn, 'Nature,' cxvi. p. 11 (1925).
(40) Nipper, 'Nature.' cxvi. p. 12 (1925).
(41) Worsnop, Proc. Phys. Soc. xxxix. p. 305 (1927).
(42) Gaertner, *Phys. Zeit.* xxviii. p. 493 (1927).
(43) Dunbar, Phil. Mag. v. p. 962 (1928).
(44) Alexander, Proc. Phys. Soc. xlii. p. 82 (1930).

IV. *On the Elastic Extension of Metal Wires under Longitudinal Stress.*—Part II. *Experimental.* By L. C. TYTE, B.Sc., A.Inst.P., *Research Department, Woolwich* *.

INTRODUCTION.

THE object of the research was the measurement of deviations from Hooke's law, for which purpose the apparatus described in a previous paper [1] was devised.

The materials investigated were steel, iron, nickel, brass, copper, aluminium, zinc, tin, and lead, some of them also being examined after different heat treatments.

THE ELASTIC AFTER-EFFECT.

It has long been known that, when stress is applied to a body, even within the "elastic limit," it suffers an immediate extension and a further small one which increases with time, the rate of increase slowly falling to zero. A similar effect has been observed in recovery from strain after the removal of stress, and has been called "Elastische Nachwirkung" or the elastic after-effect.

This phenomenon has been noted by previous investigators of the deviation from Hooke's law. Thompson [2] performed special experiments to determine its magnitude. He found on loading a wire, most of the extension occurred in the first 2 seconds, a small additional extension in the next 11 seconds, and an almost negligible increase in the next 17 seconds. His results for brass were :—

Preliminary tension.	Alteration in length		Total alteration.
	from 2–13 secs.	from 13–30 secs.	
kgm.	mm.	mm.	mm.
0·6	0·035	0·001	0·036
1·2	0·062	0·010	0·072
1·8	0·100	0·020	0·120

Further, he showed that the alteration occurring between 2–13 seconds could be considered as the heat expansion caused by loading.

Similar effects have been obtained by Grüneisen [3] for lead, tin, zinc, and bismuth, and by Schülze [4] for steel and brass. The latter, however, concludes that the adiabatic elastic modulus (determined acoustically) depends only on the load and is independent of the magnitude and duration of the after-effect.

Finally, Kyrillov [5] measured the small elongations in steel wire 16 m. long, produced by constant surcharge ($\Delta P = 2$ kgm.) of loading with different initial loads ($P = 14$–66 kgm.). The elongations (2·22–2·24 mm.) were measured by an electrical method with an accuracy of 1/2000 mm. Although the wire was kept for a long time heavily loaded, the small surcharge produced gradual but very slow elongation—in the mean about 0·0002 mm. per minute. All the measurements were reduced to the same duration (3 minutes) of action of surcharge, and to the same temperature. In a note at the end of this paper Weinberg compares the values with those of Thompson, who found that Young's Modulus diminished by 4 per cent. for elongations which were less than half those employed by Kyrillov. In the latter's experiments variations of Young's Modulus did not exceed 1 per cent. when calculated from the initial length and cross-sectional area, and were within 0·8 per cent. if based on actual values of these quantities. The variation in Thompson's values of Young's Modulus was attributed to his having excluded the possibility of hardening (écrouissage) taking place by only loading for a few seconds.

PREPARATION OF SPECIMENS.

In order to obtain consistent results, great care had to be taken to ensure that the wires were free from all kinks and curves before the commencement of an experiment. This was done by electrically heating the wires suspended vertically with a load at their lower ends sufficient to keep them taut. This treatment was continued until the wires were free from all irregularities, when they were allowed to cool slowly by reducing the current in stages. All the specimens were prepared in this manner except a few lengths of steel and brass which were used without treatment.

EXPERIMENTAL METHOD.

After this treatment the experimental wires, of length 1 and 2 metres respectively, were mounted in the chucks and then supported in their vertical position with sufficient

load to keep them taut. (For further details see Part I.) The scale reading was observed for this initial load, and a given increment was added. This stretched the wires, and the excess extension of one of them caused a scale deflexion to be observed in the telescope. The reading, however, did not remain at this new value but slowly changed, indicating a progressive extension with time. This subsequent motion gradually decreased, finally falling to zero, the time required for this depending on the load applied and the hardness of the material—for tin or lead with loads exceeding the yield-point the increase of extension with time seemed to continue indefinitely. The magnitude of this subsequent extension was comparable with the initial extension, and in the case of the soft metals many times greater. The striking contrast is exhibited by the following typical observations for steel and tin; decrease of scale reading corresponds to increase of length.

Steel: Unheated Specimen 2.

Scale reading.	Time.		Scale reading.	Time.	
cm.	h.	m.	cm.	h.	m.
19·28 (11 kilos. applied) .	2	45	14·84 (16 kilos. applied).	10	55
18·85		50	12·12	11	0
18·83		56	12·08		6
18·83 (12 kilos. applied) .	3	6	12·07		15
18·25		10	12·07		22
18·25 (13 kilos applied) .		15			
17·58		24			
17·56		34			
17·53 (14 kilos applied) .		40			
16·7		43			
16·57		55			
16·55	4	5			

Tin: Preliminary Set. 206 gm. load on wires.

Scale reading.	Time.		Scale reading.	Time.	
cm.	h.	m.	cm.	h.	m.
21·18 (load applied) ...	1	32	20·24	3	13
20·98		38	20·12		27
20·88		47	20·08		33
20·82		53	19·80	4	9
20·66	2	13	19·38		50
20·66		20	18·98	5	50
20·53		36	18·52	6	48
20·44		45	18·38	7	15
20·30		58			

The relation between the increase of excess extension and time would naturally be a complicated function and no attempt has been made to connect them, but curves between the scale readings and time are given in figs. 1 and 2 for steel and tin.

Thus in the present experiments, owing to the greatly improved method of observing the excess extension, the elastic after-effect presented a serious problem. Instead of adopting the arbitrary method employed by Thompson and Kyrillov of taking the extension after a given time interval, the wires were allowed to complete their extension before the observation was taken. This gives results for a definite state, *i. e.* complete extension, covers the difficulty of hardening—this being done automatically for each stage of the loading—and also allows the wires to take up the air temperature, thus eliminating the heat expansion caused by loading.

A typical set of observations are given below for iron.

Iron: Specimen 3.
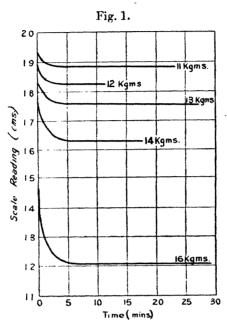
Load.	Scale reading.	Deflexion.	Temperature.	Time.	
gm.	cm.	cm.	°	h.	m.
1000	21·00	—	17·1 C.	11	50
2000	21·00	—	17·4	12	0
3000	20·97	0·03	17·5		10
4000	20·94	0·06	17·5		25
5000	20·91	0·09	17·6	1	0
6000	20·88	0·12	17·8		30
7000	20·82	0·18	17·7	2	5
8000	20·75	0·25	17·9		25
9000	20·68	0·32	17·8		50
10000	20·53	0·47	18·1	3	35
11000	20·42	0·58	17·6	4	0
12000	20·10	0·90	17·5		30
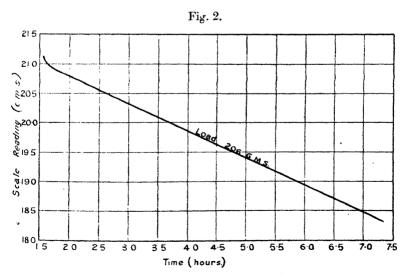
Experimental Results.

The observations have been summarized in the following tables, and are shown graphically in the corresponding figures. The load given in the tables does not include the initial load of chucks, ratio-bar, etc., but is the load applied through the ratio-bar to the two wires, and hence the load on the shorter is two-thirds and on the longer one-third

of this. Where a dash has been placed in the excess extension columns, it indicates that the corresponding load was necessary as an additional load to keep the wires taut.

Fig. 1.

Scale reading—time curves for steel.

Fig. 2.

Scale reading—time curve for tin.

STEEL.

No. 30 : s.w.g. bright drawn steel wire supplied by the London Electric Wire Company and Smith's ; a single wire would support a load of 16 kgms. without fracture.

Density = 7·689 gm./c.c.   Initial load on short wire = 153 gm.

Constant of apparatus = 0·009308.   „   long   „ = 69 „

1. *Heat Treatment A.* None : wire used as supplied.   Mean diameter = 0·304 mm.

Load (kgm.).	Load on shorter wire (kgm./sq.mm.).	Scale Deflexions (cm.).												Mean Values I.-X.	Actual excess extension of shorter wire. (10^{-3} cm.).
		I.	II.	III.	IV.	V.	VI.	VII.	VIII.	IX.	X.	Va.	VIa.		
1	9·2	—	—	—	—	—	—	—	—	—	—	—	—	—	—
2	18·4	0·03	0·02	0·03	0·04	0·03	0·02	0·03	0·02	—	—	—	—	0.02_2	0·20
3	27·6	0·06	0·05	0·06	0·11	0·07	0·06	0·10	0·08	0·03	0·03	0·01	—	0.06_5	0·60
4	36·7	0·12	0·12	0·15	0·18	0·13	0·13	0·21	0·19	0·09	0·12	0·04	0·02	0·14	1·34
5	45·9	0·25	0·24	0·24	0·32	0·25	0·23	0·36	0·36	0·20	0·24	0·11	0·08	0·27	2·50
6	55·1	0·38	0·36	0·40	0·51	0·42	0·38	0·59	0·56	0·33	0·41	0·17	0·19	0·43	4·04
7	64·3	0·56	0·54	0·55	0·72	0·64	0·66	0·81	0·82	0·51	0·65	0·25	0·31	0·64	5·92
8	73·5	0·78	0·76	0·75	1·00	0·89	0·84	1·09	1·12	0·75	0·94	0·33	0·43	0·89	8·30
9	82·7	1·02	1·02	1·02	1·31	1·22	1·15	1·41	1·48	1·04	1·24	0·45	0·56	1·19	11·09
10	91·8	1·32	1·31	1·34	1·75	1·58	1·51	1·76	1·91	1·36	1·62	0·57	0·70	1·55	14·39
11	101·0	1·71	1·70	1·77	2·25	2·00	1·95	2·17	2·39	1·78	2·08	0·73	0·89	1·98	18·44
12	110·2	2·17	2·20	2·30	2·90	2·53	2·54	2·70	2·95	2·32	2·65	0·92	1·16	2·53	23·51
13	119·4	2·76	2·85	2·94	3·58	3·16	3·21	3·32	3·62	2·99	3·41	1·15	1·50	3·18	29·64
14	128·6	3·50	3·80	3·80	4·49	3·92	4·06	4·06	4·49	3·78	4·10	1·45	1·96	4·00	37·24
15	137·8	4·46	5·33	5·01	5·62	4·92	5·22	5·00	5·50	4·95	5·15	1·82	2·51	5·12	47·62

Experiments V a. and VI a. were performed by reloading the wires used in experiments V. and VI., the maximum load used in V. being 165·3 kgm./sq.mm., and in VI. 183·7 kgm./sq.mm.

2. *Heat Treatment* B. Wires heated by a current of 3 amps. and slowly cooled, *i. e.* to a temperature of 280° C. approximately.

Mean diameter = 0·303 mm.

Load (kgm.).	Load on shorter wire (kgm./sq.mm.).	Scale Deflexions (cm.).				Mean Values.	Actual excess extension of shorter wire. (10⁻³ cm.).
		I.	II.	III.	IV.		
1	9·2	—	0·01	0·00	0·00	0·00	—
2	18·5	0·00	0·02·	0·01	0·01	0·01	0·09
3	27·7	0·01	0·04	0·02	0·02	0·02	0·19
4	37·0	0·03	0·06	0·04	0·04	0·04	0·37
5	46·2	0·06	0·08	0·06	0·07	0·07	0·65
6	55·5	0·10	0·11	0·09	0·10	0·10	0·93
7	64·7	0·15	0·15	0·13	0·14	0·14	1·30
8	74·0	0·19	0·19	0·17	0·18	0·18	1·68
9	83·2	0·25	0·24	0·22	0·22	0·23	2·14
10	92·5	0·32	0·30	—	0·28	0·30	2·79
11	101·7	0·40	0·38	—	0·34	0·37	3·44
12	111·0	0·50	0·49	—	0·42	0·47	4·37
13	120·2	0·63	0·70	—	0·52	0·61	5·68

3. *Heat Treatment* C. Wires heated by a current of 3·6 amps. and slowly cooled, *i. e.* to a temperature of 400° C. approximately.

Mean diameter = 0·303 mm.

Load (kgm.).	Load on shorter wire (kgm./sq.mm.).	Scale Deflexions (cm.).		Mean Values.	Actual excess extension of shorter wire (10⁻³ cm.).
		I.	II.		
1	9·2	—	—	—	—
2	18·5	0·00	0·01	0·00₅	0·05
3	27·7	0·02	0·03	0·02₅	0·23
4	37·0	0·05	0·06	0·05₅	0·51
5	46·2	0·09	0·10	0·09₅	0·88
6	55·5	0·14	0·14	0·14	1·30
7	64·7	0·20	0·20	0·20	1·86
8	74·0	0·27	0·27	0·27	2·51
9	83·2	0·36	0·37	0·36₅	3·40
10	92·5	0·45	0.49	0·47	4·37
11	101·7	0·60	0·63	0·61₅	5·72
12	110·0	0·81	0·84	0·82₅	7·68

4. *Heat Treatment* D. Wires heated by a current of 4 amps. and slowly cooled, *i. e.* to a temperature of 500° C. approximately.

Mean diameter = 0·302 mm.

Load (kgm.).	Load on shorter wire (kgm./sq.mm.).	Scale Deflexions (cm.).				Mean Values.	Actual excess extension of shorter wire (10⁻³ cm.).
		I.	II.	III.	IV.		
1	9·3	—	—	—	—	—	—
2	18·6	0·00	0·02	0·00	0·01	0·01	0·09
3	27·9	0·02	0·05	0·02	0·03	0.03	0·28
4	37·2	0·05	0·09	0·06	0·06	0·06₅	0·60
5	46·6	0·09	0·14	0·11	0·11	0·11	1·24
6	55·9	0·16	0·21	0·19	0·18	0·18₅	1·72
7	65·2	0·26	0·29	0·29	0·27	0·28	2·59
8	74·5	0·38	0·39	0·45	0·38	0·40	3·72
9	83·8	0·59	0·51	0·70	0·51	0·58	5·38
10	93·1	0·84	0·70	1·28	0·71	0·88	8·19

IRON.

No. 22 : s.w.g. iron wire supplied by Ormiston Bros.

Density = 7·796 gm./c.c.

Constant of apparatus = 0·009308.

Initial load on short wire = 155 gm.

,,   ,,   long   ,,   = 70   ,,

Heat Treatment. Wires heated by a current of 10·4 amps. and slowly cooled, *i. e.* to a temperature of 500° C. approximately.

Mean diameter = 0·712 mm.

Load (kgm.).	Load on shorter wire (kgm./sq.mm.).	Scale Deflexions (cm.).					Mean Values.	Actual excess extension of shorter wires (10⁻³ cm.).
		I.	II.	III.	IV.	V.		
1	1·68	—	—	—	—	—	—	—
2 ;.....	3·35	—	—	—	0·02	0·02	0·01	0·07
3 '......	5·03	0·02	0·02	0·03	0·05	0·05	0·03	0·32
4 ;.....	6·70	0·05	0·05	0·06	0·07	0·08	0·06	0·58

Heat Treatment (cont.).

Load (kgm.).	Load on shorter wire (kgm./sq.mm.).	Scale Deflexions (cm.).					Mean Values.	Actual excess extension of shorter wires (10⁻³ cm.).
		I.	II.	III.	IV.	V.		
5	8·38	0·09	0·08	0·09	0·10	0·12	0·10	0·89
6	10·06	0·13	0·11	0·12	0·14	0·17	0·13	1·25
7	11·73	0·19	0·17	0·18	0·20	0·23	0·19	1·81
8	13·41	0·26	0·25	0·25	0·25	0·30	0·26	2·44
9	15·08	0·34	0·32	0·32	0·32	0·38	0·34	3·13
10	16·76	0·50	0·46	0·47	0·46	0·54	0·49	4·52
11	18·44	0·72	0·60	0·58	0·70	0·72	0·65	6·09
12	20·11	1·20	0·86	0·90	1·18	1·04	1·06	9·83

NICKEL.

No. 24 : s.w.g. nickel wire supplied by Ormiston Bros.

Density $= 8\cdot834$ gm./c.c.

Constant of apparatus $= 0\cdot009344$.

Initial load on short wire $= 96$ gm.

,, ,, long ,, $= 48$,,

Heat Treatment. Wires heated by a current of 10 amps. and slowly cooled, *i. e.* to a temperature of 500° C. approximately.

Mean diameter $= 0\cdot561$ mm.

Load (kgm.).	Load on shorter wire. (kgm./sq.mm.).	Scale Deflexions (cm.).					Mean Values.	Actual excess extension of shorter wire (10⁻³ cm.).
		I.	II.	III.	IV.	V.		
0·5	1·35	—	—	—	—	—	—	—
1·0	2·69	0·01	0·02	0·02	0·02	0·02	0·02	0·17
1·5	4·04	0·10	0·10	0·09	0·09	0·09	0·09	0·88
1·75......	4·71	—	0·14	0·14	—	0·14	0·14	1·31
2·0	5·39	0·20	0·20	0·20	0·19	0·20	0·20	1·85
2·25......	6·06	0·32	0·29	0·28	0·28	0·30	0·29	2·75
2·5	6·73	0·43	0·41	0·39	0·39	0·41	0·41	3·79
2·75......	7·41	0·57	0·60	0·54	0·60	0·59	0·58	5·42
3·0	8·08	0·79	0·92	1·10	—	0·98	0·95	8·85

BRASS.

No. 24: s.w.g. hard brass wire supplied by Ormiston Bros.

Density = 8·410 gm./c.c.   Initial load on short wire = 15 6 gm.

Constant of apparatus = 0·009308.   ,,   ,,   long ,, = 71 ,,

1. *Heat Treatment A.* None; wire used as supplied.
2. *Heat Treatment B.* Wires heated by a current of 8 amps. and slowly cooled, *i. e.* to a temperature of 300° C. approximately. Mean diameter = 0·560 mm.

Load (kgm.).	Load on shorter wire (kgm./sq.mm.).	Scale Deflexions (cm.).			Mean Values.	Actual excess extension of shorter wire (10⁻³ cm.).
		I.	II.	III.		
1	2·70	—	—	—	—	—
2	5·40	0·05	0·04	0·04	0·04	0·40
3	8·11	0·15	0·11	0·11	0·12	1·15
4	10·81	0·30	0·25	0·23	0·26	2·42
5	13·51	0·50	0·42	0·39	0·44	4·07
6	16·21	0·70	0·60	0·59	0·63	5·86
7	18·91	0·91	0·82	0·80	0·84	7·85
8	21·62	1·16	1·10	1·08	1·11	10·36
9	24·32	1·46	1·44	1·42	1·44	13·42
10	27·02	1·83	1·80	1·86	1·83	17·04

Load (kgm.).	Load on shorter wire (kgm./sq.mm.).	IV.	Actual excess extension of shorter wire (10⁻³ cm.).
0·5	1·35	—	—
1·0	2·70	0·20	1·86
1·5	4·05	0·50	4·65
2·0	5·40	0·90	8·38
2·5	6·76	1·25	11·64
3·0	8·11	1·65	15·36
3·5	9·46	2·20	20·48
4·0	10·81	2·90	27·00

Experiments I., II., and III. were performed on wires having heat treatment A, and experiment IV. after heat treatment B.

COPPER: *Specimen 1.*— Electrolytic.

No. 24: s.w.g. bright copper wire supplied by the London Electric Wire Company and Smith's.

Density = 8·887 gm./c.c.   Initial load on short wire = 96 gm.

Constant of apparatus = 0·009344.   „ „ long „ = 48 „

1. *Heat Treatment A.* Wires heated by a current of 8 amps. and slowly cooled, *i.e.* to a temperature of 300° C. approximately. Mean diameter = 0·560 mm.

2. *Heat Treatment B.* Wires heated by a current of 11 amps. and slowly cooled, *i.e.* to a temperature of 570° C. approximately. Mean diameter = 0·559 mm.

Load (kgm.).	Load on shorter wire (kgm./sq. mm.).	Scale Deflexions (cm.).						Mean Values.	Actual excess extension of shorter wire (10⁻³ cm.).	Scale Deflexions (cm.).		Mean Values.	Actual excess extension of shorter wire (10⁻³ cm.).
		I.	II.	III.	IV.	V.	VI.			VII.	VIII.		
0·0	0·00	—	—	—	—	—	—	—	—	—	—	—	—
0·5	1·35	0·25	0·14	0·13	0·20	0·16	0·19	0·16	1·50	0·10	0·10	0·10	0·93
1·0	2·71	0·66	0·35	0·32	0·44	0·38	0·40	0·43	4·02	0·38	0·40	0·39	3·64
1·5	4·06	1·24	0·62	0·58	0·75	0·64	0·73	0·76	7·10	15·2	15·8	15·5	154·83
2·0	5·41	1·98	0·95	1·20	1·67	1·05	1·20	1·34	12·52				

As the agreement between the values was not too good, the specimen of wire being particularly difficult to free from kinks, experiments were also performed on a second specimen.

COPPER : *Specimen 2.*

No. 24: s.w.g. copper wire supplied by Ormiston Bros.

Density = 8·955 gm./c.c.

The constant of the apparatus and the initial loads were the same as for the first specimen.

Heat Treatment. Wires heated by a current of 10·5 amps. and slowly cooled, *i. e.* to a temperature of 500° C. approximately.

Mean diameter = 0·557 mm.

Load (kgm.).	Load on shorter wire (kgm./sq.mm.).	Scale Deflexions (cm.).				Mean Values.	Actual excess extension of shorter wire (10⁻³ cm.).
		I.	II.	III.	IV.		
0·5	1·37	—	—	—	—	—	—
0·75	2·05	0·00	0·03	0·00	0·00	0·01	0·07
1·0	2·74	0·03	0·05	0·03	0·06	0·04	0·40
1·25	3·42	—	0·14	—	0·16	0·15	1·40
1·5	4·10	0·20	0·25	0·21	0·28	0·24	2·20
1·75	4·79	0·46	0·45	0·49	0·48	0·47	4·39
2·0	5·47	0·96	1·10	0·89	0·86	0·95	8·90
2·25	6·16	2·22	—	1·89	—	2·06	19·21

ALUMINIUM.

No. 24: s.w.g. aluminium wire supplied by Ormiston Bros.

Density = 2·694 gm./c.c.

Constant of apparatus = 0·009344.

Initial load on short wire = 96 gm.

　　,,　　　,,　　long　　,, = 48　,,

Heat Treatment. Wires heated by a current of 6·7 amps.
and slowly cooled, *i. e.* to a temperature of 300° C.
approximately.

Mean diameter = 0·564 mm.

Load (kgm.).	Load on shorter wire (kgm./sq.mm.).	Scale Deflexions (cm.).					Mean Values.	Actual excess extension of shorter wire (10⁻³ cm.).
		I.	II.	III.	IV.	V.		
0·5	1·34	—	—	—	—	—	—	—
1·0	2·67	—	0·14	0·14	0·14	0·13	0·14	1·31
1·5	4·00	0·56	0·52	0·54	0·53	0·52	0·53	4·95
2·0	5·34	1·08	1·16	1·18	1·20	1·14	1·15	10·74
2·5	6·67	2·68	2·71	2·32	2·47	2·60	2·56	23·92

ZINC.

No. 22 : s.w.g. zinc wire supplied by the London Electric
Wire Company and Smith's Ltd.

Density = 7·181 gm./c.c.

Constant of apparatus = 0·009344.

Initial load on short wire = 96 gm.

,, ,, long ,, = 48 ,,

Heat Treatment. Wires heated by a current of 9·6 amps.
and slowly cooled, *i. e.* to a temperature of 300° C.
approximately.

Mean diameter = 0·722 mm.

Load (kgm.).	Load on shorter wire (kgm./sq.mm.).	Scale Deflexions (cm.).					Mean Values.	Actual excess extension of shorter wire (10⁻³ cm.).
		I.	II.	III.	IV.	V.		
0·0	0·000	—	—	—	—	—	—	—
0·1	0·163	0·04	0·06	0·05	0·06	0·06	0·05	0·50
0·2	0·326	0·16	0·22	0·20	0·20	0·20	0·20	·1·83
0·3	0·489	0·30	0·40	0·40	0·40	0·40	0·38	3·55
0.4	0·652	0·62	0·66	0·66	0·66	0·65	0·65	6·07
0·5	0·815	1·00	1·00	1·00	1·00	1·00	1·00	9·34
0·6	0·978	1·44	1·42	1·44	1·46	1·44	1·44	13·46
0·7	1·141	1·95	1·92	1·98	1·98	1·97	1·96	18·31
0·8	1·304	2·78	2·80	2·80	2·80	2·80	2·80	26·13
0·9	1·466	3·86	3·90	3·92	3·90	3·90	3·90	36·40
1·0	1·629	6·82	10·08	6·68	6·70	6·72	7·40	69·14

TIN.

No. 22 : s.w.g. tin wire supplied by the London Electric Wire Company and Smith's Ltd.

<div align="center">

Density = 7·292 gm./c.c.

Constant of apparatus = 0·009344.

Initial load on short wire = 53 gm.

„   „   long   „ = 26·5 „

</div>

Heat Treatment. Wires heated by a current of 6·2 amps. and slowly cooled, *i. e.* to a temperature of 200° C. approximately.

<div align="center">

Mean diameter = 0·718 mm.

</div>

Load (kgm.).	Load on shorter wire (kgm./sq.mm.).	Scale Deflexions (cm.).					Mean Values.	Actual excess extension of shorter wire (10^{-3} cm.).
		I.	II.	III.	IV.	V.		
0·00	0·000	—	—	—	—	—	—	—
0·03	0·050	0·07	0·08	0·07	0·07	0·07	0·07	0·67
0·05	0·082	0·17	0·19	0·17	0·17	0·17	0·17	1·63
0·07	0·116	0.31	0·35	0·33	0·27	0·33	0·32	2·97
0·10	0·165	0·63	0·69	0·63	0·65	0·65	0·65	6·07
0·12	0·198	0·93	1·05	1·00	0·99	1·01	1·00	9·32
0·14	0·231	2·43	5·75	1·97	2·22	2·07	2·89	26·98

LEAD.

No. 22 : s.w.g. lead wire supplied by the London Electric Wire Company and Smith's Ltd.

<div align="center">

Density = 11·344 gm./c.c.

Constant of apparatus = 0·009344.

Initial load on short wire = 53 gm.

„   „   long   „ = 26·5 „

</div>

Heat Treatment. Wires heated by a current of 5 amps. and slowly cooled, *i. e.* to a temperature of 200° C. approximately.

Mean diameter = 0·720 mm.

Load (kgm.).	Load on shorter wire (kgm./sq.mm.).	Scale Deflexions (cm.).			Mean Values.	Actual excess extension of shorter wire (10⁻³ cm.).
		I.	II.	III.		
0·00	0·000	—	—	—	—	—
0·02	0·033	0·16	0·16	0·16	0·16	1·50
0·05	0·082	0·42	0·47	0·43	0·44	4·11
0·07	0·115	0·69	0·75	0·70	0·71	6·66
0·10	0·164	1·28	1·23	1·25	1·25	11·70
0·12	0·197	1·72	1·62	1·62	1·65	15·45
0·15	0·246	2·33	2·23	2·25	2·27	21·21
0·17	0·278	3·13	2·70	2·69	2·84	26·54
0·20	0·328	3·71	3·63	3·70	3·68	34·38
0·22	0·360	4·39	4·73	4·75	4·62	43·19
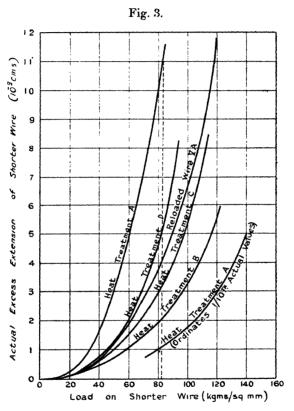
DISCUSSION OF RESULTS.

The results show that in no case is Hooke's law obeyed, excess extension of the shorter wire being observed for all loads (above that necessary to keep the wires taut), the amount of the deviation depending on the material and its treatment.

Ferrous metals.—The results for steel are shown graphically in fig. 3, the latter part of the curve for unheated steel (*i.e.* heat treatment A) being drawn with ordinates one-tenth their real size so that all the curves can be reasonably accommodated. The effect of annealing at 280° C. approximately (heat treatment B) is seen to be the reduction of the excess extension to one-fourth or one-fifth of its previous value for corresponding loads. Heating at higher temperatures, approximately 400° C. and 500° C. (heat treatments C and D), produces small increases in the excess extension for the same load, and, as will be shown later, the relation between the excess extension and load breaks down for smaller loads with increasing annealing temperature. The curve for experiment V. *a*, in which the wires were reloaded after they had been strained by a load equivalent to

165 kgm./sq.mm. on the shorter wire, shows a similar decrease in the value of the excess extension.

This is the general agreement with the change of properties of severely cold-worked steel upon subsequent annealing (*vide* Adam [6]). "There is distinct evidence that some of the effects of cold work are not permanent, even at ordinary temperature. Mere ageing undoubtedly influences the

Fig. 3.
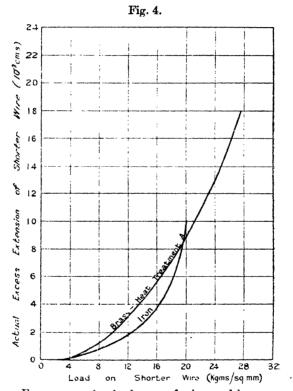
Excess extension-load curves for steel.

physical properties to some extent. The changes become more pronounced, however, as the temperature increases; thus, boiling in water produces distinctly measurable alterations in the elastic properties, and the limit of proportionality has been raised to over 80 per cent. of the ultimate strength in a cold-drawn wire heated to just under 400° C. There is little doubt that the modulus of elasticity is also affected by heat treatment after cold work. In short, up to 400° C.

there is a distinct stiffening or hardening effect, but above this point the cold-worked metal begins to soften again."¹ If this limit of proportionality is considered to be that stress at which the curve for total elongation deviates 0·025 per cent. from a straight line (Government Specification), then this statement is in accordance with the present observations.

The bright drawn steel wire (sorbitic pearlite) being a severely cold-worked material has a micro-structure of small

Fig. 4.
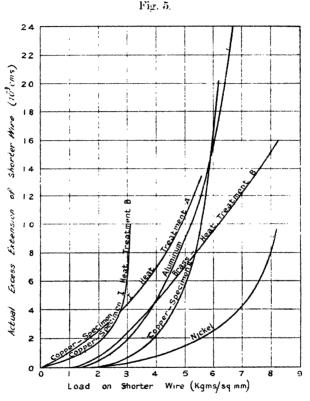
Excess extension-load curves for iron and brass.

elongated crystals, and even the highest annealing temperature used would leave the sorbite and pearlite areas distorted.

The results for iron are shown in fig. 4 ; it will be noted that the excess extension is very much greater.than that for steel for similar loads. However, in this case the annealing temperature (approximately 500° C.) is sufficient to cause recrystallization, *i. e.* large size of grain.

Non-ferrous metals.—The behaviour of unheated brass (heat treatment A) is shown in fig. 4; the values of the excess extension are numerically comparable with those of iron. The material had been subjected to considerable cold work, being hard and extremely brittle. On annealing at 300° C. approximately (heat treatment B) the brass became soft and the excess extension very much greater, being

Fig. 5.
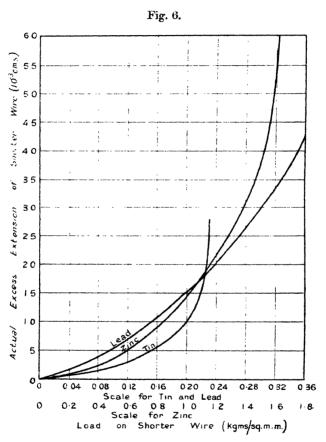
Excess extension-load curves for nickel, copper, aluminium, and brass.

similar in behaviour to copper. Fig. 5 shows the results for copper, aluminium, nickel, and the heated brass. Copper, specimen 1, was a bright drawn wire annealed at two different temperatures, 300° C. and 570° C. approximately (heat treatments A and B), the deviations from Hooke's law being much greater for the wires heated to the higher temperature. Finally, fig. 6 shows the curves for zinc, tin,

and lead, the abscissæ scale for zinc being one-fifth of that for tin and lead.

It is well known that if a metal subjected to internal stress is heated, crystal growth occurs, and, other things being equal, the higher the temperature the more complete the recrystallization and ultimate crystal size.

Fig. 6.

Excess extension-load curves for lead, tin, and zinc.

Hence, the brass and copper experiments indicate that for annealed metals the amount of deviation from Hooke's law is a function of the crystal size, suggesting that the deviation is intimately connected with the metal crystal.

Some corroboration of this view is given by the experiments of Thompson quoted by Adam (*loc. cit.* p. 168),

F 2

showing the variation with crystal size of the "true elastic limit"—a quantity, presumably, as defined above.

Dead Mild Steel.

Carbon 0·05 per cent.

Treatment.	No. of crystals per cm.	True elastic limit (tns. per sq.in.).
Annealed at 900° C.	276	9·61
Normalized.......................	343	12·0
Oil quenched at 900° C. and tempered at 650° C.	690	14·0

Open-hearth Steel.

Composition : carbon 0·26, silicon 0·05, manganese 0·57, sulphur 0·043, phosphorus 0·054 per cent.

Treatment.	No. of crystals per cm.	True elastic limit (tns. per sq.in.).
Drastically over annealed	168	less than 4·0
Normalized at 850° C.	416	15·0
Oil quenched at 850° C. and tempered at 350° C.	500	17·5

SUMMARY.

(1) It has been found that all metals investigated show deviations from Hooke's law over the whole experimental range.

(2) The amount of the deviation differs widely for different materials, and even for the same material varies greatly for different heat treatments and cold-working.

(3) For annealed metals the deviation increases with increase of crystal size.

Acknowledgment.

References.

(1) Tyte, Phil. Mag. x. p. 1043 (1930).
(2) Thompson, *Ann. der Phys.* xliv. p. 555 (1891).
(3) Grüneisen, *Verh. phys. Ges.* p. 469 (1906); *Phys. Zeitschr.* vii. p. 901 (1906); *Ann. der Phys.* xxii. p. 81 (1907); xxv. p. 825 (1908).
(4) Schülze, *Ann. der Phys.* xxxi. p. 1 (1910).
(5) Kyrillov, *Jurn. Russk. Fisik-Chimicesk Obscestva,* xxxix. No. 3, p. 64 (1907).
(6) Adam, 'Wire Drawing and the Cold Working of Steel,' p. 145 (1925). Witherby.

V. *On the Interaction of Radiation and the Electron.* By R. D. KLEEMAN, *B.A., D.Sc.**

§ 1. *Proposed Properties of the Electron.*

THE nature of the connexion between the electron and radiation is one of the outstanding problems of modern physics. Some of the experiments on the subject have led to the supposition that radiant energy does not continuously fill space, but is localized, the radiation being supposed to proceed in the form of darts. But this is almost impossible to reconcile with interference. According to other experiments the electron under certain conditions seems to behave like a wave-train, and under other conditions like a particle. In this paper we will show that certain of these apparently conflicting results, retaining the electro-magnetic theory in its orthodox form, may be reconciled if we assume that the electron and proton possess the following properties :—

(1) An electron or proton may possess internal energy apart from kinetic energy.

(2) The internal energy, or a part of it, may be converted directly into radiation, or apart from acceleration, on account of a disturbance such as a collision etc., and the process may take place according to the equation

$$\Delta u = h\nu, \quad \ldots \ldots \ldots (1)$$

where Δu denotes the change in internal energy, ν the frequency of the radiation emitted, and h Planck's constant.

(3) Radiation falling upon an electron or proton is absorbed in indefinite amounts, or not necessarily in quanta, which becomes internal energy. Temperature radiation is absorbed when the charge is in motion.

(4) The absorption of temperature radiation has a retarding effect on the motion of the charge.

(5) The force acting on a charge placed in an electric field depends on its internal energy, and when this increases the force in a general way decreases.

(6) Electrical potential energy of a charge may be converted into internal energy, and *vice versâ*.

(7) The laws of conservation of energy and momentum hold when an electron and radiation interact.

The last-named property may be taken to follow from our general knowledge of the kinetic properties of matter. Evidence that the properties (1), (3), (4), (5), (6), and the first part of (2) should hold were obtained by the writer * from considerations of the equation of a perfect gas obtained thermodynamically, and from the distribution of the velocities of the particles in a gas. Further evidence was obtained † in connexion with the application of a magnetic field to an electron gas, the axiomatic assumption ‡ that we cannot have an infinite amount of energy per c.c., the application of radiation to an electron gas §, and more evidence of a similar nature which will be published shortly.

The results obtained have been used by the writer to interpret the Bohr atom ‖. It was shown that an electron describing a Bohr orbit in an atom gradually slows down till in a stationary position on the orbit. During the process it absorbs energy from the surrounding radiation which is stored up as internal energy. It will now not be under the action of a force as far as the other charges of the atom are concerned, except when displaced from its stationary position. If an electron passes from its position to one corresponding to a smaller internal energy content, which lies on another Bohr orbit, the difference in the internal energies is emitted *directly* into

---

* Phil. Mag. vii. p. 493 (1929); *Z. anorg. allgem. Chem.* cxcvi. p. 284 (1931); *Z. Elektrochem.* xxxvii. pp. 78, 371 (1931).

† 'Nature,' cxxiv. p. 728 (1929) 'Science,' lxx. p. 478 (1929).

‡ 'Science,' lxxi. p. 340 (1930).

§ 'Science,' lxii. p. 225 (1930).

‖ Phil. Mag. vii. p. 493 (1929).

space. The frequency of the radiation emitted (following Bohr) obeys equation (1) *.

The difficulty of the nature of the process of radiation and that of the non-radiating Bohr orbit now disappear from the Bohr atom. Further, since the atom has now changed from a dynamic to a static nature, it no longer conflicts with the Lewis-Langmuir theory of the atom.

It appears also from the static Bohr atom that the force F between two electrical charges e_1 and e_2 separated by the distance r should be written

$$F = \frac{e_1 e_2}{r^2} \cdot \phi(e_1, e_2, u_1, u_2, r). \quad . \quad . \quad . \quad . \quad (2)$$

where u_1 and u_2 denote the internal energies of the charges and ϕ is a function of the quantities e_1, e_2, u_1, u_2, and r. It appears, furthermore, from the behaviour of the charges in a Bohr atom that F may be zero for certain values of u_1, u_2, and r †.

We shall now explain by means of the foregoing results three of the main experiments which have proved a difficulty in the orthodox electromagnetic theory of radiation.

§ 2. *The Velocity of the Electrons emitted from Materials subjected to Radiation.*

If radiation of a frequency ν is allowed to fall upon a material, it has been found by experiment that the velocity v of the electrons ejected is given by the equation

$$h\nu = \tfrac{1}{2}mv^2, \quad . \quad . \quad . \quad . \quad . \quad . \quad (3)$$

where m denotes the mass of an electron. Furthermore, the number ejected per sq. cm. varies inversely as the square of the distance of the material from the source of the rays. Experiments on this relation have been carried out mainly with ultra-violet light and X-rays.

To explain it let us consider first of all an electron having a store of internal energy equal to $h\nu$. It will evidently be a system possessing a resonance frequency ν, and therefore if radiation of that frequency is allowed to fall upon it

---

* For other properties of the electron, see *Z. f. Phys.* lxiii. p. 859 (1930); lxix. p. 286 (1931).

† The connexion of an atom of this nature with various physical and chemical properties has been pointed out by the writer in papers in *Z. anorg. u. allgem. Chem.* cxci. p. 201 (1930); cxciii. p. 106 (1930); cxcv. p. 164 (1931); cxcix. p. 225 (1931).

the internal energy is likely to be emitted into space as radiation of frequency ν.

Next consider two electrons separated initially by an infinite distance, one of which is brought up to a finite distance of the other. The external work performed may be written $h\nu$. Now suppose that this work, or the resultant increase in potential energy of the displaced electron, becomes internal energy. Since the total change in potential energy becomes internal energy, the work done upon the electron in transporting it again to an infinite distance would be zero. It will appear now that if potential energy and electronic internal energy may be converted into each other according to the electronic property (6), the property (5) will also hold, and *vice versâ*.

Next, suppose that the electron in the position to which it was brought (whose store of internal energy is accordingly $h\nu$) is subjected to radiation of a frequency ν, in which case it will be set radiating by resonance. This process would increase the field of the electron, and thus give rise to an increase in potential energy equal to the energy radiated, according to what has gone before. But this is impossible, or the two processes could not take place simultaneously ; and hence no energy will be radiated, but converted into potential energy. The energy will in turn be converted into kinetic energy of the electron according to equation (3) if allowed to move reely to infinity under the action of the recovered field.

Finally, consider a Bohr atom in which the electrons have assumed stationary positions. On account of the motion of the atom as a whole each electron will continually absorb radiant energy which increases the internal energy content. The stationary position of each electron may in consequence be displaced ; but a reverse displacement may also (periodically) occur, induced by radiation or some other disturbance, in which case some of the internal energy is radiated into space according to equation (1). But it may also happen that if the total available internal energy of the electron is $h\nu$, and this is equal to the potential energy it would possess on recovering its field, the internal energy may be converted into potential energy, and this in turn into kinetic energy according to equation (3), on radiation of frequency ν falling upon the electron. Thus the existence of equation (3) is explained. The underlying principles may be stated briefly in the form

that if an electron possesses an amount of internal energy equal to $h\nu$ which may become potential energy of repulsion, the process of conversion may be induced by radiation of frequency ν falling upon it.

It is evident that other possibilities in the emission of secondary electronic radiation suggest themselves. They will be treated at length in a separate paper.

The elemental amount of radiation absorbed by an electron in an atom to set it radiating at the same frequency is likely to be the same for each electron. The number of electrons liberated per c.c. in a material by a radiation of given frequency is therefore simply proportional to the energy passing through the material. The inverse square law of ionization then immediately follows.

§ 3. *The Compton Effect.*

When X-rays are allowed to fall upon a material they are scattered more or less in all directions, and undergo besides a change in wave-length according to A. H. Compton. To explain this effect he supposes * that an X-ray may be looked upon as an entity of energy $h\nu$, which may collide with a free electron as if it consisted of a particle, and that during the collision the principles of conservation of energy and momentum hold, and that the mass of the radiation and that of the electron are determined by the Principle of Relativity. These considerations give the equation

$$\Delta\lambda = \cdot0484 \sin^2 \tfrac{1}{2}\theta, \quad \ldots \quad (4)$$

where $\Delta\lambda$ denotes the increase in wave-length in passing from a direction of observation in line with the original rays to one making a direction θ with it. This equation has been found to agree well with the facts. It may, however, also be explained, as will now be pointed out, by means of the properties of the electron stated in § 1.

A free electron initially at rest may gradually absorb energy from the impinging beam of X-rays, not necessarily in quanta, till the energy absorbed is equal to $h\nu$, which is represented by the sum of the increase in internal energy of the electron and the increase in its kinetic energy $\tfrac{1}{2}mv^2$, where v denotes its final velocity, which is in the same direction as the radiation. It is now a system whose natural frequency is ν, and hence, on being further

* Phys. Rev. xxi. pp. 207, 483 (1923).

subjected to radiation of this frequency the acquired internal energy is radiated into space. This may take place in a small solid angle whose direction makes an angle θ with the original direction of the rays. This process can now easily be shown to give the same equation as (4).

It may be urged as an objection that if the orthodox electromagnetic theory holds the time of absorption of a quantum of energy $h\nu$ would be so large that it could not fail to affect the course of the experiments. But actually such an absorption is not necessary. We have seen that a free electron, on account of its motion, continually absorbs radiant energy, which is stored up as internal energy and which is periodically emitted again as radiation on being subjected to a disturbance. It will therefore happen that when X-rays of frequency ν fall upon a material some of the free electrons will have a velocity v in the direction the rays are moving *, and some will possess besides a sum of available internal energy and kinetic energy equal to or greater than $h\nu$. These would be induced by the X-rays to emit, as before, the amount of internal energy $h\nu - \frac{1}{2}mv_1^2$ in the form of radiation in a small solid angle in a direction making an angle θ with the X-rays, where v_1 denotes the final velocity of the electron.

There are evidently many other possibilities that may be predicted in this connexion †.

§ 4. *The Reflexion of Electrons from Crystals.*

De Broglie has suggested that an electron which has the velocity v represents a wave-train of frequency ν given by the equation

$$\frac{h\nu}{c} = mr, \quad . \quad . \quad . \quad . \quad . \quad . \quad (5)$$

where c denotes the velocity of light. Experiments carried out by Davisson and Germer ‡ have within certain limits proved the truth of this equation. They found that cathode rays of velocity v reflected from a crystal behave

---

* Mostly for a short time only, since the kinetic energy of the electron at the end of its free path may be largely converted into potential energy and this into internal energy.

† Thus, for example, a stationary electron having the internal energy content $2h\nu$, might be induced to radiate towards the source of the exciting radiation a beam whose energy is $h\nu$, and a beam in the opposite direction according to equation (4).

‡ Nat. Ac. of Science, xiv. p. 317 (1928).

like X-rays of frequency ν given by the above equation. Slight deviations, however, occur from the above equation under certain conditions it should be mentioned, and sometimes the reflected beam is entirely missing. But the result is notwithstanding a striking one in the light of equation (5). It is, however, difficult to see how physically an electron may consist of a wave-train and still retain its identity during the process of reflexion. For this requires that the train of waves be broken up into at least two parts which are reflected from two different layers of atoms. The result may, however, more logically be explained on the basis of the results stated in § 1.

When the electron penetrates into the crystal it may eject a beam of rays of frequency ν and energy $h\nu = cm\nu$ in the same direction as that in which it is moving. This beam may be reflected from the layers of atoms of the crystal and then be again absorbed by the now stationary electron, which then moves off with the original velocity v. Equation (5) would then be satisfied. But evidently the physical process cannot be as simple as that.

Let us therefore next suppose that the angle of incidence of the ejected radiation is less than that of the moving electron. This will in consequence not be reduced to rest, and it may now meet the reflected pencils of radiation where they join together to form the original beam. On absorbing the beam the electron would regain its original velocity and proceed in a direction corresponding approximately to that as if the electron consisted of a wave-train of frequency ν. The meeting of the reflected pencils and the electron may be ensured, since the process of reflexion of the radiation by the atoms may consist of an absorption and emission with an interval between. This would help to explain besides many anomalies in the reflexion of electrons.

But actually the electron will not emit radiation during the process of reflexion ; for as soon as this begins to happen the corresponding energy will simultaneously, altogether or in part, be converted into potential energy, similar to what happens in the process described in § 2. But this is impossible. Internal energy is therefore converted into potential energy instead of radiant energy, and *vice versâ*, or the law of force of the moving electron is temporarily changed, and this takes place in such a manner that the electron is reflected as if it consisted of a wave-

train of approximate frequency ν.   It is easy to see now
that deviations from the law expressed by equation (5)
may occur, and that these may be quite large under certain
conditions.

In this paper the interaction of radiation and the
electron is treated from a somewhat different point of
view than that put forward by de Broglie and Schrödinger,
who suppose that the electron is a packet of radiation.
But the two views are by no means antagonistic to each
other; as a matter of fact, if an electron consists of a packet
of radiation it is all the more likely to absorb and emit
radiant energy in the way described.   Possibly in the end
a combination of the various principles involved to
supplement each other might prove the desirable thing.
Since the general properties of the electron deduced from
thermodynamics do not involve any new theorems or as-
sumptions, they should form the cornerstone in these
developments.

127 Woodland Av.
Schenectady, N.Y., U.S.A.

VI. *Characteristic Curves of the Aluminium Rectifying
Cell.   By* L. L. BARNES, *M.Sc., A.K.C.**

THE aluminium cell is a serviceable rectifier for such
uses as charging storage batteries from A.C. supply,
and some of its characteristics are outlined as an indication
of the manner in which the optimum conditions for its
working can be determined.

The cell under test consists of aluminium and lead elec-
trodes in a solution of sodium borate.
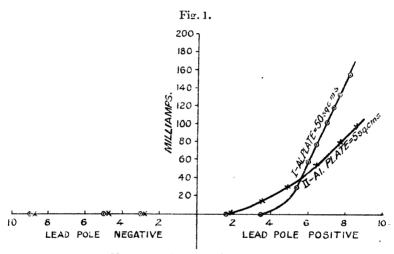
Characteristic Curve of Current and Potential.

The rectifying property is most clearly shown by the
characteristic curves in fig. 1 (Tables I. and II.).   Curve I.
is obtained using an aluminium pole of submerged area equal
to 50 sq. cm., and Curve II. with area of aluminium equal
to 5 sq. cm.

The area of lead electrode does not affect the characteristic
except in so far as it governs the purely ohmic resistance

* Communicated by the Author.

between the lead and the electrolyte. Fig. 2 shows the circuit by which the curves are obtained. The switch S is moved in one position to allow alternating current to pass through the cell (*via* the resistance R). It is then moved to the other position, and direct current from the battery B is measured by the milliameter A and the potential of the battery by the voltmeter V. The A.C. is then again applied in order to maintain the rectifying film on the aluminium) before taking the next measurements for a different value of potential from the battery. The current noted is that recorded by A instantaneously on switching over to D.C., as the direct current does not remain constant, but slowly rises.

Fig. 1.

Characteristic curve of the rectifier.

TABLE I.—Aluminium electrode = 50 sq. cm.

Lead pole positive.		Lead pole negative.	
Volts.	Milliamps.	Volts.	Milliamps.
1·8	0	3	0·0
3·5	0	5	0·0
5·4	30	9	0·0
6·0	58		
6·4	77		
7·0	102		
7·4	120		
7·8	137		
8·3	155		
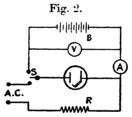
The resistance of the cell to current flowing in the direction aluminium to lead is extremely high, and even at an applied potential of 100 volts is as much as 150,000 ohms.

Effect of Area of Aluminium Plate.

The effect of variations in the area of the aluminium electrode and in temperature are examined by measuring

TABLE II.—Aluminium electrode = 5 sq. cm.
Characteristic—D.C. Current and Potential.

Lead pole positive.		Lead pole negative.	
Volts.	Milliamps.	Volts.	Milliamps.
2·0	2	3	0·0
3·5	15	5	0·0
4·8	30	9	0·0
6·5	55		
7·7	78		
8·7	100		

Fig. 2.
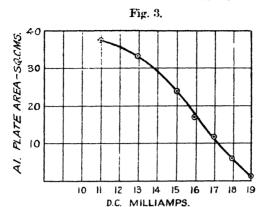
Circuit for obtaining characteristic curve of the rectifier.
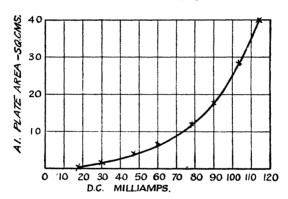
the rectified (half-wave) current for a fixed applied A.C. potential.

The curves in fig. 3 (Tables III. and IV.) are obtained by measuring the rectified current while varying the area of aluminium plate by drawing the electrode out of the electrolyte. Curve I. is taken with an impressed A.C. voltage of 5 volts, and curve II. with 8 volts. The fact that the curves slope in opposite directions shows that for smaller rectified currents the area of aluminium plate should be kept small, while for larger outputs the area should be greater. This is confirmed by reference to the characteristic curves in fig. 1, which show that up to currents of 40 milliamp. the 5 sq. cm. plate gives the more efficient rectification, while above 40 milliamp. the 50 sq. cm. plate is the more efficient.

Fig. 3.

Curve I.—5 volts A.C.
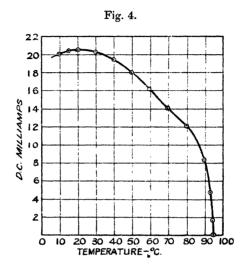
Curve II.—8 volts A.C.

Effect of variation of aluminium plate area.

TABLE III.—5 volts A.C.   TABLE IV.—8 volts. A.C.
Rectified Current and Aluminium Plate Area.

Milliamps.	Sq. cm.		Milliamps.	Sq. cm.
11	37·5		18	0·9
13	33		30	2·1
15	24		48	4·2
16	17		60	6·9
17	12		78	12·0
18	6		90	19·8
19	1·5		103	28·5
			114	40·2

Effect of Temperature.

Raising the temperature of the cell reduces its power of rectification. The curve in fig. 4 (Table V.) is obtained by

Fig. 4.

Effect of temperature on D.C. output.

TABLE V.—Rectified Current and Temperature.

° C.	Milliamps.
10	20·0
15	20·4
20	20·6
30	20·3
40	19·5
50	18·0
60	16·2
70	14·2
80	12·2
90	8·4
93	4·8
94	1·6
95	0·0

.keeping the impressed voltage and the area of aluminium constant and heating the cell externally. [The area of aluminium plate in this case is 50 sq. cm. and the applied A.C. voltage 5.]

It is noticeable that a slight heating-up of the cell is not undesirable ; experiment shows that this is due to the reduction in resistance of the electrolyte with rise of temperature more than counteracting the falling-off of rectification. In the case investigated, after 25° C. the rectification begins to decrease rapidly, and ceases completely at 95° C.

<div align="right">7 Redwing Lane, Norton-on-Tees,
Co. Durham.</div>

VII. *The Effect of Mechanical Working on the State of a Solid Surface. By* R. F. HANSTOCK, *B.Sc., A.Inst.P.**

COLD-working is known to change the physical properties of an annealed metal. Kelvin showed that a thermo-couple could be made by using two wires of the same metal, one wire being annealed by heating and the other cold-worked by drawing or hammering. This was later verified by Maclean [1], the E.M.F. generated being of the order 0·1 millivolts per centigrade degree, the current flowing generally from the annealed to the strained metal at the hot junction. Since then many other physical properties have been shown to depend on the degree of deformation of the substance. Beilby [2] repeated the thermoelectric experiment, and showed that the E.M.F. disappeared after the wires had been heated to a temperature which was about one-third of the absolute temperature of the melting-point of the metal. In the same way the elasticity of a metal depends on its previous history as regards cold-working and permanent strain. Among other properties changed by cold-working are :—

(*a*) The electrical conductivity [3]. This is usually lower in the strained than in the annealed metal.

(*b*) The magnetic susceptibility [4]. The diamagnetic susceptibility of metals belonging to the cubic system decreases on cold-working. The susceptibility of copper is changed from diamagnetic to paramagnetic by cold-working.

(c) The Laue X-ray diagram shows distortion for strained metals [5].

(d) Transparent substances become doubly refracting when strained [6].

It is evident from the above that deformation leads to considerable change in the physical properties of a substance. Similarly it is known that a change can be produced in the surface layers of a metal by parallel but less drastic methods, e. g., polishing and rubbing. In order to detect such a change it is necessary to study properties of the material which are quite different from those most influenced when the material is deformed in bulk. This is natural, since the substance as a whole is not appreciably influenced by polishing its surface. The effect of surface treatment will be rendered apparent mainly by those phenomena which are intimately connected with surface conditions.

The investigation of the effects of mechanically working a surface is considerably more difficult than for the corresponding examination of substances deformed in bulk, owing to the activity of surfaces in adsorbing gases and in forming layers of oxides and impurities. On account of this the amount of positive evidence of the formation of a layer of " strained " substance by working the surface is limited. There is, however, a certain amount of indirect evidence of such a change. In the following, reference is made to published researches which indicate that a change is produced in the nature of a surface when it is mechanically worked. It is difficult to be certain whether this change is to be attributed to a deformation of the crystal lattice comparable with that observed in treatment *en masse* or simply to disturbances and change of adsorbed films.

Microscopic examination was made by Beilby [2] of polished metallic surfaces after they had been treated with an etching liquid. He arrived at the conclusion that polishing produced a " vitreous " layer on the surface of the metal. Etching showed that the " vitreous " was more soluble than the crystalline material. A change from the " vitreous " to the crystalline state was observed on heating the surface to about one-third of the absolute temperature of the melting-point of the substance. This vitreous or amorphous layer, produced by polishing, was concluded to be of the same nature as the amorphous substance observed to form between the crystalline grains when a metal was strained in bulk, and it was suggested that the formation

of such material was due to partial liquefaction under pressure of the crystalline grains of the material. After liquefaction the solidification took place so rapidly that the metal appeared in a non-crystalline or vitreous phase. The vitreous was stronger than the crystalline material, and acted as a cement between the crystalline grains, thus giving the material as a whole a greater strength when strained than when annealed.

The theory of polishing suggested by Beilby was that a layer of this " vitreous " material was formed on the surface by liquefaction of the crystalline grains under pressure of the polishing tool. From etching observation it was shown that the vitreous layer was formed to depths of from 50 to $500\,\mu\mu$. Disturbing effects were of course produced by the polishing tool at greater depths.

This work on polishing provides the most direct evidence of the production, by mechanical working, of surface layers having different physical properties from the substance in bulk form.

Assuming the validity of the deduction that the surface layer produced by polishing is of the same nature as the substance formed between the crystalline grains of the metal when cold-worked, and that the changes in the various physical phenomena previously noted are due to the formation of such amorphous material, it is to be expected that the layer produced by polishing will affect considerably those phenomena which are most sensitive to change in surface conditions. Among those most likely to be affected by the formation of such a layer the following immediately suggest themselves : friction between solids, contact potential, frictional electricity, photoelectricity, and surface reflexion of radiation.

Friction.

Since friction probably arises in part from cohesion of the two surfaces in contact, and will thus depend on the structure of the crystal lattice at the points of contact, any deformation of the lattice by mechanical working may be expected to alter the coefficient of friction. R. B. Dow [7] measured the coefficient of friction for rods sliding *in vacuo,* and showed that it depended largely on the condition of the surfaces. He found that the coefficient of friction μ increased with the number of times the rods slid over one another, and attributed the change in μ to the formation of a vitreous layer. The experiment was carried out in air at a reduced pressure of 1·0 mm. and without heating. In later work by Shaw and

Leavey [8] the coefficient of friction was measured for rods heated up to 350° in air at a pressure of ·01 mm. They found a difference in μ for strained and annealed surfaces, μ being greater for the annealed than for the strained metals. This is exactly opposite to the effect found by Dow, but is probably a more reliable result, since the experiment is performed in better conditions.

Contact Potential.

The dependence of contact potential on surface conditions has been investigated *in vacuo* by Ende [9], who found that potentials up to 0·5 volts could be produced between similar metals. The metal surfaces were treated with acid, emery paper, worked with a harder metal, sawn, drawn, and filed. No systematic variation was noted, and the effects were attributed to differences in adsorbed gas layers. It seems possible, however, that the contact potential may in part be due to actual differences in the state of strain of the surfaces. A further point to be noted is that the adsorbed gas layer may be different for annealed and strained surfaces.

Reflecting Power.

Margenau [10] has investigated the dependence of the ultra-violet reflexion of silver on the state of the surface. The minimum of reflexion for silver occurs in the near U.V. (3160 Å.), and was examined after treating the surface in different ways, *e. g.*, after vigorous and moderate polishing, etching, and preparing by depositing the silver electro-lytically. It was shown that for highly polished plates the minimum was very low, and situated at 3160 Å. For an unstrained surface it was shifted to lower wave-lengths by 20 Å, and had a considerably higher value than for the polished plate.

Triboelectricity.

The present research is concerned mainly with the effects of mechanical working as revealed by triboelectricity and photoelectricity, and these will be considered in detail.

In 1917 Shaw [11] showed that the quantity and sometimes the sign of the charges developed when two substances were rubbed together depended to a great extent on the previous treatment of the surfaces. Two states of the surface were distinguished, termed "normal" and "abnormal," and it was shown that the position of a substance in the tribo-electric series was determined by the state of the surface.

The "abnormal" could be produced from the "normal" state by heating the substance to some temperature, usually about 250° C. The experiments were performed in air and were of a purely qualitative nature. An important point was discovered when it was shown [12], contrary to general belief, that charges could be generated by rubbing together two rods of the same material. When one rod was rubbed along another similar rod it was found that they became charged negatively and positively respectively. Continued rubbing, however, was found to influence the surfaces in such a way as to reverse the signs of the charges on the rods. This effect was permanent unless the rods were heated to some definite temperature, when they were restored to their original state. It was suggested that the strained state, *i. e.*, that produced by much rubbing, corresponded to the "normal" state in the previous work and that this changed on annealing to the state previously called "abnormal."

It was from this point that the present research was commenced, an endeavour being made to study quantitatively the changes arising in the frictional charge generated when two similar bodies were rubbed together. It is convenient at this point to give a definition of the term "mechanical working" as used in this paper. By "mechanical working" is meant the bringing of two solid surfaces into intimate contact. This may occur in the following ways:—

(*a*) Simple contact with pressure.

(*b*) Contact by rubbing.

(*c*) Contact by impact, normal or glancing.

Normal impact is probably only a more drastic form of simple contact with pressure. So far it is found that the method (*b*) is most fruitful in results.

Triboelectric Experiments.

An earlier paper [13] contains an account of the method employed in finding the relation between the triboelectric charge and the amount by which a surface has been mechanically worked. For the sake of clarity a brief *résumé* is given here. The simplest case to consider is that in which two similar insulating solids are rubbed together. If this could be done so that both solids were mechanically worked to the same degree, *e. g.*, two perfectly plane disks of the same area rubbed together with a rotary motion about an axis through their centres, there would be no reason to

expect a separation of charge. It is impossible to produce this degree of perfection in practice, and some separation of charge always takes place. Where there is pronounced differentiation in the amount of mechanical working of the two surfaces considerable charges arise. The experimental arrangement used in the previous paper is that of two cylinders in contact with their axes at right angles ; one cylinder (called the rubber) is made to slide over the other (called the rubbed), so that one spot on the first cylinder is always in contact, and slides for a definite distance along a generator of the second cylinder. The apparatus allows a known pressure to be applied between the two cylinders. The charge arising on the rubbed cylinder on separating the surfaces is indicated by a sensitive gold-leaf electroscope.

The experimental method is to anneal the two cylinders by heating to a suitable temperature, and then to take readings of the charge separated after each rub of one cylinder over the other. The cylinders are discharged after each reading. Conditions of temperature and humidity are regulated, the humidity being kept as low as possible, when it is found to have no appreciable effect on the charge separated.
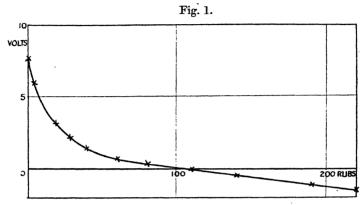
The materials used in the experiment are ebonite and celluloid as the insulators, and various metals. It is unfortunate that we are restricted to the use of such materials as ebonite and celluloid, but this is due to the difficulties arising in these experiments. The materials used must not be too hard, or very small charges are produced, presumably owing to the small amount of deformation ; also they must be of such a nature as to resist crumbling and flaking on rubbing. These restrictions limit the number of insulators which it is possible to use to these two. Most of the results are obtained using ebonite as the insulator, this being better on the whole than celluloid. There are a number of metals that may be used, but most of the work is done with copper and zinc.
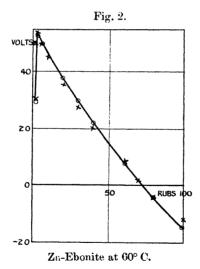
Figs. 1, 2, and 3 show typical curves for frictional charges arising between ebonite-ebonite, zinc-ebonite, and copper-ebonite as the amount of mechanical working increases (the first material of the pair represents the rubbing body in each case, *i. e.*, the one having the most mechanical working).

The use of ebonite presents one complication. It is shown [13] that the temperature at which there is a relaxation of strain for ebonite (of the quality used) is low. Complete relaxation takes place in 30 minutes at 100° C. When one piece of ebonite is made to rub over another a certain
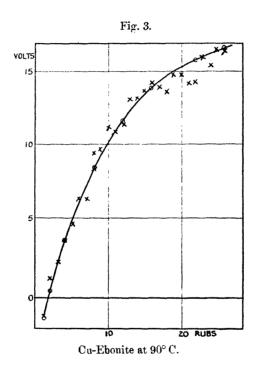
amount of heat is generated. Since ebonite is a poor heat conductor it is probable that the temperature attained by the small area of the rubber is such as to cause a certain amount of relaxation after the rubbing. This, however, does not

Fig. 1.

Ebonite-ebonite at 75° C.

Fig. 2.

Zn-Ebonite at 60° C.
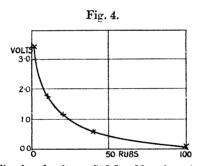
apply to so great an extent to the rubbed ebonite, since for this the area mechanically worked is much larger, and for any point on this area there is contact with the rubber for only a very short time. This relaxation effect is probably negligible for metals when they are rubbed on ebonite, since

these are good conductors of heat and also have much higher
temperatures of relaxation.   With due regard to this it is
possible to give a qualitative explanation of the curve
obtained for ebonite-ebonite (fig. 1).   Since the surfaces are
originally in the same condition (annealed by boiling
together in water) the starting-point of the curve must be
the origin (0, 0), there being no reason why electric
separation should take place between similar bodies in
simple contact.   During the first rub a positive charge is

Fig. 3.

Cu-Ebonite at 90° C.

obtained and the rubber becomes more mechanically worked
than the rubbed ebonite.   Thus the charge produced by
mechanical working, whatever its exact nature, is such as to
make ebonite charge negatively against other ebonite
mechanically worked to a lesser degree.   In most cases the
charge produced by the second is less than that produced by
the first rub, indicating that the surfaces are becoming more
like one another, *i. e.*, the rubber is changing less rapidly
than the rubbed ebonite.   Since the area of the rubber is
much less than that of the rubbed, it is probable that the

-change in the surface of the former reaches its limit during the first rub. Prolonged rubbing does not, as might be expected, lead to the two surfaces reaching the same condition. If this were so the curve would approach the zero line of charge asymptotically. What is actually observed after prolonged rubbing is the separation of a constant small negative charge on the rubbed body. This indicates a state of greater change for the rubbed ebonite than for the rubber, and is in agreement with the idea that the rubber suffers a certain amount of relaxation between the rubs, due to heating during contact with the rubbed body.

In a previous paper [13] it is demonstrated that the amount of relaxation of strain for a substance like ebonite depends not only on the temperatures of the ebonite but also on the time elapsing after straining. Thus, if a series of rubs are given the amount of relaxation of the rubber depends on the

Fig. 4.
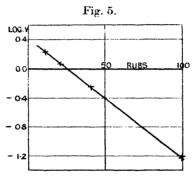
Ebonite-ebonite at 59° C. No relaxation.

intervals between the rubs. If the rubs follow one another fairly rapidly it is found that the amount of relaxation of the rubber becomes negligibly small. It is impossible, however, during a series of rubs to observe the charge and then discharge between each rub, with time intervals so small that no relaxation takes place. This difficulty may be overcome by the following procedure. The first rub is made, and the charge observed in the usual way. The next point on the curve is obtained for, say, ten rubs by starting again, with fresh places on the ebonites and giving nine rubs rapidly discharging while rubbing, and then observing the charge for the tenth rub in the usual way. Other points on the curve are obtained in a similar manner. Fig. 4 shows a curve obtained in this way, and it is seen that it now approaches the axis of zero charge asymptotically, showing that the relaxation effect has been reduced to a negligible amount.

Except for the point given by the first rub this curve may be represented by an equation of the form

$$Q = Ae^{-\lambda m},$$

where Q is the charge for any given rub m. Fig. 5 shows values of log Q plotted against m, a good straight line being obtained if the first point is neglected. It has already been stated that for ebonite-ebonite the charge obtained for the second rub is less than for the first, indicating that the rubber is approximately strained to the limit (*i. e.*, the state in which further rubbing produces no change in the tribo-electric properties) during the first rub, so that, providing no relaxation takes place, the subsequent part of the curve represents the effect of straining the rubbed body only. Thus we may say that the change in the condition of an

Fig. 5.

Ebonite-ebonite at 59° C.   No relaxation.

ebonite surface on rubbing is such as to make the charging dependent on the rubbing according to the relation $Q = Ae^{-\lambda m}$. In general the curve obtained when two pieces of ebonite are rubbed together, assuming relaxation to be eliminated, is one represented by the difference of the two exponential curves appropriate to the two surfaces. In practice this is simplified by the fact that the expression for the rubber usually reaches its limit during the first rub.

The curves obtained for copper-ebonite and zinc-ebonite suggest that the same relation may be true for these metals. It is found that the curves for zinc-ebonite may be represented by an equation of the form

$$Q + A = B(e^{-\lambda_1 m} - e^{-\lambda_2 m}),$$

where A, B, λ_1, and λ_2 are constants and λ_2 is much greater than λ_1. Except for the appearance of the constant A this

is of the same form as the equation for ebonite-ebonite, the term $Be^{-\lambda_2 m}$ representing the change of surface condition of the rubber. This cannot be neglected for zinc, since it is less easily strained than the ebonite. The change in the surface of the zinc does not reach its limit in the first rub, as happens when ebonite is used. The curve shown in fig. 2 for zinc-ebonite at 60° C. is found to be represented by

$$V + 101 \cdot 5 = 157 \cdot 3 \, (10^{-0 \cdot 0026m} - 10^{-0 \cdot 781m}),$$

V being in volts.

In the figure the circles show points calculated on the equation, the crosses being experimental observations.

From the results obtained for zinc-ebonite at different temperatures it is found that the position of the peak of the curve depends on the temperature. For 22° C. it appears at the fifth rub, for 60° C. at the third rub, for 70° C. at the second rub, and for 90° C. no peak is attained on the curve, showing that the zinc becomes fully strained during the first rub. If it is assumed [14] that plastic flow in metals begins at a temperature approximately one-third of the absolute melting-point this is explicable. The melting-point of zinc is 418° C., which gives —43° C. as the temperature at which plastic flow commences. Hence a variation of temperature from 22° C. to 90° C. should produce an appreciable effect on the rate at which the zinc is strained by rubbing.

The curve for Cu-ebonite is seen to be, in the main, a mirror image of that for zinc-ebonite, and may be represented by an equation of the form

$$Q - A = B \, (e^{-\lambda_1 m} - e^{-\lambda_2 m}),$$

only in this case λ_1 is much greater than λ_2. Indeed, for the curve for copper-ebonite at 90° C. the peak has disappeared and the term $e^{-\lambda_1 m}$ has become negligible after the first rub. The peak is quite apparent for copper-ebonite at 60° C. The curve for copper-ebonite at 90° C. may be represented by the equation

$$V - 18 \cdot 2 = 22 \cdot 2 \, . \, 10^{-0 \cdot 044m}.$$

In this case it appears to be the ebonite (*i. e.*, the rubbed body) which is strained to the limit first. This is borne out by the fact that the strain is more rapidly developed at 90° C. than at 60° C., since the peak appearing in the curve for 60° C. is not present in that for 90° C. The copper, although having a much smaller area in contact (since it is the rubber) changes more slowly than the ebonite. The temperature at which plastic flow commences for copper is about 179° C.,

which is well above the temperature of the experiment. It is to be noted that iron-ebonite gives a curve of the same form as copper-ebonite.

Consideration of the general equation given above shows that A is proportional to the charge which should arise on contact of the two materials without rubbing. It is impossible to produce charges of this order by simple contact, probably because the contact ordinarily obtained is not sufficiently intimate. Experiments have been performed with iron and ebonite in which normal impact took place between two surfaces, and the results compared with the ordinary rubbing experiments for iron-ebonite. Allowing for the differences in areas involved, it is found that the charge developed by normal impact is of the same order as that produced by the first rub in the ordinary experiment.

It will be seen that for ebonite-ebonite A is zero (or very nearly so), as would be expected. For zinc-ebonite A is negative, while for copper-ebonite it is positive. The charges, however, are those appearing on the ebonite, so that, considering the charges appearing on the metals, A is positive for zinc and negative for copper. According to this, if copper and zinc are placed in contact the copper should assume a negative potential with respect to the zinc. This is in accordance with previous observations. Also it appears probable that the potential difference between annealed copper and annealed zinc will be the same as between copper and zinc when strained to their limits, since the constant B disappears for both $m = 0$ and $m = \infty$. This may not be strictly true, since it cannot be determined with sufficient accuracy whether the coefficients of the two exponential terms in the full equation are exactly equal.

Thus the general conclusions to be drawn from these experiments are that :

(1) A mechanically worked surface charges negatively when rubbed against a surface of the same material which is mechanically worked to a lesser degree.

(2) The charge produced when a surface is rubbed on another surface which is in such a condition as to be unchanged by the rubbing is an exponential function of the number of rubs.

(3) Between similar bodies there is no separation of charge on intimate contact without rubbing.

(4) No separation of charge arises on rubbing between

similar bodies when they are mechanically worked to the limit (relaxation effects being eliminated).

(5) Between unlike bodies a charge should be separated on intimate contact without rubbing, the charges being such as to agree with the contact-potential between the two bodies.

(6) The charge separated between two unlike annealed bodies is probably the same as the charge separated between the same bodies when mechanically worked to the limit.

Photoelectric Experiments.
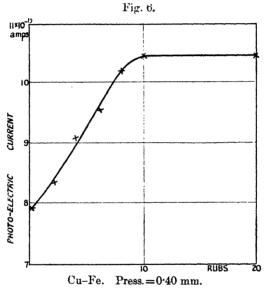
X-ray examination indicates a difference between the structures of annealed and cold-worked metals when these are treated in bulk, but fails to reveal any change in the surface layer of a polished metal. This is probably because X-rays penetrate to a depth far greater than that influenced by the working of the surface, so that the X-ray diffraction pattern is that of the bulk of the metal rather than of the surface layer. From experiments on thin metallic films short wave-length U.V. radiation is known to penetrate to and release electrons at a depth $(30 \mu\mu)$ comparable to that influenced by the mechanical working of the surface. It is therefore reasonable to suppose that the liberation of photo-electrons from the surface of a metal will depend on the amount of mechanical working of the surface.

Apparatus for testing this is described in detail in a previous paper[15]. Briefly, the apparatus consists of a photoelectric cell in which the illuminated surface is a thin flexible strip of metal. By a mechanical device the strip can be polished with a steel cylinder sliding over its surface. The cell is surrounded by a heating coil, so that the metal may be annealed *in vacuo.*

The following is a summary of the results obtained. The specimens tested are ribbons of copper, silver, gold, and platinum, and are mechanically worked *in vacuo* by sliding a steel or nickel cylinder over them. The curves obtained relating the photoelectric current to the amount of mechanical working are similar for all the metals tested and are of the form shown in fig. 6. The curve is not of simple exponential form, but is approximately linear during the increase of the photoelectric current, the surface becoming more sensitive when mechanically worked. Annealing the metals at 300° C. reduces the photoelectric current to its

original value. The annealing process begins at approximately the same temperature as that at which change in the triboelectric properties is observed. The ratio of the photoelectric current i_0 for the annealed metal to the current i_m for the worked surface shows no regular dependence on the pressure of the gas, and is of the order of 1·4 for Ag and 1·2 for Cu when polished with steel. The effect appears to be independent of the character of the radiation. It cannot be stated definitely that the effect is due to the formation of a mechanically worked layer on the surface, yet it is probable that the change, at least in part, is due to such a layer.

Fig. 6.

Cu–Fe.   Press.=0·40 mm.
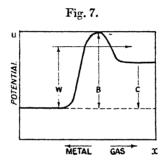
Nordheim [16] has shown that the probability of an electron passing through the surface of a metal depends on the transmission coefficient of the surface. For a metal situated *in vacuo* there is a layer at the surface in which the potential increases very rapidly in such a way that work must be done to take an electron through the surface to the outside. This corresponds to the quantity P in the Einstein equation for the photoelectric emission,

$$\tfrac{1}{2}mv^2 = h\nu - P.$$

If W is the component normal to the surface of the energy of electrons released by the incident U.V. radiation, the electrons are totally reflected if $W < P$ and totally

transmitted for $W >> P$. If, however, the potential relation
at the surface is not of the simple form considered above,
but is modified owing to the presence of a surface layer
differing in properties from the metal as a whole, the
transmission conditions are altered. If, for instance, the
layer is of material less electropositive than the metal
underneath, the potential change will be of the form shown
in fig. 7, and it has been shown that there is a definite
probability of an electron being emitted when its energy W
lies between B and C (see fig. 7). Thus, for a definite
frequency of the incident light the electron emission would
be increased by such a layer. If therefore the effect of
mechanical working is to produce a layer of metal which is
less electropositive than the metal underneath, an increase
in the emission is to be expected on rubbing. It is of course

Fig. 7.

possible that the same effect would be produced by the
formation of a layer of oxide on the surface. It is difficult
to say whether the progressive formation of such a layer
would produce the observed relation between the photo-
electric current and the amount of mechanical working.

If mechanical working does result in the formation of a
less electropositive layer on the surface it should be possible
to interpret the results of the triboelectric experiments in
terms of this change. From these experiments it is shown
that the body which is the more strained tends to charge
negatively against one which is less strained. This seems
to require the formation by mechanical working of a layer
which is more electropositive than the annealed substance.
Thus, interpreting the increase of electron emission in the
photoelectric experiments as due to the formation of a less
electropositive layer on the surfaces leads to direct conflict
with the triboelectric experiments, although it must be
remembered that the passage of electric charge across the

interface takes place in entirely different conditions in the two experiments. In the photoelectric experiments a change is observed in the electron emission from metal into vacuum, while in the triboelectric experiments flow of charge takes place between two surfaces in relative motion, the surfaces being either two insulators or an insulator and a metal. The charging during triboelectric experiments may not be due solely to electron flow across the interface, but also to the passage of charged particles split off the surface by the violent rubbing action.

On the other hand, it is possible that the change observed in the photoelectric emission is not due mainly to a change in the work of emission of electrons. Margenau [10] has shown for silver that the reflecting power depends on the state of plastic deformation of the surface layer. He finds that for wave-lengths below about 3200° A. (*i. e.*, for light of the wave-length used in the photoelectric experiments) the reflecting power is greater for an annealed than for a highly polished surface. Thus for wave-length 2000 Å. the reflecting power of an etched surface is 0·4, while for a highly polished surface it is 0·3. It is suggested that a similar effect may be present in the photoelectric experiments described in this paper. Assuming a constant intensity of incident radiation, a greater fraction of this would be reflected for an annealed than for a polished surface. Thus there would be a greater proportion of light producing photoelectrons for the polished than for the annealed surface.

Relaxation Temperatures.

Experiments have been made to determine the relaxation temperatures of some metals, as indicated by changes in the triboelectric and photoelectric properties. According to Desch [14] plastic flow in metals begins at a temperature which is approximately one-third of the absolute melting-point of the metal. If this is true, relaxation from strain would be expected to begin at about these temperatures. The following table shows the melting-points of various metals, the corresponding temperatures of commencement of plastic flow, and the relaxation temperatures as determined from triboelectric and photoelectric experiments.

In the triboelectric experiments the relaxation temperatures were determined as follows:—The metal surface was strained to the limit by burnishing. The condition of the surface was then tested by rubbing on ebonite after the metal had been heated to some definite temperature and allowed to cool.

This was done several times, through a range of temperatures. From these readings the temperature at which the triboelectric charge first showed change was estimated.

In the photoelectric experiments a similar method was employed, the photoelectric current from the polished metal surface being observed after the specimen had been heated to increasingly higher temperatures.

Experiment.	Metal.	Melting-point.	$\frac{A^\circ}{3}273.$	Observed relaxation temperature.
Triboelectric	Cu.. ...	1084° C.	179° C.	170° C.
	Fe......	1530	328	200
	Cd......	321	− 75	< room temperature.
Photoelectric	Ag......	962	139	120° C.
	Au......	1063	172	< 250
	Cu......	1084	179	< 250
	Pt	1710	388	300

Thus there is fairly good agreement between the temperatures at which change is found in triboelectric and photoelectric phenomena and the temperatures at which plastic flow commences. The observed temperatures appear to be rather lower than those calculated. It is suggested that this may be due to the presence of a comparatively large mass of the annealed metal underlying the deformed surface layer. This underlying annealed matter may help the annealing process to start in the surface layer at a lower temperature than it would if the metal were deformed throughout.

For cadmium it was found that a small amount of relaxation took place at ordinary room temperatures. This is in agreement with other observations on similar plastic metals. Rosenhain [17] has shown from ball-hardness tests on severely strained lead that slight relaxation takes place at ordinary temperatues after a few hours. Tin and zinc are also stated to undergo softening at ordinary temperatures.

Conclusions.

The experiments described in this paper and the results of other investigators in similar subjects seem to show fairly conclusively that the effect of mechanically working a surface is to produce a layer differing in physical properties from the underlying annealed material. Beilby thought of this layer as being produced by actual liquefaction of the

annealed crystalline material under pressure. This con-
clusion was arrived at from observation with the microscope.
The phenomena observed seemed to indicate a liquefaction of
the metal when polished, yet it must be remembered that
the observations were really of macroscopic dimension
compared with the lattice units of the metal. It
is probable that the apparent liquefaction observed for
Beilby may be explained simply as due to twisting and
gliding of the lattice planes under pressure of the polishing
tool. From experiments on simple metal crystals it has
been shown that the properties such as photoelectricity and
thermoelectricity depend on the particular face of the crystal
dealt with. It seems probable that the changes observed in
the physical properties discussed may, at least for the metals,
be explained as due to a change in orientation of the
crystal faces at the surface produced by mechanical working.
A certain amount of orientation may exist on the surface of
a substance owing to the intense electric field existing at the
interface.

The present research throws some light on the difficult
subject of triboelectricity in that it indicates that the
separation of charge which takes place when two substances
are rubbed together depends primarily on the contact
potential between the bodies (this assumes the existence of a
Volta effect for insulators). The potential difference on
which the separation of charge depends may be altered by
mechanically working the surface—in fact it is in general
impossible to produce frictional charges without at the same
time mechanically working the surface.

The experiments on relaxation temperatures afford evidence
that the results obtained in the triboelectric and photoelectric
experiments are related to the experiments of Beilby and
others, who find changes produced by the mechanical working
of surfaces.

This research was made possible by facilities afforded by
the Physics Department of University College, Nottingham.

Summary.

A brief account is given of published work on this and
allied subjects. The experimental research is mainly an
investigation of the effect of mechanically working a surface
as indicated by changes in the triboelectric and photoelectric
properties of the surfaces. It is concluded that in these
subjects, as well as in those investigated by others, the
condition of the surface as influenced by mechanical working

plays an important part in determining the magnitude of the effect studied. The curves obtained in the triboelectric experiments seem to indicate the existence of a definite Volta contact effect between the interfaces insulator/insulator and metal/insulator. This contact potential is influenced by the changes produced by mechanically working the surfaces. The changes produced by mechanical working may be made to disappear by heating to some definite relaxation temperature. In the triboelectric and photoelectric experiments the relaxation temperatures are approximately the same as those at which plastic flow is supposed to commence in metals.

References.

(1) Maclean, Proc. Roy. Soc. (Feb. 1899).
(2) Beilby, ' Aggregation and Flow of Solids.'
(3) Michels, *Ann. der Physik.* lxxxv. p. 6.
(4) Honda and Shimizu, ' Nature,' cxxvi. p. 990 (1930).
(5) Joffé, ' The Physics of Crystals.'
(6) Coker, Cantor Lectures.
(7) Dow, Phys. Rev. xxxiii. (Feb. 1929).
(8) Shaw and Leavey, Phil. Mag. x. (Nov. 1930).
(9) Ende, *Phys. Zeit.* (Aug. 1929).
(10) Margenau, Phys. Rev. xxxiii. (June 1929).
(11) Shaw, Proc. Roy. Soc. A, xciv. p. 16.
(12) Shaw, Proc. Phys. Soc. xxxix. p. 447.
(13) Shaw and Hanstock, Proc. Roy. Soc. A, cxxviii. p. 474.
(14) Desch, Trans. Faraday Soc. xxiv. p. 57.
(15) Hanstock, Phil. Mag. x. p. 937 (1930).
(16) Nordheim, *Phys. Zeit.* xxx. (1929).
(17) Rosenhain, ' Introduction to Physical Metallurgy,' p. 269.

VIII. *A Note on the Sound generated by a Rotating Airscrew. By* E. T. PARIS, *D.Sc., F.Inst.P.**

§ 1. *Introduction.*

AN experiment is described which was performed with the object of obtaining evidence concerning the distribution of sound round a rotating airscrew for comparison with the theoretical conclusions of E. J. Lynam and H. A. Webb † and M. D. Hart ‡. The experiment consisted of the measurement, in various directions in a horizontal

* Communicated by the Author.
† "The Emission of Sound by Airscrews," Aero. Res. Comm., R. & M., No. 624 (1919).
‡ "The Aeroplane as a Source of Sound," Aero. Res. Comm., R. & M., No. 1310 (1930).

H 2

plane, of the amplitude of the fundamental tone of the " sound of rotation " of an airscrew on a stationary aeroplane.

It is convenient to begin with a statement concerning earlier work on airscrew sound in so far as it relates to the sound of rotation, and, in particular, to the distribution round the airscrew.

§ 2. *Earlier Investigations into the Sound of Rotation of an Airscrew.*

It is well known that one of the principal sounds generated by a rotating airscrew is an harmonic series of tones having a fundamental frequency equal to the product of the number of blades with the speed of rotation [*]. This sound is called the " sound of rotation," to distinguish it from other sounds generated by an airscrew. With the aid of a hot-wire microphone A. Fage [†] investigated the relative strengths of the harmonics of the sound of rotation generated by four-bladed model airscrews, and found that in general the amplitude decreased as the order of the harmonic was increased.

Lynam and Webb, in the course of a theoretical investigation into the effect of rotational speed on the amplitude of the sound generated, obtained results which indicated certain features of interest in connexion with the acoustical field round a rotating airscrew. They made use of two alternative hypotheses concerning the representation of a rotating airscrew as a source of sound.

Their first hypothesis (*loc. cit.* p. 5) was that the airscrew could be represented as rings of sources and sinks, the strengths of which varied periodically with a frequency equal to the fundamental frequency of the sound of rotation; the sources were supposed to be in front of the airscrew and the sinks behind it. The relative phases of the sources or sinks in each ring were determined by the motion of the airscrew in such a way that the phase corresponding to any selected position of the blade lagged behind that corresponding to an earlier position by an amount equal to the

---

[*] Messrs. Lynam and Webb and M. D. Hart, *loc. cit. supra*; R. McK. Wood, "Note on some Experiments on the Sound emitted by Airscrews," Aero. Res. Comm., R. & M., No. 694, p. 18 (1920); E. Waetzmann, "Die Entstehung und die Art des Flugzeugschalles," *Z. f. techn. Phys.* no. 6, p. 167 (1921); J. Obata, "The Analysis of the Sounds emitted by Aircraft," Rep. Aero. Res. Inst., Tokyo Imp. Univ., no. 59 (March 1930).

[†] " An Experimental Study of the Vibration in the Blades and Shaft of an Airscrew," Proc. Roy. Soc. A, cvii. pp. 456–458 (1925).

time taken by the blade to move from the earlier to the later position. These sources and sinks constituted in effect a system of doublets with their axes parallel to the axis of rotation of the airscrew. Lynam and Webb found that, on this hypothesis, the amplitude of the fundamental tone of the sound of rotation at a distant point (*i. e.*, at a distance great compared with the dimensions of the airscrew) due to a single ring of sources and the corresponding ring of sinks was proportional to

$$J_m\left(\frac{m\omega r}{a}\sin\beta\right).\sin\left(\frac{m\omega b}{a}\cos\beta\right), \quad \ldots \quad (1)$$

where $J_m =$ the Bessel function of order m ;

$m =$ number of airscrew blades ;

$\omega =$ rotational speed of airscrew in radians per second;

$r =$ radius of ring of sources or sinks ;

$a =$ velocity of sound ;

$\beta =$ angle between the line joining the point of observation to the centre of the airscrew and the axis of the airscrew ;

and $b =$ distance of rings of sources and sinks from the plane of rotation.

For any harmonic other than the fundamental, for example, the pth harmonic, m would be replaced by pm.

To obtain an expression for the amplitude of the sound in a selected direction due to the emission from the whole airscrew it would be necessary to assume some radial source distribution and to integrate expressions of the type (1) along the radius. To simplify the problem, however, Lynam and Webb assumed the sources and sinks to be concentrated "at one radius only, viz., $\frac{3}{4}$ of the bladelength, approximating roughly to the centre of pressure of the blade." They also assumed that $b = \frac{1}{2}r$. On these assumptions, and with L representing the blade-length, (1) becomes

$$J_m\left(\frac{3m\omega L}{4a}\sin\beta\right).\sin\left(\frac{3m\omega L}{8a}\cos\beta\right). \quad \ldots \quad (2)$$

Lynam and Webb's second hypothesis (*loc. cit.* pp. 9 & 10) was that "while the sources are a little way in front of the airscrew, the sinks are a long way behind the airscrew, or for mathematical purposes at infinity." The problem then reduces to finding the effect at a distant point of a

single ring of simple sources having the phase-relationship referred to above, and the result, in the same notation as before, is

$$J_m\left(\frac{m\omega r}{a}\sin\beta\right). \quad \ldots \ldots \quad (3)$$

If, as before, the sources are supposed to be concentrated into a single ring of radius $3L/4$, the amplitude of the fundamental tone at a distant point should be proportional to

$$J_m\left(\frac{3m\omega L}{4a}\sin\beta\right). \quad \ldots \ldots \quad (4)$$

The hypothesis that all the sinks were at infinity was regarded as an extreme case, and Lynam and Webb suggested that the " two hypotheses might be combined, one ring of sinks being taken a little way behind the airscrew and another ring of sinks at infinity, the relative intensities of the two sinks remaining a matter for further consideration."

M. D. Hart * has written a very full discussion of aeroplane sound, including a theoretical treatment of the sound from the engine exhaust openings and of that generated by the rotation of the airscrew. So far as the distribution of sound of rotation round an airscrew is concerned he arrived at an expression, identical with (3) above, for the amplitude at a distant point due to the disturbances from an annulus of radius r swept out by an element of the blade surface. The amplitude due to the motion of the whole blade would be given by an integral which cannot at present be evaluated. It appears, however, that the resultant sound-distribution would be symmetrical about the plane of rotation †.

§ 3. *The Sound Recording Apparatus.*

It was desired to concentrate attention on the fundamental frequency (about 27∿) of the sound of rotation of a certain airscrew, and for this purpose a tuned hot-wire microphone was used.

The resonator of the hot-wire microphone had a volume of 3345 c.c. The neck was cylindrical, 22 mm. long and 6 mm. in diameter. The damping factor (h) and the conductance of the neck (c) were $15\cdot3$ sec.$^{-1}$ and $0\cdot0989$ cm. respectively at 30∿. The experimental determination of these quantities has already been described ‡.

---

* *Loc. cit.*
† *Vide* the expression at the foot of p. 16 (Hart, *loc. cit.*).
‡ Proc. Phys. Soc. xliii. pp. 74–77 (1931).

The grid of the microphone was connected in one arm of a "battery bridge" circuit, with a compensating grid as a balancer.

Two galvanometers were used in parallel ; one was of the Moll pattern, with a period of about $\frac{1}{4}$ second, and the other an Einthoven string galvanometer. The former served to record the average drop in resistance of the microphone grid, while the latter showed the alternating resistance-changes and produced a record from which the frequency of the sound affecting the microphone could be determined.

The deflexion of the Moll galvanometer was photographed continuously on a slow-speed recorder carrying a strip of sensitized paper moving at about $\frac{1}{8}$ inch per second. The shadow of the Einthoven galvanometer string was thrown on to the slit of a high-speed recording camera of the type employed with the Low-Hilger "audiometer." The shutter of this camera could be operated electromagnetically by the closing of a switch which, when records were being taken, was worked by an observer in the cockpit of the aeroplane.

The calibration of the microphone for the comparison of sound-amplitudes was effected by the stationary wave-method, whereby every observed change in average resistance δR (or the corresponding deflexion) could be interpreted as a relative pressure amplitude $\sin ky$, where $k = 2\pi/\text{wave-length}$ and y is the distance which the microphone must be displaced from a loop-position in a plane stationary wave in order to suffer the resistance change δR *.

The purpose of the frequency record was to make possible a correction for any variation in frequency of the sound which might occur between one observation and another. Since the microphone is a tuned instrument, any such variation would affect the magnitude of the steady resistance-change and might lead to false values for the amplitude. The correction was applied as follows :—

The observations yield a relative amplitude, $\sin ky$, and a frequency, n. Now if n_0 is the resonance-frequency of the microphone and q the amplitude in the neck of the resonator, then †

$$q = Q \cos \alpha, \quad \ldots \ldots \quad (5)$$

where Q is the amplitude which would occur if the sound

---

* *Cf.* Proc. Phys. Soc. xxxix. pp. 274–275 (1927) ; xliii. pp. 75–76 (1931).

† Proc. Phys. Soc. xliii. p. 74 (1931).

were exactly in tune with the microphone (*i. e.*, if $n = n_0$), and α is defined by

$$\left.\begin{array}{l} \alpha = \tan^{-1}(\Delta/2h), \\ \Delta = 2\pi n_0(n_0/n - n/n_0). \end{array}\right\} \quad \cdots \quad (6)$$

Thus, if h, n, and n_0 are known, the relative amplitude ($\sin ky'$) that would have been recorded by the microphone had it been exactly in tune can be calculated from the formula

$$\sin ky' = \sin ky \cdot \sec \alpha. \quad \cdots \quad (7)$$

The resonance-frequency (n_0) is dependent on the air-temperature, as shown by Rayleigh's formula,

$$n_0 = \frac{a}{2\pi}\sqrt{\frac{c}{V}}, \quad \cdots \quad (8)$$

a being the velocity of sound in air and V the volume of the resonator. The procedure adopted was to calculate n_0 from (8) by means of the known values of c and V on each occasion in which observations were made, the value of a appropriate to the observed air-temperature being used.

§ 4. *The Experimental Determination of the Distribution of Sound round the Airscrew.*

The aeroplane used in the experiment was a single-engined bomber with Rolls Royce "Condor" engine (700 h.p.), fitted with a two-bladed airscrew of diameter 4500 mm. (14·8 ft.) and pitch (pressure-face) 3200 mm. The gearing of engine to airscrew was 0·477. The engine was run at 1750 rev. per min. *, so that the calculated frequency of the fundamental tone of the sound of rotation was

$$(1750 \times 0.477 \times 2)/60 = 27.8 \thicksim.$$

The aeroplane was on level open ground at a distance of 760 ft. from the microphone, and records were taken with the long axis of the fuselage making different angles with the direction to the microphone. For this purpose the tail of the machine was moved round between successive observations by steps of 15°. The boss of the airscrew was above the same point on the ground during each observation.

Since the plane of rotation of the airscrew when the aeroplane was resting on level ground was inclined at an

---

* This is below the normal cruising speed of 1850–1900 rev. per min., but was the highest which could be attained under the circumstances of the experiment.

angle of about 10° to the vertical, the angle β between the direction of the microphone (as seen from the airscrew boss) and the axis of rotation had to be worked out for each position. No observations were made in this experiment at points on the axis of rotation ; the smallest value of β was 10°.

The microphone was supported on a frame at a height of 15 ft. This was to minimize possible errors arising from the upward refraction of sound-rays due to the temperature lapse-rate near the ground.

The procedure during the making of an observation was as follows :—The aeroplane being in position, with its engine running, an observer, with a switch communicating with the recording apparatus, took his place in the cockpit in a position whence he could see the engine revolution indicator. The pilot then accelerated the engine until the prearranged rev. per min. (1750) was reached, and maintained this speed as steadily as possible for a short period. During this time the observer closed the switch at what he considered a favourable moment, and a record was made.

The results of one complete set of observations are given in the following table :—
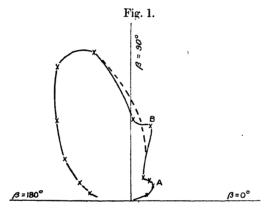
Distribution of Sound Amplitude (Airscrew Fundamental).

Record no.	Angle from axis of rotation (β).	Relative amplitude (sin ky).	Frequency (ω). cycle/sec.	Frequency correction factor (sec α).	Corrected relative amplitude.
1	10°	0	—	—	0
2	18°	0·8	27	1·11	0·9
3	32°	1·2	27	1·21	1·5
4	46°	1·3	27·5	1·15	1·5
5	60·5°	1·25	[27·5]	1·15	1·4
6	75°	4·0	27·1	1·24	5·0
7	89°	4·6	27·6	1·13	5·2
8	105°	6·6	27·1	1·24	8·2
9	120°	6·6	27·0	1·26	8·3
10	134°	4·8	27·1	1·24	6·0
11	149°	3·3	26·9	1·29	4·3
12	162°	2·4	27·1	1·24	3·0
13	170°	2·0	[27·5]	1·15	2·3

It will be seen that the frequencies recorded in the fourth column are very uniform. In the case of the records 5 and 13 there were mishaps to the high-speed recorder, and no frequency was observed. The mean of the observed frequencies (27·5∼) was therefore adopted in default of more accurate information, and is shown in square brackets in the table.

The observed relative amplitudes are plotted on a polar diagram in fig. 1. The line $\beta = 0°$ is along the axis of rotation of the airscrew and in the direction in which the aeroplane would move if it were in flight.

The curve shows that there is a tendency for the sound to die away both forward and backward along the axis of

Fig. 1.

Amplitude of the fundamental sound of rotation in various directions from a two-bladed airscrew making 13·5 rev./sec.
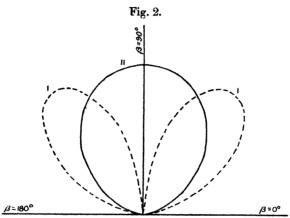
rotation, and that there is a direction of maximum amplitude between $\beta = 105°$ and $\beta = 120°$.

The irregularity which occurs between $\beta = 0°$ and $\beta = 90°$ was noticed in other sets of observations, but the exact shape was not repeated when the aeroplane occupied a different position relative to the microphone, and it seemed possible that reflexion of sound from the ground, or from parts of the machine, might be wholly or partly responsible for this effect. A maximum near the position A (fig. 1) occurred in all the observations, but not that at B, which seems to have been accidental. The true form of the curve is probably approximately along the broken line in fig. 1 *.

* This conclusion has been confirmed by subsequent experiments performed by Mr. C. F. B. Kemp in which a different method of sound-recording was employed.

§ 5. *Comparison of Observation with Theory.*

In fig. 2 the curves I and II were calculated from the theories of Lynam and Webb. The curve I corresponds to the first hypothesis and was obtained from the expression (2) of § 2, the following numerical values appropriate to the airscrew used in the experiment being employed : $m=2$, $\omega=13{\cdot}5 \sim -27\pi$ radian/sec., $L=7{\cdot}4$ ft., $a=1100$ ft./sec. With the same values curve II, corresponding to their second hypothesis, was calculated from (4) of § 2.

Fig. 2.

Theoretical curves for sound distribution round airscrew.
(Lynam and Webb.)
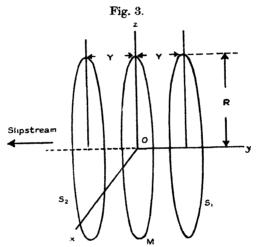
A comparison of the theoretical curves in fig. 2 with the experimental curve in fig. 1 brings out the following points :—

(i.) The experimental curve confirms the theoretical conclusion from both hypotheses of Lynam and Webb that the amount of sound projected along the axis of rotation tends to zero.

(ii.) The experimental curve confirms the conclusion of M. D. Hart * that the first hypothesis of Lynam and Webb is untenable because it gives zero sound-intensity in the plane of rotation.

(iii.) The agreement of the experimental curve with the sound distribution deduced from the second hypothesis of Lynam and Webb does not extend beyond that indicated

* Aero. Res. Comm., R. & M., No. 1310, p. 11 (1930).

in (i.), since the curve II in fig. 2 shows maximum amplitude in the plane of rotation, whereas the observations show maximum amplitude in a direction about 25° behind the plane of rotation.

(iv.) The experimental curve is not symmetrical about the plane of rotation, and hence the airscrew cannot be represented by any distribution of simple sources in the plane of rotation.

It must of course be borne in mind that the theory deals with the case of an airscrew in a homogeneous atmosphere free from reflecting surfaces, whereas in the experiments

Fig. 3.

Suggested arrangement of sources.

there must be some reflexion from the surface of the ground and from the engine and fuselage *.

The question arises whether a better representation of an airscrew as a source of sound can be arrived at by making use of the suggestion of Lynam and Webb that their two hypotheses might be combined.

In order to answer this question it is necessary first to refer to the expression for the velocity-potential at a distant point due to a ring of sources having the characteristic phase-relationship expected from the motion of the airscrew. In fig. 3 let xOz be the plane of rotation, the centre of the

* The wings, however, do not have any noticeable effect. This was shown by an experiment performed subsequently to that described in this note, in which a wingless fuselage was employed.

airscrew being at O. The potential due to a ring of sources of radius r with its centre on Oy at a distance y from O and in a plane parallel to xOz is proportional to *

$$J_m\left(\frac{m\omega r}{a}\sin\beta\right).\cos m\omega\left(t+\frac{y}{a}\cos\beta\right), \quad . \quad . \quad (9)$$

the notation being as in § 2. It is convenient to write k (equal to $2\pi/\lambda$, λ being the wave-length of the sound) for $m\omega/a$. Thus (9) may be written

$$J_m(kr\sin\beta).\cos k(at+y\cos\beta). \quad . \quad . \quad (10)$$

An arrangement of sources that has been found by trial to give a distribution of sound resembling that observed in experiments consists of a ring of sources (S_1 in fig. 3) in front of the plane of rotation, a ring of "sinks" (S_2 in fig. 3) behind it, and a ring of sources M (fig. 3) in the plane of rotation. The sources M are intermediate in phase between those at S_1 and S_2. The distinction between a "source" and a "sink" is, of course, only one of phase, a "sink" lagging behind the corresponding "source" by half a period. If R is the radius of the rings S_1 and S_2, and Y the distance of their centres from O, the potential at a distant point of the doublets constituted by the sources and sinks S_1 and S_2 is, by (10), proportional to

$$J_m(k\mathrm{R}\sin\beta)[\cos k(at+\mathrm{Y}\cos\beta)+\cos\{k(at-\mathrm{Y}\cos\beta)-\pi\}]$$

$$= -2J_m(k\mathrm{R}\sin\beta).\sin(k\mathrm{Y}\cos\beta).\sin kat. \quad (11)$$

The potential of the ring of sources of intermediate phase is found by putting $y=0$ in (10) and retarding the phase by a quarter of a period. Also it will be assumed that $r=\mathrm{R}$, as for the doublets. Thus the potential due to these sources is proportional to

$$J_m(k\mathrm{R}\sin\beta).\cos(kat-\pi/2)=J_m(k\mathrm{R}\sin\beta).\sin kat. \quad (12)$$

The total potential is found by addition of expressions proportional to (11) and (12). Thus (12) may be multiplied by a factor μ which will depend on the relative strengths of the sources in the plane of rotation compared with those composing the doublets, the strengths being equal when μ is unity. The total potential is therefore proportional to

$$J_m(k\mathrm{R}\sin\beta)\{\mu-2\sin(k\mathrm{Y}\cos\beta)\}.\sin kat. \quad . \quad (13)$$

If the values of R and Y used by Lynam and Webb are

* Lynam and Webb, *loc. cit.* p. 6.
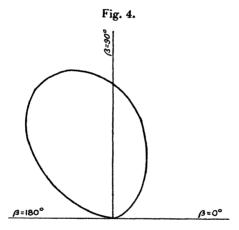
adopted, namely, $R = 3L/4$ and $Y = 3L/8$, and we assume $\mu = 2$, the amplitude of the fundamental tone generated by the two-bladed airscrew used in the experiment would be proportional to

$$2J_2\left(\frac{3kL}{4}\sin\beta\right) \cdot \left\{1 - \sin\left(\frac{3kL}{8}\cos\beta\right)\right\}, \quad . \quad (14)$$

where

$$L = 7\cdot4 \text{ ft.} \quad \text{and} \quad k = m\omega/a = (2 \times 13\cdot5 \times 2\pi) \div 1100 \text{ ft.}^{-1}.$$

The distribution of sound round the airscrew corresponding to (14) is shown by the polar diagram in fig. 4, where

Fig. 4.

Distribution of sound round airscrew calculated from (13).

relative amplitude is plotted against β. The direction of maximum amplitude is when β is about 115° and agrees approximately with that found in the experiment (*cf.* fig. 1). The calculated distribution, however, shows no secondary maximum corresponding to that at A in fig. 1, and the amplitude for directions near $\beta = 90°$ is relatively greater than that observed.
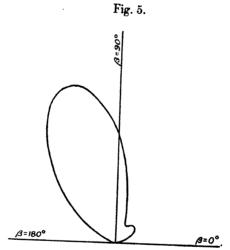
Better agreement with the observed distribution can be obtained by taking $Y = 3L$ and $\mu = 2\cdot6$. The amplitude in this case is proportional to

$$2J_2\left(\frac{3kL}{4}\sin\beta\right) \cdot \{1\cdot3 - \sin(3kL\cos\beta)\} \quad . \quad . \quad (15)$$

The corresponding polar curve is shown in fig. 5. It exhibits the main features of the observed curve (fig. 1), namely, maximum amplitude in a direction some 20° behind the plane of rotation, with a secondary maximum when β is about 45°. The observed amplitudes when β is greater than 135° are, however, considerably greater than those indicated by (15).

§ 6. *Summary and Conclusions.*

Experiment shows that the distribution of the fundamental sound of rotation round a two-bladed airscrew on a stationary

Fig. 5.

Distribution of sound round airscrew calculated from (15).

aeroplane is such that (i.) the sound tends to zero in directions forward—*i. e.*, against the slipstream—or backward along the axis of rotation, (ii.) there is a principal maximum in a direction about 25° behind the plane of rotation, and (iii.) there is a subsidiary maximum in front of this plane at about 30° to 45° from the axis of rotation.

A suggestion made by Lynam and Webb has been used to construct a formula which gives results exhibiting the principal features of the observed sound distribution so far as the fundamental sound of rotation is concerned.

IX. *Classical Energy and the Interpretation of Schroedinger's ψ-function.*   *By* A. PRESS *.

1. SUMMARY.—It is an outstanding difficulty to the classicist to regard the total energy E of a system as negative, and likewise the potential energy V. Nevertheless the power and usefulness of the Schroedinger analysis is so extraordinary that even the most ardent classicist is struck with its uncanny power. In the following, the mechanics of the so-called asymmetrical diaphragm will be taken up in the ordinary way according to the ideas of Newton and the mechanists of the old school. Later a transformation will be employed that will lead to the Schroedinger type of equation. In a sense the loaded type of diaphragm contemplated can be regarded as analogous to the linear oscillator of Planck. It should be pointed out, however, that a radiation pressure term $R dx/dt$ is here included. It will be found as a result that the ψ-function can be re-defined and led back, in its interpretation, to two components. The one is the quantity $\frac{1}{2}mv_s^2$, referring to a " steady state " value, and the other to the radiation energy $\int_0^{x_s} R dx/dt . dx$ in going from a zero position of displacement to the amplitude value x_s characterizing the energy level E_s.

2. In a centrally-weighted diaphragm of the L. V. King type we have for the d'Alembertian force of reaction the expression

$$m . \frac{d^2 x}{dt^2} : \qquad \qquad (2.1)$$

The strain energy of the system can be written down as dependent on the function

$$F_x, \qquad \qquad (2.2)$$

which in general would not be constant, but rather a function of x. The radiation pressure, on the other hand, can be assumed given by the term

$$R . \frac{dx}{dt}, \qquad \qquad (2.3)$$

whereas the three forces (2.1), (2.2), and (2.3) are to be understood as equated to an impressed force,

$$P, \qquad \qquad (2.4)$$

to satisfy the requirements of the conservation of energy
principle.

Thus we have the fundamental equation

$$m \cdot \frac{d^2x}{dt^2} + F_x + R \cdot \frac{dx}{dt} = P. \quad . \quad . \quad . \quad (2.5)$$

It may be remarked that in the asymmetrical diaphragm
it is usual to regard F as made up of terms after the following
manner :

$$F_x = \alpha x + \beta x^2 + \gamma x^3. \quad . \quad . \quad . \quad (2.6)$$

Thus for harmonic variations of the time we would have,
by way of example,

$x = x_0 + x_1,$

$x_0 = $ constant, due to an L. V. King type of bias,

$$x_1 = \Sigma_{n_1}(a_{n_1} + b_{n_1}j) \sin n_1 \omega t. \quad . \quad . \quad . \quad . \quad . \quad . \quad (2.7)$$

3. To obtain a better view of things the pressure equation
(2.5) can be multiplied by the velocity $\frac{dx}{dt}$ of the diaphragm
centre, so as to result in an activity equation. We then
have that

$$m \cdot \frac{d^2x}{dt^2} \cdot \frac{dx}{dt} + F_x \cdot \frac{dx}{dt} + R \frac{dx}{dt} \cdot \frac{dx}{dt} = P \cdot \frac{dx}{dt} \quad . \quad (3.1)$$

Clearly if a time integration is to be resorted to then the
impressed work, or energy supplied to the system, will be
given by the equation,

$$\int_{t=t_0}^{t=t} P \cdot \frac{dx}{dt} \cdot dt = \int_0^{x=x} P \cdot dx. \quad . \quad . \quad (3.2)$$

The time variable dt is brought in first since the x's are
functions of the time t.

For the force F_x producing the strain or potential energy
displacement x, it follows similarly

$$\int_{t_0}^t F_x \cdot \frac{dx}{dt} \cdot dt = \int_0^x F_x \cdot dx, \quad . \quad . \quad . \quad (3.3)$$

and for the remaining terms we need to write

$$\int_{t_0}^t \left(m \cdot \frac{d^2x}{dt^2} + R \cdot \frac{dx}{dt} \right) \frac{dx}{dt} \cdot dt = \int_0^x (\quad) dx. \quad . \quad (3.4)$$

In each of the cases (3.2), (3.3), and (3.4) a series of
frequency terms must appear on both sides for the general
problem of harmonic oscillations. If then the integrations

are to be performed at all it will be perfectly legitimate to regard the process of integration as applying to each particular frequency throughout in a separate manner. Thus, so far as the upper limit is concerned a " stationary " value x_s can be used which is discrete and characterizes the appropriate harmonic amplitude out of the infinitude of x-values possible and appropriate to (2.5). In this way therefore it s at once seen that

$$\int_0^{x_s} P \cdot dx = E_s = \text{maximum or total energy delivered}$$
$$\text{per cycle} \quad \ldots \ldots \ldots \quad (3.5)$$

$$\int_0^{x_s} F \cdot dx = V_s = \text{Total momentary strain energy}$$
(potential) occurring when E_s
attains its x_s-value, out of all the
possible x-values characterizing
the equation (2.5). . . . . (3.6)

It is justified therefore to write instead of (3.1) that

$$\int_0^{x_s} \left(m \cdot \frac{d^2x}{dt^2} + R \frac{dx}{dt} \right) dx - (E_s - V_s) = 0. \quad . \quad (3.7)$$

This condition must be satisfied for all of the infinitude of x_s's occurring in the gamut or continuum of x.

4. The Schroedinger type of equation is now easily arrived at ; for if a wave-form of equation is desired for a definite " stationary " frequency $\nu_s = \dfrac{\omega_s}{2\pi}$, it will be sufficient to define a function ψ, such that in effect

$$\int_0^{x_s} \left(m \cdot \frac{d^2x}{dt^2} + R \frac{dx}{dt} \right) dx = \frac{h^2}{8\pi^2 m} \cdot \frac{1}{\psi} \cdot \frac{d^2\psi_s}{dx_s^2}. \quad (4.1)$$

In view of (3.7) we have at once that

$$\frac{d^2\psi_s}{dx_s^2} - \frac{8\pi^2 m}{h^2}(E_s - V_s) \cdot \psi_s = 0. \quad . \quad . \quad (4.2)$$

The latter is Schroedinger's equation except for the minus sign in front of the bracketed expression $(E_s - V_s)$.

To some extent (4.2) offers an improved visualization of the radiation problem. Thus we can write

$$V_s = \frac{e^2}{r_s} \quad \ldots \ldots \ldots \quad (4.3)$$

without introducing a disconcerting minus sign. The same sort of thing is true of E_s which will be shown later is a constant, and therefore independent of x_s for any s-state.

This would not be true for the potential function V_s, which depends on the size of x_s (or rather r) according to (4.3). Such is the significance of the really parametral type of equation first brought into radiation theory by Schroedinger.

5. It is possible to give a physical meaning to the integral shown in equations (3.7) and (4.1). Thus we have that

$$\int_0^{x_s} m \cdot \frac{d^2x}{dt^2} \cdot dx = m \int_0^{x_s} \frac{dv}{dt} \cdot \frac{dx}{dt} \cdot dt$$

$$= m \cdot \int_0^{x_s} \frac{d}{dv}(v^2) dv = \tfrac{1}{2} \cdot mv_s^2 . \quad . \quad (5.1)$$

In general therefore it is to be presumed that v_s will be a function of x, and therefore ψ also. At the same time we note that

$$\int_0^{x_s} \left(\mathrm{R} \cdot \frac{dx}{dt} \right) dx = w_s, \quad . \quad . \quad . \quad (5.2)$$

where w_s expresses the energy radiated away during the s-state displacement from $x = 0$ to $x = x_s$. From the nature of the equation

$$\frac{d^2\psi_s}{dx_s^2} - \frac{8\pi^2 m}{h^2}(\mathrm{E}_s - \mathrm{V}_s) \cdot \psi_s = 0 \quad . \quad . \quad (4.2)$$

it would seem that, together with ψ_s, both w_s' and v_s are functions of x_s. Yet according to (3.7) ψ_s is essentially a function of v_s and w.

An operator method of solving the last-mentioned equation has already been given, leading to the Balmer series (see paper by writer in the Phil. Mag., July 1928, pp. 33–48).

June 1931.

X. *Additional Experiments on Moving-Coil Reproducers and on Flexible Disks.* By N. W. McLACHLAN, *D.Sc., M.I.E.E., F.Inst.P.* *

[Plates I.-V.]

SYNOPSIS.

1. The Modulus of Elasticity of Paper (E).
2. Stiffness of a Conical Sheet.
3. Influence of Reinforcing Diaphragm of Moving-coil Reproducer.
4. Combination Modes of Reed-driven Paper Disk.

---

* Communicated by the Author.

ABSTRACT.

IN this paper various details of moving-coil reproducers are discussed. The modulus of elasticity of paper is determined and used to compare the stiffness of conical sheets and disks of the same radius. A series of experiments is outlined, showing the influence of reinforcing certain portions of the diaphragm. The combination modes of a reed-driven paper disk are treated, and by comparison with theory, heterogeneity of the paper is disclosed. The exact solution of a lossless reed-driven disk vibrating *in vacuo* is given, due allowance being made for variation in the apparent mass of the reed itself. The case of a coil-driven circular aluminium disk is examined experimentally, and the frequency band occupied by the first symmetrical mode is shown to be only 5 cycles. With constant current in the coil, the output at resonance is some 2000 times greater than at non-resonant frequencies. The influence of the magnetic field upon the output and upon the coil impedance of a reproducer is analysed. The output criterion of the magnet is stipulated in terms of total gap area, air-gap flux density, and the coil space factor. It is shown that the oscillation of a coil driven by an alternating current in a non-uniform magnetic field is accompanied by a motion of translation. This is akin to the process of rectification.

Lastly, a series of impulse records showing the natural damped oscillations of moving-coil reproducers of the horn and hornless (large diaphragm) variety are given. From these records it is deduced that their field of utility lies in the determination of the main symmetrical mode in the upper register and the low frequency modes associated with the surround.

1. *The Modulus of Elasticity of Paper* (E).
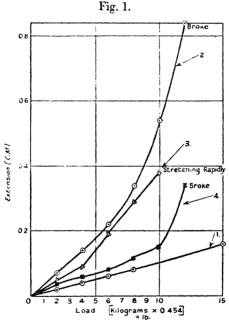
IN the course of experiments described in a former contribution *, it was necessary to find the modulus of elasticity E for certain grades of paper. The method

---

* Other properties of the disks and diaphragms treated herein will be found in Phil. Mag. xii. p. 771 (1931) and Proc. Phys. Soc. xliv. (Jan. 1932).

of procedure was the customary one of taking readings of load and extension. The results of some of the tests are

TABLE I.

Showing Young's Modulus of Elasticity (E) for paper at 20° C. Test length 50 cm. [For steel $E = 2 \times 10^{12}$ dynes cm.$^{-2}$.]

Type of paper.	Thickness (cm.).	Mass per unit. area (gm. cm.$^{-2}$).	Density. (gm. cm.$^{-3}$).	E dynes cm.$^{-2}$.
A	$1 \cdot 5 \times 10^{-2}$	$1 \cdot 0 \times 10^{-2}$	$6 \cdot 7 \times 10^{-1}$	$2 \cdot 0 \times 10^{10}$
B	$2 \cdot 1 \times 10^{-2}$	$1 \cdot 4 \times 10^{-2}$	$6 \cdot 6$	$1 \cdot 9 \times 10^{10}$
C	$4 \cdot 0 \times 10^{-2}$	$2 \cdot 5 \times 10^{-2}$	$6 \cdot 0$	$1 \cdot 9 \times 10^{10}$
D	$2 \cdot 3 \times 10^{-2}$	$1 \cdot 8 \times 10^{-2}$	$7 \cdot 8$	$4 \cdot 6 \times 10^{10}$

Fig. 1.

Load-extension curves for paper strips, width 2·54 cm., length 50 cm., thickness (1) $= 4 \times 10^{-2}$ cm., (2) $= 1 \cdot 5 \times 10^{-2}$ cm., (3) $= 2 \cdot 1 \times 10^{-2}$ cm., (4) $= 2 \cdot 3 \times 10^{-2}$ cm.

shown in Table I. In a number of cases the relationship between load and extension was substantially linear within definite limits. Curve 1, fig. 1, illustrates a typical case. By testing more than one sample of the paper it was

found that E varied, as shown in curves 3 and 4, the load/extension relationship was not always linear, whilst in some cases the paper stretched abnormally, as shown by curve 2, fig. 1. Also, the test specimen did not always return to its original length after removal of the load. Owing to variations in E, a paper cone will not act as a homogeneous sheet, so that peculiarities in nodal figures and variation in the frequencies of the modes is to be expected. Moreover, a large output from a paper diaphragm might be accompanied by harmonics due to inelasticity, especially if the wrong kind of paper or a faulty piece were used.

When the paper was baked in an oven for several hours at 110° C. the values of E were raised considerably. For example, one grade of paper in the normal state gave $E = 1.9 \times 10^{10}$ dynes cm.$^{-2}$, whilst after baking it was 3.4×10^{10} dynes cm.$^{-2}$. The latter operation was essential in making coils, since the paper formers on which they were wound had to be baked complete with the coils. For any type of paper the value of E varies with the sample and with the humidity. Moreover, the tabular data must be regarded as average values indicative of what is to be expected. In making calculations relating to a certain class of paper, it is advisable to measure the value of E at the time of the experiment rather than extract it from a table.

2. *Stiffness of a Conical Sheet.*

When a mechanical system simulates a simple loaded coil spring, both the dynamical and statical stiffness coefficients are identical, the former being defined by the relationship $k_1 = \omega^2 m$, where m is the mass and $\dfrac{\omega}{2\pi}$ the resonance frequency. This argument is valid for the simple longitudinal or torsional oscillations of a uniform bar. Where flexible disks or conical sheets are concerned, the dynamical and statical stiffness coefficients are no longer identical owing to the totally different physical conditions in the two cases.

Since it is impracticable to define the stiffness of a flexible disk on these lines, the same argument applies to a conical sheet. Moreover, other means must be sought to convey the idea of stiffness. It is proposed to find the thickness of a disk of equal radius whose first centre-moving symmetrical mode occurs at the same frequency as that of the conical sheet of like material. This must be regarded as merely illustrative, since the stresses in the two cases are of a

different nature *. The following data apply to a free-edge conical diaphragm (fig. 10 of the former paper).

<div align="center">TABLE II.</div>

Thickness of paper	$=5 \times 10^{-2}$ cm.
Radius of cone	$=16 \cdot 7$ cm.
Apical angle	$=160°$.
First symmetrical mode	$=350$ cycles per second.
Second symmetrical mode	$=664$ „ „ „

The frequency of the first mode of a paper disk equal in radius and in thickness to that of the cone is 22 cycles per second.

From Warren's analysis †

$$h^4 = bg$$

$$= 2\pi\omega^2 q \cdot \frac{6}{\pi t^3} \cdot \frac{\sigma^2 - 1}{\sigma^2} \cdot \text{E}.$$

Taking the radius a as constant, then since q the mass of the disk per unit area varies as the thickness t, we get $(ha)^4 \text{D} = \omega^2/t^2$, where D is a constant, or $t = \text{D}_1\omega/(ha)^2$. For any given value of ha corresponding to a mode, the frequency increases directly as the thickness of the disk. Applying this result to the preceding data, we find that the thickness of a disk whose first centre-moving symmetrical mode occurs at 350 cycles per second is $\frac{350}{22} \times 5 \times 10^{-2} = 0 \cdot 8$ cm., and its mass is about 15 times that of the cone. Moreover, from this view-point, the cone is equivalent to a disk $\frac{350}{22} = 16$ times as thick as the sheet of which it is constructed. The large degree of stiffness concomitant with a conical shape needs no comment.

The second symmetrical mode of the above cone occurs at 664 cycles per second, whilst that of the disk is 1380 cycles per second. For this mode, the disk $0 \cdot 8$ cm. thick is $\left(\frac{1380}{664}\right)^2 = 4 \cdot 5$ times stiffer than the cone. In other words, under our method of computation the cone is not so stiff at its second symmetrical mode as a disk $0 \cdot 8$ cm. thick. This result follows from the different nature of the stresses in the two cases.

---

* Phil. Mag. xii. p. 771 (1931). No allowance has been made for the mass of the coil.

† Phil. Mag. ix. pp. 881-901 (1930).

A second example of a diaphragm with a smaller apical angle is given in Table III. below.

TABLE III.

Thickness of paper	$=2{\cdot}1\times10^{-2}$ cm.
Radius of cone.............................	$=12$ cm.
Apical angle	$=90^{\circ}$.
E (Young's Modulus)	$=1{\cdot}9\times10^{10}$ dynes cm.$^{-2}$.
First symmetrical mode	$\doteqdot$ 900 cycles per second.

The first mode of a paper disk of equal radius is 11 cycles per second. Thus the thickness of disk having a fundamental frequency of 900 cycles is $\dfrac{900}{11}\times2{\cdot}34\times10^{-2}=1{\cdot}9$ cm., or about 57 times the mass of the cone and thrice the thickness of the equivalent disk in the preceding example. Although the grades of paper are different in Tables II. and III. these calculations show the marked increase in stiffness with decrease in apical angle.

Having given examples of conical stiffness for symmetrical modes, we now turn our attention to radial modes. The first radial mode * of a circular disk whose properties are given in the second row of Table I., occurs at 11 cycles per second, whereas that of a 90° cone, 12 cm. radius, occurs at 55 cycles per second. In this respect, the cone is equivalent to a disk of equal radius, but $55/11=5$ times as thick.

These examples are adequate to illustrate the enormous gain in stiffness which accrues from the use of a conical sheet as compared with a flat disk.
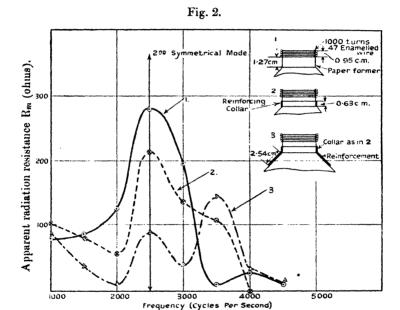
3. *Experiments showing the Effects of modifying the Diaphragm Structure of a Moving-coil Reproducer.*

In this section it is proposed to show broadly the influence of reinforcing various parts of the diaphragm structure of a reproducer. The paper was coated with aeroplane dope on each side. Only a few points were taken on the curves to show the general behaviour in each case. Moreover, some of the lesser irregularities in the curves may have been missed.

In fig. 2, curve 1, we have the case of a doped diaphragm supported on an annular rubber surround. The coil consisted of 1000 turns of 47 S.W.G. enamelled wire wound on a paper

---

* Four radial nodes or two diameters.

former and bakelized. The free length of the latter was
1·27 cm. Here the main resonance occurs at 2500 cycles.
Curve 2, fig. 2, shows the effect of reinforcing the paper
coil former (neck) near the diaphragm with a paper collar
0·63 cm. wide. The main resonance still remains at 2500
cycles. Its magnitude is reduced somewhat, whilst the
output just above 3000 cycles is increased. Curve 3, fig. 2,
shows a transformation due to a strip of paper 2·54 cm. wide,
glued round the top of the cone adjacent to the collar. The

Fig. 2.

Apparent radiation resistance of coil-driven diaphragm under
different mechanical conditions.

2500 cycle resonance persists although reduced in intensity,
whilst a more powerful resonance appears at 3500 cycles.

Curve 1, fig. 3, shows what happened when a second
reinforcing ring was added to the diaphragm 2·54 cm. from
that used for curve 3, fig. 2. The 2500 cycle resonance is
still existent, but is overshadowed by that at 3500. The
effect of removing the collar on the coil former and using
half the original free length is shown in curve 2, fig. 3; the
other conditions are as before. The result is to move the
resonance up to 3000 cycles. When large quantities of
seccotine were applied to the junction of the coil and cone

and allowed to set hard, the result is exhibited in curve 3, fig. 3. There are signs of a resonance at 2000 cycles, that at 3000 cycles remains, but others are introduced at 4000 and 5000 cycles.

By way of contrast the curve of fig. 4 is for a doped diaphragm of identical dimensions but with a free former length of only 0·3 cm., there being no reinforcement with seccotine. The addition of reinforcement to the diaphragm does not improve the reproduction, although it may extend
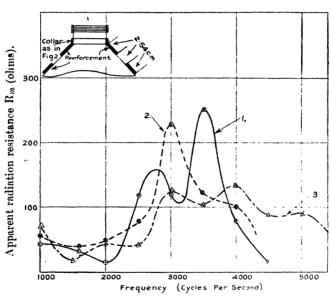
Fig. 3.
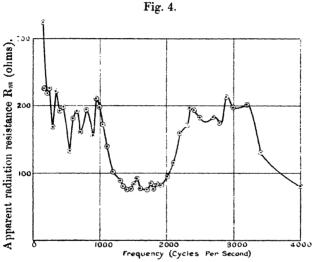
(1) See sketch inset. (2) Conditions as for (1), but collar removed and free length of former 0·48 cm. ; (3) as in (2), but with more seccotine round joint to cone.

the upper register to a degree. As a general rule, whatever artifices are adopted, the output is rapidly attenuated above 6000 cycles, and other means have to be utilized to obtain a reasonable output up to 10,000 cycles. The importance of extending the register as far as 15,000 cycles is not generally realized. The average system does not properly reproduce hand-clapping, speech, jingling of keys or coins, and transients in general, owing to attenuation of the upper frequencies. The natural frequencies of coins are of the order 10,000 cycles or more, according to the diameter. Hence

the reproducing system must be sensitive to frequencies of this order *.

4. *Combination Modes of Reed-driven Free-edge Circular Paper Disk.*

Knowing the values of E, q, and σ for paper, it is possible to calculate the *in vacuo* effective or apparent mass curves on the assumption that the paper is homogeneous and free from loss. By superposing on these the curve for the reed, as shown in a previous paper †, the frequencies of the

Fig. 4.

Apparent radiation resistance of standard doped diaphragm with 1200 turn-coil and rubber surround. Free length of coil former about 0·3 cm., there being plenty of seccotine on the joint to the cone. Main symmetrical mode from impulse test is in the neighbourhood of 2600 cycles per second as shown in fig. 18.

combination modes can at once be determined. Comparison with actual results reveals the idiosyncrasies of the paper and the influence of losses and accession to inertia.

A disk of crisp paper was mounted centrally on the reed of a "Lion" ‡ unit and securely held between two circular metal washers 0·8 cm. radius. Starting at 50 cycles, current was supplied to the unit and sand patterns were

---

* See 'Wireless World & Radio Review' (April 3, 1929).
† Phil. Mag. xi. p. 13 (Jan. 1931).
‡ Phil. Mag. xi. p. 8 (1931).

·observed up to 1300 cycles per second. The results
are indicated in fig. 5. The frequencies marked on the
horizontal axes were calculated, and the M_a curves merely
sketched in to show the trend of the results. The numbers
on the reed curve were the frequencies obtained experi-
mentally. With the exception of the second and fourth
modes at 125 and 610 cycles respectively, they fit in fairly
well. The frequencies at these modes are higher than one
would expect theoretically, and this points to heterogeneity

Fig. 5.
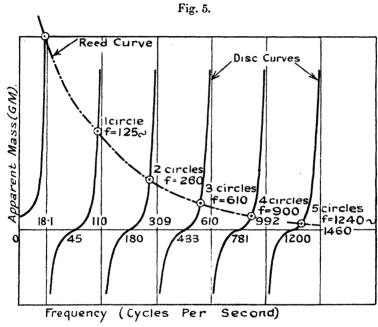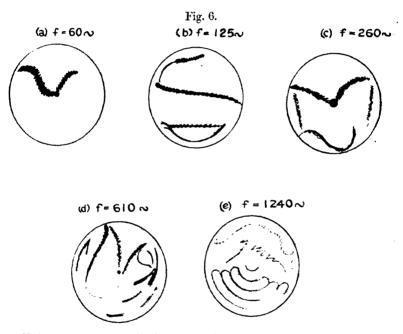
Diagram illustrating combination modes of reed-driven paper disk

of the paper. Although the modes are marked 1, 2, 3, etc.
circles, the sand-patterns are by no means as simple as this.
Some of the nodal figures are illustrated in fig. 6. Patterns
sometimes occur when they are not expected, which points to
· heterogeneity of the paper. No semblance of regularity was
seen until, at 1240 cycles, portions of five concentric circles
appeared. Owing to transmission loss the centre-stationary
modes were too obscure to be obtained with certainty, and
only the centre-moving modes were recorded. The loss may
partly account for the absence of regular sand figures. If
the effective mass curves for the disk fall below the reed

at certain frequencies no marked resonance occurs. (See Phys. Soc. paper for influence of loss on M_e curves.)

An impulse record of the combination was taken *, and it is reproduced in fig. 7 (Pl. 1.). The main frequencies are 260 and 1200 cycles per second, which correspond closely to the third and sixth modes found by sand figures. As in the case of conical diaphragms, there are two frequencies, one low, the other high, prominent on such records. Evidently the combined effect of magnetic and frictional damping is adequate to reduce the other oscillations considerably.

Fig. 6.

(a) f = 60 ∿   (b) f = 125 ∿   (c) f = 260 ∿

(d) f = 610 ∿   (e) f = 1240 ∿

Nodal patterns for reed-driven paper-disk 10 cm. radius, 5×10^{-2} cm. thick. As f increases from 60∿, the sand wanders over the surface like a snake. This effect has also been encountered in thin metal disks at low frequencies. The sand appears to flow like a fluid confined to a definite channel. At 90∿ there was one clearly defined diameter.
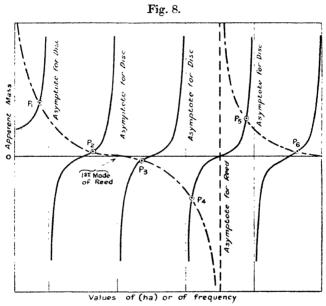
(a) Not a symmetrical mode; probably due to heterogeneity of paper.

(b) Corresponds to one circle on a homogeneous disk.

(c) Corresponds to two circles (see fig. 7) on a homogeneous disk

(d) Corresponds to three circles on a homogeneous disk.

(e) Corresponds to five circles (see fig. 7) on a homogeneous disk.

5. *Exact Solution of Combination Modes of Lossless Reed-driven disk* in vacuo.

The solution indicated in fig. 5 of the present paper and in fig. 4 of the former paper is only correct if the reed can be treated as a simple coil spring whose apparent mass is invariable. In our case, apart from losses and accession to inertia, the results are fairly accurate for three reasons : (1) the restoring force on the reed was supplied by a torsional member, thus preserving the coil-spring analogy ; (2) the modes were well below the natural frequency of the

Fig. 8.
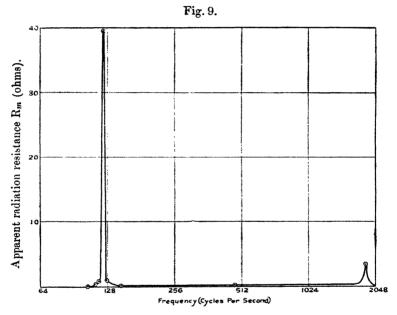
Curves (not calculated) illustrating the exact solution of the combination modes of a cantilever reed and a circular disk. It assumed that frictional and other losses are absent and the system is *in vacuo*.

reed itself (not the torsional member); and (3) the accesssion to inertia was relatively small. If, however, an ordinary reed had been used, whose first mode occurred at, say, 700 cycles, the results at the upper frequencies would have been in error. In fig. 5 the reed curve is ultimately asymptotic to a horizontal axis. Actually the reed should be represented by a family of curves similar to those for the disk, since it has an infinite number of modes.

If M_d and M_r are the apparent masses of the disk and reed respectively, the modes of the combination are given

by $M_d - M_r = 0$. Whence the solution is found by plotting M_d in the ordinary way on an ha base, whilst M_r is *inverted* and plotted on the same base, as shown in fig. 8. The abscissæ of the points of intersection of the two sets of curves provide the necessary values of frequency.

The appropriate curves are calculated from Warren's formulæ [*]. He gives the case of a disk with free and with fixed edge so that both can be treated. The cantilever reed case with a harmonic force applied to the free end is

Fig. 9.

Apparent radiation resistance of freely suspended coil-driven aluminium disk 10 cm. radius, 0·055 cm. thick, coil 2·5 cm. radius having 40 turns of 28 S.W.G.

not given, but can be deduced from expressions (6) and (7) with the conditions $D^2y = 0$ at $x = 0$ (free end), $Dy = 0$ and $y = 0$ at $x = l$ (fixed end).

Substituting in (6) and (7), we obtain the apparent mass of the reed

$$M_r = \frac{m}{\gamma} \frac{(1 + \cosh \gamma x \cos \gamma x)}{(\sinh \gamma x \cos \gamma x - \cosh \gamma x \sin \gamma x)},$$

[*] Phil. Mag. xi. p. 883 (May 1930).

where $m =$ mass of reed per unit length (assumed uniform).

$\gamma = \mu \omega^2 m$.

$\mu = 1/EI$.
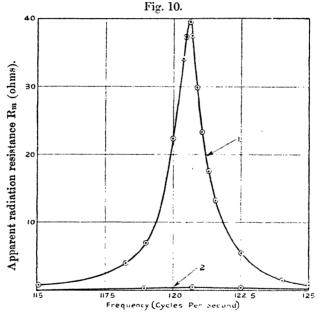
$E =$ Young's Modulus.

$I =$ Moment of Inertia about neutral axis.

$\omega = 2\pi \times$ frequency.

6. *Modes of a Coil-driven Free-edge Circular Aluminium Disk.*

A series of experiments was conducted on a thin aluminium disk driven concentrically by a bakelized 40 turn

Fig. 10.

Curve for coil-driven aluminium disk at first symmetrical mode (1) compared with that of radial mode of paper cone (2).

coil of 28 S.W.G. Using a long paper former and an elastic thread suspension, the disk was kept in a horizontal plane 2·5 cm. from the face of the electro-magnet so that eddy-current damping due to vibration in the leakage field was small.

The data obtained by measurement of the apparent radiation resistance (field off and on) are illustrated in fig. 9 and Table IV. An enormous resonance occurs at 120·6 cycles, which in appearance resembles the selectivity curves

of modern radio circuits. To exhibit this to greater
advantage, it has been plotted on the same diagram (fig. 10)
as a radial mode curve for a free edge paper cone. The
much greater damping of the paper is indicated by the
grotesque comparison of the two curves. R_m for the disk
is nearly 40 ohms, whilst that for the cone is only 0·24 ohm.
In extenuation, it should be mentioned that the mode of the
disk is symmetrical, whilst that of the cone is radial. This
partly accounts for the large difference in R_m. Accurate
location of the resonance at 120·6 cycles necessitated bridge

Table IV.

Modes of Coil-driven Free-edge Circular Aluminium Disk.
Radius = 10 cm., thickness = 0·055 cm., mass = 47 gm.
Mass of coil and former = 7·84 gm.

Frequency (cycles per second).	Nodal pattern.	R_m apparent radiation resistance (ohms).
120·6	One circle, broken twice (*a*).	39·5
200	Tendency for a curved diameter.	0·06
484	Two circles (*e*).	3·04
700	Indefinite.	0·145
950	,,	0·055
1850	Three circles outside and one inside coil.	3·31

measurements to 0·1 cycle per second, or about 1 part in
1000. On a percentage basis this resonance is not nearly
so sharp as that of a good radio circuit.
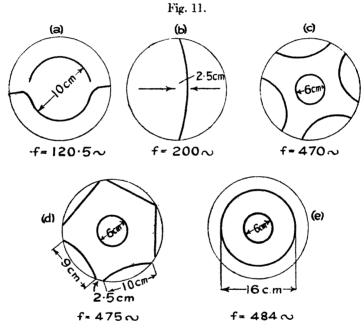
The nodal pattern for the first mode is shown in fig. 11 (*a*).
It is an approximation to a circle 5 cm. radius, and the
incompleteness at the sides is probably due to a tendency
for two radii, although it may be caused by variations in
the mechanical properties of the aluminium sheet. The
resonance at 120·6 cycles is in fair agreement with the
calculated value, due allowance being made for the mass of
the coil and the portion of the disk within it.

A minor mode occurs at 200 cycles, the corresponding
nodal figure being sketched in fig. 11 (*b*). The second centre-
moving symmetrical mode occurs at 484 cycles, but its

magnitude is only 8 per cent. of the first mode. The nodal pattern, fig. 11 (e), consists of two concentric circles, but these were irregular. At 475 cycles the outer portion of the pattern resembles a pentagon, and it is reproduced in fig. 11 (d). A few cycles below this it alters to fig. 11 (c), which manifests a tendency for radii to be formed. On the whole, the nodal patterns are rather hectic, and remind one of those pertaining to paper disks.

The next resonance of importance occurs at 1850 cycles, there being three circles outside and one inside the coil. The

Fig. 11.
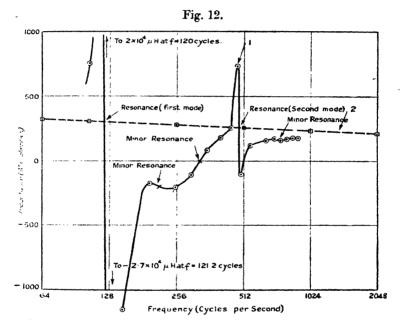
Nodal patterns for coil-driven disk of fig. 9.

circles were more clearly defined than at lower frequencies, an effect also observed with paper disks. The absence of a prominent resonance between 484 and 1850 cycles is due to the influence of the portion of the disk within the coil upsetting the phase relationship in the disk *.

There were other modes of negligible importance yielding indefinite nodal patterns. The centre fixed modes were hardly detectable, excepting from the effective mass curve *.

* Proc. Phys. Soc. *loc. cit.*

Experiments with an aluminium disk three times as thick (0·165 cm.) used in previous work, showed that the modes were not revealed so readily as those with a central reed drive. The disk could, of course, be centrally driven by attaching a small cone or a conical spider between it and the coil. It is rather a coincidence that the 1850 cycle resonance occurs in the neighbourhood of those found with 90° conical paper diaphragms about 12 to 14 cm. radius. The magnitude of R_m for the disk is about ten times that for a paper diaphragm.

Fig. 12.

Curves showing variation in inductance of coil driving aluminium disk (1) coil free L_1, (2) coil fixed L_0.

At 120·6 cycles the resistance of the coil when fixed is about 1·1 ohm, but R_m, the added resistance due to motion, is 39·5 ohms, *i. e.*, some 36 times greater. Thus the apparent radiation efficiency is $\dfrac{39·5}{40·6} \equiv 97$ per cent., which is surprisingly high *. At 250 cycles R_m is only 0·02 ohm, corresponding to an efficiency of 2 per cent. The ratio of the values of R_m at these frequencies is $\dfrac{39·5}{0·02} = 1975,$

* No baffle was used.

K 2

which demonstrates quite forcibly the increase in output due to resonance. The inductance curve of the coil "free" (L_1) is of considerable importance, since it indicates variations in the effective mass of the system *. It is plotted in fig. 12. Peculiarities in curvature correspond to resonance and the relative changes in L_1 are more pronounced than the corresponding change in resistance R_1.

7. *Influence of Magnetic Field Strength in Moving-coil Reproducer.*

From an analytical viewpoint, the mechanical and electrical systems in a moving-coil reproducer are interlinked by the quantity $C^2 = (2\pi r n H)^2$. This can conveniently be regarded as the electro-mechanical conversion factor, and it depends upon H, the strength of the magnetic field. Moreover, the influence of the latter can be predicted by examination of the various formulæ which contain C^2, provided the air-gap length and the dimensions of the moving coil remain constant.

In the absence of elastic constraint, the pure radiation resistance

$$R_a = C^2 \cos^2 \frac{\theta}{B}, \quad . \quad . \quad . \quad . \quad . \quad (1)\dagger$$

where

$$\cos\theta = \frac{B}{(B^2 + \omega^2 m^2)^{1/2}}.$$

Now B and m are independent of electrical variations since they pertain entirely to the mechanical system. Thus R_a varies directly as H^2, and therefore a strong magnetic field is desirable to enhance the sound output.

The motional capacity is given by

$$C_m = \frac{m}{C^2(1 - \cos^2\theta)} \cdot \quad . \quad . \quad . \quad . \quad . \quad (2)$$

$\cos^2\theta$ is usually small compared with unity, and is not influenced by H. Thus C_m varies inversely as H^2. Moreover, a large value of H is accompanied by a small value of C_m, and therefore by increased reactance which causes a reduction in low frequency current. In practical reproducers this is useful in limiting resonance effects when the power valve is a triode (low resistance). If a pentode is used, its resistance

---

* Proc. Phys. Soc. *loc. cit.*
† Phil. Mag. vii. p. 1017 (1929). R_m includes losses, but R_a is due to sound radiation alone.

is so high that the current is substantially constant over
a wide frequency band, and the influence of the increased
magnetic field in reducing resonances is negligible. If the
edge of the diaphragm is reinforced and there is no surround,
the lower register is relatively weak. A very strong magnetic
field will reduce it still further if the power valve is a low
resistance triode.

Hitherto we have discussed the influence of H without
reference to the area of the air-gap or the space available
for the moving coil. When the overall dimensions of
an electromagnet are restricted owing to practical and
economical considerations, a limit is set to the heat dissipation
and therefore to the ampere turns or total magnetization.
The maximum possible flux density in the gap is obtained
when the whole magnetization is utilized there, *i. e.*, the steel
path reluctance is zero (permeability $= \infty$) and there is no
leakage. Under this condition $H = 1{\cdot}257 \dfrac{ni}{l}$, where $ni =$ total
ampere turns and $l =$ length of gap. Assuming $ni = 3000$
and $l = 0{\cdot}16$ cm., $H = 23{,}600$ lines per square centimetre.
This approaches double the value in an actual case, and
indicates the influence of the magnetic reluctance of the
steel. Further information in this direction will be found
in a former paper on magnetic measurements[*].

We can approach the problem in a different manner.
Owing to magnetic leakage within and without the magnet,
experimental observation shows the total flux half-way down
the central pole to be about 1·65 times that in the air-gap.
Assuming the greatest flux density in the central iron pole
to be 16,000 lines cm.$^{-2}$, the greatest air-gap density (mean
over the axial length) [†], is

$$H = \frac{16{,}000}{1{\cdot}65} \times \frac{\text{cross-sectional area of central pole}}{\text{mean area of annular gap}}$$

(see fig. 13)

$$= \frac{\pi r^2}{2\pi r b}\, 9{\cdot}7 \times 10^3 = \frac{r}{2b}\, 9{\cdot}7 \times 10^3.$$

Taking $r = 2{\cdot}5$ cm., $b = 0{\cdot}95$ cm., then $H = 12{,}800$ lines cm.$^{-2}$
is the greatest possible air-gap flux density on the above
hypothesis. The ratio $r/2b$ cannot be increased indefinitely
by reducing b, since the pole tips would be saturated, causing
increased reluctance and leakage. These data agree with

[*] 'Wireless World,' p. 600 (Nov. 26th, 1930).
[†] *Loc. cit.*
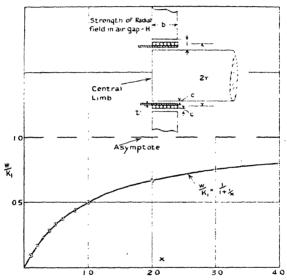
measurements on the electromagnet cited in the previous paper, which shows the argument to have some value, although it is admittedly only a cursory survey of the problem whose accurate solution is very complex.

In the preceding case we can show the influence of reluctance and leakage numerically. The ampere turns for the air-gap alone are

$$\frac{Hl}{1\cdot257} = \frac{12{,}800 \times 0\cdot16}{1\cdot257} \doteqdot 1630 \text{ or}$$

Fig. 13.

Curves illustrating the expression $W = \dfrac{K_1}{\left(1 + \dfrac{1}{x}\right)}$ or $\dfrac{W}{K_1} = \dfrac{1}{\left(1 + \dfrac{1}{x}\right)}$,

and diagram showing dimensions of air-gap of magnet.

54 per cent. of those actually required. Moreover, leakage and reluctance (mainly this) are responsible for a 46 per cent. wastage.

8. *The Output Criterion of the Magnet.*

To obtain the quantity upon which the output from any given electro- or permanent-magnet depends, it is necessary to deduce the acoustic power in terms of the flux density and the dimensions of the air-gap.

The acoustic power is

$$W = i^2 R_a, \quad \ldots \ldots \ldots \quad (1)$$

where i is the coil current and R_a the radiation resistance. For any given type of diaphragm

$$R_a = u C^2, \quad \ldots \ldots \ldots \quad (2)$$

where u is a parameter dependent upon the diaphragm and the frequency. The current is governed by the coil impedance and the resistance of the power valve. The former varies throughout the audible register. However, this is immaterial, as it can be shown that a magnet designed for greatest output at a particular frequency gives this condition at any other frequency. At the electro-mechanical resonance frequency—where the coil reactance vanishes—the impedance is purely resistive. For maximum output—not maximum efficiency—R the coil resistance referred to the anode circuit of the valve must be p times the resistance of the latter, *i. e.*, $R = p\rho_v$, where p depends upon the valve characteristics. Taking the most general case where a transformer is used and assuming it to be perfect, the turns ratio $s = [R/R_m]^{1/2}$ where R_m is the total effective resistance of the coil in the secondary circuit including radiation and diaphragm losses. For any given power valve the total resistance in the anode circuit for maximum distortionless output is

$$R + \rho_r = (p + 1)\rho_v = \text{a constant.}$$

Moreover, the alternating anode current I corresponding to a definite grid voltage swing is also constant.

Thus the coil current

$$i = Is = I[R/R_m]^{1/2}$$

or $\qquad\qquad i^2 = K_1 R_m^{-1}, \quad \ldots \ldots \ldots \quad (3)$

where K_1 is a constant $= I^2 R$ the power dissipated in the load.

Now

$$R_m = R_c + R_i + R_d + R_a,$$

where R_c = resistance due to copper of coil;

$\qquad R_i$ = resistance due to iron loss;

$\qquad R_d$ = resistance due to diaphragm loss;

$\qquad R_a$ = resistance due to radiation of sound.

The iron and diaphragm losses introduce unknown

quantities, and for the present they will be omitted so that we can write

$$R_m = R_c + R_a, \quad \ldots \ldots \quad (4)$$

From (1) and (4) the acoustic output

$$W = \frac{K_1 R_a}{(R_c + R_a)},$$

$$\text{or} \quad \frac{W}{K_1} = \frac{1}{1 + \dfrac{1}{x}}, \quad \ldots \ldots \quad (5)$$

where $x = R_a / R_c$.

Expression (5) gives a curve of the form illustrated in fig. 13. When $x = 0$, $R_a = 0$, $W = 0$, and there is no radiation (*in vacuo*), whilst as x increases so also does the radiation. Obviously the output depends upon x, and we shall regard it as the criterion of the system.

Now the d.c. resistance of the coil is

$$R_c = \frac{\rho l}{A}, \quad \ldots \ldots \quad (6)$$

where the length of wire $l = 2\pi r n$, the cross-section of the wire $A = blf_s/n$, and

$$f_s = \frac{\text{total copper cross-section}}{\text{cross-section of gap}}.$$

Substituting in (6) for l and A, we get

$$R_c = \frac{2\pi r n^2 \rho}{blf_s}. \quad \ldots \ldots \quad (7)$$

Thus from (2) and (7),

$$
\left.
\begin{aligned}
x = \frac{R_a}{R_c} &= \frac{uC^2 blf_s}{2\pi r n^2 \rho} = \frac{u(2\pi r n H)^2 blf_s}{2\pi r n^2 \rho} \\
&= \frac{u}{\rho} \cdot 2\pi r blf_s H^2 \\
&= \frac{u}{\rho} \cdot H^2 V f_s
\end{aligned}
\right\}, \quad \ldots \quad (8)
$$

where $V = 2\pi r bl$ is the volume of the annular air-gap.

So far as the magnet is concerned, the criterion is obviously

$$H^2 V f_s, \quad \ldots \ldots \quad (9)$$

this being 8π times the magnetic energy associated with the

metal of the coil. When the air-gap length l is constant, f_s can be assumed constant also, and the criterion reduces to H^2A as shown in a former paper *.

In specifying a magnet, it is obvious that a statement of the flux density by itself has no value, since the gap dimensions are left out of account. Also a statement of H^2V is meaningless, for of two magnets with equal values of H^2V the air-gap of one might be inadequate to accommodate a suitable coil. This is where the space factor becomes important. With a gap of 0·16 cm., f_s has a value of from 0·4 to 0·5, whereas for a 0·08 cm. gap f_s varies from 0·2 to 0·3. Consequently, the energy output from the smaller air-gap is less than that from the larger.

The problem can be viewed from another angle. With an air-gap of 0·16 cm., we could accommodate 50 turns of wire having a resistance R_c, whereas in the more restricted space available with a 0·08 cm. gap, the diameter of the wire would be much smaller and its resistance appreciably in excess of R_c. Thus the dead loss in the latter case would exceed that in the former, with a corresponding reduction in current and, therefore, in sound output.

It follows that the specification of a magnet should be accompanied by the quantity H^2V and the gap dimensions, so that f_s can be computed.

By hypothesis the H^2Vf_s criterion applies when the coil reactance is zero. If the best magnet is selected on the H^2Vf_s basis, it will fulfil the optimum condition in the lower register of an actual reproducer where iron and diaphragm loss occur. The output in the upper register is influenced by the mass, diameter, etc. of the coil, but no definite relationship has been established analytically. Moreover, it is out of the question to incorporate this in the preceding analysis.

A point of interest arises when economical considerations are waived. Assume we have a magnet with $l=0.96$ cm., the remaining quantities being equal to that of another magnet with $l=0.16$ cm. From the above criterion the output with the former magnet would appreciably exceed that from the latter. The ratio of the outputs is not $\dfrac{0.96}{0.16} \cdot \dfrac{f_s}{f_s'}$ since $W \propto \dfrac{1}{1+\dfrac{1}{x}}$, and it is not proportional to H^2Vf_s since the latter varies as x. With a 0·96 cm. gap a coil of 50 turns can have a very low resistance indeed, but the

---

* 'Wireless World,' p. 604 (Nov. 26th, 1930).

reactance will be unaltered. Thus the increased output will only be felt over a limited band of frequencies where the copper loss is an important fraction of the impedance. At the same time the large mass of the coil—unless aluminium were used—would restrict the amplitude causing a reduction in the output particularly at the higher frequencies. Moreover, a gap of this length is of no practical value. If $H^2 V f_s$ remains constant, an increase in radius of the coil is accompanied by a larger output. The inductive and motional capacitive reactances both increase proportionately to the square of the radius, so that the increase in output is again limited to a definite frequency band, *unless the current is constant at all frequencies.* Under the latter condition the internal resistance of the valve is so high that there is little damping of the natural oscillations, which assume undue prominence. The preceding argument shows that the quantity $H^2 V f_s$ must be used with discretion.

We are now in a position to deal with the factor $H^2 V / 8\pi$ which is sometimes cited by manufacturers as a criterion. The magnetic energy stored in the air-gap is $H^2 V / 8\pi$, but it does not immediately follow that this quantity is a panacea which incorporates all the virtues and vices of a magnet. As we have seen above, the output from a loud speaker is only proportional to $H^2 V$ when the radiation resistance is small compared with the copper resistance. This is approximately true for a number of reproducers where the resonances are relatively weak. But it is inapplicable to a moving-coil reproducer of the horn variety where the radiation resistance is 0·3 that of the total resistance. Also, we have shown by preceding examples that $H^2 V$ has to be used in conjunction with other information connected with the reproducer. Moreover, it should be clear that $H^2 V / 8\pi$ does not tell the whole story by any means, and that details of the air-gap are a necessary adjunct.

9. *Rectification Effect of Coil in Non-uniform Magnetic Field.*

Consider the arrangement sketched in fig. 14. The circular coil is immersed in a radial field whose intensity varies linearly from the point O. If A_1 is an extreme position of the coil the alternating current in it is represented by I_1, and the force urging it in the direction of the arrow A_1 is proportional to $H_1 I_1$. If A_2 be the other extreme position of the coil corresponding to current I_2, the force urging it in the direction A_2 is proportional to $H_2 I_2$.

During acceleration in the A_1 direction the mean force is greater than that during the A_2 direction. The reverse is true during the deceleration period. Thus the coil will move further in the A_1 than in the A_2 direction, which is tantamount to saying there is a translational component in the A_1 direction ; whence the coil will travel towards the zero field position, and the action can be regarded as one akin to rectification.

Fig. 14.
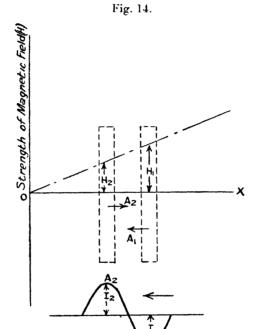
Diagram illustrating coil driven by sine wave current in non-uniform magnetic field.

This phenomenon can be demonstrated in striking fashion by aid of a moving-coil reproducer. If the diaphragm is freely suspended by four threads, the coil when supplied with alternating currrent will move out of the magnet and oscillate about an external point depending upon the gravitational restoring force due to obliquity of the threads. The larger the current the greater the distance the coil is driven from the magnet. A considerable axial force is required to restore the coil to its normal position in the

magnet, and when this force is removed the coil moves out again.

The effect is due to non-uniformity of the field distribution within and without the magnet as shown in previous papers*. The coil does not come out of the magnet until the axial amplitude exceeds a value adequate to bring it into the external leakage field to such an extent that the gravitational control is overcome. Keeping the coil current constant, the frequency must be reduced to a value where this condition is fulfilled. The greater the current the higher the frequency at which translatory motion just ceases to occur. There is obviously a limit due to heating of the coil. Under normal conditions the phenomenon is readily obtained below 100 cycles. If the diaphragm has a powerful radial mode simultaneously and is mounted horizontally, the spectacle is reminiscent of a soaring bird or a helicopter.

In the reproducer used for these tests the coil always moved out of, but not into, the magnet. This is due to the leakage field being less outside than inside the magnet. Doubtless by starting with the coil well inside the magnet it would move inwards.

The analytical expressions for this case are identical with (1) and (2) in Phil. Mag. vii. p. 1014 (1929), excepting that C, the force on the coil per unit current, is now variab.e or $C = f(x)$. Whatever simplifications are made the equations are unfortunately insoluble for a sine-wave current in the coil.

10. *Impulse Records and their uses.*

In a previous paper we saw that severe impulsing occurred when a rectangular wave form was applied to the grid of a thermionic valve having a reproducer in its anode circuit. The question now arises as to the utility of this test in studying the physical behaviour of diaphragms. Impulse records show the oscillations which are not damped out by the magnetic field or other corresponding influence. With large diaphragm moving-coil apparatus the acoustic damping is small. At low frequencies the magnetic damping is paramount, whilst at high frequencies transmission loss assists the magnetic field. In cases where small diaphragms are associated with long exponential horns, considerable damping is due to the resistive load of the horn, as well as to the magnetic field. Records illustrating the influence of the horn are given in figs. 15 *a* and 15 *b* (Pl. II.).

* Phil. Mag. xi. p. 39 (1931); also ' Wireless World,' *loc. cit.*

Probably the best way of demonstrating the use of impulse records is to give a number of typical examples. In fig. 16 *a* (Pl. III.) we have an example taken from a moving-coil reproducer. It consists of a complex oscillation having low-frequency components of 33 and 200 cycles on which is superposed an oscillation of 2000 cycles. The 33-cycle oscillation is that of the diaphragm as a whole on the surround, whilst the 200 ～ is due to the surround *per se* acting as an auxiliary resonant diaphragm *. Fig. 16 *b* (Pl. III.) shows a record of the same diaphragm after removal of the rubber surround. The 33 and 200 cycle oscillations have vanished, but the 2000 cycles oscillation due to the main symmetrical mode (2 nodal circles) of the diaphragm persists. A very strong magnetic field would be required to extinguish this mode.

Fig. 17 *a* (Pl. IV.) is a record for a free-edge paper diaphragm, 5×10^{-2} cm. thick, 16·7 cm. radius, apical angle 160°. Although this diaphragm exhibits strong radial modes when steady low-frequency alternating current is used, none is visible on the record. If excited at all by impulsing, such modes are curbed by the magnetic field. For several cycles the oscillation of fig. 17 *a* (Pl. IV.) is a fair approximation to a damped sine wave, but latterly it degenerates into a more complex type. The natural frequency is that of the main symmetrical mode corresponding to two nodal circles.

The above records were taken with the microphone on the axis of the diaphragm. When the microphone is placed at a point remote from the axis the effect is quite different, owing to the focussing or beam effect and to the velocity of propagation of sound in the diaphragm being less than that of sound in air. Fig. 17 *b* (Pl. IV.) is a record for the preceding diaphragm taken with the microphone 25 cm. *away* from the axis. At such a distance, which is approximately equal to the diameter of the diaphragm, interference is considerable, since one side of the diaphragm is much nearer to the microphone than the other. Moreover, the record must be interpreted in this sense.

The set of records in fig. 18 (Pl. V.) illustrates the influence of axial and angular distance upon the wave-form of the transient oscillation. The effect of increase in axial distance is to reduce the oscillations—due to the main symmetrical

---

* A better example of this complex type of oscillation is given in the ' Wireless World,' p. 15 (May 13, 1931). The ripples on the horizontal portions of some of the records are due to interference from a power system.

mode—which follow the first peak. A standing wave-effect arises, but it is not established until after the peak occurs. There is also diffraction at the microphone. The combination of these two may enhance the output when the microphone is near the diaphragm. The standing wave-effect decreases with increase in axial distance. The influence of angular distance is similar to that displayed in fig. 17*b* (Pl. IV.). The records of fig. 18 (Pl. V.) correspond to a standard diaphragm mounted on a rubber surround which resonated *per se* at 129·5 cycles per second. There is no trace of this on record. Moreover, if the surround resonance occurs below a certain frequency the magnetic field is adequate to render the motion aperiodic. The resonance of the diaphragm vibrating as a whole on the surround at 18 7 cycles is damped out completely. The aperiodic state is seen by the decay of the high-frequency oscillation superposed on an exponential curve. The latter represents the diaphragm being forced back to its equilibrium position by the surround, but restrained from oscillation by the magnetic field. Comparison should be made with fig. 16 *a* (Pl. III.), where both of the surround oscillations occur.

Finally, fig. 19 (Pl. I.) illustrates the case of a diaphragm in which the surround constraint was high enough to promote oscillations at 80 cycles per second. The reproduction from this instrument was accompanied by a strong boom *.

These examples demonstrate the utility of the impulse method in studying the natural oscillations of a diaphragm. Owing to irregularity in some of the records it is difficult to ascertain the frequencies of any but the more powerful oscillations. Broadly speaking, we are able to ascertain the frequency of the main symmetrical mode and to determine whether the mode due to the surround itself or that of the diaphragm on the surround is rendered aperiodic by the magnetic field †. The behaviour of the diaphragm can also be examined by the sudden application of definite frequencies to the grid of the valve, *i. e.*, interrupted sine waves of square modulation. Comparison of results at resonant and non-resonant frequencies would indicate what is to be expected in practice.

The vibrational frequencies of a diaphragm can also be

---

* A simple method of finding the resonance frequency of the diaphragm on the surround is described in ' Wireless World,' August 8th, 1928. The resonance of the surround *per se* is found by bridge measurement.

† It is interesting to reduce the magnetic field to a value where the motion becomes oscillatory.

found by the inverse of the preceding. The reproducer is set in a highly damped enclosure or in free air and impulsed acoustically. The latter can be accomplished by the impact of two bodies whose natural frequencies are much higher than those of the reproducer—supersonic preferred. The coil current is amplified and recorded in the usual way. Since the response as a microphone falls away with rise in frequency, a correction circuit may be required in the amplifier. If the wave-form is immaterial this circuit is unnecessary.

By associating a light coil or an equivalent electrostatic arrangement with any structure its vibrational frequencies can be found. It does not follow, of course, that the relative magnitudes will be identical with those when the structure is impulsed electromagnetically.

In taking impulse records care must be exercised to ensure that oscillations or aperiodic effects due to transformers or to choke-condenser combinations are not superposed upon those due to the instrument under test. This has been discussed in previous papers dealing with such tests ('Wireless World,' April 3rd, 10th, Aug. 7th, 14th, 1929).

April 1931.

XI. *The Transient Response of the Triode Valve Equivalent Network. By* W. JACKSON, *M.Sc., A.M.I.E.E., Lecturer in Electrical Engineering, College of Technology, Manchester* [*].

THE behaviour of triode valve amplifier systems in the steady state under periodic input voltages has received considerable attention, and Colebrook's generalized analysis [†] of the triode valve equivalent network permits the deduction of the general character of the variation of the important quantities of the network with the load in the anode circuit. The nature of the transient response of such a network is likely to prove an equally important consideration in design, in view of the increasing use of thermionic valves in telegraphic systems and for such special purposes as increasing the sensitivity of oscillographs, in both of which applications it is desirable that the distorting transients introduced by the elements of the triode circuit shall be of short duration in
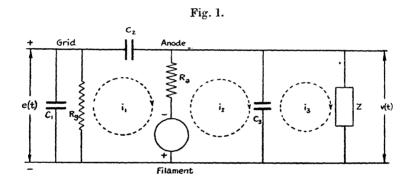
comparison with the duration of any transient voltage pulse to be amplified.

The equivalent network of a single-valve stage as developed by Colebrook is given in fig. 1. The voltage amplification factor and the internal A.C. resistance of the valve are designated μ and R_a; C_1, C_2, and C_3 are the grid-filament, anode-grid, and anode-filament self-capacities respectively ; R_g the effective resistance of the input circuit and Z the load impedance.

The problem is to derive a general expression for the voltage, $v(t)$, developed across the output or load circuit Z on the sudden application of a voltage, of the form $e(t)$, to the input circuit of the valve.

Fig. 1.

The descriptive differential equations of the network are therefore :

$$i_1 \left\{ R_a + \frac{1}{pC_2} \right\} - i_2(R_a) = (\mu + 1) \cdot e(t), \quad (1)$$

$$i_1(R_a) - i_2 \left\{ R_a + \frac{1}{pC_3} \right\} + i_3 \left(\frac{1}{pC_3} \right) = \mu \cdot e(t), \quad (2)$$

$$i_2 \left(\frac{1}{pC_3} \right) - i_3 \left\{ \frac{1}{pC_3} + Z(p) \right\} = 0, \quad (3)$$

where

$$p = \frac{d}{dt}.$$

Eliminating i_1 and i_2 from these equations gives

$$i_3 = \frac{(pR_aC_2 - \mu)}{R_a + Z(p)\{1 + pR_a(C_2 + C_3)\}} \cdot e(t). \quad (4)$$

The output voltage $v(t)$ developed across the load $Z(p)$ is therefore given in terms of the circuit parameters by

$$v(t) = Z(p) \cdot i_3 = \frac{(pR_aC_2 - \mu)Z(p)}{R_a + Z(p)\{1 + pR_a(C_2 + C_3)\}} \cdot e(t). \quad (5)$$

If the voltage $e(t)$ be applied to the system at the time $t = 0$, it may be expressed in the notation of the Heaviside Operational Calculus by $e(t) . [1]$, where $[1]$ is the unit functional voltage of value zero for time $t < 0$ and unity for time $t > 0$.

The complete expression for the output voltage $v(t)$, steady and transient, is then given as the solution of the operational equation

$$v(t) = \frac{(pR_aC_2 - \mu)Z(p)}{R_a + Z(p)\{1 + pR_a(C_2 + C_3)\}} \cdot e(t) . [1]. \quad (6)$$

The form of the operating impedance function $Z(p)$ for the load will depend on the nature of the circuit employed for coupling the triode-valve stage under consideration to a measuring device or to succeeding stages of amplification. As this circuit may contain all of the parameters resistance, inductance, and capacity, the expression for $Z(p)$ will, in general, be complex in nature. Further complexity in the solution of equation (6) results from the fact that it is not always possible to utilize the whole of the voltage developed across $Z(p)$, for application to a succeeding stage, because of the need for providing isolation of the grid of this stage from the high-tension supply.

The most convenient method of obtaining the solution of equation (6) depends upon the form of the applied voltage $e(t)$. If a convenient equivalent operator is available for $e(t)$, as is the case for periodic and exponential time variations, direct solution by the "Expansion Theorem" * may give easiest solution.

If, however, the desire is to consider the factors affecting the nature of the transient solution, this may be effected by determining the response of the system to the unit voltage $[1]$ as the solution of the operational equation

$$h(t) = \frac{(pR_aC_2 - \mu)Z(p)}{R_a + Z(p)\{1 + pR_a(C_2 + C_3)\}} \cdot [1]. \quad (7)$$
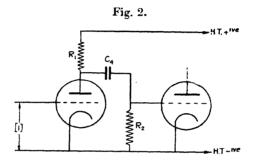
The complete response to the functional voltage $e(t)$ is then conveniently obtained by substituting the value of $h(t)$ obtained as the solution of equation (7) in the "Superposition Theorem."

* See Appendix.
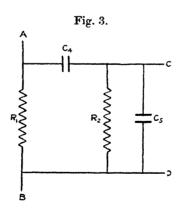
Nature of the Transient Response in typical Amplifier Networks and the Effect of the Self-capacities.

Resistance-capacity Coupling.

The resistance-capacity coupled amplifier, accepted as best for the distortionless amplification of complex periodic audio-frequency voltages, is shown diagrammatically in fig. 2, and its equivalent load circuit is drawn in fig. 3.

Fig. 2.

C_5 represents the input capacity of a succeeding triode stage, while the input resistance of this stage is included in the leak resistance R_2.

Fig. 3.

The operational equation for the voltage developed across the load terminals AB is given by equation (7), where $Z(p)$ is the generating impedance of the entire circuit between A and B, and is given by

$$Z(p) = \frac{R_1\{1 + pR_2(C_4 + C_5)\}}{1 + p\{R_2(C_4 + C_5) + R_1C_4\} + p^2(R_1R_2C_4C_5)}.$$

The voltage applied to the next stage between C and D is, however, only

$$\frac{p R_2 C_4}{\{1 + p R_2 (C_4 + C_5)\}}$$

of this voltage. The output voltage developed by the system, on the application of unit voltage [1] to the input, is therefore given by the solution of the operational equation

$$h(t) = \frac{p R_1 R_2 C_4 \{ R_a C_2 p - \mu \}}{(R_1 + R_a) + p C_4 \{ R_1 R_2 + R_2 R_a + R_a R_1 \} + p^2 C_4 R_1 R_2 R_a (C_2 + C_3 + C_5)} \ [1]. \quad (8)$$

In obtaining this equation, whenever C_2, C_3, C_5 have occurred added to C_4 they have, justifiably, been neglected as small in comparison.

Solution of this equation by the " Expansion Theorem " shows that the output voltage $h(t)$ is made up of two transient components of time constants

$$\frac{1}{a \pm \sqrt{a^2 - b}},$$

where

$$a = \frac{R_1 R_2 + R_2 R_a + R_a R_1}{2 R_1 R_2 R_a (C_2 + C_3 + C_5)}$$

and

$$b = \frac{R_1 + R_a}{R_1 R_2 R_a C_4 (C_2 + C_3 + C_5)}.$$

For normal values of the circuit constants, b is small compared with a^2, and the time constants reduce to $\dfrac{1}{2a}$ and $\dfrac{2a}{b}$; that is,

$$T_1 = \frac{R_1 R_2 R_a (C_2 + C_3 + C_5)}{R_1 R_2 + R_2 R_a + R_a R_1}$$

and

$$T_2 = \frac{C_4 (R_1 R_2 + R_2 R_a + R_a R_1)}{R_1 + R_a}.$$

For circuit constants of the following typical values :

$\mu = 20$; $R_a = 2 \times 10^4$, $R_1 = 10^5$, $R_2 = 10^6$ ohms ;
$C_2 = C_3 = 5 \times 10^{-12}$, $C_5 = 10 \times 10^{-12}$, $C_4 = 5 \times 10^{-10}$ farads,

giving a steady state amplification to periodic voltages of approximately 16·4, the solution of equation (8) is
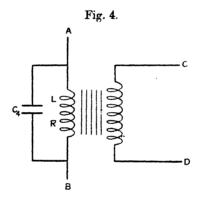
$$h(t) = 16 \cdot 4 e^{-3 \cdot 04 \times 10^6 t} - 16 \cdot 4 e^{-1968 t}$$

When the stray capacities C_2, C_3, C_5 are made equal|to zero, T_1 becomes zero. Solution of the simplified operational equation resulting from this approximation gives

$$h(t) = 16 \cdot 4e^{-1968t}.$$

It is apparent therefore that, apart from producing zero instantaneous response to the input voltage by providing instantaneously a short-circuit path through the network, the effect of the stray capacities—provided they are? of normal values—can justifiably be neglected in deriving the transient response.

Further, that for given values of R_a, R_1, and R_2, the time constant of the local transient may be reduced by reduction

Fig. 4.

in the value of the coupling condenser C_4, to which the time constant T_2 is directly proportional.

Transformer Coupling.

A simple equivalent load circuit of the transformer coupled low-frequency amplifier is shown in fig. 4, in which C_4 represents the equivalent capacity of the transformer primary and secondary windings and of the input circuit of the succeeding stage transferred to the primary. This total capacity can now be included in C_3, with which it is in parallel, given a load impedance $Z(p)$ equal to $(R + Lp)$.

From equation (4) the current i_3 through this load is the solution of

$$i_3 = \frac{(pR_aC_2 - \mu)}{R_a + (R + Lp)\{1 + pR_a(C_2 + C_3)\}} \quad [1],$$

and therefore the output voltage between C and D is given by the solution of the operational equation

$$h(t) = \frac{(pR_aC_2 - \mu)Mp}{R_a + (R + Lp)\{1 + pR_a(C_2 + C_3)\}}[1] \quad . \quad (9)$$

for the unit input voltage.

The solution of this equation shows $h(t)$ to consist of two component transients of time constants

$$\frac{1}{a \pm \sqrt{a^2 - b}},$$

where

$$a = \frac{L + RR_a(C_2 + C_3)}{2R_aL(C_2 + C_3)} \quad \text{and} \quad b = \frac{R + R_a}{R_aL(C_2 + C_3)}.$$

When, however, all self-capacities are assumed equal to zero, there appears only one transient component of time constant $\dfrac{L}{R + R_a}$. Taking the same valve as before and associating with it a typical transformer for which $L = 100$ henrys, $R = 2000$ ohms, $\dfrac{M}{L} = 3\cdot5$, and C_3 (including any condenser which may be permanently connected, inside the transformer casing, across the transformer primary winding) of value 3×10^{-10} farads, the solution of equation (9) becomes

$$h(t) = 70e^{-1\cdot66 \times 10^5 t} - 70e^{-220t}.$$

With C_2 and C_3 taken as zero, the simplified operational equation provides a solution

$$h(t) = -70e^{-220t},$$

so that the same conclusions as before can be drawn concerning the importance of stray capacities in affecting the form of the transient response.

It is at once apparent that the local disturbing transient occurring in a transformer coupled amplifier, made up of components such as are typical of those employed for the amplification of periodic voltages, is much more prolonged than that present in a resistance-capacity coupled amplifier.

Choke Coupling.

For this type of coupling the equivalent load circuit may be drawn as in fig. 5. Treating this circuit in the same
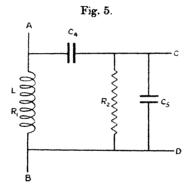
manner as with the resistance-capacity coupling, the operational equation for the output voltage between C and D is

$$h(t) = \frac{R_2 C_4 p(R_1 + Lp)\{pR_a C_2 - \mu\}}{(R_1 + R_a) + p\{L + C_4(\Sigma R_1 R_2)\} + p^2\{C_4[L(R_2 + R_a) + R_1 R_2 R_a(\Sigma C)]\} + p^3\{R_2 R_a L C_4(\Sigma C)\}} \cdot [1],$$

where

$$(\Sigma C) = C_2 + C_3 + C_5 \quad \text{and} \quad (\Sigma R_1 R_2) = R_1 R_2 + R_2 R_a + R_a R_1.$$

Since the denominator is a cubic, the output voltage $h(t)$ must consist of three component transients. Solution in the general case is, however, troublesome, and the nature of the response in the simple case of $C_2 = C_3 = C_5 = 0$ will

Fig. 5.

give the important information. The above operational equation then reduces to

$$h(t) = \frac{-\mu R_2 C_4 p(R_1 + Lp)}{(R_1 + R_a) + p\{L + C_4(\Sigma R_1 R_2)\} + p^2 C_4\{L(R_2 + R_a)\}} \cdot [1],$$

the solution of which consists of two transient terms of time constants

$$\frac{1}{a \pm \sqrt{a^2 - b}},$$

where

$$a = \frac{L + C_4(\Sigma R_1 R_2)}{2C_4 L(R_2 + R_a)} \quad \text{and} \quad b = \frac{R_1 + R_a}{C_4 L(R_2 + R_a)}.$$

Taking the circuit constants used for the resistance-capacity coupled case, with the modification that the resistance R_1 is now replaced by a choke of inductance L 100 henrys and resistance R_1 2000 ohms, the complete

expression for $h(t)$ in response to the unit input voltage given by

$$h(t) = 2 \cdot 26 e^{-220t} - 21 \cdot 86 e^{-1960t}.$$

This circuit gives a steady state amplification to 50 cycle per second input voltages of the same value as that obtained from the previously considered resistance-coupled amplifier. The first term, in spite of its smaller amplitude, is the more disturbing component because of its slower decay with time. Its time constant $\dfrac{1}{220}$ corresponds very approximately to that of the circuit composed simply of the choke and the internal resistance of the valve $\dfrac{L}{R_1 + R_a}$.

The effect on the form of this output voltage of giving different values to C_4, the intervalve coupling condenser, has been calculated. For a value of C_4 equal to 10×10^{-10} farads—*i. e.*, twice as large as before—$h(t)$ is given by

$$h(t) = 5 \cdot 20 e^{-220t} - 24 \cdot 80 e^{-975t},$$

while for a value of 1×10^{-10} farads

$$h(t) = 0 \cdot 37 e^{-220t} - 19 \cdot 97 e^{-9780t}.$$

Decreasing C_4, therefore, produces two desirable effects; it reduces the amplitude of the more troublesome transient and rapidly reduces the time constant of the other. It must be borne in mind, however, that as C_4 is decreased the voltage step up of the stage for periodic input voltages is decreased, particularly at the lower audio frequencies, because of the increasing voltage lost across C_4.

With both the transformer and choke coupled amplifier, indeterminate transient components are liable to be present in the output voltage if the inductance in the anode circuit varies with the current passing through it. This danger does not arise in parallel-fed circuits.

Parallel-fed Choke Coupling.

The equivalent load circuit of a parallel-fed choke coupled amplifier is shown in fig. 6, where the self-capacity of the choke L and of the input of the succeeding stage are represented by C_5. Proceeding as before, and taking $C_2 = C_3 = C_5 = 0$, the output response of the circuit to the unit input voltage is given as the solution of the operational equation

$$h(t) = \frac{-\mu R_1 C_4 p(R_3 + Lp)}{(R_1 + R_a) + p C_4 (\Sigma R_1 R_2) + p^2 C_4 L(R_1 + R_a)} \quad [1].$$

The solution of this equation shows $h(t)$ to be composed of two transient components of time constants
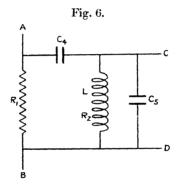
$$\frac{1}{a \pm \sqrt{a^2 - b}},$$

where

$$a = \frac{\Sigma R_1 R_2}{2L(R_1 + R_2)} \quad \text{and} \quad b = \frac{1}{C_4 L}.$$

Taking the following component values as typical of those found in circuits employed for periodic voltage amplification, $\mu = 20$; $R_a = 2 \times 10^4$, $R_1 = 10^5$, $R_2 = 2000$ ohms; $L = 100$ henrys, and $C_4 = 5 \times 10^{-8}$ farads, the complete expression for $h(t)$ is given by

$$h(t) = -\{16 \cdot 66 \cos 2\pi . 70 . t - 2 \cdot 98 \sin 2\pi . 70 . t\} e^{-88 \cdot 3t}.$$

Fig. 6.

With the large values of C_4 employed to avoid low note loss in amplifiers designed for audio-frequency amplification, it is seen that the transient response is likely to be periodic and dies away exponentially at a comparatively slow rate.

The critical value of C_4 for non-periodic transient response occurs when $a^2 = b$, that is, when

$$C_4 = 4L \left\{ \frac{R_1 + R_a}{\Sigma R_1 R_2} \right\}^2,$$

$\Sigma R_1 R_2$, as before, being $(R_1 R_2 + R_2 R_a + R_a R_1)$.

Appendix.

The operational equation given in (7) may be written in the form

$$h(t) = \frac{M(p)}{D(p)} . [1], \quad \ldots \ldots \quad (10)$$

where $M(p)$ and $D(p)$ are certain functions of p. In the cases discussed in the paper $M(p)$ is never of higher power in p than $D(p)$, so that direct solution of this equation by the " Expansion Theorem " results in the following manner.

Let $\lambda_1, \lambda_2, \ldots, \lambda_n$ be the n roots of $D(p) = 0$. Provided that none of these roots are zero and that there are no equal roots, the complete solution of (10) is given by

$$h(t) = \frac{M(0)}{D(0)} + \sum_{k=1}^{k=n} \frac{M(\lambda_k)}{\lambda_k \cdot D'(\lambda_k)} \cdot e^{\lambda_k t}$$

where $M(0)$ and $D(0)$ are the values of $M(p)$ and $D(p)$ for $p = 0$, and $D'(\lambda_k)$ is the value of $\dfrac{dD(p)}{dp}$ for $p = \lambda_k$.

If, having obtained the response of the network to the unit voltage $[1]$, it is desired to derive the response $v(t)$ to a functional input voltage $e(t)[1]$, this may be obtained by substituting for $h(t)$ and $e(t)$ in the "Superposition Theorem"

$$v(t) = e(t) \cdot h(0) + \int_0^t E(t - \phi) \cdot h'(\phi) \cdot d\phi$$

$$= e(t) \cdot h(0) + \int_0^t E(\phi) \cdot h'(t - \phi) \cdot d\phi,$$

where ϕ is a variable of integration and

$$h'(\phi) = \left[\frac{dh(t)}{dt} \right]_{t = x}.$$

If, in equation (10), $M(p)$ is of higher power in p than $D(p)$, $\dfrac{M(p)}{D(p)}$ can always be reduced to the sum of a number of terms, some of which are integral powers of p and one of which is of the form $\dfrac{x(p)}{y(p)}$, where $x(p)$ is not of higher power in p than $y(p)$. The resultant expression may then be

$$Ap[1] + B[1] + C \frac{x(p)}{y(p)}[1],$$

when the solution of equation (10) is the sum of the solutions of

$$Ap[1], \quad B[1], \quad \text{and} \quad C \frac{x(p)}{y(p)}[1].$$

XII. *Photography of Diffraction Patterns due to small Circular Apertures.* *By* L. R. Wilberforce, *M.A.,* *Lyon Jones Professor of Physics, The University of Liverpool* *.

[Plate VI.]

THE diffraction effects produced when light from a point-source passes through a circular aperture in a thin plate and is then received on a screen have been very fully investigated by Lommel †, and his paper has been frequently referred to by English writers, but the mathematical form in which his results were exhibited has left their details unfamiliar to a not inconsiderable number of physicists, and it may be of service to describe their main features in more popular language.

The changes in the diffraction pattern due to variations in the distances of the aperture from the source and from the screen, in the diameter of the aperture, and in the wavelength of the light employed, may all be summed up in two statements.

(1) The character of the pattern depends only upon the number of half-period elements (which we may abbreviate as *h–p*) which the aperture transmits ; (2) the linear dimension or " scale " of the pattern is proportional to the distance apart on the screen of the interference fringes which would be due to two imaginary identical point-sources of light at opposite ends of a diameter of the aperture. We may call this distance a " fringe-unit."

The character of the pattern may be described under two subheadings : (*a*) the positions of the maxima and minima, (*b*) the distribution of intensity at and between these positions.

Lommel's results show that if the aperture does not transmit more than about 1*h–p* the character of the pattern is absolutely constant, so far as the positions of the minima are concerned, while the positions of the maxima and the distribution of intensity tend asymptotically to constancy as the size of the aperture is decreased. Further, the radii of successive minima, starting from the centre of the picture, increase by distances which soon become practically equal. and whose value is then one fringe-unit.

---

* Communicated by the Author.
† *Abh. d. K. Bayer Akad. d. Wissensch.* xv. 1884–1886.

This statement may be made more definite numerically. Lommel's results are expressed in terms of a quantity Z, such that its relation to the distance ζ of a point from the centre of the pattern and the length f of a "fringe-unit" may readily be proved to be given by $Z = \pi\zeta/f$. The positions of the minima are given by the roots of the equation $J_1(Z) = 0$. It can readily be calculated from a table of Bessel's Functions that the corresponding values of ζ/f are: 1·298, 2·223, 3·238, 4·241, 5·243, 6·244, 7·245, 8·246, 9·246, 10·246, 11·247, 12· 247, etc.

When the aperture transmits more than 1 h–p the character of the pattern, as is well known, becomes more variable. It is then necessary to consider separately the portion of the screen in the geometrical shadow and the portion which would be fully illuminated if light travelled in straight lines, which we may call the geometrical disk. The phenomena within the disk have often been described and photographed and are so familiar that it is unnecessary to refer to them further, but it is less generally realized that in the geometrical shadow the light does not steadily decrease to zero but does so through a series of steps of minima and maxima, and that the successive values of ζ/f for the minima of these steps continue to be given by the series of numbers already written down, beginning, however, not at its first term but at such a term that the value of ζ calculated from it will correspond to the point nearest the edge of the geometrical shadow.

The fact that at points well within the geometrical shadow the character of the fringes will tend to constancy may be explained as follows. Let a plane wave pass normally through a circular aperture of radius r and let the light be received on a screen at a distance b from the aperture large compared with r, and let us consider the amplitude at a point P on the screen whose distance ζ from the axis is small compared with b but large compared with r. If N is the projection of P on the plane of the aperture, the loci of points in the aperture equidistant from P will be circular arcs with N as centre, and as the distance of N from the aperture is large compared with r it will be a good approximation to replace these arcs by parallel straight lines.

If y and $y + dy$ are the distances of two such lines from the centre of the aperture, the distance from P of the strip which they enclose is

$$\sqrt{b^2 + \zeta^2} \pm \frac{y\zeta}{\sqrt{b^2 + \zeta^2}}$$

and the area of the strip is

$$2dy\sqrt{r^2-y^2}.$$

Thus, by the usual formula, if λ is the wave-length and A the amplitude of the light at the aperture, the vibration at P is

$$\frac{2A}{\lambda}\int_{-r}^{+r}dy\frac{\sqrt{r^2-y^2}}{\sqrt{b^2+\zeta^2}}\sin\frac{2\pi}{\lambda}\left(vt-\sqrt{b^2+\zeta^2}+\frac{y\zeta}{\sqrt{b^2+\zeta^2}}\right).$$

We may write b for $\sqrt{b^2+\zeta^2}$ and, expanding the trigono-metrical term and noticing that the coefficient of $\cos\frac{2\pi}{\lambda}(vt-b)$ vanishes between the limits of integration, we reduce the expression to

$$\frac{2A}{\lambda b}\sin\frac{2\pi}{\lambda}(vt-b)\int_{-r}^{+r}dy\sqrt{r^2-y^2}\cos\frac{2\pi\zeta y}{\lambda b}.$$

If we write x for v/r, the amplitude of this vibration will be

$$\frac{2r^2A}{\lambda b}\int_{-r}^{+r}dx\sqrt{1-x^2}\cos\frac{2\pi\zeta r}{\lambda b}x.$$

This is

$$\frac{2r^2A}{\lambda b}\cdot\frac{\pi}{Z}\cdot J_1(Z),$$

where Z is written for

$$\frac{2\pi\zeta r}{\lambda b}.$$

If the aperture transmits m half-period elements

$$m\lambda=r^2/b,$$

and if the "fringe-unit" is f,

$$f=\lambda b/2r,$$

and the expression for the amplitude becomes

$$2m\pi AJ_1(\pi\zeta/f)\Big/\frac{\pi\zeta}{f}.$$

That is, in the region of the pattern where ζ is large compared with r, the character of the pattern involves the number of half-period elements merely as a factor governing the absolute intensity of illumination, while the relative

intensities at corresponding points and the positions of the maxima and minima will be the same for all values of m.

So far as I have been able to ascertain, no adequate photographs of the diffraction patterns when m is not greater than unity have been published. Arkadiew *, who gives a fine series of pictures for larger apertures and for opaque disks, has photographs for $m = \frac{1}{2}$ and $m = 1$ which show nothing outside the first considerable minimum. This is explicable by the fact that the intensity within this minimum is so great in comparison with that of the rest of the field that an exposure sufficiently long to show the outer portions of the pattern will lead to such an over-exposure of the centre that the plate will be spoilt. I therefore tried to remedy this by interposing a suitable mask in front of the photographic plate, so that a sufficiently long exposure could be given to the marginal part of the picture, and afterwards, by removing the mask, a short exposure to show the central portion. Though I naturally had expected that it would ultimately be necessary to use monochromatic light, preliminary experiments were undertaken using as a source of light a small approximately circular hole fixed a few centimetres in front of the crater of an arc. A magnified "pin-hole picture" of the crater was thus formed in the plane of the aperture, and was adjusted so that the aperture was completely within this picture. In this way a maximum of illumination was conveniently obtained. The mask, which consisted of a brass disk of suitable small diameter cemented on a thin plate of good glass, was carried by a mechanical stage, and thus could be accurately adjusted horizontally and vertically so as to be central with the pattern while observed through a suitable eye-piece.

Although the experiments were made in a darkened room the requisite exposures were often so long that further precautions against stray light became necessary. A blackened wood box about a metre long and of 20 cm. square section was made, having a sufficient opening at one end and an arrangement for holding the photographic plate at the other. The stage carrying the mask was attached to a heavy solid rod passing into the box near the bottom and close to the photographic plate attachment through a short tube which it did not touch. The mask could thus be made central with the pattern before the plate was put into position, and any slight displacement of the box due to the subsequent insertion of the plate would not disturb the adjustment of

the mask. When the marginal portion of the plate had been sufficiently exposed the mask could be lowered without disturbance of the plate by rotating the rod through a right angle about its axis, and the supplementary exposure thus obtained.

The photographic plates used were backed Wellington Ortho Process plates, and a preliminary negative obtained with an aperture transmitting about $\frac{1}{4}$ *h-p* revealed an unexpected but fortunate coincidence. A long series of maxima and minima was shown—in fact, eight or nine maxima could be measured and four or five more faintly seen, and their final disappearance even then seemed to be due to evanescent intensity rather than to any blurring due to overlapping. It appeared, therefore, that these plates were abnormally sensitive to a comparatively narrow band in the spectrum of the crater, and all the advantages of approximately monochromatic light were obtained without the serious decrease of illumination inseparable from the conventional methods.

Measurements of the diameters of some minima were made and the mean wave-length of the operative band of the spectrum thus determined, with the following results.

Aperture (1).—Diameter ·086 cm., distance from plate 335 cm., radius of 9th minimum 1·425 cm.

From the values of ζ/f for the minima previously given it follows that

$$f = 1·425/9·246 = ·154 \text{ cm.}$$

Hence $\lambda = ·086 \times ·154/335 = 3·96 \times 10^{-5}$ cm.

Aperture (2).—Diameter ·0775 cm., distance from plate 335 cm., radius of 8th minimum 1·40 cm.

Thus $f = 1·40/8·246 = ·170$ cm.

Hence $\lambda = ·0775 \times ·170/335 = 3·93 \times 10^{-5}$ cm.

Aperture (3).—Diameter ·065 cm., distance from plate 325 cm., radius of 10th minimum 2·025 cm.

Thus $f = 2·025/10·246 = ·198$ cm.

Hence $\lambda = ·065 \times ·198/325 = 3·95 \times 10^{-5}$ cm.

Aperture (4).—Diameter ·044 cm., distance from plate 335 cm., radius of 5th minimum 1·55 cm.

Thus $f = 1·55/5·243 = ·296$ cm.

Hence $\lambda = ·044 \times ·296/335 = 3·88 \times 10^{-5}$ cm.

These values for λ, which correspond to the extreme of the visible violet end of the spectrum, are in remarkable agreement, remembering that the diameters of the minima can only be measured to the nearest half millimetre.

Figs. 1, 2, & 3 (Pl. VI.) give prints from the negatives furnished by apertures (4), (3), and (1). The distance from the aperture to the source was in each case equal to its distance from the photographic plate. Considerable difficulty was experienced in making suitable apertures of the smaller diameters. The diffraction patterns were at first found to display great unsymmetrical variations of intensity even when the circular form of the aperture was beyond doubt. These irregularities were finally traced to the burr which every method of drilling which could be devised left behind it. Even the process of depositing a thick layer of copper electrolytically on each side of a piece of platinum foil, drilling completely through with a watch maker's drill, and then dissolving off the copper with nitric acid did not completely eliminate it. The technique which finally proved successful was to use platinum foil about ·08 mm. thick, which was of sufficient mechanical strength not to buckle, to work up the hole to nearly the required diameter by fine watchmakers' broaches turned rapidly in a small lathe, and to keep the burr on each side rubbed down flat on a fine Arkansas stone with water. This, of course, left the edges of the hole ragged and possibly slightly out of truth. The foil was then softened by heating to bright redness in a Bunsen burner, and, after cooling, each side of the hole was in turn just pressed squarely on to the tapering portion of a needle of slightly larger diameter than the hole while this needle was being rapidly rotated in a small lathe. This left the hole smooth and circular without producing a new burr.

The same amount of care was fortunately unnecessary for the small holes which were fixed in front of the arc to serve as approximate point-sources. It was sufficient to secure that in each case the shape should be roughly circular and, in order to avoid blurring, that the diameter should not exceed one-half of a fringe-unit multiplied by the ratio of the distance of the aperture from the source and screen respectively.

The use of an opaque mask and the consequent sharp line of demarcation produced on the negative spoils the aspect of the diffraction pattern in its immediate neighbourhood. In order to study this aspect in the neighbourhood of the centre for apertures transmitting nearly 1 *h-p* some masks

of a graduated opacity were produced photographically, and figs. 4, 5, & 6 (Pl. VI.) are prints from the negatives obtained, corresponding to $\frac{1}{2}$ $h-p$, 1 $h-p$, and $1\frac{1}{2}$ $h-p$ respectively. The same aperture was used for each at the same distance (335 cm.) from the plate, and the size of a fringe-unit is thus the same throughout ; the distances of the source were 335 cm., 112 cm., and 67 cm. respectively. The slight variations of the patterns for $\frac{1}{2}$ $h-p$ and 1 $h-p$ are fairly well brought out. The mask used for fig. 6 (Pl. VI.) transmitted too much light in its marginal portion, and the earlier minima are not well shown in consequence.

Figs. 7, 8, 9, & 10 (Pl. VI.) are the results of using a larger mask and long exposures so as to exhibit the maxima and minima far removed from the centre. They correspond to $\frac{1}{2}$ $h-p$, 1 $h-p$, and $1\frac{1}{2}$ $h-p$, obtained as explained above, and 2 $h-p$ obtained by reducing the distance of the source to 48 cm., and, as before, the fringe-unit is the same for each. The coincidence in radii of the outer maxima and minima for the various pictures is shown in fig. 11 (Pl. VI.), where half of the picture for 2 $h-p$, with its familar dark centre, and half of that for $\frac{1}{2}$ $h-p$ are put together.

The exposures for fig. 10 (Pl. VI.) were 60 minutes for the margin and 30 seconds for the centre, which indicate the rate of attenuation of the intensity ; the exposures for figs. 7, 8, & 9 (Pl. VI.) had similar ratios.

For fear of misunderstanding it should be explained that the negatives obtained diminished so greatly in density from the centre outwards that their details could not be transferred to a print by a single exposure, and two exposures, using suitable graduated masks, were needed. Thus the pictures given, while they show the *positions* of the maxima and minima, do not reproduce the relative intensities at different portions of the field.

I must not conclude without expressing my great indebtedness to my lecture-assistant, Mr. F. J. Welch, for the skill and patience which he has lavished on the development and printing of these photographs.

George Holt Physics Laboratory,
The University of Liverpool.
July 27, 1931.

XIII. *On Sensitive Flames.* *By* G. B. Brown, *M.Sc.,*
Lecturer in Physics, University College, London *.

[Plates VII.-X.]

INTRODUCTION.

SINCE its first accidental discovery by John Leconte in
1858 † the phenomenon of sensitive flames has received
the attention of a large number of investigators. In spite
of this, however, a detailed explanation of the phenomenon
has never been given, and the object of the present investi-
gation is to examine the nature of the instability of gaseous
jets more closely and to attempt to discover the causes
underlying their sensitivity to the vibrations of sound.

The first thorough examination of sensitive jets was made
by Tyndall at the suggestion of Leconte ‡. Tyndall used a
number of different kinds of jets, but the most sensitive ones
were made by drawing out ordinary glass tubing. Using
tuning-forks he found that frequencies of 3200, 2400, 2000,
and 1600, in this order of effectiveness, reacted upon his
most sensitive flames. Tyndall also showed that flames such
as the bat-wing and the fishtail, originally insensitive to
sound, could be made to jump visibly when a whistle was
sounded, if a current of air from a slit was brought against
the flame so as to make it flutter. Even a candle proved
sensitive when distorted by air from a blowpipe. Later, by
passing the gas over ammonia and then hydrochloric acid, so
as to produce a smoke of sal ammoniac, Tyndall showed that
similar effects are obtained with unlit gases. He used unlit
coal gas, hydrogen, carbon dioxide, and air. In all cases
the pitch effective was found to be much lower than in the
case of flames.

Tyndall concluded that the effect of sound on the jets of
gas was to produce a condition of turbulence similar to that
caused by increasing the pressure : "We bring it to the
verge of falling, and the sonorous pulses precipitate what
was already imminent. This is the simple philosophy of all
these sensitive flames."

Barrett, Tyndall's assistant at the Royal Institution, had
a different theory as to the cause of sensitivity in flames, and

in the 'Philosophical Magazine' for 1867 * he ventures to put it forward. He quotes Tyndall's explanation that "an external sound added to that of a gas-jet already on the point of roaring is equivalent to an augmentation of pressure on the issuing stream of gas". He then points out that the flames flare with the slightest increase in *velocity*. Since the sound waves must also throw the tubing through which the gas flows into vibration, "the flow of gas is thereby driven from the sides and urged more towards the centre of the tube, and the current, thus confined within narrower limits, must issue from the burner with an increased velocity so long as the sound continues. It is the greater rapidity thus induced in the issuing stream of gas which causes the flame to shorten and diverge . . . ."

He supports this curious hypothesis with various observations, but it does not seem to have occurred to him to test it by shielding first the tubing and then the flame itself. I find that if this is done with an efficient screen no difference is observed in the former case, while in the latter the sensitivity disappears almost entirely.

The next investigator to take up this question was Lord Rayleigh. He examined the behaviour of a sensitive flame when placed in a region of stationary waves, and observed that it was disturbed at the antinodes and not at the nodes, and consequently was affected at points where the ear would not be, and *vice versa* †.

Later Rayleigh ‡ examined phosphorus smoke-jets by intermittent vision, and noticed that the sound waves produced a "serpentine motion of the jet previous to rupture." He made use of resonators in order to increase the sensitiveness of the jets to the frequency of the tuning-fork used, which was 256. Rayleigh had difficulty in getting sufficient illumination for his stroboscopic experiments, and he repeated his observation with liquid jets. He also examined fishtail burners with liquid and found that they were sensitive, and "when much excited, throw out tall streamers in the perpendicular plane." He concludes, however, that even with the best arrangement as to sensitiveness and intermittent vision, the appearances presented by the liquid jets are difficult to interpret and also to reproduce in a drawing. Rayleigh used a "water-engine" to provide uniform rotation for his stroboscopic disk, and this no doubt prevented his examining

---

* Phil. Mag. pp. 219 & 287 (1867).
† 'Scientific Papers,' i. p. 406.
‡ *Loc. cit.* ii. p. 268.

gas flames, which require a much greater frequency than liquid jets in order to show sensitivity. He assumed, however, that the phenomena occurring in the gas flame when disturbed by sound were similar to those observed with liquid jets issuing into liquid and with smoke jets, *i. e.*, the column becomes sinuous, and when the amplitude has reached a certain value disrupts, causing "flaring," and in special cases forking. Rayleigh also wrote several mathematical papers on the stability of jets, which will be referred to later.

Present Investigation.

The investigations described below were undertaken at the suggestion of Professor E. N. da C. Andrade, and are a continuation of some research on jets originally commenced by him.

It was hoped by means of different frequencies produced by a valve oscillator, in conjunction with an amplifier and moving-coil loud-speaker, to discover the cause of the sensitivity of gas flames, and to examine, in particular, whether resonance in the jet and tubing had any effect in determining the frequencies to which the flames would most readily respond.

It has been found that the variation of sensitivity with frequency is very complex and that the range of frequencies to which different jets respond varies considerably. Nearly every jet examined has shown a marked directional effect when the direction of the sound is perpendicular to the axis, and the most sensitive ones are those in which this effect is most pronounced. In these cases the column of gas forks when in the most disturbed position, and becomes unaffected when the jet is turned about its axis through a right angle. The nature of the instability induced by sound in smoke jets has been examined stroboscopically and by means of photography. It has been found to consist of an undulatory motion of the column of smoke previous to forking, which very closely resembled that which is observed in the case of a jet of gas which is impinging on a wedge and producing edge-tones. It is suggested that there may be a close connexion between the two phenomena.

In some very rare cases flames can be made to fork without the aid of sound by introducing some form of obstruction into the jet, such as wire or cotton-wool. The flame then gives out a nearly pure note of its own, but it has not been found possible to repeat these results at will.

M 2

EXPERIMENTAL METHOD.

Source of Sound.

A heterodyne oscillator in conjunction with an amplifier and Rice-Kellogg moving-coil loud-speaker was used as the source of sound. Since it was of the first importance that the wave form given should be pure and as free as possible from harmonics, and that the amplitude should remain constant, an oscillator based on one designed by H. Kirke and described by him in the ' Wireless World ' * was constructed. It can easily be shown that if two valve oscillators are heterodyning, and if one current is stronger than the other, the resultant rectified current is proportional to the weaker of the two (assuming a linear rectifier). In other words, with a linear detector the amplitude of the rectified beats is unaltered by a change in the amplitude of the stronger oscillation. Further, harmonics can only occur in the resultant rectified current if both the high frequency oscillators have harmonics.

Consequently in this heterodyne set the weaker oscillator contains filter circuits to remove harmonics, and very weak coupling, and its frequency and amplitude are kept constant. The frequency of the stronger oscillation can be varied by means of condensers, so that when heterodyning with the weaker oscillation, frequencies from 0 to 10,000 can be obtained. If the above conditions obtain these frequencies should be free from harmonics and, moreover, of constant amplitude.

Resistance-capacity amplification is used with low resistances consisting of tapped potentiometers of 50,000 ohms. Two of these had ratios of 1 : 2, and the third a ratio of 1 : 1·05 between each tapping. A very large range of known fractions of the total output could thus be obtained by varying the tappings on the potentiometers. Care was taken that the potentiometers were non-reactively wound. This was done by winding them on a bobbin with a large number of sections, alternate sections having the winding reversed. The variable oscillator had three condensers : the first was used as a zero-adjusting condenser by setting it so that the beat frequency as indicated by the milliammeter in the detector anode circuit was zero ; the second was then used to increase the frequency from 0 to 3000, and the third from 3000 to 10,000. A ·3 μ F. air-condenser was also included in the circuit when frequencies up to 17,500 (the

* Vol. iv. no. 41, p. 67 (1927).

limit of response of the Rice-Kellogg speaker) were required.

The Rice-Kellogg speaker was fixed in the centre of a square baffle-board of 7-ply wood 3 ft. × 3 ft. This was placed on a table which also supported the oscillators and amplifier, care being taken that the oscillators, which were carefully shielded with copper-sheet, were separated by at least 5 ft. to avoid any residual interaction. Facing this table was another of the same height which supported the clamps for holding the jets, and which also had attached to it rails on which a movable board, identical with the one to which the loud-speaker was attached, could run backwards and forwards. This board, the purpose of which is explained shortly, had attached to it a small brass frame with a very fine wire stretched across it, and this moved over the surface of a wooden metre scale screwed to the table. By this means the position of the moving baffle-board could be read on the scale. At the back of this table was a large heavy felt curtain which stretched from the ceiling to the floor (15 ft.) and extended in a horizontal direction for 10 ft. This reduced the effect of reflexion to a negligible amount. (Even with the board at the distance of the curtain, the effect on the flames was very small.)

Measurement of the Frequency.

The simplest way of calibrating the condenser readings of the variable oscillator was obviously to make use of the well-known fact that sensitive flames readily indicate the positions of the antinodes when placed in a region of stationary waves. The reflecting board was placed on its rails and moved backwards, readings being taken of successive positions for maximum disturbance of the flame which was placed between it and the loud-speaker. In this manner by taking means the frequency could be obtained with 1 per cent. accuracy over the range for which the flames were sensitive. A check was obtained at lower frequencies by observing beats between tuning-forks of known frequency and the oscillator.

Apparatus for Supply of Gas and Air.

Since most jets require a pressure above that of the ordinary gas supply, some form of pressure-pump had to be employed. It was found that one of the type manufactured by Edwards and Son answered very well for this purpose. These pumps will run smoothly at speeds as low as 1 or 2

revolutions per sec., and can be used to increase the supply-gas pressure of, say, 6 cm. of water by as little as half a centimetre. The impulses of the pump were smoothed out by allowing it to discharge into a large tank to which the tubing supplying the jet was connected through a tap. In the actual apparatus used the pump was arranged so that by means of four taps it could be rapidly changed from pumping gas into one tank, to pumping air into a separate container. A water manometer was connected to the outlet from both tanks. It was always found better to regulate the pressure at the jet by altering the rheostat in series with the pump motor, rather than by means of taps or screw clips. The reason for this was the fact, first observed by Tyndall, that in some cases if the pressure on a sensitive flame is increased and the flame brought back to the condition of just not flaring by means of a tap, the flame is no longer sensitive. He came to the conclusion that an essential condition of sensitivity was "that a free way should be open for the transmission of the vibrations from the flame, *backwards*, through the gas-pipe which feeds it. The orifices of the stopcocks near the flame ought to be as wide as possible" [*].

Rayleigh [†] showed that the insensitivity produced by the stopcocks was due to the fact that flaring was prematurely produced. There are two ways in which this may be caused. Either the irregular flow through the tap may cause ricochetting of the current of gas from side to side, as Barrett suggested [‡], or sound to which the jet is sensitive may actually be produced at the tap, and the tubing act as a speaking-tube in conducting these vibrations to the orifice.

Rayleigh introduced various nozzles into the supply tube in order to deflect the stream, but he found no tendency to flare unless a hissing sound could be heard. He therefore favoured the second explanation.

To test Lord Rayleigh's theory, a high-pitched whistle to which the jet used was very sensitive, was placed in a wide-bore glass tube in series with the rubber tubing supplying the jet. It was just possible to hear when the whistle was sounding by placing the ear near to the outside of the wide-bore tube. It was invariably found that when the whistle sounded the flame became disturbed and its sensitivity much impaired.
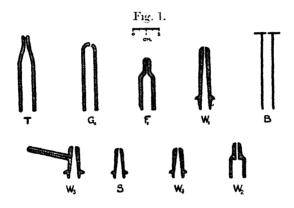
[*] Phil. Mag. 4th ser. xxxiii. p. 92 (1867).

[†] Scientific Papers,' ii. p. 101 ; also Phil. Mag. xiii. pp. 340-347 (1882).

[‡] *Loc. cit.*

This kind of disturbance is the drawback in using gas cylinders for the supply, since with these it is very difficult to avoid some sort of hissing noise at the valve or the pressure regulator. This difficulty can, however, be eliminated by packing the tubing near the jet with cotton-wool.

It was found that the diameter and the length of the metal or rubber tubing used for connecting the reservoir to the jet had no effect on the behaviour of the flame. The position of the tubing near the jet, however, makes a very great difference, since it alters the manner in which the gas streams out of the orifice. This should always be adjusted by trial for the maximum sensitivity, or for best forking, or whatever behaviour is most desired.

Fig. 1.

Types of Jets used.

As has been mentioned the original observation of sensitivity to sound was made by Leconte on a "fishtail" gasburner. Tyndall, on taking up the investigation, used drawn-out glass tubing, often with a V-shaped cut in the orifice * (fig. 1, T). Rayleigh used high-pressure pin-hole steatite gas-burner jets of the type invented by Mr. Sugg, and also drawn out glass jets.

Another kind of sensitive glass jet for low pressures has been described by Sutherland †. A glass tube of about 1 cm. diameter is rotated with one end in a blowpipe flame until the end very nearly seals itself up. While still soft it is slightly flattened, so as to make the orifice noticeably elliptical (fig. 1, G). The sensitivity is greatest in the direction of the major axis of the ellipse. "This shape

* W. F. Barrett, Phil. Mag. 4th ser. xxxiii. p. 219 (1867).
† G. A. Sutherland, 'Nature,' cviii. p. 533 (1921).

provides the sudden change of pressure on which sensitiveness depends.... As with high-pressure jets, the flame loses sensitiveness if the orifice be too nearly circular, or if its ellipticity be too great." This latter statement is not in agreement with the findings of Jordan and McClung *, who made special search for the most delicate detector of faint sounds.

According to them the orifice must be accurately circular for greatest sensitivity, and they recommend a metal jet 2 in. long, tapering from 0·113 in. diameter at the entrance down to ·043 in. at the exit. The inside must be perfectly smooth. These dimensions were the result of experiments with many different shapes and sizes of jets. In the present research a large number of jets of all kinds were examined : these are classified under several headings below.

1. *High-pressure Jets.*

    (a) *Ordinary Glass Tubing.*

        Straight pieces of ordinary glass tubing of diameter up to about half a centimetre were found to show slight sensitivity. This did not consist of ducking, but of movements of the visible yellow portion in the upper part of the flame.

            Pressures from 5 cm. to 32 cm. of water.
            Range of frequencies 850–6300.

        Independent of whether the orifice was rough or annealed.

    (b) *Capillary Tubing.*

        Glass capillary tubes 20 cm. long and 1·3 mm. diameter were tried. These showed very slight sensitivity to the rattle of keys, but if two or more tubes were bound together so that their orifices were in one plane the sensitivity was increased. Tubes of 5 cm. and 10 cm. length were also examined with the same result.

    (c) *Drawn-out Glass Jets (Tyndall type)* (fig. 1, T).

        A large number of jets of the type used by Tyndall were examined. These had a V-shaped slit filed in the orifice, and this was then annealed to prevent cracking. Glass tubing of diameter about 1 cm. was drawn out to diameters of between 1 and 2 mm.

---

* Jordan and McClung, Proc. Roy. Soc. Canada, xviii. p. 197 (1924).

The sensitivity and performance varied considerably. Some flames increased their height when disturbed by sound ; others showed very marked forking ; others showed a very pronounced directional effect, *i. e.*, when in their most disturbed state due to sound, if they were turned through 90°, they resumed their undisturbed appearance.

The range of sensitivity varied from 500–9000 in the case of the best, down to 3000–6000 for the worst. The most effective frequency varied, being either 3300, 4600, or 5850. Some were sensitive to keys but not to any noise made by the speaker, *i. e.*, sensitive above 17,500.

(d) *Round-ended Glass Tubing (Sutherland type).*

Some of these were very sensitive. The most sensitive jet used was one of this type (fig. 1, G_1). This jet forked perfectly and had very marked directional properties. If held at the entrance of the cone of the loud-speaker a turn of 90° would cause it to drop from an undisturbed flame of 40 cm. to a forked flame 7 cm. high at the fork and 12 cm. at the tips. Another turn of 90° and it became undisturbed again. It was sensitive for frequencies between 500 to 10,000. The diameter was approximately 0·13 cm.

Other jets varied in sensitivity and range, several being insensitive in the range of the loud-speaker although sensitive to keys. In some cases an unsymmetrical flame was produced, and this showed sensitivity only in one part.

G_1 was still sensitive when the amplitude was reduced to 1/2000th of the maximum output, *i. e.*, intensity reduced to 1/4,000,000th, which was scarcely audible.

(e) *Brass Jets.*

These were of two kinds : (1) Cylindrical and conical jets of various forms designed by Professor Andrade, and (2) brass tubing closed at the top by a sheet of metal in which holes of various shapes and diameters were cut.

The jets of the first kind are shown in fig. 1, nos. W_1 to W_4. These were designed specially to see whether resonance in the orifice of the jet was a factor in determining the sensitivity :

W_1. The orifice was distinctly elliptical. Major axis ·120 cm., minor axis 0·114 cm. Most sensitive

when the minor axis was parallel to the direction of sound.

> Pressure $\triangleq$ 16·4 cm. water.
> Range 3250–18,000.
> Most effective frequency 5850.
> Slight forking.

W_2. Pressure $\triangleq$ 8 cm.   Diameter 0·160 cm.
>> Range 2300–11,700.
>> Most effective frequency 5850.
>> Very sensitive.

W_3. Pressure $\triangleq$ 7 cm.   Diameter 0·219 cm.
>> Range 900–about 10,000.
>> Most effective frequency 4600.

This jet was supplied with a tube leading into the main jet through a very small hole. No difference in sensitivity was found to occur when this was placed facing the loud-speaker or in any other position.

W_4. Pressure $\triangleq$ 36 cm.   Diameter 0·112 cm.
>> Sensitive to keys, but not within the limits of the loud-speaker (0–17,500).

The jets of the second kind (fig. 1, B) were made by soldering a thin sheet of brass across the top of a brass tube 6 cm. long and diameter 0 85 cm. In the sheet were drilled circular holes of different diameters, and in some, line slits, square holes, triangular holes, etc. were punched.
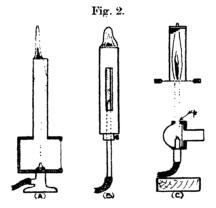
The jets with circular holes were made of different sizes in a series from nos. 52–57 (0·161 cm. to 0·110 cm.). These holes, when first made, were not polished at the edges, and it was found very difficult to get the flames to burn steadily ; some produced notes which went up and down the scale, caused originally by draught disturbance. In this state it was impossible to get some of the jets to show any sensitivity at all.

When the holes were rounded off, however, by lightly spinning a countersinking drill in them, the sensitivity appeared. The sensitivity and range varied markedly from one to the other, and no simple relation held between the pressures and the diameters of the holes or the starting frequencies, except that on the whole there was a tendency for the larger diameters to have the lower pressures and lower frequency starting-points.

This bears out the finding of Roberts [*]. By means
of a special method of Loring the holes in a sheet of
metal he succeeded in proving that the pressure for
maximum sensitivity and also for flaring decreased as
the diameter of the hole increased. But even with the
greatest care in boring the hole he never succeeded in
getting the flaring pressure the same on both sides of
the hole. It is evident that microscopic irregularities
in the construction of the jet affect the behaviour of a
stream of gas passing through it very greatly.

(f) *Sugg's Steatite Burners.*

Some of Sugg's Pinhole Steatite burners, S_1, S_2, and
S_3, were examined (fig. 1, S).

Fig. 2.

(A)   (B)   (C)

One of them (S_2) was found to be very sensitive,
while another (S_3) did not respond to any noise made
by the speaker, but was very sensitive to keys. The
orifices of these steatite burners are extremely irregular
although the insides are fairly smooth. The diameters
were 0·091 cm., 0·112 cm., and 0·069 cm. respectively.

2. *Low-pressure Jets.*

(a) *Rayleigh's Flame.*

This well-known type of flame, which is shown
diagramatically in fig. 2 (A), was examined with
regard to frequency and range. These flames can be
made very sensitive, the flame disappearing down the
tube and only returning after several seconds. They
are very sensitive to draughts, and loud sounds very

* J. H. T. Roberts, Phil. Mag. xxiii. p. 368 (1912).

easily put the flame out altogether. The actual burner used was one marketed by Messrs. Griffin and Tatlock. It was found to be sensitive to the frequencies

<div align="center">

250, 400–430, 1200–1260.

</div>

If one of these pure frequencies is maintained the flame executes a cycle of changes—disappearing into the tube, reappearing, becoming unsteady, and then disappearing again, and so on, with a period of several seconds.

(b) *Bunsen Burner.*

The ordinary Bunsen burner is obviously very much the same in construction as the Rayleigh flame, and sensitivity can sometimes be obtained, as in the Rayleigh flame, by turning down the gas pressure until the luminous flame burns lopsidedly. It can be made into a sensitive flame for low notes by attaching a diaphragm to the base of a conical sound receiver fitted to one of the air-inlet holes, any other inlet holes being tightly closed. This has been done by Mache [*].

(c) *Gauze Type.*

Jordan and McClung [†] also describe the construction of a low pressure low-frequency flame. shown in fig. 2 (C). This is similar in principle to Rayleigh's flame, except that the unlit column of gas, instead of passing through the sound-chamber into a tube, passes out through a hole, p, of the same diameter as the column, into the air, and is then lit above a gauze which is held some little distance above the top of the chamber.

A somewhat similar type has been designed by Zahradnicek [‡], fig. 2 (B). The gas passes out of a jet into a space surrounded by two concentric brass cylinders 10 cm. long and about 2 cm. in diameter. A slit in each, 5 cm. × 0·8 cm., can be varied in size by rotating one brass tube on the other, which it closely fits. At the top of the tubes is a wire grid (200 holes/cm.²). The gas is lit above the gauze, and the length of the unlit portion may be varied by sliding the jet in and out of the brass tubes. For low notes, according to the

---

[*] H. Mache, *Phys. Zeit.* xx. p. 467 (1919).
[†] *Op. cit.*
[‡] *Phys. Zeit.* xxx. p. 555 (1929).

author, this length should be about 5 cm., and for high notes about 2 cm.

A jet of this type was constructed and examined for range of sensitivity. With a distance of 7½ cm. between the jet and the gauze the range was from 1200 to 5000 ; when this was shortened to 2½ cm. the range did not commence before 3000. The sensitivity was, however, very slight, and the pressure must be adjusted very carefully. The actual range of sensitivity of the jet alone with the gas lit at the orifice was from 3850–7500.

Characteristic Behaviour of Sensitive Flames.

The behaviour of sensitive flames in general is well known. A jet of some kind with an orifice of about 1 mm. diameter is supplied with coal gas. If the pressure is increased the flame first of all burns steadily and increases in height, but a point is reached when an unsteady flickering appearance occurs, and it is in this condition that the flame exhibits sensitivity to sound. Any further increase in pressure causes the height of the flame to decrease suddenly, turbulent motion sets in, and the flame appears markedly disturbed and produces a characteristic roaring noise or "flaring." A state of turbulence can be induced by the action of sound when the flame is just on the point of flaring, and this is the cause of sensitivity. Turbulence sets in at some point in the column of the flame, and this causes the height to decrease and so exhibit the familiar "ducking" of sensitive flames. Fig. 3 (Pl. VII.) shows a flame just on the point of flaring. (Jet W₂) fig. 4 (Pl. VII.) shows the effect of shaking a bunch of keys. The height decreases from 24 cm. to 12 cm. Fig. 5 (Pl. VII.) shows the turbulent state produced by excess pressure without sound.

If instead of a noise composed of many different frequencies, a pure note is maintained, it becomes evident at once that nearly all flames show a directional effect ; as the jet is turned round the height of the flame exhibits maxima and minima, and these occur alternately along two directions which are at right angles. Further, if the positions of minimum height are examined it is found that the flame is spread out in a plane containing the axis of the jet and a line joining the jet and the loud-speaker, and the position at which this spreading occurs approaches the orifice as the amplitude increases.

This is particularly noticeable in the case of sheets of flame such as are produced by jets consisting of a straight

slit when the slit is perpendicular to the direction of propagation of the sound. Fig. 6 (Pl. VII.) shows a case of this kind. In some cases spreading may take place in two parallel planes, the flame thus behaving like two very close flames, but usually this spreading occurs in one central plane only.

Fig. 7 (Pl. VII.) shows a case of double spreading, viewed at a slight angle to the planes in which the spreading occurs ; the two sheets can be clearly distinguished towards the bottom of the flame.

The height above the orifice at which spreading occurs varies with frequency in a peculiar manner to be described later. In jets which produce a sheet of flame which is not symmetrical, being higher on one side than the other (fig. 24, Pl. X.), sensitivity may occur for different frequencies in different parts. One such jet examined was sensitive from frequencies of 700 to 1700 on one side and from 2700 to over 10,000 on the other. In special cases this spreading takes the form of a fork, and the issuing jet of flame divides into two separate jets the angle between, which increases with the amplitude of the sound (fig. 8, Pl. VII.).

In the case of flames from line jets the marked spreading or forking of the flame in the direction of propagation of the sound appears to cause the remaining parts of the flame to draw inward and coalesce, and this often causes the height of the flame to *increase* slightly when the sound occurs. The case represented in fig. 7 (Pl. VII.) shows this phenomenon, the spreading being nearly normal to the paper : the sideways contraction of the flame a short distance above the orifice which lead to the increase in height is very marked.

In some very rare cases when the jet was packed with cotton-wool and the flame was roaring, due to excess pressure, it gave out a fairly pure note. If now the frequency of the oscillator was increased gradually from zero, a very high note could be heard in the flame, whose pitch came down gradually to zero and then increased again as the frequency of the oscillator continued to rise. This note became very weak as its frequency increased and gradually became inaudible, exhibiting the characteristics of a beat note. If, however, the pitch of the oscillator was raised still further, another beat note occurred which passed through a minimum in the same manner as the first. This phenomenon was first observed with hydrogen, but was later obtained with coal-gas. In the latter case it was seen that the flame remained steadily in a fork, giving out of itself a nearly pure note of frequency

6300. If now the oscillator was started with this same frequency the fork remained undisturbed ; but if the frequency of the oscillator was either increased or decreased the arms of the fork began to close and open again in time with the beats to be expected. This of course became indistinguishable by the time that the beats became an audible note. Another vibration of the flame which gave beat notes with the oscillator occurred at a frequency of 4300, although in this case the fork was not clearly defined. A somewhat similar observation appears to have been made with a stream of ether vapour by A. T. Jones *. In general when a flame produced a nearly pure note due to excess pressure the stroboscope showed that symmetrical "bulges" starting at the jet were travelling up the flame with a frequency equal to that of the note given out. These effects, however, were very difficult to obtain and could not be repeated with any certainty.

These symmetrical swellings travelling up the flames occur with any pressure if hydrogen is used. and produce a characteristic flickering appearance. This helps to mask the effect produced by sound on the jet, and so hydrogen jets do not show great sensitivity. The swellings are always observed with coal-gas flames from jets whose diameter is greater than about half a centimetre. The well-known flickering of any form of the Bunsen flame can be shown by the stroboscope to consist of such disturbances whose wave-length seems to remain fairly constant at about 4·5 cm. and whose frequency is 3–4 a second.

This kind of disturbance can be caused in coal-gas or hydrogen streams when the orifice is less than half a centimetre by the vibrations produced by the method of the familiar singing-flame experiment in which the flame burns inside an open tube of certain length. It is only necessary to examine such flames stroboscopically to prove that this is what is occurring when the flame "sings."
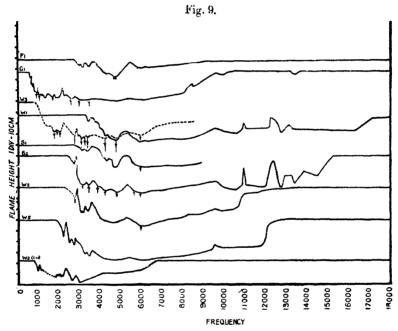
Although a sensitive flame *which is disturbed owing to the effect of sound* produces usually only a characteristic roaring noise, a note of the same pitch as that of the oscillator can be obtained if a piece of wire or other sharp obstacle is placed in the flame. The exact position is of importance and has to be found by trial In flames which fork the position extends from a point in the centre of the flame 1 cm. below the fork to points about ½ cm. up each of the branches. The effect is most marked when the direction of the wire is at

* Thesis for Degree, Clark University, Worcester, Massachusetts, 1916.

right angles to the vibration of the sound. The diameter of the wire makes very little difference.

The Effect of Frequency on the Sensitivity of Jets.

The degree of sensitivity of the flame was measured by observing the height of the flame on a centimetre scale placed near it and to one side, care being taken that its presence did not affect the behaviour of the flame by reflexion from its surface. It was found that as the oscillator was caused

Fig. 9.

to vary its frequency from zero to about 17,500 (the point at which the loud-speaker ceased to respond) the flames remained steady at first, then commenced to duck, and passed through a number of maxima and minima before becoming unresponsive again at the high frequencies.

The height of the flame was plotted against the frequency on a graph (fig. 9). Points on the graph were observed for minima and maxima, and a sufficient number in the intervals between, to show the behaviour of the flame. In the lower range of frequencies there were so many maxima and minima that these were not all measured, and only those which were most marked are shown in fig. 9. The vertical lines indicate

forking, their lengths measuring the depth of the junction of the fork below the top of the flame. Curve W_5 is for a jet exactly similar to W_2 but with the length of the narrow portion doubled (*cf.* fig. 1). The lowest curve is for jet W_2 packed up to the orifice with cotton-wool.

The results of this investigation showed :—

(1) That the different jets varied very much in regard to the range over which they were sensitive. Some begin early in the range and finish early ; some begin late and finish late. The poor jets show their lack of sensitivity by beginning late and ending early and by having much less marked maxima and minima than good jets.

(2) That provided a number of jets are all sensitive in a given range, *they all show maxima and minima at the same frequencies*, regardless of the shape of jet, the size of jet, the pressure, and the nature of the connecting tubing. Any alteration in these latter merely alters the range of the sensitivity, the sharpness of the maxima and minima, and their relative size. The most marked minima occurred at frequencies of approximately 5850, 4600, 3300, and 2400.

(3) That frequencies above those produceable by the Rice-Kellogg speaker are effective in causing disturbance in the flames. Jets were found which gave no response at all in the range 0–17,500, but which answered readily to the shaking of keys and of coins. Also some jets which were sensitive in the loud-speaker range seemed to be much more sensitive to keys, and would duck much lower when keys were sounded as well as the loud-speaker. The jet consisting of a straight slit actually *increased* its height when keys were rattled near it (see p. 174), and this was particularly noticeable when the oscillator was sounding, since for the frequencies so produced it decreased its height, as is the usual case.

It was, of course, of great importance to show that the form of the flame-height against frequency curves was a property of coal-gas jets, and not due to other causes, such as

(*a*) presence of harmonics produced by the oscillators and amplifier ;

(*b*) nature of the loud-speaker ;

(*c*) reflexion from distant parts of room, surrounding apparatus, and so on.

As regards (*a*), the behaviour of the flames was examined when the plate voltage of the oscillators and the plate voltage

and grid-bias of the amplifier were altered. No difference was observable. Duddell oscillograph records were also taken of the output of the amplifier, and the wave form proved to be a very pure sine wave up to the limit of the oscillograph (about 2000 $\sim$). Further, it is obvious that in the case of, say, the glass jet G_1, which shows many maxima and minima between 500 and 1000, the effect cannot in any case be due to harmonics lower than the 30th, since such harmonics can all be produced directly by the oscillator, and no response occurs in many cases.

To test the possibility (*b*), the Rice-Kellogg speaker was replaced by a small Stirling loud-speaker of ordinary diaphragm type, and the curve obtained showed that the behaviour of the flame was almost identical.

Finally, with regard to (*c*), the whole experiment was repeated in a different laboratory with the conditions entirely changed. The gas was supplied by a cylinder, the loud-speaker was a Brown type, the oscillator was a single LS. 5-valve, and the frequencies were measured by a bridge method. The jet used was W_3. The frequency of its maxima and minima were found to be exactly as before up to 4500, which was the limit with this particular oscillator.
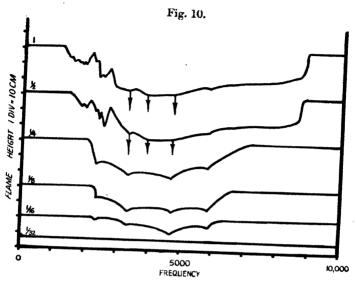
It seems therefore evident that the fact that all the different kinds of jets used showed the same flame-height against frequency curves expresses a property of gaseous jets, and not one due to causes inherent in the apparatus used.
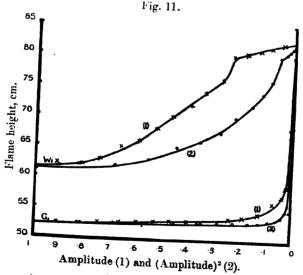
Jets of hydrogen from a cylinder were also examined. Although these flames cannot be made to show anything like the same degree of sensitiveness as coal-gas flames, nevertheless there is a small degree of " ducking," the frequencies of the minima being those most effective for the coal-gas flames, *i. e.*, 3300, 4600, 5850.

Variation of Response with Amplitude.

By means of the potentiometer tapping in the amplifier it was possible to decrease, by known fractions of the total output, the amplitude of the sound emitted by the loud-speaker. The effect of this was as would be expected : the minor fluctuation in height disappeared gradually and left only the most marked maxima and minima, viz., 2400, 3300, 4600, 5850, which also disappeared when the amplitude was decreased sufficiently. The range of sensitivity also decreased. Fig. 10 shows this effect for jet W_3, the pressure being constant at 6·7 cm. of water. When the intensity was reduced to approximately 1/1000th the jet remained undisturbed.
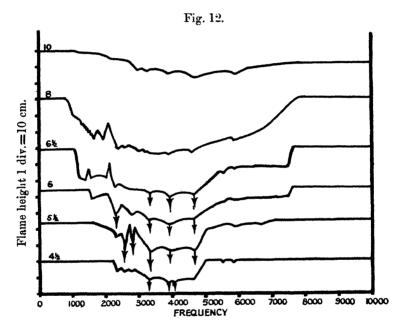
The range decreased from 1200–8900 to 2200–6300, when the amplitude was reduced to 1/16th.

Fig. 10.

Fig. 11.

Amplitude (1) and (Amplitude)² (2).

If one jet is taken and the height plotted against the amplitude for one given frequency curves such as are shown in fig. 11 are obtained. This shows the results for two jets,

N 2

W$_1$ and G$_1$, with the frequency adjusted to that for maximum sensitivity, *i. e.*, 4600 ∿. The curves marked (2) are those plotted against the amplitude squared. It will be seen on examination that there is an initial period where there is little or no response, then a period where the drop in height is very nearly proportional to the amplitude, and then a period where the height decreases very slowly, tending towards a stationary value. The initial insensitive period for the glass jet G$_1$ does not show on the scale on which fig. 11, is plotted.

Fig. 12.

Variation of Response with Pressure.
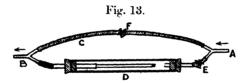
As is well known, sensitive jets show their greatest sensitiveness when just on the point of "flaring". If the pressure is now decreased or increased the response falls off; this is well illustrated by fig. 12, which shows flame height-frequency curves for jet W$_3$ for different pressures in cm. of water from 10 cm. to 4½ cm. A pressure of 8 cm. is the one for greatest sensitiveness. If the pressure is slightly in excess (10 cm.) the response is not so marked, but the range of sensitiveness extends to higher frequencies. As the pressure is reduced below 8 cm. the minor maxima and minima disappear first, leaving finally the frequencies 2400, 3300,

4600. The frequency 5850 has almost disappeared on the curve, since the range of continuous sensitivity has decreased from (800–7600) to (2200–5000). The relative importance of some maxima and minima seems to change with the pressure, *e. g.*, the minima at 2800 and the maxima on each side of it are much enhanced at a pressure of $5\frac{1}{2}$ cm. They hardly appear at all at other pressures.

Stroboscopic Examination of Smoke-jets.

In order to throw more light on the nature of the disturbance produced by sound, experiments were made with air-jets containing cigarette smoke to render them visible. The method of producing them was as follows:—Air from the large tank (pumped by the motor) was led through an arrangement of tubes shown in fig. 13.

This consisted of two glass T-pieces, A and B, connected by the rubber tubing C to act as a by-pass, and by the glass

Fig. 13.

tube D, which was about a foot long and 1 inch in diameter. Its ends were closed by rubber bungs, through which tubes were passed, one being a brass tube which acted as a cigarette holder. The cigarette was first lit and then rapidly placed in the tube D, and air allowed to flow through by opening the screw clip E, the clip F being closed. By this means a stream of air containing fine particles of smoke was obtained. The quantity of smoke could be adjusted by means of the clips E and F. Since cigarettes of ordinary length did not last sufficiently long for close examination of the jet, some cigarettes a foot long were obtained specially. It was found that the cigarettes should not be closely packed in order to give the best results, and since the density of packing varied very much in the sample tried it was important to select the cigarettes carefully first.

The jets of smoke were very unstable, and great care had to be taken to keep the space surrounding them free from draughts. The pressure was found to be much lower (1 or 2 cm. of water), and they were sensitive to notes of much lower pitch than gas-flames.

The behaviour of the smoke-jets was examined strobo-scopically. The stroboscope consisted of a brass disk radius 20 cm., with ten holes of diameter $\frac{1}{4}$ cm. The ratio of diameter of hole to opaque portion between was 1 to 7. The disk was attached to the axle of an electric motor capable of rotating at 2000 revs./min. without undue vibration. Light from a 2000 c.p. arc was focussed by condensers on a hole in the disk. Another similar hole was made in a brass plate which was held by a clamp, so that the hole was in line with the beam and close to the rotating disk. The beam was further focussed on the flame by a cylindrical lens. When the frequency of interruption of the light was that of the sound the motions of the jet could be seen with great distinctness either by reflected light or, better still, by observing in a direction opposite to that of the light and a little to one side, so as to avoid the direct glare of the lantern. There are, of course, many speeds of the motor at which the jet appears to be stationary, but vision is always clearest when the frequency of interruption coincides with that of the sound. If there is any doubt that this is the case the stroboscope can be used as a siren by blowing with a glass tube through the holes in the disk. The note heard should coincide with that of the speaker.

Photographs of the smoke-stream were taken first of all by placing the camera facing the beam from the lantern and obtaining the shadow on the plate. The smoke, however, was rarely dense enough to make this a good method, and so finally photographs were taken with scattered light by placing the camera facing the lantern but just out of the line of the main beam. Exposures of half a second were required for the stroboscopic photographs, the plates used being Ilford's Golden Iso-Zenith (speed H & D 1400).

The effect of sound on jets of cigarette smoke is shown in figs. 14 and 15 (Pl. VIII.). At a certain height above the orifice the column of smoke appears to vibrate from side to side in a direction parallel, or nearly parallel, to that of the sound, and this wave-like motion travels up the column and increases in amplitude. When the amplitude of these waves reaches a certain amount the smoke rises in a confused conical mass, the apex facing downwards. In jets, however, which show marked forking the mechanism of the process can be seen quite clearly. As the column undulates from side to side portions of approximately half a wave-length in length are broken off, and then pass on in a straight line alternately up each arm of the fork, first one to the left and then one to the right. This can be seen very clearly in fig. 15.

(Pl. VIII.). If the successive portions do not break off sharply a thin filament of smoke, extending from the top of one portion in one arm of the fork to the bottom of the portion above it in the other arm, travels up the space between the arms, causing it to have a horizontally striated appearance.

As in the case of gas-flames, the pressure must be near that of turbulent motion. If the pressure is too small the waves either do not increase in amplitude or may even decrease and die out (fig. 16 b, Pl. VIII.). If the pressure is increased the forking becomes a confused cone of smoke, the apex of which approaches the orifice of the jet. The cone has not a circular cross-section, but an elongated one, with the major axis in the direction of the sound.

As in the case of gas-flames, the height of the smoke-jets went through maxima and minima as the frequency of the oscillator was increased. The range of sensitivity extended usually from frequencies of about 80 to 900, this being, of course, very much lower than with burning gas-flames. Jets such as W_4, which, when used with gas, showed no sensitivity in the range of the loud-speaker, showed sensitivity when used with smoke in a range from 150–2900. This range included a marked minimum at 2400, a frequency which had been found very effective for gas-flames. On the whole it was found that the frequencies effective with a given jet had to be reduced about ten times if an air-stream was substituted for a burning gas-stream.

An attempt was made to see why the maxima and minima occur. The stroboscope was started, and as its rotation increased the frequency of the loud-speaker was kept in step by turning the vernier of one of the condensers. A nearly static picture of the smoke was thus obtained while the frequency increased and the maxima and minima occurred. At maxima the amplitude of the waves travelling up the stream decreased, and the point of the fork moved consequently to a point further from the orifice. *i.e.*, the stream of smoke increased in height. At minima the amplitude of the waves increased suddenly and the point of the fork moved nearer to the orifice, causing the height of the stream to decrease. But it was impossible to see any reason for the increase or decrease in amplitude, which, in most cases, occurred with the slightest turn of the vernier condenser.

The ratio of the wave-length of the undulations of the stream to its diameter varied, with different jets, from 2·8 to about 7, when the pressure was that for greatest sensitivity.

As can be seen from fig. 14 (Pl. VIII.) the amplitude of the wave in the smoke may double in one wave-length.

The wave-length in the smoke column decreases with decreasing wave-length of the sound, and also with decreasing velocity of the stream, as would be expected. For one jet (W_3) the ratio dropped from 3·7 to 2·9 on reducing the pressure slightly (figs. 16 a and 16 b, Pl. VIII.).

A series of photographs were taken as follows with one jet, a glass one of the Tyndall type (Pl. IX.) :—

Fig. 17. Stream at sensitive point but undisturbed.
„ 18. Stream disturbed by excess pressure.
„ 19. „ „ noise.
,. 20. „ „ a pure note (frequency 220).
„ 21. Case in fig. 18 examined stroboscopically
(frequency 220).
„ 22. „ fig. 19 „ „ („).
„ 23. „ fig. 20 „ „ („).

In each case the photograph was taken from a direction perpendicular to the axis of the jet and to a line joining the loud-speaker with the jet, and the line joining the V-shaped notches in the glass orifice was also perpendicular to this direction.

Fig. 17 shows how the undisturbed stream, on the point of flaring, spreads in a direction perpendicular to the line joining the notches. (The same effect is obtained with jets consisting of a slit.)

Fig. 18 shows that excess pressure caused the stream to spread at a point much nearer the orifice.

Fig. 19 was obtained by tapping on a piece of wood. The stream seems to spread outwards at a much sharper angle.

Fig. 20 shows the effect of a sound of definite frequency. Here the forking is very marked, the smoke being concentrated into the two arms, and in this case more so in one arm than the other. The frequency chosen was the one to which the stream was most sensitive (220).

Fig. 21 is a stroboscopic photograph of the condition shown in fig. 18. The stroboscope was run at the frequency to which the stream responded best (220), but no trace of periodicity can be discerned, nor was it possible to see anything but confused movements at any speed of the stroboscope. Turbulence due to excess velocity does not seem therefore to produce any definite periodicities in the motion of the stream of air.

Fig. 22, a stroboscopic photograph of disturbance produced by tapping on wood (fig. 19), only shows slight signs of periodicity, but actually these are very marked when the

stream is examined visually, although they are changing all the time, and consequently do not show well in a photograph, whose exposure is necessarily as long as half a second.

It appears that the smoke-stream selects from a noise those frequencies to which it is most sensitive.

Fig. 23 shows what is occurring in the case of a disturbance of definite frequency. This has been discussed on p. 182.

It would seem clear from this series of photographs and the observations carried out at the time that they were taken that, although the stream must be on the point of turbulence in order to be sensitive, it is not correct to say, as Tyndall did, that the effect of sound was merely to induce this state of turbulence prematurely. The turbulence due to excess velocity shows no trace of periodicity. On the other hand, the disturbance produced by sound exhibits distinct periodic sinuosities with alternate disengagement of portions of turbulence to left and to right, whether the sound is a pure note or a mixed note, the difference in the two cases being that the sinuosities are much more clearly defined for pure notes.

It is important to show that the behaviour of the stream of air is not due to the presence of particles of smoke. Smoke produced by cigarettes has been found to be composed of very fine particles which readily assume the motion of the air in which they are suspended [*]. If the smoke-stream be watched carefully as the cigarette is burnt up and for some time afterwards the number of particles decreases gradually to zero, but the sinuosities and the fork remain unchanged until the stream becomes invisible.

Further, by means of exploration with a candle-flame or other small flame in the region above an invisible air-stream it can be shown that the stream has shortened and forked when the sound is maintained.

With gas-streams the gas can be ignited above a sheet of gauze, the column below being unlit. The height of the upper burning portion indicates the sensitivity to sound of the column below. By means of screening portions of the stream from the sound it can easily be seen that it is the unlit column near the orifice which is sensitive. The frequencies to which the unlit stream responds are lower than those to which it responds when ignited, but not so low as in the case of the air-stream. The pressure for sensitivity is also lower. Sensitive flames of the type used by Jordan and McClung [†]

---

[*] E. N. da C. Andrade, Proc. Roy. Soc. A, cxxxiv. p. 445 (1931).

[†] *Op. cit.*

and by Rayleigh make use of the sensitivity of an unlit column of gas.

It seems evident therefore that the phenomena observed with columns of smoke are not due to, or affected by, the presence of fine particles.

The mechanism of the Rayleigh flame (p. 171) was examined by means of the cigarette smoke. For this purpose the brass tube which screws into the square sound-receiver with mica window was replaced by a pyrex-glass tube which rested firmly in the threaded hole and could be removed rapidly when required.

When the pressure of the smoke-stream was correctly adjusted (which requires as much care as is necessary with coal-gas) it behaved in the same manner as the gas-flame, *i.e.*, a knock on a piece of wood caused the smoke to drop within the top of the tube and, after a few seconds, recover its former position. This was due to the column shortenin and adopting the usual inverted cone appearance. If the noise was a pure note produced by the oscillator the usual wavy motion of the stream occurred, the plane of the undulations being, as usual, that which contained the direction of propagation of the sound. In either case it could be seen that when the stream was disturbed by sound there was a circulation of smoke *downwards* along the walls of the tube. This circulation is troublesome when Rayleigh's flame is used with coal-gas, as it deposits water due to combustion in the upper part of the tube on the jet below. This was observed by Rayleigh *, who got over it by coiling stout copper wire round the jet and connecting it to the hot part of the brass tube at the top.

In every case when the smoke issuing from the top "ducked," due to a note from the oscillator, it was found, by looking through the glass tube or, better, by removing this altogether, that undulations were being produced in the stream causing a certain degree of forking. Further, the pressure was just not sufficient to cause the column to break into turbulent motion, a condition for sensitivity found for all other kinds of jets.

It is quite clear therefore, that the effect of sound on a Rayleigh flame is essentially the same as in the case of ordinary jets. The important difference between Rayleigh's flame and other simple flames is that it enables the sensitiveness of an *unlit* column of gas to be detected. Such unlit columns of gas require a smaller pressure to produce turbulence, and are sensitive to lower frequencies (see p. 181).

* Proc. Roy. Inst. xv. p. 786 (1898).

The low frequency flames of Jordan and McClung * and of Zahradnicek † also make use of columns of gas which are unlit in the lower portion, which is sensitive to sound. Low pressure (and therefore low velocity) streams are very liable to disturbance from draughts, and consequently the sensitive unlit portion has to be protected by a chamber with a window of some substance which will allow the sound waves to enter. The fact that the disturbance of the column of gas is transverse shows that resonance in the tube and chamber surrounding the jet would not aid the sensitivity, but rather hinder it.

Stroboscopic Examination of Gas-jets.

The disturbance in gas-jets produced by pure notes was originally examined by means of a stroboscopic disk before the experiments with smoke-jets. It was, however, impossible to come to any definite conclusion as to what was occurring inside the flame.

With the knowledge gained from the behaviour of smoke-jets, a fresh attempt was made to see whether sinuous waves could not be detected travelling up the column of gas. Such waves were eventually found, and the difficulty of observing them explained. The pressure, and therefore the velocity, of the stream in the case of ignited gas is much higher for the sensitive condition than in the case of unlit streams such as air. Consequently the transverse effect of sound upon the stream does not in general attain such a great amplitude. Further, the outer sheath of the column is at a high temperature, and combustion is taking place within it. This appears to make it insensitive to sound ; at any rate, the wave motion that is observable takes place *inside the outer light blue sheath*, the latter remaining practically steady. The motion of the inner column would be invisible except for the fact that at its outer edge there is a yellow sheath caused by the incomplete combustion of carbon. This, of course, is surrounded on the outside by the light blue sheath, in which more vigorous combustion takes place. It is this yellow portion of the flame which, in the most favourable circumstances, shows first a wavy motion and then forking caused by alternate portions of the undulating column breaking away first on one side and then on the other. This forking does not necessarily break the outer blue sheath, and consequently the flame as a whole does not fork, but merely shortens in height and appears turbulent. In certain

* *Op. cit.* † *Op. cit.*

special cases, however, the motion of the inner column is apparently sufficient to break the outer blue sheath and cause the flame to fork. This was difficult to examine stroboscopically, since forking usually only occurs well at frequencies over one or two thousand. To observe the effects of frequencies as high as this required a very rapid rotation of the stroboscopic disk, and at high speeds a noise was produced which affected the flame considerably and prevented any clear view of the condition of the flame.

After much difficulty a photograph (fig. 28, Pl. X.) was obtained which showed the wave motion and forking of the yellow portion of a flame. In order to do this an unsymmetrical flame was used, in which the yellow portion extended much further down one side, A, than on the other, B (fig. 24, Pl. X.). B is the higher velocity side of the flame, and responds to higher frequencies than the side A. Consequently it was possible to use a frequency which produced disturbance practically entirely in the edge A, and not in the rest of the flame. And further, since the yellow portion at B was higher up than at A, it was possible to examine and photograph the portion A in the direction AA' (*i. e.*, perpendicular to the line joining speaker and jet) without being troubled by a yellow background at A', which makes observation very difficult.

A larger aluminium disk was fitted to the stroboscope, and in it were made ten holes of diameter 1 cm. equally spaced and with the ratio of opaque to open portions 7 : 1. The disk was rotated immediately in front of the camera, which had a Zeiss lens of diameter 2·2 cm. In order to get sharpness it was necessary to place a sheet of tin in front of the lens and close to the disk, with a hole in it equal in diameter to those in the disk. The photographs were taken entirely by the light given out by the flame itself, and consequently the exposure necessary was of the order of 15 sec. The stroboscope, however, would not run steadily for such a length of time, and to get over this difficulty there were obviously two methods : one was to let the stroboscope run as nearly as possible at the frequency required, and keep the waves, seen by looking at the flame through the disk, stationary by turning the vernier of one of the condensers in the oscillator, thus altering the frequency very slightly ; the other method was to keep the stroboscope constant by " braking " on the rim with the fingers. This latter method was found to be the better, although it required a good deal of practice.

Fig. 25 (Pl. X.) shows the flame in fig. 24 photographed from a direction perpendicular to that of propagation of the sound, and·shows the forking taking place at the point A due to sound of frequency 1400 ~.

Fig. 27 (Pl. X.) is a photograph taken at closer range of the same forking. This shows that the outer blue sheath of the flame is displaced slightly in the upper parts of the fork, but is otherwise undisturbed.

Fig. 26 (Pl. X.) shows the appearance of the portion of the flame shown in fig. 27, when there is no disturbance due to sound.

Fig. 28 (Pl. X.) is a photograph of the condition shown in fig. 27 viewed stroboscopically. The yellow portion of the flame enables the undulation, and then forking, of the gas-stream to be seen.

It seems therefore that the same phenomena which occur in air-streams also occur in gas-jets, although in the latter case, partly owing to the higher velocity and partly to the protecting blue sheath in which combustion is taking place, the difficulty of observation is much greater—in fact before the present investigation no record of its observation can be found.

Mathematical Considerations.

The application of hydrodynamical considerations to the problem of the stability of fluid motion in connexion with phenomena of sensitive jets was attempted by Lord Rayleigh in a series of papers [*].

Helmholtz had pointed out the possibility of the instability of a surface of separation in a non-viscous liquid where the velocity was discontinuous [†], and Rayleigh applied a method due to Kelvin [‡] in order to examine the condition of instability more closely. For the case of a cylindrical jet of fluid, of width $2l$, moving in still fluid of the same density with velocity V, and displaced in such a manner that the sinuosities of its surface are symmetrical about the axis, Rayleigh [§] shows that

$$h = \mathrm{H}e^{\pm\mu\mathrm{K}\mathrm{V}t}\cos\mathrm{K}(\mathrm{V}t - x),$$

where $h =$ amplitude of disturbance perpendicular to the jet at time t. Initially $h = \mathrm{H}\cos\mathrm{K}x$. $\mathrm{K} = 2\pi/\lambda$ and

$$\mu^2 = \mathrm{K}^2 a^2\{\log 8/\mathrm{K}a + \pi^{-\frac{1}{2}}\Gamma'(\tfrac{1}{2})\}.$$

‘Scientific Papers,’ arts. 58, 66, 144, 194, 216, 377, and 88.
† Phil. Mag. 4th ser. xxxvi. p. 337 (1868).
‡ *Loc. cit.* xlii. p. 362 (1871).
§ *Loc. cit.* vol. i. art. 58, p. 371

The case of sinuosities whose surfaces are parallel (which is the case with sensitive jets) is worked out for a jet consisting of a plane sheet of fluid. In this case $2l$ is the width of the sheet, and we then have

$$h = H\epsilon^{\pm(\sqrt{KV})KVt} \cos K(Kl \cdot Vt - x).$$

The amplitude therefore increases exponentially and disruption will occur the sooner the larger the coefficient KV. As Rayleigh points out in a further paper [*] this would lead to the conclusion that the instability would increase without limit with K ; and since $K = 2\pi/\lambda$, we should infer that the shorter the wave-length the more sensitive the jet. Experiment shows that this is not the case. The explanation of this contradiction is probably due, he suggests, to the assumption of discontinuity of velocity at the boundary, which in reality is impossible owing to viscosity. There must be a transition layer in which the velocity changes gradually, and when this layer is comparable with the wave-length of the disturbance then the solution ceases to be applicable.

Rayleigh then attempts a two-dimensional treatment of the influence of friction on stratified motion, and comes to the conclusion that, for instance, in the case of a layer of air the thickness would be $1\frac{1}{2}$ cm. at a distance from the orifice numerically equal to the velocity, however thin the layer was initially. He then goes on to attempt a solution for the case of stratification free from discontinuity of velocity, and neglecting the friction. As a result he finds that so far from instability increasing indefinitely with increasing frequency of the disturbed motion, as is the case when the transition is sudden, a diminution of the wave-length below a certain value entails an instability which gradually decreases and is finally exchanged for actual stability. For a jet of given thickness such that the velocity increases uniformly (linearly) from zero at the boundary to a maximum in the centre Rayleigh shows that there should be a maximum instability for a wave-length equal to two and a half times the thickness, and stability should set in again when the wave-length is four times the thickness. The photographs of air-jets, some of which are reproduced in this paper, show that the wave-length may be from at least three to seven times the diameter, and although there is a period of stability when the wave-length is diminished there is another disruptive period when the diminution is carried far

---

[*] 'Scientific Papers,' vol. i. art. 66, p. 474.

enough. Obviously the conditions are not so simple as Rayleigh assumes, and this is especially so in the case of gas-jets in which the sensitivity can be shown to belong to one portion of the flame only.

Rayleigh then goes on to show that if the jet is bounded by walls the motion is stable if the velocity curve is convex or concave, *i. e.*, of one curvature throughout. In a further paper * he takes a special case in which the surfaces at which the vorticity ($\frac{1}{2}dU/dy$) changes are symmetrically situated. He is then able to calculate velocity curves between whose limits the motion is unstable. Finally, Rayleigh tackled the problem of motion in two dimensions of an inviscid incompressible fluid *not* enclosed between parallel walls, but he was unable to show any sign of the amplitude of a disturbance tending to increase †. The question has also been discussed by Lord Kelvin ‡.

The essential condition of sensitivity to sound, viz., that the jet should be on the point of flaring, clearly makes any mathematical treatment very difficult, since the flow is on the point of becoming turbulent. This condition does not appear in Rayleigh's calculations, and consequently it is not surprising that his conclusions have little relation to the facts when acoustically-sensitive jets are considered. Further, the exact conditions to which Rayleigh's calculations apply are extremely difficult to gather from his papers ; even Lord Kelvin found some of them " very difficult reading, in every page, and in some ∞ly difficult §."

The Criterion for Turbulence.

Although mathematical calculations throw very little light on the nature of the instability underlying the behaviour of sensitive flames, a few general observations may be made which involve the criterion for turbulence.

First of all, there is no doubt at all that an essential condition for sensitivity is that the flame shall be on the point of " flaring," *i. e.*, that the stream is about to break up owing to turbulence of some kind. The vibrations of sound are incapable of producing a transverse oscillation of the column of gas, unless it is near the turbulence point. Consequently the initial stages of turbulence must favour the production of undulations in the column. Why this

* *Loc. cit.* iii. art. 144, p. 17.
† *Loc. cit.* iv. art. 216, p. 203.
‡ Phil. Mag. xxiv. pp. 188, 272 (1887).
§ Quoted by Rayleigh, *loc. cit.* p. 269.

should be so is not at all clear, and will be the subject of further research. If it is granted, however, that turbulence is in some way an essential to sensitivity, then by the use of Osborne Reynolds' criterion we may explain a number of facts that have been described in the preceding pages. Assuming for simplicity that the jet of gas behaves like a stream in a circular pipe, we should have for the criterion of turbulence that

$$\text{velocity} > \frac{K}{r} \cdot \frac{\eta}{\rho},$$

where K is a constant, r is the radius of the tube, η is the viscosity, and ρ is the density. For a given jet the velocity for turbulence depends only on the kinematic viscosity η/ρ. The fact that the boundary is not rigid and that the surrounding air is dragged upwards with the stream to a certain extent will make the effective value of r in the formula greater than the radius of the jet at the orifice.

Considering the radius term r first of all, it is clear that streams of small diameter can reach a greater velocity before the turbulent state is reached than streams of larger diameter. In other words. the pressure for sensitivity (*i. e.*, turbulence) will be higher the smaller the diameter of the jet. This was found to be the case. Further, it was found that for a given gas the higher velocity jets were sensitive to higher frequencies. Let us now assume that the velocity necessary for turbulence is connected in much the same way with the frequency sensitiveness when we pass from one gas to another. If now the radius is kept constant the velocity for turbulence will be greater the greater the kinematic viscosity, and, if our assumption is correct, the frequency also. We should expect then that unlit coal-gas would be sensitive to slightly higher frequencies than air, since although the ratio of the densities is 1 : 2 the ratios of the viscosities is nearer 2 : 3. This also was found to be the case (p. 185). Again, if we neglect complications arising from combustion at the outer surface only, the burning gas will have much greater kinematic viscosity, since the viscosity increases and the density decreases with temperature. If the average temperature of the flame is taken as 1500° C.[*], the ratio of the kinematic viscosity to that at 15° C. is approximately 28. The velocity for turbulence will clearly be much higher, and consequently the frequency sensitivity also. This again is what is observed. A quantitative

---

[*] A. T. Jones, *loc. cit.*

confirmation can be sought by considering water-jets in water. Here the kinematic viscosity is reduced about ten times compared with air, and if we invoke the laws of dynamical similarity, as was done by Rayleigh*, the frequency sensitivity should be reduced in the same ratio. This is well borne out by the facts :—

Most sensitive frequencies for air...... 220–700
„   „   „   „ water .. 20– 50 (Rayleigh).

It is clear, however, that simple considerations such as these only have a very subsidiary bearing on the phenomena of sensitive jets. A close examination of the photographs shown in figs. 14 and 15 (Pl. VIII.) shows that the motion of the smoke column, even before it bifurcates, is very complex. The small wisps of smoke left behind in the concave parts of the undulation, which later assume a hook-like appearance, make it very probable that the sinuosity of the column is in reality due to incipient vortices travelling alternately up the opposite sides of the column. As the vortices grow, they give a more and more hook-like appearance to the boundary of the column, until finally they separate and pass alternately up the arms of the forking stream.

There is a very close resemblance between the appearance of a column of smoke which is forking owing to the action of sound and a column of smoke from a slit which is producing edge-tones. This can be seen by comparing the diagrams given by Carrière in a paper on edge-tones † with figs. 14 and 15 (Pl. VIII.). The same hook-like appearance of the boundary occurs in the undulating column before the vortices are fully formed. At the edge the vortices separate, thus producing a fork, along the arms of which they pass alternately in a manner similar to that observed in a sensitive jet which is forking under the influence of sound. The exact mechanism of the production of edge-tones is, however, still very obscure ‡.

SUMMARY AND CONCLUSION.

The sensitivity to sound of gaseous streams issuing into air through jets of various kinds has been examined. If the size of the orifice be below about ½ mm. in diameter the stream is short and the amount of "ducking" very small.

---

* *Loc. cit.* ii. p. 273.
† *J. de Phys.* vi. p. 52 (1925).
‡ *Cf.* E. G. Richardson, "Edge-Tones," Proc. Phys. Soc. xliii. p. 397 (1931).

If the diameter of the jet exceeds about $\frac{1}{2}$ cm. the stream reaches to a great height, is very susceptible to draughts, and suffers from periodic bulbous disturbances symmetrical about the vertical axis of the jet, which travel upwards and help to mask the effect produced by sound. In between these limits all streams show some sensitivity to sound. This is always most marked when the stream is on the point of "flaring." If any roughness or obstruction in the jet causes premature "flaring," *i. e.*, turbulence at a lower velocity, then the sensitivity of the stream is markedly impaired and the range of frequencies to which it responds is lowered. If an obstruction near the orifice has the effect of splitting the column into streams of smaller diameter and higher velocity, then in this case the range of frequencies to which the flame is sensitive is displaced in the direction of greater frequency.

The position and construction of the tube supplying gas to the jet affects the sensitivity in so far as it can alter the way in which the gas streams out of the orifice. In practice the best arrangement has to be found by trial, and consequently rubber tubing serves this purpose best. If the jet contains a plug of cotton wool, the position and nature of the supply tube has no effect on the behaviour of the stream issuing from it. Taps and clips can be used provided that the gas in passing them does not produce sounds to which the stream is sensitive.

As regards the frequencies which were most effective, it was invariably found that for a given gas the frequencies producing maximum disturbance and the frequencies producing minimum disturbance were definite and did not vary with the kind of jet used : they are constants for any particular gas. The values for a hydrogen flame could not be distinguished from those for an ordinary coal-gas flame.

The *range* of frequency to which gaseous streams are sensitive varies with the gas used and with the size and nature of the jet employed. With air the range is quite low (80–900), with unlit gas somewhat higher, and with ignited coal-gas or hydrogen the range extends (with different jets) from 500 to over 18,000. The size and nature of jet affect the range by altering the velocity which leads to turbulence. If a large number of circular orifices are examined it is quite clear that the jets with high-frequency ranges are the ones where the velocity for sensitiveness is high and the ones with low-frequency sensitivity are those with low velocity. Apparent exceptions to this rule are

caused by minute irregularities in the orifice and to the position of the rubber supply tube.

The actual effect of the sound waves on a gaseous column is to cause regular undulations to proceed from the jet up the column, the upper part of the column breaking into turbulence. The wave-length of these undulations depends, as would be expected, on the velocity of the column and the frequency of the sound. The most sensitive jets are those which produce a stream which tends to break up naturally into turbulent motion in one plane rather than into turbulence symmetrical about the axis. Such jets show marked directional properties, and when the turbulent motion takes place in a plane which includes the direction of propagation of the sound wave the undulations in the lower part of the column increase to such amplitude that the stream forks. In a direction perpendicular to this the jets exhibit practically no sensitivity at all.

Although the condition of being on the point of breaking down into turbulent motion is a criterion of sensitiveness to sound for all jets, and must therefore favour the production of sinuosities in the stream, nevertheless the turbulence caused by excessive velocity does not exhibit any sinuosity or periodicity of any kind. The sound does not, as has been generally assumed, precipitate the state of turbulence into which the stream is about to fall—it produces a state of periodic disturbance which is quite distinct.

It is hoped that further research will enable the effect of sound on the motion of a gaseous column to be observed in greater detail, thereby not only throwing more light on the nature of the instability underlying the phenomenon of sensitive flames, but also perhaps on what appears to be an allied phenomenon, that of the production of edge-tones.
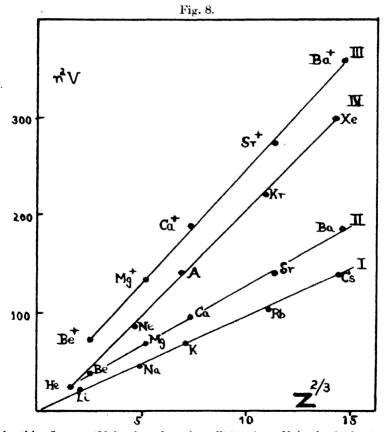
XIV. *The Electronic Energy Levels of the Elements with special reference to their Connexion with the Sizes and Electronic States of Atoms in Metallic Crystals. A Correction.*

To the Editors of the Philosophical Magazine.

GENTLEMEN,—

IN my paper, which was published under the above title in volume xi. of your Journal, some errors occur in fig. 8 on page 671. The numbers given in Table IV. below

Fig. 8.

In this figure n^2V is plotted against $Z^{2/3}$, where V is the ionization potential necessary to remove an electron of quantum number n. The curves marked I and II refer to the first ionization potentials of the alkali and alkaline earth sub-groups, whilst curve III refers to the second ionization potential of the alkaline earth group, and curve IV to the first ionization potential of the rare gas group. The data are given in Table IV.

this figure are correct, except for a misprint in the case of Krypton for which $Z^{2/3}$ equals 10·9 and not 13·9 as printed. In the drawing of the diagram some mistakes appear to have been made, and I can only suggest that the paper must have slipped when the diagrams were transferred from squared paper to Bristol board.

These mistakes are corrected in the diagram printed herewith, and it will be seen that they in no way vitiate the general conclusion of an approximately linear relation between n^2V and $Z^{2/3}$. When the corrections are made it will be found that the "fit" of the points to the best straight lines is slightly worse for line III. but equally good or even better in lines I., II., and IV. The original figure can easily be corrected by means of the data given in Table IV. on page 671, and I can only apologize for any confusion which may have been caused by my not noticing such obvious errors when correcting the proofs.

<div align="right">Yours faithfully,
W. HUME-ROTHERY.</div>

XV. *Notices respecting New Books.*

Past Years: an Autobiography. By Sir OLIVER LODGE. [Pp. 364, with portraits.] (London: Hodder and Stoughton, 1931. Price 20s. net.)

THIS is a volume of reminiscences rather than an autobiography, because it does not preserve strict historical order, but is divided into sections between which there is considerable overlapping. This makes it difficult sometimes to picture the precise order of development. The final impression produced is that of a man with many interests. The main one no doubt has been Natural Philosophy, obtained first by devouring Brewer's 'Child's Guide to Knowledge,' and by watching steam-engines, and from the tuition, by an aunt, in Astronomy. He learned nothing of science at school, and on leaving he assisted his father in business in the Potteries. A visit to an aunt in London forms a turning-point in his life; she encouraged him to attend lectures, including some by Tennant at King's College on Geology, who gave him a ticket for a course on Heat by Tyndall illustrated by a great number of experiments. These were an "eye-opener," and he absorbed the course eagerly. He attended others on various subjects at University and King's Colleges, including one by Daniell, and he at once began making experiments at home and devouring Smiles' 'Self Help' and encyclopædias; and going in for Science and Art examinations, studying Chemistry with

Frankland (or his assistant, Valentine), and, a little later, coming under the influence of Carey Foster, Clifford, and Henrici; teaching Mathematics, Physics, and Chemistry, and taking degrees.

Prior to (and leading up to) some of these events (while travelling for his father) he had attended the Bradford meeting of the British Association (1873). In Section A there were H. J. S. Smith and Glaisher ; Clerk Maxwell lectured on Molecules and W. C. Williamson on Coal Plants. The whole meeting was an experience never to be forgotten, and he never failed to attend the annual meeting until the Association went to South Africa in 1905. The Bradford meeting was the means of him breaking away from business. Soon afterwards his own publishing of original work began.

His first (and only) Professorship began in 1881 at Liverpool in the newly founded University College, and lasted till 1900, when he was appointed Principal at Birmingham. His laboratory in Liverpool was in an old building. "There was nothing sacred about the walls." They could be plugged and pulled about and holes cut in them wherever wanted. It was here that Lodge's main experimental work was done.

I first saw Lodge at a soiree, in connexion with the newly founded University College at Liverpool, somewhere about 1885. He there showed his fog-clearing experiment—in a bell-jar (p. 180). It was never a success on a large scale, but he and two of his sons have turned it to good use in connexion with smoke-dust deposition in certain factory processes (pp. 180, 248). Of his research work on oscillatory electric discharges I have a closer acquaintance. He scarcely emphasizes enough the meagre provisions at Liverpool for research. This work was largely done in the Physics Theatre, which was used for Junior as well as Senior Lectures. The lecture table had to be cleared as much as possible for these important events, research apparatus being pushed to one side. The room was surrounded by wires (stretched on posts) on which electric waves could be excited. This was all to the good so far as higher lectures were concerned, because an experimental discovery could be made on one day and shown to honours students the following day without much trouble. Probably no senior students have ever been more fortunate in that respect. They saw most of his earlier experiments (described in Chap. XVII.) "hot from the furnace" in 1888–1890.

He says little about his routine teaching. He probably had too much of it to be able to regard it with enthusiasm when there were so many more important things to do ; yet he is a born expositor, whether it be in a Junior Lecture or a popular lecture, or in summing up discussions such as that on the Universe at the recent meeting of the British Association. He knows how to supply the element of surprise. I have heard him at the Royal Institution emphasizing the need of an Æther by means of an experiment. " I wave this rod over the weight on the table ; you

do not expect to see it move." "But it does," he added, as the weight rose, lifted by an invisible connecting thread.

It is impossible in this place to detail all the phases of his active life. One, however, must be briefly mentioned. A student in his Matriculation Mechanics class—Edmund Gurney—introduced him to F. W. H. Myers.

Through Myers and Gurney, and also Barrett of Dublin, he became interested in investigations on psychical matters. The result is recorded in Chapters XXII.–XXIV. Physicists may regret that he was thus distracted from his physical investigations. On the other hand, others may rejoice that one so thoroughly acquainted with physical methods should approach psychical investigations in a sympathetic spirit. These enquiries lie outside the scope of this Journal.

Lodge has always been in favour of the use of models in explaining physical phenomena. "The abstract method of treatment at present in vogue probably represents a phase through which science has to go. It is being conducted through the haze with great ability; but in time, I believe, it will emerge on the other side and become intelligible once more, with an added perception of reality and a clearer conception of its working."

We have said nothing about the personal relations with his family and with others. The account of these fills a considerable part of the volume. The picture drawn is a very attractive one.

Dielectric Constant and Molecular Structure. By C. P. SMYTH. (The Chemical Catalog Company, New York, 1930. 4 dollars.)

THIS book is an American Chemical Society Monograph, issued by the Chemical Catalog Company of New York. By arrangement with the Inter-allied Conference of Pure and Applied Chemistry which met in London and Brussels in July 1919, the American Chemical Society undertook the production and publication of Scientific and Technologic Monographs on chemical subjects, and a long series of important publications have already appeared.

In this volume the author succeeds in correlating and organizing the relevant body of facts and the theories in terms of which they are interpreted. The book is noteworthy for the masterly way in which these theories are explained and critically examined. The summary of literature and the account of the methods of investigation cannot but be of service to those specially interested in this rapidly growing subject.

Mathematics. By B. B. LOW. (Longmans, Green and Co., 1931. Price 12*s.* 6*d.*)

THIS is a text-book designed for the use of those studying engineering or chemistry. It covers the elements of trigonometry, coordinate geometry, differential and integral calculus, and differential equations. The treatment throughout is elementary and adequate for its purpose. Mathematical tables are included.

Operational Methods in Mathematical Physics. By HAROLD JEFFREYS, F.R.S. (Cambridge Tracts in Mathematics and Mathematical Physics, No. 23.) Second Edition. (Cambridge University Press, 1931. Price 6s. 6d.)

IT is gratifying to see that this excellent Tract, first published in 1927, has already run into a second edition. There are few changes : the chapter on Bessel Functions has been re-written, and a discussion of the transmission of a simple type of telegraphic signal along a cable has been added. It remains only to repeat that this Tract can be thoroughly recommended to those who have to do with the differential equations of physics.

James Clerk Maxwell : a Commemoration Volume, 1831–1931. [Pp. 146 ; two portraits.] (Cambridge University Press, 1931. Price 6s. net.)

THIS commemoration volume is a sheer delight. It records why representatives of many nations assembled at Cambridge to celebrate the centenary of Maxwell's birth. It is introduced by a biographical essay by Sir J. J. Thomson, and followed by essays by Max Planck, Albert Einstein, Sir J. Larmor, Sir James Jeans, William Garnett, Sir Ambrose Fleming, Sir Oliver Lodge, Sir Richard Glazebrook, and Sir Horace Lamb. Garnett was the first Demonstrator in the newly opened Cavendish Laboratory ; Fleming and Glazebrook were amongst the early workers there, and Lamb attended some of Maxwell's lectures. The book is consequently punctuated with personal touches. Max Planck deals with his influence on theoretical physics in Germany and Einstein on his influence on the development of the conception of physical reality. Garnett, Fleming, and Glazebrook show most interest in the laboratory work. Lodge describes how Maxwell's speculations on electromagnetic waves led up through Hertz and his own experiments to their experimental production, and ultimately through Marconi and others to wireless telegraphy.

The book should be in the hands of every physicist and physical student.
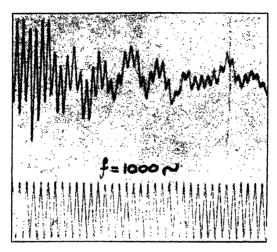
The Mysterious Universe. By Sir JAMES JEANS, F.R.S. [Pp. 142.] (Cambridge University Press. Price 2s.)

THIS is a revised edition of a book the sale of which has run into six figures. It is not a mere reprint. The first four chapters have been brought up to date and any ambiguities detected have been removed. It is a book which everyone should read whether he agrees with the point of view taken or not. It will show him the direction in which speculative scientific thought is tending at the present time.
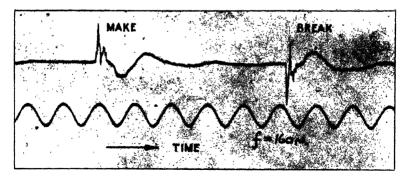
The book has not only been improved but its price is also less.

The Editors do not hold themselves responsible for the views expressed by their correspondents.

FIG. 7.

$f = 1000 \sim$
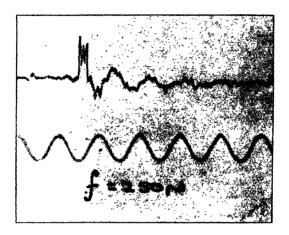
Impulse record of acoustic output from reed-driven paper disk. There are two main oscillations (1) 260 cycles, (2) 1200 cycles which correspond to the frequencies found from the sand-patterns of fig. 6.

FIG. 19.

MAKE   BREAK

TIME $f = 160 \sim$
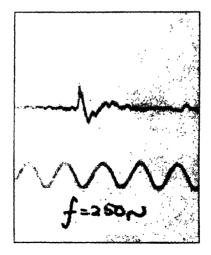
Impulse record of permanent magnet commercial reproducer with leather surround and diaphragm 7·5 cm. radius. The diaphragm oscillates on the surround at 80 cycles per second, since the magnetic field is inadequate to overcome the strong control thereof.

Fig. 15 *a.*
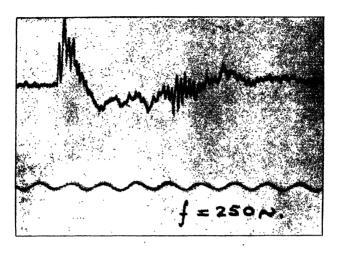
Impulse record of W. E. Co. 555 W. moving-coil receiver without horn.

Fig. 15 *b.*
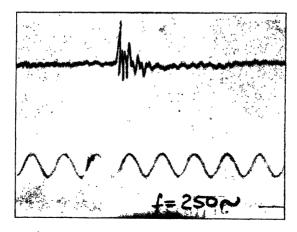
As at fig. 15 *a*, with straight exponential horn 5 feet long.
The damping effect of the horn is evident.

Fig. 16a.
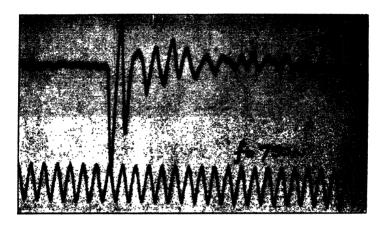
Impulse record of standard coil-driven diaphragm with tight rubber
surround.   The 33 ～ oscillation is the diaphragm moving as a
whole on the surround. The 200 ～ oscillation is due to the
surround per se, whilst the 2000 ～ oscillation is the second
symmetrical mode of the diaphragm. The coil (40 turns) was
transformer coupled, but the e.m. damping was reduced owing
to the field being 0·6 its normal value.

Fig. 16b.
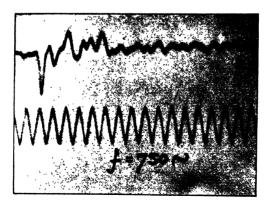
Impulse record as at fig. 16a, after removal of rubber surround.   Only
the 2000 ～ oscillation due to the main symmetrical mode remains.

Fig. 17 a.
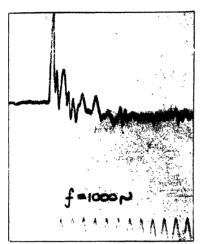
Impulse record of free-edge coil-driven paper diaphragm 16·7 cm. radius, apical angle 160°, taken with microphone on axis at a distance of 23 cm. from mouth of diaphragm. The natural frequency is that of the second symmetrical mode.

Fig. 17 b.
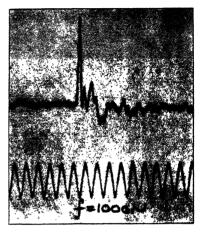
As at fig. 17 a, but microphone 25 cm. away from axis.

Fig. 18 *a*.

Fig. 18 *b*.
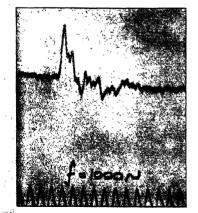
Impulse record of diaphragm of fig. 4 taken with microphone on axis at a distance of 23 cm. from mouth of cone. The motion of the diaphragm on the surround ($f = 187 \sim$) and of the surround *per se* ($129 \cdot 5 \sim$) is aperiodic. The symmetrical mode recorded is about 2600 cycles per second.
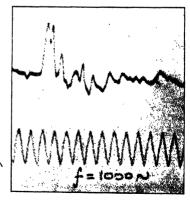
As at fig. 18 *a*. but microphone 70 cm. from mouth of cone

Fig. 18 *c*.

Fig. 18 *d*.

As at fig. 18 *a*, but microphone 25 cm. away from axis.

As at fig. 18 *a*, but microphone 28 cm. in front and 40 cm. away from axis.

FIG. 1.   FIG. 2.   FIG. 3.
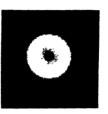
1 13·5 *h-p.*   1 6·2 *h-p.*   1/3·5 *h-p.*
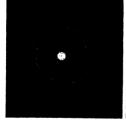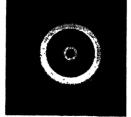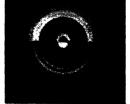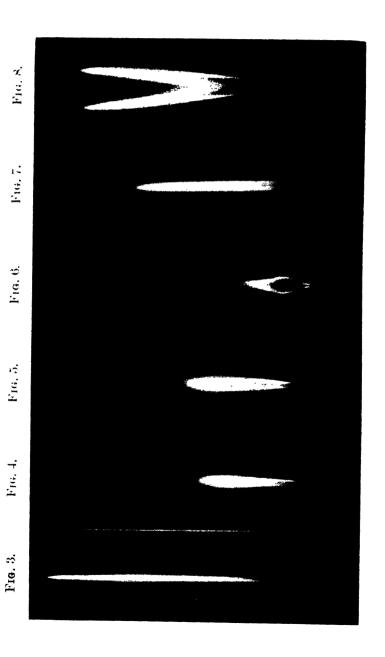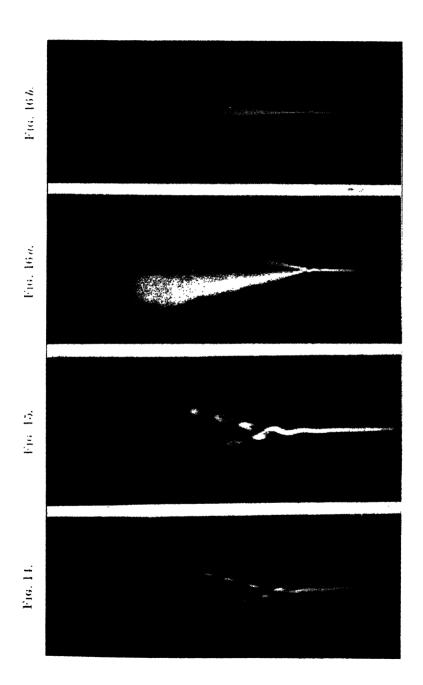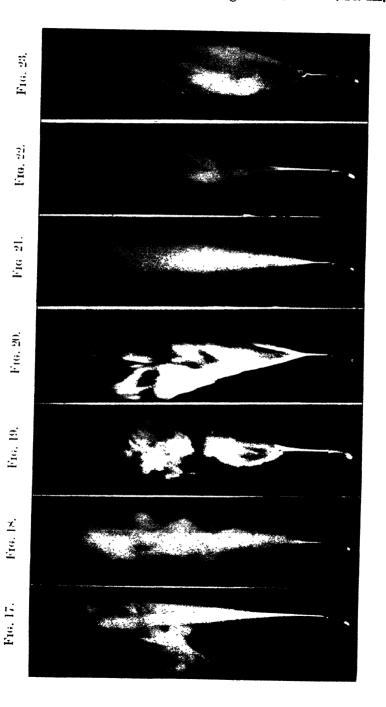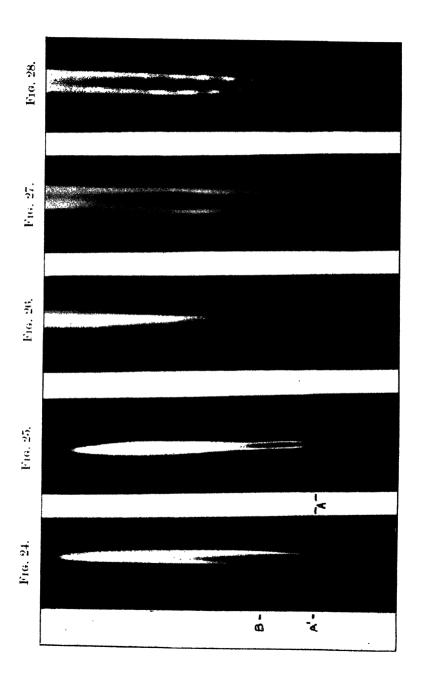
FIG. 4.   FIG. 5.   FIG. 6.

½ *h p.*   1 *h p.*   1½ *h-p.*

FIG. 7.   FIG. 8.   FIG. 9.

½ *h-p.*   1 *h p.*   1½ *h-p.*

FIG. 10.   FIG. 11.

2 *h-p.*   2 and ½ *h-p.*

Fig. 8.　Fig. 7.　Fig. 6.　Fig. 5.　Fig. 4.　Fig. 3.

Fig. 16 b.

Fig. 16 a.

Fig. 15.

Fig. 14.

BROWN.

Phil. Mag. Ser. 7, Vol. 13, Pl. IX.

Fig. 23.

Fig. 22.

Fig. 21.

Fig. 20.

Fig. 19.

Fig. 18.

Fig. 17.

Brown.

Phil. Mag. Ser. 7, Vol. 13, Pl. X.

FIG. 28.

FIG. 27.

FIG. 26.

FIG. 25.

FIG. 24.

XVI. *The Hall Effect and other Physical Properties of the Copper-Cadmium Series of Alloys.* By Wallace Richards, *M.Sc.,* and Prof. E. J. Evans, *D.Sc., Physics Department, University College of Swansea* *.

Introduction.

THE present investigation is a continuation of the experiments on the Hall effects and other physical properties of binary alloys, carried out at the Physics Department of the University College of Swansea.

In recent years much attention has been paid to theories of electrical conduction in metals, but little progress has been made in their application to alloys. In order to test such theories it is essential in the first place to carry out measurements of the various galvanomagnetic and electrical properties on the same specimen of a pure alloy. In addition, if the measurements are to be of real value the alloys must be in a definite reproduceable state, which can only be realized by annealing them at the correct temperatures. Adequate data for this purpose is usually obtained from a careful study of the equilibrium

* Communicated by the Authors.
† Stephens and Evans, Phil. Mag. (Jan. 1929) ; Stephens, Phil. Mag. (Sept. 1929).

diagram of the binary system under investigation. The experimental results obtained in investigations carried out on the various physical properties of alloys can then be examined in relation to the appropriate equilibrium diagram. With these objects in view the present investigation dealing with the Hall effect and other physical properties of the copper-cadmium series of alloys were undertaken.

The nature of the curves showing the variation of any physical property of an alloy with composition depends largely on the constituents of the alloy. In some cases the curve is continuous, but in others it shows at definite compositions singular points indicating the probable presence of intermetallic compounds at these compositions.

The results are rendered more valuable when the structures of the alloys have also been determined by X-rays, as the various physical properties can then be correlated with known changes in the arrangements and distances apart of the atoms in the alloy. Sahmen*, who examined the equilibrium diagram of the copper-cadmium system, gave two compounds corresponding to Cu_2Cd and Cu_2Cd_3, but Jenkins and Hanson † in a later investigation found evidence for four compounds corresponding to Cu_2Cd, Cu_4Cd_3, Cu_2Cd_3, and $CuCd_3$. Other investigations dealing with the physical properties considered in this paper are those of Bornemann and Wagenmann ‡ on the resistivities of the copper-cadmium alloys at high temperatures, and of Budgen ‖ on the densities of the alloys at the copper end of the series.

In the present research the Hall coefficients, the electrical resistivities, the temperature coefficients of resistance, the thermoelectric powers, the specific heats, and the densities of the copper-cadmium alloys of various compositions have been determined.

The experimental results obtained for the different physical properties will be compared with one another and considered in relation to the equilibrium diagram (fig. 1).

* R. Sahmen, *Zeitschr. Anorg. Chemie*, xlix. pp. 301-310 (May 31, 1906).
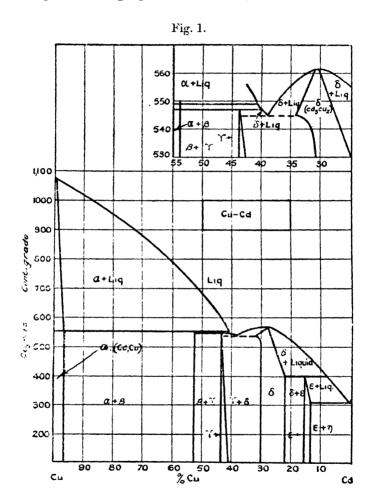
† Jenkins and Hanson, Journ. Inst. Metals, xxxi. pp. 257-270 (1924).

‡ 'Ferrum,' ii. p. 289 (1914).

‖ Budgen, 'Cadmium and its Alloys,' pp. 135-142.

Preparation and Annealing of the Alloys.

The copper-cadmium series of alloys used in this investigation was prepared in the Physical and Metallur-

Fig. 1.

gical Departments of the University College of Swansea. The copper used in their preparation was of electrolytic origin, and the cadmium, which contained 0·2 per cent. impurities, was free from iron, arsenic, and antimony. Great care was taken in the casting of the plates to prevent the formation of cracks and blow-holes.

The alloys were annealed at temperatures ascertained from the equilibrium diagram of Jenkins and Hanson * in an electric furnace, which was evacuated to a pressure of 0·01 mm. of mercury. The temperatures of the furnace were measured by means of a copper-nickel nickel-chrome couple, which had been carefully calibrated in the usual manner.

The alloys were slowly heated up to their annealing temperatures, and maintained at within a few degrees of these temperatures for periods of forty-eight hours. After each period of annealing the furnace was slowly cooled to room-temperature, and the resistivities of the alloys measured at room-temperature. This process was repeated until subsequent annealing produced no further change in the resistivities. The alloys were then considered to have reached their final state.

A great deal of attention was paid to annealing, since such accidental factors as casting temperature, rate of cooling, and composition of the mould affect the properties of the alloys. The importance of careful annealing is clearly brought out in the investigation of Jenkins and Hanson † on the Cu–Cd equilibrium diagram. They found from the study of the microstructure of the alloys that the complete γ phase could only be obtained by continuous annealing for eight days. In the present experiments the annealing of the alloys containing from 36 to 44 per cent. of copper was carried on continuously for a week, and altogether for a period of three weeks.

Analysis of the Alloys.

The percentage of copper contained in each alloy was determined by a volumetric method, and the mean of three determinations taken. The percentage of cadmium in each alloy was calculated by difference. The composition and annealing temperatures of the various alloys are given in Table I.

Measurement of Resistance.

The alloy plates were fixed across two knife edges attached to a wooden block supported on an iron base,

---

* Jenkins and Hanson, *loc. cit.*
† *Loc. cit.*

and the resistance between the knife edges was measured by a Kelvin bridge. The apparatus supporting the plates was contained in an iron box, which could be filled with ice shavings for the determination of the resistance of the plate at 0° C., and through which steam

TABLE I.

Composition and Annealing Temperatures of the Alloys.

Composition of alloys by weight.		Annealing temperatures of the alloys in degrees Centigrade.
Per cent. of copper.	Per cent. of cadmium.	
0·0	100·0	280
1·2	98·8	,,
7·0	93·0	.,
13·3	86·7	,,
16·5	83·5	350
18·0	82·0	.,
18·6	81·4	,,
20·9	79·1	.,
22·8	77·2	,,
24·7	75·3	,,
25·6	74·4	.,
27·9	72·1	450
28·9	71·1	.,
30·5	69·5	,,
31·4	68·6	,,
35·8	64·2	,,
39·3	60·7	,.
42·5	57·5	,.
44·4	55·6	,,
47·7	52·3	,,
54·2	45·8	..
63·4	36·6	500
78·5	21·5	.
93·8	6·2	.
100·0	0·0	,,

could be passed for measurements of resistance at temperatures in the neighbourhood of 100° C.

Satisfactory determinations of the resistivities of the alloys involve accurate measurements of the dimensions of the plates, and it was for this reason that the plates after preparation were rubbed down with emery paper until their dimensions were very nearly uniform. In these measurments special attention was paid to the accurate determination of the thickness of each plate, as this reading involved the greatest possibility of error. The

first set of measurements was carried out with a screw-gauge, and the mean of many readings taken.   In the second set of measurements the volume of the plate was accurately determined by weighing it in air and water, and, knowing its area, its thickness could be calculated.
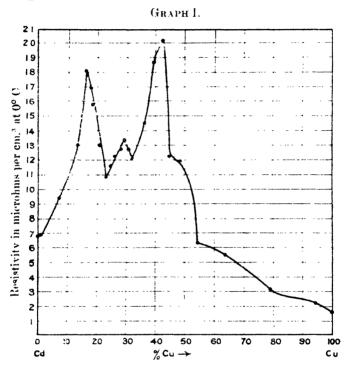
TABLE II.

Resistivities of the Alloys.

Percentage composition by weight.		Resistivities before annealing in microhms per cm.^{3} at 0° C.	Resistivities after annealing in microhms per cm.^{3} at 0° C.
Per cent. of copper.	Per cent. of cadmium.		
0·0	100·0	6·89	6·83
1·2	98·8	7·05	6·94
7·0	93·0	9·72	9·45
13·3	86·7	12·95	12·99
16·5	83·5	18·24	18·16
18·0	82·0	16·85	16·97
18·6	81·4	15·91	15·85
20·9	79·1	13·32	13·02
22·8	77·2	11·05	10·81
24·7	75·3	11·71	11·60
25·6	74·4	12·28	12·23
27·9	72·1	13·13	12·75
28·9	71·1	13·75	13·38
30·5	69·5	13·20	12·74
31·4	68·6	12·14	12·08
35·8	64·2	13·11	14·57
39·3	60·7	15·31	18·72
42·5	57·5	13·48	20·21
44·4	55·6	12·57	12·25
47·7	52·3	11·56	11·83
54·2	45·8	6·62	6·30
63·4	36·6	5·68	5·45
78·5	21·5	3·21	3·10
93·8	6·2	2·24	2·20
100·0	0·0	1·56	1·56

The values of the thickness of a plate determined by the two methods agreed to within 0·02 per cent.

The presence of serious defects in the plates, such as cracks or blow-holes, could be detected by measuring the resistance of different portions of the plate.   Although in nearly all cases the results were very consistent, it was found necessary in a few cases to discard the plates and recast new ones of the same composition.   The resistances of all the alloy plates were carefully measured

at the temperature of melting ice, and the resistivities of the alloys of various compositions calculated from the dimensions of the plates. The values of the resistivities of the various alloys in the annealed state at 0° C. are given in Table II., and, taking all factors into consideration, it is estimated that on the average the results are correct to one-third per cent. The results are plotted in Graph I.

GRAPH I.

Temperature Coefficient of Resistance.

The mean temperature coefficients of resistance of the various alloys over the range from 0° C. to about 100° C. were determined by measuring the resistances of the plates at the temperatures of ice and steam respectively. The accuracy of these determinations is not affected by the dimensions of the plates. The values of the temperature coefficients of the annealed alloys are given in Table III., and it is considered that on the average they are correct to within one-half per cent. The results are plotted in Graph II.

Thermoelectric Power of the Alloys.
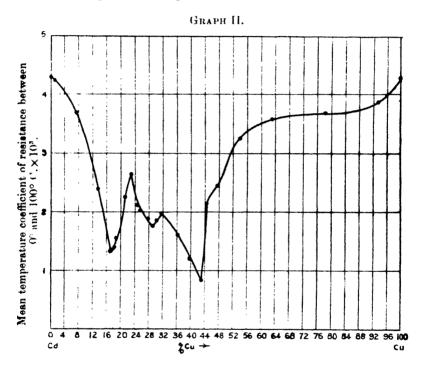
The thermoelectromotive forces of the alloys were determined with respect to copper leads clamped to the ends of the plates. The ends were jacketed, one being maintained at the temperature of steam, and the other at the temperature of running tap-water. The electro-

TABLE III.

Temperature Coefficient of Resistance of the Alloys.

Percentage composition by weight.		Mean temperature coefficient of resistance between 0 C. and 100 C. $\times 10^4$.
Per cent. Cu.	Per cent. Cd.	
0·0	100·0	42·9
1·2	98·8	42·5
7·0	93·0	37·1
13·3	86·7	24·1
16·5	83·5	13·5
18·0	82·0	13·8
18·6	81·4	15·7
20·9	79·1	22·7
22·8	77·2	26·8
24·7	75·3	21·4
25·6	74·4	20·5
27·9	72·1	19·0
28·9	71·1	17·8
30·5	69·5	18·7
31·4	68·6	19·8
35·8	64·2	15·9
39·3	60·7	12·1
42·5	57·5	8·2
44·4	55·6	21·6
47·7	52·3	24·7
54·2	45·8	32·6
63·4	36·6	35·8
78·5	21·5	37·0
93·8	6·2	39·1
100·0	0·0	43·1

motive forces of the various alloys with respect to the copper wire employed were measured over this range of temperature by means of a Tinsley vernier potentiometer in conjunction with a Weston standard cadmium cell. The mercury thermometer employed in the determination of the temperature of the cold junction was calibrated by comparing its readings with that of an accurate mercury thermometer provided with an N.P.L. certificate. Special experiments were also carried out

to determine whether the thermoelectric powers of the copper-cadmium alloys with respect to the copper wire were constant over the temperature range employed. For this purpose the temperature of the hot junction was varied by passing into the jacket a stream of water of known temperature from a Davis' constant-temperature apparatus. The experimental results showed that the thermoelectric power was constant to within 0·2 per cent. as the temperature range was varied, and it was concluded

GRAPH II.

that the thermoelectromotive force varied linearly with the temperature difference over the range from about 15° C. to 100° C.

As the thermoelectric power had been measured with respect to copper wire, which was not pure, it was decided to measure the thermoelectric power of the latter with respect to copper foil of electrolytic origin, and also with respect to pure lead. The values of the thermoelectric powers of the various alloys with respect to pure copper and pure lead were then determined by applying corrections to the experimental values. The mean

values of the thermoelectric powers of the various alloys with respect to pure copper and pure lead were then plotted with respect to composition, and the results are shown in Graph III. The values are given in Table IV., and it is estimated that, on the average they are correct to one-third per cent.

TABLE IV.

Mean Thermoelectric Power of the Alloys between 10° and 100° C. with respect to pure Lead and pure Copper.

Composition of alloy by weight.		Thermoelectric power with respect to Cu in microvolts per degree Centigrade.	Thermoelectric power with respect to Pb in microvolts per degree Centigrade.
Per cent. Cu.	Per cent. Cd.		
0·0	100·0	1·69	4·84
1·2	98·8	1·78	4·93
7·0	93·0	0·37	3·52
13·3	86·7	— 1·03	2·12
16·5	83·5	— 1·65	1·50
18·0	82·0	— 0·41	2·74
18·6	81·4	— 0·37	2·78
20·9	79·1	0·82	3·97
22·8	77·2	1·41	4·66
24·7	75·3	— 1·73	1·42
25·6	74·4	— 2·24	0·91
27·9	72·1	— 2·85	0·30
28·9	71·1	— 3·28	— 0·13
30·5	69·5	— 2·03	1·12
31·4	68·6	— 0·47	2·68
35·8	64·2	9·98	13·13
39·3	60·7	13·42	16·57
42·5	57·5	17·71	20·86
44·4	55·6	11·89	15·04
47·7	52·3	10·80	13·95
54·2	45·8	5·02	8·17
63·4	36·6	4·32	7·47
78·5	21·5	1·72	4·87
93·8	6·2	0·23	3·38
100·0	0	0·00	3·15
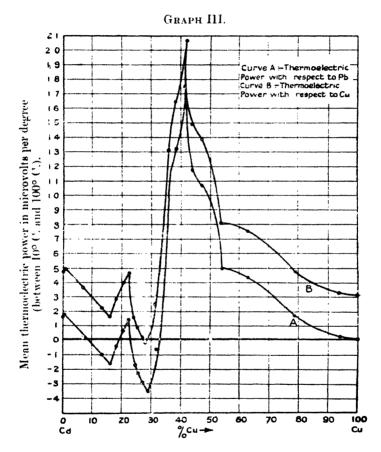
The Hall Effect of the Alloys.

When a metal plate conveying an electric current is placed in a magnetic field so that the lines of force are normal to the conducting plate and to the direction of flow of the electric current a transverse galvano-magnetic potential difference, known as the Hall effect, is set up between the edges of the plate.

It has been experimentally proved that for a given metal the Hall potential difference is given by the formula

$$E = \frac{R.H.I}{d},$$

where H is the magnetic field in gauss, I the current in absolute units, d the thickness of the plate in centimetres, and R the Hall coefficient.

GRAPH III.

The coefficient R depends on the temperature, and for some metals on the intensity of the magnetic field as well.
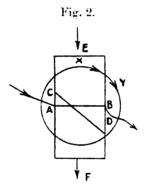
According to Ettingshausen and Nernst * the magnitude of the Hall coefficient depends to a certain extent on the length of the plates. They found during their investigations of the Hall effect in bismuth that the effect was less

* *Zeit. Phys. Chem.* ii. p. 104 (1888).

in short plates, and advocated the use of plates in which the ratio of the length to the breadth was at least 3 : 2. In the present investigation of the Hall coefficients of the copper-cadmium alloys the ratio of the length to the breadth of each plate was 5 : 1.

The Hall effect may be positive or negative, the sign differing for various metals. The convention can be readily understood from the following diagram (fig. 2) :—

The rectangle X represents the plate, and the circle Y with the arrowheads indicating the direction of the current in the electromagnet represents the magnetic field. The direction of the primary current is given by EF, the position of the equipotential line before the application of the field by AB, and the position of this equipotential

Fig. 2.

line when the field is applied by CD. If the equipotential line AB is rotated in the direction of the current in the electromagnet the effect is said to be positive, and if the equipotential line is rotated in the opposite direction the effect is said to be negative. In the present experiments the sign of the effect is found by comparison with a plate of electrolytic copper. The Hall coefficients of both copper and cadmium are small and of opposite sign, the coefficient of copper being negative and of cadmium positive. The sign of the coefficient of the intervening alloys are either positive or negative, according to the composition.

Since the Hall coefficients are small a very sensitive Paschen galvanometer was used to measure them. The galvanometer was protected from external fields by a double shield of soft iron. The instrument was mounted

on a concrete pillar built into the foundations of the laboratory and situated at a distance of about 8 metres from the powerful circular electromagnet, which had been rotated into such a position that its effect on the galvanometer was at a minimum. The pole pieces of the electromagnet were of circular cross-section, having a diameter of 9 cm., and the magnetic field between them was practically uniform over the air-gap of 1·5 cm.

The alloy under investigation was rigidly fixed in an upright wooden stand between the poles of the magnet by means of two brass clamps, which also served as leads for the plate current. The wooden frame also carried two secondary electrodes consisting of spring metallic contacts mounted on ebonite supports.

The secondary electrodes could be moved along the edges of the plate by means of two fine screws, and were connected to the galvanometer by means of well insulated flexible leads of measured resistance. Experience showed that very minute movements of the flexible leads, due to air currents and accidental vibrations, produced small induced currents in the delicate Paschen galvanometer, and, as a consequence, it was necessary to keep the leads as taut as possible, especially the portion near the electro-magnet.

In order to measure the Hall potential difference it was first necessary to set the secondary electrodes along an equipotential line. This was accomplished by adjusting the screws controlling the movement of the secondary electrodes until on reversing the current through the plate no deflexion of the galvanometer was produced. When the electromagnet was excited and the secondary circuit closed a deflexion was produced in the galvanometer due to the Hall potential difference between the edges of the plate. After the spot of light had come to rest the deflexion on reversal of the plate current was taken and recorded. The plate current was reversed several times, and the mean value of the deflexion taken. This reversal of the plate current eliminated any error in the setting of the secondary electrodes on an equipotential line, and also the potential difference set up at the edges of the plate, if there is a flow of heat in a given direction along the plate (Nernst effect). The galvanometer circuit was then broken, and after the magnetic field had been reversed a second series of readings was

obtained. The field was then re-established in its original direction, and the procedure described above was repeated. The mean of the four sets of observations was taken, the galvanometer having been calibrated before and after each set.

The calibration was effected by applying a known potential difference across the galvanometer terminals and measuring the resulting deflexion. The resistances employed in these experiments had been calibrated. From a knowledge of the resistances of the leads and galvanometer it was then possible to calculate the potential difference between the edges of the plate corresponding to the galvanometer deflexion due to a field of known strength. The maximum field employed in these experiments was 8500 gauss, which corresponded to a current of 6 amperes passing through the electromagnet coils.

The Hall potential difference was measured for various magnetic fields, and in the case of each alloy a linear relation connecting the potential difference and field was obtained. The constant value of $\dfrac{E}{H}$ was read off from a graph, an example of which for the alloy containing 16·5 per cent. copper is given in fig. 3. The value of R, the Hall coefficient, could then be calculated from

$$R = \frac{Ed}{HI}.$$
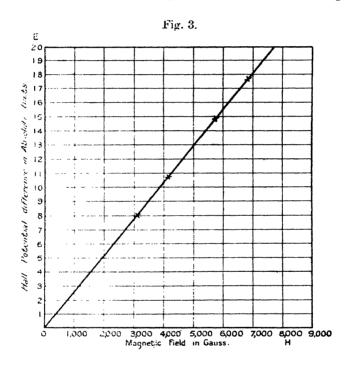
A primary current of 4 amperes was employed throughout this investigation, and it could be read to 1 part in 1200 on a delicate Weston ammeter.

The absolute value of the magnetic field, corresponding to a current of 2 amperes passing through the electromagnet coils, was determined in the usual manner by means of a search coil of known mean area and a delicate ballistic galvanometer.

The intensities of the magnetic fields corresponding to other currents passing through the coils of the electromagnet had previously been determined by means of a search coil and Grassot fluxmeter, and by making use of the ballistic galvanometer determination the various fluxmeter values could be corrected.

The accuracy of the measurement of the field was further tested by measuring the Hall coefficient of pure copper,

and comparing the results obtained with those of other observers. The result of this comparison was satisfactory, the value obtained in these experiments being $-·000523$, and the mean value found by other observers under the same conditions being $-·000520$ *. It is estimated that the magnetic fields have been determined correctly to within 1 in 200. The values of the Hall coefficients were measured at room-temperatures, the actual tempera-

Fig. 3.

ture being read from a thermometer suspended near the plate.

It is important to note that, in addition to the Hall effect, a transverse galvanomagnetic temperature difference is set up between the edges of the plate; this is the Ettingshausen effect, whose magnitude is usually very small. The difference in temperature dT is given by

$$d\mathrm{T} = \frac{\mathrm{P.H.I}}{d},$$ where H is the magnetic field in absolute

* Campbell, ' Galvanomagnetic and Thermomagnetic Effects,' p. 121.

units, I the current in absolute units, d the thickness of the plate in cms., and P the Ettingshausen coefficient.

The Hall and Ettingshausen effects are superposed, and unless the secondary electrodes are of the same material as the plate itself the Ettingshausen temperature difference dT set up between the edges of the plate

TABLE V.

The Hall Coefficient of the Alloys.
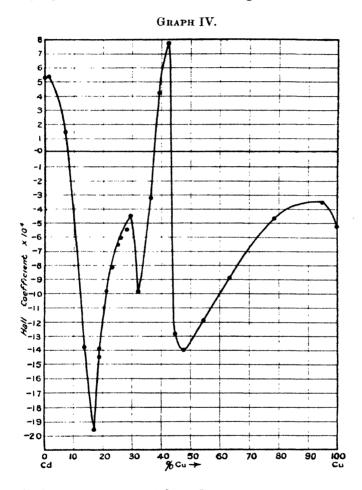
Percentage composition by weight.		Hall coefficient	Temperature
Per cent. of copper.	Per cent. of cadmium.	$\times 10^{\cdot}$.	in $^\circ$ C.
0·0	100·0	$-$ 5·30	16·8
1·2	98·8	$+$ 5·41	16·7
7·0	93·0	$+$ 1·52	15·5
13·3	86·7	$-$ 13·79	15·5
16·5	83·5	$-$ 19·61	13·2
18·0	82·0	· 14·54	13·6
18·6	81·4	$-$ 13·88	13·8
20·9	79·1	$-$ 9·86	14·2
22·8	77·2	$-$ 8·14	14·3
24·7	75·3	$-$ 6·50	15·4
25·6	74·4	$-$ 6·01	15·3
27·9	72·1	$-$ 5·43	15·0
28·9	71·1	$-$ 4·48	14·8
30·5	69·5	6·83	14·9
31·4	68·6	$-$ 9·90	12·7
35·8	64·2	·· 3·21	12·7
39·3	60·7	$+$ 4·22	13·1
42·5	57·5	$+$ 7·79	13·8
44·4	55·6	· 12·80	14·0
47·7	52·3	$-$ 14·02	15·1
54·2	45·8	$-$ 12·11	15·6
63·4	36·6	$-$ 8·95	15·3
78·5	21·5	$-$ 4·67	15·4
93·8	6·2	$-$ 3·65	15·5
100·0	0·0	$-$ 5·23	15·2

produces an electromotive force $\theta\, d$T, where θ is the thermoelectric power of the electrode with respect to the plate.

Hence the observed value for the potential difference is given by $E = E_{II} \pm \theta\, d$T, where E_{II} is the true potential difference due to the Hall effect. Then R, the Hall coefficient, becomes

$$R = \frac{E_{II}.d}{H.I} \pm P\theta.$$

The values of P are generally very small, and depend on the nature of the metal. There is comparatively little data relating to the magnitude of this coefficient for alloys, but its values for the constituent metals of the binary system examined in these experiments are very

GRAPH IV.

small, being $-1 \cdot 69 \times 10^{-9}$ and $-2 \cdot 89 \times 10^{-9}$ for copper and cadmium respectively. It is important, however, to remember that the magnitude of the potential difference also depends on the thermoelectric power of the electrode with respect to the plate.

Determinations of the Hall coefficients were made, using

secondary electrodes of copper and aluminium, and the values obtained were the same in each case. The Ettingshausen effect also takes time to reach its full value, but in these experiments there was no gradual creep in the observed deflexions during measurements of the Hall potential difference. Hence no correction for the Ettingshausen effect was necessary.

TABLE VI.

The Densities of the Alloys.

Percentage composition by weight.		Density in grams per c.c.	Temperature in 0 C.
Per cent. of copper.	Per cent. of cadmium.		
0·0	100·0	8·631	14·8
1·2	98·8	8·635	14·8
7·0	93·0	8·694	14·9
13·3	86·7	8·783	14·7
16·5	83·5	8·836	15·4
18·0	82·0	8·832	15·4
18·6	81·4	8·839	15·4
20·9	79·1	8·815	15·4
22·8	77·2	8·819	15·7
24·6	75·4	9·003	15·6
25·7	74·3	9·021	15·8
27·7	72·3	9·054	13·9
28·9	71·1	9·085	14·2
30·5	69·5	9·092	14·2
31·4	68·6	9·090	14·1
35·8	64·2	9·044	14·1
39·3	60·7	9·015	14·1
42·5	57·5	8·875	15·3
44·4	55·6	8·879	15·2
47·7	52·3	8·891	15·0
54·2	45·8	8·937	15·5
63·4	36·6	8·924	15·3
78·5	21·5	8·851	15·3
93·8	6·2	8·875	14·4
100·0	0·0	8·932	14·5

The values of the Hall coefficients for the various alloys are given in Table V. and plotted in Graph IV.

It is estimated, from a consideration of the various factors involved, that the determinations of the Hall coefficients are correct to within 1 per cent.
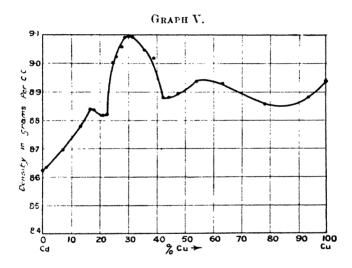
Densities of the Alloys.

The alloys were weighed in air and in pure distilled water at a known temperature. The density of the water

being known, the volumes of the plates could be determined and their densities calculated. The results are given in Table VI. and plotted in Graph V. It is considered that the densities have been determined with an error of not more than 0·1 per cent.

Specific Heats of the Alloys.

The specific heats of the alloys were determined by means of a Joly steam calorimeter in the usual manner. The thermometer employed in these experiments had been calibrated by comparison with a standard thermometer.

GRAPH V.

The mean specific heats between 18·5° C. and 100° C. are collected in Table VII. and plotted in Graph VI. It is estimated that the results are accurate to within 1 per cent. on the average.
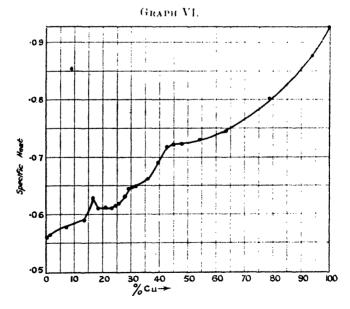
Discussion of Results.

The investigation of the electrical properties of an alloy system is a powerful method of detecting changes of phase, and the results obtained are generally in good agreement with those obtained by thermal methods. The variation of physical properties of the alloys with composition will therefore be examined for phase changes, and the results considered in relation to the equilibrium diagram.

Q 2

TABLE VII.

The Mean Specific Heats of the Alloys between 18·5° C. and 100° C.

Percentage composition by weight.		Mean specific heat between 18·5° and 100° C.	Percentage composition by weight.		Mean specific heat between 18·5° and 100° C.
Per cent. Cu.	Per cent. Cd.		Per cent. Cu.	Per cent. Cd.	
0·0	100·0	·0559	28·9	71·1	·0647
1·2	98·8	·0563	30·5	69·5	·0648
7·0	93·0	·0578	31·4	68·6	·0650
13·3	86·7	·0590	35·8	64·2	·0663
16·5	83·5	·0630	39·3	60·7	·0691
18·0	82·0	·0607	42·5	57·5	·0718
18·6	81·4	·0611	44·4	55·6	·0724
20·9	79·1	·0613	47·7	52·3	·9723
22·8	77·2	·0610	54·2	45·8	·0732
24·7	75·3	·0614	63·4	36·6	·0746
25·6	74·4	·0618	78·5	21·5	·0805
27·9	72·1	·0633	93·8	6·2	·0880
			100·0	0·0	·0934

GRAPH VI.

The curves showing the relation between the various electrical properties and composition show discontinuities near all or some of the points corresponding to CuCd₃,

Cu_2Cd_3, Cu_4Cd_3, and Cu_2Cd. These are the compounds given by Jenkins and Hanson * as the result of their investigation of the thermal properties of the alloys. At the copper end of the series the resistivity (Graph I.) at first increases gradually with addition of cadmium until the alloy containing 54·2 per cent. of copper is reached, then more rapidly to a maximum for the alloy containing 42·5 per cent. of copper. The resistivity of this alloy is 20·21 microhms per cm.³, and is about fourteen times that of copper and three times greater than that of cadmium.

At the other end of the series the addition of copper to cadmium causes at first a measurable increase in the resistivity over the small range from pure cadmium to 1·2 per cent copper, and afterwards a much more rapid increase to a maximum value of 18·16 microhms per cm.³ near the composition of the compound $CuCd_3$, which contains 15·9 per cent. of copper. This change in the slope of the resistivity curve is due to the introduction of the ε phase.

With the introduction of the δ constituent at the composition corresponding to about 16·5 per cent. of copper the resistivity decreases, and reaches a minimum at the composition 22·8 per cent. of copper, which roughly coincides with the boundary of the δ and (δ+ε) phases. At this point the ε phase disappears, and the resistivity curve rises to a second maximum at the composition 28·9 per cent. of copper, which corresponds approximately to the compound Cu_2Cd_3 †.

This maximum is followed by a second minimum which occurs near the boundary of the δ and (γ+δ) phase, at a composition corresponding to 31·4 per cent. of copper. On entering the (γ+δ) phase there is a rapid increase in the resistivity, which reaches its maximum value at the composition 42·5 per cent. of copper, which corresponds to the compound Cu_4Cd_3.

The curve shows no more well-defined singular points, but distinct discontinuities or points of inflexion occur

* *Loc. cit.*

† In the graphs connecting the electrical properties of the various alloys with composition, slight kinks corresponding to 27·9 per cent. copper have been smoothed out. These kinks may correspond to the compound Cu_2Cu_3 (27·4 per cent. copper), and the next point of inflexion at 28·9 per cent. copper is very near to the boundary δ and γ+δ phases as determined by Jenkins and Hanson.

at compositions corresponding to 44·4 and 54·2 per cent. of copper. The former composition corresponds to the boundary of the γ and the $(\beta+\gamma)$ phases and the latter to the compound Cu_2Cd, which is at the boundary between the $(\beta+\gamma)$ and the $(\alpha+\beta)$ phases. Apart from the former discontinuity the introduction of the β constituent does not materially alter the form of the resistivity-composition curve. Except at the two ends of the series (pure copper and pure cadmium) no data seems available for comparison with the results of the present investigation. However, the value of the resistivity obtained for copper ($1·561 \times 10^{-6}$ ohms per cm.³ at 0° C.) is in good agreement with that given in the International Critical Tables, and the value obtained for cadmium ($6·83 \times 10^{-6}$ ohms per cm.³ at 0°C.) with that ($6·828 \times 10^{-6}$) determined by Lees *.

The resistivities of the various alloys were not in general much affected by annealing except in the region extending from 36 to 44 per cent. of copper. In this region, as shown by an examination of Table II., large changes in the resistivities occurred. In the case of the alloy containing 42·5 per cent. of copper annealing produced an increase of 50 per cent. in the resistivity. According to the equilibrium diagram it will be seen that the region corresponds to the $(\gamma+\delta)$ and γ phases, and Jenkins and Hanson found that in order to separate out the complete γ constituent it was necessary to anneal for a considerable time at a temperature of 450° C. Annealing therefore causes a separation of the γ phase, and this explains the changes in the resistivities of the alloys in the region considered.

The mean temperature coefficient of resistance is also very sensitive to changes of phase, as shown by Graph II. No discontinuity occurs at the eutectic point (1·2 per cent. copper), and the mean temperature coefficient decreases continuously with increase of copper content to about the value $1·35 \times 10^{-3}$ for the compound $CuCd_3$, which contains 15·9 per cent. of copper. On the introduction of the δ phase at the above composition the temperature coefficient increases rapidly to a maximum at the composition (22·8 per cent. Cu) which nearly corresponds to the boundary between the δ and $(\delta+\epsilon)$ phases. With

* Phil. Trans. ccviii. p. 381 (1908).

further increase of copper content the temperature coefficient again decreases and reaches a second minimum near the compound Cu_2Cd_3, which contains 27·4 per cent. of copper. The boundary of the δ and $(\gamma + \delta)$ phases is shown by the maximum at the composition corresponding to 31·4 per cent. copper. Near this point the γ phase enters and a diminution occurs in the temperature coefficient, which reaches a minimum value for the compound Cu_4Cd_3, which contains 42·9 per cent. of copper. A further discontinuity occurs at the composition (44·4 per cent. copper), which corresponds to the boundary between the γ and the $(\gamma+\beta)$ phases. There is, however, no definite evidence in this case for the existence of the compound Cu_2Cd.

The graph (Graph III.) showing the relation between the thermoelectric power of the alloys with respect to both lead and copper, and the composition of the alloys, also show discontinuities at compositions corresponding to those of the four compounds. The various phase changes indicated by the equilibrium diagram are also shown as discontinuities on the graphs. It is interesting to note that the thermoelectric power graph for the alloy-copper junctions crosses the composition axis at the four points corresponding to 9, 19, 23, and 32·0 per cent. copper. These changes in the sign of the thermoelectric power are intimately connected with the phase changes indicated in the equilibrium diagram.

The Hall effect of the alloys is also very sensitive to phase changes. Graph IV., giving the relation between the Hall coefficients of the alloys and their composition, shows discontinuities at points corresponding to the compounds $CuCd_3$, Cu_2Cd_3, and Cu_4Cd_3, but no discontinuity at the point corresponding to the compound Cu_2Cd. The curve also shows discontinuities corresponding to all phase changes with the exception of the passage through the boundary between the δ and the $(\delta+\epsilon)$ phases. It is of interest to note that the Hall coefficients of alloys containing about 8, 37, and 43 per cent. of copper are zero. No satisfactory explanation of a zero Hall coefficient is available on present theories. From the nature of the graph it is evident that the Hall coefficient is intimately connected with the structure of the various alloys. The Hall coefficient is independent of the magnetic

field strength for all the alloys examined in this investigation.

Although the curves showing the relation between the various electrical properties and composition show many points of resemblance, it does not seem possible to draw general conclusions connecting the relative variations of these properties.

Density and specific heat are far less sensitive to changes in composition than the other physical properties investigated. In Graphs V. and VI., showing the variation of density and specific heat with composition, breaks occur at points corresponding to some of the four compounds, but they are not nearly as well defined as the marked singular points which occur in the graphs of the other physical properties. The most definite singular point in the above graphs is the one corresponding to the compound Cd_3Cu (15·9 per cent. Cu) in the specific heat graph.

Summary.

(1) The electrical resistivities, temperature coefficients of resistance, thermoelectric powers, Hall coefficients, and the specific heats and densities of the copper-cadmium series of alloys have been determined.

(2) The alloys were cast in graphite moulds in the form of plates, and their electrical resistivities at the temperature of melting ice were determined. The plates were then annealed for long periods at suitable temperatures until further annealing produced no change in their resistivities. The Hall coefficient and other physical properties were then determined in the final state.

(3) The curves giving the relation between the electrical properties and the composition of the alloys show in general singular points at compositions near those of the compounds $CuCd_3$, Cu_2Cd_3, Cu_4Cd_3, and Cu_2Cd. The presence of a compound at the composition corresponding to Cu_2Cd is not, however, indicated by the graphs showing the relation between composition of the alloy and (a) the Hall effect and (b) the temperature coefficient of resistance.

The discontinuities were much less pronounced at the points corresponding to the compositions of the above compounds in the density and the specific heat graphs.

(4) The variations of the resistivities and the thermoelectric powers of the alloys with composition were accompanied by variations in the Hall effect, and the

corresponding graphs show many points of similarity. A study of these graphs in relation to the equilibrium diagram shows that the variations in the electrical properties follow the changes of phase of the system.

(5) Annealing produced little effect on the electrical resistivity except in the region containing from 36 to 44 per cent. of copper. The comparatively large changes in resistivities of alloys in the above region produced by annealing is due, as pointed out by Jenkins and Hanson, to the separation of the γ phase.

XVII. *Kinetics of a Catalysed Isomeric Change in Solution.* *By* R. C. TRAILL, *Ph.D.*[*]

THE work of Hinshelwood and others has established the concept of kinetic activation in chemical reactions in the gaseous phase. According to this, of the total number of collisions between molecules of the reactants, the fraction which produces a chemical reaction is given by the probability that there will be available between two colliding molecules energy greater than a certain minimum, which is the energy of activation. According to Lewis[†], the velocity-coefficient of a bimolecular gaseous reaction is given (in gram molecules per litre, and minutes) by the equation

$$k = 114 \times 10^{21} \times \left(\frac{\sigma_1 + \sigma_2}{2}\right)^2 \times \sqrt{u_1^2 + u_2^2} \times e^{-E/RT},$$

where σ_1, σ_2 are the diameters, u_1, u_2 are the mean velocities (in cm. per sec.) of the reacting molecules, and E is the energy of activation calculated from the temperature coefficient of the reaction.

The applicability of this equation to a reaction in solution was tested by Norrish and Smith[‡], who introduced a correcting term to allow for the volume occupied by the solvent molecules. They investigated the reaction between trimethylamine and *m*- or *p*-nitrobenzyl chloride in benzene solution, and found a large discrepancy between the velocity-coefficient as calculated in the above manner, and that observed experimentally. The probability factor, P, being

* Communicated by T. M. Lowry, C.B.E., M.A., D.Sc., F.R.S.
† Journ. Chem. Soc. cxiii. p. 471 (1918).
‡ Journ. Chem. Soc. p. 129 (1928).

the ratio of the observed to the calculated velocity, was 2×10^{-8} for this reaction, and varied from 5×10^{-5} to 4×10^{-11} for a number of other reactions tabulated by them. They concluded that the discrepancy was due to deactivation by solvent molecules, to an extent characteristic of both the reactants and the solvent.

In the present paper some recent measurements of the velocity of catalysed mutarotation of beryllium benzyl-camphor in carbon tetrachloride and in chloroform * have been analysed on the basis of the law of Mass Action, in order to provide data for investigating the applicability of Lewis's equation to this reaction. As a result of these calculations the velocity-coefficients deduced from Lewis's equation have been found to be of the same order of magnitude as those observed experimentally, the differences being within the uncertainty of calculation. In these very simple changes, therefore, practically every collision between re-actant molecules with sufficient energy is effective, as contrasted with the extremely small probabilities in reactions involving the ionization of one of the components.

Application of the Law of Mass Action to a Catalysed Isomeric Change.

It is assumed that the isomeric change between the two forms, B_α and B_β, of beryllium benzoylcamphor can take place only through combination with the catalyst, A, to form a complex AB_α or AB_β. The change may then be formulated in three steps :

(i.) $\quad B_\alpha + A \rightleftharpoons AB_a,$

(ii.) $\quad AB_\alpha \rightleftharpoons AB_\beta,$

(iii.) $\quad AB_\beta \rightleftharpoons B_\beta + A.$

If reactions (i.) and (iii.) are fast compared with (ii.) they will be in equilibrium throughout the mutarotation and

$$[AB_\alpha] = q_\alpha[A][B_\alpha]$$
$$[AB_\beta] = q_\beta[A][B_\beta].$$

As a simplification we may take $q_\alpha = q_\beta = q$.

The velocity of change at any moment is given by

$$\frac{dx}{dt} = k_1'[AB_\alpha] - k_2'[AB_\beta].$$

* Lowry and Traill, Proc. Roy. Soc.

If a be the total concentration of catalyst,
b be the total concentration of beryllium benzylcamphor,
it can be shown that

$$k = \frac{k'}{2bq} \left\{ (aq + bq + 1) - \sqrt{(aq + bq + 1)^2 - 4abq^2} \right\}, \quad (1)$$

where k is the observed velocity-coefficient of the reaction,
and $k' = k_1' + k_2'$.

If $[AB]$ is negligible in comparison with a, this relation
can be obtained in a simpler form,

$$k = k' \frac{aq}{1 + aq}. \quad \ldots \quad \ldots \quad (2)$$

TABLE I.

Catalysis by Pyridine in Carbon Tetrachloride.

20°. $k'' = 0.132.$			25°. $k'' = 0.227.$			30°. $k'' = 0.385.$		
a	k(obs.).	k(calc.).	a.	k(obs.).	k(calc.).	a	$(k$(obs.).	k(calc.).
0.519	0.0695	0.0683	0.130	0.0322	0.0294	0.130	0.0500	0.0500
0.839	0.109	0.110	0.209	0.0535	0.0475	0.259	0.101	0.100
			0.511	0.119	0.116	0.387	0.148	0.149
			0.773	0.162	0.175			
			0.993	0.226	0.225			
			1.048	0.238	0.238			

Finally, if q be extremely small, so that aq is negligible
in comparison with unity, equation (2) reduces to

$$k = k'aq = k''a \quad \ldots \quad \ldots \quad (3)$$

where $k'' = k'q$ is a constant catalytic coefficient, or bi-
molecular velocity-coefficient for the reaction.

The results obtained for the rate of mutarotation of
beryllium benzoylcamphor in carbon tetrachloride when
catalysed by pyridine conform to equation (3), and are
shown, together with the constants deduced, in Table I.

The results obtained with alcohol as catalyst conform to
equation (1). Values of k', the unimolecular velocity-co-
efficient of the isomeric change of the complex, and of q,
the mass action constant, chosen to fit the results best, are
shown, together with the experimental figures, in Table II.

Similar results were obtained with *p*-cresol as catalyst, and are shown in Table III. The agreement here is not, however, so good, especially at low catalyst concentration, and it is possible that the effect of *p*-cresol is not so simple.

TABLE II.

Catalysis by Alcohol in Carbon Tetrachloride.

20°.	25°.	30°.
$k' = 0.105$.	$k' = 0.185$.	$k' = 0.329$.
$q = 2.2$.	$q = 2.0$.	$q = 2.0$.

b.	a.	k(obs.).	k(calc.).	b.	a.	k(obs.).	k(calc.).	b.	a.	k obs.).	k(calc.).
0.042	0.289	0.0395	0.0394	0.077	0.0037	0.0014	0.0012	0.038	0.142	0.0696	0.0695
0.037	0.710	0.0634	0.0632	0.075	0.0307	0.0092	0.0094	0.039	0.289	0.116	0.117
0.038	1.434	0.0790	0.0793	0.082	0.0450	0.0116	0.0134	0.042	0.431	0.150	0.149
				0.085	0.107	0.0320	0.0292				
				0.092	0.290	0.065	0.063				
				0.080	0.576	0.094	0.095				
				0.084	0.859	0.114	0.114				
				0.081	1.146	0.127	0.126				

TABLE III.

Catalysis by *p*-cresol in Carbon Tetrachloride at 25°.

$k' = 0.127$.	$q = 2.5$.

b.	a.	k(obs.).	k(calc.).
0.037	0.0356	0.0060	0.0096
0.037	0.0501	0.0081	0.0132
0.037	0.0540	0.0118	0.0151
0.033	0.100	0.0175	0.0257
0.036	0.110	0.0275	0.0275
0.037	0.244	0.0525	0.0483
0.037	0.358	0.0627	0.0601
0.037	0.586	0.0741	0.0756
0.037	1.18	0.0961	0.0952

Influence of the Solvent.

The isomeric change of beryllium benzoylcamphor in chloroform proceeds to an equilibrium which is different from that in carbon tetrachloride. It has been shown * that

* Burgess and Lowry, Journ. Chem. Soc. cxxv. p. 2081 (1924).

beryllium benzoylcamphor combines with two molecular proportions of chloroform to give a crystalline compound, the properties of which suggest that it contains equimolecular proportions of the α and β forms. It is therefore formulated as a "racemate," $B_\alpha B_\beta, 4CHCl_3$. The change of equilibrium in chloroform is then easily accounted for by a difference of stability of two isomeric chloroform complexes, $B\alpha, 2CHCl_3$ and $B\beta, 2CHCl_3$. These complexes are assumed to undergo isomeric change only when the chloroform has been displaced by an active catalyst such as alcohol or pyridine.

In addition to the reactions (i.), (ii.), and (iii.) (p. 226), we now write

$$\text{(iv.)} \quad B_a + 2S \rightleftharpoons B_a S_2,$$

$$\text{(v.)} \quad B_\beta + 2S \rightleftharpoons B_\beta S_2,$$

where S is a molecule of the solvent. If these reactions, like (i.) and (iii.), are fast compared with (ii.), they will be in equilibrium throughout, and

$$[B_a S_2] = p_a [B][S]^2$$

$$[B_\beta S_2] = p_\beta [B_\beta][S]^2,$$

where p_a, p_β are mass action constants for the respective forms. The velocity-coefficient k_c in chloroform is now given by the equation

$$k_c = [A]q \left\{ \frac{k_{c_1}'}{1+[A]q+p_a[S]^2} + \frac{k_{s_2}'}{1+[A]q+p_\beta[S]^2} \right\}. \quad (4)$$

If $[A]q$ is small, this reduces to

$$\left. \begin{aligned} k_c &= aq\left\{ \frac{k_c'}{1+p_a[S]^2} + \frac{k_{c_2}'}{1+p_\beta[S]^2} \right\} \\ &= ak_c'' \end{aligned} \right\} \quad . \quad (5)$$

If the ratios of the total α form to the total β form of beryllium benzoylcamphor present at equilibrium in carbon tetrachloride and chloroform be r and r_c respectively, then, for the above condition,

$$r = \frac{k_2''}{k_1''}, \quad . \quad . \quad . \quad . \quad . \quad . \quad . \quad . \quad . \quad . \quad (6)$$

and

$$r_c = \frac{k_2''}{k_1''} \frac{1+p_a[S]^2}{1+p_\beta[S]^2} = r\frac{1+p_a[S]^2}{1+p_\beta[S]^2}. \quad . \quad . \quad (7)$$

It may further be shown that

$$p_a[S]^2 = \frac{(1 + r_e)k''}{(1 + r)k_c''} - 1. \quad \cdots \quad (8)$$

$$p_\beta[S]^2 = \frac{(1 + r_c)rk''}{(1 + r)r_ck_c''} - 1. \quad \cdots \quad (9)$$

which give p_a, p_β in terms of determinable quantities.

The experimental values obtained with pyridine in chloroform are shown in Table IV.

Inserting the values $r = \dfrac{0\cdot51}{0\cdot49} = 1\cdot04$, $r_c = \dfrac{0\cdot41}{0\cdot59} = 0\cdot70$

$k''/k_c'' = 2\cdot27$ in equations (8) and (9), the mass action constants are found to be

$$p_a = 0\cdot0058 \qquad p_\beta = 0.0116.$$

TABLE IV.

Catalysis by Pyridine in Chloroform at $25°$.

$$k_c'' = 0\cdot100.$$

a.	k(obs.).	k(calc.).
0·260	0·0276	0·0260
0·642	0·0604	0·0642
0·902	0·0906	0·0902

The constants imply that, at the molecular concentration, 12·4, of pure chloroform, 46 per cent. of the α form and 64 per cent. of the β form is combined with the solvent.

Equation (4) can be obtained as

$$k_c = \frac{k_c'[A]q}{1+r} \left\{ \frac{1}{1+[A]q+p_a[S]^2} + \frac{r}{1+[A]q+p_\beta[S]^2} \right\},$$

$$\cdots \quad (10)$$

where all the quantities on the right side have been determined except $[A]$ and k_c'. Since in the experiments a is usually substantially greater than b, it is possible, by estimating $[AB]$ approximately, to obtain values of $[A]$ from the relation

$$[A] = a = [AB],$$

without introducing appreciable error. Further, by making use of the relation $k_c' = 1\cdot24\,k'$, which can be deduced theoretically from the rate of collision of the solvent molecules with those of the complex (see p. 233), the velocity of

mutarotation of beryllium benzoylcamphor in chloroform, when catalysed by alcohol or cresol, can be predicted. The nature of the agreement is shown in Tables V. and VI. It will be seen that there is good agreement between theory and experiment in the case of alcohol, but that the calculated values for cresol are some 50 per cent. too high. This

TABLE V.

Catalysis by Alcohol in Chloroform at 25°.

h.	a.	k(obs.).	k(calc.).
0·012	0·179	0·0273	0·0300
0·038	0·358	0·0492	0·0520
0·040	0·534	0·0683	0·0730
0·040	0·712	0·0871	0·0875
0·041	1·068	0·113	0·111
0·041	1·408	0·128	0·129

TABLE VI.

Catalysis by *p*-Cresol in Chloroform at 25°.

h.	a.	k(obs.).	k(calc.).
0·037	0·410	0·0294	0·0465
0·035	0·819	0·0496	0·0755
0·032	1·289	0·0692	0·0970

TABLE VII.

Catalyst.	$k_{30°}/k_{25°}$	E.
(*a*) Pyridine	2·92	18,900 cal.
(*b*) Alcohol	3·14	20,200 ,,

divergence is of the same order as that for the lower concentrations of cresol in carbon tetrachloride, and may be due to a common cause ; or is perhaps a result of association of the molecules of *p*-cresol itself.

Application of the Theory of Kinetic Activation.

The energy of activation for the isomeric change, when catalysed by pyridine and by alcohol, can be calculated from the temperature-coefficient in the usual way, and the results are shown in Table VII.

The value for pyridine is obtained from k'' of equation (3), which is a bimolecular velocity-coefficient. The velocity of isomeric change is therefore proportional to the rate of collision of the reacting molecules and the energy of activation is that for the complete reaction represented by both (i.) and (ii.) (p. 226). On the other hand the value for alcohol is calculated from k' of equation (1) which represents the unimolecular velocity-coefficient for the isomeric change of the complex, that is, for reaction (ii.) only.

(a) *Catalysis by Pyridine.*—The constant k'' of equation (3) is the bimolecular velocity-coefficient for the isomeric change catalysed by pyridine, and is therefore identical with the constant k of Lewis's equation. The values of the effective molecular diameters, that is, the mean diameters of the reactive groups of the molecules, have been taken as 4×10^{-8} cm. Since it is possible to obtain the order of magnitude only of the velocity-coefficient, it is assumed that the volume-correction introduced by Norrish and Smith is balanced by the shielding of the reactive groups of the solute and catalyst by the inert parts of their own molecules. The values of u_1 and u_2 have been deduced in the usual way from the kinetic theory. In this way the bimolecular velocity constant is calculated to be 0·084 for pyridine at 25°, compared with the experimental value of 0·227. The ratio of the observed to the calculated constant is 2·8.

(b) *Catalysis by Alcohol.*—The constant k' obtained for alcohol represents the velocity-coefficient for the isomeric change of the catalyst complex. This change may be supposed to be brought about by the acquisition of energy, by means of collision between molecules of the complex and the solvent, which may therefore be regarded as a reactant for the purpose of calculating the required constant. The bimolecular velocity-coefficient is then obtained by dividing k' by the solvent concentration. Hence, using the same values for the molecular diameters as before, the velocity constant is calculated to be 0·0072 for alcohol at 25°, and the experimental value is 0·0180, giving a ratio of observed to calculated of 2·5.

In view of the nature of the calculation, the factors 2·8 and 2·5 represent a reasonable agreement between theory and experiment, in striking contrast to the results previously obtained in solution. The reason for this difference must be sought in the nature of the reaction. It is clear that the mutarotation of beryllium benzoylcamphor, in which the activation consists merely of the opening of one, or two, rings, which are subsequently closed again in either of

two alternative positions, is a reaction of a much simpler type than the combination of trimethylamine and nitrobenzyl chloride, and similar reactions, in which a considerable rearrangement of the constituent atoms is involved.

Variation of the Velocity-Coefficient with the Solvent.

On the basis of this mechanism for the mutarotation of the complex it is easy to calculate the relative efficiencies of chloroform and carbon tetrachloride as promoters of isomeric change in presence of a catalyst. For, if the energy of activation of the complex is unaltered by the change of solvent, the relative value of k' will depend only on (i.) the diameters and (ii.) the velocities of the molecules, and (iii.) the molecular concentrations, of the solvents. If the ratio of the molecular diameters of carbon tetrachloride and chloroform is equated to the ratio of the cube roots of their parachors, the first factor will result in a diminution in the ratio 0·94 to 1 on passing from the former to the latter, the second factor produces an increase in the ratio 1·10 to 1, and the ratio of the molecular concentrations produces an increase in the ratio 1·20 to 1. The product of these three factors is 1·24, and this has been used to deduce values for the velocity-coefficients of mutarotation in chloroform when catalysed by alcohol or *p*-cresol (p. 231).

XVIII. *Magneto-Resistance and Magneto-Caloric Effects in Iron and Heusler Alloys.* By H. H. POTTER, *Ph.D., Lecturer in Physics, H. H. Wills Physical Laboratory, University of Bristol* [*].

IN a previous paper [†] the writer has shown that the suggestion of Gerlach and Schneiderhan [‡] concerning direct proportionality between change of resistance in a magnetic field and the change of magnetic energy is accurately true in the case of nickel. This change of resistance in the neighbourhood of the Curie point was measured both in transverse and longitudinal magnetic fields up to 7000 gauss, and was compared with the magneto-caloric measurements of Weiss and Forrer [§]. The resistance

---
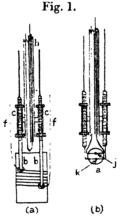
measurements have now been extended to the cases of iron and Heusler alloy, and some measurements of the magneto-caloric effect in these two substances have also been made.

IRON.
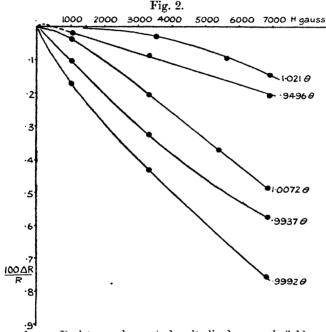
Resistance Measurements.

The resistance measurements were obtained by a voltage-current method, the specimen itself being in an evacuated tube mounted in an electric furnace between the poles of a Weiss electromagnet. The arrangements were fully described in the previous paper, so that it is necessary here to do little more than to describe a few slight modifications. In the first place, the whole apparatus had to be made of

Fig. 1.

(a)   (b)

quartz instead of pyrex glass, since the Curie point of iron is about 770° C. as compared with 360° C. for nickel ; secondly, to obtain greater reliability the temperatures were indicated by a calibrated platinum platinum-rhodium thermo-couple instead of copper-constantin ; thirdly, the earlier method of mounting the wire for the measurements in a transverse field has been dispensed with, and the mounting previously used for the measurements in a longitudinal field has been used for both sets of measurements. The wire of which the resistance was to be measured was wound on a thin quartz sheet which was supported by two thick copper leads (*b, b*) fig. 1 (*a*). These leads were bent at the ends and passed through two holes in the quartz plate, to which they were secured by copper nuts threaded on to the rods. These nuts also served to secure the iron wire, which was in one piece, with the potential leads *f, f*. The

copper leads were secured to two quartz tubes *c, c,* mounted on the main supporting tube *h.* The whole was surrounded by an evacuated quartz tube of 17 mm. diameter, the tube *h* being joined to a ground-joint which enabled the quartz plate to be turned so as to be either parallel or perpendicular to the magnetic field. It is impossible with this arrangement to have the whole of the wire either parallel or perpendicular to the field, the finite thickness of the quartz plate obviously preventing this. It will be shown, however, that the transverse and longitudinal effects are identical

Fig. 2.

Iron. Resistance change in longitudinal magnetic field.
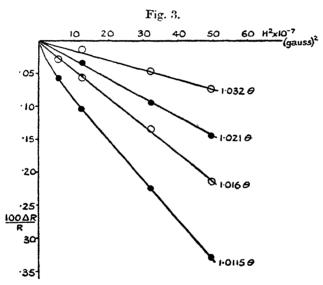
near the Curie point—to which region these results are confined—so that no error arises from this cause. The iron wire used was No. 36, S.W.G.

The relations between resistance change and applied field for the wire parallel to the lines of force are shown in fig. 2. The temperatures marked on the curves are given in terms of the Curie temperature (θ), which was 1050° K. The shapes of these curves correspond extraordinarily well with the shapes of the curves for nickel at corresponding temperatures. Near the Curie point $\frac{\Delta R}{R}$ is seen to change

less rapidly than the first power of H, but with rising temperature the curves change gradually in shape, until well above the Curie point $\frac{\Delta R}{R}$ varies as H^2. The significance of this will be indicated later in the paper. The curves in fig. 2 are all for the case of the wire parallel to the field. It was very difficult to get corresponding curves for the transverse effect, owing to the uncertainty in calculating the demagnetizing fields. In fig. 3, which is for temperatures above the Curie point, and for which therefore the demagnetizing field was much smaller, two curves for the

Fig. 3.

Iron. Resistance change in a magnetic field.
⊙ Transverse effect.
● Longitudinal effect.

transverse effect are included. In this figure $\frac{\Delta R}{R}$ is plotted against H^2, the straight line relations showing that in the quasi-paramagnetic condition $\frac{\Delta R}{R}$ is proportional to H^2 or to the change in magnetic energy $\frac{1}{2}\chi H^2$ (χ = susceptibility). The curve for the lowest temperature, $1\cdot0115\,\theta$, is not quite a straight line, showing that true paramagnetism has not been attained at this temperature.

MAGNETO-CALORIC EFFECT IN IRON.

The magneto-caloric effect is of course a direct measure of the change of magnetic energy which accompanies the application of an external field. The modifications in the apparatus required for its measurement are very slight indeed, and are shown in fig. 1 (*b*). The quartz plate of fig. 1 (*a*) was dispensed with, and its place was taken by a mass of pure iron *a* (fig. 1 (*b*)).
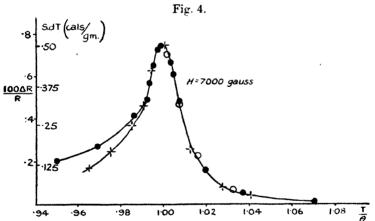
In order to examine the magneto-caloric effect two temperature measurements are necessary : (1) the temperature of the specimen, and (2) the change of temperature accompanying a given change in the value of the external field. The former was given by a platinum platinum-rhodium thermo-couple with one junction at *j* (fig. 1 (*b*)). The second junction of the thermo-couple was exterior to the apparatus and was kept at a steady temperature by immersion in water. The temperature change on magnetization was measured by a second thermo-couple of copper-constantin having one junction *k* inside the mass of iron, and the second junction only about 1·2 cm. distant but outside the iron. The latter junction was made by brazing the constantin element on to one of the copper leads *b* (fig. 1 (*a*)), the copper element being brazed on to the other lead. This thermo-couple gave practically zero e.m.f. except when the temperature of the iron was suddenly changed by a change of its magnetization. It was connected directly to a galvanometer, the deflexion on switching on the field being a direct measure of the magneto-caloric rise of temperature.

The iron specimen was an ellipsoid of revolution, with the long axis (shown perpendicular to the plane of the diagram) about twice the short axis. The long axis was parallel to the field, and consequently the demagnetizing factor was less than it would have been for a sphere, so that the effective field could be determined with greater accuracy. The thermo-junctions—although for clearness shown in the diagram placed along a short axis of the ellipsoid—were actually close together on the long axis. Contact between the iron and the junctions was obtained by jamming the thermo-junctions into tapered holes in the iron.

In fig. 4 the magneto-caloric effect for a field of 7000 gauss is shown (by the crosses) as a function of the temperature. The quantity plotted is not the rise of temperature (*d*T), but this rise multiplied by the specific heat (*s*). Obviously it is this product which represents the energy liberated, and since the specific heat changes very

rapidly in the neighbourhood of the Curie point the product $s \cdot d\mathrm{T}$ varies somewhat differently with temperature from the variation of $d\mathrm{T}$ alone. The values of the specific heat were taken from a paper by Klinkhardt [*]. On the same figure are plotted the values of $\dfrac{\Delta \mathrm{R}}{\mathrm{R}}$ both for the longitudinal effect (dots) and the transverse effect (circles), the two curves being adjusted to the same height at their peaks. The transverse effect cannot be determined very accurately on account of the large value of the demagnetizing factor— 2π for a long wire magnetized perpendicular to its length— combined with the fact that we have no accurate data concerning the intensity of magnetization in iron as a function of applied field and temperature. Consequently

Fig. 4.

Iron. Magneto-resistance and magneto-caloric effects as a function of temperature.
● Resistance change in longitudinal field.
⊙ Resistance change in transverse field.
+ Magneto-caloric effect.

no values of the transverse effect are included for temperatures below the Curie point, where the demagnetizing field will be large. Even above the Curie point the demagnetizing field is appreciable, and for the points given it has been calculated using Tyler's extension of Weiss's theory [†]. The largest correction applied (for the point at $1 \cdot 0015\,\theta$) amounted to about 20 per cent., so that the accuracy with which the point fits on to the curve would seem to justify in some measure Tyler's extension of the ordinary theory.

* Klinkhardt, *Ann. d. Physik*, 4, lxxxiv. p. 191.
† Tyler, Phil. Mag. 7, ix. p. 1026.

Although the agreement between the resistance and magneto-caloric effects is not very satisfactory below $\cdot99\ \theta$, the agreement over the rest of the curve is remarkably good, and may be taken as further evidence of the close relation between $\dfrac{\Delta R}{R}$ and the change in magnetic energy (ΔE). The proportionality factor $\dfrac{\Delta E}{\Delta R/R}$ is, however, vastly different in iron and nickel, for which curves are given in fig. 8. In iron the maximum resistance change was only $\cdot75$ per cent. and the magneto-caloric heat evolution amounted to about $\cdot50$ cal./gm. In nickel the maximum resistance change was about $1\cdot03$ per cent., but the magneto-caloric effect amounted according to the results of Weiss and Forrer to only $0\cdot1$ cal./gm. These figures all refer to a field of 7000 gauss.

HEUSLER ALLOY.
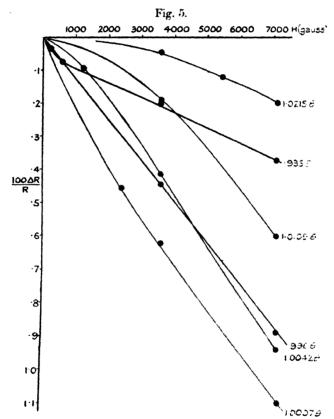
The Heusler alloy specimen used was a strongly magnetic one from a well mixed melt of constitution very near to Cu_2MnAl. The melt was cast into a narrow rod, which was annealed for 120 hours at 250° C., and then for 24 hours at 300° C. The initial long annealing at 250° C. helped to develop the strong magnetic properties, whilst the shorter annealing at 300° C. was carried out to stabilize the magnetic condition and to prevent any quick changes in properties when measurements were subsequently made at the Curie point (275° C.). A portion of the rod was ground down to about $1\cdot5$ mm. diameter, and was then further reduced in dilute nitric acid until the diameter was about $0\cdot5$ mm. This process of reducing the thickness of the specimen was carried out in two stages, since the brittleness of the alloy made reduction below $1\cdot5$ mm. on the grinding wheel somewhat hazardous. The rod was then mounted on the same apparatus as that used for the iron wire (fig. 1 (a)), except that the quartz plate was dispensed with, and the rod of alloy joined straight across between the two copper rods, b, b. Excellent contact at the junctions was obtained by electrolytic deposition of copper, the potential leads, which were also of copper, being joined in the same manner. With this arrangement the rod could be placed either parallel or perpendicular to the lines of force by merely rotating the ground-joint.

RESISTANCE MEASUREMENTS.

Unlike iron and nickel Heusler alloys show a decrease of resistance at room-temperatures in both transverse and

longitudinal fields.   (Iron and nickel both show an increase in longitudinal and a decrease in transverse fields.)   The decrease, which, when allowance is made for end demagnetizing effects, is found to be rapid for small values of the field and less rapid subsequently, amounts for both longitudinal and transverse effects to about 0·6 per cent. in a field of 7000 gauss.   This effect decreases rapidly with rise of temperature,

Fig. 5.

Heusler alloy.   Resistance change in a longitudinal magnetic field.
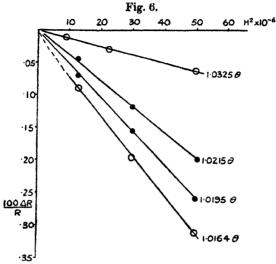
and near the Curie point gives place to effects similar to those obtained with nickel and iron.   The results for longitudinal fields are shown in fig. 5, and are in good qualitative agreement with the results for iron and nickel.   One slight difference, however, may be mentioned.   The curve at ·935 θ (fig. 5) shows a sharp initial fall of resistance followed by a less rapid linear change of resistance with the field.   The curve for iron at a corresponding temperature would show an

initial increase of resistance. This is, of course, due merely to the difference in the sign of the low temperature longitudinal effects, which have not quite disappeared at the temperature considered. If we assume that this low temperature effect has become constant where the curve is straight, then the true resistance change may be deduced from the slope of the straight part of the curve. The number of points on these curves is not as great as one would wish. The heat generated in the specimen by the magneto-caloric effect was not dissipated so rapidly as in the thin wires used in the measurements on iron and nickel. It was therefore necessary to wait some 3 or 4 minutes after every change of field before the temperature of the specimen again became steady and the resistance settled to its correct value. Owing to the difficulty of keeping the furnace temperature quite steady it was therefore necessary to cut down the number of points on a given curve to a minimum.

In fig. 6, which is for temperatures above the Curie point, and in which $\frac{\Delta R}{R}$ is plotted against H^2, two curves for the transverse effect are included. Once again it is difficult to correct the results obtained for the transverse effect for demagnetizing field. In iron the difficulty arose from our lack of knowledge of the intensity, in Heusler it arises from a different cause. It has been mentioned that owing to the brittleness of the alloy the rod was reduced in diameter by solution in nitric acid. Unfortunately the acid did not attack the rod uniformly, and the finished specimen was by no means circular in section. This irregularity made an accurate estimate of the demagnetizing factor impossible. The points for the transverse effect, which are included in figs. 6 and 7, were corrected, using a demagnetizing factor of 2π. The values of the intensity required for this correction were obtained by actual measurement on the rod before dissolving it down to the narrow diameter required for the resistance measurements. The correction amounts to about 15 per cent. at the Curie point, and of course falls off rapidly above this temperature, so that errors in estimating the demagnetizing field will not be serious for temperatures above the Curie point. This correction is somewhat greater than would be expected by comparison with iron and nickel, but is explained by the fact that the specimen used had surprisingly large susceptibility near the Curie point.
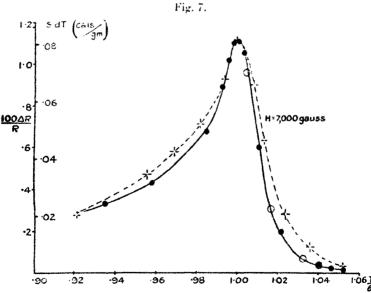
The maximum resistance change in Heusler alloy is seen to be greater than the maximum changes in either nickel or iron.

Fig. 6.

Heusler alloy.   Resistance change in a magnetic field.
⊙ Transverse effect.
● Longitudinal effect.

Fig. 7.

Heusler alloy.   Magneto-resistance and magneto-caloric effects as
a function of temperature.
● Resistance change in a longitudinal field.
⊙ Resistance change in a transverse field.
+ Magnetic-caloric effect.

MAGNETO-CALORIC EFFECT IN HEUSLER ALLOY.

The magneto-caloric effect in Heusler alloy was measured by a method identical with that used for iron. The ellipsoid used was from the same melt as the resistance specimen. It was actually the *neighbouring* piece from the cast rod, and was submitted to identical heat treatment. The specific heat measurements required in the calculation of the actual heat emission were taken from a paper by Sucksmith and the writer *. The specific heat curve (fig. 5 of that paper) was obtained for an alloy of the same composition as the one used in this experiment.

The magneto-resistance and magneto-caloric effects in Heusler alloy considered as a function of temperature are again strikingly similar (fig. 7). The heights of the two curves were adjusted to agree at the peaks, but the actual temperature at which the peaks occurred agreed accurately and also coincided with the temperature at which the spontaneous magnetization disappeared. The maximum value of the magneto-caloric effect appears to be less in Heusler alloy than in either nickel or iron.

NICKEL.

For the sake of comparison the relation between $\dfrac{\Delta R}{R}$ and T, and $s \cdot dT$ and T are given for nickel in fig. 8. These results are taken from the writer's previous paper on this subject, but the temperatures are now given in terms of the Curie temperature θ, and the results are for a field of 7000 gauss and not 5000 gauss as given previously.

DISCUSSION OF RESULTS.

The results given in figs. 2, 3. 5, and 6 show that the relation between resistance and applied field varies with the temperature. At temperatures well above the Curie point $\dfrac{\Delta R}{R}$ is proportional to H^2, at the Curie point $\dfrac{\Delta R}{R}$ varies somewhat less rapidly than H, whereas below the Curie point it is a linear function of H. Considerable evidence has been presented to show that the resistance change is proportional to the change in magnetic energy. We shall now consider how the energy varies with applied field at temperature above, at, and below the Curie point.

* Proc. Roy. Soc. A, cxii. p. 167 (1926).
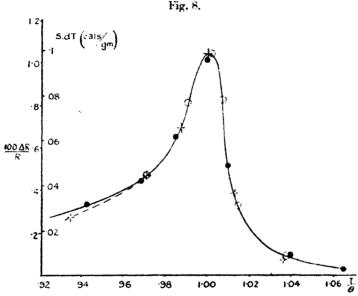
Above the Curie Point.

According to the Weiss theory a ferromagnetic body when heated above the Curie temperature behaves as a paramagnetic substance.   The energy can thus be written :

$$E = \tfrac{1}{2}\sigma H = \tfrac{1}{2}\chi H^2,$$

E = energy per c.c.,

σ = intensity of magnetization per c.c.,

χ = susceptibility.

$\dfrac{\Delta R}{R}$ should therefore be proportional to H^2 (figs. 3 and 6).

Fig. 8.

Nickel.   Magneto-resistance and magneto-caloric effects as a function of temperature.

● Resistance change in longitudinal field.

⊙ Resistance change in transverse field.

+ Magneto-caloric effect.

At the Curie Point.

The fundamental equations of the Weiss theory of ferromagnetism are

$$\sigma = \sigma_0 \tanh a, \quad \ldots \quad \ldots \quad (1)$$

$$a = \frac{\mu(H + N\sigma)}{kT} = \frac{\sigma_0 m(H + N\sigma)}{\rho RT}, \quad \ldots \quad (2)$$

$\mu =$ molecular magnetic moment,
$\sigma_0 =$ intensity per unit volume at saturation,
$m =$ molecular weight,
$k =$ Boltzman's constant,
$R =$ gas constant per gm. mol.,
$\rho =$ density,
$N =$ the constant of the intramolecular field.

At the Curie point the magnetization will be small, and so (1) can be written

$$\frac{\sigma}{\sigma_0} = \alpha - \frac{\alpha^3}{3}, \quad \ldots \ldots \quad (3)$$

and in (2) T may be replaced by θ, where θ is the Curie temperature.

Using the usual equation

$$\theta = \frac{N m \sigma_0^2}{\rho R}, \quad \ldots \ldots \quad (4)$$

from (2) and (4)

$$\alpha = \frac{\sigma}{\sigma_0} + \frac{\sigma_0 m}{\rho R \theta} H.$$

Substituting in (3)

$$\frac{\sigma}{\sigma_0} = \left(\frac{3 \sigma_0 m}{\rho R \theta} H \right)^{1/3} - \frac{\sigma_0 m}{\rho R \theta} H, \quad \ldots \quad (5)$$

$\frac{\sigma_0 m}{\rho R \theta}$ is of the order 10^{-7}, so that the second term is not appreciable unless H is large. Thus for field strengths up to several thousand gauss the intensity at the Curie point should vary as the cube root of the field.

The energy (E) is given by

$$E = \tfrac{1}{2} \sigma H_1,$$

where $H_1 =$ total field, *i.e.*, the molecular field plus the external field ;

$$\therefore \quad E = \tfrac{1}{2} \sigma (N \sigma + H). \quad \ldots \ldots \quad (6)$$

Even at the Curie temperature $N\sigma$ is still very great compared with H, so that from (5) and (6)

$$E = \tfrac{1}{2} N \sigma_0^2 \left(\frac{3 \sigma_0 m}{\rho R \theta} \right)^{2/3} . H^{2/3},$$

or, using (4),

$$E = \tfrac{1}{2} (9 N \sigma_0^4)^{1/3} . H^{2/3}.$$

If we put $\frac{\Delta R}{R} \propto E$, we have

$$\frac{\Delta R}{R} \propto H^{2/3}.$$

Analysis of the appropriate curves in figs. 2 and 5 gives fairly good agreement with this equation.

Below the Curie Temperature.

From equations (1), (2), and (6) we have

$$\left(\frac{\partial \sigma}{\partial H}\right)_T = \sigma_0 \operatorname{sech}^2 \alpha \cdot \left(\frac{\partial \alpha}{\partial H}\right)_T,$$

$$\left(\frac{\partial \alpha}{\partial H}\right)_T = \frac{\mu}{kT} + \frac{\mu N \sigma_0}{kT} \operatorname{sech}^2 \alpha \cdot \left(\frac{\partial \alpha}{\partial H}\right)_T,$$

$$E = \frac{\sigma_0}{2} \frac{kT}{\mu} \alpha \cdot \tanh \alpha,$$

$$\left(\frac{\partial E}{\partial H}\right)_T = \frac{\sigma_0 kT}{2\mu} (\alpha \operatorname{sech}^2 \alpha + \tanh \alpha) \cdot \left(\frac{\partial \alpha}{\partial H}\right)_T$$

$$= \frac{\sigma_0}{2} \frac{\alpha \operatorname{sech}^2 \alpha + \tanh \alpha}{1 - \frac{\mu N \sigma_0}{kT} \operatorname{sech}^2 \alpha}.$$

Now provided $T << \theta$, α varies only very slowly with H, and so $\left(\frac{\partial E}{\partial H}\right)_T$ may be taken as a constant. This means a linear relation between E and H. Again, if $\frac{\Delta R}{R}$ is proportional to E this is in agreement with the experimental results.
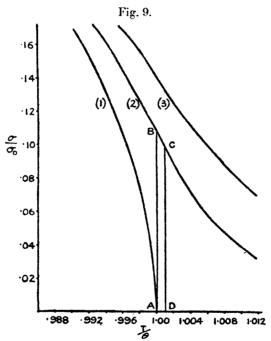
Maximum Resistance Change and Maximum Magnetocaloric Effect.

The following table shows the maximum values of $\frac{\Delta R}{R}$ and $s \cdot dT$ for iron, nickel, and Heusler alloy for a field of 7000 gauss.

	$100 \frac{\Delta R}{R}$.	$s \cdot dT$.	$\frac{s \cdot dT}{100 \frac{\Delta R}{R}}$
Iron	·76	·50	·66
Nickel	1·04	·10	·096
Heusler alloy	>1·12	·08	<·071

The ratios in the third column, although indicating clearly a very great difference between the three substances, are subject to certain sources of error which reduce their accuracy. In the first place $\frac{\Delta R}{R}$ is measured for an isothermal energy change.

whilst the quantity $s \cdot dT$ is necessarily measured adiabatically. The difference may be explained by reference to fig. 9. The curve (1) represents the variation of spontaneous magnetism with temperature, curves (2) and (3) are the magnetization curves of Ni and Fe respectively in fields of 7000 gauss. These are theoretical curves calculated by Tyler's method. Assume that initially a nickel specimen is in the demagnetized condition at the Curie point (A). If now it is magnetized isothermally in a field of 7000 gauss the new condition will be represented by the point B.

Fig. 9.

Theoretical magnetization curves for iron and nickel.

The energy is given by the expression $E = \frac{1}{2}\sigma(H_1 + H_2)$, where $H_1 =$ intramolecular field and $H_2 =$ external field. At the Curie point H_1 is still very much greater than H_2, so that $E = \frac{1}{2}N\sigma^2$, where N is the intramolecular field constant. Thus the energy change is proportional to $\overline{BA}^2$.

If, however, the specimen is magnetized adiabatically the magnetized condition will be represented by a point C, the distance AD being proportional to the magneto-caloric rise of temperature. The energy change will be proportional to $\overline{CD}^2$. Calculated from these curves, and using the experi-

mental value AD, the ratio $\dfrac{\overline{BA}^2}{\overline{CD}^2} = 1\cdot20$, or the isothermal energy change is 20 per cent. greater than the adiabatic change. An estimate can also be made from the magnetization curves of Weiss and Forrer, in which case the difference between the two effects amounts to about 16 per cent. It does not, however, change very rapidly with temperature, so that the shape of the $(s\,.\,dT,\ T)$ curve is little affected. The ratio, calculated in the same way for iron and Heusler alloy, is very near the value for nickel, so that the only effect it has on the results of this paper is to reduce all the values of $s\,.\,dT$ in the same proportion.

Secondly, in the case of Heusler alloy there is an error in the resistance measurements. The temperature changes due to the magneto-caloric effect always introduce a change of resistance opposite in direction to the magneto-resistance change. Even though a certain time was allowed for dissipation of the heat generated on applying an external field the measured ΔR was certainly slightly less than the value for an isothermal change of the field. This error is appreciable only in the case of the alloy, which was in rod form. In the cases of iron and nickel the specimens were fine wires of such low heat capacity that the heat generated by the magneto-caloric effect was lost by radiation in a few seconds.

With only three values of $\dfrac{s\,.\,dT}{\Delta R/R}$ one hesitates to make suggestions as to the cause of its variation for the three substances. It is significant that the ratio increases with increasing Curie temperature. The relation is possibly of the form $s\,.\,dT = A\theta^n\Delta R/R$, where A and n are constants, n being about 3.

Summary and Conclusions.

Measurements have been made on the magneto-resistance and magneto-caloric effects in iron and Heusler alloy. Further evidence of the direct proportionality of the magneto-resistance change to the change in magnetic energy has been obtained, but it has been shown that the proportionality factor varies considerably for different substances.

XIX. *On the Variations in the Refractive Index of Benzene during Intensive Drying.* By J. J Manley, *M.A., D.Sc., Oxon, Fellow of Magdalen College, Oxford* *.

Introductory.

IT is well known that Prof. H. B. Baker has, by intensive drying, brought about notable changes in the boiling-point B.P. of benzene. Similar and equally interesting results have been obtained with certain other liquids, as, for example, carbon tetrachloride and hexane.

The observed variations in the B.P. lead, as I have already pointed out elsewhere †, to the almost inevitable conclusion that during drying, corresponding changes, although of a much smaller order, occur in the other physical "constants" of the liquid.

Now, if such changes can be detected and measured, we acquire additional and valuable data for elucidating the underlying cause of the growths in the B.P.

Preliminary experiments having shown that the expected variations in certain constants other than the B.P. do accompany the progressive and final dehydration of benzene, effect was given to plans made for accurate determinations of the same.

In this communication we confine ourselves chiefly to a consideration of certain variations which occur in the refractive index during the intensive drying of benzene. The changes in volume also resulting from prolonged dehydration will be dealt with in another paper. We first describe the purification of the benzene used as a standard.

Preparation of a Standard Benzene.

The benzene used as a standard in this research was of the purest obtainable. Shaken for a considerable time with concentrated sulphuric acid, the latter remained colourless; but frequent shaking for some days resulted in the production of a slight tint. After treating with sulphuric acid the benzene was washed, first with water, then with sodium hydrate solution, and finally with "conductivity" water. When it had been dried over fused and pure calcium chloride it was distilled, use being made of an apparatus previously rendered chemically clean and dry. Having

* Communicated by the Author.
† 'Nature,' cxxiii. p. 907 (1929).

rejected a first small portion *, the main distillate was collected and subsequently slowly cooled until about three-quarters of it had crystallized. The residual liquid was then drained away, the crystals liquefied, and the benzene thus repurified stored in a chemically clean and dry bottle ready for use.

The Refractive Index of Standard Benzene.

(1) *The Spectrometer and Prism.*—For measuring the refractive index μ of the standard benzene, there were available the Royal Society's spectrometer and hollow quartz prism employed in former researches †. The graduated silver circle of the spectrometer, some 27 cm. in diameter, was calibrated as described elsewhere ‡. With the aid of two attached reading-microscopes fitted with micrometers, angular values were determinable with an accuracy of 2″ of arc.

For securing the parallel-plane plates to the prism, a thick oleum of metaphosphoric acid was prepared from pure phosphorus pentoxide. The oleum was smeared along the edges of the prism, the plates applied and gently pressed, and the adhesive thus made to flow towards the centre. The flow was accelerated and completed by a "Hyvac" pump operating through the aperture made for charging the prism. Superfluous oleum having been removed, the edges of the joints were coated with Canada balsam; thus the oleum was prevented from deliquescing, and at the same time the adherence of the plates increased and rendered more permanent.

Next, the newly built prism was charged with standard benzene and the aperture closed with a glass cover-slip coated beneath with the prepared oleum. Lastly, a short glass tube was luted to the prism so that it encircled the cover-slip, and into this mercury was poured and the adhesive thus protected from moisture. The prism was then placed upon the levelling-table of the spectrometer. Subsequently its refracting angle was measured and found to be $60° 6' 12''$.

Determination of the Angle of Minimum Deviation for the D line.

It will be noted that, by closing the prism as described, direct observations of the temperature of the contents were

---

* The first portion is almost invariably milky. Apparently traces of water unremovable by calcium chloride are, as the distillation begins, concentrated in the vapour of the boiling liquid. The milkiness disappears on warming or on filtering through dry paper.

† Proc. Roy. Soc. lxix. p. 108.

‡ *Annalen der Physik*, pp. 575-579 (1901).

rendered impossible. The difficulty thus presented was met as follows :—A bottle, oval in form and having thick walls, was fitted with a thermometer graduated to $0°\cdot1$ C. and filled with benzene; it was then tightly corked and placed against the vertical base of the charged prism. Finally, the whole was enclosed by an aluminium cylinder, through the lid of which the thermometer stem projected. The two windows cut in the cylinder for the transmission of light could be shuttered at will.

The reliability of this plan for ascertaining the temperature of the benzene in the prism had previously been tested when, with water in both prism and bottle, the readings of a standard thermometer in each were during an extended period wholly consistent. Doubtless this was due not only to the effectiveness of the protecting aluminium cylinder, which was polished without and blackened within, but was also largely dependent upon the fact that the spectrometer was set up in a room facing N.E. and having the daily small temperature variation of 2° C.

When the spectrometer had been adjusted, tentative experiments were made to discover remediable imperfections. These having been corrected, twelve independent measurements of the minimum deviation of the D line were made. Of these, six were carried out during the morning and the remaining six during the evening of a day for which the maximum and minimum temperatures were respectively $18°$ and $16°$ C. and the mean temperature $16°\cdot70$ C. Within these limits the variation in μ for the standard benzene was $\cdot000610$ per $1°$ C. Using this coefficient, the twelve independent values for μ were each and all reduced for the temperature of $16°\cdot70$ C. and the final mean calculated. It was thus found that

$$\mu_{16\cdot7_{[D]}} = 1\cdot50377_1 \pm \cdot000007.$$

The variation of $\pm\cdot000007$ corresponds to an error in temperature of $\mp 0°\cdot01$ C.

In all that follows $1\cdot50377_1$ was used as the standard value for μ. A brief description may now be given of the plan adopted for measuring differentially the successive increments in μ during intensive drying.

Apparatus used for the Determination of the Variations in μ during Intensive Drying.

The accuracy attainable in determining μ by the prism method is not, according to my experience, greater than that represented by five units in the sixth place of decimals ; and

as this degree was in the present instance wholly insufficient, use was made of a **Jamin** interferometer. The instrument, built by Messrs. A. Hilger, had glass containing tubes 25 cm. long ; and owing to the inadmissibility of cements in general, the parallel-plane glass windows were of the adhesed or fused-on type. One great advantage of such tubes is that they can be safely cleaned by the most efficient methods.

As a result of some preliminary measurements it was deemed necessary for the purpose in hand to modify and elaborate the interferometer. The following changes were therefore made :—

(*a*) The beam of light passing to the interferometer was greatly reduced. This was done by substituting for the makers' aperture, some 18×12 mm. in diameter, one that was circular and 1 mm. only in diameter. This aperture was cut in a bright aluminium plate.

(*b*) A 25-watt lamp used with the instrument was surrounded by a screen, and a horizontal tube projecting from this was directed towards the interferometer. The tube was fitted with a diaphragm. Also a clear glass cylinder, filled with water, was suitably placed in front of the 1 mm. aperture. Possible heating effects were thus reduced to a minimum and the lamp-light concentrated.

(*c*) The interferometer tubes were enclosed by an aluminium cell, the walls of which were bright without and black within. The required light entered and left the tubes and their contents through small circular windows cut in the two ends of the cell. These windows were fitted with shutters.

(*d*) A fine adjustment of the lever-type was added to the compensator. The lever, having an effective length of 6 inches, was, as usual, controlled by a screw working in opposition to a spring.

(*e*) A small reading-microscope was set up in conjunction with the divided circle and its vernier. Angular measurements were thus readable with an accuracy of 3′ of arc.

These several modifications added much to the convenience of working and ensured greater precision.

Determination of a Zero Reading for Standard Benzene.

As a necessary step in the determination of the variations in μ during the intensive drying of benzene, both interferometer tubes were first filled with standard benzene and their tubulures closed with caps lubricated with metaphosphoric acid (*vide supra*) ; the tubes were then placed *in situ* and compensator readings taken at various temperatures. Theoretically these readings should be invariable. Practically,

slight differences appear. With due care such differences are, however, insignificant and wholly negligible. The mean value of the whole series of readings was accepted as the true one for the standard benzene ; and with this as zero all other and subsequent readings were compared.

One interferometer tube (henceforth termed the comparison tube) was now emptied and dried; it was then attached to the ground and lubricated junction of the terminal glass spiral of the drying apparatus (*vide infra*). The other interferometer tube was left undisturbed and its contents used throughout as the standard of reference.

Plan adopted for the Drying and Periodic Examination of Benzene.

In his papers dealing with the changes in the B.P. of benzene Prof. Baker has, with the aid of illustrative figures, fully described the apparatus used by him for intensive drying. In this research his methods have in principle been strictly adhered to ; hence a brief description, unaccompanied by drawings of my own apparatus will here suffice. The apparatus used for a first series of experiments was as follows :—

To the mouth of a globular flask was fused a vertical condenser, near the upper end of which was a long side-tube. This side-tube sloped upwards for a short distance and then passed vertically downwards through a water-jacket, below which it finally ended in a spiral—this to ensure flexibility. To the end of the spiral was fused a cap, accurately ground to fit the inlet of the comparison tube of the interferometer. The exit was also fitted with a ground-on glass cap to which was fused a drying-tube filled with phosphorus pentoxide *. Both caps were lubricated with the prepared oleum (*vide supra*), firmly seated, and then enveloped with mercury. These operations having been completed, the flask was then charged by first introducing a quantity of phosphorus pentoxide and then the required benzene. Finally, the apparatus was closed by first softening and then drawing off the upper and open extremity of the reflux condenser. For the purpose of heating, the flask was immersed in a bath of medicinal paraffin. Experiments were made in the following way :—

First, the bath was suitably heated and the benzene gently and continuously boiled for a known period †. Next, the

---

* The phosphorus pentoxide used in these experiments was purified by ozonized air, as described in the J. C. S. cxxi. pp. 331–337.

† Boiling was resorted to with the object of increasing the rate of drying.

reflux condenser was rendered ineffective and the benzene vapour allowed to pass over into the side-tube, wherein it was condensed by the action of the water-jacket and delivered into the empty comparison tube.

When this was full the reflux condenser was again activated and the residual benzene boiled for a second known period. At intervals during this second period interferometer readings were taken, and from the mean value of these was calculated the first increment in μ resulting from the treatment just described. The following example will assist in making the procedure clear :—

Experiment 1.

(*a*) Both interferometer tubes filled with standard benzene. $\Big\}$ Compensator micrometer reading. $\Big\}$ 81°·7

(*b*) Reference tube filled with standard benzene and comparison tube filled with first distillate. $\Bigg\}$ Compensator micrometer reading. $\Bigg\}$ 89°·0

Difference 7°·3

From a table of calibrations the difference 7°·3 was found to be the equivalent of n fringes in sodium light. Calculating the increment according to the formula

$$\mu_1 - \mu_0 = n\lambda/l,$$

in which μ_1 and μ_0 are the respective indices of the first distillate and the standard benzene, λ the wave-length of sodium light, and l the length of the interferometer tubes in cm., we have

$$\mu_1 - 1\cdot50377_1 = \frac{20\cdot2 \times 5890 \times 10^{-8}}{25} = 4759 \times 10^{-9} \text{ *}.$$

Having thus completed the first determination the second was continued and ended as follows :—
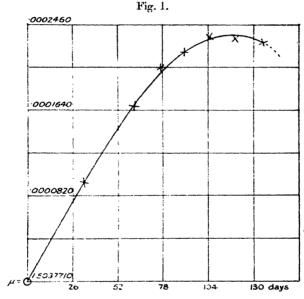
When the time assigned for the second period of boiling had elapsed the first distillate was quickly withdrawn from the comparison tube and the protecting drying-tube instantly re-attached to its tubulure. Another portion of benzene was then distilled and the comparison tube refilled. Subsequently the residual liquid was boiled during a third period ; and

---

* It was found that the temperature coefficients of the refractivities μ_0 and μ_1, $\mu_2 \ldots \mu_8$, were indistinguishable. Hence the differential method here employed and used throughout was wholly admissible.

whilst this was in progress new interferometer readings were taken. With the aid of these the second increment in μ was calculated as described above. Continuing thus, eight distillates were in the course of six months collected and the corresponding increments in μ determined. The results yielded by this series of experiments are shown graphically in fig. 1.

Second Determination of the Increments in μ.

The second series of experiments was carried out with a somewhat different and smaller apparatus. The new

Fig. 1.
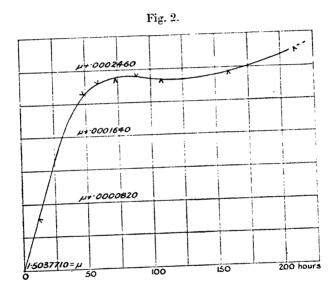
apparatus, like the other, included reflux and condensing systems. The benzene undergoing intensive drying could therefore be boiled for lengthy periods without appreciable loss, or be distilled into the comparison chamber of the interferometer. It differed, however, from the old in that the tube delivering the distillate just touched the floor of the comparison chamber and was in form capillary. Also the top of the reflux condenser, instead of being closed by fusing, was left open and fitted with a ground-in tube filled with phosphorus pentoxide. Under these circumstances the benzene which had been distilled could be re-transferred to the boiling-bulb by applying suction to the drying-tube.

The apparatus was rendered chemically clean and dry and then charged with standard benzene and phosphorus pentoxide: the drying-tube having been placed *in situ*, the second series of experiments was proceeded with and completed in accordance with the general procedure followed in the first series.

For these additional experiments the benzene was boiled for a total period of 200 hours and the distillates collected for the determination of the increments in μ at eight unequal but convenient intervals.

The results are graphically represented in fig. 2.

Fig. 2.

It may be noted that a chief advantage of the second plan lies in the fact that by its use great economy of time was effected; and that whereas in series 1, 100 days were required for the attainment by μ of a maximum value, in series 2 less than 70 hours sufficed for the same purpose. Doubtless this difference in time was partly due to the employment in the two cases of very dissimilar volumes of benzene. But it would appear that a second and contributory cause must have arisen; for in series 1 it was necessary before any one of the eight successive distillates could be withdrawn, to remove the drying-tube from the exit of the comparison chamber; and this, as Prof. Baker has clearly shown, would result in an almost immediate absorption of moisture. Thus

the time required for any given degree of intensive drying would be increased.

Next we observe that the character of the chief portion of the second graph (fig. 2) entirely conforms to that of the first (fig. 1). Hence the two are mutually confirmatory. From this we conclude that the small decline in growth which immediately follows the attainment of a maximum value by μ is to be regarded as real and not accidental.

Lastly, we have, from the terminal portion of the second graph, further evidence as to the effect produced upon μ by continued intensive drying ; and it will be seen that, after the slight decline just noted, the growth was resumed and was still proceeding when the experiments ended. Other experiments are now being made with the object of determining a limiting or major value for μ ; but in the light of Prof. Baker's work, the results cannot be known for some years to come. Meanwhile, those already obtained appear to merit publication without undue delay.

Dehydration of Benzene by Sodium and Potassium.

Having concluded the experiments just described an attempt was made to effect, by decomposing the retained water, a more rapid and possibly a more complete dehydration of benzene. For this purpose use was made of an apparatus precisely similar to that employed for the second series of experiments with phosphorus pentoxide. The procedure also was unchanged ; and therefore the two interferometer tubes were, at the outset, again filled with standard benzene and the zero of the instrument re-determined. Next, the comparison tube attached to the condenser was emptied and the new experiments commenced at a given moment by introducing into the benzene contained in the boiling-bulb some pellets of sodium *. The sodium caused an immediate but feeble evolution of gas from the calcium chloride-dried benzene ; and this persisted for some hours. The benzene was now boiled for a convenient time and then distilled into the empty interferometer chamber and the first increment in μ determined. Next, the distillate was drawn back into the bulb and boiled with the sodium

---

* For these experiments the pellets were prepared as follows :—First a piece of sodium was placed in benzene and its outer portions cut away. The metal was then repeatedly washed and finally covered with benzene : then it was cut into small pieces. Potassium pellets were prepared in the same way.

for a second period; and so on. Proceeding thus, μ assumed a constant value within about ten hours (fig. 3).

At this point the prepared potassium pellets were introduced, with the result that the evolution of hydrogen was renewed. Boiling was then resumed and the periodical measurements continued. During this additional treatment μ slowly increased and acquired a second maximum value within 140 hours. Lastly, the benzene was boiled with the sodium and potassium pellets (some of which had now formed a bright alloy), for a further period of 130 hours. In this way μ was slightly reduced. The observed reduction is,

Fig. 3.

however, consonant with the results obtained with phosphorus pentoxide in series 1 and 2. In fig. 3 the successive increments are as before, plotted against the corresponding intervals of time. On comparing the resultant graph with those of figs. 1 and 2, we see that the dehydrating powers of sodium and potassium are inferior to that of phosphorus pentoxide, and that the hoped for superiority was not realized.
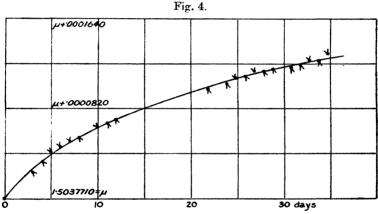
An experiment may now be described in which μ was gradually increased by the action of phosphorus pentoxide not in contact with the benzene. The experiment, the simplest possible, was as follows :—

Changes observed in μ during the Drying of Benzene Vapour.

To begin with, both interferometer chambers were charged with standard benzene, a series of compensator readings taken, and from these a mean value, regarded as zero, calculated.

Next, two drying-tubes, each filled with phosphorus pentoxide, were attached, the one to the inlet and the other to the outlet of the second interferometer chamber.

Lastly, compensator readings were again taken, now periodically, for the space of a month, the successive increments in μ determined, and the data thus obtained set out graphically (fig. 4),

Fig. 4.

In this experiment dehydration, as revealed by the continuously changing value in μ, must have been due to the passing of benzene vapour to and from the drying reagent and so back into the liquid. Under the circumstances it is perhaps surprising that μ was so markedly affected and that the growth was not irregular in form.

The next experiment to be dealt with is probably the most suggestive and informative of all.

Of the Temporary Value of μ following the Liquefaction of crystallized and partly dried Benzene.

The experiments now to be described were carried out with standard benzene made wet by shaking with " conduc-

tivity" water. Both interferometer tubes were filled with the wet liquid, placed *in situ,* and then used as follows:—

Firstly, a series of observations was taken and the zero of the instrument calculated.

Secondly, at a pre-determined moment, phosphorus pentoxide was introduced into the experimental tube, the contents shaken, and a new series of observations commenced, readings being taken at short intervals for about ten hours. These were followed by others taken daily. At the end of a week the daily growth in μ had become, for the purpose in hand, a negligible quantity.

Thirdly, it being winter, the room in which the experiments were being conducted was for a period left unheated. Consequently the temperature fell to about 2° C.; and as a result the partly-dried benzene became almost wholly crystalline, whilst the wet benzene remained entirely liquid. Attempts made to induce crystallization in the wet benzene ended in failure.

Fourthly, the experimental tube containing the crystallized benzene, was removed from the interferometer, momentarily immersed in water at 10° C., and then for a time tilted up and down, These last two operations were continuously alternated until no crystals remained. Liquefaction was thus effected at a temperature differing but slightly from the melting-point.

Finally, the experimental tube containing the liquefied benzene was replaced in the interferometer and observations again taken at short intervals until further changes in μ were insignificant. The results thus obtained are depicted in fig. 5.

In order that the legitimate conclusions, to which this graph rightly understood, leads, a few remarks may be ventured as to the conditions governing the behaviour of the benzene.

First, we observe that although care was taken to liquefy the crystals at the lowest temperature possible, there must inevitably have been some fleeting upward movements in the temperature of the liquid ; and this upward trend would be the greatest and most prolonged just at the time the last vestige of the crystalline mass became liquid. Up to that moment any slight rise in temperature would be quickly and automatically corrected by the melting benzene. Hence a determination of μ following *instantly* upon complete liquefaction, would, if measured as before in terms of the standard benzene, reveal a distinct *lessening* in value. Such a temporary depression is actually shown by the portion B C

of our graph. That this view is true will be readily granted when it is remembered that a variation of 1° C. corresponds to a change in μ of ·00066. The depression BC is equivalent to a temperature in excess of that of the standard benzene, approximating 0°·03 C. (The whole limb, CP, corresponds to about 0°·43 C.)

Secondly, viewing the graph as a whole, and for the moment neglecting the effect of temperature, we conclude that, on slowly melting dried and crystallized benzene, some
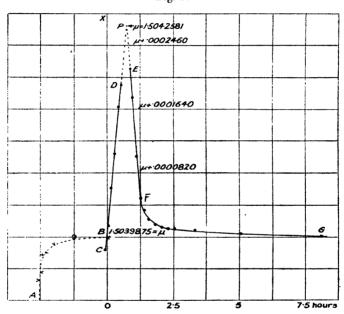
Fig. 5.

fraction of the resultant liquid consists of molecular assemblages of unusual complexity and density. Further, from the limb EG of the graph, we conclude that such assemblages, when produced as here, within *partially* dried benzene, are, owing to the disintegrating influence of residual water, more or less quickly resolved into others less dense but stable. We have no evidence of the existence of the more closely packed assemblages within wet benzene; but that before us seems clearly to indicate that as dehydration proceeds the denser assemblages are continuously formed, and that in number a maximum and permanent value is reached

with the withdrawal of the last trace of water. It will therefore be seen that if this interpretation of the results obtained interferometrically be true, then the cause of the rise in the B.P. resulting from an intensive drying of benzene is at once apparent.

Discussion of the Results.

We now take a brief review of the whole graph (fig. 5). The depression BC has already been sufficiently dealt with, and from what has been said as to the cause of the depression it will be evident that the ascending value of μ, as represented by BD, is due to a final readjustment of the temperature of the liquid benzene, following the introduction of the tube into the interferometer. The limb EFG is quite obviously representative of the rate of disintegration of the exceptionally massive assemblages already referred to. Also it will be seen that within the eight hours immediately following the complete liquefaction of the partially dried and crystallized benzene and whilst the temperature of the laboratory remained at 5° C., the whole of these assemblages, as shown by the decrease in the value of μ, had reverted to normal ones. Extrapolating both limbs of the graph, intersection occurs at P : whence a major value for μ is determinable and found to be 1·5042581, and this shows a maximum temporary increase of ·0002706. Left thus, our review would be incomplete, for upon reflection it would appear that, in respect of the more massive molecular assemblages, disintegration sets in immediately after the liquefaction of the solid benzene. Owing, however, to the initial small changes in the temperature already mentioned, the effect is not at once apparent. We approach more nearly to the true temporary value of μ by extrapolating FE in the direction of P until the curve intersects the axis OX. Doing this, we then find the increment in μ ·0006052 ; and this value is 2·23 times greater than that corresponding to the apex P. But even this new and larger increment is probably too small, for in a curve of the type shown in fig. 5 the first or upper portion is more steeply inclined than is the limb FE. Whence it follows that the altitude attained by extrapolating FE is less than the characteristic one. Consequently the true increment is greater than ·0006052, and the number of the transient and more optically dense molecules of benzene larger than a cursory glance at the graph (fig. 5) might lead one to expect. For a fuller and more critical investigation a new interferometer has been designed and built. In due course we

therefore hope to publish the results of some additional experiments which have been projected. A few brief remarks may now be made upon some observed variations in the B.P.

Variation in the B.P. during Intensive Drying.

During the progress of the several experiments with phosphorus pentoxide, and also with sodium and potassium, periodic measurements of the B.P. of the benzene were carried out and reduced for N.P.

In the case of phosphorus pentoxide there were seventeen determinations. The maximum value observed was 81°·35.

Whilst experimenting with sodium and potassium nineteen determinations of the B.P. were made. The highest value was 82°·02, the lowest 81°·28, and the mean of the whole 81°·56 C.

In both series of experiments the changes in the B.P. were chiefly irregular ; hence the impossibility of correlating them with time-intervals.

Upon one occasion only was there any well-marked *increase* in the B.P. This was observed whilst distilling benzene in the presence of sodium. The distillation commenced and continued for some time at a normal rate, whilst the liquid was to all appearance perfectly quiescent and the B.P. quite steady at 84° C. Finally, however, the benzene boiled up suddenly and the temperature fell to 82°·3 C. The pressure at the time happened to be almost exactly normal.

The above-named facts illustrate the erratic nature of B.P. determinations made during the *earlier* stages of intensive drying. They also assist in accounting for the divergences of the conclusions reached by researchers who have attempted a repetition of the original investigation. We conclude with a word upon the relative effectiveness of certain drying reagents.

Note upon the relative Dehydrating Effects of certain Reagents.
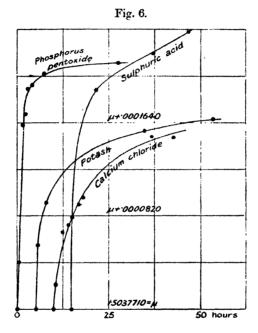
In connexion with this research it seemed desirable to compare the dehydrating effects of granular calcium chloride, and also of newly re-fused potash, with those of our pure phosphorus pentoxide. Accordingly the following experiments were made :—

Firstly, both interferometer tubes were filled with pure, but in this case damp, benzene, and the zero of the instrument determined.

Secondly, at a known moment, one of the drying reagents was dropped into the experimental tube of the interferometer and the contents agitated. Later, the increment in μ was measured and the time noted. Then the tube was again shaken and the growth in μ re-measured. Proceeding thus, experiments were continued until further changes were negligible.

Thirdly, the experimental tube was emptied, washed, and dried ; then it was re-charged, and the effect upon μ of a

Fig. 6.

second dehydrating reagent determined. The results of the several tests are graphically shown in fig. 6. It will be seen that as a drying reagent calcium chloride is inferior to potash. The effects produced by sulphuric acid are interesting ; and at first it might appear that the dehydrating power of the acid is fully equal if not superior to that of phosphorus pentoxide. The true drying effect, is, however, in some degree masked by the formation and consequent presence of benzenesulphonic acid, a minute quantity of which would augment the value of μ.

The Gables,
    Littledown Avenue,
      Bournemouth.

XX. *The Magneto-Optical Dispersion of Organic Liquids in the Ultra-violet Region of the Spectrum.*—Part IV. *The Magneto-Optical Dispersion of Acetic Anhydride, Normal Butyric Acid, and Normal Ethyl Butyrate.* By W. J. LEWIS, *B.Sc.*, *and* Prof. E. J. EVANS, *D.Sc.*, *Physics Department, University College of Swansea* *.

THE apparatus and experimental methods employed in these investigations have been described in detail in Part I. †, and consequently only a brief reference to these points is necessary.

The light from a tungsten arc falls on a Bellingham-Stanley polarizing unit designed for work in the ultra-violet, and then traverses the liquid contained in a quartz polarimeter tube, which is placed symmetrically inside the core of a solenoid. The polarized beam, after emerging from the liquid, passes through the analyser and a quartz fluorite lens, which brings it to a focus on the slit of a quartz spectrograph. As the beam of light emerging from the polarizer consists of two semicircular fields with a horizontal line of demarcation, the vibrations in one of the fields being polarized at a slight angle with those in the other, two spectra (one immediately above the other) are obtained at the camera end of the quartz spectrograph.

The analyser is set at zero by adjusting its position so that these two spectra have the same intensity throughout their length when the magnetic field of the solenoid is not excited. There are four positions of the analyser for which this is possible ; but one of the two positions of minimum intensity is chosen, as the polarimeter is then in its most sensitive position. The analyser is then rotated through an angle θ, and a photograph taken with the magnetic field excited. A second photograph was also taken on the same plate, corresponding to a rotation θ on the opposite side of the zero with the magnetic field reversed. An examination of the photograph plate shows that there is a line of definite wave-length, which has the same intensity in the upper and lower half of each spectrum. Let λ be the mean wavelength of this line, as determined from the photograph, and θ_1 the rotation at this wave-length due to the quartz ends of the polarimeter tube : then the value of Verdet's

---

* Communicated by the Authors.

† Stephens and Evans, Phil. Mag. x. p. 759 (1930).

constant δ of the liquid for wave-length λ is given by the equation

$$\theta_2 = \theta - \theta_1 = \delta \Sigma H l,$$

where the summation is taken over the length of the liquid column. The current passing through the solenoid was kept constant at two amperes, and the magnetic field H at different points along the axis of the solenoid had been accurately measured. The value of $\Sigma H l$ was 12270 cm. gauss.

The refractive indices of the three liquids in the visible region of the spectrum were determined by means of an accurate spectrometer in the usual manner, and in the ultra-violet region of the spectrum photographically by means of the quartz spectrograph in which the Cornu prism had been replaced by a hollow glass prism closed by plates of optically worked fused quartz.

The results obtained by the two methods overlapped over a region of the visible spectrum. The mode of procedure in the photographic determinations was as follows :—

Three slightly overlapping copper spectra were photographed with the hollow prism filled with (a) the standard liquid, (b) the liquid under investigation, and (c) the standard liquid. The standard liquid employed was normal butyl alcohol, whose refractive indices in the visible and ultra-violet regions of the spectrum had been determined by Stephens and Evans *. The refractive index of the liquid under investigation for a wave-length λ_2 can be determined by identifying, in the spectrum produced by the standard liquid, a line of wave-length λ_1, which coincides in position with the line of wave-length λ_2 in the spectrum of the liquid under investigation. Then the refractive index of the liquid for a wave-length λ_2 equals the refractive index of the standard liquid for the wave-length λ_1. The temperatures of the liquids were determined immediately after each exposure by means of a small calibrated mercury thermometer, and the slight shifts in the positions of the spectra were due to small temperature changes. The values of the temperature coefficients of refractive index of each liquid were found by taking photographs of two slightly overlapping copper spectra by means of the hollow prism containing the particular liquid at two known temperatures. From the resulting displacements in the positions of the

* *Loc. cit.*

spectrum lines the temperature coefficients corresponding to different regions of the spectrum could be determined. From a knowledge of the temperature coefficients the refractive indices of the liquids at temperatures differing by a few degrees from those at which they were determined could be calculated.

The liquids employed in this investigation were obtained from Dr. Schuchardt, of Görlitz, and each was subjected to a process of fractional distillation before determinations were made of the refractive indices and the magneto-optical rotations.

The experimental results have been examined in relation to Larmor's * theory of magneto-optical rotation. According to this theory Verdet's constant δ is given by the expression

$$\delta = \frac{e}{2mC^2} \cdot \lambda \cdot \frac{dn}{d\lambda}, \quad \cdots \quad (1)$$

where n is the refractive index, $\frac{e}{m}$ is the ratio of the charge to the mass of the resonators, and C the velocity of light. In the above expression the charge e is measured in electrostatic units and the magnetic field in electromagnetic units.

If the magneto-optical dispersion of each of the liquids in the region of the spectrum investigated is controlled by one absorption band in the ultra-violet, and the natural dispersion by an equation of the Ketteler-Helmholtz type, it can be shown that

$$\phi = n\delta\lambda^2 = K \left(\frac{\lambda^2}{\lambda^2 - \lambda_1^2} \right)^2, \quad \cdots \quad (2)$$

where K is a constant and λ_1 the wave-length of the absorption band in the ultra-violet.

In addition, it can be shown by combining equations (1) and (2) and the natural dispersion equation

$$n^2 - 1 = b_0 + \frac{b_1}{\lambda^2 - \lambda_1^2}, \quad \cdots \quad (3)$$

that the value of $\frac{e}{m}$ is given by $-\dfrac{2KC^2}{b_1}$.

---

* Larmor, ' Æther and Matter,' Appendix F.

EXPERIMENTAL RESULTS.

Natural Dispersion.

TABLE I. (*a*).

Visual Determinations.

Wave-length in microns.	Refractive indices.		
	Acetic anhydride at 16° C.	Ethyl butyrate at 13° C.	Butyric acid at 13° C.
·6678	1·3897	1·3936$_6$	1·3988
·5876	1·3920	1·3958$_2$	1·4011
·5016	1·3959	1·3996	1·4051
·4922	1·3966	1·4002$_6$	1·4057
·4713	1·3978	1·4015	1·4070
·4472	1·3995$_5$	1·4032$_5$	1·4086

TABLE I. (*b*).

Photographic Determinations.
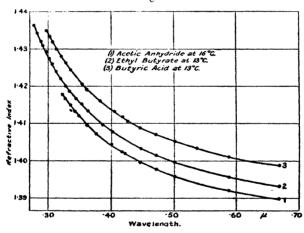
Normal Butyl Alcohol as standard.

Acetic anhydride at 16° C.		Ethyl butyrate at 13° C.		Butyric acid at 13° O.	
Wave-length in microns.	Refractive index.	Wave-length in microns.	Refractive index.	Wave-length in microns.	Refractive index.
·4226	1·4018	·4475	1·4032	·5359	1·4034
·4168	1·4023	·4212	1·4056	·4866	1·4060
·4007	1·4042$_4$	·4020	1·4077	·4651	1·4074
·3985	1·4044	·3978	1·4080	·4587	1·4078
·3759	1·4073	·3923	1·4087	·4508	1·4083
·3676	1·4085	·3860	1·4095	·4378	1·4093
·3618	1·4095	·3688	1·4120	·4260	1·4104
·3547	1·4108	·3618	1·4131	·4178	1·4113
·3493	1·4117$_5$	·3523	1·4150	·4049	1·4129
·3435	1·4131	·3413	1·4169	·3924	1·4144
·3360	1·4147	·3337	1·4184	·3824	1·4157
·3274	1·4164	·3274	1·4198	·3734	1·4169
·3220	1·4174	·3195	1·4219	·3600	1·4188
		·3126	1·4237	·3530	1·4202
		·3063	1·4257	·3464	1·4214
		·3010	1·4272	·3348	1·4241
		·2961	1·4289 .	·3274	1·4258
		·2883	1·4316	·3195	1·4277
		·2824	1·4338	·3126	1·4298
		·2766	1·4359	·3063	1·4315
				·3010	1·4330
				·2961	1·4346

TABLE I. (c).

	Wave-length in microns.	Temperature coefficient of refractive index.
Acetic anhydride	·4500	·00040 per ° C.
	·2961	·00044 ,,
Ethyl butyrate	·5100	·00041 ,,
	·3200	·00043 ,,
Butyric acid	·4560	·00040$_2$,,
	·3100	·00043$_2$,,
Normal butyl alcohol .	·4600	·00040 ,,
	·3200	·00043$_5$,,

Fig. 1.

(1) *Acetic Anhydride at 16°C.*
(2) *Ethyl Butyrate at 13°C.*
(3) *Butyric Acid at 13°C.*

Refractive indices.

Magneto-Optical Dispersion.

Acetic Anhydride.
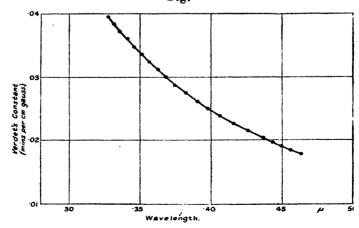
The specimen of acetic anhydride employed for the magneto-optical experiments distilled over between 139·3°C. and 139·8° C. at a pressure of 763 mm. of mercury, its correct normal boiling-point being 139·6° C. The experimental results are given in Table II. (a) and fig. 2.

Table II. (b) gives a series of values of n, the refractive index, and δ, Verdet's constant, taken from fig. 1 and

TABLE II. (a).

Temperature in ° C.	Wave-length in microns.	Verdet's constant in min./cm. gauss.
16	·4633	·0180$_0$
16	·4563	·0186$_8$
16·1	·4495	·0192$_0$
16·1	·4429	·0198$_0$
16	·4370	·0204$_0$
16	·4260	·0216$_0$
16·1	·4158	·0228$_0$
16	·4065	·0240$_0$
16	·3975	·0252$_0$
16	·3897	·0264$_0$
16	·3820	·0276$_1$
16	·3743	·0288$_1$
16	·3679	·0300$_5$
16	·3621	·0312$_1$
16·1	·3562	·0324$_1$
16	·3506	·0336$_1$
16	·3454	·0348$_1$
16	·3406	·0360$_0$
16	·3358	·0372$_3$
15·9	·3314	·0384$_1$
15·9	·3274	·0396$_1$

Fig.

Magnetic rotary dispersion of acetic anhydride at 16° C.

Table II. (a) respectively. It was found that the experimental results could be represented by a formula of the type

$$\phi = n\delta\lambda^2 = \mathrm{K}\left(\frac{\lambda^2}{\lambda^2-\lambda_1^2}\right)^2,$$

and from several pairs of values of ϕ and λ the values of λ_1 and K were obtained.

TABLE II. (b).

	λ in microns.	n.	δ in min./cm. gauss.
(a)	·4495	1·3993	·0192$_0$
(b)	·4260	1·4014	·0216$_0$
(c)	·4065	1·4035	·0240$_0$
(d)	·3406	1·4138	·0360$_0$
(e)	·3314	1·4157	·0384$_1$

The values of the function ϕ were calculated for each wave-length, and the following pairs used to obtain the constants :—

From (a) and (c) $\lambda_1 = \cdot1029\,\mu$ and $\mathrm{K} = 4\cdot875_4 \times 10^{-3}$.

,, (b) ,, (d) $\lambda_1 = \cdot1035\,\mu$,, $\mathrm{K} = 4\cdot863 \times 10^{-3}$.

,, (c) ,, (e) $\lambda_1 = \cdot1030\,\mu$,, $\mathrm{K} = 4\cdot874_7 \times 10^{-3}$.

,, (a) ,, (e) $\lambda_1 = \cdot1031\,\mu$,, $\mathrm{K} = 4\cdot872_4 \times 10^{-3}$.

The mean values of λ_1 and K are $\cdot1031\,\mu$ and $4\cdot871_4 \times 10^{-3}$ respectively, δ being measured in minutes per cm. gauss, and λ in microns.

Thus the equation representing the magneto-optical dispersion of acetic anhydride for the range of the spectrum investigated ($\cdot4633\,\mu$ to $\cdot3275\,\mu$) is

$$n\delta = 4\cdot871_4 \times 10^{-3} \cdot \frac{\lambda^2}{\{\lambda^2-(\cdot1031)^2\}^2}.$$

This equation was used to calculate the values of δ for other wave-lengths where experimental determinations had been carried out. The values of n were read off from fig. 1.

The value of δ, calculated from the equation, for sodium light is $\cdot01072_4$ at 16° C., and assuming that the value of Verdet's constant of water at $\cdot5893\,\mu$ is $\cdot0131$, the specific rotation of acetic anhydride relative to water is $\cdot818_4$.

TABLE II. (c).
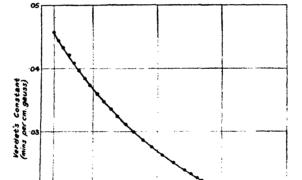
λ (microns).	δ (observed).	δ (calculated).
·4633	·0180$_0$	·0179$_7$
·4563	·0186$_0$	·0185$_8$
·4370	·0204$_0$	·0204$_2$
.4158	·0228$_0$	·0228$_1$
·3897	·0264$_0$	·0263$_9$
·3679	·0300$_5$	·0301$_0$
·3506	·0336$_1$	·0336$_4$
·3358	·0372$_1$	·0372$_2$
·3274	·0396$_1$	·0395$_4$

Normal Butyric Acid.

The butyric acid employed in the determination of Verdet's constant distilled over between 162·3° C. and 162·6° C. at a

Fig. 3.

Magnetic rotary dispersion of butyric acid at 13° C.

pressure of 758 mm. of mercury, its true normal boiling-point being 162·5° C. The experimental results are given in Table III. (*a*) and plotted in fig. 3.

In Table III. (*b*) values of Verdet's constant and the refractive indices corresponding to certain wave-lengths are given. These were employed to calculate the constants of the magneto-optical dispersion equation for butyric acid.

TABLE III. (a).

Temperature in ° C.	Wave-length in microns.	Verdet's constant in min./cm. gauss.
13·1	·4802	·0180$_3$
13	·4663	·0192$_3$
13·1	·4593	·0198$_7$
12·9	·4535	·0204$_3$
13·1	·4472	·0210$_3$
13·1	·4419	·0216$_4$
13·2	·4358	·0223$_5$
13·1	·4316	·0228$_4$
13·2	·4265	·0234$_8$
13·1	·4217	·0240$_4$
13·3	·4128	·0252$_4$
13·1	·4041	·0264$_4$
13·1	·3960	·0276$_4$
13·1	·3889	·0288$_6$
13·1	·3818	·0300$_6$
13	·3755	·0312$_6$
13·2	·3683	·0324$_8$
13	·3638	·0336$_7$
13·1	·3585	·0348$_7$
13	·3532	·0360$_7$
13·1	·3483	·0372$_9$
13·1	·3437	·0384$_7$
13	·3393	·0396$_8$
13·1	·3353	·0408$_8$
13·2	·3312	·0420$_8$
13·1	·3272	·0432$_8$
15·1	·3236	·0444$_9$
13·1	·3202	·0456$_9$

TABLE III. (b).

	Wave-length in microns.	Verdet's constant.	Refractive index, n.
(a)	·4419	·0216$_4$	1·4090
(b)	·4041	·0264$_4$	1·4129$_6$
(c)	·3638	·0336$_7$	1·4183$_3$
(d)	·3272	·0432$_8$	1·4258

From (a) and (b) $\lambda_1 = ·1065\ \mu$ and $K = 5·28_2 \times 10^{-3}$.

„ (b) „ (c) $\lambda_1 = ·1068\ \mu$ „ $K = 5·27_7 \times 10^{-3}$.

„ (c) „ (d) $\lambda_1 = ·1059\ \mu$ „ $K = 5·29_6 \times 10^{-3}$.

„ (a) „ (d) $\lambda_1 = ·1063\ \mu$ „ $K = 5·28_4 \times 10^{-3}$.

The mean values of λ_1 and K are $\cdot1064 \mu$ and $5\cdot28_5 \times 10^{-2}$ respectively, and the equation representing the magneto-optical dispersion of normal butyric acid over the region of the spectrum investigated ($\cdot4802 \mu$ to $\cdot3208 \mu$) is

$$n\delta = 5\cdot28_5 \times 10^{-3} \cdot \frac{\lambda^2}{\{\lambda^2 - (\cdot1064)^2\}^2} \cdot$$

This equation was used to calculate δ for a few wavelengths at which experimental determinations had been carried out. The values of n used were read off from fig. 1. Table III. (c) shows a comparison of the observed and calculated values.

The equation was also employed to calculate Verdet's constant for sodium light, and the value obtained $= \cdot0116_1$

Table III. (c).

λ (in microns).	δ (observed).	δ (calculated).
$\cdot4802$	$\cdot0180_3$	$\cdot0180_3$
$\cdot4535$	$\cdot0204_3$	$\cdot0204_4$
$\cdot4316$	$\cdot0228_4$	$\cdot0228_1$
$\cdot4128$	$\cdot0252_4$	$\cdot0252_1$
$\cdot3818$	$\cdot0300_6$	$\cdot0301_0$
$\cdot3532$	$\cdot0360_7$	$.0360_6$
$\cdot3353$	$\cdot0408_8$	$\cdot0408_1$
$\cdot3202$	$\cdot0456$	$\cdot0456_3$

at $13\cdot1^\circ$ C. Perkin * found the specific rotation of butyric acid to be $\cdot8803$ at $19\cdot9^\circ$ C. and $\cdot8826$ at 18° C. Assuming the temperature coefficient deduced from these results, the value of the specific rotation at 13° C. is $\cdot888$, and taking the value of Verdet's constant of water for sodium light to be $\cdot0131$, the value deduced from Perkin's results is $\cdot01163$. This compares satisfactorily with the value $\cdot0116_1$ calculated from the equation.

Lowry and Dickson †, who determined the magnetic rotations of butyric acid for a number of wave-lengths in the visible spectrum, have compared the rotary powers at various wave-lengths with that at $\lambda = \cdot5461 \mu$. A comparison of their results with those calculated from the magneto-optical dispersion equation, which represents the present results, is given in Table III. (d).

---

* Journ. Chem. Soc. i. p. 483 (1884).
† Journ. Chem. Soc. ciii. p. 1067 (1913).

TABLE III. (d).

Wave-length in microns.	Magnetic rotary power relative to that at ·5161 μ.	
	Lowry and Dickson.	Present results.
·6708	·645	·647
·5893	·853	·850
·4359	1·634	1·634

Normal Ethyl Butyrate.

The ethyl butyrate employed for the determination of the magneto-optical rotations distilled over at the correct normal
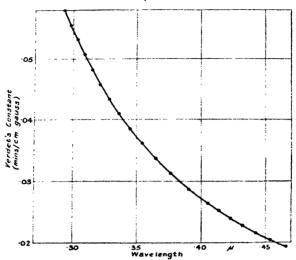
TABLE IV. (a).

Temperature in ° C.	Wave-length in microns.	Verdet's constant in min./cm. gauss.
12·9	·4669	·0192$_8$
13·3	·4542	·0204$_3$
13·1	·4427	·0216$_3$
13·2	·4320	·0228$_4$
13	·4224	·0240$_4$
13·1	·4134	·0252$_4$
13·1	·4050	·0264$_4$
13·1	·3899	·0288$_6$
13·1	·3763	·0312$_6$
13·1	·3648	·0336$_7$
13·2	·3541	·0360$_7$
13·2	·3445	·0384$_7$
13·1	·3360	·0408$_8$
13·1	·3282	·0432$_8$
13·1	·3210	·0456$_9$
13·1	·3144	·0480$_9$
13·1	·3082	·0505$_0$
13·1	·3026	·0529$_0$
13·1	·2973	·0553$_1$
13·1	·2925	·0577$_2$

boiling-point 121·4° C. when the pressure was 761 mm. of mercury. The experimental results are given in Table IV.(*a*) and fig. 4.

Table IV.(*b*) contains results read off from fig. 1 and Table IV.(*a*), and these were made use of in solving the magneto-optical dispersion equation.

Fig. 4.

Magnetic rotary dispersion of ethyl butyrate at $13°$ C

TABLE IV. (b).

	Wave-length in microns.	Refractive index, n.	Verdet's constant in min./cm. gauss.
(a)	·4427	1·4036	·0216$_9$
(b)	·3763	1·4110	·0312$_6$
(c)	·3541	1·4146$_4$	·0360$_7$
(d)	·2925	1·4299	·0577$_2$

From (a) and (b) $\lambda_1 = ·1073 \mu$ and $K = 5·272 \times 10^{-3}$.

„ (a) „ (c) $\lambda_1 = ·1080_3 \mu$ „ $K = 5·262 \times 10^{-3}$.

„ (b) „ (d) $\lambda_1 = ·1086 \mu$ „ $K = 5·249 \times 10^{-3}$.

„ (c) „ (d) $\lambda_1 = ·1085 \mu$ „ $K = 5·252 \times 10^{-3}$.

„ (a) „ (d) $\lambda_1 = ·1082_4 \mu$ „ $K = 5·260 \times 10^{-3}$.

The mean value of $\lambda_1 = ·1081 \mu$ and $K = 5·25_9 \times 10^{-3}$, and the equation representing the magneto-optical dispersion of ethyl butyrate over the region ·4669 μ to ·2925 μ is

$$n\delta = 5·25_9 \times 10^{-3} \frac{\lambda^2}{\{\lambda^2 - (·1081)^2\}^2}.$$

The accuracy of the representation of the results by the equation is shown in Table IV. (c), where a comparison is

made of the experimental values of Verdet's constant and
the values calculated from the equation.

TABLE IV. (c).

λ (microns).	δ (observed).	δ (calculated).
·4669	·0192$_3$	·0192$_1$
·4224	·0240$_4$	·0240$_2$
·3648	·0336$_7$	·0336$_2$
·3360	·0408$_8$	·0408$_7$
·3210	·0456$_9$	·0456$_7$
·3026	·0529$_4$	·0529$_0$
·2973	·0553$_1$	·0553$_1$

The value of Verdet's constant for sodium light calculated
from the above equation is ·0116$_2$ at 13·1° C. Perkin[*] has
measured the specific rotation of ethyl butyrate relative to
water, and found the value to be ·8889 at 13° C. Taking the
value of Verdet's constant for water to be ·0131, the value
of Verdet's constant for ethyl butyrate at 13° C. is ·01164.
This is in good agreement with the value calculated above.

The Natural Dispersion Equations.

The experimental results have shown that the magneto-
optical dispersion of each liquid over the range of the
spectrum investigated can be explained by the presence of a
single absorption band. A satisfactory natural dispersion
equation can be obtained for each of these liquids if the
assumption is now made that the same absorption band is
responsible for the natural dispersion of the liquid over the
same range of wave-length.

The constants of the equation of the form

$$n^2 - 1 = b_0 + \frac{b_1}{\lambda^2 - \lambda_1^2}$$

can be obtained from two values of the refractive index
corresponding to two wave-lengths.

Acetic Anhydride.

The mean values of b_1 and b_0 are ·921$_3 \times 10^{-10}$ and ·9101$_8$
respectively, and the natural dispersion equation of acetic
anhydride is

$$n^2 = 1·9101_8 + \frac{·921_3 \times 10^{-10}}{\lambda^2 - (1·031 \times 10^{-5})^2}.$$

[*] Journ. Chem. Soc. i. p. 499 (1884).

The pairs of values used are given below :—

TABLE V. (a).

λ (cm. $\times 10^5$).	*n*.	b_1.	b_0.
6·678	1·3897		
4·226	1·4017$_8$	·922$_2 \times 10^{-10}$	·9100$_3$
5·016	1·3959		
3·493	1·4117$_5$	·921$_7 \times 10^{-10}$	·9102$_0$
4·472	1·3995$_5$		
3·220	1·4174	·920$_0 \times 10^{-10}$	·9101$_6$

This equation was used to calculate *n* for a number of wave-lengths where experimental values had been obtained. Table V. (*b*) contains a comparison of the calulated and experimental values.

TABLE V. (*b*).

λ (microns).	*n* (observed).	*n* (calculated).
·5876	1·3920	1·3920
·4922	1·3966	1·3964
·4713	1·3978	1·3977$_7$
·4168	1·4023	1·4024
·3985	1·4044	1·4044
·3547	1·4107$_6$	1·4107$_4$
·3435	1·4131	1·4128
·3274	1·4164	1·4162

Butyric Acid.

The constants b_1 and b_0 of the natural dispersion equation for butyric acid were calculated from the pairs of values given in the following table :—

TABLE VI. (a).

λ (cm. $\times 10^5$).	*n*.	b_1.	b_0.
6·678	1·3988		
4·508	1·4083	·916$_5 \times 10^{-10}$	·9355$_6$
5·876	1·4011		
3·924	1·4144	·932$_0 \times 10^{-10}$	·9351$_6$
5·016	1·4051		
3·530	1·4202	·914$_5 \times 10^{-10}$	·9362$_4$
4·713	1·4070		
3·010	1·4330	·938$_3 \times 1^{-1}$	·9351$_4$
4·472	1·4086		
2·961	1·4346	·948$_1 \times 10^{-10}$	·9339$_1$

The mean value of $b_1 = \cdot930_0 \times 10^{-10}$ and of $b_0 = \cdot9352_0$, and the equation representing the natural dispersion of butyric acid is

$$n^2 = 1\cdot9352_0 + \frac{\cdot930_0 \times 10^{-10}}{\lambda^2 - (1\cdot064 \times 10^{-5})^2}.$$

Values of n calculated from this equation are compared in Table VI.(*b*). with the observed values at certain wavelengths.

TABLE VI. (*b*).

λ (microns).	n (observed).	n (calculated).
·5359	1·4034	1·4032
·4922	1·4057	1·4055
·4651	1·4074	1·4073
·4178	1·4113	1·4114
·3734	1·4169	1·4170
·3464	1·4214	1·4216
·3274	1·4258	1·4256
·3063	1·4315	1·4311

Ethyl Butyrate.

The following pairs of values of the refractive indices were used in calculating the constants of the natural dispersion equation for ethyl butyrate :—

TABLE VII. (*a*).

λ (cm. × 10⁵).	n.	b_1.	b_0.
6·678	1·3936₆	$\cdot900_6 \times 10^{-10}$	·9215₅
4·020	1·4077		
5·876	1·3958₂	$\cdot900_5 \times 10^{-10}$	·9213₂
3·618	1·4131		
5·016	1·3996	$\cdot912_6 \times 10^{-10}$	·9208₁
3·126	1·4237		
4·713	1·4015	$\cdot921_3 \times 10^{-10}$	·9204₂
2·824	1·4338		
4·472	1·4032₅	$\cdot916_3 \times 10^{-10}$	·9204₅
2·766	1·4359		

The mean values of b_1 and b_0 are $\cdot910_3 \times 10^{-10}$ and $\cdot9209_2$ respectively, and the natural dispersion equation is

$$n^2 = 1\cdot9209_2 + \frac{\cdot910_3 \times 10^{-10}}{\lambda^2 - (1\cdot081 \times 10^{-5})^2}.$$

Table VII. (*b*) contains a comparison of the observed results at certain wave-lengths and the values calculated from the above equation.

TABLE VII. (*b*).

λ (microns).	*n* (observed).	*n* (calculated).
·4922	1·4002$_8$	1·4001$_4$
·4475	1·4032	1·4033
·3860	1·4095	1·4097
·3413	1·4169	1·4170
·3274	1·4198	1·4199
·3063	1·4257	1·4255
·2961	1·4289	1·4286

CALCULATION OF $\dfrac{e}{m}$.

As pointed out in the introduction, the value of $\dfrac{e}{m}$ can be obtained from the relation

$$\frac{e}{m} = -\frac{2C^{\prime 2}K}{b_1}.$$

The values of K given in this paper have been calculated when δ is expressed in minutes per cm. gauss and λ in microns. For the purpose of evaluating $\dfrac{e}{m}$ from the above equation the values of K must be calculated when δ is expressed in radians per cm. gauss and λ in cm. The absolute values of K for acetic anhydride, butyric acid, and ethyl butyrate are $1·417 \times 10^{-14}$, $1·537_3 \times 10^{-14}$, and $1·529_8 \times 10^{-14}$ respectively. The corresponding values of b_1 are $·921_3 \times 10^{-10}$, $·930_0 \times 10^{-10}$, and $·910_3 \times 10^{-10}$. On substituting these in the above equation the calculated values of $\dfrac{e}{m}$ for acetic anhydride, butyric acid, and ethyl butyrate are $·923 \times 10^7$, $·992 \times 10^7$, and $1·00_8 \times 10^7$ e.m.u. respectively.

DISCUSSION OF RESULTS.

The magneto-optical dispersion of acetic anhydride, butyric acid, and ethyl butyrate over the range of the spectrum extending from about $·46\,\mu$ to about $·30\,\mu$ can be represented by the equation

$$n\delta = K \cdot \frac{\lambda^2}{\{\lambda^2 - \lambda_1^2\}^2},$$

where δ and n are the values of Verdet's constant and the refractive index of the liquid for a wave-length λ, K a constant which varies from liquid to liquid, and λ_1 the wavelength corresponding to the free period of the resonators. It is of interest to compare the values of K and λ_1 for butyric acid and ethyl butyrate with those obtained by Stephens and Evans * and Jenkins and Evans † for propionic acid and some of its esters. These results are collected in Table VIII. The magneto-optical rotations of acetic acid and formic acid in the ultra-violet region of the spectrum have not yet been examined in this laboratory, and unpublished results on the magneto-optical rotation of propyl acetate suggest the necessity of repeating with greater accuracy the previous results of Evans and Evans ‡ on

TABLE VIII.

Liquid.	Molecular weight.	λ_1 (microns).	K.	Temp. in °C.
Propionic acid.......... (C$_2$H$_5$. COOH)	74	·1051	$5.00_8 \times 10^{-3}$	13
Methyl propionate ... (C$_2$H$_5$. COOCH$_3$)	88	·1066	$4.77_1 \times 10^{-3}$	17·1
Ethyl propionate...... (C$_2$H$_5$. COOC$_2$H$_5$)	102	·1075	$5.06_5 \times 10^{-3}$	15·8
Butyric acid............ (C$_3$H$_7$. COOH)	88	·1064	$5.28_5 \times 10^{-3}$	13·1
Ethyl butyrate......... (C$_3$H$_7$. COOC$_2$H$_5$)	116	·1081	$5.25_3 \times 10^{-3}$	13·1

methyl and ethyl acetates. These substances are now being investigated, and the comparison of the results for similar compounds can then be extended.

An examination of the above table shows that, in general, values of λ_1 increase with increasing molecular weight, the value for propionic acid being $\cdot 0013 \mu$ below that of butyric acid, the next member of the homologous series. It is interesting to note that the value of λ_1 for butyric acid is practically the same as that for methyl propionate, which has the same molecular weight.

The value of K is greater for butyric acid than for propionic acid, and the same is true when ethyl and methyl propionates are compared. It is, however, seen that the

---

* *Loc. cit.*
† Phil. Mag. xi. pp. 377–396 (Feb. 1931).
‡ Phil. Mag. viii. (August 1929).

increase of molecular weight in passing from propionic acid to methyl propionate and in passing from butyric acid to ethyl butyrate is accompanied by a diminution in the value of K.

The natural dispersion of three liquids over the range of spectrum extending from $\cdot6678\,\mu$ to $\cdot2800\,\mu$ is represented within experimental error by an equation of the type

$$n^2 - 1 = b_0 + \frac{b_1}{\lambda^2 - \lambda_1{}^2},$$

where λ_1 is the wave-length of the absorption band calculated from the magneto-optical experiments, and b_0, b_1 are constants, which vary from liquid to liquid.

A comparison of the values of b_0 and b_1 for the liquids included in Table VIII. are given in Table IX. The values of $\frac{e}{m}$ are also included in the same table.

TABLE IX.

Liquid.	b_0.	$b_1 \times 10^{10}$.	$\frac{e}{m}$ (e.m.u.).
Propionic acid	·9042	·8716	$1\cdot00 \times 10^7$
Methyl propionate	·8717	·8680	·96 $\times 10^7$
Ethyl propionate	·8918	·8990	·99 $\times 10^7$
Butyric acid	·9352	·9300	·99 $\times 10^7$
Ethyl butyrate	·9209	·9103	$1\cdot00 \times 10^7$

An examination of the table shows that, if the two acids are compared, the values of b_0 and b_1 increase with increasing molecular weight, and also that the value of $\frac{e}{m}$ tends to diminish as the molecular weight increases. If the esters are compared, the values of b_0, b_1, and $\frac{e}{m}$ increase with increasing molecular weight. The replacement of hydrogen in propionic acid by the CH_3 group to form methyl propionate reduces the value of $\frac{e}{m}$, and the replacement of hydrogen in butyric acid by the C_2H_5 group slightly increases the value of $\frac{e}{m}$.

From the values of $\frac{e}{m}$ deduced in the present experiments on acetic anhydride, butyric acid, and ethyl butyrate, it can be seen that the resonators controlling the magneto-optical

dispersion in the visible and ultra-violet regions of the spectrum are the electrons. However, the values obtained for $\frac{e}{m}$ are much lower than the accepted value 1.77×10^7 e.m.u.

SUMMARY.

1. The magneto-optical dispersion of acetic anhydride, normal butyric acid, and normal ethyl butyrate in the visible and ultra-violet regions of the spectrum ($.46\,\mu$ to about $.30\,\mu$) can be represented by equations of the type

$$n\delta = K \cdot \frac{\lambda^2}{(\lambda^2 - \lambda_1^2)^2},$$

where δ is Verdet's constant, n the refractive index for wave-length λ, K a constant, and λ_1 the wave-length of the absorption band.

The values of λ_1 for acetic anhydride, butyric acid, and ethyl butyrate are $.1031\,\mu$, $.1064\,\mu$, and $.1081\,\mu$ respectively.

2. The natural dispersion of acetic anhydride, butyric acid, and ethyl butyrate in the visible and ultra-violet regions of the spectrum ($.6678\,\mu$ to about $.2800\,\mu$) can be represented within experimental error by equations of the type

$$n^2 - 1 = b_0 + \frac{b_1}{\lambda^2 - \lambda_1^2},$$

where b_0 and b_1 are constants and λ_1 has for each liquid the value determined from the magneto-optical dispersion experiments.

3. The values of $\frac{e}{m}$ for acetic anhydride, butyric acid, and ethyl butyrate, calculated from the results of the magneto-optical and natural dispersion experiments, are $.923 \times 10^7$, $.992 \times 10^7$, and $1.00_8 \times 10^7$ e.m.u. respectively.

July 1931.

XXI. *Activities and the Standard State.*—I. *Activity Co-efficients.* By ANGUS MACFARLANE, *B.A.,* and OLIVER GATTY, *B.A.*[*]

THE concentrations of solutions have been variously expressed in terms of a given volume or weight either of solvent or solution. For dilute aqueous solutions there is

no appreciable difference between concentrations measured on the weight or the volume normality scale. But in other solvents, where the density is not unity, this is no longer the case, and, in consequence, confusion has sometimes arisen in investigations of the thermodynamical properties of solutions. This paper and the following one deal with the choice of suitable concentration scales when the free energy contents of solutions are to be considered.

Since only differences in free energy can be measured, the partial molal free energy of a solute in solution at a given temperature and pressure is defined by reference to a standard state. For convenience in correlating the partial molal free energies of a solute in different solvents, this standard state should be so chosen as to be independent of the nature of the medium. This was done by G. N. Lewis, in dealing with fugacities, which he referred to the rarefied vapour of the pure solute. The term fugacity will be employed in what follows as simply implying any absolute standard of this type. In practice the simplest fugacity system would take as the standard the pure solute at a given temperature, but reference even to this is difficult owing to our general ignorance of the properties of saturated solutions. In consequence, free energies are referred to a separate standard state for each solvent. The activities a_1 and a_2 of a solute in any one solvent at two concentrations are related to the partial molal free energies by the expression

$$\bar{F}_2 - \bar{F}_1 = RT\, ln \frac{a_2}{a_1}. \quad \ldots \ldots \quad (1)$$

An activity so defined can be related to a fugacity, α, and to the fugacity of the solute in the standard state, α_0, by the expression

$$a = \frac{\alpha}{\alpha_0}. \quad \ldots \ldots \ldots \quad (2)$$

Since all solutions approach ideal behaviour at very high dilutions, the standard state is usually chosen so that

$$\underset{c \to 0}{\mathrm{Lt}} \frac{a}{c} = 1.$$

But this standard state is dependent on the concentration scale selected which may be any one of six that have been used from time to time. Thus the concentration of a given solution may be expressed in :—

(1) Gram molecules of solute per 1000 c.c. of solution.

(2) Gram molecules of solute per 1000 c.c. of solvent.

(3) Gram molecules of solute per 1000 gm. of solution.

(4) Gram molecules of solute per 1000 gm. of solvent.

(5) Gram molecules of solute per gram molecule of solution (*i. e.*, molar fraction).

(6) Gram molecules of solute per gram molecule of solvent.

Let the concentrations on these six scales be denoted by c, c', m, m', x, and x' respectively, and the activites by

$$(1)\ a_c = fc\ ; \qquad (2)\ a_{c'} = f'c'\ ; \qquad (3)\ a_m = \gamma m\ ;$$

$$(4)\ a_{m'} = \gamma' m'\ ; \qquad (5)\ a_x = \xi x\ ; \qquad (6)\ a_{x'} = \xi' x'\ ;$$

where f, f', γ, γ', ξ, and ξ' are the activity coefficients, and the six standard states are chosen so that

$$\underset{c\to 0}{\text{Lt}}\ \frac{a_c}{c} = 1\ ; \qquad \underset{m\to 0}{\text{Lt}}\ \frac{a_m}{m} = 1\ ; \qquad \underset{x\to 0}{\text{Lt}}\ \frac{a_x}{x} = 1\ ; \tag{3}$$

$$\underset{c'\to 0}{\text{Lt}}\ \frac{a_{c'}}{c'} = 1\ ; \qquad \underset{m'\to 0}{\text{Lt}}\ \frac{a_m}{m'} = 1\ ; \qquad \underset{x'\to 0}{\text{Lt}}\ \frac{a_{x'}}{x'} = 1\ ;$$

The various concentration units used are simply related to each other :—

$$\frac{c}{m} = \Delta_s, \quad \text{where } \Delta_s = \text{the density of the solution.}$$

$$\frac{c'}{m'} = \Delta, \quad \text{where } \Delta = \text{the density of the solvent.}$$

$$\frac{m}{m'} = \frac{1000}{1000 + W}, \quad \text{where } W = \text{the number of grams of solute dissolved per 1000 gms. of solvent.}$$

$$\frac{c}{c'} = \frac{1000}{1000 + V}, \quad \text{where } V = \text{the volume change after the addition of W gm. of solute to 1000 c.c. of solvent.}$$

$$\frac{x}{x'} = 1 - x.$$

$$\frac{m'}{x'} = \frac{1000}{M}, \quad \text{where } M = \text{the molecular weight of the solvent.}$$

$$\left. \begin{array}{c} \ \end{array} \right\} \ . \ (4)$$

The properties of the solution tend towards those of the

pure solvent at low concentrations, and it is clear from expression (4) that

$$\operatorname{Lt}_{c \to 0} \frac{c}{c'} = 1 ; \qquad \operatorname{Lt}_{m \to 0} \frac{m}{m'} = 1 ; \qquad \operatorname{Lt} \frac{x}{x'} = 1. \quad . \quad (5)$$

Thus it follows in the limit that

$$\operatorname{Lt}_{c \to 0} \left[\frac{\alpha}{\alpha_{0_c}} = a_c = c = c' = a_{c'} = \frac{x}{\alpha_{0_{c'}}} \right],$$

and therefore

$$\alpha_{0_c} = \alpha_{0_{c''}} \quad . \quad . \quad . \quad . \quad . \quad . \quad (6)$$

similarly

and

$$\left. \begin{array}{c} \alpha_{0_m} = \alpha_{0_{m'}} \\[2mm] \alpha_{0_x} = \alpha_{0_{x'}} \end{array} \right\} \quad . \quad . \quad . \quad . \quad . \quad . \quad (7)$$

Thus it is seen that for any solvent the concentration scales (1) and (2) lead to the same standard state; the scales (3) and (4) both lead to another, and scales (5) and (6) to yet a third. Therefore the following equations hold for a given solution *at all concentrations* : —

$$\left. \begin{array}{c} a_c = a_{c'}, \\[2mm] a_m = a_{m'}, \\[2mm] a_x = a_{x'}, \end{array} \right\} \quad . \quad . \quad . \quad . \quad . \quad . \quad (8)$$

and from equation (4)

$$\left. \begin{array}{c} \dfrac{f'}{f} = \dfrac{1000}{1000 + V}, \\[4mm] \dfrac{\gamma'}{\gamma} = \dfrac{1000}{1000 + W}, \end{array} \right\} , \quad . \quad . \quad . \quad (2)$$

so that the activity coefficients of a given solution will differ according to whether the concentration scale refers to the solvent or the solution.

When a solution in which the solute has fugacity α is considered, the standard states and activity coefficients on the weight, volume, and molecular fraction scales can be related to each other by a similar type of reasoning.

$$\operatorname{Lt}_{m \to 0} a_m \equiv \gamma m \equiv \frac{\alpha}{\alpha_{0_m}} = m,$$

$$\operatorname{Lt}_{c \to 0} a_c \equiv f.c \equiv \frac{\alpha'}{\alpha_{0_c}} = c,$$

$$\mathop{Lt}_{x\to 0} a_x \equiv \xi x \equiv \frac{\alpha}{\alpha_{0_x}} = x,$$

$$\mathop{Lt}_{m\to 0} \frac{c}{m} = \Delta \quad \text{and} \quad \mathop{Lt}_{m\to 0} \frac{m}{x} = \frac{1000}{M}.$$

$$\therefore \quad \Delta = \frac{\alpha_{0_m}}{\alpha_{0_c}} = \frac{a_c}{a_m} = \frac{a_{c'}}{a_{m'}} \quad (\text{at all concentrations}), \quad (10)$$

and

$$\frac{1000}{M} = \frac{\alpha_{0_x}}{\alpha_{0_m}} = \frac{a_m}{a_x} = \frac{a_{m'}}{a_x} \quad (\text{at all concentrations}). \quad (11)$$

Now from the definition of the activity coefficients it is evident, since

$$\frac{c'}{m'} = \Delta \quad \text{and} \quad \frac{m'}{x'} = \frac{1000}{M} \quad \text{at all concentrations,}$$

that

$$f' = \gamma' = \xi'. \quad . \quad . \quad . \quad . \quad . \quad (12)$$

So that activity coefficients when referred to concentration scales (2), (4), or (6) are always the same. At finite concentrations this relationship does not hold for concentration scales (1), (3), and (5).

Equations (6), (7), and (8) show that the standard state is dependent on the unit of concentration employed, but is independent of whether these units refer to the solvent or to the solution ; while equation (12) gives a strong reason for using a concentration scale that refers to the solvent rather than the solution. It is customary to look on the activity coefficient as a property of a solution which measures its departure from the ideal. If so, an activity coefficient that is independent of the units of concentration is desirable so that it may really be said to be a property of the solution. It is accordingly suggested that the concentration scales employed when determining activity coefficients should refer to the solvent rather than the solution. In dilute solutions, of course, the difference is negligible.

The Debye-Hückel * expression represents the electrical contribution to the work function A (constant volume function) of the solution. Since it is only valid in regions where it may be equated to the true free energy F without appreciable error, they were able to deduce an equation for the activity coefficient of the solute which was necessarily in

* Debye and Hückel, *Phys. Zeit.* xxiv. pp. 185, 305 (1923).

terms of c. This expression can only be expected to hold in solutions more dilute than hundredth normal, in which range concentrations calculated in terms of quantity of solvent or of solution are practically indistinguishable. But equation (12) shows that only activity coefficients referred to the solvent basis have a simple physical significance in strong solution. To avoid the use of separate scales for dilute and concentrated solutions, it is therefore suggested that the c' unit of concentration be employed. This scale has the additional advantage, when testing the theory in non-aqueous solutions, of being ascertainable without a knowledge of the density of the solution.

By referring the concentration to the solvent and not to the solution it is possible to examine the temperature and pressure coefficients of the activity coefficients for a solution of constant composition. A more detailed analysis of Bjerrum's equation for the heats of dilution can be made by this means, and the method leads eventually to expressions for the fugacity in the standard state as a function of pressure and temperature.

Consider a solution containing N_1 gram molecules of solvent and N_2 of solute. From ordinary thermodynamics the partial molal heat-content and volume of the solute in any such solution may be calculated from the following equations:

$$\left(\frac{ln\ a}{T}\right)_{p,\ N} = -\frac{\overline{H}}{RT^2}, \quad \cdots \quad (13)$$

$$\left(\frac{ln\ a}{p}\right)_{T,\ N} = \frac{\overline{V}}{RT}, \quad \cdots \quad (14)$$

where the subscript N implies that both N_1 and N_2 are kept constant. The equations hold also for a solution which is in the standard state at the initial temperature and pressure, but after any infinitesimal change in these variables the solution does not necessarily correspond to the standard state in the new conditions. Thus, although these equations give the partial molal heat-content and volume of the solute in a solution which is a standard at the given temperature and pressure, information of the change of standard state with temperature and pressure must be obtained by an indirect method.

Let a_1 and a_2 be the activities of the solute at concentrations 1 and 2 on any scale. Then the ratios $\dfrac{a_2}{a_1}$ and $\dfrac{c_2'}{c_1'}$

can be determined without reference to the standard state. Accordingly the ratio $\dfrac{f_2'}{f_1'}$ is independent of any knowledge of the standard state and we may write

$$\left(\frac{\partial \ln a_2/a_1}{T}\right)_{p,\,N} = \left(\frac{\ln \alpha_2/\alpha_1}{T}\right)_{p,\,N}$$

$$= \left(\frac{\ln c_2'/c_1'}{T}\right)_{p,\,N} + \left(\frac{\ln f_2'/f_1'}{T}\right) = \frac{\overline{H}_1 - \overline{H}_2}{RT^2} .$$

A similar set of equations holds for all the other concentration scales. Only on the volume scale is the concentration a function of temperature and pressure, but by reference to the volume of pure solvent the concentration ratio $\dfrac{c_2'}{c_1'}$ is independent of these variables, although the ratio $\dfrac{c_2}{c_1}$ is not. Therefore

$$\left(\frac{\partial \ln f_2'/f_1'}{\partial T}\right)_{p,\,N} = \left(\frac{\partial \ln \gamma_2'/\gamma_1'}{\partial T}\right)_{p,\,N}$$

$$= \left(\frac{\partial \ln \xi_2'/\xi_1'}{\partial T}\right)_{p,\,N} = \frac{\overline{H}_1 - \overline{H}_2}{RT^2} ,$$

since, by equation (12), $f' = \gamma' = \xi'$ at all temperatures, pressures, and concentrations.

Now let f_2' refer to any solution that is at a limitingly great dilution. Then f_2' is sensibly equal to unity at all temperatures and $\overline{H}_2$ becomes $\overline{H}_{c=0}$, which has a constant value at all limitingly low concentrations. Equation (14) then becomes

$$-\left(\frac{\partial \ln f'}{\partial T}\right)_{p,\,N} = \frac{\overline{H} - \overline{H}_{c=0}}{RT^2} , \quad \cdot \quad \cdot \quad \cdot \quad (15)$$

and there are two corresponding equations for γ' and ξ'. Thus $-RT^2\left(\dfrac{\ln f'}{T}\right)_{p,\,N}$ gives the partial molal heat of dilution of the solute to infinite dilution, and the expression is independent of the concentration units employed as long as they refer to the pure solvent and not to the solution. This result must hold at any concentration.

Similarly, by differentiating with respect to pressure, it is found that

$$\left(\frac{\ln f'}{p}\right)_{T,\,N} = \frac{\overline{V} - \overline{V}_{c=0}}{RT} , \quad \cdot \quad \cdot \quad \cdot \quad (16)$$

where $\overline{V}$ is the partial molal volume of the solute at concentration c and $\overline{V}_{c=0}$ its value at infinite dilution. This result is also independent of the concentration units and holds at any concentration.

Returning now to solutions in the standard state, the variation of the fugacities may be examined to find whether their concentrations also depend on the temperature and pressure. Since

$$
\begin{aligned}
\alpha_{0_c} &= \frac{\alpha}{c'f'}, \\[2mm]
\alpha_{0_m} &= \frac{\alpha}{m_0'\gamma'}, \\[2mm]
\alpha_{0_x} &= \frac{\alpha}{x_0'.\xi'},
\end{aligned}
\qquad \cdots \cdots \quad (17)
$$

$$
\begin{aligned}
\left(\frac{\ln \alpha_{0_c}}{\partial T}\right)_p &= \left(\frac{\partial \ln \alpha}{\partial T}\right)_{p,\,N} - \left(\frac{\partial \ln c'}{\partial T}\right)_{p,\,N} - \left(\frac{\partial \ln f'}{\partial T}\right)_{p,\,N} \\[2mm]
&= -\frac{H}{RT^2} - \left(\frac{\partial \ln c'}{\partial T}\right)_{p,\,N} + \frac{H - \overline{H}_{c=0}}{RT^2} \\[2mm]
&= -\frac{\overline{H}_{c=0}}{RT^2} - \left(\frac{\partial \ln c'}{\partial T}\right)_{p,\,N} \\[2mm]
&= -\frac{H_{c=0}}{RT^2} + \left(\frac{\partial \ln V}{\partial T}\right)_{p,\,N}, \quad \cdots \cdots \quad (18)
\end{aligned}
$$

where V is the molal volume of the solvent.

Similarly, since m' and x' are independent of T,

$$
\left(\frac{\ln \alpha_{0_m}}{T}\right)_p = -\frac{\overline{H}_{c=0}}{RT^2}, \qquad \cdots \cdots \quad (19)
$$

$$
\left(\frac{\ln \alpha_{0_x}}{\partial T}\right)_p = -\frac{H_{c=0}}{RT^2}, \qquad \cdots \cdots \quad (20)
$$

while, for the pressure variation, the expressions are :

$$
\left(\frac{\partial \ln \alpha_{0_c}}{\partial p}\right)_T = \frac{\overline{V}_{c=0}}{RT} + \left(\frac{\partial \ln V}{\partial p}\right)_{T,\,N}, \quad \cdots \quad (21)
$$

$$
\left(\frac{\partial \ln \alpha_{0_m}}{\partial p}\right)_T = \frac{\overline{V}_{c=0}}{RT} = \left(\frac{\partial \ln \alpha_{0_x}}{\partial p}\right)_T. \quad \cdots \quad (2\,2)
$$

Since $\overline{V}_{c=0}$ is not in general equal to $\overline{V}$, nor $\overline{H}_{c=0}$ to $\overline{H}$, it is clear, on comparing equations (13) and (14) with (18)

to (20) and (21) to (22) respectively, that the actual concentrations of the solutions in the standard states c_0', m_0', x_0', which, of course, are the reciprocals of the activity coefficients, are functions of both the pressure and temperature of the system. Thus, for a given temperature and pressure, α_0 is completely determined, but α is a function of the concentration as well.

Summary.

The relationships between the standard states and activity coefficients of a solute in solution have been investigated for a number of concentration scales. It is recommended that the concentration should be expressed in gram-molecules of salt in a fixed quantity of solvent. The physical interpretation of the activity coefficient is thereby simplified, while definite relationships can be obtained between it and the partial molal heat and volume of dilution of the solute to infinite dilution. The concentration of solute in the standard states is, in general, a function of the temperature and pressure of the solution. When testing the Debye-Hückel expression in solvents whose density is not unity, a volume normality scale should be used.

Physical Chemistry Laboratory,
    Balliol College and Trinity College,
            Oxford.

XXII. *Activities and the Standard State.*—II. *Electrode Potentials. By* Oliver Gatty, *B.A., and* Angus Macfarlane, *B.A.*[*]

THE potential difference between an element and a solution of its ions which are at unit activity, *i. e.,* in the standard state, is defined as its single electrode potential. In the preceding paper it was shown in equations (6) and (7) that the standard state is the same whether the concentration unit refers to quantity of solvent or of solution, but in equations (10) and (11) that it is dependent on whether a weight, volume, or molecular scale is chosen. This choice will correspondingly affect the single electrode potentials.

Thus, if π is the electrostatic potential in volts of an

element in contact with a solution of its ions, whose activity is a_m on the weight and a_c on the volume scale,

$$\pi = \pi_{0_c} + \frac{RT}{n\mathbf{F}} \ln a_c$$

$$= \pi_{0_m} + \frac{RT}{n\mathbf{F}} \ln a_m. \quad \ldots \quad (23)$$

Therefore, from equation (10),

$$\pi_{0_m} - \pi_{0_c} = \frac{RT}{n\mathbf{F}} \ln \Delta, \quad \ldots \quad (24)$$

where π_{0_m} and π_{0_c} are the standard single potentials on the two scales, Δ is the density of the solvent, n is the valency of the ion, and $\mathbf{F}$ the value of the Faraday in coulombs.

¶ Since the exact magnitude of the absolute zero of potential is still uncertain, electrode potentials are referred to the standard hydrogen electrode, where hydrogen gas at atmospheric pressure is in equilibrium with a solution containing hydrogen ions at unit activity. The standard electrode potential of an element A, which gives rise to anions in solution, can be calculated from measurements of the e.m f., E_1, of the cell :

$$H_2 \qquad HA \qquad A,$$
$$a_c \text{ or } a_m$$

(1 atmosphere),

since

$$E_1 = {}^{A}\pi_{0_c} - \frac{RT}{\mathbf{F}} \ln a_c^- - \left[{}^{H_2}\pi_{0_c} + \frac{RT}{\mathbf{F}} \ln a_c^+ \right]$$

$$= {}^{A}\pi_{0_m} - \frac{RT}{\mathbf{F}} \ln a_m^- - \left[{}^{H_2}\pi_{0_m} + \frac{RT}{\mathbf{F}} \ln a_m^+ \right]. \quad . \quad (25)$$

But, by definition, ${}^{A}\pi_0 - {}^{H_2}\pi_0$ is the standard electrode potential of the anion, and if the product $a_+ . a_-$ is denoted by $a_{\pm}^2$, equation (25) may be rewritten :

$$E_1 = {}^{A}E.P._{.c} - \frac{2RT}{\mathbf{F}} \ln a_{\pm_c}$$

$$= {}^{A}E.P._{.m} - \frac{2RT}{\mathbf{F}} \ln a_{\pm_m}; \quad \ldots \quad (26)$$

$$\therefore \quad {}^{A}E.P._{.c} - {}^{A}E.P._{.m} = \frac{2RT}{\mathbf{F}} \ln \frac{a_{\pm_c}}{a_{\pm_m}} = \frac{2RT}{\mathbf{F}} \ln \Delta. \quad . \quad (27)$$

This equation is valid even for a weak electrolyte, since the standard states are fixed by extrapolation of $E_1 + \frac{2RT}{\mathbf{F}} \ln c$

or $E_1 + \dfrac{2RT}{F} \ln m$ to infinite dilution where dissociation is complete.

The electromotive force, E_2, of the corresponding cell with a metallic electrode in equilibrium with a solution of the metallic salt, MA :

$$M \qquad \underset{a_c \text{ or } a_m}{MA} \qquad A,$$

is given by the equation

$$E_2 = {}^A\pi_{0_c} - {}^M\pi_{0_c} - \frac{2RT}{F} \ln a_{\pm c}$$

$$= {}^A\pi_{0_m} - {}^M\pi_{0_m} - \frac{2RT}{F} \ln a_{\pm m} ;$$

$$\therefore \quad {}^A\pi_{0_c} - {}^A\pi_{0_m} = {}^M\pi_{0_c} - {}^M\pi_{0_m} + \frac{2RT}{F} \ln \triangle.$$

But from (25)

$$\quad {}^A\pi_{0_c} - {}^A\pi_{0_m} = {}^{H_2}\pi_{0_c} - {}^{H_2}\pi_{0_m} + \frac{2RT}{F} \ln \triangle ;$$

$$\therefore \quad {}^M\pi_{0_c} - {}^{H_2}\pi_{0_c} = {}^M\pi_{0_m} - {}^{H_2}\pi_{0_m},$$

or $\qquad\qquad {}^M E.P._c = {}^M E.P._m.$ . . . . . . (28)

Thus the result of employing different activity scales is to change the potentials of the electrodes in the standard states. Since the potential of the standard hydrogen electrode is taken as zero, the differences for both ions are included in the standard potentials of the anions, those of the cations remaining unchanged.

To compare the partial molal free energy contents of a solute in two different solvents some fugacity system must be employed. Let the fugacity of the solute in solvent I be α and its fugacities in the standard states be $\alpha_{0_c} \ldots \alpha_{0_m} \ldots, \alpha_{0_x} \ldots$, then the activities in that solution are given by

$$a_c = \frac{\alpha}{\alpha_{0_c}}, \quad a_m = \frac{\alpha}{\alpha_{0_m}}, \quad a_x = \frac{\alpha}{\alpha_{0_x}}.$$

Similarly, for a given solution of the same solute in the second solvent if the fugacity be β,

$$b_c = \frac{\beta}{\beta_{0_c}}, \quad b_m = \frac{\beta}{\beta_{0_m}}, \quad b_x = \frac{\beta}{\beta_{0_x}},$$

where the activities of the solute are $b_c \ldots, b_m \ldots, b_x \ldots$ in that solution and the fugacities $\beta_{0_c} \ldots, \beta_{0_m} \ldots, \beta_{0_x} \ldots$ in the standard state. Then the free energy change on transferring one gram-molecule of solute from the first solution to the second is, by definition, equal to $RT \ln \dfrac{\alpha}{\beta}$. Under the special condition that $a_c = b_c$, and therefore $\dfrac{\alpha}{\beta} = \dfrac{\alpha_{0_c}}{\beta_{0_c}}$, the free energy of transfer will be the same as when the transfer is made between solutions in the standard states in both solvents. If, on the other hand, the concentration is the same in the two solvents while the activities are now denoted by $_c a$ and $_c b$, then

$$\operatorname*{Lt}_{c \to 0} \frac{_c a}{_c b} = \frac{c}{c} = 1.$$

This, as infinite dilution is approached, reduces to the special condition previously mentioned, and hence

$$\frac{\alpha}{\beta} = \frac{\alpha_{0_c}}{\beta_{0_c}}, \quad \cdots \cdots \quad (30)$$

that is, the free energy of transfer between solutions of equal concentration becomes in the limit the same as that between solutions at the respective standard states. This result holds whatever concentration scale is chosen.

When one Faraday is passed through the cell

A	HA	$H_2 - H_2$	HA	A
	in solvent I		in solvent II	
	a		b	

one gram-molecule of solute is transferred from solvent I to solvent II. The e.m.f. of the cell, E_3, is given by the equation

$$E_3 = {}^A\text{E.P.}_{\text{II}} - {}^A\text{E.P.}_{\text{I}} - \frac{2RT}{F} \ln \frac{b}{a}. \quad \cdots \quad (31)$$

Thus ${}^A\text{E.P.}_{\text{II}} - {}^A\text{E.P.}_{\text{I}}$ is a measure of the change in partial molal free energy of the solute HA when transferred at unit activity from solvent I to solvent II. But from equation (30) it follows that this is also the limiting value as infinite dilution is approached of the change in partial molal free energy of the solute when it is transferred from a solution of concentration c in solvent I to the same concentration in solvent II.

Though this result is equally true whatever the concentration scale, the numerical values are not independent of

the choice of standard states (27), because the allocation of all the standard states involves an extrapolation to infinite dilution, where the partial molal free energy becomes an infinite negative quantity. Moreover, the free energy of transfer from a solution of concentration c to one of $\frac{c}{2}$ becomes, as c tends to zero,

$$RT \ln \frac{c}{\frac{c}{2}},$$

and thus is equal to $RT \ln 2$, independently of the value of c. All properties at infinite dilution must be expressed in terms of an appropriate ratio which can be made to retain a finite value in the limit where the concentration approaches zero, so that the interpretation of results dependent on extrapolation to infinite dilution must be made with proper regard for the method by which the limit is approached.

Thus the limiting values of the free energy change are given by the following expressions :—

$$\text{From } c \text{ in solvent I to } c \text{ in solvent II} = RT \ln \frac{\beta_{0_c}}{\alpha_{0_c}},$$

$$\text{,, } m \text{ ,, ,, } m \text{ ,, ,, } = RT \ln \frac{\beta_{0_m}}{\alpha_{0_m}},$$

$$\text{,, } x \text{ ,, ,, } x \text{ ,, ,, } = RT \ln \frac{\beta_{0_x}}{\alpha_{0_x}}. \quad (32)$$

Born [*] has deduced the free energy in calories of solvation of an ion as the difference in work done in conferring on it a charge $z\epsilon$, first *in vacuo* and then in a solvent of dielectric constant D :

$$F_i = \frac{z_i^2 \epsilon^2}{2r \cdot J} \left[1 - \frac{1}{D} \right], \quad \cdots \quad (33)$$

where J is the mechanical equivalent of heat.

Hence the free energy of transfer of a gram-molecule of a binary electrolyte, the radius of whose ions are r_1 and r_2, from a solvent of dielectric constant D_1 to another in which it is D_2, is given by the equation

$$\Delta F = \frac{N \cdot z^2 \epsilon^2}{2 \cdot J} \left[\frac{1}{D_2} - \frac{1}{D_1} \right] \left[\frac{1}{r_1} + \frac{1}{r_2} \right], \quad \cdots \quad (34)$$

where N is Avogadro's number.

In comparing this equation with the observed electrode potentials it is important to decide which concentration

---

[*] Born, *Z. Physik.* xlv. p. 1 (1920).

scale may be appropriately used, as equation (32) shows that their values will depend on the standard state chosen. The derivation of the Born equation merely implies an ion in a large bulk of solvent. The expression is in fact the electrical contribution to the work function, A, of solvation of the ions in very dilute solution, and is independent of the concentration. It thus provides a correction for the deviation from ideal behaviour analogous to the Debye-Hückel activity coefficient, which, in the terms of the previous paper, was shown to be a property of the solution independent of the concentration scale.

The arguments there adduced in favour of the adoption of the volume concentration scale, c', are therefore equally cogent in this case. To these may be added an additional reason. Dalton's law is a statement that the partial molal free energy of one of a mixture of perfect gases depends, at a given temperature, only on its own partial pressure, *i. e.*, its volume concentration. The volume concentration therefore represents a true fugacity scale, being the one on which the free energy of transfer from one mixture to another of the same concentration can, under ideal conditions, be equated to zero. In any solution where a liquid is the solvent, even when the solute is a rare gas, some correction for deviation from ideal behaviour will be necessary. In the case of an electrolyte the Born equation provides another such correction; clearly then it must be applied to measurements based on such a scale that reference to the ideal state might ultimately be possible.

Summary.

The choice of units of expressing the concentration of solutions has been shown to affect the values of the standard electrode potentials of the anions. From a knowledge of their magnitudes in different solvents the partial molal free energies of transfer of electrolytes in infinitely dilute solution may be calculated and compared with results derived from the Born equation. It is therefore important that a standard unit of concentration be adopted, and, in this connexion, the use of the volume normality scale is advocated.

We wish to express our thanks to Sir Harold Hartley, to whom we are indebted for his advice and criticism in the preparation of these papers.

Physical Chemistry Laboratory,
   Balliol College and Trinity College,
     Oxford.

XXIII. *An Application of Piezo-electricity to Microscopy. By* E. H. SYNGE*.

A METHOD was suggested by the writer (Phil. Mag. Jan. 1931) by which a microphotograph might be built up on the principle of a telephotograph. It was proposed to obtain the investigating spot of light by using a colloidal particle situated at one focus of an ellipsoid of glass as an illuminating source. Light scattered by the particle and reflected by the surface of the ellipsoid would come to an image, small compared with a wave-length, at the other focus, which was supposed to lie within the microscopic section, and the section was to be moved in two senses, at right angles to one another, relatively to this spot. Reference may be made to the diagram in the article mentioned.

The method was proposed as a photographic one only, but its usefulness would, of course, be greatly increased if it could be converted into a visual one. Practically speaking, the method might be termed a visual one if a picture of the field could be formed on a phosphorescent screen or on very sensitive photographic printing paper, in the course of a few seconds. As the writer proposed it, the motion, in two senses, of the section was dependent on the turning of screws driven by clockwork, and mechanical considerations seemed to set a limit to the rapidity with which a picture might be built up. If we take as the standard size of a picture a square each of whose sides is one hundred times the resolution aimed at, the whole picture would perhaps take half an hour or more to construct. One of the two motions would, of course, be slow and regular, but the other, a to-and-fro motion, would be a hundred times as rapid, and there would be obvious mechanical difficulties to giving this motion by means of screws with any considerable speed, having regard to the regularity and evenness which would be necessary.

No method suggested itself to the writer at that time as an alternative to a mechanical method, but he believes now that the principle of piezo-electricity might be used, and that it would supply all the *desiderata* in the case. Taking formula (7) on page 29 of P. Vigoureux, ' Quartz Resonators and Oscillators ' (1931), we have $dt = -\mathrm{H}\dfrac{t}{e}\mathrm{V}$, where dt is

* Communicated by the Author.

the dilation along the third axis of a quartz crystal, t and e are the thicknesses of the crystal along that axis and the electric axis respectively, H is a constant having the value $6\cdot32 \times 10^{-8}$, and V is the difference of potential between plates in contact with the crystal along faces perpendicular to the electric axis. Setting $t = 5$ cm. and $e = \cdot15$ cm., it appears that the change in t for each volt of difference of potential will be about 2×10^{-6} cm. Thus, if the difference of potential increase regularly and constantly through 250 volts, the length of t will change regularly through about 5×10^{-4} cm, which one may take as the dimensions of the field aimed at, in a typical case.

It would therefore only be necessary to incorporate two quartz crystals in the frame (HG in diagram) which carried the section M, in such a way that changes of potential in plates in contact with them would produce changes in the lengths of the crystals, which would have the effect of giving M the motions desired. Or one crystal only might be used to give the more rapid to-and-fro motion, a mechanical method—a screw actuating a wedge—being perhaps more convenient for the slower motion.

The rapidity aimed at is, of course, not very great, and it is easy to suggest mechanical devices by means of a varying resistance by which the potential could be made to vary regularly in whatever way was desired. An electrometer designed for an automatic compensation or null method would no doubt be best for the automatic recording, and it should be noted that the light by which the picture is built up, and which might most conveniently be a strong beam of ultra-violet light, need not be proportional in intensity to the light from F_2, but small differences could be accentuated as desired, which would give the method, either as a visual or a photographic one, a very real advantage over ordinary microscopic methods, in the case of delicate stains, quite apart from the increased resolution attainable. One or two difficulties which might seem to be involved in the writer's suggestion are really not essential ones. Various contact methods are certainly available to test the dimensions of an ellipsoid to well beyond 10^{-6} cm.; while, to avoid a problem in glass manufacture, the colloidal particle at F_1 might be brought into position on a second glass rod, carried into a hollow in the ellipsoid, the particle simply resting on the surface of the rod, and all interstices being filled with immersion fluid of the right refractive index. It seems worth raising the question also whether a fluorescent particle might not be more advantageous to use than a metal

particle. The light scattered by the former is probably not subject to Rayleigh's law as the size of the particle decreases.

Where rapid results were aimed at, as by the method suggested in the present paper, it might be best that the rod R should be carried right through the ellipsoid and the rapid to-and-fro motion given in the direction of the rod. No doubt various other modifications and improvements would suggest themselves to technicians engaged in constructing the apparatus. But these are matters of detail, and everything required seems to be essentially within the range of present-day technique. The attainable rapidity in the recording apparatus is one of those questions which need hardly be raised at the outset, although it would become of great importance at a later stage. It would presumably depend on the amount of light available, and hence on the resolution.

Note on Fluorescent Particles.—Since writing the above, the writer has found an account by Zsigmondy ('Colloids and the Ultra-Microscope,' p. 196) of the examination of fluorescent substances in extreme dilution which seems remarkable. Zsigmondy, apparently using a not very strong illuminating system (*op. cit.* p. 122), and with heavy losses of light in polarization, found that a light-cone, only 1μ to 2μ thick, was visible, in the case of fluorescein and some other substances, down to a dilution which corresponds to little more than one fluorescent molecule per μ^3 of the aqueous solution. He was, however, unable to see the molecules separately in any case.

In the circumstances it is difficult to think of any reason for his failure except that the molecules were in too rapid and irregular motion for the eye to retain more than an averaged effect. It would certainly seem worth repeating the experiment, using a viscous solution, *e. g.*, of glycerine, in which the molecules would move very slowly, instead of an aqueous one, employing a stronger illuminating system, and perhaps replacing polarization, as a means of separating fluorescent from other scattered light, by a prismatic separation of the different parts of the spectrum, the illuminating beam, of course, in this case, consisting of short wave-lengths only.

Various interesting consequences would follow if the molecules should prove to be visible separately in a sufficiently viscous solution. As regards the microscopic method proposed, it seems a fair conclusion, even from Zsigmondy's

results, that one might look forward to an ultimate development in which a single fluorescent molecule might be the illuminating source, and a resolution of 10^{-7} cm. be attained. It may be remarked that where a fluorescent particle was used it would not be necessary to limit the angle, and hence the intensity of the illuminating beam (supposed of short wavelengths), since the two parts of the spectrum could be separated afterwards by a prism, even if the original beam were reflected back through the microscopic section M. But, as can easily be seen, the latter contingency might be avoided by the choice of an immersion fluid which, while homogeneous with the glass for the longer wave-lengths, was different for the shorter wave-lengths, a minute prism of this fluid being interposed somewhere in the path of the beam after it had left F_1.

It may also be worth remarking that, if a fluorescent particle were used, the whole method might be inverted— corresponding to dark-field microscopy—the illuminating beam then converging to F_2 and the particle at F_1 being under observation.

XXIV. *An Attempt to Detect High Photoelectric Absorption in Cæsium Vapour at Double the Series Limit.* By E. T. S. APPLEYARD, *Ph.D.*, *H. H. Wills Physical Laboratory, University of Bristol* *.

Introduction.

BERGEN DAVIS † ‡ has, in two recent papers, reported a very high probability of electron capture when α-particles are projected through a cloud of free electrons having certain discrete velocities relative to the α-particle. Briefly, if the kinetic energy of the electron referred to axes fixed in the α-particle is the same as the kinetic energy corresponding to the movement of an electron in a Bohr orbit about the doubly charged helium nucleus, then the electron will be captured into this orbit with a very high degree of probability. In fact, the quantitative work of Barnes suggests that the effective target area for capture under these circumstances can be of the order of 10^{-7} cm.^{2}, which is hundreds of millions of times any known gas kinetic target area.

This unusually large effective target area is astonishing; for Mohler's * experiments on recombination spectra have shown that capture of electrons, even those whose energy is as small as 1/20 equivalent volt, is relatively improbable when the positive ions of the alkalis are in question. In fact, for electrons of this energy captured into the vacant ground orbit of a cæsium ion the effective target area is about 10^{-20} cm.^{2}.

Moreover (assuming for the moment a stationary helium nucleus), when the electron is captured by a process such as Bergen Davis suggested, there is an energy change in the system which is equal to twice the ionization energy of the orbit into which the electron is captured. This energy must pass out as radiation of double the frequency corresponding to the series limit of ionized helium. There is an exact thermodynamical inverse to this process, viz., the absorption of this frequency by an ionized helium atom and the ejection of a free electron whose kinetic energy is equal to the ionization energy of singly ionized helium. In other words, if we could examine the absorption spectrum of ionized helium, we ought to find, in addition to the ordinary continuous absorption at the series limit, a very powerful absorption band at double this frequency †.

To perform this inverse experiment with ionized helium is, of course, impracticable, but there is no reason to suppose that this process is restricted to ionized helium ; for Barnes (*loc. cit.*) reports double capture when the kinetic energy of two electrons is equal to that energy of the ground state of neutral helium. This paper describes an attempt to detect absorption by cæsium vapour in the far ultra-violet in the neighbourhood of twice its series limit.

Experimental.

The series limit of cæsium lies at $\lambda 3184$. We must therefore look for absorption between $\lambda 1500$ and $\lambda 1600$—that is to say, in the region of the spectrum where air begins to to absorb strongly.

This circumstance brought with it some technical problems which were not easy to resolve. The method finally adopted was to place a few drops of cæsium metal in an evacuated

---

* Mohler and Boëkner, *B. a. Stand. J. Res.* iii. p. 303 (1929).
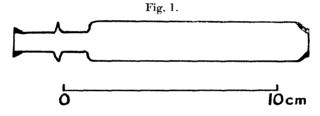
† The band must be fairly broad, for if an exact relative velocity had been necessary for capture, Davis and Barnes (*loc. cit.*) could never have detected it, owing to the distribution-in-velocity of his thermionic electrons and the straggling of his α-particles.

cell with thin quartz windows, and to place this cell (which was provided with a heating element) in the optical axis of a vacuum spectrograph between the slit and a suitable light source.

The absorption cell is shown in fig. 1. The body of the cell was made from pyrex, but its ends were closed by thin quartz windows stuck on with hard enamel. Thin quartz transmits quite satisfactorily down to λ 1430 provided it is freshly polished.

The cell was evacuated by means of a diffusion pump and a mercury trap. To remove the water vapour and volatile organic matter from the enamel it was baked out for some time at 200° C. Cæsium was prepared by heating a small quantity of cæsium chromate and misch-metal filings in a metal capsule by electron bombardment. The metallic cæsium produced by the reaction was distilled from the reaction vessel into the cell at about 200° C., and the cell was then

Fig. 1.
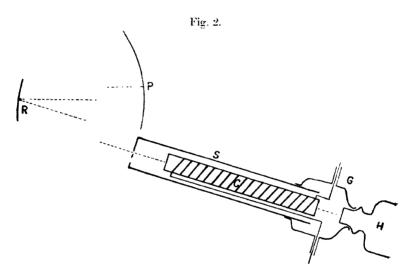
sealed off from the reaction vessel and from the pumps. During the distillation the windows were kept free from cæsium metal by local heating, so that finally the cæsium formed a dense mirror in the middle portion of the cell.

The optical arrangements are shown schematically in fig. 2. To produce the spectra the large vacuum grating spectrograph of the laboratory * was employed in the first order spectrum. The source of light was a water-cooled hydrogen discharge tube, H, dissipating about 1 kilowatt. Pure hydrogen was circulated over charcoal in liquid air and through the tube during the exposures, so as to prevent impurities from showing up in the spectrum.

The absorption cell fitted snugly into a copper tube, C, wound with "nichrome" strip, which was insulated from the body of the tube by mica. Thermocouples at the centre of the tube and at the ends gave the temperature maintained by the heating current, and the windings were arranged to give a temperature difference of about 20° C. between the

* To be described by H. W. B. Skinner elsewhere.

windows and the centre of the cell, so as to keep the former clear from a dew of cæsium metal, which caused much trouble in the earlier experiments. The cell, with its oven, fitted into a water-cooled jacket (not shown), and this into the slit-tube, S, of the spectrograph. The oven was insulated thermally and electrically from the slit-tube by means of glass washers (not shown). Leads for the oven windings and for the thermocouples were taken out to air through the glass adapter, G, which was attached by means of a water-cooled wax joint to the slit-tube. All joints were made vacuum-tight by wax.

Fig. 2.

Spectra were photographed in the first order of the grating R on the curved photographic plate P. The dispersion was about 8·7 A per mm. in the region under consideration, and was ample for the purpose in hand. Oiled plates were used *, and during the exposures the pressure in the spectrograph was kept down to a few thousandths of a millimetre of mercury by means of a fast rotary oil-pump.

Much difficulty was experienced in obtaining suitable conditions for the exposures. The cæsium vapour gradually attacked the quartz windows, producing a surface film which, though transparent to the visible spectrum, absorbed strongly beyond λ 1800.

---

* Jeantet and Duclos (*cf.* Lyman, 'Spectroscopy of the Extreme Ultraviolet,' p. 61).

The method finally employed was to take an exposure through the cold cell, one through the cell warmed to 100° C., and another again through the cold cell. In this way serious darkening of the windows could be detected. An exposure was also taken with the cell removed from the path of the beam. The lines on the resulting spectra were identified by means of a carbon comparison spectrum and Lyman's * tables.

The best exposed and most uniform plate shows no detectable difference between the second and third spectra mentioned above, and all the spectra examined line for line show a similar intensity distribution. In particular the line λ 1591·5 of molecular hydrogen showed no preferential absorption. Calculation shows that under these experimental conditions an atomic absorption coefficient greater than 10^{-15} would have been readily detected.

Discussion.

If preferential capture of an electron into the ground state of a cæsium ion occurs when the kinetic energy of the electron approaching is equal to the mean kinetic energy of an electron in this orbit, then, just as for capture into a hydrogen-like orbit, radiation of twice the frequency of the series limit must be emitted ; for the calculation demands only that the potential energy of such an orbit shall be double its kinetic energy, and this is always true for a system of electrons and protons †.

An exact argument allows us to calculate the magnitude of the absorption coefficient which we should expect in this neighbourhood.

Let $\psi(\nu_1)$, $\psi(\nu_2)$ be the atomic absorption coefficients in the continuous absorption region of some atom at frequencies ν_1 and ν_2. Then an argument from the "Principle of Detailed Balance" ‡ shows

$$\frac{\psi(\nu_1)}{\psi(\nu_2)} = \frac{\nu_2{}^3}{\nu_1{}^3} \cdot \frac{\nu_1 - \nu_0}{\nu_2 - \nu_0} \cdot \frac{F(\eta_1)}{F(\eta_2)},$$

where $F(\eta_1)$ and $F(\eta_2)$ are the "target areas" for the exact inverse of the absorption process, viz., for the capture of an electron of energy $\eta = \eta(\nu - \nu_0)$, where ν_0 is the frequency of the series limit.

---

* Lyman, *loc. cit.*

† Sommerfeld, *Atombau u-Spektrallinien*: *Anhang.* The above assumption neglects the small perturbation of the core during the core-entering part of the orbit.

‡ Fowler, 'Statistical Mechanics,' p. 478 (Cambridge, 1930).

Let us take for the values of $F(\eta_1)$, $F(\eta_2)$ the values derived from Bergen Davis's experiment and from Mohler's results on the recombination of slow electrons with ions.

Consider absorption of $\lambda\,3130$ of mercury by cæsium vapour. This will eject from the 1^2S state of cæsium an electron of energy ·06 volts. The target area for recombination of such an electron is at most 10^{-21} cm.^{2}.

This gives (taking the very conservative estimate of 10^{-10} cm.^{2} for the target area in a process such as Bergen Davis describes)

$$\frac{\psi(\nu_1)}{\psi(\nu_2)} \sim 10^{12},$$

if we take ν_1 as the frequency at double the series limit and ν_2 as the frequency corresponding to $\lambda\,3130$ of mercury. In other words, the absorption at the double series limit should be colossally greater than any previously known continuous absorption. To give numerical values, if we take Mohler's * value for the atomic absorption coefficient of cæsium at $\lambda\,3130$, viz., $K = 1\cdot85 \times 10^{-19}$, we obtain for the atomic absorption coefficient at double the series limit

$$K \sim 2 \times 10^{-7}.$$

As we have previously mentioned in the experimental part of the paper a coefficient of absorption $> 10^{-15}$ would have been readily detectable.

We conclude that if capture of this type exists in cæsium vapour it must be less than one ten-millionth the magnitude of the effect claimed for α-particles. Davis's results are therefore difficult to understand. They have not been reproduced by Webster†, and a recent note from Bergen Davis‡ and Barnes appears to throw grave doubt on the validity of his original experimental results; and since this work was begun Korff and Nickerson§ have published a short note in which they report that a similar experiment to the foregoing, using sodium vapour, gave a negative result.

Thanks are due to the various members of this laboratory for help at different times, and to Professor Tyndall for his continued interest. I must particularly thank Dr. H. Jones for helpful discussion. Thanks are also due to the Department of Scientific and Industrial Research for an award, without which this work could not have been performed.

* Mohler and Boëkner, *loc. cit.*
† Webster, Proc. Camb. Phil. Soc. xxvii. p. 116 (1931).
‡ Bergen Davis and Barnes, Phys. Rev. xxxvii. p. 1367 (1931).
§ Korff and Nickerson, Phys. Rev. xxxv. (1930).

XXV. *On the Raman Effect from the Standpoint of Unimolecular Reactions.* By A. GANGULI, *Benares Hindu University, Benares* *.

SINCE the discovery of the Raman effect, various theories to explain the mechanism and intensity relationship of Raman lines have been proposed by several authors. Of course, the most satisfactory explanation will be in the line of the dispersion theories developed by Smekal (*Naturw.* xi. p. 873 (1923)), and by Kramers and Heisenberg (*Zeit. f. Phys.* xxxi. p. 684 (1925)). A more powerful method is the wave mechanical (as well as the quantum mechanical) one. A. Carelli (*Atti Acad. Lincei*, ix. p. 165 (1929)) deduces a relationship between the intensities of the anti-Stokes and the Stokes lines from wave mechanics as well as by Dirac's quantum mechanics (see also E. Amaldi, *Atti Acad. Lincei*, ix. p. 876 (1929)). Born (*Naturw.* xvi. p. 673 (1928)), however, suggests that the observed intensities can very well be explained by the statistical application of quantum mechanics. E. G. Kemble and E. C. Hill (Proc. Nat. Acad. Sci. 15, xv. p. 387 (1929)) derive a general formula for the perturbed electric moment associated with the Raman lines using matrix mechanics.

Now a review of the literature indicates two different views of the ratios of the Stokes and the anti-Stokes lines in the Raman effect. Raman (Ind. J. Phys. ii. p. 387 (1928)) believes that the intensities will be proportional to the number of normal and the excited molecules as calculated from the Maxwell-Boltzmann distribution law. Carelli (*loc. cit.*), on the other hand, suggested that the same are proportional to the square of the number of molecules in the normal and the excited states. Again, the fourth power law of intensities was suggested by Cabbanes and Rocard (*J. de Phys. et le Radium*, x. p. 52 (1929)), and later by Mandelstam and Landsberg (*Zeit. f. Phys.* lx. p. 366 (1930)), Tamm (*Zeit. f. Phys.* lx. p. 363 (1930)), and Orstein and Rekveld (*Zeit. f. Phys.* lxiii. p. 257 (1931)). According to these

$$\frac{I_s}{I_{AS}} = \frac{(\nu - \nu)^4}{(\nu + \nu_i)^4} \, e^{\frac{h\nu_i}{kT}}, \quad . \quad . \quad . \quad . \quad (1)$$

where ν is the incident frequency, and ν_i is the difference between the incident and the modified frequencies. Orstein,

---

* Communicated by K. C. Kar, D.Sc.

as well as Mandelstam and Landsberg, introduces the transition probabilities of Einstein (*Phys. Z.* xviii. p. 123 (1917)), whereas Tamm uses a quantum mechanical expression and deduce the intensities from electric moments.

In the present investigation the Raman effect will be considered from an entirely different aspect. In a previous paper (Phil. Mag. xii. p. 583 (1931)) a mechanism of unimolecular reactions was suggested, and, subsequently, it was pointed out that the Raman effect may be considered as unimolecular reaction, according to the following scheme :

$$A_m \xrightarrow{h\nu} A_{a_1} \longrightarrow A_n + h(\nu - \nu_i) \qquad \text{Stokes lines, . . (2)}$$

$$A_n \xrightarrow{h\nu} A_{a_2} \longrightarrow A_m + h(\nu + \nu_i) \qquad \text{Anti-Stokes line, \quad (3)}$$

where A_m and A_n stand for a molecule in the mth and nth states. In the first case the normal molecule passes to an intermediate active state by the absorption of radiation of initial frequency ν, and, subsequently, to the excited state by giving out radiation of frequency $\nu - \nu_i$. Thus the excited molecule has absorbed infra-red radiation of frequency ν_i in passing from the state $m \longrightarrow n$. This is in line with the radiation hypothesis of chemical reactions. The difference between the Raman effect and the ordinary chemical reaction is, that, in the first case, the excited (or active) molecules do not further decompose, as in the case of ordinary active molecules, in chemical reactions (*cf.* Phil. Mag. *loc. cit.*). In the case of the anti-Stokes lines we have the reverse process. The molecule already excited absorbs again a quantum of initial frequency ν and thus passes into a second activated state, but immediately returns to the normal state by the emission of radiation of frequency $\nu + \nu_i$.

In order to calculate the number of molecules N_n in the excited state, we will follow a method due to Christiansen (*Zeit. f. Phys. Chem.* ciii. p. 91 (1923)), who advanced arguments similar to that of Einstein (*Phys. Z.*, loc. cit.) in the derivation of Planck's radiation law from the Bohr model. The number of molecules N_{a_1} obtained by the absorption of $h\nu$ by the normal molecules

$$N_{a_1} = N_m \frac{p_{a_1}}{p_m} e^{-\frac{E_{a_1} - E_m}{kT}} = N_m \cdot \frac{p_{a_1}}{p_m} \cdot e^{-\frac{h\nu}{kT}}, \quad . \quad . \quad (4)$$

where the *à priori* probabilities for the two states are p_{a_1} and p_m and $\dfrac{p_{a_1}}{p_m}$ may be taken to be unity. Now, the number of molecules N_n are obtained by the emission of radiation

of frequency $\nu' = \nu - \nu_i$. Hence, we have, after Einstein, the number of excited molecules,

$$N_n = N_m e^{-\frac{h\nu}{kT}} (A_{a_1}^n + B_{a_1}^n \cdot \rho_{\nu'}), \quad \cdots \quad (5)$$

where $A_{a_1}^n$ is the probability of spontaneous emission, and $B_{a_1}^n$ is the probability of emission proportional to the radiation density $\rho_{\nu'}$. Now, we know that (Einstein, *loc. cit.*)

$$\rho_{\nu'} \cdot B_{a_1}^n = \frac{A_{a_1}^n}{e^{\frac{h\nu'}{kT}} - 1}, \quad \cdots \quad (6)$$

and hence from (5) and (6),

$$N_n = N_m e^{-\frac{h\nu}{kT}} \cdot \frac{A_{a_1}^n}{1 - e^{\frac{h\nu'}{kT}}} . \quad \cdots \quad (7)$$

If, along with Christiansen, we identify $A_{a_1}^n$ with the frequency ν', then

$$N_n = N_m e^{-\frac{h\nu}{kT}} \cdot \frac{\nu'}{1 - e^{\frac{h\nu'}{kT}}} . \quad \cdots \quad (8)$$

For small values of $\dfrac{h\nu'}{kT}$, from equation (8), we have

$$N_n = N_m \cdot e^{-\frac{h\nu}{kT}} \cdot \frac{kT}{h}, \quad \cdots \quad (9a)$$

while for larger values of $\dfrac{h\nu'}{kT}$,

$$N_n = N_m \cdot e^{-\frac{h\nu}{kT}} \cdot \nu'. \quad \cdots \quad (9b)$$

Hence the total energy due to the Stokes lines

$$E_S = N_n \cdot \rho_{\nu,}$$
$$= N_m \cdot \frac{k^2 T^2}{c^3 h} \cdot 8\pi\nu'^2 \cdot e^{-\frac{h\nu}{kT}} . \quad \cdots \quad (10a)$$

for high temperatures or small $\dfrac{h\nu'}{kT}$ (Rayleigh-Jeans). Again,

$$E_S = N_m \cdot \frac{8\pi h\nu_1^4}{c^3} \cdot e^{-\frac{h\nu}{kT}} e^{-\frac{h\nu'}{kT}} \quad \cdots \quad (10b)$$

for large values of $\dfrac{h\nu'}{kT}$ for low temperatures (Wien).

For the case of anti-Stokes transitions we have, similarly, for the number of normal molecules which are brought back to the normal state from the excited state,

$$N_m' = N_n' \cdot {}^{-}e^{\frac{h\nu}{k\mathrm{T}}} \cdot \frac{k\mathrm{T}}{h},$$

or

$$N_m' = N_n' \cdot e^{-\frac{h\nu}{k\mathrm{T}}} \cdot \nu'',$$

where N_n' are the number of previously excited molecules which give rise to N_m' normal molecules by the emission of frequency ν''. Again, since N_n' are obtained by the absorption of energy corresponding to $h\nu_i$, by the normal molecules N_m, we have from Boltzmann's distribution law,

$$N_n' = N_m e^{-\frac{h\nu_i}{k\mathrm{T}}} \cdot = N_m e^{-h(\nu-\nu')} ; \text{ since } \nu' = \nu - \nu_i.$$

Thus

$$N_m' = N_m \cdot e^{-\frac{h(\nu-\nu')}{k\mathrm{T}}} \cdot e^{-\frac{h\nu}{k\mathrm{T}}} \cdot \frac{k\mathrm{T}}{h} \quad . \quad . \quad (11a)$$

or

$$N_m = N_m \cdot e^{-\frac{h(\nu-\nu')}{k\mathrm{T}}} \cdot e^{-\frac{h\nu}{k\mathrm{T}}} \cdot \nu''. \quad . \quad . \quad (11b)$$

$$\therefore E_{AS} = N_m \cdot e^{-\frac{h(\nu-\nu')}{k\mathrm{T}}} \cdot e^{-\frac{h\nu}{k\mathrm{T}}} \cdot \frac{8\pi\nu''^2 k^2 \mathrm{T}^2}{c^3 h} \quad . \quad (12a)$$

for high temperatures or small $\dfrac{h\nu''}{k\mathrm{T}}$, and

$$\therefore E_{AS} = N_m \cdot e^{-\frac{h(\nu-\nu')}{k\mathrm{T}}} \cdot e^{-\frac{h\nu}{k\mathrm{T}}} \cdot \frac{8\pi k\nu''^4}{c^3} e^{-\frac{h\nu''}{k\mathrm{T}}} \quad . \quad (12b)$$

for low temperatures or large $\dfrac{h\nu''}{k\mathrm{T}}$.

Hence, from (10a) and (12a),

$$\therefore \frac{I_S}{I_{AS}} = \frac{E_S}{E_{AS}} = \frac{\nu'^2}{\nu''^2} \cdot e^{\frac{h(\nu-\nu')}{k\mathrm{T}}} = \frac{(\nu-\nu_i)^2}{(\nu+\nu_i)^2} e^{\frac{h\nu_i}{k\mathrm{T}}}. \quad (13a)$$

for high temperatures or small ν and ν_i, and from (10b) and (12b),

$$\frac{I_S}{I_{AS}} = \frac{\nu'^4}{\nu''^4} \cdot e^{\frac{\{h(\nu-\nu_1)+(\nu''-\nu')\}}{k\mathrm{T}}} = \frac{(\nu-\nu_i)^4}{(\nu+\nu_i)^4} e^{\frac{3h\nu_i}{k\mathrm{T}}} \quad . \quad (13b)$$

for low temperatures or large ν and ν_i, since $\nu' = \nu - \nu_i$ and $\nu'' = \nu + \nu_i$.

If, on the other hand, we take the intensities to be proportional to the number of molecules in the excited and in the normal state as suggested by Raman (*loc. cit.*), we obtain from equations (9 *a*) and (11 *a*).

$$\frac{I_S}{I_{AS}} = e^{-\frac{h\nu_i}{kT}}, \quad \ldots \ldots \quad (14a)$$

and from equations (9 *b*) and (11 *b*),

$$\frac{I_S}{I_{AS}} = \frac{(\nu - \nu_i)}{(\nu + \nu_i)} e^{-\frac{h\nu_i}{kT}}. \quad \ldots \ldots \quad (14b)$$

Again, taking the intensities to be proportional to the square of the number of normal and excited molecules (Carelli, *loc. cit.*), we have from the above equations

$$\frac{I_S}{I_{AS}} = e^{-\frac{2h\nu_i}{kT}} \quad \ldots \ldots \quad (15a)$$

for high temperature or low frequency, and

$$\frac{I_S}{I_{AS}} = \frac{(\nu - \nu_i)^2}{(\nu + \nu_i)^2}. \; e^{-\frac{2h\nu_i}{kT}} \quad \ldots \ldots \quad (15b)$$

for low temperature or large frequency. It is interesting to note that the above equation resembles (13 *a*), although these are valid for different cases. We shall, however, prefer the fourth power formula (13 *b*) for Raman lines in the visible region at ordinary temperature, since *ν* is sufficiently large. This is in agreement with the results of Mandelstam and others. It may, however, be pointed out that we have $3h\nu_i$ instead of simply $h\nu_i$, in our equation (13 *b*), but this does not make any material difference if $h\nu_i$ is large compared to kT.

My thanks are due to Dr. K. C. Kar for helpful criticism.

Chemical Laboratory,
  Benares Hindu University,
    Benares, June 1931.

XXVI. *The more Accurate Calculation of the Deflexion of Beams and Struts.* By H. H. JEFFCOTT, Sc.D. *

1. IN engineering design it is often required to determine by calculation the deflexion of a beam or of a strut, and in some instances this is required with accuracy.

We shall suppose the beam or strut to be straight and of uniform section, and to be long compared with the cross-sectional dimensions. Then the solution is to be derived from the formula

$$\frac{EI}{\rho} = M,$$

where M is the value of the bending moment at a point in the axis of the beam where the radius of curvature of the neutral axis is ρ and EI is the flexural rigidity of the beam, E being Young's modulus of elasticity and I the moment of inertia of the cross-section about a line through the neutral axis perpendicular to the plane of bending.

If x and y be the rectangular coordinates of a point on the neutral axis where the radius of curvature is ρ, then

$$\rho = \frac{\left\{1 + \left(\frac{dy}{dx}\right)^2\right\}^{3/2}}{\frac{d^2y}{dx^2}}.$$

Hence

$$EI\frac{d^2y}{dx^2} = M\left\{1 + \left(\frac{dy}{dx}\right)^2\right\}^{3/2}.$$

Now in general the elastic deformation is small and the slope $\frac{dy}{dx}$ is also small. Accordingly in ordinary calculations it is permissible to neglect the term $\left(\frac{dy}{dx}\right)^2$ compared with unity in the expression

$$\left\{1 + \left(\frac{dy}{dx}\right)^2\right\}^{3/2}.$$

The equation

$$EI\frac{d^2y}{dx^2} = M$$

is then usually easily soluble.

When high accuracy is desired this omission is not justifiable, and we shall see, particularly for struts, that the calculated deflexion may be seriously different when such omission is made.

It is proposed in this paper to discuss the deflexion of a simple strut and also of a simple case of bending under lateral load.

In these examples an approximate method will be put forward and illustrated for solving the more exact equation, and it will be found that the results of this method are fully

justified by comparison with the accurate solutions of the exact equations obtained in terms of elliptic integrals.

2. The method of approximation to be employed here has been used by the writer in other * applications.
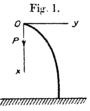
It consists in first finding the solution of the simple equation

$$\mathrm{EI}\frac{d^2y}{dx^2} = \mathrm{M}.$$

The value of y thus obtained is substituted in the small term $\left(\frac{dy}{dx}\right)^2$ yielding $\left(\frac{dy}{dx}\right)'^2$, and a solution is sought of

$$\mathrm{EI}\frac{d^2y}{dx^2} = \mathrm{M}\left\{1+\left(\frac{dy}{dx}\right)'^2\right\}^{3/2}.$$

The value of y thus obtained is a closer approximation to the true value than that derived by the complete omission of the small term. If desired this new and more accurate

Fig. 1.

value of y may be substituted in the small term $\left(\frac{dy}{dx}\right)^2$, and a still more accurate value will result.

Successive approximations of this kind may be carried out, but usually only one or at most two will suffice.

The application of the method will be clear from the examples to be given, and its accuracy will be tested by comparison with their exact solutions.

3. Let us take as the first example the case of a long, thin, straight rod clamped vertically at its lower end and subjected to a vertical load P at its upper end.

It is required to study the deflexion, the weight of the rod being negligible (fig. 1).

Take axes of x and y vertically and horizontally through the upper end of the rod as origin, and let x_1 and y_1 be the coordinates of the lower or fixed end.

---

* See Sci. Proc. R. D. S. xviii. no. 6, pp. 63–66 (1924); and Phil. Mag. vol. viii. p. 66 (July 1929).

Let s be the length measured along the neutral axis of the rod from the origin to the point x, y, and let the whole length of the rod be l. Bending in a single loop will only be considered.

The bending moment at the point xy is Py. The form of the neutral axis is given by

$$EI\frac{d^2y}{dx^2} = -Py\left\{1+\left(\frac{dy}{dx}\right)^2\right\}^{3/2},$$

or, using dots to denote differentiation,

$$EI\ddot{y} + Py(1+\dot{y}^2)^{3/2} = 0.$$

Put $$\mu^2 = \frac{P}{EI};$$

therefore $$\ddot{y} + \mu^2 y(1+\dot{y}^2)^{3/2} = 0.$$

The solution of this equation gives the x, y equation to the neutral axis.

We proceed now to solve this equation in three ways.

4. Firstly, we seek the simple and inexact solution obtained by omitting $\dot{y}^2$. The equation is

$$\ddot{y} + \mu^2 y = 0.$$

This is satisfied by

$$y = y_1 \sin \mu x.$$

The end conditions are

at $x=0$, $y=0$, at $x=x_1$, $y=y_1$ and $\dot{y}=0$.

Hence we require

$$\mu x_1 = \frac{\pi}{2}.$$

4 (a). We next find an expression for the length of arc s in this simple case.

$$\frac{ds}{dx} = (1+\dot{y}^2)^{1/2} = (1+\mu^2 y_1^2 \cos^2 \mu x)^{1/2}.$$

Now the term $\dot{y}^2$ is always small ; hence we observe that $\mu^2 y_1^2$ is small.

Put $\mu y_1 = 2k$, and expand the radical in powers of k. Therefore

$$\frac{ds}{dx} = 1 + 2k^2 \cos^2 \mu x - 2k^4 \cos^4 \mu x + \ldots$$

Regard the fourth and higher powers of k as being negligibly small.

Therefore

$$s = (1 + k^2)x + \frac{k^2}{2\mu}\sin 2\mu x,$$

the constant of integration being zero, since $s = 0$ at $x = 0$.

Now $s = l$ when $x = x_1$, and $\mu x_1 = \dfrac{\pi}{2}$.

Therefore $\qquad l = (1 + k^2)x_1 + \dfrac{k^2}{2\mu}\sin 2\mu x_1$;

$$\therefore \quad \mu l = (1 + k^2)\frac{\pi}{2}.$$

For comparison with other solutions it is convenient to put $y = y_1\cos\theta$, so that here $\sin\mu x = \cos\theta$ and $\mu x = \dfrac{\pi}{2} - \theta$
Accordingly

$$\mu s = (1 + k^2)\left(\frac{\pi}{2} - \theta\right) + \frac{1}{2}k^2\sin 2\theta.$$

5. For the second method of solution we use successive approximations.

In the equation

$$\ddot{y} + \mu^2 y(1 + \dot{y}^2)^{3/2} = 0$$

we substitute in the small term $\dot{y}^2$ the value $y = y_1\sin\mu x$ obtained in paragraph 4, and solve the resulting equation for y, namely

$$\ddot{y} + \mu^2 y(1 + \mu^2 y_1^2\cos^2\mu x)^{3/2} = 0.$$

Now this equation is not readily soluble, and it is more convenient to transform the original equation to one having y as the independent variable, i.e., to an equation in

$$\frac{dx}{dy} \quad \text{and} \quad \frac{d^2x}{dy^2}.$$

The equation $\qquad \ddot{y} + \mu^2 y(1 + \dot{y}^2)^{3/2} = 0$

then becomes $\qquad \ddot{x} + \mu^2 y\dot{x}^3\left(1 + \frac{1}{\dot{x}^2}\right)^{3/2} = 0.$

We observe that $\ddot{x} = \mu^2 y\dot{x}^3$ is satisfied by $\mu x = \sin^{-1}\dfrac{y}{y_1}$.

As an approximation we substitute this value of x in the small term $\dfrac{1}{\dot{x}^2}$, and we obtain

$$\frac{\ddot{x}}{\dot{x}^3} = \mu^2 y\{1 + \mu^2(y_1^2 - y^2)\}^{3/2}.$$

Now we know that the term $\mu^2(y_1{}^2-y^2)$ is always small compared with 1.

Expanding the radical we have

$$\frac{\ddot{x}}{\dot{x}^3} = \mu^2 y \left\{ 1 + \frac{3}{2}\mu^2(y_1{}^2-y^2) + \ldots \right\}.$$

Hence

$$-\frac{1}{2}\frac{d}{dy}\left(\frac{1}{\dot{x}^2}\right) = \mu^2 y \left\{ 1 + \frac{3}{2}\mu^2(y_1{}^2-y^2) \right\}$$

if powers of $\mu^2(y_1{}^2-y^2)$ higher than the first be omitted.

Integrating we obtain

$$-\frac{1}{\mu^2\dot{x}^2} = y^2\left(1 + \frac{3}{2}\mu^2 y_1{}^2\right) - \frac{3}{4}\mu^2 y^4 + C.$$

When $y = y_1$, $\dot{x} = \infty$;

$$\therefore \quad C = -y_1{}^2 - \frac{3}{4}\mu^2 y_1{}^4 ;$$

$$\therefore \quad \frac{1}{\mu^2\dot{x}^2} = (y_1{}^2 - y^2) + \frac{3}{4}\mu^2(y_1{}^2-y^2)^2.$$

Put $y = y_1\cos\theta$, and $\mu y_1 = 2k$;

then

$$\frac{1}{\dot{x}^2} = 4k^2\sin^2\theta + 12k^4\sin^4\theta ;$$

$$\therefore \quad \frac{1}{\dot{x}} = 2k\sin\theta.(1 + 3k^2\sin^2\theta)^{1/2},$$

or

$$\mu dx = \frac{-2k\sin\theta\, d\theta}{2k\sin\theta.(1+3k^2\sin^2\theta)^{1/2}},$$

since

$$dy = -y_1\sin\theta\, d\theta ;$$

$$\therefore \quad \mu dx = -\{1 + 3k^2\sin^2\theta\}^{-1/2}\, . \, d\theta.$$

Expanding the radical in powers of k, and omitting k^4 and higher powers, since k is small, we obtain

$$-\mu dx = \left(1 - \frac{3}{2}k^2\sin^2\theta\right)d\theta ;$$

$$\therefore \quad -\mu x = \left(1 - \frac{3}{4}k^2\right)\theta + \frac{3}{8}k^2\sin 2\theta + C.$$

At $\quad x = x_1, \quad y = y_1, \quad \cos\theta = 1, \quad \theta = 0$;

$$\therefore \quad C = -\mu x_1 ;$$

$$\therefore \quad \mu(x_1 - x) = \left(1 - \frac{3}{4}k^2\right)\theta + \frac{3}{8}k^2\sin 2\theta.$$

When $x = 0$, $y = 0$ and $\theta = \dfrac{\pi}{2}$;

therefore

$$\mu x_1 = \left(1 - \frac{3}{4}k^2\right)\frac{\pi}{2}.$$

5 (a). Next we find an expression for the length of arc *s*. We have

$$\left(\frac{ds}{d\theta}\right)^2 = \left(\frac{dx}{d\theta}\right)^2 + \left(\frac{dy}{d\theta}\right)^2 :$$

$$\therefore \quad \mu^2\left(\frac{ds}{d\theta}\right)^2 = \left\{1 - \frac{3}{4}k^2 + \frac{3}{4}k^2\cos 2\theta\right\}^2 + 4k^2\sin^2\theta$$

$$= 1 + k^2\sin^2\theta ;$$

$$\therefore \quad -\mu\frac{ds}{d\theta} = 1 + \frac{1}{2}k^2\sin^2\theta \text{ approximately ;}$$

$$\therefore \quad -\mu s = \left(1 + \frac{1}{4}k^2\right)\theta - \frac{1}{8}k^2\sin 2\theta + C.$$

When $y = 0$,   or $\theta = \dfrac{\pi}{2}$, $s = 0$;

therefore

$$C = -\left(1 + \frac{1}{4}k^2\right)\frac{\pi}{2};$$

$$\therefore \quad \mu s = \left(1 + \frac{1}{4}k^2\right)\left(\frac{\pi}{2} - \theta\right) + \frac{1}{8}k^2\sin 2\theta.$$

$$s = l \text{ when } \theta = 0 ;$$

$$\therefore \quad \mu l = \left(1 + \frac{1}{4}k^2\right)\frac{\pi}{2}.$$

This result differs seriously from that obtained by the simple though rough method of paragraph 4 (a). In that case

$$k^2 = \frac{2\mu l}{\pi} - 1$$

or

$$y_1^2 = \frac{4}{\mu^2}\left(\frac{2\mu l}{\pi} - 1\right).$$

The more approximate method followed in this paragraph eads to

$$y_1^2 = \frac{16}{\mu^2}\left(\frac{2\mu l}{\pi} - 1\right).$$

In other words, the value of the maximum deflexion is double that obtained by the simple method.

It is therefore important to investigate the matter with still greater accuracy.

Incidentally this great difference in the deflexion as determined from the two equations suggests the carrying out of an experiment of this kind to determine if $\dfrac{EI}{\rho} = M$ is in fact the more accurate formula. It is to be noted, however, that in this position the deflexion is very sensitive to small changes in the value of the load, which must therefore (as well as E and I) be determined with accuracy.

6. We now turn to finding a more exact solution of the equation

$$\ddot{y} + \mu^2 y(1+\dot{y}^2)^{3/2} = 0.$$

Obviously we can write down a first integral.

Multiply across by $\dfrac{2\dot{y}}{(1+\dot{y}^2)^{3/2}}$, and we obtain on integration

$$\frac{1}{(1+\dot{y}^2)^{1/2}} = \frac{1}{2}\mu^2 y^2 + C.$$

Now $\dot{y} = 0$ at $y = y_1$; therefore $C = 1 - \dfrac{1}{2}\mu^2 y_1^2$.

Hence

$$\frac{1}{(1+\dot{y}^2)^{1/2}} = 1 - \frac{1}{2}\mu^2(y_1^2 - y^2).$$

Put $y = y_1 \cos\theta$, $\mu y_1 = 2k$, and reduce.
Therefore

$$-\mu dx = \frac{1-2k^2\sin^2\theta}{\sqrt{1-k^2\sin^2\theta}}\,d\theta$$

$$= 2\sqrt{1-k^2\sin^2\theta}\,.\,d\theta - \frac{d\theta}{\sqrt{1-k^2\sin^2\theta}}\;;$$

$$\therefore\;\; \mu x = F(k,\,\theta) - 2E(k,\,\theta),$$

where F and E are elliptic integrals of the first and second kinds.

Since k is small compared with unity, we may expand the radicals, and if we omit powers of k higher than the second we find

$$-\mu x = \int \left(1 - \frac{3}{2}k^2\sin^2\theta\right)d\theta$$

$$= \left(1 - \frac{3}{4}k^2\right)\theta + \frac{3}{8}k^2\sin 2\theta + C.$$

When $x = x_1, \quad y = y_1, \quad \cos\theta = 1, \quad \theta = 0$;

therefore $C = -\mu x_1$;

$$\therefore \quad \mu(x_1 - x) = \left(1 - \frac{3}{4}k^2\right)\theta + \frac{3}{8}k^2 \sin 2\theta.$$

When $x = 0, \quad y = 0 \quad$ and $\quad \theta = \dfrac{\pi}{2}$;

$$\therefore \quad \mu x_1 = \left(1 - \frac{3}{4}k^2\right)\frac{\pi}{2}.$$

6 (a). To find an expression for the length of arc s we proceed precisely as in paragraph 5 (a).

Since the values of x and y in terms of θ are exactly the same in paragraphs 5 and 6 to the second power of k, we obtain the same results for s and l as in paragraph 5 (a), namely

$$\mu s = \left(1 + \frac{1}{4}k^2\right)\left(\frac{\pi}{2} - \theta\right) + \frac{1}{8}k^2 \sin 2\theta,$$

and $\mu l = \left(1 + \dfrac{1}{4}k^2\right)\dfrac{\pi}{2}$ *.

Accordingly to the second power of k the value of the maximum deflexion y_1 obtained from the equation

$$\ddot{y} + \mu^2 y(1 + \dot{y}^2)^{3/2} = 0$$

agrees with that obtained by the method of approximation described, using but one stage in the approximation, and is double that obtained by solving the simpler equation

$$\ddot{y} + \mu^2 y = 0.$$

In like manner the solution may be carried to higher powers of k than the second, and the exact solution be compared with that obtained by the method of approximations, employing one or more successive stages as desired.

7. We now turn to a second example and consider a simple case of lateral loading.

We shall find the deflexion of a long, thin, straight beam clamped horizontally at one end and subjected to a single load W at the other end, the weight of the beam being negligible (fig. 2).

Take axes of x and y horizontally and vertically through the loaded end of the beam, $x_1 y_1$ being the coordinates of the clamped end.

Let s be the length of the arc of the neutral axis from

---
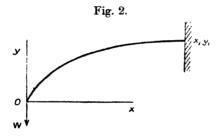
* This result has recently been given by M. Bertrand de Fontviolant.

the origin to the point $x_1 y_1$, and let the whole length of the beam be l.

The bending moment at the point xy is Wx, and accordingly the form of the neutral axis is given by

$$\text{EI}\frac{d^2y}{dx^2} = -Wx\left\{1+\left(\frac{dy}{dx}\right)^2\right\}^{3/2},$$

or

$$\ddot{y} + 2\mu x(1+\dot{y}^2)^{3/2} = 0,$$

if

$$\mu = \frac{W}{2\text{EI}}.$$

We proceed to solve this equation in three ways in paragraphs 8, 9 and 10.

8. First we take the simple and usual method of omitting the term $\dot{y}^2$. The equation is then $\ddot{y} + 2\mu x = 0$.

We readily find the solution complying with the terminal conditions is

$$y = \frac{1}{3}\mu x(3x_1^2 - x^2).$$

Hence

$$y_1 = \frac{2}{3}\mu x_1^3.$$

8 (*a*). To find s

$$ds = (1+\dot{y}^2)^{1/2}.dx,$$
$$\dot{y} = \mu(x_1^2 - x^2).$$

Hence

$$ds = \left\{1 + \frac{1}{2}\dot{y}^2 - \frac{1}{8}\dot{y}^4 + \dots\right\}dx$$

$$= \left\{1 + \frac{1}{2}\mu^2(x_1^2 - x^2)^2 - \frac{1}{8}\mu^4(x_1^2 - x^2)^4 + \dots\right\}dx;$$

$$\therefore \quad s = x + \frac{1}{2}\mu^2 x \left(x_1^4 - \frac{2}{3} x_1^2 x^2 + \frac{1}{5} x^4 \right)$$

$$- \frac{1}{8}\mu^4 x \left(x_1^8 - \frac{4}{3} x_1^6 x^2 + \frac{6}{5} x_1^4 x^4 - \frac{4}{7} x_1^2 x^6 + \frac{1}{9} x^8 \right) + \dots ;$$

$$\therefore \quad l = x_1 + \frac{4}{15}\mu^2 x_1^5 - \frac{16}{315}\mu^4 x_1^9 + \dots .$$

9. We next apply the method of approximations to this problem.

In the equation

$$\ddot{y} + 2\mu x (1 + \dot{y}^2)^{3/2} = 0$$

we substitute in the small term $\dot{y}^2$ the approximate value of y already obtained in paragraph 8.

Hence

$$\ddot{y} + 2\mu x \{1 + \mu^2 (x_1^2 - x^2)^2\}^{3/2} = 0.$$

As $\dot{y}^2$ and therefore $\mu^2 (x_1^2 - x^2)^2$ is always small, we may expand and omit the higher powers of the small quantity.

Hence

$$\ddot{y} + 2\mu x \left\{ 1 + \frac{3}{2}\mu^2 (x_1^2 - x^2)^2 \right\} = 0.$$

Integrating and substituting the terminal conditions we readily find

$$y = \frac{1}{3}\mu x (3x_1^2 - x^2)$$

$$+ \frac{1}{70} \mu^3 x (35x_1^6 - 35x_1^4 x^2 + 21x_1^2 x^4 - 5x^6),$$

and

$$y_1 = \frac{2}{3} x_1^3 + \frac{8}{35} \mu^3 x_1^7.$$

9 (a).

$$ds = (1 + \dot{y}^2)^{1/2} dx$$

$$= \left(1 + \frac{1}{2}\dot{y}^2 - \frac{1}{8}\dot{y}^4 + \dots \right) dx$$

$$= \left\{ 1 + \frac{1}{2}\mu^2 (x_1^2 - x^2)^2 + \frac{3}{8} \mu^4 (x_1^2 - x^2)^4 + \dots \right\} dx,$$

since y has the value found in paragraph 9.

$$\therefore \quad s = x + \frac{1}{2}\mu^2 x \left(x_1^4 - \frac{2}{3} x_1^2 x^2 + \frac{1}{5} x^4 \right)$$

$$+ \frac{3}{8}\mu^4 x\left(x_1^8 - \frac{4}{3}x_1^6 x^2 + \frac{6}{5}x_1^4 x^4 - \frac{4}{7}x_1^2 x^6 + \frac{1}{9}x^8\right) + \dots,$$

and

$$l = x_1 + \frac{4}{15}\mu^2 x_1^5 + \frac{16}{105}\mu^4 x_1^9 + \dots .$$

10. Finally, in verification of the method of approximation just employed we seek a more exact solution of the original equation

A first integral of the equation

$$\ddot{y} + 2\mu x(1 + \dot{y}^2)^{3/2} = 0$$

is

$$\frac{\dot{y}}{(1 + \dot{y}^2)^{1/2}} + \mu x^2 = C.$$

At $x = x_1$, $y = 0$; therefore $C = \mu x_1^2$.
Therefore

$$\frac{\dot{y}}{(1 + \dot{y}^2)^{1/2}} = \mu(x_1^2 - x^2).$$

Hence

$$\dot{y} = \frac{\mu(x_1^2 - x^2)}{\{1 - \mu^2(x_1^2 - x^2)^2\}^{1/2}}.$$

The solution of this equation can be expressed in elliptic integrals.

Since the term $\mu^2(x_1^2 - x^2)^2$ is small it will suffice to obtain an approximate solution of the first integral by expansion and the omission of small quantities. It then becomes approximately

$$\dot{y} = \mu(x_1^2 - x^2)\left\{1 + \frac{1}{2}\mu^2(x_1^2 - x^2)^3\right\}.$$

Hence

$$y = \frac{1}{3}\mu x(3x_1^2 - x^2) + \frac{1}{70}\mu^3 x(35x_1^6 - 35x_1^4 x^2 + 21x_1^2 x^4 - 5x^6),$$

and

$$y_1 = \frac{2}{3}\mu x_1^3 + \frac{8}{35}\mu^3 x_1^7.$$

10 (a).

$$ds = (1 + \dot{y}^2)^{1/2}\,dx,$$

$$1 + \dot{y}^2 = \frac{1}{1 - \mu^2(x_1^2 - x^2)} \text{ from paragraph 10;}$$

$$\therefore \quad ds = \left\{1 + \frac{1}{2}\mu^2(x_1^2 - x^2)^2 + \frac{3}{8}\mu^4(x_1^2 - x^2)^4 + \dots \right\} dx;$$

$$\therefore \quad s = x + \frac{1}{2}\mu^2 x \left(x_1^4 - \frac{2}{3} x_1^2 x^2 + \frac{1}{5} x^4 \right)$$
$$+ \frac{3}{8} \mu^4 x \left(x_1^8 - \frac{4}{3} x_1^6 x^2 + \frac{6}{5} x_1^4 x^4 - \frac{4}{7} x_1^2 x^6 + \frac{1}{9} x^8 \right)$$
$$+ \dots,$$

and

$$l = x_1 + \frac{4}{15}\mu^2 x_1^5 + \frac{16}{105}\mu^4 x_1^9 + \dots .$$

11. Thus we find that the results of the method of approximation of paragraph 9, even when employing only one stage of approximation, are the same as those given by the more exact method of paragraph 10, so far as the terms up to μ^4 are concerned.

The usual simple method of paragraph 8 gives agreement only so far as terms in μ^2.

For obtaining exact results in deflexion problems the usual method involving the omission of the term $\dot{y}^2$ is insufficient, and the employment of the method of successive approximation described above, even when carried only to one stage, is advocated as a method of general utility.

June 1931.

XXVII. *Notices respecting New Books.*

L'Introduction des théories de Newton en France au XVIIIͤ *siècle.* By PIERRE BRUNET. (Paris: Librairie Albert Blanchard. Price 55 francs.)

IN this book the learned author describes the protracted struggle between the followers of Des Cartes and Newton which preceded the general acceptance of the latter's philosophy, to use the old term, in France. The action-at-a-distance of Newton offered grave difficulties to philosophers accustomed to think of space as filled with vortices which carried the planets round; as Voltaire wrote in 1733: "Un Français qui arrive à Londres trouve les choses bien changées en philosophie .... Il a laissé le monde plein, il le trouve vide. A Paris, on voit l'univers composé de tourbillons de matière subtile : à Londres, on ne voit rien de cela. Chez nous, c'est la pression de la lune qui cause le flux de la mer ; chez les Anglais, c'est la mer qui gravite vers la lune." The Cartesians reproached Newton with bringing back, in the force of gravity, the doctrine of occult qualities, although as Cotes (whom M. Brunet, with that pleasant variation which the French always bring to our names, calls Côtes) and Newton himself

pointed out, the term would be more properly applied to the vortices of fictive material than to a force which was manifest to everybody, however little its true nature was understood.

Newton's criticism of the vortices, on the ground that they were incompatible with the known laws of astronomy, was met with a host of ingenious, but mechanically unsound, arguments, hypotheses, and analogies, described by M. Brunet in his first chapter. The next chapter deals with the period 1720 to 1728, in which appeared not only Keill's famous exposition of the Newtonian doctrine, written in Latin, Coste's French translation of the 'Opticks,' and 's Gravesande's textbook of Newtonian philosophy, but also a host of books defending various aspects of the Cartesian theory. In 1728 the Académie des Sciences awarded a prize to Bülffinger for a Cartesian disquisition on gravity, and Privat de Molières defended the vortex scheme, while in the next few years other writers showed that the Cartesian philosophy still had a firm hold in France. We then find the great names of Maupertius and Voltaire, who were to bring about the ultimate triumph of Newton in France. Meanwhile, however, Jean Bernoulli defended the Cartesian system, of which he was an upholder until his death in 1748. M. Brunet deals at length with these matters, bringing to their discussion a wealth of knowledge, and closes his book in the year 1738, when Voltaire's 'Eléments de la Philosophie de Newton' appeared. to give the controversies a new direction. He promises to continue the history of the subject in a further volume.

M. Brunet's book is of very great interest, showing, as it does, how great is the force of a tradition, and how possible it is for men of great learning, nay even of genius, to adhere to a theory which has, seen from a distance, clearly been shown to be untenable. Every student of the history of science will find his subject one of great fascination. Many of the arguments of the Cartesians would be easier to follow if M. Brunet had given us a few drawings in illustration of their contentions, which are, no doubt, perfectly clear to him, saturated as he must be in the Cartesian literature of the time. A copious bibliography will aid the reader who wishes to go more deeply into any particular point.

A Comprehensive Treatise upon Inorganic and Theoretical Chemistry. By J. W. MELLOR. Vol. IX. (London : Longmans, Green & Co. Price 63s.)

DR. MELLOR's monumental undertaking is by now so well known to all physicists and chemists that praise, or expressions of wonder at so colossal a task so well carried out, are superfluous. The present volume deals with the elements tellurium, chromium, molybdenum, and tungsten, all of great interest to physicists. The tradition of excellence and completeness which already attaches to the work appears to be well maintained.

The Nature of a Gas. By LEONARD B. LOEB. (New York: John Wiley & Sons. Price 12s. 6d.)

THE plan of this book is somewhat unusual. It owes its origin to a Committee on Electrical Insulation of the American National Research Council, which, in view of the fact that gases are commonly used as insulators, asked Professor Loeb to treat of the nature and electrical properties of a gas. It is probably as a consequence of the fact that the book is not primarily intended for physicists that it contains not only, for example, a general account of some of the latest researches on the probability of ionization of different gases and vapours by the impact of electrons of different primary velocity, but also a simple description of the kinetic theory of gases, including the significance of mean free path and other elementary conceptions which would generally be supposed to be familiar to readers seeking information on ionization. The matter is, from the point of view of the ordinary text-book or monograph, miscellaneous, but the exposition is at all points very good and the diagrams excellent.

The book is divided into three sections. The first one presents a general outline of the modern theory of atomic structure, in terms of electron orbits, and of the elementary features of molecular structure, as seen by the physicist. The second gives a description of the chief features of the kinetic theory of gases, while in the third the mechanism of ionization is discussed, with special reference to critical potentials. Throughout the language is simple and the mathematics elementary. There are useful appendices and a short and practical bibliography. The peculiar object with which the book was written seems to have been well fulfilled.

Molecular Rays. By RONALD G. J. FRASER, Ph.D. (Aberd.). [Pp. xii+204.] (Cambridge University Press, Fetter Lane, London, E.C. 4. Price 12s. 6d. net.)

THE increasingly large number of experimental results that have been obtained by using molecular rays makes Dr. Fraser's book particularly welcome at the present stage. The earlier part of the book deals in considerable detail with the technique of the production and measurement of the rays, and gives valuable information on laboratory experience which has not yet appeared in the original papers on the subject. A considerable amount of the research recorded has been carried out at the Hamburg Institute of Physical Chemistry, in which the author himself worked for three years.

A good account is given of the important bearing of the method of molecular rays on the fundamental postulates of the gas kinetic theory. Attention is drawn to the direct and primitive nature of the method which enables it to attack problems of a fundamental character. This is strikingly demonstrated by the fact that it has been found possible to diffract beams of atoms and molecules

at the cross grating of a crystal cleavage, and thus to establish
directly the wave properties demanded by the new mechanics.
The last chapter touches many applications of molecular rays, but
gives rather a brief account of the processes involved. Mathe-
matical data are treated where possible in an elementary manner,
and are everywhere as concise as is possible to bring out the full
significance of the results. Diagrams, graphs, and photographs
are used freely throughout the book with a very pleasing effect.
Full references to researches carried out until 1930 are given as
footnotes, and the subject matter is developed up to and including
that year. A specialist will find ' Molecular Rays ' a useful text-
book, while other people, with but a slight knowledge of the
subject, will read it with enjoyment and profit.

Numerical Examples in Physics. By W. N. BOND, M.A.
(Cantab.), D.Sc. (Lond.). [Pp. 127.] (Edward Arnold & Co.,
London. Price 4s. net.)

ELEMENTARY students of physics have no difficulty in finding sets
of examples which enable them to test their understanding of the
formal results of the subject. An urgent need has, however, been
felt for similar typical examples in the more advanced parts,
particularly in the modern developments. The present little
volume sets out to supply this need. There are 450 examples in
all, of which 141 are of the standard to be expected in an Honours
Degree, 227 of a somewhat lower standard, and the remainder
elementary. The examples have been well selected, and there are
but few that should cause difficulty to a student who has studied
his text-books intelligently. It is particularly gratifying to find
a chapter of numerical questions on atomic physics, and it is to be
hoped that in future editions this last chapter will be considerably
enlarged. It would also be desirable to add a group of questions
on spectral theory and spectro-photometry, so as to familiarize the
student with energy and term values and modern spectroscopic
notation. A table of constants and useful formulæ would also
be an advantage. For teaching purposes this book should be
invaluable.

Acoustics : a Text on Theory and Application. By GEORGE W.
STEWART, Ph.D., and ROBERT B. LINDSAY, Ph.D. [Pp. iv + 358,
142 figures.] (Messrs. Chapman & Hall, Ltd., 11 Henrietta St.,
Covent Garden, London, W.C. 2. Price 25s. net.)

THIS book sets out to give a detailed theoretical survey of the
advance of acoustics during the last decade as a result of the
many new applications to which acoustical devices have been put,
e. g., subaqueous signalling, loud-speakers, and the use of sound
in national defence. A clear exposition is given of the theory
underlying the modern applications, as may be seen in the chapters
dealing with acoustic transmission through conduits, the effects of
branch lines, acoustic coupling, and so forth. The analogy with

electrical circuits is emphasized and skilfully used. On the other hand, the chapters on physiological acoustics, acoustics of buildings, and atmospheric acoustics give the impression of having been dealt with rather cursorily.

The idea inspiring the work, however, seems to be rather to deal with problems from their theoretical aspect, and to leave the field clear to others to give detailed descriptions of the practical devices already used or which can be constructed on the lines predicted by theory. Much of the practical information regarding acoustic impedance, filtration of sound, and so forth is the result of research by the authors.

Although in the preface the authors deny a thread of mathematical continuity throughout the book, and maintain that each application stands alone, yet in reading the work the impression is conveyed of a central mathematical idea which is enlarged and explained from Chapter I. to Chapter X. In some cases, where the full theory is already given in Rayleigh's ' Sound,' it has only been considered necessary to give a shortened synopsis and references. From Chapter IX. to the end the theory is obviously introduced only to explain certain special applications, and here gives the impression of discontinuity. Since, however, this is not a treatise on mathematics, but on the most concrete of the modern sciences, the feeling of physical unity must be the ultimate goal.

The claim put forward by the authors in the preface, that " the present work is unique in its stress on the important researches of the past decade and in the useful combination of material both from the theoretical and practical viewpoints," can hardly be substantiated in the light of the appearance of Dr. A. B. Wood's treatise on the subject.

Some useful examples are appended to each chapter. This will be found helpful to students entering the higher examinations, while much of the theory will inspire researchers in radio-telephony and telegraphy and many other subjects which have sprung up during the last decade.

XXVIII. *Proceedings of Learned Societies*

GEOLOGICAL SOCIETY.

November 4th, 1931.—Prof. E. J. Garwood, M.A., Sc.D., F.R.S., President, in the Chair.

1. Mr. E. J. WAYLAND, A.R.C.S., F.G.S., gave a brief description, illustrated by lantern-slides, of the Katwe crater-lake, Uganda. He remarked that Lake Katwe occupies the bottom of an explosion crater of the caldera type, and is one of many in southern Busongora lying between Lakes Edward and George, on the south and east respectively, and Ruwenzori

on the north-west. Not only is it of interest as a type example, but also because it is the source and centre of a flourishing native-managed salt industry, the improvement of which is being considered by the Government.

The level of Lake Katwe in relation to that of Edward, was wrongly determined by the Boundary Commission of 1906, and, very recently, was quite differently, and again erroneously, given by a railway survey party. The lecturer's own figures differed from the first of these determinations by nearly 170 feet, and from the second by about 102 feet. The difference in each case was enormous and very important, for upon it, in his view, depended the true geological and economic significance of Katwe. Precise re-levelling undertaken by the railway authorities had shown the lecturer's figures to be correct.

Lake Edward, it had been found, oscillates in accordance with the sunspot cycle, while Lake Katwe does not. While the level of the former is above the water-table, that of the latter is determined and maintained by it. It had been further shown that, although the volcanic vent passes through the saturation zone, its upper parts are more or less completely sealed off from the surrounding ground-water by deposits of the less soluble salts thrown out of solution at successively lower levels as temperature decreased with time. Within the tube so formed, aqueous circulation is produced by the temperature gradient, and the most soluble of the salts, derived at depth from decomposing alkali lavas, are thereby brought to the surface and, as a consequence of solar evaporation, are deposited in the shallow lake.

2. ' Petrology of the Volcanic Fields East and South East of Ruwenzori, Uganda.' By Prof. Arthur Holmes, D.Sc., D.I.C., F.G.S., and Henry Francis Harwood, Ph.D., M.Sc., F.G.S.

The various suites of rocks with which this paper deals were collected in 1924 and 1930 by members of the Geological Survey of Uganda, and were sent to the Authors for description and analysis, together with relevant field-notes and a geological map.

Towards the close of the period in which the Kaiso lacustrine beds were deposited, volcanic activity broke out along a series of belts extending north and south of Fort Portal and north and south of the Kazinga Channel. The first phase (Lower to Middle Pleistocene) is represented by sub-aqueous tuffs. Post-Kaiso rifting movements followed, and were succeeded in turn by a second phase of vulcanism, in which explosion-vents were blown through the rift-valley floor, the bordering scarps, and the adjoining plateau. The rocks of this stage

include tuffs and agglomerates, ejected blocks, and volcanic bombs.

Throughout the area the earlier tuffs appear to represent melilite-basalts. They contain fragments of biotite-pyroxenites and related types which constitute a well-defined suite of sub-volcanic rocks. The tuffs are followed by others having compositions transitional towards that of leucitite. The later cognate ejected blocks include melanocratic varieties of potash-nephelinite and leucitite, most of which are referred to as potash-ankaratrite or leucite-ankaratrite. Accompanying them are bombs of leucitite and olivine-leucitite, some of the latter being sufficiently rich in olivine to be regarded as a volcanic equivalent of kimberlite.

The volcanic belts together constitute a co-magmatic region of a highly individualized kind. Positive evidence is provided by the community of field occurrences, rock assemblages, mineral associations, and geochemical characters. Negative evidence includes the absence of quartz, plagioclase, and amphiboles from the suite of minerals, and of basalts and basaltic derivatives from the rocks. An attempt is made to show that the rocks could not have been derived from basaltic magma by any known process of differentiation, with or without assimilation. On the other hand, the rarer constituents revealed by five chemical analyses, and in particular the abundance of BaO and SrO, suggest community of origin with kimberlite, a new and detailed analysis of which has been made by Mr. L. S. Theobald for comparison.

It is shown that both kimberlite and olivine-leucitite could be derived from a magma having the composition of average peridotite or stony meteorites by abstracting from it the constituents of dunite and eclogite in reasonable proportions. Continued abstraction of olivine and pyroxene would lead to leucitite. Enstatite is found to be an early product of crystallization from olivine-leucitite; it also occurs as phenocrysts in melilite-basalt. These facts suggest the possibility that the abstraction of olivine and enstatite from a primary peridotite magma would serve to provide a melilite-basalt magma. The early separation of enstatite leaves the magma markedly deficient in silica, while under conditions of higher pressure the separation of chloromelanite (in eclogite) removes soda and leaves a relatively potash-rich magma. The hypothesis is proposed that the rocks described, together with kimberlite, represent various stages in the high-pressure crystallization-differentiation of a parent magma having a composition akin to that of average peridotite. The substratum that underlies the ' basaltic layer ' is regarded as the probable source of this magma.

XXIX. *nhν Emission in Xenon and Thallium iii.*
By W. M. Hicks, *F.R.S.*†

THERE is now considerable evidence for the existence
of *nhν* emissions in spectra, suggested by me in this
Journal ‡ two years ago. Further evidence for their presence
is given here in connexion with the spectra of X and Tl iii.
The discussion was originally undertaken in connexion with
a more complete determination of spectral constants. These
require an accurate value of the lowest *p*-term as a starting-
point, and the determination of this requires a knowledge of
several consecutive orders of one of the typical series. In
many cases those in *hν* emission lie in a region outside the
observed, while any in 2*hν* or 3*hν* come within. Unfor-
tunately the drastic excitations required to bring out clearly
the spectra of ionized atoms as a rule produce a considerable
amount of disruption of normal lines, so that it is often diffi-
cult to distinguish between their different collaterals. This
is specially the case in the very valuable and extended
measures of J. A. Carroll §, not only in Tl but also in Ga,
In, and Hg, observed by him. Very definite evidence of
such displacements in his data in Hg ii has been adduced ‖.

† Communicated by the Author.
‡ Phil. Mag. 8, 108, 29. In all references the numbers in order give
the volume, the page, and the last two digits of the year.
§ Trans. Roy. Soc. 225, 357, 25.
‖ Phil. Mag. 9, 673, 30.

The present discussion is restricted to (1) allocation of S.P. series in the blue spectrum of X and in Tl iii and some D sets in the latter, (2) evidence for the existence of these higher order emissions, and (3) direct evidence for collaterals in directly observed *hv* emissions and in assumed *2hv, 3hv*. An * is appended to *nhv* emissions, $n > 1$.

The theory is that the energy of fall of an exterior electron is transmitted to the nucleus, which then radiates it either as *hv, 2hv, 3hv*. The probability of any particular event happening with *2hv* or *3hv* increases with the amount of energy to be radiated. As the nucleus in H is the proton, the proton must be a radiator. It is tempting to suppose that it can only radiate *hv*, and that in other elements any *hv* emission comes from one proton only in the nucleus, but the nucleus can pass on the whole energy to one proton (*hv* emission) or can divide it equally between two (two *2hv* emissions) or between three (three *3hv* emissions).

Xenon †.

In xenon the triplet P series, after P1, runs down into the ultra-violet beyond any observed region. It is easy to get a rough idea as to where P2 should be, but the separations are not known, and it is hopeless to guess whether *nhv* emissions can be allocated. But the $p1 - p2$ combinations should lie within Baly's region, and would put themselves in evidence at once by reproducing the ν_1, ν_2 separations 1778, 816. Thence P2 can be deduced. As a fact, such combinations are found. Indeed, a whole series of $p1 - pm$ occur with indications up to $m = 9$, those for $m > 2$ being either found amongst Déjardin's ‡ latest measures (up to $n = 53400$) or in *2hv* emissions. We make this our starting-point. We shall denote the series $p1 - pm$ by $Q(m)$, with the usual Rydberg subscripts. With Qm given it is now possible to reconstruct Pm, and we find it established, with representatives up to $P_1 9$ at least, by means of *2hv, 3hv* emissions. Further, certain considerations published in 1926 § had led me to expect a second S1 set with *s1* a fraction of a volt above, *i. e.*, a W.N. about 1000 to 2000 greater, but unfor-

† Messrs. Meggers, de Bruin, and Humphreys, in a paper on the first spectrum of xenon, Bureau of Standards, no. 115, state (p. 733): "Hicks and —— have also discussed the structure of the first spectrum of xenon, but their results, too, are mostly spurious." I cannot understand this statement, as I have never at any time discussed, or even attempted to discuss, the constitution of the red spectrum. My attention has been given exclusively to the blue or second spectrum.

‡ *Ann. de Physique*, 14, 82, 30.

§ *Ann. de Physique*, 6, 294, 26.

tunately at that date they all lay outside the observed region. Now there are Déjardin's measures considerably beyond, and a complete triplet reproducing the ν_1, ν_2 separations is found at 2095 ahead. With this is found another series parallel to the above P with a limit $s1 + 2095$. The existence of these series therefore affords a very considerable amount of data involving $2h\nu$, $3h\nu$ emissions. We begin by reproducing the data of the S series in Table I., adding to it also a few $2h\nu$ as well as lines since observed by Déjardin which establish the old formulæ—and sounded—values.

A note may here be advisable as to the significance of the classification adopted by the Blochs and Déjardin. Their excitation is the method of bombardment, the classification depends on the velocity of the electrons when the line first appears, and it is supposed that the lines in any one class are due to one and the same degree of ionization. But this is doubtful. The method of bombardment does not, for example, seem favourable for the production of the lowest spark lines B.B.D. fail to observe a very considerable proportion of Baly's lines in the blue spectrum, and many of the lines classified by them as E_2, E_3 certainly belong to series lines of class E_1. This is quite definitely shown by their presence in exact positions in the series which I denoted as the 1864 F, remarkable not only for its regularity up to high orders but as possessing a summation series even more regular than the corresponding difference one. There are, of course, in analogy with all other spectra, many instances of displaced, linked, and summation lines produced by a higher excitation than that of the normal lines. But here there are several instances of normal series lines in which the allotted class is higher than E_1. It would appear that the bombardment excitation is not always favourable for the production of all E_1 lines. For their production it is necessary to ionize the atom. This then proceeds to emit its particular radiation, leaving it neutral but in an excited state. This excited atom then emits the Baly E_1 line in question.

In the following tables are given at the head the series formula, the triplet separations, together with the oun shifts, and in XS the link values of e, u, v. The oun shift on a term t is indicated by $t \rightarrow$. Thus in Table I. $p_1 1 \rightarrow\ = 10\cdot819$ is the change in the limit when the denominator of the term is altered by the addition or subtraction of δ_1. In X, δ_1 is $155\cdot42$ †. The shifts in the current terms are entered

† This is considerably larger than the value $152\cdot72$ given in the 'Analysis,' estimated from the $p1$ terms alone. The new value is settled by the new data afforded by the present discussion.

TABLE I.—(XS).

$$n = 51026\cdot99 - R/\{m + \cdot096726 - \cdot011826/m\}^2.$$

$\nu_1 = 1777\cdot96.$ $\nu_2 = 816\cdot14.$ $\nu_1 + \nu_2 = 2594\cdot10.$

$p_1 1 \rightarrow = 10\cdot819.$ $p_2 1 \rightarrow = 11\cdot389.$ $p_3 1 \rightarrow = 11\cdot654.$

$e = 7316\cdot13.$ $u = 4133\cdot64.$ $v = 4428\cdot53.$

Note.—All $\lambda > 2414$ are in R.A., those below 2414 in I.A.

26·730.

1.	<1 i	2869·71.*e*	−42154·07 [54·73]		
	{ 5 ii	3023·99.*e*	−40376·73		
	⎩ 10 i	2476·02	− 76·83	**1777·90**	
	4 i	2527·10	−39560·78	**816·05**	**2593·95**

3·730.

2.	{ 3 i	5368·30.*e*	25939·51		
	⎩ 4 iii	3854·44	37·76	−	
	5 i	3607·17	27715·72	**1779·96**	
	{ 3 i	4712·78.*e*	28529·95		
	⎩ 1 i	3505·99	31·86	**816·14**	**2594·10**

1·152

3.	4 i	2526·97	39562·82	−	
	{ <1	2938·38.*e*	41339·89	**1777·07**	
	⎩ 1	2418·47	37·53		
			(42156·8)		**2594·1**

·496

4.	{ 1*n* i	2689·82.*e*	44483·79 [82·54]		
	⎩ 1*n* i	2247·22	85·60	−	
	{ 4 i ½×4321·95		46264·22 *	**1778·62**	
	⎩ 0 iii	2160·9	62·4		
	1*n*	2514·16.*e*	47080·46	**816·24**	**2594·86**

·258.

5.	4 iii ½×4272·74		46797·00 * [800·89]		
	1 i	2423·08.*e*	48575·04	**1778·04**	
	{ <1	2884·39.2*e*	49392·81	**817·77**	**2595·81**
	⎩ 0*n* i ?	2023·82	95·51		**2594·62**
					from [ ]

6.	2 iii ?	2452·76.*e*	48075·63 [74·37]	−	
	1*n* i	2623·31.*e.v*	49854·53	**1778·90**	
	1 i	2549·05.*e.u*	50669·84	**815·31**	**2594·21**

7.	{ <1	2921·74.2*e*	48849·74 [48·22]	−	
	{ 1 i ½×4093		52 *		
	⎩ 1 iii	2046·5	48·4		

TABLE I. (cont.).

	4 ii	2777·10.2*e*	50631·90		
	1 i	2308·20.*e*	26·58		
	2*n* i	1975·92	25·99	**1776·25**	
	1 i	2715·91.2*e*	51442·85		
	2 i ½×3886·88	42·58 *	**816·59**	**2592·84**
	0 iii	1944·67	39·54		
8.	2 iii	2658·37.*e.v*	49352·10 [53·38]		
	<1*n* ½×4051·36	54·12 *	–	
	3*n* iii	2519·17.*e.u*	51135·04	**1780·92**	
	2*n* i	2468·54.*e.u*	948·91	**813·87**	**2594·79**
	1 i	2239·81.*e*	48·88		
	2 i ½×3848·75 ?	52·22 *		

9.	1 iii	2850·41.2*e*	49706·01 [01·20]		
	0 i ?	2011·5	698·0 02·0 (mean)		
		– – –	– – –		
	1 i ½×3823·34	52297·34 *	–	**2595·3**

| 10. | 2 i ½×4002·51 | 49956·46 * [50·11] | – |
| | | – – – | – – – | |

| | 2 iii | 2636·58.2*e* | 52550·37 | – | **2593·91** |
| | 0 i | 2210·3.*e* | 44·7 | | [**94·6**] |

11.	1 i	2584·04.*e.u*	50138·77 [36·13]	–	
	2 i	2470·30.*e.u*	51920·07	**1781·30**	
	5 iii ½×3791·82	52732·14 *	**812·07**	**2593·37**

12.	1 i	3202·17.2*e.v*	50281·70 [77·35]	–	
	1 iii (−δ₁) 1989·94	50280·0		
	1 iii ?	2479·98.*e.v*	52056·74	**1775·04**	
	3 iii ?	2614·13.2*e*	875·65	**818·91**	**2593·95**

13.	2 i	1985·25	50387·99 [87·43]	–	
	2 i	2663·43.2*e*	52168·09		
	0 i	1917·59	66·20	**1778·21**	
		– – –	– – –	

$m=3$.—3 i 2369·7 42188·3 as $(-3)S_3(-3)$ gives $S_3 = 42156·8$, with exact $\nu_1 + \nu_2$.

$m=4$.—Déj. gives two lines,

$$0\,\text{iii} ?\ 2247·5 \qquad 44480·0,$$
$$1n\,\text{i, iii} ?\ \ 7·22 \qquad 85·60.$$

These seem to be $S_1 4(\mp\delta)$, giving

$$S_1 4 = 44485·60 - 1·98 = \ldots 83·62,$$

agreeing with the *e* linked line and the formula.

$m=7$.—The $2h\nu$ line for S_1 is a rough measure by B.B.D., and is within O.E. of the 2*e* linked line.

above the corresponding values of *n*, except when less than O.E. In the P series the shifts for p_1, p_2, p_3 are entered in this order. Small Roman numerals denote Déjardin's classification. Numbers in [ ] denote calculated values and in ( ) those considered in the notes following the tables.

In my original paper † and in the 'Analysis' the orders above S3 were outside the then observed region. Their approximate positions were determined from the formula and sustained by sounding. The method of sounding is particularly applicable here, *e. g.*, using the *e*-link we find a parallel series with few lacunæ at aW.N. $e = 7316$ less. The consequence is that several successive orders of this parallel series are continued on in the observed region, while the real S are, so to say, out of sight. This enables us to reconstruct S4, S5, S6. $S7 - e$ is now beyond, but $2e$, $e + u$, $e + v$ come in. The table, as given here, contains additional data from Déjardin's extended region, including also new *e*-linked lines and several $2h\nu$ emissions. That Déjardin has not observed all the required lines may probably be put down to the unfavourable effect of his excitation. For exact comparison the sounding method is subject to a slight uncertainty due to small shifts often accompanying it. In $S_1 1$, $S_2 1$ they closely agree. In $S_1 4$ the old linked value and a new Déj. line agree within the considerable OE, but their mean is the calculated value. Again, in S6, with no directly observed lines, the sounded agree with the calculated $(d\lambda = \cdot 05)$ and give the true $\nu_1 + \nu_2$ separation $2594 \cdot 10 + \cdot 11$. In $S_2 4$, $S_1 7$ the *hν*, *2hν* are both observed and agree.

The next table gives the data of the $p1$ - $pm \equiv Qm$ lines. There is clear evidence of the presence of displacements, not to be unexpected when "forbidden" lines are in question. Consider first the Q2. $Q_{11} 2$ or 32960 gives the denominator of $p_1 2 = 2 \cdot 463873$ compared with $1 \cdot 466115$ for $p_1 1$, and the two give the formula at the top of the table. Further, the displacement for $\nu_1 + \nu_2 = 566 \cdot 87$ is of the same order of magnitude as that for $p1$, viz., 37767 compared with 35903, *i. e.*, $60\frac{3}{4} \delta$ compared with $57\frac{3}{4} \delta$. But the $\nu_1 + \nu_2$ of Q_1 is $2595 \cdot 20$, or $1 \cdot 20$ larger than the normal value, suggesting that in this set $p1$ is displaced by $- \delta_1$ or $- 2\delta_1$. However, taking it as undisplaced, the above formula gives the series of values entered in [ ] in the table for each order. They give values slightly less than the observed, $m = 3$ excepted, for which see the notes. But the formula is sufficiently good to settle the general correctness of the allocations of the Q.

† Trans. Roy. Soc. 220, 335, 19.

From Table II. the positions of the P lines can be indicated. As beyond $m=1$ they all lie in the far ultra-violet, they can only be identified by their $nh\nu$ emissions. The results are contained in Table III. The values as calculated from the Q are inserted in [ ]. The agreement is seen to be very good except in the case of P2, where the triplet is reproduced with the same separations but shifted -20. With $Q_{11}2 = 32960$, P_12 should be 75114, whereas the $2h\nu$ data definitely give a value 20 less. Those entered are clearly the representatives of P2, and they reproduce the same $p2$ separations as Q2. Again, this supports the supposition above that in Q2 the $p1$ terms are displaced to $p1(-2\delta_1)$. It will be seen that the agreement is remarkably close. That the march of the separations is a natural one is seen by a comparison of the displacements of the $\nu_1 + \nu_2$. They are, with the order of magnitude of the multiples of δ :—

m.	$\nu_1+\nu_2$.	Δ.	$m\delta$.
1	2594·1	35903	57¾
2	566·47	37741	60¾
3	216·80	40470	65
4	102·0	40649	65½
5	56·48	41488	66¾

To deal with the supposed preparatory potential, and with electrons passing from p_1 to a level in the sheath, equivalent to a small fraction of a volt, the spectrum must be examined for sets giving ν_1, ν_2 in the near region ahead of 42154. One such is found and is given in the right-hand column of Table III., 2095 ahead of P1. If, however, it represent the expected system, we must get lines corresponding to falls from the upper p levels to this lower one. In other words, there will appear a parallel P system 2095 ahead of the old. We shall denote it by P'. Their wave-numbers with intensities are given on the right hand, with the separations in heavy type. The order of emission of each line, *i. e.*, the n in $nh\nu$, is given in ( ) after each W.N., and the λ are appended at the end of the table. It is specially to be noted that $P_1'2$ agrees with P_12, and not with that calculated from Q2. Some confidence can be felt therefore that they correspond to the normal set, and that Q2 is abnormal. There is, however, evidence for displacement in the other P'2 lines adduced.

Although not bearing on the present discussion, it may be pointed out that 2095 is equivalent to ·258 volts, so that the

$$\text{TABLE II.}—(Q(m) \equiv p1-pm).$$

$$n = 51026\cdot99 - R/\{m + \cdot461631 + \cdot004484/m\}^2.$$

$$p_1 1 \rightarrow = 10\cdot819. \qquad p_2 1 \rightarrow = 11\cdot389. \qquad p_3 1 \rightarrow = 11\cdot645.$$

2·387. $m = 2.$

$p_3 2$ {	<1	*32398·98*	**1779·08**	<1	34178·07	**817·25**	1 i	*34995·33*
		- - -		<1	75·29	**816·74**	1 iii	89·33
2·353.		- - -	*164·14*		**176·64**	*161·13*		**176·35**
$p_2 2$ {	2 i	*563·12*	**76·08**	<1	*339·20*			
	1	578·83	**70·40**	1 i	349·23	**816·45**	<1 i	(35165·68)
2·279		381·19	*396·90*		**389·83**	*399·86*		**389·54**
$p_1 2$	2 i	960·02	**79·04**	1 i	739·06	**816·16**	3 iii	35555·22
		- - -	*561·04*		**566·47**	*560·99*		**565·89** 559·90

λλ. *3085 74*; *70·19*; *68·71*; *33·22.*——*2925·11*; *25·58*; *11·33*; *10·54*;
        2877·87.——*2856·80*: *57·29*; *11·81.*

·846. $m = 3.$

$p_3 3$ {	1 *n* i	41685·60 *	**1778·49**	3 i	43464·09			
			80·32	1 *n*	465·92 *s*			
·823		85·64			77·33	75·50		
$p_2 3$	1 *n* i	71·24 *	**1770·18**	6 iii	541·42 *	**820·12**	1 i	44361·54 *
·818.		133·52			141·30			
$p_1 3$		(41904·76)	**1777·96**	6 i	682·72 *			
		219·16			219·20	216·80		

λλ. ½×4796·66; ½×4786·83.——*2300·04*; ½×4600·20; ½×4592·22;
        ½× ...77·36.——½×4507·32.

·394. $m = 4.$

$p_3 4$	2 iii	45396·02	**1788·40**	10 i	47176·50 *	**815·83**	0 iii	47992·33
·387					41·35			46·93
$p_2 4$		- - -		1 i	217·85	**821·41**	3 i	48039·26 *
·384						80·29		75·70
$p_1 4$		(45520·18)	**1774·06**	{ 1 i	294·24	**820·72**	<1	114·96 *
		[18·74]		{ 2 ii	302·04 *	(98·14) (mean)		
		124·16				121·63		122·63

λλ. 2202·05.——½×4238·37; 2117·17; 13·75; ½×4227·12.——*2083·00*;
        ½×4162·25; ½×55·70.

$m = 5.$

$p_3 5$	2 iii	47302·04 *	**1782·32**	1	49084·36 *		- - -
					12·94		
$p_2 5$		- - -		2 i	097·40		- - -
		[51·34]			41·75		
$p_1 5$	3 *n* i	47363·92	**1775·23**	1 i	139·15	**819·6**	0 iii	49958·7
					54·79		

λλ. ½×4227·12; 2110·64.——½×4073 62; 2036·11; 34·38.——2001·0.

TABLE II. (*cont.*).

$m = 6$.

$p_3 6$	2 iii	48360·27		- - -		{ 1 i	50959·57
		13·57				{ 2n ii	61·64 *
$p_2 6$ {	1 i	373·84	**1778·11**	3 i	50151·95		- - -
	1 i	378·32 *					
		25					
$p_1 6$ {	1 i	398·66 [00·7]		0 i?	64·30	0 i?	95·7
	1 i	401·36 *		3 iii	62·06 *		
		38·39, 41·09					**36·2**

λλ. 2067·15; 66·57; $\frac{1}{2} \times 4133$·08; 2065·51; $\frac{1}{2} \times 4131$·11.——1994·59; 94·1;
$\frac{1}{2} \times 3986$·10.——1962·99; $\frac{1}{2} \times 3923$·56; 1961·6.

$m = 7$.

$p_2 7$	2 ii	49044·42		- - -		- - -	
		17·4					
$p_1 7$ {	1 iii	61·74	**1781·5**	0 i	50843·23	**823·54**	2n i	51666·77
		[57·4]		2	43·86 *		2 i	69·82 ×

λλ. 2038·31; 37·59.——1967·48; $\frac{1}{2} \times 3932$·63.——1935·48; $\frac{1}{2} \times 3869$·79.

$m = 8$.

$Q_{11} 8$	0 i	2020·5,	49476·7

				$m = 9$.		
		hν.				*2hν.*
$Q_{11} 9$	0 iii	2006·8.	49814·4	1 $\frac{1}{2} \times 4014$·27,	49810·48 *
			1755·9		**1761·56**
$Q_{21} 9$	0 i	1939·74,	51570·32	1 $\frac{1}{2} \times 3877$·12,	51572·04 *
					835·38
$Q_{31} 9$				1 i$\frac{1}{2} \times 3815$·32.	52407·42 *
					2596·94

$m = 2$. The lines in italics are clearly related to a corresponding Q_{13}, although there is no Q_{13} for the given set ("forbidden"). There is also no direct line for Q_{32}, but there is an apparent collateral, < 1 i, 2841·46, 35149·32 as $(1/-2)$ gives $Q_{32} = 35165$·68. This gives the correct $\nu_2 = 816$·45 within O.E.

$m = 3$. The formula value for Q_{11} is 41881·43. The (41904) entered as Q_{11} is the $Q_{12} + \nu_1$, and it will be found to give rise to a corresponding $P_1 3$. The 41881·43 is 23·33 less than this. The shift is due to displacement $2/-2 = 21$·638 + 1·636 = 23·27. There is a great deal of disruption of Q3 present in the spectrum which is of interest for collateral theory, but as it does not bear on the present discussion of $nh\nu$ emissions it is omitted.

1 i 2253·10, 44384·28 as $(-3\delta_1)Q_{32}$ gives $Q_{32} = 44360$·97, *i. e.*, is the $2h\nu$ line ... 61·54.

$m = 4$. The $2h\nu$ line for Q_{23} seems too strong. Possibly it covers a $Q_{23} = 47177$·42 giving the $\nu_1 + \nu_2$ separation $= 121$·43, the same as the others.

ionization potential for the S.D sets should be $11{\cdot}50 + {\cdot}26$ $= 11{\cdot}76$ volts †.

The separation 2095 can be due only—so far as our present knowledge reaches—to (1) a displacement in the $s1$ term (not in $p1$, since ν_1, ν_2 are unaltered), (2) to a linkage effect, or (3) to the replacement of s by an independent term-type:

(1) The displacement on $s1$ to produce $2095{\cdot}61 + d\nu$ is $11997 + 11{\cdot}26\,d\nu$. This cannot be met by an oun multiple.

(2) There is no linkage effect explicable on the basis of e, u, v links at least.

(3) These two results point to the last supposition as correct, such as would occur if the new s term depends on a level in the sheath.

It is curious that if Déjardin's readings for $\lambda < 2414$ had been treated as in RA, the agreements would have been much closer.

TABLE III.—(X, P. and P').

$$s1 = 93181{\cdot}72.$$

$$s1 \rightarrow\,= 26{\cdot}730.$$

P.

$m=1$, 10·819; 11·389; 11·645.

[2371·57]	[42154·73]		**2094·11**	2 i	44248·94	
10 i	2476·02	40376·83	**1777·90**	1 i	42459·40	**1779·54**
4 i	2527·10	39560·78	**2593·95**	0 i	41654·50	**2594·44**

$m=2$, 2·280; 2·353; 2·387.

	[75114·7]				[77210·3]	
				4 i	198·22(3) *┐	
<1	½×2662·60	75094·84 *	**2095·64**	1	190·48(3) *	**381·2**
<1	½× 76·22	74712·98 *	**381·86**	2	76829·10(3) *	
1n i	½×−82·84	528·68 *	**566·16**	3 ii	636·78(2) *	**561·44**

$m=3$, ·818; ·831; ·846.

{ 0 iii	½×2378·9	84046·8±4 *	–	**2097·0±4**	0 iii 86143·8(2) *	
{ 1 iii?	¼×4757·48	57·76±1[57·77] *				
{ 0 iii?	½×2383·2	83898·0±4 *			- - -	
{ 1 i	½×3574·56	905·74 *	**141·1**			
1	⅓×3578·14	821·80 *	**225·0**		1 iii 85917·10(2) *	**226·7**

---

† *Ann. de Physique*, 6, 301, 26.

TABLE III. (cont.).

	P.			P′.		
m=4, ·384						
4 i	⅓×3420·89	87674·76[74·77] *	**2100·45**	1	89775·21(3) *	
	- - -	- - -		1	699·60(3) *	**75·6**
{4 i	½×2283·15	87571·18 *		1 iii	660·91(3) *	**114·3**
{1	⅓×3424·88	72·67 *	**102·09**			
m=5, ·209.						
1n i	⅓×3850·53	89515±2[15·0] *	**2096**	3 i	91611·42(3) *	
	- - -	- - -		1 i	578·39(3) *	**33·03**
1 i	½×2234·97	458·78 *	**56**			
m=6, ·126.						
<1 i	⅓×3311·95	90558·66±1·5[55·0] *	**2095·8**	1	92640·87(3) *	
3 i	⅓×2208·27	40·32±3 *	**18·3**			
1n i {	⅓×3313·64	512·46 *				
2 i {	¼×4418·10	514·68 *	**43·9**		- - -	
m=7.						
5 iii	½×3288·03	91217·28±1·5[16·4]*	**2092**	4 iii	93309·60(3) *	
m=8.						
3 i {	½×3273·06	91634·6[31·4] *	**2095**			
1 {	½× 71·35	82·5(58·6) *		1	93730·29(3) *	
m=9.						
1 i {	½×3262·18	91940·19[69]				
<1 {	½× 60·81	78·80(59·50) *	**2096·3**	<1	94055·85(3) *	

λλ of P′. (1) 2259·24; 2353·91; 99·97.——(2) 3885·15; 5·54; 3903·82; 2609·04.——(3) 2321·0; 27·11.——(4) 3340·85; 44·41; 45·11.——(5) 3273·89; 75·07.——(6) 3237·50.——(7) 3214·30.—— (8) 3199·87.——(9) 3188·80.

These large W.N. have a very considerable $dn/d\lambda$, but this will be less than if they had been directly observed. $dn/d\lambda$ is found by bringing the decimal point back four places and squaring the first two or three significant figures. But in $nh\nu$ emissions the observed W.N. is $1/n^2$ of that in the table, and the correction on the observed λ is $1/n$ of this. The final W.N. is found by multiplying by n. Hence the correction is $1/n$th of that deduced directly from the tabulated wave-number. Thus in $P_1 3$ the O.E. in W.N. in the first is not $(8 . 4)^2 d\lambda = 70·5 d\lambda$, but $35 d\lambda$, whereas in the second, with its $4h\nu$, it is $17·6 d\lambda$.

$m=1$. Déjardin, with the electron bombardment excitation, appears to have seen a collateral of $P_1 1$, viz., 4 i, 2369·68, 42186·89 as $P_1(\delta)$, gives $P_1 = 42153·62$.

$m=2$. The observed P is not that dependent on $Q_{11}2$ but about 20 less, but they give the same separations, and P_1' agrees with P_1. Again, this fits in with the conclusion arrived at that Q(2) belongs to a set with $p_1(-2\delta_1)$. The line given for P_2' gives the correct ν_1 with that related to the $Q_{11}2$. P_3', giving one of the ν_1 in Q2 with a line 77198, is really $P_3'2(5\delta_1)$, giving $P_3' = ...624·85$ and $\nu_1 + \nu_2 = 565·63$.

The presence of classes higher than i should not be unexpected in the "forbidden" Q, but if such appear here they are probably collaterals. It is seen that they predominate in the odd orders 3 and 7. That entered as $P_3'4$ may be incorrectly allocated, or it may be a collateral. As $P_3'(4)(-6\delta_1)$ it would give a separation 102. $m=8$ and 9 are merely suggestions of equal and opposite collaterals.

Tl iii.

Carroll allocated from his measures the first doublets $p2-s2$ and $p2-d3$, besides suggestions for $d3-f4$ and $f4-g5$. To these J. C. McLennan, A. B. McLay, and M. F. Crawford † added $p2-s3$, $p3-s3$, $p3-s4$, $p3-d3$, and $p3-d4$. In the present attempt to extend the series to higher orders it was found that $D(3.4)$ formed part of a clear quartic set, and a reconsideration showed at once that the whole S, D, and P sets belonged, with a few lacunæ, to quartet configurations, with separations following Landé's rules with great closeness. It is possible Carroll's allocation of S2 does not belong to this set, but is the doublet $p^2 2-s^2 2$, for there appears no $p_3^4 2-s^4 2$ related to it. Moreover, its $s2$ term is not in good step with the $s^4 m$. It is included, however, in the tables.

The observed ν_1 separations due to $p2$ vary between 14805 and 14816 or over. The variations are too large to be attributed to O.E. They may be due to displaced sets (one oun changes ν_1 by about 7), *or* we may be in the presence of satelloids ($y=7$), and there seems some uncertain evidence for this in S3 (see notes). The uncertainty renders it impossible to determine quite definitely the limit $p_1 2$ from Sm or Dm. The P series, however, seems better suited for this. This series is sustained by sets of pp combinations. The allocations are given in the following tables, but the whole interest of the discussion centres in the notes attached to each. These notes in each order (m) take first the evidence for collaterals, and second that for $nh\nu$ emissions—with other special points arising.

Tables IV.-VII. contain the allocations for $S(2.m)$, $S(3.m)$——$P(2.m), P(3.m)$——$Qm\equiv p1-pm$——$D(2.m)$, $D(3.m)$. The O.E. in the higher W.N. are naturally rather large. In addition there may be some doubt in certain cases as to normal values when collaterals are present. These facts explain why in the determination of the limits of each series some discrepancies appear, *e.g.*, the values of $p2$ found are: from S 162339, from P 162096, from D 162158. The differences 181, 62 at first sight appear very large. Really, in comparison with similar determinations in neutral series, these are analogous to 20 and 7, amounts not unknown in the latter and due to combined O.E., abnormalities, and formula weakness. More definite values of the ν_1, ν_2 separations would enable us to get closer values of $p2$, from considerations of the oun values, known from the Tl i series. This is, however,

outside the scope of the present discussion. Indeed, so also is the discussion of collaterals in Tl iii, but I have given way to the temptation to include it because the oun shifts are very large and agreements with observation are very striking; moreover, they afford additional $nh\nu$ data.

A similar discussion of Carroll's measures in Ga and In, in connexion with the spectra of Ga ii and In ii is also found to extend the series allocations by means of these multiple emissions, but the details are not here given.

<div align="center">

TABLE IV.—(Tl S2 . m ; S3 . m).

$n = 162339$; $77775 \cdot 89 - 9R / \{m + \cdot 156156 - \cdot 140464/m\}^2$.

</div>

$p_1 2 \rightarrow = 49 \cdot 617.$	$p_1 3 \rightarrow = 16 \cdot 453.$
$p_2 2 \rightarrow = 56 \cdot 560.$	$p_2 3 \rightarrow = 18 \cdot 306.$
$p_3 2 \rightarrow = 61 \cdot 389.$	$p_3 3 \rightarrow = 19 \cdot 543.$

The oun shifts on the sm are placed above each order. Cols. 5, 8 give the last digits of the doublet separations and col. 6 those of $p_1 2 - p_2 3$.

S(2 . m).   84563 ±   S(3 . m).

14808. 9943.   5682. 3784

           148... 845...   56 –

           99...   57...

$m = 2.$ 89·94.

8	C 1266·33	−78968·36	**60·0**			
15	C 1558·60	−64160·14	**08·22**	−163528·3*	$\frac{1}{3} \times 1223 \cdot 03$, 00	
	– – –	– – –		– – –	near $\frac{1}{2}$P$_1$(2 . 3)	

$m = 3.$ 24·788.

8	L 1660·06	60238·78	**63·78**	−24325·00	4109·85,	10 L
4	L 1332·36	75054·80	**16·02**	**81·81** −18643·19		
1	1176·50	84997·9	**43·1**	ultra red	5362·40,	8 L

$m = 4.$ 10·634.

1	$\frac{1}{2} \times 2877 \cdot 74$	104217·96*	**65·43**	19652·53	5086·99,	6n L
0	$\frac{1}{2} \times 1680 \cdot 3$	119026·4*	**08·4**	**82·31** 25334·84		
2	$\frac{1}{2} \times 1550 \cdot 75$	128969·84*	**43·4**	**87·22** (29122·06)	3946·02,	6 L

$m = 5.$ 5·520.

	(124798·)	[124802]	**65**	(40233·2)	see
5	$\frac{1}{2} \times 1602 \cdot 38$	814·3*			notes
		(139627·0) **12·7**	**81**	(45913·96)	
	$\frac{1}{2} \times 1337 \cdot 19$	149567·36* **40·4**	**70**	(49684·0)	

TABLE IV. (*cont.*).

$m=6.$ $3\cdot225.$

2	$\frac{1}{2}\times1469\ 59$	$136092\cdot4*$	62		$51530\cdot4$	$1940\ 6,$	0
00	$\frac{1}{2}\times1325\cdot52$	$150884\cdot2*$		$84\cdot4$	$57214\cdot8$	$1747\cdot8,$	0
	(0/5)	$(900\cdot3)$ 08		84	$(60999)?$		
		$(160855\cdot1)$ 54					

$m=7.$ $2\cdot048.$ $[91\cdot87]$

	- - -	$[142953\cdot8]$	$65\cdot2$		$58390\cdot8*$	$\frac{1}{2}\times3425\cdot2,$	0
		$[157761\cdot9]$		$83\cdot0$	$64073\cdot8*$	$\frac{1}{2}\times3121\cdot4.$	0
		$[167707]$			- - -	- - -	

$m=8.$ $1\cdot381.$

	- - -	$\left\{\begin{array}{}[147434\cdot2]\end{array}\right.$	$61\cdot0$		$[62873\cdot19]$	- - -	
				84	68558	$1458\cdot6,$	00
				84	$(72343\cdot20)$	$(-c_1)1382\cdot70(c_1),$	3
5	$\frac{1}{2}\times1358\cdot58$	$147212\cdot5*$	$48\cdot0$		$62664\cdot5$	$1595\cdot8,$	00
1	$\frac{1}{2}\times1234\cdot25$	$162041\cdot7*$	$29\cdot2$		- - -	- - -	
00	$\frac{1}{3}\times1744\cdot3$	$171988\cdot8*$	$47\cdot1$		- - -	- - -	

$m=9.$ $\cdot972.$ $[61\cdot27]$

	$(150522\cdot0)$	$66\cdot3$		$65955\cdot70*$	$\frac{1}{2}\times3031\cdot55,$	$3n$
	$(165331\cdot1)$ 09·0		$87\cdot8$	$71643\cdot5$	$1395\cdot8,$	0
	(175273) 42			- - -	- - -	

Allocations by Carroll are indicated by C, by McLennan, McLay, and Crawford by L. The others are by the author. Owing to some uncertainty as to S5, the formula has been found from $m=3, 4, 6.$

Notes to Table IV.

The possible collateral and *nhv* emissions are considered under each order. The lines adduced are successive in Carroll's list, without selection. The W.N. for the S_1, S_2, S_3 sets with intensities are arranged in three parallel columns with the separation from the normal S lines below when it is above S, and above when it is below S. The $O-C\ d\lambda$ are calculated on the supposition that the normal lines have no error and are entered after each W.N. A $\times$ means that the line is not a collateral, and a ? that it is a doubtful one. The oun shifts for $p2, s2$ are so large that allowance must be made for change with increasing multiples. The values of the oun shifts given are for negative displacement.

An asterisk attached means that the line occurs as a direct *nhv* without displacement.

The $p \rightarrow$ are given at the top of the table.

The $S(2.m)$, $S(3.m)$ series are separated by about 84564.

$$m = 2. \quad s2 \rightarrow = 89\cdot94.$$

1.	1	$-79293\cdot97$	$\cdot1?$	1	$-64387\cdot77$	$\cdot03$		
		$325\cdot61(1/-3)=319\cdot7$			$227\cdot6(\delta/0)=226\cdot2$			
2.	2	$142\cdot10$	$\cdot1?$	3	$349\cdot65$	?		
		$173\cdot7(0/-2)=179\cdot9$			$189\cdot5(0/-2)=180$			
3.	8	$-78968\cdot36$ $S_1 14808\cdot22$		15	$160\cdot14$	S_2	no S_3.	
		$318\cdot0(-1/3)=318\cdot4$			$118\cdot74$		see P2.2 for collaterals.	
4.	0	$650\cdot36$	0	8	$041\cdot40$	$\times$		
					$221\cdot5(-\delta/0)=226\cdot2$			
5.				1	$-63938\cdot6$	$\cdot1$		

$\lambda\lambda$. $1261\cdot13$; $63\cdot55$; $66\cdot33$; $71\cdot45$.——$1553\cdot09$; $54\cdot01$: $58\cdot60$; $61\cdot49$; $64\cdot0$.

$$2h\nu.$$

6.	0	$-79159\cdot64$	$\cdot06$	4	$=64383\cdot66*$	$\cdot1$		
		$191\cdot13(2/-1)=189\cdot2$			$223\cdot5(\delta/0)=225\cdot9$			
7.	7	$000\cdot16$	$-\cdot1?$	5	$353\cdot40*$	?		
		$31\cdot8(6/3)=28\cdot26$			$193\cdot3$			
		S_1		5	$241\cdot56$	$\times$	$9n$ $54404\cdot54$	$\cdot2$
					$81\cdot42$			
		$117\cdot4(-6/-2)=117\cdot4$					$187\cdot5(3/0)=184\cdot2$	
8.	0	$-78850\cdot94$	0	5	$219\cdot26$	$\cdot1$	6 $280\cdot50$	$\cdot1$
		$274\cdot1(0/3)=270\cdot36$			$59\cdot2(1/0)=56\cdot6$		$63\cdot5(1/0)=61\cdot39$	
9.	$0n$	$694\cdot22$	$\cdot1$		S_2		$S_3[54217\cdot0]$	

$2\lambda\lambda$ (air) $2526\cdot10$; $30\cdot88$; $35\cdot67$; $40\cdot72$.——$3105\cdot48$; $06\cdot94$; $12\cdot35$; $13\cdot43$.——$3675\cdot12$; $83\cdot52$.

If S_1 is about $2\cdot3$ larger ($d\lambda=\cdot04$), nos. 1, 3, 4 in $h\nu$ and 6, 7, 9 in $2h\nu$ have $O-C$ $d\lambda=\cdot06, 04, 0$, and $\cdot01, 03, \cdot03$, but no. 7 *may* be due to a y-effect referred to under S3, also no. 9 is possibly related to $Q_{12}3$.—Note the very exact pairs ($\pm\delta_1/\mp3\delta_1$) in S_1 and $\pm\delta/0$ in S_2, and $1/0$ in S_2 and S_3.

There are no observed S_3 under $h\nu$. In $2h\nu$ emissions the $d\lambda$ vanish if $[S_3]$ is calculated from the corrected S_1.

The parallel series $S(3.2)$ requires values

$$78968\cdot36+84564+x=163532\cdot36+x=2(81766\cdot18+\tfrac{1}{2}x)$$
$$\dots-5682 \rightarrow =157850 \qquad =2\times78925$$
$$-3795 \rightarrow =154055 \qquad =2\times77027$$

For the $2h\nu$ are found

$$00 \; 1223\cdot03, \; 81764\cdot15*=163528\cdot30=-\tfrac{1}{2}S_1(3.2)=\tfrac{1}{2}P(2\cdot3)$$
$$108\cdot24(1/-1)=106\cdot3$$
$$00 \; 1223\cdot84 \quad 710\cdot03 \quad =163420\cdot06 \quad 0$$

78925 is close to $P_1 2=78970$ and would be weak.

Also $3h\nu$, 0, $1834\cdot3$, $163550\cdot1\pm9=S_1 2(\delta_1)$ within O.E.

$$m=3. \quad s3\!\to\!=24\!\cdot\!788.$$

Here $p_1 2\!\to\!(49\!\cdot\!62)$ is almost identical with $2 \times s3\!\to\!(49\!\cdot\!57)$, so that it is not always possible to settle uniquely a displacement in S_1.

1.				3 74862·04 †	·03	**9941·3**	2 84803·3	·03
				192·8(3/−1)=194·5			194·7(2/−3)=197·1	
2.	2 60107·0	·01	**14822**	2	929·37†	·02		
	131·7(2/−1)−y=131·9				125·4(0/−5)=123·9			
3.	3	204·7						
	34·0, −5y=34·4							
4. 10	238·7	S_1	**14816**	4 75054·80		S_2 **9943·18**	1 84997·98	S_3
	34·9, 5y=34·4						46·2(0/2)=49·6	
5. 0	273·6						1 85044·14	·04
	116·1(−2/1)−y=117·1			110·03(−2/0)=113·1,			101·26(0/4)=99·15	
6. 0	354·77	·02	**14810**	2 164·80	·05	**9934·34**	0 099·14	·03

λλ. 1663·7; 61·0; 60·06; 59·1; 54·87.——1335·79 C; 34·59 C; 32·36; 30·41.——1179·2; 76·50 : 75·86 : 75·1.

† See also $S_3 5$.

$$2h\nu.$$

7.	4 60031·30	×	0 75013·2	0	2 84882·4	·01
	207·4(3/−3)=223·2			41·6 6y=41·34	115·6(2/0)−y=115·7	
8.	4 096·98	0	0	S_2		S_3
	141·7(3/0)+y=141·8			40·0 6y=41·34		
9.	4 160·08	0	0 094·8	·02		
	78·6(2/0)+3y=78·4		80·34(−1/1)=81·36			
10.	S_1		3 135·14	·02		

2λ (air), 3330·64; 27·00 ; 23·51.——2666·2 ; 63·3(vac); 61·08.——2356·2.

Those λ marked C are close to carbon lines, but the displacements fit them in closely as belonging to Tl.

Here are found three sets close to ν_1 separations, differing successively by about 7. At first sight this suggests oun changes in the limit with the last as true S_1, but the changes are in the wrong direction for this explanation to hold good. Moreover while the shifts in S_2 are met by oun displacements, those in S_1 definitely cannot be thus explained. The equal separations 34 of nos. 3, 4, 5 point to the lines being collaterals, but the separation 34 cannot be met by oun shifts on the p, s terms. They are close to $5y$, where y denotes the satelloid separation referred to above. If this is so, the $34\cdot0 + 34\cdot9 = 68\cdot9 = 10y$ gives a close value for y of 6·89 and nos. 2, 6 are simultaneously met, as well as the $2h\nu$ representatives. Nos. 1, 6 are $\pm 2/\mp 1 - y$. It would seem that

the line taken as S_1 is normal S_1-y. This would make the ν_1 separation correct, and explain also the abnormal 14822 of no. 2. The S_2 collaterals all have close agreement without y, but there is some difficulty in those in $2h\nu$ for S_2. The three adduced depend on multiples of 40·2, which itself cannot be expressed as oun shifts. Nos. 7, 9 separated by 81·2 may be mutual collaterals $1/-1$, but there is no direct collateral relation with S_2. They may be $S_2 \pm 67$, but as we shall see later, No. 9 is $p_1 2 - p_2 3$. No. 10 is $(-1)S_2(+1)$.

In the region of $\frac{1}{2}S_1$, the λ are > 2900, and therefore in a region in which Carroll has unfortunately not published measures of lines with intensities < 3.

$$S(3.3).$$

1.	10	-2432495	S_1	**5681·76**	8	-1864319	S_2	$-[14854]$	S_3

1. 10 -2432495 S_1 **5681·76**   8 -1864319 S_2 $-[14854]$ S_3
      60·28 $121·64(-4/2)=122·80$ outside Carroll's region

2. 6n 385·23 $\times$ $2n$ 784·83   ·3   in the red.
      80·81

3. 6n 405·76 $\times$
      $139·8(-4/3)=140·2$

4. 1   464·8   ·07

     $\lambda\lambda.$ 4109·85 ; 4099·69 ; 96·24 ; 87·5.——5362·40 ; 21·97.——

$$m=4. \quad s4 \to\ =10·634.$$

From here on the $h\nu$ emissions produce lines beyond the observed region. The $nh\nu$ are entered as $h\nu$, *i.e.*, $n\times$ the observed W.N.

1. 0   104015·0   ·08
     $203·0(4/0)=198·5$

2. 0   052·8   ·04
     $165·1(2/-6)=163·0$

3. 0   085·4   ·04
     $132·6(2/-3)=131·1$

4. 0   177·6   ·01   1   118885·6   0
     $40·2(1/1)=39·0$ $137·8(3/3)=137·78$

5.   217·96 S_1 **14808·4**   0   119026·4 $S_2[23·4]$ **9943·4**   2   128969·84 S_3
     $46·4(-1/0)=49·6$ $166·0(-2/5)=166·29$ $211·60(4/3)=213·65$

6. 00   264·4   ·06   0   189·4   0   3   129181·44   ·02
     $106·2(-2/1)=109·9$ $230·4(-2/11)=230·09$

7. 1   324·2   ·06   0   253·4   0
     $138·8(-2/4)=141·7$ The separations are measured

8. 0   356·8   ·05   from $[S_2]$.
     $329·8(-6/3)=329·6$

9. 1   547·8   00

   $2\lambda\lambda.$ 1922·8 ; 22·1 ; 21·5 ; 19·8 ; $\frac{1}{2}\times2877·74$; 1918·2 ; 17·1 ; 16·5 ; 13·0.——1682·29
       80·3 ; 78·0 ; 77·1.——1550·75 C; 48·21 C.

S(3.4).

1.   5*n* 29001·36   0
                                                                              120·70(4/−4)=120·71

2. 6*n* 19652·53   S$_1$ **5682**   6 25334·84   S$_2$ **3787**   [29122·06]   S$_3$
          31·15(0/3)=31·90   11·31(0/1)=10·63

3 7*n*   683·68   ·19 ?   5   346·15   ·1

                λλ. 5086·99; 78·94.——3946·02; 44·26.·——3447·13

$$m=5. \quad s5 \to =5·520.$$

$9 \times s \to =49·68$, so that again $p_1 1 \to$ and $s \to$ are commensurable.

1. 0 124533   0   6 139401·0   0   2 149397·50   ·02
          281(6/3)=280·76   226(4/0)=226·27   169·80(2/−8)=169·9
2.   [802]   [S$_1$]   [610·5]   [S$_2$]
3. 5   814·4   S$_1$ **14812·6**   (627·0)   S$_2$ **9940·3**   4   567·36   S$_3$
          216·8(−4/3)=215·23   355(−6/3)=356·4   156·75(−2/6)=155·9
4. 0 125031·2   ·02   0   782·0   ·01   3   724·12†   0
          322·8(−6/3)=325·64   399·6(−7/0)=396·5   291·38(−5/−3)=290·8
5. 1   137·2   ·05   0 140026·6   ·03   2   858·74†   0
          424·4(−8/5)=425·2   527(−9/3)=526·4
6. 6   238·8   ·01   0   154   0

        2λλ. 1606·0; 02·38; 1599·6; 98·4; 96·95.——1434·71; 30·8; 28·3;
              27·0.——1338·71; 37·19; 35·79; 34·59.

† These also occur as *hv* collaterals of S$_2$3. Both cannot be accepted.

This gives an observed v_1+v_2 correct within O.E. No line for the formula value of $\frac{1}{2}$S$_1$ is observed. It may be noted that the line taken as S$_1$ is 16·4 ahead of 124798, *i.e.*, no. (3) is [S$_1$](3δ$_1$). It follows that if the true S$_1$ is that of the formula the displacements in (1, 4, 5, 6) become 6/0, −4/6, −6/6, −8/8. It will be noticed that all the displacements are exact within very small O.E., although the individual oun shifts are so large. This means that the sets are all really S5 collaterals, *i.e.*, depend on $p1$, $s5$ terms. Note especially how the same displacements −6/3 in S$_1$, S$_2$ agree, although the actual shifts differ by 41.

S(3.5).

No direct lines for S$_1$(3.5) are found, but clear collaterals are seen. Although no *hv* emissions of S$_2$ or its collaterals are found it is curious that 2*hv* which meet the conditions are present. S$_3$ is represented by collaterals.

1.   1*n* 49353·5   ·03
                                                                              330·5(17/0)=331·3
2. 2 40070·5±2   ·1   4 45786·36   ·05   1*n*   490·2   ·06
          162·7(10/0)=164·3   127·60(7/0)=128·14   193·8(10/0)=195·15
3.   (233·2) S$_1$ **5680·7**   (913·96) S$_2$ **3770·0**   (684·0) S$_3$
          162·7(−10/0)=164·8   36·34(2/0)=36·71   193·8(−10/0)=195·88
4. 1 395·9±2   ·1   4   950·50   ·03   1*n*   877·8   ·03
          λλ. 2495·6; 75·5.——$\frac{1}{2}$ 4366·89; $\frac{1}{2}$ 4357·29.——2026·21; 20·6; 04·9.

Here no 1, in S_3, was included, because the similar character $(1n)$ of the three lines suggested that they were all collaterals. Direct calculation for the large displacement shows that the shift is exactly met within O.E. Note again how the same displacements $(\pm 10/0)$ in the S_1, S_3 agree although the shifts differ by 31.

$$m = 6. \quad s6 \rightarrow = 3\cdot 225.$$

1. 0 150723·9 0
    160·3(3/3)=160·0

2. 00 884·2 1 160796·26 0
    16·1(0/5)=16·1 58·86(1/1)=58·32

3. 2 136092·4 S_1 **14808** (900·3) (S_2) **9955** (855·12) S_3?
   473(−9/9)=476·5 58·86(−1/−1)=58·32

4. 1 565·4 ·04 00⎤ 914·0
                    ⎥ 329·5(6/12)=330·59?
5.   00⎦ 161243·52

2λλ, 1469·59; 64·5.——1326·93; 25·52.——1243·82; 42·9; 40·36.

The *s*-shifts from now on are comparable with O.E., so that definite displacements in the *s*-term cannot be settled. Those entered above, no. 5 excepted, satisfy the equal or equal and opposite conditions. The correctness of the S_1 is certified by the S3 . 6, definitely observed. The (S_2) depends on the real value of ν—it is an exact $5\delta_1$ on *s* in no. 2. In S_3 nos. (2, 4) are displaced $(\pm 1/\pm 1)$ from their mean, and this is taken as S_3, although the ν_2 is abnormally large. It is $(0/4)$ on the true S_3. No. (5) is entered as being of the same character as (4), but the evidence with the small $s\rightarrow$ is not conclusive.

S(3.6).

For the S_1, S_2 a set is found which fits with the S(2.6):

0 51530·4 S_1 **5684·4** 00 57214·8 S_2
101·2(−6/1)=101·9 114·8(−5/6)=110·8 no obs. S_3

0 631·6 ·01 00 329·6 ·12

λλ, 1936·3.——1744·3.

$$m = 7. \quad s7 \rightarrow = 2\cdot 048.$$

The formula value of $S_1 7$ is 142953·28. No direct $2h\nu$ representatives of the set for S(2.7) are found, nor $h\nu$ for S(3.7); but curiously the $2h\nu$ for S(3.7) are, and are given

in the table. For the sake of comparison with foregoing orders the adjoining lines are here given :

1. 3 142694·1   ·01   0 157300·1   0
      259·2(5/−5)=258·3   462·8(8/−5)=463·6

2.   [953·28] S₁ **14809·6**   [762·9] S₂   **9943** [167706]
      210·6(−4/4)=206·7   173·8(−3/2)=173·8   53·9(−1/−4)=53·2

3. 1 143163·9   ·05   8   936·7   0 ??   1 167759·90   0

      2λλ. 1401·60 ; 1397·00.——1271·45 ; 66·33.——1192·18.

of which no. 3 in S₂ (1266·33), although numerically exact, is S2, and is a coincidence.

$$m=8. \quad s8\rightarrow=1\text{·}381.$$

The formula gives S₁2.8=147434·19, but no representatives for the S2.8 set are found, though a remnant for the S3.8 appears ; but S₂3.8 is coincident with P₂3.5. For S₃(3.8) there is a possible collateral (1)S(−1)=72322·27 (λ=1382·70), giving S₃=72343·20, entered in ( ).

There seem also indications of a set depending on 147212. If this were about 21, or 3*y* larger, the *v* becomes 14808, the separation from the S3.8 would be 84569, *i. e.*, 62664 is a good S₁(3.8), but no S₂ if found either in *hv* or 2*hv*. The 2*hv* would lie in a region where Carroll has omitted weak lines. The chief interest of this allocation lies in its indicating a p_1 limit considerably less than that given above.

$$m=9.$$

1. 2 150329·6   ·01   00 165275·6   0   1 175146·6
      192·4(4/4)=194·5   56·5(1/0)=56·5   122·9(2/0)=122·8

2.   [522·0] S₁ **14810**   [332·1] S₂ **9941·3**   (273·4) S₃
      201·8(−4/4)=202·4   84·3

3. 0   723·8   ·0   1   416·4   ×

      2λλ 1330·41 ; 26·93.——1210·1 ; 09·07.——1141·9. The first two coincide
      with 6 in S₂3 and 1 in S₂6 respectively.

In S(3.9) S₂ is observed in *hv*, as given in the table. S₁ is not in *hv*, but in 2*hv* are found

$$3n \tfrac{1}{2}\times 3031\text{·}55 \qquad 65955\text{·}70$$
$$3n \tfrac{1}{2}\times \quad 29\text{·}95 \qquad 988\text{·}54$$

The lines have the same character and small O.E. Their separation is 32·84, while 2/0 shifts 32·90.

TABLE V.—(TlP2ι. m ; P3 . m).

$n = 241064\cdot3$; $101857 - 9R/\{m + \cdot621344 - \cdot157480m\}^2$.

$s2\!\to\! = 89\cdot84$. $s3\!\to\! = 24\cdot657$.

P(2.m).   **139207**. P(3.m).

139...

$m = 2$. 49·549 ; 56·468 ; 61·317.

10	C 1266·33	78968·36		**207**	−60238·78	8 L	
8	O 1558·60	64160·14	**14808·22**		−75054·80	4 L	**14816·0**
		(54217·28)	**9942·86**		−84997·9	1	**9943·1**

$m = 3$. 16·453 ; 18·306 ; 19·543.

00	½×1223·03	163528·30*		**203**	24325·00	10 L	
		[157844]			18643·19	8 L	**5681·9**
		— — —			[14859]		

$m = 4$. 7·726 ; 8·431 ; 8·910.

3	⅓×1030·86	194012·7*		**155**	54857·6	1	
1	½×1046·02	191201·0*	**2811·7**		52042·7	0	**2814·9**
1	½×1056·34	189333·0*	**1868·0**		(50175·0)		**1867·7**

$m = 5$. 4·254 ; 4·607 ; 4·863.

		[209491]		**207**	70283·9	1	
		[207766]			68558·9	00	**1725·0**
					67335·5	0 ?	**1223·4**

$m = 6$. 2·594 ; 2·755 ; 2·844.

				240	[79162·26]		
00	⅓×1373·61	218402·67*		**260**	42·10	2	
	— — —	— — —			78205·64	1	**936·46**
3	⅓×1382·70	216966·61*	**1436**		77701·29	2	**504·35**

$m = 7$.

					[84761·50]		
					37·14	0	
					84203·4	00	**558·1**

λλ for P3 . m.——1660·60 ; 1332·36 ; 1176·50.——4109·25 ; 5362·40 ; [6728].
——1822·9 ; 1921·5.——1422·8 ; 58·6 ; 85·1.——1263·55 ; 78·68 ; 86·98.——
1180·12 ; 87·6.

The formula is calculated from $m = 3, 4, 5$ in P(3 . m). The value of $s2 - s3 = S3 - S2 = 60238\cdot78 + 78968\cdot36 = 139207 \pm ?$. This is the separation between the P(2 . m) and P(3 . m) series.

$m = 2$. $P_3(2.2)$ should be about 54217. There is no direct line here, but it is possibly disrupted $0/\pm5$, shift $\pm306\cdot29$ into

| 4, | 1854·91, | 53910·99 | as P(-5) gives P = 54217·28 |
| 0, | 34·3, | 54516·7 ± 3 as P(5) | „ | 10·4± |

The collateral relation being granted, the first is a reliable measure, and it

gives the correct ν_2. The second has O.E.$=6\cdot7$ or $d\lambda=2$ on $1834\cdot3$—quite possible. $P_3(3.2)$ is given by Carroll as close to a C line.
$m=3$. For $P(2.3)$ see $S(3.2)$.
$m=4$. The two series sets are separated by 139155, definitely not the value given above. The sets are both clearly related to the normal sets and displacement exists; but the $p_1 1 - p_1 4$ combination $115065\cdot9 \pm 5$, given below, would indicate that the $P(2.4)$ set are really $P(-3\delta_1)$ and the $P(3.4)$ are $P(3\delta_1)$; see notes to this combination below. The separations $2811\cdot80$, $1868\cdot00 = 3 \times 937$, 2×934 are in the normal ratio for quartets. Next to $P_3(2\cdot4)$ are

2, $\tfrac{1}{2} \times 1057\cdot56$ $189114\cdot58$ $(228\cdot40)$ $(2/-5)=224\cdot23$ $d\lambda=\cdot01$

1, $\tfrac{1}{2} \times$ $56\cdot34$ $332\cdot98$ P_3

00, $\tfrac{1}{2} \times$ $54\cdot80$ $609\cdot40$ $(276\cdot42)$ $(3/-1)=278\cdot79$ $d\lambda=\cdot01$

With the above ν_2, $P_3(3.4)$ should be about $50174\cdot7$, but there is no direct line. There are, however, two apparent collaterals of similar character:

00, $1999\cdot1$ $50022\cdot5$ as (4) $P_3(-6)$ gives $S_3 = 50174\cdot6$

00, $89\cdot1$ $50274\cdot0$ as (-4) P_3 ,, $75\cdot4$

The mean is entered in the table in ( ).
$m=5$. The separations are in the correct ratio. The formula value is 209491, and with this goes the observed $P_2(3.5)$ within O.E. $P_2(3.5)$ is coincident with $S_2 3\cdot8$. We are now outside the observed $2h\nu$ region for $P(2 \cdot m)$, but the energies are so large that $3h\nu$ emissions appear. There are found:

0, $\tfrac{1}{3} \times 1430\cdot8$ $209673\cdot0$ as (-2) S_1 gives $S_1 = 209493\cdot7$

1, $\tfrac{1}{3} \times$ $44\cdot9$ $207629\cdot7$ as (1) $S_2(-10)$,, $S_2 = 207965\cdot6$ $1728\cdot1$

$m=6, 7$. The sets entered in P3 . m are seen to be both definitely less than the formulæ values, and must be regarded as very doubtful, although it is possible the limit may be about $20=9 \times 2\cdot2$ too large. Also 79142 is a possible collateral of $S_1 2$. The lines given in the table for $P_1 2.6$, $P_3 2.6$ give the $\nu_1 + \nu_2$ separation, but the separation from the $P(3.6)$ is 53 too large, compared with the 52 too small in the order $m=4$. They seem related, but the actual connexion is not evident.

TABLE VI.

$p2 - pm \equiv Q(m)$ combinations.

$m = 3$.

			as	gives Q	$d\lambda$
$Q_{13}[$ $75094\cdot8]$	0 $\tfrac{1}{2} \times 2663\cdot3$			$75094\cdot8*$	
$Q_{12}[$ $78882]$	0 $\tfrac{1}{2} \times 2535\cdot67$		$78850\cdot96$ $(1/1)$	$78882\cdot3$	0
$Q_{11}[$ $84564\pm2]$	$\begin{cases} 00\ \tfrac{1}{2} \times 2365\cdot8 \\ 0\ \ \ 1182\cdot31 \end{cases}$		$84538\cdot0$ $(0/-1)$ $84580\cdot18$ $(0/+1)$	$84554\cdot4$? $84563\cdot75$	$\cdot14$ 0

In the notes to $S(3.2)$ is given a $3h\nu$ line $n=163550\cdot1 +9$. Calculated from this gives $Q_{11}=84581\cdot7 \pm$, or the last line above.

$Q_{23}[$ $89904\pm]$	$\begin{cases} 0\ \ \ 1112\cdot0 \\ 4\ \tfrac{1}{2} \times 3339\cdot56 \end{cases}$		$89928\cdot1$ $(0/1)$	$89908\cdot5$ $89906\cdot44*$	$\cdot05$
$Q_{22}[$ $93690]$	5 $\tfrac{1}{3} \times 3201\cdot37$			$93682\cdot98*$	
$Q_{21}[$ $99372]$	- - -			- - -	
$Q_{33}[$ $99848]$	$4n$ $\tfrac{1}{3} \times 3002\cdot44$		$99889\cdot68$ $(0/-3)$	$99848\cdot06$	0
$Q_{32}[103635]$	1 $\tfrac{1}{2} \times 1930\cdot7$		$103589\cdot4$ $(1/1)$	103631	$\cdot08$
$Q_{31}[109316]$	$0n$ $\tfrac{1}{3} \times 2743\cdot5$		$109349\cdot4$ $(0/2)$	$109316\cdot7$	0

(left margin brace annotations: 14814 / 14801 ; 9940 / 9948)

TABLE VI. (*cont.*).

$m = 4$.

			as	gives Q	$d\lambda$
$l_{11}[115044\cdot4]$	00 $\frac{1}{2}\times2607\cdot2$			$115065\cdot9*$	
$96\cdot4]$	00 $\frac{1}{4}\times2605\cdot2$	$115154\cdot4$	$(0/-1)$	$115061\cdot1$	
	0 $\frac{1}{2}\times1736\cdot7$	$115161\cdot0$	$(-2/0)$	073	$\cdot05$

This is the order in which P(2·4), P(3.4) show anomalies. The first [Q] is deduced from P(2.4) and the second from P(3.4). The assumption is here made that the normal $p1- p4$ is the directly observed $3h\nu$ line. In this case (since $p_14\rightarrow=7\cdot72$)

$$Q(-3\delta_1)=115042\cdot8 \qquad d\lambda=\cdot01$$
$$Q(3\delta_1)=115089 \qquad d\lambda=\cdot05$$

These agree within O.E. with the two from the two P series. The other $3h\nu$, $2h\nu$ may refer to the same line ($d\lambda=\cdot05$) *or* they may be relatively displaced one oun in $p4$. The 115161 is 95·1 ahead of Q, which is $(-2\delta_1)Q$ numerically.

$Q_{21}[129873]$	00 $\frac{1}{3}\times2309\cdot1$	$129920\cdot7$	$(0/6)$	$129874\cdot4$	
			or $(-1/0)$	$871\cdot2$	

(left margin: 14808·5)

$m = 5$.

$Q_{13}[127574]$	6 $\frac{1}{4}\times1568\cdot45$	$127514\cdot42$	$(1/-2)$	$127573\cdot7$	0
$Q_{12}[128797]$	1 $\frac{1}{2}\times1553\cdot09$	$128775\cdot54$	$(0/5)$	$128798\cdot5$	0
$Q_{11}[130522]$	5 $\frac{1}{3}\times2298\cdot09$	$130502\cdot71$	$(0/-5)$	130524	0
$Q_{23}[142382]$	8 $\frac{1}{3}\times1404\cdot60$			$142389\cdot3*$	$\cdot03$
$Q_{33}[152325]$	1 $\frac{1}{3}\times1313\cdot20$	$152299\cdot72$	$0/5$	$152324\cdot0$	0

(left margin: 14815·6 ... 9935)

The shifts on $p5$ are so small compared with O.E. that no weight can be attached to these agreements quite apart from the fact that three of them are too strong for this combination.

$m = 6$.

$Q_{11}[139401\cdot04]$	6 $\frac{1}{2}\times1434\cdot71$			$139401\cdot00*$ 0

The calculated value is determined from the formula value of P(3.6). The $2h\nu$ line is exact, but again is too strong for acceptance.

No doubt several of these allocations depend on chance coincidences; but the number, especially in the first two orders, exclude the supposition that they can all be thus explained.

TABLE VII.—(Tl D2 . m ; D3 . m).

$n = 162158$; $77594 \cdot 40 - 9R/\{m + 1 \cdot 339730 - \cdot 214164/m\}^2$.

$p_1 2 \rightarrow = 49 \cdot 617.$ $p_2 2 \rightarrow = 56 \cdot 560.$ $p_3 2 \rightarrow = 61 \cdot 389.$

$p_1 3 \rightarrow = 16 \cdot 453.$ $p_2 3 \rightarrow = 18 \cdot 306.$ $p_3 3 \rightarrow = 19 \cdot 543.$

[NOTE.—The digits **148** are represented by !.]

$d \rightarrow$ $m = 2.$

71·431				−4, 30015·65	9947·4	−8n, 20068·2
				1072·31		
70·886	−0,	43771·3	!28·0	−6, 28943·34		− [19000]
		1759·8		1741·07		
69·979	−0n,	42011·5	!09·2	−9n, 27202·27		
		2510·8				
68·692	−8,	39500·7				

		84577		—		
				− [123720]	3782	−1, (119938·83)
				1072		1072
	−	[128331]	5683	− [122648]	3782	−0, (118865·90)
		1738		1741		
	−00,	(126593·1)	5686·3	−0. 120906·84*		
		2515				
	−00,	124077·2*				

$2510 \cdot 8$; $1741 \cdot 0$; $1041 \cdot 0 = 7 \times 358 \cdot 7$; $5 \times 348 \cdot 2$; $3 \times 347.$

$\lambda.$ $2284 \cdot 6$; $2380 \cdot 3$; $2531 \cdot 6.$——$3330 \cdot 64$; $3454 \cdot 04$; $3675 \cdot 12.$——$4981 \cdot 60.$

$\lambda.$ $\frac{1}{2} \times 1611 \cdot 9.$——$\frac{1}{3} \times 2480 \cdot 50.$

$m = 3.$

22·995				0, 79728·28	9940·38	4. (89668·62)*
				528·58		525·58
22·810		– – –		0, 80256·82	9937·65	0n, (90194·47)*
				940·36		
22·497	4,	66391·81 C	!05·37	6, 81197·18 C		
		1315·75				
22·018	9,	67707·56 C				

		84572·6	In ultra red.	
	−2,	18178·7 L	5683·7	4, −12495 L
		1313·7		
	−6,	16865·0 L		

$1315 \cdot 7$; $940 \cdot 4$; $528 = 7 \times 187 \cdot 9$; 5×188 ; $3 \times 176.$

$\lambda.$ $1506 \cdot 21$; $1476 \cdot 94.$——$1254 \cdot 26$; $46 \cdot 00$; $31 \cdot 57.$——$\frac{1}{3} \times 3343 \cdot 83$; $\frac{1}{2} \times 2217 \cdot 1.$

$\lambda.$ $5499 \cdot 4$; $5927 \cdot 8.$——8001 ; all by L.

TABLE VII. (*cont.*).

$$m = 4.$$

9·798		4, (121914)* (2)			– – –
		107			
9·769	1, (107208·2)* (2)	!13	0, (122021·1)* (3)		– – –
	177 6				
9·721	2, (385·8)* (2)		– – –		
	249				
9·564	0n, 107634·9* (3)				
	84564·4		———		

					– – –		– – –
5,	22644·18	**5681**	5,	28325·04	**3784·59**	5,	32109·63
	177·51			**177·90**			
7,	821·69 L	**5681·25**	9n,	28502·94 L			
	248·84						
4,	23070·53						

248·84 ; 177·6 ; ?$= 7 \times 35·5$; $5 \times 35·5$; $3 \times 35·5 = 106$.

λ. $\frac{1}{3} \times 2787·2$.

λ. 4414·91 ; 4380·57 ; 33·32.——3529·44 ; 07·41.——3113·43.

In each order the first set give D(2.m), the second D(3.m). The **845** .. give the separations of the two.

$m = 2$. For the D(3.m) set only D_{11}, D_{22} in 2$h\nu$ are directly observed, but they are probably displaced one oun on p_1 since the separation from $D_1(2.2) - 84577$ is 16 too large. There seem collaterals for D_{33}, D_{34}. Thus

$$D_{34}, \tfrac{1}{3} \times 2504·33 \quad -119756·43 \text{ as } -2.2 \text{ gives } 119938·38$$
$$D_{33}, \tfrac{1}{3} \times 26·10 \quad -118729·14 \text{ as } -7/0 \text{ ., } 118865·9$$

There are two 2$h\nu$ lines which look like equal and opposite displacements of D_{12} :

$$1, \tfrac{1}{2} \times 1580·63 \quad -126531·82$$
$$0, \tfrac{1}{2} \times 79·1 \quad - 654·4$$ mean 126593·1,

The separation is 122·6. Treated as displaced $\pm \delta$ on the $p_1 3$ the double shift $= 131·62$. The O.E. $dn = 80 d\lambda$, so that the difference 9 corresponds to $d\lambda = ·1$ between the two lines.

$m = 3$. The D_3 lines appear displaced. Landé's rules suggest $\sigma_3 = 3 \times 188 = 564$, *i. e.*, larger than 528. The following are found for D2.3 :—

$$D_{34} \begin{cases} 1109·43 & 4 \ 90126·37 \text{ as } 0/-3 \text{ gives } D_{33} = 90194·80 \\ \tfrac{1}{3} \times 3327·00 & 4 \quad 45·47 \text{ as } 0/-2 \quad ,, \quad 91·09* \\ \tfrac{1}{3} \times 23·51 & 4 \ 90240·15 \text{ as } 0/2 \quad ,, \quad 94·53* \\ \tfrac{1}{3} \times 30·64 & 4 \ 90046·95 \text{ as } 2/-1 \quad ,, \quad 92·54* \end{cases}$$

$$D_{34} \begin{cases} \tfrac{1}{3} \times 3339·56 & 4 \ 89806·44 \text{ as } 0/6 \quad ., \ D_{34} = 89668·45* \\ \tfrac{1}{3} \times 43·83 & 4 \quad 691·78 \text{ as } 0/1 \quad ,, \quad 68·79* \\ \tfrac{1}{3} \times 47·65 & 4 \quad 589·30 \text{ as } 2/2 \quad ., \quad 66·06* \\ \tfrac{1}{3} \times 48·48 & 5 \quad 567·22 \text{ as } 2/1 \quad ,, \quad 67·0* \end{cases}$$

$$D_{24} \begin{cases} D_{24} & & 79728·28 \\ \tfrac{1}{3} \times 2511·04 & 0n \ 79624·30 \text{ as } 1/-2 \quad ,, \quad 26·85* \end{cases}$$

The three sets are very striking examples of displacement. The oun shifts are all large and different in each set. L's readings for D_{11}, D_{12} give wave numbers 7 less than those of O. Is this due to a satelloidal effect, as suggested above due to the presence of $p_1 2$?

$m=4$. The allocations for D3.4 seem justified, with separations in normal ratio. The absent D_{24}, D_{34} are in a region where Carroll has not recorded lines with intensities <3. They should probably be about 3542·7, 3123·3. For D2.4 the D_{11} alone appears, and as a $3h\nu$ emission. Its separation from D_{11}3.4——84562 is the same as that given by the S2 . *m*, S3 . *m* series. Those inserted in brackets may show collaterals, but as the oun shift on *d*4 is now of the order 9 the evidence cannot have much value. But data are here given as possibilities:

$$D_{12} \begin{cases} 2 & \frac{1}{2}\times1862\cdot95 & 107356\cdot62 & \text{as } 0/-3 & \text{gives } D_{12}=107385\cdot78 \\ 3 & \frac{1}{2}\times \ \ 61\cdot6 & 434\cdot4 & \text{as } 0/5 & \text{,,} \qquad\qquad 385\cdot8 \end{cases}$$

$$D_{13} \begin{cases} 1 & \frac{1}{2}\times1865\cdot9 & 107186\cdot8 & \text{as } 1/3 & \text{gives } D_{13}=107207\cdot1 \\ 1 & \frac{1}{2}\times \ \ 66\cdot9 & 129\cdot4 & \text{as } 1/-3 & \text{,,} \qquad\qquad 208\cdot2 \end{cases}$$

$$D_{23} \quad 0 \ \ \frac{1}{4}\times2458\cdot5 \qquad 122030\cdot9 \quad \text{as } 0/1 \quad \text{gives } D_{22}=122021\cdot1$$

$$D_{24} \quad 4 \ \ \frac{1}{2}\times1640\cdot1 \qquad 121943 \qquad\ \text{as } 0/3 \quad \text{,, } D_{24}=121914$$

This table gives allocations up to $m=4$ on the supposition of the existence of quartic systems, for which the evidence seems good. There are indications for orders above m, but I have not been able to satisfy myself as to definite allocations for higher orders, and their uncertainties could add little evidence for the *nhν* effect—the object of this communication. The table ends therefore at $m=4$. It must be noted, however, that for D3.4 L. allocates as the doublet set

$$7 \quad 22821\cdot69 \qquad D_{12}{}^2 \text{ my } D_{12}{}^4$$
$$10 \quad 23413\cdot68 \qquad D_{11}{}^2$$
$$9n \quad 28502\cdot94 \qquad D_{22}{}^2 \text{ ,, } D_{22}{}^4,$$

whilst I have taken for $D_{11}{}^4$ 4, 23070·53. It will be noted that the intensities in their allocation are in a normal order, and, moreover, the satellite separation of **591·99** is in step with the **1313** of $m=3$. But no quartic separations are found to go with this. If both allocations are correct, the p_1, p_2 terms must have the same values in both the doublet and quartic types. Although a similar effect exists in Cu †, one would accept its reality with considerable doubt, and, indeed, I do not feel satisfied with my own allocation. Possibly the correct allocation depends on the measures of the weaker lines which C. did not publish.

---

† Phil. Mag. 4, 1167, 27.

XXX. *Lattice Distortion and Hardness of Heat-treated Tungsten Magnet Steels.* *By* W. A. WOOD, *M.Sc., Physics Department, National Physical Laboratory, Teddington, Middlesex*[*].

[Plate XI.]

Introduction.

THE behaviour of tungsten magnet steels on heat treatment is a matter of some industrial importance, because the hardness and the magnetic properties undergo peculiar modification. Thus the coercive force may be reduced to a fifth of its optimum value by heating at about 950° C. and then restored by reheating at 1250° C [1]. The hardness varies in a similar way. The steels are said to have been "spoiled" and "recovered" respectively.

The object of the present work was (i.) to determine the relative importance, if any, of lattice distortion as a contributory factor to a final explanation of the spoiling and recovery of tungsten magnet steels, and (ii.) to obtain some experimental evidence of the relation, as developed by Rosenhain [2], between hardness and lattice distortion under conditions unlikely to introduce extraneous complications. We imply by the lattice distortion of steel solely a permanent irregular displacement of the iron atoms from the centres and corners of the body-centred cubic unit cells which constitute the space lattice of iron. The only criterion of such distortion is that it should cause a broadening of the lines of the X-ray spectrum of the distorted material.

Results on the relation of lattice distortion to the hardness of a metal may be complicated because, in the first case, the hardness can be changed without any variation in the degree of lattice distortion present or in the breadth of the lines of the X-ray spectrum. Thus the deformation of metals due to development of slip planes in the grains will change the hardness, but as shown by Dehlinger for the metals aluminium and zinc, this type of deformation does not alter the sharpness of the X-ray lines nor therefore cause any lattice distortion. In the second case, the X-ray lines may broaden as a result of another factor besides that of lattice distortion, namely, in consequence of the presence of grains in the metal less than about 10^{-5} cm. in size. These might very well be produced in specimens which have been quenched from high temperatures. The broadening due to distortion

* Communicated by Dr. G. W. C. Kaye, O.B.E.

and that due to small grain-size depend in a different way upon the angles of diffraction of the spectral lines. Despite this fact, however, it is not easy, unless the broadening is very large, to differentiate between the two types. These considerations may have a bearing on the results of W. L. Fink and K. R. Van Horn [3], who find that, contrary to the usual view, an increase in hardness of α-brass, deformed by bending, is accompanied by a decrease in lattice distortion. Advantage is taken in the present work of the fact that, in the steels investigated, increase as well as decrease in hardness can be produced merely as a result of heating and slow cooling. Thus the complications of deformation by slip and the formation of very small crystals are avoided.

Experimental Procedure.

The specimens were in the form of small blocks about 2 cm. square and 1 cm. thick. They were cut from the same bar of steel to ensure uniform composition. A typical bar of the steel contained 6 per cent. by weight of tungsten, 0·7 per cent. of carbon, 0·19 per cent. of nickel, 0·28 per cent. of manganese, 0·14 per cent. of silicon, 0·023 per cent. of sulphur, and 0·027 per cent. of phosphorus, the remainder being iron.

For the heat treatment the specimens were placed in a quartz tube, which could be inserted into an electric furnace maintained at any desired temperature. After a given interval of time the tube was withdrawn from the furnace, allowed to cool to room temperature, and then the specimen taken out. A stream of purified argon was passed through the tube during the periods of heating and cooling, in order to prevent oxidation and minimize decarbonization. The times of heating of fourteen different specimens at various temperatures are given in the table on p. 357.

The hardness of the specimens, 0 to 14, was determined in the Engineering Department of the National Physical Laboratory. The tests were made by the static indentation method in a Vickers Hardness Testing Machine using a 136° diamond pyramid as indenting tool and a load of 10 kgm. The diamond pyramid hardness number is given in terms of the ratio of the load applied in kgm. to the pyramidal area of impression in sq. mm. The results are recorded in the table opposite the particular specimens to which they refer. The different values for each specimen are the results of tests made at different points of the surface.

X-ray diffraction photographs were taken of the surface of the specimens. Each photograph was secured under

identical experimental conditions, so that any changes in the breadths of the diffraction lines were due only to changes in the steels themselves. The surface of the specimen was mounted to coincide with the axis of a cylindrical camera of radius 5 cm. The incident beam was rendered approximately parallel by passage along a slit 5 cm. long and 1 mm. wide, and fell perpendicularly on the face of the specimen. Under these conditions the photographic film, wrapped round the circumference of the camera, recorded the reflexion from the (220) planes in a state of suitable

Specimen.	Temperature.	Time.	Hardness.	Nature of (220) line.
Original.	—	—	342, 339, 342, 312	Very diffuse.
1	700° C.	½ hour.	278, 284	Diffuse.
2	700° C.	1 hour.	282, 300, 292, 290	,,
3	700° C.	1½ ,,	268, 262	Sharp doublet.
4	830° C.	10 min.	336, 325	Very diffuse.
5	830° C.	15 ,,	258, 264	Sharp doublet.
6	830° C.	20 ,,	256, 240	,, ,,
7	830° C.	30 ,,	250, 248	Doublet *.
8	830° C.	50 ,,	240, 230	,, *
9	830° C.	1 hour.	248, 250	,, *
10	830° C.	2½ ,,	227, 226	,, *
11	900° C.	10 min.	252, 250, 254, 282	,, *
12	900° C.	2 hours.	266, 264	,, *
13	950° C.	10 min.	260, 274	,, *
14	1250° C.	2 hours.	336, 339	Very diffuse.
14A	1250° C.	Few min.	382 (Brinell)	,, ,,

* Oscillated.

focus. The (220) reflexion in the case of a steel free from lattice distortion was a sharp doublet, and the two component lines, due to the α1 and α2 wave-lengths of the incident iron Kα radiation, were separated by about 0·7 mm. The appearance of lattice distortion was accompanied by a coalescence of the components into a single diffuse line, the change in breadth of which signified the degree of distortion present. In the table is given a description of the nature of the line opposite the corresponding specimen. In addition photographs showing the (220) line for particular cases are reproduced herewith.

It is important to note that reflexions from metals containing few large grains could give an apparent breadth of line which was entirely misleading. For each grain, if set at the correct angle for reflexion from particular planes, will produce one spot, an image of the slit, as its contribution to the reflected line. If the number of grains thus arranged are few then the line appears broken up into spots, and the distribution of spots over the width of the line, corresponding to the finite width of the slit, is a matter of chance. Thus the spots might be concentrated on the edges of the line where normally the line would be fading away, and give therefore an illusion of breadth. Consequently, in the case of specimens which, when photographed stationary, gave spotted lines, an oscillatory motion of 10° about the normal position was imparted, so as to bring more grains into the reflecting position and render the lines continuous. Photographs 10 *a*, 10 *b* (Pl. XI.) illustrate a broad spotted line made to resolve into a doublet by oscillation of the steel.

Results.

From the observations recorded in the table and the illustrative photographs of specimens, 0, 1, 3, 4, 5, 10 and 14 (Pl. XI.) we are able to conclude, in the first case, that the fundamental factor resulting in the spoiling and recovery of this type of steel is the variability of lattice distortion of the iron. Thus the hardness value of the initial untreated specimen is 334, taking the mean of the four tests, and this specimen gives a diffuse system of spectral lines. When heated to temperatures in the spoiling region the hardness value falls to 250 or 220, according to the time of spoiling, and the spectra of these specimens now show sharp lines; the (220) line becomes a definite doublet. This shows that the spoiling of the steel and the removal of lattice distortion are mutually associated. The evidence is not final as it stands, however, because it is usual for lattice distortion to disappear on heating a metal owing to removal of previous stress; but we have the next observation that when the specimen is further heated to 1250° C. the lattice distortion reappears, the (220) line becomes very diffuse, as shown in photograph of specimen no. 14. Moreover, the hardness recovers the value of 337. Also it was found that specimens which had been spoiled, and which gave a sharp spectrum, exhibited after reheating for a short time at 1250° C. the very diffuse spectrum associated with the recovered state. It is not usual for heating thus to re-introduce distortion. We have then the discovery that

spoiling is connected with the removal of the lattice distortion and recovery with the introduction of distortion.

Magnetic data of a batch of steels of similar composition were known, and confirmatory results were obtained from this batch. Thus, before treatment the Brinell hardness of specimen 14 A in the table was 375 and the magnetic coercive force 34. Spoiling at 900° C. reduced the hardness to 260 or 211 and the coercive force to 17 or 12 according to the time of spoiling. Recovery by heating at 1250° C. brought back the value of the hardness to 382 and the coercive force to 32. (This coercive force could, of course, be increased by quenching ; but since the broadening of the line, likewise found to increase, might involve the small crystal effect, the process was avoided for purposes of the present argument.) The changes in line breadth occurred as before. The magnetic quality of the steel appears therefore with hardness to be determined by the degree of lattice distortion.

In the second case we are able to conclude that a change in lattice distortion is shown to cause a corresponding change in hardness under conditions free from the complicating factors of slip deformation and small crystal effect. This follows from the above consideration of the re-introduction of distortion and the recovery of the hardness by the further heat treatment at 1250° C. This treatment would hardly re-introduce slip-deformed grains or submicroscopic crystals. It is interesting also to compare specimens 4 and 5. The sudden decrease in hardness of specimen 5, due only to an extra five minutes' heating, is accompanied by an equally sudden change in the appearance of the (220) line. Very diffuse in the case of specimen 4, it becomes a sharp doublet in the case of specimen 5. This would appear to prove that, whatever other factors may be influencing the hardness, they are certainly minor compared with the effect of lattice distortion. The only difference between the various specimens heated in the spoiling region is that the lower the temperature the slower the specimen is to exhibit the decrease of the hardness and of the lattice distortion.

Conclusion.

Of the possible factors associated with the phenomena of spoiling of tungsten magnet steels we have isolated that of lattice distortion and shown that it plays a fundamental and leading part. This narrows down the enquiry for a final explanation. Why the lattice should become distorted under the treatment must be bound up with the influence of

the foreign atoms and carbide compounds [4]. It is proposed to consider these in a separate paper.

The association of magnetic coercive force with lattice distortion opens up an interesting field. It is usually accepted that it is atomic phenomena which are primarily concerned with magnetic quantities. The derangement of atoms upon lattice distortion presumably influences the distribution of electric charge in the atom. Possibly a sufficiently sensitive determination of the " F-curves," giving this distribution, might show a difference between results for a single crystal of iron, say, before and after distortion. The greater the range of distortion a lattice will withstand, the greater the variation in associated physical properties the substance will show as a result of some treatment ; and possibly the effect of introduction of elements like tungsten into the iron lattice affects this range.

As a result of this and other work, we emphasize the importance of the determination of the degree of distortion the lattice of a metal or alloy will withstand whilst remaining stable. This value appears to be a fundamental physical quantity characteristic of that metal or alloy.

Finally, the author wishes to express his thanks to Mr. C. Wainwright, M.Sc., for help in the heating of specimens, to Dr. W. H. Hatfield for supplying the steels, and to Dr. G. W. C. Kaye for his interest in the researches of which this is part.

Summary.

The changes in lattice distortion in tungsten magnet steels are followed as the steels are subjected to various heat treatments. It is found that the decrease in magnetic quality and hardness on heating about 900° C. is due to disappearance of lattice distortion, and that the recovery of these properties by heating at 1250° C. is due to re-introduction of the distortion. Lattice distortion is advanced as the main factor underlying the spoiling and recovery of this type of steel. It is further shown that the particular nature of the changes exclude possible complications arising from the deformation of grains by slip or the formation of submicroscopic crystals.

References.
(1) Evershed, Journ. Inst. Elec. Eng. lxiii. p. 725 (1925).
(2) W. Rosenhain, Trans. Am. Inst. Min. Met. Eng. lxix. p. 1003 (1923).
(3) W. L. Fink & K. R. Van Horn, Inst. Met. xliv. p. 241 (1930).
(4) W. A. Wood, Phil. Mag. x. p. 659 (1930).

Aug. 18, 1931.

XXXI. *A Note on the Transport Phenomena in a Degenerate Gas.—Part I. By* D. S. KOTHARI *.

IN view of the numerous recent applications of the Fermi-Dirac statistics to physical [1] and astrophysical [2] problems, it may be of interest to study the allied phenomena of diffusion, viscosity, and conduction of a degenerate gas. The purpose of this paper is to deal with these allied phenomena, following the classical method of Boltzman and Lorentz. The results here obtained regarding electrical and thermal conduction are in no way more general than those derived by Sommerfeld, except that the form in which they are here obtained is more suited to their astrophysical applications.

The present part is concerned with a derivation of the various formulæ for diffusion, viscosity, etc. The applications of these results to stellar conditions will be discussed in Part II. The chief results are summarized at the end in a tabular form.

§ 1.

The three phenomena of diffusion, viscosity, and conduction are related to one another, and are commonly called the mean-free-path phenomena. The conception of the mean-free-path enables one to obtain to a first approximation expressions for these various phenomena in a very simple way. We can easily extend this simple treatment to a degenerate gas. Let us consider a gas composed of free electrons and ionized atoms. If D, η, σ, and λ denote the coefficients of diffusion, viscosity, electrical and thermal conductivity respectively, then, as is easily shown [3],

$$\left.\begin{array}{l} D = \frac{1}{3}\bar{c}l(\bar{c}), \\ \eta = \frac{1}{3}nm\bar{c}l(\bar{c}), \\ \sigma = \frac{1}{2}\frac{e^2}{m}\left(\frac{1}{c}\right)l(\bar{c}), \\ \lambda = \frac{1}{3}C_v\bar{c}l(\bar{c}), \end{array}\right\} \quad \ldots \ldots (1)$$

where c denotes the velocity of an electron and a dash over it signifies its value averaged for all the electrons, C_v is the specific heat (at constant volume) per unit volume, n, e, and m denote the number of electrons per unit volume, the charge and the mass of an electron respectively ; $l(\bar{c})$ denotes the

* Communicated by Prof. E. A. Milne, M.A., F.R.S.

Phil. Mag. S. 7. Vol. 13. No. 84. *Suppl. Feb.* 1932.   2 B

mean-free-path for the electron, which may be a function of $\bar{c}$.

We can rewrite (1), leaving aside the numerical coefficients, in terms of E_k, the average kinetic energy per electron,

$$
\left.
\begin{aligned}
D &= \sqrt{\frac{\overline{E_k}}{m}}\, l(E_k), \\[2mm]
\eta &= n\sqrt{\overline{E_k m}}\, l(E_k), \\[2mm]
\sigma &= \frac{e^2 n}{\sqrt{E_k m}}\, l(E_k), \\[2mm]
\lambda &= n\sqrt{\frac{E_k}{m}}\left(\frac{dE_k}{\partial T}\right)_v l(E_k).
\end{aligned}
\right\} \quad \ldots \ldots (2)
$$

In the classical case, which corresponds to non-degeneracy in the Fermi-Dirac statistics, we take

$$
E_k = \tfrac{3}{2}kT. \quad \ldots \ldots \ldots (3)
$$

The corresponding formulæ for the degenerate case are obtained when we put for E_k the value it has in the degenerate state [4],

$$
E_k = \frac{3}{10}\frac{h^2}{m}\left(\frac{3n}{8\pi}\right)^{2.3}\left[1 + \frac{5}{12}\left(\frac{2\pi m kT}{h^2}\right)^2\left(\frac{3n}{8\pi}\right)^{-4/3} \ldots \right]. \quad (4)
$$

We need to show, however, that in the degenerate case no other modification except this interpretation for E_k is necessary. This is a point which is discussed in § 2 *.

Now let us find a rough value for $l(E_k)$. The electrons will be deflected mainly by encounters with ionized atoms. A deflexion of 90° may be taken as a fair equivalent to the termination of a free path. Therefore† the radius of the apparent target is easily found to be, for the inverse square law of force,

$$
\sigma_1 = \frac{Ze^2}{2E_k}, \quad \ldots \ldots \ldots (5)
$$

and the mean-free-path $l(E_k)$ is

$$
l(E_k) = \frac{4E_k^2}{\pi Z e^4 n}, \quad \ldots \ldots \ldots (6)
$$

---

* See also the Appendix.

† From the well-known relation for the inverse-square law of force :

$$
\tan \phi = \frac{mpv^2}{Ze^2}
$$

(see Eddington, 'Constitution of Stars,' equation (153·7)).

where Ze is the charge on the ionized atom. From (2), (3), (4), and (6) we obtain the values of D, η, ... for the non-degenerate and the degenerate case. These values are given in the following table. As we are here concerned with only the orders of magnitude, the numerical co-efficients are replaced by unity. The last column gives the ratio of D, η, ... in the degenerate state to that in the non-degenerate state. This ratio is expressed in terms of A, the degeneracy discriminant [4],

$$A = \frac{nh^3}{2(2\pi m\,kT)^{3/2}}, \quad \ldots \ldots \quad (7)$$

$$A \ll 1, \quad \text{Non-deg.}$$

$$A \gg 1, \quad \text{Deg.}$$

It is seen at once that the values of D, η, σ, and λ are greater for the degenerate state than for the non-degenerate one at the same temperature and concentration.

	Non-deg.	Deg.	$R* = \dfrac{\text{Deg.}}{\text{Non-deg.}}$
Diffusion D	$\dfrac{(kT)^{1/2}}{e^4 m^{1/2}Zn}$	$\dfrac{n^{2/3}h^5}{e^4 m^3 Z}$	$A^{5/3}$
Viscosity η	$\dfrac{m^{1/2}(kT)^{5/2}}{e^4 Z}$	$\dfrac{n^{5/3}h^5}{e^4 m^2 Z}$	$A^{5/3}$
Electric conductivity σ	$\dfrac{(kT)^{3/2}}{e^2 m^{1/2}Z}$	$\dfrac{nh^3}{e^4 m^2 Z}$	A
Thermal conductivity λ	$\dfrac{k(kT)^{5/2}}{e^4 m^{1/2}Z}$	$\dfrac{nh^3k^2T}{e^4 m^2 Z}$	A

§ 2 †.

We proceed now to a more rigorous derivation of the above results. The method here used is essentially the same, with, of course, the necessary modifications, as that followed

---

* A better approximation for R is

$$R = \frac{3\pi^{1/2}}{2}\frac{1}{(3+x)|\frac{3+x}{2}}\left[\frac{3\pi^{1/2}}{4}A\right]^{x,3},$$

where $x=5$ for the case of D and η, and $x=3$ for the case of σ and λ.

† We consider the velocities small enough to render any relativity correction negligible.

by Jeans' 'Dynamical Theory of Gases,' 4th ed. chap. viii., and hence, to avoid needless repetition, we use, whenever practicable, Jeans's notation and results. We will refer to the equations given there only by their number.

Let us consider a system formed of a mixture of particles in which we distinguish the different kind of particles by the suffixes 1, 2, etc. Let the number of particles of, say, the kind 1, whose centres at any instant t lie within an element of volume $dx\,dy\,dz$, when their velocity components lie within an interval $du\,dv\,dw$, be denoted by

$$F_1(u, v, w, x, y, z, t)\,du\,dv\,dw\,dx\,dy\,dz. \quad . \quad . \quad (8)$$

The particles denoted by (8) will have their kinetic energies within the range E_{s_1}, $E_{s_1} + dE_{s_1}$. If m_1 be the mass of the particle, then F_1/m_1^3 will denote the density of the representative points in the part of the phase-space which corresponds to the energy E_{s_1}. The number of phase-cells per unit extension of the phase-space is g_1/h^3, g_1 being the statistical weight of the particle. We shall denote

$$\frac{m_1^3 g_1}{h^3} = Z_1.$$

In the case of the Fermi-Dirac statistics no two representative points can occupy the same phase-cell.

The representative points in the phase-space are always jumping into and out of the cells, and this can be regarded as brought about by two causes:

    (i.) due to the acceleration produced by external forces;

    (ii.) due to the collision-like interaction between the particles themselves.

In the steady state the density of the representative points does not vary with time, *i. e.*, the total time-rate of variation of F_1 is to be zero. Thus, following Jeans, we write the fundamental Boltzman equation for the classical case

$$\frac{\partial}{\partial t}F_1 = -\left[X\frac{\partial}{\partial u} + Y\frac{\partial}{\partial v} + Z\frac{\partial}{\partial w} + u\frac{\partial}{\partial x} + v\frac{\partial}{\partial y} + w\frac{\partial}{\partial z}\right]F_1$$

$$+ \sum \iiint\!\!\iiint [\bar{F}_1\bar{F}_2' - F_1F_2']V\,du'\,dv'\,dw'\,p\,dp\,d\epsilon,$$

$$. \quad . \quad . \quad (9)$$

where $p, \epsilon, u', v', w', V$ have the same meaning as in Jeans' (519) and the dash on F_1, F_2' has the same significance as it has with regard to f_1, f_2' in (519).

The terms [5] in the first bracket on the right-hand side in (9) remain apparently unaltered in the new statistics. The terms under the integrals need modification, and, following Nordheim [6], we replace (9) in the new statistics by

$$\left[\frac{\partial}{\partial t}+X\frac{\partial}{\partial u}+Y\frac{\partial}{\partial v}+Z\frac{\partial}{\partial w}+u\frac{\partial}{\partial x}+v\frac{\partial}{\partial y}+w\frac{\partial}{\partial z}\right]F_1$$

$$=\Sigma\int\int\int\int\int\left\{\overline{F}_1\left(1\pm\frac{F_1}{Z_1}\right)\overline{F}_2'\left(1\pm\frac{F_2'}{Z_2}\right)\right.$$

$$\left.-F_1\left(1\pm\frac{\overline{F}_1}{Z_1}\right)F_2\left(1\pm\frac{\overline{F}_2'}{Z_2}\right)\right\}V\,du'\,dv'\,dw'\,p\,dp\,d\epsilon,$$

$$\qquad\qquad\qquad\qquad\qquad\qquad\qquad \cdot\;\cdot\;\cdot\;(10)$$

where $+$ is to be used if the particles obey the Bose-Einstein statistics and $-$ if they obey the Fermi-Dirac.

Now we consider the system to consist of only two kinds of particles, and that of these the particles of the second kind are enormously heavier than those of the first. The heavy particle may be treated as a massive centre of force which deflects the light particle without altering its velocity, *i. e.*, no energy is transferred between them during an encounter. We shall neglect the effect of the encounters of the light particles with one another. Because of the above restrictions we can put

$$F_2'=F_2',\qquad\ldots\ldots\quad(11)$$

and hence, as has been shown by Nordheim [7], (10) reduces to

$$\left[\frac{\partial}{\partial t}+X\frac{\partial}{\partial u}+Y\frac{\partial}{\partial v}+Z\frac{\partial}{\partial w}+u\frac{\partial}{\partial x}+v\frac{\partial}{\partial y}+w\frac{\partial}{\partial z}\right]F_1$$

$$=n_2\int\int(\overline{F}_1-F_1)Vp\,dp\,d\epsilon;\quad(12)$$

n_2 is the number of the heavier particles per unit volume.

It must be noticed that for the particular case we are considering, *i. e.*, the imposition of the condition (11), makes some important terms in (10) cancel out, and the equation (12) so obtained shows immediately that the procedure we are to follow now reduces to that of Boltzman and Lorentz, with the modification that we have to use here a different distribution function, *i. e.*, that of Fermi-Dirac.

To search for a solution of (12) we assume

$$F_1=F_{01}+\phi_1(x,y,z,u,v,w),\quad\ldots\quad(13)$$

where ϕ_1 is a small quantity of the first order when compared to F_{01}, and

$$F_{01} = \cfrac{1}{\cfrac{1}{A_1} \exp\left[(u-u_0)^2 + (v-v_0)^2 + (w-w_0)^2\right]\beta_1 + 1} ; \quad (14)$$

u_0, v_0, w_0 denote the components of the velocity of mass motion of the gas and $\beta_1 = \dfrac{m_1}{2k\mathrm{T}}$.

The solution in (13) is not definite unless we subject it to the restriction that u_0, v_0, w_0, β_1, and A_1 are to have the same physical meaning in (13) as they have in the steady-state solution when $\phi_1 = 0$. We express these restrictions in terms of the five relations

$$\iiint u\phi_1 \, du \, dv \, dw = 0, \quad (15\,\mathrm{i.})$$

$$\iiint v\phi_1 \, du \, dv \, dw = 0, \quad (15\,\mathrm{ii.})$$

$$\iiint w\phi_1 \, du \, dv \, dw = 0, \quad (15\,\mathrm{iii.})$$

$$\iiint \phi_1 \, du \, dv \, dw = 0, \quad (15\,\mathrm{iv.})$$

$$\iiint (u^2 + v^2 + w^2)\phi_1 \, du \, dv \, dw = 0. \quad (15\,\mathrm{v.})$$

The limits for the integrals are $+\infty$ to $-\infty$. These conditions correspond to Jeans' (531), (533), and (535) in the classical case.

Further, if we represent the force * between a particle of the first kind and another of the second kind, a distance r apart, as

$$m_1 m_2 \mathrm{K}/r^s, \quad \ldots \ldots \quad (16)$$

then

$$p \, dp \, d\epsilon = \left[(m_1 + m_2)\mathrm{K}\right]^{\frac{2}{s-1}} \mathrm{V}^{-\frac{4}{s-1}} \alpha \, d\alpha \, d\epsilon, \quad (17)$$

where

$$\alpha = p\left[\cfrac{\mathrm{V}^2}{(m_1+m_2)\mathrm{K}}\right]^{\frac{1}{s-1}}. \quad \ldots \ldots \quad (17)$$

[Jeans' (552) and p. 218, first equation.]

---

* In § 1 we considered only the case of inverse-square force, *i.e.*, $s = 2$.

Noting that for the case we are considering

$$V = c = \sqrt{u^2 + v^2 + w^2} \quad [\text{Jeans } \S 288].$$

we obtain from (12), (13), and (17),

$$\left[\frac{\partial}{\partial t} + X\frac{\partial}{\partial u} + Y\frac{\partial}{\partial v} + Z\frac{\partial}{\partial w} + u\frac{\partial}{\partial x} + v\frac{\partial}{\partial y} + w\frac{\partial}{\partial z}\right] F_{01}$$
$$= n_2\left[(m_1 + m_2)K\right]^{\frac{2}{s-1}} c^{\frac{s-5}{s-1}} I_p, \quad (19)$$

where

$$I_p = \iint (\bar{\phi}_1 - \phi_1)\alpha \, d\alpha \, d\epsilon. \quad . \quad . \quad . \quad (20)$$

It is readily shown [Jeans' $\S\S$ 289–294] that

$$I_p = -[I_1(s)\psi_1 + 3I_2(s)\psi_2], \quad . \quad . \quad (21)$$

where ϕ has the solution

$$\phi = \psi_1 + \psi_2, \quad . \quad . \quad . \quad . \quad (22)$$

and ψ_1 is any function of u, v, w, and c, which is linear in u, v, and w; and ψ_2 is a function of u, v, w, c of degree 2 in u, v, and w, and such that the sum of the coefficients of u^2, v^2, w^2 vanishes. Both ψ_1 and ψ_2 are spherical harmonics,

$$\left.\begin{array}{l} I_1(s) = 4\pi \displaystyle\int_0^\infty \cos^2\frac{\theta'}{2}\, \alpha \, d\alpha, \\[2mm] I_2(s) = \pi \displaystyle\int_0^\infty \sin^2\theta'\alpha \, d\alpha, \end{array}\right\} \quad . \quad . \quad (23)$$

where θ' is the angle through which the asymptotes of the relative paths of the particles are deflected, when the distance between the initial asymptotes is p and their initial relative velocity is V [Jeans' (570) and (575)].

From (14) we obtain

$$\frac{\partial}{\partial u} F_{01} = -A_1 \frac{\partial F_{01}}{\partial A_1} 2u\beta_1, \quad . \quad . \quad . \quad . \quad . \quad (24)$$

$$\frac{\partial}{\partial x} F_{01} = -A_1 \frac{\partial F_{01}}{\partial A_1}\left[-\frac{1}{A_1}\frac{\partial A_1}{\partial x} - 2\beta_1\left(u\frac{\partial u_0}{\partial x} + v\frac{\partial v_0}{\partial x} + w\frac{\partial w_0}{\partial x}\right)\right.$$
$$\left. + c^2\frac{\partial \beta_1}{\partial x}\right], \quad . \quad . \quad (25)$$

and further, the hydrodynamical equation of continuity is [Jeans' (536)]

$$\frac{\partial}{\partial t}\log n_1 = -\left[\frac{\partial u_0}{\partial x} + \frac{\partial v_0}{\partial y} + \frac{\partial w_0}{\partial z}\right]. \quad . \quad . \quad (26)$$

Hence, for a steady state of motion which does not vary with time, we obtain from (19), (20), (21), (24), (25), and (26)

$$
\begin{aligned}
\bigg\lfloor 2\beta_1(u\mathrm{X}+v\mathrm{Y}+w\mathrm{Z}) &- \Big(u\frac{\partial}{\partial x}+v\frac{\partial}{\partial y}+w\frac{\partial}{\partial z}\Big)\log \mathrm{A}_1 \\
&+ c^2\Big(u\frac{\partial\beta_1}{\partial x}+v\frac{\partial\beta_1}{\partial y}+w\frac{\partial\beta_1}{\partial z}\Big)-2\beta_1\Big\{(u^2-\tfrac{1}{3}c^2)\frac{\partial u_0}{\partial x} \\
&+ \ldots +uv\Big(\frac{\partial v_0}{\partial x}+\frac{\partial u_0}{\partial y}\Big)+\ldots\Big\}\bigg]\mathrm{A}_1\frac{\partial \mathrm{F}_{01}}{\partial \mathrm{A}_1} \\
&= n_2[(m_1+m_2)\mathrm{K}]^{s-1}c^{s-5}[\mathrm{I}_1(s)\psi_1+3\mathrm{I}_2(s)\psi_2].
\end{aligned}
$$
$$\cdots \quad (27)$$

This equation is satisfied by taking *

$$
\psi_1 = \frac{u\Big[2\beta_1\mathrm{X}-\dfrac{\partial\log\mathrm{A}_1}{\partial x}+c^2\dfrac{\partial\beta_1}{\partial x}\Big]+\cdots}{n_2[(m_1+m_2)\mathrm{K}]^{\frac{2}{s-1}}c^{\frac{s-5}{s-1}}\mathrm{I}_1(s)}\,\mathrm{A}_1\frac{\partial\mathrm{F}_{01}}{\partial\mathrm{A}_1}, \quad (28)
$$

$$
\psi_2 = -\frac{2\beta_1\Big[\Big(u^2-\dfrac{1}{3}c^2\Big)\dfrac{\partial u_0}{\partial x}+\ldots+uv\Big(\dfrac{\partial u_0}{\partial y}+\dfrac{\partial v_0}{\partial x}\Big)+\cdots\Big]}{3n_2[(m_1+m_2)\mathrm{K}]^{s-1}c^{s-5}\mathrm{I}_2(s)}
$$
$$
\times\,\mathrm{A}_1\frac{\partial\mathrm{F}_{01}}{\partial\mathrm{A}_1}. \quad (29)
$$

Having obtained (28) and (29), we can proceed immediately to their various applications. In what follows, the lighter particles are to be taken as electrons, and we denote this specifically by dropping out the suffix I.

§ 3.

Electric and Thermal Conduction.

(a) *Electric conduction.*

Suppose the electric current to flow along the x-axis and to be produced by the electric intensity E,

$$
\mathrm{E}=\frac{m}{e}\,\mathrm{X}.
$$

* As seen before [equations (21) and (22)], ψ_1 and ψ_2 are functions of u, v, w, and c. ψ_1 is linear in u, v, and w, and ψ_2 is of degree 2. Hence, in equation (27) we identify ψ_1 with those terms that are linear in u, v, w, and ψ_2 with terms of degree 2 in u, v, w, and c.

Therefore, in this case,

$$\phi = \psi_1 = \frac{2\beta e u c^{-\frac{s-5}{s-1}}}{m\Delta_1} A \frac{\partial F_0}{\partial A}, \quad . \quad . \quad . \quad (30)$$

$$\Delta_1 = n_2 [m_2 K]^{\frac{2}{s-1}} I_2(s).$$

The electric current[8] J is

$$J = e \int u\phi \, d\Omega, \quad . \quad . \quad . \quad . \quad (31)$$

$$d\Omega = 8\pi \left(\frac{m}{h}\right)^3 c^2 \, dc. \quad . \quad . \quad . \quad (32)$$

Therefore, we obtain from (30) and (31) the value for σ, the specific conductivity,

$$\sigma = \frac{8\pi}{3} \frac{e^2}{m} \left(\frac{m}{h}\right)^3 \frac{A}{\Delta_1} \frac{\frac{2}{s-1}+2}{\beta^{\frac{2}{s-1}+1}} \frac{\partial}{\partial A} U_{\frac{s+1}{s-1}}, \quad . \quad . \quad (33)$$

where $U_{\frac{s+1}{s-1}}$ stands for the Sommerfeld integral[4] of the form

$$U_\rho = \frac{1}{\rho+1} \int_0^\infty \frac{u^\rho \, du}{\frac{1}{A} e^u + 1}. \quad . \quad . \quad . \quad (34)$$

We note that in the case of non-degeneracy $(A \ll 1)$

$$A = \frac{nh^3}{2(2\pi mkT)^{3/2}}, \quad . \quad . \quad . \quad (35)$$

$$U_\rho = -\frac{A^2}{2^{\rho+1}} + \frac{A^3}{3^{\rho+1}}, \quad . \quad . \quad . \quad (36)$$

$$\frac{\partial U_\rho}{\partial A} = 1 - \frac{A}{2^\rho} + \frac{A^2}{3^\rho}. \quad . \quad . \quad . \quad (37)$$

In the case of degeneracy $(A \gg 1)$

$$\log A = \frac{h^2}{2mkT} \left(\frac{3n}{8\pi}\right)^{2/3}, \quad . \quad . \quad . \quad . \quad (38)$$

$$U_\rho = \frac{(\log A)^{\rho+1}}{\lfloor \rho+2} + 2\left\{ c_2 \frac{(\log A)^{\rho-1}}{\lfloor \rho} + \ldots \right\}, \quad . \quad (39)$$

$$A \frac{\partial U_\rho}{\partial A} = \frac{(\log A)^\rho}{\lfloor \rho+1} + 2\left\{ c_2 \frac{(\log A)^{\rho-2}}{\lfloor \rho-1} + \ldots \right\}, \quad . \quad (40)$$

$$c_2 = \frac{\pi^2}{12}.$$

Hence, we obtain from (33)

$$\sigma_N = \frac{4}{3\sqrt{\pi}} \frac{e^2 n}{\Delta_1 m} \left(\frac{2kT}{m}\right)^{\frac{1}{2}\frac{5-s}{s-1}} \left| \frac{2}{s-1} + 2 \right. \qquad \text{Non-deg.,} \quad (41\,\text{i.})$$

$$[\text{Jeans' (609)}]$$

$$\sigma_D = \frac{8\pi e^2}{3\Delta_1 m} \left(\frac{h}{m}\right)^{\frac{5-s}{s-1}} \left(\frac{3n}{8\pi}\right)^{\frac{2s+1}{3s-1}} \qquad \ldots \qquad \text{Degenerate,} \quad (41\,\text{ii.})$$

and

$$\frac{\sigma_D}{\sigma_N} = \left[\frac{nh^3}{2(2\pi m kT)^{3/2}}\right]^{\frac{1}{3}\frac{5-s}{s-1}} \left[\left(\frac{3\pi^{1/2}}{4}\right)^{\frac{2s+1}{3s-1}} \frac{1}{\left|\dfrac{2}{s-1}+2\right.}\right]. \quad \cdot (42)$$

(b) *Thermal conduction.*

Let the gas be devoid of mass-motion and the temperature gradient exist along the x-axis. We obtain, therefore,

$$\phi = \psi_1 = u c^{-\frac{s-5}{s-1}} \left[-\frac{\partial \log A}{\partial x} + c^2 \frac{\partial \beta}{\partial x}\right] \frac{A}{\Delta_1} \frac{\partial F_0}{\partial A}, \quad (43)$$

subject to the restriction [Jeans' (598)]

$$\iiint u\psi_1 \, du \, dv \, dw = 0, \quad \ldots \quad (44)$$

for there are to be no convection currents. Combining (43) and (44), we have

$$\psi_1 = \frac{A}{\Delta_1} \frac{\partial F_0}{\partial A} u c^{-\frac{s-5}{s-1}} \left[-\frac{1}{\beta} \frac{2s}{s-1} \frac{\dfrac{\partial}{\partial A} U_{\frac{2}{s-1}+2}}{\dfrac{\partial}{\partial A} U_{\frac{2}{s-1}+1}} + c^2\right] \frac{\partial \beta}{\partial x}. \quad (45)$$

The heat-current [8] W is given by

$$W = \tfrac{1}{2} m \int c^2 u \psi_1 \, d\Omega, \quad \ldots \quad (46)$$

and hence we obtain for the thermal conductivity λ

$$\lambda = \frac{2\pi m}{3} \left(\frac{m}{h}\right)^3 \frac{A}{\Delta_1} \left[-\frac{1}{\beta^2} \frac{2s}{s-1} \frac{\dfrac{\partial}{\partial A} U_{\frac{2}{s-1}+2}}{\dfrac{\partial}{\partial A} U_{\frac{2}{s-1}+1}} \right| \frac{\dfrac{2}{s-1}+3}{\beta^{\frac{2}{s-1}+2}} \frac{\partial}{\partial A} U_{\frac{2}{s-1}+2}$$

$$+ \frac{\sqrt{\frac{2}{s-1}+4}}{\beta^{\frac{2}{s-1}+4}} \frac{\partial}{\partial A} U_{\frac{2}{s-1}+3} \Bigg] . \quad . \quad (47)$$

After some reduction we get

$$\lambda_N = \frac{2}{3\sqrt{\pi}} \frac{nk}{\Delta_1} \left(\frac{2kT}{m}\right)^{\frac{1}{2}\frac{s+3}{s-1}} \Big| \frac{2}{s-1} + 3 \quad \text{Non-deg.,} \quad . \quad (48\,\text{i.})$$

$$[\text{Jeans' (602)}]$$

$$\lambda_D = \frac{32}{3} \frac{\pi c_2}{\Delta_1} \frac{k^2T}{m} \left(\frac{h}{m}\right)^{\frac{5-s}{s-1}} \left(\frac{3n}{8\pi}\right)^{\frac{2s+1}{3s-1}} \quad \text{Degenerate,} \quad . \quad (48\,\text{ii.})$$

and

$$\frac{\lambda_D}{\lambda_N} = \left[\frac{nh^3}{2(2\pi m kT)^{3/2}}\right]^{\frac{5-s}{3(s-1)}} \left[\frac{\pi^2}{3}\left(\frac{3\pi^{1/2}}{4}\right)^{\frac{2s-1}{3s-1}} \frac{1}{\sqrt{\frac{2}{s-1}+3}}\right]. \quad (49)$$

From (41) and (48) we have

$$\frac{\lambda_N}{\sigma_N} = \frac{2s}{s-1} \frac{k^2}{e^2} T, \quad . \quad . \quad . \quad . \quad (50\,\text{i.})$$

$$[\text{Jeans' (610)}]$$

$$\frac{\lambda_D}{\sigma_D} = 4c^2 \frac{k^2}{e^2} T = \frac{\pi^2}{3} \frac{k^2}{e^2} T. \quad . \quad . \quad (50\,\text{ii.}) \, {}^{(9)}$$

Diffusion.

For this case we take u_0, v_0, w_0, all constant, and

$$X = Y = Z = 0.$$

Hence,

$$\phi = \psi_1 = \frac{u \frac{\partial}{\partial x} \log A}{\Delta_1 c^{\frac{s-5}{s-1}}} A \frac{\partial F_0}{\partial A}. \quad . \quad . \quad (51)$$

The flow of electrons parallel to the axis of x per unit area and time is

$$\iiint \left[F_0 - \frac{u \frac{\partial}{\partial x} \log A}{\Delta_1 c^{\frac{s-5}{s-1}}} A \frac{\partial F_0}{\partial x}\right] u \, d\Omega. \quad . \quad (52)$$

Therefore the coefficient of diffusion D is

$$D = \frac{4\pi}{3}\left(\frac{m}{h}\right)^3 \frac{\sqrt{\frac{2}{s-1}+2}}{\beta^{\frac{2}{s-1}+2}} \frac{1}{\Delta_1} \frac{\partial}{\partial A} U_{\frac{2}{s-1}+1} \frac{\partial A}{\partial n}. \quad . \quad (53)$$

Hence we obtain

$$D_N = \frac{2}{3\sqrt{\pi}\,\Delta_1}\left(\frac{2kT}{m}\right)^{\frac{1}{2}\frac{s+3}{s-1}}\sqrt{\frac{2}{s-1}+2} \quad \text{Non-deg.,} \quad . \quad . \quad (54\,\text{i.})$$
$$[\text{Jeans' (613)}]$$

$$D_D = \frac{1}{3\Delta_1}\left(\frac{h}{m}\right)^{\frac{s+3}{s-1}}\left(\frac{3n}{8\pi}\right)^{\frac{1}{3}\frac{s+3}{s-1}} \quad . \quad . \quad \text{Degenerate,.} \quad . \quad (54\,\text{ii.})$$

and

$$\frac{D_D}{D_N} = \left[\frac{nh^3}{2(2\pi mkT)^{3/2}}\right]^{\frac{1}{3}\frac{s+3}{s-1}}\left[\frac{2}{3}\left(\frac{3\pi^{1/2}}{4}\right)^{\frac{4s}{3(s-1)}}\frac{1}{\sqrt{\frac{2}{s-1}+2}}\right]. \quad (55)$$

Viscosity.

We follow essentially the same method as in Jeans' § 297. His equation (591), when modified in accordance with the present treatment, stands as

$$P_{xx} = p - \frac{2\beta m}{\Delta_2}\left(\frac{m}{h}\right)^3 A \frac{8\pi}{45}$$
$$\times \left[2\frac{\partial u_0}{\partial x} - \frac{2}{3}\left(\frac{\partial u_0}{\partial x} + \frac{\partial v_0}{\partial y} + \frac{\partial w_0}{\partial z}\right)\right]\frac{\partial}{\partial A}\int F_0 c^{6-\frac{s-5}{s-1}}dc,$$

where
$$\quad . \quad . \quad . \quad (56)$$

$$\Delta_2 = n_2(m_2 K)^{\frac{2}{s-1}} I_2(s). \quad . \quad . \quad . \quad (57)$$

If η denotes the viscosity, we have from hydrodynamics [Jeans' (593)]

$$P_{xx} = p - 2\eta\frac{du_0}{dx} + \tfrac{2}{3}\eta\left[\frac{\partial u_0}{\partial x} + \frac{\partial v_0}{\partial y} + \frac{\partial w_0}{\partial z}\right]. \quad . \quad (58)$$

From (56) and (58)

$$\eta = \frac{8\pi}{45}\left(\frac{m}{h}\right)^3 \frac{m}{\Delta_2}\frac{\sqrt{\frac{2}{s-1}+3}}{\beta^{\frac{2}{s-1}+2}} A \frac{\partial}{\partial A} U_{\frac{2}{s-1}+2}. \quad . \quad . \quad (59)$$

Hence

$$\eta_N = \frac{4mn}{45\sqrt{\pi}\Delta_2}\left(\frac{2kT}{m}\right)^{\frac{s+3}{2(s-1)}}\sqrt{\frac{2}{s-1}+3} \quad \text{Non-deg.,} \quad (60\,\text{i.})$$

[Jeans' (595)]

$$\eta_D = \frac{8\pi}{45}\frac{m}{\Delta_2}\left(\frac{h}{m}\right)^{\frac{s+3}{s-1}}\left(\frac{3n}{8\pi}\right)^{\frac{4}{3}\frac{s}{(s-1)}} \quad . \quad . \quad \text{Degenerate,} \quad (60\,\text{ii.})$$

and

$$\frac{\eta_D}{\eta_N} = \left[\frac{nh^3}{2(2\pi m kT)^{3/2}}\right]^{\frac{s+3}{3(s-1)}}\left[\left(\frac{3\pi^{1/2}}{4}\right)^{\frac{4s}{3(s-1)}}\frac{1}{\sqrt{\frac{2}{s-1}+3}}\right]. \quad (61)$$

We may note the relation between thermal conductivity, viscosity, and the constant volume specific heat.

Let C_v' denote the specific heat per unit mass, then in the non-degenerate case,

$$C_v' = \frac{3}{2}\frac{k}{m}.$$

and we have from (48 i.) and (60 i.),

$$\frac{\lambda_N}{C_v'\eta_N} = 5\frac{I_2(s)}{I_1(s)}. \quad . \quad . \quad . \quad (62\,\text{i.})$$

In the degenerate case, from (4)

$$C_v' = \frac{\pi^2 k^2}{h^2}\left(\frac{8\pi}{3n}\right)^{2/3}T,$$

and hence we have from (48 ii.) and (60 ii.)

$$\frac{\lambda_D}{C_v'\eta_D} = 5\frac{I_2(s)}{I_1(s)}, \quad . \quad . \quad . \quad (62\,\text{ii.})$$

the same ratio as in the non-degenerate case.

In connexion with (60) we must note that it represents only the contribution made by free electrons to viscosity, and does not take account of the contribution due to the ionized atoms, which in the case of non-degeneracy may be considerable. We can easily show that for the degenerate case this correction is never serious. As the non-degenerate case has been fully treated by Chapman [10], we do not concern ourselves here beyond making a very rough calculation for the multiplying factor to (60 i.), necessary to give the actual viscosity of an ionized gas.

The ionized atoms will be deflected by encounters with other ionized atoms only. As in § 1, we can calculate the

mean-free-path for the ionized atom. If l_2 and l_1 denote the mean-free-path for the ion and the electron respectively in the case of the inverse-square forces, i. e., $s = 2$, we have

$$\frac{l_2}{l_1} = \frac{1}{Z^2}\left(\frac{E_{k_2}}{E_{k_1}}\right)^2,$$

where E_{k_2} and E_{k_1} are the respective mean kinetic energies for the ion and the electron. Hence, if η_2 and η_1 denote the viscosity due to the ions and the electrons separately, we have from (62),

$$\frac{\eta_2}{\eta_1} = \frac{1}{Z^3}\left(\frac{m_2}{m_1}\right)^{1/2}\left(\frac{E_{k_2}}{E_{k_1}}\right)^{5/2}. \quad\quad\quad (63)$$

This gives for non-degenerate case, when

$$E_{k_1} = E_{k_2},$$

$$\frac{\eta_2}{\eta_1} = \frac{1}{Z^3}\left(\frac{m_2}{m_1}\right)^{1/2}, \quad\quad\quad\quad (64)$$

giving for the multiplying factor to (60 i.)

$$\left[1 + \frac{1}{Z^3}\left(\frac{m_2}{m_1}\right)^{1/2}\right].$$

In the case of degeneracy (64) gives

$$\frac{\eta_2}{\eta_1} = \left(\frac{5}{3}\frac{1}{A}\right)^{5.2}\frac{1}{Z^3}\left(\frac{m_2}{m_1}\right)^{1/2}, \quad\quad\quad (65)$$

and as $A \gg 1$, the correction is never serious. Thus, in a degenerate ionized gas the viscosity can be considered as due almost entirely to the free electrons.

§ 4.

We now summarize the various results for $s = 2$, a case with which alone we shall be concerned in astrophysical applications. The gas is supposed to consist of ionized atoms of charge Ze and free electrons. Whenever numerical values are given, Z has been taken to be 26 (fully ionized iron atom), and $\mu = 2\cdot5$ (density $\rho = \mu m_H n$).

The formulæ involve the integrals (23). These, for the case of $s = 2$, reduce to

$$I_1(s) = 4\pi\int_0^\infty \cos^2\frac{\theta'}{2}\,\alpha\,d\alpha = 2\pi\log_e(1+\alpha^2)\Big]_0^\infty, \quad (66\text{ i.})$$

$$I_2(s) = \pi\int_0^\infty \sin^2\theta'\alpha\,d\alpha = 2\pi\left[\log_e(1+\alpha^2)+\frac{1}{1+\alpha^2}\right]\Big]_0^\infty,$$

$$\cdots \quad (66\text{ ii.})$$

and thus tend to infinity. This difficulty was overcome by Chapman [11] by assuming an upper limit for α ($= \alpha_0$). E. Persico's [12] more refined treatment, involving some numerical integrations, has shown that no serious error is involved in Chapman's simpler treatment.

Following Chapman, we can immediately write for α_0,

$$\alpha_0 = \frac{E_{k_1}}{2Z^{2/3}e^2 n^{1/3}}, \quad \ldots \quad (67)$$

which, in the non-degenerate case, reduces to Chapman's result,

$$\alpha_0 = \frac{3}{4} \frac{kT}{e^2 Z^{2/3} n^{1/3}} = 8 \cdot 45 \times 10^{-7} \frac{T}{\rho^{1/3}}, \quad \ldots \quad (68)$$

where ρ is the density in gm./cm.^{3}

In the degenerate case we obtain from (4),

$$E_{k_1} = \frac{4\pi}{5} \frac{h^2}{mn} \left(\frac{3n}{8\pi}\right)^{5/3} = 3 \cdot 57 \times 10^{-27} n^{2/3},$$

$$\alpha_0 = 5 \cdot 55 \times 10^{-2} \rho^{1/3}.$$

We tabulate for ready reference the values of α_0, I_1, and I_2 for the degenerate case :—

TABLE I.

ρ.	α_0.	I_1.	I_2.
10^6	5·55	21·7	21·9
10^5	2·58	12·8	13·6
10^4	1·20	5·6	8·2
10	0·56	1·7	6·5
10^2	0·26	0·43	6·3
10	0·12	0·09	6·3
1·0	0·06	0·02	6·3
0·1	0·03	0·006	6·3

The various values of the transport phenomena for the cases of non-degeneracy and degeneracy are summarized in Table II. The astrophysical applications of these results will be detailed in Part II.

TABLE II.

	Non-Degenerate.		Degenerate.	
	(13) E.S.U.		E.S.U.	C.G.S.
Electric conduction .	$\dfrac{2^{9/2}}{\pi^{1/2}}\dfrac{k^{3/2}}{e^2 m^{1/2}}\dfrac{T^{3/2}}{ZI_1}$	$1.28 \times 10^{-4}\,\dfrac{T^{3/2}}{I_1}$ (ohm)$^{-1}$	$\dfrac{3}{8\pi}\dfrac{h^3}{e^2 m^2 m_{\mathrm{H}}}\dfrac{\rho}{\mu Z I_1}$	$1.28 \times 10^3\,\dfrac{\rho}{I_1}$ (ohm)$^{-1}$
Thermal conduction .	$\dfrac{2^{13/2}k^{7/2}}{\pi^{1/2}e^4 m^{1/2}}\dfrac{T^{5/2}}{ZI_1}$	$3.81 \times 10^{-5}\,\dfrac{T^{5/2}}{I_1}$ C.G.S.	$\dfrac{8}{\pi}\dfrac{h^3 k^2}{e^4 m^2 m_{\mathrm{H}}}\dfrac{T\rho}{\mu Z I_1}$	$4.56 \times 10^2\,\dfrac{T\rho}{I_1}$ C.G.S.
Diffusion . .	$\dfrac{2^{1/2}k^{3/2}m_{\mathrm{H}}}{\pi^{1/2}e^4 m^{1/2}}\dfrac{\mu T^{5/2}}{ZI_1\rho}$	$2.88 \times 10^{-13}\,\dfrac{T^{5/2}}{\rho I_1}$	$\dfrac{1}{3}\left(\dfrac{3}{8\pi}\right)^{5/3}\dfrac{h^5}{e^4 m^3 m_{\mathrm{H}}{}^{2/3}}\dfrac{\rho^{2/3}}{\mu^{2/3}ZI_1}$	$4.55 \times 10^{-1}\,\dfrac{\rho^{2/3}}{I_1}$
Viscosity . .	$\dfrac{2^{15/2}m^{1/2}k^{5/2}}{15\pi^{1/2}e^4}\dfrac{T^{5/2}}{ZI_2}$	$3.33 \times 10^{-17}\,\dfrac{T^{5/2}}{I_2}$	$\dfrac{1}{15}\left(\dfrac{3}{8\pi}\right)^{5/3}\dfrac{h^5}{e^4 m^3 m_{\mathrm{H}}{}^{5/3}}\dfrac{\rho^{5/3}}{\mu^{5/3}ZI_2}$	$1.97 \times 10^{-5}\,\dfrac{\rho^{5/3}}{I_2}$

APPENDIX.

On the Mean-free-path and Degeneracy.

In § 1 we have used the conception of the mean-free-path to find approximate expressions for the transport phenomena in the degenerate case. We found

$$l(E_k) \sim \frac{E_k^2}{Z^3 e^4 n}, \quad \cdot \quad \cdot \quad \cdot \quad \cdot \quad \cdot \quad (1)$$

and stated that $l(E_k)$ in the non-degenerate and the degenerate case is obtained by putting for E_k the corresponding values, *i. e.*, $3/2\,k\mathrm{T}$ for non-degenerate and $\dfrac{3}{40}\left(\dfrac{3}{\pi}\right)^{2/3}\dfrac{h^2 n^{2/3}}{m}$ for the degenerate case respectively. The justification for this, *i. e.*, for the degenerate case $l(E_k)$ is still given by (1), is clear from § 2, but it is interesting to examine this point further in detail.

Let us consider an assembly of free electrons and ionized atoms in isothermal steady state subject to no external forces. Generally, the important deflexions in the path of an electron will occur when it encounters an ion, and we shall, as a first approximation, neglect the encounters of the electrons amongst themselves. Further, as has been seen in § 2, no appreciable energy interchange will take place between the electron and the atom during their encounter, *i. e.*, the electron will possess the same kinetic energy before and after the encounter.

If V be the volume of the assembly and p_x, p_y, p_z the components of momentum for an electron, then

$$\mathrm{V}\,dp_x\,dp_y\,dp_z = h^3 \quad \text{(volume of a phase-cell)}.$$

So long as an electron continues to move undeflected, its representative point remains in the same phase-cell; but when it suffers a deflexion the representative point jumps from the initial cell to another unoccupied cell corresponding to the same energy as the initial one.

We estimate that a deflexion of 90° in the path of an electron is a fair equivalent to the termination of a free-path. Therefore the radius of the apparent target for an ion is easily shown to be (see § 1)

$$\sigma = \frac{Z^2 e^2}{2E_e},$$

where E_e is the kinetic energy of the encountering electron.

Therefore the probability of collision for an electron with energy E_s is

$$\frac{\pi n \sigma^2}{Z}(1-n_s), \quad \ldots \ldots \quad (2)$$

where n_s is the number of electrons per unit volume of the phase-space already present in that region of the phase-space which corresponds to the energy E_s. The factor $(1-n_s)$ is essentially a feature of the new statistics, and would be absent in a purely classical treatment.

Noting that

$$n_s = \frac{1}{\frac{1}{A}e^{E_s/kT}+1},$$

we obtain at once for l,

$$l = \frac{16\left|\overline{7/2}\,(2m)_{3/2}\right.}{Z^3 e^4 n^2 h^3}(kT)^{7/2}A, \quad \ldots \ldots \ldots \quad (3)$$

$$l_N = \frac{15(kT)^2}{\pi Z^3 e^4 n} \quad \ldots \ldots \ldots \ldots \text{Non-deg..} \quad (4)$$

$$l_D = \frac{16\left|\overline{7/2}\,(2m)^{3/2}\right.}{Z^3 e^4 n^2 h^3}(kT)^{7/2}e^{\frac{h^2}{2mkT}\left(\frac{3n}{8\pi}\right)^{2/3}} \quad \text{Degenerate.} \quad (5)$$

Equation (5) shows that for a completely degenerate system the mean-free-path tends to infinity. This, however, holds true only for an isothermal assembly subject to no external forces, and it is wrong to assume that (3) is valid in the case of an assembly when external forces are present, *i. e.*, for instance, it will be wrong to conclude from (5) that the electrical conductivity for a completely degenerate assembly becomes infinitely large.

To take the other case, let us, for simplicity, consider the case of electric conduction alone, *i. e.*, we take an assembly in isothermal steady state subject to an external electric field and let it be completely degenerate. Because of the presence of the external force, the kinetic energy of an electron (in general) no longer remains constant, but is changing as the electron describes its path. Let us consider at instant t those electrons (n_s') which at instant $t+\Delta t$ will all have the same kinetic energy, say * E_s. At instant t these electrons will possess kinetic energy different from E_s, and the phase-cells (a_s) corresponding to the energy E_s are

* Strictly lying between the interval E_s, E_s+dE_s.

all occupied (at instant t) by other electrons. However, at time $t + \Delta t$ the a_s cells are all empty, as the electrons they contained at t have all moved out (because of the action of the external force their kinetic energy is now no longer E_s), and thus they are free to be occupied by the n_s' electrons. It is, therefore, easily seen that the factor $(1 - n_s)$ in (2), which took account of the already-occupiedness of the cells, is now no longer necessary, and thus the mean-free-path *which is to determine the conductivity* is given by

$$l = \frac{4}{\pi Z^3 e^4 n} \int \frac{E_s^2 E_s^{1/2} d E_s}{\frac{1}{A} e^{E_s/kT} + 1} \bigg/ \int \frac{E_s^{1/2} dF_s}{\frac{1}{A} e^{E_s/kT} + 1} \qquad . \quad . \quad (6)$$

$$= \frac{15(kT)^2}{\pi Z^3 e^4 n} \frac{U_{5/2}}{U_{1/2}}, \qquad . \quad . \quad . \quad . \quad . \quad . \quad . \quad (7)$$

$$l_N = \frac{15(kT)^2}{\pi Z^3 e^4 n}, \qquad . \quad . \quad . \quad . \quad . \quad \text{Non-deg.,} \qquad (8)$$

$$l_D = \frac{15}{4\pi} \frac{1}{Z^3 e^4 n} \left[\frac{h^2}{m} \left(\frac{3n}{8\pi} \right)^{2/3} \right]^2 . \quad . \quad \text{Degenerate.} \quad (9)$$

These are the expressions which (neglecting the numerical coefficients as a rough approximation) we have already used in § 1.

My best thanks are due to Prof. E. A. Milne for his kind interest and many valuable suggestions.

References.

(1) Darrow, Phys. Rev. Supp. i. p. 90 (1929).
(2) Milne, M. N. R. A. S. xci. p. 1 (1930).
(3) Loeb, 'Kinetic Theory of Gases,' p. 181.
(4) Sommerfeld, *Zs. f. Phys.* xlvii. p. 1 (1928).
(5) Darwin, Proc. Roy. Soc. cxvii. p. 258 (1927).
(6) Nordheim, Proc. Roy. Soc. cxix. p. 693 (eqn. 7) (1928).
(7) Nordheim, *loc. cit.* (6) [see p. 697].
(8) Sommerfeld, *loc. cit.* (See his eqn. (46 a).)
(9) Sommerfeld, *loc. cit.* (See his eqn. (50 b).)
(10) Chapman, Phil. Trans. ccvii. p. 189 (1917); M. N. R. A. S. lxxxii. p. 294 (1922).
(11) Chapman, M. N. R. A. S. lxxxii. p. 293 (1922).
(12) Persico, M. N. R. A. S. lxxxvi. p. 93 (1926).
(13) Compare with Chapman, eqn. (6), M. N. R. S. lxxxix. p. 55 (1929).

Cavendish Laboratory,
Cambridge.

XXXII. *A Determination of the Stefan-Boltzmann Radiation Constant, using a Callendar Radio-balance. By* F. E. HOARE, *M.Sc., A.R.C.S.* [*]

1. *Introduction.*

IN a former paper † details and results of a determination of the Stefan-Boltzmann radiation constant, using as the source of radiation a wire-wound electric furnace operated between the temperatures 716·55° C. and 981·51° C., were given. The accuracy and consistency of the results obtainable with the instruments used in that investigation made it appear that an extension of the range of observation would be of value. The present paper describes such an extension to a source temperature of approximately 100° C.

Through the kindness of the authorities of the Royal College of Science a radio-balance, constructed for the late Professor Callendar according to a new design, was available, and made this investigation possible. As this instrument has proved to have advantages over the older design, a description is given here.

2. *Description of the Radio-balance.*

In essentials the radio-balance is the same as that described by Callendar in his original paper ‡, but the mounting has been modified in many respects. Fig. 1 gives a sectional view of the instrument through the centre, approximately to scale.
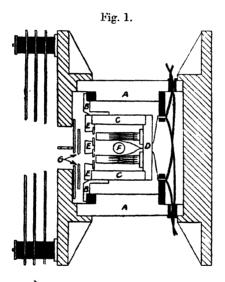
Two plates of aluminium, shown cross-shaded in the figure, 12·5 cm. square, have circular holes cut a part of the way through through them to locate a hollow aluminium cylinder, A, of external diameter 7·2 cm. and 5·5 cm. length. The maximum thickness of this cylinder is just greater than 1 cm., but it is partially turned out at each end to make steps 0·5 cm. in width. On the step so formed at the foremost end of the cylinder, left-hand side in figure, is fastened a vulcanized fibre ring to which are screwed three brass lugs, B, supporting a central brass ring of 3·5 cm. internal diameter. At the rear two pieces of fibre screwed to the aluminium step serve as mountings to which the electrical connexions are brought. Through the brass ring already

---

mentioned passes a hollow copper cylinder, C, with walls
0·5 cm. thick. This cylinder is closed at one end by a copper
plate, D, of the same thickness as the walls, to which are
attached the copper block mountings of the thermopiles
supporting the thin copper receiving cups. At the other
end a copper plate, E, having two conical holes, blackened
on the inside, is screwed to the cylinder. Behind these
conical holes and let into the copper plate are two disks of
stainless steel with bevelled apertures of about 2 mm.
diameter, arranged so as to be one in front of each receiving
cup.

Fig. 1.

A brass tube, F, let into the copper cylinder allows a
mercury in glass thermometer to be introduced right into
the body of the instrument and the temperature in the
immediate neighbourhood of the cups to be taken. This is
important, as a difference of $\frac{1}{10}°$ C. makes a difference of
nearly one in a thousand in reducing the results.

Two holes through the front aluminium plate admit the
radiation, which can be screened from either cup by a mov-
able shutter, G, working in close contact with the aluminium
plate and the copper plate E. (The separation of the shutter
from the copper plate has been exaggerated in the diagram
in order to show the components more clearly.) The double
shutter is made up from two pieces of brass, separated from
one another at the top by a small piece of fibre. The side of

the shutter exposed to the radiation is nickel-plated, and the other blackened with a dull black paint. Small conical apertures in the shutter admit the radiation, and a single lever outside the aluminium cylinder allows the shutter to be moved so as to screen either cup. On the front of the instrument are three screens, nickel-plated on one side and blackened on the other, to shield the instrument. These have concentric holes of increasing diameter, as shown in the figure, and are mounted on four ebonite bushes, so that there is poor thermal contact between them.

In the present instrument the couples both for the Peltier junctions and the thermopiles were copper-constantan instead of iron-constantan as in the original instrument. Although it means a slight lowering of the sensitivity, this change was made as it was thought that such couples would keep more constantly to their calibrations than couples using iron, which might suffer from atmospheric corrosion. All junctions are hard soldered, the thermopiles being insulated from the cups and the blocks as before with thin paper and shellac. The leads from the thermopiles and Peltier junctions are brought away through small pieces of ebonite let into the copper plate D, and thence to the fibre mounts screwed to the aluminium cylinder. Twin flex soldered to the appropriate points leads away from here through ebonite bushes in the aluminium cylinder A for the external connexions.

This method of construction with massive metal parts and a wide air space between the aluminium and copper cylinders keeps the temperature of the whole instrument very constant, it being found much steadier in working than that used in the previous investigation.

The edges of the holes in the front nickel-plated screens were not sharp originally, and some difficulty was occasioned by reflexion of radiation from these points into the receiving cups. This was successfully overcome, however, by fastening tin-foil over these holes in the front and then cutting it away so as to leave a small width projecting all the way round, this being blackened on the side towards the cups. As an added precaution, and to facilitate screening both apertures together, an additional movable shutter with conical apertures was put at the front of the aluminium plate.

The method of using this radio-balance is exactly the same as for that of the older design. The thermopiles surrounding the cups are connected in opposition and the circuit completed through a sensitive galvanometer. The Peltier junctions in the bottoms of the cups are also

connected in opposition, and this circuit completed through a source of electric current, a variable resistance, and some apparatus for measuring the current. Means are also provided in this circuit for reversing the current.

As before, the amount of radiation incident in either cup is given by

$$E = 2PC + (D' - D'')s \text{ microwatts,}$$

where P is the value of the Peltier coefficient in millivolts, C the balancing current passed through the couples in milliamps, $(D' - D'')$ the galvanometer deflexion on transferring the radiation from cup 1 to cup 2, measured in the direction of the deflexion due to passing from cup 1 to cup 2 exposed to the radiation with no current through the junctions, and s the scale sensitivity of the galvanometer, *i. e.*, the microwatts necessary to be generated at the Peltier junctions to cause one scale division deflexion. This quantity is obtained by shielding both of the cups from radiation and reversing a known current of C milliamps through the junctions, the galvanometer deflexion D being taken. The scale sensitivity is then given as

$$s = \frac{2PC}{D} .$$

3. *Calibration of the Radio-balance.*

The method adopted for determining the values of the Peltier coefficient was the same as that previously employed [*]. Two small heating coils, approximately 11 ohms each, and agreeing in resistance to about one part in a thousand, were constructed from manganin wire and fitted one into each cup. A current was made to pass through one coil and a pair of dummy leads attached to the other coil, in this way compensating for any heating effect in the leads. The heating effect in one coil was balanced against the cooling effect of the Peltier couple in that cup and the heating effect in the other. The current being sent through the second coil and the current in the Peltier circuit being reversed, the Peltier coefficient at the temperature of the radio-balance is given by

$$P = \frac{W - (D' - D'')s}{C} \text{ millivolts,}$$

where W is the energy in microwatts expended in the coil

* *Loc. cit.* p. 831.

and C the current in milliamps through the Peltier junctions.

The currents in the coil and Peltier circuits were found by measuring the potentials across standard resistances of approximately 1 ohm each with a Cambridge Inst. Co. direct-reading 0–90 millivolts potentiometer. One of the standard resistances used was supplied by the same company and the other was an oil-immersion resistance made specially for this work and compared with the former. The scale of the potentiometer was adjusted by a Weston standard cell the E.M.F. of which was taken as 1·0183 volts at 20° C. with a temperature correction given by

$$V_t = V_{20} - 0 \cdot 0000406\,(t - 20).$$

It was found that the values of the Peltier effect could be represented with an accuracy slightly greater than one part in a thousand by the equation

$$P_t = P_{20} + 0 \cdot 0726\,(t - 20),$$
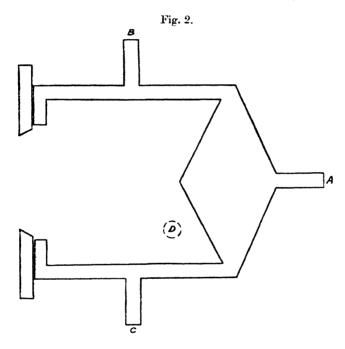
the value at 20° C. being 11·528 millivolts.

4. *Experimental Arrangement.*

The source of radiation used in these experiments was a double-walled vessel, made up from 16 gauge tin-plate, as shown in fig. 2. The tubes A and B served to admit steam from an electrically heated boiler, whilst C and D were connected to water traps and condensers which allowed the condensed steam to reflux into the boiler. Electrical heating was adopted in preference to gas in order to minimize the amount of carbon dioxide in the room where the experiments were conducted, and the consequent risk of absorption of radiation. The inside walls of the radiator were blackened with a thin coat of a dull black paint, made by mixing lampblack with very dilute shellac, and afterwards had a thin layer of soot from burning benzene deposited upon them. It was found that the initial coating of lampblack and shellac enabled a more even deposit of benzene soot to be obtained. The apex of the cone in the radiator being towards the radiating aperture prevents direct reflexion of radiation into the receiving apparatus. The outside of the " black body " was well lagged with felt to minimize condensation of steam within.

In front of, and fitting closely to, the radiator was a water-cooled diaphragm with a central bevelled aperture with a sharp edge of approximately 10 cm. diameter defining the

radiating aperture. This diaphragm was made of copper, the central aperture being turned from a gun-metal casting, and blackened in the same way as the interior of the radiator. The water space between the back and front was half an inch, which allowed a rapid circulation of water to be maintained. The aperture in the diaphragm could be closed with a water-cooled shutter mounted directly in the front of the diaphragm, its back surface being in close contact with the latter. The size of the diaphragm was sufficient to prevent any radiation

Fig. 2.

being received by the radio-balance from the surroundings other than this at the distances used.

The water circulating in the diaphragm entered at the bottom and flowed out at the top, afterwards passing through the shutter in the same direction. The temperature of the water was taken on inflow and outflow with sensitive mercury thermometers, totally immersed in the stream, which could be estimated to $\frac{1}{100}°$ C.

The radio-balance was mounted on a microscope carriage which had an attached vernier moving over a brass scale on a massive iron base. The original scale belonging to the

microscope was removed and a longer one from a catheto-- meter put in its place. The end of this scale was carefully cut off at the zero mark and then screwed to the iron micro- scope base, so that a length of about 10 cm. projected at the foremost end. It was arranged that the end of the scale was in the same plane as the radiating aperture. By means of steel rules and spirit-levels the iron base was so adjusted that in all positions the centre of the radio-balance was on the horizontal axis through the centre of the radiating aperture.

Unfortunately owing to the dimensions of the radio- balance it was impossible to work with the receiver at a smaller distance from the source than about 20 cm. If the distance is increased very much the radiation received is greatly diminished, as this varies inversely as the square of the distance, and therefore the distances actually employed varied only from 22·902 cm. to 26·902 cm., it being thought more advantageous to obtain a large number of observations where the readings were relatively accurate than a few readings at widely varying distances with consequent loss of percentage accuracy in the measurements of the radiation received.

5. *Method of taking Observations.*

The procedure followed in taking observations was similar to that previously used. The radio-balance having been set with the plane of its apertures at a known distance from, and parallel to, the plane of the aperture in the water-cooled diaphragm, the latter was covered with the water-cooled shutter. First one cup of the receiver and then the other was exposed to the radiation from these water-cooled surfaces, and the small galvanometer deflexion D_0 on changing over was noted. The shutter then being removed, one cup of the radio-balance was exposed to radiation from the "black body," and the current through the Peltier junctions adjusted to maintain a very small difference of temperature between the cups. It was found unnecessary to take readings at one minute intervals for five minutes, as was done when using the old instrument, for conditions were much steadier with the new radio-balance. On each reading, therefore, five minutes was allowed for equilibrium to be established, and readings of the galvanometer and potential difference across the standard resistance in the Peltier circuit taken at the end of this period. The second cup was then exposed to the radiation, the Peltier current reversed, and after a further period of five minutes similar readings again taken.

The temperature of the radio-balance and the inflow and outflow temperatures of the water were taken before and after each set of readings, the mean values being used in reducing the results. It was sufficiently accurate to take the water temperature to $\frac{1}{20}°$ C.

It was considered that by taking a number of readings at certain fixed distances, and averaging the results at each of these distances, any systematic variation of the radiation constant with distance would be more likely to make itself apparent. Consequently the distances used were in centimetre steps from $22 \cdot 902$ to $26 \cdot 902$ cm.

The net radiation received by the radio-balance from a source at an absolute temperature T_1 in surroundings at temperature T_2, *i. e.*, that of the water in the diaphragm and shutter, is given by

$$E = 2PC + (D' - D'' - D_0)s \text{ microwatts.}$$

The temperature of the source of radiation was obtained by reading the barometric height during the course of each observation, and then deducing the boiling-point of water from tables.

As the radiator was made of stout tinplate it was thought that a temperature gradient might exist through the metal, especially as the surfaces exposed to the steam soon became coated with rust. At the conclusion of the work, in order to test if such a temperature gradient existed, a copperconstantan thermocouple was made, and one junction put into the steam space of the radiator and the other junction soldered to the front surface of the radiating cone and covered with black paint as before. The aperture was closed with the movable shutter, and steam from the same boiler passed through this to prevent radiation from the rear of the thermocouple with consequent cooling. To compensate for any lack of symmetry the couples were then reversed, the galvanometer deflexions being noted in each case. It was found that the total change in the galvanometer scale reading on reversal of the couples was $2 \cdot 80$ cm., the deflexion in each case being in a direction to indicate that the front surface of the metal was at a lower temperature than the steam. As a deflexion of $4 \cdot 76$ cm. corresponded to a difference of temperature of $1°$ C., the difference between the steam and the front surface of the radiator was $0 \cdot 29°$ C. This has been subtracted from the temperature of the source, as obtained from readings of the barometric height, in reducing the results.

6. *Reduction of Observations.*

It has been shown by Keene [*] and others [†] that the energy exchange between two fully radiating coaxial circular apertures, separated by a distance of the same order as the diameters of the apertures themselves, is given by

$$E = \tfrac{1}{4}\pi R(r_1 - r_2)^2,$$

where E is the energy passing through one of the apertures in one second, R is the total stream of radiation, r_1 and r_2 the greatest and least distances between two points, one on each circle bounding the apertures.

If a and b are the radii of the two apertures and d is the perpendicular distance between them, this expression may be written as

$$E = \tfrac{1}{4}\pi R\{(d^2 + x^2)^{\frac{1}{2}} - (d^2 + y^2)^{\frac{1}{2}}\}^2,$$

if x and y are substituted for $(a+b)$ and $(a-b)$ respectively. On expansion this becomes

$$E = \pi R \cdot \frac{a^2 b^2}{d^2} \left\{ 1 - \frac{x^2 + y^2}{d^2} + \frac{1}{8} \cdot \frac{x^4 + x^2 y^2 + y^4}{d^4} \right.$$
$$\left. - \frac{5}{64} \cdot \frac{x^6 + x^4 y^2 + x^2 y^4 + y^6}{d^6} + \dots \right\}^2.$$

With the apparatus used in this investigation the value of b, i. e., the radius of the radio-balance apertures, is about 0·1 cm., whilst a, the radius of the radiating aperture, is approximately 5 cm. Further, since d is always greater than 20 cm., it is sufficiently accurate to regard x and y within the bracket as being the same and each equal to a. The expression then becomes

$$E = \pi R \cdot \frac{a^2 b^2}{d^2} \left\{ 1 - \frac{a^2}{2d^2} + \frac{3a^4}{8d^4} - \frac{5a^6}{16d^6} + \dots \right\}^2$$
$$= \frac{\pi R a^2 b^2}{d^2 + a^2}.$$

As the radio-balance has two apertures which are arranged to be equidistant on either side of the horizontal axis passing through the centre of the radiating aperture, and at the same distance from this aperture, the above expression has to be multiplied by the ratio $\dfrac{d^2}{d^2 + c^2}$, on

* Proc. Roy. Soc. A, lxxxviii. p. 59 (1913).
† Phil. Mag. vii. pp. 273 & 1092 (1929).

account of the increase of distance between the source and receiver centres, and in the same ratio again because of the obliquity of the apertures, c being the displacement of the centre of either receiving aperture from the axis. This correction is applied with sufficient accuracy by the addition of the constant $2c^2$ to the factor $(d^2 + a^2)$ in the above expression. We thus have

$$E = \pi R a^2 b^2 / d^2 + a^2 + 2c^2.$$

According to Stefan's law for a black body at a temperature T_1 radiating to surroundings at a temperature T_2, the value of R is given by

$$R = \sigma(T_1^4 - T_2^4),$$

and therefore

$$E = \frac{\sigma(T_1^4 - T_2^4)\pi a^2 b^2}{d^2 + a^2 + 2c^2}:$$

and substituting for E from our former expression,

$$\sigma = \frac{\{2PC + (D' - D'' - D_0)s\}\{d^2 + a^2 + 2c^2\}}{\pi a^2 b^2 (T_1^4 - T_2^4)}.$$

7. *Measurements.*

The diameters of the apertures in front of the cups were measured with a Hilger measuring microscope reading to 0·0001 cm.

The mean of fifty measurements for each aperture diameter gave 0·2123 cm. and 0·2089 cm., corresponding to areas of 0·03540 sq. cm. and 0·03428 sq. cm. respectively. The mean area was taken as 0·03484 sq. cm.

The displacement of the radio-balance apertures from the central axis, c, as obtained by measurement with a microscope, was 0·593 cm.

The diameter of the radiating aperture was measured with vernier calipers (Starrett) reading to 0·001 cm. The mean of twenty equally-spaced measurements was 10·289 cm.

The radio-balance was set at one of five fixed distances from the source by means of the vernier and scale. It was necessary to ascertain how far behind the plane of the receiving apertures lay the zero of the vernier. This was accomplished by measuring the distance of these aperture planes below the front aluminium plate by focussing a microscope, first on one and then on the other. A piece of plane rigid brass was then clamped to the front of the radio-balance with part projecting downwards to be just in contact

with the brass scale. One side of the brass being in the same plane as the front surface of the aluminium plate, it was set to correspond exactly with various division marks on the scale, and the vernier read. Subtraction then gave the distance from the vernier zero to the plane of the receiving apertures. The maximum variation in these readings was 0·008 cm., the probable accuracy of the measurements of the distance of source from receiver being of the same order.

The method of measuring the current through the Peltier functions and the required temperatures has already been indicated.

8. *Results.*

The following table gives the results of fifty measurements of the Stefan-Boltzmann constant σ in ergs/sec./cm.^{2}/degree^4 :

TABLE.

Date, 1931.	Temp. source.	Temp. water.	Temp. rad. bal.	Total microwatts.	Distance.	Value of $\sigma \times 10^5$.
	° C.	° C.	° C.			
April 9 ...	99·72	10·35	12·6	123·24	22·902	5·732
10 ...	99·88	11·30	13·6	122·72	,,	5·733
11 ...	99·87	11·35	12·8	122·64	,,	5·732
18 ...	99·40	10·55	10·2	121·78	,,	5·700
21 ...	99·61	10·70	14·0	122·09	,,	5·703
21 ...	99 60	10·70	14·1	121·7	,,	5·689
22 ...	99·52	11·15	15·0	121·80	,,	5·716
24 ...	99·05	11·60	14·1	121·02	,,	5·741
May 1 ...	99·51	12·80	15·3	120·80	,,	5·739
5 ...	99·48	11·85	12·3	121·65	,,	5·742
April 9 ...	99·73	10·55	12·8	114·07	23·902	5·762
10 ...	99·89	11·25	13·4	112·40	,,	5·693
13 ...	99·96	10·80	11·0	114·61	,,	5·779
17 ...	99·41	11·05	11·4	112·10	,,	5·713
21 ...	99·61	10·40	13·3	112·59	,,	5·694
22 ...	99·57	10·80	13·7	113·06	,,	5·737
22 ...	99·53	11·15	14·9	112·91	,,	5·747
24 ...	99·05	11·60	14·5	111·47	,,	5·736
28 ...	99 69	11·60	14·7	113·28	,,	5·772

TABLE (*cont.*).

Date, 1931.	Temp. source.	Temp. water.	Temp. rad.-bal.	Total microwatts.	Distance.	Value of $\sigma \times 10^5$.
	° C.	° C.	° C.			
May 5 ...	99·49	11·85	12·7	112·01	,,	5·735
April 9 ...	99·73	10·55	13·0	104·80	24·902	5·726
10 ...	99·89	11·15	13·1	104·86	,,	5·741
13 ...	99·96	10·85	11·1	105·71	,,	5·765
17 ...	99·41	11·05	11·5	104·83	,,	5·766
21 ...	99·61	10·25	13·0	104·44	,,	5·706
21 ...	99·60	10·65	14·2	104·25	,,	5·713
22 ...	99·53	11·15	14·8	103·89	,,	5·720
24 ...	99·05	11·60	14·8	102·83	,,	5·724
28 ...	99·69	11·60	14·5	104·21	,,	5·742
May 1 ...	99·49	12·90	16·2	102·87	,,	5·741
April 10 ...	99·92	10·95	13·1	97·86	25·902	5·765
13 ...	99·96	10·90	11·5	98·32	.,	5·787
13 ...	99·96	11·15	11·9	97·33	,,	5·738
20 ...	99·51	10·05	12·0	97·51	,,	5·746
22 ...	99·57	10·85	14·0	96·86	,,	5·735
22 ...	99·54	11·10	14·6	96·65	,,	5·736
24 ...	99·04	11·60	15·0	95·64	,,	5·742
28 ...	99·70	11·60	14·4	97·22	,,	5·776
May 1 ...	99·49	12·90	16·3	95·04	,,	5·721
5 ...	99·51	12·10	12·9	96·44	,,	5·768
April 9 ...	99·73	10·45	13·5	90·79	26·902	5·750
10 ...	99·92	10·80	12·9	90·27	,,	5·714
13 ...	99·96	11·15	11·6	91·52	,,	5·804
18 ...	99·41	10·55	10·6	89·51	,,	5·703
22 ...	99·57	11·00	14·3	89·90	,,	5·733
22 ...	99·54	11·05	14·1	90·22	,,	5·757
24 ...	99·04	11·60	15·0	88·50	,,	5·715
28 ...	99·70	11·60	14·1	90·26	,,	5·768
May 1 ...	99·51	12·85	15·7	88·38	,,	5·718
5 ...	99·51	12·10	13·0	89·06	,,	5·729

Mean value of $\sigma = 5.737 \times 10^{-5}$ ergs/sec./cm.^{2}/degree^4.

9. *Discussion.*

In reducing the above results no correction has been made for atmospheric absorption, it having been found to be negligible by Gerlach [*] for a source at 100° C. The mean values at the five distances used show no systematic variation with distance, and thus add confirmation to Gerlach's result.

The effect of not making the correction for the drop of temperature through the metal of the radiator would be to decrease the results by a little more than 0·4 per cent., varying, of course, according to the temperature limits.

The almost exact numerical agreement of the mean of the above results with that obtained in the previous investigation, namely, 5·735, cannot be regarded as other than accidental, as the values of the Peltier coefficients were measured in each case with a little greater accuracy than one part in a thousand. All the other measurements, however, have been made with an accuracy usually considerably greater than one part in a thousand.

Treating the results by the method of least squares we have the following as the data from the two investigations [†] :—

Former investigation ... $\sigma = 5\cdot735 \pm 0\cdot014 \times 10^{-5}$,

Present investigation ... $\sigma = 5\cdot737 \pm 0\cdot017 \times 10^{-5}$,

and combining the two ...... $\sigma = 5\cdot736 \pm 0\cdot016 \times 10^{-5}$.

10. *Summary.*

The present paper describes a determination of the Stefan-Boltzmann radiation constant using a Callendar radiobalance, and a source of radiation operated at approximately 100° C. The experimental procedure is very similar to that previously employed and described elsewhere [‡]. The mean of fifty measurements of this constant gives the value as $5\cdot737 \times 10^{-5}$ ergs/sec./cm.^{2}/degree^4.

In conclusion, I have to thank the Government Grants Committee of the Royal Society for a grant, with which the major part of the apparatus used in this investigation was purchased, and Dr. F. H. Newman for his encouragement and advice during the course of the experiments.

[*] *Ann. der Phys.* 1. p. 233 (1916).
[†] The P.E. of a *single* observation is given in each case.
[‡] *Loc. cit.*

XXXIII. *The Thermoelectric Properties of Ferromagnetic Substances. By* L. F. BATES, *B.Sc., Ph.D., Reader in Physics, University College, London* *.

Introduction.

IT has long been known that the thermoelectric powers of certain ferromagnetic elements show anomalies in the regions of their ferromagnetic Curie points. Recently, however, these anomalies have acquired a greater interest, since Dorfmann and Jaanus † suggested that the variation of the Thomson coefficient of a ferromagnetic substance represented the behaviour of its specific heat, assuming that its ferromagnetism is due entirely to the action of free electrons. It has been shown by Bloch‡ that, theoretically, at any rate, free electrons may adequately account for the existence of ferromagnetism. Briefly, we may suppose that ferromagnetism arises from the interaction of spinning electrons belonging to different atoms within a group of atoms which forms a kind of magnetic particle. On heating a ferromagnetic substance, some of these electrons may be supposed to leave the groups and to become free or conduction electrons. Accordingly energy must be supplied to produce this liberation of electrons, and the substance must possess a kind of additional specific heat, which, as the temperature rises, must disappear in the neighbourhood of the ferromagnetic critical point §. As a basis for their treatment of the problem, Dorfmann and Jaanus assumed that each ferromagnetic atom liberated one electron when it passed from the ferromagnetic to the paramagnetic state, and we shall adopt this hypothesis as a basis in what follows.

Let us suppose that we have a thermoelectric circuit consisting of a ferromagnetic metal M and a normal metal C, their Thomson coefficients being σ_M and σ_C respectively. We will assume that the ferromagnetic metal possesses a positive Thomson coefficient when the Thomson E.M.F. between a point at a temperature T and a point at $T + dT$ is $-\sigma_M . dT$, i. e., this E.M.F. acts from hot to cold, and an amount of heat equal to $\sigma_M . dT$ is reversibly absorbed when unit quantity of positive electricity flows from the first point to the second.

* Communicated by Prof. E. N. da C. Andrade.
† Dorfmann and Jaanus, *Zeit. für Phys.* liv. p. 277 (1929).
‡ Bloch, *Zeit. für Phys.* lvii. p. 545 (1929).
§ Weiss, *Journ. de Physique*, vii. p. 249 (1908); Bates, *Proc. Phys. Soc.* xlii. p. 441 (1930).

From the latter statement arises the conception of the specific heat of electricity. The above definition is not that adopted in the "International Critical Tables," but it is the more common in the literature of the subject. Now the difference in the Thomson coefficients of the two metals, $\sigma_M - \sigma_C$, is equal to $T \cdot \frac{d^2}{dT^2} (_M E_C)$ or $T \cdot \frac{d^2 E}{dT^2}$, and if this quantity is positive the thermoelectric current must flow from M to C across the colder junction. If the current is carried by free electrons, then the nett heat absorbed by the passage of one electron round the circuit is $e \cdot T \cdot d^2 E/dT^2$, heat being absorbed in M and liberated in C. Now, in the neighbourhood of the ferromagnetic Curie point we observe a sudden decrease in the specific heat of the substance M. Hence, on the assumption that free electrons are responsible for ferromagnetism, we should observe a sudden decrease in $\sigma_M - \sigma_C$, *i. e.*, the sign of $d^2 E/dT^2$ should be negative, so that $e \cdot T \cdot d^2 E/dT^2$ may be positive just before M changes from the ferromagnetic to the paramagnetic state, after which we may expect $d^2 E/dT^2$ to remain practically constant.

Consequently, a sudden change in the value of $e \cdot T \cdot d^2 E/dT^2$ in the neighbourhood of the ferromagnetic Curie point, denoted in what follows by S, should represent the sudden change, or "step-down," in specific heat which occurs in that region.

A careful survey of the behaviour of thermoelements of nickel and platinum and of nickel and copper in the neighbourhood of the ferromagnetic Curie point of nickel has been made by Dorfmann and Kikoin [*]. They find an effect of sufficient magnitude to account for the major portion of the change in the specific heat of nickel. Unfortunately, however, this does not establish the correctness of the free electron theory of ferromagnetism as pictured by Dorfmann and Jaanus, for, as Stoner [†] has pointed out, the change of specific heat deduced from these electrical measurements is of opposite sign to that found by direct calorimetric measurements of the specific heat of nickel.

The free electron theory obviously needs considerable modification before it can possibly represent the true state of affairs. Firstly, it is difficult to see how the electrons responsible for metallic conduction can possibly be free in the full meaning of the word. Their passage through a metallic lattice is probably much more adequately represented

---

[*] Dorfmann and Kikoin, *Zeit. für Phys.* liv. p. 289 (1929).
[†] Stoner, 'Nature,' cxxv. p. 973 (1930).

by the picture given by Lennard-Jones *. Secondly, as Stoner † points out, free electrons would require ferromagnetism to persist at temperatures enormously higher than the Curie points known to us. Thirdly, the phenomena are not likely to be strictly reversible. So far, then, the experimental facts are that the specific heat changes found by direct experiment are of opposite sign to those predicted on the free electron theory of ferromagnetism, at any rate in the case of nickel and iron. It is therefore desirable to know whether this is true for all ferromagnetic substances. For this purpose the following investigation of the thermoelectric behaviour of thermocouples made of copper and manganese arsenide was carried out. The latter substance exhibits very pronounced and sharply defined specific heat changes ‡ in the neighbourhood of a ferromagnetic critical point at 42·2° C., so that it appeared to be a very suitable substance for examination.

Preparation of Manganese Arsenide.

The method of preparing manganese arsenide in a powdered form has been fully described elsewhere. and it is sufficient to state here that black metallic manganese was heated with excess arsenic in a wide, evacuated, quartz tube at a temperature of about 750° C. for about forty hours. The available stock of pure (pre-war) arsenic having been used up, arsenic was obtained from other sources. This was found to be rather impure, and had to be purified by successive distillations in a wide pyrex tube with a long, narrow, outlet-tube. through which the main tube was evacuated and sealed. The wide tube was placed inside a furnace at 550° C., with the outlet-tube outside the furnace, so that the impurities were driven off and condensed in the latter. To make rods of manganese arsenide the substance thus prepared was powdered, digested for days in concentrated hydrochloric acid, washed thoroughly with water and with alcohol, and dried. Samples of this arsenide were placed in long quartz tubes which were evacuated and sealed. These tubes were suspended vertically in a furnace and subjected to the heat treatments as outlined in the particular cases described below. As this work was in the nature of a preliminary survey, the number of rod specimens successfully prepared was not large. In general, they were exceedingly brittle,

---

* Lennard-Jones, Trans. Farad. Soc. xxv. p. 668 (1929).
† Stoner, Proc. Leeds Phil. Soc. ii. p. 50 (1930).
‡ Bates, Proc. Roy. Soc. A, cxvii. p. 680 (1927) ; Proc. Phys. Soc *loc. cit.*
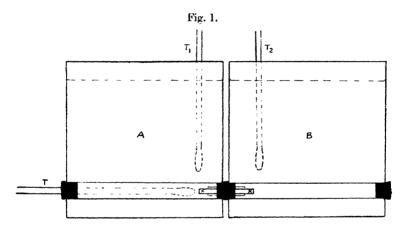
and their porous nature made it unsafe to dissolve in hydrofluoric acid the quartz tubes in which they were made, in order to obtain the metallic specimens. The latter were therefore removed by dissolving the tubes in hydrofluoric acid until they were very thin, and then by carefully breaking the tubes. The general conclusions to be drawn from this work are that it is advisable to get rid of traces of excess arsenic remaining in the arsenide by continued preliminary heating, so that the former is condensed in the upper end of the tube. To do this effectively, a sufficiently wide quartz tube must be used. It is also inadvisable to heat the substance above 1000° C. for any considerable interval of time.

Although some rods over 10 cm. long were obtained by these methods, they were usually so brittle, that, even with very careful handling, a specimen more than 4 cm. long was rarely successfully mounted. The majority of the thermoelectric measurements were carried out with specimens 2·5 to 3·5 cm. long. In some ways this was an advantage, for there was a greater probability that a shorter rod was of more uniform composition than a longer one. In order to make thermoelectric measurements it was necessary to make electrical contacts at the two ends of the specimen. It was possible to electroplate the ends with copper to which copper leads could be soldered, but there was danger that the porous substance would absorb the electrolyte, and this method was discarded. A small phosphor bronze clip was therefore fixed tightly on each end of the specimen and thin double silk covered copper leads were soldered to the clips.

The specimen XX. (fig. 1) was supported in a quartz tube which passed through a cork. The latter was inserted into a thick copper tube which passed through the copper tank A and into a similar tube in the tank B, so that one end of the specimen was inside A and the other inside B. The tanks were partly filled with suitable liquids, which were vigorously stirred and electrically heated. The temperature inside the tube in A was recorded by a sensitive mercury thermometer whose bulb was almost in contact with the end of the specimen. Thermometers T_1 and T_2 were used to read the temperatures of the tanks A and B. All thermometers were read by means of special eyepieces, and the heating arrangements were such that with a little practice it was comparatively easy to maintain the temperatures of the tanks constant to within 0·01° C. The tanks were in electrical contact to assist in preventing leak currents, and, of course, the electrical insulation of the specimen was satisfactorily tested.

The tanks were well lagged, but in view of the average length of the specimens used, there was little lagging in the space between them.

The temperature difference between the tanks was usually maintained at 2° C., or, more accurately, 2° C. as indicated by the thermometers T_1 and T_2. These thermometers were only used in maintaining the temperatures of the tanks constant, and the actual difference in temperature of the two ends of the specimen was found by means of a copper constantan thermocouple. The copper leads of this thermocouple were taken to a mercury cup commutator, which was kept in a constant temperature bath, and thence to a galvanometer called G_2. The copper leads from the ends of the

Fig. 1.

specimen also passed to a similar commutator, and thence to a galvanometer called G_1. Hence galvanometer G_1 measured the actual thermoelectric electromotive force between the ends of the specimen, whilst G_2 measured the difference in temperature between the ends. It was found to be absolutely necessary to have two separate galvanometers for these purposes in order to avoid errors due to the very slight fluctuations in temperatures, which were important when the temperature difference was so small. Both galvanometers were of sufficiently high resistance for their readings to be used directly ; the resistance of the specimen was usually a fraction of an ohm, so that any changes in its resistance were negligible. It should be mentioned that the copper constantan thermojunctions were not actually cemented to the ends of the specimen, but were placed as close to them

as possible. This, of course, was not entirely satisfactory, but it was necessary to avoid straining the specimen, and reference is made to the appropriate corrections below.

Experimental Procedure.

The following experimental procedure was adopted. The specimen was cooled to 0° C. by packing the tanks with ice at least one day before the electrical measurements were taken, in order always to start with the specimen in the same magnetic state. At the commencement of a set of readings the tank A was raised to a suitable temperature, say 29·1° C., whilst the tank B was simultaneously raised to 27·1° C., as recorded by the thermometers T_1 and T_2. After allowing sufficient time for the ends of the specimen to acquire stationary temperatures, the deflexions of G_1 and G_2 were recorded. It is easy to see that the appropriate value of $d\mathrm{E}/d\mathrm{T}$ for the specimen with respect to copper is given by

$$\frac{\text{Deflexion of } G_1}{\text{Deflexion of } G_2} \times \frac{\text{Voltage Sensitivity of } G_1}{\text{Voltage Sensitivity of } G_2} \times P,$$
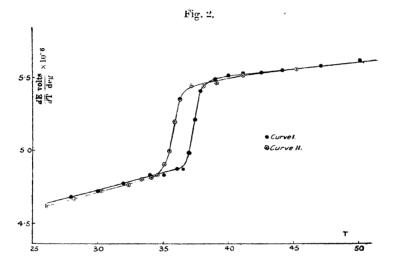
where P is the thermoelectric power of the copper-constantan couple. The ratio of the voltage sensitivities was easily found from the deflexions of G_1 and G_2 when the two were connected in parallel to the same difference of potential. The determination of P also presented no difficulty. The mean value of the absolute temperature T recorded by the thermometer inside the copper tube in tank A was noted. Hence, by taking a series of values of $d\mathrm{E}/d\mathrm{T}$ with different temperatures T a graph of $d\mathrm{E}/d\mathrm{T}$ was obtained. On completion of a series of readings extending above the ferromagnetic Curie point, the specimen was usually allowed to cool slowly to room temperature overnight. The following day it was cooled to 0° C. and at a later date the above experiment was repeated, but with tank B at a temperature higher than tank A.

Results.

We will first discuss the results obtained with a specimen called Aa. This specimen was prepared by heating the arsenide in the lower half of a vertical quartz tube 3 mm. in diameter, so that the latter could be raised or lowered through holes in the furnace. It had been hoped that in this manner a single crystal of the arsenide would have been formed. A little free arsenic was present in the upper part of the tube. After several hours of preliminary heating and shaking at
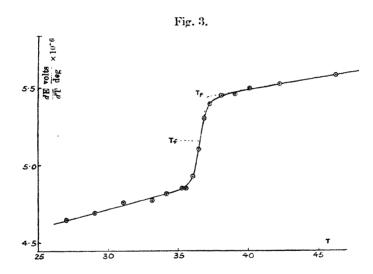
temperatures between 550 and 600° C., the tube was heated for several hours at 750° with the upper end protruding from the furnace. Eventually the temperature was raised to 860° C., the furnace current was switched off, and the tube allowed to cool *in situ.* In the lower end of the tube a very compact rod, the specimen Aa, was formed. Most of the remaining arsenide was in the form of a long porous rod.

The specimen Aa was mounted as already described, and fig. 2 gives the results of two sets of measurements, the points on Curve I. being obtained when T_1 recorded a higher temperature than T_2, and Curve II. when T_2 recorded a higher

Fig. 2.

temperature than T_1, the abscissæ being the readings recorded by the thermometer inside the tube in tank A. Thus Curves I. and II. should be displaced through exactly 2° with respect to one another. If this were the case, then the value of d^2E/dT^2 obtainable from fig. 3, which is obtained directly as the mean of the experimental points plotted in Curves I. and II. of fig. 2, would not be subject to correction, for we should then know that the copper-constantan thermojunctions actually indicated the true temperatures of the ends of the specimen. The curves are, however, only displaced by 1·5° C. This is a very extreme case, and such a large discrepancy was never obtained in similar experiments with other specimens ; in fact, it is hard to believe that it represents the true state of affairs, unless the short specimen

was very much displaced towards one tank. The maximum value of d^2E/dT^2 obtained from fig. 3 must therefore be multiplied by 4/3, the corrected value then being $+6\cdot4\times10^{-7}$ volt per deg.², whence S, the sudden change, or "step-down," in specific heat calculated on the above theory, is $-7\cdot6\times10^{-24}$ cal. per deg. per molecule, assuming that one electron per molecule is responsible for the ferromagnetism. The point of inflexion, T_f, in fig. 3 cannot be found with great accuracy, but it may be taken to be at $T=36\cdot45°$ C. We will denote by T_F the temperature at which the tangent to the steep portion of the curve and the tangent to the high temperature portion of the curve intersect; from fig. 3, $T_F=37\cdot2°$ C.

Fig. 3.
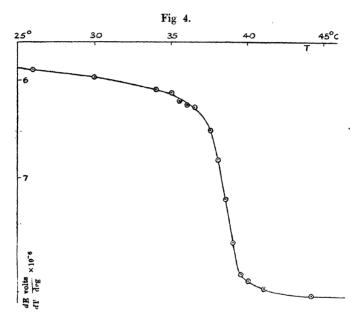
The value of $e\,.\,T\,.\,d^2E/dT^2$ when the arsenide is in the paramagnetic state is practically equal to zero, so that the sudden change in specific heat near the Curie point may be considered, with a sufficient degree of accuracy, to be the value of $e\,.\,T\,.\,d^2E/dT^2$ at the temperature T_f. All the values of d^2E/dT^2 quoted below therefore refer to this temperature.

Before the importance of the displacement of Curves I. and II. was realized, a change in the specimen was produced, so that, unfortunately, the above results could not be checked after readjustment of the specimen. After heating the specimen above its ferromagnetic Curie point it was suddenly cooled by replacing the liquids in the tanks with ice. The value of d^2E/dT^2 then obtained was $+5\cdot75\times10^{-7}$ volt per
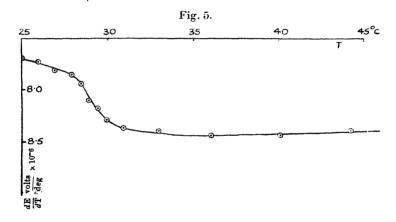
deg.^{2}, whence S was $-6\cdot8 \times 10^{-24}$ cal. per deg. per molecule, the corresponding values of T_f and T_F being $36\cdot6$ and $37\cdot3°$ C. respectively. On the whole, then, the result of rapid cooling was a slight rise in the values of dE/dT, T_f and T_F, and in S.

The specimens used in another series of experiments were made by partly filling a quartz tube 3 mm. in diameter with arsenide containing a little free arsenic. After much preliminary heating to expel this free arsenic to the upper part

Fig 4.

of the tube, it was kept at $900°$ C. for eight hours, after which the furnace current was switched off and the tube allowed to cool *in situ*. A long but very brittle and porous rod was obtained. Several portions of this rod were used in the following experiments. The first portion, called ABa 1, gave the mean curve shown in fig. 4, where the change in sign of dE/dT should be noted, from which it follows that d^2E/dT^2 was $-9\cdot1 \times 10^{-7}$ volt per deg.^{2} and S was $+10\cdot7 \times 10^{-24}$ cal. per deg. per molecule. The values of T_f and T_F were respectively $38\cdot5$ and $39\cdot7°$ C. Incidentally, no correction was found necessary for difference of temperature between the thermojunctions and the ends of the

specimen. This particular specimen showed the need for
great care in the thermal treatment. After it had been
raised to a temperature of 44·5° C. it was cooled com-
paratively quickly to 0° C., by using ice in the tanks, the
cooling process lasting about an hour and a quarter. The
result was a striking change, the new values of dE/dT
below the transition point being algebraically much decreased,
whilst above it the values remained practically the same
as those previously obtained. The value now obtained for
d^2E/dT^2 was $-4\cdot3 \times 10^{-7}$ volt per deg.^{2}, whence S was
$+5\cdot1 \times 10^{-24}$ cal. per deg. per molecule, so that by sudden
cooling, the value of the specific heat per molecule had
apparently been decreased by more than one half its initial
value. At the same time the values of T_f and T_F were

Fig. 5.
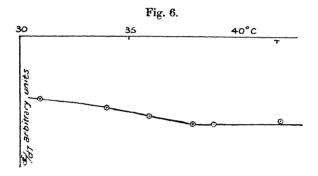
respectively decreased to 37·65 and 38·7° C. Incidentally,
fig. 5 shows a mean cooling curve, obtained by heating
the specimen above its ferromagnetic Curie point and
taking readings as it cooled, in a manner similar to that
employed in obtaining the previous graphs. The nature
of the temperature hysteresis observed with manganese
arsenide is clearly shown,

A second portion, called ABa 2, gave a value of d^2E/dT^2
equal to $+4\cdot6 \times 10^{-7}$ volt per deg.^{2}, whence S was equal
to $-5\cdot5 \times 10^{-24}$ cal. per deg. per molecule, the values of
T_f and T_F being respectively 36·9 and 37·8° C.

Again, a third specimen, called ABa 3, gave a value of
d^2E/dT^2 equal to $+6\cdot4 \times 10^{-7}$ volt per deg.^{2}, whence S was
equal to $-7\cdot6 \times 10^{-24}$ cal. per deg. per molecule, the values
of T_f and T_F being respectively 36·6 and 37·3° C.

A further series of measurements was made with specimens prepared by heating manganese arsenide containing a little free arsenic in a vertical quartz tube, which, after much preliminary heating, was slowly introduced into the furnace when the latter was at 1000° C. The tube was kept at this temperature for about ten minutes, the furnace current was then reduced and the tube allowed to cool slowly *in situ*. As a small hole was open in the lower end of the furnace, the lower end of the specimen was somewhat cooler than the upper end. When the cold tube was opened, a series of short and polished rods coated with black powder were obtained, *i. e.*, some of the manganese had apparently volatilized. It would appear desirable to repeat the preparation with a wider tube and to allow longer time for annealing.

Fig. 6.
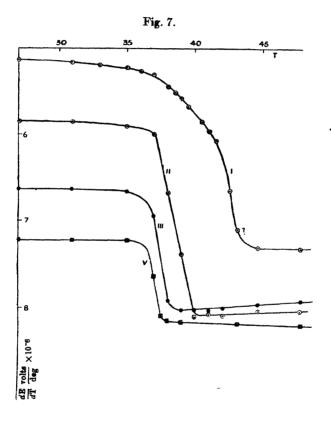
Two of the above rods were examined. The first, *Bd* 1, gave very unsatisfactory results, for it was very brittle and easily fractured at an angle with its axis, much after the fashion of single crystals. The value of d^2E/dT^2 was roughly $-1·9 \times 10^{-7}$ volt per deg.[2], whence S was equal to $+2·3 \times 10^{-24}$ cal. per deg. per molecule.

By repeatedly heating this specimen to above 45° C. and cooling it rapidly to 0° C., it was possible to obtain a curve which showed very little sign of a sudden change in thermoelectric power with temperature ; one such curve is reproduced in fig. 6. Yet the specimen remained ferromagnetic at low temperatures.

The second rod, called *Bd* 2, gave some striking results. The first curve (fig. 7, Curve I.) was obtained with the temperature of the tank A 2° higher than that of B, and was quite different in shape to any subsequently obtained with the same specimen. After the readings for this curve had been obtained the specimen was slowly cooled to 0° C. in the usual manner.

The next time the experiment was repeated, Curve II., fig. 7, was obtained.   Again, the specimen was cooled slowly to 0° and later Curve III. was obtained.   This appeared to be rather stable, for Curve IV., shown together with Curve III. in fig. 8, was obtained when tank B was 2° higher than tank A.   From the mean curve given by the values of Curves III.

Fig. 7.

and IV. the value of d^2E/dT^2 was $-11\cdot8 \times 10^{-7}$ volt per deg.[2], whence S was $+12\cdot9 \times 10^{-24}$ cal. per deg. per molecule, whilst T_f and T_F were respectively $36\cdot5$ and $37\cdot2°$ C. The specimen was then raised to 50° C. and cooled very quickly to 0° C., whereupon Curve V., fig. 7, was later obtained : this, again, was a curve which was relatively stable and reproducible   It will be noted that whilst the Curves II., III., and V. give values of d^2E/dT^2 which are practically identical, the total change in dE/dT which occurs when the substance

passes from the ferromagnetic to the paramagnetic state is much greater for Curve II. than for Curves III. and V., and, on the whole, there is a tendency for dE/dT to become more negative as the substance is repeatedly heated and cooled. At the same time the values of T_f and T_F become lower and lower.

For convenience, the values of the quantities for the several specimens are collected in the table below, in which the last column contains the appropriate values of (dE/dT), *i. e.*, the approximate value of dE/dT at the point of inflexion, corrected for any difference of temperature between the ends of the specimen.

Fig. 8.
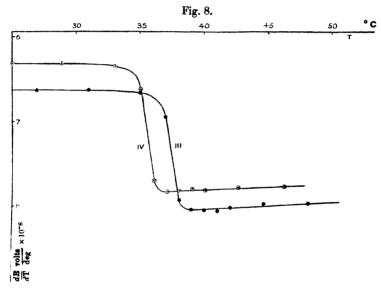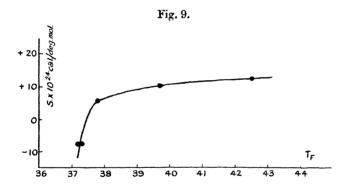
TABLE.

Specimen.	d^2E/dT^2.	S.	Tf.	TF.	$(dE/dT)_f$.
	Volts per deg.^{2} ×10^{-7}.	Cal. per deg. per mol. ×10^{-24}.	°C.	°C.	Volt per deg. ×10^{-6}.
Aa	+ 6·4	− 7·6	36·45	37·2	+6·8
Aa (later)*	+ 5·75	− 6·8	36·6	37·3	+6·7
ABa 1	− 9·1	+10·7	38·5	39·7	−7·2
ABa 1 (later) *	− 4·3	+ 5·1	37·65	38·7	−7·4
ABa 2	+ 4·6	− 5·5	36·9	37·8	+2·9
ABa 3	+ 6·4	− 7·6	36·6	37·3	+3·4
Bd 2	−11·8	+12·9	36·5	$\left\{ \begin{matrix} 42·5 \\ *(37·2) \end{matrix} \right\}$	−7·5

In this table two values for T_F are given for specimen $Bd\,2$. The first was obtained from Curve I. fig. 7, when the specimen had not been subjected to any thermal treatment since its preparation, and the second was obtained after the thermal treatment which eventually gave rise to the curves of fig. 8. In fig. 9 the values of S, or $e.\mathrm{T}.\,d^2\mathrm{E}/d\mathrm{T}^2$, for the several specimens are plotted against the corresponding values of T_F, the sets of readings marked with an asterisk being omitted, as they refer to specimens which have been cooled quickly.

Discussion of Results.

The above results are sufficient to show that the phenomena are complex, and that more experimental work with well-annealed specimens is required. In particular, at this stage

Fig. 9.

it was not possible to make experiments to try to correlate the changes in the thermoelectric properties with changes in the intrinsic or spontaneous magnetization of the substance, for which special apparatus would be necessary. Moreover, no attempt was made at this stage to examine the bearing of the thermoelectric phenomena upon the problem of the two Curie points *. We see, however, that the sign of $d^2\mathrm{E}/d\mathrm{T}^2$, just before the transition from the ferromagnetic to the paramagnetic state occurs, may be positive or negative according to the specimen investigated, and that it is possible to produce large changes in the actual value of $d^2\mathrm{E}/d\mathrm{T}^2$ by means of quite simple thermal treatment of a given specimen. Again, such thermal treatment may also produce large changes in T_F and reduce considerably the total change in

* Forrer, *Journ. de .Phys.* i. p. 49 (1930); Bates, Proc. Phys. Soc. xliii. p. 87 (1931); Bitter, Phys. Rev. xxxvii. pp. 91 and 1176 (1931).

$d\mathrm{E}/d\mathrm{T}$ which occurs on transition from the ferromagnetic to the paramagnetic state. In all cases where the value of $d^2\mathrm{E}/d\mathrm{T}^2$ under consideration is negative, the effect of rapid cooling of the specimen is to cause this total change in $d\mathrm{E}/d\mathrm{T}$ to be considerably decreased, the value of $d\mathrm{E}/d\mathrm{T}$ in the ferromagnetic state approaching more and more nearly to the value in the paramagnetic state ; the value in the latter state does not change to any great extent in the majority of cases. The effect of sudden cooling in these cases must be similar to the effects produced by quenching in the case of steels ; the substance tends to persist in the form in which it exists before cooling takes place. The existence of a temperature hysteresis shows that manganese arsenide is peculiarly liable to exhibit such changes.

On the whole, then, the effect of sudden cooling is to reduce the extent to which $d\mathrm{E}/d\mathrm{T}$ may change in a negative sense. The experimental results, and more especially those set forth in fig. 9, make it appear reasonable to suppose that a perfectly annealed specimen, not subjected to disturbing thermal treatment, would show a very considerable negative change or decrease in $d\mathrm{E}/d\mathrm{T}$ extending over a rather large temperature range as the specimen passes from the ferromagnetic to the paramagnetic state. There must obviously be an upper limit to the magnitude of $d^2\mathrm{E}/d\mathrm{T}^2$ or S, as is indicated by the shape of the curve of fig. 9 at the higher values of $\mathrm{T_F}$.

It is noteworthy that the highest recorded value of $\mathrm{T_F}$ was $42 \cdot 5°$ C., whereas the values of the ferromagnetic critical point and the ferromagnetic Curie point of the specimen actually used in the earlier specific heat measurements were $42 \cdot 2$ and $43 \cdot 2°$ C. respectively. Now, it is generally accepted that the presence of impurities causes a lowering of the ferromagnetic Curie point, and, at this stage, it is most reasonable to suppose that they produce a lowering of the temperatures $\mathrm{T_f}$ and $\mathrm{T_F}$, which, it is considered, should coincide with the ferromagnetic critical point and the ferromagnetic Curie point respectively. It will be noted that specimens of the type $\mathrm{AB}a$, which have all undergone the same initial thermal treatment, show that the higher these temperatures the higher is the value of S. Impurities are also considered to cause a decrease in the intrinsic or spontaneous magnetization of a substance, and, again, it is reasonable to assume that they produce a change in $d\mathrm{E}/d\mathrm{T}$. It will be noted, too, that, in the case of the specimens $\mathrm{AB}a$, the lower the values of $\mathrm{T_f}$ and $\mathrm{T_F}$ the greater algebraically are the values of $(d\mathrm{E}/d\mathrm{T})_f$. On the classical electron theory

this would mean that the lower T_f and T_F the greater would be the number of free electrons present.

The question now arises whether the presence of impurity can be sufficient to destroy the difference between dE/dT in the ferromagnetic and in the paramagnetic state, or even to reverse the sign of that change. There appears to be no reason to suppose that this cannot happen. It is generally accepted that the effect of impurities is to produce distortion of the metallic lattice. We should expect a limit to the effects which distortion can have on the ferromagnetic properties and, consequently, on the thermoelectric properties of the substance ; this is taken to be the explanation of the sudden fall in the values of S, in fig. 9, where the values of T_F appear to be approaching a lower limit.

Distortions may also be produced by mechanical stress or by improper heat treatment, and, undoubtedly, distortions are to be considered responsible for the changes which we have recorded as produced by sudden cooling. There must obviously be a limit to the amount of distortion which can be produced by sudden cooling, and this is probably the reason for the relative stability of such curves as Curve V., fig. 7. Again, when considerable distortion has already been produced by the presence of impurities, we should expect that this distortion would not greatly be increased by the effects of· sudden cooling. This appears to be precisely the case with specimen Aa, where the changes in T_f, T_F, and $(dE/dT)_f$ produced by cooling are very small indeed, and it is a little surprising that there is such a marked change in the value of S, but we have already expressed doubt that the change is really as large as stated. The specimen Aa was one of the earliest to be prepared, and there is no doubt that it contained considerable traces of free arsenic.

At this point reference may conveniently be made to some experiments [*] carried out with manganese arsenide, in which the change of contact difference of potential, E', between an electrode of powdered manganese arsenide and a solution of hydrochloric acid and manganese chloride was measured as a function of the temperature of the system. The manganese arsenide used was that actually employed in the specific heat determinations, and it was naturally prepared under more favourable conditions than were possible in the preparation of the rods. It was found that at a temperature of about 42° C. the value of d^2E'/dT^2 showed a maximum negative value. Hence we may conclude from these experiments

[*] Bates, Phil. Mag. vi. p. 593 (1928).

that S is positive for the purest manganese arsenide so far used, although, unfortunately, it is not possible to deduce its value.

It is therefore considered that we may safely conclude that in the absence of serious traces of impurity and with properly-annealed specimens, a large negative value of d^2E/dT^2 takes place on the passage of the substance from the ferromagnetic to the paramagnetic state. Hence the value of $e.T.d^2E/dT^2$ should be positive for manganese arsenide, corresponding to a decrease in the specific heat of the substance on passing through its ferromagnetic critical point. Thus we have a case in which the sign of S is in agreement with the specific heat change as found by direct calorimetric measurements, as required by the Dorfmann and Jaanus theory. Now, the maximum value of S was obtained with specimen Bd2, namely, $12 \cdot 9 \times 10^{-24}$ cal. per deg. per molecule. The maximum value obtained by direct experiment[*] was approximately 170×10^{-24} cal. per deg. per molecule.

It should, however, be noted that in the electrical measurements a difference of some 2° C. existed between the ends of the specimen, whereas a difference of only a small fraction of a degree could have existed between the different portions of the powdered specimen used in the specific heat measurements. It is known, too, that a large change in volume occurs as the substance passes through its ferromagnetic critical point, and the value of the specific heat was measured at constant pressure, whilst the theory assumes constant volume. Further, the electrical calculations suppose that the phenomena are reversible, which the existence of a temperature hysteresis shows to be incorrect. Moreover, we have every reason to suppose that the specimen used in the specific heat measurements was purer than the specimens obtained in the form of rods. Hence, all the circumstances tend to render the value obtained from the electrical measurements too low, so that the above discrepancy is not so unreasonable as it may appear at first sight.

In the case of nickel we have no evidence that the value of S does or does not change with sudden cooling, etc., and we must therefore confine our attention to the available data which gives a negative value for S. To explain this, Stoner[†] has suggested that the nickel atoms are associated in groups of five, and that three out of the five atoms have

---

[*] Bates, Proc. Roy. Soc. A, *loc. cit.*
[†] Stoner, Proc. Leeds Phil. Soc. ii. p. 149 (1931).

each lost one electron. Now each electron has a definite spin moment associated with it, and since the group has lost three such electrons, the remainder must possess a spin moment equivalent and opposite to that of the missing electrons   Experiments on the gyromagnetic effect of ferromagnetic substances by the author and others have definitely proved that the spin of the electron is responsible for ferromagnetism. Hence the nickel group pictured above must exhibit ferromagnetism.   On this view, the addition of a free electron to a nickel atom results in the formation of an uncharged, diamagnetic atom, with a corresponding decrease in the magnetic moment of the group, and a change in the magnetic energy associated with the group. As this energy is negative, we shall have at the ferromagnetic critical point a large decrease in the amount of heat required to neutralize the remainder of the negative energy associated with the substance, *i. e.*, a large decrease in the specific heat.

The explanation given by Stoner certainly seems adequate to explain the phenomena observed with nickel. The idea of the association of nickel atoms or ions in groups of five was first put forward to explain the existence of the different magneton numbers associated with nickel at very low temperatures and at temperatures above the ferromagnetic Curie point. As the writer has shown *, a logical extension of this conception provides an explanation of the existence of non-coincident ferromagnetic and paramagnetic Curie points, which are observed with most ferromagnetic substances. Evidence of the correctness of Stoner's explanation is also provided by the experiments of Bidwell † on the thermo-electric properties of the alkali metals with respect to platinum. The magnetic evidence shows that a solid alkali metal consists of an assemblage of diamagnetic positive ions and free electrons. On passage to the liquid state we should expect some of these ions to take up their valency electrons. Consequently, if the Stoner hypothesis may be employed here, then, just before an alkali metal passes into the liquid state, we should expect to find a large positive increase in the thermoelectric power of the metal with respect to platinum. This increase is observed with all the alkali metals. It extends over a range of temperature of some $10°$ C. just below the melting-point, even with very pure materials, and it is accompanied by an increase of resistance and a fading-out of the X-ray diffraction patterns. It

---

* Bates, Proc. Phys. Soc. xliii. p. 87 (1931).
† Bidwell, Phys. Rev. xxiii. p. 357 (1924).

is interesting that the values of $e.T.d^2E/dT^2$ observed in these experiments on the alkali metals are of the same order of magnitude as those obtained with manganese arsenide and nickel in the transition region. We know, further, that nickel also exhibits a continuous increase of resistance as it approaches its ferromagnetic critical point, a phenomenon which has been the subject of several recent investigations [*]. Unfortunately, data for the resistance of manganese arsenide have not yet been obtained.

The writer has previously used the conception of atoms associated in groups in presenting an explanation of the variation of the magnetic susceptibility of manganese arsenide above the ferromagnetic Curie point. It now remains to show that the conception does not fail when applied to the thermoelectric behaviour of this substance. We have to explain the occurrence of positive and negative values of S, positive values requiring the ferromagnetic groups to lose electrons, and negative values requiring the groups to gain them, on passing into the paramagnetic state. We are aided in our explanation by the knowledge that manganese is unique, in that it only exhibits ferromagnetic properties when in combination with another substance. In support of this statement we may point out that various workers have suggested that the ferromagnetism of metallic manganese is due to the presence of hydrogen or of nitrogen. In our case, whilst hydrogen and nitrogen contamination cannot be entirely ruled out of account, it appears most unlikely that the ferromagnetism is due to anything but combination with arsenic. Again, manganese is peculiar in that it forms very complicated structures, and it has been suggested [†] that the atom may exist in four different states, in which the interatomic distances are markedly different. There is therefore nothing against the assumption that two or more kinds of groups may be formed in the case of manganese arsenide, one of which may gain electrons whilst the others may lose electrons on passing from the ferromagnetic to the paramagnetic state. We should naturally expect their formation to be markedly influenced by the presence of impurities. What is surprising in these experiments is the sharpness with which the thermoelectric changes occur and the comparatively small range of temperature in which the transition may occur. It would appear to indicate that only one type of group is responsible for the ferro-

* *Vide* 'Science Progress,' xxvi. p. 11 (1931).
† Hume-Rothery, 'The Metallic State,' p. 321 (1931).

magnetism, whilst two or more kinds of groups may exist in the paramagnetic state.

So much success has attended the conception of the group, in the case of nickel consisting of five atoms or ions, that the size of this group has more or less governed the writer's conception of the size of the group in other materials. Recently, however, evidence has been put forward by Bitter * in support of what is termed the block theory of ferromagnetism. According to this theory the ferromagnetic substance is built up of blocks, each consisting of some 10^5 or 10^6 atoms. Although the theory has much to commend it, unfortunately, it is not possible, in the opinion of the writer, to test it by means of thermoelectric experiments so narrowly confined to the region of the ferromagnetic Curie point, and it is hoped that experiments over a greater range of temperature above this point will give us further information of value in the solution of the problem.

Summary.

A series of experiments have been made on the thermoelectric properties of short rods of manganese arsenide. The results show that there is a marked change in the thermoelectric power when the substance passes from the ferromagnetic to the paramagnetic state, some specimens exhibiting positive and others negative Thomson coefficients. It is shown that a rod of the pure substance exhibits a negative Thomson coefficient at the ferromagnetic critical point, and thus, on the basis of the free electron theory of ferromagnetism put forward by Dorfmann and Jaanus, a decrease in the specific heat is predicted at this point; this is in agreement with the results of direct calorimetric measurements. The experimental results are discussed in the light of recent contributions to the theory of ferromagnetism.

* Bitter, Phys. Rev. *loc. cit.*

XXXIV. *A Simple Harmonic Continuous Calculating Machine.* By J. MONTEATH ROBERTSON, *M.A., Ph.D.*[*]

[Plate XII.]

THE apparatus (see Pl. XII.) consists of three plungers of equal diameter, A, B, and R, operating in cylinders C, D, and E, which are completely filled with oil and interconnected at the bottom with a pipe. Thus the sum of any displacements given by the plungers A and B is continuously indicated by the motion of the recording plunger R. Any rotation given to the shaft FG imparts a simple harmonic motion to the plungers by means of cranks and slides, and the amplitude of the motion can be varied by adjusting the positions of the crank-pins on the scales H and I. The shaft FG which connects the two components carries two large gear wheels at J and K, each provided with a scale and clamp to lock them in any position. The gear wheel J is fixed to the shaft, but the wheel K is free to turn on the shaft and carries a differential gear situated between the two components. Thus if the clamp at K is locked as in the illustration, and a certain rotation α is given to the wheel J, then an equal but opposite rotation $-\alpha$ is transmitted to the component B through the operation of the differential gear ; but if the clamp at K is unlocked, and a certain rotation $-\dfrac{\beta}{2}$ is given to the gear wheel at K at the same time as the rotation α is given to the gear wheel at J, then the rotation transmitted to the second component B is $-(\alpha+\beta)$. Thus the phase difference between the two components can be continuously varied.

The scale on the wheel J is graduated in degrees. This variable will be denoted by x. The scale on the wheel K, denoted by y, is, however, graduated to read one degree for every half degree around its circumference, i.e., this scale reads from zero up to 360° twice in the course of a revolution, and, further, it is graduated in the opposite sense to the graduations on the wheel J. These scales read zero when the cranks are turned vertically downwards[†]. The amplitudes which can be set on the scales provided on the crank arms of the two components will be denoted by A_1

---

[*] Communicated by Sir W. H. Bragg, O.M., K.B.E., M.A., F.R.S.

[†] If these scales are made to read zero when the cranks are in a horizontal position, an adjustment easily effected, the machine then deals with sines instead of cosines.

and A_2 respectively. If the volume of oil in the apparatus is kept constant (it is assumed to be incompressible) the following equation is always satisfied :

$$A_1 \cos x + A_2 \cos (x+y) = S,$$

where S, the sum of the displacements given by the two components, is indicated by the reading on the scale S. The periodic surface given by this equation may be represented by a series of contour lines which can be drawn very readily with the aid of the machine ; for let the plunger R be moved to a certain desired contour level on the scale S, equal to S_K, and clamped in that position. One degree of freedom now remains between the two components A and B. For every position given to the x-scale the y-scale must take up another position which satisfies the equation

$$A_1 \cos x + A_2 \cos (x+y) = S_K.$$

In this way, with a simple mechanical extension which is not shown in Pl. XII., the contour lines can be drawn out automatically. It should be noted, however, that during these operations whenever any crank comes to a vertical or nearly vertical position it must be assisted past the turning-point, otherwise the machine will jam. Thus the process is really only semi-automatic.

The machine can also be used to explore the whole surface systematically. The y-scale may be locked, the x-scale moved round, and readings on S taken at definite intervals of x, or readings on x taken at definite intervals of S. The y-scale may then be moved to a new position, and the operations repeated. The points through which the contour lines pass may be plotted on a chart directly from the readings. These points can, of course, be taken as close together as we please, depending on the accuracy desired. Fig. 1 was prepared in this way with the machine. It is part of the periodic surface given by

$$42 \cos x + 32 \cdot 5 \cos (x+y) = S,$$

where S is the coordinate perpendicular to the paper. The contour lines are drawn at intervals of 20, negative lines being dotted. An accuracy of about 1 per cent. can easily be obtained.
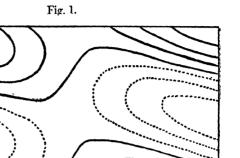
It is of some interest to consider the operations of which the machine would be capable if extended to a number of components instead of only two as used in the present model. Imagine first a two-dimensional array or net of components, as in fig. 2. Each circle is supposed to represent a component
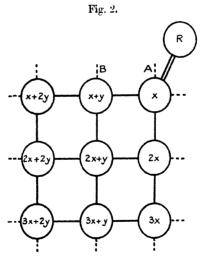
like A or B, or any similar reversible contrivance for pro-
ducing and adding simple harmonic motions, and between
each component in the rows is placed a differential gear.

Fig. 1.

Fig. 2.

The shafts connecting up each row are geared together to
turn in the ratios 1 : 2 : 3 etc., but all the differentials are
connected to turn together at the same speed, and alter-
nately in positive and negative directions. These movements
can be achieved very simply by means of idle intermediate

wheels and shafts. If x is the rotation imparted to the first component A and $\pm y/2$ the rotation given to all the differential gears simultaneously, then the rotation transmitted to each component in the net is that shown in fig. 3 *. For begin with a rotation x on the first row at A ; the differential gear between A and B adds a rotation y to this, and the rotation transmitted to B and beyond is $x+y$. The next differential adds another rotation y, so that the rotation transmitted to the third component in the first row is $x+2y$, and so on. The second and succeeding rows are exactly the same, only they begin with rotations $2x$, $3x$, etc.

It is clear, then, that a net of components of this kind will continuously indicate the sum of the double Fourier series

$$\Sigma\Sigma A_{pq}\cos{(px+qy)}$$

throughout the range $x=0$, $y=0$, to $x=360°$, $y=360°$, the number of terms dealt with being equal to the number of components. In the same way, if we built up a three-dimensional array or lattice of components, succeeding layers or nets of the lattice being connected by a second independent set of differential gears, whose motions may be denoted by z, then the machine would continuously indicate the sum of the triple Fourier series

$$\Sigma\Sigma\Sigma A_{pqr}\cos{(px+qy+rz)}.$$

We might extend this to any number of independent variables, the value of each new independent variable being fed in by a new set of connected differential gears.

The form of the machine outlined above is, of course, only diagrammatic, and need not be adhered to in the actual construction of a model. For example, the adjustment of the amplitude on a component in the centre of the lattice would be inconvenient in practice.

The machine might also be used to obtain the solutions of certain sets of simultaneous equations. In fig. 3 let R_1, R_2, and R_3 be three recording plungers connected to the three columns of components. Each column now represents a separate tank, connexions with the other columns being cut off, *e. g.*, by turning a stop-cock. All gear wheels are removed or put out of action, and the components forming each row are connected together simply by shafts, so that each component in any one row takes the same rotation and the rotations of the different rows are independent. Let

---
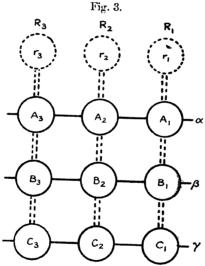
* The symbols indicate the magnitude of the rotation, the sign being neglected, as it makes no difference to the cosine displacement.

these independent rotations be α, β, and γ, and let the amplitudes be set to A_1, A_2, B_1, etc., as shown in fig. 3. Now give a displacement r_1 by the recording plunger R_1. This displacement must distribute itself in the first column according to the equation

$$A_1 \cos\alpha + B_1 \cos\beta + C_1 \cos\gamma = r_1,$$

the total volume in this tank remaining constant. The values of α, β, and γ may be anything that satisfy the equation, there being two degrees of freedom. Next give a displacement r_2 to the second column or tank by the plunger R_2. The equation satisfied is

$$A_2 \cos\alpha + B_2 \cos\beta + C_2 \cos\gamma = r_2,$$

Fig. 3.

one degree of freedom remaining. When we finally give a displacement r_3 to the third column the equation satisfied by it is

$$A_3 \cos\alpha + B_3 \cos\beta + C_3 \cos\gamma = r_3,$$

and in the general case no degrees of freedom remain, the three equations being satisfied simultaneously. Writing x for $\cos\alpha$, y for $\cos\beta$, and z for $\cos\gamma$, we have solved the three linear equations

$$A_1 x + B_1 y + C_1 z = r_1,$$
$$A_2 x + B_2 y + C_2 z = r_2,$$
$$A_3 x + B_3 y + C_3 z = r_3,$$

the values of x, y, and z being simply the cosines of the angles to which the shafts have turned in their final positions.

The number of equations and unknowns again depends simply on the number of components used. If instead of connecting up the components in each row by shafts we connect them by gears, to give the ratios $a_1 : a_2 : a_3$, $b_1 : b_2 : b_3$, and $c_1 : c_2 : c_3$, the apparatus will then deal with equations of the type

$$A_1 \cos a_1 \alpha + B_1 \cos b_1 \beta + C_1 \cos c_1 \gamma + \ldots = r_1,$$

$$A_2 \cos a_2 \alpha + B_2 \cos b_2 \beta + C_2 \cos c_2 \gamma + \ldots = r_2,$$

$$A_3 \cos a_3 \alpha + B_3 \cos b_3 \beta + C_3 \cos c_3 \gamma + \ldots = r_3,$$

$$\ldots \text{etc},$$

or, if differential gears are employed as well in connecting up the components in each row, then another degree of freedom can be attached to each component, and the terms in the equations become of the type $A \cos (a\alpha + b\beta)$, where α and β are unknowns. It seems unlikely, however, that transcendental equations could be dealt with in general except for small values of the unknowns, unless additional mechanisms were employed to assist the cranks past their vertical turning-points.

It has been pointed out that the above descriptions are intended to be diagrammatic, and various types of mechanism might be used in the actual construction of such a machine with many components. Thus any reversible method for continuously indicating the sum of a number of separate independent motions might be employed instead of the hydraulic method used in the model (Pl. XII.) ; for example, the addition of displacements given to a string passing over pulleys, as in the Kelvin tide predictor. Another very compact method, which does not appear to have been used before, would be to convert all translations into rotations, and combine them by means of a further set of differential gears, similar to those used for feeding in the values of the independent variables in the present model.

Summary.

A mechanical method is described for summing single, double, and triple Fourier series, and solving sets of linear and certain transcendental simultaneous equations. In principle it amounts to a generalization of Kelvin's tide predicting machine and his equation solving machine, with an extension to several dimensions. A simple model consisting of two components has been made, and is used to illustrate the method of working.

XXXV. *An X-ray Examination of Iron-Chromium Alloys. By* G. D. PRESTON, *B.A., the National Physical Laboratory* *.

[Plate XIII.]

PREVIOUS investigation †, by X-ray methods, of the Iron Chromium system has shown that it consists of a continuous series of solid solutions, the parameter of the body-centred cubic unit increasing from 2·861 Å. for iron to 2·878 Å. for chromium. The present paper contains an account of an investigation which has been confined to the accurate determination of the parameter changes which take place in the series of solid solutions. The opportunity of making these observations has arisen from the preparation in the Metallurgy Department of a series of alloys of iron and chromium ‡ of high purity.

Material.

The material for X-ray examination was prepared from ingots which had been annealed *in vacuo* to remove " coring " for 12 hours at a temperature of 1300° C. to 1350° C. The large-grain size of the annealed ingots of chromium content exceeding 20 atomic per cent. necessitated the preparation of a powder for the X-ray work. Filings were accordingly made, and these were sealed off in exhausted silica tubes and then annealed for a few minutes at about 1000° C. to remove the effect of cold work. In the composition range extending from 0 to 12 atomic per cent. chromium the alloys, during

cooling, undergo the γ to α transformation at some temperature exceeding 850° C. Since the filings annealed at 1000° C. were rather rapidly cooled, a second series was annealed *in vacuo* for 24 hours at 600° C. These alloys are marked (a) in Table I. giving the values of the parameters. It will be seen that in every case the parameter is the same,

TABLE I.

Alloy No.	a.	$\check{a}$.	$a-\check{a}$.	Alloy No.	a.	$\check{a}$.	$a-\check{a}$.
	Å.	Å.	Å.		Å.	Å.	Å.
Pure Iron	2·860₀	2·8600	0·0000	42 A0	2·868₂	2·8678	0·0005
„ (a)	2·860₁			43 A2	2·868₅	2·8680	0·0005
2 A1	2·861₃	2·8604	0·0009	44 A2	2·868₅	2·8682	0·0003
4 A1	2·862₃	2·8608	0·0016	46 A8	2·869₈	2·8687	0·0011
„ (a)	2·862₅			48 A8	2·869₃	2·8691	0·0002
6 A5	2·863₇	2·8612	0·0025	50 A5	2·869₄	2·8694	0·0000
8 A4	2·864₃	2·8616	0·0027	53 A0	2·869₅	2·8699	−0·0004
„ (a)	2·864₃			59 A2	2·871₀	2·8710	0·0000
11 A9	2·865₁	2·8622	0·0028	65 A7	2·871₈	2·8722	−0·0004
„ (a)	2·864₉			69 A4	2·872₁	2·8729	−0·0008
14 A8	2·865₇	2·8628	0·0028	76 A2	2·873₁	2·8742	−0·0011
„ (a)	2·865₄			79 A2	2·874₀	2·8747	−0·0007
16 A7	2·865₈	2·8631	0·0027	„	2·874₉		
19 A2	2·866₂	2·8636	0·0026	85 A4	2·875₂	2·8759	−0·0007
„ (a)	2·866₃			89 A0	2·875₆	2·8766	−0·0010
23 A2	2·866₈	2·8643	0·0025	93 A1	2·876₂	2·8773	−0·0011
25 A0	2·867₄	2·8647	0·0027	95 A7	2·877₀	2·8778	−0·0008
30 A2	2·866₆	2·8656	0·0010	98 A9	2·878₁	2·8784	−0·0003
„	2·866₇			Pure Chromium	2·878₆	2·8786	0·0000
35 A9	2·867₉	2·8667	0·0012				

(a) These specimens have been annealed for 24 hours at 600° C., the remainder a few minutes at 1000° C.

within the limits of error of experiment, as that found for the alloy annealed at the higher temperature. The necessity for using filings is unfortunate because it introduces the possibility of contamination of the specimen by carbon from the file. When the material under examination is non-magnetic the particles broken from the file during the preparation of the powder can be separated by a magnet.

In the present case this was not possible, as the alloys up to about 70 atomic per cent. chromium are all ferromagnetic at room temperatures. The file used in the preparation of the specimens was an old one which had been frequently used for a similar purpose, and judging by the behaviour of the alloys of high chromium content when the filings, spread on a sheet of paper, were exposed to the field of a magnet the contamination is believed to be very small. Some support is given to this view by the good agreement between the values of the parameters of those alloys which have been subjected to different heat treatments. If serious contamination of the metal were taking place during filing it is improbable that two specimens prepared at different times would be contaminated to the same extent and a difference in the observed parameters would be noticed.

Method of Experiment.

The method of experiment has been described in another connexion *, and will here be referred to only with a view to estimating the accuracy of the results. The camera consists of a circular cylinder of diameter about 10 cm. which carries the specimen and slit at opposite ends of a diameter. The photographic film, of length about one half the circumference of the camera, is wrapped round the cylinder and held against it by elastic bands, the X-ray beam being admitted to the camera through a hole punched in the middle of the film. The object of this arrangement is to record reflexions at high angles, and to satisfy the well-known "focussing principle" which requires the slit, specimen, and photographic film to lie on the circumference of a circle. If s is the distance between corresponding lines on the film and r is the radius of the camera, the angle of reflexion θ is given by

$$\frac{s}{8r} = \frac{\pi}{2} - \theta.$$

In the present case we are concerned with a body-centred cubic lattice of side a Å., and the spacing d of the plane hkl is given by

$$d = \frac{a}{\sqrt{h^2 + k^2 + l^2}}.$$

Radiation from a chromium target has been used throughout the investigation, and the film records reflexions of the

---

* Gayler and Preston, Journ. Inst. of Metals, xli. p. 191 (1929).

Kα doublet from the planes (211) at an angle, θ, which lies near to 78° for iron. Substituting the values of d and θ from the above expressions in the relation

$$\lambda = 2d \sin \theta,$$

where λ is the wave-length, we obtain

$$\frac{\delta a}{a} = \tan \frac{s}{8r} \, \delta \left(\frac{s}{8r} \right),$$

or if $\frac{s}{8r}$ is small,

$$\frac{\delta a}{a} = \left(\frac{s}{8r} \right) \frac{\delta s}{s} .$$
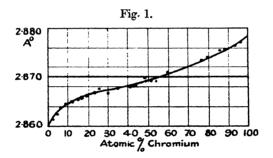
In the present case s is in the neighbourhood of 90 mm., and $8r$ approximately 400 mm., so that tan $s/8r$ may be put equal to $s/8r$ for our purpose. Using these values of s and $8r$ the expression for δa is

$$\delta a = \frac{9}{16,000} a \delta s = 1 \cdot 6 \times 10^{-3} \, \delta s,$$

when a is about 2·86 Å. Thus every tenth millimetre error in the determination of s introduces an error 0·00016 Å. in the value of a.

The measurement of the films was carried out by means of a travelling stage microscope, the distance between the lines and the total length of the exposed part of the film being recorded in each case. The total length of the exposed part of the film varied from 155·4 to 155·9 mm., and the values of s have been corrected for a mean length of 155·66 mm. on the assumption that the shrinkage of the film is uniform throughout its length. The distance between the lines on the film was measured twice on each film, and in no case did these two values differ by more than 0·2 mm., so that if the mean difference were computed from these measurements it would be less than ±0·1 mm. An accuracy of this degree is not claimed, but it is believed that the position of the lines can be determined to ±0·3 mm., and that the relative values of the parameters are therefore susceptible to an error not exceeding 0·0005 Å. A further source of error against which precautions have been taken is the position of the specimen in the camera. The filings are attached by an adhesive to a small sheet of thin celluloid, and this is held against the circumference of the camera by a pair of springs. In the preparation of these specimens attention has been directed to keeping the layer of filings as thin as possible, consistently with obtaining photographs with a reasonable

exposure. It was found that the thickness of the layer
could be conveniently diminished until it was not quite
opaque and that good photographs could be obtained with
exposures of from one to one and a half hours, the tube
being operated at 30 k.v. and about 10 m.a. The thickness
of the layer of filings is thus of the same order of mag-
nitude as the individual grains of metal and is so small that
errors arising from the penetration of the X-ray beam into
the material have been regarded as negligible. Parameter
changes due to the natural variation of room temperature
during the exposures and from day to day have also been
treated as negligible. The coefficient of expansion of iron
is of the order of 10^{-5} per degree Centigrade, so that a
parameter change of 0.00016 Å., corresponding to a displace-
ment of 0.1 mm. of the line on the film, would be produced

Fig. 1.
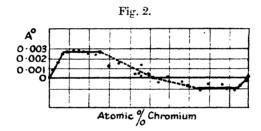
by a temperature change of $5°$ C. The measurements may
be taken as referring to a temperature of $17°$ C.

Results.

The results of the computation of the parameter from the
measurements made on the films are given in Table I.
The first column contains a symbol which serves to
identify the alloy and to give its composition, thus the
alloy 6A5 contains 6.5 atomic per cent. chromium. As
mentioned above, the filings of those alloys marked (*a*) have
been annealed for 24 hours at $600°$ C., the remainder for a
few minutes at about $1000°$ C. The values of the parameter
are plotted against composition in fig. 1, and a smooth curve
has been drawn to fall as near the points as possible. Each
observed point has been surrounded by a circle whose
diameter on the scale of the figure represents 0 0004 Å., and
it will be seen that, with the exception of three points (alloys
25 A0, 30 A2, and 46 A8), all the circles are touched or

intersected by the curve, *i. e.*, the observed points fall within
±0·0002 Å. of the curve—a deviation of half the expected
experimental error. Of the three exceptions, the first
deviates from the line by just the expected error, and the
other two by about one and a half times this amount. The
photograph of the alloy 30 A2 was the worst of the whole
series, the lines being distinctly broader than in the others,
as may be seen from Pl. XIII., where a few typical
films are reproduced. The discrepancy in this case is no
doubt due to the difficulty of measuring the films with the
necessary degree of accuracy. With regard to the alloy
46 A8, the point for which departs from the curve by
0·0008 Å., it has been assumed that some other error has
vitiated the result. It is possible that it is due to segrega-
tion in the ingot, and that the region from which the filings
were taken was deficient in chromium.

Fig. 2.

Atomic % Chromium

Although the experimental points fall close to the curve
in fig. 1, an alternative interpretation of the results will now
be briefly considered. Denoting by a the ordinate to the
straight line joining the points for iron and chromium its
equation is

$$\bar{a} = 2\cdot8600 + 0\cdot000186\ x,$$

where x is the atomic percentage of chromium. The differ-
ence between the observed parameters a and the value of
$\bar{a}$ for each alloy has been plotted in fig. 2, the values of a and
$a-\bar{a}$ being given in the table. In fig. 2 the points could be
joined by a continuous curve just as in fig. 1, and this curve
would not depart from any point by more than the correspond-
ing curve in fig. 1. The way in which the points lie in fig. 2
suggests, however, that the parameter does not vary contin-
uously with composition. In the range from 0 to 25 atomic
per cent. chromium the value of $a-\bar{a}$ increases very rapidly
up to about 6·5 atomic per cent. chromium, and then remains
constant. A pair of straight lines can be drawn so as to lie

within ± 0.0001 Å. of the observed points. In the remainder of the diagram the evidence for discontinuity is not so marked. In assessing the error of the parameter determination at ± 0.0005 Å. it was assumed that the position of the diffraction lines on the film could be measured to ± 0.3 mm., although from repetitions of the measurements it appeared that the error might be as small as ± 0.1 mm., and in those cases where duplicate photographs have been taken the parameters do, in fact, agree to within ± 0.0001 Å. While this high degree of accuracy is not claimed in the present investigation, it appears justifiable to draw attention to the fact that there may be discontinuities in the variation of parameter with composition.

Acknowledgments.

The material used in this investigation has been prepared by Mr. Frank Adcock, and I have pleasure in acknowledging my indebtedness to him and also to Mr. Harvey.

30th June, 1931.

XXXVI. *Standard Electrode Potentials in Ethyl Alcohol.* *By* Angus Macfarlane, *B.A., and* Sir Harold Hartley, *F.R.S.**

THERE have been numerous isolated measurements of the electromotive forces of cells containing non-aqueous solutions, but few systematic attempts to determine the standard electrode potentials of the elements in solvents other than water. In ethyl alcohol the only extensive investigation recorded is that of Neustadt and Abegg [1], which permits the calculation of the electrode potentials of the three halogens, of silver, and of five divalent metals. Such are the uncertainties involved in their experimental procedure, however, that no great reliance can be placed on their results. The errors inherent in this and other earlier work have been reviewed by Buckley and Hartley [2], who have established the electrode potentials of nine elements in methyl alcohol. This paper describes the extension of their methods to the investigation of solutions in ethyl alcohol.

The electromotive force, E, of a cell, consisting of two electrodes each reversible to one of the ions of the electro-

lytic solution with which they are in equilibrium, is given by the expression

$$E = E_0 - \frac{2RT}{F} \ln f.c, \quad . \quad . \quad . \quad . \quad (1)$$

where c is the concentration of the electrolyte and f the activity coefficient, expressing its deviation from ideal behaviour. E will become equal to E_0 when the product fc is equal to unity ; the point at which this condition is fulfilled is termed the standard state.

If one of the ions of the electrolyte is the hydrion and one electrode a surface in equilibrium with hydrogen gas under 760 mm. pressure, the value of E_0 is defined as the standard electrode potential of the anion. The standard electrode potentials of the metals can then be found from the electromotive forces of the corresponding cells containing a metallic cation and the same anion. But in order to evaluate E_0 measurements must be made in very dilute solution, so that extrapolation to zero concentration, where the activity coefficient is unity, may be justified. Such a self-contained determination is not always possible, even in aqueous solution.

In methyl and ethyl alcohols measurements of activity coefficients have been confined to solutions of hydrogen chloride. Wolfenden, Wright, Ross-Kane, and Buckley[3] attempted the investigation of sodium chloride solutions in methyl alcohol, but found the behaviour of the sodium amalgam electrode to be anomalous. In consequence it has been assumed in this paper that the activity coefficients of all the strong uni-univalent electrolytes employed are equal to those of hydrogen chloride at the same concentration, which have been interpolated from the results of Woolcock and Hartley[4]. As explained by them, it is convenient to express the concentration of non-aqueous solutions in grammolecules per thousand grams of solution, denoted by the symbol m. In consequence, equation (1) must be rewritten in the form

$$E = E_{0_m} - \frac{2RT}{F} \ln m.\gamma, \quad . \quad . \quad . \quad . \quad (2)$$

where γ is the molal activity coefficient. The influence of this convention on the standard state and on the value of E_{0_m} will be discussed later.

REFERENCE ELECTRODES.

The hydrogen electrode is accepted as the ultimate reference standard, the electrode potential of hydrogen being

defined as zero in each solvent. As a practical standard, however, this electrode is inconvenient, and it has been generally replaced by the mercury-calomel or silver-silver chloride systems. It has recently been shown by Randall and Young[5] and by Güntelberg[6] that both these electrodes are liable to oxidation, particularly in acid solution ; they maintain steady potentials only if the chloride solutions with which they are in contact have been carefully freed from air. That the potential difference between these electrodes is independent of the nature of the chloride solution has been demonstrated by measurements in tenth molal solution of lithium chloride in ethyl alcohol. It was found to be 0·0457 volts, in agreement with Gerke's value in water, 0·0455 volts. A slow rise in the e.m.f. occurred, which was reproduced in hydrogen chloride solution, where, moreover, the initial potential difference was greater. Disturbance due to oxidation might be expected to be more pronounced at the calomel electrode, and indeed silver-silver chloride electrodes were found to exert potentials steady to a tenth of a millivolt in acid and in neutral solutions, which had not been specially purified from oxygen.

Several forms of precipitated silver and silver chloride were tested, but the greater convenience of the electrolytic type described by Nonhebel and Hartley[8], and the fact that these were the electrodes whose potential against hydrogen has been established by Woolcock, led to their adoption as practical reference standards. For each run electrodes, which had been silvered some time previously and in the meanwhile had been carefully washed free from traces of cyanide, were freshly chloridized. It was rare to find a potential difference of more than a hundredth of a millivolt between electrodes prepared at the same time. and their reproducibility was proved by duplicate experiments.

LIQUID JUNCTION POTENTIALS.

Most of the cells investigated contained at least one liquid junction ; it was therefore important to estimate their magnitude accurately. All the junctions were formed between two equally concentrated solutions of uni-univalent electrolytes, possessing one common ion. Lewis and Sargent[9] showed that this type of junction is reproducible and that its magnitude is accurately represented by the formula

$$E = \frac{RT}{F} \ln \frac{\Lambda_1}{\Lambda_2}, \quad \ldots \ldots (3)$$

where Λ_1 and Λ_2 are the equivalent conductivities of the two

electrolytes at that concentration. This equation can only be expected to hold as long as the activities of the two solutes are the same. It was found that the liquid junction potential between tenth molal solutions of lithium and hydrogen chlorides is less than that calculated from the formula. Since it appears from the work of Woolcock and Hartley that hydrogen chloride is appreciably associated in such strong solutions, this result is not surprising.

Two separate measurements of the cell,

$$\text{Ag}.\text{AgCl} \quad \begin{array}{c} \text{HCl} \\ 0.01 \text{ m}. \end{array} \Bigg| \begin{array}{c} \text{LiCl} \\ 0.01 \text{ m}. \end{array} \quad \text{AgCl}.\text{Ag},$$

gave e.m.f.'s of 14·8 mv. and 15·3 mv.; the junction potential calculated from equation (3) is 15·0 mv. At this dilution, then, the activity coefficients are more nearly equal, and the junction potentials may be safely calculated from the Lewis-Sargent formula. Interposition of a bridge of saturated potassium iodide solution only reduced the e.m.f. to 4 mv.

During the progress of this work the researches of Guggenheim [10] on the more complicated junctions,

$$\begin{array}{c} \text{HCl} \\ c_1 \end{array} \Bigg| \begin{array}{c} \text{KCl}, \\ c_2 \end{array}$$

in water, were published, in which the importance of the junctions possessing cylindrical symmetry is stressed. In our later measurements this condition was attained by forming the junctions within the vertical side-tubes of the half-cells, and not at the tip.

The conductivity measurements required were made in a small Washburn cell. The results are assembled in Table I. The volume concentrations used in the calculation of Λ_c have been obtained by multiplying the molality by the density of the pure solvent.

EXPERIMENTAL PROCEDURE.

The potentiometer, thermostats, and equipotential shield were the same as those used by Nonhebel and Hartley [8], and the form of the durosil glass cells has already been described by them. Modifications of this apparatus are referred to in the descriptions of the particular experiments for which they were made. Ethyl alcohol was prepared by the method described by McKelvy [11]. The salts were pure specimens prepared for conductivity work. The measurements were carried out at a temperature of $25° \pm 0.01°$ C.

The cadmium cell used as a working standard of e.m.f. was frequently compared with one calibrated by the N.P.L.

The European convention of the sign of electrode potentials, which is the opposite of that advocated by G. N. Lewis, has been used throughout ; in the diagrammatic representation of the cells the pole on the left is that bearing the negative charge.

TABLE 1.

Electrolyte.	Molality.	Equivalent conductivity at 25° C.
HCl	0·01	49·2
HClO₄	0·01	58·2
LiCl	0·01	27·6
„	0·005	29·4
„	0·003	31·0
LiBr	0·01	28·6
LiI	0·01	36·2
LiCNS	0·01	37·0
LiClO₄	0·01	38·9
„	0·005	38·3
„	0·003	42·3
NaClO₄	0·01	27·4
AgClO₄	0·01	37·0
„	0 005	38·4
TlClO₄	0·003	42·9
LiOEt	0·01	22·6

EXPERIMENTAL RESULTS.

Hydrogen.

The electromotive force of the cell,

$$\text{H}_2 \quad 0\text{·}01 \text{ m. HCl} \quad \text{AgCl.Ag},$$

was determined in order to check the technique against the previous measurements of Woolcock and Hartley. The e.m.f. was found to be 0·1930 volts, in reasonable agreement with the value interpolated from the smoothed curve, 0·1940 volts. The e.m.f., E_{0m}, of the cell,

$$\text{Ag.AgCl} \quad \text{HCl} \quad \text{H}_2,$$
$$a = 1$$

is 0·0759 volts, the hydrogen being here the more positive electrode.

Lithium.

The potential of lithium metal against a 0·035 per cent. lithium amalgam has been measured by Lewis and Keyes [12] in conjunction with their determination of the standard electrode potential in water. Experiments with the cell,

> Lithium amalgam   LiCl in EtOH   AgCl.Ag,
> 0·035 per cent.   0·01 m.

were therefore sufficient to establish the electrode potential in ethyl alcohol. Since the amalgam reacts readily with alcohol provision was made for the rapid renewal of the amalgam surface and of the solution in contact with it. An overflowing electrode was used in the type of cell described by Philpot [13]. The amalgam was prepared by electrolysis and was purified and analyzed by the method of Richards and Conant [14]. In all measurements with amalgam electrodes the solutions were freed from dissolved air by bubbling pure nitrogen, previously saturated with alcohol vapour, through them for some days.

From the first experiment a provisional value of 2·28 volts, accurate to about a centivolt, was obtained for the e.m.f. of the cell. A prolonged series of measurements was impossible, because solution crept up the inside of the dropper and, by liberation of hydrogen, broke up the falling column of amalgam. A new form of electrode, which obviated this difficulty and had the additional merit of maintaining more constant dropping rates, was therefore devised. Using this, much more satisfactory results were obtained; the extreme variation of potential was less than a millivolt, and renewal of the solution was without appreciable effect. The value of the e.m.f. was 2·287 volts, which is within the limits of uncertainty of the previous measurement. As the possible sources of error would tend to lower the e.m.f., it was to be expected that the more accurate measurement should give the higher reading.

Assuming the activity coefficient of lithium chloride in hundredth molal solution to be 0·518, that of hydrogen chloride at the same molality, the e.m.f. of the cell at unit activity, E_{C_m}, can be calculated from the equation

$$E_{0_m} = E + \frac{2RT}{\mathbf{F}} \ln a \quad . \quad . \quad . \quad . \quad (4)$$

$$= 2·287 - 0·271 \text{ volts.}$$

On adding 0·950 volts, the Lewis and Keyes value for the difference in potential between amalgam and metal, and

0·076 volts to refer it to the standard hydrogen electrode, it is found that the standard electrode potential of lithium is −3·042 volts in ethyl alcohol.

Sodium.

The solubility of sodium chloride in ethyl alcohol is not sufficient to permit the measurement of the cell analogous to that used for lithium. The electrode potential of sodium was therefore measured with the combination

Sodium Amalgam $NaClO_4$ | $LiClO_4$ | $LiCl$ $AgCl.Ag$,
                   + 9·0 mv.—   + 8·8 mv.—

the molalities of all three solutions being 0·01.

The amalgam electrode was similar to that just described, but the cell was modified to permit the establishment of the liquid junctions. Two experiments were made with different strengths of amalgam ; in both the e.m.f. remained steady over a wide range of dropping rates and was but little altered by change of solution. In the first the amalgam strength was found by titration to be 0·247 per cent , in the second 0·466 per cent. ; the corresponding e.m.f.'s were 1·9943 and 2·0316 volts. Lewis and Kraus[15] found that the potential difference between sodium metal and a 0·205 per cent. amalgam is 0·8456 volts ; interpolation with Richards and Conant's results[14] provides the corrections, 0·0069 and 0·0414 volts, for the strength of the amalgams here employed. After adding the liquid junction potential and reducing the e.m.f.s to the standard state, these figures give −2·6557 and −2·6584 volts as the two values of the standard electrode potential of sodium. The mean is, to the nearest millivolt, −2·657 volts.

Thallium.

It has been shown by measurements in water that anomalous results are obtained with thallium electrodes unless oxygen is carefully excluded from the apparatus. A probable explanation is that a sparingly soluble oxide is formed as a film over the amalgam surface, and consequently the potential of the electrode attains a more negative value than corresponds to true equilibrium with the thallium ion content of the bulk of the solution.

Measurements in ethyl alcohol with solutions initially freed from oxygen, but in an apparatus which did not preclude its slow diffusion to the electrode, confirmed this view. Owing to the low solubility of thallium salts in this solvent the concentration of the solutions in the cell

Two-phase
Thallium Amalgam $\quad$ TlClO$_4$ $\quad$ | $\quad$ LiClO$_4$ $\quad$ | $\quad$ LiCl $\quad$ AgCl.Ag,
$$-0.4 \text{ mv.} + \qquad + 8\cdot0 \text{ mv.} -$$

was only three hundredth molal. The e.m.f. rose slowly but continuously by some five millivolts in the course of two days; on stirring the amalgam with a glass rod it fell momentarily towards the original value. Such behaviour is compatible with the explanation advanced, since dissipation of the oxide film by stirring would bring the amalgam into contact with solution possessing a higher thallium ion activity. The initial value of the e.m.f. was 0·573 volts.

Further experiments were conducted in which the formation of oxide was avoided by bubbling pure nitrogen through the amalgam and solution. The saturated amalgam was prepared by warming the elements in an atmosphere of hydrogen. It was delivered into the cell, without having come in contact with the air, through a capillary filter. The e.m.f. of the cell varied only by a few tenths of a millivolt over a period of several hours. Since its value, 0·5710 volts, was slightly lower than that recorded previously, greater reliance can be placed upon it, and it has been used to calculate the electrode potential. Interpolation of Woolcock's results shows the activity coefficient of hydrogen chloride at this dilution to be 0·675 ; hence 0·314 volts must be subtracted from the observed e.m.f. to give E_{0_m}. After addition of 7·6 mv. for the liquid junction potential, 2·6 mv, for the potential difference between the two-phase amalgam and thallium metal, and 0·076 volts to refer the measurements to the standard hydrogen electrode, the standard electrode potential of thallium is found to be $-0\cdot343$ volts.

Silver.

Three series of determinations, at two dilutions, were made with the cell,

$$\text{Ag.AgCl} \quad \text{LiCl} \mid \text{LiClO}_4 \mid \text{AgClO}_4 \quad \text{Ag.}$$

Three kinds of silver electrode were used :—platinum grids silvered electrolytically, and granular silver prepared by the reduction of silver nitrate (i.) with ammonium formate and (ii.) with ferrous sulphate solutions. Electrodes of the first and second types exerted the same potential, but, both in 0·01 and in 0·005 m. solution, the third type was found to be 1·7 mv. positive to the electrolytic grids, two of which were used in each case. The cells maintained constant

e.m.f.s, which are embodied in the table, over periods exceeding twenty-four hours.

	Observed e.m.f. in volts.		
Silver electrode.	Expt. I. at 0·01 m.	Expt. II. at 0·01 m.	Expt. III. at 0·005 m.
Electrolytic.........	0·5622	0·5626	0·5311
Granular (i.)	...	0·5626	...
Granular (ii.)	0·5638	...	0·5328

A difference in potential between electrodes of the same metal may be attributed to variations in the state of strain of their surfaces. The form exerting the highest positive potential is that possessing the minimum energy content, and therefore the measurements with the second specimen of granular silver should be used to calculate the electrode potential. The algebraic sum of the liquid junction potentials, 10·1 mv. in hundredth and 6·8 mv. in two hundredth molal solution, is to be subtracted in each case from the gross e.m.f. of the cell. The standard electrode potential of silver, as calculated from the first experiment, is 0·7485 volts, and, from the third, 0·7500 volts. The agreement between these measurements at different molalities justifies the assumption that the activities of strong electrolytes of the same valency type are approximately equal in solutions of the same concentration.

Chlorine.

The standard electrode potential of chlorine in ethyl alcohol can be calculated from that of silver and the solubility product of silver chloride. Since the e.m.f. of the cell,

$$Ag \quad AgCl \quad Cl_2,$$

is a measure of the free energy change of the reaction

$$Ag + \tfrac{1}{2}Cl_2 = AgCl,$$
(solid) (1 atmosphere) (solid)

it is independent of the solvent in which the silver chloride is dissolved. Gerke[7] has measured the e.m.f. of this cell in water, and has found it to be 1·1362 volts; it can be represented by the equation

$$E = E.P._{Cl} - E.P._{Ag} - \frac{RT}{F} \ln L_{AgCl}, \quad . \quad . \quad . \quad (5)$$

which holds whatever the solvent in which the quantities on the right-hand side have been obtained. (Substitution of the data for water gives $E = 1.135$ volts, in agreement with experiment.) The solubility product of silver chloride in ethyl alcohol, calculated below, is 1.16×10^{-14}, while the electrode potential has just been found to be 0.749 volts. Hence the standard electrode potential of chlorine is calculated to be $+1.060$ volts.

Bromine.

The same procedure may be followed to obtain the standard electrode potential of bromine. The e.m.f. of the cell,

$$Ag \qquad AgBr \qquad Br_2,$$

will again be independent of solvent, and from the measurements in water should be 0.986 volts. Since the solubility product of silver bromide in ethyl alcohol is 1.04×10^{-16}, the standard electrode potential of bromine is $+0.789$ volts.

Iodine.

The e.m.f. of the cell,

$$Ag \qquad AgI \qquad I_2,$$

is found, on substituting the values in water ($E.P._{Ag}$ 0.7995, $E.P._I$ 0.5357, L_{AgI} 1.0×10^{-16}), in the equation

$$E = E.P._I - E.P._{Ag} - \frac{RT}{F} \ln L_{AgI}$$

to be 0.6802 volts. This value is in fair agreement with that obtained through direct measurement by Jones and Hartman [16], 0.685 volts. The solubility product of silver iodide is 1.41×10^{-19}, whence it is deduced that the standard electrode potential of iodine in ethyl alcohol is $+0.317$ volts.

The Solubility Products of Sparingly Soluble Salts.

Silver Chloride.

The e.m.f. of the hydrogen-silver chloride cell can be represented, when the activity of the hydrogen chloride is unity, by the equation

$$E_{0m} = -E.P._{Ag} + \frac{RT}{F} \ln L_{AgCl}. \quad . \quad . \quad (7)$$

Substituting the values of these quantities, the solubility product of silver chloride can be calculated,

$$0.05915 \log L_{AgCl} = 0.749 + 0.0759,$$

and is thus found to be 1.16×10^{-14}, and therefore the solubility is 1.08×10^{-7} gram-molecules in 1000 grams of solvent.

Silver Bromide.

The solubility product of silver bromide was deduced from measurements of the e.m.f. of the combination,

$$\text{Ag.AgBr} \quad \text{LiBr} \mid \text{LiCl} \quad \text{AgCl.Ag,}$$
$$-0.9 \text{ mv.} +$$

in hundredth molal solution. Silvered platinum grids, bromidized in a decinormal solution of potassium bromide for an hour with a current of 0.01 amperes per electrode, maintained potentials constant to a fifth of a millivolt. Two silver-silver bromide electrodes were compared with two silver-silver chlorides. The e.m.f. of the cell was 0.1203 volts, while a repetition with fresh materials gave a value of 0.1204 volts. Thence the potential of the Ag.AgBr, 0.01 m. LiBr electrode is calculated to be 0.0617 volts negative to the standard hydrogen electrode. Substituting this figure in the equation,

$$E = \text{E.P.}_{\text{Ag}} + 0.05915 \log a_{\text{Ag}} +$$

a value of 2.01×10^{-14} is obtained for the silver ion activity of this solution. Since the bromide activity is 0.518×10^{-2}, the solubility product of silver bromide is 1.04×10^{-16} and the solubility 1.02×10^{-8} gram-molecules in 1000 grams of solvent.

Silver Iodide.

Owing to the formation of complex salts it is difficult to procure a coherent and regular deposit on a silvered anode from an aqueous solution of potassium iodide. Possibly for this reason electrodes compounded of granular silver and precipitated silver iodide failed to maintain a constant potential in contact with a solution of lithium iodide.

Partington and Isaacs [17], in their measurements of iodide concentration cells, found that steady and reproducible results could be obtained by using simple silver electrodes, uncoated with iodide. When such electrodes were placed in the cell,

$$\text{Ag.AgI} \quad 0.01 \text{ m. LiI} \mid 0.01 \text{ m. LiCl} \quad \text{AgCl.Ag,}$$
$$+ 6.9 \text{ mv.} -$$

an e.m.f. of 0.2839 volts was recorded, constant to a fifth of

a millivolt over a period of eighteen hours. From this reading, by the same process as before, the solubility product of silver iodide is calculated to be 1.41×10^{-19}. The solubility is therefore 3.8×10^{-10} gram-molecules in 1000 grams of solvent.

Silver Thiocyanate.

Using silvered electrodes, coated electrolytically with silver thiocyanate, the e.m.f. of the cell,

Ag.AgCNS   LiCNS | LiCl   AgCl.Ag,
+ 7·5 mv.—

in hundredth molal solution, remained constant for eight hours. Its gross value was 0·0157 volts, whence the solubility product is calculated to be 4.73×10^{-15} and the solubility 6.9×10^{-8} gram-molecules in 1000 grams of solvent.

Thallium Chloride.

The solubility of thallium chloride in ethyl alcohol was investigated by means of the cell,

Two-phase
Thallium Amalgam TlCl   0·01 m. LiCl   AgCl.Ag.

The e.m.f. of the combination quickly reached an equilibrium value of 0·5639 volts, which was well maintained over a period of seven hours. Referred to the hydrogen standard, the potential of the thallium-thallium chloride electrode is therefore 0·508 volts, and the thallium ion activity in the solution 1.9×10^{-7}.

In calculating the solubility product it is no longer legitimate, as was the case with the less soluble silver salts, to assume that the total chloride ion activity is unaffected by the solution of thallium chloride. It should rather be equated to the sum of the activities of the lithium and thallium ions. Hence

$$a_{Cl^-} = 0.00518 + 0.00190 = 0.00708,$$

and the solubility product of thallium chloride is 1.34×10^{-5}.

The solubility products of these salts in the three solvents, water, methyl, and ethyl alcohols, are given in Table II. It will be seen that the solubility products of the silver halides are about a thousandfold less in methyl alcohol than in water. There is a further decrease by about a factor of five in passing from methyl to ethyl alcohol.

THE DISSOCIATION CONSTANT OF ETHYL ALCOHOL.

Two series of determinations of the hydrogen ion activity in alkaline alcoholic solutions were carried out in the cell,

$$H_2 \quad 0\text{·}01 \text{ m. LiOEt} \quad | \quad 0\text{·}01 \text{ m. LiCl} \quad AgCl.Ag.$$
$$-5\text{·}2 \text{ mv.} +$$

Lithium ethylate solutions were prepared by dissolving the clean metal in air-free alcohol through which a current of dry nitrogen was passing. Their concentrations were determined by weight titration and adjusted by weight addition of pure solvent. Iridized gold plates were used as hydrogen electrodes, the gas being generated by electrolysis of baryta solution, freed from oxygen by passing over a heated tungsten filament, dried with sulphuric acid, soda-lime, and.

TABLE II.

The Solubility Products of Sparingly Soluble Salts.

Salt.	L_{H_2O}.	L_{MeOH}.	L_{EtOH}.
AgCl	$1\text{·}8 \times 10^{-10}$	$8\text{·}9 \times 10^{-14}$	$1\text{·}2 \times 10^{-14}$
AgBr	$6\text{·}5 \times 10^{-13}$	$5\text{·}8 \times 10^{-16}$	$1\text{·}0 \times 10^{-16}$
AgI	$1\text{·}0 \times 10^{-15}$	$6\text{·}0 \times 10^{-19}$	$1\text{·}4 \times 10^{-19}$
AgCNS	$1\text{·}44 \times 10^{-12}$	$1\text{·}8 \times 10^{-14}$	$4\text{·}7 \times 10^{-15}$
TlCl	$2\text{·}25 \times 10^{-4}$	$4\text{·}4 \times 10^{-5}$	$1\text{·}3 \times 10^{-5}$

phosphorus pentoxide, and saturated with alcohol vapour before admission to the cell.

The e.m.f. of the cell was 1·0355 volts in the first experiment and 1·0360 volts in the second. To these figures 1·1 mv. and 0·9 mv. respectively must be added to correct the partial pressure of the hydrogen gas to 760 mm. Deduction of 5·2 mv., the liquid junction potential, yields values of 1·0314 and 1·0317 volts for the corrected e.m.f. of the cell. The silver-silver chloride electrode in hundredth molal lithium chloride solution is 0·0594 volts positive to the standard hydrogen electrode ; hence the mean value of the potential difference between hydrogen electrodes in 0·01 m. lithium ethylate solution and in hydrogen chloride solution of unit activity is 0·9721 volts. The hydrogen ion activity of the former solution is therefore $3\text{·}66 \times 10^{-17}$, and since that of the ethylate ion may be taken as $5\text{·}18 \times 10^{-3}$, their product, the dissociation constant of ethyl alcohol, is found to be $1\text{·}9 \times 10^{-19}$.

Danner [18] has measured this quantity by two separate methods. From the conductivity of a pure specimen of ethyl alcohol he obtained the value $2 \cdot 89 \times 10^{-16}$. To this method, however, he does not attach much importance, but considers his e.m.f. measurements to be more significant. To avoid liquid junction potentials he based his calculations on investigations of the three cells

H_2	HCl	$Hg_2Cl_2 \cdot Hg,$
$Hg \cdot Hg_2Cl_2$	Saturated NaCl	Na amalgam,
Na amalgam	NaOEt	$H_2.$

The sum of the processes occurring in these cells is the reaction

$$EtOH = EtO^- + H^+,$$

and the e.m.f. corresponding to it is also obtained by addition. Owing to the unreliability of calomel electrodes he was forced to measure the second cell, whose e.m.f. should be independent of solvent, in aqueous solution. His measurements extended over a range of concentration, but he adopted the doubtful assumption that the ratio of the equivalent conductivity in very dilute solution to that at infinite dilution represents the activity coefficient. He obtained in this way a value of $0 \cdot 73 \times 10^{-19}$ for the dissociation constant of ethyl alcohol. Since his concentrations are expressed on a volume scale, it is not strictly comparable with the present determination.

A more natural basis of comparison with this, and also with the corresponding data in other solvents, is provided by calculation of the molecular fraction of the solvent dissociated into ions, N. The relation between this factor and the dissociation constant, K, is given by the expression

$$N = \frac{\sqrt{\overline{K}} \cdot M}{1000 \cdot \Delta}$$

when the concentration has been calculated in gram-molecules per litre, and by

$$N = \frac{\sqrt{\overline{K}} \cdot M}{1000}$$

when the solution has been made up by weight. M is the molecular weight and Δ the density of the solvent. Danner's value for the molecular fraction of ethyl alcohol dissociated is $1 \cdot 6 \times 10^{-11}$, in fair agreement with the present figure, $2 \cdot 0 \times 10^{-11}$.

DISCUSSION.

It has been pointed out in an earlier paper [19] that the choice of a weight instead of a volume concentration scale, and the corresponding use of molal activity coefficients, alters the values of the calculated electrode potentials unless the density of the solvent is unity. If the electrode potentials on the volume scale are denoted by the symbol E.P.$_c$ and those calculated on a weight basis by E.P.$_m$, then, while for cations

$$\text{E.P.}_c = \text{E.P.}_m,$$

for anions

$$\text{E.P.}_c = \text{E.P.}_m + \frac{2RT}{F}\ln \Delta, \quad . \quad . \quad . \quad (9)$$

TABLE III.

Element.	E.P.$_c$ in			Differences.	
	H$_2$O.	MeOH.	EtOH.	MeOH/H$_2$O.	EtOH/H$_2$O.
Li	−2·958	...	−3·042	...	0·084
Na	−2·7125	−2·728	−2·657	0·015	−0·056
Tl	−0·3363	−0·379	−0·349	0·043	0·013
H	0	0	0	0	0
Ag	0·7995	0·764	0·749	0·036	0·051
I	0·5357	0·357	0·305	0·179	0·231
Br	1·0659	0·837	0·777	0·229	0·289
Cl	1·3594	1·116	1·048	0·243	0·301

where Δ is the density of the solvent. Reasons, related to the purpose of this discussion, were there adduced for the adoption of the volume concentration standard. In Table III. the electrode potentials of the anions have therefore been adjusted in accordance with equation (9), which at 25° C. takes the form

$$\text{E.P.}_c = \text{E.P.}_m - 0·0123_4 \quad \text{for methyl alcohol,}$$

and $\quad \text{E.P.}_c = \text{E.P.}_m - 0·0124_5 \quad$ for ethyl alcohol.

Since the density correction for water is inappreciable the electrode potentials in that solvent have been taken directly from Lewis and Randall's 'Thermodynamics.'

In general the electrode potentials of the elements are the more negative the lower is the dielectric constant of the solvent. To this rule two exceptions appear in the table ; the electrode potential of thallium is lower in ethyl than in

methyl alcohol, while that of sodium is highest in methyl but lowest in ethyl alcohol. The elements maintain the same relative positions in the three solvents, and the specific differences are in the main small. That they are greater for the anions than for the cations arises from the adoption of hydrogen as the standard electrode in each solvent.

The difference in the electrode potentials of an anion in two solvents is the e.m.f. of the cell,

HA in solvent I.   HA in solvent II.

A $H_2 - H_2$ A

$a = 1$ $a = 1,$

and is therefore a measure of the partial molal free energy of transfer of the acid HA from the first solvent to the second when at unit activity in both. This free energy change can be calculated in 15° C. calories from the equation

$$\Delta \overline{F}_{HA}^{25°} = 23059 \left[E.P._{A_{II}} - E.P._{A_I} \right]. \quad . \quad . \quad (10)$$

The partial molal free energy of transfer of the corresponding metallic salt MA is deduced from the e.m.f., E, of the cell,

MA in solvent I.   MA in solvent II.

A $M - M$ A

$a = 1$ $a = 1,$

and is therefore represented in calories by the equation

$$\Delta \overline{F}_{MA} = 23059 \left[E.P._{A_{II}} - E.P._{M_{II}} - E.P._{A_I} + E.P._{M_I} \right].$$

$$. \quad . \quad . \quad (11)$$

It was also demonstrated in the previous paper that this quantity is the limiting value, as the concentration sinks to zero, of the partial molal free energy of transfer of the electrolyte between equally concentrated solutions in the two solvents. Since Born[20] has calculated the free energy of solvation of an ion of radius r in a solvent of dielectric constant D at infinite dilution as

$$F_i = \frac{z^2 \epsilon^2}{2r} \left[1 - \frac{1}{D} \right], \quad . \quad . \quad . \quad . \quad (12)$$

the observed values of the free energy of transfer may be properly compared with those deduced from the equation,

$$\Delta \overline{F} = \frac{N z^2 \epsilon^2}{2} \left[\frac{1}{D_2} - \frac{1}{D_1} \right] \left[\frac{1}{r_1} + \frac{1}{r_2} \right], \quad . \quad . \quad (13)$$

by substitution of N, Avogadro's number, D_1 and D_2, the dielectric constants of the two solvents, and the radii of the ions, r_1 and r_2, obtained from the crystal lattice.

Table IV. contains the values for the transfer of a number of electrolytes from water to methyl and also to ethyl alcohol calculated from this equation, and also those obtained by means of equations (10) and (11) from the observed electrode potentials. The data for the thiocyanates were

<center>TABLE IV.</center>

<center>Partial Molal Free Energies of Transfer at 25° C.
in Calories.</center>

<center>H_2O—MeOH.</center>

	Calculated.			Observed.			
	Cl.	Br.	I.	Cl.	Br.	I.	CNS.
Li	6570	6360	6160	...	...	...	...
Na	5370	5160	4960	5260	4970	3820	3390
Tl	4270	4060	3860	4610	4280	3130	2700
H	...	...	...	5610	5280	4130	3700
Ag	5270	5060	4860	4780	4450	3400	2970

<center>H_2O—EtOH.</center>

	Cl.	Br.	I.	Cl.	Br.	I.	CNS.
Li	8970	8690	8410	5010	4730	3390	2900
Na	7270	6990	6710	8260	7980	6640	6160
Tl	5670	5390	5110	6650	6370	5030	4540
H	...	...	...	6950	6670	5330	4840
Ag	7070	6790	6510	5770	5490	4150	3660

deduced from the solubility product measurements by use of the conception of a hypothetical thiocyanogen electrode, as described by Buckley and Hartley. There is a general correspondence between the observed and calculated values. It will be seen from the figures for the hydrogen halides that the free energy change in both solvents decreases with increasing ionic radius. The observed differences between the chloride and the bromide are of the calculated magnitude, but those between the bromide and the iodide are considerably greater. The partial molal free energies of transfer of the metallic chlorides from water to methyl alcohol are also in the inverse order of the ionic radii of the cations. The

observed value is less than the calculated except in the case of thallium, where the measurement is a little uncertain and the result may be too low; but there is considerable divergence from a quantitative agreement. Thus the difference between sodium and silver chlorides is greater than was to be expected from their ionic radii, which are almost equal. The electrode potential of lithium has not yet been determined in methyl alcohol, but, judging from its values in the other solvents, it is probably more negative than the Born equation demands.

Turning to the transfers of the metallic chlorides from water to ethyl alcohol, it is seen that the irregularities, incipient in methyl alcohol, are here more pronounced. Thus the free energy change is greater for sodium than for hydrogen chloride, while that of thallium is nearly as great, and is larger than that of silver, the ionic radius of which is two-thirds smaller. The results for the lithium salts correspond to a much greater ionic radius than the metal possesses in the crystal.

The Born equation can only be regarded as an approximate expression for the free energy of solvation of the ion. It fails to take into account the change in the properties of the medium due to the electrical charge on the ion. The solvent dipoles around the ion must be orientated in the electrical field with a consequent alteration in dielectric properties. Such factors may be expected to be dependent on the ionic radius for ions of equal charge, and cannot therefore be sufficient to account for the specific differences in the observed free energies of transfer.

There is, however, the further possibility of the formation of physical or chemical links between the ions and the solvent molecules. Abundant evidence for the existence of solvation in this sense exists; indeed, it is calculated from conductivity data that the ionic radii of the alkali metals in solution in these solvents decrease as the atomic weight increases, implying that the lighter ions, such as lithium, are the more heavily solvated. Not only the effective ionic radius, but also the degree of solvation of the ion, may therefore be expected to vary from solvent to solvent, so that its partial molal free energy of transfer will be modified accordingly.

The low values for the transfer of the lithium salts may thus be taken as confirmation of the existence of a high or uniform degree of solvation of the lithium ion. The anomalous position of sodium and thallium, the largest of these cations, would seem to indicate that their solvation, initially smaller in extent, decreases with the dielectric constant of

the solvent. In this connexion it is significant that the solubility of the soluble salts of these metals is much smaller in the alcohols than in water, in contrast to the high solubilities of lithium salts which solvation would be expected to promote. These measurements of electrode potentials in ethyl alcohol show, then, that the electrical contribution of the Born equation is not the only factor in determining the free energy of solvation, and serve to support the view that the ion is associated, to an extent dependent on its size and on the dielectric constant of the medium, with molecules of the solvent in which it is dissolved.

SUMMARY.

(1) A study has been made of reference electrodes and of liquid junction potentials in ethyl alcohol.

(2) The electrode potentials of seven elements and the solubility products of five sparingly soluble salts have been measured.

(3) The results have been used to calculate the partial molal free energies of transfer of a number of electrolytes, which have been compared with values derived from the Born equation.

(4) The dissociation constant of ethyl alcohol has been determined.

BIBLIOGRAPHY.

(1) Neustadt and Abegg, *Zeit. Electr.* xvi. p. 866 (1910); Neustadt, *Zeit. Phys. Chem.* lxix. p. 486 (1909).
(2) Buckley and Hartley, *Phil. Mag.* viii. p. 320 (1929).
(3) Wolfenden, Wright, Ross-Kane, and Buckley, *Trans. Farad. Soc.* xxiii. p. 491 (1927).
(4) Woolcock and Hartley, *Phil. Mag.* v. p. 1133 (1928).
(5) Randall and Young, *J. A. C. S.* l. p. 989 (1928).
(6) Güntelberg, *Zeit. Phys. Chem.* cxxiii. p. 202 (1926).
(7) Gerke, *J. A. C. S.* xliv. p. 1684 (1922).
(8) Nonhebel and Hartley, *Phil. Mag.* l. p. 729 (1925).
(9) Lewis and Sargent, *J. A. C. S.* xxxi p. 363 (1909).
(10) Guggenheim, *J. A. C. S.* lii. p. 1315 (1930).
(11) McKelvy, *Bull. Bur. Standards,* ix. p. 327 (1913).
(12) Lewis and Keyes, *J. A. C. S.* xxxv. p. 340 (1913).
(13) Philpot, *Phil. Mag.* (in the press)
(14) Richards and Conant, *J. A. C. S.* xliv. p. 601 (1922).
(15) Lewis and Kraus, *J. A. C. S.* xxxii. p. 1459 (1910).
(16) Jones and Hartman, *J. A. C. S.* xxxvii. p. 756 (1915).
(17) Partington and Isaacs, *Trans. Farad. Soc.* xxv. p. 53 (1929).
(18) Danner, *J. A. C. S.* xliv. p. 2824 (1922).
(19) Macfarlane and Gatty, *Phil. Mag.* xiii. pp. 283, 291 (1932).
(20) Born, *Z. Physik,* xlv. p. 1 (1920).

Physical Chemistry Laboratory,
    Balliol and Trinity Colleges, Oxford.

XXXVII. *The Effect of Electrolytes on the Dielectric Constant of Water.*—Parts III. and IV. *By* R. T. LATTEY *and* W. G. DAVIES *.

PART III.

Results for Salts of other than the Uni-univalent Type.

WE have previously described our application of the " Voltage Tuning " resonance method to the determination of the dielectric constants of electrolytic solutions [6].

Measurements were carried out on four uni-univalent salts at temperatures of 18° C. and 25° C. up to concentrations of about 0·01 N. It was found that the dielectric constant increased linearly with concentration, and that within the limit of experimental error the effect of each salt was the same if the concentration was expressed in gram equivalents per 1000 grams of water.

We have now completed the investigation of a few multivalent salts at a temperature of 18° C.
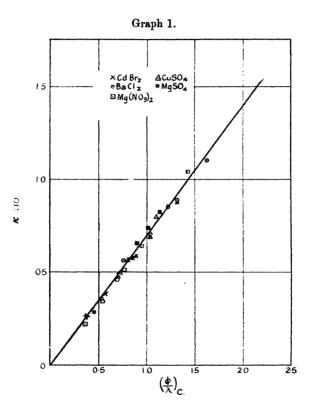
All the salts used were supplied by Kahlbaum. The magnesium sulphate contained water of crystallization, estimated by heating the salt and converting it into the anhydrous state. Cadmium bromide was analyzed by the estimation of bromine as silver bromide. The nitrates of magnesium, lanthanum, thorium and zirconium were analyzed by conversion into their oxides on heating.

It was pointed out by us [6] that our values of $\dfrac{\Delta\phi}{\lambda}$ should vary linearly with κ, the specific conductivity of the solution. In Graph 1 we have plotted the values of $\dfrac{\Delta\phi}{\lambda}$ for our smallest condenser against κ for solutions of $CdBr_2$, $BaCl_2$, $Mg(NO_3)_2$, $CuSO_4$, and $MgSO_4$. The values of κ are interpolated from Kohlrausch's values [7]. The slope of the line obtained is identical with that obtained for the uni-univalent salts, as would be expected. No values appear to be available for variation of Λ, the equivalent conductivity, with concentration for lanthanum nitrate. Heydweiller [4] gives the equivalent conductivity at infinite dilution $\Lambda_0 = 111\cdot7$. If the values of κ are determined from our experimental values of $\dfrac{\Delta\phi}{\lambda}$ by the aid of the relation obtained between

* Communicated by the Authors.

$\dfrac{\Delta\phi}{\lambda}$ and κ for other salts, then we obtain values of $\Lambda\left(=\dfrac{\kappa}{\text{conc.}}\right)$ varying between 106·6 and 111·6. The values of κ are not sufficiently accurate to obtain a value of Λ_0, but the values of $\dfrac{\Delta\phi}{\lambda}$ are at least of the right order.

Graph 1.

Heydweiller [4] measured the conductivities of $ThCl_4$ solutions. He calculated that for $\frac{1}{4}ThCl_4$ $\Lambda_0 = 23\cdot5$. The value of Λ_0 for NO_3 being 61·7, the calculated value for $\frac{1}{4}Th(NO_3)_4$ is $\Lambda_0 = 85\cdot2$. Our values of $\dfrac{\Delta\phi}{\lambda}$ give a value of Λ_0 which is considerably greater than this. This is probably explained by the hydrolysis of $Th(NO_3)_4$ in solution according to the equation

$$Th(NO_3)_4 + 4H_2O = 4HNO_3 + Th(OH)_4$$

the high conductivity of HNO_3 giving an abnormal experimental value for Λ_0. No data seem to be available for $Zr(NO_3)_4$ solutions, but with this salt also there is an unexpectedly high value for the conductivity.

The values obtained for the dielectric constants of the various solutions are given in Table I. and are plotted against the concentration in Graphs 2–5. The concentration is expressed in gram equivalents per 1000 gram of solution. The second column gives the number of independent values which were obtained, while the third column gives the mean value.

TABLE I.

1 : 2 Salts.

CdBr$_2$.			BaCl$_2$.		
Conc.	No.	D.	Conc.	No.	D.
0	—	80·79	0	—	80·79
000,839	12	81·24	000,907	12	81·37
1,577	16	81·71	1,927	11	82·13
2,759	14	82·57	1,974	5	82·49
4,198	8	83·07	3,124	6	83·62
5,651	9	84·14	3,348	9	82·97
6,993	5	84·55	5,198	10	84·83
7,215	9	85·60	6,488	10	86·20
8,177	8	85·44	6,944	10	86·86
			7,926	6	87·37
			10,415	3	88·20

Mg(NO$_3$)$_2$.		
Conc.	No.	D.
0	—	80·79
000,713	10	80·86
1,311	15	81·40
2,189	14	81·90
3,490	11	82·86
4,748	9	84·10
5,263	8	84·28
6,638	4	84·66
9,430	5	85·70
11,091	3	86·13

Table I. *(cont.).*

2 : 2 Salts.

CuSo₄.			MgSO₄.		
Conc.	No.	D.	Conc.	No.	D.
0	—	80·79	0	—	80·79
001,145	12	81·47	000,870	11	81·46
2,281	15	82·40	1,867	13	82·16
4,239	15	84·44	3,614	12	83·53
6,333	11	85·26	6,930	18	85·91
7,384	9	86·30	8,292	10	86·26
9,534	9	86·68	9,608	4	86·48
11,114	18	87·79	10,887	10	87·29
13,239	4	88·21			
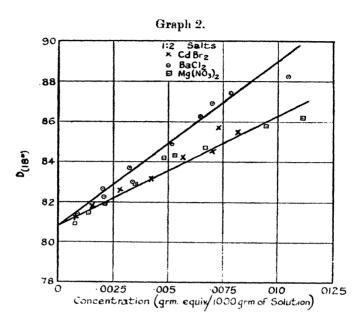
1 : 3 Salts.
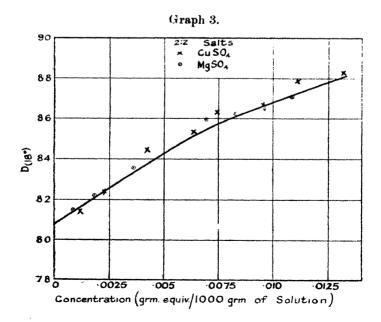
La(NO₃)₃.		
Conc.	No.	D.
0	—	80·79
000,983	10	81·43
2,008	10	82·20
3,141	11	83·83
3,906	10	84·29
5,090	8	86·00
6,303	8	86·72
7,932	5	88·82
10,194	5	90·33

1 : 4 Salts.
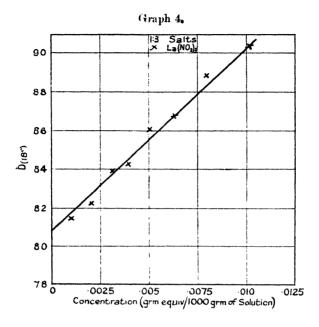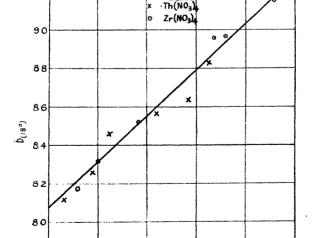
Th(NO₃)₄.			Zr(NO₃)₄.		
Conc.	No.	D.	Conc.	No.	D.
0	—	80·79	0	—	80·79
000,819	11	81·21	001,452	9	81·70
2,137	8	82·59	2,447	7	83·08
3,079	11	84·54	4,566	9	85·11
4,669	8	85·10	8,358	5	89·51
5,473	7	85·61	8,922	3	89·59
7,123	7	86·34	11,432	3	91·70
8,079	5	88·21			

Graph 2.

Graph 3.

Graph 4.

Graph 5.

PART IV.

It is found that for each salt there is an increase of dielectric constant with concentration. The increase is linear except in the cases of $CuSO_4$ and $MgSO_4$ solutions, for which the rise in dielectric constant falls off from linearity with increasing concentration. For salts of $1:2$ type, $CdBr_2$ and $Mg(NO_3)_2$ show increases of the same amount, but these are considerably less than the values for $BaCl_2$. The $1:3$ salts and $1:4$ salts have increases of the same amount within the limit of experimental error.

The increase with concentration which we observe is contrary to the observations of most recent investigations. Sack[8], Walden and Werner[9], Carman and Schmidt[1], and others have explained the decrease of the dielectric constant with concentration which they have found experimentally by supposing the existence of intense electric fields in the neighbourhood of the ions in the solution, thus rendering some volume of the solution inactive to an externally applied field. The volumes of these electrically saturated cavities around the ions can be calculated from Sack's experimental results. For KCl solutions they would have a volume equal to 1000 times that of the ions[2]. Using Walden and Werner's results the volumes would be 10,000 times.

A rise of dielectric constant on further increase of concentration is predicted, due to the formation of doublets which would be oriented by the external field. Carman and Schmidt account for their observed rise in this way.

As we have shown[6] the results of various observers are in such great disagreement that no definite conclusions can be reached about any of these hypotheses.

The measurements of Heydweiller[5] on the refractions of electrolytic solutions show that the refractive index of a solution increases as the concentration is increased. Defining the refraction by $\dfrac{\mu^2-1}{\mu^2+2} \cdot \dfrac{G}{d}$, where μ is the refractive index, G the weight of the solution, and d its density, he deduces the ionic refractions, and shows that at infinite dilution the ionic refractions are additive, *i. e.*, the molar refraction of KCl is the sum of the ionic refractions of K^+ and Cl^-. It is interesting to apply a treatment similar to that of Heydweiller to the dielectric constant.

We will consider 1000 grams of a solution in which are dissolved C gram mols. of a solute. Then if the density of the solution $=d$ its volume $=1000/d$.

Let the mass of 1 gram mol of solute $= m_1$, so that Cm_1 is the mass of solute dissolved in 1000 grams of solution.

If the mass of 1 gram mol of solvent $= m_2$, then the number of gram mols of solvent in 1000 grams of solution

$$= \frac{1000 - Cm_1}{m_2}.$$

Let $p_1 =$ molar polarization of the solute and $p_2 =$ molar polarization of the pure solvent.

We will assume that the value of p_2 is unaffected by the presence of the solute.

Then the total polarization

$$= Cp_1 + \frac{1000 - Cm_1}{m_2} \cdot p_2 \quad \text{in a volume } 1000/d$$

$$= \frac{D-1}{D+2} \cdot \frac{1000}{d} \qquad \text{(Clausius -Mosotti)},$$

where D is the dielectric constant of the solution.

When $C = 0$, then

$$\frac{10^3 \cdot p_2}{m_2} = \frac{D_0 - 1}{D_0 + 2} \cdot \frac{10^3}{d_0},$$

where d_0 is the density and D_0 is the dielectric constant of the pure solvent.

$$Cp_1 = \frac{D-1}{D+2} \cdot \frac{1000}{d} - \frac{(1000 - Cm_1)}{d_0} \cdot \left(\frac{D_0 - 1}{D_0 + 2} \right)$$

$$= 10^3 \left\{ \frac{D-1}{D+2} \cdot \frac{1}{d} - \frac{(10^3 - Cm_1)}{1000 d_0} \cdot \frac{D_0 - 1}{D_0 + 2} \right\}$$

$$= 10^3 (P_1 - P_0),$$

where

$$P_1 = \frac{D-1}{D+2} \cdot \frac{1}{d}$$

and

$$P_0 = \frac{(10^3 - Cm_1)}{1000 d_0} \cdot \frac{D_0 - 1}{D_0 + 2};$$

p_1, the molar polarization of the solute, is related to the polarizability α by the relation

$$p_1 = \frac{4\pi N}{3} \alpha,$$

where N is the Avogadro number.

In the case of a dissociated solute p_1 and α would refer to the sum of the polarizations and the polarizabilities of the ions.

It is possible to determine P_1 and P_0 from our experimental data, so that p_1 may be calculated.

The values of p_1 have been calculated for potassium chloride solutions over the range allowed by our experimental data.

TABLE II.

$T = 18°$ C. $D_0 = 80·79$. $m_1 = 74·56$.

$d_0 = 0·99862$. $\dfrac{D_0 - 1}{D_0 + 2} = 0·96376$.

C.	Cm_1.	D.	d.	P_1.	P_0.	$P_1 - P_0$.	p_1.	D (calc.).
000,963	·07	81·09	0·99866	0·96518	0·96503	0·00015	(155·76)	81·40
2,133	·16	82·28	99872	96563	96496	67	314·11	82·21
2,830	·21	82·54	99876	96572	96492	80	282·69	82·71
3,983	·30	83·76	99882	96616	96483	133	333·92	83·48
4,783	·36	83·71	99885	96612	96476	136	284·34	83·96
6,658	·50	85·50	99895	96674	96463	211	316·92	85·30
7,452	·56	85·58	99899	96670	96457	213	285·83	85·81
8,658	·65	86·28	99905	96694	96448	246	284·13	86·70
9,303	·69	87·04	99909	96718	96443	275	295·61	87·21
10,225	·76	88·00	99913	96749	96439	310	303·18	87·96
12,092	·90	90·22	99923	96820	96423	397	328·36	89·32

Mean value of $p_1 = 302·91$ c.c.

$$p_1 = \frac{4\pi}{3} N\alpha \quad \therefore \quad \alpha = 119·26 \times 10^{-24}.$$

Using the value $p_1 = 302·91$, the values of D at the various concentrations are calculated and are given in the last column.

The values of the density are interpolated from those of Hartley and Barrett [3].

The assumption that was made that p_2, the polarization of the solvent, would be unaffected by the introduction of the solute could only be expected to hold at infinite dilution. At higher concentrations forces between the ions themselves and between the ions and the solvent molecules might be expected to affect the dielectric constant, causing p_1 to vary in a regular manner with concentration, but this is not borne out by the experimental data. Any change of polarization due to inter-ionic action would probably be masked by experimental errors at the low concentration at which

we worked. The polarization has been calculated for the other salts at 18°, and the values obtained are given below:—

TABLE III.

Salt.	Molar polarization (p_1).	Salt.	Molar polarization (p_1).
KCl	302·9	BaCl$_2$	673·2
NaCl	268·7	Mg(NO$_3$)$_2$	513·0
NaF	266·7	CuSO$_4$	573·8
KIO$_3$	302·9	MgSO$_4$	574·0
CdBr$_2$	510·0	La(NO$_3$)$_3$	1406·6
		Th(NO$_3$)$_4$	1478·6
		Zr(NO$_3$)$_4$	1879·8

Both the refraction and the polarization of an ion may be considered as due to the deformation of the electron orbits on the application of the external field.

Debye [2] has worked out the case of the hydrogen atom. Here we have one electron with an orbit of radius a. Debye shows that a, the radius of the distorted orbit, is connected to the polarizability by the relation

$$a^3 = \frac{2}{9}\alpha.$$

The values of the polarization given in Table III. are the sum of the ionic polarizations of the ions in solution. For KCl 302·9 represents the sum of the polarizations of the K ion and the Cl ion. For CdBr$_2$ 510·0 represents the sum of the polarizations of the Cd ion and two Br ions.

We may apply the Debye relation to the KCl molecule, with the reservation that α represents the sum of the polarizabilities of the K and Cl ions and a_1 and a_2 represent for each ion the mean of a number of radii of orbits which undergo a shift.

We may put

$$a_1^3 + a_2^3 = \frac{2}{9}\alpha = \frac{p_1}{6\pi N}.$$

The ionic radii have been calculated for crystals by Wasastjerna [10] and for aqueous solutions by Webb [11].

In Table IV. are given their values of $a_1{}^3 + a_2{}^3$ against our values of $\dfrac{p_1}{6\pi N}$.

The values of $\dfrac{p_1}{6\pi N}$ are greater in each case than $a_1{}^3 + a_2{}^3$. The values of p_1 for any given salt, and the values of a which are calculated from them can at present only be regarded as approximate. Also the factor $\dfrac{2}{9}$ used in the Debye relation only holds for the hydrogen atom. Nevertheless the theory which we have adopted seems tenable—that the increase in dielectric constant with concentration which is observed for electrolytic solution in a field of frequency 10^7 is due to the distortion which the electronic orbits undergo.

TABLE IV.

Salt.	$\dfrac{p_1}{6\pi N}$.	$a_1{}^3 + a_2{}^3$.	
		Webb [11].	Wasastjerna [10].
$K^+ + Cl^-$	$26 \cdot 52 \times 10^{-24}$	$17 \cdot 778 \times 10^{-24}$	$7 \cdot 29 \times 10^{-24}$
$Na^+ + Cl^-$	$23 \cdot 52$	$14 \cdot 616$	$6 \cdot 12$
$Na^+ + F^-$	$23 \cdot 35$	$8 \cdot 767$	$3 \cdot 38$
$Ba^+ + 2Cl^-$	$55 \cdot 94$	......	$12 \cdot 92$
$Cd^+ + 2Br^-$	$44 \cdot 65$	$28 \cdot 555$	......

It is proposed to improve the experimental method and to redetermine the dielectric constants with greater accuracy. This may be done in two ways—by increasing the frequency and decreasing the size of the condenser in which the electrolytic solution is contained. Both methods introduce difficulties which are not easy to overcome. More accurate measurements of the polarization of ions and its variation with concentration should establish its analogy with optical refraction, and should throw light on the forces between the ions and between the ions and the solvent molecules.

The improved method could also be applied to acids where the conductivity is very high.

The polarizability of the hydrogen ion, consisting only of a proton (unless it is really H_3O in aqueous solution), equals zero, and consequently the polarizabilities of the individual ions could be calculated.

References.

(1) Carman and Schmidt, Phys. Rev. xxx. p. 925 (1927).
(2) Debye, ' Polar Molecules ' (1929).
(3) Hartley and Barrett, J. C. S. cxxiii. p. 398 (1923).
(4) Heydweiller, *Zeit. phys. Chem.* lxxxix. p. 281 (1915).
(5) Heydweiller, *Phys. Zeit.* xxvi. p. 256 (1925).
(6) Lattey and Davies, Phil. Mag. xii. Dec. 1931.
(7) Kohlrausch and Holborn, ' Das Leitvermögen der Elektrolyte.'
(8) Sack, *Phys. Zeit.* xxviii. p. 199 (1927).
(9) Walden and Werner, *Zeit. phys. Chem.* cxxix. p. 389 (1927).
(10) Wasastjerna, Comm. Phys. Math. Soc. Scient. Fennicæ, i. p. 38.
(11) Webb, T. J., J. Am. C. S. xlviii. p. 2589 (1926).

XXXVIII. *Raman Spectra in Liquid and Gaseous* CH_4.
By Susil Chandra Biswas [*].

RAMAN spectra in the vibrational and the rotational vibrational states of CH_4 molecule have been examined by McLennan, Smith, and Wilhelm (Roy. Soc. Canada, T. xxiii. p. 279, 1929), and those for the gaseous state by Dickinson, Dilton, and Rasetti (Phys. Rev. xxxiii. p. 582, 1929). For the liquid state the frequency differences from the incident radiation are as given $\nu = 2909$ and 3071 cm.$^{-1}$ in addition to a weak band with lines at 2953, 2989, 3023, and 3047 cm.$^{-1}$, whereas for the gaseous state the frequency differences are 2914 cm.$^{-1}$ (strong and sharp), 3071 cm.$^{-1}$ (weak), and the rotation vibration band 3022·1 with a number of equally spaced lines (weak).

Apparently the rotation vibration lines in the liquid state of methane are found with a shift of about ± 23 cm.$^{-1}$, whereas in the gaseous state the frequency shifts are of about ± 20 cm.$^{-1}$. There also appears quite a small frequency change in the vibrational Raman lines, 2909 (liquid) and 2914 cm.$^{-1}$ (gas). The other frequency, 3071 cm.$^{-1}$, remains practically the same in both the liquid and the gaseous states.

Arguing on different lines, Rankine, Langmuir, Dennison, Brusche, and others attributed to the outer shell of CH_4 molecule the same symmetrical electron configuration as that of a rare gas atom, krypton. It has also been shown by an examination of the crystal structure of solid methane by McLennan and Plummer (Phil. Mag. vii. p. 761, 1929) that the methane molecule showed a symmetrical tetrahedral

structure. They obtained in their experiments no evidence of the existence of a pyramidal modification.

Presumably such a symmetrical molecule may have no permanent electric moment (or ignoring for the present the small electric moment that it may have), and we may believe that the reaction of the radiation field in producing any change in the energy of the molecule by the quantum-mechanical effect that is set up in the liquid state, due to the interaction of the neighbouring molecules, may vanish altogether or may be inappreciable, as CH_4 molecules are known to be optically isotropic. It may thus be pointed out that Dadieu and Kohlrasch (*Naturw.* xviii. p. 154, 1930) expressed the same frequency for both the liquid and gaseous CH_4.

As, contrary to this view, the small displacements in the frequency shifts observed in the Raman spectra of the two states might be explained if a small di-pole moment ($K = 0.048 \times 10^{-18}$) may be considered as really substantive (Riegger, *Ann. der Phys.* 1919 ; Ebert and Hartel, *Naturw.* 1927). On this view a change in frequency in the two states of a molecule must be expected. Breit and Salant have already derived an expression showing a change in frequency $\Delta \nu = \dfrac{Ne^2}{6\pi m \nu}$, where N is the number of resonating electrons per unit volume, m is the mass, ν the free vibration frequency of a molecule, and e is Dennison's effective electronic charge for a molecule. This equation shows the change due to Lorenz-Lorentz shift only, and contributes only a part to the total frequency shift. Due to the small di-pole moment of the molecule this expected change must be very small.

In the foregoing considerations two types of CH_4 molecules—(1) symmetrical and (2) slightly unsymmetrical—have been brought in evidence. This may be more aptly shown by considering from the examination of the Raman spectra that the frequency 3071 cm.$^{-1}$ (equivalent possibly to $\nu_3 = 3014$ cm.$^{-1}$ (intensity 20) in absorption) should be considered as the fundamental frequency of the symmetrical methane molecule. It thus indicates no change in frequency due to a change of state. The other frequency, 2914 cm.$^{-1}$, should be considered as the fundamental of the second type. This line does not appear as an absorption line, but appears as a difference combination of Dennison's two frequencies $\nu_4 = 1304$ (intensity 50) and $\nu_1 = 4217$ (intensity 1). If, in preference to 4217 cm.$^{-1}$ as a fundamental frequency, 2914 cm.$^{-1}$ is considered as fundamental, the analysis of the

absorption lines of Cooley and Ellis within the range 1.15μ to 7.7μ may satisfactorily be explained. It may also be pointed out that this fundamental frequency is closely related to C–H bond.

The appearance of the frequency 2914 cm.$^{-1}$ as a Raman line shows that it must be characteristic of a symmetrical vibration of the C–H parts within a molecule and must be associated with no change of electric moment, that is, the vibration that will be produced in different vibrating centres will not produce any oscillation among them.

Conclusion.

The small asymmetry that is mentioned in one form of CH₄ molecule may be obtained by only a slight change in the angular position of a hydrogen atom in the tetrahedron of the other form, which is perfectly symmetrical with respect to the four hydrogen positions. There is enough evidence to show the existence of two types of NH₃ molecules which, though they may not differ chemically, are supposed to differ in their geometrical or other physical entities. Thus Tronsted (*Zs. f. Phys. Chem.* cxxxv. p. 333, 1929) showed that, like the two types of para- and ortho-hydrogen existing in a mixture, molecules of NH₃ also exist in two different forms with different heat conductivities and specific heats. Spectroscopic evidences of two types of NH₃ molecules have also been cited by Ellis, Barker, and Mecke (Phys. Rev. 1930–1931).

It has been a moot question with several investigators to attribute to the CH₄ molecule an asymmetric form at least in the presence of a radiation field (*cf.* Henri, Chem. Rev. vol. iv.). Presumably, then, the two forms of CH₄ molecules, under the action of light and collision undergoing interchanges from one form to another (Hund), may safely be postulated, with the result that the frequency difference in the two fundamentals of the Raman spectra of the two types represents the energy of activation due to the geometrical or other physical changes. Such a sort of dynamic i-omerism in the geometry of two types of CH₄ molecules with the hydrogen positions respectively at (1), (3), (6), and (8) (symmetrical tetrahedron), and at (1), (3), (4), and (6) (unsymmetrical tetrahedron) have been worked out by Morse (Proc. Nat. Acad. of Sc. xiv. p. 166, 1928), and the moment of inertia of different types are calculated and checked with Cooley's results on band spectra.

The view outlined here may also possibly be shared by a study of the ionization processes of CH₄ molecules, where

two distinct but nearly identical values of ionization potential have been observed at 14·5 and 15·5 volts, producing respectively the ions (CH_4^+) and (CH_3^+) without the production of H^+ ions (Hogness and Kvalness, Phys. Rev. xxxii. p. 942, 1928), but at the higher voltage free H atom is liberated.

Physics Department,
    Dacca University.

XXXIX. *The Stabilizing Effect of Imposed Oscillations of High Frequency on a Dynamical System.* By E. R. LOWENSTERN, *M.A., Dip.Ed. (Melbourne), Lecturer in Mathematics at the University of Tasmania* *.

THE investigations given below, of the stabilizing effect of imposed oscillations of high frequency on a dynamical system, are concerned with imposed motions of such high frequency and small amplitude that the equations of motion for the system at any instant may be obtained by introducing mean values over a period of time of the same order as the period of the rapid oscillation.

The problem arose from the fact that an inverted pendulum may be stabilized by the application of a rapid vertical oscillation of the point of support, and will oscillate about the initially unstable position under these conditions.

The effect of forced oscillations of finite frequency on a system with one degree of freedom has been discussed by previous writers, most of whom have used Hill's method involving infinite determinants ((1) and (2) below). They have then made approximations corresponding to the assumption of rapid forced oscillations, to determine conditions of stability in special cases. The stability of a spinning-top acted on by a periodic vertical force through a point in the axis is considered by Mr. A. Stephenson ((2) (ii.), (iii.)), but general equations of motion are not obtained.

By a similar method Mr. Stephenson has also determined the conditions of stability of two and of three rods linked together end to end and originally in a position of unstable equilibrium, if the point of support is given rapid vertical oscillations ((2) (v.)).

In another paper ((2, (iv.)) he has investigated the case of a pendulum of which the pivot is supposed to receive a series

of impulses which keep it moving with constant speed in a line making a small angle with the rod of the pendulum. He determines a "mean" motion, which is stable. In a similar way he obtains the condition of stability for the inverted pendulum if the pivot is given rapid, vertical, simple harmonic oscillations.

Van der Pol and Strutt (3) have discussed the conditions under which a "rectangular ripple" may produce stability in an otherwise unstable system.

In a recent paper (4) Mr. Paul Hirsch has considered, by an elementary process of taking means, the case of a pendulum whose point of suspension has a small imposed oscillation, rectilinear or not, of high frequency.

Thus the conditions of stability of certain systems with imposed rapid oscillations have been determined, but no general equations of motion have been obtained.

In the present paper the equations of motion are found for a general Lagrangian system which receives rapid oscillations, and the equations for small oscillations about an equilibrium position. From these the equations of motion and conditions for stability have been determined in certain special cases, which will be enumerated later.

[The publication of this investigation has been long delayed. Since its completion the paper (4) by Mr. P. Hirsch has appeared, of which the underlying idea is the same as that in the general discussion of the present paper.]

The method adopted differs from those previously used, in that the forced oscillations are taken to be of high frequency and small amplitude from the beginning, and modifications consequent on this assumption are made immediately, in the general Lagrangian equations of motion. Thus we assume that the imposed oscillations have indefinitely short periods, but finite accelerations, which necessitate the introduction of some limit method in order to solve the equations of motion of the system.

Consideration of the case of the simple inverted pendulum shows that the corresponding equations of motion should be obtainable by some such means. The pendulum has a finite oscillation about the vertically upright position, but the rapid vibration, with small period, of the point of support must cause some corresponding variation in the angular coordinate of the pendulum. This is imperceptible, the position of the rod that is observed at any instant being the mean position for the small vibrations that are taking place at the instant. The equation of motion for the rod in terms of the angle defining this *observed* position at any instant (that

is, excluding the local changes in position) is obtained by the immediate modification of the Lagrangian equations of motion of the system by means of the assumptions to which reference has been made. Thus the process involves the introduction of new coordinates to eliminate the effect of the rapid oscillations on those coordinates which do not receive the rapid periodic variations, and the taking of mean values over a period or a finite multiple of the periods of the imposed oscillations—that is, over an infinitesimal period of time. By this means equations of motion are obtained free from the variations in the order of magnitude of the terms which occur in the original Lagrangian equations.

The method is due to Professor J. H. Michell, of Melbourne, who has supervised the work and suggested the lines of development. The investigation was carried out in 1928 under the terms of a research grant from the University of Melbourne.

The general Lagrangian equations of motion and the equations for small oscillations have been obtained, and the equations of motion deduced for the following special cases :—

(i.) An inverted simple pendulum with two degrees of freedom, which receives rapid vertical oscillations at the point of support.

(ii.) Two rods linked end to end, and given rapid vertical oscillations at the point of support when in a position of unstable equilibrium. [The condition of stability determined agrees with that obtained by Mr. Stephenson ((2) (v.)).]

(iii.) Three rods connected as in (ii.).

The small oscillations of

(a) three equal simple pendulums pivoted so that they move in a horizontal plane,

(b) three pendulums of unequal length but of the same mass, free to move horizontally,

are discussed in greater detail.

(iv.) A spinning-top, the pivot of which is given rapid vertical oscillations.

The case of the simple pendulum with one degree of freedom is omitted, as it has been discussed in other papers.

List of previous Papers.

(1) Rayleigh.—Scientific Papers, iii.
(2) Stephenson.—(i.) "On a Class of Forced Oscillations," Quarterly Journal of Pure and Applied Mathematics (1905–6).
    (ii.) "The Forcing of Oscillations by Disturbances of Different Frequencies,"Phil. Mag.(July 1907).
    (iii.) "On Induced Stability," Phil. Mag. (1908).
    (iv.) "A New Type of Dynamical Stability," Proceedings of the Manchester Literary and Philosophical Society (1908).
    (v.) "On Induced Stability," Phil. Mag. (1909).
(3) Van der Pol and Strutt.—"The Stability of the Solutions of Mathieu's Equation," Phil. Mag. (Jan. 1928).
(4) Hirsch.—"Das Pendel mit oszillierendem Aufhängepunkt," *Zeitschrift für Angewandte Math. u. Mechanik.* (Feb. 1930).

The Stabilizing Effect of small Oscillations of High Frequency on a Lagrangian System.

Consider any general dynamical system, defined by co-ordinates $\xi_1, \xi_2 \ldots \xi_n, \theta_1, \theta_2 \ldots \theta_m$, of which the ξ-coordinates have given periodic variations, of small amplitude and high frequency. These are taken to be such that, though the variations ξ are indefinitely small, the velocities $\dot{\xi}$ are of the same order as the velocities $\dot{\theta}$, which are supposed finite, and the accelerations $\ddot{\xi}$ are indefinitely great.

[*E. g.* If

$$\xi = a \sin\left(\frac{2\pi}{\tau} t + \epsilon\right),$$

where a and τ are indefinitely small, but a/τ is finite of the order of the velocities $\dot{\theta}$,

$$\dot{\xi} = \frac{2\pi}{\tau} a \cos\left(\frac{2\pi}{\tau} t + \epsilon\right),$$

$$\ddot{\xi} = -\left(\frac{2\pi}{\tau}\right)^2 a \sin\left(\frac{2\pi}{\tau} t + \epsilon\right).$$

Hence $\dot{\xi}$ is finite and $\ddot{\xi}$ is infinitely great, being of order $1/\tau$.]

Following Lagrange's method, the kinetic energy is of the form

$$T = \tfrac{1}{2}(\Sigma_{r,\,s}A_{rs}\dot{\xi}_r\dot{\xi}_s + 2\Sigma_{r,\,s}B_{rs}\dot{\xi}_r\dot{\theta}_s + \Sigma_{r,\,s}C_{rs}\dot{\theta}_r\dot{\theta}_s),$$

with

$$A_{rs} = A_{sr}, \text{ etc.,}$$

and the work function may be written as

$$W = f(\xi_1 \ldots \xi_n, \ \theta_1 \ldots \theta_m).$$

The θ_r equation of motion is

$$\frac{d}{dt}\left(\frac{\partial T}{\partial \dot{\theta}_r}\right) - \frac{\partial T}{\partial \theta_r} = \frac{\partial W}{\partial \theta_r},$$

which gives, on substituting for T,

$$\frac{d}{dt}(\Sigma_s C_{rs}\dot{\theta}_s + \Sigma_s B_{sr}\dot{\xi}_s) - \tfrac{1}{2}\left(\Sigma_{p,\,s}\frac{\partial A_{ps}}{\partial \theta_r}\dot{\xi}_p\xi_s + \Sigma_{p,\,s}2\frac{\partial B_{ps}}{\partial \theta_r}\dot{\xi}_p\dot{\theta}_s\right.$$
$$\left. + \Sigma_{p,\,s}\frac{\partial C_{ps}}{\partial \theta_r}\dot{\theta}_p\dot{\theta}_s\right) = \frac{\partial W}{\partial \theta_r}.$$

In order to eliminate the infinite terms due to the high-frequency oscillations, we first introduce new quantities γ, defined by the m equations

$$\Sigma_s C_{rs}\theta_s + \Sigma_s B_{sr}\xi_s = \Sigma_s C_{rs}\gamma_s, \quad \ldots \quad (1)$$

so that

$$\Sigma_s C_{rs}(\theta_s - \gamma_s) + \Sigma_s B_{sr}\xi_s = 0. \quad \ldots \quad (1')$$

These make the $(\theta - \gamma)$ vanish when there are no ξ-oscillations.

Replacing

$$\theta_s - \gamma_s \ \text{ by } \ \eta_s. \quad \ldots \ldots \quad (2)$$

(1') becomes

$$\Sigma_s C_{rs}\eta_s + \Sigma_s B_{sr}\xi_s = 0. \quad \ldots \ldots \quad (3)$$

In these equations the η's vanish when there are no ξ-oscillations, and are of the same character as the ξ coordinates (*i. e.*, η is of the same order as ξ, and its derivatives are of the same order as the corresponding derivatives of ξ).

From the equation (1') we have

$$\Sigma_s C_{rs}\theta_s + \Sigma_s B_{sr}\xi_s = \Sigma_s C_{rs}\gamma_s.$$

Hence, differentiating with respect to t, and using the relation (2),

$$\Sigma_s C_{rs}\dot{\theta}_s + \Sigma_s B_{sr}\dot{\xi}_s = \Sigma_s C_{rs}\dot{\gamma}_s - (\Sigma_s \dot{C}_{rs}\eta_s + \Sigma_s \dot{B}_{sr}\xi_s),$$

and

$$\frac{d}{dt}(\Sigma_s C_{rs}\dot{\theta}_s + \Sigma_s B_{sr}\dot{\xi}_s)$$

$$= \Sigma_s \dot{\gamma}_s \left\{ \Sigma_u \frac{\partial C_{rs}}{\partial \theta_u}\dot{\eta}_u + \Sigma_u \frac{\partial C_{rs}}{\partial \theta_u}\dot{\gamma}_u + \Sigma_v \frac{\partial C_{rs}}{\partial \xi_v}\dot{\xi}_v \right\}$$

$$+ \Sigma_s C_{rs}\ddot{\gamma}_s - \frac{d}{dt}(\Sigma_s C_{rs}\eta_s + \Sigma_s \dot{B}_{sr}\xi_s).$$

Taking the ξ's, and hence the η's, to be indefinitely small, we now modify the functions C_{rs}, expressing them in terms of the new variables γ.

Thus, if $C_{rs} = f(\theta_1 \ldots \theta_m, \xi_1 \ldots)$, we consider the modified function $C_{rs}^* = f(\gamma_1 \ldots \gamma_m, 0, \ldots)$, obtained by replacing the θ's by the corresponding γ's and the ξ's by zero.

Then

$$\frac{\partial C_{rs}}{\partial \theta_u} = \frac{\partial C_{rs}^*}{\partial \gamma_u},$$

and all terms which do not have to be differentiated with respect to the time can be so modified.

Hence

$$\frac{d}{dt}(\Sigma_s C_{rs}\dot{\theta}_s + \Sigma_s B_{sr}\dot{\xi}_s)$$

$$= \Sigma_s \frac{d}{dt}(C_{rs}^*\dot{\gamma}_s) + \Sigma_s \left\{ \Sigma_u \left(\frac{\partial C_{rs}}{\partial \gamma_u}\eta_u\right) + \Sigma_v \left(\frac{\partial C_{rs}}{\partial \xi_v}\right)^* \dot{\xi}_v \right\} \dot{\gamma}_s$$

$$- \frac{d}{dt}(\Sigma_s \dot{C}_{rs}\eta_s + \Sigma_s \dot{B}_{sr}\xi_s),$$

where $\left(\dfrac{\partial C_{rs}}{\partial \xi_v}\right)^*$ means that the θ's are replaced by the γ's and the ξ's are put equal to zero after differentiation.

$\dfrac{\partial T}{\partial \theta_r}$ must also be expressed in terms of ξ, $\dot{\xi}$, η, $\dot{\eta}$, γ, $\dot{\gamma}$, by means of the relations

$$\theta = \gamma + \eta, \qquad \dot{\theta} = \dot{\gamma} + \dot{\eta}.$$

For this term the coefficients A_{rs} etc. of T may be modified by putting $\theta = \gamma$ and $\xi = 0$, since the ξ's (and hence the η's) are to be considered indefinitely small, and derivatives with respect to time of these coefficients will not occur.

Thus, since

$$T = \tfrac{1}{2}(\Sigma_{rs}A_{rs}\dot{\xi}_r\dot{\xi}_s + 2\Sigma_{rs}B_{sr}\dot{\xi}_s\dot{\theta}_r + \Sigma C_{rs}\dot{\theta}_r\dot{\theta}_s).$$

$$T^* = \tfrac{1}{2} \{ \Sigma_{rs} A^*_{rs} \dot{\xi}_r \dot{\xi}_s + 2\Sigma_{rs} B^*_{sr} \dot{\xi}_s (\dot{\gamma}_r + \dot{\eta}_r)$$
$$+ \Sigma_{rs} C^*_{rs} (\dot{\gamma}_r + \dot{\eta}_r)(\dot{\gamma}_s + \dot{\eta}_s) \},$$

with the same symbolism as before.

The work function W may also be modified in this way.

Then $\dfrac{\partial T}{\partial \theta_r}$ is replaced by

$$\frac{\partial T^*}{\partial \gamma_r} = \frac{1}{2} \left\{ \Sigma_{ps} \frac{\partial A^*_{ps}}{\partial \gamma_r} \dot{\xi}_p \dot{\xi}_s + 2\Sigma_p \left(\Sigma_s \frac{\partial B^*_{sp}}{\partial \gamma_r} \dot{\xi}_s + \Sigma_s \frac{\partial C^*_{ps}}{\partial \gamma_r} \dot{\eta}_s \right) \dot{\gamma}_p \right.$$
$$\left. + \Sigma_{ps} \frac{\partial C^*_{ps}}{\partial \gamma_r} \dot{\gamma}_p \dot{\gamma}_s + \Sigma_{ps} \frac{\partial C^*_{ps}}{\partial \gamma_r} \dot{\eta}_p \dot{\eta}_s + 2\Sigma_{ps} \frac{\partial B^*_{sp}}{\partial \gamma_r} \dot{\xi}_s \dot{\eta}_p \right\},$$

and the θ_r (or γ_r) equation of motion becomes

$$\Sigma_s \frac{d}{dt}(C^*_{rs} \dot{\gamma}_s) + \Sigma_s \left\{ \Sigma_u \frac{\partial C^*_{rs}}{\partial \gamma_u} \dot{\eta}_u + \Sigma_v \frac{\partial C^*_{rs}}{\partial \xi_v} \dot{\xi}_v \right\} \dot{\gamma}_s$$
$$- \frac{d}{dt}(\Sigma \dot{C}_{rs} \eta_s + \Sigma_s \dot{B}_{sr} \xi_s) - \frac{1}{2} \left\{ \Sigma_{ps} \frac{\partial A^*_{ps}}{\partial \gamma_r} \dot{\xi}_p \dot{\xi}_s \right.$$
$$+ 2\Sigma_{ps} \frac{\partial B^*_{sp}}{\partial \gamma_r} \dot{\xi}_s \dot{\gamma}_p + 2\Sigma_{ps} \frac{\partial B^*_{sp}}{\partial \gamma_r} \dot{\xi}_s \dot{\eta}_p + \Sigma_{ps} \frac{\partial C^*_{ps}}{\partial \gamma_r} \dot{\gamma}_p \dot{\gamma}_s$$
$$\left. + 2\Sigma_{ps} \frac{\partial C^*_{ps}}{\partial \gamma_r} \dot{\gamma}_p \dot{\eta}_s + \Sigma_{ps} \frac{\partial C^*_{ps}}{\partial \gamma_r} \dot{\eta}_p \dot{\eta}_s \right\} = \frac{\partial W^*}{\partial \gamma_r}. \quad (4)$$

Hence the θ's do not now occur explicitly in the equation of motion. From equation (4) it may be seen that the $\ddot{\gamma}$'s are of finite order at most, since all the other terms are at most of that order.

Further modification is necessary to free the equation of motion from terms such as the $\dot{\eta}$'s, which, though themselves finite, have infinite derivatives.

To do this mean values are taken over an interval of time τ, which is the lowest common multiple of the periods of the ξ and η coordinates (τ is taken to be of the same order as the periods as ξ and η, *i. e.*, infinitesimal). The finite parts of the expressions may be taken as constant throughout the interval, so that the mean value over such an interval of

time τ, of $\dfrac{\partial C^*_{rs}}{\partial \gamma_u} \dot{\eta}_u \dot{\gamma}_s$, is $\dfrac{1}{\tau} \displaystyle\int_t^{t+\tau} \dfrac{\partial C^*_{rs}}{\partial \gamma_u} \dot{\eta}_u \dot{\gamma}_s dt$, in which $\dfrac{\partial C^*_{rs}}{\partial \gamma_u} \dot{\gamma}_s$

may be regarded as constant during the interval τ, since its rate of change is finite ($\dot{\gamma}$ and $\ddot{\gamma}$ being finite).

Therefore the mean value is $\dfrac{1}{\tau}\dfrac{\partial C^*_{rs}}{\partial \gamma_u}\dot{\gamma}_s\bar{\dot{\eta}}_u\tau$, where $\dot{\eta}$ is the mean value of $\dot{\eta}$ for the interval τ. But $\bar{\dot{\eta}}_u = 0$, since τ is a multiple of the period of η_u, and hence of $\dot{\eta}_u$.

Thus the mean value of $\dfrac{\partial C^*_{rs}}{\partial \gamma_u}\dot{\eta}_u\dot{\gamma}_s$ is zero.

Similarly the mean values of the other terms may be found. (If all the ξ coordinates have the same period, the η coordinates also have this period, so that the interval over which the mean is taken is a single period of the ξ (or η) oscillations.)

Hence, taking mean values throughout the equation, we obtain

$$\Sigma_s \frac{d}{dt}(C^*_{rs}\dot{\gamma}_s) - \frac{1}{2}\left\{ \Sigma_{ps}\frac{\partial A^*_{ps}}{\partial \gamma_r}\overline{\dot{\xi}_p\dot{\xi}_s} + 2\Sigma_{ps}\frac{\partial B^*_{ps}}{\partial \gamma_r}\overline{\dot{\xi}_p\dot{\eta}_s} \right.$$
$$\left. + \Sigma_{ps}\frac{\partial C^*_{ps}}{\partial \gamma_r}\overline{\dot{\gamma}_p\dot{\gamma}_s} + \Sigma_{ps}\frac{\partial C^*_{ps}}{\partial \gamma_r}\overline{\dot{\eta}_p\dot{\eta}_s} \right\} = \frac{\partial W}{\partial \gamma_r} \quad (5)$$

as the equation for γ_r, which now defines some mean position in the interval τ. (In this equation no modification of symbolism has been made to denote the modification of the $\dot{\gamma}$'s due to the taking of mean values. These symbols now have a different meaning from the corresponding ones in (4).)

The γ's of the equation (4) are equal to the original coordinates θ to the degree of approximation employed.

The γ's of equation (5) gives the position at some instant of an infinitesimal period of time τ, and hence, to the degree of approximation adopted, are the same as the γ's given by (4).

Hence (5) gives the position of the body at any instant.

The $\dot{\gamma}$'s of equation (5) and those of (4) are equal. For, if $\bar{\gamma}$ is the mean value of γ in the period τ,

$$\bar{\gamma} = \frac{1}{\tau}\int_t^{t+\tau}\gamma\,dt,$$

$$\dot{\gamma} = \frac{1}{\tau}(\gamma_{t+\tau} - \gamma_t)$$

$$= \dot{\bar{\gamma}}, \quad \text{the mean velocity for the interval } \tau.$$

$\ddot{\gamma}$ is finite (by equation (4)), hence to the order of approximation used above,

$$\dot{\gamma} = \dot{\bar{\gamma}}, \quad \text{so that} \quad \dot{\bar{\gamma}} = \dot{\gamma} \quad \text{to the same order.}$$

The $\dot{\gamma}$'s of equation (4) differ from the $\dot{\theta}$'s by the finite amounts $\dot{\eta}$, which may be found by means of the relations

(3). Thus the velocity at any instant can be obtained when these equations are solved.

The $\ddot{\gamma}$'s are of the same order in equations (4) and (5), but differ by a finite amount.

Higher derivatives differ in order, those obtained from (4) being indefinitely large, while those from (5) remain finite.

Hence equations (5) give the position and velocity in the dynamical problem considered.

Small Oscillations about an Equilibrium Position.

Suppose the kinetic energy is given by an expression of the form

$$2T = \Sigma_{rs}A_{rs}\dot{\xi}_r\dot{\xi}_s + 2\Sigma_{rs}B_{sr}\dot{\xi}_s\dot{\theta}_r + \Sigma_{rs}C_{rs}\dot{\theta}_r\dot{\theta}_s,$$

and the work function by

$$2W = 2W_0 + 2\Sigma D_r\theta_r + 2\Sigma E_r\xi_r + \Sigma_{rs}F_{rs}\theta_r\theta_s + \dots,$$

the notation for the coordinates being the same as before. (If the coordinates are zero for the position of equilibrium, the D's are zero ; in any case they are small.)

As before, the θ_r equation of motion is

$$\frac{d}{dt}\left(\frac{\partial T}{\partial \dot{\theta}_r}\right) - \frac{\partial T}{\partial \theta_r} = \frac{\partial W}{\partial \theta_r},$$

or

$$\frac{d}{dt}(\Sigma_s C_{rs}\dot{\theta}_s + \Sigma_s B_{sr}\dot{\xi}_s)$$
$$-\frac{1}{2}\left(\Sigma_{ps}\frac{\partial A_{ps}}{\partial \theta_r}\dot{\xi}_p\dot{\xi}_s + 2\Sigma_{ps}\frac{\partial B_{sp}}{\partial \theta_r}\dot{\xi}_s\dot{\theta}_p + \Sigma_{ps}\frac{\partial C_{ps}}{\partial \theta_r}\dot{\theta}_p\dot{\theta}_s\right)$$
$$= \frac{\partial W}{\partial \theta_r}. \quad (1)$$

The coefficients A_{rs}, B_{rs}, C_{rs}, etc. are all functions of the θ's and ξ's. The oscillations are taken to be so small that all powers of the coordinates are rejected except the lowest which occur, except in terms which are to be differentiated with respect to time. In these the order will rise with the differentiation ; *e. g.*, since $\dot{\theta}$ and $\dot{\xi}$ are finite in the small oscillations, some of the terms involved in $\dfrac{\partial T}{\partial \theta_r}$ are finite and some of order θ. Hence the coefficients A_{rs} etc. cannot be considered as constants, but may be taken to be of the second degree in the θ's and ξ's, so that $\dfrac{\partial A_{ps}}{\partial \theta_r}$ etc. are

of the first degree in θ and ξ, and equation (1) contains terms down to the order of θ and ξ.

Corresponding to the modification of the general equations of motion, we put

$$\Sigma_s C_{rs}\theta_s + \Sigma_s B_{sr}\xi_s = \Sigma_s C_{rs}\gamma_s \quad . \quad . \quad . \quad (2)$$

or

$$\Sigma_s C_{rs}\eta_s + \Sigma_s B_{sr}\xi_s = 0, \quad . \quad . \quad . \quad . \quad (2')$$

where

$$\eta_s = \theta_s - \gamma_s.$$

Equations $(2')$ are sufficient to determine the η's, which vanish when there are no ξ oscillations and are of the same character as the ξ's. Proceeding as in the general theory above, we differentiate equation (2) and obtain

$$\frac{d}{dt}(\Sigma_s C_{rs}\dot{\theta}_s + \Sigma_s B_{sr}\dot{\xi}_s)$$

$$= \Sigma_s \frac{d}{dt}(C_{rs}^*\dot{\gamma}_s) + \Sigma_s \left\{ \Sigma_u \frac{\partial C_{rs}^*}{\partial \gamma_u}\dot{\eta}_u + \Sigma_v \left(\frac{\partial C_{rs}}{\partial \xi_v}\right)^* \dot{\xi}_v \right\} \dot{\gamma}_s$$

$$- \frac{d}{dt}(\Sigma \dot{C}_{rs}\eta_s + \Sigma \dot{B}_{sr}\xi_s),$$

where C_{rs}^* is the modified function obtained by replacing the θ's by γ's, and the ξ's by zero, in C_{rs}.

In the same way $\dfrac{\partial T}{\partial \theta_r}$ is replaced by

$$\frac{\partial T}{\partial \gamma_r} = \frac{1}{2} \left\{ \Sigma_{ps} \frac{\partial A_{ps}^*}{\partial \gamma_r}\dot{\xi}_p\dot{\xi}_s + 2\Sigma_p \left(\Sigma_s \frac{\partial B_{sp}^*}{\partial \gamma_r}\dot{\xi}_s + \Sigma_s \frac{\partial C_{ps}^*}{\partial \gamma_r}\dot{\eta}_s \right)\dot{\gamma}_p \right.$$

$$\left. + \Sigma_{ps} \frac{\partial C_{ps}^*}{\partial \gamma_r}\dot{\gamma}_p\dot{\gamma}_s + \Sigma_{ps} \frac{\partial C_{ps}^*}{\partial \gamma_r}\dot{\eta}_p\dot{\eta}_s + \Sigma_{ps} \frac{\partial B_{sp}^*}{\partial \gamma_r}\dot{\xi}_s\dot{\eta}_p \right\},$$

where the coefficients $\dfrac{\partial A_{rs}^*}{\partial \gamma_r}$ etc. are taken to be partly constant and partly of the first degree in γ_r.

The equation of motion then becomes

$$\frac{d}{dt}(\Sigma_s C_{rs}^*\dot{\gamma}_s)$$

$$+ \Sigma \left\{ \Sigma_u \frac{\partial C_{rs}^*}{\partial \gamma_u}\eta_u + \Sigma_v \left(\frac{\partial C_{rs}}{\partial \xi_u}\right)^* \dot{\xi}_v \right\} \dot{\gamma}_s - \frac{d}{dt}(\Sigma \dot{C}_{rs}\eta_s + \Sigma \dot{B}_{sr}\xi_s)$$

$$- \frac{1}{2} \left\{ \Sigma_{ps} \frac{\partial A_{ps}^*}{\partial \gamma_r}\dot{\xi}_p\dot{\xi}_s + 2\Sigma_{ps} \frac{\partial B_{sp}^*}{\partial \gamma_r}\dot{\xi}_s\dot{\gamma}_p + 2\Sigma_{ps} \frac{\partial B_{sp}}{\partial \gamma_r}\dot{\xi}_s\dot{\eta}_p \right.$$

$$\left. + \Sigma_{ps} \frac{\partial C_{ps}^*}{\partial \gamma_r}\dot{\gamma}_p\dot{\gamma}_s + 2\Sigma_{ps} \frac{\partial C_{ps}}{\partial \gamma_r}\dot{\gamma}_p\dot{\eta}_s + \Sigma_{ps} \frac{\partial C_{ps}}{\partial \gamma_r}\dot{\eta}_p\dot{r}_s \right\} = \frac{\partial W}{\partial \gamma_r}.$$

$$(3)$$

From equation (3) it appears that the ˙'s are finite, since all the other terms of the equation are finite at most.

Therefore, if the motion is from the equilibrium position, $\dot\gamma$ is small in a small oscillation, and the terms such as $\dfrac{\partial C^*_{ps}}{\partial\gamma_r}\dot\gamma_p\dot\gamma_s$ may be neglected.

Taking mean values over a period of time τ, which is a multiple (supposed infinitesimal) of the periods of the ξ and η oscillations, the variation in terms such as $\dfrac{\partial A^*_{ps}}{\partial\gamma}$ and $\dot\gamma$ may be neglected, as in the previous work, and the equation becomes

$$\Sigma_s C^*_{rs}\ddot\gamma_s - \frac{1}{2}\left\{\Sigma_{ps}\frac{\partial A^*_{ps}}{\partial\gamma_r}\overline{\xi_p\xi_s} + 2\Sigma_{ps}\frac{\partial B^*_{ps}}{\partial\gamma_r}\overline{\dot\xi_p\eta_s}\right.$$
$$\left. + \Sigma_{ps}\frac{\partial C^*_{ps}}{\partial\gamma_r}\overline{\dot\eta_p\eta_s}\right\} = \frac{\partial W}{\partial\gamma_r}, \quad (4)$$

which is the γ_r equation of motion.

(The term $\dfrac{dC^*_{rs}}{dt}\dot\gamma_s$ is omitted, since it is of the second degree in $\dot\gamma$, and therefore is of the second order of smallness.)

The terms $\dfrac{\partial A^*_{ps}}{\partial\gamma_r}$ etc. in general involve the γ's to the first power, as well as a constant term.

(4) may be written

$$\Sigma_s C^*_{rs}\ddot\gamma_s$$
$$= \frac{\partial}{\partial\gamma_r}\{W + \tfrac{1}{2}\Sigma_{ps}A^*_{ps}\overline{\dot\xi_p\dot\xi_s} + \Sigma_{ps}B^*_{ps}\overline{\dot\xi_p\eta_s} + \tfrac{1}{2}\Sigma_{ps}C^*_{ps}\overline{\dot\eta_p\eta_s}\} = \frac{\partial W'}{\partial\gamma_r},$$

say, where $2W' = 2(W + \tfrac{1}{2}\Sigma A_{ps}\overline{\dot\xi_p\dot\xi_s} + \ldots)$
$$= 2W'_0 + 2\Sigma_r D'_r\gamma_r + \Sigma_{rs}F'_{rs}\gamma_r\gamma_s + \ldots;$$

∴ the equations of motion are of the form

$$\Sigma_s C^*_{rs}\ddot\gamma_s = D'_r + \Sigma_s F'_{rs}\gamma_s,$$

the coefficients D'_r, F'_{rs}, involving $\overline{\dot\xi_r\dot\xi_s}$ etc.

The coefficients D'_r will be small (since the D's are small); hence with a suitable change of variable the equations take the form

$$\Sigma_s C^*_{rs}\ddot\gamma_s = \Sigma_s F_{rs}\gamma_s$$
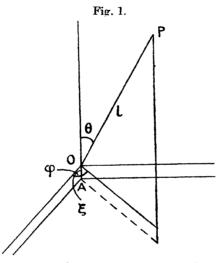
(with the necessary modification of the coefficients), and the conditions for small oscillations may be determined.

Deduction of Equations of Motion and Conditions of
Stability for some Special Cases.

(The case of a simple pendulum with one degree of
freedom has been investigated in some of the papers men-
tioned below, and therefore will be omitted here.)

(i.) *The case of an inverted simple pendulum with two*
degrees of freedom, which receives rapid vertical oscillations at
the point of support.

The position of the bob P is defined by the polar co-
ordinates (l, θ, ϕ).

Fig. 1.

The coordinates of the point of support O at any instant
are $(0, 0, \xi)$ referred to axes as in fig. 1.

The kinetic energy is given by

$$T = \tfrac{1}{2}m(\dot{\xi}^2 - 2l\dot{\xi}\dot{\theta}\sin\theta + l^2\dot{\theta}^2 + l^2\sin^2\theta\,\dot{\phi}^2). \quad . \quad . \quad (1)$$

Hence, substituting in the general equation of motion (5) (on
p. 465), the γ_1 equation of motion is

$$\frac{d}{dt}(ml^2\dot{\gamma}_1) - \tfrac{1}{2}(-2ml\dot{\xi}\dot{\eta}_1\cos\gamma_1 + 2ml^2\dot{\gamma}_2{}^2\sin\gamma_1\cos\gamma_1)$$
$$= mgl\sin\gamma_1, \quad (2)$$

and the γ_2 equation of motion is

$$\frac{d}{dt}(ml^2\dot{\gamma}_2\sin^2\gamma_1) = 0. \quad . \quad . \quad . \quad . \quad (3)$$

The equations for η_1 and η_2 are

$$l\eta_1 - \xi \sin\theta = 0, \qquad l^2\eta_2 \sin^2\theta = 0.$$

Hence $\qquad l\dot{\eta}_1 = \dot{\xi}\sin\gamma_1, \qquad\qquad \eta_2 = 0,$

$$l\dot{\eta}_1\dot{\xi} = \dot{\xi}^2 \sin\gamma_1,$$

$$l\overline{\dot{\xi}\dot{\eta}_1} = \overline{\dot{\xi}^2}\sin\gamma_1 \quad \text{(taking the mean over a period}$$
$$\text{of the } \xi \text{ oscillation),}$$

and (2) becomes

$$l\ddot{\gamma}_1 + \frac{1}{l}\overline{\dot{\xi}^2}\cos\gamma_1\sin\gamma_1 = g\sin\gamma_1 + l\dot{\gamma}_2{}^2\sin\gamma_1\cos\gamma_1,$$

and (3) gives

$$\dot{\gamma}_2\sin^2\gamma_1 = \text{constant}, \;\; = \sqrt{C}, \text{ say.} \quad . \quad . \quad . \quad (4)$$

Therefore the γ_1 equation of motion is

$$l\ddot{\gamma}_1 - \frac{Cl\cos\gamma_1}{\sin^3\gamma_1} + \frac{\overline{\dot{\xi}^2}}{l}\cos\gamma_1\sin\gamma_1 - g\sin\gamma_1 = 0.$$

Hence, integrating with respect to γ_1, and dividing by l, we obtain

$$\dot{\gamma}_1{}^2 + \frac{C}{\sin^2\gamma_1} - (\overline{\dot{\xi}^2}/l^2)\cos^2\gamma_1 = -\frac{2g}{l}\cos\gamma_1 + C_1. \quad . \quad (5)$$

To simplify this equation, put

$$x = \cos\gamma_1, \qquad \dot{x} = -\dot{\gamma}_1\sin\gamma_1,$$

which gives

$$\dot{x}^2 + (1-x^2)\left(-\frac{x^2\overline{\dot{\xi}^2}}{l^2} + \frac{2g}{l}x - C_1\right) = -C. \quad . \quad (5')$$

Assume as a solution

$$x = \cos\alpha + P\cos\overline{\lambda t + f},$$

where α is a constant determined by initial conditions and P is so small that P^3 can be neglected; *i.e.*, we assume a small disturbance from motion in a cone, as in festoon motion. Then

$$\dot{x} = -\lambda P\sin(\lambda t + f),$$

and the equation (5′) becomes

$$\lambda^2P^2\{1 - \cos^2(\lambda t + f)\} + \{1 - \cos^2\alpha - 2P\cos\alpha\cos(\lambda t + f)$$

$$-P^2 \cos^2(\lambda t + f)\} \left[\frac{-\bar{\xi}^2}{l^2} \{\cos\alpha + P\cos(\lambda t + f)\}^2 \right.$$

$$+ \frac{2g}{l} \{\cos\alpha + P\cos(\lambda t + f)\} - C_1 \left] = -C. \right.$$

Hence, equating coefficients of powers of $\cos(\lambda t + f)$, and solving the resulting equations,

$$C_1 = -Z(2\cos^2\alpha - 1) + \frac{g(3\cos^2\alpha - 1)}{l\cos\alpha},$$

where Z replaces $\dfrac{\bar{\xi}^2}{l^2}$;

$$\therefore \qquad \lambda^2 = 4Z\cos^2\alpha - \frac{g(3\cos^2\alpha + 1)}{l\cos\alpha}.$$

If $\cos\alpha$ is negative (*i. e.*, the steady motion is as in fig. 2), λ^2 is positive. If $\cos\alpha$ is positive (the steady motion being as in fig. 3), λ^2 is positive if

$$4Z\cos^2\alpha > \frac{gl(3\cos^2\alpha + 1)}{\cos\alpha} \quad \ldots \quad \ldots \quad (6)$$

Fig. 2.

Fig. 3.

(This reduces to the condition of stability of a pendulum with one degree of freedom, if $\alpha = 0$.) Also

$$P^2 = \frac{1}{\lambda^2} \left[-C + \sin^4\alpha \left(Z - \frac{g}{l\cos\alpha} \right) \right];$$

$\therefore$ P^2 is positive if

$$C < \sin^4\alpha \left(Z - \frac{g}{l\cos\alpha} \right), \quad \ldots \quad \ldots \quad (7)$$

λ^2 being positive.

[(i.) If $\alpha = 0$,

$$\lambda^2 = 4Z - 4g/l, \qquad C_1 = -Z + 2g/l, \qquad P^2 = -C/\lambda^2 \, ;$$

$\therefore$ if λ^2 is positive, $C = 0$, since C cannot be negative ; *i.e.*, $\dot{\phi} = 0$, and motion reduces to that of a pendulum with one degree of freedom.

(ii.) If $\alpha = \pi$,

$$\lambda^2 = 4Z + 4g/l, \qquad C_1 = -Z - 2g/l, \qquad P^2 = -C/\lambda^2 \, ;$$

i.e., is negative unless $C = 0$.

(iii.) If $\alpha = \pi/2$, C_1 is infinite.

(iv.) $P = 0$ if

$$C = \sin^4\alpha \left(Z - \frac{g}{l\cos\alpha} \right),$$

giving steady motion.]

If conditions (6) and (7) are satisfied, a festoon motion takes place. To find the limits for the zone or zones of such motion, put $\dot{\gamma}$ equal to zero in the equation for $\dot{\gamma}$.

Equation (5) becomes

$$\frac{C}{\sin^2\gamma_1} - Z\cos^2\gamma_1 = -2\frac{g}{l}\cos\gamma_1 + C_1, \quad . \quad . \quad (5'')$$

which gives the extreme values of γ_1. Or, replacing $\cos\gamma$ by x, and clearing the equation of fractions, this becomes

$$Zx^4 l - 2gx^3 - (Z - C_1)lx^2 + 2gx + Cl - C_1 l = 0.$$

Substituting for C_1, the equation becomes

$$lZx^4 - 2gx^3 - \left[2Zl\cos^2\alpha - g\frac{3\cos^2\alpha - 1}{\cos\alpha} \right]x^2 + 2gx$$
$$+ Zl(2\cos^2\alpha - 1) - g\frac{3\cos^2\alpha - 1}{\cos\alpha} = -Cl, \quad (8)$$

which determines the extreme positions of the pendulum.

From the relation

$$\dot{\phi}^2\sin^4\gamma = C$$

we see that if C is not zero and $\dot{\phi}$ is finite γ cannot be zero or π ; *i.e.*, quantities β_1, β_2 exist, such that

$$0 < \beta_1 \leqq \gamma_1 \leqq \beta_2 < \pi,$$

and for the values β_1, β_2 of γ_1, $\dot{\gamma}_1$ will be zero.
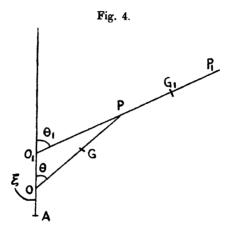
Thus, if $\cos\beta_1=b_1$ and $\cos\beta_2=b_2$, b_1 and b_2 are roots of equation (8), which therefore has at least two real roots.

If $x=0$, *i. e.*, $\gamma=\pi/2$, the equation (5′), which may written

$$\dot{x}^2 l + Cl - Zx^2(1-x^2)l = -2gx(1-x^2) + C_1(1-x^2)l,$$

becomes $\qquad\qquad \dot{x}^2 = C_1 - C ;$

∴ if $C_1 > C$, this value of γ_1 is possible.

(ii.) *Two rods linked together end to end are given rapid vertical oscillations at the point of support when in a position of unstable equilibrium.*

Suppose that the rods OP, PP′ are of mass m, m_1 and of length l, l_1, and that the centres of mass G, G_1 are distant

Fig. 4.

h, h_1 from O and P respectively. Let k be the radius of gyration of the rod OP about G, and k_1 be the radius of gyration of PP′ about G_1.

$$T = \tfrac{1}{2}[\{m(k^2+h^2)+m_1 l^2\}\dot{\theta}^2 + m_1(k_1^2+h_1^2)\dot{\theta}_1^2 + (m+m_1)\dot{\xi}^2$$
$$-2(mh+m_1l)\dot{\xi}\dot{\theta}\sin\theta - 2m_1 h_1\dot{\xi}\dot{\theta}_1\sin\theta_1$$
$$+2m_1 h_1 l\dot{\theta}\dot{\theta}_1\cos(\theta_1-\theta)]$$

$$W = g(mh+m_1l)(1-\cos\theta) + m_1 g h_1(1-\cos\theta_1).$$

Substituting in the general equations of motion, the γ equation of motion is

Phil. Mag. S. 7. Vol. 13. No. 84. *Suppl. Feb.* 1932. 2 I

$$\frac{d}{dt}\left[\{m(k^2+h^2)+m_1l^2\}\dot{\gamma}+m_1h_1l\cos(\gamma_1-\gamma)\dot{\gamma_1}\right]$$

$$-\tfrac{1}{2}\left[-2(mh+m_1l)\overline{\dot{\xi}\eta}\cos\gamma+2m_1h_1l\dot{\gamma}\dot{\gamma_1}\sin(\gamma_1-\gamma)\right.$$

$$\left.+2m_1h_1l\overline{\dot{\eta}\dot{\eta_1}}\sin(\gamma_1-\gamma)\right]=g(mh+m_1l)\sin\gamma,$$

and the γ_1 equation of motion is

$$\frac{d}{dt}\left[h_1l\dot{\gamma}\cos(\gamma_1-\gamma)+(k_1^2+h_1^2)\dot{\gamma_1}\right]$$

$$-\tfrac{1}{2}\left[-2h_1\overline{\dot{\xi}\eta_1}\cos\gamma_1-2h_1l\dot{\gamma}\dot{\gamma_1}\sin(\gamma_1-\gamma)\right.$$

$$\left.-2h_1l\overline{\dot{\eta}\dot{\eta_1}}\sin(\gamma_1-\gamma)\right]=gh_1\sin\gamma_1.$$

The equations for η and η_1 are

$$\left.\begin{aligned}
[m(k^2+h^2)+m_1l^2]\eta+m_1h_1l\eta_1\cos(\theta_1-\theta)\\
-(mh+m_1l)\xi\sin\theta=0,\\
m_1h_1l\eta\cos(\theta_1-\theta)+m_1(k_1^2+h_1^2)\eta_1-m_1h_1\xi\sin\theta_1=0
\end{aligned}\right\}\quad.\quad.\quad(1)$$

Therefore the equations to determine $\overline{\dot{\xi}\eta}$ etc. are

$$[m(k^2+h^2)+m_1l^2]\dot{\eta}+m_1h_1l\dot{\eta_1}\cos(\gamma_1-\gamma)=(mh+m_1l)\dot{\xi}\sin\gamma,$$

$$m_1h_1l\dot{\eta}\cos(\gamma_1-\gamma)+m_1(k_1^2+h_1^2)\dot{\eta_1}=m_1h_1\dot{\xi}\sin\gamma_1.$$

To find the form of the terms such as $\overline{\dot{\xi}\eta}$, we put

$$\eta=\xi f(\theta,\theta_1)=\xi f,\qquad \eta_1=\xi f_1(\theta,\theta_1)=\xi f_1.$$

Then

$$\dot{\xi}\eta=\dot{\xi}^2 f+\xi\dot{\xi}\dot{f},\qquad \dot{\xi}\eta_1=\dot{\xi}^2 f_1+\xi\dot{\xi}\dot{f_1},$$

$$\dot{\eta}\dot{\eta_1}=ff_1\dot{\xi}^2+\xi\dot{\xi}(f\dot{f_1}+f_1\dot{f})+\xi^2\dot{f}\dot{f_1}.$$

Taking mean values over a period τ of the rapid oscillation,

$$\dot{\xi}\eta=\frac{1}{\tau}\int_t^{t+\tau}f(\theta,\theta_1)\dot{\xi}^2dt+\frac{1}{\tau}\int_t^{t+\tau}\xi\dot{\xi}\dot{f}dt.$$

The variations in θ and θ_1 are of the order τ in this interval; therefore $f(\theta,\theta_1)$ may be regarded as constant. The second term on the right-hand side is of the order τ, since the integrand is of order τ (ξ being of that order, and the other terms being finite).

Hence, to finite order,

$$\overline{\dot{\xi}\eta}=f(\theta,\theta_1)\overline{\dot{\xi}^2}=f(\gamma,\gamma_1)\overline{\dot{\xi}^2}.$$

Similarly

$$\overline{\dot{\xi}\eta_1}=f_1(\theta,\theta_1)\overline{\dot{\xi}^2}=f_1(\gamma,\gamma_1)\overline{\dot{\xi}^2}\ \text{etc.}$$

where f, f_1, are obtained by solving the equations (1).

Stability of Two Equal Uniform Rods in a Vertical Position.

The equations of motion for small oscillations are

$$\tfrac{1}{2}l^2\ddot{\gamma} + \tfrac{1}{3}l^2\ddot{\gamma}_1 - \tfrac{27}{14}\overline{\xi^2}\gamma + (\tfrac{17}{7}\overline{\xi^2} - \tfrac{1}{2}gl)\gamma_1 = 0 \quad . \quad . \quad (1)$$

$$\tfrac{4}{3}l^2\ddot{\gamma} + \tfrac{1}{2}l^2\ddot{\gamma}_1 + (\tfrac{27}{7}\overline{\xi^2} - \tfrac{3}{2}lg)\gamma - \tfrac{27}{14}\overline{\xi^2}\gamma_1 = 0. \quad . \quad . \quad (2)$$

Put $\gamma = \mathrm{L}\sin(pt + \epsilon)$, $\qquad \gamma_1 = \mathrm{M}\sin(pt + \epsilon)$.

Then the equation for p is

$$\tfrac{7}{36}p^4 - (\tfrac{11}{2}Z - \tfrac{7}{6}g/l)p^2 + \tfrac{81}{28}Z^2 - \tfrac{9}{2}Zg/l + \tfrac{3}{4}g^2/l^2 = 0$$

$$\left(\text{where Z replaces } \frac{\overline{\xi^2}}{l^2} \right).$$

The discriminant of this equation reduces to $28(Z - \tfrac{1}{6}g/l)^2$, and therefore is positive; so that real values of p^2 are obtained.

These are positive, *i.e.*, the motion is stable if

(1) $\quad (\tfrac{11}{2} + 2\sqrt{7})Z > (\tfrac{7}{6} + \tfrac{1}{3}\sqrt{7})g/l,$

$\quad$ *i.e.*, $\qquad Z > \cdot1898g/l,$

(2) $\quad (\tfrac{11}{2} - 2\sqrt{7})Z > (\tfrac{7}{6} - \tfrac{1}{3}\sqrt{7})g/l$ (these being the conditions corresponding to the two roots);

$\quad$ *i.e.*, $\qquad Z > 1\cdot367g/l.$

[If $\xi = 2a\cos nt$, $\quad \overline{\xi^2} = 2(an)^2,$

and the condition for stability is

$$a^2n^2/l^2 > \cdot6835g/l.$$

The condition given by Stephenson (1909) was

$$a^2n^2/l^2 > \cdot683g/l.]$$

Small Oscillations of Two Rods which are Pivoted so that they are free to move in a Horizontal Plane.

The equations of motion are

$$\mathrm{K}[lh_1\ddot{\gamma} + (k_1^2 + h_1^2)\ddot{\gamma}_1]$$
$$= \overline{\xi^2}lh_1^2(h + m_1l/m)\gamma - \overline{\xi^2}h_1^2(k^2 + h^2 + m_1l^2/m)\gamma_1,$$

and

$$\mathrm{K}[(k^2 + h^2 + m_1l^2/m)\ddot{\gamma} + m_1lh_1\ddot{\gamma}_1/m]$$
$$= \{\overline{\xi^2}m_1h_1^2l(h + m_1l/m)/m\}\gamma_1 - \overline{\xi^2}(k_1^2 + h_1^2)(h + m_1l/m)^2\gamma,$$

where

$$\mathrm{K} = (k_1^2 + h_1^2)(k^2 + h^2) + m_1l^2k_1^2/m.$$

Let $\gamma = M \sin (pt + \epsilon)$, $\qquad \gamma_1 = N \sin (pt + \epsilon)$.

The equation for p is

$$K^2 p^4 - p^2 \bar{\xi}^2 [2 m_1 l^2 h_1^2 (h + m_1 l/m)/m + h_1^2 (k^2 + h^2 + m_1 l^2/m)^2$$
$$+ (k_1^2 + h_1^2)^2 (h + m_1 l/m)^2] + (\bar{\xi}^2)^2 h_1^2 (h + m_1 l/m)^2 = 0.$$

Solving for p^2, we get as discriminant an expression which is positive for any dimensions of the rods ; hence there are two real positive values for p^2 and four real roots for p, *i.e.*, the two rods have oscillatory motion about the position $\gamma = 0$, $\gamma_1 = 0$.

For the case of two equal uniform rods of length l, the values of p^2 are

$$2(2\sqrt{2} + 3)\bar{\xi}^2/l^2, \quad 2(3 - 2\sqrt{2})\bar{\xi}^2/l^2.$$

(iii.) *The Equations of Motion of Three Rods linked end to end, if one end of the System is given Rapid Oscillations.*

The rods are supposed capable of motion in one plane, which is taken to be vertical, and are initially in the position of unstable equilibrium. The rapid oscillations are vertical.

Suppose the rods OP, PQ, QR are of mass m_1, m_2, m_3 and of length l_1, l_2, l_3, and that the centres of mass G_1, G_2, G_3 are distant h_1, h_2, h_3 from O, P, and Q respectively. Let the radii of gyration of the rods about their centres of mass be k_1, k_2, k_3.

The rapid oscillation is measured by ξ, and the coordinates are θ, ϕ, ψ, as in the figure.
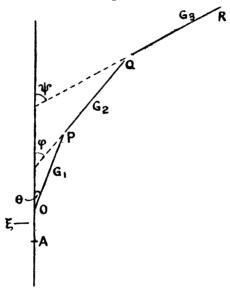
Proceeding as in the previous cases, the γ_1 equation of motion is

$$\frac{d}{dt} \left[\{ m_1 (k_1^2 + h_1^2) + (m_2 + m_3) l_1^2 \} \dot{\gamma}_1 \right.$$
$$+ (m_2 h_2 + m_3 l_2) l_1 \dot{\gamma}_2 \cos (\gamma_1 - \gamma_2) + m_3 l_1 h_3 \cos (\gamma_3 - \gamma_1) \dot{\gamma}_3]$$
$$- \tfrac{1}{2} [-2 \{ m_1 h_1 + (m_2 + m_3) l_1 \} \bar{\dot{\xi} \dot{\eta}_1} \cos \gamma_1$$
$$- 2 l_1 (m_2 h_2 + m_3 l_2) \dot{\gamma}_1 \dot{\gamma}_2 \sin (\gamma_1 - \gamma_2)$$
$$+ 2 m_3 l_1 h_3 \dot{\gamma}_3 \dot{\gamma}_1 \sin (\psi - \theta) - 2(m_2 h_2 + m_3 l_2) l_1 \overline{\dot{\eta}_1 \dot{\eta}_2}$$
$$\sin (\gamma_1 - \gamma_2)$$
$$+ 2 \overline{m_3 l_1} h_3 \dot{\eta}_3 \dot{\eta}_1 \sin (\gamma_3 - \gamma_1)]$$
$$= m_1 h_1 g \sin \gamma_1 + (m_2 + m_3) l_1 g \sin \gamma_1. \quad . \quad . \quad (1)$$

The γ_2 equation of motion is

$$\frac{d}{dt}\left[(m_2h_2+m_3l_2)l_1\dot{\gamma}_1\cos(\gamma_1-\gamma_2)+\{m_2(k_2^2+h_2^2)+m_3l_2^2\}\dot{\gamma}_2\right.$$
$$\left.+m_3l_2h_3\dot{\gamma}_3\cos(\gamma_2-\gamma_3)\right]$$
$$-\tfrac{1}{2}\left[-2(m_2h_2+m_3l_2)\overline{\ddot{\xi}\eta}_2\cos\gamma_2\right.$$
$$+2(m_2h_2+m_3l_2)l_1\dot{\gamma}_1\dot{\gamma}_2\sin(\gamma_1-\gamma_2)$$
$$-2m_3l_2h_3\dot{\gamma}_2\dot{\gamma}_3\sin(\gamma_2-\gamma_3)$$
$$+2(m_2h_2+m_3l_2)l_1\overline{\dot{\eta}_1\dot{\eta}_2}\sin(\gamma_1-\gamma_2)$$
$$\left.-2m_3l_2h_3\sin(\gamma_2-\gamma_3)\overline{\dot{\eta}_2\dot{\eta}_3}\right]=g(m_2h_2+m_3l_2)\sin\gamma_2. \quad (2)$$

Fig. 5.

The γ_3 equation of motion is

$$\frac{d}{dt}\left[m_3l_1h_3\dot{\gamma}_1\cos(\gamma_3-\gamma_1)+m_3l_2h_3\dot{\gamma}_2\cos(\gamma_2-\gamma_3)\right.$$
$$\left.+m_3(k_3^2+h_3^2)\dot{\gamma}_3\right]-\tfrac{1}{2}\left[-2m_3h_3\overline{\ddot{\xi}\eta}_3\cos\gamma_3\right.$$
$$+2m_3l_2h_3\dot{\gamma}_2\dot{\gamma}_3\sin(\gamma_2-\gamma_3)-2m_3l_1h_3\dot{\gamma}_3\dot{\gamma}_1\sin(\gamma_3-\gamma_1)$$
$$+2m_3l_2h_3\overline{\dot{\eta}_2\dot{\eta}_3}\sin(\gamma_2-\gamma_3)-2m_3l_1h_3\overline{\dot{\eta}_3\dot{\eta}_1}\sin(\gamma_3-\gamma_1)\right]$$
$$=m_3h_3g\sin\gamma_3. \quad . \quad . \quad . \quad (3)$$

The equations for η_1, η_2, η_3, are

$$[m_1(k_1^2+h_1^2)+(m_2+m_3)l_1^2]\eta_1+(m_2h_2+m_3l_2)\eta_2$$
$$+m_3l_1h_3\cos(\psi-\theta)\eta_3-\{m_1h_1+(m_2+m_3)l_1\}\xi\sin\theta=0, \quad (4)$$

$$(m_2h_2+m_3l_2)l_1\cos(\theta-\phi)\eta_1+[m_2(k_2^2+h_2^2)+m_3l_2^2]\eta_2$$
$$+m_3l_2h_3\cos(\phi-\psi)\eta_3-(m_2h_2+m_3l_2)\,\xi\sin\phi=0, \quad (5)$$

$$l_1h_3\cos(\psi-\theta)\eta_1+l_2h_3\cos(\phi-\psi)\eta_2+(k_3^2+h_3^2)\eta_3$$
$$-h_3\xi\sin\psi=0. \quad (6)$$

Solving for η_1, η_2, η_3, the values for $\overline{\eta_1\xi}$ etc. may be obtained.

The equations of motion for small oscillations about a vertically upright position (which is taken as the zero position of the coordinates) are

$$[m_1(k_1^2+h_1^2)+(m_2+m_3)l_1^2]\ddot{\gamma}_1+(m_2h_2+m_3l_2)l_1\ddot{\gamma}_2+m_3l_1h_3\ddot{\gamma}_3$$
$$+[m_1h_1+(m_2+m_3)l_1]\overline{\xi^2}[\{m_1h_1+(m_2+m_3)l_1\}$$
$$\{m_2(k_2^2+h_2^2)(k_3^2+h_3^2)+m_3k_3^2l_2^2\}\gamma_1$$
$$+(m_2h_2+m_3l_2)\{-(k_3^2+h_3^2)m_2h_2-m_3l_2k_3^2\}l_1\gamma_2$$
$$+m_3m_3h_3^2l_1(h_2l_2-k_2^2-h_2^2)\gamma_3]/A$$
$$=g\{m_1h_1+(m_2+m_3)l_1\}\gamma_1, \quad . \quad . \quad (7)$$

$$(m_2h_2+m_3l_2)l_1\ddot{\gamma}_1+[m_2(k_2^2+h_2^2)+m_3l_2^2]\ddot{\gamma}_2+m_3l_2h_3\ddot{\gamma}_3$$
$$+(m_2h_2+m_3l_2)\overline{\xi^2}[\{m_1h_1+(m_2+m_3)l_1\}\{-m_2h_2(k_3^2+h_3^2)$$
$$-m_3l_2k_3^2\}l_1\gamma_1+\gamma_2(m_2h_2+m_3l_2)[(k_3^2+h_3^2)\{(k_1^2+h_1^2)m_1$$
$$+m_2l_1^2\}+k_3^2m_3l_1^2]$$
$$+m_3h_3^2[m_2h_2l_1^2-l_2\{m_1(k_1^2+h_1^2)m_1+m_1l_1^2\}]\gamma_3]/A$$
$$=g(m_2h_2+m_3l_2)\gamma_2, \quad . \quad . \quad (8)$$

$$m_3l_1h_3\ddot{\gamma}_1+m_3l_2h_3\ddot{\gamma}_2+m_3(k_3^2+h_3^2)\ddot{\gamma}_3$$
$$+m_3h_3^2\overline{\xi^2}[\{m_1h_1+(m_2+m_3)l_1\}\{m_2h_2l_2-m_2k_2^2+h_2^2)\}l_1\gamma_1$$
$$+(m_2h_2+m_3l_2)[m_2l_1^2h_2-m_1l_2(k_1^2+h_1^2)-m_3l_1^2l_2]\gamma_2$$
$$+[\{m_1(k_1^2+h_1^2)+(m_2+m_3)l_1^2\}\{m_2(k_2^2+h_2^2)+m_3l_2^2\}$$
$$-l_1^2(m_2h_2+m_3l_2)^2]\gamma_3]/A=m_3h_3g\gamma_3, \quad . \quad . \quad (9)$$

where A is given by the determinant

$$\begin{vmatrix} m_1(k_1^2+h_1^2)+(m_2+m_3)l_1^2 & (m_2h_2+m_3l_2)l_1 & m_3l_1h_3 \\ (m_2h_2+m_3l_2)l_1 & m_2(k_2^2+h_2^2)+m_3l_2^2 & m_3l_2h_3 \\ l_1h_3 & l_2h_3 & k_3^2+h_3^2 \end{vmatrix}.$$

Small oscillations of three equal simple pendulums, pivoted so that they move in a horizontal plane. (The equations are deduced from the general equations for three rods, given above.)

In this case

$$h_1 = l_1 = h_2 = l_2 = h_3 = l_3 = l,$$

$$m_1 = m_2 = m_3 = m,$$

and $\quad k_1 = k_2 = k_3 = 0,$

so that the equations become

$$3ml^2\ddot{\gamma}_1 + 2ml^2\ddot{\gamma}_2 + ml^2\ddot{\gamma}_3 + 3ml\xi^2[3m^2l^5\gamma_1 - 2m^2l^5\gamma_2]/A = 0,$$

$$2ml^2\ddot{\gamma}_1 + 2ml^2\ddot{\gamma}_2 + ml^2\ddot{\gamma}_3 + 2ml\xi^2[-3m^2l^5\gamma_1 + 4m^2l^5\gamma_2 - m^2l^5\gamma_3]/A = 0,$$

$$ml^2\ddot{\gamma}_1 + ml^2\ddot{\gamma}_2 + ml^2\ddot{\gamma}_3 + ml\xi^2[-2m^2l^5\gamma_2 + 2m^2l^5\gamma_3]/A = 0,$$

where $A = m^2l^6$;

i.e., $\quad 3\ddot{\gamma}_1 + 2\ddot{\gamma}_2 + \ddot{\gamma}_3 + 3Z(3\gamma_1 - 2\gamma_2) \qquad = 0,$

$$2\ddot{\gamma}_1 + 2\ddot{\gamma}_2 + \ddot{\gamma}_3 + Z(-6\gamma_1 - 8\gamma_2 - 2\gamma_3) = 0,$$

$$\ddot{\gamma}_1 + \ddot{\gamma}_2 + \ddot{\gamma}_3 + Z(-2\gamma_2 + 2\gamma_3) = 0,$$

where Z has the same meaning as before.

(The γ's are measured from the equilibrium position, as before.)

Put

$$\gamma_1 = L \sin(pt + \epsilon), \quad \gamma_2 = M \sin(pt + \epsilon), \quad \gamma_3 = N \sin(pt + \epsilon).$$

The equation for p is

$$p^6 - 45p^4Z^2 + 216p^2Z^4 - 36Z^6 = 0 ;$$

or, replacing p^2 by Z^2P, it becomes

$$f(P) \equiv P^3 - 45P^2 + 216P - 36 = 0.$$

The signs of $f(P)$ corresponding to different values of P are shown by the table below :—

P	—	0	1	10	∞
$f(P)$	—	—	+	—	+

Thus there are three real positive values for p^2, and therefore real values for p.

Hence there is stability for small oscillations.

Other positions about which there may be small oscillations. The general equations of motion for three equal pendulums are

$$3l\ddot{\gamma}_1 + 2l\ddot{\gamma}_2 \cos(\gamma_1 - \gamma_2) + 2l\dot{\gamma}_2^2 \sin(\gamma_1 - \gamma_2)$$
$$+ l\ddot{\gamma}_3 \cos(\gamma_3 - \gamma_1) - l\dot{\gamma}_3^2 \sin(\gamma_3 - \gamma_1) + 2l\overline{\dot{\eta}_1\dot{\eta}_2} \sin(\gamma_1 - \gamma_2)$$
$$- l\overline{\dot{\eta}_3\dot{\eta}_1} \sin(\gamma_3 - \gamma_1) + 3\overline{\ddot{\eta}_1\xi} \cos\gamma_1 = 0, \quad \ldots \quad (1)$$

$$2l\ddot{\gamma}_1 \cos(\gamma_1 - \gamma_2) + 2l\ddot{\gamma}_2 + l\cos(\gamma_2 - \gamma_3)\ddot{\gamma}_3$$
$$- 2l\dot{\gamma}_1^2 \sin(\gamma_1 - \gamma_2) + l\dot{\gamma}_3^2 \sin(\gamma_2 - \gamma_3) - 2l\overline{\dot{\eta}_1\dot{\eta}_2} \sin(\gamma_1 - \gamma_2)$$
$$+ l\overline{\dot{\eta}_2\dot{\eta}_3} \sin(\gamma_2 - \gamma_3) + 2\overline{\ddot{\xi}\eta_2} \cos\gamma_2 = 0, \quad \ldots \quad (2)$$

$$l\ddot{\gamma}_1 \cos(\gamma_3 - \gamma_1) + l\ddot{\gamma}_2 \cos(\gamma_2 - \gamma_3) + l\ddot{\gamma}_3$$
$$+ l\dot{\gamma}_1^2 \sin(\gamma_3 - \gamma_1) - l\dot{\gamma}_2^2 \sin(\gamma_2 - \gamma_3) - l\overline{\dot{\eta}_2\dot{\eta}_3} \sin(\gamma_2 - \gamma_3)$$
$$+ l\overline{\dot{\eta}_3\dot{\eta}_1} \sin(\gamma_3 - \gamma_1) + \overline{\ddot{\eta}_3\xi} \cos\gamma_3 = 0. \quad \ldots \quad (3)$$

Consider motion about the position $\gamma_1 = 0$, $\gamma_2 = \pi$, $\gamma_3 = 0$.
Let $\gamma_2 = \pi + \gamma_2'$.
Then the equations of motion are

$$3\ddot{\gamma}_1 + 2\ddot{\gamma}_2' \cos(\gamma_1 - \pi - \gamma_2') + 2\dot{\gamma}_2'^2 \sin(\gamma_1 - \pi - \gamma_2')$$
$$+ \ddot{\gamma}_3 \cos(\gamma_3 - \gamma_1) - \dot{\gamma}_3^2 \sin(\gamma_3 - \gamma_1)$$
$$+ 2\overline{\dot{\eta}_1\dot{\eta}_2} \sin(\gamma_1 - \pi - \gamma_2') - \overline{\dot{\eta}_3\dot{\eta}_1} \sin(\gamma_3 - \gamma_1)$$
$$+ (3/l)\overline{\ddot{\xi}\eta_1} \cos\gamma_1 = 0, \quad \ldots \quad (1)$$

$$2\ddot{\gamma}_1 \cos(\gamma_1 - \pi - \gamma_2') + 2\ddot{\gamma}_2' + \ddot{\gamma}_3 \cos(\pi + \gamma_2' - \gamma_3)$$
$$- 2\dot{\gamma}_1^2 \sin(\gamma_1 - \pi + \gamma_2') + \dot{\gamma}_3^2 \sin(\pi + \gamma_2' - \gamma_3)$$
$$- 2\overline{\dot{\eta}_1\dot{\eta}_2} \sin(\gamma_1 - \pi + \gamma_2') + \overline{\dot{\eta}_2\dot{\eta}_3} \sin(\pi + \gamma_2' - \gamma_3)$$
$$+ (2/l)\overline{\ddot{\xi}\eta_2} \cos(\pi + \gamma_2') = 0, \quad \ldots \quad (2)$$

$$\ddot{\gamma}_1 \cos(\gamma_3 - \gamma_1) + \ddot{\gamma}_2' \cos(\pi + \gamma_2' - \gamma_3) + \ddot{\gamma}_3$$
$$+ \dot{\gamma}_1^2 \sin(\gamma_3 - \gamma_1) - \dot{\gamma'}_2^2 \sin(\pi + \gamma_2' - \gamma_3)$$
$$- \overline{\dot{\eta}_2\dot{\eta}_3} \sin(\pi + \gamma_2' - \gamma_3) + \overline{\dot{\eta}_3\dot{\eta}_1} \sin(\gamma_3 - \gamma_1)$$
$$+ (1/l)\overline{\ddot{\xi}\eta_3} \cos\gamma_3 = 0. \quad \ldots \quad (3)$$

For small oscillations the equations become

$$3\ddot{\gamma}_1 - 2\ddot{\gamma}_2' + \ddot{\gamma}_3 + 3Z(3\gamma_1 + 2\gamma_2') = 0, \quad \ldots \quad (1)$$

$$2\ddot{\gamma}_1 - 2\ddot{\gamma}_2' + \ddot{\gamma}_3 - 2Z(3\gamma_1 + 4\gamma_2' + \gamma_3) = 0, \quad \ldots \quad (2)$$

$$\ddot{\gamma}_1 - \ddot{\gamma}_2' + \ddot{\gamma}_3 + Z(2\gamma_2' + 2\gamma_3) = 0. \quad \ldots \quad (3)$$

On putting

$$\gamma_1 = \mathrm{L} \sin (pt + \epsilon), \quad \gamma_2' = \mathrm{M} \sin (pt + \epsilon), \quad \gamma_3 = \mathrm{N} \sin (pt + \epsilon),$$

the equation for p^2 is the same as the one obtained in small oscillations about the position $\gamma_1 = \gamma_2 = \gamma_3 = 0$.

Hence the small oscillations about the position $\gamma_1 = \gamma_3 = 0$, $\gamma_2 = \pi$, are stable.

Motion about the position $\gamma_1 = \gamma_2 = 0, \quad \gamma_3 = \pi$.

Let $\gamma_3 = \pi + \gamma_3'$.

Then the equations for small oscillations are

$$3\ddot{\gamma}_1 + 2\ddot{\gamma}_2 - \ddot{\gamma}_3' + 3Z(3\gamma_1 - 2\gamma_2) = 0, \quad . \quad (1)$$

$$2\ddot{\gamma}_1 + 2\ddot{\gamma}_2 - \ddot{\gamma}_3' + 2Z(-3\gamma_1 + 4\gamma_2 + \gamma_3') = 0, \quad . \quad (2)$$

$$\ddot{\gamma}_1 + \ddot{\gamma}_2 - \ddot{\gamma}_3' - Z(2\gamma_2 + 2\gamma_3') = 0, \quad . \quad (3)$$

and these give rise to the same determinant to determine p^2 as do the previous cases.

Therefore the position is stable for small oscillations.

Similarly it may be shown that there can be small oscillations about the position $\gamma_1 = 0, \quad \gamma_2 = \pi, \quad \gamma_3 = \pi$.

Three Pendulums of unequal Length, and equal Mass, free to move Horizontally.

Let
$$l_3 = a^2 l_1, \quad l_2 = a l_1, \quad l_1 = l,$$
$$h_3 = a^2 l, \quad h_2 = a l, \quad h_1 = l.$$

The equations of motion are

$$3\ddot{\gamma}_1 + 2a\ddot{\gamma}_2 \cos (\gamma_1 - \gamma_2) + a\dot{\gamma}_2{}^2 \sin (\gamma_1 - \gamma_2)$$
$$+ a^2 \ddot{\gamma}_3 \cos (\gamma_3 - \gamma_1) - a^2 \dot{\gamma}_3{}^2 \sin (\gamma_3 - \gamma_1)$$
$$+ a\dot{\eta}_1 \eta_2 \sin (\gamma_1 - \gamma_2) - a^2 \dot{\eta}_3 \eta_1 \sin (\gamma_3 - \gamma_1)$$
$$+ (3/l)\xi \eta_1 \cos \gamma_1 = 0, \quad . \quad . \quad . \quad . \quad . \quad . \quad (1)$$

$$2a\ddot{\gamma}_1 \cos (\gamma_1 - \gamma_2) + 2a^2 \ddot{\gamma}_2 + a^3 \ddot{\gamma}_3 \cos (\gamma_2 - \gamma_3)$$
$$- 2a\dot{\gamma}_1{}^2 \sin (\gamma_1 - \gamma_2) + a^3 \dot{\gamma}_3{}^2 \sin (\gamma_2 - \gamma_3)$$
$$- 2a\dot{\eta}_1 \eta_2 \sin (\gamma_1 - \gamma_2) + a^3 \dot{\eta}_2 \eta_3 \sin (\gamma_2 - \gamma_3)$$
$$+ (2a/l)\xi \eta_2 \cos \gamma_2 = 0, \quad . \quad . \quad . \quad . \quad . \quad . \quad (2)$$

$$a^2 \ddot{\gamma}_1 \cos (\gamma_3 - \gamma_1) + a^3 \ddot{\gamma}_2 \cos (\gamma_2 - \gamma_3)$$
$$+ a^4 \ddot{\gamma}_3 + a^2 \dot{\gamma}_1{}^2 \sin (\gamma_3 - \gamma_1) - a^3 \dot{\gamma}_2{}^2 \sin (\gamma_2 - \gamma_3)$$
$$- a^2 \dot{\eta}_2 \eta_3 \sin (\gamma_2 - \gamma_3) + a^2 \dot{\eta}_3 \eta_1 \sin (\gamma_3 - \gamma_1)$$
$$+ (a^2/l)\xi \eta_3 \cos \gamma_3 = 0. \quad . \quad . \quad . \quad . \quad . \quad (3)$$

For small oscillations, from the position $\gamma_1 = 0 = \gamma_2 = \gamma_3$, these reduce to

$$3\ddot{\gamma}_1 + 2a\ddot{\gamma}_2 + a^2\ddot{\gamma}_3 + (3/l)\eta_1\xi = 0, \quad \ldots \quad (1)$$

$$2\ddot{\gamma}_1 + 2a\ddot{\gamma}_2 + a^2\ddot{\gamma}_3 + (2/l)\eta_2\xi = 0, \quad \ldots \quad (2)$$

$$\ddot{\gamma}_1 + a\ddot{\gamma}_2 + a^2\ddot{\gamma}_3 + (1/l)\eta_3\xi = 0 ; \quad \ldots \quad (3)$$

or

$$3\ddot{\gamma}_1 + 2a\ddot{\gamma}_2 + a^x\ddot{\gamma}_3 + 3Z(3\gamma_1 - 2\gamma_2) = 0, \quad . \quad (1)$$

$$2\ddot{\gamma}_1 + 2a\ddot{\gamma}_2 + a^2\ddot{\gamma}_3 + 2Z(-3\gamma_1 + 4\gamma_2 - \gamma_3) = 0, \quad . \quad (2)$$

$$\ddot{\gamma}_1 + a\ddot{\gamma}_2 + a^2\ddot{\gamma}_3 + Z(-2\gamma_2 + 2\gamma_3) = 0. \quad . \quad (3)$$

If

$$\gamma_1 = L\sin(pt+\epsilon), \quad \gamma_2 = M\sin(pt+\epsilon), \quad \gamma_3 = N\sin(pt+\epsilon),$$

the equation for p is

$$a^6p^6 - p^4Z(9a^6 + 12a^5 + 16a^4 + 4a^3 + 4a^2)$$
$$+ 6p^2Z^2(6a^4 + 6a^3 + 10a^2 + 8a + 6) - 36Z^3 = 0$$

(which reduces to the equation obtained for three equal simple pendulums if $a = 1$).

Writing P for p^2/Z,

$$f(P) \equiv a^6P^3 - P^2(9a^6 + 12a^5 + 16a^4 + 4a^3 + 4a^2)$$
$$+ 12P(3a^4 + 3a^3 + 5a^2 + 4a + 3) - 36 = 0.$$

The equation has no negative roots, and has at least one positive root. To find if it has three real roots the values of P for which $\dfrac{df}{dP} = 0$ are found, and, if these are P_1 and P_2, the sign of $f(P_1)f(P_2)$ is determined. If this is positive there is only one real root, if it is negative there are three real roots.

$\dfrac{df}{dP} = 0$, if

$$P = (9a^4 + 12a^3 + 16a^2 + 4a + 4)/3a^4 \pm \frac{1}{3a^4} \times$$

$$\sqrt{(9a^4 + 12a^3 + 16a^2 + 4a + 4)^2 - 36a^2(3a^4 + 3a^3 + 5a^2 + 4a + 3)}$$
$$= P_1 \text{ or } P_2.$$

The discriminant can be shown to be positive ; therefore there are real turning points of the function for positive values of P.
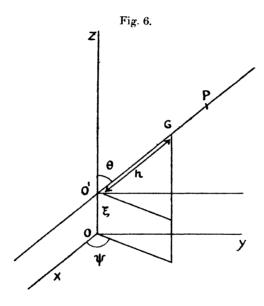
On substituting the values P_1 and P_2 in $f(P)$, it was found that $f(P_1)f(P_2)$ is negative, so that the equation has three real positive roots. Therefore the system is stable for any value of a.

The Equations of Motion of a Spinning Top, if the Peg is given rapid vertical Oscillations.

Let GP be the axis of symmetry of the top,

„ GA „ „ perpendicular to GP in the plane ZO'P,

„ GB „ „ „ „ the plane ZO'P,

and take coordinates θ, ψ, ξ, as marked.

Fig. 6.

Then the angular velocities about GA, GB, GP are

$$p = \dot{\psi}\sin\theta, \quad q = -\dot{\theta}, \quad r = \dot{\phi} + \dot{\psi}\cos\theta,$$

where ϕ is the angle which a plane through O'P, fixed in the top, makes with ZO'P.

If A' is the moment of inertia about GA or GB, and C the moment of inertia about GP,

$$T = \tfrac{1}{2}A'(\dot{\psi}^2\sin^2\theta + \dot{\theta}^2) + \tfrac{1}{2}C(\dot{\phi}^2 + 2\dot{\phi}\dot{\psi}\cos\theta + \dot{\psi}^2\cos^2\theta)$$
$$+ \tfrac{1}{2}M(\dot{\xi}^2 - 2h\dot{\xi}\dot{\theta}\sin\theta + h^2\dot{\theta}^2\sin^2\theta + h^2\dot{\psi}^2\sin^2\theta + h^2\dot{\theta}^2\cos^2\theta)$$
$$= \tfrac{1}{2}(A\dot{\psi}^2\sin^2\theta + A\dot{\theta}^2 + M\dot{\xi}^2 - 2Mh\dot{\xi}\dot{\theta}\sin\theta + Cr^2),$$

where A is the moment of inertia of the top about axes through O parallel to GA or GB.

The equations of motion are

$$\frac{d}{dt}(A\dot{\gamma}) - \tfrac{1}{2}[-2Mh\cos\gamma\overline{\xi\eta} + (A-C)\dot{\gamma}_3{}^2\sin 2\gamma - 2C\dot{\gamma}_2\dot{\gamma}_3\sin\gamma$$
$$+ (A-C)\overline{\dot{\eta}_3{}^2}\sin 2\gamma - 2C\overline{\dot{\eta}_2\dot{\eta}_3}\sin\gamma] = Mgh\sin\gamma, \quad (1)$$

$$\frac{d}{dt}(C\dot{\gamma}_2 + C\dot{\gamma}_3\cos\gamma) = 0, \quad\ldots\ldots\ldots \quad (2)$$

or $\dot{\gamma}_2 + \cos\dot{\gamma}_3$ is constant, $= n$, say,

$$\frac{d}{dt}[C\dot{\gamma}_2\cos\gamma + (A\sin^2\gamma + C\cos^2\gamma)\dot{\gamma}_3] = 0, \quad\ldots \quad (3)$$

or

$A\dot{\gamma}_3\sin^2\gamma + C\cos\gamma(\dot{\gamma}_2 + \dot{\gamma}_3\cos\gamma)$ is constant, $= K$, say,

and

$$\eta_2 = 0 = \eta_3, \quad (\eta_2 = \gamma_2 - \phi, \quad \eta_3 = \gamma_3 - \psi),$$

$$\eta = \theta - \gamma = \frac{1}{H}\xi\sin\theta, \quad \text{where } H = A/Mh.$$

Hence (1) reduces to

$$\ddot{\gamma} - \dot{\psi}^2\sin\gamma\cos\gamma + (\overline{\xi\eta}/H)\cos\gamma + (Cn/A)\dot{\psi}\sin\gamma = (g\sin\gamma)/H,$$
$$\ldots \quad (4)$$

which is the equation of motion for the top.

Also, $\qquad\qquad \overline{\dot{\xi}\eta} = (\overline{\dot{\xi}^2}/H)\sin\gamma,$

so that the equation of motion becomes

$$\ddot{\gamma} - (K - Cn\cos\gamma) \cdot [(K - Cn\cos\gamma)\cos\gamma - Cn\sin^2\gamma]/A^2\sin^3\gamma$$
$$+ (\overline{\dot{\xi}^2}/H^2) \cdot \sin\gamma\cos\gamma = (g/H) \cdot \sin\gamma;$$

i. e.,

$$\frac{d}{d\gamma}(\tfrac{1}{2}\dot{\gamma}^2) - [(K^2 + C^2n^2)/A^2]\cos\gamma\,\mathrm{cosec}^3\gamma$$
$$+ KCn(1 + \cos^2\gamma)/A^2\sin^3\gamma$$
$$+ (\overline{\dot{\xi}^2}/H^2)\sin\gamma\cos\gamma = (g/H)\sin\gamma. \quad (5)$$

Integrating with respect to γ, and replacing $\cos\gamma$ by x and $-\dot{\gamma}\sin\gamma$ by $\dot{x}$, (5) becomes

$$\dot{x}^2 + (\overline{\dot{\xi}^2}/H^2)x^4 - 2(g/H)x^3 - [(2\overline{\dot{\xi}^2} - C_1H^2)x^2/H^2]$$
$$- 2[(KCn/A^2) - (g/H)]x$$
$$+ (K^2 + C^2n^2)/A^2 + (\overline{\dot{\xi}^2}/H^2) - C_1 = 0. \quad (6)$$

Assume, as a solution,

$$x = \cos\alpha + P\cos(\lambda t + f), \qquad \dot{x} = -P\lambda\sin(\lambda t + f),$$

where P is so small that P^3 may be neglected (as in festoon motion). Then (6) becomes

$$P^2\lambda^2[1 - \cos^2(\lambda t + f)] + \dot{\xi}^2[\cos\alpha + P\cos(\lambda t + f)]^4/H^2$$
$$- 2g[\cos\alpha + P\cos(\lambda t + f)]^3/H$$
$$- (2\dot{\xi}^2 - C_1 H^2)[\cos\alpha + P\cos(\lambda t + f)]^2/H^2 - 2[(KCn/A^2)$$
$$- (g/H)][\cos\alpha + P\cos(\lambda t + f)][(K^2 + C^2 n^2)/A^2]$$
$$+ (\dot{\xi}^2/H^2) - C_1 = 0.$$

Fig. 7.

Fig. 8.

Equating coefficients of powers of $\cos(\lambda t + f)$ to zero, we deduce

$$C_1 = -(2\dot{\xi}^2/H^2)\cos^2\alpha + (3g/H)\cos\alpha$$
$$+ (2\dot{\xi}^2/H^2) + \sec\alpha[(KCn/A^2) - (g/H)],$$
$$\lambda^2 = (4\dot{\xi}^2/H^2)\cos^2\alpha - (3g/H)\cos\alpha$$
$$+ \sec\ [(KCn/A^2) - (g/H)],$$
$$P^2\lambda^2 = (\dot{\xi}^2/H^2)\cos^4\alpha - (g/H)\cos^3\alpha - (2\dot{\xi}^2/H^2)\cos^2\alpha$$
$$+ [(KCn/A^2) + (2g/H)]\cos\alpha - [(K^2 + C^2 n^2)/A^2]$$
$$+ (\dot{\xi}^2/H^2) + \sec\alpha[(KCn/A^2) - (g/H)].$$

Thus, (i.) If $\cos\alpha$ is negative, *i.e.*, $\alpha > \pi/2$ (fig. 7), λ^2 is positive if

$$|4\dot{\xi}\cos^3\alpha - 3gH\cos^2\alpha - gH|/H^2 > KCn/A^2.$$

(ii.) If $\cos\alpha$ is positive, *i.e.*, $\alpha < \pi/2$ (fig. 8), λ^2 is positive if

$$4\dot{\xi}^2 A\cos^3\alpha + KCnH^2 > 3gAH\cos^2\alpha + gAH$$

Existence of Positions of Steady Motion.

If $\cos\alpha = 1$,

$$\lambda^2 = (4\bar{\xi}^2/H^2) - (3g/H) + (KCn/A^2) - g/H,$$

i. e., is positive or negative as

$$(4\bar{\xi}^2/H^2) + KCn/A^2 > \quad \text{or} \quad < 4g/H,$$

and

$$P^2 = -(K - Cn)^2/\lambda^2 A^2,$$

which is negative if λ^2 is positive (unless $K = Cn$, when $P^2 = 0$, giving conical motion).

If $\cos\alpha = 0$,

$$P^2 = 1.$$

Therefore there is at least one positive value of $\cos\alpha$ satisfying the equation $P^2 = 0$. Hence there exists a position of steady motion for some value of α less than $\pi/2$.

If $\cos\alpha = -1$,

$$\lambda^2 = (4\bar{\xi}^2/H^2) + (4g/H) - KCn/A^2,$$
$$P^2 = -(K + Cn)^2/\lambda^2 A^2,$$

and therefore is negative if λ^2 is positive, *i. e.*, if

$$KCn/A^2 < (4\bar{\xi}^2/H^2) + 4g/H$$

(this is compatible with the previous condition for a positive λ^2), in which case there is at least one negative value of $\cos\alpha$ which satisfies $P^2 = 0$. Thus there is a position of steady motion for some value of α greater than $\pi/2$.

Limits of the Zone or Zones in which Motion occurs.

At the extremes of the zones $\dot{\gamma} = 0$, *i. e.*, $\dot{x} = 0$. Therefore the values of x, for which $\dot{\gamma} = 0$, are obtained from equation (6), and are given by

$$(\bar{\xi}^2/H^2)x^4 - (2g/H)x^3 - [(2\bar{\xi}^2/H^2) - C_1]x^2 - 2[(KCn/A^2)$$
$$- (g/H)]x + (K^2 + C^2 n^2)/A^2 + (\bar{\xi}^2/H^2) - C_1 = 0. \quad (7)$$

Since γ is not equal to 0 or π, there must be some values β_1, β_2 of γ, such that
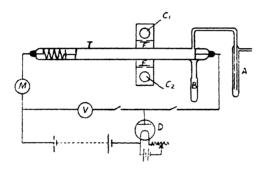
$$0 < \beta_1 \leq \gamma \leq \beta_2 < \pi,$$

and for these values $\dot{\gamma} = 0$. Therefore, if $a = \cos\beta_1$, $b = \cos\beta_2$, a and b are roots of equation (7), which therefore has at least two real roots.

XL. *Light Intensities of Neon Discharges. By* P. JOHNSON,
M.A., Fellow of Magdalen College Oxford *.

1. THE following is an account of an experimental
investigation of the relative intensities of the
light emitted by direct-current discharges in neon at
different pressures. It is a continuation of the work already
published on the light emitted by a high-frequency discharge
in helium †.

The apparatus which was used is represented in the accom-
panying figure. The discharge-tube, T, was of transparent
silica with aluminium electrodes. The internal diameter of
the tube was 3 cm. and the maximum distance between the
electrodes was 26 cm. The gas was carefully purified, and was

admitted to the discharge-tube through the tube A, contain-
ing charcoal which was cooled with liquid air. The tube T
had a side-tube B near the cathode, which contained charcoal,
so that if there were any easily ionized impurities in the gas
they would be carried with the current towards the cathode
and would be absorbed by the charcoal in the tube B.
These precautions were considered advisable, although the
impurities were removed from the discharge-tube before
any measurements were made. For this purpose pure gas
was admitted to the apparatus, and the tube T heated
strongly ; the gas which thus became impure was pumped
out, and the process was repeated several times. Eventually
a stage was reached in which no appreciable amount of
impurity was given off unless the tube was brought to a red

* Communicated by Prof. J. S. Townsend, F.R.S.
† J. S. Townsend and F. Llewellyn Jones, Phil. Mag. xi. (March
1931).

heat. The discharge was maintained by a battery of accu-mulators, the potential difference between the electrodes was measured by the voltmeter V, and the current, which was adjusted to any required value by the two-electrode valve D, was measured by the milliammeter M.

The positive electrode in the discharge-tube was movable, so that the force in the positive column could be determined by measuring the potentials for different distances between the electrodes. The values of these forces agreed closely with those obtained in a previous research *, where it was found that the force in the positive column of a direct-current discharge was the same as the mean force in the luminous column of a high-frequency discharge.

The intensity of the light was measured by two photo-electric cells C_1 and C_2, either of which could be connected to an electrometer, and the photoelectric currents measured by an induction balance. A series of screens limited the light entering the cells to that from a small section of

TABLE I.

p.	X/p.	R.	Y.	G.	B.
7·9	·58	100	100	100	100
17·0	·47	67	66	100	152
38·2	·41	35·5	37	163	331

the uniform positive column of the discharge, and effectively prevented any light from the room or from the space near the electrodes of the discharge-tube from reaching the cells. The light entering each cell passed through an aperture in the screen which was covered by a filter F. The cell C_1 was sensitive over a wide range of wave-lengths covering the red, yellow, and green parts of the spectrum ; the other cell, C_2, was most sensitive in the blue region. Three filters were used to cover the aperture in front of the cell C_1 which were transparent to the light of three different ranges of wave-lengths in the red, the yellow, and the green parts of the spectrum respectively ; one filter was used to cover the aperture in front of C_2, which was transparent to blue light.

2. The results of the experiments at different pressures are given in Table I., where p is the pressure of the neon in millimetres of mercury, X/p the ratio of the electric force X

* P. Johnson, Phil. Mag. x. (Nov. 1930).

in volts per centimetre in the discharge to the pressure, and the remaining four columns give the intensities of the red, yellow, green, and blue light respectively. The intensity of the light of each colour is expressed in terms of its intensity at the lowest pressure, which is taken as 100. The current in the discharge tube was 4·7 milliamperes.

The light that passed through the red filter included a number of lines in the neon spectrum from the orange line 6182 Å. down to the red end of the spectrum. The light that passed through the yellow filter had wave-lengths from 6305 Å. to 5500 Å., and therefore contained a number of orange and yellow lines, in particular the strong yellow line at 5853 Å. In neither of these two ranges of wavelengths can any continuous spectrum be observed by a direct-vision spectroscope. The green filter allowed light whose wave-lengths lay between 5500 Å. and 4840 Å. to pass through; in this region there is a continuous spectrum, which becomes more prominent in comparison with the line spectrum as the pressure is increased. The total intensity in the green region of the neon spectrum is very small compared with the intensities in other parts of the spectrum. The blue filter allowed light of wavelengths between 4840 Å. and 4000 Å. to pass. In this region there was a continuous spectrum in the discharges at all the pressures at which the above measurements were made, and the total amount of light of the lines in this region appeared to be small compared with that of the continuous spectrum.

The results show that for a given current in the discharge-tube the intensity of the light emitted in the red and yellow regions of the spectrum diminishes as the pressure is increased. In the range of pressures given in Table I. the rate at which the intensity of the red light changes with change of pressure is the same as the rate at which the intensity of the yellow light changes. At lower pressures the intensity of the yellow light increases more rapidly than that of the red as the pressure is reduced. The intensity of the green light increases as the pressure is increased above 12 millimetres ; at this point the intensity of the green light attains a minimum value, and at pressures lower than 8 millimetres it shows a marked increase as the pressure is reduced. The intensity of the blue light increases as the pressure is increased from 7·9 to 38 millimetres.

3. The light intensities were not exactly proportional to the currents in the discharge-tube. When the current was

increased from 2·5 to 5 milliamperes the intensities, as measured by the photoelectric cell of the red and yellow light, were increased by a factor of 2·2, whereas that of the blue light was increased by the factor 1·85. At the pressure of 38 millimetres the intensity of the green light varies with the current in the same manner as that of the blue light, but at 17 and 7·9 millimetres pressure the intensity is directly proportional to the current.

The manner in which the light intensities vary with the current in the discharge-tube is what would be expected if the density of the gas diminished as the current was increased, assuming that the intensity of the light would be proportional to the current if the density were constant. The required change in density is, however, greater than the change to be expected from the increase of the temperature with the increase of the current.

4. The intensities of the ultra-violet light emitted by discharges in neon have also been determined by measuring

TABLE II.

p.	I_1.	I_2.
10	100	197
17	113	227
23	148	292
33	226	417

the photoelectric currents from a copper plate which was placed about 6 centimetres away from the discharge-tube. Copper was used in preference to zinc, as its sensitivity remained constant during the time required to make a series of measurements with the gas at different pressures. The area of the plate was about 20 square centimetres, and a gauze was fixed in front of it, leaving a space of about 4 millimetres between the gauze and the plate. The plate was connected to the electrometer and the gauze was maintained at a positive potential of 80 volts by a battery of accumulators.

In order to obtain photoelectric currents from copper the exciting radiation must be of wave-lengths less than 3000 Å ; consequently it was in that region of the spectrum that the light intensities were measured. The copper plate was completely unaffected by light from the room, and the photoelectric current was reduced to zero when the light from the tube was filtered with a sheet of pyrex glass.

The results of experiments with ultra-violet light are given in Table II. The pressure p of the neon is given in the first column in millimetres of mercury. The intensities I_1 of the light obtained with a current of 4 milliamperes in the discharge-tube are given in the second column. The intensities I_2 obtained with a current of 8 milliamperes are given in the third column. The numbers in these two columns are the photoelectric currents in arbitrary units.

It appears from these results that, for a given current in the discharge-tube, the intensity of the ultra-violet light increases as the pressure is increased from 10 to 33 millimetres. As in the case of the blue light the intensity is approximately proportional to the pressure at the highest pressures. Further experiments show that intensity has a minimum value when the pressure in the discharge-tube is about 8 millimetres.

5. The light in the ultra-violet spectrum has also been examined by Mr. J. Keyston. He took photographs of the spectra of the luminous columns of high-frequency discharges in two quartz tubes, one containing neon at 11·6 millimetres pressure and the other at 1 millimetre pressure.

In the ultra-violet region a continuous spectrum and a line spectrum were obtained in each case. At the higher pressure the continuous spectrum predominated, and at the lower pressure the line spectrum predominated. The results obtained from observations of the green and blue regions of the visible spectrum, where the intensity of the continuous spectrum was seen to increase in comparison with that of the line spectrum as the pressure was increased, are thus extended to the ultra-violet region.

6. From the spectroscopic observations and from the measurements of the light intensities in the different parts of the spectrum the conclusion is arrived at that, when the current in the discharge-tube remains constant, the intensity of light in the line spectrum diminishes and that the light in the continuous spectrum increases as the pressure is increased. The yellow and red parts of the spectrum are examples of line spectra only. The light in the green, blue, and ultra-violet parts of the spectrum when the pressure is high is almost entirely due to the continuous spectrum. In the ultra-violet and green regions minimum values of the intensity were obtained at pressures where the continuous spectrum was disappearing and the line spectrum becoming appeciable. There is, presumably, also a pressure at which

the intensity of the blue light has a minimum value, but it has not been determined experimentally.

7. According to the theory of the positive column given by Townsend * there is no recombination between electrons and positive ions, and the light is due to collisions of electrons with molecules or atoms of the gas. The energies of the electrons which excite light of a given wave-length have a certain mean value E_x, and the intensity I of the light is approximately proportional to the number N_x of electrons having energies greater than E_x. The energy E_x is different for lights of different wave-lengths, and it has been found that in most cases the values of E_x are greater than the mean energy E_1 of all the electrons N_1 in discharges in wide tubes where the gas is at high pressures, such as those which are here investigated. The ratio $\dfrac{N_x}{N_1}$ is a function of $\dfrac{E_x}{E_1}$ which depends on the distribution of the energies of agitation. If the probability of an electron exciting an atom increases abruptly when the energy of the electron exceeds a certain value, then this value will only be very slightly less than E_x.

The formula for calculating E_x is

$$\frac{I_1}{I_2} = \frac{p_1 W_2 \phi\left(\dfrac{E_x}{E_1}\right)}{p_2 W_1 \phi\left(\dfrac{E_x}{E_2}\right)}.$$

In this formula I_1 and I_2 are the intensities of the light of given wave-length emitted by the discharge-tube at the pressures p_1 and p_2, and when the current is kept constant. W_1 and W_2 are the velocities of the electrons in the direction of the electric force in each case. $\phi\left(\dfrac{E_x}{E_1}\right)$ is the function which gives the ratio $\dfrac{N_x}{N_1}$. The values of E_1 and E_2, the mean energies of agitation of all the electrons at the two pressures, depend only upon the ratio $\dfrac{X}{p}$ †.

* J. S. Townsend, Phil. Mag. xi. (May 1931).

† J. S. Townsend, ' Motion of Electrons in Gases ' (Clarendon Press).

8. The intensities of the red and yellow light that have been measured are not those of single spectral lines but of two groups of lines, so that values of E_x calculated from these results will give mean values for the groups. Since between pressures of 8 and 38 millimetres the intensity of the red light changes in the same proportion as that of the yellow light as the pressure changes, it follows that over this range of pressure the mean value of E_x must be the same for each group of lines. These experiments may therefore be explained on the hypothesis that the light is excited by single impacts of electrons with ordinary atoms of the gas, and that the mean energy of the electrons in these collisions is the same when yellow or red light is excited.

The method of calculating the energies is only approximate, as the distribution of the energy of the electrons is not known exactly. It has been shown that the distribution is not the same as the Maxwellian distribution, and if this distribution be used to calculate E_x two widely different values are obtained from the measurements of the intensities at different pressures. From the intensities at 17 and 38 millimetres pressure we obtain an energy corresponding to 45 volts, and from those at 7·9 and 17 millimetres pressure 24 volts. If we use a distribution formula given by Townsend * the corresponding values are 12·4 volts and 11·4 volts.

These two values agree quite well with each other, but are considerably below the value 16 volts which is generally considered to correspond to the smallest amount of energy that an ordinary neon atom can absorb.

Another theory of the radiation from discharges has been suggested which depends on the formation of metastable atoms. According to this theory the atoms of neon are first raised to a metastable state by collisions with electrons which have large energies, and the radiation is due to subsequent collisions of electrons with metastable atoms. In order to account for the experimental results on this hypothesis it would be necessary to assume that the number of metastable atoms in the gas is independent of the current.

Below 8 millimetres pressure it was found that the rate of increase of the yellow light as the pressure was reduced was greater than that of the red light. It is difficult to account for this result without assuming that some of the electrons attain sufficient energy to excite atoms by single impacts.

* J. S. Townsend, Phil. Mag. ix. (June 1930).

9. The measurements made of the intensities of the continuous parts of the spectrum show that the energies required to excite them are much the same in the blue parts of the spectrum as in the ultra-violet, since the rate at which the intensity changes with change of pressure is approximately the same in each case.

Whatever distribution is used in the formula to calculate E_x, its value for the continuous spectrum is much less than that for the line spectrum, and appears to be about 5 volts.

The average loss of enegy of electrons in collisions with atoms of neon is very small when the energy is about 5 volts. There may, however, be losses of energy in large amounts in a very small proportion of these collisions, which would account for the continuous spectrum.

The continuous spectrum cannot be due to the recombination of electrons with positive ions, because in that case the intensity would be proportional to the square of current. The experiments showed that the intensity was almost directly proportional to the current.

I should like to express my thanks to Professor Townsend for his advice and help throughout this research, and also to Mr. J. E. Keyston for the photographs he took of the neon spectrum, and to Mr. M. H. Pakkala who assisted in the measurements of the intensities of the ultra-violet light.

XLI. *On the Distribution of Space-potential in Striated and other Forms of High-frequency Discharge.* By D. BANERJI, *M.Sc., Lecturer in Physics, University College of Science, and* R. GANGULI, *M.A., M.Sc., Lecturer in Physics, Serampore College* *.

[Plate XIV.]

INTRODUCTION.

IN a previous communication † on high-frequency glow discharge it has been shown that by using the Langmuir "Exploring Collector" method in combination with a third "bobbin" electrode the space-potential at any point of the glow in high-frequency discharge could be ascertained along with the concentration and average energy of the electrons.

The theory and working of the method have been fully given in the previous paper. The type of discharge investigated was the non-striated positive column glow of air and oxygen in cylindrical tubes. The main results that were obtained may be summarized as follows :—

(1) The space-potential at any point in or outside the luminous column depends to a great extent on the gas pressure inside the tube ;

(2) the space-potential-distance curve (under a fixed pressure and fixed exciting voltage on the electrodes) shows a maximum in the middle of the positive or luminous column. There are two minima lying near about the region of the electrodes, which behave as if they are both cathodes ; and

(3) the concentration of the electrons near the electrodes is less than that in the middle of the luminous column.

On the accepted notions of potential distribution under steady applied voltage in an evacuated tube in which a definite small amount of ionization is maintained a distribution of space-potential, such as described above, may seem to be qualitatively valid when the applied voltage is a high-frequency oscillatory one *. The accumulation of positive ions near the cathodes, and the consequent partial neutralization of the negative space-charge there, is borne out by (3).

In the present communication, by using the same method, it is proposed to give the results of space-potential measurements along with the derived values of electron concentration and energy in different parts of discharge in (i.) a conical tube—which is intended to serve as a check on the derived data, and (ii.) cylindrical tubes in stages of (*a*) striated, (*b*) low-pressure non-striated, and (*c*) " splasmoidal " discharge. The last two present interesting features which are not ordinarily found in D.C. discharge.

* In a private communication to one of the authors Dr. K. G. Emeléus has questioned the applicability of the method in its present form, as the position of the third " bobbin " electrode, with reference to which the space-potential measurements are made was not very clearly defined. It has been observed since that the measured values of the space-potential, ionic-concentration, etc., are independent of the exact location of the third electrode, provided it is placed so far away from the external electrode as not to alter visibly the nature of the discharge. The formation of an ionic " sheath " on the " bobbin," which keeps it at zero-potential, also seldom escapes observation.
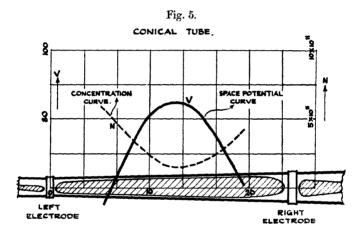
The apparatus used and the procedure followed were essentially the same as in the previous work, excepting that the oscillatory circuit was changed to one having frequency about three million cycles per second. The collector-current was measured by a Kipp and Zonen galvanometer, shunted by a suitable resistance.

RESULTS.

(i.) *Experiments with Conical Tube.*

Fig. 1 (Pl. XIV.) gives the picture of the discharge in a conical tube (length 25 cm., diameter of the wider end 4 cm. and of the constricted end 2 cm.). The portion between the

Fig. 5.

CONICAL TUBE.

electrodes is fitted with three identical "collectors" of tungsten wire—one in the middle and the other two symmetrical about it and 5 cm. distant from the edges where the external electrodes (made out of aluminium sheet) are fitted.

In our previous communication on space-potential distribution in cylindrical tubes it was observed that the value of the space-potential is higher in the middle of the glow than that near the region of the electrodes. With a conical tube one would therefore expect a similar higher potential at the centre and lower ones near the electrodes, but of the latter two the one at the wider end might reasonably be expected to be higher than the other at the constricted end. This is what has been found in the present measurement with the conical tube (fig. 5). The greater concentration of electrons

at the constricted end is natural to expect, and accords well with the present observation (Table I.).

(ii.) *Experiments with Cylindrical Tubes.*

(a) & (b). *Striated and non-striated Discharge.*

The types of discharge in a cylindrical tube which appear when the pressure inside is being gradually reduced from about a mm. to values such as 10^{-2} mm. of Hg are often striated, and the number of striations, which to start with may be ten, becomes less and less in number till it is reduced

TABLE I.—Conical Tube.

Pressure inside the tube 0·2 mm. of Hg.
Distance between electrodes 25 cm.
Frequency 3×10^6 cycles/sec.

Distance of collector from left electrode (cm.).	Diameter of section (cm.).	Space-potential (volts).	Average electron-energy (electron volts).	Current density (amp.).	Concentration of electrons per c.c.
5	2·0	−22	0·09	$37\cdot8 \times 10^{-2}$	$5\cdot80 \times 10^{11}$
12·5	2·5	98	0·10	$11\cdot0 \times 10^{-2}$	$1\cdot61 \times 10^{11}$
20	3·0	0	0·14	$23\cdot7 \times 10^{-2}$	$3\cdot54 \times 10^{11}$
...	...	...	...	...	...

to one. These striated forms of discharge present sharply-defined glow regions and dark spaces in hydrogen with mercury vapour as an impurity. The gas for the purpose was obtained by electrolysis, and was fed on to the discharge-tube by osmo-regulation through a heated platinum tube, so as to maintain a steady pressure of 7×10^{-2} mm. of Hg inside the tube while the pump was running. Fig. 2 (Pl. XIV.) gives an appearance of the discharge with a single striated dark space in the middle. This form of the discharge is somewhat unstable, and by a slight alteration of the exciting voltage may easily pass to a stage presented in fig. 3 (Pl. XIV.), in which the striation is absent. Tables II. and III. (figs. 6 and 7) give the data obtained for the two stages respectively. It is to be observed that in the striated discharge

(A) the maxima of the electric force occur at the bright heads of the striation and the minima at the dark part;

(B) the temperature is greater in the luminous part than in the dark ; and

(C) the concentration of electrons is minimum in the dark part.

Some of the above features are in common with those corresponding to D.C. discharge. In the other stable form of discharge mentioned above (fig. 3, Pl. XIV.), in which

TABLES II. and III.—Cylindrical Tube.
Distance between the electrodes = 10 cm.
Frequency 3×10^6 cycles/sec.

	Distance of collector from left electrode (cm.).	Space potential (volts).	Average electron-energy (electron volts).	Current density (amp.).	Concentration of electrons per c.c.	Temperature O_x.
Striated discharge.	0	−6	0·19	$36·1 \times 10^{-3}$	$3·94 \times 10^{10}$	1573
	1	13	0·30	$44·8 \times 10^{-3}$	$3·87 \times 10^{10}$	2484
	2·5	13	0·20	$38·9 \times 10^{-3}$	$4·00 \times 10^{10}$	1656
	5 (in striation)	6	0·19	$25·9 \times 10^{-3}$	$2·76 \times 10^{10}$	1573
	...	...	...	...	...	...
	...	...	...	...	...	...
Nonstriated discharge.	−1	−18	0·25	30×10^{-3}	$2·76 \times 10^{10}$	2070
	0	12	0·12	17×10^{-3}	$2·30 \times 10^{10}$	1035
	2	11·8	0·20	40×10^{-3}	$4·14 \times 10^{10}$	1656
	5	12	0·15	33×10^{-3}	$3·68 \times 10^{10}$	1242
	...	...	...	...	...	...
	...	...	...	...	...	...

the whole tube is filled with glow with a very condensed extension of it through the region of external electrodes, both the cathode glow and the dark space are absent. It is to be remembered here that in the above forms of discharge, except when it is striated, the potential in the central portion remains appreciably constant, or, in other words, the electric field there is low. In the case of striation, however, there is a sudden drop of potential between the edge and the centre of the striation, resulting in an appreciable electric field, which is responsible for the ionization outside the dark space. The increased electric field causes the electrons to drift away from the striated region and produces a diminution of electronic concentration there in agreement with observation.

(c). "*Splasmoidal*" *Discharge.*

As the pressure in the discharge-tube is further reduced by cutting off the supply of hydrogen and keeping the pump

Fig. 6.

CYLINDRICAL TUBE.

LEFT
ELECTRODE.

RIGHT
ELECTRODE

Fig. 7.

CYLINDRICAL TUBE

LEFT
ELECTRODE.

RIGHT
ELECTRODE
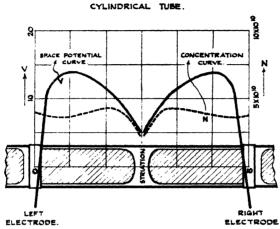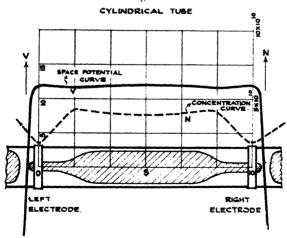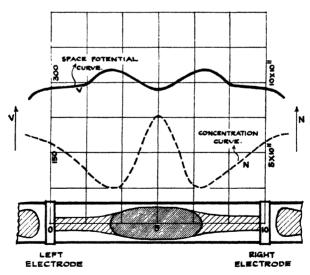
running a state of discharge is obtained which is akin to that of the "splasmoidal discharge." Remarkable egg-ball-, and pear-shaped bodies are formed. Fig. 4 (Pl. XIV.)

shows an egg-shaped glow between the electrodes. The most striking feature of such a discharge is that the space-potential is very high (Table IV.) as compared to that for

TABLE IV.

Distance of collector from left electrode (cm.).	Space-potential (volts).	Average electron energy (electron volts).	Current density (amp.).	Concentration of electrons per c.c.
−1	280	0·0135	15×10^{-2}	$5·91 \times 10^{11}$
0	290	0·0137	$4·5 \times 10^{-2}$	$5·88 \times 10^{11}$
2	290	0·015	$8·4 \times 10^{-2}$	$3·14 \times 10^{11}$
3 (edge of the egg)	320	0·020	$7·6 \times 10^{-2}$	$2·48 \times 10^{11}$
5 (middle of the egg)	290	0·130	19×10^{-2}	$7·66 \times 10^{11}$
...	...	...	...	...

Fig. 8.

CYLINDRICAL TUBE

other forms of discharge (fig. 8). The transition to this value of the space-potential is abrupt from the stage of non-striated glow studied under (ii. *b*). The concentration and the average energy of the electrons are shown in Table IV.

SUMMARY AND CONCLUSION.

Measurements have been made by the Langmuir "Exploring Collector" in combination with a third "bobbin" electrode (a method developed by the authors in a previous paper) of the space-potential, energy, and concentration of the electrons in striated and other forms of high-frequency discharges. The types of discharge now studied are those occurring in conical and cylindrical tubes. The results with the conical tube conform to what might be presumed on *à priori* considerations, and thus confirm the correctness of the "Exploring Collector" method in its modified form as applied to high-frequency discharge.

In the case of the cylindrical tube striated, non-striated (at low pressure), and splasmoidal forms of discharge have been studied. In all the non-striated forms of discharge the electronic concentration falls with the rise of the space-potential. In the case of striated discharge, however, the space-potential as well as the electronic concentration drops to a minimum value in the dark space. The splasmoidal discharge is characterized by abnormally high value of the space-potential as compared to that of the former two. The electric field of force in the glow is nevertheless low and comparable with the other cases.

In conclusion, we desire to express our best thanks to Prof. S. K. Mitra for suggesting the investigation and for his kind help and guidance.

Wireless Laboratory,
  University College of Science,
    Calcutta, 24th July, 1931.

XLII. *A Search for the Band Spectra of Boron Fluoride. By* N. R. TĀWDE, *B.A., M.Sc.(Bombay), and* R. C. JOHNSON, *M.A., D.Sc., Lecturer in Physics, University of London, King's College* *.

Introduction.

OUR knowledge of the band spectra of diatomic molecules such as CO, N_2 is very extensive. The investigation of the band spectra of boron fluoride (BF) therefore arose in view of the close similarity which it should exhibit with

* Communicated by the Authors.

CO and N_2 from the point of view of electronic structure. Attempts at the investigation of BF spectra were previously made by Johnson and Jenkins [*], who reported failure of their attempts due to the presence of SiF_4. The band systems of the latter have now been fully classified by those authors. The work of the classification of BF spectra offered therefore a simplified prospect, and has led the writers to the present attempts.

Very little is known of the band spectra of this compound beyond certain bands found by Plücker, Ciamician, and others (see Kayser and Konen, ' Handbuch der Spektroscopie,' vols. v. and vii. on boron) by the discharge through BF_3 and some others measured by Kühne referred to collectively without distinction as the "boron bands." They were subsequently identified by Mulliken [†] as due to boron oxide (BO) molecule.

Experimental.

Two methods were tried for the preparation of BF_3, one involving the use of calcium fluoride (CaF_2) and the other potassium fluoborate (KBF_4). The use of either method gave the same type of spectra. The methods used were as follows:—

(i.) A mixture of finely powdered boron trioxide (boric anhydride, B_2O_3) and calcium fluoride was treated with concentrated sulphuric acid, and the resulting gas was passed over sodium fluoride and then made to scrub with vitreous boric oxide. The purpose of the former was to free the gas from HF, and the latter to avoid the impurity of silicon fluoride (SiF_4). The free gas was then dried by passing over calcium chloride and P_2O_5 before it finally entered the discharge tube.

(ii.) In the second method a mixture of KBF_4 and finely powdered B_2O_3 was treated with conc. H_2SO_4, and the resulting gas was then purified and dried as above. The discharge tube, to which two side bulbs of P_2O_5 and KOH were attached, was kept on the pump system throughout the exposure, and fresh supplies of gas were admitted continuously at a constant pressure without interrupting the exposure. The tubes used were both wide bore and capillary. The exciting current was kept approximately constant and the pressure of gas in the tube at about 1 mm. of mercury. The photographs have been taken on a Hilger E_1 glass spectrograph giving a dispersion of 14·2 cm. from $\lambda\lambda$ 7000–

* Proc. Roy. Soc. A, cxvi. p. 327 (1927).
† Phys. Rev. xxv. p. 259 (1925).

4700 and the same from λλ 4700–3900. On the quartz spectrograph the dispersion was 20·7 cm. from λλ 7000–3200 and 18·7 cm. from λλ 3100–2431.

Bands Examined.

On close examination of the several plates obtained in the different regions it was noticed that the photographs showed a number of double-headed doublet bands between λλ 5600–3500. These on measurement and comparison were, however, found to belong to the α-system analyzed by Mulliken (*loc. cit.*) and ascribed by him to the BO molecule. Besides these a few strong and very diffuse bands degraded to the violet were obtained near the red region which cannot be assigned to any of the known systems. There is some evidence of structure in these diffuse groups suggesting that each may, in fact, be a close sequence ; but it is impossible to say this with any certainty, in view of the low dispersion. These are tabulated below. The wave-lengths are measured correct to 1 Å.U.

TABLE I.

Intensity.	Wave-length in I.A.	
3	6399·7	?
1	6395·5	
3	6327·1	?
2	6323·5	
4	6176·1	
4	6112·2	
8	5993·7	
6	5983·9	
4	5975·6	
10	5822·1	
8	5814·3	
6	5806·9 ?	
6	5803·5	
6	5663·8	
3	5655·9	
1	5649·8 ?	
1	5646·3	

Apart from those above, some miscellaneous band groups degraded to the red are recorded below which seem to be

interesting and may perhaps be due to BF molecule; but in the absence of sufficient evidence nothing definite can be said as to their structure and origin.

TABLE II.

Intensity.	Wave-length in I.A.
2	5476·3 ⎫
6	5471·8 ⎰
10	5460·8 ⎫
8	5457·7 ⎰
4	5451·1 ⎫
4	5447·9 ⎰
1	5441·5 ⎫
3	5437·2 ⎰
2	5425·5 ⎫
2	5421·6 ⎰
8 d	4465·0
8 d	4461·7 ⎫
6 d	4460·4 ⎰ ?
8 d	4443·5
6 d	4440·2 ⎫
6 d	4438·8 ⎰ ?

d = diffuse.

In all the plates taken we have not obtained any of the band systems of SiF molecule except a very faint trace of the strongest band at λ 4368. With regard to the formation of the BO bands, we can only infer the presence of a trace of oxygen mixed with BF_3 which entered the discharge-tube. The data presented in this paper are clearly inadequate for purposes of any analysis, but it has been thought desirable to place on record the only band data which are found in the optical region of the spectrum associated with boron fluoride. We can offer no explanation of the contrast presented by this molecule with those of CO and N_2.

One of the authors (Mr. Tawde) is indebted to the Government of Bombay for offering due facilities to carry on the work.

XLIII. *On the Absorption of X-Rays in Gases and Vapours.*
Part II. *By* J. A. Crowther, *M.A., Sc.D., F.Inst.P.,*
Professor of Physics in the University of Reading, and
L. H. H. Orton, *B.Sc.* *.

§1. *Experimental Method and Results.*

IN a previous communication † we described some measure-
ments on the absorption of a homogeneous beam of
X-rays in various gases. The primary object of these
experiments was to investigate the relation between the total
ionization produced by the complete absorption of the
beam in a gas and the ionization potential of the gas—
that is, between the average energy spent in producing
a pair of ions and the minimum energy necessary to produce
ionization. The choice of gases for experimentation was
therefore limited to those gases for which the ionization
potentials had been determined. It became clear, however,
in the course of the work that we had at our disposal a
means of investigating with some accuracy absorptions in
a part of the X-ray spectrum which so far had not been
too thoroughly explored, and it was decided to extend the
observations to other gases and vapours.

One of the main sources of uncertainty in the measure-
ment of the absorption of soft X-rays by substances in the
solid or liquid form lies in the difficulty of preparing films
sufficiently thin to transmit a suitable fraction of the incident
beam and at the same time sufficiently uniform for the
purpose. This difficulty does not arise in the case of gases
or vapours. The actual path of the X-rays through the
gas may be as much as 50 cm., and can therefore be
measured with great accuracy, and the mass per unit area
can be adjusted and measured by altering and measuring the
pressure of the gas.

The apparatus and method of working, fully described in
the previous communication, was adopted without material
alteration in the present work. A close investigation of the
beam transmitted through the apparatus indicated that
greater consistency might be obtainable in the measurements
if the dimensions of the various slits in the collimating
system were slightly altered, and these adjustments were
made before the new measurements were undertaken.
As it was found that this increased consistency was actually

attained, fresh measurements were undertaken on most of the gases previously investigated. The new determinations, however, did not differ as a rule by more than 1 per cent. from those previously quoted.

In some of the more highly absorbent vapours the absorption in the 50 cm. absorption chamber was too high to be measured accurately unless the pressure of the vapour was reduced to an inconveniently low value. For these vapours a shorter absorption chamber was substituted for the original one. Test experiments, made with air as the absorbing medium, showed that the two chambers gave identical results.

Most of the measurements were made using copper K_α radiation obtained by analyzing the radiation from a Shearer tube, fitted with a copper anticathode, using a simple spectrometer furnished with a rock-salt crystal. A certain number of experiments were also made using iron K_α radiation, obtained in a similar manner. Although the primary object of the research was to determine coefficients of absorption, determinations of the relative ionization produced by the beam in different gases and vapours was also measured, as it was thought that the results might have some practical value. The whole of the experimental results are contained in Table I. The first column gives the value assumed for the density of the gas or vapour at standard temperature and pressure. For gases we have usually been able to use experimentally determined values. The values given for the vapours have been calculated from their molecular weights, as we were unable to trace any direct determinations.

The second column gives μ_m, the mass coefficient of absorption of the substance for the radiation employed. It includes both the true mass absorption τ_m and the mass scattering σ_m. The third column gives the ionization per unit volume relative to air at the same temperature and pressure. The final column (which is calculated from the previous column and the assumed density of the gas) gives the relative ionization in equal masses of the given substance and air.

§2. *Discussion of the Order of Accuracy of the Results.*

Before attempting to discuss the results given in Table I. it is necessary to form some estimate of the accuracy of the work. A balance method was employed, the ionization in two oppositely charged ionization chambers being adjusted, by altering the pressure in one of them, until an electroscope

TABLE I.

	Density ×10³.	μ_m.	I_v.	I_m.	T.
CuK$_\alpha$ radiation ($\lambda = 1.539$ Å.).					
Air......................	1·293	9·44	1·00	1·00	1·00
N$_2$	1·254	7·33	0·743	0·766	0·99$_3$
O$_2$	1·429	11·10	1·438	1·301	1·10$_3$
CO$_2$	1·977	9·15	1·535	1·004	1·03$_5$
H$_2$S	1·538	82·7	14·96	12·58	1·41
A	1·781	112·5	21·80	15·83	1·32$_0$
C$_5$H$_{12}$	3·214	3·58	1·32	0·53$_1$	1·45
C$_6$H$_{14}$	3·839	3·62	1·65	0·55$_4$	1·50
C$_2$H$_5$Cl	2·87	60·0	18·74	8·44	1·31
CHCl$_3$	5·328	92·4	52·7	12·79	1·28$_5$
CCl$_4$	6·87	96·9	73·8	13·89	1·33
Zn(CH$_3$)$_2$	4·258	39·3	18·9	5·74	1·37
C$_2$H$_5$Br	4·864	66·2	35·3	9·38	1·31
CH$_3$I	6·337	259·8	187·3	38·2	1·36
Al	—	47·9	—	—	—
Wax n(CH$_2$)	—	3·74	—	—	—
FeK$_\alpha$ radiation ($\lambda = 1.935$ Å.).					
Air......................	—	18·81	1·00	1·00	1·00
O$_2$	—	22·20	1·439	1·302	1·10$_1$
CO$_2$	—	18·27	1·550	1·013	1·04$_2$
C$_5$H$_{12}$	—	7·36	1·34	0·53$_3$	1·41
C$_6$H$_{14}$	—	7·04	1·64	0·55$_2$	1·50
(C$_2$H$_5$)$_2$O	3·307	10·48	1·98	0·77$_3$	1·40
C$_2$H$_5$Cl	—	107·5	—	—	—
Al	—	93·8	—	—	—
Wax	—	7·47	—	—	—

μ_m = mass coefficient of absorption ; I_v = relative ionization per unit volume ; I_m = relative ionization per unit mass of gas ; T = total (integrated) ionization, relative to air.

connected to both gave no deflexion when the rays were passing. The chamber which is to contain the absorbing substance lies between the two ionization chambers, and a balance is obtained with this chamber evacuated. The chamber is then filled with the absorbing vapour, and the decreased ionization in the further ionization chamber is compensated by reducing the pressure in the nearer one. The accuracy of the work thus depends primarily on the accuracy with which this change in pressure can be measured.

In practice the method was found to work extremely well. It was found that a variation of less than $\frac{1}{2}$ mm. in the pressure in the ionization chamber was sufficient to produce a perceptible steady drift in the leaf of the electroscope. Since each balance point could be fixed with certainty to $\frac{1}{2}$ mm., the extreme error in measuring the change in pressure should not exceed 1 mm. For the majority of the substances used it was possible to arrange that the total change in pressure to be measured was of the order of 20 cm. Individual measurements made on the same material should thus be consistent to $\frac{1}{2}$ per cent. These expectations were in the main realized. Thus four independent sets of measurements on the absorption of iron K_α radiation in oxygen gave values for the coefficient of absorption of 22·34, 22·19, 22·10, and 22·16, with a mean value of 22·20 and a maximum variation from the mean of 0·6 per cent. The measurements on air provide a more searching test; they were taken at intervals throughout the course of the research, and should therefore be subject to any errors which might be introduced by the various readjustments of the apparatus and by the presence of impurities remaining in the apparatus from previous experiments. The actual values obtained were 9·45, 9·48, 9·43, 9·48, 9·39, 9·46, and 9·41, giving a mean value of 9·44, with a maximum variation from the mean of just over $\frac{1}{2}$ per cent. The consistency of the measurements indicates that, in the absence of systematic error, the calculated coefficients should be accurate to at least $\frac{1}{2}$ per cent., and probably better. The only exceptions to this statement are the coefficients of absorption of copper K_α radiation in pentane and hexane. Owing to a small absorption coefficient, coupled with a comparatively low vapour pressure, the absorption of the radiation in these vapours was less than 10 per cent. of the initial energy of the beam, and the pressure change to be measured was less than 5 cm. The uncertainty in these two values may be as high as 3 per cent.

Consistency in the readings does not of course preclude the possibility of systematic error. A point of some importance is the purity of the materials used. The methods of preparation of most of the gases used has been described in the earlier communication. The argon was obtained from the British Oxygen Company, and was stated to contain less than 1 per cent. of nitrogen. The various liquids whose vapours were employed in the experiments were obtained from Kahlbaum, and were described by them as pure (with the exception of the chloroform which was stated to contain 1 per cent. of alcohol). The aluminium foil was the ordinary commercial product. It was analyzed, and found to contain 0·56 per cent of iron. The values for aluminium given in Table I. have been corrected for the presence of this quantity of iron.

In the case of vapours some uncertainty is introduced by the assumption, necessarily made in the calculations, that these vapours could be treated as perfect gases and that their density could be calculated from the molecular weight. These assumptions are certainly not rigorously true, but the error introduced is probably small. For saturated water vapour, for which the data necessary for testing the matter exist, the error is rather less than 1 per cent. at 27° C. As the vapours in our experiments were always used at pressures considerably below the saturation pressure, the error introduced is not likely to be larger than this, unless the vapour is one which shows partial polymerization. This source of uncertainty of course does not exist in the measurements on gases.

A question which is always important in absorption measurements is the homogeneity of the radiation used. The radiation used in our experiments was the K_α radiation of the target of the tube, sorted out from the general radiation by means of a rock-salt crystal. No attempt was made to eliminate either of the two K_α lines, but the resolving power was sufficiently high to allow of the complete removal of the K_β lines. As the tube was excited at a voltage of 45,000 volts, the beam emerging from the simple spectrometer would contain, in addition to the K_α radiation required (which was reflected as a first order spectrum), the second and third order reflexions of portions of the general radiation from the tube. Fortunately, as experiment shows, nearly half the X-ray energy emitted from a Shearer tube under the conditions employed is in the line radiation, the general radiation being everywhere comparatively weak. Moreover the efficiency of the second and

third order reflexions is only about 7 per cent. of that of the first order. Calculations made on the data obtained by Treloar * showed that at most the admixture of high-frequency radiation in our beam should not amount to more than $1\frac{1}{2}$ per cent. This should not have any appreciable effect on the absorption measurements until the absorption reached about 80 per cent. of the initial energy of the beam.

To test the matter, however, absorption measurements were made with varying numbers of sheets of aluminium foil. The coefficient of absorption of copper K_α radiation in aluminium was found to be 49·4 using a single sheet, 49·4 using two sheets, and 49·2 using three sheets. The three sheets together absorbed 89 per cent. of the radiation, and it will be seen that up to an 89 per cent. absorption there is no significant change in the coefficient of absorption. If we assume that the drop from 49·4 to 49·2 is significant (it is probably just within the possible experimental error) it would indicate an admixture of harder radiation amounting to 1·2 per cent. of the whole. The error introduced into our results by this percentage of hard radiation would not exceed about 0·2 per cent., and may safely be disregarded.

§3. *Molecular and Atomic Absorptions.*

The molecular absorption of a compound or element may be calculated by multiplying the mass coefficient of absorption by the actual mass of the molecule. The latter can be obtained by multiplying the molecular weight by the mass, in grams, of an atom of unit atomic weight. We have taken this constant as $1·65 \times 10^{-24}$ gram. The molecular absorption, $\mu_{mol.}$, so calculated is recorded in the first column of Table II. It includes both the true molecular absorption, $\tau_{mol.}$, and the molecular scattering, $\sigma_{mol.}$ To obtain the true absorption it is therefore necessary to know the molecular scattering.

A difficulty here arises which has caused us some anxious consideration. In spite of many careful and elaborate experiments there is still much uncertainty as to the precise values of the coefficients of scattering, the uncertainty being particularly great in the long wave-length end of the X-ray spectrum. There seems to be some consensus of opinion that the mass coefficient of scattering in the neighbourhood of the molybdenum K radiation is of the order of 0·2 for carbon, that it increases with increasing wave-length, and, further, that, particularly in the long wave-length part of the

* Treloar, J. Brit. Inst. Rad. ii. p. 188 (1929).

spectrum it also increases fairly rapidly with increasing atomic number of the scattering element. The actual numerical estimates, however, are very discordant, and, as far as we are aware, no absolute measurements of scattering have been made in the region of the spectrum with which we are concerned.

TABLE II.

	CuK_α radiation. $\lambda = 1\cdot539 \times 10^{-8}$ cm.			FeK_α radiation. $\lambda = 1\cdot935 \times 10^{-8}$ cm.		
	$\mu_{mol.} \times 10^{22}$.	$\sigma_{mol.} \times 10^{22}$.	$\tau_{mol.} \times 10^{22}$.	$\mu_{mol.} \times 10^{22}$.	$\sigma_{mol.} \times 10^{22}$.	$\tau_{mol.} \times 10^{22}$.
N_2	3·38	0·11	3·27	—	—	—
O_2	5·86	0·15	5·71	11·69	0·19	11·50
CO_2	6·69	0·18	6·51	13·26	0·23	13·03
C_5H_{12}	4·26	0·29	3·97	8·64	0·37	8·27
C_6H_{14}	5·14	0·33	4·81	10·00	0·42	9·58
n(CH_2). wax	n(0·854)	n(0·054)	n(0·80)	n(1·72₅)	n(0·068)	n(1·65)
$(C_2H_5)_2O$	—	—	—	12·79	0·37	12·42
Al	21·3	0·20	21·1	41·8	0·25	41·5
H_2S	47·0	0·31	46·7	—	—	—
C_6H_5Cl	63·6	0·5	63·1	114·5	0·6	113·9
$CHCl_3$	183·7	1·1	182·6	—	—	—
CCl_4	245·1	1·4	243·7	—	—	—
A	73·9	0·4	73·5	—	—	—
$Zn(CH_3)_2$	61·9	1·0	60·9	—	—	—
C_2H_5Br	119·0	2·6	116·4	—	—	—
CH_3I	608·2	4·1	604	—	—	—

$\mu_{mol.}$ = absorption per molecule; $\sigma_{mol.}$ = scattering per molecule (assumed) $\tau_{mol.}$ = true absorption per molecule (= $\mu_{mol.} - \sigma_{mol.}$).

The increase in the scattering coefficient is generally ascribed to the effect of cooperation between the electrons in the atom when the wave-length of the incident radiation becomes comparable to the distance apart of the electrons.

In the absence of such cooperation—that is to say, when the
wave-length of the radiation is small in comparison with
the distance between the electrons—the scattering should be
calculable from the formula given by Compton or from the
more complicated formula of Klein and Nishina.   Hertzog [*]
has recently made some very careful measurements of the
relative scattering of a beam consisting largely of copper
K radiation for a number of gases, including many of those
used in our experiments.   We have assumed that the
scattering for hydrogen can be calculated from the Klein-
Nishina formula—that is to say, that the two electrons in the
hydrogen molecule act as independent scattering centres for
the copper K_α radiation,—and obtained the scattering
coefficients for other substances from this value by using
Hertzog's measurements of the relative scattering.   The
values of $\sigma_{mol.}$ thus obtained are given in Table II. ; they are
clearly minimum values.   Experiments published recently
by Coade [†] might be taken as justifying appreciably higher
values for the scattering coefficients.

Fortunately the scattering for absorbable radiation such
as we have been using in our experiments is relatively small
compared with the true absorption.   For the hydrocarbons,
where the correction is most important, it only amounts to
7 per cent. ; for oxygen it is already as low as 2 per cent.,
and for elements of higher atomic number it is practically
negligible ; for the lighter elements, however, the correction
is certainly not known to the accuracy with which we
believe we have been able to make the measurements of the
absorption.

§4. *Atomic Absorptions.*

If we make the usual assumption that X-ray absorption
is an atomic effect and that the molecular absorption is the
sum of the absorptions of the individual atoms, we can
calculate the atomic absorptions of a considerable number
of the lighter elements from the molecular absorptions given
in Table II. ; the values so obtained are given in Table III.
One or two points may be worth further discussion.

A considerable amount of time was spent in accumulating
data for the calculation of the atomic absorption of carbon,
the difficulty being of course the very small absorption
of this element.   As indicated in a previous section of the
paper the measurements on pentane and hexane for copper
radiation are somewhat uncertain.   Those on carbon dioxide

---

[*] Hertzog, *Helvet. Phys.* Acta ii. p. 3 (1929)
[†] Coade, Phys. Rev. xxxvi. p. 1110 (1930).

and oxygen are probably accurate to at least $\frac{1}{2}$ per cent., as each of these gases was easy to prepare in a state of purity and produced sufficient absorption in the beam to make accurate measurements possible. An error of $\frac{1}{2}$ per cent. in either would, however, produce an error of 5 per cent. in the value for carbon, since this is the difference between the two molecular absorptions. It was for this reason that the experiments on paraffin wax were undertaken. This

TABLE III.

Atomic Absorption, $\tau_a \times 10^{22}$.

Element.	CuK_α.	FeK_α.	CuK_α (Colvert).	$\dfrac{Fe}{Cu}$.
6. Carbon	0·80	1·62	—	2·02
7. Nitrogen	1·63	—	—	—
8. Oxygen	2·86	5·75	—	2·01
10. Neon	—	—	7·64	—
13. Aluminium	21·1	41·5	21·8	1·97
16. Sulphur	46·7	—	46·3	—
17. Chlorine	60·7	110·7	59·8	1·82
18. Argon	73·5	—	74·6	—
30. Zinc	59·3	—	—	—
35. Bromine	114·8	—	—	—
53. Iodine	603·3	—	—	—

was measured in the solid state, the wax being pressed out into sheets of uniform thickness between two surface plates. We have assumed in our calculations that the molecular formula of the wax may, with sufficient accuracy, be taken as $n(CH_2)$. The results of the various estimations of the atomic absorption of carbon are given below:—

Copper K_α *radiation.*

(1) C_6H_{12} ; $C = \dfrac{1}{5}(3·97) = 0·79.$

(2) C_6H_{14} ; $C = \dfrac{1}{6}(4·81) = 0·80.$

(3) Wax; $C = \dfrac{1}{n} n(0{\cdot}80) = 0{\cdot}80.$

(4) $CO_2 - O_2$; $C = 6{\cdot}51 - 5{\cdot}73 = 0{\cdot}80.$

Iron K_α *radiation.*

(1) C_5H_{12}; $C = \dfrac{1}{5}(8{\cdot}27) = 1{\cdot}65.$

(2) C_6H_{14}; $C = \dfrac{1}{6}(9{\cdot}58) = 1{\cdot}60.$

(3) Wax; $C = \dfrac{1}{n}(1{\cdot}65) = 1{\cdot}65.$

(4) $CO_2 - O_2$; $C = 13{\cdot}03 - 11{\cdot}56 = 1{\cdot}53.$

(5) $C_4H_{10}O - O$; $C = \dfrac{1}{4}(12{\cdot}42 - 5{\cdot}75) = 1{\cdot}67.$

It may be noted that we have assumed that the absorption of hydrogen, as distinct from its scattering, which has already been allowed for in calculating the molecular absorption, is negligibly small. This seems justifiable, as the atomic absorption varies approximately as the fourth power of the atomic number. The measure of agreement shown by the results is eminently satisfactory, especially when we consider that the measurements on the hydrocarbons are the least certain of our measurements. The maximum discrepancy shown is in the calculation of the atomic coefficient for iron radiation from the difference between the molecular absorptions of CO_2 and O_2. This would be accounted for by an error of only $\frac{1}{2}$ per cent. in either of the readings, or by an error in $\frac{1}{4}$ per cent. in both. It is, therefore, probably not significant.

The values of the atomic absorption of chlorine as deduced from the three chlorine compounds are 61·5 from ethyl chloride, 60·7 from chloroform, and 60·6 from carbon tetrachloride. The value from ethyl chloride seems rather high compared to the other two, the discrepancy amounting to 1·3 per cent. It is possible that there may be slight polymerization in this vapour. As the two lower results are very consistent we have taken 60·7 as the best value.

While these experiments were in progress measurements on X-ray absorption in certain gases were published by Colvert[*]. The values of τ_a calculated from his measurements for the elements with which we are concerned are

---

[*] Colvert, Phys. Rev. xxxvi. p. 1619 (1930).

given in the third column of Table III. Colvert took very
elaborate precautions to ensure the purity of his radiation.
His paper gives very little information as to the method of
measuring the absorption. As far as we can judge from
his paper he seems to have relied on being able to maintain
a constant output from his X-ray tube. If so his results
should be rather less certain than ours. The agreement
between the two sets of values is, on the whole, satisfactory.

§5. *X-ray Absorption Formulæ. Variation of Atomic Absorption with Atomic Number.*

It is well known that the atomic absorption of X-rays can
be represented approximately over a very wide range of
wave-lengths and a very wide range of absorbing substances
by an empirical relation of the form

$$\tau_a = Z^4\lambda^3(C_\kappa + C_L + \ldots),$$

where λ is the wave-length of the radiation, Z the atomic
number of the absorbing element, and C_κ, C_L, ... are
constants representing the contributions of the K, L, ..
absorption bands. For radiation of sufficiently high fre-
quency to stimulate all the absorption bands the formula
reduces to the simple form

$$\tau_a = CZ^4\lambda^3.$$

A relation of this type was developed by Kramers[*] on
theoretical grounds. He showed, that on certain assump-
tions the atomic absorption should be represented by the
relation

$$\tau_a = \frac{32\pi^4 e^{10} m}{3\sqrt{3}c^4 h^6}\left(1 + \frac{1}{6} + \frac{1}{18} + \ldots\right)Z^4\lambda^3,$$

m and e being the mass and charge of an electron and c the
velocity of light.

Somewhat earlier de Broglie[†], by an entirely different
mode of attack, had suggested the relation

$$\tau_a = \frac{\pi e^2}{mc^2}\lambda^3\left\{\eta_\kappa\frac{N_\kappa}{\lambda_\kappa^2} + \eta_L\frac{N_L}{\lambda_L^2} + \ldots\right\},$$

where e, m, and c have the same significance as before, N_κ is
the number of electrons in the K ring, λ_κ is the critical
K absorption wave-length, and η_κ is an undetermined
constant of the order of magnitude unity. The two formulæ

[*] Kramers, Phil. Mag. xlvi. p. 836 (1923).
[†] de Broglie, *Journ. de Phys.* iii. p. 33 (1922).

agree in predicting a variation in the absorption proportional to the third power of the wave-length of the incident radiation. On Kramer's theory the atomic absorption varies as the fourth power of the atomic number. In de Broglie's formula the atomic number is involved indirectly, since the critical absorption wave-lengths are a function of the atomic number. Assuming Moseley's relation, $\frac{1}{\lambda_{\kappa}^{2}} \propto (Z-k)^4$, where k is a constant which varies from one absorption band to another. For the elements with which we are mainly concerned, from carbon to argon λ_{L}^{2} is very large compared with λ_{κ}^{2}, and the L absorption term can be neglected. Hence we should expect that for these elements $\frac{\tau_a}{(Z-k)^4}$ should be constant. The distinction between the two theories is obviously most pronounced for elements of low atomic number, such as those investigated in the present experiments.

If the actual values of the critical absorption wave-lengths are known we can of course substitute the values directly in the de Broglie formula. If the available data are reliable this is the more satisfactory method, since Moseley's law does not hold with absolute accuracy. We can thus estimate the value of the undetermined constant η_{κ}. In the following discussion we shall confine our attention to the results obtained with copper K radiation, deferring until a later section the consideration of the results obtained with iron K radiation.

If the logarithm of τ_a is plotted against the logarithm of Z the graph falls into two parts, since the copper radiation does not excite the K absorption of zinc and elements of higher atomic number. In the first portion of the graph, from carbon to argon, we are dealing with the $K + L + \ldots$ absorption, in the latter, from zinc to iodine, only with the $L + M + \ldots$ absorption. Each portion appears very nearly linear if the graph is plotted on a sufficiently small scale. If we ignore the deviations from exact linearity, and draw two straight lines to represent the points as accurately as possible, each of these lines has a slope of 4·00 within the limits of experimental error. Thus, if the atomic absorption is to be represented by a relation of the form $\tau_a \propto Z^n$, the best value of n does not differ appreciably from 4. It may be mentioned, in passing, that the value of the quantum absorption jump in the neighbourhood of the absorption discontinuity is given by $(K + L + \ldots)/(L + M + \ldots) = 8\cdot9$.

Plotting on a large scale, however, reveals that the first portion of the graph (and possibly the second also) is not

exactly linear, but shows an unmistakable concavity to the Z axis which is certainly greater than our experimental error. Since the graph is not rectilinear the results cannot be expressed by a simple power law, such as that of Kramers. This is shown quite clearly by evaluating the ratio τ_a/Z^4 for the different elements. The result of the calculation is given in the first column of Table IV. We have included in this table, together with our own observations, a value for neon

TABLE IV.

	$\dfrac{\tau_a}{Z^4} \times 10^{26}$.	$\dfrac{\tau_a \times 10^{26}}{(Z-0.7)^4}$.	$\dfrac{\tau_a \times 10^{26}}{(Z+0.5)^4}$.
6. Carbon	6·18	10·14	—
7. Nitrogen	6·72	10·11	—
8. Oxygen	6·96	10·04	—
10. Neon	7·64	10·21	6·29
13. Aluminium	7·38	9·22	6·35
16. Sulphur	7·12	8·50	6·29
17. Chlorine	7·27	8·62	6·21
18. Argon	7·00	8·20	6·29
26. Iron	6·58	7·35	6·11
30. Zinc	0·732	0·805	—
35. Bromine	0·765	0·829	—
53. Iodine	0·764	0·806	—

τ_a = atomic absorption coefficient for Cu K_α radiation.
Z = atomic number.

calculated from Colvert's * data, and a possibly somewhat less certain value for iron calculated from measurements by S. J. Allen †. It will be seen that the ratio increases fairly rapidly from carbon to neon, and then decreases slowly but definitely with increasing atomic number. It is quite clear

* Colvert, *loc. cit.*
† Allen, Phys. Rev. vol. **xxviii**. p. 907 (1926).

from these figures that the relation is not of the form $T_a \propto Z^4$.

If the values of $\tau_a^{\frac{1}{4}}$ are plotted against Z it is found that the points from carbon to neon lie very accurately on a straight line which intercepts the Z axis at about 0·7 on the positive side of zero. A formula of the type $\tau_a \propto (Z-k)^4$, suggested by de Broglie's theory, should therefore fit the experimental results over this range. The value of k which appeared to fit the results most closely was 0·7. The values of $\tau_a/(Z-\cdot7)^4$ are given in the third column of Table IV.

It will be seen that this ratio is constant to an accuracy of nearly 1 per cent. for the four elements carbon, nitrogen, oxygen, and neon. This constancy seems too close to be fortuitous. After passing neon, however, the value of the ratio steadily declines, the decline being much greater than the possible error in the determinations of τ_a.

The graph of $\tau_a^{\frac{1}{4}}$ against Z shows a distinct change in slope at neon, and it is interesting to notice that the second portion of the graph, from neon to argon, also appears to be linear, the straight line through the points cutting the axis of Z at about 0·5 on the negative side of the zero. It is very difficult to conceive of any theoretical basis for a relation of the form $\tau_a \propto (Z+k)^4$, but the fact remains that the ratio $\tau_a/(Z+\cdot5)^4$ is constant to 1 per cent. for the elements from neon to argon. The figures are given in column 3 of Table IV.

These results make it evident that the atomic absorption cannot be represented over the whole range of atomic numbers covered by our measurements by either of the formulæ proposed, although that of de Broglie appears to be of the right form for elements in the first group of the periodic table—that is to say, until the completion of the L ring. To test the de Broglie formula in more detail we can substitute the observed values for the critical absorption frequencies in the equation. Holweck [*] has made an accurate survey of the absorption levels of most of the lighter atoms, and his values for the K and L absorption levels are given in columns 2 and 3 of Table V., where they are expressed in " volts." The corresponding value of ν_κ (where ν_κ is the critical absorption frequency and is equal to c/λ_κ) are given in column 4. It will be seen that $\nu_L^2 \nu_\kappa^2$ is completely negligible for aluminium and elements of lower atomic number, and is only 0·006 for argon. If η_L is of the same order of magnitude as η_κ, the

---

[*] Holweck, *C. R.* clxxiii. p. 709 (1921); clxxxii. p. 1339 (1923).

L absorption for argon only amounts to about 2·5 per cent. of the K absorption, and is a still smaller fraction for the lighter elements. The L term in the formula can thus be neglected. Since $1/\lambda_\kappa^2 \propto \nu_\kappa^2$, the ratio τ_a/ν_κ^2 should thus be constant if de Broglie's formula holds good. The values of this ratio are given in the last column of Table V.

The agreement is very good for the first four elements in the list, but again there is a marked change after neon is passed, the ratio showing a steady decline as the atomic number increases. The effect of taking into account the

TABLE V.

	λ_κ (volts). λ_L (volts). (after Holweck).		$\nu_\kappa \times 10^{16}$.	$\left(\dfrac{\nu_L}{\nu_\kappa}\right)^2$.	$\dfrac{\tau_a}{\nu_\kappa^2} \times 10^{56}$.
Carbon	280 5	—	6·79	—	1·74
Nitrogen	397	—	9·63	—	1.76
Oxygen	528	—	12·74	—	1·76
Neon	864	16·5	20·90	4×10^{-4}	1·75
Aluminium.....	1555	70·6	37·6	2×10^{-3}	1·49
Sulphur	2464	59·6	59·6	4×10^{-3}	1·32
Chlorine.........	2817	203	68·2	5×10^{-3}	1·31
Argon............	3195	246·5	77·3	6×10^{-3}	1·23
Iron	7100	—	171·5	—	1·02

$\lambda_\kappa, \lambda_L$. Critical K. L absorption wave-lengths (in volts).

ν_κ, ν_L. Critical absorption frequencies, per sec.

L absorption would be to decrease these later values slightly, and thus to make the decline rather more rapid.

Taking $1·75 \times 10^{-56}$ as the constant value of τ_a/ν_κ^2 for the first four elements, and substituting in de Broglie's equation the value of the undetermined constant, η_κ is found to be 2·44. This seems in reasonable accord with de Broglie's statement that it should be of the order unity. The relation thus appears to fit the results for elements up to an atomic number of 10. It seems clear, however, that some other factor comes into play for elements of higher atomic number which reduces the atomic absorption to a value below that to be expected on the theory. It is as if the

accumulation of the outer electrons produced a kind of screening effect on the K electrons and prevented them from exercising their full absorptive powers. The fact that the break appears to take place at the point where the L ring becomes closed may not be without significance.

In the previous paragraphs we have been dealing only with the K absorption of the elements. For the elements zinc, bromine, and iodine the radiation employed is of too low a frequency to stimulate the K absorption, and we are here dealing mainly with the L absorption. It will be seen on consulting Table IV. that the ratio τ_a/Z^4 is much more nearly constant for the L absorption than for the K absorption. The values are, in fact, identical for bromine and iodine ; that for zinc is about 4 per cent. lower.

The value given by our experiments for the atomic absorption of zinc may possibly be slightly low. Zinc methyl reacts very readily with water vapour, oxygen, and many other substances. Although the apparatus was washed out with carefully dried nitrogen before introducing the zinc methyl vapour it is possible that there may have been sufficient traces of water vapour or other substances adsorbed on the walls to cause the precipitation of a little of the zinc. Although we had no evidence from our measurements that such decomposition had occurred, it is impossible to attach quite the same weight to this measurement as to those on ethyl bromide and methyl iodide.

A relation of the form $\tau_a \propto (Z-k)^4$ is evidently not applicable to this part of the absorption curve. It is true that if k were small we should not, owing to the fact that we are now dealing with high atomic numbers, be able to discriminate between the two relations ; on the other hand, the form $(Z-k)^4$ arises from the application of Moseley's relation for λ_L, and as we are dealing now with the L absorption band, k should have a value of the order of 7 or more. The values for $\tau_a/(Z-0\cdot7)^4$ are already less constant than those of τ_a/Z^4. Any higher value of k is clearly impossible.

It is unfortunately impossible to test de Broglie's theory by inserting values for λ_L, since the L level is complex, and it is not known what contribution each of the sub-levels makes to the absorption. The critical L absorption wavelengths for iodine are given as $2\cdot38$, $2\cdot55$, and $2\cdot71 \times 10^{-8}$ cm. If we take a mean of $2\cdot55$ the undetermined constant η_L becomes $1\cdot5$. This is of the right order of magnitude. The failure of the relation, however, makes it unlikely that de Broglie's theory fits this part of the work. We must conclude then that the portion of the absorption curve from

zinc to iodine can be represented most adequately by the relation $\tau_a \propto Z^4$, with possibly a slight tendency for the absorption to fall below the normal value in the immediate neighbourhood of the absorption band.

§6. *Variation of Atomic Absorption with Wave-length.*

Both Kramers' and de Broglie's theories agree in predicting that the atomic absorption of a given element should vary as the cube of the wave-length of the incident radiation. The theoretical basis for this relation seems fairly strong. The experimental evidence, however, seems against it. Allen was the first to suggest that the exponent was somewhat less than 3, and he suggested that a figure of 2·92 would more nearly represent his very extensive observations. Colvert gives values for the exponent ranging from 2·77 for argon to 2·92 for neon. The question is complicated by the scattering, which, in the case of measurements made with fairly penetrating radiation, becomes an important factor in the whole absorption, and may account for as much as one quarter of the whole. In the absence of more precise knowledge of the magnitude of the scattering and its variation with wave-length and atomic number, the actual relation between τ_a and λ must remain somewhat doubtful

Our own experiments are not sufficiently extensive at present to enable us to draw any very certain conclusions. The copper K_a radiation has a mean wave-length of 1·539 Å.; the iron K_a one of 1·935 Å. The ratio $(Fe/Cu)^3$ is thus 1·986, or very nearly 2. If we take the measured coefficient of absorption μ the ratio μ_{Fe}/μ_{Cu} is almost exactly 2 for all the substances measured with the exception of ethyl chloride, for which the ratio falls to 1·80. Excluding this compound the mean value of the ratio from all the other measurements is 1·988.

The coefficient μ, however, includes the scattering. As it is extremely unlikely that the coefficient of scattering varies as rapidly as the cube of the wave-length, the ratio τ_{Fe}/τ_{Cu} will be somewhat greater than this value. The values for $(\tau_a)_{Fe}/(\tau_a)_{Cu}$ are given in the last column of Table III. Considering the uncertainty of the scattering correction the values for carbon, oxygen, and aluminium do not differ from $(\lambda_{Fe}/\lambda_{Cu})^3$ by more than the possible errors of experiment. The value for chlorine, however, is distinctly lower, the discrepancy being certainly greater than the experimental error. It is probably significant that the λ^3 law holds for those elements of low atomic number which were found in

the previous section to fit de Broglie's theory, and breaks down at approximately the same point in the atomic table.

§7. *Relative Ionization and Total Ionization.*

The relative ionizations of equal volumes of the different gases and vapours, compared with air as a standard, are given in the second column of Table I. The relative ionization for equal masses of gas are given in the third column. The total or integrated ionization, T, is obtained by dividing the relative ionization per unit mass by the true mass coefficient of absorption. It is given in the fifth column of the table. The agreement between the values for copper radiation and iron radiation is very close, in some cases quite surprisingly close. The only marked discrepancy is for pentane, where, as has already been explained, the absorption measurements were difficult. Consideration of all the data suggests that the mass absorption coefficient of copper radiation in pentane is probably 2 per cent. higher than the value given in the table. We may conclude that over the limited range of wave-lengths employed the total ionization is independent of the wave-length.

As we pointed out in our previous paper the relative efficiency of the ionization process in the different gases may be represented by the product P.T., where P is the minimum ionization potential of the gas and T is the total ionization. Our latest measurements allow us to add two further determinations of this product to the list given in our previous communication. Argon, with an ionization potential of 15·7, gives a value for P.T. of 20·7, and chloroform, with an ionization potential of 11·5, a value of 14·8. The complete list runs: argon 20·7, nitrogen 16·6, carbon dioxide 14·8, chloroform 14·8, sulphuretted hydrogen 14·7, ethylene 14·4, and oxygen 14·1. As pointed out in the previous communication, the points of interest are, firstly, that the efficiency is high for the gases argon and nitrogen, which have a low electron affinity, and, secondly, the surprising constancy of the values for the remaining gases.

In conclusion, we wish to express our thanks to the Government Grants Committee of the Royal Society for the continued loan of X-ray apparatus and to the Board of Scientific and Industrial Research for a maintenance grant to one of us.

Summary.

The mass absorption coefficients and relative ionizations of a number of gases and vapours have been measured with

CuK and FeK radiation. Atomic absorption coefficients have been deduced for eleven elements, and have been used to test the relation between atomic absorption and atomic number and between atomic absorption and wave-length.

It is found that de Broglie's formula agrees well with the observations for elements in the first series of the atomic table, but breaks down for elements of higher atomic number, the measured absorptions being less than the values given by de Broglie's theory, the presence of the outer electrons appearing to produce a screening effect on the absorption of the K electrons.

The relative total ionization in different gases is found to be independent of the wave-length of the radiation employed. The efficiency of the ionizing process is found to be high for elements which show little electron affinity, and is practically constant for other substances.

Department of Physics,
University of Reading.
August 1931.

XLIV. *The Theory of Coagulation of Homogeneous Aerosols.* *By* H. S. PATTERSON [*].

IT has previously been shown (Patterson, Whytlaw-Gray, and Cawood, Proc. Roy. Soc. A, cxxiv. p. 502 (1929)) that the experimental relationship between particulate volume and time for a coagulating aerosol may be expressed by the relationship

$$\sigma = \sigma_0 + \mathrm{K}t,$$

in which σ is the particulate volume at time t, σ_0 that at zero time obtained by extrapolation, and K is a constant for a definite material dispersed at a fixed concentration. With change of concentration or material, however, K alters, becoming smaller the higher the concentration.

On the theoretical side (*loc. cit.* p. 513) the Smoluchowski theory of coagulation of sols gives for the rate of coagulation the expression

$$-\frac{dn}{dt} = 2\pi \mathrm{DS}n^2, \quad \ldots \ldots \quad (1)$$

where n is the number of particles per unit volume, D the relative diffusion coefficients for any two particles, and S the average radius of the sphere of attraction between any two

particles. For a homogeneous aerosol, the particles of which only unite when they touch, we have shown that

$$2\pi DS = \frac{4}{3}\frac{RT}{\eta N}\left(1 + A\frac{l}{r}\right),$$

where R is the gas constant, T the absolute temperature, η the viscosity of the medium (air), N the Avogadro number, A a constant determined experimentally by Millikan, l the mean free path in air, and r the radius of the average particle. Equation (1) becomes accordingly

$$-\frac{dn}{dt} = \frac{4}{3}\frac{RT}{\eta N}\left(1 + A\frac{l}{r}\right)n^2. \quad \ldots \quad (2)$$

Now r obviously depends on n and may be calculated from the mass concentration and number at any given time by the expression

$$\frac{4}{3}\pi r^3\rho = \frac{m \cdot 10^{-9}}{n} = m\sigma \cdot 10^{-9},$$

where m is the mass of aerosol in milligrams per cubic metre, ρ the density of the particles, and n the number of particles per c.c. For an accurate solution of equation (2) r should be expressed in terms of n and the equation then integrated. Since, however, for many of the aerosols which we investigated the term $A\frac{l}{r}$ is fairly small compared with unity an approximate solution of the equation was obtained in which $A\frac{l}{r}$ was regarded as a constant during integration. We thus find

$$\frac{1}{n} = \frac{1}{n_0} + \frac{4RT}{3\eta N}\left(1 + A\frac{l}{r}\right)t.$$

Substituting $r = \left(\frac{3m \cdot 10^{-9}}{n}\Big/4\pi\rho\right)^{1/3}$, and writing particulate volume for numbers, *i. e.*, putting $\sigma = \frac{1}{n}$ and $\sigma_0 = \frac{1}{n_0}$, we have

$$\sigma = \sigma_0 + \frac{4}{3}\frac{RT}{\eta N}\left[1 + \frac{Al}{(3m\sigma \cdot 10^{-9}/4\pi\rho)^{1/3}}\right]t$$

or

$$t = \frac{\sigma - \sigma_0}{\frac{4}{3}\frac{RT}{\eta N}\left[1 + \frac{Al}{(3m\sigma \cdot 10^{-9}/4\pi\rho)^{1/3}}\right]} \quad \ldots \quad (3)$$

This equation gave results in fair agreement with many of

our experimental data. Latterly, however, the accuracy of the experimental methods has been increased, and has rendered a complete solution of the coagulation equation of importance. This may be deduced in the following way :—

Reverting to equation (2), and substituting

$$r = (3m \cdot 10^{-9}/4\pi\rho n)^{1/3},$$

we have

$$-\frac{dn}{dt} = \frac{4}{3}\frac{RT}{\eta N}\left[1 + \frac{A\ln^{1/3}}{(3m \cdot 10^{-9}/4\pi\rho)^{1/3}}\right]n^2. \qquad (4)$$

For simplification we will put

$$\frac{4}{3}\frac{RT}{\eta N} = B, \qquad \frac{Al}{(3m \cdot 10^{-9}/4\pi\rho)^{1/3}} = C.$$

Equation (4) then becomes

$$-\frac{dn}{dt} = B(n^2 + Cn^{7/3}).$$

The integral of this equation obtained by putting $n = y^3$ and resolving into partial fractions is

$$\frac{1}{3}\left(\frac{1}{n} - \frac{1}{n_0}\right) - \frac{C}{2}\left(\frac{1}{n^{2/3}} - \frac{1}{n_0^{2/3}}\right) + C^2\left(\frac{1}{n^{1/3}} + \frac{1}{n_0^{1/3}}\right)$$

$$- C^3 \log_e \frac{(1 + Cn^{1/3})n_0^{1/3}}{(1 + Cn_0^{1/3})n} = \frac{B}{3}t,$$

where n is the number of particles at time t and n_0 that at zero time. Transforming to particulate volumes, we have

$$\frac{1}{3}(\sigma - \sigma_0) - \frac{C}{2}(\sigma^{2/3} - \sigma_0^{2/3}) + C^2(\sigma^{1/3} - \sigma_0^{1/3})$$

$$- C^3 \log_e \frac{\sigma^{1/3} + C}{\sigma_0^{1/3} + C} = \frac{B}{3}t, \quad . \quad (5)$$

This equation gives the relationship between particulate volume and time for an aerosol initially homogeneous with the same degree of accuracy as that deduced by Smoluchowski for a coagulating sol. The equation is obviously not linear, and consequently the course of coagulation cannot be represented by a straight line. Actually the curvature is generally beyond the limit of error of experiment. It may be noted that if $C = 0$, that is, for sufficiently large particles, the equation becomes

$$\sigma = \sigma_0 + Bt,$$

where B is the constant deduced by Smoluchowski for sols (*Z. f. physikal Chem.* xxix. p. 129 (1918)). The numerical

value of the constant is of course different for sols and aerosols, owing to the viscosity coefficient in the denominator.

The difference in the rate of coagulation given by equations (3) and (5) is best shown from a few numerical examples. Thus, if we put

$$R = 8\cdot3.10^7 \text{ ergs,}$$
$$T = 293^\circ \text{ C. abs.,}$$
$$\eta = 1\cdot82.10^{-4} \text{ C.G.S. units,}$$
$$N = 6\cdot1.10^{23},$$
$$Al = 9\cdot10^{-6} \text{ çm.,}$$

we obtain

$$B = 2\cdot92.10^{10} \text{ cm.}^3/\text{sec.} = 1\cdot75.10^{-8} \text{ cm.}^3/\text{min.,}$$
$$C = 1\cdot450.10^{-2} \frac{\rho^{1/3}}{m^{1/3}}.$$

We will now use these values of B and C to calculate the times at which aerosols of unit density and of various weight concentrations in milligrams per cubic metre will attain to certain particulate volumes, assuming, as is frequently the case, that the initial number of particles tends to be indefinitely large, *i. e.*, that $\sigma_0 = 0$.

Time in minutes.

$\sigma.10^6$.	Calculated from equation (5).			Calculated from equation (3).		
	$m = 1$ mgm.	$m = 10$ mgm.	$m = 100$ mgm.	$m = 1$ mgm.	$m = 10$ mgm.	$= m 100$ mgm.
0	0	0	0	0	0	0
0·5	8	13	18	10	15	20
1·0	19	29	39	23	34	43
2·0	45	65	84	53	74	91
4·0	101	142	177	115	160	190

It will be seen that the rate of coagulation deduced from the more exact formula (equation 5) is faster than that found from the approximate form (equation 3). With increase of weight concentration, however, the values given by the two equations become closer, since the term $A\dfrac{l}{r}$ becomes smaller. For very small concentrations equation (3) would of course give entirely wrong results, as $A\dfrac{l}{r}$ would become large compared with unity. The figures deduced from equation (5) are in much closer agreement with experiment than those calculated from equation (3). Thus we have shown (*loc. cit.* p. 522) that equation (3) gives a fair agreement with a resin aerosol of concentration 15 mgm

per cubic metre. Reference to the diagram shows, however, that the calculated rate of coagulation is too slow in the later stages of the system. Using equation (6), on the other hand, the agreement is quite satisfactory. More recently the equation has been tested on other aerosols, and has been found to reproduce the experimental results as closely as could be expected when account is taken of the fact that the system, even if initially homogeneous, tends to become heterogeneous owing to coagulation. This latter effect, as has been shown previously, will tend to increase slightly the rate of coagulation.

The University, Leeds.
　3rd August, 1931.

XLV. *Notices respecting New Books.*

The Physical Properties of the Soil. By B. A. KEEN. (Longmans, Green & Co., Ltd., 1931. Price 21*s*. net.)

AT even the mention of soil research our minds have grown accustomed to conjure up the name of Rothamsted, an institution of world renown. Dr. Keen, who by the way has now assumed the Directorship of the Imperial Agricultural Research Institute of Pusa, India, for many years held the posts of Assistant Director and Head of the Soil Physics Department of Rothamsted Experimental Station, and we welcome his valuable addition to the Rothamsted monographs.

Although trials had been carried out during the domestic farming of earlier centuries, we learn from the historical introduction that it was not until after the advent of industrial methods, in fact, not until the present century, that really systematic investigations of the physical properties of soils were initiated.

Particle size naturally occupies an important section dealing with its measurement and distribution. All methods of mechanical analysis are based upon Stokes' law or its elaborations, and of these the best is that employing the Odén-Keen automatic self-recording balance, possessing a self-evident advantage where a large number of samples have to be analyzed.

Perhaps as important as the soil particles is the water associated with them, and the chapter dealing with the distribution and movement of water in the soil affords a very good illustration of the importance of applying strict mathematical reasoning to simplified cases. Haines and others considered an ideal soil of spheres of uniform size, regularly packed, either openly (simple cubic) or closely (face-centred cubic). Interest centred, of course, not in the spheres but in the pore space, and the agreement between theoretical results for moisture content and experiments is very encouraging. The existence of the phenomenon of

hysteresis in the moisture content-pressure deficiency relation must be of the utmost importance.

In Chapter V. the viscosities of soil and clay pastes are surveyed and evidence is advanced for assigning four stages in the velocity-pressure curve, indicating with increasing pressure, firstly, static rigidity, secondly, plug motion, and thirdly, a central plug motion surrounded by a cylindrical stream-line shell, which finally, in the fourth stage, entirely replaces the plug motion.

Naturally the colloidal aspect of soils is included, but determinations of physical properties in a laboratory are only stepping-stones to the better understanding of soil properties under field conditions. The text is well balanced, and the later chapters are devoted to such matters as soil resistance (as determined by the dynamometer) and its correlation with drainage and yield data, a full account of ploughing, crop rotation, soil temperature, and aeration.

Dr. Keen is to be congratulated on producing so critical and instructive an account of soil physics. Its presentation should assure its appeal to his fellow physicists and its indispensability to all interested in agricultural science.

Vorlesungen aus dem Gebiete der angewandten Mathematik. By Dr. RICHARD VON MISES, Professor at the University of Berlin. Band 1. *Wahrscheinlichkeitsrechnung und ihre Anwendung in der Statistik und Theoretischen Physik.* [Pp. 574.] (Leipzig und Wien: Franz Deuticke. 1931.)

THIS is the first text-book on the calculus of probabilities written from the physicist's point of view: but it is evidently not only useful for the physicist, but also of value to anybody interested in the theory of probabilities and the various problems of mathematical statistics.

The author has divided his book into four sections. The first part contains the elements of the calculus of probabilities, the second the theorems about limits in probabilities, the third the applications of the calculus of probabilities in statistics and in the theory of errors, and the last the elements of statistics in physics.

In the first section Prof. von Mises develops his own new conceptions of the theory of probability, which he had described before in a little book in 1928 *.

His notion of probability is based on the notion of a "collectivum" (Kollektiv), which is an infinite sequence of homogeneous observations of an irregular type. The probabilities are the limits, as the collectivum tends to infinity, of the empirical frequencies of that part of the collectivum which contains all elements having a certain attribute. The totality of the probabilities of a

* *Cf.* Prof. Richard von Mises, 'Wahrscheinlichkeit, Statistik und Wahrheit,' Wien, 1928 (Band III. Der Schriften zur wissenschaftlichen Weltauffassung, herausgegeben, von Phil. Frank und M. Schlick).

-collectivum is its distribution (Verteilung). These distributions may be continuous or discontinuous, and it is possible to characterize them by moments. The four elementary operations for the construction of new collectiva are : the selection (Auswahl), the combination (Mischung), the division (Teilung), and the conjunction (Verbindung). By the combination of these operations it is possible to solve all problems occurring in the calculus of probabilities.

In the second section of his book Prof. von Mises shows the derivation of the laws of large numbers under very restricted conditions. Here is to be found the most original and outstanding part of his book.

In the third section is contained the discussion of the main problems of the application of the calculus of probabilities in statistics and the theory of errors. Here are described the method of moments, the various ways of describing distributions (Bruns, Charlier, Pearson), Lexis' criterion of dispersion, the methods of comparison of an empirical distribution with a supposed theoretical one, a few problems of correlation analysis, and the Gaussian error law with its consequences and applications.

The last section of the book contains the elements of statistics in physics. This book clearly demonstrates that the knowledge of the calculus of probabilities and the use of statistics are of great importance for the modern scientist, that these methods are used now with great success for the solution of a wide variety of problems, and, in fact, that in the future the statistical methods may become increasingly important in all branches of science. This book is of outstanding value, and it is very desirable that it should be translated into English, so as to render it more accessible for English and American scientists.

Traité de Pyrométrie Optique. By GUSTAVE RIBAUD, Directeur du Laboratoire de Pyrométrie de la Fondation Edmond de Rothschild. [Pp. xvi + 488. with 163 figures in the text.] (Editions de la Revue d'Optique. Paris, 1931. Price 95 francs.]

THIS book forms part of an Encyclopædia of Photometry which the Société de la Revue d'Optique proposes to publish in 27 volumes. So far only one other part has been issued, namely, the ' Introduction générale à la Photométrie,' written by Prof. Ch. Fabry and published in 1927. Other volumes are promised for the near future.

The bulk of the book is concerned with the theory and use of instruments based on the Wien-Planck distribution law, since measurements with full radiation pyrometers are too much affected by extraneous circumstances to be reliable. Consideration of these instruments is, however, by no means lacking, for 60 pages are devoted to descriptions of the familiar types devised by Féry, Foster, Thwing, and others. Prof. Ribaud has had a very wide experience of optical pyrometry in all its aspects, and he has been allowed ample space to treat the subject in the fullest detail, so

that it is unlikely that anyone will go to the book for information on any point within its scope without obtaining full satisfaction. The references are very complete and extend to papers published early in 1931. It is most unfortunate that the work of the Bureau of Standards, Washington, on the freezing-point of platinum and the realization of the Waidner-Burgess standard of luminous intensity should have been published just too late for inclusion. Prof. Ribaud gives as the "most probable value" of this freezing-point $1767 \pm 5°$ C., while the very careful determination by Messrs. Roeser, Caldwell, and Wensel gives $1773 \cdot 5 \pm 1°$ C.

The book contains subject and author indices and 72 tables of data. Those interested in optical pyrometry as an industrial appliance will probably find sufficient for their purpose in one of the several English text-books on temperature measurement. For the specialist and the science library this book is indispensable.

Spektroskopie der Röntgenstrahlen. By MANNE SIEGBAHN. 2nd edit. (Berlin: Julius Springer, 1931. Price 47 R.M.; bound 49.60 R.M.)

To anyone interested in X-rays, Siegbahn's X-ray Spectroscopy needs no introduction. Since its first appearance in 1923 and that of the revised English translation two years later it has held unassailed its position as the work of reference on the subject.

The production of the second edition has afforded an opportunity of bringing the contents completely up to date. The subject matter is restricted to much the same limits as in the previous edition, *e. g.*, the Compton effect and associated phenomena are excluded; but even so, the volume has grown to twice its previous size. It has been liberally revised throughout and extended to include recent developments, and it would be difficult to select any particular section for special mention except that dealing with the Optics of X-rays. This now includes reflexion, refraction, and dispersion, together with diffraction and interference phenomena corresponding to those familiar in the "older optics." Some very fine reproductions of fringe systems are given.

Diffraction of X-rays by line gratings is now a common phenomenon. It leads to an absolute value for wave-lengths slightly greater by a few tenths of 1 per cent. than those determined by crystal measurements—a discrepancy which remains unexplained. Involved in this comparison is the deviation from Bragg's law, a subject now much amplified. The use of line gratings in vacuum spectrographs has opened up a new field, that of the long wave-lengths, and results are recorded up to about 300 A.U. The results of these researches naturally find their places in many sections, *e. g.*, in extending largely the K, L, M, etc. emission series, the list of which, previously thirty pages, now occupies over one hundred, and in disclosing more absorption discontinuities etc. Energy-level schemes have now been suitably modified to include the new results.

The experimental aspect is carefully considered, and a useful account of the apparatus used is given both for soft-ray work as

well as for the more usual range. Absorption edges and their dependence upon chemical constitution, together with secondary absorption, form another section, whilst such matters as intensity relations, multiply-ionized atoms and fine structure all find their respective places in the volume.

Unfortunately attention can be drawn here to only a few of the most important alterations. The volume concludes with an exhaustive bibliography and some very useful appendices and indices. An atmosphere of refined accuracy has always pervaded Siegbahn's book—the present edition is even more impressive. The volume is very well produced, and it is to be hoped that the present state of our exchange will not deter anyone from purchasing such an indispensable volume.

The Law of Gravitation in Relativity. By HORACE C. LEVINSON, Ph.D., and ERNEST BLOOMFIELD ZEISLER, Ph.D. Second Edition. (The University of Chicago Press, Chicago, Illinois, 1931. Cambridge University Press, Fetter Lane, London, E.C. 4. Price 16s.)

THOSE already conversant with the tensor calculus will find many results of interest in the first five chapters of this book, in which the authors have presented the subject from the point of view that tensors are linear matrices obeying a special type of transformation law. The reader is introduced to covariant differentiation and the Riemann-Christoffel tensor, without reference to the concept of parallelism, but by the consideration of the second partial derivatives of the transformation functions of a fundamental tensor, $g_{\mu\nu}$. Considerable space is then devoted to the determination of the most general form of tensor in a space of four dimensions, which does not contain derivatives of the $g_{\mu\nu}$ beyond the second order and which is linear in these derivatives.

The remainder of the book is devoted to showing that Einstein's law of gravitation, $G_{\mu\nu} = 0$, ($G_{\mu\nu}$ the contracted Riemann-Christoffel tensor), is not the only law which agrees with the postulates of general relativity. An alternative law is considered, which is obtained by equating to zero the components of a certain tensor of the fourth rank. In addition, however, the assumption is made that the average Gaussian curvature of the space vanishes. The spherically symmetrical solution of these equations is applied to the case of the field of the sun, and yields results with regard to the advance of the perihelion of Mercury and the bending of light rays which are not in agreement with experiment.

Novius Organum. By J. C. MCKERROW. (Longmans, Green & Co., Ltd., 1931. Price 9s. net.)

'NOVIUS ORGANUM, or Essays in a new Metaphysic,' a collection of twelve papers written by the author within the last few years, is "an attempt to import more order into a somewhat disorderly system of modern knowledge."

If we understand Mr. McKerrow's point of view correctly, he desires to substitute accident for volition in the initiation of habit. Habitual repetition would represent a stationary state of affairs, while pure accident would permit changes of habit, and thereby evolution, either as an advance or degeneration. In brief, any system, animate or inanimate, would exist by repetition, entirely by habit, until purely accidentally something new happened, affording the possibility of its repetition as a new habit or of its rejection. The scientifically-minded would generally infer the existence of some cause to account for the occurrence of this unusual event, but in McKerrow's opinion this procedure is wrong metaphysically—it is placing the cart before the horse. He denies the existence of any cause, and considers the unusual event to occur accidentally.

In the attempt to demonstrate the truth of his logic McKerrow has applied it to matters so diverse and extensive that it is impossible to give any coherent account in a short review. It is interesting to consider in how many cases this logic is acceptable, and by not advancing any bias here the reader will be left free to form his own opinion.

Handbuch der Experimentalphysik. Band IV. 1 Teil. *Hydro- und Aerodynamik. Strömungslehre und Allgemeine Versuchs- technik.* (Leipzig : Akademische Verlagsgesellschaft. Brosch. R.M. 66, geb. R.M. 68.)

THIS volume of the ' Handbuch der Experimentalphysik ' repre- sents a very important addition to the literature on hydrodynamics. Although its title indicates that it is mainly concerned with the experimental aspects of the subject, one finds that the theoretical treatment included is adequate at any rate for the large majority of physicists who are likely to consult this book.

The more or less theoretical aspects are separately treated by L. Prandtl, H. Falkenhagen, W. Tollmien, A. Busemann, and J. Ackeret, who respectively contribute articles on the fundamental concepts of fluid motion, classical hydrodynamics, the theory of surface films and turbulence, the dynamics of gases, and cavitation.

These articles are all excellently illustrated, the photographs included in the section on vortex motion being particularly good. The " Schlieren " method of examination of moving gases is, of course, well described, and many excellent pictures showing its range of application are given throughout the book.

The more strictly experimental aspects of the subject are treated in five additional sections. In the first of these H. Peters describes the procedure necessary for the measurement of pressure in a flowing liquid, whilst A. Betz describes the micromanometers which are employed in such measurements. H. Mueller and H. Peters are jointly responsible for the description of the apparatus used in measuring the velocities of liquids.

J. M. Burgers deals with the use of hot wires for the measure- ment of the flow of gases. This section was completed in April

1928, but in a footnote references to later work, including such measurements with liquids, are given. The final section, by O. Tietjens, is devoted to the description of methods of recording stream lines. This article is also excellently illustrated.

The printing and binding are of the same high quality which has characterized the earlier publications in this 'Handbuch.' In addition, one gains the impression that in this particular volume much more attention has been devoted to English sources of information than appeared to be the case in some of the earlier volumes.

XLVI. *Proceedings of Learned Societies.*

GEOLOGICAL SOCIETY.

November 18th, 1931.—Prof. E. J. Garwood, M.A., Sc.D., F.R.S., President, in the Chair.

THE following communication was read:—

'The British Carboniferous Reticulate Spiriferidæ.' By Thomas Neville George, M.Sc., Ph.D., F.G.S.

The short-hinged Spirifers which are customarily referred to the genus *Reticularia* fall into two main groups. These are probably not intimately related, and the presence of a reticulate ornament in both is a homœomorphic and not a genetic similarity.

One group, constituting *Reticularia* proper (genotype *Terebratula imbricata* Sowerby), is characterized by relatively large forms which possess a coarse shell-structure and an apparent absence of biramous spines. They display a morpho-genetic seriation from a rectimarginate stage through various plicate stages to divergent end-forms, which may be parasulcate, or acutely uniplicate, or feebly sulciplicate. In these changes of shell-shape, they develop along lines parallel with those of other brachythyrid spiriferid stocks, and in particular have been confused with lævigate species of *Martinia* and similar genera. The ornament, however, serves as a means of distinction from such species, and does not appear to be catagenetically lost, as Buckman contended. Internally, also, *Reticularia* differs from all other known British Avonian non-costate brachythyrid Spirifers in possessing apical plates and a euseptoid in the ventral valve.

The second group, referred to a new genus, contains relatively small forms with a fine shell-structure which do not advance beyond an incipiently uniplicate stage in the development of shell-sculpture. The ornament is characteristically gemino-spinous ; a detailed examination reveals each spine to be armoured laterally with doubly-spiked hooklets. This

extremely specialized ornament shows only minor variation throughout the group, and is considered to warrant the inclusion of the species within the one genus, despite the fact that some species are wholly aseptate, others possess minute ventral apical plates, and still others are strongly septate (though a euseptoid is never present). That is, while members of *Reticularia* (*sensu stricto*) are progressive in shell-shape and conservative in septal changes, the reverse condition holds with the new genus.

Reticularia (*sensu stricto* is confined to the Avonian, and it appears that most of the acutiplicate forms are characteristic of the upper portion of the Dibunophyllum Zone. The new genus, a cryptogenetic type, also first appears commonly in the upper portion of the Dibunophyllum Zone, but extends upwards into the Upper Carboniferous. The stratigraphical distribution of the species suggests that the Settle and Clitheroe reef-knolls are of approximately mid-Dibuno phyllum age, despite the conclusions of Hudson and Parkinson

The paper concludes with a detailed description of the species of the two genera.

December 2nd, 1931.—Prof. E. J. Garwood, M.A., Sc.D., F.R.S., President, in the Chair.

Dr. W. F. Hume, A.R.C.S., A.R.S.M., F.G.S., delivered a lecture, illustrated by lantern-slides, on ' The Pre-Cambrian Rocks of Egypt : their Nature, Classification and Correlation.'

Metamorphic and plutonic rocks form the main feature of the mountainous regions of the Eastern Desert of Egypt and Sinai, where they occupy an area of 93,000 square kilo-metres—larger than the whole of Scotland. They are but a small extension of the rocks of similar nature which form the backbone of ' High Africa '. In composition, the meta-morphic rocks vary from coarse-grained gneisses to the finest-grained siliceous schists or clay-slates, while the plutonic rocks are represented by every type from the most basic of peri-dotites to the most acid of granites. Dykes also occur in the greatest variety and abundance.

The fundamental rocks of Egypt are considered as Pre-Cambrian for the following reasons :—(1) The absence of evidence of life, with the one exception of certain minute *Archœocyathus*-like bodies noted by Barthoux in the schistose series of Wadi Hammamat ; (2) the nearest Middle Cambrian strata, those at the southern end of the Dead Sea, are markedly unconformable to the rocks of the fundamental series ; (3) they resemble, in nature and sequence, Pre-Cambrian formations in America, Europe, India, and other places.

The succession of Pre-Cambrian events in Egypt can be

-separated into three major episodes or cycles, all possessing features in common, but each having characteristics of its own. The sequence in each cycle appears to have been : (*a*) sedimentation ; (*b*) minor dyke or sill injection, leading on to volcanic extrusion ; (*c*) plutonic intrusions, with development of land forms ; and (*d*) erosion of the hill-features during a prolonged internal, giving rise to the sedimentation of the next succeeding episode or cycle.

All students of the Pre-Cambrian formations are aware of the difficulties which have arisen over the use of the terms ' Huronian,' ' Algonkian,' and ' Proterozoic '. Consequently, the formation in Egypt has been divided into four series, these being, beginning with the oldest, (1) Archæan (*sensu stricto*), (2) Metarchæan, (3) Eparchæan, and (4) Galtarian. The last-named is derived from Gebel Galtar, a conspicuous granitic range in Eastern Egypt. Under the term Archæan (*sensu stricto*) is included a very ancient series of schists, in which calcareous and magnesian members are at times prominent. With these are associated widespread plutonic intrusions. The latter give rise to some of the main gneisses present in Egypt, while the schists have at times been subject to intense pressure and metamorphism. The dips are frequently high, often approaching the vertical, there is much crumpling, and, in the case of the gneiss, the foliation is regional in its extent. Apart from the biotites and hornblende-gneiss, the Archæan includes the hornblende-gneisses of the Ereier complex, the Sikait beryl (emerald) schists, the Baramia serpentines, and the Haimur and Amara calcareous schists.

The beds of Metarchæan age most probably mainly correspond to strata elsewhere classed as Algonkian, Huronian, or Proterozoic. The schists are for the larger part paraschists, with dips more moderate than those of the Archæan. Minor igneous activity is very marked, the sheets and sills being basic. The plutonic intrusions into the Metarchæan are mainly diorites or hornblende-granites, and the gold yielding areas in Egypt seem intimately associated with them. The main characteristics of the Eparchæan are, on the one hand, absence of intrusive granites in batholiths and of basic rocks in sills, and, on the other hand, the marked development of siliceous schists, tuffs, breccias, and conglomerates. These contain fragments of granites, andesites, and tuffs, and the most typical example is the Hammamat schist with its associated breccias and conglomerates. This period of erosion and sedimentation is terminated by the intrusion of minor intrusive or volcanic rocks (porphyrites, dacites, etc.), of which the Imperial Porphyry is the best-known member.

The Galtarian may be regarded as the plutonic intrusive phase of the Eparchæan, but is on so vast a scale that it appears to have affected the whole of Egypt and Sinai. Its most

characteristic member is the Red Granite, which gives rise to some of the finest mountain ranges in the country. A very varied series of dykes is of younger date, but is, in the main, long anterior to the deposition of the Carboniferous Sandstones.
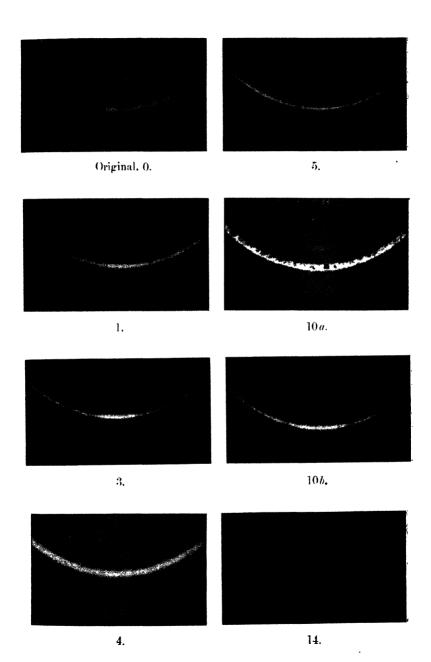
An attempt has been made to correlate these different divisions in Egypt with those of Pre-Cambrian formations elsewhere.
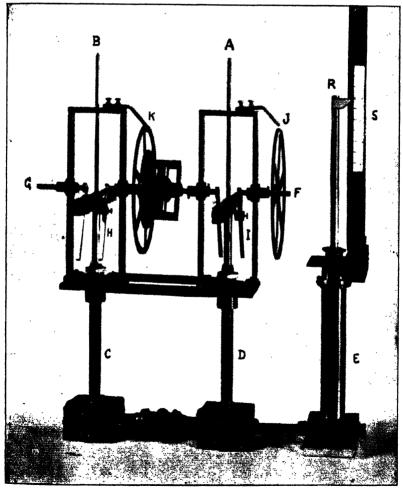
For England and Wales, it is provisionally concluded that the nearest representatives of the Egyptian Archæan plutonic rocks are the Lewisian types of gneiss present in Anglesey and the Lleyn Peninsula, at Malvern, and possibly in Cornwall on the English Channel coast. It is very difficult to determine precise equivalents for the Metarchæan series of events. On the other hand, Eparchæan characteristics are very marked in the whole of the Pebidian system 'from Pembrokeshire and Carnarvonshire into Anglesey on the one side, and into Shropshire and farthest east in the Midlands on the other.' The eastern Longmyndian and Charnian rocks are equally of Eparchæan type, while the western Longymndian rocks, correlated definitely by Prof. W. W. Watts with the Torridonian of Scotland, would also be Eparchæan.

Comparing the Egyptian Pre-Cambrian with that of Scotland, the Archæan gneisses of Egypt agree very closely with those of the Lewisian series. There are no marked equivalents of the gneissose flagstones of the Moine series, but the Dalradian has features which recall the Metarchæan characteristics. In both cases these systems as a whole consist of altered sediments, which have been invaded by granites, diorites, and quartz-porphyries, and also contain bands of hornblende-schist due to the foliation of basic igneous rocks. At the base of both are green beds, which are epidotic in character, and albite-gneisses or schists are common to the series in both countries. The Lennoxian can also be correlated with the Eparchæan in the dominance of its slates and grits, the former being associated with bands of quartz-felspar breccias. These differ from the Hammamat breccias of Egypt in the absence of granitic, andesitic, and tuff fragments. This may, perhaps, indicate that the erosion in Scotland had not proceeded as far as in Egypt. In Ireland, the early gneisses and schists bear close resemblances to those of the Egyptian Archæan, while the abundant basic intrusions of the Irish Dalradian recall Metarchæan conditions. It has not been found possible to correlate any of the Irish formations with the Eparchæan, but the latest intrusive granites proved to be of definitely Pre-Cambrian age may probably correspond with the Galtarian.

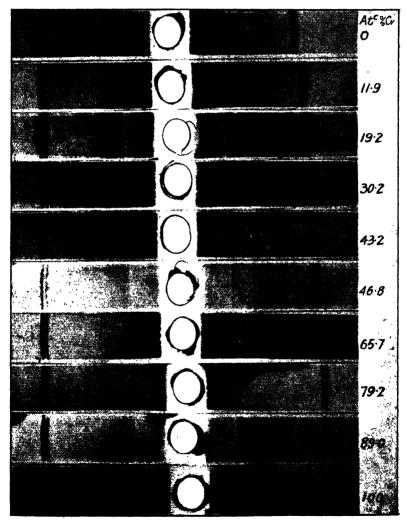Original. 0.

5.

1.

10 *a*.

3.

10 *b*.

4.

14.

Lattice Distortion and Hardness of Heat-treated Tungsten Magnet Steels.

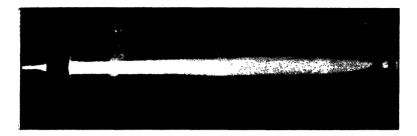Two components of calculating machine.

Fe-Cr Alloys.

Fig. 1.

Fig. 2.
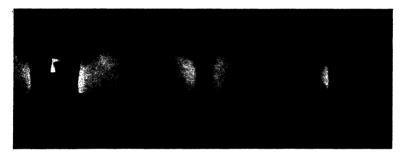
Fig. 3.
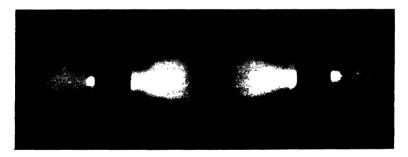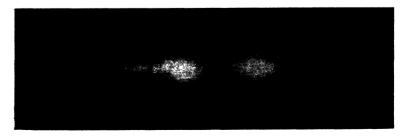
Fig. 4.

Types of High Frequency Discharge.

XLVII. *Symbolic Calculus.* By BALTH. VAN DER POL, *D.Sc., and* K. F. NIESSEN, *D.Sc., Natuurkundig Laboratorium der N. V. Philips' Gloeilampenfabrieken, Eindhoven, Holland* *.

INTRODUCTION.

BY symbolic calculus we mean the operational calculus of Heaviside in the form given by Carson † and extended by the first of us to the solution of ordinary differential equations (*a*) with constant coefficients ‡ and (*b*) with variable coefficients §. In the title above we use the name *symbolic* instead of *operational* calculus, since, with a view to the rigour of the method, we consider it advisable to abandon the idea of an operator and an operand in the original sense of Heaviside. Instead we base our considerations on Carson's foundation of the calculus, by means of which a given

---

* Communicated by the Authors.

† John R. Carson, 'Electric Circuit Theory and the Operational Calculus' (McGraw Hill, New York, 1926).

‡ Balth. van der Pol, Phil. Mag. vii. p. 1153 (1929) ; viii. p. 861 (1929); referred to as P.

§ We also draw attention to a recent book by G. A. Campbell and R. M. Foster (Bell Telephone System, Monograph B 584) which will be of interest for those who study operational methods.

function $h(x)$ is related symbolically to another function $f(p)$, given by the Laplace transform

$$f(p) = p \int_0^\infty e^{-px} h(x) dx, \quad \ldots \quad (1)$$

where it is assumed that the integral converges.

We will speak of an "original" function $h(x)$ and its "image" $f(p)$. The integral relation (1) between $f(p)$ and $h(x)$ we denote as

$$f(p) \doteqdot h(x).$$

When the image $f(p)$ is known, then the original $h(x)$ is found back by means of the Bromwich-Wagner theorem

$$h(x) = \frac{1}{2\pi i} \int_{c-i\infty}^{c+\infty} \frac{f(p)}{p} e^{px} dp, \quad \ldots \quad (2)$$

which is a consequence of the Mellin-Fourier theorem *.

In (2) the straight path of integration is so chosen that all singularities lie to the left.

The relation (2) between $h(x)$ and $f(p)$ will also be indicated by

$$h(x) \doteqdot f(p),$$

where again the symbol $\doteqdot$ is used, although the process to derive $f(p)$ from $h(x)$ (as in (2)) is entirely different from the process to derive $h(x)$ from $f(p)$ (as in (1)).

Confusion between original and image is impossible, since the image always contains the symbolic parameter p. Therefore it is perfectly immaterial whether we write

$$h(x) \doteqdot f(p) \quad \text{or} \quad f(p) \doteqdot h(x):$$

both mean $h(x)$, transformed symbolically, gives $f(p)$, and $f(p)$, interpreted backwards, gives $h(x)$.

In this respect we remark that Dalzell † uses a slightly different nomenclature. He speaks of $F(p)$, which is the convert of $h(x)$, and of $h(x)$, which is the revert of $F(p)$. Moreover, his $F(p)$ is not quite identical with our $f(p)$ of (1), but he uses $F(p) = \dfrac{f(p)}{p}$. He too points out that the new method, on account of its exactness, is to be preferred to the original Heaviside operational calculus.

We would like to keep to our own notations of "original"

---

* Courant und Hilbert, 'Methoden der Mathematischen Physik,' i. s. 90.
† D. P. Dalzell, Proc. Phys. Soc. London, xlii. p. 75 (1929).

$h(x)$ and " image " $f(p)$, where the parameter p is connected with the variable x in the sense of (1).

For instance, to $h(x) = x$ belongs, according to (1), $f(p) = \dfrac{1}{p}$. The fact that functions of p represent functions of x may therefore be indicated by means of

$$\frac{1}{p} \doteqdot x \quad \text{or} \quad x \doteqdot \frac{1}{p}.$$

If we deal with a function of two variables x, y, it is sometimes useful to represent it as a function of x by means of $f(p)$, but as a function of y by means of a function of another symbolic parameter q,

$$\frac{1}{p} \doteqdot x, \quad \frac{1}{q} \doteqdot y.$$

Then we will have a case of simultaneous symbolic calculus.

Now several rules have been derived, partly by Carson, partly by van der Pol, which are of very frequent use in symbolic calculations.

For convenience of the reader we collect these rules in Part I. and repeat some results found in P and again to be used in this paper. Moreover, a new rule and some considerations of a general character will be given in Part I. In Part II. we intend to show again how these rules can be used in a very simple way for the derivation of many new relations.

<p style="text-align:center">I.—THEORETICAL PART.</p>

<p style="text-align:center">*Fundamental Rules.*</p>

1. Carson pointed out that from (1) we may conclude

$$f\left(\frac{p}{s}\right) \doteqdot h(sx), \qquad \text{if } s = \text{constant} > 0, \quad \text{(R1)}$$

$$pf(p) \doteqdot \frac{d}{dx} h(x), \qquad \text{if } h(0) = 0, \quad \text{(R2)}$$

$$\frac{1}{p} f(p) \doteqdot \int_0^x h(x)\,dx, \qquad \text{(R3)}$$

$$\frac{p}{p+a} f(p+a) \doteqdot e^{-ax} h(x), \qquad \text{(R4)}$$

<p style="text-align:center">2 N 2</p>

$$e^{-\lambda p} f(p) \doteqdot \begin{Bmatrix} 0, & \text{for } x < \lambda \\ h(x-\lambda), & \text{for } x > \lambda \end{Bmatrix} \text{ if } \lambda > 0, \quad . \quad (\mathrm{R}\,5)$$

$$e^{+\lambda p} f(p) \doteqdot h(x+\lambda), \quad \text{if } \lambda > 0 \text{ and } h(x) = 0$$
$$\text{for } 0 < x < 1. \quad . \quad . \quad (\mathrm{R}\,6)$$

Van der Pol added to this list

$$\left(-p\frac{d}{dp}\right)^n f(p) \doteqdot \left(x\frac{d}{dx}\right)^n h(x), \quad n > 0, \quad . \quad (\mathrm{R}\,7)$$

$$p\left(-\frac{d}{dp}\right)^n \frac{f(p)}{p} \doteqdot x^n h(x), \qquad n > 0, \quad . \quad (\mathrm{R}\,8)$$

$$\int_p^\infty \frac{f(p)}{p} dp \doteqdot \int_0^x \frac{h(x)}{x} dx, \quad . \quad . \quad . \quad (\mathrm{R}\,9)$$

$$\int_0^p \frac{f(p)}{p} dp \doteqdot \int_x^\infty \frac{h(x)}{x} dx, \quad . \quad . \quad . \quad (\mathrm{R}\,10)$$

and also the following ordinary equalities :

$$\int_0^\infty \frac{f(p)}{p} dp = \int_0^\infty \frac{h(x)}{x} dx, \quad . \quad . \quad . \quad (\mathrm{R}\,11)$$

$$\operatorname*{Lim.}_{p \to \infty} f(p) = \operatorname*{Lim.}_{x \to 0} h(x), \quad . \quad . \quad . \quad (\mathrm{R}\,12)$$

$$\operatorname*{Lim.}_{p \to 0} f(p) = \operatorname*{Lim.}_{x \to \infty} h(x), \quad . \quad . \quad . \quad (\mathrm{R}\,13)$$

provided the integrals and limits exist.
Proofs of these rules were given in P.

2. The rule we now wish to add is

$$\frac{h(x)}{x^n} \doteqdot p \int_p^\infty \int_p^\infty \dots \int_p^\infty \frac{f(p)}{p} (dp)^n, \quad . \quad (\mathrm{R}\,14)$$

provided the multiple integral converges, *i. e.*, if

$$\operatorname*{Lim.}_{x \to 0} h(x) = x^m, \qquad m > n-1.$$

This rule can be proved as follows :—
We have

$$\frac{e^{-px}}{x} = \int_p^\infty e^{-px} dp ;$$

$$\therefore \quad p\int_0^\infty e^{-px} \frac{h(x)}{x} dx = p\int_0^\infty h(x) \int_p^\infty e^{-px} dp \, dx$$

$$= p\int_p^\infty \int_0^\infty e^{-px} h(x) dx \, dp = p\int_p^\infty \frac{f(p)}{p} dp.$$

In the same way we have

$$\frac{e^{-px}}{x^2} = \int_p^\infty \int_p^\infty e^{-px} dp\, dp\,;$$

$$\therefore\ p \int_0^\infty e^{-px} \frac{h(x)}{x^2} dx = p \int_0^\infty h(x) \int_p^\infty \int_p^\infty e^{-px} dp\, dp\, dx$$

$$= p \int_p^\infty \int_p^\infty \frac{f(p)}{p} dp\, dp,$$

from which the general rule can easily be established.

Moreover, the rule is also proved by repeated application of (R 2) on (R 9).

3. Another rule mentioned by Carson (*l. c.* p. 41) without proof and which can be based upon Volterra's theorem of a " produit de composition " * is

$$\left. \begin{aligned} \frac{1}{p} \cdot f_1(p) \cdot f_2(p) &\doteqdot \int_0^x h_1(\xi) h_2(x-\xi) d\zeta, \\ \text{or} \qquad &\doteqdot \int_0^x h_1(x-\xi) h_2(\xi) d\xi, \end{aligned} \right\} \quad . \quad \text{(R 15)}$$

where $h_1(x)$ and $h_2(x)$ are the originals of $f_1(p)$ and $f_2(p)$.
A new and very direct proof of this rule is as follows :—
By (1) we have the ordinary equation

$$\frac{1}{p} f_1(p) = \int_0^\infty e^{-p\lambda} h_1(\lambda) d\lambda.$$

Multiplying with $f_2(p)$ we get

$$\frac{1}{p} f_1(p) f_2(p) = \int_0^\infty e^{-p\lambda} f_2(p) h_1(\lambda) d\lambda. \quad . \quad . \quad \text{(3)}$$

We now assume p to belong to a variable x in the sense of (1) ; therefore

$$\frac{1}{p} \doteqdot x\,;$$

then by (R 5)

$$e^{-p\lambda} f_2(p) \doteqdot \begin{cases} 0. & \text{for } \lambda > x, \\ h_2(x-\lambda), & \text{for } \lambda < x. \end{cases} \quad . \quad . \quad \text{(4)}$$

We substitute this result in the right-hand side of (3),

* Volterra-Péres, 'Leçons sur la composition et les fonctions permutables' (Paris, 1924).

which thus becomes " the original " of the left-hand side, so that we obtain

$$\frac{1}{p} f_1(p) f_2(p) \doteq \int_0^x h_2(x-\lambda) h_1(\lambda) d\lambda.$$

The upper limit of the last integral is written x instead of ∞, because of (4).

4. Of the results obtained in P by application of the rules above we mention here a few, which we will afterwards have to use :

$$\frac{1}{p^n} \doteq \frac{x^n}{\Pi(n)}, \quad \ldots \ldots \ldots \text{(F 1)}$$

$$\frac{p}{p+1} \doteq e^{-x}, \quad \ldots \ldots \ldots \text{(F 2)}$$

$$\frac{p}{p^2+1} \doteq \sin x, \quad \ldots \ldots \ldots \text{(F 3)}$$

$$\frac{p^2}{p^2+1} \doteq \cos x, \quad \ldots \ldots \ldots \text{(F 4)}$$

$$x^{\frac{n}{2}} J_n(2\sqrt{x}) \doteq p^{-n} e^{\frac{1}{p}}, \quad \ldots \ldots \text{(F 5)}$$

$$x^n J_n(x) \doteq \frac{2^n \Pi(n-\frac{1}{2})}{\sqrt{\pi}} \frac{p}{(p^2+1)^{n+\frac{1}{2}}}, \quad \text{(F 6)}$$

$$J_n(x) \doteq \frac{p}{\sqrt{p^2+1}} (\sqrt{p^2+1}-p)^n, \quad \text{(F 7)}$$

$$P_n(1-x) \doteq e^{-p} p^{n+1} \left(\frac{1}{p} \frac{d}{dp}\right)^n \left(\frac{e^p}{p}\right), \quad \ldots \text{(F 8)}$$

$$L_n^x(x) \doteq \Pi(n) \left(1-\frac{1}{p}\right)^n, \quad \ldots \ldots \text{(F 9)}$$

$$p \doteq \delta(x). \quad \ldots \ldots \ldots \ldots \text{(F 10)}$$

$\delta(x)$ is the impulsive function, being ∞ for $x = 0$ and 0 for $x \neq 0$ in such a way that

$$\int_{-\infty}^{+\infty} \delta(x) dx = 1.$$

Considerations of a General Character.

5. It may be instructive to analyze the definition (1) of the symbolic calculus in the following way :

Write

$$h(x) \doteq p \int_0^\infty e^{-ps} h(s)\, ds. \quad \ldots \quad (5)$$

Now p is the image of an impulsive function having its maximum at $x = 0$, and therefore by means of (R5) the image pe^{-sp} corresponds to an impulsive function, being infinite at $x = s$ and denoted by $\delta(x-s)$:

$$pe^{-ps} \doteq \delta(x-s). \quad \ldots \ldots \quad (6)$$

Substituted in (5) this gives the confirmation

$$h(x) = \int_0^\infty \delta(x-s) h(s)\, ds = h(x).$$

6. It is possible to give the relation between original and image in another form. We have, according to (R 8) and $h(x) = 1 \doteq 1 = f(p)$,

$$x^n \doteq p\left(-\frac{d}{dp}\right)^n \left(\frac{1}{p}\right);$$

$$\therefore \quad h(x) \doteq ph\left(-\frac{d}{dp}\right)\left(\frac{1}{p}\right), \quad \ldots \ldots \quad (7)$$

provided $h(x)$ can be expressed as a finite or infinite sum of positive integral powers of x. In this case we have

$$f(p) = ph\left(-\frac{d}{dp}\right)\left(\frac{1}{p}\right). \quad \ldots \ldots \quad (8)$$

Suppose now, that we found already (*e.g.*, by means of (1)) the image of an original.

For instance, for

$$h(x) = J_0(x) \text{ we know } f(p) = \frac{p}{\sqrt{p^2+1}},$$

$$h(x) = \cos x \text{ ,, ,, } f(p) = \frac{p^2}{p^2+1},$$

$$h(x) = J_n(x) \text{ ,, ,, } f(p) = \frac{p}{\sqrt{p^2+1}}(\sqrt{p^2+1}-p)^n.$$

Then equation (8) leads to

$$J_0\left(\frac{d}{ds}\right)\left(\frac{1}{s}\right) = \frac{1}{\sqrt{s^2+1}}, \quad \ldots \ldots \quad (9)$$

$$\cos\left(\frac{d}{ds}\right)\left(\frac{1}{s}\right) = \frac{s}{s^2+1}, \quad \ldots \ldots \quad (10)$$

$$J_n\left(\frac{d}{ds}\right)\left(\frac{1}{s}\right) = \frac{1}{\sqrt{s^2+1}}(s-\sqrt{s^2+1})^n, \quad . \quad (11)$$

etc.,

where we replaced p by s, because in these ordinary analytical relations s may represent any positive variable $s > 1$.

7. Further, we draw attention to the fact that the symbolic calculus may provide the solution of several integral (or differential integral) equations.

A simple example may first illustrate the idea.

We know

$$f(p) = \frac{p}{p^2+1} \doteqdot \sin x. \quad . \quad . \quad . \quad (12)$$

Now

$$\frac{p}{p^2+1} = \frac{1}{p+\frac{1}{p}}.$$

In connexion herewith we apply successively the following application of the rules (R) to (12).

$$p f(p) \doteqdot \frac{d}{dx}\sin x, \text{ since } \sin 0 = 0,$$

$$\frac{1}{p}f(p) \doteqdot \int_0^x \sin x\, dx ;$$

$$\therefore \left(p+\frac{1}{p}\right)f(p) = 1 \doteqdot \frac{d}{dx}\sin x + \int_0^x \sin x\, dx.$$

But

$$1 \doteqdot 1;$$

therefore

$$y = \sin x$$

is a solution of the differential integral equation

$$1 = \frac{dy}{dx} + \int_0^x y\, dx.$$

Another example is more complicated. Take

$$f(p) = \frac{p}{\sqrt{p^2+1}} \doteqdot J_0(x).$$

Now

$$f(p) = \frac{1}{\sqrt{1 + \dfrac{1}{p^2}}} = \frac{1}{1 + \dfrac{1}{2}\dfrac{1}{p^2} - \dfrac{1}{8}\dfrac{1}{p^4} + \ldots}.$$

Thus we get

$$y = \mathrm{J}_0(x)$$

as a solution of the integral equation

$$1 = y + \frac{1}{2}\int_0^x \int_0^x y(dx)^2 - \frac{1}{8}\int_0^x \ldots \int_0^x y(dx)^4 + \ldots$$

8. We conclude our considerations of definition (1) of the symbolic calculus by the remark that we expect this formulation in the future to be extended in some way, so as to cover still more functions. Two of the reasons we will mention here :

First we have the fact that with the definition (1) it is in general not legitimate to derive from

$$f(p) \doteqdot h(x) \quad \ldots \quad \ldots \quad (13)$$

the relation

$$f(-p) \doteqdot h(-x). \quad \ldots \quad \ldots \quad (14)$$

We would have, according to (1),

$$h(-x) \doteqdot p \int_0^\infty e^{-pt} h(-t)\, dt,$$

which would imply the knowledge of h for negative values of the argument. Supposing these known, and changing t in $-\tau$, we still would get

$$h(-x) \doteqdot (-p)\int_0^{-\infty} e^{-(-p)\tau} h(\tau)\, d\tau,$$

which, however, is not identical with $f(-p)$, the upper limit being $-\infty$ instead of $+\infty$. There are pairs $h(x)$ and $f(p)$ in (13) for which (14) is valid.

One might further suggest to use instead of (1) the definition

$$f(p) = \int_0^\infty e^{-x} h\!\left(\frac{x}{p}\right) dx, \quad \ldots \quad \ldots \quad (15)$$

which has *some* advantage.

But secondly there remain many other difficulties—for instance, the fact that in practical symbolic calculus the relation

$$x^{-\frac{3}{2}} \doteqdot \Pi\!\left(-\frac{3}{2}\right) p^{\frac{3}{2}} \quad \ldots \quad \ldots \quad (16)$$

can often be used without any trouble, although the integral definition (1) with $h(x) = x^{-\frac{3}{2}}$ would diverge.

For x^{-n}, where n is a positive integer, we are faced with the same difficulties which are encountered by Volterra in defining his " composition " *.

However, we will base our further considerations strictly on the definition (1), and apply only the rigid rules which could be derived from it, thus avoiding any uncertainty in the exactness of our results.

It was already shown in P that the present formulation of the symbolic calculus is already of an amazing fertility, and in Part II. of this paper we will come to the same conclusion on account of the great number of known and unknown relations found by the application of our rules.

II.—Practical Part.

In Part I. we dealt with general methods ; here we will treat less general methods. Some *special* methods of procedure will be discussed which make use of *peculiarities* of image functions. There are a great number of those special methods, giving us the opportunity of deriving many known and unknown relations between several functions. Nevertheless we can divide several manipulations into groups.

A few of these types may already be found in P, namely :

I. Obtaining relations from summation of images.

II. Using the theorem (R15) mentioned in P, p. 864, as " produit de composition," and here called product theorem.

Some further examples of these groups will be given below. In addition we present here a number of new groups :

III. The evaluation of integrals by introducing a parameter, which is transformed symbolically.

IV. Finding new relations by using a known integral with a parameter α, for which will be substituted a function of the symbolic parameter p. After transformation of the total function of p and interpretation of p backwards again, we get the new relations.

In this group we may distinguish especially two sub-groups :

* Volterra, *l. c.*

IV. *a.* Where the original formula is so changed that a factor $e^{-\frac{1}{p}}$ appears, and

IV. *b.* Where the manipulation brings a factor

$$\frac{p}{\sqrt{p^2+1}}\, e^{-\lambda \sqrt{p^2+1}}.$$

Some very simple examples of the kind (III.) and (IV.*a*) can already be found in Heaviside *.

All these groups will appear to be of a very fertile nature. Finally we put together in group

V. All those applications of the symbolic calculus which do not belong to one of the preceding groups.

(i.) *Relations from Summation of Images.*

1. For the Laguerre polynomials $L_n(x)$, we have †

$$L_n(x) \doteqdot n!\left(1-\frac{1}{p}\right)^n ; \quad \ldots \quad \text{(F 9)}$$

$$\therefore \sum_{n=0} (-1)^n \frac{L_n(x)}{n!} = 1 - \left(1-\frac{1}{p}\right) + \left(1-\frac{1}{p}\right)^2 - \ldots = \frac{1}{2}\frac{p}{p-\frac{1}{2}}$$

Now,

$$\frac{p}{p-\frac{1}{2}} \doteqdot e^{\frac{1}{2}x}.$$

and thus

$$\sum_{n=0}^{\infty} (-1)^n \frac{L_n(x)}{n!} = \frac{1}{2}e^{\frac{1}{2}x}. \quad \ldots \quad \text{(17)}$$

2. Another example is

$$\sum_{n=0}^{\infty} \frac{L_n(x)}{(n!)^2} \doteqdot \sum_{n=0}^{\infty} \frac{\left(1-\frac{1}{p}\right)^n}{n!} = e^{1-\frac{1}{p}},$$

and thus, by interpretation of the right-hand member,

$$\sum_{n=0}^{\infty} \frac{L_n(x)}{(n!)^2} = e J_0(2\sqrt{x}). \quad \ldots \quad \text{(18)}$$

3. Still another example with Laguerre polynomials :

$$\frac{e^{-\frac{x}{2}}L_n(x)}{n!} \doteqdot \frac{p}{p+\frac{1}{2}}\left(\frac{p-\frac{1}{2}}{p+\frac{1}{2}}\right)^n,$$

---

* O. Heaviside, ' Electromagnetic Theory,' iii. pp. 237, 238.
† P. p. 892.

resulting from application of (R 4) upon (F 9). And by (R 1):

$$\frac{e^{-x}L_n(2x)}{n!} \doteq \frac{p}{p+1}\left(\frac{p-1}{p+1}\right)^n, \quad \cdots \quad (19)$$

$$\therefore \quad e^{-x}\sum_{n=0}^{n=\infty}\frac{(-1)^n L_{2n}(2x)}{(2n)!}$$

$$\doteq \frac{p}{p+1}\left[1-\left(\frac{p-1}{p+1}\right)^2+\cdots\right] = \frac{1}{2}\frac{p^2+p}{p^2+1}.$$

Hence by interpretation of the right-hand side by means of (F 3) and (F 4):

$$e^{-x}\sum_{n=0}^{n=\infty}\frac{(-1)^n L_{2n}(2x)}{(2n!)} = \frac{1}{2}(\cos x + \sin x). \quad . \quad (20)$$

4. Some examples with Hermite polynomials are based upon the image of $\mathrm{He}_n(\sqrt{x})$, which can be found from the differential equation for the Hermite functions in an analogous way as the image of $J_0(2\sqrt{x})$ from the differential equation for Bessel functions (*cf.* P. p. 877). In that way we get for the image of $\mathrm{He}_{2n+1}(\sqrt{x})$:

$$\mathrm{He}_{2n+1}(\sqrt{x}) \doteq \frac{(2n+1)!}{n!}\frac{\sqrt{\pi}}{\sqrt{p}}\left(\frac{1}{p}-1\right)^n, \quad . \quad (21)$$

$$\therefore \quad \sum_{n=0}^{n=\infty}\frac{(-1)^n}{(2n+1)!}\mathrm{He}_{2n+1}(\sqrt{x}) \doteq \frac{\sqrt{\pi}}{\sqrt{p}}e^{1-\frac{1}{p}} \doteq e\sqrt{\pi}x^{\frac{1}{2}}J_{\frac{1}{2}}(2\sqrt{x}).$$

Put.

$$2\sqrt{x}=y,$$

then

$$\sum_{n=0}^{n=\infty}\frac{(-1)^n}{(2n+1)!}\mathrm{He}_{2n+1}\left(\frac{y}{2}\right) = e\sqrt{\frac{\pi}{2}}y\,J_{\frac{1}{2}}(y) = e\sin y. \quad (22)$$

5. In another example, now for Bessel functions, the process is one of reversed direction. We decompose a p-function into a sum of others. Thus we can prove symbolically why Bessel functions of half-integral order can be written in the form

$$J_{n+\frac{1}{2}}(x) = A(x)\sin x + B(x)\cos x, \quad . \quad (23)$$

where $A(x)$ and $B(x)$ represent finite polynomials.

We multiply first by $x^{n+\frac{1}{2}}$, and use (F 6) for half-integer indices

$$x^{n+\frac{1}{2}}J_{n+\frac{1}{2}}(x) \doteqdot \frac{2^{n+\frac{1}{2}}\Pi(n)}{\sqrt{\pi}}\frac{p}{(p^2+1)^{n+1}} \quad . \quad . \quad (24)$$

It is seen that only integral powers of p^2+1 occur when the order of the Bessel functions is a half integer. We can write

$$\frac{1}{(p^2+1)^{n+1}} = \sum_{m=0}^{m=n} \frac{A^{n+1}_{n+1-m}}{(p+i)^{n+1-m}} + \sum_{m=0}^{m=n} \frac{B^{n+1}_{n+1-m}}{(p-i)^{n+1-m}},$$

where the coefficients A are easily obtained by expanding the left-hand member in ascending powers of $(p+i)$, when we let p approach $-i$ and the coefficients B by expanding the same side in ascending powers of $p-i$, provided we take p close to $+i$. We thus find

$$A^{n+1}_{n+1-m} = (-1)^{n+m+1}B^{n+1}_{n+1-m} = \frac{(-1)^m(n+m)!}{m!\,n!\,(-2i)^{n+m+1}}.$$

The typical functions of p we thus get to interpret in the right-hand side of (24) are

$$\frac{p}{(p+i)^k} \doteqdot h_1(x) \quad \text{and} \quad \frac{p}{(p-i)^k} \doteqdot h_2(x).$$

Applying (R 4) we derive for $h_1(x)$ and $h_2(x)$ respectively,

$$e^{ix}h_1(x) \doteqdot \frac{1}{p^{k-1}}, \qquad e^{-ix}h_2(x) \doteqdot \frac{1}{p^{k-1}},$$

$$\therefore \quad h_1(x) = e^{-ix}\frac{x^{k-1}}{\Pi(k-1)}, \qquad h_2(x) = e^{ix}\frac{x^{k-1}}{\Pi(k-1)}.$$

In this way we obtain the ordinary equation

$$x^{n+\frac{1}{2}}J_{n+\frac{1}{2}}(x)$$
$$= \frac{2^{n+\frac{1}{2}}n!}{\sqrt{\pi}}\sum_{m=0}^{m=n}\frac{(-1)^m(n+m)!}{m!\,n!}\frac{e^{-ix}+(-1)^{n+m+1}e^{ix}}{(-2i)^{n+m+1}}\frac{x^{n-m}}{(n-m)!}.$$

Dividing again by $x^{n+\frac{1}{2}}$ and introducing cos and sin functions, we have for even $n(n=2\nu)$

$$J_{2\nu+\frac{1}{2}}(x)$$
$$= \frac{1}{\sqrt{\pi}}\left[\cos x.\sum_{\mu=0}^{\nu-1}(-1)^{\nu+\mu}\frac{(2\nu+2\mu+1)!\,2}{(2\mu+1)!\,(2\nu-2\mu-1)!}\frac{1}{(2x)^{2\mu+\frac{3}{2}}}\right.$$
$$\left.+\sin x.\sum_{\mu=0}^{\nu}(-1)^{\nu+\mu}\frac{(2\nu+2\mu)!\,2}{(2\mu)!\,(2\nu-2\mu)!}\frac{1}{(2x)^{2\mu+\frac{1}{2}}}\right],$$

$$. \quad . \quad . \quad (25)$$

and for n odd $(n=2\nu+1)$

$J_{2\nu+\frac{3}{2}}(x)$

$$= \frac{1}{\sqrt{\pi}} \left[\cos x \cdot \sum_{\mu=0}^{\nu} (-1)^{\nu+\mu+1} \frac{(2\nu+2\mu+1)! \, 2}{(2\mu)! \, (2\nu-2\mu+1)!} \frac{1}{(2x)^{2\mu+\frac{3}{2}}} \right.$$

$$\left. + \sin x \cdot \sum_{\mu=0}^{\nu} (-1)^{\nu+\mu} \frac{(2\nu+2\mu+2)! \, 2}{(2\mu+1)! \, (2\nu-2\mu)!} \frac{1}{(2x)^{2\mu+\frac{3}{2}}} \right].$$

$$\cdots \quad (26)$$

6. In another example we expand the image function into an infinite series. The following image is known :

$$\frac{p}{\sqrt{p^2+1}} e^{-\lambda \sqrt{p^2+1}} \doteqdot \begin{cases} J_0(\sqrt{x^2-\lambda^2}) & \text{for} \quad x > \lambda, \\ 0 & \text{for} \quad x < \lambda, \end{cases}$$

from which, by application of (R 5),

$$\frac{p}{\sqrt{p^2+1}} e^{-\lambda(\sqrt{p^2+1}-p)} \doteqdot J_0(\sqrt{x^2+2\lambda x}) \quad \text{for} \quad x > 0. \quad (27)$$

This last image can be expanded as

$$\frac{p}{\sqrt{p^2+1}} \left[1 - \lambda(\sqrt{p^2+1}-p) + \frac{\lambda^2}{2!}(\sqrt{p^2+1}-p)^2 - \ldots \right],$$

and since by (F 7)

$$J_n(x) \doteqdot \frac{p}{\sqrt{p^2+1}} (\sqrt{p^2+1}-p)^n,$$

we have

$$J_0(\sqrt{x^2+2\lambda x}) = J_0(x) - \lambda J_1(x) + \frac{\lambda^2}{2!} J_2(x) - \ldots,$$

giving for $J_n(x)$:

$$J_n(x) = \left[\frac{d^n}{d\lambda^n} J_0(\sqrt{x^2-2\lambda x}) \right]_{\lambda=0} \cdot \quad \cdot \quad (28)$$

(ii.) *Applications of the " Product Theorem."*

1. From the identity

$$\frac{1}{p} \cdot \frac{\Pi(m)}{p^m} \cdot \frac{\Pi(n)}{p^n} = \frac{\Pi(m)\Pi(n)}{p^{m+n+1}},$$

we conclude with the aid of the product theorem (R 15)

$$\int_0^x \xi^m (x-\xi)^n \, d\xi = \frac{\Pi(m)\Pi(n)}{\Pi(m+n+1)} x^{m+n+1}.$$

Thus we find for the Beta function, defined by

$$B(n+1, m+1) = \int_0^1 \xi^m (1-\xi)^n d\xi,$$

immediately its value, expressed in Gamma functions:

$$B(n+1, m+1) = \frac{\Pi(m)\Pi(n)}{\Pi(m+n+1)}$$

or

$$B(n, m) = \frac{\Gamma(m)\Gamma(n)}{\Gamma(m+n)}. \quad \cdots \quad (29)$$

2. As another application of the product theorem we consider the image (F 3) of the Laguerre function $L_n(x)$, now with $\Pi(n)$ instead of $n!$, from which, by means of (R 3), we get

$$\int_0^x L_n(\xi) d\xi \doteq \frac{\Pi(n)}{p} \left(1 - \frac{1}{p}\right)^n. \quad \cdots \quad (30)$$

The right-hand side can be written as

$$\frac{\Pi(n)}{\Pi(n-m)\Pi(m)} \frac{1}{p} \cdot \Pi(n-m)\left(1 - \frac{1}{p}\right)^{n-m} \cdot \Pi(m)\left(1 - \frac{1}{p}\right)^m$$

so that the product theorem leads here to

$$\int_0^x L_n(\xi) d\xi = \frac{\Pi(n)}{\Pi(n-m)\Pi(m)} \int_0^x L_{n-m}(\xi) L_m(x-\xi) d\xi. \quad (31)$$

3. Another example connects the polynomials of Hermite with those of Laguerre. We used already (21), which we now write in the form

$$He_{2n+1}(\sqrt{x}) \doteq \frac{(2n+1)!}{n!} \frac{\sqrt{\pi}}{\sqrt{p}} \left(\frac{1}{p} - 1\right)^n$$

$$= (-1)^n \frac{(2n+1)!}{(n!)^2} \frac{1}{p} \cdot \sqrt{p} \cdot \sqrt{\pi} \, n! \left(\frac{p-1}{p}\right)^n.$$

From (F 9) and $\sqrt{p} \doteq \dfrac{1}{\sqrt{\pi x}}$ it follows at once, by the product theorem, that

$$He_{2n+1}(\sqrt{x}) = \frac{(-1)^n(2n+1)!}{(n!)^2} \int_0^x \frac{1}{\sqrt{\xi}} L_n(x-\xi) d\xi,$$

or, by introducing new variables,

$$He_{2n+1}(x) = (-1)^n \frac{(2n+1)!}{n! \, n!} 2 \int_0^x L_n(x^2 - \xi^2) d\xi. \quad (32)$$

4. There is also a connexion between Bessel and Laguerre functions. Take

$$x^{n+\frac{1}{2}}J_{n+\frac{1}{2}}(x) \doteqdot \frac{2^{n+\frac{1}{2}}\Pi(n)}{\sqrt{\pi}} \frac{p}{(p^2+1)^{n+1}}. \quad . \quad . \quad (33)$$

In order to compare this with the image of a Laguerre function, we first transform (33) so as to get a denominator $(p^2-1)^{n+1}$, *i. e.*, one with real roots. This can be done by means of (R 1) with $s=i$, giving

$$x^{n+\frac{1}{3}}I_{n+\frac{1}{2}}(x) \doteqdot \frac{2^{n+\frac{1}{2}}\Pi(n)}{\sqrt{\pi}} \frac{p}{(p^2-1)^{n+1}}, \quad . \quad (34)$$

where

$$I_n(y) = \frac{1}{i^n}J_n(iy). \quad . \quad . \quad . \quad . \quad (35)$$

We now apply rule (R 4), giving

$$e^{-x}x^{n+\frac{1}{3}}I_{n+\frac{1}{2}}(x) \doteqdot \frac{2^{n+\frac{1}{2}}}{\sqrt{\pi}} \Pi(n) \frac{1}{(p+2)^{n+1}p^n},$$

or, applying (R 1) with $s=\frac{1}{2}$,

$$e^{-\frac{x}{2}}x^{n+\frac{1}{3}}I_{n+\frac{1}{2}}\left(\frac{x}{2}\right) \doteqdot \frac{\Pi(n)}{\sqrt{\pi}} \frac{1}{(p+1)^{n+1}p^n}$$
$$= \frac{1}{\sqrt{\pi}} \cdot \frac{1}{p} \cdot \frac{1}{p^{2n}} \cdot \frac{\Pi(n)p^{n+1}}{(p+1)^{n+1}}.$$

The factor $\left(\dfrac{p}{p+1}\right)^{n+1}$ can be related to Laguerre functions by means of an application of (R 4) to (F 9) giving

$$\frac{e^{-x}L_n(x)}{\Pi(n)} \doteqdot \left(\frac{p}{p+1}\right)^{n+1}. \quad . \quad . \quad . \quad (36)$$

Applying the product theorem, we obtain

$$e^{-\frac{x}{2}}x^{n+\frac{1}{3}}I_{n+\frac{1}{2}}\left(\frac{x}{2}\right) = \frac{1}{\sqrt{\pi}} \int_0^x \frac{\xi^{2n}}{\Pi(2n)} e^{-(x-\xi)}L_n(x-\xi)\,d\xi,$$

or

$$e^{\frac{x}{2}}x^{n+\frac{1}{3}}I_{n+\frac{1}{2}}\left(\frac{x}{2}\right) = \frac{1}{\sqrt{\pi}\,\Pi(2n)} \int_0^x e^\xi \xi^{2n}L_n(x-\xi)\,d\xi. \quad (37)$$

5. A great number of the integrals, derived recently by J. G. Rutgers [*], can be obtained very directly by means of

[*] J. G. Rutgers, Proc. Royal Soc. Amsterdam, xxxiv. p. 239 (1931).

the product theorem. It might be sufficient to show this for only one specimen, taken out of his collection, namely, for

$$\int_0^x J_n(x-\xi)J_{-n-1}(\xi)(x-\xi)^n\xi^{-n}d\xi = \frac{\cos x}{\sin(n+\frac{1}{2})\pi}. \quad (38)$$

The left-hand side has the form

$$\int_0^x h_1(x-\xi)h_2(\xi)\,d\xi,$$

where

$$h_1(x) = x^n J_n(x) \doteq \frac{2^n \Pi(n-\frac{1}{2})}{\sqrt{\pi}}\cdot\frac{p}{(p^2+1)^{n+\frac{1}{2}}} = f_1(p)$$

and

$$h_2(x) = x^{-n}J_{-n-1}(x) = x\cdot x^{-n-1}J_{-n-1}(x).$$

By (R8) and (F6), we have

$$x\cdot x^{-n-1}J_{-n-1}(x)$$

$$\doteq p\left(-\frac{d}{dp}\right)\left\{\frac{2^{-(n+1)}\Pi(-n-\frac{3}{2})}{\sqrt{\pi}}\frac{1}{(p^2+1)^{-n-\frac{1}{2}}}\right\},$$

hence

$$h_2(x) \doteq \frac{2^{-n}\Pi(-n-\frac{1}{2})}{\sqrt{\pi}}\frac{p^2}{(p^2+1)^{-n+\frac{1}{2}}} = f_2(p).$$

Thus the left-hand side of (38) is symbolically represented by

$$\frac{1}{p}\cdot f_1(p)\cdot f_2(p) = \frac{\Pi(n-\frac{1}{2})\Pi(-n-\frac{1}{2})}{\pi}\frac{p^2}{p^2+1}$$

$$= \frac{1}{\sin(n+\frac{1}{2})\pi}\frac{p^2}{p^2+1},$$

being just the image of the right-hand side of (38). Thus the relation (38) is proved.

6. A last application of the product theorem can be based upon the known images

$$\sqrt{\pi p}\,e^{-\frac{1}{p}}I_n\left(\frac{1}{p}\right) \doteq \frac{1}{\sqrt{x}}J_{2n}(2\sqrt{2x}), \quad \cdot \quad \cdot \quad (39)$$

$$e^{-\frac{1}{p}}I_n\left(\frac{1}{p}\right) \doteq J_n^2(\sqrt{2x}), \quad \cdot \quad \cdot \quad \cdot \quad (40)$$

which follow immediately from known integrals (see Watson, 'Bessel Functions,' pp. 394, 395).

Writing the identity,

$$e^{-\frac{1}{p}} I_n\left(\frac{1}{p}\right) = \frac{1}{p} \cdot \sqrt{p}\, e^{-\frac{1}{p}} I_n\left(\frac{1}{p}\right) \cdot \sqrt{p},$$

and applying the product theorem, we get the relation

$$J_n^2(\sqrt{2x}) = \int_0^x \frac{1}{\sqrt{\pi\xi}} J_{2n}(2\sqrt{2\xi}) \frac{1}{\sqrt{\pi(x-\xi)}} d\xi,$$

or by an obvious transformation,

$$J_n^2(\alpha) = \frac{2}{\pi} \int_0^{\frac{\pi}{2}} J_{2n}(2\alpha \sin\theta)\, d\theta. \quad . \quad . \quad . \quad (41)$$

Some of the formulæ in the foregoing groups, namely, (17), (18), (31), and (32), were already published else-where *.

<center>(iii.) Symbolic Evaluation of Integrals.</center>

In connexion herewith we mention that the ordinary equation (R 11) may already give a means to evaluate integrals : If the integral on the left- or on the right-hand side is known, we find the other, as was shown already in P.†
But here we mean another symbolic method, which is best explained again with the aid of some examples.

Suppose we wish to prove the formulæ

$$\int_0^\infty \frac{\sin s}{s}\, ds = \frac{\pi}{2},$$

$$\int_0^\infty \frac{\cos s}{1+s^2}\, ds = \frac{\pi}{2}\frac{1}{e},$$

$$\int_0^\infty \frac{\cos s}{\sqrt{s}}\, ds = \sqrt{\frac{\pi}{2}}.$$

We can consider the integrals

$$\int_0^\infty \frac{\sin\alpha s}{s}\, ds, \qquad \int_0^\infty \frac{\cos\alpha s}{1+s^2}\, ds, \qquad \int_0^\infty \frac{\cos\alpha s}{\sqrt{s}}\, ds,$$

---

* Balth. van der Pol, *Handelingen XXIIIe Ned. Natuur- en Geneesk. Congres*, April 1931, Delft.
† P. pp. 872, 887.

where the introduced parameter α will be treated symbolically :

$$\alpha \doteq \frac{1}{p}.$$

Thus we get functions of p, which in the above cases allow immediate integration with respect to s, and the resulting functions of p can thereupon be interpreted backwards into functions of α, where, in order finally to obtain the required result, $\alpha = 1$ is to be taken.

For illustration, we take

$$\int_0^\infty \frac{\cos \alpha s}{1+s^2} ds \doteq \int_0^\infty \frac{p^2}{p^2+s^2} \frac{ds}{1+s^2} = \frac{\pi}{2} \frac{p}{p+1} \doteq \frac{\pi}{2} e^{-\alpha} ;$$

hence

$$\int_0^\infty \frac{\cos s}{1+s^2} ds = \frac{\pi}{2} \frac{1}{e}.$$

Sometimes it is advisable to introduce two parameters, α and β, and to treat them both symbolically :

$$\alpha \doteq \frac{1}{p}; \quad \beta \doteq \frac{1}{q},$$

as is, *e. g.*, the case for the evaluation of

$$\int_0^\infty \frac{\sin^2 s}{s^2} ds \quad \text{by means of} \quad \int_0^\infty \frac{\sin \alpha s}{s} \cdot \frac{\sin \beta s}{s} ds,$$

or in the more complicated cases in the authors' paper on simultaneous symbolic calculus [*].

However, here we study the symbolic evaluation by means of *one* parameter only.

Often the integral, whose value has to be determined, must be put in a form more suitable for the introduction of α and its interpretation. This occurs, *e. g.*, in the following integral :

$$S = \int_0^\infty \frac{J_n(s)\, ds}{s^{n-m+1}}.$$

Writing $s = 2\sqrt{t}$, we get

$$2^{n-m+1} S = \int_0^\infty \frac{J_n(2\sqrt{t})\, dt}{t^{\frac{n-m+2}{2}}} = \int_0^\infty \frac{t^{\frac{n}{2}} J_n(2\sqrt{t})\, dt}{t^{\frac{2n-m+2}{2}}}.$$

* Balth van der Pol and K. F. Niessen, Phil. Mag. xi. p. 368 (1931).

Introduce and treat, now, α in the following way :

$$2^{n-m+1}S(\alpha) = \int_0^\infty \frac{(\alpha t)^{\frac{n}{2}}J_n(2\sqrt{\alpha t})}{t^{\frac{2n-m+2}{2}}}\, dt,$$

$$\alpha \doteqdot \frac{1}{p},$$

$$2^{n-m+1}S(\alpha) \doteqdot \int_0^\infty \left(\frac{p}{t}\right)^{-n} e^{-\frac{t}{p}} t^{-\frac{2n-m+2}{2}}\, dt = \frac{\Pi\left(\frac{m}{2}-1\right)}{p^{n-\frac{m}{2}}}$$

where we first used (F 5) with (R 1), and secondly Euler's formula for the Π-function. Hence

$$2^{n-m+1}S(\alpha) = \frac{\Pi\left(\frac{m}{2}-1\right)}{\Pi\left(n-\frac{m}{2}\right)}\alpha^{n-\frac{m}{2}}.$$

With $\alpha=1$ and $2\sqrt{t}=s$, this gives

$$\int_0^\infty \frac{J_n(s)\,ds}{s^{n-m+1}} = \frac{1}{2^{n-m+1}}\frac{\Pi\left(\frac{m}{2}-1\right)}{\Pi\left(n-\frac{m}{2}\right)}. \quad\quad . \quad (42)$$

being Weber's integral (see Watson, 'Bessel Functions,' p. 391).

(iv. a.) *Transformation of the Original Relation into one with the Factor* $e^{-\frac{1}{p}}$.

In the following examples a predominant role is played by the relation (F 5) :

$$\frac{1}{p^n}e^{-\frac{1}{p}} \doteqdot x^{\frac{n}{2}} J_n(2\sqrt{x}).$$

1. We start with a known integral, *e. g.*, with

$$\int_0^\infty e^{-\alpha s}s^n J_n(s)\,ds = \frac{2^n}{\sqrt{\pi}}\Pi(n-\tfrac{1}{2})\frac{1}{(\alpha^2+1)^{n+\frac{1}{2}}}. \quad (43)$$

Substitute

$$\alpha = \beta + \frac{1}{p},$$

thus

$$\int_0^\infty e^{-\beta s} e^{-\frac{s}{p}} s^n J_n(s)\,ds$$

$$= \frac{2^n}{\sqrt{\pi}}\frac{\Pi(n-\frac{1}{2})}{(\beta^2+1)^{n+\frac{1}{2}}}\frac{p^{2n+1}}{\left[\left(p+\frac{\beta}{\beta^2+1}\right)^2+\left(\frac{1}{\beta^2+1}\right)^2\right]^{n+\frac{1}{2}}}. \quad (44)$$

For a later purpose we prefer to write (44) first in the form

$$\int_0^\infty \frac{e^{-\beta s}}{s^n}\frac{s^{2n}}{p^{2n}}e^{-\frac{s}{p}}J_n(s)\,ds$$

$$= \frac{2^n}{\sqrt{\pi}}\frac{\Pi(n-\frac{1}{2})}{(\beta^2+1)^{n+\frac{1}{2}}}\frac{p}{\left[\left(p+\frac{\beta}{\beta^2+1}\right)^2+\left(\frac{1}{\beta^2+1}\right)^2\right]^{n+\frac{1}{2}}}. \quad (45)$$

So far, p was introduced and treated as an ordinary constant, but from here we will consider p as a symbolic parameter, used in a symbolic calculus, where $\frac{1}{p}$ is the image of some quantity x :

$$\frac{1}{p}\doteq x.$$

Thanks to the symbolic nature we ascribed to p, we can interpret backwards both members of (45) into functions of x. For the interpretation of the left-hand side we use

$$\frac{s^{2n}}{p^{2n}}e^{-\frac{s}{p}}\doteq (xs)^n J_n(2\sqrt{xs}), \quad \ldots \quad (46)$$

originating from (F 5) and (R 1), so that the integral belongs to the original :

$$x^n\int_0^\infty e^{-\beta s} J_{2n}(2\sqrt{xs}) J_n(s)\,ds.$$

To find the original $h(x)$ of the right-hand side of (45), we apply (R 4) and determine $h(x)$ by means of

$$e^{\frac{\beta}{\beta^2+1}x}h(x)\doteq \frac{2^n}{\sqrt{\pi}}\frac{\Pi(n-\frac{1}{2})}{(\beta^2+1)^{n+\frac{1}{2}}}\frac{p}{\left[p^2+\left(\frac{1}{\beta^2+1}\right)^2\right]^{n+\frac{1}{2}}},$$

hence,

$$h(x) = e^{-\frac{\beta}{\beta^2+1}x}(\beta^2+1)^{n-\frac{1}{2}}\left(\frac{x}{\beta^2+1}\right)^n J_n\left(\frac{x}{\beta^2+1}\right).$$

The original functions belonging to both members of (45) being equal, we have the new relation,

$$\int_0^\infty e^{-\beta s}J_{2n}(2\sqrt{sx})J_n(s)\,ds = \frac{1}{\sqrt{\beta^2+1}}e^{-\frac{\beta}{\beta^2+1}x}J_n\left(\frac{x}{\beta^2+1}\right),$$

$$\ldots \; (47)$$

yielding the value of an infinite integral in whose integrand appear two Bessel functions with arguments of a different kind with respect to the integration variable.

Substituting $\beta=0$ in (47), we have the special case

$$\int_0^\infty J_{2n}(2\sqrt{sx})J_n(s)\,ds = J_n(x). \quad \ldots \; (48)$$

2. In another example we consider the known integral [*],

$$\int_0^\infty e^{-\alpha\frac{s^2}{4}}s^{n+1}J_n(s)\,ds = \frac{2^{n+1}}{\alpha^{n+1}}e^{-\frac{1}{\alpha}}. \quad \ldots \; (49)$$

We substitute again

$$\alpha = \beta + \frac{1}{p},$$

thus,

$$\int_0^\infty e^{-\beta\frac{s^2}{4}}e^{-\frac{s^2}{4p}}s^{n+1}J_n(s)\,ds = \left(\frac{2}{\beta}\right)^{n+1}\frac{p^{n+1}}{\left(p+\frac{1}{\beta}\right)^{n+1}}e^{-\frac{1}{\beta}\frac{p}{p+1}\frac{1}{\beta}}.$$

Divide both members by p^n in order to get easily interpretable functions of p,

$$\int_0^\infty e^{-\beta\frac{s^2}{4}}\frac{4^n}{s^{n-1}}\left(\frac{s^2}{4p}\right)^n e^{-\frac{s^2}{4p}}J_n(s)\,ds = \left(\frac{2}{\beta}\right)^{n+1}\frac{p}{\left(p+\frac{1}{\beta}\right)^{n+1}}e^{-\frac{1}{\beta}\frac{p}{p+1}\frac{1}{\beta}}.$$

$$\ldots \; (50)$$

Ascribing now a symbolic nature to p,

$$\frac{1}{p} \doteqdot x,$$

we can interpret backwards both members of (50).

For the first one we use

$$\left(\frac{s^2}{4p}\right)^n e^{-\frac{s^2}{4p}} \doteqdot \left(\frac{xs^2}{4}\right)^{\frac{n}{2}}J_n\left(2\sqrt{\frac{xs^2}{4}}\right), \qquad . \; (51)$$

---

* Watson, ' Bessel Functions,' p. 394, (4).

originating from (F 5) and (R 1), whereupon the whole first member can be easily interpreted.

In order to find the original $h(x)$, corresponding to the second member in (50), we apply (R 4) and have to determine $h(x)$ from

$$e^{\frac{1}{\beta}x}\, h(x) \doteqdot 2^{n+1}\beta^{n-1}e^{-\frac{1}{\beta}}\frac{1}{(\beta^2 p)^n}e^{\frac{1}{\beta^2 p}}.$$

Now,

$$\frac{1}{p^n}e^{\frac{1}{p}} \doteqdot x^{\frac{n}{2}}\mathrm{I}_n(2\sqrt{x}),$$

where

$$\mathrm{I}_n(y) = \frac{1}{i^n}\mathrm{J}_n(iy).$$

Thus

$$e^{\frac{1}{\beta}x}\, h(x) = 2^{n+1}\beta^{n-1}e^{-\frac{1}{\beta}}\left(\frac{x}{\beta^2}\right)^{\frac{n}{2}}\mathrm{I}_n\left(2\sqrt{\frac{x}{\beta^2}}\right),$$

and thus $h(x)$ is known.

Equating the original functions we found to belong to the first and second member of (50), we obtain, with

$$\sqrt{x} = \alpha.$$

$$\int_0^\infty e^{-\beta\frac{s^2}{4}}s\,\mathrm{J}_n(s)\mathrm{J}_n(\alpha s)\,ds = \frac{2}{\beta}e^{-\frac{\alpha^2+1}{\beta}}\mathrm{I}_n\left(\frac{2\alpha}{\beta}\right), \quad . \quad (52)$$

thus deriving in a very simple way Weber's second exponential integral (*cf.* Watson, ' Bessel Functions,' p. 395, form (1)).

3. It is not advisable to take $\beta = 0$ in this formula, for the right-hand member then would take the form $0 \times \infty$. In connexion herewith two formulæ can easily be derived, again with symbolic methods :

    a. The value of (52) for $\beta = 0$.

    b. A discontinuous integral of a different nature.

For their derivation it is better to go back to (49), where the substitution

$$\alpha = \frac{1}{p}$$

gives

$$\int_0^\infty e^{-\frac{s^2}{4p}}s^{n+1}\mathrm{J}_n(s)\,ds = 2^{n+1}p^{n+1}e^{-p}. \quad . \quad . \quad (53)$$

From this we can derive two results.

a. For the evaluation of (52) with $\beta = 0$ we divide both members of (53) by p^n, just as in the case $\beta > 0$,

$$\int_0^\infty \frac{1}{p^n} e^{-\frac{s^2}{4p}} s^{n+1} J_n(s)\, ds = 2^{n+1} p e^{-p}. \quad . \quad . \quad (54)$$

The right-hand member now containing the factor e^{-p} is of a form entirely different from that in the case $\beta > 0$, since, according to (6), $p e^{-p}$ is the image of an impulsive function with its maximum at $x = 1$, which is indicated by the Dirac δ-function, $\delta(x-1)$.

The left-hand member of (54) can again be interpreted by means of (51). Thus we obtain for the integral (52) with $\beta = 0$ (by substituting again $\sqrt{x} = \alpha$),

$$\int_0^\infty s J_n(\alpha s) J_n(s)\, ds = \frac{2}{\alpha^n} \delta(\alpha^2 - 1). \quad . \quad . \quad (55)$$

b. Returning to (53) we divide both members by p^{m+1}, where we suppose

$$m > n.$$

In the relation, thus obtained,

$$\int_0^\infty \frac{1}{p^{m+1}} e^{-\frac{s^2}{4p}} s^{n+1} J_n(s)\, ds = 2^{n+1} \frac{e^{-p}}{p^{m-n}} ; \quad . \quad . \quad (56)$$

p is understood again to be a symbolic parameter. The first member then can be interpreted with the aid of

$$\left(\frac{s^2}{4p}\right)^{m+1} e^{-\frac{s^2}{4p}} \doteqdot \left(\frac{s^2 x}{4}\right)^{\frac{m+1}{2}} J_{m+1}\left(2\sqrt{\frac{s^2 x}{4}}\right).$$

The second member by means of

$$e^{-p} \frac{1}{p^{m-n}} \doteqdot \begin{cases} 0 & \text{for } x < 1, \\[2mm] \dfrac{(x-1)^{m-n}}{\Pi(m-n)} & \text{for } x > 1, \end{cases}$$

which is based upon (F 1) and (R 5).

Equating the original functions belonging to the first and second member of (56), we get (again with $x = \sqrt{\alpha}$)

$$\int_0^\infty \frac{J_{m+1}(\alpha s) J_n(s)}{s^{m-n}}\, ds = \begin{cases} 0 & \text{for } \alpha < 1, \\[2mm] \dfrac{(\alpha^2 - 1)^{m-n}}{2^{m-n} \Pi(m-n) \alpha^{m+1}} & \text{for } \alpha > 1, \end{cases}$$

$$. \quad . \quad . \quad (57)$$

in accordance with Watson, 'Bessel Functions,' p. 401, (2).

4. In another example of this group the term $e^{-\frac{1}{p}}$ originates from the substitution $\alpha = \dfrac{1}{p}$ in the known integral,

$$\int_0^x \frac{J_0(s)\,s\,ds}{\sqrt{s^2 + \alpha^2}} = e^{-\alpha}$$

giving

$$\int_0^\infty J_0(s)\frac{\mu s}{\sqrt{p^2 s^2 + 1}}\,ds = e^{-\frac{1}{p}}.$$

Considering here, again, p as a symbolic parameter for which

$$\frac{1}{p} \doteq x,$$

we obtain by interpretation of both members,

$$\int_0^\infty J_0(s) J_0\left(\frac{x}{s}\right) ds = J_0(2\sqrt{x}), \quad (x > 0). \quad (58)$$

a relation already known to Heaviside [*].

5. One may also start from

$$\int_0^\infty e^{-\alpha s} s^n ds = \frac{\Pi(n)}{\alpha^{n+1}}.$$

Substitute

$$\alpha = 1 + \frac{1}{p},$$

$$\int_0^x e^{-\left(1+\frac{1}{p}\right)s} s^n ds = \Pi(n)\left(1 + \frac{1}{p}\right)^{-(n+1)}. \quad (59)$$

Now from (36) we know

$$e^{-x}L_n(x) \doteq \Pi(n)\left(1 + \frac{1}{p}\right)^{-(n+1)}. \quad (36)$$

Interpretation of both members of (59) leads therefore to

$$L_n(x) = e^x \int_0^\infty e^{-s} s^n J_0(2\sqrt{sx})\,ds. \quad (60a)\dagger$$

---

* O. Heaviside, *l. c.* iii. p. 281, form 295.

† In a recent paper by Sommerfeld (*Ann. d. Phys.* xi. p. 272, 1931) we found this equation ascribed to Epstein and Muskat (**Proc. Nat. Acad.** xv. p. 405, 1929).

In order to obtain a similar expression for Hermite's polynomials we transform the original function by means of our rules, so that the image contains a factor $\left(1+\dfrac{1}{p}\right)^{-n}$, and then replace this by means of (59) by an integral containing $e^{-\frac{s}{p}}$.

We use (21 a) for polynomials of odd order

$$\mathrm{He}_{2n+1}(\sqrt{x}) \doteqdot 2^{2n+1}\Pi(n+\tfrac{1}{2})\frac{1}{\sqrt{p}}\left(\frac{1-p}{p}\right)^n \quad . \quad (21\ a)$$

and by application of (R 4),

$$e^{-s}\mathrm{He}_{2n+1}(\sqrt{x}) \doteqdot 2^{2n+1}\Pi(n+\tfrac{1}{2})(-1)^n\frac{1}{\sqrt{p+1}}\left(\frac{p}{p+1}\right)^{n+1}$$

$$,, \qquad \doteqdot 2^{2n+1}\Pi(n+\tfrac{1}{2})(-1)^n\frac{1}{\sqrt{p}}\left(1+\frac{1}{p}\right)^{-(n+\frac{3}{2})}$$

$$,, \qquad \doteqdot 2^{2n+1}(-1)^n\frac{1}{\sqrt{p}}\int_0^x e^{-\left(1+\frac{1}{p}\right)s}s^{n+\frac{1}{2}}ds$$

$$,, \qquad \doteqdot 2^{2n+1}(-1)^n\int_0^x e^{-s}s^n\left(\frac{s}{p}\right)^{\frac{1}{2}}e^{-\frac{s}{p}}ds,$$

from which, by interpretation backwards,

$$\mathrm{He}_{2n+1}(\sqrt{x})=(-1)^n 2^{2n+1}x^{\frac{1}{4}}e^x\int_0^\infty e^{-s}s^{n+\frac{1}{4}}\mathrm{J}_{\frac{1}{2}}(2\sqrt{sx})ds, \quad (60\ b)$$

expressing Hermite polynomials of odd order as an integral containing a Bessel function.

Using

$$\mathrm{J}_{\frac{1}{2}}(x) = \sqrt{\frac{2}{\pi x}}\sin x$$

and introducing $\xi=\sqrt{x}$ and $t=\sqrt{s}$, we can write the expression (60 b) also in the form

$$\mathrm{He}_{2n+1}(\xi) = \frac{(-1)^n 2^{2n+2}}{\sqrt{\pi}}e^{\xi^2}\int_0^\infty e^{-t^2}t^{2n+1}\sin(2\xi t)\,dt.$$

7. The images (36) and (21 a) lend themselves also very well to an application of the product theorem.

First combining two images of the type (36), we have

$$\frac{1}{p}\cdot n!\left(1+\frac{1}{p}\right)^{-(n+1)}\cdot m!\left(1+\frac{1}{p}\right)^{-(m+1)}$$

$$= n!\, m!\, \frac{1}{p}\left(1+\frac{1}{p}\right)^{-(n+m+2)}$$

$$= \frac{n!\, m!}{(n+m+1)!}\int_0^{'\infty} e^{-s}s^{n+m}\frac{s}{p}\epsilon^{-\frac{s}{p}}\,ds.$$

By application of the product theorem we get

$$\int_0^x e^{-\xi}\mathrm{L}_n(\xi)e^{-(x-\xi)}\mathrm{L}_m(x-\xi)\,d\xi$$

$$= \frac{n!\, m!}{(n+m+1)!}\int_0^{'x} e^{-s}s^{n+m}(sx)^{\frac{1}{2}}\mathrm{J}_1(2\sqrt{sx})\,ds,$$

or

$$\int_0^x \mathrm{L}_n(\xi)\mathrm{L}_m(x-\xi)\,d\xi$$

$$= \frac{n!\, m!}{(n+m+1)!}x^{\frac{1}{2}}e^x\int_0^{'x} e^{-s}s^{n+m+\frac{1}{2}}\mathrm{J}_1(2\sqrt{sx})\,ds. \quad (60\,aa)$$

8. Now combining an image (36) with an image (21 a) we construct the identity.

$$\frac{1}{p}\cdot n!\left(1+\frac{1}{p}\right)^{-(n+1)}\cdot(-1)^m 2^{2m+1}\Pi(m+\tfrac{1}{2})\frac{1}{\sqrt{p}}\left(1+\frac{1}{p}\right)^{-(m+\frac{1}{2})}$$

$$= (-1)^m 2^{2m+1}\Pi(n)\Pi(m+\tfrac{1}{2})\frac{1}{p^{\frac{3}{2}}}\left(1+\frac{1}{p}\right)^{-(n+m+\frac{5}{2})}$$

$$= (-1)^m 2^{2m+1}\frac{\Pi(n)\Pi(m+\tfrac{1}{2})}{\Pi(n+m+\tfrac{3}{2})}\frac{1}{p^{\frac{3}{2}}}\int_0^\infty e^{-\left(1+\frac{1}{p}\right)s}s^{n+m+\frac{3}{2}}\,ds.$$

Application of the product theorem gives

$$\int_0^x e^{-\xi}\mathrm{L}_n(\xi)e^{-(x-\xi)}\mathrm{He}_{2m+1}(\sqrt{x-\xi})\,d\xi$$

$$= (-1)^m 2^{2m+1}\frac{\Pi(n)\Pi(m+\tfrac{1}{2})}{\Pi(n+m+\tfrac{3}{2})}\int_0^{'x} e^{-s}s^{n+m}(sx)^{\frac{1}{2}}\mathrm{J}_{\frac{1}{2}}(2\sqrt{sx})\,ds$$

or

$$\int_0^x \mathrm{L}_n(\xi)\mathrm{He}_{2m+1}(\sqrt{x-\xi})\,d\xi$$

$$= (-1)^m 2^{2m+1}\frac{\Pi(n)\Pi(m+\tfrac{1}{2})}{\Pi(n+m+\tfrac{3}{2})}x^{\frac{1}{2}}e^x\int_0^x e^{-s}s^{m+n+\frac{3}{2}}\mathrm{J}_{\frac{1}{2}}(2\sqrt{sx})\,ds.$$

$$\qquad\qquad\qquad\qquad\cdots\quad (60\,ab)$$

9. Finally, combining two images both of the type (21 *a*), we start with the identity :

$$\frac{1}{p} \cdot (-1)^n 2^{2n+1} \Pi(n+\tfrac{1}{2}) \frac{1}{\sqrt{p}} \left(1+\frac{1}{p}\right)^{-(n+\frac{3}{2})} \times$$

$$(-1)^m 2^{2m+1} \Pi(m+\tfrac{1}{2}) \frac{1}{\sqrt{p}} \left(1+\frac{1}{p}\right)^{-(m+\frac{3}{2})}$$

$$= (-1)^{m+n} 2^{2(m+n+1)} \Pi(n+\tfrac{1}{2}) \Pi(m+\tfrac{1}{2}) \frac{1}{p^2} \left(1+\frac{1}{p}\right)^{-(m+n+3)}$$

$$= (-1)^{m+n} 2^{2(m+n+1)} \frac{\Pi(n+\tfrac{1}{2})\Pi(m+\tfrac{1}{2})}{\Pi(m+n+2)} \frac{1}{p^2}$$

$$\int_0^x e^{-\left(1+\frac{1}{p}\right)s} s^{m+n+2} ds,$$

which, interpreted backwards, means

$$\int_0^x e^{-\xi} \mathrm{He}_{2n+1}(\sqrt{\xi}) e^{-(x-\xi)} \mathrm{He}_{2m+1}(\sqrt{x-\xi}) d\xi$$

$$= (-1)^{m+n} 2^{2(m+n+1)} \frac{\Pi(n+\tfrac{1}{2})\Pi(m+\tfrac{1}{2})}{\Pi(m+n+2)} \times$$

$$\int_0^\infty e^{-s} s^{m+n}(sx) J_2(2\sqrt{sx}) ds,$$

or

$$\int_0^x \mathrm{He}_{2n+1}(\sqrt{\xi}) \mathrm{He}_{2m+1}(\sqrt{x-\xi}) d\xi$$

$$= (-1)^{m+n} 2^{2(m+n+1)} \frac{\Pi(n+\tfrac{1}{2})\Pi(m+\tfrac{1}{2})}{\Pi(m+n+2)} xe^x \times$$

$$\int_0^\infty e^{-s} s^{m+n+1} J_2(2\sqrt{sx}) ds. \quad . \quad (60\,bb)$$

We further remark, that in $(60\,aa)$, $(60\,ab)$, and $(60\,bb)$ the factor containing the Π-functions can also be expressed as a Beta-function, for we have (see (29))

$$B(n+1, m+1) = \frac{\Pi(m)\Pi(n)}{\Pi(m+n+1)} \cdot$$

(iv.*b*.) *Transformation of the Original Relation into one containing the Factor* $\dfrac{p}{\sqrt{p^2+1}} e^{-\sqrt{p^2+1}\,\lambda}$.

In this group the following relation is used :

$$\frac{p}{\sqrt{p^2+1}} e^{-\sqrt{p^2+1}\,s} \doteq \begin{cases} J_0(\sqrt{x^2-s^2}) & \text{for } x > s \\ 0 & \text{for } x < s. \end{cases} \quad . \quad (61)$$

We will now give a few examples, arranged according to an increasing complication of the known integrals with which we start.

1. In the simplest case we begin with

$$\int_{0}^{\infty} e^{-as}\,ds = \frac{1}{a},$$

wherein we substitute

$$a = \sqrt{p^2+1},$$

whereupon we multiply both members with $\frac{p}{\sqrt{p^2+1}}$, so that

$$\int_{0}^{\infty} \frac{p}{\sqrt{p^2+1}} e^{-s\sqrt{p^2+1}}\,ds = \frac{p}{p^2+1}.$$

Considering now p again as a symbolic parameter for which

$$\frac{1}{p} \doteq x,$$

we get, by application of (61) for the interpreted members, the equation

$$\int_{0}^{x} J_0(\sqrt{x^2-s^2})\,ds = \sin x, \quad . \quad . \quad . \quad (62)$$

a well-known integral, where the upper limit became $s = x$ on account of the fact that the function on the right-hand side of (61) is zero for $s > x$.

2. In the same way we obtain, from the known integral

$$\int_{0}^{\infty} e^{-as} \cos s\,ds = \frac{a}{a^2+1}$$

by substitution of $a = \sqrt{p^2+1}$ and multiplication with $\frac{p}{\sqrt{p^2+1}}$,

$$\int_{0}^{\infty} \frac{p}{\sqrt{p^2+1}} e^{-s\sqrt{p^2+1}} \cos s\,ds = \frac{p}{p^2+2},$$

which, interpreted backwards, in a calculus, where

$$\frac{1}{p} \doteq x,$$

leads, by means of (F 3), to

$$\int_0^x J_0(\sqrt{x^2 - s^2}) \cos s\, ds = \frac{1}{\sqrt{2}} \sin (x \sqrt{2}), \quad . \quad (63)$$

being a special case of Sonine's formula (Watson, 'Bessel Functions,' p. 376, (1)).

3. New formulæ can be obtained, if we apply this method together with the product theorem.

E. g., the known integral,

$$\int_0^\infty e^{-\alpha s} \sin s\, ds = \frac{1}{\alpha^2 + 1},$$

leads, after the above transformation, to

$$\int_0^x \frac{p}{\sqrt{p^2 + 1}} e^{-s \sqrt{p^2 + 1}} \sin s\, ds = \frac{1}{p} \cdot \frac{p}{\sqrt{p^2 + 1}} \cdot \frac{p}{p^2 + 2},$$

or by interpretation, if

$$\frac{1}{p} \doteq x$$

and application of (F 6), (F 3), and (R 15) to

$$\int_0^x J_0(\sqrt{x^2 - s^2}) \sin s\, ds = \frac{1}{\sqrt{2}} \int_0^x J_0(x - \xi) \sin (\xi \sqrt{2})\, d\xi.$$

$$. \quad . \quad . \quad (64)$$

4. Or we may start with the given integral,

$$\int_0^\infty e^{-\alpha s} J_0(s)\, ds = \frac{1}{\sqrt{\alpha^2 + 1}},$$

which leads to

$$\int_0^\infty \frac{p}{\sqrt{p^2 + 1}} e^{-s \sqrt{p^2 + 1}} J_0(s)\, ds = \frac{p}{\sqrt{p^2 + 1}} \cdot \frac{p}{\sqrt{p^2 + 2}} \cdot \frac{1}{p}.$$

Hence,

$$\int_0^x J_0(\sqrt{x^2 - s^2}) J_0(s)\, ds = \int_0^x J_0(x - \xi) J_0(\xi \sqrt{2})\, d\xi. \quad (65)$$

5. Take, for a last example, the known integral,

$$\int_c^{\infty} e^{-as}\,ds = \frac{e^{-ca}}{\alpha}.$$

Replace $\alpha = \sqrt{p^2+1}$ and multiply with $\dfrac{p}{\sqrt{p^2+1}}$, then

$$\int^{\infty} \frac{p}{\sqrt{p^2+1}} e^{-\sqrt{p^2+1}\,s}\,ds = \frac{1}{p}\cdot\frac{p}{\sqrt{p^2+1}}\cdot\frac{p}{\sqrt{p^2+1}} e^{-c\sqrt{p^2+1}}.$$

$$\cdots\ (66)$$

Relating symbolically

$$\frac{1}{p} \doteq x,$$

and using (61), the original, belonging to the left-hand side of (66), will be

$$\int_c^x J_0(\sqrt{x^2-s^2})\,ds \quad \text{for } x > c. \quad . \quad (67)$$

The last condition is necessary, since for $x < c$ we would have $x <$ all values of s, available in the left-hand side of (66), so that its image would disappear on account of (61). The original of the right-hand side will be of the form

$$\int_0^x h_1(x-\xi)h_2(\xi)\,d\xi,$$

where

$$h_1(\xi) = J_0(\xi),$$

$$h_2(\xi) = \begin{cases} J_0(\sqrt{\xi^2-c^2}) & \text{for } \xi > c, \\ 0 & \text{for } \xi < c. \end{cases}$$

The original thus becomes

$$\int_c^x J_0(x-\xi)J_0(\sqrt{\xi^2-c^2})\,d\xi. \quad . \quad . \quad (68)$$

Equating (67) and (68) we get

$$\int_c^x J_0(\sqrt{x^2-s^2})\,ds = \int_c^x J_0(x-\xi)J_0(\sqrt{\xi^2-c^2})\,d\xi. \quad (69)$$

For $c = 0$,

$$\int_0^x J_0(\sqrt{x^2-s^2})\,ds = \int_0^x J_0(x-\xi)J_0(\xi)\,d\xi,$$

being in accordance with (62), since by P 883 we have

$$\int_0^x J_0(x-\xi)J_0(\xi)\,d\xi = \sin x.$$

(v.) *The Mixed Group.*

1. In the theory of propagation of radiowaves over the earth, an important role is played by the integral S :

$$S = \int_0^\infty \frac{J_0(\lambda r)e^{-\sqrt{\lambda^2-k^2}\,z}\lambda d\lambda}{\sqrt{\lambda^2-k^2}} = \frac{e^{ik\sqrt{r^2+z^2}}}{\sqrt{r^2+z^2}}, \quad . \quad (70)$$

where k is a complex quantity in the first quadrant. The root $\sqrt{\lambda^2-k^2}$ is to be taken with a positive real part. The symbolic calculus provides a proof of this formula in a very simple way.

We prefer here to use a symbolic calculus, where it is not r, but r^2, which is represented by $\dfrac{1}{p}$,

$$r^2 \doteqdot \frac{1}{p},$$

so that a function $h(r^2)$ of r^2 is represented by

$$h(r^2) \doteqdot p \int_0^\infty e^{-pr^2}h(r^2)d(r^2). \quad . \quad . \quad . \quad (71)$$

To evaluate the integral S by means of the symbolic calculus, we first write

$$J_0(\lambda r) = J_0\left(2\sqrt{\frac{\lambda^2}{4}r^2}\right) \doteqdot e^{-\frac{\lambda^2}{4p}}$$

on account of (F 5), where x is to be replaced by r^2. Therefore

$$S \doteqdot \int_0^\infty e^{-\frac{\lambda^2}{4p}}e^{-z\sqrt{\lambda^2-k^2}}\frac{\lambda d\lambda}{\sqrt{\lambda^2-k^2}}.$$

We transform this function of p by the substitution,

$$\lambda = 2p\sqrt{u},$$

giving

$$S \doteqdot p\int_0^\infty e^{-pu-2pz\sqrt{u-\left(\frac{k}{2p}\right)^2}}\frac{du}{\sqrt{u-\left(\frac{k}{2p}\right)^2}}.$$

Putting

$$u - \left(\frac{k}{2p}\right)^2 = v^2,$$

we get

$$S \doteqdot 2p\int_{-\frac{ik}{2p}}^\infty e^{-pv^2-\frac{k^2}{4p}-2pzv}\,dv.$$

Defining a new variable t by means of

$$v = -i\frac{k}{2p} + \sqrt{t^2 + z^2} - z,$$

we have

$$S \doteq p \int_0^{\infty} e^{-pt^2}\frac{e^{ik\sqrt{t^2 + z^2}}}{\sqrt{t^2 + z^2}}\, d(t^2),$$

and, therefore, by means of (71)

$$S = \frac{e^{ik\sqrt{r^2 + z^2}}}{\sqrt{r^2 + z^2}}.$$

2. The heuristic value of the symbolic calculus appears, *e.g.*, clearly from the following examples.

We can from the known relation

$$H^{(2)}_{n+\frac{1}{2}}(ix) = \sqrt{\frac{2}{\pi}}\, i^{n+\frac{1}{2}}x^{n+\frac{1}{2}}\left(\frac{1}{x}\frac{d}{dx}\right)^n\left(\frac{e^x}{x}\right), \quad . \quad (72)$$

derive another expression for the Hankel function $H^{(2)}_{n+\frac{1}{2}}(ix)$. From (F 8) we know, on the one hand, that the harmonic $P_n(1-x)$ in a symbolic calculus where

$$x \doteq \frac{1}{p},$$

is represented by

$$P_n(1-x) \doteq e^{-p}p^{n+1}\left(\frac{1}{p}\frac{d}{dp}\right)^n\left(\frac{e^p}{p}\right), \quad . \quad . \quad (F\,8)$$

where the image shows a remarkable similarity with the right member of (72).

On the other hand, Rodrigues's formula

$$P_n(y) = \frac{1}{2^n n!}\frac{d^n}{dy^n}(y^2-1)^n,$$

gives

$$P_n(1-x) = \frac{1}{n!}\frac{d^n}{dx^n}\left(x - \frac{x^2}{2}\right)^n, \quad . \quad . \quad (73)$$

being a polynomial in x with positive powers. For such a polynomial $h(x)$ we found already (see (7))

$$h(x) \doteq p\, h\left(-\frac{d}{dp}\right)\frac{1}{p}.$$

Hence

$$\left(x - \frac{x^2}{2}\right)^n \doteq p\left(-\frac{d}{dp} - \frac{1}{2}\frac{d^2}{dp^2}\right)^n \frac{1}{p}. \quad . \quad . \quad (74)$$

The function on the left-hand side, and also its first $(n-1)$ differential quotients disappear for $x=0$. Therefore, we may apply rule (R 2) n-times to (74), giving in connexion with (73),

$$P_n(1-x) \doteq \frac{1}{n!} p^n p\left(-\frac{d}{dp} - \frac{1}{2}\frac{d^2}{dp^2}\right)^n \frac{1}{p}$$

or
$$P_n(1-x) \doteq p^{n+1}\left(1 + \frac{1}{2}\frac{d}{dp}\right)^n \frac{1}{p^{n+1}}, \quad . \quad . \quad (75)$$

which is a new symbolic representation of $P_n(1-x)$ *. We thus have two images (F 8) and (75) for the same original $P_n(1-x)$, and these always being identical, we have

$$e^{-p} p^{n+1}\left(\frac{1}{p}\frac{d}{dp}\right)^n \left(\frac{e^p}{p}\right) = p^{n+1}\left(1 + \frac{1}{2}\frac{d}{dp}\right)^n \frac{1}{p^{n+1}}.$$

This equation being an identity, we may replace here p by any arbitrary value $s > 0$, so that we have in general the identity :

$$e^{-s}\left(\frac{1}{s}\frac{d}{ds}\right)^n \left(\frac{e^s}{s}\right) = \left(1 + \frac{1}{2}\frac{d}{ds}\right)^n \frac{1}{s^{n+1}} \dagger \quad . \quad . \quad (76)$$

We now apply this result to (72) and obtain a new expression for $H_{n+\frac{1}{2}}^{(2)}(is)$:

$$H_{n+\frac{1}{2}}^{(2)}(is) = \sqrt{\frac{2}{\pi}}(is)^{n+\frac{1}{2}} e^s\left(1 + \frac{1}{2}\frac{d}{ds}\right)^n \frac{1}{s^{n+1}} \quad . \quad (77)$$

In an analogous way we derive from

$$H_{n+\frac{1}{2}}^{(1)}(is) = \sqrt{\frac{2}{\pi}} i^{n+\frac{1}{2}} s^{n+\frac{1}{2}}\left(\frac{1}{s}\frac{d}{ds}\right)^n \left(\frac{e^{-s}}{-s}\right), \quad . \quad (78)$$

---

* The image (75) could, contrary to Rodrigues's formula (73), be used for a definition of spherical harmonics with fractional index. One would only have to expand the binomial and to interpret backwards the individual terms on the right-hand side of (75). Thus a solution is obtained of the differential equation for $P_n(1-x)$ with fractional index. A similar remark can be made with respect to (72) and (77) below.

† It might be of interest to show how this identity, which was found easily in a symbolic way, can also be proved by using ordinary analysis. We have

$$\frac{1}{s}\frac{d}{ds}\left(\frac{e^s}{s}\right) = \frac{1}{s}\frac{d}{ds}\int_{-1}^{\infty} e^{-s\xi} d\xi = \frac{1}{s}\int_{-1}^{\infty} e^{-s\xi}(-\xi)d\xi$$

$$= \frac{1}{s}\int_{-1}^{\infty} e^{-s\xi} d\left(\frac{1}{2} - \frac{\xi^2}{2}\right) = \int_{-1}^{\infty}\left(\frac{1}{2} - \frac{\xi^2}{2}\right) e^{-s\xi} d\xi.$$

the new expression

$$\mathrm{H}^{(1)}_{n+\frac{1}{2}}(i\,s) = (-1)^{n+1}\sqrt{\frac{2}{\pi}}\,(i\,s)^{n+\frac{1}{2}}\,e^{-s}\left(1 - \frac{1}{2}\frac{d}{ds}\right)^n\frac{1}{s^{n+1}}. \quad (79)$$

3. The symbolic calculus may also very successfully be applied to prove theorems, in which in some direct or indirect way an impulsive function (or Dirac function) occurs. For instance, as an example of relations based upon orthogonal functions we can easily prove the relation

$$\mathrm{F}(x) = \int_{s=0}^{s=\infty}\mathrm{F}(s)\,s\int_{\lambda=0}^{\lambda=\infty}\mathrm{J}_0(\lambda s)\,\mathrm{J}_0(\lambda x)\,\lambda d\lambda\,ds\ . \quad (80)$$

in the following way.

It will be sufficient to show that

$$s\int_{\lambda=0}^{\lambda=\infty}\mathrm{J}_0(\lambda s)\,\mathrm{J}_0(\lambda x)\,\lambda d\lambda$$

is an impulsive function $\delta(x-s)$ being infinite at $s=x$. This can be done by using the symbolic calculus again, where

$$x \doteq \frac{1}{p}.$$

In this way we have

$$s\int_{\lambda=0}^{\lambda=\infty}\mathrm{J}_0(\lambda s)\,\mathrm{J}_0(\lambda x)\,\lambda d\lambda \doteq s\int_{\lambda=0}^{\lambda=\infty}\mathrm{J}_0(\lambda s)\,\frac{p}{\sqrt{p^2+\lambda^2}}\,\lambda d\lambda = p\,e^{-sp},$$

$$\cdots \quad (81)$$

the last step being based upon a known integral.

By repeating this transformation n-times, one obtains

$$\left(\frac{1}{s}\frac{d}{ds}\right)^n\left(\frac{e^s}{s}\right) = \frac{1}{n!}\int_{-1}^{\infty}\left(\frac{1}{2} - \frac{\xi^2}{2}\right)^n e^{-s\xi}\,d\xi,$$

and with

$$\xi = -1 + x,$$

$$e^{-s}\left(\frac{1}{s}\frac{d}{ds}\right)^n\left(\frac{e^s}{s}\right) = \frac{1}{n!}\int_0^{\infty}e^{-sx}\left(x - \frac{x^2}{2}\right)^n dx.$$

Now

$$\int_0^{\infty}e^{-sx}x^k\,dx = \frac{k!}{s^{k+1}} = \left(-\frac{d}{ds}\right)^k\frac{1}{s}.$$

Hence:

$$e^{-s}\left(\frac{1}{s}\frac{d}{ds}\right)^n\left(\frac{e^s}{s}\right) = \frac{1}{n!}\left(-\frac{d}{ds} - \frac{1}{2}\frac{d^2}{ds^2}\right)^n\frac{1}{s} = \left(1 + \frac{1}{2}\frac{d}{ds}\right)^n\frac{1}{s^{n+1}}.$$

Now from (6) we know that $p\,e^{-sp}$ corresponds to an impulsive function $\delta(x-s)$ with its maximum at $x=s$. This was just what we had to prove in order to establish the theorem (80).

It was perhaps instructive to speak here of impulsive functions, but this was not necessary. We need only to prove the symbolic relation (81), since substituted into (80), it leads to

$$\mathrm{F}(x) \doteqdot p \int_0^{\infty} e^{-ps} \mathrm{F}(s)\, ds,$$

which is the basic definition of the symbolic calculus, and hence (80) has been proved*.

4. In conclusion we give a few remarks concerning the examples in the groups IV. *a* and IV. *b*. There the positive constant α was replaced by $\alpha = \beta + \dfrac{1}{p}$ or by $\alpha = \sqrt{p^2 + 1}$. It will be obvious that the possibilities are not exhausted by this choice, since any substitution

$$\alpha = f(p)$$

may be used as long as $f(p) > 0$ for $p > 0$.

The practical question, however, is to use such transformations, that functions of p emerge, the original functions of which are known. Therefore the substitutions we used in IV. *a* and IV. *b* were successful.

Nevertheless, we shall now show that some other substitutions may also be of use sometimes.

In integrals of the type

$$\alpha \int_0^{\cdot} e^{-\alpha s} h(s)\, ds = f(\alpha), \qquad \dots \quad (82)$$

it can be useful to substitute for instance :

$$\alpha = \sqrt{p},$$

giving

$$\int_0^{\infty} \sqrt{p}\, e^{-s\sqrt{p}} h(s)\, ds = f(\sqrt{p}). \quad \dots \quad (83)$$

Considering now again p as a symbolic parameter,

$$\frac{1}{p} \doteqdot x,$$

* Compare also a similar consideration in Part I.

we use, for the   terpretation of the left-hand side *,

$$\sqrt{p}\,e^{-s\sqrt{p}} \doteq \frac{1}{\sqrt{\pi x}}\,e^{-\frac{s^2}{4x}}. \quad \ldots \quad (84)$$

The applied substitution, therefore, will be successful only if we happen to know also the interpretation $X(x)$ of $f(\sqrt{p})$ in the right-hand side of (83),

$$f(\sqrt{p}) \doteq X(x).$$

In that case we will have derived the relation

$$\int_0^{\infty} \frac{1}{\sqrt{\pi x}}\,e^{-\frac{s^2}{4x}} h(s)\,ds = X(x). \quad \ldots \quad (85)$$

There is a multitude of known integrals of the type (82), namely, those expressing the relation

$$h(x) \doteq f(p),$$

between an original $h(x)$ and its known image $f(p)$. We have, of course, to select those pairs $h(s)$ and $f(\alpha)$, where $f(\alpha)$ is of such a form that $f(\sqrt{p})$ can easily be interpreted too.

For example, take in (82)

$$h(s) = \cos s \quad \text{with} \quad f(\alpha) = \frac{\alpha^2}{\alpha^2 + 1}.$$

Now in this case

$$f(\sqrt{p}) = \frac{p}{p+1} \doteq e^{-x} = X(x).$$

Thus we find by substitution into (85) at once the relation

$$\frac{1}{\sqrt{\pi x}} \int_0^{\infty} e^{-\frac{s^2}{4x}} \cos s\,ds = e^{-x}. \quad \ldots \quad (86)$$

5. Another substitution which sometimes is useful for integrals of the type (82) is

$$\alpha = p + \frac{1}{p}$$

giving

$$\int_0^{\infty} e^{-ps - \frac{s}{p}} h(s)\,ds = \frac{f\left(p + \frac{1}{p}\right)}{p + \frac{1}{p}}, \quad \ldots \quad (87)$$

---

* See, *e.g.*, J. R. Carson, 'Electric Circuit Theory and the Operational Calculus,' p. 39, formula (g).

which can be considered as an equation between two symbolic images.

For the interpretation of the first one we use

$$\frac{1}{p} \doteqdot x,$$

$$e^{-\frac{s}{p}} \doteqdot J_0(2\sqrt{sx}),$$

and by (R 5)

$$e^{-ps}\, e^{-\frac{s}{p}} \doteqdot \begin{cases} 0 & \text{for } s > x, \\ J_0(2\sqrt{s(x-s)}) & \text{for } s < x, \end{cases} \quad . \quad (88)$$

so that the first member of (87) corresponds to the original :

$$\int_0^x J_0(2\sqrt{s(x-s)})\, h(s)\, ds,$$

where the upper limit $s = x$ follows from the fact that the original in (88) was zero for $s > x$.

Suppose, now, that we also know the original $Y(x)$ of the right-hand side of (87) :

$$\frac{f\left(p + \dfrac{1}{p}\right)}{p + \dfrac{1}{p}} \doteqdot Y(x).$$

Then we find the new relation

$$\int_0^x J_0(2\sqrt{s(x-s)})\, h(s)\, ds = Y(x). \quad . \quad . \quad (89)$$

For instance, we may take in (82)

$$h(s) = 1, \text{ to which belongs } f(\alpha) = 1$$

for

$$1 \doteqdot 1.$$

In this case we have

$$\frac{f\left(p + \dfrac{1}{p}\right)}{p + \dfrac{1}{p}} = \frac{p}{p^2 + 1} \doteqdot \sin x = Y(x).$$

Thus we find by means of (89)

$$\int_0^x J_0(2\sqrt{s(x-s)})\, ds = \sin x. \quad . \quad . \quad (90)$$

The above examples clearly show the great variety of successful substitutions as well as the freedom in the choice of the original integrals, from which one can start to derive new ones. It is hoped that the many examples treated above may again show the great heuristic value of the symbolic calculus.

List of some Results obtained above.

$$\sum_{n=0}^{\infty} (-1)^n \frac{L_n(x)}{n!} = \tfrac{1}{2} e^{\frac{1}{2}x}. \quad \ldots \quad (17)$$

$$\sum_{n=0}^{\infty} \frac{L_n(x)}{n! \, n!} = e\, J_0(2\sqrt{x}). \quad \ldots \quad (18)$$

$$\sum_{n=0}^{\infty} \frac{(-1)^n L_{2n}(x)}{(2n)!} = \tfrac{1}{2} e^{\frac{x}{2}} \left(\cos\frac{x}{2} + \sin\frac{x}{2}\right). \quad (20)$$

$$\sum_{n=0}^{\infty} \frac{(-1)^n}{(2n+1)!} He_{2n+1}(x) = e\sin 2x, \quad \ldots \quad (22)$$

$$\int_0^x L_{n-m}(\xi) L_m(x-\xi)\, d\xi = \frac{\Pi(n-m)\,\Pi(m)}{\Pi(n)} \int_0^x L_n(\xi)\, d\xi. \quad (31)$$

$$He_{2n+1}(x) = (-1)^n \frac{(2n+1)!}{n! \, n!} 2 \int_0^x L_n(x^2-\xi^2)\, d\xi. \quad (32)$$

$$\int_0^x e^{\xi} \xi^{2n} L_n(x-\xi)\, d\xi = \sqrt{\pi}\, \Pi(2n)\, e^{\frac{x}{2}} x^{n+\frac{1}{2}} I_{n+\frac{1}{2}}\left(\frac{x}{2}\right). \quad (37)$$

$$J_n^2(\alpha) = \frac{2}{\pi} \int_0^{\frac{\pi}{2}} J_{2n}(2\alpha\sin\theta)\, d\theta. \quad \ldots \quad (41)$$

$$\int_0^{\infty} e^{-\beta s} J_{2n}(2\sqrt{s\alpha}) J_n(s)\, ds = \frac{1}{\sqrt{\beta^2+1}}\, e^{-\frac{\beta}{\beta^2+1}\alpha} J_n\left(\frac{\alpha}{\beta^2+1}\right).$$
$$\ldots \quad (47)$$

$$\int_0^{\infty} J_{2n}(2\sqrt{s\alpha}) J_n(s)\, ds = J_n(\alpha). \quad \ldots \quad (48)$$

$$\int_0^{\infty} e^{-\beta\frac{s^2}{4}} s J_n(s) J_n(\alpha s)\, ds = \frac{2}{\beta} e^{-\frac{\alpha^2+1}{\beta}} I_n\left(\frac{2\alpha}{\beta}\right) \quad \text{(Weber).} \quad (52)$$

$$\int_0^{\infty} s J_n(\alpha s) J_n(s)\, ds = \frac{2}{\alpha^n} \delta(\alpha^2-1). \quad \ldots \quad (55)$$

$$\int_0^{\infty} \frac{J_{m+1}(\alpha s) J_n(s)}{s^{m-n}}\, ds = \frac{(\alpha^2-1)^{m-n}}{2^{m-n} \Pi(m-n)\, \alpha^{m+1}} \binom{\alpha>1}{m>n}$$
$$\text{(Sonine and Schafheitlin).} \quad \ldots \quad (57)$$

$$\int^{\infty} J_0(s) J_0\left(\frac{a}{s}\right) ds = J_0(2\sqrt{a}) \quad (\alpha > 0) \quad \text{(Heaviside)}.$$
$$\text{. . . (58)}$$

$$L_n(x) = e^x \int_0^\infty e^{-s} s^n J_0(2\sqrt{sx}) ds. \quad \text{. . . (60 a)}$$

$$He_{2n+1}(\sqrt{x}) = (-1)^n 2^{2n+1} x^{\frac{1}{4}} e^x \int_0^\infty e^{-s} s^{n+\frac{1}{4}} J_{\frac{1}{2}}(2\sqrt{sx}) ds.$$
$$\text{. . . (60 b)}$$

$$\int_0^x I_n(\xi) L_m(x-\xi) d\xi$$
$$= \frac{\Pi(n)\Pi(m)}{\Pi(n+m+1)} x^{\frac{1}{2}} e^x \int_0^x e^{-s} s^{m+n+\frac{1}{2}} J_1(2\sqrt{sx}) ds. \quad \text{(60 aa)}$$

$$\int_0^x L_n(\xi) He_{2m+1}(\sqrt{x-\xi}) d\xi$$
$$= (-1)^m 2^{2m+1} \frac{\Pi(n)\Pi(m+\frac{1}{2})}{\Pi(m+n+\frac{3}{2})} x^{\frac{1}{4}} e^x \times$$
$$\int_0^\infty e^{-s} s^{m+n+\frac{3}{4}} J_{\frac{1}{2}}(2\sqrt{sx}) ds. \quad \text{. . . (60 ab)}$$

$$\int_0^x He_{2n+1}(\sqrt{\xi}) He_{2m+1}(\sqrt{x-\xi}) d\xi$$
$$= (-1)^{m+n} 2^{2(m+n+1)} \frac{\Pi(n+\frac{1}{2})\Pi(m+\frac{1}{2})}{\Pi(m+n+2)} x e^x \times$$
$$\int_0^x e^{-s} s^{m+n+1} J_2(2\sqrt{sa}) ds. \quad \text{. . . (60 bb)}$$

$$\int_0^a J_0(\sqrt{a^2-s^2}) \cos s\, ds = \frac{1}{\sqrt{2}} \sin(a\sqrt{2}) \quad \text{(Sonine)}. \quad \text{(63)}$$

$$\int_a^x J_0(x-\xi) J_0(\sqrt{\xi^2-a^2}) d\xi = \int_a^x J_0(\sqrt{x^2-s^2}) ds. \quad \text{(69)}$$

$$H_{n+\frac{1}{2}}^{(1)}(is) = (-1)^{n+1} \sqrt{\frac{2}{\pi}} (is)^{n+\frac{1}{2}} e^{-s} \left(1 - \frac{1}{2}\frac{d}{ds}\right)^n \frac{1}{s^{n+1}}, \quad (79)$$

$$H_{n+\frac{1}{2}}^{(2)}(is) = \sqrt{\frac{2}{\pi}} (is)^{n+\frac{1}{2}} e^s \left(1 + \frac{1}{2}\frac{d}{ds}\right)^n \frac{1}{s^{n+1}}. \quad \text{. . . (77)}$$

The following new images were found :—

$$He_{2n+1}(\sqrt{x}) \doteqdot \frac{(2n+1)!}{n!} \frac{\sqrt{\pi}}{\sqrt{p}} \left(\frac{1}{p} - 1\right)^n, \quad \text{. . . (21)}$$

$$P_n(1-x) \doteq \begin{cases} e^{-p}p^{n+1}\left(\dfrac{1}{p}\dfrac{d}{dp}\right)^n\left(\dfrac{e^p}{p}\right), \\[2mm] p^{n+1}\left(1+\dfrac{1}{2}\dfrac{d}{dp}\right)^n\dfrac{1}{p^{n+1}}, \end{cases} \text{identical.} \quad (75)$$

Note added in the Proof.—In order to prove formula (41) (for the special case of n being an integer) by means of ordinary analysis, one may start with Graf's generalization of Neumann's addition theorem, given in the form *

$$\sum_{m=-\alpha}^{m=+\infty} J_{\nu+m}(Z)J_m(z){\cos \atop \sin}m\phi = J_\nu(\tau){\cos \atop \sin}\nu\psi, \quad . \quad . \quad (91)$$

where τ and ψ follow from Z, z, and ϕ in a geometrical way :

If Z and z represent the length of two sides of a triangle and ϕ the included angle, then τ is the length of the other side, and ψ the angle between Z and τ.

From (91) we obtain

$$\int_0^\pi J_\nu(\tau){\cos \nu\psi \cos m\Phi \atop \sin \nu\psi \sin mt}d\phi = \frac{\pi}{2}J_{\nu+m}(Z)J_m(z).$$

For $Z = z = \alpha$, we have

$$\psi = \frac{\pi}{2} - \frac{\phi}{2}, \qquad \tau = 2\alpha\sin\frac{\phi}{2}.$$

Choosing further the case $m = -n$ and $\nu = 2n$, where n is an integer, so that the relation

$$J_{-n}(\alpha) = (-1)^n J_n(\alpha)$$

can be used, we get with $\dfrac{\phi}{2} = \theta$

$$2\int_0^{\frac{\pi}{2}} J_{2n}(2\alpha\sin\theta){\cos^2(2n\theta) \atop \sin^2(2n\theta)}d\theta = \frac{\pi}{2}J_n^2(\alpha).$$

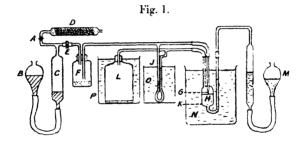Adding these two formulæ, we arrive at (41).

Eindhoven,
    October 29, 1931.

* Watson, ' Bessel Functions,' p. 361.

XLVIII. *The Surface Tensions of Mixtures of Normal Propyl Alcohol and Benzene.* By R. C. BROWN, *B.Sc., Lecturer in Physics, University College, London* *.

Introduction.

THE purpose of this paper is to describe an apparatus and technique for the accurate measurement of the surface tensions of mixtures of volatile liquids and to record the results obtained for mixtures of normal propyl alcohol and benzene. These two liquids were chosen in order to investigate whether there was any connexion between the surface tension-composition curve and viscosity-composition curve published by Dunstan †, which shows that, over the range from 0 to 10 per cent. of propyl alcohol, the viscosities of the mixtures are less than that of either of the pure

Fig. 1.

substances. The minimum occurs in Dunstan's curve at about 5 per cent.; the number of results which he determined in this neighbourhood was, however, small. The present measurements of surface tension cover the whole range from 0 to 100 per cent.

Method and Apparatus.

The method used for measuring the surface tensions was Jaeger's "maximum bubble-pressure" method, the principle of which needs no discussion here.

The apparatus was so designed that the liquid under test was not in direct communication with the atmosphere, so that changes of composition due to evaporation of the mixture and contamination were almost completely avoided.

Fig. 1 shows diagrammatically the arrangement employed.

The tap, A, was opened and the mercury reservoir, B, was first raised and then lowered so that the tube, C, was filled with air which had been drawn through calcium chloride and glass wool packed in D. A being then closed, the air in C could be made to flow into the rest of the apparatus through a piece of pressure tubing constricted by a screw-clip, E, at a rate which could be controlled by alterations in the height of B. The air thus flowing passed over anhydrous phosphorus pentoxide in F, and reached the jet, G, where it formed bubbles in the liquid in the usual way in the liquid under test, H, contained in a special glass apparatus, K. The space above H communicated with one arm of a manometer, J, and a large bottle, L. The other arm of J was connected to the tube leading to the jet. Thus the difference of level in the two arms of J gave the excess pressure inside the bubble above that in the space above H, and was independent of the actual pressure inside the apparatus. The function of L was merely to increase the volume of the space into which the bubbles escaped. Evaporation from the surface of H into this space was reduced by introducing a small quantity of the test liquid into L.

The jet was set with its plane actually coincident with the free surface of H, adjustment of the level of H being made by raising or lowering the reservoir, M, which was provided with a slow-motion movement. After a little practice and with convenient lighting of the jet and liquid this adjustment could be made quite easily and consistently repeated. The escape of a bubble caused the surface of H to be lowered slightly, so that it was necessary to bring it back to the plane of the jet before each reading of maximum pressure was taken.

The glass apparatus, K, was connected to the rest of the apparatus by pressure tubing at the three points shown in the diagram. The bulb in which the bubbles were formed was of about 4·5 cm. diameter. N was a large glass beaker containing water maintained at a temperature of $20·00 \pm ·02°$ C., and O was a vessel with optical glass sides also containing water at the same temperature. Finally, the large bottle L was kept at approximately 20° C. by the water-bath P.

The liquid used in the manometer was butyl phthalate, and proved thoroughly satisfactory, having a very low vapour pressure at 20° C. The same liquid was also used in the reservoir M. The levels of liquid in the manometer arms were measured by means of a large Casella cathetometer supported in a 6 ft. iron frame and provided with a micrometer cross-wire, one graduation on the screw-head of which

corresponded to 0·0094 mm. This method was extremely convenient, since by means of the cross-wire the slow changes of level of the meniscus could be followed right up to the maximum pressure point.

The jet, G, was made by drawing down a piece of medium-walled glass tubing and cutting at the constricted part in the usual way. After a number of attempts a very satisfactory jet was produced and no grinding was necessary. The mean diameter of the jet was obtained from measurements made by means of a microscope fitted with an eye-piece scale and a stage micrometer, several different objectives (and therefore magnifications) being used. The glass apparatus, K, into which the jet was sealed, could be tilted so as to ensure that the plane of the jet was horizontal—a state of affairs which could be judged accurately by eye when the jet was just below the surface of the liquid.

Before each new mixture was introduced into K the latter was completely filled with chromic acid, allowed to stand, washed in running tap-water and conductivity water, and dried by passing dust-free air into each of the three inlets in turn whilst it was heated to well above 100° C.

Special features of the apparatus and method were therefore : —

1. Total enclosure of the liquid prevented

    (*a*) evaporation and consequent changes in composition of mixture, and

    (*b*) contamination from the atmosphere.

2. By setting the tip of the jet in the free surface of the liquid the measurement of its depth below the surface was obviated, and it was not necessary to know accurately the densities of the mixtures used, since in this circumstance the density occurs only in a small correcting term.

3. The mixtures were made up by weighing actually in the glass apparatus, K, before the latter was connected to the remainder of the apparatus.

Materials used.

The normal propyl alcohol was supplied by British Drug Houses, Ltd., and one bottle sufficed to complete all the measurements. The surface tension of the alcohol suffered no measurable change throughout the whole research.

Kahlbaum benzene was used, fresh quantities being re-distilled and partially frozen (the liquid being rejected) for each mixture. The boiling-point of the benzene thus prepared was 79·9° C. at 76·0 cm. Hg and the freezing-point was 5·5° C.

Results.

The following equation was used in calculating the surface tensions :

$$T = \frac{rg}{2}(H\rho - \tfrac{2}{3}r\sigma),$$

where r = mean radius of the jet = ·0142(3) cm.

g = acceleration due to gravity = 981·2 cm./sec.²

H = maximum bubble-pressure in cm. of butyl phthalate.

ρ = density of butyl phthalate at 20·0° C. = 1·0458 gm./c.c.

σ = density of test liquid.

Benzene.

The surface tension of each specimen of benzene used in making up the mixtures was determined. In this way seventeen values of the maximum bubble pressure for benzene were obtained. They ranged from 3·9623 to 3·9660 cm. of butyl phthalate, the mean value being 3·9642 ± ·0002 cm.

The density of benzene at 20° C. was taken as 0·88 gm./c.c.

Using these figures, and assuming a probable error of ± ·00002 cm. in the above value for the radius of the jet, we get :—

The surface tension of benzene at 20·00 ± ·02° C. against air saturated with vapour = 28·89 ± ·04 dyne/cm.

The "standard" value quoted in the International Critical Tables, and based upon the results of Richards and Coombs [*], Richards and Carver [†], and Harkins and Brown [‡], all of whom used the capillary rise method, is 28·88 ± ·03 dyne/cm.

Normal Propyl Alcohol.

Two determinations of the surface tension of the sample of propyl alcohol used in the research were made with an interval of one month between them. The results differed by only one part in 3000, the value being 23·78 dyne/cm. at 20° C. The density of the alcohol was assumed to be

* Journ. Amer. Chem. Soc. xxxvii. p. 1656 (1915).

† *Ibid.* xliii. p. 827 (1921).

‡ *Ibid.* xli. p. 499 (1919).

0·80 gm./c.c. The International Critical Tables give as the most probable result $23·8 \pm ·2$ dyne/cm., based on the work of Morgan and Owen *, Ramsay and Shields †, Renard and Guye ‡, Richards and Mathews §, and Schiff ‖.

Mixtures of Benzene and Normal Propyl Alcohol.

The densities of the various mixtures were not known, but it was estimated that a change of density from, say, 0·90 to 0·75 gm./c.c. (within which range all the densities certainly lie) makes a difference of only one part in 3000 to the surface tension as calculated from the formula already given, since

Fig. 2
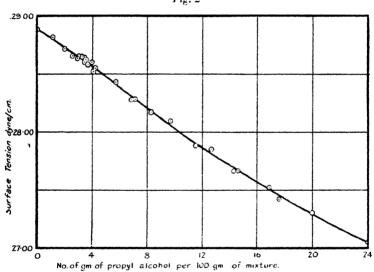
the term $\frac{2}{3}r\sigma$ is of the order of 0·008, whilst the magnitude of $H\rho$ is 4·0.
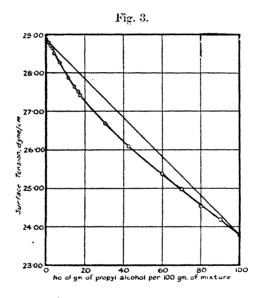
1. *For low concentrations of alcohol :*

As explained before, it was intended to investigate as carefully as possible the surface tension-concentration curve for low concentrations of alcohol. Fig. 2 shows the results obtained up to 24 per cent. of alcohol. A considerable number of these were determined in the neighbourhood

---

* *Ibid.* xxxiii. p. 1713 (1911).
† Journ. Chem. Soc. lxiii. p. 1089 (1893).
‡ *Journ. de Chim. Phys.* v. p. 81 (1907).
§ Journ. Amer. Chem. Soc. xxx. p. 8 (1908).
‖ *Ann. der Chem.* (Justus Leibig) ccxxiii. p. 47 (1884).

between 2 and 5 per cent., and a sufficient number throughout the rest of the region to fix the general trend of the curve. A definite reversal of curvature is shown by the graph at about 7 per cent., the portion between the pure benzene point and the point of inflexion being convex upwards. The centre of this region therefore lies at about 3·5 per cen

2. *For all concentrations of alcohol* :

Fig. 3 shows the surface tension-concentration curve over the whole range 0 to 100 per cent. of alcohol. The curve closely resembles that found by Morgan and Scarlett[*] for mixtures of ethyl alcohol and benzene, and presents no unexpected features.

Fig. 3.

between 2 and 5 per cent., and a sufficient number throughout

Discussion of Results.

Fig. 2 establishes definitely that the curvature of the graph undergoes a reversal at 7 per cent. of alcohol, the effect being outside the limit of experimental error. This region corresponds to the range over which Dunstan found that the viscosities of mixtures are below those of the pure substances[†].
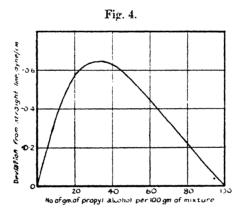
It has been suggested by Denison[‡] that the deviation from a straight line of a property-composition curve can be

---

[*] Journ. Amer. Chem. Soc. xxxix. p. 2275 (1917).

[†] *Loc. cit.*

[‡] Trans. Farad. Soc. viii. pp. 20 & 35 (1912).

accounted for by postulating a combination of some nature between the molecules of the two substances concerned. The degree of combination is a maximum when the percentage composition of the mixture is such that the ratio of the total numbers of molecules of the two substances is equal to the ratio of their numbers in the compound molecule. At this percentage composition the maximum deviation from the straight line law will take place. Denison showed that a maximum deviation often does occur at a percentage which represents some simple numerical ratio between the numbers of the molecules of the two simple substances present. Morgan and Scarlett * have determined the surface tension-concentration curves for various mixtures together with their deviations from the corresponding straight lines,

Fig. 4.

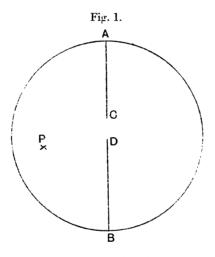No of gm. of propyl alcohol per 100 gm of mixture

and each mixture shows a maximum deviation at a percentage composition giving a simple ratio.

Fig. 4 shows the deviation-composition curve for mixtures of propyl alcohol and benzene obtained from the present measurements by reading deviations directly from the surface tension-concentration curve (fig. 3). The maximum deviation occurs at 34 per cent. (to the nearest whole number). A proportion of three molecules of benzene to two molecules of propyl alcohol would correspond to 33·9 per cent., so that, assuming Denison's theory, the present research provides evidence that molecular groups having a composition $3C_6H_6 . 2C_3H_8O$ are formed in the mixture.

It gives me great pleasure to thank Professor E. N. da C. Andrade, D.Sc., for the helpful interest with which he has followed the course of this research.

* *Loc. cit.*

XLIX. *Note on the Slow Motion of Fluid.*
By W. R. DEAN, *M.A., Trinity College, Cambridge* *.

1. IN a recent paper † Prof. A. E. H. Love has developed a method of biharmonic analysis and applied it to the solution of some important problems of the theory of elasticity. The analytical method is a general one, and its employment appears to make possible the solution of a wide class of problems not only of elasticity but also of the theory of the slow motion of viscous fluids, of special interest among the latter being some cases of two-dimensional motion past various types of obstacle. There are, for instance, some

Fig. 1.

examples of fluid motion considered in general terms by Rayleigh ‡, who concludes from them that "the formation of eddies observed in practice is not wholly due to the influence of the terms involving the squares of the velocities, but would persist in certain cases even though the motion were made infinitely slow."

Rayleigh considers an elastic plate (shown as circular in fig. 1) clamped along its circumference and along barriers AC, DB which nearly divide it into two independent parts. Suppose that pressure normal to the plane of the plate is applied at some isolated point P. The part of the plate near
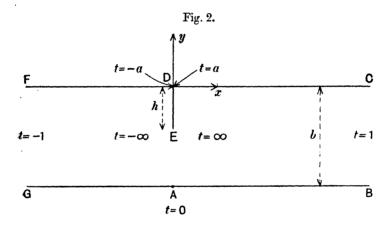
---

* Communicated by the Author.
† Proc. London Math. Soc. (2) xxix. pp. 189–242 (1929).
‡ 'Scientific Papers,' iv. pp. 78–93.

P will move in the direction (say downwards) of the applied force, but Rayleigh points out that the plate will, as it were, pivot about the supports C and D, with the result that parts of the plate on the right of the barriers will move upwards. There will be two sets of closed contours. In the corresponding fluid motion there will be an eddy on the right of the barriers. As another example * Rayleigh concludes that an eddy will be formed by fluid moving along a barrier into which a channel at right angles to the barrier opens.

Love's work should make it possible to examine such problems in detail. However, it seemed to be a desirable preliminary to apply the method, which makes use of somewhat heavy analysis, to a problem of a simpler character

Fig. 2.

than, for instance, the second of those cited above, which is certain to present difficulty. In this paper is therefore considered the two-dimensional motion of fluid in a channel in which there is (as shown in fig. 2) a projection, although there is clearly no possibility of an eddy in this example. The analysis shows that, although it would be exceedingly difficult to reach results of great numerical accuracy, the work involved in ascertaining the general character of the motion is not specially heavy. In the more important problems, like that mentioned above, no more than the general character of the motion is required, for the question is whether in given conditions an eddy does or does not exist, and we can conclude that the solution of some problems of this type is practicable by Love's method of analysis.

* *Loc. cit.* p. 89.

2. The simplest type of fluid motion is obtained in the channel represented in fig. 2 if it is supposed that the boundary GAB is moved in its own line with constant velocity (and therefore imparts the same velocity to the fluid in contact with it) while the boundary CDEF is held fixed. Let D be the origin of Cartesian coordinates (x, y), let DC be the x axis, and let GB be the line $y = -b$, $b > 0$. The stream-function ψ must then satisfy the differential equation

$$\left(\frac{\partial^2}{\partial x^2} + \frac{\partial^2}{\partial y^2}\right)^2 \psi \equiv \nabla_1{}^4\psi = 0 \quad . \quad . \quad . \quad . \quad (1)$$

at all points of the channel, the boundary conditions

$$\psi = \frac{\partial \psi}{\partial \nu} = 0 \quad . \quad . \quad . \quad . \quad . \quad (2)$$

on CDEF, $\dfrac{\partial}{\partial \nu}$ denoting as usual differentiation with respect to distance measured normal to the boundary; and the boundary conditions

$$\psi = k, \qquad \frac{\partial \psi}{\partial \nu} = k', \qquad y = -b, \quad . \quad . \quad . \quad (3)$$

k and k' being constants whose values depend on the velocity of GB.

3. Love's analysis starts from the fact that if $u + iv$ is a function of $z \, (= x + iy)$ then $xv - yu$ is a biharmonic function of the variables x, y. It is clear that

$$xv - yu = \mathrm{I}[(x - iy)(u + iv)] = -\mathrm{I}[(x + iy)(u - iv)], \quad (4)$$

where $\mathrm{I}[f]$ denotes the imaginary part of f. The problem of finding a suitable biharmonic function is therefore reduced to that of finding a suitable function of z, and the first step in this process is, according to Love's work, the conformal representation of the interior of the region concerned on the interior of a circle of unit radius.

The region ABCDEFG in the plane of z can be represented conformally on a half-plane (t) by the transformation of Schwarz and Christoffel. Let the new variable t be such that at B and C $t = 1$; at F and G $t = -1$; at D $t = \pm a$, where a is real and greater than unity and the positive or negative sign is appropriate, according as D is approached

from C or F ; at E $t = \pm \infty$, with the same sign convention. The required relation between z and t is then such that

$$\frac{dz}{dt} = \frac{C}{(1-t^2)(a^2-t^2)^{1/2}}, \quad \cdots \quad (5)$$

where C is a positive real constant.

The upper half of the plane of t can be represented conformally on the interior of the circle $|\zeta| = 1$ by the relation

$$\zeta = \frac{i-t}{i+t}. \quad \cdots \cdots \quad (6)$$

The relation between z and ζ necessary to transform ABCDEFG into the interior of the circle is consequently such that

$$\frac{dz}{d\zeta} = -\frac{iC}{\sqrt{a^2+1}} \frac{1+\zeta}{(1+\zeta^2)\left(1+\zeta^2+\dfrac{a^2-1}{a^2+1} 2\zeta\right)^{1/2}}, \quad (7)$$

and can be expressed in finite terms if necessary. If an acute angle α determined by

$$\cos\alpha = \frac{a^2-1}{a^2+1}, \qquad \sin\alpha = \frac{2a}{a^2+1} \quad \cdots \quad (8)$$

is introduced, equation (7) can be written

$$\frac{dz}{d\zeta} = -\frac{iC}{\sqrt{a^2+1}} \frac{1+\zeta}{(1+\zeta^2)(1+\zeta e^{i\alpha})^{1/2}(1+\zeta e^{-i\alpha})^{1/2}}. \quad (9)$$

The correspondence between the walls of the channel and the circumference of the circle is shown in fig. 3.

If $\zeta = r(\cos\theta + i\sin\theta)$ one side of the projection DE corresponds to the circumference of the circle between $\theta = \pi - \alpha$ and $\theta = \pi$, and it can be seen from equation (9) that the y coordinates of points of the projection are given in terms of θ by
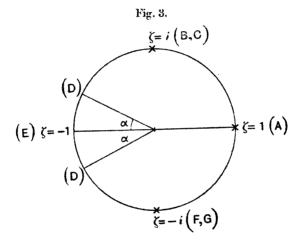
$$y = \frac{C}{2\sqrt{a^2+1}} \int_{\pi-\alpha}^{\theta} \frac{\cos\dfrac{\theta}{2}\,d\theta}{\cos\theta\sqrt{-\cos\dfrac{\theta-\alpha}{2}\cos\dfrac{\theta+\alpha}{2}}}$$

$$= -\frac{C}{2\sqrt{a^2+1}} \int_{\pi-\theta}^{\alpha} \frac{\sin\dfrac{\theta}{2}\,d\theta}{\cos\theta\sqrt{\sin\dfrac{\alpha+\theta}{2}\sin\dfrac{\alpha-\theta}{2}}} ; \quad (10)$$

the integral can, if required, be expressed in finite terms. For h, the height of the projection, and b, the breadth of the channel, we have

$$h = \frac{C}{2\sqrt{a^2+1}} \int_0^a \frac{\sin\frac{\theta}{2}\, d\theta}{\cos\theta \sqrt{\sin\frac{\alpha+\theta}{2} \sin\frac{\alpha-\theta}{2}}}, \quad (11)$$

and

$$b = \frac{C\pi}{2\sqrt{a^2-1}}.$$

Fig. 3.

4. Love * takes as a typical biharmonic function

$$-I[(x-iy)\zeta^n],$$

where n is a positive integer. Since ζ^n is a function of z, this expression is of the form (4) ; moreover, since any function of z of the kind required can be expanded as a power series in ζ, convergent when $|\zeta| < 1$, any biharmonic function of the kind required can be expanded as a series of these typical solutions. An expression alternative to that above is, since $\zeta = re^{i\theta}$,

$$I[(x+iy)r^n e^{-ni\theta}].$$

From equation (7) z is given in terms of ζ by a series of the form

$$z = i(c_0 + c_1\zeta + c_2\zeta^2 + \ldots),$$

* *Loc. cit.* § 1.51.

the coefficients c being real, and the solution can accordingly be expressed as

$$
I\left[i\left(\sum_{m=0}^{\infty} c_m r^m e^{mi\theta}\right) r^n e^{-ni\theta}\right]
$$
$$
= \sum_{m=0}^{n} c_m r^{n+m} \cos(n-m)\theta + \sum_{m=n+1}^{\infty} c_m r^{m+n} \cos(m-n)\theta. \quad (12)
$$

A harmonic function may clearly be added, and Love accordingly uses solutions such as

$$
\sum_{m=0}^{n} c_m (r^{n+m} - r^{n-m}) \cos(n-m)\theta
$$
$$
+ \sum_{m=n+1}^{\infty} c_m (r^{m+n} - r^{m-n}) \cos(m-n)\theta,
$$

which vanish at the boundary $r = 1$. The use of solutions of this type in the problem of the present paper led to some difficulty, which arose from the circumstance that the region we are concerned with is unbounded ; the typical solution, say ψ_n, will therefore be left in the form

$$
\psi_n = \sum_{m=0}^{n} (c_m r^{n+m} + d_m r^{n-m}) \cos(n-m)\theta
$$
$$
+ \sum_{m=n+1}^{\infty} (c_m r^{m+n} + d_m r^{m-n}) \cos(m-n)\theta, \quad (13)
$$

the coefficients d being arbitrary.

5. When the boundary GAB is moved in its own line with constant velocity the fluid is set into uniform shearing motion, somewhat modified by the projection. It is therefore convenient to write

$$
\psi = -y^2 + \phi \quad \ldots \ldots \quad (14)
$$

for the stream-function. The first term which corresponds to the motion of uniform shear does not vanish on the projection DE, but otherwise, since DE is in the direction of the y axis, satisfies all the conditions of § 2.

The function ϕ must therefore satisfy the differential equation

$$
\nabla_1^4 \phi = 0, \quad \ldots \ldots \quad (15)
$$

and the condition

$$
\frac{\partial \phi}{\partial \nu} = 0,
$$

or the equivalent * condition

$$\frac{\partial \phi}{\partial r} = 0, \quad \ldots \ldots \ldots \quad (16)$$

at all points of the boundary; lastly, ϕ must equal y^2 on DE and must vanish elsewhere on the boundary, so that when $r=1$

$$\begin{aligned} \phi &= y^2, \quad &\pi - \alpha \leq \theta \leq \pi + \alpha, \\ &= 0, \quad &\begin{cases} 0 \leq \theta < \pi - \alpha, \\ \pi + \alpha < \theta \leq 2\pi. \end{cases} \end{aligned} \quad \right\} \quad \ldots \quad (17)$$

The required function ϕ is the sum of a series of the functions ψ_n of the preceding paragraph. Let the constants d of expression (13) be chosen so that the differential coefficients with respect to r of the coefficients of the cosines vanish when $r=1$; accordingly, in the first sum

$$d_m = -\frac{n+m}{n-m} c_m, \quad \ldots \ldots \quad (18)$$

and in the second

$$d_m = -\frac{m+n}{m-n} c_m. \quad \ldots \ldots \quad (19)$$

When $m=n$, d_m is not defined by (18), and we take $d_n=0$. The reason for this is that the last term $(m=n)$ of the first sum in (12) is $c_n r^{2n}$; the corresponding harmonic function is therefore a constant and cannot be used to nullify the boundary value of the derivative. After the above step we consequently have only a biharmonic function whose normal derivative is constant at the boundary, not one with a zero derivative. These constants are eliminated below (§ 7) by combining the functions ψ_n in pairs. We then have a series of functions which satisfy (15) and (16) and which can be combined to satisfy the last condition (17) after the boundary values of ϕ have been expanded as a cosine series.

6. It is now assumed that the height h of the projection is small in comparison with b, the breadth of the channel. The assumption is, at least in theory, unnecessary, for it would certainly be possible to continue at the expense of some heavy algebra without it; but it introduces a very considerable simplification into the subsequent arithmetical work without interfering in any way with the main object

---

* See § 9.

of this paper, which is to assess the practical difficulty or applying Love's method of analysis to problems of the kind mentioned in § 1.

The assumption that h/b is small implies that the angle α of § 3 is small, and hence from (8) that $1/a$ is small. To expand the boundary values of ϕ as a cosine series the values of y^2 at all points of the projection must be expressed in terms of θ. Since α is small and θ varies between $\pi - \alpha$ and π on one side of the projection, the variable in integral (10) is small throughout the range of integration ; equation (10) can therefore be replaced by

$$y = -\frac{C}{2a} \int_{\pi-\theta}^{\alpha} \frac{\theta \, d\theta}{(\alpha^2 - \theta^2)^{1/2}}$$

$$= -\frac{C}{2a} \left[\alpha^2 - (\pi - \theta)^2 \right]^{1/2} ;$$

replacing α by $\sin\alpha$ and $\pi - \theta$ by $\sin\theta$, we can write

$$y^2 = \frac{C^2}{4a^2} \left[\sin^2\alpha - \sin^2\theta \right]. \quad \ldots \quad (20)$$

We have now to expand as a Fourier series, say

$$\sum_{0}^{\infty} f_n \cos n\theta,$$

the function which is equal to y^2 when $\pi - \alpha < \theta < \pi + \alpha$, and which vanishes for all other values of θ ; from equation (17) ϕ must be equal to this function when $r = 1$. Consequently we must have

$$\phi = f_0 + f_1 \cos\theta + \ldots + f_n \cos n\theta + \ldots, \, r = 1, \quad . \quad (21)$$

where

$$f_0 = \frac{C^2}{8\pi a^2} \left[\frac{1}{2} \sin 2\alpha - \alpha \cos 2\alpha \right],$$

and generally

$$f_n = \frac{(-1)^n}{n} \frac{C^2}{4\pi a^2} \left[\frac{\sin(n-2)\alpha}{n-2} - \frac{\sin(n+2)\alpha}{n+2} \right], \, n = 1, 2, 3, \ldots,$$

$$. \quad . \quad (22)$$

the first term in the bracket being α when $n = 2$.

It is still easier to calculate the coefficients c of § 4. When $r = 1$,

$$y = c_0 + c_1 \cos\theta + c_2 \cos 2\theta + \ldots,$$

and to a first approximation (in which the values of y on the

projection can be assumed zero) the boundary values of
y are given by

$$y = -\frac{C\pi}{2a}, \quad -\frac{\pi}{2} < \theta < \frac{\pi}{2}, \quad \ldots \quad (23)$$

$$= 0, \quad \frac{\pi}{2} < \theta < \frac{3\pi}{2}. \quad \ldots \ldots \quad (24)$$

All that is needed is the expansion of this function as a
cosine series. Approximately then the coefficients c with
even suffixes vanish and

$$c_{2n+1} = \frac{(-1)^{n+1}}{2n+1}\frac{C}{a}. \quad \ldots \ldots \quad (25)$$

The effect of these approximations is that terms of the
second and higher powers of α are ignored.

7. Inserting the values of the coefficients c and d given
by equations (18), (19), and (25) in expression (13), we
arrive at a series of functions ϕ_1, ϕ_3, ... given by

$$\frac{a\phi_1}{C} = r^2 - \frac{\cos 2\theta}{3}(r^4 - 2r^2)$$
$$+ \frac{\cos 4\theta}{5}\left(r^6 - \frac{3r^4}{2}\right) - \frac{\cos 6\theta}{7}\left(r^8 - \frac{4r^6}{3}\right) + \ldots,$$

$$\frac{a\phi_3}{C} = \cos 2\theta(r^4 - 2r^2)$$
$$- \frac{r^6}{3} + \frac{\cos 2\theta}{5}(r^8 - 4r^2) - \frac{\cos 4\theta}{7}\left(r^{10} - \frac{5r^4}{2}\right) + \ldots,$$

$$\frac{a\phi_5}{C} = \cos 4\theta\left(r^6 - \frac{3r^4}{2}\right)$$
$$- \frac{\cos 2\theta}{3}(r^8 - 4r^2) + \frac{r^{10}}{5} - \frac{\cos 2\theta}{7}(r^{12} - 6r^2) + \ldots,$$

and similar equations. These functions are biharmonic, but
do not satisfy the boundary condition (16), nor can they
be made to do so by the addition of harmonic functions.
However, it is clear that the functions $(\phi_1 + \phi_3)$, $(\phi_3 + \phi_5)$,
$(\phi_5 + \phi_7)$, ... do satisfy the condition. The difficulty does
not arise with the functions ϕ_2, ϕ_4, ϕ_6, ... which are given by

$$\frac{a\phi_2}{C} = \cos \theta(r^3 - 3r) - \frac{\cos \theta}{3}(r^5 - 5r)$$
$$+ \frac{\cos 3\theta}{5}\left(r^7 - \frac{7r^3}{3}\right) - \frac{\cos 5\theta}{7}\left(r^9 - \frac{9r^5}{5}\right) + \ldots,$$

$$\frac{a\phi_4}{C} = \cos 3\theta \left(r^5 - \frac{5r^3}{3} \right) - \frac{\cos\theta}{3}(r^7 - 7r)$$
$$+ \frac{\cos\theta}{5}(r^9 - 9r) - \frac{\cos 3\theta}{7}\left(r^{11} - \frac{11r^3}{3} \right) + \dots,$$

$$\frac{a\phi_6}{C} = \cos 5\theta \left(r^7 - \frac{7r^5}{5} \right) - \frac{\cos 3\theta}{3}\left(r^9 - \frac{9r^3}{3} \right)$$
$$+ \frac{\cos\theta}{5}(r^{11} - 11r) - \frac{\cos\theta}{7}(r^{13} - 13r) + \dots,$$

and similar equations; these functions are biharmonic and satisfy condition (16).

If then we assume for ϕ an expression of the form

$$\phi = A_1\phi_2 + A_2(\phi_1 + \phi_3) + A_3(\phi_2 + \phi_4) + A_4(\phi_3 + \phi_5) + \dots,$$

where the coefficients A are constant, the problem is reduced to finding the values of A_1, A_2, A_3, ..., so that

$$(\phi)_{r=1} = \sum_{n=0}^{\infty} f_n \cos n\theta. \quad \dots \quad (26)$$

It is easily seen that when $r = 1$

$$\frac{a\phi_2}{2C} = \left[-1 + \left(1 - \frac{1}{3} \right) \right]\cos\theta - \left(\frac{1}{3} - \frac{1}{5} \right)\cos 3\theta$$
$$+ \left(\frac{1}{5} - \frac{1}{7} \right)\cos 5\theta - \dots,$$

$$\frac{a(\phi_2 + \phi_4)}{2C} = -\left(\frac{1}{3} - \frac{1}{5} \right)\cos\theta + \left[-\frac{1}{3} + \left(\frac{1}{5} - \frac{1}{7} \right) \right]\cos 3\theta$$
$$- \left(\frac{1}{7} - \frac{1}{9} \right)\cos 5\theta + \dots,$$

$$\frac{a(\phi_1 + \phi_3)}{2C} = \frac{1}{1.3} - \left[\frac{1}{2} + \left(\frac{1}{3} - \frac{1}{5} \right) \right]\cos 2\theta + \left(\frac{1}{5} - \frac{1}{7} \right)\cos 4\theta$$
$$- \left(\frac{1}{7} - \frac{1}{9} \right)\cos 6\theta + \dots,$$

$$\frac{a(\phi_3 + \phi_5)}{2C} = -\frac{1}{3.5} + \left(\frac{1}{5} - \frac{1}{7} \right)\cos 2\theta - \left[\frac{1}{4} + \left(\frac{1}{7} - \frac{1}{9} \right) \right]\cos 4\theta$$
$$+ \left(\frac{1}{9} - \frac{1}{11} \right)\cos 6\theta - \dots,$$

Consequently the problem is formally solved if coefficients A_1, A_3, A_5, ... are found such that

$$\left[-1 + \left(1 - \frac{1}{3}\right)\right] A_1 - \left(\frac{1}{3} - \frac{1}{5}\right) A_3 + \left(\frac{1}{5} - \frac{1}{7}\right) A_5 - \ldots = \frac{af_1}{2C},$$

$$-\left(\frac{1}{3} - \frac{1}{5}\right) A_1 + \left[-\frac{1}{3} + \left(\frac{1}{5} - \frac{1}{7}\right)\right] A_3 - \left(\frac{1}{7} - \frac{1}{9}\right) A_5 + \ldots = \frac{af_3}{2C},$$

and coefficients A_2, A_4, A_6, ... such that

$$-\left[\frac{1}{2} + \left(\frac{1}{3} - \frac{1}{5}\right)\right] A_2 + \left(\frac{1}{5} - \frac{1}{7}\right) A_4 - \left(\frac{1}{7} - \frac{1}{9}\right) A_6 + \ldots = \frac{af_2}{2C},$$

$$\left(\frac{1}{5} - \frac{1}{7}\right) A_2 - \left[\frac{1}{4} + \left(\frac{1}{7} - \frac{1}{9}\right)\right] A_4 + \left(\frac{1}{9} - \frac{1}{11}\right) A_6 - \ldots = \frac{af_4}{2C},$$

and so on. The constant term on each side of equation (26) is ignored.

8. Before it can be concluded that the formal solution as obtained above does in fact satisfy the conditions of the problem some difficult questions of convergence must first be settled. But in practice there is no difficulty, for only a finite number of terms of the ϕ-series can be handled numerically, and it is a straightforward matter to estimate the extent to which such an expression for ϕ fails to satisfy the imposed conditions. A good deal of preliminary work showed that a reasonable approximation could be expected from the first fourteen terms of the series. We therefore write

$$\phi = A_1\phi_2 + \sum_{m=2}^{14} A_m(\phi_{m-1} + \phi_{m+1}), \qquad . \quad . \quad (27)$$

and choose A_1, A_2, ... so that the first fourteen of the equations of §7 are satisfied.

The problem has been completed numerically only in the case in which the angle α is 20°, the height of the projection being then rather more than one-tenth (0·113) of the breadth of the channel. To ensure that the projection exerts a pronounced influence on the fluid motion a value has been assigned to α that is somewhat large in view of the approximation of §6.

The values of the coefficients f_1, f_2, ... of equation (26) are given for $\alpha = 20°$ in the following table, in which

$$f_r' = \frac{4\pi a^2 f_r}{C^2}. \; . \cdot$$

TABLE I.

f_1'	$-·0533$	f_6'	$·0339$	f_{11}'	$-·0069$
f_2'	$·0514$	f_7'	$-·0281$	f_{12}'	$·0030$
f_3'	$-·0483$	f_8'	$·0223$	f_{13}'	$·0001$
f_4'	$·0443$	f_9'	$-·0167$	f_{14}'	$-·0023$
f_5'	$-·0394$	f_{10}' ...	$·0115$		

Solution of the equations of §7 then gives the values for A_1, A_2, ... shown in Table II., wherein

$$A_r' = \frac{8\pi a A_r}{C}.$$

TABLE II.

A_1'	$·1835$	A_6'	$-·1997$	A_{11}'	$·0285$
A_2'	$-·0920$	A_7'	$·1362$	A_{12}'	$-·0373$
A_3'	$·0552$	A_4'	$-·1810$	A_{13}'	$·0421$
A_4'	$-·1834$	A_9'	$·2036$	A_{14}'	$·0322$
A_5'	$·2689$	A_{10}'	$-·1135$		

9. The detailed working out of the stream-lines would be a difficult matter, and one which is in the present problem scarcely necessary, since the general pattern of the flow is obvious. The only detailed work that has been undertaken is consequently the evaluation of the stream-function ψ at points of the line EA, the continuation of the projection.

The functions ϕ_1, ϕ_2, ... are most easily evaluated in terms of the coordinates r, θ of the ζ-plane. The line of the projection corresponds to the real axis of the ζ-plane, and there is the following relation, derived from integration of equation (7), between the ordinates of points of EA and the corresponding values of r,

$$y = -\frac{C}{\sqrt{a^2-1}} \tan^{-1}\left(\frac{1+a^2t^2}{a^2-1}\right)^{1/2},$$

where

$$t = \frac{1+r}{1-r},$$

and negative values of r are assigned to points of the line $\theta = \pi$.

Setting $a = 20°$ in equation (8), we have $a^2 = 32·17$, whence the relation between y and r shown in Table III.

TABLE III.

r...	$-1\cdot00$	$-\cdot95$	$-\cdot90$	$-\cdot80$	$-\cdot50$	0
$-\sqrt{a^2-1}\,y/C$...	$\cdot1773$	$\cdot1791$	$\cdot1848$	$\cdot2086$	$\cdot3658$	$\cdot8009$

r...	$\cdot50$	$\cdot80$	$\cdot90$	$\cdot95$	$1\cdot00$
$-\sqrt{a^2-1}\,y/C$...	$1\cdot2543$	$1\cdot4619$	$1\cdot5190$	$1\cdot5456$	$1\cdot5708$

Table IV. shows the values of the functions ϕ for several values of r, θ being equal to π. To obtain the corresponding values when $\theta = 0$, such functions as $\phi_2 + \phi_4$ should be reversed in sign and such functions as $\phi_1 + \phi_3$ left unchanged. When $r = 0$ all the functions vanish.

TABLE IV.

	$r=1\cdot00$.	$r=\cdot95$.	$r=\cdot90$.	$r=\cdot80$.	$r=\cdot50$.
$a\phi_2/C$	$\cdot8584$	$\cdot8556$	$\cdot8472$	$\cdot8144$	$\cdot6022$
$a(\phi_1+\phi_3)/C$	$-\cdot5251$	$-\cdot5206$	$-\cdot5080$	$-\cdot4626$	$-\cdot2404$
$a(\phi_2+\phi_4)/C$	$\cdot8584$	$\cdot8513$	$\cdot8315$	$\cdot7633$	$\cdot4571$
$a(\phi_3+\phi_5)/C$	$-\cdot5584$	$-\cdot5492$	$-\cdot5248$	$-\cdot4472$	$-\cdot1754$
$a(\phi_4+\phi_6)/C$	$\cdot3251$	$\cdot3141$	$\cdot2864$	$\cdot2061$	$-\cdot0009$
$a(\phi_5+\phi_7)/C$	$-\cdot3156$	$-\cdot3028$	$-\cdot2719$	$-\cdot1892$	$-\cdot0179$
$a(\phi_6+\phi_8)/C$	$\cdot3251$	$\cdot3105$	$\cdot2770$	$\cdot1936$	$\cdot0475$
$a(\phi_7+\phi_9)/C$	$-\cdot2576$	$-\cdot2416$	$-\cdot2062$	$-\cdot1254$	$-\cdot0124$
$a(\phi_8+\phi_{10})/C$	$\cdot1981$	$\cdot1807$	$\cdot1440$	$\cdot0671$	$-\cdot0162$
$a(\phi_9+\phi_{11})/C$.........	$-\cdot1961$	$-\cdot1773$	$-\cdot1396$	$-\cdot0664$	$\cdot0008$
$a(\phi_{10}+\phi_{12})/C$	$\cdot1981$	$\cdot1781$	$\cdot1396$	$\cdot0705$	$\cdot0141$
$a(\phi_{11}+\phi_{13})/C$	$-\cdot1690$	$-\cdot1478$	$-\cdot1091$	$-\cdot0448$	$-\cdot0019$
$a(\phi_{12}+\phi_{14})/C$	$\cdot1421$	$\cdot1200$	$\cdot0812$	$\cdot0220$	$-\cdot0093$
$a(\phi_{13}+\phi_{15})/C$	$-\cdot1414$	$-\cdot1183$	$-\cdot0796$	$-\cdot0248$	$\cdot0008$

The corresponding values of ψ are tabulated below. A constant has been added to the values of ϕ given directly by equation (27) so that ψ may vanish when $r = -1$, that is, at the end of the projection.

TABLE V.

r...	$-1\cdot00$	$-\cdot95$	$-\cdot90$	$-\cdot80$	$-\cdot50$	0
$-8\pi a^2\psi/C^2$ ...	0	$\cdot0371$	$\cdot1387$	$\cdot5031$	$3\cdot1307$	$16\cdot499$

r...	$\cdot50$	$\cdot80$	$\cdot90$	$\cdot95$	$1\cdot00$
$-8\pi a^2\psi/C^2$ ...	$40\cdot749$	$55\cdot393$	$59\cdot816$	$61\cdot924$	$63\cdot965$

In fig. 4 is shown the relation between ψ and y, and, as a comparison, the relation between y and the stream-function, $-y^2$, of the undisturbed flow at great distance from the projection. About a quarter of the breadth b of the channel is covered by the figure; elsewhere on the section considered the influence of the projection is small, and the curves representing the two stream-functions are nearly coincident.

Fig. 4.

$$\psi = -y^2$$

The point of most interest in the figure is the fact that $\partial\psi/\partial y$ does not vanish when $y = -h$, which implies that there is a finite velocity of slip at the end of the projection; but there is no reason to suppose that this is merely a consequence of the approximations that have been made, for when $r = 1$ of the two conditions

$$\frac{\partial\psi}{\partial r} = 0, \quad \frac{\partial\psi}{\partial \nu} = 0,$$

the first implies the second at all points except those at which the modulus of the transformation $\left|\dfrac{d\zeta}{dz}\right|$ is infinite. The end E of the projection is from (7) one of these exceptional points, and this is the mathematical reason for the existence of the velocity of slip.

From a more general point of view it may be observed that such a velocity is not precluded by the generally accepted boundary condition governing the motion of viscous fluids; nor, in the problem of elasticity which corresponds to that of this paper, is the fact that a thin plane plate ABCFG, clamped on the edge CDEF, is actually inclined at E contrary to the usual definition of a clamped edge; for the ideas of velocity of slip and of clamping alike presuppose a boundary with finite curvature and a definite normal, while at E the boundary has no definite normal. These remarks evidently apply only to a sharp internal corner; with an external corner no difficulty of this kind arises.

10. It is not necessary to examine in the general case the convergence of the process of §7; for consider the function

$$\psi = -y^2 + \phi, \quad \ldots \ldots \quad (28)$$

where ϕ is given by (27) and is therefore the sum of a finite number of the functions $\phi_1, \phi_2, \ldots$ The expression is biharmonic, and its derivative satisfies the boundary condition, but it does not itself exactly attain the required values on the boundary. It is convenient to write (28) in the equivalent form

$$\psi = [-y^2 + f(\theta)] + [\phi - f(\theta)],$$

where

$$f(\theta) = \overset{\infty}{\underset{0}{\Sigma}} f_n \cos n\theta.$$

The term in the first bracket attains the correct boundary values, so that the boundary values of the term in the second bracket represent the error in the expression for ψ. The function ϕ has been chosen so that there are no terms in $\cos\theta$, $\cos 2\theta$, ... or $\cos 14\theta$ in $\phi - f(\theta)$, which therefore consists first of the difference between $f(\theta)$ and the first 15 terms of its expansion as a Fourier series, and then of the terms in $\cos 15\theta$, $\cos 16\theta$, ... in ϕ. But these last terms are very small: the coefficient of $\cos 15\theta$ in ϕ is

$$-\frac{C^2}{8\pi a^2}(\cdot 005),$$

the coefficient of $\cos 16\theta$ still smaller, while the successive coefficients are on the whole decreasing. We can conclude that the error arises almost entirely from the replacement of $f(\theta)$ by the first 15 terms of the series, and is quite small.

The errors introduced by the assumption that h/b is small are ignored in the preceding remarks; these are more difficult to assess, since it is one of the consequences of this assumption that the functions ϕ_1, ϕ_2, ... are not exactly biharmonic. But the magnitudes of these errors depend merely on the value assigned to α, the whole assumption being, moreover, avoidable. This matter has therefore no bearing on the general question of the practical difficulty of applying this analysis to such problems as those mentioned in §1. In those problems the important thing is to decide whether eddies do or do not exist—to determine, that is to say, the general character of the fluid motion; no great accuracy is demanded. The work of this paper is enough to show that questions of this kind can be answered by Love's method of analysis without special difficulty.

L. *An X-ray Investigation of the Crystals of o-Azotoluene.* *By* Mata Prasad, *D.Sc.,* and K. V. Desai, *M.Sc.*[*]

THE crystals of azo-benzene

$$(\langle\ \ \rangle-N=N-\langle\ \ \rangle)$$

have been studied by Prasad (Phil. Mag. x. p. 306 (1930)), who found that they belong to the space group C_{2h}^5 and that the unit cell contains four molecules, contrary to the results of Becker and Jancke (*Zeit. Phys. Chem.* xcix. p. 242 (1921)). He further found that there exists nearly complete symmetry about the $(20\bar{1})$ plane both in respect to the geometrical relation and to the intensities of reflexions by corresponding planes.

o-Azotoluene,

$$(\langle\ \overset{CH_3}{\underset{|}{\ }}\ \rangle-N=N-\langle\ \overset{CH_3}{\underset{|}{\ }}\ \rangle),$$

is similar to azobenzene except for the two methyl groups attached to the benzene rings in an ortho-position to the nitrogen atoms. Also the crystals of azobenzene and *o*-azotoluene belong to the monoclinic prismatic class of

* Communicated by Sir W. H. Bragg, O.M., K.B.E., M.A., F.R.S.

crystals. An X-ray examination of the crystals of *o*-azotoluene was, therefore, undertaken to determine if they bear any structural identity with the crystals of azobenzene.

The crystals of *o*-azotoluene were prepared by the slow evaporation of its solution in alcohol. The *c*(001) face is a prominent face; other faces found to develop are *r*(40$\bar{1}$), *p*(111) and *o*(11$\bar{1}$). The axial ratios found by crystallographers are

$$a:b:c \ :: \ 2.2254:1:1.7077$$
$$\text{and} \ \angle\beta = 101°4'$$

(*cf.* Groth, *Chemische Krystallographie*, v. p. 65).

The crystals were examined by the rotating crystal method. With a Shearer tube fitted with a copper anti-cathode and a Universal Photogoniometer, designed by J. D. Bernal and manufactured by W. G. Pye & Co., Cambridge, the rotation photographs about the *a* and *b* axes were taken, and the lengths of these axes were calculated. Assuming $\angle\beta$ to be 101°4' (Groth's value), the length of the *c* axis was determined from (002) and (004) planes, which appeared as very strong spots on both the *a* and *b* rotation photographs.

The dimensions of the unit cell were thus found to be

$$a = 13.93 \text{ Å.U.}, \quad b = 6.604 \text{ Å.U.}, \quad c = 14.55 \text{ Å.U.}$$

The axial ratios are

$$a:b:c \ :: \ 2.109:1:2.204.$$

The various reflecting planes were identified from the oscillation photographs taken about *a* and *b* axes at intervals of 15 degrees. The indices of the planes, corresponding to the spots which appeared on the oscillation photographs, were worked out by Bernal's method of analysis (Proc. Roy. Soc. A, cxiii. p. 117 (1926)). Tables I. and II. give the indices of the planes observed together with a rough idea of their relative intensities. The intensities of the spots were evaluated by eye-estimation in the same way as described by Prasad (*loc. cit.*) and the same symbols have been used.

Table I. shows that the planes (*h0l*) are halved when *h* is odd and (*0kl*) are halved when *k* is odd. Also (010) is halved. These halvings correspond to the space group C_{2h}^5 and Γm lattice.

The number of the molecules in the unit cell required by the space group is four; the number of the molecules calculated from the dimensions of the unit cell and the

density of the crystal being also four, the molecules in the unit cell are asymmetric. The elements of symmetry of the unit cell are, in accordance with the space group, a glide

TABLE I.

Axial planes.	(*hol*) planes.	(*okl*) planes.	(*hko*) planes
020 m.s.	201 v.w.	021 m.s.	110 m.s.
002 v.s.	203 m.s.	022 w.	130 w.
004 v.s.	20$\bar{2}$ v.s.	023 w.	220 s.
005 w.	20$\bar{3}$ s.	024 m.s.	310 m.s.
007 w.	20$\bar{4}$ s.	025 m.s.	330 m.s.
200 v.s.	20$\bar{5}$ m.s.	026 w.	420 w.
400 v.w.	20$\bar{6}$ w.		510 w.
600 w.	401 m.s.		710 w.
	403 m.s.		
	40$\bar{2}$ s.		
	40$\bar{5}$ w.		
	40$\bar{6}$ w.		
	60$\bar{1}$ m.s.		

TABLE II.

111 w.	215 w.	311 w.	411 m.s.	511 w.
112 v.s.	21$\bar{4}$ v.s.	312 w.	41$\bar{2}$ v.w.	512 m.s.
113 v.s.	221 m.s.	313 w.	41$\bar{4}$ v.w.	513 w.
114 m.s.	22$\bar{2}$ w.	314 m.s.	41$\bar{5}$ m.s.	514 m.s.
115 w.	223 m.s.	31$\bar{1}$ w.	41$\bar{6}$ m.s.	51$\bar{1}$ w.
116 w.	224 w.	31$\bar{2}$ m.s.	421 v.w.	51$\bar{2}$ w.
11$\bar{1}$ m.s.	225 w.	31$\bar{3}$ m.s.	422 w.	51$\bar{4}$ w.
11$\bar{2}$ s.	226 v.w.	31$\bar{4}$ m.s.	423 w.	51$\bar{7}$ w.
11$\bar{3}$ v.s.	22$\bar{1}$ s.	32$\bar{4}$ w.	424 w.	52$\bar{3}$ v.w.
11$\bar{4}$ v.s.	22$\bar{2}$ m.s.	32$\bar{5}$ w.	42$\bar{1}$ w.	62$\bar{3}$ v.w.
11$\bar{5}$ s.	22$\bar{3}$ w.	32$\bar{6}$ w.	42$\bar{2}$ w.	71$\bar{4}$ v.w.
11$\bar{6}$ w.	22$\bar{4}$ w.	331 w.	42$\bar{3}$ w.	
11$\bar{7}$ v.w.	22$\bar{5}$ w.	332 w.	42$\bar{5}$ m.s.	
12$\bar{3}$ m.s.	22$\bar{6}$ w.	333 w.	42$\bar{6}$ m.s.	
12$\bar{4}$ m.s.	22$\bar{7}$ w.		43$\bar{3}$ v.w.	
133 w.				
13$\bar{1}$ w.				

plane of symmetry parallel to the (*ac*) face and a screw axis parallel to *b* axis (*cf.* Astbury and Yardley, Phil. Trans. A, ccxxiv. pp. 221–257).

These results show that the crystals of azobenzene and *o*-azotoluene are identical in the following respects : (1) the

crystals belong to the space group C_{2h}^5 ; (2) the planes (*hol*) are halved if *h* is odd and (010) is also halved ; (3) the molecules in the unit cell are four and they are asymmetric; and (4) the value of $c \sin \beta$, *i. e.* the spacing of (001) planes is 14·29 Å. The same value of $c \sin \beta$ in the two crystals may indicate that the molecules in the unit cell lie with their length along the direction $c \sin \beta$; as the lengths of the molecules of the two substances, represented according to their chemical formula, are identical.

The crystals of *o*-azotoluene show no geometrical symmetry about the direction of ($20\bar{1}$) plane in (010) face. Table III. gives the strongly reflected planes referred to this direction as one of the coordinate axes and shows that the intensities of reflexion of the corresponding planes, *i.e.* of the ($h'k'l'$) and

TABLE III.

202 v.s.	$20\bar{2}$ v.s.	1113 w.	$111\bar{3}$ w.
204 v.w.	$20\bar{4}$ m.s.	222 s.	$22\bar{2}$ m.s.
208 m.s.	$20\bar{8}$ m.s.	224 m.s.	$22\bar{4}$ m.s.
406 m.s.	$40\bar{6}$ w.	226 w.	$22\bar{6}$ w.
111 m.s.	$11\bar{1}$ m.s.	228 m.s.	$22\bar{8}$ w.
113 w.	$11\bar{3}$ s.	2210 w.	$221\bar{0}$ w.
115 v.s.	$11\bar{5}$ v.s.	2212 w.	$221\bar{2}$ w.
117 v.s.	$11\bar{7}$ v.s.	311 w.	$31\bar{1}$ m.s.
119 m.s.	$11\bar{9}$ s.	313 m.s.	$31\bar{3}$ m.s.
1111 w.	$111\bar{1}$ w.	315 w.	$31\bar{5}$ m.s.

($h'k'\bar{l}'$) in the crystal of *o*-azotoluene, are not so completely identical as in that of azobenzene.

Summary.

The structure of crystals of *o*-azotoluene has been examined by the rotating crystal method. The dimensions of the unit cell are found to be

$$a = 13{\cdot}93 \text{ Å.U.}, \quad b = 6{\cdot}604 \text{ Å.U.}, \quad c = 14{\cdot}55 \text{ Å.U.}$$
$$\angle \beta = 101^{\circ}{\cdot}4'.$$

The cell contains four molecules. The crystal belongs to space group C_{2h}^5 and Γm lattice. No complete symmetry about ($20\bar{1}$) has been observed as in the case of azobenzene, but the value of $c \sin \beta$ in this crystal is the same as in that of azobenzene.

Chemistry Laboratory,
The Royal Institute of Science,
Bombay.

LI.—*On the Theory of Equations of State.* By T. S.
Wheeler, *Ph.D., F.R.C.Sc.I., F.I.C., Principal, Royal
Institute of Science, Bombay* *.

Summary.

A GENERAL expression for the work of dilution of a system
of charged particles in thermal equilibrium is deduced from
thermodynamic and dimensional considerations. Some
special applications of this expression are considered.

Notation.

$a =$ van der Waals's pressure constant.

$a', a_1',$ etc. $=$ constants for a given system of particles.

$B_{s+1} =$ the virial coefficient corresponding to V^{-s}.

$\overline{B}_L =$ the value of B_2, $(s = 1)$, calculated on the
Leiden system, multiplied by 10^4.

$\overline{B}_y =$ a constant for a given system of ions.

$b', b_1' =$ constants.

$c =$ concentration of a salt in gram-mols. per
litre.

$C', C, C_1, C_2 =$ constants occurring in the expressions for
virial coefficients.

$D =$ a function of a temperature-variable property
of the medium separating the particles.
(Dielectric constant.)

$e =$ a function of an intrinsic property (charge)
of each of the particles which is indepen-
dent of temperature.

$E =$ electrical internal energy change associated
with W.

$\overline{E} =$ value of E when D is independent of tempe-
rature.

$f, F =$ functions.

$G_{yz} =$ a constant for a given system of ions.

$g =$ osmotic coefficient.

$i =$ van't Hoff factor.

$k =$ Boltzmann's constant.

$k_2 =$ constant.

$m =$ number of ions in a molecule.

$m =$ index expressing the variation of a force with inverse distance.

$n =$ index expressing the variation of a force with inverse distance.

$N =$ total number of particles in volume V.

$N_y =$ number of particles of the yth kind in volume V.

$N =$ number of molecules in 1 gram-mol.

$p =$ pressure.

$q =$ constant $(= 3\gamma)$.

$r =$ distance between two particles.

$s =$ index of V.

$T =$ absolute temperature.

$\bar{U} =$ mutual potential of the particles.

$V =$ volume containing N particles.

$W =$ electrical work of dilution.

$w =$ Debye and Hückel's valency factor.

$w_y =$ valency of the yth kind of ion.

x refers to one of the forces between a particle of the yth and a particle of the zth kind.

$\alpha, \beta, \gamma, \delta =$ constants.

$\theta =$ deviation of osmotic coefficient $= (1-g)$.

$\lambda, \mu =$ force coefficients.

$\sigma =$ diameter of a particle.

$\phi =$ function equivalent to W.

Introduction.

IN a recent paper[1] the author has shown that for a dilute solution of a salt yielding small ions the electrical work done by the interionic forces can be expressed as the product of a potential energy corresponding to the law of force specified, multiplied by a sum of a series, each term of which consists of a power of the ratio of the potential energy to a thermal kinetic energy.

In this paper an attempt is made to generalize somewhat this result and to consider some particular applications of it.

The System of Particles Considered.

We consider a volume V containing at temperature T and pressure p N small spherically symmetrical gaseous

particles. There are i kinds of these particles present, and N is given by

$$N = N_1 + N_2 + N_3 + \dots N_y \dots N_z \dots N_i. \quad \dots \quad (1)$$

Each particle is present in sufficient numbers to permit of statistical treatment.

We assume that the xth of the separate forces between a particle of the yth kind and a particle of the zth kind at a distance r from each other can be expressed by

$$f_{yz,x}(r) = \lambda_{yz,x}/r^{n_{yz,x}} = e_{yz,x}/(\mathrm{D}.r^{n_{yz,x}}), \quad \dots \quad (2)$$

where e is a function of an intrinsic property of each of the particles which is independent of temperature and D is a function of a temperature-variable property of the medium separating the particles.

The Electrical Work of Expansion.

We define the " electrical " work of expansion W as the work done by the forces between the particles when the gaseous system is reversibly and isothermally expanded to infinity [*].

If $W_{yz,xr}$ is the electrical work done by the xth force between a particle of the yth kind and a particle of the zth kind at an initial distance r from each other, then the total work done by the xth forces between all the yz pairs is given by

$$W_{yz,x} = \sum_r W_{yz,xr}. \quad \dots \dots \quad (3)$$

The work done by the total forces between all the yz pairs is given by

$$W_{yz} = \sum_x W_{yz,x}. \quad \dots \dots \quad (4)$$

The total electrical work is given by

$$W = \sum_y \sum_z W_{yz} = \sum_y \sum_z \sum_x \sum_r W_{yz,xr}, \quad \dots \quad (5)$$

the summation being taken over all pairs in the usual manner. It is convenient in what follows to replace the suffix yz,x by a dash, for example, $W_{yz,x}$ is written W'.

The General Form of the Work Function.

We *assume* that we can put

$$W' = \phi(\bar{e}', D, T, V) = \phi', \quad \dots \dots \quad (6)$$

---

[*] It is assumed that it is unnecessary formally to distinguish between expansion at constant volume and at constant pressure [2].

where $\bar{e}'$ is a function of all the e properties (charges) and involves e' in some special manner.

W will be the sum of a number of ϕ functions; we have, in fact, ((4), (5)),

$$W = \underset{y \; z \; r}{\Sigma\Sigma\Sigma} \phi' = \bar{\Sigma}\phi',$$

where $\bar{\Sigma}$ is equivalent to

$$\underset{y \; z \; x}{\Sigma\Sigma\Sigma}. \qquad \ldots \ldots \quad (7)$$

We can apply to ϕ' considerations similar to those applied to the work function in the simpler case previously discussed [1].

We have :—

1. ϕ' must vanish when V is indefinitely increased.

2. ϕ' must vanish when D is indefinitely increased.

3. ϕ' must vanish when e' vanishes.

4. The general charging and discharging process described by Debye [3] enables us to write

$$pV = NkT - V(\delta W/\delta V)_{T, D} \quad \ldots \ldots \quad (8)$$

$$= NkT - V\bar{\Sigma}(\delta\phi'/\delta V)_{T, D}, \quad \ldots \quad (9)$$

and to deduce that $V(\delta\phi'/\delta V)_{T, D}$ has the dimensions of energy.

5. Writing

$$-E/T^2 = (\delta(W/T)\delta T)_V = \bar{\Sigma}(\delta(\phi'/T)/\delta T)_V, \quad . \quad (10)$$

we can deduce that $T(\delta\phi'/\delta T)_{V, D}$ must have the dimensions of energy, since the expansion of (10) gives

$$E = \Sigma\left[[\phi' - T(\delta\phi'/\delta T)_{V, D}]\left[1 - \frac{T(\delta\phi'/\delta D)_{V, T}(\delta D/\delta T)_V}{\phi' - T(\delta\phi'/\delta T)_{V, D}}\right]\right].$$
$$\ldots \quad (11)$$

6. Employing the general method which Bjerrum [4] applied to two particles attracting according to the inverse square law, it can readily be shown that

$$[1 + (T/D)(\delta D/\delta T)_V]$$

must be a factor of E and E′.

Hence from (11)

$$D(\delta\phi'/\delta D)_{V, T} = -\phi' + T(\delta\phi'/\delta T)_{V, D}. \quad . \quad (12)$$

Consequently $D(\delta\phi'/\delta D)_{V, T}$ must have the dimensions of energy.

We can satisfy the six conditions set out above if we put

$$\phi' = a_1' T^{\alpha_1'} D^{\beta_1'} V\gamma_1' e'^{\delta_1'} + a_2' T^{\alpha_2'} D^{\beta_2'} V\gamma_2' e'^{\delta_2'} + . \quad (13)$$

$$= \Sigma a_1' T^{\alpha_1'} D^{\beta_1'} V\gamma_1' e'^{\delta_1'}, \quad . . . . . . (14)$$

where a_1', a_2', etc. are such functions of all the "charges" that they do not become infinite when e' vanishes, and α_1', β_1', γ_1' δ_1', etc. are constants of which the β' and γ' constants are negative and the δ' constants are positive.

The Relations between the Indices occurring in ϕ'.—The relations between the α', β', γ', and δ' constants can be deduced in a manner similar to that previously described for the simpler case then considered [1]; the treatment is modified in that the Clausius virial equation is here directly applied.

From (12) it follows that

$$\beta_1' = \alpha_1' - 1 \; ; \; \beta_2' = \alpha_2' - 1 \; ; \; \text{etc.} \quad . . (15)$$

The Clausius virial equation, assumed to be valid for the system considered, is

$$pV = NkT + (1/3)\Sigma\Sigma\Sigma rf'(r). \quad . . . (16)$$

From (2)

$$\Sigma\Sigma rf'(r) = (e'/D)\Sigma\Sigma(1/r^{n'-1}). \quad . . . (17)$$

The mutual potential of the particles at a given instant as regards the xth force between the yth and the zth particles is given by

$$U' = -(e'/D)\Sigma\Sigma \int_x^r (1/r^n)dr \quad . . . . (18)$$

$$= (e'/D)(1/(n'-1))\Sigma\Sigma(1/r^{n'-1}). \quad . . (19)$$

When D is independent of temperature this mutual potential is equal to the internal energy of the solution corresponding to the force under consideration ($\bar{E}'$), so that from (11), (14), (19), and (17) we have

$$\bar{E}' = \phi'\Sigma(1 - \alpha_1') = \bar{U}' = (1/(n'-1))\Sigma\Sigma rf'(r). \quad (20)$$

and (16) becomes

$$pV = NkT + (1/3)\bar{\Sigma}(n'-1)\phi'\Sigma(1 - \alpha_1'). \quad . (21)$$

From (9) and (14)

$$pV = NkT - \Sigma\phi'\Sigma\gamma_1'. \quad . . . . (22)$$

From (15), (21), and (22) we can deduce relations between α', β', and γ', which enable us to write

$$\phi' = \Sigma a_1' T^{1+3\gamma_1'/(n'-1)} D^{3\gamma_1'/(n'-1)} V\gamma_1' e'^{\delta_1'}. \quad . (23)$$

If now we put

$$\delta_1' = -3\gamma_1'/(n'-1), \quad \ldots \quad (24)$$

we can write (23)

$$\phi' = \frac{e'}{\mathrm{D} \mathrm{V}^{(n'-1)/3}} \sum b_1' \left(\frac{e'}{\mathrm{D} \mathrm{V}^{(n'-1)/3}(k\mathrm{T})}\right)^{-1-(3\gamma_1'/(n'-1))} \quad (25)$$

by a suitable choice of the b' constants.

The right-hand side of (25) is of the form of a static potential energy corresponding to the law of force under consideration, multiplied by a series, each term of which consists of a power of the ratio of the static potential energy to a kinetic energy. Since this expression is of the correct energy dimensions, the b' constants will be of zero dimensions in energy, and will contain expressions involving only the particle charges, the numbers of the various kinds of particles, and pure numerical constants, *e.g.*, π.

If we put $q_1' = 3\gamma_1'$, $q_2' = 3\gamma_2'$, etc. where the q constants are always negative, we can write (23)

$$\phi' = \Sigma a_1'(e'/\mathrm{D})^{-q_1'/(n'-1)} \mathrm{T}^{1+(q_1'/(n'-1))} \mathrm{V}^{q_1'/3} \quad . \quad (26)$$

$$= \Sigma a_1' \lambda'^{-q_1'/(n'-1)} \mathrm{T}^{1+(q_1'/(n-1))} \mathrm{V}^{q_1'/3}, \quad . \quad (27)$$

and

$$\mathrm{W} = \Sigma \Sigma a_1' \lambda'^{-q_1'/(n'-1)} \mathrm{T}^{1+(q_1'/(n'-1))} \mathrm{V}^{q_1'/3}. \quad . \quad (28)$$

We may now consider some applications of the general expression given in (28).

Solutions of Strong Electrolytes with Small Ions.

Putting $n' = 2$ and $\lambda' = w_y w_z e^2/\mathrm{D}$, where w_y is the valency of the yth kind of ion, and assuming that ϕ' is a one-termed function, we have, if q_1' is put arbitrarily equal to $-3/2$,

$$\phi' = a'(w_y w_z e^2/\mathrm{D})^{3/2} \mathrm{T}^{-1/2} \mathrm{V}^{-1/2}. \quad . \quad . \quad (29)$$

And if ϕ'' is the dilution work evolved by the electrical forces between the yth kind of ions and all the ions in the solution we can write

$$\phi'' = \mathrm{B}_y(e^2/\mathrm{D})^{3/2} \mathrm{T}^{-1/2} \mathrm{V}^{-1/2} (\mathrm{G}_{y1} + \mathrm{G}_{y2} + \ldots + \mathrm{G}_{yz} + \ldots + \mathrm{G}_{yi}),$$
$$\ldots \quad (30)$$

where B, G_{y1}, etc. are functions of numerical constants such as π, of the valencies of the various ions and the number of ions present. B_y will contain $k^{-1/2}$ as a factor

(see (25)), and the various functions will also be related by equations of the type

$$\bar{B}_y G_{yz} = a'(w_y w_z)^{3/2}. \quad . \quad . \quad . \quad . \quad (31)$$

Debye's [5] actual expression for ϕ'' is given by

$$\phi'' = \frac{-2\pi^{1/2} w_y^2 N_y}{3k^{1/2}} \left(\frac{e^2}{D}\right)^{3/2} T^{-1/2} V^{-1/2} (\Sigma N_1 w_1^2)^{1/2}, \quad (32)$$

to which ϕ'' is equivalent if we put

$$\bar{B}_y = (-2\pi^{1/2}/3)(w_y^2 N_y/k^{1/2}), \quad . \quad . \quad . \quad (33)$$

and

$$\Sigma G_{y1} = (\Sigma N_1 w_1^2)^{1/2}. \quad . \quad . \quad . \quad . \quad (34)$$

It will be seen that ΣG_{y1} is independent of y. It was by their brilliant use of the Poisson equation that Debye and Hückel were able to express the work function for one kind of ion as a function of the properties and numbers of that kind of ion, and a separate function of the properties of the solution as a whole, which did not involve the properties of the one kind of ion in any special fashion.

We will return later to the case of ions with a definite radius.

Potential of Crystal Lattices.

To obtain the work function for a uniform system in which the ions have no thermal motion we make the index of T in (28) equal to zero wherever it occurs.

The expressions for the work function corresponding to each force then reduce each to one term, since there is only one possible value for each q index. For example, in (26)

$$q_1' = q_2' = q_3' = \ldots = -(n'-1), \quad . \quad . \quad (35)$$

so that (26) becomes

$$\phi' = a'(e'/D) V^{-(n'-1)3}, \quad . \quad . \quad . \quad (36)$$

and (28) may be written

$$W = \bar{\Sigma} a'(e'/D) V^{-(n'-1)3}, \quad . \quad . \quad . \quad (37)$$

which is the general expression for the work function, and in this case for the potential function (*cf.* (20), d_1' etc. $= 0$), of a crystal lattice.

The Gaseous Equation of State.

From (8) and (28) we have

$$pV = NkT - \bar{\Sigma}\Sigma(q_1'/3)a_1'\lambda'^{-q_1'/(n'-1)} T^{1+(q'_1/(n'-1))} V^{q_1'/3}, \quad (38)$$

which is the general form of the equation of state.

We can derive from this equation expressions for the related functions g, i, etc. in the manner described in the previous paper [1].

We can also deduce expressions for the various virial coefficients [6]; these we will now consider.

We have

$$pV = NkT(1 + B_2/V + \ldots + B_{s+1}/V^s + \ldots, \quad (39)$$

where B_{s+1} is the virial coefficient corresponding to V^{-s}.

Putting $q_1'/3 = -s$, we have from (38)

$$B_{s+1} = \Sigma\, C'(e'/D)^{3s/(n'-1)}T^{-3s/(n'-1)} \quad . \quad . \quad (40)$$

$$= \Sigma\, C'(\lambda'/T)^{3s/(n'-1)}, \quad . \quad . \quad . \quad . \quad (41)$$

C' will contain expressions involving the particle charges, and the numbers of the various kinds of particles.

Debye's result for W with small ions (see (32)) corresponds to $s+1 = 3/2$.

From (41), if the particles are all of one kind, with a force given by λ/r^n between each pair, the second virial coefficient B_2 is given by

$$B_2 = C\left(\frac{\lambda}{T}\right)^{3/(n-1)} \quad . \quad . \quad . \quad . \quad (42)$$

Jeans' expression for the second virial coefficient (repulsive force) in this case can be written [7]

$$B_2 = (2\pi/3)N(\lambda/(n-1)\,kT)^{3/(n-1)}\,\Gamma((n-4)/(n-1)). \quad (43)$$

so that

$$C = (2\pi/3)N(1/(n-1)\,k)^{3/(n-1)}\,\Gamma((n-4)/(n-1)). \quad (43')$$

If the particles are all of one kind, with forces given by λ/r^n and μ/r^m between them, (41) gives

$$B_2 = C_1(\lambda/T)^{3/(n-1)} + C_2(\mu/T)^{3/(m-1)}. \quad . \quad . \quad (44)$$

No assumption is made as regards the signs of λ and μ, which will depend on the direction of the forces.

The expression developed by Lennard-Jones [7] for B_2 in the case under consideration is of the form

$$B_2 = K_2((\lambda/T)(T/\mu))^{3/(n-m)}\,F[(\mu/T)(T/\lambda)^{(m-1)/(n-1)}], \quad (45)$$

where the function F consists of the sum of a series of powers of the expression involved. λ here corresponds to a repulsive, and μ to an attractive force. In this expression the effect of each force is not separated; whether it will ever be possible to develop a method of analysis which

will give an expression of the type of (44) with definite values for C_1 and C_2 remains to be seen.

As an example of the utilization of (44) Table I. shows the application of the equation

$$\overline{B}_L = 78\cdot2/T^{3/(21-1)}-11{,}200/T^{3/(4-1)}, \quad . \quad . \quad (46)$$

that is,

$$\overline{B}_L = 78\cdot2/T^{\cdot15}-11{,}200/T, \quad . \quad . \quad . \quad . \quad (47)$$

to the calculation of the second virial coefficient of argon. ($\overline{B}_L$ is the value of B_2 calculated on the Leiden system [8] multiplied by 10^4.)

TABLE I.

Second Virial Coefficient of Argon [9].

Temperature ° C.	Log $\overline{B}_L$ observed.	Log B_L calculated (47).
−121·21	1·57 (n) *	1·57 (n)
−120·24	1·56 (n)	1·56 (n)
−119·2	1·56 (n)	1·56 (n)
−115·86	1·55 (n)	1·54 (n)
−113·8	1·53 (n)	1·53 (n)
−109·88	1·51 (n)	1·51 (n)
−102·51	1·46 (n)	1·47 (n)
−87·05	1·38 (n)	1·39 (n)
−57·72	1·22 (n)	1·23 (n)
0	·87 (n)	·86 (n)
20·39	·75 (n)	·68 (n)

* (n) indicates that $\overline{B}_L$ is negative and that the log $-\overline{B}_L$ is given.

As will be clear from (46), the value of n, the index for the repulsive force, is 21, and of m, the index for the attractive force, is 4 (*cf.* (51)).

Lennard-Jones[10] found that values for $(n;m)$ of $(14\cdot3;5)$, $(21;5)$, and $(25;5)$ gave satisfactory results with (45). (44) appears to be more sensitive than (45) to variations in the values of n and m. An expression of this form may therefore be of use in the determination of the values of these indices.

The van der Waals Equation.

If in (44) we take λ/r^n as a repulsive force, and observe that a rigid spherical particle corresponds to the repulsive force λ/r^n when $n \to \infty$, the diameter being given by

$$\underset{n \to \infty}{\text{Lt.}} \quad \lambda^{1/(n-1)} = \sigma \; [11], \quad . \quad . \quad . \quad . \quad (48)$$

we obtain
$$B_2 = C_1\sigma^3 + C_2(\mu/T)^{3/(m-1)} *. \quad . \quad . \quad . \quad (49)$$

Now van der Waals's equation can be written, ignoring virial coefficients higher than the second,
$$pV = NkT\left[1 + \frac{(2/3)\pi\sigma^3 N}{V} - \frac{a}{VNkT}\right]. \quad . \quad (50)$$

Hence B_2 from (50) is given by
$$B_2 = (2/3)\pi\sigma^3 N - a/(NkT), \quad . \quad . \quad . \quad (51)$$

which is equivalent in form to (49) if $m = 4$.

Van der Waals's cohesive force can thus be regarded as varying as the inverse fourth power of the distance [12].

Solutions of Strong Electrolytes with Ions of Finite Size.

If in (28) we assume that all the particles have the diameter σ, and if we represent this condition by making one of the n indices infinite as in (48), we can write (28)
$$W = \overline{\Sigma}\Sigma a_1' \lambda'^{-q_1'(n'-1)}T^{1+(q_1'/(n'-1))}V^{q_1'/3} + \Sigma a_1\sigma^{-q_1}TV^{q_1/3};$$
$$\quad . \quad . \quad (52)$$

(38) then becomes
$$pV = NkT - \overline{\Sigma}\Sigma(q_1'/3)a_1'\lambda'^{-q_1'(n'-1)}T^{1+(q_1'/(n'-1))}V^{q_1'/3}$$
$$- \Sigma(a_1q_1/3)\sigma^{-q_1}TV^{q_1/3}. \quad . \quad . \quad . \quad (53)$$

If we put $q_1 = -3$, $a_1 = (2/3)\pi N^2 k$, and suppress the Σ sign, the correction for the size of the ions in (53) becomes similar to the van der Waals correction given in (50).

Inserting as a first approximation Debye and Hückel's value for the electrical work of dilution and the van der Waals values for a_1 and q_1, (53) becomes (*cf.* (32))
$$pV = NkT - \Sigma\left(\frac{\pi^{1\,2}w_y^2 N_y}{3k^{1/2}}\left(\frac{e^2}{D}\right)^{3/2}T^{-1/2}V^{-1/2}\right)\left(\Sigma N_1 w_1^2\right)^{1/2}$$
$$+ (2/3)\pi N^2 k\sigma^3 TV^{-1}. \quad . \quad . \quad . \quad (54)$$

We assume now that we are dealing with 1 gram-mol. of a salt which yields $\overline{m}$ ions per molecule, so that we can put
$$N = \overline{m}\overline{N}, \quad . \quad . \quad . \quad . \quad (55)$$

where $\overline{N}$ is the number of molecules in 1 gram-mol.

If now
$$pV = g\overline{m}\overline{N}kT, \quad . \quad . \quad . \quad . \quad (56)$$

* Keesom's [13] value for B_2 in this case is related to (45)..

comparing (54) and (56) we can write (for $T = 273 \cdot 1^\circ$)

$$\theta = 1 - g = [\cdot 263 w \sqrt{mc}] - (2/3)\pi \bar{m}\bar{N}\sigma^3\bar{c}\, 10^{-3}, \quad (57)$$

where $\bar{c}$ is the concentration of the salts in gram-mols. per litre, and w is Debye and Hückel's valency factor. (For the calculation of the term in square brackets see Debye and Hückel [14].)

From (57)

$$\sigma = \left[\frac{\cdot 263 w \sqrt{mc} - \theta}{(2/3)\pi \, \overline{mc}\bar{N}\, 10^{-3}} \right]^{1 \cdot 3} \quad \ldots \quad (58)$$

$$= \left[\frac{7 \cdot 876 \times 10^{-22}}{\sqrt{mc}}\left(\cdot 263 w - \frac{\theta}{\sqrt{mc}} \right) \right]^{1 \cdot 3} \ldots \quad (59)$$

As an example of the application of (59) we take values for potassium sulphate given by Debye and Hückel [14].

TABLE II.

w for potassium sulphate $= 2\sqrt{2}$.

$\sqrt{mc}$.	θ observed.	$\sigma \times 10^8$ (cm.) calculated from (59).
·0906	·0647	6·3
·110	·0729	8·3
·136	·0776	9·9
·176	·101	9·1
·229	·128	8·6
·280	·147	8·5
·369	·178	8·2
·516	·220	7·9
·600	·238	7·7

The values of σ obtained are larger than the value calculated by Debye and Hückel ($2 \cdot 7 \times 10^{-8}$ cm.), but they are of the right order and show the approximate validity of (54). No great accuracy can be expected, since the values inserted for the second and third terms in the general equation (53) can only be regarded as first approximations to the correct values.

References.

(1) Wheeler, *Phys. Zeit.* xxxii. p. 674 (1931).
(2) Gatty, Phil. Mag. (7) xi. p. 1082 (1931); Scatchard, J. Amer. Chem. Soc. liii. p. 2037 (1931).
(3) Debye, *Phys. Zeit.* xxv. p. 98 (1924); Fowler, Trans. Faraday Soc. xxiii. p. 440 (1927) ; 'Statistical Mechanics,' pp. 197, 319 (1929).

(4) Bjerrum, *Zeit. Phys. Chem.* cxix. p. 150 (1926).
(5) Debye, *loc. cit.* p. 99.
(6) Kamerlingh-Onnes, Proc. Sect. Sciences, Amsterdam, iv. p. 125 (1902).
(7) See Lennard-Jones, Proc. Roy. Soc. cvi. A, p. 466 (1924).
(8) Lennard-Jones, 'Statistical Mechanics' (Fowler), p. 220 (1929).
(9) Kamerlingh-Onnes and Crommelin, Com. Phys. Lab. Leiden, no. 118 B, p. 24 (1910); Lennard-Jones, Proc. Roy Soc. cvi. A, p. 470 (1924).
(10) Lennard-Jones, *loc. cit.* p. 469.
(11) Lennard-Jones, *loc. cit.* p. 452.
(12) *Cf.* Keesom, Com. Phys. Lab. Leiden, Supp. no. 26, p. 4 (1912).
(13) Keesom, *loc. cit.*, Supp. no. 24 B, p. 32 (1912); Lennard-Jones, *loc. cit.* p. 467.
(14) Debye and Hückel, *Phys. Zeit.* xxiv. p. 200 (1923); Fowler, 'Statistical Mechanics,' p. 321 (1929).

LII. *The Equations of Motion of a Viscous Fluid.*
By J. Prescott, *M.A., D.Sc.*[*]

AFTER searching in several places for a simple and at the same time satisfying proof of the equations of viscous flow, I felt that there was room for another one. In some books the writers borrow all the fundamental equations of elasticity, and then deduce those of viscous flow by an analogy which they do not prove to exist. Other writers, and these the best, produce very good proofs with rather a greater call on mathematics than is necessary. Still others use more doubtful methods than the analogy with elasticity. Even Stokes's proof, which has the great merit of starting from one physical assumption, has the drawback that few people would be willing to grant the truth of this physical assumption.

My object in this paper is to derive the equations of viscous flow by easy logical steps from the simplest physical assumption that we know about the subject, and one that can be tested quite easily. This assumption is the law of viscosity in the simplest case of all—that of laminar flow.

In the general case of flow of a fluid the particle which is at the point (x, y, z) at time t has component velocities u, v, w, which may be functions of x, y, z, and t. We get the simplest case of laminar flow if we take

$$u = f(z), \quad v = 0, \quad w = 0.$$

This means that all the particles which are in a plane perpendicular to the z-axis move with the same velocity parallel to

the x-axis. This velocity u is, of course, different in different planes, or there would be no relative motion and no viscous flow.

Our one physical assumption, apart from the laws of mechanics, is that the friction per unit area between two planes of particles separated by the geometrical plane at z s proportional to the velocity gradient $\frac{\partial u}{\partial z}$—that is, the frictional drag, in the direction δx, of the upper plane on the lower plane across an element of area δA perpendicular to the z-axis at the point (x, y, z), is

$$\delta F = \mu \frac{\partial u}{\partial z} \delta A,$$

where μ is a constant, called the coefficient of viscosity. The friction per unit area is therefore

$$f = \mu \frac{\partial u}{\partial z}. \quad \ldots \quad \ldots \quad (1)$$

Now let us consider what is happening to a rectangular element $\delta x \times \delta y \times \delta z$, at the point (x, y, z), due to the motion we are considering, on the assumption that $f(z)$ is a function increasing as z increases. (This last assumption leads to the same equations as the contrary assumption.)

In consequence of the difference of velocities at z and $(z + \delta z)$ the rectangle $\delta x \times \delta z$ is changing into a parallelogram. Suppose the line of particles which was along δz at time t has turned through a small angle $d\theta$ in a further interval dt; then, since the relative velocity of the two opposite faces at z and $(z + \delta z)$ is $\frac{\partial u}{\partial z} \delta z$, it follows that the relative displacement in time dt is

$$\left(\frac{\partial u}{\partial z} \delta z \right) dt = \delta z \times d\theta,$$

from which

$$\frac{\partial u}{\partial z} = \frac{\partial \theta}{\partial t}.$$

If we write ϕ for the angle inside the parallelogram (fig. 1) we see that

$$\frac{\partial \theta}{\partial t} = - \frac{\partial \phi}{\partial t},$$
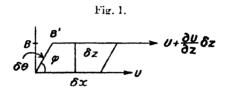
and so

$$\frac{\partial u}{\partial z} = - \frac{\partial \phi}{\partial t}.$$

Consequently the frictional drag per unit area is
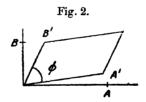
$$f = -\mu \frac{\partial \phi}{\partial t}. \qquad \dots \qquad (2)$$

We shall now turn to the general case where u, v, w, are all functions of x, y, z, t, and shall find the equations of motion which are consistent with (2).

Fig. 1.

We have a further assumption to make, but one about the truth of which there is no doubt : it is that the viscous drag depends on the relative motion of the parts of the liquid, and not at all on any uniform translation or bodily rotation, in which there is no relative motion.

When neither u nor w is zero we must still suppose that the relative *slip* of the two planes of particles at z is $-\dfrac{\partial \phi}{\partial t}$, ϕ being the angle inside the parallelogram in fig. 1. Actually

Fig. 2.

the true displacement is now shown in fig. 2, since all the sides of the parallelogram rotate.

It is easy to show in this case that

$$-\frac{\partial \phi}{\partial t} = \frac{\partial u}{\partial z} + \frac{\partial w}{\partial x}.$$

If the component velocity v exists at the same time it will be granted that this will have no effect on the component drag in any plane perpendicular to v. Therefore we conclude that
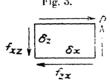
the frictional drag per unit area, in the *x*-direction, on a plane perpendicular to the *z*-axis, is

$$f_{zx} = -\mu \frac{\partial \phi}{\partial t}$$

$$= \mu \left(\frac{\partial u}{\partial z} + \frac{\partial w}{\partial x} \right). \quad \ldots \ldots (3)$$

This equation is the natural and logical extension of (1) to the general case of flow.

If we interchange *z* and *x* in (3), and consequently *w* and *v*, we get, for the frictional drag in the *z*-direction per unit of area perpendicular to the *x*-axis.

$$f_{xz} = \mu \left(\frac{\partial w}{\partial x} + \frac{\partial u}{\partial z} \right)$$

$$= f_{zx}. \quad \ldots \ldots \ldots \ldots (4)$$

Fig. 3.

The result $f_{xz} = f_{zx}$ is the same relation as for shear stresses in elasticity, and could be proved by statics, as is usual in the subject of elasticity. The statical proof consists in taking moments about the point D for the equilibrium of the element shown in fig. 3. The normal forces are left out of the figure ; when these are taken into account it will be found that their contribution to the moment equation is a quantity of smaller order than the contribution of the frictions. The moment equation is therefore

$$(f_{xz} \delta z \, \delta y) \, \delta x = (f_{zx} \delta x \, \delta y) \times \delta z,$$

from which

$$f_{xz} = f_{zx}. \quad \ldots \ldots \ldots (5)$$

This last result, deduced from statics, affords a verification of (3) ; for from (1) we may surely assume that, when *w* is not zero,

$$f_{zx} = \mu \frac{\partial u}{\partial x} + s_1, \quad \ldots \ldots (6)$$

where s_1 is something depending on w. From this last equation we get, by interchanging the axes of x and z,

$$f_{xz} = \mu \frac{\partial w}{\partial x} + s_2, \quad \ldots \ldots \quad (7)$$
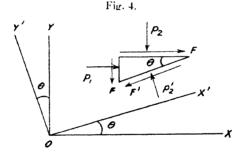
where s_2 similarly depends on u.

Since $f_{zx} = f_{xz}$ by (5), the simplest, though not perhaps the only, conclusion from (6) and (7), is that

$$f_{zx} = \mu \left(\frac{\partial u}{\partial z} + \frac{\partial w}{\partial x} \right).$$

All our assumptions, taken together, are completely expressed in the typical equation

$$f_{xy} = f_{yx} = \mu \left(\frac{\partial u}{\partial y} + \frac{\partial v}{\partial x} \right), \quad \ldots \ldots \quad (8)$$

where μ is a constant called the coefficient of viscosity.

Fig. 4.

So far we have found no connexion between the normal pressures on the faces and the viscosity. We shall next show that (8) and the two corresponding equations will give us all we seek.

Let p_1, p_2, p_3, be the normal pressures in the liquid at the point x, y, z, in the direction OX, OY, OZ. We shall find that these are, as a rule, unequal in a viscous fluid. It is only in a frictionless fluid that the pressure at a point is the same in every direction.

Let us consider the stresses on faces which are perpendicular to a set of rectangular axes OX', OY', OZ, the axes OX' and OY' making an angle θ with the old axes OX and OY respectively, while OZ is the same in both sets of axes. We shall write F for f_{xy}.

2 S 2

Let p_1', p_2', and $f_{x'y'}$ (for which we shall write F') be the stresses relative to the new axes which correspond to p_1, p_2, and F relative to the old axes. The pressure p_3 is, of course, the same for both sets of axes. Also let u' and v' be the component velocities relative to the new axes corresponding to u and v relative to the old. For shortness we shall write l and m for $\cos\theta$ and $\sin\theta$.

Now since

$$\frac{F}{\mu} = \frac{\partial u}{\partial y} + \frac{\partial v}{\partial x},$$

it follows that

$$\frac{F'}{\mu} = \frac{\partial u'}{\partial y'} + \frac{\partial v'}{\partial x'};$$

but

$$u' = lu + mv, \qquad v' = lv - mu,$$
$$x = lx' - my', \qquad y = ly' + mx',$$

from which

$$\delta u' = \frac{\partial u'}{\partial x}\delta x + \frac{\partial u'}{\partial y}\delta y$$
$$= \frac{\partial u'}{\partial x}(l\delta x' - m\delta y') + \frac{\partial u'}{\partial y}(l\delta y' + m\delta x').$$

Therefore

$$\frac{\partial u'}{\partial y'} = -m\frac{\partial u'}{\partial x} + l\frac{\partial u'}{\partial y}$$
$$= -m\left(l\frac{\partial u}{\partial x} + m\frac{\partial v}{\partial x}\right) + l\left(l\frac{\partial u}{\partial y} + m\frac{\partial v}{\partial y}\right)$$
$$= l^2\frac{\partial u}{\partial y} - m^2\frac{\partial v}{\partial x} + lm\left(\frac{\partial v}{\partial y} - \frac{\partial u}{\partial x}\right). \quad \cdots \quad (9)$$

Similarly

$$\frac{\partial v'}{\partial x'} = l^2\frac{\partial v}{\partial x} - m^2\frac{\partial u}{\partial y} + lm\left(\frac{\partial v}{\partial y} - \frac{\partial u}{\partial x}\right). \quad \cdots \quad (10)$$

Consequently

$$\frac{F'}{\mu} = (l^2 - m^2)\left(\frac{\partial u}{\partial y} + \frac{\partial v}{\partial x}\right) + 2lm\left(\frac{\partial v}{\partial y} - \frac{\partial u}{\partial x}\right)$$
$$= (l^2 - m^2)\frac{F}{\mu} + 2lm\left(\frac{\partial v}{\partial y} - \frac{\partial u}{\partial x}\right). \quad \cdots \quad (11)$$

Again, if A denotes the area of that face of the triangular prism in fig. 4 on which F' acts, then the areas of the other faces are lA and mA. Consequently, by resolving the forces

which act on the prism in the direction of F′ we get, after division by A,

$$F' = (lF + mp_1)\cos\theta - (mF + lp_2)\sin\theta$$
$$= (l^2 - m^2)F + lm(p_1 - p_2). \quad\quad\quad (12)$$

In equations (11) and (12) we have got two expressions for F′ which must be identical for all values of θ, and therefore for all possible values of *lm*. By equating the coefficients of *lm* in the two values of F′ we find *

$$p_1 - p_2 = 2\mu\left(\frac{\partial v}{\partial y} - \frac{\partial u}{\partial x}\right), \quad\quad\quad (13)$$

whence

$$p_1 + 2\mu\frac{\partial u}{\partial x} = p_2 + 2\mu\frac{\partial v}{\partial y}.$$

By rotating the axes about OY instead of about OZ we should have found

$$p_1 + 2\mu\frac{\partial u}{\partial x} = p_3 + 2\mu\frac{\partial w}{\partial z}.$$

Let Q be written for each of the quantities such as $p_1 + 2\mu\dfrac{\partial u}{\partial x}$, that is,

$$Q = p_1 + 2\mu\frac{\partial u}{\partial x} = p_2 + 2\mu\frac{\partial v}{\partial y} = p_3 + 2\mu\frac{\partial w}{\partial z}; \quad (14)$$

then

$$3Q = p_1 + p_2 + p_3 + 2\mu\Delta, \quad\quad\quad (15)$$

where

$$\Delta = \frac{\partial u}{\partial x} + \frac{\partial v}{\partial y} + \frac{\partial w}{\partial z}, \quad\quad\quad (16)$$

which can be proved to be the rate at which the density of the fluid at (x, y, z) is decreasing divided by the density at that point—that is, if ρ is the density,

$$\Delta = -\frac{1}{\rho}\frac{d\rho}{dt}. \quad\quad\quad (17)$$

Next, by resolving the forces on the triangular prism in the direction of p_2', we find

$$p_2' = (lF + mp_1)\sin\theta + (mF + lp_2)\cos\theta$$
$$= l^2p_2 + m^2p_1 + 2lmF. \quad\quad\quad (18)$$

In like manner we could prove that

$$p_1' = l^2p_1 + m^2p_2 - 2lmF \quad\quad\quad (19)$$

* Or merely by puttin $\theta = 45°$, so that $l = m$, we get the same result.

Therefore

$$p_1' + p_2' = (l^2 + m^2)(p_1 + p_2)$$

$$= p_1 + p_2. \quad \cdots \quad \cdots \quad (20)$$

Consequently, since p_3' is the same as p_3,

$$p_1' + p_2' + p_3' = p_1 + p_2 + p_3. \quad \cdots \quad (21)$$

Now, as we can bring the axes into any possible directions by three successive rotations about three lines, say about OZ, then about OX', and next about the new axis OY'', and as the relation (21) would persist after each rotation, it is clear that this relation is true for all rectangular axes.

Let us now put

$$3p = p_1 + p_2 + p_3, \quad \cdots \quad \cdots \quad (22)$$

so that p denotes the arithmetic mean of the normal pressures in three perpendicular directions at the point (x, y, z). Then equation (15) gives

$$Q = p + \tfrac{2}{3}\mu\Delta. \quad \cdots \quad \cdots \quad (23)$$

and therefore

$$p_1 = Q - 2\mu \frac{\partial u}{\partial x}$$

$$= p + \tfrac{2}{3}\mu\Delta - 2\mu \frac{\partial u}{\partial x}, \quad \cdots \quad (24)$$

with similar expressions for the other two component pressures.

Since Δ and p have the same values for all sets of rectangular axes, it should be observed that the same is true also for Q.

The completion of the problem from this point—that is, the derivation of the dynamical equations—is much the same in all books. Since the rest is quite short, we may as well complete the proof here.

Let α_x denote the x-component acceleration of the particle of fluid which is at (x, y, z) at time t. This same particle will be at the point $x + u\delta t$, $y + v\delta t$, $z + w\delta t$, at time $t + \delta t$. If, then,

$$u = F(x, y, z, t), \quad \cdots \quad \cdots \quad (25)$$

and if Δu is the increase of the velocity of this particular particle in the interval δt, then

$$u + \Delta u = F(x + u\delta t, y + v\delta t, z + w\delta t, t + \delta t)$$
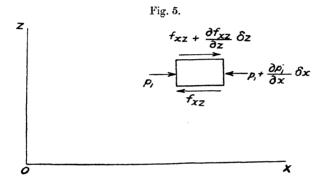
$$= F(x, y, z, t) + u\delta t \frac{\partial u}{\partial x} + v\delta t \frac{\partial u}{\partial y} + w\delta t \frac{\partial u}{\partial z} + \delta t \frac{\partial u}{\partial t}.$$

Consequently

$$\alpha_x = \lim \frac{\Delta u}{\delta t}$$

$$= u\frac{\partial u}{\partial x} + v\frac{\partial u}{\partial y} + w\frac{\partial u}{\partial z} + \frac{\partial u}{\partial t} \quad \cdots \quad (26)$$

Now let us consider the motion of an element of fluid of dimensions $\delta x . \delta y . \delta z$ of density ρ under the action of a force which has components X, Y, Z, per unit mass. Fig. 5 shows all the stresses in the x-direction except the frictions of the type f_{xy}, and these can be inferred from the other pair of frictions shown in the figure.

Fig. 5.

Resolving in the direction OX, we get

$$(\rho\,\delta x\,\delta y\,\delta z)\alpha_x = (\rho\,\delta x\,\delta y\,\delta z)X + \delta x\,\delta y\left(\frac{\partial f_{xz}}{\partial z}\delta z\right)$$

$$+ \delta x\,\delta z\left(\frac{\partial f_{xy}}{\partial y}\delta y\right) - \delta y\,\delta z\left(\frac{\partial p_1}{\partial x}\delta x\right),$$

from which

$$\rho(\alpha_x - X) = \frac{\partial f_{zx}}{\partial z} + \frac{\partial f_{xy}}{\partial y} - \frac{\partial p_1}{\partial x} \quad \cdots \quad (27)$$

The substitution of the values of the stresses from equations (8) and (24) in this last equation gives

$$\frac{\partial p_1}{\partial x} - \mu\left(\nabla^2 u + \frac{1}{3}\frac{\partial\Delta}{\partial x}\right) = -\rho(\alpha_x - X). \quad \cdots \quad (28)$$

Two similar equations are got by resolving in the directions of the other two axes. These three are the equations of viscous flow of a fluid.

College of Technology,
    Manchester.

LIII. *The Effect of Surface Changes on the Photoelectric Emission of Silver and Gold. By* T. E. CLARKE, *B.Sc., University College, Nottingham* *.

A GREAT deal of work has been done on the effect of "outgassing" on the photoelectric properties of various metals ; something has also been done on the effect on the photoelectric emission caused by alterations in the physical state of the metal. Yet no attention appears to have been paid to the possibility that the observed effects may be due to the two causes acting jointly.

The present work was undertaken to investigate the changes in photoelectric emission, produced by alternately straining and annealing a metal ; and to determine how far the observed changes were due to physical change of the metal itself and how far to changes in the adsorbed gas layer on the metal surface. We use the word strain to indicate the state of the metal surface after being mechanically polished by rubbing with a polished steel surface.

Beilby † has shown that a thin $(50\,\mu\text{-}500\,\mu)$ modified layer (vitreous layer) can be produced on the surface of an annealed metal by polishing, and that this layer returns to the original state on heating to a certain temperature. This fact has been used ‡ to explain an increase in photoelectric sensitivity observed on polishing a metal in air at a pressure of 10^{-3} mm. Hg.

The Photoelectric Cell.

This consists of a cylindrical glass vessel, A, about a foot long, closed at one end by a glass disk having an optically worked quartz window, C, at its centre, and at the other end by a glass-stopper-like arrangement, B, which is made to fit into A by means of a large vacuum-tight ground-joint. The glass disk and window C are attached by means of hard wax seals. The part B carries two stout copper leads which pass out through two copper-glass joints H, O, and support across their inner extremities (*i. e.*, the ends projecting into the main part A) the thin metal strip P constituting the cathode. This strip is screwed down to the ends of the two leads by means of small screws tapped axially into them, and is held taut by a spring, J, fixed

between the two leads and insulated from one of them
by a glass sleeve. The anode consists of a shallow copper
cylinder, G, supported rigidly in the centre of the cell
on a stout copper rod which passes out of the cell through
a copper-glass joint on the side-tube, D. A large copper
cylinder, F, completely screens the anode G except near
the cathode P, where a circular aperture in the screen
admits the electrons from the cathode. The lead from the
screen F passes through the side-tube and copper-glass
joint E. Parallel slits cut in the ends of the two cylinders
F and G serve to define a narrow beam of the ultra-violet
light which enters through the quartz window. A constant
beam is incident on the cathode strip, since constant
parallelism of the slits is ensured by fixing the outer
cylinder F firmly by means of phosphor-bronze spring-
clips. The firmness of the inner cylinder G is maintained
by its stout supporting rod. The leakage path from the
cathode to the anode is very large, and is further increased
by the glass sleeve K projecting into the cell from the
ground-joint. The dotted circle round the cathode strip
in fig. 1 *a* indicates another side-tube M of wider diameter
which enters the main tube perpendicular to the plane of
fig. 1 *a*, carrying the polishing lever N. This section of the
cell is shown in plan in fig. 1 *b*.

By means of a large copper-glass joint a flexible metal
tube, I, of the type used for "vacuum levers"* is fitted
as an extension to the side-tube as shown in fig. 1 *b*. A thick
steel rod N (4 mm. diam.) passes through into the cell,
the outer end being soldered to the outer end of the flexible
tube and the inner end, which is highly polished, resting
on the cathode strip. Thus, by up and down movements
of the flexible tube the polished steel end can be moved
to and fro over the strip, at the same time sufficient pressure
being exerted to produce a polish. In this manner the
metal is polished *in vacuo* without any scratching or tearing
of the surface and without introducing any complicated
and troublesome mechanism.

Experimental Arrangement.

The tube L is connected to the pumping system and
vapour-trap, and to a McLeod gauge. The pump used is a
Gaede two-stage steel diffusion-pump backed by a "Hyvac,"
and the pumping speed is 2500 c.c. per sec. with a backing
pressure of only 2 mm. ; thus it may be expected to deal

---

* Brose and Keyston, Journ. Sci. Instr. i. p. 19 (1930).

effectively with any vapours given off within the system. The outer half of the ground-joint is greased with Leybold's stiff "Ramsayfett."

The anode lead is carried directly through a short, wide, brass tube, which is earthed, to a quadrant electrometer situated close to the cell. The capacity of the system is thus kept at a small value, so that the rate of deflexion for a given current is as large as possible. The "time of

Fig. 1 *a*.
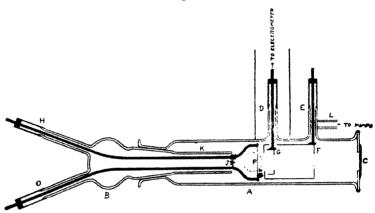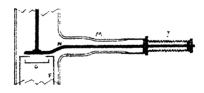
Fig. 1 *b*.
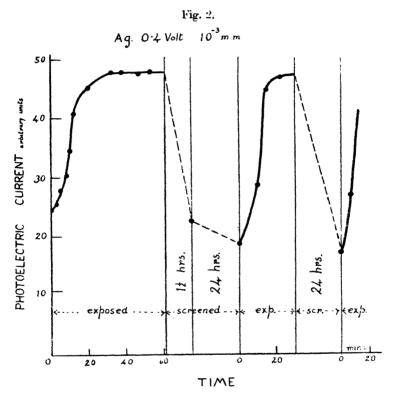
deflexion" method was used in measuring the photoelectric current, the cathode P being maintained at a negative potential, and the screen F at a smaller negative potential, so that the emitted electrons are collected on G and so charge up the electrometer.

A quartz mercury-vapour-lamp in an earthed metal housing is used as the source of U.V. radiation, the full radiation being used. It is found necessary to connect a variable resistance in series with the lamp, so that slight changes occurring in the electricity supply can be compensated for. The ends of the cathode strip are

connected by way of the copper-glass joints to a battery
of large storage cells which provide the 25 amps. or so
necessary to raise the strips of silver and gold to red heat.

Procedure and Results.

Since the specimen had of necessity to be illuminated
for a short time at intervals during the course of an

Fig. 2.

experiment, for the purpose of measuring the emission,
the possibility of the occurrence of so-called "fatigue"
effects was not overlooked. Accordingly a preliminary
series of experiments was undertaken to investigate how
the photoelectric emission for silver and gold was influenced
by continued exposure to ultra-violet light.

The variation of current with time of exposure was
observed (1) when the current was saturated (-30 volts
on cathode), and (2) when there was practically no acceler-
ating potential ($-0\cdot4$ volts on cathode). In the second

case, *i. e.*, for unaccelerated emission, at a pressure of 10^{-3} mm., the current increased rapidly at first, and reached a maximum, which was twice the initial value, in about 40 minutes. On screening the source of light the emission gradually resumed its original value in about 90 minutes. At a pressure of 10^{-6} mm. Hg. no such increase occurred, and at both pressures the saturated current showed no appreciable change on continued exposure of the metal to ultra-violet light.

At this point it is worthy of note that, in the case of unaccelerated emission at a pressure of 10^{-3} mm., the first " recovery" value of the current was appreciably lower than the initial value, and after a second exposure and rest the second " recovery " value was lower than the first but to a less marked degree : this is seen from fig. 2. It thus appears that, although there is a negative " fatigue " while the metal is exposed, there is also a small resultant positive " fatigue."

It was concluded that the " fatigue " observed at relatively high pressure was due in some way to the presence of adsorbed gas, and that the adsorbed gas still present at 10^{-6} mm. was inoperative in producing " fatigue." This eliminates one possible cause of change in sensitivity in the next series of observations.

We now go on to the investigation of the effect of heat treatment and subsequent polishing, and to the separation of the effect due to physical change in the metal from secondary effects due to adsorbed gas.

The metal strip cathode was highly polished by means of fine emery cloth, pumice powder, and opticians' rouge, thoroughly washed in benzene, and then placed in the apparatus. The latter was quickly exhausted and heated, together with connecting tubing etc., until the pump maintained a constant pressure of the order of 10^{-6} mm. Hg. Now the work of Werner [*] shows that when the pressure is maintained at a low value there is an increase in emission up to a constant value, consistent with the assumption that the adsorbed gas layer is gradually diminished in thickness to a limiting value. Accordingly the pumps were allowed to run for several hours under constant conditions before any readings were taken. Current measurements taken at intervals during this time of standing confirmed Werner's results, showing a regular increase with time up to a constant value. It was thus reasonable to assume that,

* J. Werner, *Zeit. für. Phys.* lxvii. p. 211 (1931).
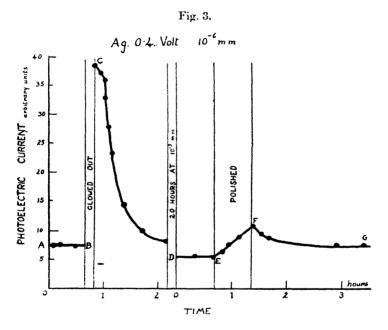
after a sufficient time of standing under the same vacuum
conditions, a residual gas layer existed in a state of equi-
librium at the surface of the metal. Having reached a
stable state in which the photoelectric emission remained
constant, the problem then was to investigate the effect
of annealing the metal, assuming it to be originally in
the polished or strained state. The cathode was heated
to the point of redness for four minutes, after which the
heating current was slowly decreased to zero. During this
heating a positive restraining potential of 30 volts was
applied to the strip to prevent any thermionic emission.
Measurements of the photoelectric current were taken at
intervals from the time at which the heating current was
switched off, and the time at which each measurement was
taken was noted. When the variation with time became small
the apparatus was left for a period of 20 hours, the pressure
being 10^{-3} mm., after which the pressure was again reduced
to 10^{-6} mm. and the same conditions as at the beginning
were maintained for an hour. After this time the readings
had become constant. The annealed strip was then polished
in vacuo, the emission being measured at intervals during
the process, and was finally allowed to stand under exactly
the same conditions as before. The emission again assumed
a constant value.

Explanation of Curves.

Fig. 3 is a graphical representation of the complete
cycle for silver. The part AB represents the constant
emission for the polished metal under equilibrium conditions
(stable adsorbed gas layer at 10^{-6} mm.). Heating the
strip produces a sudden increase in emission to the value
at C. This may be the resultant effect due to a change
in the metal and also in the adsorbed gas layer. The effect
of standing with the pressure at 10^{-6} mm. is shown by
the fall from C to D, which is attributed to a return of
gas to the surface of the silver. After 20 hours standing
at 10^{-3} mm. and subsequent evacuation at 10^{-6} mm. for
an hour a constant value, represented by DE, is attained.
Now, since the vacuum conditions leading up to the point
A have been repeated before the point D of the cycle, it
is reasonable to assume that the stable adsorbed gas layer
is the same at both points : this assumption is justified by
subsequent results. Then the difference between the
ordinates of AB and DE must be entirely due to a
change in the primary emission, *i. e.*, to a change in

the metal itself due to annealing. The ordinate of AB represents the emission for the polished metal and that of DE the emission for the annealed metal.
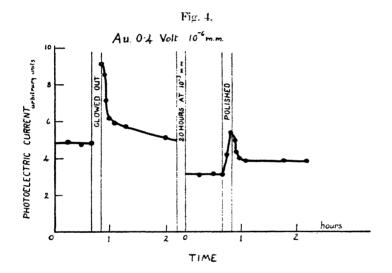
The part EF of the curve shows the effect of re-polishing *in vacuo* and indicates a roughly linear increase in emission with time of polishing, up to a maximum at F. Now, after standing to allow complete re-formation of the disturbed gas layer, a constant value is again reached at G, and the fact that the value of emission at G is approximately the

Fig. 3.

same as that for the polished metal at A shows that the conditions prevailing at A have been repeated at G. This strengthens our assumption that the surface gas always returns to the same extent, under the same pressure conditions, provided that sufficient time is allowed for a state of equilibrium to be established.

The second peak, F, in the curve, brought about by re-polishing, is also explained in the same way as that due to heating, *i.e.*, it is due both to a change in state of the metal itself and to a removal of gas from the surface by the polishing process. In standing this gas ultimately returns to its former stable condition.

Fig. 4 represents a similar cycle for gold. This shows the same characteristics as the curve for silver, although in this case the re-polishing has not quite brought the emission up to the initial value for polished gold. There is, however, quite a definite change in the emission accompanying the change from the annealed to the polished state. The slight discrepancy is probably due to the fact that the same degree of polish as that existing initially, was not quite obtained by means of the polished steel cylinder. This is borne out by the fact that subsequent annealing and polishing *in vacuo* produced repetition of the lower value.

Fig. 4.

Au. 0·4 Volt 10⁻⁶ m.m.

Saturation Current Experiments.

Observations have also been made on the saturation current, the procedure being the same as for the unaccelerated emission. The results show no effects similar to those described above, which may be attributed to changes in the adsorbed gas layer, but there is a marked increase in sensitivity on polishing and a decrease of the same magnitude on annealing.

Conclusion.

It is apparent from this work that the photoelectric emission of a metal, in the absence of a strong accelerating field, can be used as an indicator of changes occurring in the adsorbed gas layer on the surface of the metal.

The probable explanation is that, since under these con-ditions the emitted electrons will have energies ranging from a very small value up to a maximum, a change in depth of the adsorbed gas layer will produce a corre-sponding change in the proportion of slower electrons restrained by the layer. Such a change will have very little effect on the saturated emis-ion, owing to the higher energy of the electrons. The saturation current is, in fact, only affected by an alteration in the true contact potential (and therefore in the long wave limit) : since no " gas " effects occur in the saturation current experiments, it is apparent that the removal of adsorbed gas in the manner described has no effect on the contact potential, while the polishing and annealing processes alter it to a definite extent which can be repeated.

An investigation of the behaviour of the long wave limit under the above conditions is desirable, and it is intended to carry on the work in this direction for a series of metals.

In conclusion, I wish to express my thanks to Professor P. E. Shaw for facilities provided for this work and for valuable advice during the course of the experiments.

LIV. *Some Properties of Porous Building Materials.*— Part III. *A Theory of the Absorption and Transmission of Water by Porous Bodies. By* E. MADGWICK, *M.C., M.Sc., Ph.D.*[*]

Introduction.

THIS section is concerned with an elucidation of the laws governing the flow of water in porous bodies under certain conditions, and the expression of those laws in terms of definite physical constants which can be determined experi-mentally. The flow is always considered to take place from a plane surface of the material, initially dry, and to proceed in a direction normal to the surface. It may occur under the action of capillary or applied forces, or both. Capillary forces are always operative when absorption is proceeding ; transmission is due solely to applied forces. Three cases of practical importance will be considered :—

    (*a*) Entering surface horizontal, the direction of flow being vertically downwards. Absorption is assisted

by a head of water equal to the depth of penetration added to the pressure (if any) which is applied at the surface ; when the water flows through the material the capillary forces are no longer effective.

(*b*) Absorption from a horizontal surface, the flow being vertically upwards. The absorption is retarded by a head of water equal to the height of penetration, and proceeds until the opposing forces are equal.

(*c*) Absorption from a vertical surface, the flow being horizontal. If the surface in question is that of a wall the absorption is generally due to capillarity only, but may be assisted to some slight extent by wind pressure ; if it forms the side of a tank filled with water the pressure arising from the head of water will also be of consequence.

The porosity has been defined as the volume of water which is absorbed by unit volume of the material under the experimental conditions to be described. Although experiments on some specimens are completed within the short space of an hour, it has been found that very little further absorption takes place over a much longer period ; and it is probable that the amount of water which is absorbed under these conditions approximates closely to that which is absorbed in the course of the slow immersion test of Hirschwald or the four days' immersion test of Kreüger.

The Fundamental Equation.

In deriving the fundamental equation we shall take the case of vertically downward flow. Let the pressure at the surface of the material be gh, i. e., that due to a head of h centimetres of water, and consider the conditions for equilibrium at the moment the depth of penetration is x. The applied pressure is then $gh + gx$. For unit area of cross-section of the material let α be the total area of cross-section of the pores normal to the direction of flow, and β the sum of their perimeters. Then the force due to the applied pressure is $(gh + gx)\alpha$ per unit area, and that due to capillarity is $\beta T \cos \theta$, where T is the surface tension and θ the angle of contact. Thus the force assisting the motion is

$$(gh + gx)\alpha + \beta T \cos \theta \text{ per unit area.}$$

Assume that the resistance to flow is proportional to the

average velocity—which is proportional to the rate of penetration $\frac{dx}{dt}$. It will be proportional also to the average length of the path of the water within the material, and this is proportional to the depth of penetration x. The force resisting the motion is then $C'x\frac{dx}{dt}$, where C' is a constant for the material, and the total force per unit area is

$$(gh + gx)\alpha + \beta \mathrm{T}\cos\theta - C' \cdot x\frac{dx}{dt}.$$

This is equal to the rate of change of momentum of the water contained within a prism of the material of unit cross-section and height x. Let the porosity be B. The mass of this water is Bx and its average velocity is $k\frac{dx}{dt}$, where k is a constant; hence the rate of change of momentum is

$$\frac{d}{dt}\left(\mathrm{B}kx\frac{dx}{dt}\right).$$

Thus
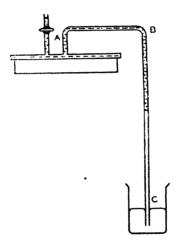
$$gh + gx + \frac{\beta \mathrm{T}\cos\theta}{\alpha} - \frac{C'}{\alpha}\cdot x\frac{dx}{dt} = \frac{\mathrm{B}k}{\alpha}\cdot\frac{d}{dt}\left(x\frac{dx}{dt}\right).$$

$\frac{\beta \mathrm{T}\cos\theta}{\alpha}$ can be written gh', i. e., capillarity is in effect equivalent to a head h' of water. Hence, writing also $\frac{C'}{\alpha} = C$,

$$gh + gx + gh' - cx\frac{dx}{dt} = \frac{\mathrm{B}k}{\alpha}\cdot\frac{d}{dt}\left(x\frac{dx}{dt}\right).$$

The term on the right-hand side of this equation can be neglected if it is small in comparison with $gh + gx + gh'$. To get some idea of the order of magnitude of h' the arrangement shown in the accompanying figure was used. The specimen was fixed to a brass cap of the type which is employed for the air permeability and water absorption tests, and the space enclosed by the specimen and the cap, together with the tube A B C, was filled with water. After the lapse of a few minutes the end C of the tube was allowed to dip into mercury, so that as water was absorbed by the specimen mercury was drawn up the tube to a height which remained steady for some time. It was found that the absorption of water was then accompanied by the withdrawal of air, a result which is to be

anticipated from the following considerations. In consequence of the rise of mercury in the vertical tube there is applied to the stone a definite negative pressure which opposes the flow. If all the pores were similar this pressure would increase until it just balanced the capillary forces, and would give a direct measure of h'. But since the pores vary in size and shape, a state of affairs is reached such that the capillary forces in the finer pores are sufficient, but those in the larger pores insufficient, to overcome the opposing pressure. Thus the value of the pressure which is measured in this way is a property of the largest pores and is less than the average value gh' as defined above. Expressed in centimetres of water it is always large compared with unity and

often equal to several hundreds. Thus gh' is great compared with 1000. Now $\dfrac{B}{\alpha}$ and k are greater than unity, but of that order of magnitude; they each, in fact, represent the ratio of the length of the average tortuous path followed by the water to that of the shortest possible path. It only remains to show that $\dfrac{d}{dt}\left(x\,\dfrac{dx}{dt}\right)$ is small. This is estimated roughly as follows. In the absorption experiments to be described the total quantity of water absorbed at any time may readily be obtained from the curves; then, from a knowledge of the porosity, the distance penetrated at that time may be calculated. It is found that the results are well

2 T 2

represented by the equation $t = mx^n$, where m and n are constants, m of the order some hundreds and n in the region of 2. This equation gives, by successive differentiation,

$$\frac{d}{dt}\left(x\frac{dx}{dt}\right) = (2-n)\bigg/ n^2 m^{\frac{2}{n}} t^{2-\frac{2}{n}}, \text{ or } (2-n)/n^2 m^2 x,$$

which is seen to be extremely minute compared with 1000 for any appreciable value of t or x and for permissible values of m and n. Leaving out the term in question, the equation of motion becomes simply

$$gh + gx + gh' = cx\frac{dx}{dt}. \quad \ldots \quad (10)$$

The Capillary Pressure.

h' will be termed the *capillary head* and gh' the *capillary pressure*. The term $gh + gx + gh'$ represents the total pressure, capillary plus applied. Calling this p, we may write equation (10)

$$p = cx\frac{dx}{dt}. \quad \ldots \quad \ldots \quad (11)$$

Regarding the factor $\frac{dx}{dt}$ generally as the rate of movement of the water normally to the entering surface, which may vary, as in the case of absorption, or be constant, as in the case of transmission, it is clear that equation (11) applies equally to the three cases of downward, upward, and horizontal flow for both absorption and transmission. Whenever absorption is proceeding the value of the capillary pressure is included in the term p ; for all cases of transmission gh' is zero.

The Permeability.

Let q be the rate of absorption or transmission in cubic centimetres per second per square centimetre of material. Then

$$q = B\frac{dx}{dt}, \text{ or } \frac{dx}{dt} = \frac{q}{B},$$

and substituting in equation (11),

$$q = \frac{B}{c}\frac{p}{x} = P\frac{p}{x}, \quad \ldots \quad \ldots \quad (12)$$

writing $P = \dfrac{B}{c}$; or, if Q is the rate of absorption or transmission over an area A,

$$Q = A.P.\frac{p}{x}. \quad . \quad . \quad . \quad . \quad . \quad (13)$$

The constant P represents the rate of flow through unit area of the material of unit thickness under the action of unit pressure, and is termed the *permeability*. (In these definitions a definite temperature is implied, since the surface tension and viscosity vary with temperature.)

The Resistivity.

Equation (13) is similar to that representing the corresponding case of the steady flow of heat or electricity, and, by analogy, P might be called the conductivity. $\dfrac{1}{P} = \sigma$ will be referred to as the *resistivity*. Equation (13) may thus be written

$$Q = \frac{Ap}{\sigma x}. \quad . \quad . \quad . \quad . \quad . \quad (14)$$

The Absorptivity

A case of considerable practical importance is that in which absorption occurs under the action of capillarity only— that is, in which the value of p is gh'. Inserting this value in equation (13), we have

$$Q = A.P.\frac{gh'}{x},$$

and when $A = 1$ and $x = 1$,

$$q = Pgh',$$

which gives the rate of absorption per square centimetre of surface under the action of capillarity only at the moment when the depth of penetration is 1 centimetre. This will be termed the *absorptivity*, Z. Thus

$$Z = Pgh', \quad . \quad . \quad . \quad . \quad . \quad (15)$$

and the rate of absorption in the absence of any applied pressure is given simply by

$$Q = \frac{AZ}{x}. \quad . \quad . \quad . \quad . \quad . \quad (16)$$

The Rate of Penetration.

The time which is taken for the water to penetrate to a given distance can be calculated from equation (11).

(a) *Vertically Downward Flow.*—In the case of vertically downward flow we have

$$p = gh + gx + gh' = gH + gx,$$

writing $H = h + h'$, the sum of the pressure in centimetres of water at the entering surface and the capillary head. Hence, remembering that $c = B\sigma$,

$$H + x = \frac{B\sigma}{g} \cdot x \cdot \frac{dx}{dt}, \quad . \quad . \quad . \quad . \quad (17)$$

whence

$$t = \frac{B\sigma}{g} \left\{ x - H \log\left(1 + \frac{x}{H}\right) \right\} \quad . \quad . \quad . \quad (18)$$

By expanding the logarithmic term this is converted into the form

$$t = \frac{B\sigma}{2gH} \cdot x^2 \left\{ 1 - \frac{2}{3}\frac{x}{H} + \frac{2}{4} \cdot \frac{x^2}{H^2} \cdots \right\}$$

$$= D \cdot \frac{h'}{H} \cdot x^2 \left\{ 1 - \frac{2}{3}\frac{x}{H} + \frac{2}{4} \cdot \frac{x^2}{H^2} \cdots \right\}, \quad . \quad (19)$$

where

$$D = \frac{B\sigma}{2gh'}.$$

When x is small compared with H equation (19) simplifies to

$$t = D \cdot \frac{h'}{H} x^2. \quad . \quad . \quad . \quad . \quad . \quad (20)$$

and when $h = 0$ it further reduces to

$$t = Dx^2. \quad . \quad . \quad . \quad . \quad . \quad . \quad (21)$$

(b) *Vertically Upward Flow.*—Vertically upward flow is generally due solely to capillarity, i. e., $h = 0$ and $H = h'$. Also, the head of water inside the material acts against the capillary forces and $p = gh' - gx$. Hence (*cf.* equation (17))

$$h' - x = \frac{B\sigma}{g} \cdot x \cdot \frac{dx}{dt}$$

and

$$t = -\frac{B\sigma}{g} \left\{ x + h' \log\left(1 - \frac{x}{h'}\right) \right\}, \quad . \quad . \quad (22)$$

or, by expanding the logarithmic term,

$$t = D.x^2 \left\{ 1 + \frac{2}{3}\frac{x}{h'} + \frac{2}{4}\frac{x^2}{h'^2} \cdots \right\}, \quad . \quad . \quad . \quad (23)$$

which also simplifies to equation (21) when x is small in comparison with h'.

(c) *Horizontal Flow.*—For horizontal flow

$$p = gh + gh' = gH$$

and (*cf.* equation (17))

$$H = \frac{B\sigma}{g}x\frac{dx}{dt} :$$

whence

$$t = \frac{B\sigma}{2gH}x^2 = D\frac{h'}{H}x^2, \quad . \quad . \quad . \quad . \quad (24)$$

and when $h=0$,

$$t = Dx^2. \quad . \quad . \quad . \quad . \quad . \quad . \quad . \quad (25)$$

D may be termed the *penetration constant.* It is equal to the time taken for the water to penetrate to unit distance under the action of capillarity only. Under these conditions, which are very common in practice, a simple expression emerges for the rate of absorption at any given time; for, from equations (25) and (16),

$$Q = AZ\sqrt{\frac{D}{t}}. \quad . \quad . \quad . \quad (26)$$

Different Materials in Contact.

We now proceed to examine the flow of water into and through a series of slabs of different materials in intimate contact with one another.

(1) *Absorption and Transmission.*

Let p = the total pressure across the slabs,

$p_1, p_2 \ldots$ = the pressures across slabs 1, 2, ...,

$l_1, l_2 \ldots$ = their thicknesses,

$\sigma_1, \sigma_2 \ldots$ = their resistivities.

We have the conditions that the total pressure is the sum of the pressures across the separate slabs, and that q at any moment is constant throughout. Therefore

$$p = p_1 + p_2 + \ldots$$
$$= \sigma_1 l_1 q + \sigma_2 l_2 q \ldots \quad \text{by equation (14)}$$
$$= q\Sigma\sigma l,$$

and
$$q = \frac{p}{\Sigma \sigma l},$$

or
$$Q = A\frac{p}{\Sigma \sigma l}, \quad \ldots \ldots \ldots \quad (27)$$

in further conformity with the thermal and electrical analogies. This equation applies equally to absorption or transmission in the same manner as equation (14). For absorption it is merely necessary to include in p the capillary pressure of the medium into which the water is penetrating.

(2) *Penetration.*

In investigating the rates of penetration into the successive slabs, we consider each separately and determine the time the water takes to penetrate to a given distance from the moment it enters.

(a) *Vertically Downward Flow.*—Let h' represent the capillary head in the nth medium. When the water has penetrated to a distance x in that medium,

$$q = \frac{p}{\sigma_1 l_1 + \sigma_2 l_2 + \ldots + \sigma_n x} \quad \text{by equation (27),}$$

and
$$p = g(h + l_1 + l_2 + \ldots + l_{n-1}) + gx + gh'$$
$$= gH + gx,$$

writing $H =$ the sum of the applied head at the surface of the medium under consideration and the capillary head of that medium. Then

$$q = \frac{gH + gx}{\sum_1^{n-1} \sigma l + \sigma_n x};$$

also,
$$q = B_n \cdot \frac{dx}{dt},$$

where B_n is the porosity of the nth medium. Thus

$$B_n \frac{dx}{dt} = \frac{gH + gx}{\sum_1^{n-1} \sigma l + \sigma_n x},$$

whence

$$t = \frac{B_n \left(\sum_1^{n-1} \sigma l - \sigma_n H \right)}{g} \log\left(1 + \frac{x}{H}\right) + \frac{B_n \sigma_n}{g} \cdot x. \quad (28)$$

(b) *Vertically Upward Flow.*—For upward flow we have, similarly,

$$B_n \cdot \frac{dx}{dt} = \frac{gh' - g(l_1 + l_2 + \ldots + l_{n-1}) - gx}{\sum_1^{n-1} \sigma l + \sigma_n x}$$

$$= \frac{gH - gx}{\sum_1^{n-1} \sigma l + \sigma_n x},$$

whence

$$t = -\frac{B_n \left(\sum_1^{n-1} \sigma l + \sigma_n H \right)}{g} \log\left(1 - \frac{x}{H}\right) - \frac{B_n \sigma_n x}{g}. \quad (29)$$

(c) *Horizontal Flow.*—When the flow is horizontal we have simply

$$B_n \frac{dx}{dt} = \frac{gh + gh'}{\sum_1^{n-1} \sigma l + \sigma_n x} = \frac{gH}{\sum_1^{n-1} \sigma l + \sigma_n x},$$

which gives

$$t = \frac{B_n \sum_1^{n-1} \sigma l}{Hg} \cdot x \frac{B_n \sigma_n}{2Hg} \cdot x^2. \quad \ldots \quad (30)$$

When x is small in comparison with H, equations (28) and (29) approximate to (30).

The constants h', p, σ, Z, D, and B will be referred to as the absorption constants. It will be observed that only three of them (h', σ, and D, for example) are independent; and, if the theory holds, these are sufficient to predict the circumstances of the flow of water under the conditions which have been described.

LV. *Some Properties of Porous Building Materials.*—Part IV. *The Determination of the Absorption Constants of a Homogeneous Specimen.* By E. MADGWICK, *M.C., M.Sc., Ph.D.* *
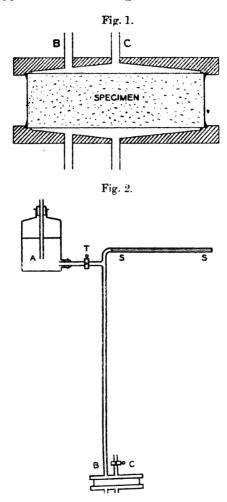
The Experimental Method.

THE specimen which has been used in the air permeability test (Part II.) is already prepared for the water absorption test. The holders were designed primarily in this

* Communicated by Sir F. E. Smith, K.C.B., C.B.E., Sec.R.S.

connexion, and are shown in fig. 1. Before the specimen is placed between them they are heated to a temperature just above the melting-point of Faraday wax, a little of which is applied around the edges to render the joints air-

Fig. 1.

Fig. 2.

and water-tight. If the test is to be carried out at a pressure greater than about 50 cm. of water, the holders are clamped together while the wax is still soft.

The specimen so prepared is connected to the apparatus shown in fig. 2. A is an aspirator containing water, T a

glass tap, SS a capillary tube in front of a millimetre scale.
To fill the space above the specimen the tap T is turned on
while the tube C is left open, so that as water enters at B
the air is driven out through C (see also fig. 1). When the
space is completely filled with water C is closed, and
the vertical tube and the capillary tube are also filled. The
tap T is now closed, and the meniscus in the capillary tube
moves along the scale as absorption proceeds. By observing
the time taken to move through any distance the rate of
absorption or transmission can be calculated from a know-
ledge of the bore of the capillary tube. The sensitivity of
the apparatus can be altered by using capillary tubes of
different bores. These are carefully selected so as to show
no appreciable variation in cross-section throughout their
lengths. At the beginning of an experiment it is usual
to work with a movement of 50 cm., which may be reduced
to as little as 2 cm. towards the end. The vertical glass
tube is readily detachable in order that the head of water
may be adjusted.

The time is noted the moment the specimen is wetted, and
the rate of absorption is measured as soon as possible
afterwards. Immediately one reading is finished another is
commenced, the process being repeated until the rate of flow
attains a constant value. The rate q at which water enters
each square centimetre of the specimen, or the rate Q at
which it enters the whole specimen of area A, is plotted
against the time t.

The Theoretical Absorption Curve.

While absorption is proceeding the value of the pressure p
is $g(h' + h + x)$, where h' is the capillary head, h the head of
water at the entering surface, and x the depth of pene-
tration. A convenient value of h is 50 cm.; h' is rarely less
than 100 cm., and is sometimes greater than 1000 cm. The
thickness of the specimen is generally between 1 and 4 cm.
Thus p is nearly constant and approximately equal to gH
where $H = h' + h$. Then we have from equation (14)

$$x = \frac{AgH}{\sigma Q},$$

and from equation (20)

$$t = \frac{B\sigma}{2gH} \cdot x^2.$$

These give for the equation to the absorption curve in the case of a thin specimen

$$t = \frac{K_1}{Q_2}, \quad \ldots \ldots \quad (31)$$

where

$$K_1 = \frac{BA^2 g H}{2\sigma} \quad \ldots \ldots \quad (32)$$

Assuming the water front to be perfectly uniform, absorption should proceed according to equation (31) until the under face of the specimen is reached and transmission commences. At that moment the capillary forces cease to operate and the value of the pressure p falls from $g(h' + h + l)$ to $g(h + l)$.

By equation (13) this results in a drop in the rate of flow from

$$Q_0 = \frac{AP g(h' + h + l)}{l}, \quad \ldots \ldots \quad (33)$$

representing the rate of absorption for a depth of penetration equal to the thickness of the specimen, to

$$Q_1 = \frac{AP g(h + l)}{l}, \quad \ldots \ldots \quad (34)$$

representing the steady rate of transmission. Further, this occurs at time

$$t_0 = D \cdot \frac{h'}{H} \cdot \left(1 - \frac{2}{3} \cdot \frac{l}{H} \ldots\right) l^2 \quad \ldots \quad (35)$$

by equation (19).
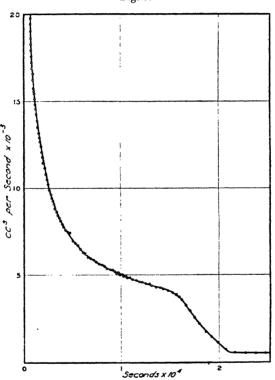
The Experimental Absorption Curve.

Many tests have been carried out on natural stones, bricks, and plasters. A set of typical results for a specimen of Box Ground stone are plotted in fig. 3, which depicts the three characteristic features of absorption, the transition between absorption and transmission and steady transmission.

Box Ground is a stone of unusual homogeneity, in which absorption takes place in excellent agreement with equation (31). Generally there are between the theoretical and experimental absorption curves slight divergences which may either be random in character or, in the cases of certain materials, tend to conform to type. A number of causes may contribute to such divergences. All the materials with which we are concerned are unhomogeneous to some extent. Specimens have been examined in this connexion by allowing

them to absorb a staining solution of potassium perman-
ganate and breaking them across after a suitable penetration
had taken place. The advancing surface of the liquid is
always characterized by irregularities, which in most cases
are fairly uniform with regard to magnitude and distribution,
but occasionally are so marked as to indicate definite
discontinuities in the rates of penetration. Progressive

Fig. 3.

variations in the properties of such artificial test pieces as
plasters are to be anticipated from the manner of their
preparation. An edge effect is also present, the absorption
being retarded somewhat in the vicinity of the waxed sides
of the specimen. This, however, can be reduced to neglig-
ible proportions by using specimens sufficiently wide in
proportion to their thickness. Corresponding to thick-
nesses of 1 and 2 inches, widths of 8 and 12 inches.

respectively are adequate. In consequence of the drying out of a specimen there may be present at the surface a "skin" of appreciable resistance, which is not necessarily constant throughout the course of a test. To isolate any such effect would require sufficient experimental data for each material to eliminate the random consequences of unhomogeneity. Moreover, tests on different specimens of the same material reveal such variations in properties as to render a refinement of this sort unnecessary within the scope of our present investigation. In other connexions the skin effect is of considerable importance and will be examined in the next section.

The average depth of penetration may be defined as the depth to which the absorbed water would have reached had the penetration been uniform. Also, the total amount of water which has been absorbed at any stage is represented by the area under the curve up to the appropriate time.

The transition between absorption and transmission is gradual, due to the irregularity in the water front which has been remarked. The portion of the curve corresponding to this phase is shown in fig. 4. Transmission commences at b and absorption ends at c, the flow at any intermediate point comprising absorption and transmission together. In a thicker specimen absorption would continue according to equation (31), and be represented by the prolongation of the curve ab. Thus, if ab be extrapolated to a point d at which the area under the curve represents the quantity of water which is actually absorbed by the specimen throughout the whole course of the test, the point d will indicate the rate of absorption Q_0 (equation (33)) corresponding to an average depth of penetration equal to the thickness of the specimen and the time t_0 (equation (35)) taken to penetrate to that depth. The steady rate of transmission Q_1 (equation (34)) is given by the rate of flow beyond c.
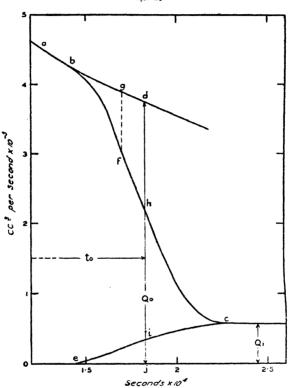
To separate the contributions which absorption and transmission make to the rates of flow between b and c, consider a point f on bc, and let g be the point corresponding to the same time on the prolongation of ab. Suppose X to be the area over which transmission takes place; then the rate of transmission is $Q_1 \dfrac{X}{A}$, where Q_1 is the rate of transmission over the whole specimen of area A, and the rate of absorption is $Q_2 \cdot \dfrac{A-X}{A}$, where Q_2 represents what would be the rate of absorption over the whole area of the specimen corre-

sponding to the momentary average depth of the water front. Thus, if Q' is the total rate of flow at j,

$$Q' = Q_1 \cdot \frac{X}{A} + Q_2 \cdot \frac{A - X}{A},$$

Fig. 4.

whence

$$X = \frac{A(Q_2 - Q')}{Q_2 - Q_1},$$

and the rate of transmission

$$\frac{Q_1 X}{A} = \frac{Q_1(Q_2 - Q')}{Q_2 - Q_1}.$$

Provided the irregularities in the water front are not too great the rate at which the average depth of penetration

increases during the period of combined absorption and transmission is approximately half that at which it would increase were absorption to proceed uninterrupted. Q_2 decreases from the value of Q at b to that at d, and at any moment approximates to the mean of the values at b and g. The rates of transmission as calculated in this way are shown by the line *ec*.

The total amount of water absorbed by the specimen is represented by the area under the experimental curve which is bounded by the line *ce*, and also by that under the extrapolated curve up to d. Thus, if the perpendicular dj to the time axis cut bc in h and ce in i, we see that the area *hic* is equal to the sum of the areas *hbd* and *eij*. The point d is determined by this condition.

Calculation of the Constants.

The values of Q_0, t_0. and Q_1 having been determined, the absorption constants may be calculated from equations (33), (34), and (35). From equations (33) and (34) the capillary head

$$h' = \frac{(Q_0 - Q_1)(h + l)}{Q_1}. \quad \dots \quad (36)$$

From equation (34) the permeability

$$P = \frac{Q_1 l}{A(h + l)g}. \quad \dots \quad (37)$$

The resistivity

$$\sigma = \frac{1}{P} = \frac{A(h + l)g}{Q_1 l}. \quad \dots \quad (38)$$

The absorptivity

$$Z = Ph'g = \frac{l(Q_0 - Q_1)}{A}. \quad \dots \quad (39)$$

From equation (35) the penetration constant

$$D = \frac{t_0}{l^2} \cdot \frac{H}{\left(1 - \frac{2}{3}\frac{l}{H} \cdots\right)h'}$$

$$= \frac{t_0}{l^2} \cdot \frac{\left(1 + \frac{2}{3} \cdot \frac{l}{H}\right)H}{h'},$$

since l is small in comparison with H,

$$= \frac{t_0}{l^2} \cdot \frac{(h + l) + h'}{h'}.$$

writing $\qquad$ (H + l) $\quad$ for $\quad$ (H + $\frac{2}{3}l$)

$$= \frac{t_0 Q_0}{l^2 (Q_0 - Q_1)} \quad \ldots \ldots \quad (40)$$

by equation (36).

Also, from our definition of D_1 the porosity

$$B = \frac{2gh'D}{\sigma} = \frac{2t_0 Q_0}{Al}. \quad \ldots \ldots \quad (41)$$

When the ordinates of the absorption curve represent the rates of flow q per sq. cm., equations (36)–(41) are modified by substituting $q_0 . A$ for Q_0 and $q_1 . A$ for Q_1.

The expression (41) is susceptible to inaccuracy from the causes which, as mentioned above, may affect equation (31). In practice a more precise value of the porosity, which is required in connexion with the determination of the saturation coefficient (Part I.), is obtained by estimating, from the area under the curve, the total amount of water absorbed by the specimen. After the specimen has been wetted two or three minutes elapse before observations are taken. The quantity of water absorbed during this period is determined as follows :—For purposes of extrapolation portions of the curve conform accurately enough to the equation $Q^n . t = $ constant, where n is in the region of the theoretical value 2. n is evaluated for the first part of the curve by plotting $\log Q$ against $\log t$. Then the amount of water absorbed at time t is

$$\int_0^t Q dt = \frac{n}{n-1} Q_t . t,$$

where Q_t is the rate of absorption at time t. The area under the curve beyond t is measured by means of a planimeter.

The results of some tests are set out below. The series of values for Whitbed are selected to illustrate the extent to which the absorptive properties of a stone may vary. Of the six specimens the last two were cut from the same block, the remainder collected at random.

The method here described has been extensively applied to the routine testing of various kinds of building materials. The calculations are based on the assumptions that the specimen is homogeneous and that absorption is unaccompanied by chemical changes. An examination of the absorption curve readily reveals whether these conditions are approached sufficiently closely to justify the expressions of the absorptive properties of the material in terms of the

constants which have been defined. Even when such is not the case the curve invariably yields information of value.

Application to the Weathering Problem.

It has been remarked that the weathering of stone is intimately associated with the flow of water in it. Observations on structures built with the same stone have shown discrepancies in their weathering qualities, and from

Specimen.	Capillary head h'. cm. of water.	Resistivity. C.G.S. units $\times 10^8$.	Penetration Constant D. C.G.S. units.	Porosity.
Portland Whitbed .	276	10·7	365	·175
	135	4·01	189	·118
	167	4·25	153	·114
	275	20·7	523	·131
	249	11·1	350	·142
	264	10·5	320	·148
Portland Roach ...	196	49·3	1290	·101
Beerstone	556	4·46	871	·208
Monks Park	906	36·4	391	·195
Box Ground	1355	100·0	671	·178
Darley Dale	228	69·9	1170	·078
Longridge	514	48·7	3530	·073
Bath Stone	1078	43·3	446	·225
Wire-cut brick	201	5·46	277	·198
Sand-faced brick ...	95	0·336	24	·130
Gypsum plaster ...	684	20·8	374	·228

the table we see that the absorptive properties of the same material show considerable variations. The possible coordination of there two facts suggests a new avenue of investigation. Specimens for weathering tests may be selected to differ in their absorption constants but in other respects to be as nearly as possible similar.

LVI. *On the Effective Capacity of the Quadrant Electrometer.* *By* J. J. McHenry, *M.A., D.Sc.*[*]

THE theory of the effective capacity of the quadrant electrometer has been treated theoretically by Sir J. J. Thomson, O.M.[†], who showed that the motion of the

---

[*] Communicated by the Author.
[†] Phil. Mag. vol. xlvi. p. 536 (Dec. 1898).

needle, when at a high potential, caused an apparent increase in the effective capacity of the instrument. The effective capacity may be defined as the quantity of electricity necessary to increase by unity the potential of the insulated quadrants, the other pair of quadrants being earthed and the needle maintained at a given potential. In what follows the earthed pair of quadrants, together with the case of the instrument and screening tubes for connexions, will be called the first conductor ; the other pair of quadrants, with wires leading to them, will be called the second conductor ; and the needle will be called the third conductor.

Thomson's treatment is given here, with a slight change of notation.

If Q_2 is the charge on the second conductor,

$$Q_2 = q_{12}V_1 + q_{22}V_2 + q_{32}V_3,$$

where q_{22} is a coefficient of capacity and q_{12}, q_{32} coefficients of induction of the conductors. They depend on the position of the needle, and are therefore functions of the angle θ, which is the deflexion of the needle from the zero position in which it rests when $V_1 = V_2 = 0$ for all values of V_3.

When $V_1 = V_2 = 0$, $(Q_2)_0 = (q_{32})_0 V_3$.

When $V_1 = 0$, and $V_2 \neq 0$, $Q_2 = q_{22}V_2 + q_{32}V_3$.

The effective capacity

$$= \frac{Q_2 - (Q_2)_0}{V_2} = q_{22} + \frac{V_3}{V_2}\{q_{32} - (q_{32})_0\}.$$

Now

$$\frac{d}{d\theta}(q_{12} + q_{22} + q_{32}) = 0$$

when the needle is originally in the symmetrical position, and also, when θ is small, $\frac{d}{d\theta}(q_{12}) = 0$; so that

$$\frac{d}{d\theta}(q_{22}) = - \frac{d}{d\theta}(q_{23}).$$

Thus, neglecting powers of θ higher than the first,

$$q_{22} = (q_{22})_0 - b_1\theta ; \quad q_{32} = (q_{32})_0 + b_1\theta,$$

and the effective capacity is

$$(q_{22})_0 - b_1\theta + b_1\theta\left(\frac{V_3}{V_2}\right),$$

or

$$(q_{22})_0 + b_1\theta\left(\frac{V_3}{V_2} - 1\right).$$

2 U 2

Now $\theta = k V_2 V_3$, and the effective capacity is therefore

$$(q_{22})_0 + b_1 k (V_3{}^2 - V_2 V_3).$$

If $\dfrac{V_2}{V_3}$ is small, as is usual when the instrument is used heterostatically, the effective capacity is $(q_{22})_0 + b_1 k V_3{}^2$.

The object of the present paper is to investigate the importance of the term $b_1 k (V_3)^2$ in ordinary use, and to find out how far it explains the behaviour of the instrument in measuring currents or quantities of electricity. Now it is well known that the coefficient k in the above treatment is not a constant, but depends itself on the value of V_3, and this alters the form of the expression for the effective capacity. This alteration is due to the necessity of expanding the coefficient of capacity q_{33} to a higher power of θ than the first *.

When $\dfrac{V_2}{V_3}$ is small,

$$\theta = \frac{b_1 V_2 \left(V_3 - \dfrac{V_2}{2} \right)}{F + b_2 V_3{}^2},$$

where b_1, as before, is $-\dfrac{d}{d\theta}(q_{22})$, or $+\dfrac{d}{d\theta}(q_{32})$; and b_2 is $\dfrac{d^2}{d\theta^2}(q_{23})$, or $-\frac{1}{2}\dfrac{d^2}{d\theta^2}(q_{33})$. F is the modulus of torsion of the suspending fibre. If we use the above expression for θ in finding the effective capacity we get, as before,

$$(q_{22})_0 + b_1 \theta \left(\frac{V_3}{V_2} - 1 \right)$$

or $\qquad (q_{22})_0 + \dfrac{b_1{}^2 (V_3 - V_2) \left(V_3 - \dfrac{V_2}{2} \right)}{F + b_2 V_3{}^2}.$

Thus the effective capacity becomes, when V_2 is neglected,

$$m + \frac{b_1{}^2 V_3{}^2}{F + b_2 V_3{}^2}.$$

Here m is written instead of $(q_{22})_0$.

---

* Walker, Phil. Mag. (6) vi. p. 238 (Aug. 1903); Anderson, Phil. Mag. p. 380 (March 1912).

When the instrument is used idiostatically and $V_3 = V_1 = 0$,

$$\theta = \frac{-b_1 V_2^2}{2(F - a_2 V_2^2)},$$

where a_2 is $\dfrac{1}{2}\dfrac{d^2}{d\theta^2}(g_{11})$, or $\dfrac{1}{2}\dfrac{d^2}{d\theta^2}(q_{22})$. The charge on the insulated quadrants is Q_2, where

$$Q_2 = (q_{22})V_2 = (m - b_1\theta)V_2.$$

The effective capacity

$$= \frac{Q_2}{V_2} = m - b_1\theta = m + \frac{b_1^2 V_2^2}{2(F - a_2 V_2^2)}.$$

Here, in practice, the term $\dfrac{b_1^2 V_2^2}{2(F - a_2 V_2^2)}$ is small and may be neglected. It amounts in the electrometer studied here to about ·06 cm. when $V_2 = 5$ volts and θ about 50 divisions. The capacity m was 52·2 cm. The coefficients b_1 and b_2 may be easily compared with F, the modulus of torsion of the fibre suspending the needle, by finding in radians the values of θ for different values of V_2, V_3, and substituting in the formula $\theta = \dfrac{b_1 V_2 V_3}{F + b_2 V_3^2}$. Here V_2 must be small compared with V_3, and both must be expressed in electrostatic units. If $(V_3)_m$ is that potential of the needle which makes the angle θ a maximum for a given value of V_2,

$$\frac{b_2}{F} = \frac{1}{(V_3)_m^2}.$$

With the needle at a potential $(V_3)_m$,

$$\theta = \frac{b_1 V_2 (V_3)_m}{2F},$$
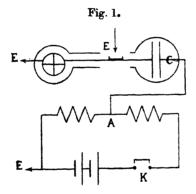
and by substitution of experimentally found values for θ and V_2, $\dfrac{b_1}{F}$ may be found. The effective capacity may then be expressed in terms of V_3 and F, and is equal to

$$m + \left\{ \frac{\left(\dfrac{b_1}{F}\right)^2}{\dfrac{1}{(V_3)^2} + \left(\dfrac{b_2}{F}\right)} \right\} F, \quad \text{or} \quad m + xF,$$

where x can be calculated for different values of V_3. The expression for the increase in the effective capacity due to the motion of the needle may therefore be tested by plotting the values of x for given values of V_3 against the corresponding increases in the effective capacity of the electrometer as measured by experiment. It will be seen below that the graph so obtained is a straight line passing through the origin. In addition, F may be obtained by dividing the factor x into the observed value of the increase in the effective capacity for a given value of V_3.

The Experiments.

The effective capacity of the electrometer, called hereafter c, was found by comparison with a fixed condenser,

Fig. 1.

which will be denoted by C, and whose capacity was known to be approximately ·0000466 microfarads, or 41·94 e.s.u. The exact value of C is of no great importance in the experiments described here, as all the values of the quantity c are measured in terms of it. The value obtained for F depends on the value of C, and therefore also the values of b_1 and b_2. The experimental arrangements are shown in fig. 1. The condenser C is placed in series with the electrometer, one plate being joined to the insulated quadrants through the usual earthing key. The other plate of C is connected to the point A of a potentiometer. To begin with, both quadrants were earthed and the key K was open, so that A was also at zero potential. The needle was raised to the required potential and the earthing key raised so as to leave the working quadrants insulated, the

needle being in the zero position. When the key K was closed the point A and one plate of C was raised to a potential V and the other plate of the condenser and the insulated quadrants assumed a potential v. Since the quadrants and that plate of C connected to them were insulated, it is clear that

$$cv + C(v - V) = 0, \quad \text{or} \quad cv = C(V - v),$$

so that

$$\frac{c}{C} = \frac{V - v}{v}.$$

When the electrometer is used idiostatically

$$V_1 = v_3 = 0, \quad \text{and} \quad \frac{c}{C} = \frac{\sqrt{\theta_1} - \sqrt{\theta_2}}{\sqrt{\theta_2}},$$

where θ_1 and θ_2 are the deflexions caused by the potentials V and v respectively. When used heterostatically and when V_3 is large compared with V or v

$$\frac{c}{C} = \frac{\theta_1 - \theta_2}{\theta_2}.$$

It must be noted that to make $V_3 = 0$ it is not in general sufficient to join the needle to earth, on account of the contact difference of potential between the material of the needle and that of the quadrants. To make $V_3 = 0$, or, in other words, to make sure that the potential at a point in air just outside the needle is the same as that at a point in air just outside the earthed quadrants, a small potential must be applied to the needle, until with $V_1 = 0$ a reversal of the sign of V_2 causes no change in the deflexion observed. The electrometer used in these experiments had a needle made of silvered paper which was ·076 volts electronegative to the brass quadrants. Another electrometer had an aluminium needle which was ·263 volts electropositive to the quadrants.

In the above method the potential V is fixed and the deflexion θ_1 may be read at leisure, but the deflexion θ_2, which depends on v and which takes a minute or two to read, will be affected by any defect in the insulation of the electrometer or of the condenser. A leak in the electrometer makes θ_2 too small and a leak in the condenser makes it too big. When the readings given below were being taken the insulation was satisfactory, the deflexion θ_2 being steady. A variation of the method in which, with the electrometer system insulated and at zero potential, the potential of the point A is changed from V to zero, could also be used. In this case the insulated system has an original

charge $= -CV$, the charge due to the potential of the needle being, of course, left out of account. When V is changed to zero by opening the key K, the potential of the insulated system changes to v where v and V have now opposite signs. The charge on the insulated system remaining constant, we have

$$-CV = Cv + cv,$$

or

$$\frac{c}{C} = \frac{V + v}{-v}.$$

When the potential of the needle, V_3, is zero, the sign of v makes no change in θ_2, and we have, as before,

$$\frac{c}{C} = \frac{\sqrt{\theta_1} - \sqrt{\theta_2}}{\sqrt{\theta_2}}.$$

When $V_3 \neq o$ and $\dfrac{V_2}{V_3}^2$ is small we have

$$\frac{c}{C} = \frac{\theta_1 + \theta_2}{-\theta_2},$$

where θ_2 is the deflexion due to the potential v and is of opposite sign to θ_1. If we disregard the sign of θ_2 and deal in absolute values of the deflexions we get, as before,

$$\frac{c}{C} = \frac{\theta_1 - \theta_2}{\theta_2}.$$

In this second method when the insulated system has attained the potential v it may leak to earth either across the electrometer system or the condenser, so that the defective insulation of both c and C conspire to make the absolute value of v too small, and therefore the absolute deflexion θ_2 too small.

In our case the insulation of c and C was good, and the first method described gave steady values of θ_2, so that it alone was used. In cases where the condenser insulation is worse than that of the electrometer both methods should be used and means taken.

Table I. shows the values of V_3, θ_1, θ_2, and $\dfrac{c}{C}$. The values of V_3 go from zero to 250 volts. The deflexions given were not those read directly from the straight scale of the electrometer, but were reduced to readings on a circular scale having the mirror as centre. The deflexions
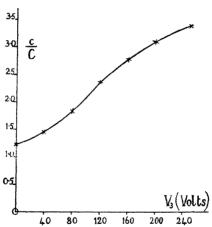
θ_1 and θ_2 are proportional to the angles of deflexion of the needle.

The values of V_3 and $\dfrac{c}{C}$ are shown in the graph of fig. 2.

The last reading given in the table, in which $\dfrac{c}{C} = 2\cdot74$, was

TABLE I.

V_3 (volts).	θ_1.	θ_2.	$\dfrac{c}{C}$.
0	191·5	38	1·244
40·5	143	58	1·47
81	118·4	41	1·86
119	137·5	40·5	2·40
161	142	37·2	2·82
200	137	33	3·15
250	126·3	28·3	3·46
157 (by sharing charges)................................			2·74

Fig. 2.

obtained by the method of "sharing the charges." The electrometer was charged to a given potential which was read from the value of the deflexion, and then was connected to the condenser, so that the charge was shared between c and C. The value 2·74 differs from that of the corresponding point on the graph (2·80) by about 2 per cent.

It will be observed that the effective capacity when V_3 is about 125 volts is double the capacity when $V_3 = 0$.

The increase in the effective capacity of the electrometer with V_3 is a very important factor in its behaviour when used to measure charges or currents. Let a quantity of electricity Q be given to the insulated quadrants, causing their potential to increase by V_2. Then $Q = cV_2$, where c is the effective capacity. Now $\dfrac{V_2}{V_3}$ being small,

$$V_2 = \frac{(F + b_2 V_3^2)\theta}{b_1 V_3}$$

or

$$V_2 = \frac{\theta}{\gamma},$$

where

$$\gamma = \frac{b_1 V_3}{F + b_2 V_3^2},$$

and may be called the sensitivity of the electrometer for measuring potentials. Q therefore is $\dfrac{c\theta}{\gamma}$, where $\dfrac{\gamma}{c}$ may be called the sensitivity for measuring charges. Table II. shows the deflexions (θ) observed for a value of $V_2 = \cdot505$ volts, with different values of V_3. A graph of θ against V_3, V_2 being kept constant, shows how γ varies with V_3. This graph is shown in curve B of fig. 3. When these values of γ are divided by numbers proportional to c we obtain quantities proportional to the sensitivity of the electrometer in measuring charges, that is, to $\dfrac{\gamma}{c}$. These numbers are also shown in Table II. and plotted on curve A of fig. 3. The points obtained in this way are indicated by crosses. Curve B shows that the electrometer is most sensitive in measuring potentials when $V_3 = 157$ volts approximately. Curve A shows that the electrometer when used to measure charges is most sensitive when V_3 is in the neighbourhood of 80 volts, when no external loading condenser is added to increase the electrometer capacity. If this is done it is obvious that the value of V_3, which causes greatest sensitivity in measuring charges, will increase and approach the value of V_3, which causes the electrometer to be most sensitive in measuring potentials, the two values coinciding when the loading condenser is very big.

The variation with V_3 of the sensitivity of the electrometer in measuring charges was also studied by measuring
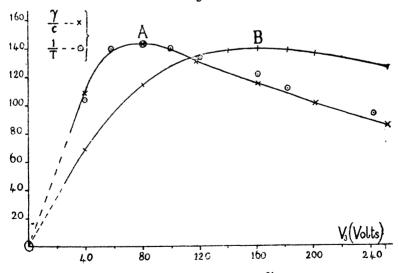
the time, T, necessary for a constant current, I, to produce a given deflexion, θ. Here

$$Q = I \times T = \frac{c\theta}{\gamma}, \quad \text{and} \quad \frac{\gamma}{c} = \frac{\theta}{IT};$$

TABLE II.

V_3 (volts).	$\gamma \times$ const.	$\frac{\gamma}{c} \times$ const.	T (secs.).	$\frac{1}{T} \times$ const.
40·5	70	111	94	106
58·5	—	—	70·2	143
81	116·4	146	68·3	146
101	—	—	70·5	142
119	137·3	133·2	—	—
121	—	—	73·4	136
141	140·4	—	—	—
161	141·6	117·3	80·4	124
182	140·8	—	88·5	113
200	138	102·2	—	—
243	—	—	105·5	95
250	128	86·3	—	—

Fig. 3.

so that when I and θ are kept constant $\frac{\gamma}{c}$ is proportional to the reciprocal of T. A small quantity of uranium oxide

was placed on the lower of two plates inside an earthed box.
The lower plate was joined to the electrometer, the upper
being maintained at a constant potential of about 180 volts.
T was the time taken, when the electrometer system was
disconnected from earth, for the spot of light on the scale
to move over seventy divisions. The values of $\frac{1}{T}$ are indi-
cated by circles on fig. 3. The constants by which $\frac{\gamma}{c}$ and
$\frac{1}{T}$ were multiplied were so chosen that their values, so
multiplied, were made equal when $V_3 = 81$ volts. It will
be seen that the values of $\frac{1}{T}$ lie near, but not quite on,
curve A. In curve A, which shows the values of $\frac{\gamma}{c}$, c is the
capacity of the electrometer and leads, but in measuring T
this capacity is necessarily increased somewhat by the
addition of the ionization chamber. This additional capacity
was small, but not negligible. The addition of an external
capacity to the effective capacity of the electrometer makes
curve A alter in form towards that of curve B, with which
it would coincide when the additional capacity is made very
big. The small deviation of the values of $\frac{1}{T}$ from curve A
may therefore be attributed to the addition of the extra
capacity of the ionization chamber.

The experimental values of c therefore explain the
variation with V_3 of the sensitivity of the instrument
in measuring quantities of electricity. It remains now
to find how these observed values agree with the theoretical
expression for the effective capacity,

$$m + \frac{b_1{}^2 V_3{}^2}{F + b_2 V_2{}^2}, \quad \text{or} \quad m + \frac{b_1{}^2}{b_2 + \dfrac{F}{V_3{}^2}}.$$

Here m is, with sufficient accuracy, the value of the effective
capacity when $V_3 = 0$, which may be seen from Table I.
to be $1\cdot244$ C. Subtracting this from the full values of the
effective capacity we obtain the increase in the latter values
due to the motion of the needle or values of $c - m$. Now
$c - m$, experimentally obtained, should be equal to

$$\frac{b_1{}^2}{b_2 + \dfrac{\mathrm{F}}{\mathrm{V_3}^2}} \quad \text{or} \quad \left\{ \frac{\left(\dfrac{b_1}{\mathrm{F}}\right)^2}{\dfrac{b_2}{\mathrm{F}} + \dfrac{1}{\mathrm{V_3}^2}} \right\} \mathrm{F}.$$

If $\mathrm{V_3}$ be expressed in volts instead of electrostatic units we have

$$c - m = \left\{ \frac{\left(\dfrac{b_1}{\mathrm{F}}\right)^2}{\dfrac{b_2}{\mathrm{F}} + \dfrac{300}{\mathrm{V_3}^2}} \right\} \times \mathrm{F}.$$

The ratios $\dfrac{b_2}{\mathrm{F}}$ and $\dfrac{b_1}{\mathrm{F}}$ were obtained from the following data :—

The electrometer is most sensitive in measuring potentials when $\mathrm{V_3} = 157$ volts ; therefore $b_2 \times \left(\dfrac{157}{300}\right)^2 = \mathrm{F}$; from which $\dfrac{b_2}{\mathrm{F}} = 3\cdot65$.

When $\mathrm{V_3} = 157$ volts and $\mathrm{V_2} = \cdot2526$ volts, $\theta = 70\cdot9$ divs. on a scale 1 metre from the mirror ; 800 divisions on the scale were equal to 795 mm. Substituting in the formula,

$$\theta = \frac{b_1 \mathrm{V_2} \mathrm{V_3}}{2\mathrm{F}(300)^2} = \frac{70\cdot9 \times 795}{2000 \times 800} \text{ radians,}$$

we get $\dfrac{b_1}{\mathrm{F}} = 160$.

Substituting these values in the formula given above, we have

$$c - m = \left\{ \frac{(160)^2}{3\cdot65 + \left(\dfrac{300}{\mathrm{V_3}}\right)^2} \right\} \times \mathrm{F}$$

$$= x\mathrm{F}.$$
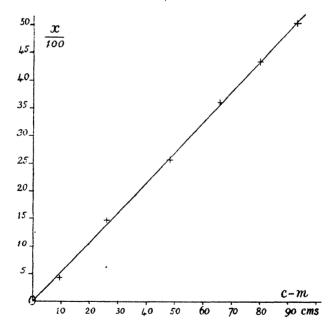
The measured values of $c - m$ are given, in terms of the capacity C, in the second column of Table III. In the third column they are expressed in electrostatic units. The fourth column gives the corresponding values of the factor x. Fig. 4 shows $c - m$ plotted against x. The graph so obtained is a straight line passing through the origin, which shows that the theoretical expression for the effective capacity is verified by experiment.

Taking a point on the graph, $c - m = 73.4$ cm.; $x = 4000$.

Hence $F = \dfrac{73 \cdot 4}{4000} = \cdot 0184$ dynes × cm. per radian. This

TABLE III.

V_3 (volts).	$\dfrac{c-m}{C}$.	$(c-m,$ in e.s.u.	x.
0	Negligible.	—	—
40·5	·226	9·48	437
81	·616	25·8	1474
119	1·156	48·5	2558
161	1·576	66·1	3595
200	1·906	80·0	4338
250	2·216	93·0	5029

Fig. 4.

gives $b_1 = 2 \cdot 94$ cm./radian; $b_2 = \cdot 0672$ cm./(radian)^2. The modulus of torsion of the suspension, F, was also found directly by hanging from it a small cylinder of aluminium and measuring the period of the torsional oscillations. The axis of rotation was perpendicular to the axis of the cylinder

and passed through its centre of gravity. The mass of the cylinder was 2·771 grm. ; its length was 3·72 cm. and diameter ·594 cm. The period was 81·7 seconds. From these data F was found to be ·0193 c.g.s. units, which differs from the value determined above by about $4\frac{1}{2}$ per cent., which is not greater than the possible error in the assumed value of the capacity C.

The four constants of the electrometer, viz., b_1, b_2, m, and F, may therefore be found easily by electrical methods provided a suitable standard condenser is available. Here it will be remembered

$$b_1 = \frac{d}{d\theta}(q_{23}) = -\frac{d}{d\theta}(q_{13}),$$

$$b_2 = \frac{d^2}{d\theta^2}(q_{23}) = \frac{d^2}{d\theta^2}(q_{13}) = -\frac{1}{2}\frac{d^2}{d\theta^2}(q_{33}),$$

$$m = (q_{22})_0,$$

and F is the modulus of torsion of the fibre suspending the needle. These four constants determine to a reasonable degree of accuracy the whole behaviour of the instrument. We may, for example, find in terms of them the potential $(V_3)_\mu$ which makes the electrometer most sensitive in measuring charges, and an expression for this maximum sensitivity, as follows :—

$$\frac{\theta}{Q} = \frac{\theta}{cV_2} = \frac{b_1 V_3}{\left(m + \frac{b_1^2 V_3^2}{F + b_2 V_3^2}\right)(F + b_2 V_3^2)}$$

$$= \frac{1}{\frac{mF}{b_1 V_3} + \left(\frac{mb_2 + b_1^2}{b_1}\right)V_3}.$$

$\frac{\theta}{Q}$ is greatest when the denominator is least, V_3 alone being variable, or $\frac{\theta}{Q}$ is maximum when

$$V_3^2 = \frac{mF}{mb_2 + b_1^2} = \frac{F}{b_2 + \frac{b_1^2}{m}}$$

$$= (V_3)_\mu^2.$$

Thus, $\qquad (V_3)_\mu = \sqrt{\dfrac{F}{b_2 + \dfrac{b_1^2}{m}}}.$

The sensitivity for measuring potentials is

$$\frac{\theta}{V_2} = \frac{b_1 V_3}{F + b_2 V_3{}^2} = \frac{b_1}{\dfrac{F}{V_3} + b_2 V_3}.$$

$\dfrac{\theta}{V_2}$ is greatest when

$$V_3 = (V_3)_m = \sqrt{\frac{F}{b_2}}.$$

When m or $(q_{22})_0$ becomes very big $(V_3)_\mu = (V_3)_m$.

The maximum value of $\dfrac{\theta}{Q}$ is

$$\frac{1}{2\sqrt{\dfrac{m^2 F b_2 + m F b_1{}^2}{b_1{}^2}}} = \frac{b_1}{2\sqrt{m F(m b_2 + b_1{}^2)}}.$$

The fact that b_2, in electrometers of the usual pattern, is positive is shown by Walker (*loc. cit.*) to be due to the air gaps separating the quadrants. He thinks it probable that b_2 could be made to vanish by altering the angle of the needle, which is usually made in the form of a double sector of a circle. If this can be realized there is no theoretical limit to the sensitivity of the instrument in measuring potentials, but $\dfrac{\theta}{Q}$, the sensitivity for measuring charges, has still a maximum value $\dfrac{1}{2\sqrt{mF}}$ when $V_3 = \dfrac{\sqrt{mF}}{b_1}$.

University College, Galway.

LVII. *A Continuous Atomic Matrix.*
By W. R. MORGANS, *M.Sc.* [*][†].

1. *Introduction.*

THE recent developments in the quantum theory enable us to calculate the intensity of the spectral lines which are emitted by the transition between two electronic states. For a theoretical treatment of many phenomena, however, such as rates of recombination, the intensity of continuous X-rays, and the photoelectric effect, further

knowledge of continuous matrices is required. Oppenheimer [3] gave a general treatment of hydrogen-like atoms, but his final results are not satisfactory in numerical computation. Epstein and Muskat [1] and Sugiura [2] have given the Schroedinger matrices for the affinity spectrum of hydrogen-like atoms in a more amenable form. The evaluation of the matrices for the capture of a cathode ray electron travelling in a definite direction, the z axis, by a bare nuclear charge Ze, has not yet been suitably determined. It appears that, from Temple's [4] work, it is convenient to use parabolical coordinates in such an investigation. The problem is essentially an analytical one, and it is proposed here to evaluate the matrices for such a collision problem, using parabolical coordinates. The method follows that given by Epstein [5].

2. *The Wave Functions.*

If we use the parabolical coordinates

$$x=\sqrt{\xi\eta}\cos\phi, \qquad y=\sqrt{\xi\eta}\sin\phi, \qquad z=\frac{\xi-\eta}{2},$$

$$0\leq\xi<\infty, \qquad 0\leq\eta\leq\infty, \qquad 0\leq\phi\leq 2\pi,$$

and assume the cathode ray electron and the nucleus as one system, then the Schroedinger wave equation for the electron travelling in the direction of the nuclear charge Ze is given by

$$\frac{\partial}{\partial\xi}\left(\xi\frac{\partial\psi}{\partial\xi}\right)+\frac{\partial}{\partial\eta}\left(\eta\frac{\partial\psi}{\partial\eta}\right)+\frac{1}{4}\left(\frac{1}{\xi}+\frac{1}{\eta}\right)\frac{\partial^2\psi}{\partial\phi^2}$$

$$+\frac{2\pi^2\mu\mathrm{E}}{h^2}(\xi+\eta)\psi+4\pi^2\frac{\mu e^2 Z}{h^2}\psi=0$$

where ψ is the amplitude function, μ and e the mass and charge of the electron, E the energy of the atomic system, and h is Planck's constant.

In order to obtain the wave function corresponding to the electron moving in the direction of the z axis with energy $\mathrm{E}>0$, Temple solved the above wave equation by omitting the angular term, and obtained a solution corresponding to the initial state of the electron, in which the wave associated has symmetry about the z axis. If we make the substitutions

$$\frac{k^2}{4}=\frac{2\pi^2\mu\mathrm{E}}{h^2}, \qquad a=\frac{h^2}{4\pi^2\mu e^2 Z}, \qquad n=\frac{1}{ak},$$

the solution found for the initial state becomes

$$\psi(n) = A(n) e^{\frac{ik}{2}(\xi - \eta)} F(in, 1, ik\eta),$$

where

$$F(\alpha, j, x) = \sum_{p=0}^{x} \frac{\alpha(\alpha + 1) \dots (\alpha + p - 1) \, x^p}{j(j + 1) \dots (j + p - 1) \, p!},$$

and n is a parameter characterizing the continuous state. $A(n)$, the normalization factor, can be determined by Fues'[6] method of normalization, and has been shown by Oppenheimer to have the value

$$|A(n)|^2 = \frac{2\pi\mu n}{h} \cdot e^{\pi n} n\Gamma(1 - in)\Gamma(1 + in).$$

The wave function for the final state of the electron, in which the energy $E_1 < 0$, is more complex, and is given by the general solution of the wave equation above. If we make the substitution

$$-\frac{(k')^2}{4} = \frac{2\pi^2\mu E_1}{h^2},$$

we find the solution to be

$$\psi(n_1 n_2 m) = A(n_1 n_2 m)(\xi\eta)^{\frac{|m|}{2}} e^{-\frac{k'}{2}(\xi + \eta)}$$
$$F(-n_1, |m| + 1, k'\xi) F(-n_2, |m| + 1, k'\eta) \frac{\cos}{\sin} m\phi,$$

where $|m| = 0, 1, 2, \dots, \infty$, and $k'(|m| + 1 + n_1 + n_2) = \frac{1}{a}$, and $A(n_1, n_2, m)$ is the normalization factor for the final state.

3. *The Matrices.*

We proceed with the evaluation of the Heisenberg matrices for transitions from the initial continuous state to the final state. It has been shown by Schroedinger that the components of the matrices are given by the expressions

$$q_x(n ; n_1 n_2 m) = \iiint x\psi(n)\psi^*(n_1 n_2 m) dx \, dy \, dz$$

(with analogous expressions for z and y), where $\psi^*(n_1 n_2 m)$ denotes the conjugate value of $\psi(n_1 n_2 m)$ and the integration is extended over the whole of space. If we introduce the coordinates ξ, η, ϕ, we obtain

$$'q_{x,y}(n \; ; \; n_1 n_2 m) = \tfrac{1}{4} \mathrm{A}(n) \mathrm{A}(n_1 n_2 m) \iiint \sqrt{\xi\eta}(\xi+\eta)(\xi\eta)^{\frac{|m|}{2}}$$

$$e^{-\frac{k'}{2}(\xi+\eta)} \mathrm{F}(-n_1, |m|+1, k'\xi) \mathrm{F}(-n_2, |m|+1, k'\eta)$$

$$e^{-\frac{ik}{2}(\xi-\eta)} \mathrm{F}(-in, 1, -ik\eta) \genfrac{}{}{0pt}{}{\cos}{\sin} m\phi \genfrac{}{}{0pt}{}{\cos}{\sin} \phi \, d\xi \, d\eta \, d\phi.$$

The integration with respect to ϕ can be carried out immediately, giving a finite value $\pm\frac{\pi}{2}$ only when $m=\mp 1$. Hence

$$|q_{x,y}(n \; ; \; n_1 n_2 \pm 1)| = \frac{\pi}{8} \mathrm{A}(n) \mathrm{A}(n_1 n_2 \pm 1) \iint (\xi+\eta)\xi\eta$$

$$\mathrm{F}(-n_1, 2, k'\xi) \mathrm{F}(-n_2, 2, k'\eta) e^{-\frac{k'}{2}(\xi+\eta)} e^{-\frac{ik}{2}(\xi-\eta)}$$

$$\mathrm{F}(-in, 1, -ik\eta) d\xi \, d\eta.$$

Also q_z is finite only when $m=0$, so that

$$|q_z(n \; ; \; n_1 n_2 0) = \frac{\pi}{8} \mathrm{A}(n) \mathrm{A}(n_1 n_2 0) \iint (\xi^2-\eta^2) e^{-\frac{k'}{2}(\xi+\eta)}$$

$$\mathrm{F}(-n_1, 1, k'\xi) \mathrm{F}(-n_2, 1, k'\eta) e^{-\frac{ik}{2}(\xi-\eta)} \mathrm{F}(-in, 1, -ik\eta) d\xi \, d\eta.$$

For aid in the evaluation of these matrix integrals we introduce the function $\mathrm{H}^{\delta}_{\beta\gamma}(nn'\alpha\alpha')$, defined such that

$$\mathrm{H}^{\delta}_{\beta\gamma}(nn'\alpha\alpha') = \int_0^\infty e^{-\frac{(\alpha+\alpha')}{2}\xi} \xi^{\delta+\beta} \mathrm{F}(-n, \delta+1, \alpha\xi)$$

$$\mathrm{F}(-n', \delta+1-\gamma, \alpha'\xi) d\xi. \qquad (1)$$

With this definition the expressions for the matrix elements become

$$|q_{xy}(n \; ; \; n_1 n_2 \pm 1) = \frac{\pi}{8} \mathrm{A}(n) \mathrm{A}(n_1)[\mathrm{H}^{1}_{11}(n_1 o k' ik) \mathrm{H}^{1}_{01}(n_2 in k' - ik)$$

$$+ \mathrm{H}^{1}_{11}(n_2 in k' - ik) \mathrm{H}^{1}_{01}(n_1 o k' ik)], \quad . \quad . \quad (2)$$

$$|q_z(n \; ; \; n_1 n_2 0)| = \frac{\pi}{8} \mathrm{A}(n) \mathrm{A}(n_1)[\mathrm{H}^{0}_{20}(n_1 o k' ik) \mathrm{H}^{0}_{00}(n_2 in k' - ik)$$

$$- \mathrm{H}^{0}_{20}(n_2 in k' - ik) \mathrm{H}^{0}_{00}(n_1 o k' ik)]. \quad . \quad . \quad (3)$$

4. *Evaluation of the Integrals.*

The integrals occurring in the matrix components come under the general form

$$\mathrm{H}^{\delta}_{\beta\gamma}(nn'\alpha\alpha'),$$

where $\qquad \gamma = 1 \; ; \qquad \delta = 0, 1 \; ; \qquad \beta = 0, 1, 2.$

2 X 2

By a number of reduction formulæ the above forms can be reduced to one suitable for evaluation. If we use the relation

$$F(\alpha, \gamma, x) = \frac{(\gamma-1)}{x} [F(\alpha, \gamma-1, x) - F(\alpha-1, \gamma-1, x)],$$

then

$$H_{\beta 1}^{\delta}(nn'\alpha\alpha') = \frac{\delta}{\alpha} [H_{\beta 0}^{\delta-1}(nn'\alpha\alpha') - H_{\beta 0}^{\delta-1}(n+1, n', \alpha, \alpha')]. \quad (4)$$

Again, the integral $H_{\beta 0}^{\delta}(nn'\alpha\alpha')$ may be written as

$$H_{\beta 0}^{\delta}(nn'\alpha\alpha') = \int_{0}^{\infty} y(n)y'(n')d\xi,$$

where

$$y(n) = e^{-\frac{\alpha}{2}\xi} \xi^{\frac{\delta+\beta}{2}} F(-n, \delta+1, \alpha\xi),$$

$$y'(n') = e^{-\frac{\alpha'}{2}\xi} \xi^{\frac{\delta+\beta}{2}} F(-n', \delta+1, \alpha'\xi).$$

It can be shown that $y(n)$ and $y'(n')$ are solutions of the following differential equations:

$$\xi\frac{d^2y}{d\xi^2} + (1-\beta)\frac{dy}{d\xi} + \left[-\frac{\alpha^2}{4}\xi - \frac{(\delta^2-\beta^2)}{4\xi} + \alpha\left(\frac{\delta+1}{2}+n\right)\right]y = 0, \quad . \quad (5)$$

$$\xi\frac{d^2y'}{d\xi^2} + (1-\beta)\frac{dy'}{d\xi} + \left[-\frac{\alpha'^2}{4}\xi - \frac{(\delta^2-\beta^2)}{4\xi} + \alpha'\left(\frac{\delta+1}{2}+n'\right)\right]y' = 0. \quad . \quad (6)$$

Multiply (5) by $y'(n')$ and (6) by $y(n)$ and subtract; then

$$y\frac{d}{d\xi}\left(\xi\frac{dy}{d\xi}\right) - y'\frac{d}{d\xi}\left(\xi\frac{dy'}{d\xi}\right) - \beta\left(y'\frac{dy}{d\xi}-y\frac{dy'}{d\xi}\right) + \frac{(\alpha'^2-\alpha^2)}{4}\xi yy' + \left[\alpha\left(\frac{\delta+1}{2}+n\right) - \alpha'\left(\frac{\delta+1}{2}+n'\right)\right]yy' = 0.$$

Integrating the expression between zero and infinity, and omitting terms that vanish at these limits, we find, after a little rearrangement, that

$$-2\beta\int_{0}^{\infty} y'\frac{dy}{d\xi}d\xi + \frac{(\alpha'^2-\alpha^2)}{4}H_{\beta+1, 0}^{\delta}(nn'\alpha\alpha') + \left[\alpha\left(\frac{\delta+1}{2}+n\right) - \alpha'\left(\frac{\delta+1}{2}+n'\right)\right]H_{\beta 0}^{\delta}(nn'\alpha\alpha') = 0. \quad . \quad (7)$$

Again,

$$\frac{d}{d\xi}y(n) = -\frac{\alpha}{2}y(n) + \frac{(\delta+\beta)}{2\xi}y(n)$$
$$+ e^{-\frac{\alpha}{2}\xi}\xi^{\frac{\delta+\beta}{2}}\frac{d}{d\xi}F(-n, \delta+1, \alpha\xi).$$

If we use the relation

$$\frac{d}{d\xi}F(-n, \delta+1, \alpha\xi) = -\frac{n}{\xi}[F(-n+1, \delta+1, \alpha\xi)$$
$$-F(-n, \delta+1, \alpha\xi)],$$

we may write

$$\int_0^\infty y'(n)\frac{dy}{d\xi}d\xi = -\frac{\alpha}{2}H_{\beta 0}^\delta(nn'\alpha\alpha') + \frac{(\delta+\beta)}{2}H_{\beta-1,0}^\delta(nn'\alpha\alpha')$$
$$+ nH_{\beta-1,0}^\delta(nn'\alpha\alpha') - nH_{\beta-1,0}^\delta(n-1, n'\alpha\alpha').$$

Substituting this value in (7), we have

$$H_{\beta+1,0}^\delta(nn'\alpha\alpha') = \frac{4}{(\alpha^2-\alpha'^2)}\left[\left\{\alpha\left(\frac{\delta+1}{2}+n\right) - \alpha'\left(\frac{\delta+1}{2}+n'\right)\right\}\right.$$
$$H_{\beta 0}^\delta(nn'\alpha\alpha') - \beta(\delta+\beta+2n)H_{\beta-1,0}^\delta(nn'\alpha\alpha')$$
$$\left. + 2n\beta H_{\beta-1,0}^\delta(n-1, n'\alpha\alpha')\right].$$

In particular

$$H_{10}^\delta(nn'\alpha\alpha') = \frac{4}{(\alpha^2-\alpha'^2)}\left[\alpha\left(\frac{\delta+1}{2}+n\right)\right.$$
$$\left. -\alpha'\left(\frac{\delta+1}{2}+n'\right)\right]H_{00}^\delta(nn'\alpha\alpha'), \quad (8)$$

$$H_{20}^\delta(nn'\alpha\alpha') = \frac{4}{(\alpha^2-\alpha'^2)}\left[\frac{4}{(\alpha^2-\alpha'^2)}\left\{\alpha\left(\frac{\delta+1}{2}+n\right)\right.\right.$$
$$\left. -\alpha'\left(\frac{\delta+1}{2}+n'\right) + \alpha\right\}\left\{\alpha\left(\frac{\delta+1}{2}+n\right)\right.$$
$$\left. -\alpha'\left(\frac{\delta+1}{2}+n'\right)\right\} \times H_{00}^\delta(nn'\alpha\alpha') - (\delta+1+2n)$$
$$H_{00}^\delta(nn'\alpha\alpha') + 2nH_{00}^\delta(n-1, n'\alpha\alpha')\right]. \quad \cdot \quad \cdot \quad (9)$$

If we use the relations (4), (8), (9) in the expressions

(2), (3), the x, y matrix components, for which $k'(2 + n_1 + n_2) = \dfrac{1}{a} = kn$, can be reduced to the form

$$|q_{x,y}(n; n_1 n_2 \pm 1)| = \frac{\pi A(n) A(n_1)}{2k'(k^2 + k'^2)} \Big[H^0_{00}(n_1 + 1, ok'ik)$$

$$H^0_{00}(n_2 + 1, in\, k' - ik) - H^0_{00}(n_1\, ok'ik)$$

$$H^0_{00}(n_2\, in\, k' - ik) \Big].$$

Likewise the z matrix component, for which $k'(1 + n_1 + n_2) = \dfrac{1}{a} = kn$, reduces to

$$q_z(n; n_1 n_2\, 0)| = \frac{\pi A(n) A(n_1)}{(k'^2 + k^2)} \Big[\Big\{ (n_1 - n_2) \frac{(k'^2 - k^2)}{(k'^2 + k^2)}$$

$$- \frac{2ikk'}{(k'^2 + k^2)} (1 + in) \Big\} H^0_{00}(n_1 ok'ik) H^0_{00}(n_2 in\, k' - ik)$$

$$+ n_1 H^0_{00}(n_1 - 1, 0, k'\, ik) H^0_{00}(n_2\, in\, k' - ik)$$

$$- n_2 H^0_{00}(n_1\, ok'ik) H^0_{00}(n_2 - 1, in\, k' - ik) \Big].$$

The computation of the matrix components will be determined if the integral

$$H^\delta_{00}(nn'\alpha\alpha') = \int_0^\infty e^{-\frac{(\alpha + \alpha')}{2}\xi} \xi^\delta F(-n, \delta + 1, \alpha\xi)$$

$$F(-n', \delta + 1, \alpha'\xi) d\xi \quad \ldots \quad (10)$$

can be evaluated, where n', α' are imaginary and n, α are real. We can represent the function

$$y(n) = \xi^{\delta/2} e^{-\frac{\alpha}{2}} F(-n, \delta + 1, \alpha\xi)$$

in the following form :

$$y(n) = \frac{e^{(-\frac{\alpha}{2}\xi - i\pi n)} \Gamma(\delta + 1)\Gamma(n + 1)}{2\pi i(-\alpha)^{\delta/2} y^{\frac{\delta + 2n}{2}}}$$

$$\int_{\odot} J_\delta(2\sqrt{-\alpha y \xi t}) t^{-\frac{(\delta + 2n + 2)}{2}} e^{-yt} dt, \quad (11)$$

where the path of integration is a loop around the pole $t = 0$.

Likewise

$$y'(n') = \xi^{\frac{\delta}{2}} e^{-\frac{\alpha'}{2}} F(-n', \delta+1, \alpha'\xi)$$

$$= \frac{e^{(-\frac{\alpha'}{2}\xi - i\pi n')}\Gamma(\delta+1)\Gamma(n'+1)}{2\pi i(-\alpha')^{\frac{\delta}{2}} y^{\frac{\delta+2n'}{2}}}$$

$$\int_c J_\delta(2\sqrt{-\alpha' y \xi t}) t^{-\frac{(\delta+2n'+2)}{2}} e^{-yt} dt, \quad (12)$$

where the path of integration is a complex loop coming from $+\infty$ along the real axis, making a positive circuit around the point $t=0$ and going back to $+\infty$. If we substitute (11), (12) in the integrand (10), and use the following relation from the theory of Bessel Functions,

$$\int_0^\infty J_\delta(2\sqrt{a\xi}) J_\delta(2\sqrt{b\xi}) e^{-c\xi} d\xi = \frac{1}{c} e^{-\frac{(a+b)}{c} - i\frac{\delta\pi}{2}} J_\delta\left(\frac{2i\sqrt{ab}}{c}\right), \quad ^{(7)}$$

the integrations can be carried out to give the result

$$H_\infty^\delta(nn'\alpha\alpha') = (-1)^n \left(\frac{2}{\alpha+\alpha'}\right)^{\delta+1} \Gamma(\delta+1) u^{n+n'}$$

$$F\left(-n, -n', \delta+1, 1-\frac{1}{u^2}\right),$$

where $u = \frac{\alpha-\alpha'}{\alpha+\alpha'}$ and $F\left(-n, -n', \delta+1, 1-\frac{1}{u^2}\right)$ is a hypergeometric function.

With this determination the matrix components become, after slight reductions and the use of the relation,

$$F(a+1, b, c, z) - F(a, b, c, z) = \frac{bz}{c} F(a+1, b+1, c+1, z).$$

$$|q_{x,y}(n; n_1 n_2 \pm 1) = 2\pi A(n) A(n_1) \frac{(-1)^{n_1+n_2}}{k'(k^2+k'^2)^2}$$

$$v^{n_1-n_2-in} in(1-v^2) F(-n_2, 1-in, 2, 1-v^2),$$

$$|q_z(n; n_1 n_2 0) = 4\pi A(n) A(n_1) \frac{(-1)^{n_1+n_2}}{(k^2+k'^2)^2} v^{n_1-n_2-in}$$

$$[\{(n_1+n_2+1)+v(n_1+1)\}F(-n_2, -in, 1, 1-v^2)$$

$$+ n_2 v F(-n_2+1, -in, 1, 1-v^2)],$$

where $v = \frac{k'-ik}{k'+ik}$.

5. *The Normalization factor* $A(n_1n_2m)$.

The factor $A(n_1n_2m)$ for the discrete Eigenfunction is defined by the relation

$$\frac{1}{4}\iiint (\xi+\eta)\psi^2(n_1n_2m)\,d\xi\,d\eta\,d\phi=1,$$

where the integration is extended throughout space. If we integrate with respect to ϕ, and make use of relation (1), we find

$$\frac{\pi}{4}A^2(n_1n_2m)\big[H_{10}^{|m|}(n_1n_1k'k')H_{00}^{|m|}(n_2n_2k'k')$$

$$+H_{10}^{|m|}(n_2n_2k'k')H_{00}^{|m|}(n_1n_1k'k')\big]=1. \quad (13)$$

But

$$H_{10}^{|m|}(nn'\alpha\alpha')=\frac{4}{(\alpha^2-\alpha'^2)}\left[\alpha\left(\frac{|m|+1}{2}+n\right)\right.$$

$$\left.-\alpha'\left(\frac{|m|+1}{2}+n'\right)\right]H_{00}^{|m|}(nn'\alpha\alpha'),$$

which gives in the limit

$$\underset{\substack{a\to a'\\n\to n'}}{Lt}\ H_{10}^{|m|}(nn'\alpha\alpha')=\frac{2}{\alpha'}\left(\frac{|m|+1}{2}+n'\right)H_{00}^{|m|}(n'n'\alpha'\alpha').$$

The equation (13) becomes therefore

$$\frac{\pi}{4}A^2(n_1n_2m)\frac{2}{k'}(|m|+n_1+n_2+1)$$

$$H_{00}^{|m|}(n_1n_1k'k')H_{00}^{m}(n_2n_2k'k')=1.$$

Furthermore, as

$$H_{00}^{|m|}(nn'\alpha\alpha')=(-1)^n\left(\frac{2}{\alpha+\alpha'}\right)^{|m|+1}\Gamma(|m|+1)u^{n+n'}$$

$$F\left(-n',-n,|m|+1,1-\frac{1}{u^2}\right),$$

where

$$u=\frac{\alpha-\alpha'}{\alpha+\alpha'}$$

and

$$F(a,b,c,z)=\frac{\Gamma(c)\Gamma(c-a-b)}{\Gamma(c-a)\Gamma(c-b)}F(a,b,a+b+1-c,1-z),$$

when a, b are discrete numbers, then

$$H_{00}^{|m|}(n_1 n_1 k' k') = \frac{(-1)^{n_1}}{(k')^{|m|+1}} \frac{\Gamma(|m|+1)^2 \Gamma(|m|+2n_1+1)}{\Gamma(|m|+1+n_1)^2} \underset{u \to 0}{\mathrm{Lt}} u^{2n_1}$$

$$F\left(-n_1, -n_1, -2n_1-|m|, \frac{1}{u^2}\right),$$

$$= \frac{(-1)^{n_1}}{(k')^{|m|+1}} \frac{\Gamma(|m|+1)^2 \Gamma(|m|+2n_1+1)}{\Gamma(|m|+1+n_1)^2} \underset{u \to 0}{\mathrm{Lt}}$$

$$\sum_{p=0}^{n_1} (-1)^p \frac{n_1{}^2 (n_1-1)^2 \ldots (n_1-p+1)^2 u^{2(n_1-p)}}{p!\,(2n_1+|m|)\ldots(2n_1+|m|-p+1)}$$

$$= \frac{1}{(k')^{|m|+1}} \frac{\Gamma(|m|+1)^2 \Gamma(n_1+1)}{\Gamma(|m|+n_1+1)}.$$

Using this result in equation (13) we find that

$$A(n_1 n_2 m) = \sqrt{\frac{2a}{\pi}} \frac{(k')^{|m|+2}}{\Gamma(|m|+1)^2}$$

$$\sqrt{\frac{\Gamma(|m|+n_1+1)\Gamma(|m|+n_2+1)}{\Gamma(n_1+1)\Gamma(n_2+1)}}.$$

For the particular cases $m = \pm 1$ and $m = 0$ we find

$$A(n_1 n_2 \pm 1) = (k')^3 \sqrt{\frac{2a}{\pi}(n_1+1)(n_2+1)},$$

$$A(n_1 n_2 0) = (k')^2 \sqrt{\frac{2a}{\pi}}.$$

The matrices are now completely determined.

In conclusion, I wish to express my thanks to Prof. P. S. Epstein for suggesting this and related problems, and for his advice while the work was in progress.
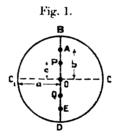
REFERENCES.

(1) Epstein and Muskat, Proc. Nat. Acad. Sciences, vol. xv. no. 5 (1929).
(2) Y. Sugiura, Phys. Rev. vol. xxxiv. no. 6 (1929).
(3) J. R. Oppenheimer, *Zeits. f. Phys.* xli. p. 268 (1927).
(4) G. Temple, Proc. Roy. Soc. A, cxxi. (1928).
(5) P. S. Epstein, Phys. Rev. vol. xxviii. no. 4 (1926).
(6) E. Fues, *Ann. Phys.* p. 80 (1926).
(7) N. Nielsen, 'Cylinderfunktionen,' p. 184.

LVIII. *Current Flow in a Circular Disk. By* J. H. AWBERY,
*B.A., B.Sc., F.Inst.P., Physics Department, National
Physical Laboratory, Teddington, Middlesex* *.

Introduction.

IT is proposed in this paper to determine the electrical
resistance of a circular disk when current is led in at
two points, A and E (see fig. 1), the potential difference
being observed at two other points, P, Q, on the same
diameter as A, E. The current terminals and also the
potential terminals are to be disposed symmetrically with
respect to the centre O of the disk. (In fig. 1, A and E are
shown further from the centre than P and Q, but the results
obtained will still apply if they are nearer.) The electrodes
project through the whole thickness of the disk.

Fig. 1.

In the theory the potentials at A and E will be infinity,
but this does not affect the application of the theory to cases
where the potential electrodes do not coincide with the
current electrodes ; the former will lie on an equipotential
curve which is unaffected by any change occurring within
the curve marked out by any equipotential which completely
surrounds the current terminal. In theory, as in practice,
we may take the diameter OC to be at zero potential, where
OC is perpendicular to OB.

Calculation of Potential at any Point of Disk.

To solve the problem just enunciated we shall use
the method of conformal representation, and to simplify
the calculations we restrict ourselves to the hemisphere
BCDEOPB. The resistance of the whole disk will be
one-half of that found for the hemisphere.

Let $OB = OC = a$, $OA = OE = b$, $OP = OQ = c$, and let the potentials at B, D be $\pm V_0$.

It is clear that AE is one flow-line and that ABCDE is another. We use a flow function U such that $U = 0$ along ABCDE and $U = U_0$ along AE. Then writing $w = U + iV$, the electrical diagram is that of fig. 2, where potential $\overline{V}$ is measured vertically and U is measured horizontally.

To convert this figure into the hemisphere of fig. 1 we transform each into a straight line as an intermediary, as shown in fig. 3, which is lettered to correspond to figs. 1 and 2.

Fig. 2.
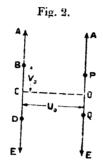
Fig. 3.

Consider first the transformation

$$t = (z + ia)^2/(z - ia)^2, \quad \ldots \ldots \quad (1)$$

where t is the variable, say $(r + is)$, in fig. 3, and $z = (x + iy)$ is that in fig. 1.

Then

$$r + is = [x + i(y + a)]^2/[x + i(y - a)]^2$$

$$= [(x^2 + y^2 - a^2) + ix(2a)]^2/[x^2 + (y - a)^2]^2,$$

or, equating the real and the imaginary parts,

$$r = [(x^2 + y^2 - a^2)^2 - 4a^2x^2]/[x^2 + (y - a)^2]^2,$$

$$s = 4ax(x^2 + y^2 - a^2)/[x^2 + (y - a)^2]^2.$$

It follows at once that s is zero or t is a real quantity if either $x = 0$ or $x^2 + y^2 = a^2$, *i.e.* the figure in the t plane is the real axis (fig. 3) when the z figure is the semicircle $x^2 + y^2 = a^2$, with the diameter $x = 0$ (BD in fig. 1). The corresponding values of t and z for the points with which we are concerned are found (by substitution in equation 1) to be :—

At   B. $z = ia$ and $t = \pm\infty$.

      A. $z = ib$,, $t = (b+a)^2/(b-a)^2$.

      P. $z = ic$,, $t = (c+a)^2/(c-a)^2$.

      O. $z = 0$,, $t = 1$.

      Q. $z = -ic$,, $t = (a-c)^2/(a+c)^2$.

      E. $z = -ib$,, $t = (a-b)^2/(a+b)^2$, which is $1/t_A$.

      D. $z = -ia$,, $t = 0$.

      C. $z = a$,, $t = (1+i)^2/(1-i)^2 = -1$.

Thus it appears that equation (1) transforms fig. 1 to fig. 3. To establish a correspondence between figs. 1 and 2 we must transform the latter also to the straight line fig. 3.

To effect this we have the theorem of Schwarz and Christoffel (see Jeans, ' Electricity and Magnetism,' 3rd edition, p. 271), which gives the differential relation between w and t for the present case in the form

$$dw/dt = A(t - t_A)^{-1}(t - t_E)^{-1} = A t_A/(t - t_A)(t t_A - 1),$$

using t_A to represent the quantity $(b+a)^2/(b-a)^2$, the value of t at the point A.

From this equation

$$w = B + A t_A \int \frac{dt}{(t - t_A)(t t_A - 1)},$$

where A and B are constants to be subsequently determined. Now

$$\int \frac{dt}{(t - t_A)(t t_A - 1)} = \frac{1}{(t_A^2 - 1)} \log_e \left(\frac{t - t_A}{t t_A - 1} \right),$$

so that, taking a new constant C, we find

$$w = B + C \log_e \left(\frac{t - t_A}{t t_A - 1} \right). \quad \cdots \quad (2)$$

We require the diagrams to correspond as follows :—

Point.	Value of w.	Value of t.
A	i	t_A
B	i	∞
C	0	-1
D	$-i$	0
E	$-i$	$1/t_A$
O	U_0	1

and it will be found that all these are satisfied if $C = -iU_0/\pi$ and $B = 0$, together with the condition

$$\pi V_0 = U_0 \log t_A. \quad \ldots \quad \ldots \quad (2\,a)$$

Eliminating t from the equations (1) and (2), we find the relation between w and z in the form

$$e^{i\pi w/U_0} = \frac{(z+ia)^2 - t_A(z-ia)^2}{(z+ia)^2 t_A - (z-ia)^2}. \quad \ldots \quad (3)$$

Writing $w = u + iv$, the real part of the left-hand side is

$$e^{-\pi V/U_0} \cos \pi U/U_0,$$

and the imaginary part is

$$ie^{-\pi V/U_0} \sin \pi U/U_0.$$

Similarly, substituting $(x+iy)$ for z, and rationalizing the denominator, the right-hand side of equation (3) reduces to the form $F(x, y) + iG(x, y)$, where

$$\Delta \cdot F(x, y) = [\{x^2(1-t_A) - (y+a)^2 + t_A(y-a)^2\} \times \\ \{x^2(t_A - 1) - (y+a)^2 t_A + (y-a)^2\} \\ + 4x^2\{a^2(1+t_A)^2 - y^2(1-t_A)^2\}],$$

and

$$\frac{\Delta}{2x} \cdot G(x, y) = [\{y(1-t_A) + a(1+t_A)\}\{x^2(t_A - 1) \\ - (y+a)^2 t_A + (y-a)^2\} \\ - \{x^2(1-t_A) - (y+a)^2 + t_A(y-a)^2\}\{a(1+t_A) - y(1-t_A)\}].$$

Here Δ has been written as an abbreviation for

$$[x^2(t_A - 1) + (y-a)^2 t_A + (y+a)^2]^2 \\ + 4x^2[a(t_A + 1) - y(1-t_A)]^2.$$

By equating the real and imaginary parts of equation (3), and then squaring and adding the resulting equations, we obtain an expression for the potential V at any point of the disk,

viz., $$e^{-2\pi\overline{V}/U_0} = \{F(x, y)\}^2 + \{G(x, y)\}^2.$$

Resistance of Disk when all Electrodes lie on one Diameter.

At present, however, we are interested only in the potential along the diameter BD, so that, setting $x = 0$, the equation simplifies to

$$\Delta_0^2 \, e^{-2\pi\overline{V}/U_0} = [\{t_A(y-a)^2 - (y+a)^2\}\{(y-a)^2 + (y+a)^2 t_A\}]^2,$$

or

$$\Delta_0 \, e^{-\pi\overline{V}/U_0} = \pm [t_A(y-a)^2 - (y+a)^2][(y-a)^2 - (y+a)^2 t_A],$$

where Δ_0 is the value of Δ when $x = 0$, so that

$$\Delta_0 = [(y-a)^2 - t_A(y+a)^2]^2.$$

Thus

$$e^{-\pi\overline{V}/U_0} = \pm [t_A(y-a)^2 - (y+a)^2]/[(y-a)^2 - (y+a)^2 t_A],$$

. . . (4)

where the ambiguous sign is to be interpreted so that the right-hand side is positive, since the exponential of a real number cannot be negative. In fact, the negative sign must be taken if $y < b$ and the positive if $y > b$. The limiting point is the point A, fig. 1, where

$$\overline{V} = \infty \quad \text{or} \quad e^{-\pi\overline{V}/U_0}$$

vanishes; on passing this point we move from one flow-line to another.

Taking logarithms of equation (4) we find finally that

$$\overline{V} = \frac{U_0}{\pi} \log_e \pm \left[\frac{(y-a)^2 - (y+a)^2 t_A}{t_A(y-a)^2 + (y+a)^2}\right], \quad . \quad . \quad (5)$$

an explicit expression for the potential $\overline{V}$ at any point y on the diameter BD.

U_0 is, of course, the total current flowing in the hemisphere between the two points A and E, whilst $\overline{V}$ is the potential of any point P in the diameter. The potential difference between P and Q, fig. 1, is twice this, so that inserting the resistivity ρ and thickness l of the material, the resistance of the hemisphere is $2\rho\overline{V}/lU_0$, or substituting

the value of t_A, writing c for y, and halving the value so as to obtain the resistance R of the whole circle, we find

$$ \mathrm{R} = \frac{\rho}{\pi l} \log \pm \left[\frac{(c-a)^2(b-a)^2 - (c+a)^2(b+a)^2}{(b+a)^2(c-a)^2 - (c+a)^2(b-a)^2} \right], $$

where a, b, c are the dimensions, as marked in fig. 1.

It is of interest to notice that this result gives an example of a reciprocal theorem ; the resistance is unaltered if the current is led in at the points which were originally potential terminals, and the potential measured at the original current terminals. A second point of interest is to note that for a constant thickness the resistance is independent of the size of the disk, provided that geometrical similarity is maintained.

Particular Cases : *Solution by " Point Charges."*

Among particular cases we notice that if $c = 0$ the resistance reduces to zero, as it should do since the potential difference vanishes.

If $c = b$ it becomes

$$ \frac{\rho}{\pi l} \log \pm \left[\frac{(c-a)^4 - (c+a)^4}{(c^2-a^2)^2 - (c^2-a^2)^2} \right] = \infty . $$

This is to be expected, since now the potentials at the measuring points are infinitely great.

Finally, when $b = a$, the current terminals being now attached on the circumference of the circle,

$$ \mathrm{R} = \frac{\rho}{\pi l} \log \pm \frac{4a^2(a+c)^2}{4a^2(c-a)^2} = \frac{2\rho}{\pi l} \log \frac{a+c}{a-c} . $$

This result, as a matter of fact, may be very easily deduced by the method of "sources and sinks." Taking a point source of strength Q at B, and one of strength $-$Q at D, the potential due to the former at the point (x, y) is

$$ - \frac{Q}{2\pi} \log r = - \frac{Q}{4\pi} \log \left[x^2 + (y-a)^2 \right], $$

where r is the distance of (x, y) from B. Thus the potential due to the two together is

$$ \frac{Q}{4\pi} \log \left[\frac{x^2 + (y+a)^2}{x^2 + (y-a)^2} \right], $$

which clearly makes the circumference a flow-line. On the diameter BD it reduces to

$$ \frac{Q}{2\pi} \log \frac{y+a}{y-a}, $$

or in the previous notation to

$$(Q/2\pi) \log \left(\frac{c+a}{c-a}\right).$$

Now the source Q at B emits quantity Q per unit time, of which only Q/2 flows within the circle, the remainder flowing outside. Thus the current in the whole circle is Q/2, and the potential difference between P and Q (fig. 1) is

$$\frac{Q}{\pi} \log \frac{c+a}{c-a}.$$

Consequently the resistance of the whole circle is

$$\frac{2\rho}{l\pi} \log \frac{c+a}{c-a},$$

as found by the other method.

Error due to slight Displacement of Electrodes.

Reverting to the general problem, we may pertinently enquire, with a view to practical application, what will be the effect on the resistance if any of the points is slightly displaced from its assumed position. These errors could of course be found by direct calculation, since the general expression for the potential is known, but such numerical calculation gives no clue as to the general effect of a displacement.

If the point P is slightly displaced laterally, so that its co-ordinates are $(\delta x, c)$, it will be seen that the real part of the right-hand side of equation (3) is not affected to the first order, whilst the imaginary part contains δx as a factor. Thus, on squaring and adding these, the potential difference is affected only to the second order of small quantities. Physically this is, of course, due to the fact that the equipotentials cut BD at right angles, so that any slight lateral variation moves a point along a single equipotential. Clearly the same applies to a lateral displacement of the point A.

If the displacement of P from the symmetrical position takes place along the diameter, so that y becomes $(c+\delta c)$, then expression (5) will hold for the potential at P, but with $(c+\delta c)$ written in place of y.

We thus find that $\pi \bar{V}/U_0$ is approximately

$$\log \pm \left[\frac{(c^2+a^2-2ac-2a\,\delta c - 2c\,\delta c) - t_A(c^2+2c\,\delta c + a^2 + 2ac + 2a\,\delta c)}{t_A(c^2+2c\,\delta c + a^2 - 2ac - 2a\,\delta c) - (c^2+2c\,\delta c + a^2 + 2ac + 2a\,\delta c)}\right],$$

which reduces to

$$\log \pm \left[\frac{(c^2+a^2)(1-t_A) - 2ac(1+t_A)}{(c^2+a^2)(t_A-1) - 2ac(1+t_A)} \right] \times$$

$$\left[1 + \frac{\delta c\,(2c - 2a - 2ct_A - 2at_A)}{(c^2+a^2)(1-t_A) - 2ac(1+t_A}\right.$$

$$\left. - \frac{\delta c\,(2ct_A - 2at_A - 2c - 2a)}{(c^2+a^2)(t_A-1)2ac(t_A+1)} \right],$$

or, expanding the logarithm of the second factor, $\pi \overline{V}/U_0$ is approximately

$$\log \pm \left[\frac{(c^2+a^2)(1-t_A) - 2ac(1+t_A)}{(c^2+a^2)(t_A-1) - 2ac(1+t_A)} \right]$$

$$+ \delta c \left[\frac{2(c-a) - 2t_A(c+a)}{(c^2+a^2)(1-t_A) - 2ac(1+t_A)} \right.$$

$$\left. - \frac{2(c-a)t_A - 1(c+a)}{(c^2+a^2)(t_A-1) - 2ac(t_A+1)} \right].$$

Thus the potential difference between P and Q (since Q is unaltered) is increased * by

$$\frac{2U_0\,\delta c}{\pi} \left[\frac{(c-a) - t_A(c+a)}{(c^2+a^2)(1-t_A) - 2ac(1+t_A)} \right.$$

$$\left. - \frac{(c-a)t_A - (c+a)}{(c^2+a^2)(t_A-1) - 2ac(1+t_A)} \right].$$

or the resistance is increased by

$$\frac{\rho\,\delta c}{l\pi} \left[\frac{(c-a) - t_A(c+a)}{(c^2+a^2)(1-t_A) - 2ac(1+t_A)} \right.$$

$$\left. - \frac{(c-a)t_A - (c+a)}{(c^2+a^2)(t_A-1) - 2ac(1+t_A)} \right],$$

i. e.. by

$$\frac{2a\rho\,\delta c(a^2-c^2)(1-t_A^2)}{\pi l[2t_A\{(a^2+c^2)^2 + 4a^2c^2\} - (1+t_A^2)(a^2-c^2)^2]}.$$

This vanishes if $a = c$ (it is impossible to make $t_A^2 = 1$ in practice), so that the best disposition of electrodes would seem to be reached by placing the potential terminals on the circumference of the circle, as their position will not then be sensitive to slight inaccuracies of construction.

* This result also follows by differentiating equation (5) with respect to *y*.

LIX. *Langmuir Probe Measurements in the Normal Copper Arc. By* ERVIN H. BRAMHALL *.

ABSTRACT.

LANGMUIR'S theory of a collector in an ionized gas is applied to the normal arc in air, the collector being a fine platinum wire which is made to swing horizontally through a section of the arc. The volt-ampere probe characteristic is obtained by interposing between the cathode and probe a small alternating potential superimposed on a direct potential of suitable magnitude, and recording the current on an oscillograph used in conjunction with an amplifier. The complete characteristic is thus obtained on a single oscillogram. It is found that the density of the drift current is of the order of 100 times that of the random current, which leads to the conclusion that the temperature motion of the electrons is relatively unimportant. This complicates the interpretation of the probe characteristic according to the collector theory, so that, although satisfactory measurements of space potentials in the arc are secured, it is found possible to obtain only rough approximations to the electron density and energy. The results indicate a density of the order of 7×10^{11} cm.$^{-3}$ and an average energy of 2 volts.

The voltage gradient between the cathode fall space and the anode glow is found to be non-uniform, increasing greatly close to the electrodes. By extrapolation a cathode fall within the range, 11 to 13 volts, which is considerably below that generally accepted, is obtained.

Equations for the arc characteristics based on a uniform gradient, such as those of Steinmetz and Ayrton, are shown to be untenable at short lengths.

1. INTRODUCTION.

AS long ago as 1888 Letcher † used a small electrode or probe, introduced into the arc discharge, to ascertain what was known as the back e.m.f. of the arc. Since then probe methods have been used by a series of investigators ‡ to determine space potential, arc gradient, cathode and

anode falls, and arc resistance ; employing, however, either a capacity or high resistance in series. Their results for the most part were rendered invalid by Langmuir and Mott-Smith *, who showed that under the condition of practically zero probe current the probe assumes a potential at which the number of positive ions absorbed is equal to the number of electrons, and that this potential differs considerably from the space potential.

It was shown that if the ions collected by a probe have a random or Maxwellian distribution the logarithm of the probe current is a linear function of the probe potential with respect to space, if this potential is such that arriving electrons are retarded, *i. e.*, negative. The slope of this line and the point where this slope changes provide information from which the space potential, the electron concentration, and the distribution temperature may be calculated.

The Langmuir probe (utilizing the above principle) is most readily adapted to the study of low-pressure discharges in which the temperature is not too high to permit the continuous immersion of the probe. It has been used thus by Emeléus†, Uyterhoeven‡, and others in the low-pressure glow discharge, and by Compton, Van Voorhis §, and others in the mercury arc. Nottingham ‖ has recently extended its use to arcs between metal electrodes at normal pressure by swinging the probe at a known rate through the arc and measuring the total charge through the probe circuit at different voltages on a ballistic galvanometer.

The present investigation deals with the conditions existing in the arc between copper electrodes at atmospheric pressure. The principle of the Langmuir probe is utilized in so far as limitations imposed on it by the experimental conditions allow.

It is realized that the collector theory of Langmuir and Mott-Smith is not strictly applicable to the study of high-pressure discharges in which the electronic mean free path is so short that collisions in the ion sheath surrounding the collector can no longer be neglected. An application of the theory is, however, of importance if for no other reason than to indicate to what extent it may be relied upon to elucidate the complicated processes occurring in the normal

* Phys. Rev. xxviii. p. 727 (1926); Gen. Elect. Rev. xxvii. pp. 449, 538, 616, 762, 810 (1924).
† Camb. Phil. Soc. Proc. xxiii. p. 531 (1927).
‡ Nat. Acad. Sci. Proc. xv. p. 32 (1929).
§ *Ibid.* xiii. p. 336 (1927).
‖ Franklin Inst. Journ. ccvi. p. 43 (1928); ccvii. p. 299 (1929).

arc ; for it is indisputable that the probe method is the most powerful yet available for this purpose.

2. Theoretical Considerations.

The Collector Characteristic.

The complete current-voltage characteristic consists of three distinct parts :—

(*a*) When the probe is sufficiently negative to repel all electrons its current is small and consists entirely of positive ions which form a sheath around it of such a thickness that the probe exerts no influence beyond its boundaries.

(*b*) As the potential is made less negative, so that some electrons are able to pierce the sheath in spite of the retarding potential, the net positive ion current falls off and finally changes sign. This is the region where the Langmuir probe characteristic,

$$i = \mathrm{I} A \epsilon^{\left(\frac{e V}{KT}\right)}, \quad \ldots \ldots \quad (1)$$

obtains. I is the random electron current density [*] in amps./cm.^{2} (*i. e.*, the random electron current at space potential divided by the area of contact, A, between the probe and the ionized gas), V is the probe potential with respect to that of space, *e* is the electronic charge, 1.59×10^{-19} coulombs, K is the Boltzmann constant, 1.37×10^{-16} ergs per degree, and T is the temperature corresponding to the Maxwellian distribution of electrons.

(*c*) When the space potential is reached the sheath, which has been decreasing in thickness, vanishes. The collector then receives the random, electron, and positive ion currents. The latter is so small as to be practically negligible compared with the former because of the relatively low speeds of the heavy positive ions ; and the total current is therefore negative.

The above considerations apply in their entirety only to the ideal case of ions having a purely thermal distribution. Actually this condition is never strictly fulfilled in any electric discharge, since there is always a drift of electrons

---

[*] The random current density is defined as the current in one direction due to the random motion of electrons through unit area of a plane perpendicular to that direction, and is given by the relation

$$\mathrm{I} = \frac{nev}{4},$$

n being the electron concentration, and *v* the mean velocity of thermal agitation.

and ions towards the electrodes, this constituting the current through the external circuit. In low-pressure discharges * the random and drift currents seem to be of about the same magnitude, but no previous determination of the relative magnitudes of these quantities has been made for the normal arc discharge between metal electrodes. It is therefore important to estimate the ratio of drift to random current densities, I_d/I, and to allow for its influence in the interpretation of results.

Fig. 1.

SWITCH AND PROBE

3. EXPERIMENTAL PROCEDURE.

The arc is drawn between $\frac{1}{8}$-in. copper electrodes arranged in a vertical position as in fig. 1, the lower electrode being the cathode (negative). An insulated platinum probe, 0·012 in. diam., swings horizontally through the arc at the rate of 13 cm./sec., which remains practically constant for the short period it is in contact with the arc. The probe potential is adjusted by means of a battery interposed between the probe and cathode.

The entire sequence of operation necessary to draw the arc, record the transient phenomena, and break the circuit

* Emeléus, ' Conduction of Electricity through Gases,' p. 50.

is performed automatically by a series of contacts operated by a falling weight. The total time elapsing between the make and break of the arc is thus made a small fraction of a second, thereby minimizing contact oxidation and other effects which tend toward non-uniformity of operation.

Methods of Measurement.

(a) *Using the Ballistic Galvanometer.*

To obtain the Langmuir probe characteristic, the method of Nottingham * was first tried. A ballistic galvanometer measures for different potentials the total charge, Q, picked up by the probe as it swings through the arc. Q is propor-

Fig. 2.

POSITIVE ION SATURATION CHARACTERISTIC

tional to i_p, the current per unit length of the probe, in accordance with the relation
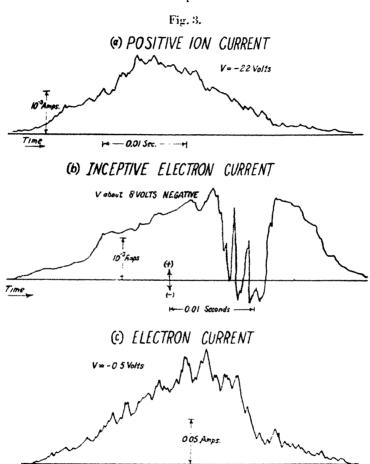
$$Q = \pi R_a{}^2 i_p/u,$$

where R_a is the arc radius and u is the probe velocity.

The positive ion saturation characteristic (fig. 2) could be obtained by this method, but in the region where equation (1) applies the results were too erratic to be satisfactory.

It is observed in connexion with this experiment that even with a probe potential 140 volts negative from space, that is, more negative by a value in excess of 100 volts than the cathode itself, the discharge is not interrupted. This

* *Loc. cit.*

illustrates the importance of a high cathode temperature in the low voltage arc, since the existence of such a temperature, producing an electron source in the cathode, is the only real distinction between it and the probe.

Fig. 3.

(a) POSITIVE ION CURRENT

V = -22 Volts

10^{-3}Amps.

Time

┣— 0.01 Sec. ——┤

(b) INCEPTIVE ELECTRON CURRENT

V about 8 VOLTS NEGATIVE

10^{-3}Amps

(+)

Time

(-)

┣—0.01 Seconds ——┤

(c) ELECTRON CURRENT

V = -0 5 Volts

0 05 Amps.

Time

┣ 0004Sec. ┤

(b) *Using the Oscillograph with Amplifier.*

Alternatively the oscillograph was used in conjunction with a resistance coupled amplifier. Fig. 3 represents typical examples of records taken at different probe potentials. In (a) only positive ions are being collected—the probe potential is sufficiently negative to repel all electrons, so that

the current is small and positive. In (c) the current consists almost entirely of electrons, so that the current is large and negative.

As the probe voltage with respect to the cathode is raised in successive steps, approaching space potential, it is interesting to note the effect on the probe current. The maximum current (fig 3 (a)) decreases slightly, due to the decreasing thickness of the positive ion sheath and the consequent reduction in the contact area between the probe and arc; otherwise there is little disturbance until the potential is about 10 volts below that of space. Then indentations appear, due to the penetration of electrons into the sheath, particularly toward the centre of the arc, where the electron energy is maximum, as is evident in fig. 3 (b). Finally, the
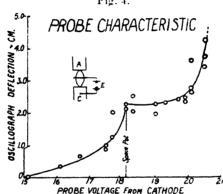
Fig. 4.

current completely reverses in direction and increases greatly in magnitude, its character being generally irregular (fig. 3 (c)). This explains the erratic behaviour of the ballistic galvanometer when used to measure the electron current.

By measuring the variation of probe current near the centre of the arc as the potential is raised it was found possible to obtain the characteristic (fig. 4) provided that a sufficient number of records were taken   However, a more promising and less laborious method was devised. making use of an alternating probe potential.

When the peak of the alternating voltage is high enough to intersect the space potential the resulting current is represented in fig. 5. This oscillogram shows clearly the rapid variation of probe current as the space potential is approached, and suggests that the Langmuir probe characteristic might be obtained directly if, in the proximity of

space potential, the probe voltage were to vary more slowly.

This condition is fulfilled by the superposition of a small alternating potential on to a relatively high continuous voltage. Fig. 6 is an oscillogram thus obtained, the probe

Fig. 5.

PROBE CURRENT *with* ALTERNATING P. D.
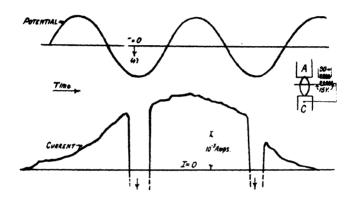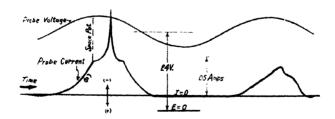
Fig. 6.

OSCILLOGRAM *of* PROBE CURRENT *and* VOLTAGE

24 Volts D C and 3 Volts A.C. on Probe
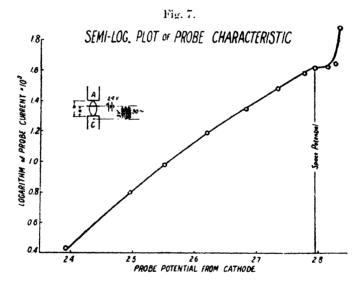
voltage being 3 volts, r.m.s., and 24 volts, d.c., with respect to the cathode. It was taken with the probe at a distance, *a*, 0·34 cm. from the cathode, with an overall arc length, *b*, of 0·39 cm., and an arc current of 7·5 amp. On this oscillogram the voltage vibrator measures the total probe voltage. Actually greater accuracy is attainable when this vibrator is connected only across the alternating potential.

4. EXPERIMENTAL RESULTS.

The Ratio of Drift to Random Currents.

Fig. 7 shows that the semi-logarithmic plot of section (*a*) (fig. 6) is noticeably convex towards the voltage axis. According to the theory of Langmuir and Mott-Smith such a deviation from a straight line relationship signifies the existence of a ratio of drift to random currents high enough to influence the interpretation on the assumption of a purely thermal electron distribution of the probe characteristic. Consequently it is necessary to estimate this ratio.

Fig. 7.

SEMI-LOG. PLOT OF PROBE CHARACTERISTIC

The drift current density,

$$I_d = \frac{I_a}{\pi R_a^2},$$

depends on the arc current, I_a, and the arc radius, R_a, at the section where the probe is introduced. The probe velocity being known, it is possible to estimate the arc diameter by noting the time on the oscillogram of probe current during which there is an observable deflexion. The result depends on the contribution of the region, consisting of ionized gases, surrounding the central nucleus towards the total current, the probe potential with respect to space, and the amplifier sensitivity. Therefore, since there is no evident manner of correlating the probe position with time on the oscillogram,

to obtain an unambiguous measure of R_a it is necessary to resort to a roundabout method.

As the probe enters the region surrounding the arc nucleus the current density to it should increase slowly at first, due to the increasing temperature and ion density. A greater increase should be noted as soon as the nucleus is reached, and thereafter the density of the probe current should remain more or less uniform. Consequently a study of the variation of probe current density, i, with the distance, X, between the centre-lines of probe and arc should afford a means of calculating R_a.

For a constant arc area the area of contact between the probe and arc depends on the effective probe radius which is the probe radius, c, plus a positive ion sheath of thickness, σ, which varies with the probe potential with respect to space. It is found that the experimental positive ion saturation characteristics correspond roughly to $\sigma = 0\cdot017\,cV$ when $V < -15$ volts, *i. e.*, sufficient to repel practically all electrons. The theory * for a plane collector gives

$$\sigma = \frac{k V^{3\cdot4}}{\sqrt{I_p}},$$
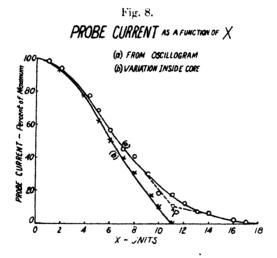
where I_p is the positive ion current density and k is constant. The difference between the two relations may be attributed to high pressure effects, probe curvature, and sheath distortion due to the drift.

From the foregoing the quantity $(c + \sigma)$ is known for a specific example, and for convenience is made equal to unity. Then oscillograms such as fig. 3 (*a*) are readily convertible to curves giving the variation of positive ion current with X in units. Since, according to fig. 10, the increase of the area of contact, A, with X is almost linear until A is about 60 per cent. of the maximum, in this region the total current as a function of X should have the same form as that of the current density. In the example (fig. 8) the curve (*a*) is the total current. At P, the point where the slope changes, $X = 11$ units and $i = 11$ per cent This latter represents the contribution of the region surrounding the arc nucleus, and must be subtracted from the total current to obtain that part which may properly be ascribed to the nucleus alone. Subtracting 11 per cent. from the ordinates of (*a*) and multiplying by 100/89 (to make the maximum current 100 per cent.) curve (*b*) is obtained, which is the true

---

* Emeléus, *ibid.* p. 43.

variation of i with X. The arc radius is in this case $(11-1)$, or 10 units.

The calculation of R_a by the method of fig. 8 at different sections along the arc stream does not produce very consistent results, especially when a, the distance from the cathode, is large. The data for the conditions, $I_a = 8$ amp., $b = 1\cdot2$ cm., and a from $0\cdot1$ to $0\cdot5$ cm., conform roughly to the equation

$$B = 0\cdot005 + 0\cdot21\,a,$$

where B is the arc area and is πR_a^2. This gives a current density at the cathode, $(a=0)$, of 1600 amp./cm.^{2}, which, however, is unreliable because practical considerations impose

Fig. 8.

PROBE CURRENT AS A FUNCTION OF X

(a) FROM OSCILLOGRAM
(b) VARIATION INSIDE CORE

a lower limit of about 1 mm. on a, this being insufficiently close to justify extrapolation to the cathode. Otherwise the cathode current might be obtained directly. The drift current density calculated from (10) varies from 310 at $a = 0\cdot1$ cm. to 70 amp./cm.^{2} at $a = 0\cdot5$ cm.

The literature on the subject is singularly lacking in directly comparable data, and the current density at the cathode is not known even approximately. It undoubtedly lies between 250 and 7000 amp./cm.^{2}, the values given by Compton * for carbon and iron, and is probably within the range given for tungsten, viz., 700 to 3200 amp./cm.^{2}. Compton's value for the current density in the middle of a *carbon* arc is 50 amp./cm.^{2}.

* Phys. Rev. xxi. p. 266 (1923); Journ. A. I. E. E. xlvi. p. 1192 (1927).

Since for short arcs any sectional area, and consequently the current density, varies with the total arc length, it is next to impossible to formulate a general law, and it becomes necessary to determine the area experimentally for each set of conditions. By the method described an accuracy not greater than 50 per cent. could be expected.

In the absence of a drift velocity, *i. e.*, for a purely thermal distribution, the electron current at space potential divided by the contact area would be the random current density, I. This amounts to between 1 and 5 amperes per square cm. in the present experiments, which, however, may differ considerably from the true random current because of the electron drift. In lieu of more accurate experimental data it can only be concluded that the ratio, (I_d/I), appears to be very high, and may exceed 100. This is much higher than in the low-pressure discharge, where the ratio seems to be about unity [*].

Analysis of the Probe Characteristic.

The work of Langmuir and Mott-Smith [†] shows that, due to such a high ratio, the probe characteristic should approach one of two limiting forms corresponding to the case of ions having a large drift velocity on which is superimposed a relatively small temperature motion :

(1) When the retarding voltage, V, is small compared to V_0, the voltage equivalent of the drift velocity, in the limit as the temperature decreases,

$$i = 2cl\mathrm{I}\sqrt{1 + \mathrm{V}/\mathrm{V}_0} \quad \text{for V greater than } -\mathrm{V}_0,$$

$$= 0 \quad \text{for V less than } -\mathrm{V}_0,$$

in which c and l are the radius and length of the cylindrical collector.

(2) When the retarding voltage is nearly equal to or greater than V_0, the temperature motion though, small, becomes important as $-\mathrm{V}$ approaches V_0. For λ positive

$$\left(\lambda = \sqrt{\frac{e}{\mathrm{K}\mathrm{T}}}(\sqrt{\mathrm{V}_0} - \sqrt{-\mathrm{V}})\right),$$

the current is approximately a parabolic function of $(\mathrm{V}_0 - \mathrm{V})$. while with λ negative the current decreases rapidly, $\log i$ becoming nearly a linear function of λ^2.

* Eméléus, 'Conduction of Electricity through Gases,' p. 50.
† Phys. Rev. xxviii. p. 727 (1926); Gen. Elect. Rev. xxvii. pp. 449, 528, 616, 762, 810 (1924).
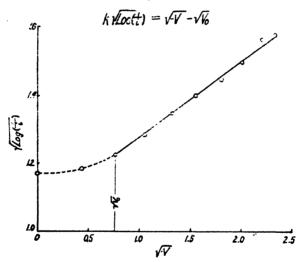
From the form of the probe current-voltage curve (fig. 7), it is evident that the relative importance of the temperature and drift motions in the arc is such that (2) is the limiting form. This means that the temperature motion is great enough to become important when the retarding voltage, V, is small. The plot of

$$\sqrt{\log\left(\frac{1}{i}\right)} \ vs \ \sqrt{-V}$$

should be approximately linear when V is less than $-V_0$. Fig. 7 is replotted, using these coordinates as in fig. 9. The curve is linear for $\sqrt{-V} > 0.8$, so that the theory gives

$$V_0 = (0.8)^2 = 0.64.$$

Fig. 9.

$$k \sqrt{\log\left(\frac{t}{i}\right)} = \sqrt{V} - \sqrt{V_0}$$

Electron Density and Energy.

If u_0 is the drift velocity and e is in e.s.u., it follows that

$$V_0 = \frac{mu_0^2}{2e}.$$

Thus,

$$u_0 = \left(\frac{2eV_0}{m}\right)^{1/2} = 0.82 \times 10^9 \ \text{cm./sec.}$$

Since the drift current density is

$$J_d = \frac{neu_1}{3 \times 10^9},$$

the electron density is

$$n = \frac{3 \times 10^9}{eu_0} I_d.$$

Taking $I_d = 100$ amp./cm.^{2}, $n = 7.7 \times 10^{11}$. This compares with 1.8×10^{10} and 11.4×10^{10} given by Emeléus† for low-pressure mercury discharges.

The approximate slope of the curve (fig. 7) near space potential is 0.55 ; so that the apparent electron distribution temperature, neglecting the influence of the drift velocity, is

$$T = \frac{e}{0.55 \, K} = 20,900° \text{ C.,}$$

and the equivalent energy is 2.7 volts. These and other representative data similarly obtained for different conditions in the arc are incorporated in the following table.

I_d (amp.).	a (cm.).	b (cm.).	e_a (volts).	e_s (volts).	T (° C.).	e_s*.	e_s.	T.
				Column 1 (central).			Column 2 (side).	
7.5	0.05	0.39	37.8	20.1				
	0.05	...	..	19.5	...	18.5		
	0.11	...	...	24.0	18.300	22.0	22.8	
	0.26	...	...	24.1				
	0.26	...	...	23.8	...	23.0		
	0.34	...	...	28.1	...	...	27.9	10,300
	0.34	...	...	27.2	16,700	26.5	27.7	8.850
	0.34	...	...	28.0	20.900			
4.1	0.18	0.32	46.0	25.5	7.900	23.5		
	0.26	0.49	58.0	30.5	...	29.4		
2.9	0.26	0.49	70.0	...	...	38.0	38.9	

* Indicated space potential corrected for voltage rise due to the introduction of the probe.

b is the arc length and a is the distance between the cathode and the plane section covered by the probe as it swings through the arc. The data of column 1 correspond to a probe position nearly central in the arc, while that of column 2 is for a lateral position.

The electron energy calculated from the temperatures of the table varies from 2.1 to 2.7 volts, but this is merely an

† 'Conduction of Electricity through Gases,' pp. 40, 51.

indication of its magnitude, since the error due to neglecting the drift velocity is indeterminate.

Effect of Variation of Contact Area.

Equation (1) shows that the total probe current depends on the contact area between probe and arc, so that the above analysis is valid only on the assumption of constant A. If the voltage variation is sufficiently rapid, or if the probe moves sufficiently slowly, the entire characteristic can be obtained in such a short time that the probe may be considered stationary in the arc for this period, in which case A is constant. However, the accuracy of measuring the current variation on the oscillogram decreases as the time is made shorter, and this factor limits the optimum rate of change of probe voltage. A lower limit for the probe velocity is fixed by its melting-point and the relative sizes of probe and arc. With a velocity of 13 cm./sec. and a 90-cycle voltage the complete characteristic is obtained within $\frac{1}{8}$ of a cycle or $\frac{1}{720}$ sec. The distance moved by the probe during this time is 0·018 cm., which is not more than $\frac{1}{6}$ of the arc radius extant in most of the experiments.
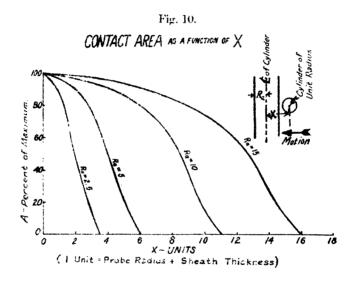
In order to estimate the change in contact area due to a motion of this magnitude the probe and arc are assumed to behave as cylinders, and the variation of surface contact area between them for different relative sizes is obtained graphically as a function of the distance between their centre-lines. It is convenient in fig. 10 to plot areas, A, as percentage of maximum, and distances, X, in units, one unit being the radius of the smaller cylinder.

Fig. 10 shows that if the probe position is near the centre of the arc A is practically constant over a period corresponding to $\frac{1}{6}$ of the arc radius. On the other hand, for a lateral position A may vary as much as 30 per cent. In the latter case it is necessary to allow for the variation of A in obtaining the true probe characteristic. This process entails considerable labour and is of doubtful accuracy, so that with few exceptions only the former case is considered when estimating the electron energy.

Potential Distribution.

From the tabulated data the potential distribution and the potential drops at the anode and cathode can be studied First, however, the effect on the indicated space potential of the introduction of the cold, cylindrical probe should be

considered. The most obvious consequences are : (1) distortion or lengthening of the arc stream by impeding the natural motions of the ions ; (2) a high local cooling of the gases near the probe. The magnitude of the disturbance caused by both of these depends on the relative sizes of probe and arc, and is manifested by an increased overall voltage. Oscillograms of probe current, taken as the probe is traversing the arc, are generally symmetrical, and not unlike the curve of A as a function of X (fig. 10). This constitutes evidence that (1) is not important. The explanation probably lies in the high thermal motion of the electrons.

Fig. 10.

considered.

The actual rise in overall potential varies from 1 to 6 volts in the various experiments, depending on divers factors. It is necessary therefore to correct the indicated space potential for the voltage rise due to the introduction of the probe.

It seems unquestionable that the rise caused by (2) is entirely localized. In the steady state the loss of ions by diffusion and recombination at any section is exactly balanced by the number generated in that section by collisions of electrons with gas molecules. The introduction of the probe, by cooling the gas, increases the coefficient of recombination, which depends approximately on the third power of the temperature, and upsets the balance, necessitating an increased ion generation in its vicinity. This means that the

local gradient must be increased so that a higher percentage of the electrons acquire sufficient energy in the field to ionize on collision.

In accordance with this view, in obtaining the best values for space potential, half of the total voltage rise is assumed to occur between the probe and cathode, and is added to the indicated space potentials of the table.

The indicated space potential in the example (fig. 7) is 28 volts, and it is interesting to note that this is about 4 volts higher than would be obtained by the old method of measuring the potential assumed by a probe taking zero current.

Fig. 11.
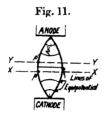
Fig. 12.

INFLUENCE of HIGH CENTRAL SPACE POTENTIAL
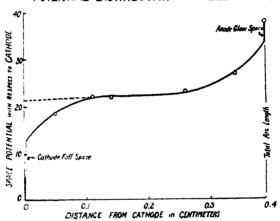
It is observed that e_s depends on the instantaneous probe position and may vary throughout the same section. There is definitely an increase or decrease in e_s when this position is towards the outer edge of the arc, according as the section considered is further from or closer to the cathode than the section bisecting the axis. The lines of equipotential in the arc are probably somewhat similar to those indicated in fig. 11. If the plane X–X is that covered by the probe it is evident that e_s is less at point p than at the axis, while the reverse is true in the plane Y–Y. This view is confirmed by an oscillogram (fig. 12) representing the former case. The arc current is 8 amperes, and the probe voltage with respect to the cathode remains constant at $+23\cdot5$ volts, which is slightly less than the space potential at the axis in

the section covered by the probe. The electron current is markedly higher towards the sides than at the centre, showing that the corresponding space potentials must be lower. At increased distances from the centre the current is naturally limited by the lower temperature and density of the electrons.

The potential distribution along the axis is plotted in fig. 13 for $I_e = 7\cdot5$ amp. and $b = 0\cdot39$ cm. The gradient U, which is the slope of this curve, evidently increases greatly towards the electrodes, though it becomes uniform a short distance away from them. This curve illustrates the fallacy

Fig. 13.

POTENTIAL DISTRIBUTION ʙᴇᴛᴡᴇᴇɴ ELECTRODES

in the assumption of a uniform gradient which is commonly made *.
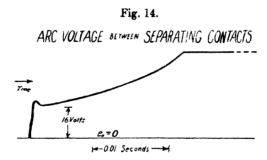
The increased gradient near the electrodes can be attributed to the cooling of the gas immediately adjacent, affecting the loss of ions and the gradient in the same way as did the introduction of the cold probe.

It is apparent from fig. 13 that large errors are likely to accrue if the cathode and anode falls are obtained by extrapolation to the electrodes on the basis of a uniform gradient. Particularly is this true if the gradient used is that obtaining midway between the electrodes. The closer to the cathode the potential is measured the less becomes the resulting

* Chrisler, Astrophys. Journ. liv. p. 273 (1921), also notes a non-uniform gradient.

error; but the proximity of the probe to the cathode is limited by practical considerations, so that accuracy is difficult to obtain.

If the central gradient be continued to the cathode (dotted lines, fig. 13) the present example gives 21 volts as the cathode fall. A facile experiment disproves such a high value, showing that it may be 50 per cent. or more in error. Fig. 14 reproduces an oscillogram of arc voltage taken as the contacts are separating. The minimum overall potential is only about 16 volts, and this remains practically the same for arc currents varying from 4 to 50 amperes, increasing at lower currents. The same is true for $\frac{1}{2}$-in. electrodes, so that size is not an important factor. The fact that the voltage is initially higher than this may be explained by the theory of collisions * when the arc length is less than the

Fig. 14.

ARC VOLTAGE *between* SEPARATING CONTACTS

16 Volts

$e_o = 0$

↦-*0·0i* Seconds —↦

molecular mean free path. The minimum should occur when the length is equal to the thickness of the cathode fall space, in which case there is no positive column and the arc voltage is the sum of the anode and cathode falls †.

---

* J. J. Thomson, ' Conduction of Electricity through Gases,' p. 381 ; J. S. Townsend, ' Electricity in Gases,' chap. 8, 9.

† It has recently been stated (Bruce. Journ. I. E. E. lxix. p. 557 (1931)) that e_c, the contact voltage drop, which is the sum of anode and cathode falls, approaches 30 volts ; and supporting experimental data are cited which give values of e_c ranging from 18 to 40 volts. However, in most of these cases the measurement was made on a low sensitivity scale—that is, the constants of the oscillograph circuit were not adjusted to give an accurate low voltage reading. The value, 16 volts, obtained above for *non-oxidized* contacts of pure copper, is probably more nearly correct, since the maximum oscillograph deflexion was made to correspond to a low voltage (about 20 volts) by limiting the arc length to a very small value. It must be remembered, however, that this value is not absolute, since the anode fall particularly is to some extent influenced by the experimental conditions.

The above fact and observations of the trend of the potential curves, similar to fig. 13, indicate a probable cathode fall within the range, 11 to 13 volts, and an anode fall from 3 to 5 volts. This latter value is applicable only for the particular experimental conditions.

As Compton * points out, the cathode fall is not necessarily the ionizing potential of the medium in which the arc is drawn, but it is interesting to note that Wahlin † gives 10·9 volts as the ionizing potential of copper vapour. In a copper arc in air at reduced pressure Hagenbach ‡ gives a cathode fall of 13·7 volts, which is nearly within the range determined. Nottingham § finds a value of 20·5 volts, but on the assumption of a uniform gradient between the probe and cathode. Chrisler ‖ gives a value of 16 volts.

Another instance occurs in the literature where the accepted cathode fall in a *tungsten* arc is greater than the overall voltage. Compton ¶ gives 16·2 volts for tungsten in hydrogen, while arcs have been obtained ** having an overall voltage less than 14 volts at 12 amperes and 17 volts at 2 amperes, the arc length being extremely short. Incidentally, if the cathode fall depends on the electron work function of the cathode material, as appears to be the case in the glow discharge ††, copper, which has a lower work function than tungsten, should also have a lower cathode fall.

Further evidence is forthcoming to show how the electrodes affect the gradient in their vicinity. After the source voltage, E, and the initial current, I_0, in a low-inductance circuit have been adjusted to the desired values, records of arc voltage similar to fig. 14 are taken as the contacts separate with an acceleration predetermined by adjustment of the spring, S, fig. 1. Then at any instant after the contacts start to separate the arc voltage and length are known. The corresponding arc current is obtained graphically or by the relation

$$I_a = I_0 \left(I - e_a/E\right).$$

The data from a number of such records taken at different initial currents, and voltages when necessary, give the characteristics at different arc lengths. For the present

---

* Phys. Rev. xxi, p. 266 (1923); Journ. A.I.E.E. xlvi. p. 1192 (1927).
† Phys. Rev. xxxii. p. 277 (1928).
‡ *Handb. d. Phys.* Springer, xiv. p. 335.
§ Franklin Inst. Journ. ccvi. p. 43 (1928); ccvli. p. 299 (1929).
‖ *Loc. cit.*
¶ *Loc. cit.*
** Anderson and Kretchmar, Phys. Rev. xxvi. p. 33 (1925).
†† 'International Critical Tables,' vi. (1929).

purpose it is convenient to plot e_a as a function of l for constant currents, as in fig. 15.
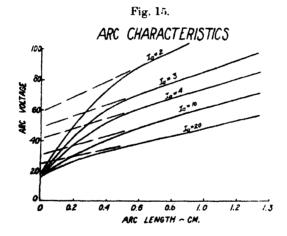
When l is large these curves are linear, indicating a uniform gradient, but as l decreases they become concave towards its axis. This curvature at short lengths means an increase in gradient which may undoubtedly be attributed to the proximity of the electrodes

The average gradient, which is $(e_a - \mathrm{C})/l$, where C is the sum of anode and cathode falls, is obtained as a function of current with other parameters constant. The results, plotted on logarithmic paper, as in fig. 16, while not conforming exactly to the relation

$$ \mathrm{U} = k\mathrm{I}_a{}^{-n}, $$

Fig. 15.

ARC CHARACTERISTICS

where U is the gradient and k and n are constants, do approximate to it in the range, 0·5 to 15·0 amperes. The best value of n is about 0·6. Then, since the arc area, B, varies as I_a, U varies as $\mathrm{B}^{-0·6}$. Assuming that B varies as some power, p, of l within definite limits, $\mathrm{U} = k_2 l^{-0·6p}$. Then

$$ e_a = \int \mathrm{U} dl = k_3 l^{(1 - 0·6p)}. $$
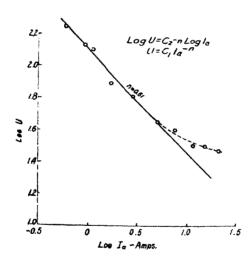
It follows that a straight line should connect $\log e_a$ and $\log l$, having a slope $(1 - 0·6p)$. Values of e_a and l from fig. 20 fulfil this condition very closely in the range 3 to 20 amperes, and l up to 0·25 cm. The slopes correspond to values of p from 0·92 to 0·99, decreasing with current. Therefore

within the specified limits the average arc area is approximately proportional to l, while the average gradient depends on the 0·6 power of this quantity.

For this reason equations such as those of Ayrton * and Steinmetz †, expressing the arc voltage in terms of current and length, which are based on a uniform gradient, are untenable when the arc length is short—that is, when the influence of the electrodes is important. Moreover, referring to fig. 13, the average gradient between the cathode fall space and any point in the arc depends in no simple manner on their distance apart, and has no physical significance.

Fig. 16.

VARIATION OF GRADIENT WITH ARC CURRENT

$$Log\ U = C_2 - n\ Log\ I_a$$
$$U = C_1\ I_a^{-n}$$

5. SUMMARY OF RESULTS AND CONCLUSIONS.

1. It may be concluded from the experimental results that the theory of the collector in an ionized gas may be applied to the case of the normal arc in air to obtain space potentials, but that extraneous factors prevent an accurate interpretation of the volt-ampere probe characteristic for the purpose of estimating the electron density and energy on the basis of this theory.

* H. Ayrton, ' The Electric Arc,' p. 186.
† C. P. Steinmetz, Trans. A. I. E. E. xxv. p. 802 (1906).

2. The probe characteristic is shown to approach a certain limiting form corresponding to a relatively small temperature motion of the electrons in the arc superimposed on a high drift velocity.

3. Measurements of sectional area in the arc stream by means of the probe give current densities from 70 to 310 amperes per square centimetre, increasing beyond this near the electrodes; and rough estimates of the actual ratio of drift to random currents show that this may exceed 100.

4. The electron density in the arc is found to be of the order of 7×10^{11} cm.$^{-3}$, and the average energy about 2 volts.

5. From measurements of space potential at various points in the arc it may be concluded that—

(*a*) The potential may not be the same throughout any sectional area. It may be higher or lower at the axis than towards the sides depending on the position of the area considered relative to the electrodes.

(*b*) The assumption of a uniform gradient between the cathode fall space and the anode glow is unjustified, the gradient increasing greatly near the electrodes.

(*c*) The cathode fall is probably within the range, 11 to 13 volts, which is comparable with the ionizing potential of copper vapour.

6. It is shown that equations similar to those of Ayrton and Steinmetz for the arc characteristics are untenable when the arc length is short, due to the variation of the average gradient with length.

LX. *Special Examples of the Elastic Ring acted upon by Equal and Equiangular Radial Forces.* *By* C. E. LARARD, *M.Inst.C.E.* *

IN an investigation dealing with a circular elastic ring of uniform cross-section acted upon by any number of equal and equiangular forces the author obtained general equations for the two maximum flexural moments† on radial sections of the ring and also for the two maximum radial strains.

It is of some importance to calculate the particular values of the above quantities when N, the number of forces, is 2, 3, 4 ... to 16.

The general equation given for the maximum negative flexural moment ‡ is

$$M_1 = \frac{PR}{2}\left(\cot\alpha - \frac{1}{\alpha}\right), \quad \ldots \ldots \quad (1)$$

and for the maximum positive moment §

$$M_c = \frac{PR}{2}\left(\operatorname{cosec}\alpha - \frac{1}{\alpha}\right). \quad \ldots \ldots \quad (2)$$

Reference to the illustrations in column 2 of Table I. will make clear the particular cases here considered.

The angle α in the above equations (1) and (2) is half the angle between any two adjacent forces, and is therefore equal to π/N. Thus α takes successively the values $\pi/2$, $\pi/3$, ... $\pi/16$. Substituting these values in turn in equations (1) and (2) the results in columns 3 and 4 of Table I. are obtained. They are also plotted in the accompanying figure.

The numerical values of K_1 in column 3 give the maximum negative flexural moments per unit values of PR, and the values of K_2 in column 4 the maximum positive flexural moments per unit of PR.

The first of these maximum moments occurs at radial sections of the ring containing the line of action OP, and the second maxima at the radial sections midway between the lines of action of any two adjacent forces.

Comparing the values given in columns 3 and 4 of Table I. it will be noticed that the moments at the OP

---

* Communicated by the Author.
† Phil. Mag. xii. (July 1931), equations (6) and (8), p. 132.
‡ *Loc. cit.*
§ *Loc. cit.*

Table I.
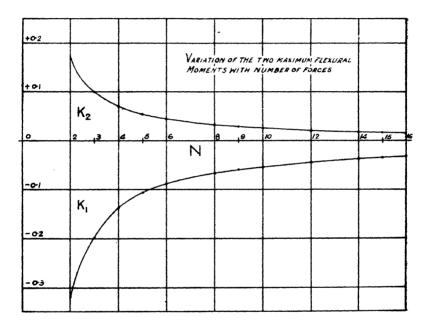
1.	2.	3.	4.
			Maximum flexural moments.
Number of forces. N.	System of N equal forces. $\alpha = \dfrac{\pi}{N}$.	M_1 at section of each P $= \dfrac{PR}{2}\left(\cot\alpha - \dfrac{1}{\alpha}\right)$ $= K_1 PR$. Values of K_1.	M_c at mid-section between two adjacent P s $= \dfrac{PR}{2}\left(\operatorname{cosec}\alpha - \dfrac{1}{\alpha}\right)$ $= K_2 PR$. Values of K_2.
2........		−0·31831	0·18169
3........		−0·18879	0·09969
4........		−0·13662	0·07049
5........		−0·10758	0·05487
6........		−0·08890	0·04507
8........		−0·06613	0·03332
9.... ..		−0·05866	0·02951
10........		−0·05271	0·02648
12........		−0·04386	0·02199
15...		−0·03501	0·01754
16........		−0·03281	0·01644

sections of the ring do not differ much from twice the values of those for the mid-sections between the forces.

Consider next the two maximum radial strains.

Equation (24)* in the author's original paper gives the general expression for the alteration in the length of each radius joining the centre, O, of the ring to the point of application of each force P ; and this is the maximum radial strain.

This equation is written again with the three terms near the head of columns 2, 3, and 4 in Table II.

For the special cases here considered α takes successively the values $\pi/2$, $\pi/3$, . . . $\pi/16$, and therefore the equation for any one of these values takes the form

$$y_{OP} = K_3 \frac{PR^3}{EI} + K_4 \frac{PR}{EA} + K_5 \frac{CRP}{GA} . \quad . \quad . \quad (3)$$

The numerical values of K_3, K_4, and K_5 for the different values of $\alpha = \pi/N$ are given in columns 2, 3, and 4 of Table II.

* *Loc. cit.* p. 134.

Thus the numerical values of K_3 represent the alteration in the lengths of the radius OP for unit value of $\dfrac{PR^3}{EI}$, when bending alone is considered. K_4 gives the additional strain on OP due to hoop-stress per unit value of $\dfrac{PR}{EA}$, and K_5 the extra strain per unit of $\dfrac{CRP}{GA}$ when shear is also taken into account.

TABLE II.

Total alteration in length of radius OP due to flexure, hoop-stress, and shear.

1. Number of forces. N.	2. Strain due to bending $\frac{1}{4}\left(a\operatorname{cosec}^2 a+\cot a-\frac{2}{a}\right)\dfrac{PR^3}{EI}$ or $K_3\dfrac{PR^3}{EI}$ +	3. Strain due to hoop-stress $+\frac{1}{4}(a\operatorname{cosec}^2 a+\cot a)\dfrac{PR}{EA}$ $K_4\dfrac{PR}{EA}$ +	4. Strain due to shear-stress. $+\frac{1}{4}(a\operatorname{cosec}^2 a)\dfrac{CRP}{GA}$ $K_5\dfrac{CRP}{GA}.$
	Values of K_3.	Values of K_4.	Values of K_5.
2.........	0·07439	0·39270	0·39270
3........	0·01594	0·49340	0·20473
4.........	0·00608	0·64270	0·14270
5.........	0·00298	0·79875	0·11056
6.........	0·00168	0·95661	0·09059
8.........	0·00069	1·27393	0·06683
9.........	0·00048	1·43287	0·05914
10.........	0·00035	1·59190	0·05306
12......	0·00020	1·91006	0·04404
15......	0·00010	2·38743	0·03511
16.........	0·00008	2·54657	0·03289

It may be stated that for most values of P, R, and A the second and third terms in equation (3) become numerically very small compared with the value of the first term, which considers flexure only.

The minimum radial strain occurs along a radius OC, where C is the mid-point on the arc between any two of the adjacent forces P, and the alteration in the length of OC is given by equation * (45 a) + (45 b) + (45 c) in the original

* *Loc. cit.* pp. 139, 140.

paper after Q has been written $=0$. Substituting $\alpha = \pi/N$, where N takes in turn the values $2, 3, \ldots 16$, the equation above simplifies to the terms given in columns 2, 3, and 4 of Table III., and these may be written

$$y_{OC} = K_6 \frac{PR^3}{EI} - K_7 \frac{PR}{EA} + K_8 \frac{CPR}{GA}.$$

The values of the three coefficients K_6, K_7, and K_8 are evaluated and given in the table.

TABLE III.

1.	2.	3.	4.
	Total alteration in length of radius OC due to flexure, hoop-stress, and shear.		
	Strain due to bending	+ Strain due to hoop-stress	+Strain due to shear-stress.
Number of forces.	$\frac{1}{4}\left[\frac{2}{\alpha} - \operatorname{cosec}\alpha(\alpha\cot\alpha+1)\right]\frac{PR^3}{EI}$ or $K_6\frac{PR^3}{EI}$	$+\frac{1}{4}[-\operatorname{cosec}\alpha(1+\alpha\cot\alpha)]\frac{PR}{EA}$ $-K_7\frac{PR}{EA}$	$+\frac{1}{4}[\operatorname{cosec}\alpha(1-\alpha\cot\alpha)]\frac{CRP}{GA}$ $+K_8\frac{CRP}{GA}.$
	Values of K_6.	Values of K_7.	Values of K_8.
2.........	0·06831	0·25	0·25
3.........	0·01426	0·46321	0·11414
4.........	0·00539	0·63123	0·07587
5.........	0·00263	0·79315	0·05750
6.........	0·00148	0·95345	0·04655
8.........	0·00061	1·27263	0·03393
9.........	0·00042	1·43197	0·02993
10.........	0·00031	1·59124	0·02679
12.........	0·00017	1·90968	0·02217
15.........	0·00009	2·38725	0·01763
16.........	0·00007	2·54640	0·01651

In this case also it is the first term, due to flexure, which accounts for most of the strain, the other two terms, due to hoop-stress and shear-stress, being relatively small for most ordinary values of P, R, and A.

A comparison of the coefficients K_4 (Table II.) and K_7 (Table III.) show, on plotting with N as the other variable, that after the value $N=4$ a close and approximate linear relationship exists between the variables; thus strain along

OP due to hoop-stress is given closely by $0{\cdot}15915\,\mathrm{N}\,\dfrac{PR}{EA}$ and strain along OC due to hoop-stress is $-0{\cdot}15915\,\mathrm{N}\,\dfrac{PR}{EA}$.

Comparing the effects of the shear-stresses on the two strains along OP and OC it will be seen that the values of K_s in column 4 Table II. are roughly twice the values of K_8 in column 4 Table III.

In conclusion, the author expresses his indebtedness to Dr. J. Ward and Mr. C. K. Larard for independently working out the numerical values given in the three tables.

Sept. 30, 1931.

LXI. *Periodic Orbits in a Field of Force defined by a certain Potential. By* M. A. HIGAB, *M.Sc., Ph.D., Lecturer in Mathematics in the Egyptian University, Cairo* *.

IN discussing the motion of an electron in the field of a non-neutral atom (Phil. Mag. vii. pp. 31–52, Jan. 1929, and vii. pp. 783–792, May 1929) the following problem arose :—

To find the condition for the existence of periodic orbits when a particle of unit mass moves in a field of force whose potential is

$$V = \mu \int F(r)\,dr + \frac{\lambda}{r^2} \int f(\theta)\,d\theta,$$

where r and θ are the usual polar coordinates and λ and μ are constants.

The object of the present paper is to establish that condition.

The equations of motion are

$$\ddot{r} - r\dot{\theta}^2 = -\mu F(r) + \frac{2\lambda \int f(\theta)\,d\theta}{r^3}, \quad . \quad . \quad . \quad (1)$$

$$\frac{1}{r}\frac{d}{dt}(r^2\dot{\theta}) = -\frac{\lambda f(\theta)}{r^3}. \quad . \quad . \quad . \quad . \quad (2)$$

* Communicated by the Author.

Equation (2) admits the integral

$$r^4\theta^2 = A - 2\lambda \int f(\theta)d\theta, \quad \ldots \ldots \quad (3)$$

where A is constant.

Since the left-hand side of equation (3) is positive, the right-hand side must also be positive.

Eliminating $\dot{\theta}$ between equations (1) and (3), we get

$$r = \frac{A}{r^3} - \mu F(r) ;$$

$$\therefore \quad \dot{r}^2 = -\frac{A}{r^2} - 2\mu \int F(r)dr + B, \quad \ldots \quad (4)$$

where B is constant.

To obtain the significance of the constant B we have

$$\tfrac{1}{2}(\dot{r}^2 + r^2\dot{\theta}^2) + \mu \int F(r)dr + \frac{\lambda \int f(\theta)d\theta}{r^2} = \frac{B}{2},$$

i. e., B is twice the total energy.

The Differential Equation of the Path.

From equations (3) and (4) we get

$$\frac{1}{r^4}\left(\frac{dr}{d\theta}\right)^2 = \frac{-\dfrac{A}{r^2} - 2\mu \int F(r)dr + B}{A - 2\lambda \int f(\theta)d\theta}.$$

Putting $u = \dfrac{1}{r}$, and writing $\dfrac{du}{d\theta} = u_1$, we get

$$u_1^2 = \frac{-Au^2 + 2\mu \int F\left(\dfrac{1}{u}\right)\dfrac{du}{u^2} + B}{A - 2\lambda \int f(\theta)d\theta}$$

as the differential equation of the path.

Periodic Orbits.

Two types of periodic orbits are to be discussed separately :—

    (*a*) Circular periodic orbits.

    (*b*) Periodic orbits in general motion.

(a) *Circular Periodic Orbits.*

Let $r=a$, where a is constant, the equations (1) and (3) give

$$a^4\dot\theta^2 = \mu a^3 F(a) - 2\lambda \int f(\theta)d\theta$$

and

$$a^4\dot\theta^2 = A - 2\lambda \int f(\theta)d\theta$$

respectively.

These two equations are identical if $A = \mu a^3 F(a)$.

Thus circular periodic orbits exist if

$$\mu a^3 F(a) - 2\lambda \int f(\theta)d\theta$$

is positive.

The time is given by

$$t + E = \sqrt{\frac{a}{\mu F(a)}} \int \sqrt{\frac{d\theta}{1 - \frac{2\lambda}{\mu a^3 F(a)}\int f(\theta)d\theta}} \cdot$$

where E is constant.

(b) *Periodic Orbits in General Motion.*

A necessary condition for periodic orbits is that u must be oscillatory. Putting $\dfrac{du}{d\theta} = 0$, we get

$$B - Au^2 + 2u\phi(u) = 0. \quad\dots\quad (5)$$

where

$$\phi(u) = \int F\left(\frac{1}{u}\right)\frac{du}{u^2}.$$

Let α and β be two positive roots of equation (5), where $\alpha > \beta$;

$$\therefore \quad A = 2\mu \frac{\phi(\alpha) - \phi(\beta)}{\alpha^2 - \beta^2}$$

and

$$B = 2\mu \frac{\beta^2\phi(\alpha) - \alpha^2\phi(\beta)}{\alpha^2 - \beta^2}.$$

The motion in this case is included between two circles of radii α and β.

The equation of the path can be put in the form

$$\int_{u_0}^{u} \frac{du}{\sqrt{2\mu\frac{\beta^2\phi(\alpha) - \alpha^2\phi(\beta)}{\alpha^2 - \beta^2} - 2\mu\frac{\phi(\alpha) - \phi(\beta)}{\alpha^2 - \beta^2}u^2 + 2\mu\phi(u)}}$$

$$= \sqrt{\frac{\alpha^2 - \beta^2}{\phi(\alpha) - \phi(\beta)}} \int_{\theta_0}^{\theta} \sqrt{1 - \frac{2\lambda(\alpha^2 - \beta^2)}{\phi(\alpha) - \phi(\beta)}\chi(\theta)},$$

where $\chi(\theta) = \int f(\theta)d\theta$, i.e.,

$$\Phi(u)-\Phi(u_0) = \sqrt{\frac{\alpha^2-\beta^2}{\phi(\alpha)-\phi(\beta)}} \int_{\theta_0}^{\theta} \sqrt{\frac{d\theta}{1-\dfrac{2\lambda(\alpha^2-\beta^2)}{\phi(\alpha)-\phi(\beta)}\chi(\theta)}}.$$

The remaining conditions for periodic orbits are

$$\sqrt{\frac{\alpha^2-\beta^2}{\phi(\alpha)-\phi(\beta)}} \int_{\theta_0}^{k\pi+\theta_0} \sqrt{\frac{d\theta}{1-\dfrac{2\lambda(\alpha^2-\beta^2)}{\phi(\alpha)-\phi(\beta)}\chi(\theta)}} = 2m\pi,$$

and $\Phi(u)$ must be an inverse function obeying the law

$$\Phi^{-1}[\Phi(u)+2m\pi] = \Phi^{-1}\Phi(u) = u,$$

where k and m are integers.

If these conditions are satisfied, then we have

$$\Phi(u) = \Phi(u_0) + 2m\pi \; ;$$
$$\therefore \quad \Phi^{-1}\Phi(u) = \Phi^{-1}[\Phi(u_0)+2m\pi]$$
$$= \Phi^{-1}\Phi(u_0),$$

i.e., $\qquad\qquad u = u_0.$

This means that as θ increases from θ_0 to $\theta_0+k\pi$, then u returns to its original value and periodic orbits are formed.

As an example, take the case of an electron moving in the field of a non-neutral atom (Phil. Mag. vii. p. 786 (1929)). The equation of the path is

$$\cos^{-1}\frac{l/r-1}{e} - \cos^{-1}\frac{l/r_0-1}{e} = 2\sqrt{\frac{A}{A+2\lambda}} F\left(\psi, \sqrt{\frac{4\lambda}{A+2\lambda}}\right).$$

Then, if

$$2\sqrt{\frac{A}{A+2\lambda}} F\left(k\pi, \sqrt{\frac{4\lambda}{A+2\lambda}}\right) = 2m\pi,$$

then

$$\cos\cos^{-1}\frac{l/r-1}{e} = \cos\left[\cos^{-1}\frac{l/r_0-1}{e}+2m\pi\right],$$

i.e., $\qquad\qquad \dfrac{l/r-1}{e} = \dfrac{l/r_0-1}{e},$

i.e., $\qquad\qquad r = r_0,$

i.e., the electron returns to its point of projection and periodic orbits are formed.

LXII. On the Stability of Laminar Motion of Viscous Fluids. By ALFRED ROSENBLATT [*].

THE problem of the stability of the laminar motion of incompressible viscous fluids has been treated by many eminent authors, especially by Lord Kelvin and Lord Rayleigh ; but, so far as I am aware, it is only Mr. F. Noether[†] who has made an attempt to investigate *finite* disturbances without giving rigorous proofs. I think therefore that it will not be without interest to examine rigorously the simpler case of *exponentially vanishing disturbance*. Having already treated the case of *initial rest*, I shall now investigate the case of fundamental motion of the form

$$u_0 = \frac{U y}{H}, \quad \dots \dots \quad (1)$$

$y = 0$, $y = H$ being the equations of the walls, U the velocity of the latter.

1. I suppose the Stokes function to be of the form

$$\Psi = \Psi_0 + \overset{\alpha}{\underset{k=1}{\Sigma}} \epsilon^k \Psi_k(x, y, t), \quad \dots \quad (2)$$

$$\Psi_k = e^{-k(\lambda x + \mu t)} f_k(y), \quad k = 1, 2, \dots \quad (3)$$

In order to obtain dimensionless quantities we introduce, with Mr. Sommerfeld, the expressions

$$\xi = \frac{x}{H}, \quad \eta = \frac{y}{H}, \quad \tau = \frac{U}{H} t, \quad \gamma = \lambda H, \quad \delta = \frac{\mu H}{U}, \quad R = \frac{U H}{\nu}$$

$$\dots \quad (4)$$

(R number of Reynolds). We have now

$$\Psi_k = e^{-k(\gamma \xi + \delta \tau)} f_k(\eta).$$

Writing

$$\phi_k(\eta) = f_k''(\eta) + k^2 \gamma^2 f_k(\eta),$$

we obtain the following set of differential equations :

$$\phi_k{''}(\eta) + \left[k^2\gamma^2 + kR(\delta + \gamma\eta) \right]\phi_k(\eta) = \frac{\gamma}{\nu} \sum_{\substack{l+m=k; \\ l,\, m=1,\,\ldots k-1}} , \\ \left[-l f_l \phi_m' + m f_l' \phi_m \right] = D_k(\eta), \\ k = 1, 2, \ldots \tag{5}$$

We replace now in the equations which determine $f_k(\eta)$, $\phi_k(\eta)$ the independent variable η by the variable z_k,

$$z_k = \frac{k^2\gamma^2 + kR(\delta + \gamma\eta)}{(k\gamma R)^{\frac{2}{3}}} \ \ldots \ \ldots \ \ldots \tag{6}$$

The limits of η being 0 and 1, the limits $z_k{}^0$, $z_k{}^1$ of z_k are

$$z_k{}^0 = \frac{k^2\gamma^2 + kR\delta}{(k\gamma R)^{\frac{2}{3}}}, \quad z_k{}^1 = \frac{k^2\gamma^2 + kR(\delta + \gamma)}{(k\gamma R)^{\frac{2}{3}}}.$$

Writing

$$f_k(\eta) = \overline{f}_k(z_k), \qquad \phi_k(\eta) = \overline{\phi}_k(z_k),$$

$$D_k(\eta) = \overline{D}_k(z_k), \qquad g_k = -\frac{(k\gamma)^{\frac{2}{3}}}{R^{\frac{1}{3}}},$$

we obtain the following two sets of equations :

$$f_k{''}(z_k) + g_k{}^2 \overline{f}_k(z_k) = \frac{g_k{}^2}{k^2\gamma^2} \overline{\phi}_k(z_k), \ . \ \ . \ \ . \ \ . \tag{7}$$

$$\overline{\phi}_k{''}(z_k) + z_k \phi_k(z_k) = \frac{g_k{}^2}{k^2\gamma^2} D_k(z_k) . \ . \ \ . \ \ . \ \ . \tag{8}$$

2. The equations (7) are integrated by the formulæ

$$f_k(z_k) = \frac{g_k}{k^2\gamma^2} \int_{z_k{}^0}^{z_k} \sin g_k(z_k - u) \overline{\phi}_k(u)\, du, \quad . \ \ . \tag{9}$$

and the equations (8) by the formulæ

$$\overline{\phi}_k(z_k) = A_k \sigma_1(z_k) + B_k \sigma_2(z_k) + \frac{g_k{}^2}{k^2\gamma^2}$$

$$\int_{z_k{}^0}^{z_k} \left[\sigma_1(u)\sigma_2(z_k) - \sigma_2(u)\sigma_1(z_k) \right] . \overline{D}_k(u)\, du. \tag{10}$$

3 A 2

$\sigma_1(z_k)$, $\sigma_2(z_k)$ are the following independent integrals of the *linear homogeneous equations* belonging to (8):

$$\left.\begin{array}{l}\sigma_1(z) = (\tfrac{1}{3})^{\frac{1}{3}}\Gamma(\tfrac{2}{3})\sqrt{z}\,\mathrm{I}_{-\frac{1}{3}}(\tfrac{2}{3}z^{\frac{3}{2}}),\\[1mm]\sigma_2(z) = (\tfrac{1}{3})^{-\frac{1}{3}}\Gamma(\tfrac{4}{3})\sqrt{z}\,\mathrm{I}_{\frac{1}{3}}(\tfrac{2}{3}z^{\frac{3}{2}}),\end{array}\right\}\quad . \quad (11)$$

I being the Bessel functions.

We have therefore

$$\begin{aligned}\overline{f}_k(z_k) = \frac{g_k}{k^2\gamma^2}\int_{z_k^0}^{z_k}&\sin g_k(z_k-u)\Big\{\mathrm{A}_k\sigma_1(u)+\mathrm{B}_k\sigma_2(u)\\&+\frac{g_k^2}{k^2\gamma^2}\int_{z_k^0}^{u}[\sigma_1(\zeta)\sigma_2(u)-\sigma_2(\zeta)\sigma_1(u)]\,\overline{\mathrm{D}}_k(\zeta)\,d\zeta\Big\}\,du.\end{aligned}$$

$$. \quad . \quad . \quad (12)$$

The limit conditions are

$$\overline{f}_k(z_k^1) = 0, \qquad \overline{f}_k{}'(z_k^1) = 0.$$

3. We introduce the integrals

$$\mathrm{I}_i(a, b) = \int_a^b \sin g_k(b-u)\sigma_i(u)\,du, \quad i=1, 2, \quad (13)$$

$$\mathrm{J}_i(a, b) = \int_a^b \cos g_k(b-u)\sigma_i(u)\,du, \quad i=1, 2, \quad (14)$$

A_1, B_1 are determined by the equations

$$\left.\begin{array}{l}\mathrm{A}_1\mathrm{I}_1(z_1^0, z_1^1)+\mathrm{B}_1\mathrm{I}_2(z_1^0, z_1^1) = 0,\\[1mm]\mathrm{A}_1\mathrm{J}_1(z_1^0, z_1^1)+\mathrm{B}_1\mathrm{J}_2(z_1^0, z_1^1) = 0,\end{array}\right\}\quad . \quad . \quad (15)$$

which give the *transcendental equation* determining γ, δ

$$\mathrm{D}_1(z_1^0, z_1^1) \equiv \mathrm{I}_1(z_1^0, z_1^1)\mathrm{J}_2(z_1^0, z_1^1)-\mathrm{I}_2(z_1^0, z_1^1)\mathrm{J}_1(z_1^0, z_1^1) = 0.$$

$$. \quad . \quad . \quad (16)$$

We have

$$\mathrm{A}_1 = -\mathrm{C}_1\mathrm{I}_2(z_1^0, z_1^1), \qquad \mathrm{B}_1 = \mathrm{C}_1\mathrm{I}_1(z_1^0, z_1^1), \quad . \quad (17)$$

C_1 being an arbitrary constant.

Inverting in (12) the order of integration, we obtain the following equations which determine A_k, B_k, $k \geq 2$:—

$$\left.\begin{array}{l}\mathrm{A}_k\mathrm{I}_1(z_k^0, z_k^1)+\mathrm{B}_k\mathrm{I}_2(z_k^0, z_k^1)\\[1mm]\quad+\dfrac{g_k^2}{k^2\gamma^2}\displaystyle\int_{z_k^0}^{z_k^1}\overline{\mathrm{D}}_k(\zeta)[\sigma_1(\zeta)\mathrm{I}_2(\zeta, z_k^1)-\sigma_2(\zeta)\mathrm{I}_1(\zeta, z_k^1)]\,d\zeta = 0,\\[4mm]\mathrm{A}_k\mathrm{J}_1(z_k^0, z_k^1)+\mathrm{B}_k\mathrm{J}_2(z_k^0, z_k^1)\\[1mm]\quad+\dfrac{g_k^2}{k^2\gamma^2}\displaystyle\int_{z_k^0}^{z_k^1}\overline{\mathrm{D}}_k(\zeta)\,[\sigma_1(\zeta)\mathrm{J}_2(\zeta, z_k^1)-\sigma_2(\zeta)\mathrm{J}_1(\zeta, z_k^1)]\,d\zeta = 0.\end{array}\right\}$$

$$. \quad . \quad (18)$$

Writing

$$D_k(z_k^{t0}, z_k^1) = I_1(z_k^0, z_k^1) J_2(z_k^0, z_k^1) - I_2(z_k^0, z_k^1), J_1(z_k^0, z_k^1),$$

. . . (19)

we have

$$A_k = \frac{g_k^2}{D_k(z_k^0, z_k^1) . k^2 \gamma^2} \left\{ I_2(z_k^0, z_k^1) \right.$$

$$\int_{z_k^0}^{z_k^1} \overline{D_k}(\zeta) [\sigma_1(\zeta) J_2(\zeta\ z_k^1) - \sigma_2(\zeta) J_1(\zeta, z_k^1)] d\zeta - J_2(z_k^0, z_k^1)$$

$$\int_{z_k^0}^{z_k^1} D_k(\zeta) [\sigma_1(\zeta) I_2(\zeta, z_k^1) - \sigma_2(\zeta) I_1(\zeta, z_k^1)] d\zeta \left. \right\},$$

$$B_k = \frac{g_k^2}{D_k(z_k^0, z_k^1) . k^2 \gamma^2} \left\{ J_1(z_k^0, z_k^1) \right.$$

$$\int_{z_k^0}^{z_k^1} D_k(\zeta) [\sigma_1(\zeta) I_2(\zeta, z_k^1) - \sigma_2(\zeta) I_1(\zeta, z_k^1)] d\zeta - I_1(z_k^0, z_k^1)$$

$$\int_{z_k^l}^{z_k^1} D_k(\zeta) [\sigma_1(\zeta) J_2(\zeta, z_k^1) - \sigma_2(\zeta) J_1(\zeta, z_k^1)] d\zeta \left. \right\}.$$

. . . (20)

We obtain therefore the following recurrent expressions for the $\bar{\phi}_k(z_k)$:—

$$\bar{\phi}_k(z_k)$$

$$= \frac{g_k^2}{D_k(z_k^0, z_k^1) . k^2 \gamma^2} \left\{ \int_{z_k^0}^{z_k^1} D_k(\zeta) [\sigma_1(\zeta) \sigma_1(z_k) \{ I_2(z_k^0, z_k^1) J_2(\zeta, z_k^1) \right.$$

$$- I_2(\zeta, z_k^1) J_2(z_k^0, z_k^1) \} - \sigma_2(\zeta) \sigma_2(z_k) \{ I_1(\zeta, z_k^1) J_1(z_k^0, z_k^1)$$

$$- I_1(z_k^0, z_k^1) J_1(\zeta, z_k^1) \} + \sigma_2(\zeta) \sigma_1(z_k) \{ I_1(\zeta, z_k^1) J_2(z_k^0, z_k^1)$$

$$- I_2(z_k^0, z_k^1) J_1(\zeta, z_k^1) \} - \sigma_1(\zeta) \sigma_2(z_k) \{ I_1(z_k^0, z_k^1) J_2(\zeta, z_k^1)$$

$$- I_2(\zeta, z_k^1) J_1(z_k^0, z_k^1) \}] d\zeta$$

$$+ D_k(z_k^0, z_k^1) \int_{z_k^0}^{z_k} D_k(\zeta) [\sigma_1(\zeta) \sigma_2(z_k) - \sigma_2(\zeta) \sigma_1(z_k)] . d\zeta \left. \right\}.$$

. . . (21)

4. In order that the expressions (21) may have a sense the expressions (19) for $k \geq 2$ must be different from zero We must therefore first of all calculate the *limit* of (19) for k tending to $+\infty$.

We have for large values of z the formulæ

$$
\begin{aligned}
\sigma_1(z) &= \left(\frac{1}{3}\right)^{\frac{1}{3}} \Gamma\left(\frac{2}{3}\right) \cdot \frac{1}{z^{\frac{1}{4}}} \left\{ \sqrt{\frac{3}{\pi}} \cos\left(\frac{2}{3} z^{\frac{3}{2}} - \frac{\pi}{12}\right) + \left(\frac{1}{z}\right) \right\}, \\
\sigma_2(z) &= \left(\frac{1}{3}\right)^{-\frac{1}{3}} \Gamma\left(\frac{4}{3}\right) \cdot \frac{1}{z^{\frac{1}{4}}} \left\{ \sqrt{\frac{3}{\pi}} \sin\left(\frac{2}{3} z^{\frac{3}{2}} - \frac{\pi}{12}\right) + \left(\frac{1}{z}\right) \right\}.
\end{aligned} \quad\quad (22)
$$

Introducing the integrals

$$
I_{1,2,3,4} = \int_{z_k^0}^{z_k^1} {\sin \atop \cos} \Big\} \; g_k(z_k^1 - u) \cdot {\cos \atop \sin} \Big\} \left(\frac{2}{3} u^{\frac{3}{2}} - \frac{\pi}{12}\right) \frac{du}{u^{\frac{1}{4}}}, \quad (23)
$$

we have for large values of k

$$
D(z_k^0, z_k^1) = \frac{3}{\pi} \cdot \Gamma\left(\frac{2}{3}\right) \Gamma\left(\frac{4}{3}\right) (I_1 I_4 - I_2 I_3) + \epsilon(k). \quad (24)
$$

Writing

$$
v = g_k(z_k - u) + \frac{2}{3} u^{\frac{3}{2}} - \frac{\pi}{12},
$$

$$
v' = g_k(z_k - u) - \frac{2}{3} u^{\frac{3}{2}} + \frac{\pi}{12},
$$

$$
u = \frac{k^2 \gamma^2 + k R(\delta + \gamma\eta)}{(k\gamma R)^{\frac{2}{3}}},
$$

we can replace the integrals $I_1 \ldots I_4$ by the integrals

$$
I'_{1,4} = \frac{\sqrt{R}}{2} \int_0^1 (\sin v \pm \sin v') \, d\eta,
$$

$$
I'_{2,3} = \frac{\sqrt{R}}{2} \int_0^1 (\cos v' \pm \cos v) \, d\eta.
$$

But we have

$$
\frac{dv}{d\eta} = 2k\gamma\left(1 + \left(\frac{1}{k}\right)\right), \qquad \frac{dv'}{d\eta} = -\frac{R(\delta + \gamma\eta)}{2\gamma} + \left(\frac{1}{k}\right);
$$

we can therefore consider only the integrals containing v, and write

$$
D_k(z_k^0, z_k^1) = -\frac{3R}{4\pi} \Gamma\left(\frac{2}{3}\right) \Gamma\left(\frac{4}{3}\right)
$$

$$
\left\{ \left(\int_0^1 \sin v' \, d\eta\right)^2 + \left(\int_0^1 \cos v' \, d\eta\right)^2 \right\} + \epsilon(k). \quad (25)
$$

But we have

$$v' = g_k z_k + \frac{\pi}{12} + \frac{1}{3}\frac{(k\gamma)^2}{R} - \frac{R}{4}\frac{(\delta+\gamma\eta)^2}{\gamma^2} + \left(\frac{1}{k}\right)$$

$$= m - \frac{R}{4}\left(\eta+\frac{\delta}{\gamma}\right)^2 + \left(\frac{1}{k}\right).$$

We have therefore

$$\left(\int_0^1 \sin v'\, d\eta\right)^2 + \left(\int_0^1 \cos v'\, d\eta\right)^2$$

$$= \left(\int_0^1 \sin\frac{R}{4}\left(\frac{\delta}{\gamma}+\eta\right)^2 d\eta\right)^2 + \left(\int_0^1 \cos\frac{R}{4}\left(\frac{\delta}{\gamma}+\eta\right)^2 d\eta\right)^2 + \epsilon(k),$$

and the limit D_x of $D_k(z_k^0, z_k^1)$ is

$$D_x = -\frac{3R}{4\pi}\Gamma\left(\frac{2}{3}\right)\Gamma\left(\frac{4}{3}\right)$$

$$\left\{\left(\int_0^1 \sin\frac{R}{4}\left(\frac{\delta}{\gamma}+\eta\right)^2 d\eta\right)^2 + \left(\int_0^1 \cos\frac{R}{4}\left(\frac{\delta}{\gamma}+\eta\right)^2 d\eta\right)^2\right\}.$$

$$\cdots \quad (26)$$

5. The integrals in the parenthesis are the well-known *Fresnel integrals.* Introducing the variable of integration,

$$\xi = \sqrt{\frac{2}{\pi}}\sqrt{\frac{R}{4}}\left(\frac{\delta}{\gamma}+\eta\right),$$

we have

$$\int_0^1 \sin\frac{R}{4}\left(\frac{\delta}{\gamma}+\eta\right)^2 d\eta = \sqrt{\frac{2\pi}{R}}\,[S(b)-S(a)],$$

$$\int_0^1 \cos\frac{R}{4}\left(\frac{\delta}{\gamma}+\eta\right)^2 d\eta = \sqrt{\frac{2\pi}{R}}\,[C(b)-C(a)],$$

where $S(\xi)$, $C(\xi)$ are the Fresnel integrals

$$S(\xi) = \int_0^\xi \sin\frac{\pi}{2}u^2\,du, \qquad C(\xi) = \int_0^\xi \cos\frac{\pi}{2}u^2\,du, \quad (27)$$

and a, b are

$$a = \sqrt{\frac{R}{2\pi}\frac{\delta}{\gamma}}, \qquad b = \sqrt{\frac{R}{2\pi}\left(1+\frac{\delta}{\gamma}\right)}. \quad (28)$$

We have, finally.

$$D_\infty = -\sqrt{3}\cdot\pi\{(S(b)-S(a))^2 + (C(b)-C(a))^2\}. \quad (29)$$

But it is well known that the *Cornu spiral,* whose equations are

$$x = \mathrm{C}(\xi), \quad y = \mathrm{S}(\xi), \quad . \quad . \quad . \quad . \quad (30)$$

has *no double point.* We obtain therefore our first result:

Theorem 1.—" The determinants (19), which appear in the denominators of the expressions (21) for the $\phi_k(z_k)$, converge with $k \to +\infty$ to a number D_∞ given by (29), which is *always different from zero.*"

Writing

$$\mathrm{F}(\xi) = \mathrm{C}(\xi) + i\mathrm{S}(\xi),$$

we have for large ξ

$$\mathrm{F}(\xi) = \tfrac{1}{2}(1+i) + \frac{e^{i\frac{\pi}{2}\xi^2}}{i\pi\xi}\,(1+\epsilon(\xi')).$$

D_∞ tends therefore to zero if R or if $\dfrac{\delta}{\gamma}$ increases indefinitely.

If R and if $\dfrac{\delta}{\gamma}$ are contained in finite intervals D_∞ is absolutely superior to a positive number l and $\mathrm{D}_k(z_k^0, z_k^1)$ tends *uniformly* to D_∞. Suppose now that $\mathrm{R}_0, \delta_0, \gamma_0$ satisfy the transcendental equation (16). We choose a number k_0, such that for the finite intervals containing R_0 and $\dfrac{\delta_0}{\gamma_0}$ and for any $k > k_0$ $\mathrm{D}_k(z_k^0, z_k^1)$ is absolutely superior to $l > 0$ The roots $\mathrm{R}_0, \delta_0, \gamma_0$, common to two equations,

$$\mathrm{D}_{k'}(z_{k'}^0, z_{k'}^1) = 0, \quad \mathrm{D}_{k''}(z_{k''}^0, z_{k''}^1) = 0, \quad . \quad . \quad (31)$$

form an *exceptional set,* and for a given R_0 there is only a *finite number* of roots, γ_0, δ_0, in limited intervals. In closed intervals not containing these exceptional values the $\mathrm{D}_k(z_k^0, z_k^1)$ are *for all* k uniformly absolutely superior to a *fixed* positive number $m > 0$.

6. We shall now establish the *convergence* of the series

$$s_\phi = \sum_{k=1}^{\infty} \epsilon^k e^{-k(\gamma\xi + \delta\tau)} . \overline{\phi_k}(z_k), \quad . \quad . \quad . \quad (32)$$

and therefrom also the convergence of the series

$$s_f = \sum_{k=1}^{\infty} \epsilon^k e^{-k(\gamma\xi + \delta\tau)} . f_k(\eta). \quad . \quad . \quad . \quad (33)$$

Consider the expressions (21). The integrals I, J are *uniformly* limited with respect to k. The interval of integration is of the order $k^{\frac{1}{2}}$ and the σ are of order $k^{-\frac{1}{2}}$. The formulæ (9) show that the $f_k(z_k)$ are of the order of the $\overline{\phi}_k(z_k)$ multiplied by k^{-1}, while the $f'_k(z_k)$ are of the order of $\overline{\phi}_k(z_k)$ multiplied by $k^{-\frac{1}{2}}$. The $\phi'(z_k)$ are of the order of the $\overline{\phi}_k(z_k)$ multiplied by $k^{\frac{1}{2}}$. Indeed, the $\sigma'(z_k)$ are of the order of $\sigma(z_k)$ multiplied by $k^{\frac{1}{2}}$, since we have

$$\sigma'(z) = \frac{1}{2z}\sigma(z) + Az I_n'\left(\frac{2}{3}z^{\frac{3}{2}}\right),$$

$$I_n'\left(\frac{2}{3}z^{\frac{3}{2}}\right) = -\frac{3n}{2z^{\frac{3}{2}}}I_n\left(\frac{2}{3}z^{\frac{3}{2}}\right) + I_{n-1}\left(\frac{2}{3}z^{\frac{3}{2}}\right).$$

Let us now suppose that the functions

$$\overline{\phi}_1, \ \overline{\phi}_2, \ \dots \ \overline{\phi}_{k-1}$$

have the majorant numbers

$$\Phi_1, \ \Phi_2, \ \dots \ \Phi_{k-1},$$

and that the functions

$$\overline{\phi}_i', \overline{f}_i, \overline{f}_i', \quad i = 1, \dots k-1$$

have respectively the majorant numbers

$$\Phi_i.i^{\frac{2}{3}}, \quad \Phi_i.\frac{1}{i}, \quad \Phi_i.i^{-\frac{1}{3}}.$$

Let us consider the expressions (21). It is easily seen that $\overline{D}_k(\zeta)$ is a sum of terms whose majorant numbers are

$$\frac{\gamma}{\nu}(\gamma R)^{\frac{1}{2}}m\Phi_l\Phi_m.$$

It follows that there exists a positive number N *independent of* k, such that Φ_k, given by the formula [*]

$$\Phi_k = N \sum_{i=1}^{k-1} \Phi_i\Phi_{k-i}, \quad \dots \quad \dots \quad (34)$$

is a majorant number of the function $\overline{\phi}_k(z_k)$, and that majorant numbers of the functions

$$\overline{\phi}_k'(z_k), \quad \overline{f}_k(z), \quad f_k'(z_k)$$

---

[*] *Cf.* the interesting papers of Mr. Odquist: "Die Randwertaufgaben der Hydromechanik zäher Flüssigkeiten," Dissertation, Stockholm, 1928; "Über die Randwertaufgaben der Hydromechanik zäher Flüssigkeiten," *Math. Zeits.* 1930, p. 32.

are respectively the numbers

$$k^{\frac{2}{3}}\Phi_k, \quad \frac{1}{k}\Phi_k, \quad k^{-\frac{2}{3}}\Phi_k.$$

The series

$$\left.\begin{array}{l} S_\phi = \sum\limits_{k=1}^{\infty} \epsilon^k E_k \Phi_k, \\[2mm] E_k = e^{-k(\gamma\xi + \delta\tau)}, \end{array}\right\} \quad \cdots \quad (35)$$

is therefore a *majorant series* of s_ϕ. The radius ρ of convergence is found considering that S_ϕ satisfies the equation of second degree,

$$NS_\phi^2 - S_\phi + E_1 \epsilon \Phi_1 = 0. \quad \cdots \quad (36)$$

We obtain

$$\rho = \frac{1}{4NE_1\Phi_1} \quad \cdots \quad \cdots \quad (37)$$

We have therefore the theorem :

Theorem 2.—" The series (2) for Ψ is absolutely and uniformly convergent with all derivatives for $|\epsilon| < \rho$, and satisfies the equation of 4th order for viscous fluids."

Cracow,
    August 1931.

───────────────

LXIII. *Relativistic Precession of Periodic Orbits in Central Force Fields. By* M. A. Omara, *Docteur ès Sciences (Grenoble), Lecturer in Applied Mathematics in the Egyptian University* [*].

1. **I**T is a well-known fact that the path of a particle in a Newtonian field of force, when the relativistic variation of mass is taken into consideration, is no longer a Keplerian ellipse. It may be considered as an ellipse whose perihelion is advancing. The aim of this paper is to establish that this advance or precession of the perihelion is common to all periodic orbits described under central forces depending on the distance. The orbit is supposed nearly circular and the apsidal angles are compared, in Newtonian and in relativistic dynamics   It is found that, for a given field of force, the relativistic apsidal angle

exceeds slightly the corresponding Newtonian one. This slight excess depends, as well as in the case of the inverse square law of force, upon the inverse of the square of the velocity of light and may be interpreted in the same manner, and can be calculated to any degree of approximation.

2. A particle whose rest mass is m moves in a central force field derived from a potential $V(r)$. Let r and θ be the polar coordinates of the particle, referred to the centre of force as origin. The corresponding relativity Hamilton-Jacobi equation is:

$$\left(\frac{\partial S}{\partial r}\right)^2 + \frac{1}{r^2}\left(\frac{\partial S}{\partial \theta}\right)^2 = 2m(E - V) + \frac{1}{c^2}(E - V)^2, \quad (1)$$

E being the constant of energy. The equation of the path is then

$$\beta = \frac{\theta}{2\sqrt{\alpha}} - \frac{1}{2}\int_r \frac{dr}{\sqrt{\Phi(r)}},$$

where

$$\Phi(r) = 2mr^2(E - V) + \frac{r^2}{c^2}(E - V)^2 - \alpha,$$

α, β are arbitrary constants, α having the dimensions of the square of a moment of momentum.

Take a new variable $u = \frac{1}{r}$, and put $V(r) = W(u) = W$. The equation of the path becomes

$$\beta = \frac{\theta}{2\sqrt{\alpha}} + \frac{1}{2}\int \frac{du}{\sqrt{\Psi(u)}}, \quad \dots \quad (2)$$

where $\Psi(u) = 2m(E - W) + \frac{1}{c^2}(E - W)^2 - \alpha u^2$.

As the orbit is supposed periodic, r, and consequently u, must remain between two finite limits. Let the limits for u be u_1 and u_2 ($> u_1$). The values u_1 and u_2 are consecutive roots of the equation

$$\Psi(u) = 0.$$

The apsidal angle is then

$$\Theta = \int_{u_1}^{u_2} \frac{-\sqrt{\alpha}\,du}{\sqrt{\Psi(u)}} \quad \dots \quad (3)$$

A proposition of integral calculus, easy to prove, states that when u_1 and u_2 tend to a common limit a, such that $u_1 < a < u_2$, the limiting value of the integral $\displaystyle\int_{u_1}^{u_2} \frac{du}{\sqrt{\Psi(u)}}$ is

$$\pi\sqrt{\frac{-2}{\Psi''(a)}},$$

where $\Psi''(a)$ stands for $\dfrac{d^2\Psi}{du^2}$ for $u = a$.

Suppose the initial conditions so chosen that the orbit is nearly a circle of radius $\dfrac{1}{a}$, and take for approximate value of Θ the limiting value when u_1 and u_2 tend to a.

In order to calculate $\Psi''(a)$, we have

$$\frac{d\Psi}{du} = -2\left(m + \frac{E-W}{c^2}\right)\frac{dW}{du} - 2au,$$

and, for a circular motion,

$$\Psi'(a) = -2\left(m + \frac{E-W(a)}{c^2}\right)W'(a) - 2aa = 0.$$

Also

$$\Psi''(a) = -2\left(m + \frac{E-W(a)}{c^2}\right)W''(a) + \frac{2}{c^2}W'^2(a) - 2a.$$

Substituting for E from the preceding equation, we have

$$\Psi''(a) = -2a\left(1 - a\frac{W''(a)}{W'(a)}\right) + \frac{2}{c^2}W'^2(a),$$

and then

$$\Theta = \frac{\pi}{\sqrt{1 - a\dfrac{W''}{W'} - \dfrac{W'^2}{ac^2}}} = \frac{\pi}{\omega}\text{(say)}. \quad . \quad . \quad . \quad (4)$$

W', $W'' \dots$ are written for $W'(a)$, $W''(a)$.

3. Another method of computing the apsidal angle is to pass by the differential equation of the path. This method has the advantage of showing the degree of approximation admitted.

From equation (2) we get

$$a\left(\frac{du}{d\theta}\right)^2 = \Psi(u) = 2m(E-W) + \frac{1}{c^2}(E-W)^2 - au^2.$$

Differentiating again with respect to θ, dividing both sides by $a\dfrac{du}{d\theta}$, and arranging, we get

$$\frac{d^2u}{d\theta^2} + u = -\frac{m}{a}\left(1 + \frac{E - W}{mc^2}\right)\frac{dW}{du}.$$

Put $u = a$, then

$$a = -\frac{m}{a}\left(1 + \frac{E - W(a)}{mc^2}\right)W'(a). \quad . \quad . \quad . \quad (5)$$

Eliminating E between these two equations, we have

$$\frac{d^2u}{d\theta^2} + u = \left[\frac{a}{W'(a)} + \frac{W(u) - W(a)}{ac^2}\right]W'(u).$$

Put $u = a + x$, where x is a small quantity. Expanding by Taylor's theorem, and arranging, the equation becomes

$$\frac{d^2x}{d\theta^2} = -\omega^2 x + \left(a\frac{W'''}{W'} + 3\frac{W'W''}{ac^2}\right)\frac{x^2}{2}$$

$$+ \left(a\frac{W^{IV}}{W'} + \frac{4W'W''' + 3W''^2}{ac^2}\right)\frac{x^3}{6} + \ldots \quad (6)$$

This equation can be integrated by successive approximations; but if we confine ourselves to the first order of small quantities, equation (6) may be written

$$\frac{d^2x}{d\theta^2} + \omega^2 x = 0,$$

and is satisfied by

$$x = A\cos(\omega\theta - \epsilon),$$

where A and ϵ are arbitrary constants. The approximation to the path is given by

$$u = a + A\cos(\omega\theta - \epsilon), \quad . \quad . \quad . \quad . \quad (7)$$

and the apsidal angle is again $\dfrac{\pi}{\omega}$.

4. When a particle of mass m describes a circle of radius $\dfrac{1}{a}$, with velocity v, the square of the moment of momentum,

$$a = \frac{m^2 v^2}{a^2},$$

also,

$$\frac{d\mathrm{W}}{du} = \frac{d\mathrm{V}}{dr}\frac{dr}{du} = \frac{\mathrm{F}}{u^2},$$

where F is the force acting on the particle. We have in this case

$$\mathrm{F} = mar^2,$$

and, therefore,

$$\mathrm{W}'(a) = \frac{mv^2}{a},$$

and then

$$\omega^2 = 1 - a\frac{\mathrm{W}''}{\mathrm{W}'} - \frac{v^2}{c^2}.$$

Put

$$\lambda^2 = 1 - a\frac{\mathrm{W}''}{\mathrm{W}'}, \quad \text{and} \quad \gamma^2 = 1 - \frac{v^2}{c^2\lambda^2};$$

then the apsidal angle may be written

$$\Theta = \frac{\pi}{\gamma\lambda}.$$

The ratio $\frac{v}{c}$ being in general very small, γ differs slightly from unity.

In Newtonian dynamics $\gamma = 1$, and the apsidal angle is

$$\Theta_1 = \frac{\pi}{\lambda}.$$

We have therefore the relation

$$\Theta\gamma^{-1}\Theta_1.$$

Let the angle θ be measured from a perihelion. During a radial vibration the angle θ increases in relativistic dynamics by an amount 2Θ, while in Newtonian dynamics the increment is $2\Theta_1$. We see that during this radial vibration the perihelion has a relative advance

$$2\Theta_1 = (\gamma^{-1} - 1).$$

Now suppose that the Newtonian orbit is a closed one, *i. e.*, there exists two integers, m and n, such that

$$m\Theta_1 = n\pi.$$

Then, in relativistic dynamics, while the radius vector reverts to its original value θ increases by an amount

$2m\Theta$, and the perihelion from which θ is measured will have advanced by

$$2m\,\Theta_1(\gamma^{-1}-1).$$

It is evident that this advance or precession of the perihelion is uniform.

If we refer the motion of the particle to a system of coordinates which participates in the motion of the perihelion, *i. e.*, to the system

$$r=r, \qquad \phi=\gamma\theta,$$

we have again the same Newtonian orbit, as can be easily verified by substitution in equation (7).

5. As application consider (*a*) the case of the Keplerian ellipse: the potential is

$$V=-\frac{\mu}{r},$$

and then $\qquad W=-\mu u, \qquad W'=-\mu, \qquad W''=0.$

The correction factor γ has the meaning

$$\gamma^2=1-\frac{\mu^2}{\alpha c^2},$$

and the advance of the perihelion during a radial vibration is approximately

$$\frac{\pi\mu^2}{\alpha c^2}.$$

(*b*) The case of the central ellipse, *i. e.*, the one described under a force proportional to the distance. We have

$$V=\frac{\mu r^2}{2}, \quad \text{and therefore} \quad W=\frac{\mu}{2}u^{-2};$$

then $\qquad W'=-\mu a^{-3}, \qquad W''=3\mu a^{-4},$

and $\qquad\qquad \Theta_1=\frac{\pi}{2}.$

The correction factor γ is given by

$$\gamma^2=1-\frac{\mu^2}{4\alpha^6 c^2}, \quad \cdot \quad \cdot \quad \cdot \quad \cdot \quad \cdot \quad \cdot \quad (8)$$

and the advance of the perihelion during a radial vibration is approximately

$$\frac{\pi \mu^2}{8 x a^6 c^2}.$$

6. The case of the central ellipse can be treated directly. The Hamilton-Jacobi equation is

$$\left(\frac{\partial S}{\partial r}\right)^2 + \frac{1}{r^2}\left(\frac{\partial S}{\partial \theta}\right)^2 = 2m\left(E - \frac{\mu r^2}{2}\right) + \frac{1}{c^2}\left(E - \frac{\mu r^2}{2}\right)^2.$$

The equations of motion are

$$t - t_0 = \int \left[m + \frac{E}{c^2} - \frac{\mu r^2}{2c^2} \right] \frac{r\,dr}{\sqrt{\Phi(r)}},$$

$$\beta = \frac{\theta}{2\sqrt{\alpha}} - \int \frac{dr}{2r\sqrt{\Phi(r)}},$$

where

$$\Phi(r) = 2m\left(E - \frac{\mu r^2}{2}\right)r^2 + \frac{r^2}{c^2}\left(E - \frac{\mu r^2}{2}\right)^2 - \alpha.$$

Put $r^2 = z$, these equations become

$$t - t_0 = \frac{1}{2}\left(m + \frac{E}{c^2}\right)\int \frac{dr}{\sqrt{\Psi(z)}} - \frac{\mu}{4c^2}\int \frac{z\,dr}{\sqrt{\Phi(z)}}, \quad (9)$$

$$2\left(\frac{\theta}{\sqrt{\alpha}} - 2\beta\right) = \int \frac{dr}{2\sqrt{\Psi(z)}}, \quad \cdots \quad (10)$$

where

$$\Psi(z) = \frac{z}{c^2}\left(E - \frac{\mu z}{2}\right)^2 + 2m\left(E - \frac{\mu z}{2}\right)z - \alpha$$

$$= \frac{z}{c^2}\left(E - \frac{\mu z}{2}\right)^2 - m\mu\left(z - \frac{E}{\mu}\right)^2 + \frac{mE^2}{\mu} - \alpha;$$

$\Psi(z)$ being a polynomial of the third degree the problem can be integrated in terms of elliptic functions. Take an auxiliary variable y defined by the equation

$$y = \int^z \frac{dr}{\sqrt{\Psi(z)}},$$

from which we have

$$\left(\frac{dz}{dy}\right)^2 = \Psi(z). \quad \cdots \cdots \quad (11)$$

The equation $\Psi(z) = 0$ has three real and positive roots, as $\Psi(z)$ is negative for $z = -\infty$, 0, and $\frac{2E}{\mu}$, and positive for

$z = \dfrac{E}{\mu}$ and $+\infty$. If the three roots be designated by z_1, z_2, z_3, we have

$$z_1 > \frac{2E}{\mu} > z_2 > \frac{E}{\mu} > z_3 > 0.$$

In the actual motion z lies between z_2 and z_3.
Define a new variable by the equation

$$z = Mx + N.$$

The constants M and N are to be so chosen that equation (11) takes the form

$$\left(\frac{dx}{dy}\right)^2 = \frac{\Psi(Mx+N)}{M^2}$$
$$= 4(x - e_1)(x - e_2)(x - e_3),$$

with the condition that $e_1 + e_2 + e_3 = 0$.

e_1, e_2, e_3 are the roots corresponding to z_1, z_2, z_3 respectively. We find by identification

$$M = \frac{16\mu^2}{c^2}, \qquad N = \frac{\mu}{3}\left(m + \frac{E}{c^2}\right).$$

The inversion of the integral defining y gives

$$x = \wp(y + \gamma),$$

where γ is a constant and $\wp$ is the Weierstrassian elliptic function formed with the roots e_1, e_2, e_3. Since z lies between the roots z_2 and z_3, it follows that x lies between e_2 and e_3, and therefore the constant γ is of the form $\omega' + \gamma_0$, where ω' is the half period corresponding to the root e_3, *i.e.*, a purely imaginary quantity, and γ_0 is a real quantity depending on the lower limit of the integral defining y. If this limit be z_3, γ_0 is null.
The real half period ω will be given by

$$\omega = \int_{e_3}^{e_2} \frac{dx}{\sqrt{4(x - e_1)(x - e_2)(x - e_3)}}.$$

The equations of motion become

$$t - t_0 = \frac{1}{2}\left(m + \frac{E}{c^2}\right)\int dy - \frac{\mu}{4c^2}\int [M\wp(y + \omega') + N]\,dy, \quad (12)$$

$$2\left(\frac{\theta}{\sqrt{\alpha}} - 2\beta\right) = \int \frac{dy}{M\wp(y + \omega') + N} \quad \cdot \quad \cdot \quad (13)$$

Integrating (12) we have

$$t - t_0 = \frac{1}{2}\left(m + \frac{E}{c^2}\right)\left(1 - \frac{\mu^2}{6c^2}\right)y + \frac{M\mu}{4c^2}\zeta(y + \omega').$$

In order to integrate (13), take a constant k defined by

$$\wp(k) = -\frac{N}{M},$$

so that from equation (11) we have

$$\wp'(k) = \frac{i\sqrt{\alpha}}{M}.$$

Equation (13) becomes

$$2\left(\frac{\theta}{\sqrt{\alpha}} - 2\beta\right) = \frac{1}{i\sqrt{\alpha}}\int \frac{\wp'(k)}{\wp(y + \omega') - \wp(k)}\,dy.$$

Integrating, we get

$$2i(\theta - \theta_0) = \log\frac{\sigma(y + \omega' - k)}{\sigma(y + \omega' + k)} + 2y\zeta(k),$$

where θ_0 is a new constant.

Or $\qquad\qquad e^{2i(\theta - \theta_0)} = e^{2y\zeta(k)}\dfrac{\sigma(y + \omega' - k)}{\sigma(y + \omega' + k)}.$ . . . (14)

We have also

$$\wp r^2 = M(y + \omega') + N. \quad . \quad . \quad . \quad (15)$$

Equations (14) and (15) determine the path.

When y increases by 2ω, r reverts to its original value and θ increases by the quantity

$$2i[\eta \cdot k - \omega\zeta(k)], \quad . \quad . \quad . \quad . \quad (16)$$

which evidently differs from π. The constant $\eta = \zeta(\omega)$.

We can obtain an approximate value for the increment (16) of the angle θ in the following manner. Equation (10) may be written

$$d\theta = \frac{\sqrt{\alpha}}{2}\frac{dz}{z\sqrt{\frac{\mu^2}{4c^2}(f - z)(z - g)(h - z)}}; \quad . \quad (17)$$

f and g are two finite quantities between which z lies, and h the third root of the cubic. Suppose the motion nearly circular

of radius $\frac{1}{a}$, and let b be the mean value of $z = r^2 = \frac{1}{a^2}$. Let

$$f = b - e \quad \text{and} \quad g = b + e,$$

e being a small quantity.

From the equation

$$\Psi(z) = 0$$

we have

$$f + g + h = \frac{4c^2}{\mu}\left(m + \frac{E}{c^2}\right);$$

therefore

$$h = \frac{4c^2}{\mu}\left(m + \frac{E}{c^2}\right) - 2b.$$

Take another variable ϕ defined by

$$z = \frac{f+g}{2} + \frac{g-f}{2}\cos\phi = b + e\cos\phi.$$

Substituting in (17), we get

$$d\theta = \frac{\sqrt{\alpha}}{2} \cdot \frac{d\phi}{(b + e\cos\phi)\sqrt{H^2 - \frac{\mu^2 e}{4c^2}\cos\phi}}, \quad . \quad (18)$$

where

$$H^2 = \mu\left(m + \frac{E}{c^2}\right) - \frac{3b\mu^2}{4c^2}$$

$$= \alpha a^4 - \frac{\mu^2}{4a^2 c^2},$$

as is easily verified on substituting for E from equation (5), where we put

$$W(a) = \frac{\mu}{2a^2} \quad \text{and} \quad W'(a) = -\frac{\mu}{a^2}.$$

Expanding the two expressions in the denominator of (18), neglecting squares and higher powers of e, and integrating between 0 and π, we get

$$\Theta = \frac{\pi}{2}\left(1 - \frac{\mu^2}{4\alpha a^6 c^2}\right)^{-\frac{1}{2}};$$

we have the same expression for γ as from (8).

7. Returning to equation (6), it will be easily seen that for a second approximation the apsidal angle is still $\frac{\pi}{\omega}$.

For a third approximation the coefficient of θ is no longer a multiple simply of ω. The differential equation may be written

$$\frac{d^2x}{d\theta^2} = -\omega^2 x + \mathrm{K}x^2 + \mathrm{L}x^3,$$

the meanings of K and L being evident.

This equation is satisfied by

$$x = \mathrm{A}\cos p(\theta-\epsilon) + \mathrm{A}^2[\mathrm{B}+\mathrm{C}\cos 2p(\theta-\epsilon)] + \mathrm{A}^3\mathrm{D}\cos 3p(\theta-\epsilon).$$

The constants B, C, D, and p are to be determined by substituting in the differential equation, neglecting powers of A higher than the third and equating coefficients on both sides. It will be found that

$$p^2 = \omega^2 - \frac{\mathrm{A}}{12}\left\{10\frac{\mathrm{K}^2}{\omega^2} + 9\mathrm{L}\right\} = \Gamma^2\Lambda^2,$$

where

$$\Lambda^2 = 1 - a\frac{\mathrm{W}''}{\mathrm{W}'} - \frac{\mathrm{A}^2 a}{24\mathrm{W}'}\left\{\frac{5a\mathrm{W}'''^2}{\mathrm{W}'(\mathrm{W}'-a\mathrm{W}'')} + 3\mathrm{W}''''\right\},$$

$$\Gamma^2 = 1 - \frac{1}{ac^2\Lambda^2}\left[\mathrm{W}''^2 + \frac{\mathrm{A}^2}{24}\left\{3(3\mathrm{W}''^2 + 4\mathrm{W}'\mathrm{W}''')\right.\right.$$
$$\left.\left. + \frac{5\mathrm{W}'}{\mathrm{W}'-a\mathrm{W}''}\left(6a\mathrm{W}'''\mathrm{W}'''' + \frac{a^2\mathrm{W}''^2\mathrm{W}'''^2}{\mathrm{W}'(\mathrm{W}'-a\mathrm{W}'')}\right)\right\}\right] + \ldots,$$

and the apsidal angle is then

$$\Theta = \frac{\pi}{p} = \frac{\pi}{\Gamma\Lambda}.$$

In Newtonian dynamics the correction factor Γ, as well as γ, reduces to unity, and the apsidal angle is

$$\Theta_1 = \frac{\pi}{\Lambda}.$$

Summary.

It has been proved that a Newtonian periodic orbit described under central forces depending on the distance may be considered in relativistic dynamics as if it were revolving in its own plane about the centre of forces. The angular displacement for a radial libration has been calculated, and applications to fields proportional to the distance and to the inverse square of the distance have been given. The case of the first field has been treated fully, in terms of elliptic functions.

LXIV. *On the Electrical Oscillations of very short Wave-length.*

To the Editors of the Philosophical Magazine.

GENTLEMEN,—

IN a note published in the Phil. Mag., October 1931, Mr. E. W. B. Gill gave an account of some observations made on a three-electrode valve, oscillating with positive grid. The valve, inserted in a Lecher circuit of fixed length, gave oscillations of several different periods, corresponding to the harmonics of the circuit, for different intervals of values in the grid tension (V) and in the emission current (i). Oscillations of greatest intensity for a given period were obtained by well determined couples of values of V and i; in four cases recorded by the author these conformed approximately to the relations

$$(\cdot) \quad \lambda^2 V = \text{const.},$$

$$(\cdot\cdot) \quad \frac{V^{3/2}}{i} = \text{const.}$$

If instead of varying V and i simultaneously V is kept constant and i is varied continuously, oscillations of different periods are also obtained. The values of i which, with given values of V, give rise to oscillations of the greatest strength having a wave-length λ, satisfy the relation

$$(\cdot\cdot\cdot) \quad \lambda^2 i = \text{const.}$$

The author remarked that none of the generally accepted theories were capable of explaining these results, and he therefore put forward an ingenious new model.

I think that all the facts observed by E. W. B. Gill can be also explained by the more extensive and precise scheme that I have developed in three notes in the *R. Acc. delle Scienze di Torino* during the year 1931 [*].

In these I showed that the electrons contained between the plate and the grid of the valve, with positive grid, as a whole form an oscillating system whose frequency is a function of the total number N of the electrons. It follows therefore as a fundamental relation that

$$(a) \quad \lambda^2 N \text{ must be constant.}$$

If N is calculated to a first approximation, by neglecting

* Vol. lxvi. pp. 123, 217, 383 (1st semester): Notes I., II., III.

space-charge effects, under the supplementary condition that V=const., then (a) clearly becomes

$$\lambda^2 i = \text{const.},$$

as I showed in Note I.

It is just this relation ($\cdots$) that E. W. B. Gill found experimentally by V = constant.

A method of calculating N, taking into account the space-charge effects, is developed in Note III. I obtain an expression of the form

$$N = V f\left(\frac{V^{3.2}}{i}\right),$$

f being a numerically calculable function of $\frac{V^{3.2}}{i}$. It follows that, if $\frac{V^{3/2}}{i}$ remains constant, as in the experiments of E. W. B. Gill ($\cdot\cdot$), then $\lambda^2 V =$ const. ($\cdot$) is an immediate consequence of the relation (a) $\lambda^2 N =$ const.

In a series of experiments (to be published shortly) which I have carried out with valves of many types the relation $\lambda^2 N =$ const., predicted by the theory, has proved itself valid in all cases as a satisfactory approximation. In special cases, when $\frac{V^{3/2}}{i}$ does remain constant, it is found that $\lambda^2 V$ is constant too.

Physical Institute,
    University of Turin.
January 28th, 1932.

Yours faithfully,
Antonio Rostagni.

LXV. *On the Electrical Oscillations of very short
Wave-length.*

To the Editors of the Philosophical Magazine.

Gentlemen,—

PROFESSOR ROSTAGNI has most kindly sent me a copy of his note to you on short-wave oscillations, and I should like to make a few remarks thereon. I do not think Professor Rostagni and I are very far apart ; his very interesting calculations, which I had not seen before, are the result of approaching the problem in a rather different manner. Where I am not in agreement with him is as to whether his theory affords a complete explanation of what is happening. He has proved that the space charges between the grid

and anode of a valve have natural periods of oscillation obeying observed laws, but that is a very different thing from proving that the electrons passing across the valve will maintain these oscillations. The theory I put forward tried to explain exactly how this regeneration occurred.

An analogy from sound illustrates the difference. The natural period of the air in an organ-pipe can be calculated ; this corresponds to Prof. Rostagni's work. The explanation of how a uniform stream of air blowing past the orifice can keep the pipe sounding corresponds to what I published.

Mr. Morrell has pointed out to me that my explanation of the valve's action corresponds exactly to the well-known explanation of the maintenance of sound in an organ-pipe, and it is therefore not surprising that Prof. Rostagni and I ultimately reach the same type of equation for the frequencies.

Yours faithfully,

Merton College, Oxford.
February 8, 1932.

E. W. B. GILL.

LXVI. *Transient Response of the Triode Valve Equivalent Network.*

To the Editors of the Philosophical Magazine.

GENTLEMEN,—

AN introductory remark in my paper on " The Transient Response of the Triode Valve Equivalent Network " in the January issue of your Journal, and its relation to the subsequent subject-matter of the paper, is liable to lead to difficulty and misinterpretation, and calls therefore for extension. It is stated that the distorting transient introduced by the elements of the triode network should be of short duration in comparison with the duration of the transient. This, however, is only a partial statement of the case. Taking the resistance capacity coupled amplifier example, in which the coupling condenser C_4 is given a value of $\cdot 5 \times 10^{-10}$ farads, the output voltage response to the unit input voltage consists of two components of time constants

$$T_1 = 1/3 \cdot 04 \times 10^6 \text{ sec.} \quad \text{and} \quad T_2 = 1/1968 \text{ sec.}$$

The output voltage is zero at time $t=0$, and then rises to a maximum at a rate governed mainly by T_1, after which it dies away at a rate determined by T_2. For an approach to perfect reproduction of the unit voltage pulse the duration of the transient rise must be as short as possible compared with

the duration of the applied pulse, so that T_1 must be small. On the other hand, the rate of output voltage decay after the maximum is attained must be as slow as possible, a consideration which calls for a large value of T_2 and therefore a large value of C_4, although a small value may appear to be indicated in the paper. This statement also relates in some measure to the C_4 value in the choke-coupled case considered. The effect on the nature of the response curves of decreasing T_1 and increasing T_2 is well demonstrated by C. W. Oatley in the 'Wireless Engineer,' viii. pp. 204 & 307 (1931). A comparison of the transformer-coupled amplifier with a resistance-capacity coupled circuit employing a value of $1\,\mu\mathrm{f}$. for C_4 shows that not only is the voltage rise in the former case less rapid, but, further, that the voltage decays much more quickly. This emphasizes the superiority of a correctly adjusted resistance-capacity coupled amplifier—a point somewhat hidden by the value of C_4 chosen in the paper.

College of Technology,
　　Manchester.
22nd January, 1932.

Yours faithfully.
　　W. JACKSON.

LXVII. *The Theory of the Electrification of Aerosols.*

To the Editors of the Philosophical Magazine.

GENTLEMEN,

I SHOULD like to point out that in a recent communication to the Philosophical Magazine (p. 1175, Dec. 1931) on the "Theory of the Electrification of Aerosols," equation (4), giving the relationship between the particulate volumes of the electrified and total particles in a coagulating system, was wrongly printed. The correct form of equation (4) is

$$\sigma_e = 1 \cdot 5\sigma + \left[\frac{e^{b^2(\sigma^2 - \sigma_0{}^2)}}{\sigma_{e_0} - 1 \cdot 5\sigma_0} - \frac{b^2}{0 \cdot 75} e^{b^2\sigma^2} \left(\int_0^\sigma e^{-b^2\sigma^2}\,d\sigma - \int_0^{\sigma_0} e^{-b^2\sigma^2}\,d\sigma \right) \right]^{-1}. \quad (4)$$

The numerical calculations quoted in the paper were, of course, made from the correct form of the equation as given above.

Yours faithfully,
　　H. S. PATTERSON.

Leeds University.
9th February, 1932.

LXVIII. *Notices respecting New Books.*

Die Quantenstatistik und ihre Anwendung auf die Elektronentheorie der Metalle. By L. BRILLOUIN. Translated by E. RABINOWITSCH. *Struktur der Materie*, XIII. [Pp. x+530.] (Springer, Berlin, 1931. R.M. 42; bound 43.80.)

THE present book is a translation of 'Les statistiques quantiques' which has fitly been added to the 'Struktur der Materie' series. The author has taken advantage of the German edition to make a number of modifications and improvements in the treatment, and he has extended the account of the electron theory of metals, bringing it completely up-to-date.

The book opens with a lucid summary of the classical treatment of temperature radiation, involving the laws of Kirchhoff, Stefan, and Wien. The photon hypothesis is then introduced and the fundamental ideas of wave mechanics are outlined. After an account of classical statistical methods the quantum modifications, embodied in the Einstein-Bose and Fermi-Dirac statistics, are fully discussed, and applications are made to radiation and to emission and absorption processes. This first part of the book, clear and comprehensive without being unduly detailed, is admirably adapted to bridge the somewhat difficult gap between such a book as Rice's 'Introduction to Statistical Mechanics' and Fowler's large treatise.

The kernel of the book, for which the first part paves the way, is a detailed critical account, in two chapters occupying over two hundred pages, of the application of the Fermi-Dirac statistics to free electrons in metals by Sommerfeld, and of the later theoretical developments. An outstanding weakness of Sommerfeld's theory lay in the lack of precision as to the "mean free path of the electrons" which entered into the formulæ. Much of the later work may be regarded (though somewhat artificially) as being directed at a determination of this free path. Starting with free electrons. the problem is to determine the effect of the periodic field of the crystal lattice on the electron waves, and the effect of interchange of energy between them and the thermal motions of the crystal when electric (and magnetic) fields are applied. The discovery that there are allowed and disallowed energy bands has shed an entirely new light on the problem of conduction. In an alternative procedure the electrons, in the first approximation, are treated as bound to particular atoms. The work that has been carried out in this difficult field by Brillouin himself, Bloch, Peierls, and others is admirably discussed. The unified presentation, co-ordinating a multiplicity of original papers, will be invaluable, giving, as it does, a comprehensive account of developments which seem destined to be of fundamental significance for the understanding of the metallic and semi-metallic state.

In the last two chapters the distribution of electrons in atoms, and inside and near the surface of metals, and the distribution of atoms between different states under various conditions, are discussed. An appendix deals with formulæ for dispersive media, with the fundamentals of combinatory analysis, and with some very recent work by Nordheim and Peierls on the electron theory of metals.

The book will be of the greatest value to those who require either an introduction to recent developments in quantum statistics, or a full account of one of its most important applications.

Cours D'Electricité Théorique professé a l'école professionelle supérieure des postes et télégraphes. Par J. B. Pomey, Ingénieur en chef des postes et télégraphes. Tome III. [Pp. 315.] (Gauthier-Villars et Cie. Paper cover, fr. 90.)

This well-printed book gives a pretty complete account up to recent times of the mathematical theory of telegraphy and telephony.

After a short opening chapter on the equations of the electromagnetic field, the author plunges at once into his subject, and devotes a chapter to radiation from antennæ and wave propagation and reflection.

There follow several chapters on the Theory of Relativity with the necessary mathematical introductions.

This first half of the book is very largely mathematical, but the latter part is concerned in the main with the more technical task of giving an account of the theory of telephone transmission. Thus we have, in Chapter 8, an excellent treatment of the loaded line which gives particular attention to the questions of phase and frequency distortion. Other subjects dealt with in this section include the balancing of paired circuits, the localization of faults by impedance-frequency tests, and the theory of the repeater considered as a four-terminal network. The treatment of the subject as a whole may be said to be unusually comprehensive.

The following chapter develops the theory of artificial lines and frequency filters, the homographic transformation being also presented, while in the remaining sections we find the theory of the valve oscillator, the Gulstad relay, and a useful account of the latest work on operational circuit analysis. In this latter section the author makes frequent reference to the work of Carson in America, and manages to present, in a comparatively small space, a very clear statement of the theory as it stands at present.

Quartz Resonators and Oscillators. By P. Vigoureux, M.Sc., National Physical Laboratory. [Pp. 217+figs. 125.] (H.M. Stationery Office. Boards, 7s. 6d.)

This monograph has been produced under the auspices of the Radio Research Board, and will be found to be a most useful

and up-to-date account of Piezo-electricity in general and its applications.

The first of the five chapters is given up to a short general account of the physical properties of quartz, and here the first hint is given of the extraordinarily rapid war-time development of the subject initiated by the brothers Curie in 1880 by their discovery that some strained crystals exhibit electrical polarity.

This chapter is perhaps rather too condensed to permit the author to do justice to his subject. Terse dismissal of well-known properties is understandable under such self-imposed conditions of brevity, but many readers would have welcomed an extra line or two for a definition of such a term as " Permittivity " for example.

The section on the static Piezo electric effect is most useful, and the practical details for the preparation of quartz plates will be found specially useful to experimentalists.

The next section, on Piezo Electric Resonators, deals with a mass of interesting detail, both theoretical and experimental, and appears to be a very specially complete account of this most interesting subject.

Numerous circuits are given for oscillation maintenance, and a sub-section is devoted to quartz resonators as frequency standards and other applications.

The book closes with a chapter on the structure of quartz.

The book is sufficiently well printed and the numerous diagrams have been well and clearly prepared, while the references at the end of the book are very complete.

A most useful and welcome book, not only for the physicist, but for those on the look-out for the technical applications of Physics.

Die Maxwellsche Theorie. By H. A. LORENTZ. Translated by Dr. H. STÜCKLEN. [199 pp.] (Leipzic, Akademische Verlags-gesellschaft.)

THIS book (of which there is an English version, translated by Dr. L. Silberstein and A. P. H. Trivelli) is a continuation of the publication of the lectures on Theoretical Physics delivered by H. A. Lorentz at the University of Leiden.

The title "Maxwell's Theory" covers all the elements of electromagnetic theory. The first chapter proper (following an excellent summary of vector analysis) is devoted to a derivation of the equations of the electromagnetic field, and these are subsequently applied to the separate branches of electrostatics; current electricity, stationary and induced ; the last two chapters being given to a short account of the energy of the electromagnetic field and the electromagnetic theory of light. The mathematics is treated vectorially, although where the condensed form of the vector notation is liable to render the assimilation of the equation difficult, the Cartesian form is given as well, so that even the amateur mathematician will find the book well within his powers.

The treatment is throughout logical, compact, and complete, howbeit the physical aspect of the fundamental equations is given rather scanty consideration; in particular, the account of the displacement current is so brief as to be almost breathless—but to one who wishes merely to appreciate the mathematical development this is no disadvantage.

Like all reprinted courses of lectures it is intended for serious study rather than for reference on particular problems; and for the purpose of acquiring a knowledge of electromagnetic theory it would be difficult to recommend a better treatise.

The Dipole Moment and Chemical Structure. Edited by P. DEBYE. Authorised translation by WINIFRED M. DEANS. [Pp. x+134.] (London : Blackie & Son Ltd. Price 10s.)

THE relation between molecular structure and the magnitude of the electric dipole moment was the subject of discussion at a recent conference at Leipzig, and the present volume is a collection of papers communicated by various workers in this particular field.

The theoretical considerations of Debye relative to the influence of permanent dipoles on the dielectric capacity of liquids and gases has given a marked impetus to the further investigation of dielectric properties, and the accuracy attainable in such measurements has been greatly increased in consequence. This, indeed, may be regarded as essential for the application of dipole moment data to various problems.

Results thus far obtained justify the view that dipole moments provide valuable information relative to the spacial configuration of molecules, and that such data afford a basis for the correlation of many physical and chemical properties of related compounds.

The collected papers describe recent advances in theory and experiment from both the physical and chemical standpoint. Particular interest attaches to those which deal with (1) the influence of temperature on the dielectric constants of gases and vapours, (2) the application of the molecular-beam method of observation, and (3) the connexion between dipole moment and reaction velocity.

To those physicists and chemists who are concerned with problems involving molecular polarization effects the book should be of value as a convenient source of information relative to the problems which are in course of investigation, although it does not in any way serve the purpose of a monograph on the subject. The translator's work has been thoroughly well done.

H. M. DAWSON.

LXIX. *Proceedings of Learned Societies.*

GEOLOGICAL SOCIETY.

December 16th, 1931.—Prof. W. W. Watts, LL.D., Sc.D.,
F.R.S., Vice-President, in the Chair.

THE following communication was read :—

' The Tertiary Ring Complex of Slieve Gullion (Ireland).'
By James Ernest Richey, M.C., B.A.I., F.G.S., with petro-
logical notes by Herbert Henry Thomas, M.A., Sc.D., F.R.S.

The Tertiary intrusive complex of Slieve Gullion lies west
of the Mourne Mountains and north-west of the Carlingford
peninsula. Topographically, it consists of a ring of curving
ridges and hills, 7 miles in diameter, which is bisected by
a mountainous belt extending to the north-west. The ring
and the North-West Belt mark the outcrops of a very simple
ring-dyke complex and later Tertiary plutonics (not described
in the present paper). The area was mapped by J. Nolan,
F. W. Egan, and W. A. Traill of the Geological Survey over
60 years ago, and their work has now been extended by the
Authors.

The Slieve Gullion Tertiary rocks are intruded around the
western portion of the Newry Granite. This, in its composition
and in its relations to Silurian country rocks, resembles the
Lower Old Red Sandstone granites of the Southern Uplands
of Scotland.

The Ring Complex forms a complete ring, except to the
south-west, where it is broken through by the North-West
Belt. It includes the following rocks, in order of age :—
(1) Lavas of olivine-basalt, basalt with felspar phenocrysts,
and trachyte, associated with (2) agglomerates, chiefly formed
of fragments of Newry Granite and lying in vents along the
south-western part of the ring. These, the Forkhill vents,
are intruded by (3) an elongate vent-intrusion and an arcuate
ring-dyke of porphyritic felsite. The remainder of the ring
is constituted of (4) remarkable breccias, due largely to
crushing and partly to explosion, associated with (5) an exten-
sive ring-dyke of porphyritic granophyre, in part a double
or triple intrusion. This ring-dyke is intruded to the north-
west and south-east by masses belonging to the North-West
Belt. The Ring Complex is perhaps entirely earlier than the
North-West Belt.

The olivine-basalts are identical with the Hebridean plateau type, and predominate over the other lavas. All appear to be downslipped masses within the vents. The agglomerate-fragments consist of various other rocks in addition to granite, and are evidently well mixed together. They include locally all the Tertiary lava-types mentioned, as well as a glassy andesite. The felsite sometimes penetrates the agglomerates so intimately as to form a matrix for the fragments, as Nolan observed, and the vent-brecciation is ascribed to gases given off from the uprising felsite magma. Age-relations of the felsite and granophyre ring-dykes are proved at contacts. The crush-breccias include flinty crush-rock, and the crushing affects the granite-wall as well as the granophyre ring-dyke itself. The brecciation is most intense around the north and west sides of the ring-dyke. It suggests movement of the central block enclosed by the ring-fissure, but no marked subsidence can be proved.

The almost exact coincidence of the ring-fissure with the margin of the western portion of the Newry Granite is perhaps the most remarkable feature of the Ring Complex. A local magma-reservoir underlying the Tertiary complex would seem to owe its position to the Newry Granite. If so, the reservoir should perhaps be ascribed to crustal-subsidence rather than to crustal re-melting, since it was, mainly at least, filled with magma of normal Tertiary affinities.

January 13th, 1932.—Dr. H. H. Thomas, M.A., Sc.D., F.R.S., Vice-President, and afterwards

Prof. E. J. Garwood, M.A., Sc.D., F.R.S., President, in the Chair.

The following communication was read :—

'The Geological Structure of the Eastern Mendips.' By Francis Brian Awburn Welch, B.Sc., Ph.D., F.G.S.

The area here termed the Eastern Mendips comprises the Beacon Hill pericline, the most southerly situated of the four echeloned Mendip periclines and that bordering the Radstock Coalfield. As in the other three cases, the structure is anti-clinal with a steeply folded north limb : the core is formed of Old Red Sandstone and Silurian, the Avonian outcropping on the flanks. The south limb is much concealed by Mesozoic strata, which also stretch across the eastern part of the area, so that the Avonian can only be seen in deep ravines.

The region can be divided into three parts—the eastern, the western, and the central. The western area is relatively

simple in structure and calls for little comment, except that on the north limb the D$_3$ Subzone has been detected. The eastern area is extensively faulted along the southern limb, the limestones being thrust along the line of the K-shales against the Old Red Sandstone. The central area forms a great thrust-block bordered by two north-and-south tear-faults which run through Downhead on the west and Chantry on the east. The beds on the north limb show little signs of faulting, whilst the limestones of the south limb were apparently thrust northward over the K-shales. The result was the production of a gigantic overfold on the north side (resembling in shape a. breaking wave) under which the Coal Measures were thrust. All that remains of this overfold, which was shattered by minor thrusting, are the inliers of Vobster and Luckington, which lie in a due north line between the two tear-faults.

The whole sequence of events appears to have been the northward drive of the east-and-west pericline against the southern ' nose ' of the Coal Measure basin (with a north-and-south axis). Maximum resistance was offered to this movement along the line of this axis, and in this line lies the Central Fault Block. Consequently, the Coal Measures to the west are little disturbed, except for slight overfolding which gradually increases eastwards and reaches a maximum between the two tear-faults.

January 27th, 1932.—Prof. E. J. Garwood, M.A., Sc.D., F.R.S., President, in the Chair.

The following communication was read :—

' The Geology of the Ruhuhu Coalfields, Tanganyika Territory.' By Gordon Murray Stockley, A.R.C.S.. D.I.C.. F.G.S. ; with a report on some Fossil Plants from the Karroo Beds in the Ruhuhu River Depression, by Prof. John Walton, D.Sc., F.R.S.E., F.G.S. (Read by Mr. L. R. Cox, M.A., F.G.S., in the absence of the Author.)

The paper gives an outline of the geology of an area of some 1500 square miles situated east of Lake Nyasa, and drained by the Ruhuhu and its tributary rivers. The area, which is occupied by Karroo rocks, forms a depression between the mountains which lie to the north and south ; these are composed of gneisses and other rocks of the Primitive System, which are brought into juxtaposition with the Karroo rocks by faults of considerable magnitude—in one case at least 10,000 feet. The boundary of the gneiss is marked by steep

fault scarps. The whole area is also cut up into numerous fault blocks. The faults, which date from the period of rift faulting, mostly range in direction from north-east and south-west to north-north-west and south-south-east.

The rocks of the Primitive System fall into three groups : (a) highly altered felsitic and acid volcanic rocks ; (b) metamorphosed sedimentary rocks, consisting of quartzites, marbles, ophicalcites, phyllites, and mica-schists ; (c) gneisses and granulites.

The following classification of the Karroo rocks is proposed :—

		Feet.
(Lower Stormberg)	MANDA BEDS. Felspathic sandstones and marls with *Unio* and one bone bed ...	440
(Middle and Upper Beaufort ?)	KINGORI SANDSTONES. Current-bedded grits and sandstones, conglomeratic in part	1200
(Lower Beaufort)	LOWER BONE BED. Mudstones with limestone nodules and sandstone beds, and containing reptilian bones and fossil wood	300
(Upper Ecca ? to Lower Beaufort)	RUHUHU BEDS. Fine-grained sandstones. shales, etc., with beds and nodules of magnesian limestone, and with occasional fossil wood (*Dadoxylon*); *Palæomutela* and *Glossopteris* present in the upper beds ....700 to	1000
(Ecca)	UPPER COAL MEASURES. Clay-shales with coal seams. ironstones, and sandstone beds	335
(Do.)	INTERMEDIATE MARLS AND SANDSTONES.	450
(Do.)	LOWER COAL MEASURES. Sandstones with coal seams, carbonaceous shales, and limestones	450
(Do. ?)	BASAL SANDSTONES AND CONGLOMERATE.	1690

Approximate total thickness...... 5865

The correlation of the Karroo Beds with the standard South African succession is based upon the evidence of the reptilian remains, mollusca, and plants described in the following papers. An account is given of the exposures of the two bone beds.

A report on the fossil plants from the Karroo rocks is added.

LXX. *Electrodeless Discharges.* By J. S. TOWNSEND, *M.A.,*
F.R.S., Wykeham Professor of Physics, Oxford *.

1. IN previous papers on high-frequency discharges I have
shown that the theory which I gave to explain the
uniform positive column in direct-current discharges † also
explains the uniform luminous column of high-frequency
discharges in cylindrical tubes.

The theory may be applied in general to various other
types of discharge, such as electrodeless discharges in
spherical bulbs, provided the pressure of the gas is within
certain limits.

The experiments on direct-current discharges show that
the force in the uniform positive column is independent of
the current, when the increase of temperature of the gas
due to the current is negligible. It is therefore necessary
to assume that the numbers of electrons and positive ions
per cubic centimetre of the gas are proportional to the
current. It is also assumed that the supply of electrons and
positive ions is maintained by the process of ionization by
collision at a rate proportional to the number of electrons
per cubic centimetre. In the steady state the rates at which
the electrons and positive ions disappear from the gas are

---

* Communicated by the Author.
† ' Electricity in Gases Section,' p. 302 (1915).

also proportional to the current, since these rates must be the same as the rate of ionization.

The effect of recombination of electrons and positive ions in the gas is small and may be neglected, since the rate at which electrons and positive ions disappear due to this process is proportional to the square of the current. According to this theory the electrons and positive ions disappear by diffusing to the sides of the tube.

2. In order to apply the theory to electrodeless discharges in a spherical bulb it may be supposed that the bulb is placed midway between two large parallel plates connected to the ends of the inductance of an oscillatory circuit which performs oscillations of constant amplitude.

When a continuous oscillatory discharge is thus maintained in the bulb, the oscillating force Z in the gas is less than the mean force V/*b* between the plates, V being the oscillating potential and *b* the distance between the plates. The difference between these forces depends on the current.

As in the ordinary uniform columns, it may be assumed that the effect of recombination may be neglected and that the force Z is independent of the amplitude of the current through the gas, but the difference between the forces Z and V/*b* increases with the current.

3. The theoretical investigation of high-frequency discharges involves several coefficients which depend on the energy of agitation of the electrons. Under certain conditions, depending on the pressure *p* of the gas and the periodic time T of the oscillations, there may be appreciable periodic variations in the energy of the electrons but in general these variations are small, and the mean values of the coefficients, which are independent of the time, may be used in the equations of motion.

Let K_1 be the coefficient of diffusion of the electrons, w_1Z the velocity in the direction of the electric force, K_1 and w_1 being the mean values of the coefficients during the time T. Let K_2 and w_2 be the corresponding coefficients for positive ions.

The electrons perform oscillations about their mean positions under the action of the force Z and the distances z_1 traversed by the electrons on either side of their mean positions is $w_1Z_1T/2\pi$ where Z_1 is the amplitude of the force Z.

In discharges in helium and neon at pressures of about 5 mm. the velocity w_1Z_1 is of the order 10^6 cm. per second, so that if the wave-length of the oscillations be about

100 metres the distance z_1 is about half a millimetre. The corresponding distance traversed by the positive ions is negligible. Thus in spheres of diameter of about 8 cm. the rate at which the electrons are brought into contact with the surface by the oscillatory motion is very small. In tubes the rate at which electrons come into contact with the surface depends on the inclination of the force Z to the axis. This was observed by Gill and Donaldson in tubes 3 cm. in diameter containing air at low pressures *. They found that the loss of conductivity due to this cause was greatest when the force was perpendicular to the axis. In the following theory this effect will be neglected, and it will be supposed that the electrons and positive ions come into contact with the surface of the bulb by the process of diffusion.

4. Let n_1 be the number of electrons per cubic centimetre of the gas when the electrons are in their mean positions, a the radius of the bulb, and r the distance of a point in the gas from the centre of the bulb. The electrons are distributed symmetrically about the centre so that n_1 is a function of r except at points near the surface of the bulb. Let N_1 be the number of electrons in the sphere of radius r,

$$N_1 = 4\pi \int_0^r n_1 r^2 dr,$$

and let n_2 and N_2 be the corresponding numbers of positive ions.

In the high-frequency discharges which are here considered the electric force is comparatively small and the mean velocity of the electrons in the direction of the electric force is small compared with the velocity of agitation. The rate at which molecules of the gas are ionized therefore depends on the energy of agitation of the electrons. Thus the mean rate of ionization in unit volume of the gas during the time T is proportional to the number of electrons n_1 and to a factor which is a function of the mean energy of agitation E_1. The rate of increase of n_1 may therefore be expressed in the form $n_1 \phi(E_1)$. For the purposes of this investigation it is convenient to express $n_1 \phi(E_1)$ in terms of the electric force and the ordinary coefficient of ionization α.

5. In the method of measuring this coefficient which is usually adopted electrons are set free from a plate P_1 by the

* E. W. B. Gill and R. H. Donaldson, Phil. Mag. xii. p. 719 (Sept. 1931).

action of ultra-violet light, and move under a constant force Z through a distance z to a parallel plate P_2. The increase in the number of electrons n that arrive at the plate P_2 due to an increase dz in the distance between the plates is expressed in terms of α by the equation $dn = \alpha n\, dz$. Thus the rate of increase of the number n in the time dt is $\alpha n\, dz/dt$ where dz/dt is the velocity wZ of the electrons in the direction of the force. The rate of increase of n due to ionization by collision may therefore be expressed in the form $\alpha n wZ$.

It will be shown that the mean energy of agitation of the electrons in an oscillating discharge is the same as the mean energy E_1 of electrons moving under a constant force of intensity $Z_1/\sqrt{2}$, Z_1 being the amplitude of the oscillating force.

When the ionization is maintained in a spherical bulb by an oscillating force the mean rate of ionization in a sphere of radius r may therefore be represented by the expression $\alpha N_1 w_1 \overline{Z}$, where $\overline{Z}$ is the mean force $Z_1/\sqrt{2}$.

6. Since the electrons diffuse more rapidly than the positive ions the number of electrons left in the gas is less than the number of positive ions in the initial stages of the development of the current. There is therefore a positive charge in the gas giving rise to a force R along the radius, which retards the motion of the electrons and accelerates the motion of the positive ions towards the surface of the bulb ($R = e(N_2 - N_1)/r^2$).

In general $(N_2 - N_1)$ is small compared with N_1 or N_2. In the steady state where the amplitude of the oscillating current is constant, the rates at which the electrons and positive ions pass outwards through the surface of a sphere of radius r is equal to the rate of ionization of the gas in the sphere. These conditions are expressed by the following equations :

$$\alpha N_1 w_1 \overline{Z} = -4\pi r^2 K_1 dn_1/dr - 4\pi r^2 n_1 w_1 R, \quad . \quad . \quad (1)$$

$$\alpha N_1 w_1 \overline{Z} = -4\pi r^2 K_2 dn_2/dr + 4\pi r^2 n_2 w_2 R. \quad . \quad . \quad (2)$$

If $(n_2 - n_1)$ be neglected in comparison with n_1 an equation is obtained for n_1 by eliminating R which may be written in the form

$$\frac{d^2 n_1}{dr^2} + \frac{2}{r}\frac{dn_1}{dr} + c^2 n_1 = 0, \quad . \quad . \quad . \quad (3)$$

where c^2 is the constant $\alpha w_1(w_1 + w_2)\overline{Z}/(K_1 w_2 + K_2 w_1)$.

Since w_1 is large compared with w_2 and $K_1 w_2$ large compared with $K_2 w_1$, the value of c^2 is approximately

$$c^2 = a w_1{}^2 \bar{Z}/K_1 w_2 \quad \cdots \cdots (4)$$

The solution of equation (3) is

$$n_1 = A \sin cr/cr \quad \cdots \cdots (5)$$

and for a first approximation this equation may be taken as

$$n_1 = A(1 - c^2 r^2/6). \quad \cdots \cdots (6)$$

A being the value of n_1 at the centre of the sphere. The total number of electrons in the sphere of radius r is

$$N_1 = \tfrac{4}{3}\pi r^3 A(1 - c^2 r^2/10). \quad \cdots \cdots (7)$$

Assuming the value of n_1 near the surface of the sphere to be $A/2$ the product $c^2 a^2$ is 3, and the mean value of n_1 throughout the gas is ·7 A. If the ratio of the values of n_1 at the centre and at the surface of the bulb, and the force $\bar{Z}$ were known, a would be determined by equation (4), since the coefficients w_1, w_2, and K_1 have been found in terms of the ratio $\bar{Z}/p$. The theory may thus be tested by comparing these values of a with those found by the ordinary method [*].

7. Since K_1 and w_1 are large compared with K_2 and w_2, the value of R is obtained directly from equations (1) and (2) without considering the solution given by equations (4), (5), and (6). The value of n_1 is a maximum at the centre of the bulb so that dn_1/dr is negative. In equation (1) the quantity on the left is expressed as the difference of two large quantities, and in equation (2) the same quantity on the left is expressed as the sum of two small quantities. The first equation therefore shows that the two quantities on the right are approximately equal, so that the following equation is obtained for R :

$$R = -\frac{K_1}{w_1} \times \frac{1}{n_1} \times \frac{dn_1}{dr}, \quad \cdots \cdots (8)$$

and the difference between the potential at the centre and that at the surface of the bulb is

$$-\int_0^a R \, dr = (K_1 \log A/A^1)/w_1. \quad \cdots \cdots (9)$$

---

[*] *Comptes Rendus*, clxxxvi. p. 55 (Jan. 1928).

According to the theory * of the motion of electrons which has been given to explain the lateral diffusion of a stream, the ratio K_1/w_1 is $mu_1^2/3e$ where e is the atomic charge, so that if the kinetic energy of the electron be expressed in the form eE_1 where E_1 is a potential, the ratio K_1/w_1 is $2E_1/3$, and the potential

$$-\int_0^a R\,dr \text{ is } (2E_1 \log A/A')3.$$

If A' be one half of A this potential is $\cdot 46\,E_1$.

Thus the potential $\int_0^a R\,dr$ depends only on the energy of agitation of the electrons and on the ratio of the values of n_1 at the centre and at the surface of the bulb †.

In ordinary discharge-tubes containing helium or neon at pressures exceeding 2 or 3 mm. the mean energy of agitation of the electrons is about 3 or 4 volts, so that the potential at the centre of the bulb exceeds that at the surface by about 1·5 or 2 volts.

The oscillating force increases with the pressure of the gas, and at high pressures (exceeding 2 or 3 mm.) the force R is small compared with the mean force $\overline{Z}$. At lower pressures the force R becomes comparable with the mean force $\overline{Z}$, so that it would be necessary to modify the theory in order to take into consideration the effect of the force R on the energy of agitation of the electrons.

8. The force R is not oscillatory, since the periodic variations in the numbers n_1 and n_2 are negligible. This may be seen by considering the rate of increase of n_1 due to ionization by collision given by equation (1).

In discharges in helium in a tube 3 cm. in diameter, the value of α is $7\cdot7 \times 10^{-3}$ when the pressure is 6 mm. and $1\cdot8 \times 10^{-3}$ when the pressure is 22 mm.‡

The velocity $w_1\overline{Z}$ is of the order 10^6 cm. per second, so that the rate of increase of n_1 due to ionization by

---

* Proc. Roy. Soc. A, lxxxi. p. 464 (1908).

† A similar result is obtained for the uniform column of a discharge in a cylindrical tube. This may be deduced in the same way from equation (1), p. 1115, of the paper on "Uniform Columns in Electric Discharges" (Phil. Mag. vol. xi., May 1931). In this case also, the potential at the centre of a section exceeds that at the surface of the tube by the amount ·46 E_1 when the value of n_1 near the surface is one half the value at the centre of a section.

‡ Phil. Mag. vol. xi. p. 1118 (May 1931).

collision is of the order $5 \times 10^{8} \times n_1$. In the half period T/2 of an oscillation of 100 metres in wave-length the number of electrons generated by collisions is therefore of the order $n_1 \times 10^{-3}$. This shows that during the time T, the periodic variations in the numbers n_1 and n_2 are very small so that the force R which depends on the difference may be considered constant for oscillations of wave-lengths of the order of 100 or 1000 metres.

9. Although the periodic changes in the numbers n_1 and n_2 are small there may be appreciable periodic changes in the energy of agitation of electrons.

In each complete oscillation there are two intervals during which the force is small, and the electrons lose more energy in collisions with molecules of the gas than they gain by moving in the direction of the force.

The periodic variations in the energy of agitation of the electrons arising from this cause depend on the mean free path of the electrons and on the mean loss of energy in a collision.

The calculation of the variations of energy is simplified by adopting the results of the investigations that have been made to determine the steady motion of electrons in a direct current moving under the action of a constant force. Let E_1 be the mean energy of agitation of electrons in the steady motion maintained by a constant force of intensity $\overline{Z}$, u_1 the velocity $\sqrt{2E_1/m}$, and $w_1\overline{Z}$ the velocity of the electrons in the direction of the force. The energy E_1 and the velocity $w_1\overline{Z}$, have been determined experimentally for a large number of gases, and from these determinations the mean free path and the mean loss of energy of an electron in a collision are obtained by formulæ based on the kinetic theory of gases *. These formulæ involve numerical coefficients which depend on the specification of a collision, and also on the distribution of the energies of the electrons about the mean energy.

Thus if l be the mean free path, and E the kinetic energy of an electron, λE the mean loss of energy of the electron in a collision, and u the velocity $\sqrt{2E/m}$, the number of collisions made by the electron in the time dt is $u\,dt/l$ and the loss of energy is $\lambda E u\,dt/l$. The mean loss of energy in the time dt of electrons in a stream where the energies are distributed about the mean energy E_1 is therefore

---

* ' Motion of Electrons in Gases ' (Clarendon Press, Oxford, 1925).

$c_1 \lambda E_1 u_1 / l$, where c_1 is a constant depending on the distribution of the energies about the mean energy. The mean gain of energy in the time dt of the electrons in the stream due to the motion in the direction of the electric force is $e w_1 \overline{Z}^2 dt$. In the steady state where E_1 is constant these two quantities are equal, so that the relation between the constants is given by the equation

$$2 \lambda' E_1{}^2 / ml = e w_1 u_1 \overline{Z}^2, \quad . \quad . \quad . \quad . \quad (10)$$

where λ' is the product $c_1 \lambda$. The product $w_1 u_1$ is a constant proportional to l.

10. The preceding results may be used in investigating the energy of agitation of the electrons in high-frequency discharges. In these cases it is necessary to consider the periodic variations in the energy. Let E be the mean energy at any time t, u the velocity $\sqrt{2E/m}$, wZ the velocity in the direction of the electric force, $Z = Z_1 \sin qt$ the force, and T the periodic time $2\pi/q$. The coefficient w is inversely proportional to u, so that $w_1 u_1 / u$ may be substituted for w. In this case the rate at which the mean energy of the electrons increases due to the motion in the direction of the force is $e w Z^2$, and the rate at which the mean energy is reduced by the collisions of the electrons with molecules is $\lambda' E u / l$. The rate of change of the energy is the difference between these quantities, so that the equation * for dE/dt is

$$u \, dE/dt = e w_1 u_1 Z^2 - \lambda' E u^2 / l . \quad . \quad . \quad (11)$$

which gives E in terms of t since $u = \sqrt{2E/m}$.

Substituting for Z^2 its value $\overline{Z}^2 (1 - \cos 2qt)$ and for $e w_1 u_1 \overline{Z}^2$ the value given by equation (10), the differential equation for E in terms of t becomes

$$\sqrt{2E/m} \, dE/dt = 2\lambda'(E_1{}^2(1 - \cos 2qt) - E^2)/lm . \quad (12)$$

Under an oscillating force of constant amplitude there is a steady state where the mean energy of the electrons may be expressed in the form of a series where one term is a constant and the other terms periodic functions of the time with constant amplitudes. The cases of particular interest are those where the amplitudes of the periodic terms are small compared with the constant term. Under these

---

* This equation also gives the rate of change of the mean energy E of a group of electrons, moving in a uniform field where the force Z is constant, before the steady motion is attained.

conditions the solution of equation (12) representing the steady state is obtained by substituting $E_1^2 + h$ for E^2 where h is a function of the time. The following equation connecting E, h, and t, is thus obtained :—

$$\sqrt{\frac{ml^2}{2\lambda^{12}E}}\ \frac{dh}{dt} + h = -E_1^2 \cos 2qt \ . \ . \ . \ (13)$$

If the variations in E be small compared with E_1, E_1 may be substituted for E in the first term of this equation, and since the first term is large compared with the second the function h is obtained in the simple form

$$h = -\frac{QE_1}{4\pi} \sin 2qt \ . \ . \ . \ . \ (14)$$

where Q is the constant $\lambda' u_1 E_1 T/l$, which is the mean loss of energy of electrons in collisions with molecules of the gas during the time T. Thus $E^2 = E_1^2 + h$, and in cases where $Q/4\pi$ is small compared with E_1, the energy E at any time is given by the equation

$$E = E_1 - (Q/8\pi) \sin 2qt \ . \ . \ . \ . \ (15)$$

11. It will be noticed that the frequency of the periodic term is twice that of the oscillating force, and the mean values of E is the energy in a continuous current maintained by a constant force of intensity $Z_1/\sqrt{2}$ *.

The amplitude of the periodic term is small compared with E_1 and may be neglected when the wave-length of the oscillations and the pressure of the gas are below certain limits.

The energy E_1 is obtained directly in terms of the ratio Z/p from experiments on the lateral diffusion of a stream of electrons, and the quantity Q may also be found directly from similar experiments, without considering the values of λ and l. The rate at which electrons lose energy in collisions with molecules in oscillatory currents is the same as in direct currents maintained by a constant force $\overline{Z}$, since the mean energy of agitation is the same in both cases. In direct currents when the motion is steady the amount of energy lost by electrons in collisions with molecules in the

---

* On this point there is an error in the previous papers, where it is stated that the theory indicates that the effects obtained in oscillatory discharges are the same as those obtained in direct currents maintained by a constant force of intensity $2Z_1/\pi$.

time T is the same as the energy gained by moving the distance w_1 $\bar{Z}T$ in the direction of the force. Thus the value of Q in volts is $w_1\bar{Z}^2T$.

In helium the energy of agitation E_1 is $2\bar{Z}/p$, approximately, and the velocity $w_1\bar{Z}$, is 10^6 $\sqrt{\bar{Z}/2p}$ cm. per sec. for values of $\bar{Z}$ and p in ordinary uniform columns of discharges in wide tubes when the pressure is greater than 1 mm., $\bar{Z}$ being in volts per centimetre.

Under these conditions the value of Q in volts is $10^6 \times p \cdot T \cdot E_1^{3/2}/4$. The value of E_1 depends on the diameter of the tube and on the pressure of the gas.

If E_1 be 4 volts, the pressure of the gas 5 mm., and the wave-length of the oscillations 100 metres, the value of Q is $\cdot8\,E_1$.

Thus with oscillations of wave-lengths less than 100 metres, the periodic term is small compared with the constant E_1 in discharges in helium at pressures less than 10 mm., and the mean values u_1 and w_1 may be used instead of u and w in considering the motion of the electrons.

In these cases the distribution of the energies of the electrons about the mean energy E_1 in the oscillatory discharge should be the same as the distribution about the mean energy in a direct current maintained by a constant force of intensity $Z_1/\sqrt{2}$. The coefficient of ionization and the intensities of the principal lines in the spectrum of the gas should therefore be the same as the coefficient of ionization and the intensities of the lines in the direct current, since the rate of ionization and the intensity of the lines depend both on the value of the mean energy of the electron and on the distribution of the energies about the mean [*].

There is a large range of pressures and wave-lengths where this general agreement is obtained between oscillatory discharges and direct current discharges.

12. With large pressures and long wave-lengths the periodic variations in the energy of the electrons become appreciable. In addition to the corresponding periodic variations in the rate of ionization and in the intensity of the light there may also be changes in the mean values of these quantities, similar to those which would be obtained in a direct current if the distribution of the energies of the electrons about the mean energy were increased. In these

* Phil. Mag. vol. ix. p. 1145 (June 1930).

discharges, therefore, the coefficient of ionization a and the intensities of the lines in the spectrum of the gas would be somewhat greater than in a direct current maintained by a force $\overline{Z}$.

It will be noticed that there are also lower limits to the pressures and wave-lengths for which the energy of the electrons in the oscillatory discharge is obtained accurately from equation (11). In that equation it is assumed that the velocity of the electrons in the direction of the oscillating force is proportional to Z. This implies that each electron makes several collisions with molecules in the time T. This condition is not satisfied with very short wave-lengths when the pressure is low and the mean free path is not small compared with the distance $u_1 T$. It may be generally assumed that equation (11) represents the value of dE/dt accurately when the wave-length of the oscillation exceeds 50 metres, and the pressure of the gas exceeds one-tenth of a millimetre.

13. In order to determine the mean energy of agitation in electrodeless discharges it is necessary to find the force in the gas. The simplest cases are those in which the gas is contained in a sphere or a long cylindrical tube placed midway between two parallel plates. The potential difference V between the plates may be measured experimentally, but the force Z in the gas differs both in amplitude and in phase from the mean force V/b between the plates, b being the distance between the plates. These differences are due to the periodic motion of the electrons under the action of the force Z. If z be the displacement of the electrons from their mean positions the velocity dz/dt is $w_1 Z$, and the distance z is $-w_1 dZ/q^2 dt$, $2\pi/q$ being the periodic time of the oscillations. The displacement z of the electrons is independent of the shape of the vessel containing the gas. For an approximate determination of the force Z, it may be assumed that the electrons are uniformly distributed in the gas.

14. If the gas be contained in a spherical bulb of radius a and Br^3 the number of electrons in a sphere of radius r, the total charge on the electrons is $-eBa^3$ and the centre of the distribution is at a distance z from the centre of the sphere. The displacement gives rise to a uniform force eBz in the gas in the direction normal to the plates, and outside the gas the force is the same as that due to positive and negative charges $\pm eBa^3$ at points at a distance apart z and approximately at a distance $b/2$ from the plates.

The force F due to the displacement of the electrons therefore comprises the term eBz, and, in addition, a number of terms representing the effect of the images of the charges $\pm eBa^3$ in the plates. The principal images give rise to a force $4eBza^3/b^3$ at the centre of the sphere, so that when b is greater than $3a$ the value of F in the gas is approximately $eBz(1-4a^3/b^3)$.

In general the mean value of the force F in the gas may be expressed in the form

$$F = eB'z = eB'w_1 dZ/q^2 dt.$$

15. A similar result is obtained for discharges in cylindrical tubes when the axis of the tube is parallel to the plates, and midway between the plates. In this case, if r be the distance of a point in the gas from the axis of the tube, a the radius of the tube, Br^2 the number of electrons in unit length of a cylinder of radius r, the mean positions of the electrons in sections of the tube at any time during the oscillations are along a line at a distance z from the axis of the tube. The principal term in the expression for the force F in gas due to the displacement of the electrons is $2eBz$, which represents a force proportional to z. The other terms are due to the images in the plates of a uniform distribution of positive electricity eBa^2 per unit length, along the axis of the tube, and a similar distribution of negative electricity on a parallel line at a distance z from the axis. The principal images give rise to the force $4eBza^2/b^2$, so that when b is greater than $3a$ the force F in the tube is $2eBz(1-2a^2/b^2)$, which may be written in the form $eB'z$ or $eB'w_1 dZ/q^2 dt$, which is similar to the expression obtained for F in a spherical bulb.

15. In these cases the value of Z is obtained from the equation

$$Z = V/b - eB'w_1 dZ/q^2 dt, \quad . \quad . \quad . \quad . \quad (16)$$

from which the following relation is obtained between the amplitude Z_1 and the amplitude V_1 of the oscillatory potential

$$Z_1(1+T^2I^2)^{\frac{1}{2}} = V_1/b, \quad . \quad . \quad . \quad . \quad (17)$$

where I represents the quantity $eB'w_1/2\pi$, which is proportional to the number of electrons per cubic centimetre of the gas. The intensity of the light from the discharge is therefore proportional to I, so that I may be measured in

arbitrary units by a photoelectric cell. The value of Z_1 is thus obtained from the values of I corresponding to different values of V_1.

Experiments are being made to determine the force by this method in gases at different pressures.

Equation 17 shows that in general if V_1 be the potential difference between the external electrodes and b the distance between them, Z_1 is less than V_1/b, but the difference diminishes with the current.

16. As the theory of radiation is related to the theory of conductivity it is of interest to consider some points which we observed in connexion with the different types of spectra obtained in helium at high pressures. They relate principally to the continuous spectrum and were not mentioned in the accounts of the experiments which we have already given.

In order to obtain a consistent explanation of the conductivity of a gas in the part of the discharge where the force is independent of the current, it is necessary to assume that the electrons do not recombine with the positive ions. This hypothesis is in agreement with the experiments which show that with small currents the intensity of the light from the uniform column of a discharge is proportional to the current. It thus appears that the simplest explanation of the radiation from the uniform column is that in which the light is attributed to collisions of electrons with atoms of the gas.

There are three types of spectra to be considered—the line spectrum, the band spectrum, and the continuous spectrum.

In high-frequency discharges the band spectrum in helium is seen with the line spectrum in spaces near the electrodes, and in continuous discharges in the negative glow, where there are several bright bands in the visible spectrum and the discharge has a bright purple colour *.

It has been suggested that the bands are due to unstable molecules formed by the action of the discharge, but these investigations do not give direct evidence as to the origin of this spectrum, as the method of measuring the energies of the electrons does not apply to the electrons in the negative glow.

17. In tubes about 3 cm. in diameter the light in the positive column comprises only the line spectrum when the gas is at low pressures, but at pressures of 7 or 8 mm.

* J. S. Townsend and S. P. McCallum, Phil. Mag. xiii. p. 1168 (Dec. 1931).

a continuous light is obtained in the visible spectrum which increases in intensity in comparison with the line spectrum as the pressure is increased. A few bands are also obtained in the positive column, but they are very faint.

In order to test whether the continuous spectrum was due to impurities the helium was admitted to a long quartz cylinder with parallel plate electrodes at one end. If the gas contained small traces of impurities they would be removed by passing an electrodeless discharge in the other end of the cylinder and the effect would be indicated by a large change in the sparking potential between the parallel plates. This method of testing for impurities has been found to be very sensitive *.

In helium at high pressures the line spectrum and the continuous spectrum were observed in the electrodeless discharge, but the discharge had no effect on the sparking potential between the plates. It may therefore be concluded that the continuous spectrum is not due to impurities.

18. According to this theory, the change in the relative intensities of the continuous spectrum and the line spectrum obtained with a change of pressure is due to the energy of the electrons which excite the line spectrum being greater than the energy of those which excite the continuous spectrum.

When the pressure is increased the electric force required to maintain the discharge is also increased, but the ratio $\overline{Z}/p$ diminishes. The proportion in which this ratio is changed is very small compared with the change of pressure. Thus, in tubes about 3 cm. in diameter, if the pressure of the helium be increased from 4 to 12 mm. the value of $\overline{Z}/p$ is reduced from 1·8 to 1·56 and the mean energy of agitation of the electrons is reduced from 3·6 volts to 3·1 volts. This reduction in the mean energy of agitation gives rise to a large reduction (about 6 : 1) in the number of electrons per cubic centimetre with the large energies required to excite the line spectrum when the same current flows through the gas.

The corresponding reduction in the number of electrons with the energies required to excite the continuous spectrum is much less.

Thus the intensity of the line spectrum diminishes in comparison with the continuous spectrum when the pressure is increased.

* J. S. Townsend and S. P. McCallum, Phil. Mag. vi p. 858 (Nov. 1928).

In the experiments * which were made to determine the intensity of the light in the visible spectrum of helium, the intensity was measured by a photoelectric cell, and light-filters were used in order to examine the changes of intensity in different parts of the spectrum due to changes of pressure.

The light passing through the filters included light in the different types of spectrum, so that the reduction in the photoelectric effect due to an increase of pressure was less than the reduction in the intensity of the light in the line spectrum. This may account for the fact that at the higher pressures from 13 to 38 mm. the reduction in the intensity of the photoelectric effect due to an increase of pressure was so small, and the energies of the electrons that excite the light which were calculated from the experiments are so much less than the values to be expected if all the light emitted from the discharge were in the line spectrum.

19. Further experiments have recently been made in which the photoelectric effect due to the ultra-violet spectrum was compared with the photolectric effect due to the light in the visible spectrum from the same discharge. It has been found that the intensity of the green light diminishes in comparison with the ultra-violet as the pressure increases. This shows that the energies of the electrons which excite the ultra-violet light in helium at high pressures is less than the energies of those which excite the green light.

The explanation according to this theory is that the ultra-violet light contains a larger proportion of radiation in the continuous spectrum than the green light †.

The spectra of the discharges in the tubes which were used for these experiments have been photographed by Mr. Keyston. The tubes were in quartz, without electrodes, so that the gas should not become impure due to the long exposure required to obtain the photographs. The plates show the continuous spectrum in the ultra-violet region, which increases in intensity in comparison with the line spectrum, and becomes noticeable in the visible region as the pressure of the gas is increased. A set of photographs showing the effects obtained at different pressures will shortly be published.

---

* J. S. Townsend and F. Llewellyn Jones, Phil. Mag. xii. p. 815 (Oct. 1931).
† These experiments have been made in collaboration with Mr. Pakala, and a more complete account of them will be given in another paper.

LXXI. *On Potential Dividers for Cathode Ray Oscillographs. By* F. P. BURCH, *B.A., Metropolitan-Vickers Electrical Company, Ltd., Manchester* *.

SUMMARY.

IN Gábor's oscillographic method a known fraction of the voltage to be measured has to be transmitted over a long line and reproduced without distortion, the division of voltage being effected by condensers or condensers and resistances. If the low voltage impedance of the system is divided between the two ends of the line, the condensers may be made from six to eight times smaller than when it is concentrated at one end only. The field of application of the method is thus greatly extended.

I. *Introduction.*

THE principal problem of high speed cathode ray oscillography is that of recording on a stationary photographic film transients of which the moment of occurrence cannot be controlled. This has been solved in two ways. In the first, which may properly be associated with the name of Norinder†, the time-element of the record is introduced by making the cathode ray spot oscillate continually, at a known frequency, to and fro along the axis of abscissæ. To prevent fogging before the transient arrives, the beam is normally blocked by a target, and the transient is applied to a system of plates so arranged as to bend the beam past the target and cause it to reach the film with an ordinate deflexion proportional to the voltage. On the other hand, in the second method, introduced by Gábor ‡, the time-motion is a single sweep of the beam across the film, once only. The transient is first made to operate a relay near the oscillograph, and then conveyed to the voltage deflexion plates by wires which are made long enough to delay its arrival until after the relay has released the beam from a " blocking chamber " and initiated the time-sweep.

For certain problems Norinder's system has very great advantages, but it gives no record of voltages near zero, and

---

the replotting of the oscillatory trace in Cartesian coordinates is a great trouble. Gábor's method is therefore being increasingly adopted, especially for high-voltage work. Its weakness, of course, lies in the energy required by the delay wires, which are indispensable if the start of the transient—nearly always the most interesting part—is to be recorded. When the voltage to be measured is of the same order as that required for the oscillograph deflexion (usually a few hundred volts *), Gábor's method is only applicable to those problems in which the transmission of the entire transient over wires is required or can be tolerated. But when the voltage is high the delay wires can be connected to the tapping of a potential divider, and then under certain conditions the disturbance of the source becomes negligible. The nature of these conditions is most easily understood by considering the case in which the high voltage rises suddenly from zero to a constant value—the Heaviside " unit function." Faithful reproduction of this is a necessary and sufficient condition for faithful reproduction of any wave-form ; the unit voltage function is therefore as important theoretically as its close realization is common in practice. To reproduce the sudden rise, a surge current of some 5 to 20 amperes must enter the delay wires. An initial current of at least this amount must therefore be drawn from the high-voltage source. Now in most problems the surge impedance of the high-voltage circuit is of the same order as that of the delay wires, so that at some hundreds or thousands of kilovolts the immediate effect of a load of several amperes is negligible. Accordingly the reproduction of a sudden rise, or a high-frequency change, usually presents no difficulty. But to reproduce a constant voltage, following a sudden rise, the current must continue for long enough to provide the whole charge required by the wires (a few microcoulombs, for a delay time of $\frac{1}{2}$ microsecond) and, indeed, much more. For when we seek to limit the total charge taken from the high-voltage circuit, by including condensers in the potential divider, we find that it must always be fairly large compared with the charge on the wires, otherwise a sufficiently faithful reproduction cannot be obtained. Thus, if the capacity of the high-voltage circuit is limited, phenomena of moderate or long duration will be seriously affected. In most laboratory impulse circuits a drainage of 100 microcoulombs produces a considerable fall of voltage, and in many of the most interesting

---

* In high speed work. For medium speeds amplifiers can be used; also the oscillograph can be made more sensitive.
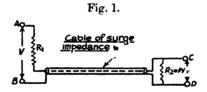
oscillographic problems, such as the study of the electro-
magnetic fields of thunderstorms, the quantity of electricity
available is much smaller.

It is therefore important to cut down the capacities of the
condensers in the potential divider to the minimum value
consistent with reasonably faithful reproduction. In the
present paper potential divider circuits are discussed in
which they may be made over six times smaller than in the
circuit used by Gábor. For some kinds of work, *e. g.*, the re-
cording of surges on power transmission lines, condensers
must in any case be included in the potential divider, to
reduce the power current taken ; and a minimum capacity
is always desirable, not only electrically, but also because of
the great bulk and cost of high-voltage condensers.

II. *Types of Potential Divider.*

Fig. 1 shows the first and simplest potential divider
system used by Gábor. The delay wires take the form of

<div align="center">Fig. 1.</div>
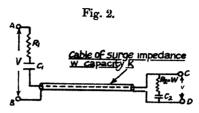
a concentric rubber insulated cable, commonly 50 yards
long, in which the velocity of propagation is about half the
speed of light. When the voltage across the terminals AB
is suddenly raised from zero to unity, a wave enters the
cable raising it to a voltage $W/(R_1 + W)$. On reaching
the end CD it meets a resistance equal to the surge im-
pedance W of the cable and accordingly suffers no reflexion.
Thus the voltage across the terminals CD jumps suddenly
from zero to $W/(R_1 + W)$ and thereafter remains constant.

For cases where condensers must be included, Gábor used
the circuit of fig. 2 with R_1C_1 approximately equal to WC_2 ;
and pointed out that C_2 must be large compared with the
capacity K of the cable, the error of reproduction being of
order K/C_2.
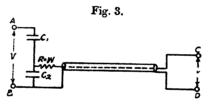
The improvements to be described in this paper arose from
the consideration of fig. 3, which is the simplest arrangement
employing condensers, instead of resistances, to effect the
initial division of potential. Under unit applied voltage
a wave of magnitude $C_1/2(C_1 + C_2)$ enters the cable and is

doubled by reflexion at CD, but is absorbed without sensible reflexion when it again reaches the input end. Thus the voltage at CD jumps initially to $C_1/(C_1 + C_2)$. But after

Fig. 2.
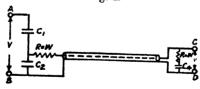
infinite time it has fallen to $C_1/(C_1 + C_2 + K)$; as in fig. 2, there is an error of amount K/C_2 (C_1 being $\ll C_2$). For the reduction of this error the circuit of fig. 4 suggested itself. Here a part of the low-voltage capacity has been transferred to the "receiving" end of the cable, being connected in series with a resistance W between the output terminals.

Fig. 3.

The "tailing off" of the first voltage wave, due to the charge drained from C_2 by the cable, is now more or less compensated by the fact that C_4 is simultaneously charging up. Moreover, if we make

$$C_1 + C_2 = C_4 + K$$

Fig. 4.

the initial value of output voltage will be the same as the value after infinite time. A very much more faithful reproduction may then be expected.

3 D 2
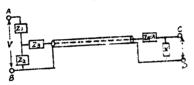
This principle of connecting shunt impedance across both
ends of the cable, instead of only one, can of course be
applied also to fig. 2. We will now discuss the performance
of the various circuits mathematically.

III. *General Equations.*

The application of Heaviside's methods to a line with
terminal impedances has been explained by Carson [*]. It
will suffice here to give the principal formulæ, which we
shall do for the rather general circuit of fig. 5. The output
voltage v, due to an applied voltage V, is given by the
solution of the operational equation

$$v = \frac{S \cdot e^{-p\tau}}{1 - \mu_1\mu_2 e^{-2p\tau}} \cdot V, \quad \cdots \quad (1)$$

Fig. 5.

in which

$$S = \frac{X}{Z_4} \cdot \frac{Z_2}{Z_1 + Z_2} \cdot \frac{(1 + \mu_1)(1 - \mu_2)}{2}, \quad \cdots \quad (2)$$

$$\mu_1 = \frac{W(Z_1 + Z_2) - (Z_1 Z_2 + Z_2 Z_3 + Z_3 Z_1)}{W(Z_1 + Z_2) + (Z_1 Z_2 + Z_2 Z_3 + Z_3 Z_1)}, \quad \cdots \quad (3)$$

$$\mu_2 = \frac{W - Z_4}{W + Z_4}. \quad \cdots \quad (4)$$

The impedances X, Z_1, Z_2, Z_3, Z_4, and in general also the
applied voltage V, are functions of the operator $p = \dfrac{d}{dt}$.
The cable is assumed to be non-dissipative, and $\tau = WK$ is
the time taken by an electric wave to travel from one end to
the other.

Equation (1) may also be written

$$v = V \cdot S\{e^{-p\tau} + \mu_1\mu_2 e^{-3p\tau} + (\mu_1\mu_2)^2 e^{-5p\tau} + \ldots\}, \quad (5)$$

---

[*] Carson, 'Electric Circuit Theory and Operational Calculus,' McGraw
Hill, Chap. X.

and the solution, giving v as a function of time, is

$$v = v_0(t-\tau) + v_1(t-3\tau) + v_2(t-5\tau) + \dots, \quad . \quad . \quad (6)$$

where $v_0(t)$, $v_1(t)$, etc., are the solutions of the operational equations,

$$\left.\begin{aligned} v_0 &= S.V, \\ v_1 &= \mu_1\mu_2\,S.V, \\ v_2 &= (\mu_1\mu_2)^2.S.V, \\ &\text{etc.} \end{aligned}\right\} \quad . \quad . \quad . \quad . \quad (7)$$

The terms of (6) represent, of course, the effects produced at the "receiving" end by the original wave and the successive reflected waves. For the most part we shall be interested in the response to a "unit voltage function," that is, $V=0$ when $t<0$, $V=1$ when $t>0$, which may be called, following Carson, the "indicial response."

IV. *Indicial Response of Simple Capacity Circuit.*

For the circuit of fig. 3, writing

$$\left.\begin{aligned} \frac{1}{2W(C_1+C_2)} &= \frac{K}{2(C_1+C_2)}\cdot\frac{1}{\tau} = a, \\ m &= \frac{C_1}{C_1+C_2}, \end{aligned}\right\} \quad . \quad . \quad (8)$$

we have

$$S = m\cdot\frac{p}{p+a}, \quad \mu_1 = -\frac{a}{p+a}, \quad \mu_2 = -1. \quad . \quad . \quad (9)$$

The terms of the indicial response are

$$\left.\begin{aligned} v_0(\xi_0) &= m\,e^{-a\xi_0}, \\ v_1(\xi_1) &= m.(a\xi_1).e^{-a\xi_1}, \\ v_n(\xi_n) &= m.\frac{(a\xi_n)^n}{n!}e^{-a\xi_n}, \end{aligned}\right\} \xi_n = t-(2n+1)\tau. \quad (10)$$

They are, of course, zero for negative values of ξ_n. Fig. 7 shows the result for the case

$$K/(C_1+C_2) = \eta = 1/10;$$

the final value of output voltage, $C_1/(C_1+C_2+K)$, being taken as unity. It will be seen that there is a sharp discontinuity of slope at $t=3\tau$, but not elsewhere. The second reflected wave is inappreciable.

V. *Split Capacity Circuit.*

For this circuit (fig. 4) we take first the simplest case namely,

$$C_4/(C_1 + C_2) = f = 1.$$

Writing

$$\frac{1}{2W(C_1 + C_2)} = \frac{1}{2WC_4} = \frac{K}{(C_1 + C_2 + C_4)\tau} = a, \quad m_0 = \frac{C_1}{C_1 + C_2},$$
$$\ldots \quad (11)$$

we have

$$S = \frac{m_0}{2} \cdot \frac{p(p + 2a)}{(p + a)^2}, \quad \mu_1 = \mu_2 = -\frac{a}{p + a}, \quad (12)$$

and the terms of the indicial response are

$$\left.\begin{array}{l} v_0(\xi_0) = \dfrac{m_0}{2} e^{-a\xi_0}(1 + a\xi_0), \\[2mm] v_1(\xi_1) = \dfrac{m_0}{2} \cdot \dfrac{(a\xi_1)^2}{2!} e^{-a\xi_1}\left(1 + \dfrac{a\xi_1}{3}\right), \\[2mm] v_n(\xi_n) = \dfrac{m_0}{2} \cdot \dfrac{(a\xi_n)^{2n}}{(2n)!} e^{-a\xi_n}\left(1 + \dfrac{a\xi_n}{2n+1}\right), \end{array}\right\} \quad \xi_n = t - (2n+1)\tau.$$
$$\ldots \quad (13)$$

This is shown in fig. 7, for a total condenser capacity

$$C_1 + C_2 + C_4 = 10K,$$

as before ($\eta = 1/10$, $f = 1$). Though the initial error is, of course, just as great as with fig. 3, the fall of voltage is much more gradual, as was expected. There is now no discontinuity of slope anywhere; the existence of reflexions could not be inferred from the curve alone.

For the general case,

$$C_4/(C_1 + C_2) = f \neq 1,$$

we put

$$\frac{1}{2W(C_1 + C_2)} = a, \quad \frac{1}{2WC_4} = b, \ldots \quad (14)$$

and obtain

$$S = \frac{m_0}{2} \cdot \frac{p(p + 2b)}{(p + a)(p + b)}, \quad \mu_1 = -\frac{a}{p + a}, \quad \mu_2 = -\frac{b}{p + b}.$$
$$\ldots \quad (15)$$

The first three terms of the indicial response are

$$v_0(\xi_0) = \frac{m_0}{2}\left\{\frac{2b-a}{b-a}e^{-a\xi_0} - \frac{b}{b-a}e^{-b\xi_0}\right\},$$

$$v_1(\xi_1) = \frac{m_0}{2}\left\{\begin{array}{l} \dfrac{ba(3b-a)}{(b-a)^3}(e^{-b\xi_1}-e^{-a\xi_1}) \\[2mm] + \dfrac{b(2b-a)}{(b-a)^2}(a\xi_1).e^{-a\xi_1} + \dfrac{ba}{(b-a)^2}(b\xi_1).e^{-b\xi_1}\end{array}\right\},$$

$$v_2(\xi_2) = \frac{m_0}{2}\left\{\begin{array}{l} \dfrac{3b^2a^2(3b-a)}{(b-a)^5}(e^{-a\xi_2}-e^{-b\xi_2}) \\[2mm] - \dfrac{b^2a(5b-2a)}{(b-a)^4}(a\xi_2)e^{-a\xi_2} \\[2mm] - \dfrac{ba^2(4b-a)}{(b-a)^4}(b\xi_2)e^{-b\xi_2} \\[2mm] + \dfrac{b^2(2b-a)}{(b-a)^3}\dfrac{(a\xi_2)^2}{2!}e^{-a\xi_2} - \dfrac{ba^2}{(b-a)^3}\cdot\dfrac{(b\xi_2)^2}{2!}e^{-b\xi_2}\end{array}\right\}.$$

$$\ldots \quad (16)$$

If we make

$$C_1 + C_2 = C_4 + K,$$

to correct the "initial overshooting," we have, putting

$$\eta = K/(C_1 + C_2 + C_4),$$

$$a = \frac{\eta}{(1+\eta)\tau}, \quad b = \frac{\eta}{(1-\eta)\tau}, \quad f = \frac{1-\eta}{1+\eta}.$$

Fig. 7 shows the result for this case, η being 1/10 as before.

At $t=7\tau$ one is dealing with the differences of numbers over 700, but calculation beyond 7τ is as unnecessary as it would be tedious. There is still no discontinuity of slope, and the maximum error is now only 1·6 per cent. To obtain an equally small error with the circuit of fig. 3 a total capacity

$$C_1 + C_2 = 62K$$

would be required, i. e., 6·2 times larger than with fig. 4. The advantage of fig. 4 is even greater than this number suggests, for in practice one would make $C_1 + C_2$ somewhat greater than $C_4 + K$, to distribute the error symmetrically about the final value ; and this cannot be done with fig. 3.

VI. *Resistance-capacity Circuits.*

These are greatly to be preferred to the corresponding capacity circuits, figs. 3 and 4, primarily on account of their finite input impedance at infinite frequency, but also because they are capable of more accurate response curves._

For fig. 2, Gábor calculated the response up to 5τ, assuming

$$m_0 = W/(R_1 + W)$$

to be small, and
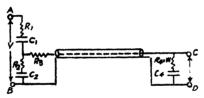
$$R_1 C_1 = W C_2.$$

The initial voltage is then m_0 and the final voltage $m_0/(1+\eta)$, where

$$\eta = K/(C_1 + C_2).$$

The voltage falls to $m_0(1-\eta)$ at $t=3\tau$, passes through a minimum between $t=3\tau$ and $t=5\tau$, and returns to $m_0(1-\eta)$

Fig. 6.

at $t=5\tau$. The subsequent oscillations can be ignored. Thus the maximum error is η approximately. Gábor pointed out that if

$$R_1 C_1 = W C_2 (1+\eta)$$

the initial value of voltage would be the same as the final value. It is easy to calculate that in this case the voltage at $t=3\tau$ is

$$m_0 \left[1 - \frac{\eta(1-\eta)}{1+\eta} \right] \quad \text{approximately.}$$

Clearly, a minimum total fluctuation roughly equal to η is the best that fig. 2 will give.

We shall not give the equations for fig. 2, but shall pass to the consideration of fig. 6. Here we have an extra condenser, so that in addition to making the initial voltage bear any desired ratio to the final voltage, we can satisfy some other condition for the improvement of the response. Further, we have included an extra resistance R_3, and, as

will appear later, still another possibility of improvement lies in the alteration of the ratio $R_2 : R_3$. We shall confine ourselves to cases in which the condition

$$R_3 + \frac{R_1 R_2}{R_1 + R_2} = W \quad . \quad . \quad . \quad . \quad (17)$$

is satisfied, so that the reflexion of very high frequencies is zero. Writing

$$\frac{1}{R_1 C_1} = \alpha, \qquad \frac{1}{R_2 C_2} = \beta, \qquad \frac{1}{W C_4} = \gamma,$$

$$\frac{R_2}{R_1 + R_2} = m_0, \qquad 1 - \frac{R_3}{W} = \kappa, \quad . \quad . \quad . \quad . \quad (18)$$

$$\frac{K}{C_1 + C_2 + C_4} = \eta,$$

we have, taking (17) into account,

$$\mu_1 = - \frac{\kappa \{ p [m_0 \alpha + (1 - m_0)\beta] + \alpha\beta \}}{2 p^2 + p \{ [(2 - \kappa)(1 - m_0) + \kappa]\alpha + [(2 - \kappa) m_0 + \kappa]\beta \} + \kappa \alpha \beta}, \quad (19)$$

while

$$\mu_2 = - \frac{\gamma}{2p + \gamma}. \quad . \quad . \quad . \quad . \quad . \quad . \quad (20)$$

$$\frac{Z_2}{Z_1 + Z_2} = m_0 \cdot \frac{p + \beta}{p + (1 - m_0)\alpha + m_0 \beta}. \quad . \quad . \quad (21)$$

If $m_0 \ll 1$, (19) and (21) become, approximately

$$\mu_1 = - \frac{\kappa\beta}{2p + \kappa\beta}, \quad . \quad . \quad . \quad . \quad (22)$$

$$\frac{Z_2}{Z_1 + Z_2} = m_0 \frac{p + \beta}{p + \alpha}, \quad . \quad . \quad . \quad . \quad (23)$$
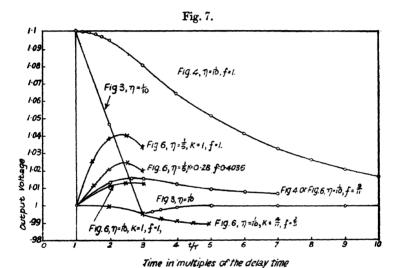
so that

$$S = \frac{m_0}{2} \cdot \frac{p(p + \beta)(p + \gamma)}{(p + \alpha)\left(p + \frac{\kappa\beta}{2}\right)\left(p + \frac{\gamma}{2}\right)} \quad \text{approximately.} \quad (24)$$

We first notice that if $\alpha = \beta$ the response functions take the same form as those of equations (15) and (16) and are, in fact, identical with them, for $\kappa\beta$ is approximately equal to $1/W(C_1 + C_2)$ and $\gamma = 1/WC_4$, while $\alpha = \beta$ is equivalent

to $m_0 = C_1/(C_1 + C_2)$. The whole response is then the same, independently of the value of κ, as that of a split-capacity circuit (fig. 4) having the same values of capacity, and the curve of fig. 7 again serves for the case where $\eta = 1/10$ and the initial overshooting is corrected.

$\alpha = \beta$ does not, however, represent the best that can be done. To obtain a general analytical expression for the conditions giving minimum error would be impracticable, but we shall obtain some insight into the possibilities by considering how far the initial rate of change of voltage and its

Fig. 7.

Time in multiples of the delay time

Response curves of potential dividers. Constant voltage
suddenly applied.

derivative can be controlled. Dropping the scale factor $m_0/2$ and writing (24) in the form

$$S = \frac{p(p+m)(p+n)}{(p+a)(p+b)(p+c)},$$

we have, operationally,

$$v_0'(t-\tau) = \frac{d}{dt} v_0(t-\tau) = pSe^{-p\tau}$$

$$= \frac{p^2(p+m)(p+n)}{(p+a)(p+b)(p+c)} \cdot e^{-p\tau},$$

and it is easy to show that

$$v_0'(0) = m+n-(a+b+c). \quad \dots \quad (25)$$

Similarly,

$$v_0''(0) = mn - (m+n)(a+b+c) + (a+b+c)^2 - (ab+bc+ca).$$
$$\qquad \qquad \qquad \qquad \qquad \qquad \cdots \quad (26)$$

α, β, and γ are connected with τ through η, κ, and m_0 by the relation

$$\tau = \eta \left(\frac{m_0}{\kappa\alpha} + \frac{1-m_0}{\kappa\beta} + \frac{1}{\gamma} \right). \quad \cdots \quad (27)$$

We shall be interested in cases in which $\kappa\alpha$, $\kappa\beta$, and γ are of the same order of magnitude (27) then becomes

$$\tau = \eta \cdot \frac{\kappa\beta + \gamma}{\kappa\beta\gamma}, \quad \cdots \cdots \quad (28)$$

and if $f = \kappa\beta/\gamma$ ($= C_4/C_2$ approximately),

$$\kappa\beta = \frac{\eta}{\tau}(1+f), \quad \Bigg\}$$
$$\gamma = \frac{\eta}{\tau}\left(1+\frac{1}{f}\right), \quad \Bigg\} \qquad \cdots \cdots \quad (29)$$

We shall suppose that the initial overshooting is corrected; this requires

$$\frac{C_1}{C_1 + C_2 + C_4 + K} = \frac{m_0}{2},$$

which is equivalent to

$$\alpha = \frac{\beta\gamma[2 - m_0(1+\eta)]}{(1+\eta)[\kappa\beta + (1-m_0)\gamma]}, \quad \cdots \quad (30)$$

or, using (28), since $m_0 \ll 1$,

$$\alpha = \frac{2\eta}{\kappa(1+\eta)\tau} \quad \text{approximately.} \quad \cdots \quad (31)$$

Putting these values in (25) and (26), we obtain

$$\tau \cdot v_0'(0) = \frac{\eta}{2\kappa} \cdot \frac{(2-\kappa)f^2 - \dfrac{2(1-\eta)}{1+\eta} \cdot f + \kappa}{f}, \quad \cdots \quad (32)$$

$$\tau^2 \cdot v_0''(0) = \eta^2 \left[\frac{\eta}{\kappa(1+\eta)} - \frac{1}{4} \right] \left(2 + f + \frac{1}{f} \right)$$
$$- \left[\frac{2\eta}{\kappa(1+\eta)} + \frac{\eta}{2}\left(2 + f + \frac{1}{f}\right) \right] \cdot \tau \cdot v_0'(0). \quad (33)$$

When $\kappa > (1-\sqrt{\eta})^2/(1+\eta)$, $v_0'(0)$ is always positive. For a given value of κ it has a minimum value,

$$v_0'(0)_{\min.} = \eta \left\{ \sqrt{\frac{2-\kappa}{\kappa}} - \frac{1-\eta}{\kappa(1+\eta)} \right\} \quad \text{when } f = \sqrt{\frac{\kappa}{2-\kappa}}.$$

. . . (34)

As κ diminishes from unity this minimum rises from

$$v_0'(0)_{\min.} = \frac{2\eta^2}{(1+\eta)\tau} \quad \text{for } \kappa = 1, \quad f = 1 \quad . \quad . \quad (35)$$

up to a stationary value

$$v_0'(0)_{\min.} = \frac{2\eta^2}{(1-\eta^2)\tau} \quad \text{for } \kappa = \frac{(1-\eta)^2}{1+\eta^2}, \quad f = \frac{1-\eta}{1+\eta}, \quad (36)$$

and then falls to

$$v_0'(0)_{\min.} = 0 \quad \text{for } \kappa = \frac{(1-\sqrt{\eta})^2}{1+\eta}, \quad f = \frac{1-\sqrt{\eta}}{1+\sqrt{\eta}}. \quad (37)$$

$f = (1-\eta)/(1+\eta)$ corresponds to $\alpha = \beta$, when

$$v_0'(0) = 2\eta^2/(1-\eta^2)\tau$$

for all values of κ. If $\kappa = 1$, the best result is given by $f = 1$. Fig. 7 shows the first wave in this case, both for $\eta = 1/10$ and also for $\eta = 1/5$. With $\eta = 1/10$ the maximum error is 1·4 per cent., as compared with 1·6 per cent. when $\alpha = \beta$; and even with $\eta = 1/5$ the error is only 4·1 per cent.

However, if we are prepared to use small values of κ, we can do better still ; in fact, if

$$\kappa < \frac{(1-\sqrt{\eta})^2}{1+\eta}, \quad . \quad . \quad . \quad . \quad (38)$$

$v_0'(0)$ vanishes for

$$f = \frac{1}{2-\kappa} \left\{ \frac{1-\eta}{1+\eta} \pm \sqrt{\left(\frac{1-\eta}{1+\eta}\right)^2 - \kappa(2-\kappa)} \right\} \quad .. \quad (39)$$

Further, if $\eta < 1/9$, (38) is satisfied by

$$\kappa = \frac{4\eta}{1+\eta},$$

and with this value of κ, if f is chosen to make $v_0'(0)$ vanish, $v_0''(0)$ vanishes also. The first two waves are given in fig. 7 for the case $\eta = 1/10$, $\kappa = 4\eta/(1+\eta) = 4/11$, and $f = 2/3$, corresponding to the positive sign in (39). The maximum

error is now $-1\cdot1$ per cent. approximately, occurring in the neighbourhood of $t=5\tau$.

Obviously some value of κ intermediate between $4\eta/(1+\eta)$ and unity will give the best result. In the case $\eta=1/10$, the error could thus be brought down to a fraction of 1 per cent. But if we attempt to use larger values of η, the value of κ necessary to give a better result than $\kappa=1$, $f=1$ may become so small as to require an undesirably low high-voltage resistance R_1. To test this point the first wave has been calculated for $\eta=1/5$, $\kappa=0\cdot28$, $f=[\kappa/(2-\kappa)]^{\frac12}=0\cdot4035$. It will be seen that the error is thus reduced from $4\cdot1$ per cent. to $2\cdot5$ per cent. Values of κ as low as $0\cdot28$ will often be permissible; to take a practical example, consider a potential divider to reduce from 1,000,000 volts to 500 volts, a ratio u of 1/2000. If the surge impedance of the cable is 50 ohms, the circuit of fig. 2 has a resistance $R_1=(1-u)W/u=99,950$ ohms, while fig. 6, with $\kappa=0\cdot28$, requires $R_1=\kappa W/2u=14,000$ ohms. If the surge impedance of the high-voltage circuit is, say, 500 ohms, this value of R_1 is not unduly small. For a $\frac12$ microsecond delay time the capacity of the cable is $K=\tau/W=\cdot01$ microfarad. Assuming the initial overshooting to be corrected in each case, fig. 2 requires, to limit the error to $2\cdot5$ per cent., $\eta=1/40$, $C_1=200$ micromicrofarads approximately; while with fig. 6, $\eta=1/5$, $C_1=25$ micromicrofarads suffices. In cases where a high value of R_1 is required, it will be best to make $\kappa=1$, $f=1$, and distribute the error symmetrically by under-correcting the initial overshooting.

Results quite similar to the above are obtained if the resistance R_3 is inserted at the "receiving" instead of the "sending" end, *i.e.*, in the position Z_4-X of fig. 5. But when R_1 is small, *i. e.*, κ small, the arrangement of fig. 6 has the advantage that the cable is not subjected to a higher voltage than is required by the oscillograph. It is sometimes convenient on practical grounds to be able to use quite a low resistance R_1; further, when R_1 is low, the error caused by the stray capacities which are effectively in parallel with it is reduced.

Fig. 6 is, of course, very far from being the most general arrangement. Each of the impedances might consist of a quite complicated arrangement of resistances and condensers. I have not, however, investigated these possibilities; nor have I investigated the effect of departing from the condition (17). Such a departure ($R_S=0$, $R_2>W$) might be useful when a high value of R_1, together with a moderately high value of η, was required.

VII. *Response to Other Wave-Forms.*

It is of practical interest to consider how the errors affect the reproduction of other wave-forms. If a constant voltage is applied for a very short time, δt, and then removed, the output voltage rises at $t = \tau$ to $v_0(0)$, but returns at $t = \tau + \delta t$ to $\delta t . v_0'(0)$ instead of zero, and the subsequent contribution of the first term is $\delta t . v_0'(t - \tau)$. To this is added, at $t = 3\tau$, a square peak of amplitude $v_1(0)$, duration δt, followed by a contribution $\delta t . v_1'(t - 3\tau)$; and so on.

In practice, at least one end of the cable is made reflexion-free to high frequencies, so that $v_1(0)$, $v_2(0)$, etc., are all zero, *i. e.*, the repetitions of the square peak do not occur. $v_2'(0)$, $v_3'(0)$, etc., are also zero. $\delta t . v_1'(0)$ vanishes if both ends are reflexion-free; otherwise there is a discontinuity of this amount at $t = 3\tau$. Elsewhere there is a smooth fluctuation of voltage.

The steady state response to a sinusoidal e.m.f. is calculated by putting $V = V_0 e^{i\omega t}$ in equation (1), and writing $i\omega$ instead of p. If $S = G + iH$, $\mu_1\mu_2 = g + ih$, we have

$$\left| \frac{v}{V_0} \right| = \frac{(G^2 + H^2)^{\frac{1}{2}}}{(1 + g^2 + h^2 - 2g\cos 2\omega\tau - 2h\sin 2\omega\tau)^{\frac{1}{2}}}.$$

For the circuits of fig. 4 or fig. 6, with $\eta = 1/10$, $f = (1 - \eta)/(1 + \eta)$, we calculate:

$2\pi/\omega\tau$.	$\left\lvert\frac{v}{V_0}\right\rvert$.	$2\pi/\omega\tau$.	$\left\lvert\frac{v}{V_0}\right\rvert$.
∞	1	8/3	1·0056
20	1·0305	2	1·0009
11·1	1·0372	4/3	1·0023
9·884	1·0375	1	1·0001
8	1·0359	0	1
4	1·0198		

Thus the maximum error is 3·75 per cent., occurring, as might be expected, at a period $2\pi/\omega$ equal not to some integral multiple of τ, but to the resonant period of the condensers C_2, C_4 in series acting with the inductance $W\tau$ of the cable ($2\pi/\omega = 9.884\,\tau$).

VIII. *Acknowledgement.*

LXXII. *Some Experimental Support for Stern's Theory of the Electrolytic Double Layer.* By JOHN ST. LEGER PHILPOT, *B.A.* (*from the Physical Chemistry Laboratory, Balliol and Trinity Colleges, Oxford*).[*]

INTRODUCTION.

THE special type of electrical double layer which exists between an electrode and a solution of an electrolyte has been called by Stern [(1)] an "electrolytic double

Fig. 1.
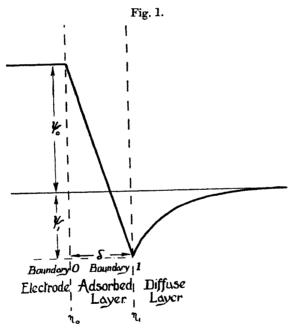
Diagram (after Stern) of an electrolytic double layer.

layer." Stern has studied theoretically the distribution of electrically charged particles in it. He represents his conception of the distribution by means of diagrams similar to that shown in fig. 1. The ordinates represent the electrical potential with respect to the interior of the solution, and the abscissæ represent the distance from a " boundary 0 " defining the electrode surface. On the electrode side of

boundary 0 the excess of positive over negative electricity is η_0 per cm.^{3}, assumed to be concentrated at boundary 0. On the solution side there is an "adsorbed" layer of ions, with net charge $-\eta_1$, assumed to be concentrated at boundary 1, distant δ from boundary 0. Beyond this there is a "diffuse" layer, of net charge $-\eta_2$, arranged in an ion atmosphere whose charge density decreases rapidly as the distance from boundary 1 increases.

If the system as a whole is electrically neutral $\eta_0 = \eta_1 + \eta_2$. The electrical potentials are zero in the interior of the solution ψ_1 at boundary 1, and ψ_0 at boundary 0. The special case shown in fig. 1 is a complex one, where η_1 is of opposite sign to η_2 owing to "specific adsorption" of a negative ion. Stern's theory is a combination of the simple Helmholtz theory of the "adsorbed" layer, corresponding to $\eta_2 = 0$, and the Gouy-Chapman theory of the "diffuse" layer corresponding to $\eta_1 = 0$.

Making the above and some further assumptions, Stern has derived an equation connecting the potentials ψ_0 and ψ_1 with the charges η_0, η_1, and $-\eta_2$. The experimental work described in the present paper provides support for the belief that Stern's theory and equation are fundamentally correct. The evidence is not, however, direct, since none of the quantities concerned are directly measurable. An understanding of the relation between the theoretically and experimentally accessible quantities requires a precision of definition which is not easily attained, and whose discussion must be postponed till a later paper. For the present it must suffice to state :—

(*a*) In a case where no charged particles can cross "boundary 0" (and not necessarily in any other), Stern's "η_0" must be identical with the experimental quantity ϵ which is defined below.

(*b*) When an electrode is such that over a large range of potential no electrochemical change can occur, there is considerable *a priori* justification for the belief that over part of this range no charged particles can cross boundary 0.

(*c*) Mercury in specially purified solutions of hydrochloric acid or sodium chloride, as used in the present work, forms a close approximation to such an electrode.

(*d*) The belief expressed in (*b*) is strengthened by th fact that ϵ, measured on the electrode described in (*c*), varies with potential and concentration in the same way as in Stern's equation.

(*e*) The same fact provides evidence that Stern's equation is an approximation to the truth.

Definition of ϵ *or* $\left(\dfrac{\partial q}{\partial s}\right)_{\psi_s}$.—Consider a pair of electrodes. R and S, immersed in a solution of electrolyte, and connected with each other through an external circuit.

Electrode S is perfectly polarizable, *i. e.*, its electrical potential ψ_S is uniquely determined by its area S and by the quantitity of electricity q which has flowed through the external circuit from R to S.

Electrode R is a non-polarizable "reference electrode," *i. e.*, its electrical potential ψ_R with respect to the solvent is independent of q and dependent only on the composition of the system.

If ψ_S is kept constant the current flowing from R to S is given by

$$\left(\frac{\partial q}{\partial t}\right)_{\psi_s} = \left(\frac{\partial q}{\partial s}\right)_{\psi_s} \frac{ds}{dt} \quad \ldots \ldots \quad (1)$$

$\left(\dfrac{\partial q}{\partial s}\right)_{\psi_s}$ is the "capacity per unit of surface at constant potential" as defined by Lippmann [11], and is generally written ϵ for short. At a perfectly polarizable electrode no continuous electrochemical change can occur. This is an unattainable ideal, and for all actual electrodes $\left(\dfrac{\partial q}{\partial s}\right)_{\psi_s}$ will have a value greater than that for the corresponding ideal electrode. If q_a refers to an actual electrode and q_i and ϵ_i to the corresponding ideal one, and if I is the current corresponding to unavoidable electrochemical change, then

$$\left(\frac{\partial q_a}{\partial t}\right)_{\psi_s} = \left(\frac{\partial q_i}{\partial s}\right)_{\psi_s} \frac{ds}{dt} + I = \epsilon_i \frac{ds}{dt} + I. \quad . \quad . \quad (1\,a)$$

In the present work, I has been made quite small compared with $\epsilon_i \dfrac{ds}{dt}$, and a correction has been applied for what remains. Thus fairly reliable values for ϵ_i have been obtained for comparison with η_0.

Potentials.—The potential ψ_S will, in the present paper, be identified with Stern's "ψ_0." This involves the acceptance of Stern's assumption that the charge on the electrode side is concentrated entirely at "boundary 0." The quantities "ψ" are electrical potential differences between two phases, which according to Guggenheim [2], [3] have individually

no physical significance. The measured potential difference E is equal to $\psi_R - \psi_S$, if ψ_R is defined so as to include all liquid or metal junction potentials.

Stern's equation.—The theoretical equation derived by Stern is

$$\overbrace{K_0(\psi_0 - \psi_1)}^{\eta_0} = FZ\left(\overbrace{\frac{1}{2 + \dfrac{1}{c}e^{\frac{\psi_- - F\psi_1}{RT}}} - \frac{1}{2 + \dfrac{1}{c}e^{\frac{\phi_+ + F\psi_1}{RT}}}}^{\eta_1} \right)$$

$$+ \overbrace{\sqrt{\frac{DRTc}{2\pi \times 18}}\left(e^{\frac{F\psi_1}{2RT}} - e^{-\frac{F\psi_1}{2RT}} \right)}^{\eta_2}. \quad (2)$$

where the quantities η and ψ have been defined,

$K_0 = \dfrac{d}{4\pi\delta} =$ the capacity per cm.^{2} of the "adsorbed" layer by virtue of its being separated from the electrode by a space of thickness δ and dielectric constant d.

$F =$ the value of the Faraday in electrostatic units.

$Z =$ the number of moles on 1 cm.^{2} area of water, assumed to equal $1\cdot7 \times 10^{-9}$.

ϕ_+ and $\phi_- =$ the "specific adsorption potentials" of the ions defined as the free energy of formation of an "adsorbed layer" from one pole of positive or negative ion, respectively, under conditions where $\psi_1 = 0$.

$D =$ the dielectic constant of water.

$c =$ the concentration expressed as mole fraction.

C will denote the concentration in moles per thousand grams and is equal to $0\cdot018\,c$ if the molecular weight of water is given its simple value 18.

The electrical quantities are expressed in absolute electrostatic units. Converting to practical electromagnetic units, replacing c by C, and inserting the values of the constants, transforms the equation to

$$\eta_0 = 8\cdot15\left(\frac{1}{2 + \dfrac{1}{0\cdot036\,C}e^{\frac{\phi_- - F\psi_1}{RT}}} - \frac{1}{2 + \dfrac{1}{0\cdot036\,C}e^{\frac{\phi_+ + F\psi_1}{RT}}} \right)$$

$$+ 5\cdot73\,\sqrt{C}\left(e^{\frac{F\psi_1}{2RT}} - e^{-\frac{F\psi_1}{2RT}} \right) \quad . \quad . \quad (2\,a)$$

$$= K_0(\psi_0 - \psi_1). \quad . \quad . \quad . \quad . \quad . \quad . \quad . \quad . \quad (3)$$

η_0 is now expressed in microcoulombs per cm.^{2}, ψ_1 and ψ_0 in volts, ϕ_+ and ϕ_- in joules per gram ion, and K_0 in microfarads per cm.^{2}

For values of η_0 up to 10, and of C up to 0·1, which is the experimental range of the present work, the 2 in the denominators in equation $(2\,a)$ can be neglected. Doing this, and writing

$$x = e^{\frac{F\psi_1}{2RT}} \qquad\qquad A = 2·93$$

$$X_+ = e^{\frac{-\phi_+}{RT}} \qquad\qquad B = 5·73$$

$$X_- = e^{\frac{-\phi_-}{RT}}$$

$$\eta_0 = \overbrace{AC\left(X_-x^2 - \frac{X_+}{x^2}\right)}^{\eta_1} + \overbrace{B\sqrt{C}\left(x - \frac{1}{x}\right)}^{\eta_2}. \quad . \quad (2\,b)$$

η_0 may be separated for mathematical convenience into η_+ and η_-, the portions which correspond respectively to positive and negative ions on the solution side of boundary 0. Thus, within the present experimental range,

$$-\eta_+ = AC\frac{X_+}{x^2} + \frac{B\sqrt{C}}{x}. \quad . \quad . \quad . \quad (2\,b_+)$$

$$\eta_- = ACX_-x^2 + B\sqrt{C}x. \quad . \quad . \quad . \quad (2\,b_-)$$

When ψ_1 is numerically large, X is much greater or smaller than 1, according to the sign of ψ_1. η_0 then becomes equal to η_- and η_+ in the two cases respectively.

It is readily deducible from Stern's equation that

$$\underset{(\eta_0 \to \pm\infty)}{Lt} \frac{d\eta_0}{d\psi_0} = K_0,$$

and that, for a constant and numerically large value of η_0,

$$\psi_0 = \text{const.} \pm \frac{RT}{F}\log C,$$

the sign of $\frac{RT}{F}\log C$ being opposite to that of η_0. In other words, the theoretical curve representing η_0 in terms of ψ_0, has two nearly linear portions of slope approximately equal to K_0, which move apart along the axis of η_0 with increasing dilution, at a rate of $\frac{2RT}{F}\log C$. They are joined by

a non-linear portion. This form of curve is peculiar to Stern's theory. By suitable adjustment of constants the linear or non-linear portions can be made to predominate, giving in the two limiting cases tho wholly linear curve of the Helmholtz theory, and the wholly non-linear curve of the Chapman-Gouy theory.

Stern's equation in its present form applies only to univalent ions and to a constant value of K_0. Uni-univalent electrolytes were used in the present work, but it was found that K_0 was different for the two ions. In applying Stern's equation, therefore, the value of K_0 was chosen to correspond with the predominant ion, or if neither predominated, equation (3) was written

$$\psi_0 = \frac{\eta_+}{K_{0+}} + \frac{\eta_-}{K_{0-}} + \psi_1, \quad \ldots \quad (3\,a)$$

where K_{0+} and K_{0-} are the values of K_0 corresponding with each ion.

The measurement of ϵ.—If a dropping mercury electrode is kept at a constant potential, $\frac{ds}{dt}$ of equation (1 a) can be identified with the area of fresh electrolytic double layer which is formed per second by the expanding drops, and this must equal the area of a drop at the moment of detachment multiplied by the number of drops per second. If r is the radius of a drop (assumed to be approximately spherical at the moment of detachment) and if x is the number of drops per second, then

$$\frac{ds}{dt} = 4\pi r^2 x.$$

If n drops fill a volume V in time T, then

$$r = \left(\frac{V}{\frac{4}{3}\pi n}\right)^{\frac{1}{3}}$$

and

$$x = \frac{n}{T}.$$

Hence, from equation (1 a),

$$\epsilon_i = \left(\frac{\partial q_a}{\partial t}\right)_{\psi_s} \times \frac{I}{(4\pi)^{\frac{1}{3}}\left(\frac{V}{3}\right)^{\frac{2}{3}} n^{\frac{1}{3}}} - I. \quad \ldots \quad (1\,b)$$

All the quantities on the right-hand side are directly

measurable except I. Heyrowsky [12] has shown that I, if small, is independent of potential except in the neighbourhood of the discharging potential of the substance undergoing electrochemical change. Therefore, if I is ignored the experimental curve of ϵ against E will be shifted along the ϵ axis without change of shape except in the neighbourhood of a discharging potential. Also it is fairly certain that as $\frac{ds}{dt}$ is increased the ratio of $\epsilon \frac{ds}{dt}$ to I increases, so that for extremely high values of $\frac{ds}{dt}$ I, is negligible in equation (1 b) provided the concentration of reducible substances is small. Enormous dropping-rates introduce difficulties in measuring $\frac{ds}{dt}$, but it is possible to measure the limiting value (as $\frac{ds}{dt}$ increases) of the potential where $\epsilon = 0$. This is, in fact, Freundlich's "electrokinetic potential," relative to the reference electrode R.

ϵ_a can now be converted to ϵ_i ; it is only necessary to plot ϵ_a against E and shift the curve along the ϵ-axis till it cuts the E-axis at the "electrokinetic potential." The extent of the shift is equal to I, and will be seen from figs. 5 and 6 to be quite small in the present case. The above correction is only valid at potentials between the electrokinetic potential and the discharging potential of a substance present. There is, however, no evidence for a discharging potential occurring over the range of the curves shown.

Electrolytic purification.—In the present work the final purification from reducible substances was done electrolytically in the cathode compartment of the cell itself. A pool of mercury was maintained at a potential sufficient to reduce impurities, but not hydrogen or sodium ions. Extremely efficient stirring was necessary, which was achieved by bubbling hydrogen under reduced pressure through the mercury. An estimate of the quantity of impurities reduced was obtained from the area under the curve, obtained by plotting current against time. The ratio of initial to final concentration of reducible impurities was found from the current required to maintain a stationary mercury surface at a given potential. Combination of these data gave absolute values for the initial and final concentrations, which were of the order 10^{-7} and 10^{-9} normal respectively.

EXPERIMENTAL DETAILS.

Water was distilled at a pressure of 20 mm. in a stream of nitrogen and condensed on silica, the aim being to remove oxygen and other reducible impurities as completely as possible. The low temperature permitted the use of rubber bungs, which had been boiled in alkali and distilled water, dried, and soaked in molten paraffin wax for an hour. (The rubber imbibes the paraffin, which fills the pores and prevents the slow diffusion of sulphurous impurities from the interior). During the distillation samples were run into a test cell containing a gold cathode and platinum anode. Roughly speaking, the current at 1-volt applied potential was a measure of the reducible impurities and at 8 volts a measure of the ordinary conductivity. The water was collected when it gave below 10^{-8} amp. for 1 volt and 3×10^{-6} amp. for 8 vols. (The cathode area was 5 cm.^{2}). The specific conductivity of the yield as a whole was generally measured in an Ostwald cell and was from 2 to 4×10^{-7} reciprocal ohm.

Hydrochloric acid.—The gas was transferred *in vacuo* from the concentrated acid to pure water, after letting the first portion go to waste and filtering the gas through glass wool. The strong solution thus obtained was titrated, and diluted as required without contact with air.

Sodium chloride.—Some Kahlbaum *pro analysi* material was used without further purification.
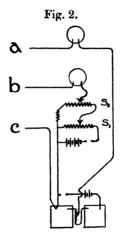
Mercury.—The mercury was washed for 12 hours in an acid column with air-lift, and distilled in a Hulett still, with an air-stream at 40 mm. pressure. It was filtered through silk immediately before use.

Hydrogen.—Cylinder hydrogen was passed over an incandescent tungsten filament, to remove oxygen, then through soda-lime, and filtered through a thick plug of glass wool.

Handling of solutions.—Water and solutions were stored, and dilutions made, in ½-2-litre durosil flasks, fitted with paraffined rubber bungs (described above), containing tubes for filling, emptying, and evacuating or filling with hydrogen. For fear of a possible effect of traces of sodium and other ions on the measurements in hydrochloric acid, the flasks were coated inside with paraffin wax containing a minute trace of pure "crepe" rubber (free from sulphur). The paraffin was deposited as a thin layer from carbon tetrachloride solution and warmed in the air-oven; the trace of

rubber prevents flaking. As a precaution against contamination the coated flasks were left filled with distilled water for some hours before they were first used, but there was no detectable increase in either reducible impurity or conductivity of water kept for months in them. The results obtained with sodium chloride show that a trace of sodium ion would have no effect on measurements in hydrochloric acid, so the paraffin lining is unnecessary, at any rate if pyrex flasks are used.

The solutions on entering the cell contained apparently about the same amount of reducible impurity as those of Bowden and Rideal [6], but more than those of Bowden [7] in

Fig. 2.
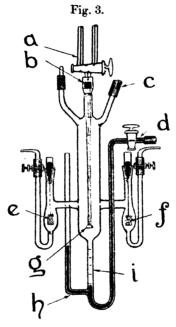
The electrical circuit :
a, to reference electrode ; *b*, to anode ; *c*, to cathode.

later work on overvoltage. In view of the success of the final electrolytic purification described above the sources of impurities were not investigated further.

The electrical circuit.—A wiring diagram is given in fig. 2. The potentiometer circuit was identical with that described by Nonhebel [8]. In the current circuit the only notable feature was the adjusting device consisting of two sliding resistances, S_1 and S_2, and a hundred-ohm coil. S_1 gave a coarse and S_2 a fine adjustment of the applied potential, which was altered till the potentiometer was balanced at a chosen value. The potentiometer galvanometer was a mirror instrument sensitive to 10^{-10} amp., while the currents were measured with a bifilar pointer instrument, with the smallest

division equal to 5×10^{-8} amp., which could be multiplied by 10 or 100, or 1000 by a universal shunt.

The cell.—The final form of cell is shown in fig. 3. The cathode compartment is a vertical cylinder ending in an outlet for mercury and solution, which has a straight graduated portion *i* and a platinum contact *h* at the bottom, and communicates through a tap *d* and rubber tube with an evacuated filter flask. The anode *f* (of silver gauze) and reference electrode *e* (electrolytic silver-silver chloride as

Fig. 3.

The cell.

a. Dropper bubbler tap.
b. Contact for dropper.
c. To pump or hydrogen train.
d. Exit for mercury and solution.
e. Reference electrode.

f. Anode
g. Dropper and bubbler.
h. Contact for bubbling cathode.
i. Graduated tube.

described by Nonhebel [8]) are in compartments on opposite sides of the cathode compartment and separated from it by perforated diagrams, which give high conductivity while preventing mixing of unpurified solution with the purified contents of the cathode compartment. The anode and reference compartments have exit tubes for emptying, and the electrodes

themselves are fixed in by means of ground-glass joints. At the top of the cathode compartment are three tubes, one for filling with solution, another for admitting or removing hydrogen, while the third admits the combined dropping electrode and hydrogen bubbler. This consists of a fine-drawn capillary, ending in an inverted cup *g* at the bottom, and joined at the top to a two-way tap *a*, which admits either mercury, or hydrogen which has passed through a fine capillary, to control the rate. A platinum seal *b* provides contact with the drops. The inverted cup is a new type of dropper which gives large drops (about 3 mm. diameter), while allowing the capillary to be of such small bore (tapering slightly upwards) that solution does not creep up when the mercury is turned off. (The usual practice seems to be to use a capillary which tapers downwards. This not only gives drops too small for the present purpose, but also causes the dropping to be unstable below a critical rate.)

The "run" procedure with this cell was as follows :— After being cleaned with nitric and chromic mixture and rinsed finally with the solution to be used, the cell was immersed in the thermostat (paraffin, 25° C. $\pm 0.1°$). The anode and freshly chloridised reference electrode were inserted, and the necessary connexions made. The cell was then evacuated and filled with hydrogen at an excess pressure of 100 mm. The rubber tube on the solution inlet was unplugged and hydrogen allowed to stream out while the solution storage flask was connected. (The outlet from this flask is narrow enough to fit inside the inlet to the cell so that entering solution does not touch the rubber.) The cell was then evacuated and solution allowed to enter. It was again filled with hydrogen and the storage flask removed and the inlet plugged. Bubbles of hydrogen in the side compartments were removed by running solution out of the exits and ground joints. The cathode compartment was filled with mercury to just above the bottom of the dropper, and a turn of the dropper-bubbler tap, followed by evacuation of the cell, caused the bubbling process to occur. A suitable potential (about 1 volt) was then applied to the pool of mercury and electrolysis continued until a potential of 0.6 volt gave 10^{-8} amp. or less on a stationary surface. The current during bubbling was still above 5×10^{-7}. This state was reached in $\frac{1}{2}$–3 hours. The rubber tube supplying hydrogen to the bubbler was then pinched and hydrogen admitted to the cell by the side-tube. When the mercury had risen above the dropper-bubbler tap the latter was closed. The remaining mercury was sucked out of the

cathode compartment into the waste until the meniscus was below the graduated portion of the exit. The solution exits in the side compartments were opened momentarily to allow purified solution to run through the diaphragms, and thus prevent further the diffusion of impurities into the cathode compartments. The cathode lead was changed over to the dropper, the latter turned on, and measurements started.

To take a reading the dropping-rate was adjusted to about 2 drops per sec. and allowed a few minutes to become steady. The potentiometer was adjusted to the desired value, the applied potential was brought up to this by means of the sliding resistances, and the current was read. The dropped-mercury was sucked to the bottom of the graduated tube, and the time and number of drops required to fill a certain number of graduations were noted. The current was then read again, and if it had altered (through change in dropping-rate) the process was repeated, or, if the alteration was small the mean was taken. The potentiometer was then adjusted to a new potential and all the above measurements repeated. The whole range of potential was traversed rapidly at first and in detail later. Thus any general drift with time could be detected, but was never found in well-purified solutions. After a "run" the solution was blown out of the cell and fresh solution introduced. At least two "runs" were done at each concentration. At each change of concentration the cell was well rinsed with the new solution without dismantling, and a freshly chloridized reference electrode was introduced. Whenever a new substance was used the cell was dismantled and cleaned.
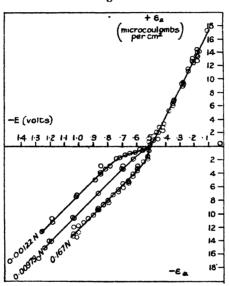
Results.

Measurements of ϵ were made in hydrochloric acid of molar concentration 0·1, 0·01, 0·0001, 0·00005, and in sodium chloride of concentration 0·1, 0·002, 0·0002. In the most dilute solution of each substance the resistance of the electrolyte in the cathode compartment affected the measured potential, so the only significant results obtained in these two solutions were the potentials for the zero ϵ (*i. e.*, the electrokinetic potentials), which are independent of the resistance of the solution. In the other solutions the dilution caused no difficulties except that for some reason the negative half of the curve for 0·002 N sodium chloride could not be measured.

The values of ϵ are shown plotted against E (the potential referred to silver-silver chloride in the same solution) in figs. 4–6. Fig. 6 shows inset the effect of using different

dropping-rates and degrees of purification, and the method of correcting for I. Fig. 4 shows the effect of concentration in the case of hydrochloric acid (uncorrected, as the method of correcting had not yet been developed). Results were obtained with three different dropping electrodes : the first, in which mercury ran down an amalgamated platinum wire, was used in a preliminary run with a different type of cell, and gave a value for " K_+ " (see Table I. on p. 789), agreeing closely with those obtained with the two "inverted cup" electrodes in the final cell.

Fig. 4.
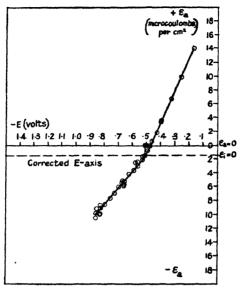
Capacity per cm.^{2} (at constant potential) of a mercury electrode, measured in hydrochloric acid at different concentrations.

Table I. gives values derived from the graphs, which are used in the subsequent discussion. They are E_0, E_+, and E_- (the values of E for $\epsilon = 0$, -10, and $+10$ respectively), and K_+ and K_- (the slopes of the lines when $q = -10$ and $+10$ respectively). The K values are given in microfarads per cm.^{2}, and the E values in volts.
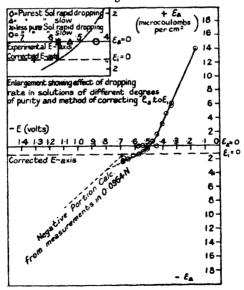
The agreement of K_+ for hydrochloric acid and sodium chloride is unexpected, since K_+ is supposed to depend on the radius of the positive ion. K_-, on the other hand, which is supposed to depend on the negative ion (chloride in both

Fig. 5.

Capacity per cm.² of a mercury electrode, measured in 0·0964 N. sodium chloride.

Fig. 6.

Capacity per cm.² of a mercury electrode, measured in 0·00185 N. sodium chloride.

TABLE I.

0. Graph.	I. Substance.	II. Concentration.	III. K+	IV. K−	V. −E₀		VI. −E+		VII. −(E+ − 0·11 log c)		VIII. −E−	
					A. uncorr.	B. corr.	A. uncorr.	B. corr.	A. uncorr.	B. corr.	A. uncorr.	B. corr.
—	HCl	0·1613†	21·5	—	0·425	—	·866	—	·772	—	—	—
4	,,	0·1613	22·0	43·4	0·464	—	·856	—	·762	—	·240	—
4	,,	0·00980	21·8	44·7	0·510	—	·964	—	·736	—	·250	—
4 and 7	,,	0·00122	21·6	45·1	0·578	—	1·109	—	·774	—	·259	—
—	,,	0·00004	—	—	0·578	—	—	—	—	—	—	—
5	NaCl	0·0964	21·8	48·8	0·475	0·512	·859	·929	·739	·809	·262	·293
6	,,	0·00185	—	47·6	0·498	0·575	—	(1·171)*	—	—	·252	·279
—	,,	0·000168	—	—	0·476	0·529	—	(1·295)*	—	—	—	(·279)*
			(Const.).	(Const.).							(Const.).	(Const.).

† Using another type of dropper and cell. * Calc. from measurements at higher concentrations.

cases), shows a slight change. The two series were done with different dropping electrodes, which may have caused this apparent reversal of the expected behaviour, but the discrepancy between the two chloride-ion values is not nearly as big as the difference in radius of the hydrogen and sodium ions. It might be thought that K_+ is due to the hydrogen ion in both cases; but this is discounted by the positions of the linear regions along the E axis.

COMPARISON OF THEORY AND EXPERIMENT.

The following tests show that Stern's theory gives a truer picture of the electrolytic double layer than any other, and that under the conditions of these measurements η_0 and ϵ_i are probably identical :—

(1) The Helmholtz theory gives $\eta_0 =$ a linear function of Ψ_0 at all potentials.

The Chapman-Gouy theory gives $\eta_0 =$ an exponential function of ψ_0 at all potentials.

Stern's theory gives $\eta_0 =$ an exponential function of ψ_0 when ψ_0 and C are small, and a linear function when they are large. A glance at the series of experimental curves shows that Stern's theory is the only one which can fit them.

(2) Stern's theory gives that if ψ_0 is large, ψ_0 for a given value of η_0 = const. $-$ RT/F log C if η_0 is positive,

or   = const. $+$ RT/F log C if η_0 is negative.

Hence, for a given value of η_0, E = const. independent of C, if η_0 is positive, and $(E - 2\ RT/F\ \log C) =$ const. if η_0 is negative (since $\psi_R =$ const. $- \dfrac{RT}{F} \log C$).

The quantities E_- and $(E_+ - 2RT/F \log C)$ in Table I.* should therefore be constant, and so they are, within the limits of error. The series of graphs in fig. 4 shows clearly the shift of the negative portion of the curve along the axis with dilution, while the positive portion is stationary.

(3) The theoretical curve for C=0·001 has been evaluated, using the values of K_0 and ψ_R, obtained as described below, and neglecting ϕ_+ and ϕ_-. It is plotted beside the experimental curve in fig. 7, and the correspondence is striking.

(The slopes of the straight portions are experimental, not theoretical, as they depend on K_0, and by adjusting ϕ_+ and ϕ_- they can be moved along the axis till they coincide with the experimental curve.)

---
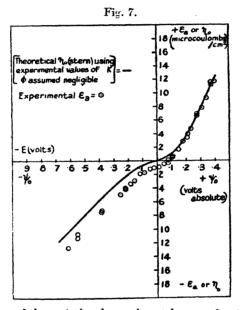
* E_- corresponds to an excess of negative ions on the solution side, and so to a positive value of η_0.

The features (1) and (2) above were noticed in the experimental curves independently of Stern's theory, which was only studied after the results in hydrochloric acid had been obtained.

CALCULATION OF K_0, ψ_R, ϕ_+ AND ϕ_-, FROM THE EXPERIMENTAL CURVES, USING STERN'S EQUATION.

Calculation of K_0.

K_0, the capacity per cm.^{2} of the adsorbed portion of the double layer, is the limiting slope of the curve of η_0 against

Fig. 7.

Comparison of theoretical and experimental curves for electrolytic double layer in 0·00122 N hydrochloric acid.

ψ_0 at very high potentials. Such potentials are nearly but not quite obtainable in practice, so a small correction must be applied to the measured value of $\dfrac{d\eta_0}{d\psi_0}$, called K, as follows :—

From equation (3) above

$$K_0 = \frac{K}{1 - \dfrac{K}{d\eta_0/d\psi_1}}. \quad \cdots \quad (4)$$

From equations $(2\,b_+)$ and $(1\,b_-)$,

$$\frac{d\eta_+}{d\psi_1} = \frac{-\mathrm{F}}{\mathrm{RF}}\,(\eta_+ - \tfrac{1}{2}\eta_{2_+}),$$

$$\frac{d\eta_-}{d\psi_1} = \frac{\mathrm{F}}{\mathrm{RT}}\,(\eta_- - \tfrac{1}{2}\eta_{2_-}),$$

where η_{2_+} and η_{2_-} = charge in diffuse layer due to positive

and negative ions, $= -\dfrac{\mathrm{B}\sqrt{c}}{x}$ and $+\mathrm{B}\sqrt{c}x$ respectively.

Taking values of η_0 large enough to be equal to η_+ or η_-,

and substituting $\dfrac{d\eta_+}{d\psi_1}$ and $\dfrac{d\eta_-}{d\psi_1}$ for $\dfrac{d\eta_0}{d\psi_1}$ in equation (4),

$$\mathrm{K}_{0_+} = \frac{\mathrm{K}_+}{1 + \dfrac{\mathrm{K}_+\mathrm{RT}}{\mathrm{F}(\eta_+ - \tfrac{1}{2}\eta_{2_+})}},$$

$$\mathrm{K}_{0_-} = \frac{\mathrm{K}_-}{1 - \dfrac{\mathrm{K}_-\mathrm{RT}}{\mathrm{F}(\eta_- - \tfrac{1}{2}\eta_{2_-})}},$$

where K_+ is the experimental slope when η_0 is large and
negative (see footnote on p. 790), K_- is the experimental
slope when η_0 is large and positive and K_{0_+} and K_{0_-} are the
capacities of the adsorbed layer when composed solely of
positive or solely of negative ions. When η_0 is large the

term involving it is small and $\dfrac{\eta_0}{\eta_2}$ is large. Therefore, η_2

need only be estimated approximately from the simple
theoretical curve, ignoring ϕ_+ and ϕ_-. If the experimental
data justified great accuracy η_2 could be obtained more
exactly by successive approximation after calculating the
other quantities.

From the values in Table I. of K_+ and K_- for the most
dilute solutions in which they were successfully measured
(where the above approximations are best justified) the
following values of K_0 were found :—

Table II.

For hydrochloric acid $\mathrm{K}_{0_+} = 23\cdot3 \pm 0\cdot5$ microfarads per cm.²

$\mathrm{K}_{0_-} = 53\cdot7 \pm 1\cdot7$,,   ,,   ,,

For sodiumchloride $\mathrm{K}_{0_+} = 23\cdot6$,,   ,,   ,,

$\mathrm{K}_{0_-} = 57\cdot3 \pm 1\cdot4$,,   ,,   ,,

(The limits of error given represent the maximum variation in the measurements of K at all concentrations.)

Stern calculated from the electrocapillary measurements of Krüger and Krumreich [4] in KNO_3, $K_0 = 29$ for both ions.

A check on the above calculation is provided by the fact that the theoretical curve for hydrochloric acid using these values of K_0, which is given in fig. 7, runs parallel to the experimental one at $\eta_0 = +10$ and -10, while when K is used instead of K_0 the lack of parallelism is quite apparent.

The values of ψ_R, ζ, ϕ_+, and ϕ_-.

ψ_R, the absolute * electrical potential of the reference electrode, is nearly equal, at low concentrations, to $-E_0$, the electrokinetic potential relative to the reference electrode. The two quantities differ by ζ, the absolute value of the electrokinetic potential. If Stern's equation is assumed to be correct, ζ can be calculated from the experimental curves, and is found to be of the order -0.003 volt in $N/500$ sodium chloride. The same calculation yields values for the specific absorption potentials ϕ_+ and ϕ_- of the order of -0.02 volt for the hydrogen, sodium, and chloride ions. The calculation depends very much on exact values of E_0, which the present apparatus was not specially designed to give, so the above figures are only provisional. A similarly provisional value of $+0.47 \pm 0.03$ volt can be given for the absolute potential ψ_R of the silver-silver chloride electrode in decinormal sodium chloride. The theoretical significance of this quantity, and its relation to results of other workers (*e. g.*, Bennewitz and Schulz [6], Billiter [9], Bodforss [10]), will be discussed in a later paper.

Calculation of η_0 for the sodium amalgam electrode at its equilibrium potential.—An approximate calculation from the experimental curves shows that if a is the activity of sodium in an amalgam, taking that in a 0.1 per cent. amalgam as unity, then

$$\eta_0 = -37.1 + 1.29 \log a \pm 1.5 \text{ microcoulombs per cm.}^2$$

at the equilibrium potential in sodium chloride of any concentration. The assumption is made that the electrolytic double layer on sodium amalgam is arranged as on mercury if the solution is sodium chloride in both cases.

---

* In this paragraph potentials arising from a possible orientation of solvent dipoles are neglected.

SUMMARY OF NUMERICALLY DETERMINED CONSTANTS.

1. The capacity of the adsorbed layer when consisting of only one kind of ion is —

For the hydrogen ion $23 \cdot 3 \pm 0 \cdot 5$ mfds. per cm.^{2}.

„ „ sodium ion $23 \cdot 6$ „ „ „

„ „ chloride ion $53 \cdot 7 \pm 1 \cdot 7$ „ „ „ (measured in HCl).

or $57 \cdot 3 \pm 1 \cdot 4$ „ „ „ (measured in NaCl).

2. The specific adsorption potentials of the hydrogen, sodium, and chloride ions are probably negative and of the order $0 \cdot 02$ volt.

3. The "absolute" electrokinetic potential of mercury in N/500 sodium chloride is probably negative and of the order $0 \cdot 003$ volt.

4. The "absolute" potential of the silver-silver chloride electrode in decinormal sodium chloride is $+ 0 \cdot 47 \pm 0 \cdot 03$ volt.

5. The charge in the double layer of a sodium amalgam electrode in equilibrium with a solution of sodium chloride of any concentration is

$$-37 \cdot 1 + 1 \cdot 29 \log a \pm 1 \cdot 5 \text{ microcoulombs per cm.}^2$$

where a is the activity of sodium in the amalgam, taking that in a $0 \cdot 1$ per cent. amalgam as unity.

SUMMARY.

1. The "capacity per cm.^{2} at constant potential" of the electrolytic double layer on mercury has been measured in hydrochloric acid and sodium chloride, over a wide range of concentration and potential.

2. The results show good agreement with the theoretical equation of Stern.

3. Stern's equation has been used to calculate various quantities from the experimental data.

I wish to express my sincere thanks to Sir Harold Hartley, F.R.S., to Mr. O. Gatty, and to others, for helpful advice and criticism throughout the course of this work.

References.

(1) Stern, *Zeit. für Electrochem.* xxx. p. 508 (1924).
(2) Guggenheim, J. Phys. Chem. xxxiii. p. 842 (1929).
(3) Guggenheim, J. Phys. Chem. xxxiv. p. 1540 (1930).
(4) Krüger and Krumreich, *Zeit. für Electrochem.* xix. p. 617 (1913).

(5) Bowden and Rideal, *Proc. Roy. Soc. A*, cxx. p. 59 (1928).
(6) Bennewitz and Schulz, *Zeit. Phys. Chem.* cxxiv. p. 115 (1926).
(7) Bowden, *Trans. Far. Soc.* xxiv. p. 473 (1928).
(8) Nonhebel, *Phil· Mag.* ii. p. 1085 (1926).
(9) Billiter, *Zeit. Phys. Chem.* xlviii. p. 513 (1904).
(10) Bodforss, *Zeit. für Electrochem*, xxix. p. 121 (1923).
(11) Lippmann, *Ann. de Chim. et de Phys.* v. ser. 5, p. 515 (1875).
(12) Heyrowsky, *Papers in Bull. Soc. Chim.* (1923 onwards).

LXXIII. *The Problem of the Sodium Amalgam Electrode in Dilute Solutions. By* J. St. L. Philpot, *B.A.*, N. L. Ross-Kane, *B.A., B.Sc., and* J. H. Wolfenden, *M.A., Fellow of Exeter College, Oxford* *.

IN the determination of the activity of an electrolyte by measurements of the E.M.F. of a cell with electrodes reversible to cation and anion respectively, it is well known that a self-contained determination is only possible if measurements are extended into the range of concentration in which the limiting equation of Debye and Hückel holds. This condition must always be fulfilled if an unequivocal linear extrapolation to determine E° is to be made. The extent of the limiting range of concentration is not well defined, but for strong uni-univalent electrolytes its upper limit is about $0.01\,N$ in water and $0.002\,N$ in methyl alcohol, and diminishes with the dielectric constant of the solvent.

Precision in E.M.F. measurement becomes progressively more difficult as the dilution of the electrolyte increases, and in the case of amalgam electrodes the disturbing effects at high dilution take a particularly aggravated form. Comparatively few workers have extended their measurements with alkaline amalgam electrodes below $N/100$, and their measurements have usually been made with double cells of the type

$$Ag : AgCl/Na\ Cl/NaHg_x\text{———}NaHg_x/Na\ Cl/AgCl : Ag,$$
$$c_1 \qquad\qquad\qquad c_2$$

in which the disturbing effects at the two intermediate amalgam electrodes cancel one another to an unknown extent.

Wolfenden, Wright, Ross-Kane, and Buckley [1] showed that the E.M.F. of the cell

$$Na\ Hg_x/NaCl\ in\ MeOH/AgCl : Ag$$

* Communicated by Sir Harold Hartley, F.R.S.

3 F 2

falls off rapidly from the true equilibrium value below a concentration of ·005 N. This leaves no intermediate range of concentration free from both the complex interionic effects at high concentration and the disturbing electrode effects at low concentration, and therefore yields no results susceptible to linear extrapolation. A recent paper by Scatchard and Tefft [2] describes the anomalous behaviour of the calcium amalgam electrode and stresses the complexity of the problem.

The experiments described in the present paper refer to the sodium amalgam electrode in aqueous solution and were undertaken in the hope of throwing some light on the nature of the disturbing effects at high dilution and on the conditions under which they are likely to be insignificant. In particular we wished to examine the influence on the potential of the amalgam electrode of such factors as the form of electrode, the rate of amalgam flow, and the presence of reducible impurities in the solution.

After an account of the experimental results a mechanism of the electrode processes is suggested and is applied to interpret the results obtained, and finally the conditions most favourable to precise measurement are discussed.

Experimental.

The E.M.F. of the cell

$$NaHg_x/aqueous\ NaCl,/AgCl : Ag$$

was measured with sodium chloride solutions ranging in concentration from normal to $0·0001\ N$, the amalgam concentration being varied from $0·3$ per cent. to $0·005$ per cent. by weight. Each cell consisted of a single compartment containing the amalgam and silver-silver chloride electrodes, connected by thick rubber tubing to a container for waste amalgam (see fig. 1) ; the cells were immersed in a paraffin thermostat at $25°\pm0·1°$. To save time three cells were used simultaneously, the three amalgam electrodes being supplied from the same reservoir. Of these three electrodes one was a fine capillary dropping electrode, another was a capillary dropping electrode of wider bore, while the third consisted of an overflowing capillary electrode.

The solutions were made up from water distilled in a stream of nitrogen and condensed on tin. Before the introduction of solution into flasks or cells, the air was displaced from the latter by a stream of nitrogen.
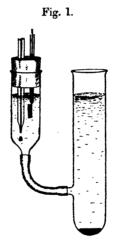
A continuous flow of solution past the electrodes was

dispensed with in these measurements, since interest was focussed primarily on the amalgam electrode itself.

The E.M.F. of each cell was measured over a range of dropping-rates from 1 drop per second to that giving a continuous column of amalgam 1 cm. in length. Measurements were continued for about an hour, when a rapid fall of E.M.F. began, which indicated alteration in composition of the solution. The effect of dissolved oxygen was occasionally studied by bubbling the gas through the solution.

A few later experiments were made with the cell described in the accompanying paper on the electrolytic double layer[3].

Fig. 1.
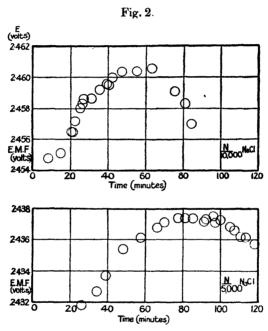
One of the triplet cells.

The solution could be purified electrolytically from reducible impurities down to a molar concentration of 10^{-9} before turning on the amalgam. Alternatively the cell could be emptied and rapidly refilled from a storage flask with solution containing 10^{-7} gram-equivalents per litre of reducible impurity, while the amalgam was dropping steadily; this was equivalent to using flowing solution. The instantaneous potential at any stage of drop formation or immediately after switching off a small current was measured on a few occasions with a capillary electrometer of the Keith-Lucas type used in physiological work. For these later experiments an overflowing electrode was used exclusively.

Results.

From the work as a whole the following empirical generalizations may be made :—

(1) In stationary solutions containing a considerable quantity of reducible impurity, such as were used for all the earlier experiments, the E.M.F. rises rapidly at first, stays constant for a time, and then falls rapidly. The height of the initial rise increases, and the length of the period of

Fig. 2.
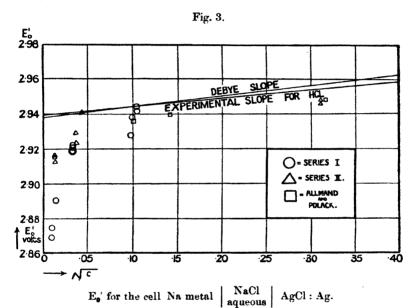
Variation of E.M.F. with time.

constancy decreases, with decrease in concentration of sodium chloride. The initial rise was not observed in the few experiments with solutions containing 10^{-7} to 10^{-9} gram-equivalents per litre of reducible impurity, but it is premature to say that it does not occur in them. The graphs of the E.M.F. plotted against time (fig. 2) show the effect in question.

(2) In water, as in methyl alcohol, the deviation from the true equilibrium E.M.F. begins to occur above the range of concentration in which the logarithm of the activity coefficient is a linear function of $\sqrt{c}$, so that the necessary

extrapolation of E_0' to $c=0$ cannot be carried out. This was shown by plotting the function "E_0'" against the square root of the concentration. To calculate E_0' [4] the maximum E.M.F. of the overflowing electrode cell was first corrected to give the E.M.F relative to sodium metal by graphic interpolation from the combined data of Lewis and Kraus [5] and Richards and Conant [6]. By subtracting $\frac{2RT}{F} \ln c$ from this corrected E.M.F., the function E_0' i

Fig. 3.

E_0' for the cell $\;$ Na metal $\;\left|\; \begin{array}{c} \text{NaCl} \\ \text{aqueous} \end{array} \;\right|\;$ AgCl : Ag.

obtained whose limiting value at infinite dilution represents the E.M.F. of the cell :—

Na metal/aqueous NaCl of unit activity/AgCl : Ag.

The curve obtained by plotting E_c' against $\sqrt{c}$ is everywhere concave to the concentration axis. Fig. 3 gives these values, together with lines showing the Debye-Hückel limiting slope and that observed for hydrochloric acid by Nonhebel and Hartley [7], both drawn through our experimental value for $c=0.01$ N. The results of Allmand and Polack [8], recalculated to a common basis, are given in the range where they overlap. The Table gives the numerical values.

(3) At concentrations of 0·001 N and 0·0002 N solutions containing 10^{-7} to 10^{-9} gram-equivalents/litre of reducible impurity have an E.M.F. a few millivolts higher than the less carefully purified solutions used at first ; but this higher

Concentration of solution in mols per litre, c.	$\sqrt{c}$	Amalgam concentration in grams per cent.	Observed E.M F.	E_0' referred to metal.	
0·00011	0·0105	0·0734	2·4613	2·8747	Series I. Triplet cells as described in text ; solutions not specially freed from reducible impurities.
,,	,.	,,	2·4558	2·8692	
0·00021	0·0145	0·0739	2·4445	2·8909	
0·00107	0·0327	0·0246	2·3563	2·9185	
0·00108	0·0329	0·3060	2·4399	2·9184	
0·00109	0·0330	0·0471	2·3774	2·9223	
,,	,,	,,	2·3756	2·9205	
0·00957	0·0978	0·3000	2·3377	2·9282	
0·00989	0·0994	0·0246	2·2617	2·9381	
0·0110	0·1049	0·0471	2·2780	2·9417	
,,	,,	,,	2 2809	2·9446	
0·9801	0·9900	0·0233	2·0418	2·9557	
0·9972	0·9985	0·3000	2·1293	2·9586	
0·000168	0·0139	0·0550	2·4692	2·9129	Series II. Cell as described in previous paper ; solutions purified down to 10^{-7} or 10^{-9} gram-equivalents of reducible impurity per litre.
,,	,,	,,	2·4722	2·9159	
,,	,,	0·1320	2·5011	2·9164	
0·00133	0·0365	,,	2·4009	2·9232	
,,	,,	,,	2·4073	2·9296	
0·00185	0·0430	0·0550	2·3737	2·9408	
0·0964	0·3105	,,	2·1782	2·9485	
,,	,,	0·0058	2·1156	2·9463	
0·100	0·3162	0·1389	(Calomel used as reference electrode.)	2·9486	Allmand and Polack's results.
0·0200	0·1414	,,		2·9399	
0·0100	0·1000	,,		2·9361	

E.M.F. is still well below the probable equilibrium value inferred from the Debye-Hückel slope and from the experimental E_0' curve for hydrochloric acid in aqueous solution.

4. In 0·001 N solutions, with dropping-rates down to 0·5 per sec., the instantaneous potential during drop formation, as measured with the capillary electrometer, is lowest

when a drop has just fallen leaving a fresh surface ; it rises rapidly by about 20 mv. to a value which remains constant during the rest of the life of the drop.

(5) When a current of 10^{-5} amps. is passed in 0.0001 N solution containing 10^{-7} gram-equivalents per litre of reducible impurity, the potential immediately after switching off the current is about 1 mv. higher than normal, and persists for the whole life of the drop.

(6) The agreement between the values of E_0' calculated from measurements of E.M.F. made with the same sodium chloride solution but with amalgam electrodes of widely different concentration is fairly satisfactory.

(7) The comparison of a silver–silver chloride electrode in the presence of a trace of alkali with a similar electrode in neutral solution showed that the alkali produced by the amalgam in a stationary solution might have a considerable effect on the reference electrode. The following are typical results, the electrode in neutral solution being negative :—

Concentration of NaCl ... 0·01   0·001   0·0001

Change in potential due to 0·00017 N :

NaOH .... 0·3 mv.   30 mv.   60 mv.

(8) The overflowing electrode gives a far steadier E.M.F. than either a coarse or a fine dropping electrode, though the last often gives a higher value by as much as 2 mv.

(9) The variation of E.M.F. with dropping-rate was scarcely detectable, and the small effect (ca. 0·1 mv.) was irregular in sign. Below 2 drops per sec. readings became erratic in the earlier experiments, but in the later ones steady readings were obtained down to 0·4 drops per sec. This is probably connected with the fact that in the later experiments the bore of the electrode increased towards the orifice so that there was no tendency for the amalgam column to retreat from the end under the influence of surface tension. With this type of electrode the slowest dropping-rate gave the highest E.M.F.

(10) When oxygen was bubbled through the cell the E.M.F. fell rapidly and continued falling for a short time after the bubbling was stopped. Bubbling for 5 minutes lowered the E.M.F. by 1 mv. in N solution. and 8 mv. in N/100.

Discussion.

The electrode process may be described in the following manner :—When a fresh drop of amalgam is formed, sodium ions enter the electrolytic double layer from the amalgam and continue to do so till the potential is sufficient to maintain equilibrium. At this potential, however, two constituents of the solution are not in equilibrium—reducible impurities and hydrogen ions. The former are reduced at a rate proportional to their concentration, if small, and independent of potential, while the latter are reduced to hydrogen at a rate determined by one of the two equations for overvoltage [9]. The current required for these processes must be supplied by sodium ions passing from the double layer into the solution and being replaced from the amalgam. If some part of this compensating process goes too slowly the E.M.F. will fall below the equilibrium value. The shape of the curve of E_0' against c (fig. 3) can be explained on the assumption that the departure of the E.M.F. from equilibrium which is required to produce the compensating current increases to appreciable values at low concentrations.

The formation of the double layer requires quite a large quantity of sodium ions which is calculated in the accompanying paper [3] and is equivalent to -34 microcoulombs per sq. cm. The capillary electrometer measurements showed that this double layer is not formed instantaneously, and the low potential during its formation must contribute to the mean potential as ordinarily measured to an increasing extent as the dropping-rate is increased. This sets an upper limit to the permissible dropping-rate. A lower limit is set by the reduction processes described above, for if the sodium, which must dissolve in compensation during the life-time of a drop, exceeds a certain quantity per cm.^{2} surface, then the thickness of the amalgam layer supplying it is such that the process of diffusion becomes too slow, quite apart from the effects in the solution described below. The same consideration of diffusion also sets a limit to the permissible dilution of the amalgam.

So much for occurrences in the amalgam. The adjacent layer of solution is probably even more prominent in determining the measured E.M.F. In the fraction of a second which is the life of a drop not much diffusion or mixing can occur. There will, therefore, be rapid changes, confined to a thin layer near the electrode surface and little affected by flowing solution, as well as the slow steady changes in the bulk of the solution if stationary. The changes consist in

(*a*) diminution of concentrations of hydrion and reducible impurities, which raises the E.M.F. by allowing nearer approach to equilibrium in the double layer, and (*b*) increase in concentration of sodium ion, which lowers the E.M.F., according to Nernst's equation. (Since $dE/dc \propto 1/c$ this effect is very prominent at low concentrations.) As the process continues therefore the E.M.F. will tend first to rise towards the equilibrium value as hydrion and impurities disappear, and then to fall off as sodium ion accumulates. Consideration of the solution as a whole in this way provides the simplest explanation of the shape of the E.M.F.-time curves shown in figs. 1 and 2 and described in section 1. The same process should occur in miniature in the surface-film of solution during the life of each drop of amalgam, but so far only the initial rise has been observed even with a drop lasting 2 secs. (see section 4). Probably, however, if the capillary electrometer measurements were made with solutions more dilute than 0·001 N, both the initial rise and the final fall would be evident in the life of a single drop at the normal dropping rates. A contributing factor in the final fall must be the liquid junction potential due to the accumulation of hydroxyl ions round the amalgam electrode (see section 7). If the hydroxyl ion had a direct action on the silver-silver chloride equilibrium it would, on the other hand, raise the E M.F. after the considerable time required for diffusion from the amalgam electrode. This has never been observed, but might have been masked by the final fall described above.

Most of the results have thus received a qualitative explanation :—

(1) The initial rise and final fall in the E.M.F. are due to removal of hydrion and reducible impurities and to accumulation of sodium ion respectively.

(2) The abnormally low E.M.F. in dilute solutions is due to the overlapping of all the factors described, in such a way that under no conditions can they all be absent as is possible in stronger solutions.

(3) The rate of reduction of impurities is independent of potential, while that of hydrion increases with it. Therefore with increasing dilution the lowering of E.M.F. will be due more to hydrion and less to impurities, and purification will be less effective in restoring the equilibrium value.

(4) The initial rise of the instantaneous potential of a fresh drop is due to the slowness of formation of the electrolytic double layer, either because of the slowness with which

sodium ions leave the amalgam, or because an abnormal number must leave it to compensate for the reduction processes. A final fall of potential of a long-lived drop should be observed under some conditions for reasons given above.

(5) Passage of a current compensates the reduction processes without dissolving sodium, so it should be possible in this way to separate the initial rise and the final fall at concentrations where they normally overlap. But it is impossible at present to tell how much current to pass, as the rate of reduction of hydrogen in neutral unbuffered solutions is extremely erratic, especially at these high potentials.

(6) It is impossible to calculate the influence of amalgam concentration without data as to the rates of dissolution of sodium from amalgams of various concentrations at various potentials, but the amalgam can certainly be too dilute, and it is possible that it may be too strong.

(7) Two ways have been suggested in which alkali can affect the reference silver-silver chloride electrode. Of these the liquid junction potential is believed to be the more important.

(8) The steadiness of the overflowing electrode is probably due to its greater mechanical stability. The higher E.M.F.s of the fine dropping one cannot be lightly dismissed, but have so far been unmeasurably erratic.

(9) Theoretically a very slow dropping-rate should give a low mean potential because of the predominance of the local "final fall," while a very high rate should give a low potential because of the predominance of the "initial rise," and intermediate rates should give a higher potential nearly independent of rate. It seems that the rates normally used are in this sense "intermediate" or slightly "high."

(10) When oxygen was bubbled through the solution it increased the reducible impurity, and the stirring brought up outlying portions of the solution which had not been reduced. Both these factors set back the "initial rise," *i. e.*, caused a fall of potential.

Conclusions.

Our observations lead us to suggest that the following conditions are the most likely to lead to values approximating to the true equilibrium potential of the sodium amalgam electrode :—

(1) The use of an external current or of some equivalent

device is necessary if E.M.F measurements are to be extended to concentrations below N/1000.

(2) Reducible impurities should not exceed 10^{-7} gram-equivalents/litre. This requires carefully prepared water and rigid exclusion of air. Purification beyond this point is unnecessary.

(3) An intermittently renewed solution should be used in preference to a flowing one. The former will yield more information, and the latter will not necessarily give the highest E.M.F.

(4) The overflowing type of electrode is probably best. It should be of narrow bore throughout. If the dropping-rate is controlled with a tap the bore of the electrode must increase slightly towards the orifice. Dropping-rates down to 0·5 per sec. should be used if the amalgam is between 0·005 and 0·1 per cent.

(5) Although they require higher dropping-rates and rapid renewal of solution, concentrated amalgams are probably better than the dilute ones which have often been used.

Summary.

Measurements of electromotive force have been made with the sodium amalgam electrode in aqueous solutions of sodium chloride at high dilution. The nature of the various disturbing factors is discussed in the light of the phenomena observed and conditions likely to minimize their influence are suggested.

References.

(1) Wolfenden, Wright, Ross-Kane, and Buckley, Trans. Faraday Soc. xxiii. p. 491 (1927).
(2) Scatchard and Tefft, Journ. Amer. Chem. Soc. lii. p. 2272 (1930).
(3) Philpot, Phil. Mag. 1932 (preceding paper).
(4) Lewis and Randall, 'Thermodynamics' p. 334 (1923).
(5) Lewis and Kraus, Journ. Amer. Chem. Soc. xxxii. p. 1459 (1910).
(6) Richards and Conant, Journ. Amer. Chem. Soc. xliv. p. 601 (1922).
(7) Nonhebel and Hartley, Phil. Mag. l. p. 729 (1925).
(8) Allmand and Polack, Journ. Chem. Soc. cxv. p. 1020 (1919).
(9) Bowden, Trans. Faraday Soc. xxiv. p. 473 (1928).

Balliol and Trinity College Laboratory,
    Oxford.

LXXIV. *On Gibbs's Adsorption Equation for the Case of Binary Mixtures. By* R. K. SCHOFIELD, *M.A., Ph.D., and* E. K. RIDEAL, *F.R.S.*[*]

IN recent years some confusion has arisen in the application of Gibbs's equation to binary mixtures. In developing a kinetic theory of surface films (Proc. Roy. Soc. A, cix. p. 57, 1925) the authors made use of the Gibbs equation

$$d\sigma = -\Gamma_1 d\mu_1 - \Gamma_2 d\mu_2 - \text{etc.,}$$

for examining the nature of the surface phase of solutions. In the equation σ is the surface tension and μ_1, μ_2, etc., are the thermodynamic potentials of the independently variable components. Γ_1, Γ_2, etc., are the excess surface concentrations used in Gibbs's sense, namely : the number of moles of these components in excess per unit area of the interface, the excess being reckoned with respect to an imaginary geometrical surface which is parallel to, but not necessarily coincident with, the physical surface of discontinuity. Gibbs called this imaginary surface the " dividing surface."

The value of the individual terms on the right-hand side of the equation depends on the position chosen for the dividing surface, any one being made zero by a suitable choice ; but their sum is independent of its position.

Use was made of this equation to analyze data for binary mixtures of ethyl alcohol and water. It was concluded, in the case of mixtures rich in alcohol, that the existence at the surface of a layer of closely packed alcohol molecules (which appears probable on other grounds) can only be conceded if at the same time it is supposed that a layer relatively rich in water exists below it.

Recently, W. F. K. Wynne-Jones [†] has put forward a treatment which, it is claimed, shows the existence of the close-packed alcohol layer without requiring the presence of the water-rich layer below it. In his paper, the essential importance of the imaginary " dividing surface " to the whole of Gibbs's theory is overlooked, the term " surface excess " being used without reference to this ꜞ" dividing surface."

In the present case it is convenient to choose the position of the dividing surface, so that Γ for water is zero. To
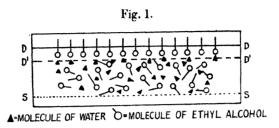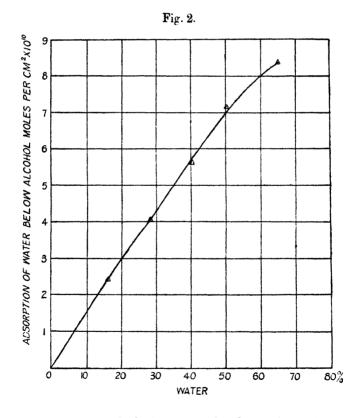
make clear the method of fixing the dividing surface, D,
let us imagine another surface, S, represented by the
dotted line, to be described parallel to the physical surface
but sufficiently far from it to be in the homogeneous liquid
phase. D is so placed that the total quantity of water pre-
sent in the system would be correctly computed by supposing
the water concentration existing below S to continue
unchanged to D, and there change abruptly to that obtaining
in the vapour phase. If such an accumulation as we have
suggested is present, the dividing surface will cut through
the outermost layer of alcohol in somewhat the way indicated
in the figure. To calculate Γ we must first calculate how
much alcohol would be present if the alcohol concentration
between S and D were the same as it is below S, and at D
changed abruptly to the concentration in the vapour. This
calculation would give an amount of alcohol less than that
actually present, and the difference (reckoned per unit area
of interface) is Γ. It should be clear from this that, with
an accumulation of water molecules below the surface layer
of alcohol, Γ will be less than the amount of alcohol in one
square centimetre of the outermost layer. If, on the other
hand, no such accumulation exists and the water and alcohol
concentrations are uniform as far as the underside of the
alcohol layer, then the dividing surface will be at D', and Γ
will be equal to the amount of alcohol in one square centi-
metre of the outermost layer. There appears to be no
escape from this conclusion.

If, following Wynne-Jones, we assume that from 30 per
cent. to 100 per cent. ethyl alcohol the surface is covered
by a layer of alcohol amounting to $U = 8 \cdot 2 \times 10^{-10}$ moles/cm.^{2},
it is easy to calculate the excess of water immediately below
this layer, since $U - \Gamma$ is equal to the amount of alcohol
which could be accommodated between D and D' if the
concentration were the same as in the bulk. What we
require is the amount of water that could be similarly
accommodated, and this is evidently given by $(U - \Gamma)R$,
where R is the ratio of water molecules to alcohol molecules
in the bulk. Using the values of Γ calculated by Wynne-
Jones from the vapour-pressure data of Dobson and the
surface-tension data of Morgan and Neidle, we obtain the
figures in the table and the curve, which give us a water
adsorption falling to zero in pure alcohol and approaching
one molecule of water to each of the adsorbed alcohol
molecules in a mixture containing 60 per cent. of water.

No great accuracy can be claimed for these figures, as,

for one thing, they depend on the value chosen of U, the
amount of alcohol in the surface layer, the very existence
of which is only inferred from general considerations, and

Fig. 1.

▲-MOLECULE OF WATER   Ỗ-MOLECULE OF ETHYL ALCOHOL

Fig. 2.

cannot be established from purely thermodynamic con-
siderations. But any explanation involving the existence
of this outermost layer must, to be thermodynamically
consistent, also take account of the water accumulation.

Turning finally to the relation $U = \Gamma + kc$ proposed by Wynne-Jones, it might be asked why c has been taken as the percentage by weight, rather than by volume or molecular volume. But such questions are really beside the point, seeing that the relation has no thermodynamic foundation and cannot, therefore, give results of any value.

Summary.

The theory advanced by Wynne-Jones relating to the figures published by the authors for the adsorption of alcohol at the surface of alcohol-water mixture is criticized.

TABLE.

Per cent. Water.	Per cent. Ethyl Alcohol.	Ratio by weight r.	Ratio by moles. R ($r \times 2{\cdot}55$).	Γ moles. per sq. cm. $\times 10^{10}$.	$(U-\Gamma)$ $[U=8{\cdot}2]$ $\times 10^{10}$.	Adsorption of water below alcohol moles. per. cm.$^2 \times 10^{10}$.
65	35	1·86	4·74	6·45	1·75	8·3
50	50	1·0	2·55	5·4	2·8	7·1
40	60	0·666	1·70	4·9	3·3	5·6
28	72	0·389	0·99	4·2	4·0	4·0
16	84	0·191	0·487	3·3	4·9	2·4
0	100	0	0	0	0	0

The view originally advanced by the authors that the fall in the surface excess in strong alcohol solutions is due to the formation of a layer relatively rich in water below a closely packed surface-layer of alcohol is reasserted, and a calculation based on the experimental figures preferred by Wynne-Jones indicates that this accumulation of water rises from zero in pure alcohol to a value of the order of one water molecule to every adsorbed alcohol molecule in the neighbourhood of 60 per cent. water.

No theoretical foundation can be found for the relation $U = \Gamma + kc$ proposed by Wynne-Jones.

LXXV. *Application of the Law of Photo-elastic Extinction to some Problems.* By J. KUNO, *Assistant Professor of Civil Engineering, Kyushu Imperial University, Fukuoka* *.

[Plates XV. & XVI.]

I. *Introduction.*

THE law of photo-elastic extinction—that is, the principal stress difference at a point in a specimen multiplied by the thickness of the specimen is proportional to the order of extinction—has been obtained by the author with specimens of phenolite under simple stress †. In order to examine whether the law holds generally true at the point where both the principal stresses are not equal to zero it is attempted in the present paper to compare the values of stresses experimentally obtained by this law with the theoretical values in a roller and in a rectangular thick plate of two-dimensional stress.

II. *A Roller Diametrically Compressed.*

(1) *Theory.*

A number of mathematical solutions and photo-elastic experiments have been carried out for a roller diametrically compressed ‡. The solution given in this article is somewhat different from others and will be compared with the photo-elastic test performed by using a specimen of phenolite.

We may take a system of curvilinear orthogonal co-ordinates α, β defined by the equation

$$z = a\, e^{-w},$$

where

$$z = x + iy, \quad w = \alpha + i\beta, \quad \alpha \geq 0, \quad \beta^2 \leq \pi^2.$$

Here the condition $\alpha = 0$ represents the circumference of a circle whose radius is a, and the condition $\alpha = \infty$ its centre,

* Communicated by the Author.

† Phil. Mag. xii. p. 503 (1931).
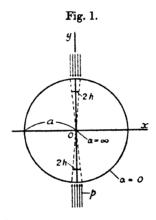
‡ Hertz, *Ges. Werk.* i. p. 285; Michell, *Proc. London Math. Soc.* xxxii. p. 35 (1900); Mesnager, *Ann. P. et Ch. Mém.* (71) iv. p. 160 (1901); Huber and Fuchs, *Phys. ZS.* xv. p. 298 (1914); König, *Ann. der Phys.* (4) lii. p. 553 (1917); Steinheil, *Diss. Giesen* (1920); Filon, Brit. Assoc. Report, Liverpool, p. 354 (1923); Föppl, *Drang und Zwang,* i. p. 320 (1924); Arakawa, Proc. Phys. Math. Soc. Japan, (3) vii. p. 174 (1925); Birth, *Ann. der Phys.* (4) lxxix. p. 145 (1926); Tuzi, Scientific Papers, I. P. C. R. (Tokyo) viii. p. 251 (1928).

as shown in fig. 1. If we refer to such a system of coordinates, Prof. S. Yokota's general expression for stress-components in two-dimensional problems of elasticity [*] becomes

$$\widehat{\alpha\alpha} - \widehat{\beta\beta} - 2i\widehat{\alpha\beta} = (1 - e^{-2i\beta})f_1'(w) - e^{\alpha - i\beta}f_2(w), \\ \widehat{\alpha\alpha} + \widehat{\beta\beta} = \text{Real part of } 2f_1(w), \quad \Bigg\} \quad (1)$$

where $f_1(w)$ and $f_2(w)$ are arbitrary functions of w. Let the load P be distributed on the area $2hab$ with the uniform radial intensity p, where b is the length of the roller and $2h$ is a small angle at the centre in radians intercepting the

Fig. 1.

loaded arc. Then the boundary conditions in the first quadrant must be

$$[\widehat{\alpha\beta}]_{\alpha=0} = 0,$$

$$[\widehat{\alpha\alpha}]_{\alpha=0} = 0 \quad \text{for} \quad (-\beta) < \left(\frac{\pi}{2} - h\right),$$

$$\qquad\qquad = -p \quad \text{for} \quad (-\beta) > \left(\frac{\pi}{2} - h\right), \quad \Bigg\} \quad (2)$$

or

$$[\widehat{\alpha\alpha}]_{\alpha=0} = -\frac{2p}{\pi}\left[h + \sum_{n=1}^{\infty} (-1)^n \frac{1}{n} \sin 2nh \cos 2n\beta\right].$$

The boundary conditions in the other quadrants are naturally fulfilled from symmetry.

* Journ. Soc. Mech. Eng. Japan, xxix. (April 1915).

Now put

$$f_1(w) = \frac{2p}{\pi} \sum_{n=0}^{\infty} A_{2n} e^{-2nw},$$

$$f_2(w) = \frac{2pa}{\pi} \sum_{n=0}^{\infty} B_{2n+1} e^{-(2n+1)w}.$$

$$\left.\right\} \quad \dots \quad (3)$$

Inserting (2) and (3) into (1), we find

$$A_0 = -h,$$

$$A_{2n} = (-1)^{n+1} \sin 2nh \quad \text{for} \quad n > 0,$$

$$B_{2n+1} = 2nA_{2n} - 2(n+1)A_{2(n+1)}.$$

Then we have, finally,

$$\widehat{\alpha\alpha} - \widehat{\beta\beta} - 2i\widehat{\alpha\beta} = -\frac{4p}{\pi}(e^{2a}-1) \sum_{n=1}^{\infty} (-1)^n e^{-2nw} \sin 2nh,$$

$$\widehat{\alpha\alpha} + \widehat{\beta\beta} = -\frac{4p}{\pi} \left[h + \sum_{n=1}^{\infty} (-1)^n \frac{1}{n} e^{-2na} \sin 2nh \cos 2n\beta \right].$$

$$\left.\right\} \quad \dots \quad (4)$$

These equations enable us to obtain the stress-components at any point. In the circular domain excepting the circumference (4) can be transformed into

$$\widehat{\alpha\alpha} - \widehat{\beta\beta} = \frac{4p}{\pi D}(1-e^{-2a})\sin 2h[(1+e^{-4a})\cos 2\beta + 2e^{-2a}\cos 2h],$$

$$\widehat{\alpha\alpha} + \widehat{\beta\beta} = \frac{2p}{\pi} \left[\text{arctg} \frac{\sin 2(h+\beta)}{e^{2a}+\cos 2(h+\beta)} \right.$$

$$\left. + \text{arctg} \frac{\sin 2(h-\beta)}{e^{2a}+\cos 2(h-\beta)} - 2h \right],$$

$$\widehat{\alpha\beta} = \frac{2p}{\pi D}(1-e^{-2a})(1-e^{-4a})\sin 2h \sin 2\beta,$$

where

$$D = \{1 + e^{-4a} + 2e^{-2a}\cos 2h \cos 2\beta\}^2$$

$$- \{2e^{-2a}\sin 2h \sin 2\beta\}^2.$$

In the case where $2h$ is very small we may put approximately

$$\sin 2h = 2h, \qquad \cos 2h = 1,$$

$$\text{arctg} \left[\frac{\sin 2h}{(e^{2a}+\cos 2h)} \right] = \frac{2h}{(1+e^{2a})}.$$

Then we have on the horizontal and vertical diameters

$$[\widehat{\alpha\alpha}]_{\beta=0} = \frac{P}{\pi ab}\left(\frac{1-\xi^2}{1+\xi^2}\right)^2,$$
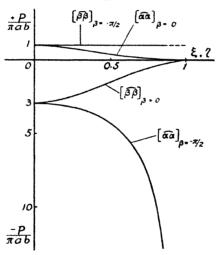
$$[\widehat{\beta\beta}]_{\beta=0} = -\frac{P}{\pi ab}\left\{\left(\frac{2\,\xi}{1+\xi^2}\right)^2 - 1\right\},$$

$$[\widehat{\alpha\alpha}]_{\beta=-\pi/2} = -\frac{P}{\pi ab}\frac{3+\eta^2}{1-\eta^2},$$

$$[\widehat{\beta\beta}]_{\beta=-\pi/2} = \frac{P}{\pi ab},$$

Fig. 2.

where $\xi = x/a$ and $\eta = y/a$. The results of these calculations, plotted in fig. 2, show that they agree with the results given by Hertz and others under the assumption that each load acts at a point. As a measure of the accuracy of the above reduction we have the total pressure on the horizontal diameter as follows :

$$2\int_0^a b[\widehat{\beta\beta}]_{\beta=0}\,dx = -P.$$

Let γ be the angle which the normal at (α, β) to the line of the α-family that passes through this point makes with

the axis of x, and θ be the angle which a principal axis at (α, β) makes with the axis of x. Then we have generally

$$2(\gamma - \theta) = \text{Amplitude of } (\widehat{\alpha\alpha} - \widehat{\beta\beta} - 2i\widehat{\alpha\beta}) \ *.$$

In the present case it becomes

$$\text{tg } 2(\theta + \beta) = \frac{(1 - e^{-4\alpha}) \sin 2\beta}{(1 + e^{-4\alpha}) \cos 2\beta + 2e^{-2\alpha} \cos 2h}$$

which may be shown to be transformed into

$$y^2 - x^2 + 2xy \cot \theta = a^2$$

provided that $\cos 2h = 1$. Turn the axes through an angle
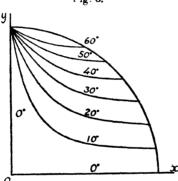
Fig. 3.

$(\theta/2 - \pi/4)$, the origin remaining the same. Referring to the new axes we get

$$Y^2 - X^2 = a^2 \sin \theta.$$

This equation represents the isoclinic lines, θ being a parameter. Such lines are shown in fig. 3 for one quadrant of the section, the others being deducible from symmetry.

Next, denoting the difference of the two principal stresses at a point by S, we have generally

$$S^2 = \{\widehat{\alpha\alpha} - \widehat{\beta\beta}\}^2 + \{2\widehat{\alpha\beta}\}^2 \dagger.$$

In the present case we have

$$S = 4p(1 - e^{-2\alpha}) \sin 2h / \pi D^{1/2}, \quad . \quad . \quad . \quad (5)$$

---

* Tech. Rep. Kyushu Imp. University, v. p. 265 (Feb. 1931)
† *Loc. cit.*

where p may be expressed in the form $p = P/2hab$. If we insert the law of photo-elastic extinction $Sd = nK$ into (5), and put approximately

$$D^{1/2} = 1 + e^{-4a} + 2e^{-2a}\cos 2\beta \quad \text{and} \quad \sin 2h = 2h,$$

we have

$$n = \frac{4P}{\pi aK} \frac{1 - e^{-2a}}{1 + e^{-4a} + 2e^{-2a}\cos 2\beta}$$

where n is the order of extinction and K is the coefficient of photo-elastic extinction. Fig. 4 shows the isochromatic
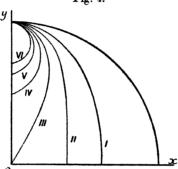
Fig. 4.

lines calculated from the above equation for the case $\frac{4P}{\pi aK} = 3$. On the axis of y the equation (5) becomes

$$S = \frac{4p \sin 2h}{\pi} \frac{1 - \eta^2}{1 + \eta^4 - 2\eta^2 \cos 2h},$$

where $\eta = y/a$. Differentiating S with respect to η, and equating the result to zero, we get a special value of η given by

$$\eta_0^2 = 1 - \sqrt{(2 - 2\cos 2h)}$$
$$= 1 - 2h + \frac{1}{24}(2h)^3 + \dots \qquad \cdot \quad \cdot \quad (6)$$

S is maximum at the point indicated by η_0, showing that the highest order of extinction or the maximum of the maximum shearing stress does not occur on the periphery.

(2) *Distribution of Stresses on the Contact Area.*

The elastic problems of stresses which arise when two cylinders, running parallel with each other, are pressed

together was solved by M. T. Huber and S. Fuchs [*] in accordance with Hertz's general theory of contact. In the case where a cylinder (E_1, μ_1) is pressed on a plate (E_2, μ_2), where the bodies in the unstressed state are in contact at the origin of (x, y), and where the axis of x is directed along the common tangent, we may show that the stress-distribution on the contact area can be expressed by the equations

$$w^2 = \frac{4ap'}{\pi} \left\{ \frac{1-\mu_1^2}{E_1} + \frac{1-\mu_2^2}{E_2} \right\},$$

$$\sigma_x = \frac{2p'}{\pi} \frac{y}{w^2} \left[\sqrt{\frac{v+w^2}{v}} \left\{ 2 - \frac{w^2 y^2}{v^2 + w^2 y^2} \right\} - 2 \right],$$

$$\sigma_y = \frac{2p'}{\pi} \frac{y^3}{v^2 + w^2 y^2} \sqrt{\frac{v+w^2}{v}},$$

$$\tau = \frac{2p'}{\pi} \frac{xy^2}{v^2 + w^2 y^2} \sqrt{\frac{v}{v+w^2}},$$

where

$$2v = (x^2 + y^2 - w^2) + \sqrt{[(x^2 + y^2 - w^2)^2 + 4w^2 y^2]}.$$

$2w =$ the width of the contact area,

$a =$ the radius of the cylinder,

$p' =$ the applied force per unit length of the cylinder,

$E, \mu =$ Young's modulus and Poisson's ratio.

On the axis of y we have, putting $x = 0$,

$$\sigma_x = \frac{2p'}{\pi w^2} \left[\sqrt{y^2 + w^2} \left(2 - \frac{w^2}{y^2 + w^2} \right) - 2y \right],$$

$$\sigma_y = \frac{2p'}{\pi} (y^2 + w^2)^{-1/2}, \qquad \tau = 0.$$

At the origin we get the greatest stress :

$$\sigma_x = \sigma_y = \frac{2p'}{\pi w}.$$

The principal stress difference on the axis of y may be expressed by the equation

$$S = [\sigma_y - \sigma_x]_{x=0},$$

or

$$S = \frac{4p'y}{\pi w^2} \left[1 - \frac{y}{\sqrt{(y^2 + w^2)}} \right].$$

* *Phys. ZS.* xv. p. 298 (1914).

Differentiating S with respect to y, and equating the result to zero, we have $y_0 = 0\cdot7861\,w$, where y_0 is the value of y, giving the maximum of S.

As an example, let a phenolite cylinder ($a = 17\cdot5$ mm., $E_1 = 4\cdot3 \times 10^4$ kg./cm.^{2} *, $\mu_1 = 0\cdot36$) be pressed on a steel plate ($E_2 = 2 \times 10^6$ kg./cm.^{2}, $\mu_2 = 0\cdot3$) so that the pressure p' (P/b) between them is $72\cdot8$ kg. (or $P = 43\cdot7$ kg., $b = 0\cdot6$ cm.). Then calculation gives us

$$2w/a = 0\cdot068, \qquad y_0/a = 0\cdot027, \qquad \eta_0 = 1 - y_0/a = 0\cdot973,$$

the mean intensity of load on the contact area $= 610$ kg./cm.^{2}, the value of stress at the origin $= 780$ kg./cm.^{2}.

In our notation $2w/a = 2h$. If we insert $2h = 0\cdot068$ into the equation (6), we find

$$\eta_0 = 0\cdot965$$

as the position of maximum S for the case where the uniform pressure p is distributed radially over the contact area.

(3) *Experiment.*

Figs. 5 and 6 (Pl. XV.) show the apparatus employed by the author for measuring the stress-optical effect. For the light source Dr. Nagaoka's mercury lamp is used. The Glan-Thompson's prisms, $2 \times 2 \times 5$ cm., are employed in the polarizer and analyzer instead of Nicol's prisms. The ray of light from the source reaches the specimen after passing through a condenser, a photographic lens, the polarizer, and another lens in succession. The specimen is then projected by a lens on a photographic plate. The analyzer and a Wratten light filter No. 77 A are placed in front of the camera, which is fitted with a Compur shutter. The lenses used are F/4·5 and $f = 30$ cm. The quarter-wave plates are removable from the polarizer and the analyzer.

A circular disk of phenolite, 35 mm. in diameter and 6 mm. in thickness, was tested, the initial stresses in it being removed before the test. The disk, placed in the beam of circularly polarized monochromatic light and compressed, as shown in fig. 6 (Pl. XV.), was photographed at the instant so that just one minute had elapsed after being loaded (see fig. 7, Pl. XV.), the applied load being 43·7 kg. (refer to the numerical example in the last article). Since the

---

* This value was determined recently and corresponds to K_1.

value of the coefficient K_1 for phenolite may be taken as 10·6 kg./cm. *, we have in this case

$$4P/\pi a K_1 = 3.$$

Hence fig. 7 (Pl. XV.) should be compared with the theoretical result shown in fig. 4. Fig. 8 (Pl. XV.) was taken at the instant just 15 minutes after being loaded, the load remaining constant. Comparing fig. 7 with fig. 8 (Pl. XV.) proves that isochromatic lines undergo an enormous amount of time effect.

On removing the quarter-wave plates from the apparatus the isoclinic lines were photographed, fig. 9 (Pl. XV.) and fig. 10 (Pl. XVI.), being the typical examples. These should be compared with the theoretical lines as shown in fig. 3.

Measurement on the photographic plate of fig. 7 (Pl. XV.) indicates that the nucleus of the isochromatic lines is inside the periphery, its position being $\eta_0 = 0.964$.

For photographing the isochromatic and isoclinic lines the Ilford Screened Chromatic Plates were used, the time of exposure being a tenth of a second. The plates were developed for two and a half minutes at 20° C. with the hydroquinone developer recommended by Ilford Ltd. for their process plates.

III. *A Rectangular Thick Plate compressed on its Two Opposite Sides.*

(1) *Theory.*

In the case where a rectangular thick plate is compressed by forces applied on its two opposite sides, the stress-components may be expressed in terms of the stress-function F by the formula

$$\sigma_x = \frac{\partial^2 F}{\partial y^2}, \qquad \sigma_y = \frac{\partial^2 F}{\partial x^2}, \qquad \tau = -\frac{\partial^2 F}{\partial x\, \partial y}, \quad \cdot \quad (7)$$

where F must satisfy the equation

$$\frac{\partial^4 F}{\partial x^4} + \frac{\partial^4 F}{\partial y^4} + 2\frac{\partial^4 F}{\partial x^2\, \partial y^2} = 0.$$

In a rectangular plate, as shown in fig. 11, there are the eight boundary conditions

$$[\sigma_x]_{x=0\,\text{or}\,a} = 0, \qquad [\sigma_y]_{y=0\,\text{or}\,b} = -P(x),$$

$$[\tau]_{x=0\,\text{or}\,a} = 0, \qquad [\tau]_{y=0\,\text{or}\,b} = 0.$$

* Phil. Mag. xii. p. 503 (1931).

The load $P(x)$ may be generally developed in a sine series for each value of x between $x=0$ and $x=a$, namely,

$$P(x) = \frac{4p}{\pi} \sum_{n=1}^{\infty} S_n \sin \frac{n\pi x}{a},$$

where $p =$ the intensity of load at any chosen point,

$$S_n = \frac{\pi}{2pa} \int_0^a P(x) \sin \frac{n\pi x}{a} dx.$$

We may introduce a stress-function F by means of the form

$$F = F_1 + F_2 + F_3,$$

Fig. 11.

where

$$F_1 = \frac{4p}{\pi} \sum_{n=1}^{\infty} A_n \frac{a^2}{n^2\pi^2} \operatorname{Sech} n\pi\phi_1 \operatorname{Cosh} \frac{n\pi}{a}(y-b/2),$$

$$F_2 = \frac{4p}{\pi} \sum_{n=1}^{\infty} B_n (n\pi\phi_1 + \operatorname{Sinh} n\pi\phi_1)^{-1} \frac{a^2}{n^2\pi^2} \left\{ \frac{n\pi y}{a} \operatorname{Sinh} \frac{n\pi}{a}(y-b) \right.$$
$$\left. + \frac{n\pi}{a}(y-b) \operatorname{Sinh} \frac{n\pi y}{a} \right\} \sin \frac{n\pi x}{a},$$

$$F_3 = \frac{4p}{\pi} \sum_{n=1}^{\infty} C_n (n\pi\phi + \operatorname{Sinh} n\pi\phi)^{-1} \frac{b^2}{n^2\pi^2} \left\{ \frac{n\pi x}{b} \operatorname{Sinh} \frac{n\pi}{b}(x-a) \right.$$
$$\left. + \frac{n\pi}{b}(x-a) \operatorname{Sinh} \frac{n\pi x}{b} \right\} \sin \frac{n\pi y}{b},$$

$$\phi = a/b, \qquad \phi_1 = b/a.$$

Then we have by some calculations

$$\left[\frac{\partial^2 F}{\partial y^2} \right]_{x=0} = \left[\frac{\partial^2 F}{\partial y^2} \right]_{x=a} = 0,$$

$$\left[\frac{\partial^2 F}{\partial x^2} \right]_{y=0} = \left[\frac{\partial^2 F}{\partial x^2} \right]_{y=b} = -\frac{4p}{\pi} \sum_{n=1}^{\infty} A_n \sin \frac{n\pi x}{a},$$

$$-\left[\frac{\partial^2 F}{\partial x \partial y}\right]_{x=0} = \left[\frac{\partial^2 F}{\partial x \partial y}\right]_{x=a}$$

$$= \frac{4p}{\pi} \sum_{n=1}^{\infty} \left[\sum_{r=1}^{\infty} A_r(Y_{nr}) \right.$$

$$\left. + \sum_{r=1}^{\infty} B_r(_nZ_{r\phi_1}) + C_n \right] \cos\frac{n\pi y}{b},$$

$$-\left[\frac{\partial^2 F}{\partial x \partial y}\right]_{y=0} = \left[\frac{\partial^2 F}{\partial x \partial y}\right]_{y=b}$$

$$= \frac{4p}{\pi} \sum_{n=1}^{\infty} \left[A_n \operatorname{Tanh}\frac{n\pi}{2\phi} \right.$$

$$\left. + B_n + \sum_{r=1}^{\infty} C_r(_nZ_{r\phi}) \right] \cos\frac{n\pi y}{a},$$

where

$$(Y_{nr}) = \frac{4}{\pi} \frac{1-\cos n\pi}{2} \frac{r\phi_1}{n^2 + r^2\phi_1^2},$$

$$(_nZ_{r\phi}) = \frac{8}{\pi} \frac{1-\cos n\pi}{2} \frac{n^2 r\phi}{(n^2 + r^2\phi^2)^2} \frac{1+\operatorname{Cosh} r\phi\pi}{r\phi\pi + \operatorname{Sinh} r\phi\pi}.$$

The boundary conditions are satisfied if we put

$$A_n = S_n,$$

$$C_n + \sum_{r=1}^{\infty} B_r(_nZ_{r\phi_1}) = -\sum_{r=1}^{\infty} A_r(Y_{nr}), \quad . \quad . \quad (8)$$

$$B_n = -\sum_{r=1}^{\infty} C_r(_nZ_{r\phi}) - A_n \operatorname{Tanh}\frac{n\pi}{2\phi}. \quad . \quad . \quad (9)$$

To make the calculation simpler we eliminate B from (8) and (9). Then we have the formula for C

$$C_n - \sum_{s=1}^{\infty} \sum_{r=1}^{\infty} (_nZ_{r\phi_1})(_rZ_{s\phi})C_s = \sum_{r=1}^{\infty} A_r\left[(_nZ_{r\phi_1})\operatorname{Tanh}\frac{n\pi}{2\phi} - (Y_{nr}) \right].$$

These equations give us three systems of constants, A, B, and C. Now all the constants being known, the expressions for the stress-components can be found from (7).

(2) *Numerical example.*

A square plate, as shown in fig. 12, is considered.

The intensity of load for $0 \leq x < 0\cdot4\,a$ is zero,

,, ,, $0\cdot4\,a \leq x \leq 0\cdot6\,a$ is p,

,, ,, $0\cdot6\,a < x \leq a$ is zero.

The load may be expressed by the equation

$$P(x) = \frac{4p}{\pi} \sum_{n=1}^{\infty} \frac{1}{n} \sin\frac{n\pi}{2} \sin\frac{n\pi}{10} \sin\frac{n\pi x}{a}.$$

Calculation gives us the coefficients and stresses as shown in Table I. and figs. 13 and 14.

Fig. 12.
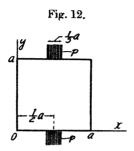
TABLE I.

n.	A_n.	$-B_n$.	$-C_n$.
1............	0·3091	0·2652	0·0396
3............	−0·2697	−0·2803	0·0112
5............	0·2	0·1923	0·0139
7............	−0·1156	−0·1211	0·0099
9............	0·0343	0·0292	0·0071
11............	0·0281	0·0238	0·0056
13............	−0·0622	−0·0660	0·0045
15............	0·0667	0·0634	0·0038
17............	−0·0476	−0·0504	0·0032
19............	0·0163	0·0137	0·0028
21............	0·0147	0·0123	0·0025
23............	−0·0352	−0·0373	0·0023
25............	0·04	0·0381	0·0020

As a measure of the accuracy of these calculations the value of $\int_0^a \sigma_y dx$ is measured graphically at the sections parallel to the axis of x, which must be compared with $P = 0·2\,ap$.

TABLE II.

Measure of Accuracy.

Sections.	Measured values.	Errors in percentage.
$y = 0.2\,a$	$0.2008\,ap$	$+0.4$
$y = 0.3\,a$	$0.2002\,ap$	$+0.1$
$y = 0.4\,a$	$0.1984\,ap$	-0.8
$y = 0.5\,a$	$0.1992\,ap$	-0.4

Thus the error is comparatively small.

Fig. 13.
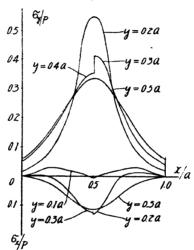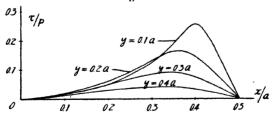
Fig. 14.

‧‧ The principal stress difference S at a point may be expressed by the form $S = mp$, where p is the intensity of load as before and m is the numerical coefficient calculated from the stress-components. If we insert the two relations

$$p = \mathrm{P}/0.2\,ad, \qquad Sd = n\mathrm{K},$$

into the above expression, $S = mp$, we get
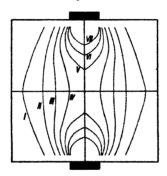
$$n = 5mP/aK.$$

Further, assuming

$$P/aK = 2, \quad \ldots \ldots \quad (10)$$

and calculating the values of m at various points, the values of n at various points are then found. The loci of the integral values of n (the theoretical isochromatic lines) are finally traced as shown in fig. 15, where the Roman numerals show the order of extinction or the values of n.

Fig. 15.

(3) *Experiment.*

A square plate of phenolite, $33 \times 33 \times 6$ mm., was tested. The isochromatic lines were photographed at the instant just one minute after being loaded, the load being 70 kg. (fig. 16, Pl XVI.). Since the coefficient K_1 for phenolite may be taken as 10·6 kg./cm., we have in the present specimen

$$P/aK_1 = 2,$$

which is nothing but the equation (10). Hence fig. 16 (Pl. XVI.) should be compared with the theoretical lines shown in fig. 15.

Figs. 17, 18, 19, and 20 (Pl. XVI.) show the typical examples of isoclinic lines. In fig. 17 we may find that the directions of principal axes at the section $x = 0.5\,a$ or $y = 0.5\,a$ are vertical and horizontal, which agrees clearly with the theory.

IV. *Conclusion.*

1. In the scope of this paper it may be concluded that the values of stresses experimentally obtained by *the law of photo-elastic extinction* are in fairly good agreement with the theoretical values.

2. Further investigations are needed to determine whether the accuracy and usefulness of this law may be established for general purposes of studying two-dimensional elastic systems.

N.B.—Dr. Z. Tuzi, Research Member of the Institute of Physical and Chemical Research in Tokyo, recently informed the author that the elastic properties of phenolite seem to differ to some extent according to the baking temperature in its finishing stage, and that the higher the temperature (limits being 100°–140° C.) the harder and brittler becomes phenolite. If it is really so, the value of the coefficient K may also differ. Hence the value of K should be determined whenever a new plate of phenolite is used.

LXXVI. *Arc, Spark, and Glow: a Note on Nomenclature. By* JOHN THOMSON, *M.A., B.Sc., Ph.D., Lecturer in Natural Philosophy at the University of Glasgow* *.

THE purpose of this note is two-fold. First, it is proposed to call attention to ambiguities of terminology which exist with regard to the electric discharge. Three classes of investigators—the electrical engineers, those engaged in research upon the mechanism of the gaseous discharge, and the spectroscopists—employ the terms "arc" and "spark" to define certain discharge phenomena. Unfortunately, the connotation of each term varies considerably from one class to the other, so that auxiliary definition is always required, but too seldom given. By physicists in general the terms are used in the sense which was originally intended by the electrical engineers, but, as the progress of research has shown that the phenomena described by them are complex, the words have become not only ambiguous but definitely misleading. The attempt will therefore be made to indicate · clearly what each of the three classes mentioned intends to be understood when the term "arc" or "spark" is employed.

* Communicated by the Author.

Secondly, it is proposed to describe a simple experiment which exhibits at atmospheric pressure all the types of electric discharge. From a consideration of the conditions under which each type appears it should be possible to suggest some more exact definitions which will rationalize the nomenclature and destroy the confusion which at present exists.

Electrical Engineering Nomenclature.

In the ' Dictionary of Applied Physics' an electric " spark " is defined as " the sudden discharge of electricity across an air-gap accompanied by the production of light and heat," and the " arc " as " a stream of hot gases carrying an electric current across a gap between two electrodes." Surely these two definitions are not mutually exclusive ; it is easy to imagine a spark (so defined) taking the form of an arc (so defined). Yet in practice a distinction between the two is implied. This may be well exemplified with reference to the phenomena exhibited by an induction coil or high-tension magneto.

I. *Induction Coil Discharges without a Secondary Condenser.*—Suppose the secondary terminals of a coil to be connected to an air-gap with no condenser in parallel, and the primary current to be arranged so that a bright discharge across the gap takes place. Then the evidence of the rotating mirror[1] is that at each break in the primary circuit there is a series of secondary discharges. The first of these is bright, particularly at the outset, and the others are faint. The current is pulsating but unidirectional. A simultaneous oscillograph record of the potential across a secondary coil is of the form shown in fig. 1[2], where the ordinate measures the square of the secondary potential and the abscissa the time.

The potential peak A gives rise to the first bright discharge, while B, C, D, E are the cause of the fainter, more diffuse ones. In accordance with the customary terminology of electrical engineering, discharge A is called a " spark " and B, C, D, E are called " arcs." The number of arcs which follow the spark depends, of course, upon experimental conditions ; it is even possible, by using larger primary currents and small gaps, to obtain a decaying aperiodic arc instead of the pulsations of fig. 1.

It is difficult to say exactly what is the distinguishing characteristic of the spark in this discharge. Certainly A is considerably brighter than B, C, D, E. In fact, the aggregate intensity of the last four is usually small compared with

the intensity of the spark. There is also evidence that the
initial part of discharge A is of a different nature from the
rest—it is the earlier stage which is most brilliant. But
neither of these qualities is of much use in forming a defini-
tion. Perhaps the best properties of the spark which can be
used to distinguish it from the arc are the potential difference
required for its production and the time which it takes to
occur. A is associated with a very large potential difference
between the electrodes—something of the order of 20,000
volts/cm. in air at atmospheric pressure, while in B, C, D, E
the corresponding inter-electrode potential difference is less
than one-tenth of this. Also, the initial spark is of very

Fig. 1.
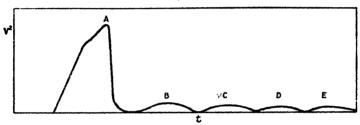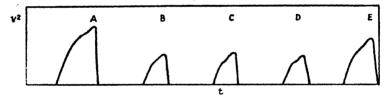
Fig. 2.

short duration. It is a sudden rush of electricity accom-
panied, as is seen from fig. 1, by a very rapid decrease of
potential.

II. *Induction Coil Discharge with a Secondary Condenser.*
—Suppose, now, a condenser to be placed in parallel with
the air-gap, and the primary current again arranged so that
bright discharges are obtained. In this case one break of
the primary circuit gives rise to a series of discharges of a
different type. These, when examined by means of the
rotating mirror, prove to be all fairly bright, the first and
last being slightly brighter than the others. An oscillo-
graph record of the secondary potential is of the general
appearance of fig. 2.

In this case each discharge A, B, C, D, E is called a spark, and each presents the general appearance of A of the discharge without a condenser. Often each discharge of this type contains more than one spark—there may be as many as six associated with one potential peak. If the primary current is greatly increased, a time comes when the *régime* of fig. 1 begins in a modified way. The pulsating arc makes its appearance, and the number of sparks is reduced to one or two, corresponding to one or two distinct potential peaks. Again, it is evident that the most constant property of the spark is the high associated potential. All the peaks A, B, C, D, E are of the order 20,000 volts/cm., although in general they are not so large as A of fig. 1. Hence it seems that the common usage of electrical engineering terminology is simply to associate the name "spark" with a bright high-potential discharge.

Nomenclature employed in connexion with the Gaseous Discharge.
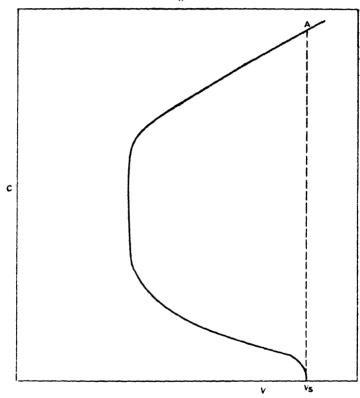
The mechanism of what has been called by modern physicists the "spark discharge" has been the subject of innumerable investigations. In this connexion the word "spark" is seldom used as a substantive, the "sparking potential" being the important concept. If, however, the spark is to be defined at all, then it must be as *the initial stage of any discharge of electricity through a gas, where the current is carried entirely by gaseous ions between cold electrodes.* The "sparking potential" is the minimum steady potential which, when applied for an indefinite time between the electrodes, produces an appreciable current through the gas ; it is a function of the nature and pressure of the gas, the shape of the electrodes and their distances apart, and, probably, the photoelectric emissivity of the electrode surfaces.

These definitions imply a considerable knowledge of the nature of the discharge, and the wording of the definition of the spark is particularly significant. It is now well known that the general shape of the current-potential characteristic of a gas discharge between cold electrodes is as shown in fig. 3, where the abscissa measures the potential difference between the electrodes, and the ordinate the current flowing in the discharge. Such characteristics have been carefully studied by Taylor, Penning, and Clarkson[a].

It follows from the nature of this curve that although the potential difference between the electrodes must be raised to

3 H 2

V_s (fig. 3) to start the discharge, the latter may be maintained at a much smaller voltage.   Hence, if, the current in any experiment is not controlled by resistance in the circuit, immediately after the discharge commences the conditions correspond to point A on the characteristic.   This is the reason for defining the spark as the *initial stage* of the discharge.   The curve shown in fig. 3 is really a corona and

Fig. 3.

glow characteristic; the spark is represented by an infinitesimally small portion of the curve at V_s.

It is rather more difficult to suggest a definition of the arc which will be representative of the nomenclature employed in connexion with the gaseous discharge.   As distinct from the spark, the arc in this connexion is to be associated with a hot cathode at which thermionic emission is taking place.   In practice, however, unless a heated filament of tungsten or some other metal of high boiling-point

is intentionally used as the cathode, thermionic emission requires that the latter should be at such a temperature that it will be partly vaporized. Hence, leaving out of account special techniques, an arc is a discharge in which the current is carried by the metal vapour as well as the gas. This definition forms a sufficiently marked contrast to that of the spark.
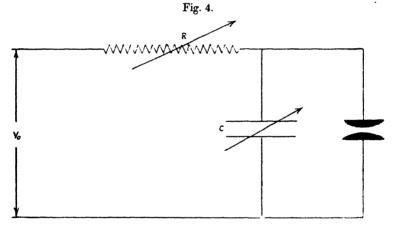
Comparing these definitions with the loose ideas acquired from a study of the engineer's use of the terms arc and spark, it is immediately obvious that some readjustment of nomenclature is necessary. The rather ghostly spark of the researcher on the mechanism of the discharge is so faint as to be almost invisible, and the maximum current passing during such a *régime* is of the order of microamperes. The typical engineer's spark results from the discharge of a large condenser. It is of enormous light-intensity, and the current in it is of the order of hundreds of amperes.

The Nomenclature of Spectroscopy.

Only a word is required in this connexion. The "arc" spectrum of an element is that produced when the atom or molecule is returning to its normal state from one of higher energy. It is therefore typical of the un-ionized element, or in the extreme case of the recombination of an electron with a singly ionized atom or molecule. The "spark" spectrum or enhanced spectrum is that produced by the ionized element returning to its most stable ionized state. In the extreme case it is produced by a multiply-ionized atom or molecule recombining with an electron. The use of the terms "arc" and "spark" in this manner arose from the empirical study of spectra before the analysis given above was understood. It was found that certain lines in the complete spectrum of an element were not present when the substance was excited by an arc discharge, but were present in the spark. The arcs and sparks which are meant are, of course, those defined by the terminology of the engineers. It is now known that the excitation of the enhanced spectrum depends upon high current density and high electric field strength. These are characteristic of the engineer's spark—hence the connexion. Yet the spectra exhibited by a typical spark discharge are indeed varied. Four spectra are obtained with varying degrees of intensity: (a) the arc spectrum of the gas between the electrodes; (b) the spark spectrum of the gas; (c) the arc spectrum of the metal of the electrodes; (d) the spark spectrum of the metal. In no case is the total intensity of the two spark spectra as large as that of the

other two. The spark actually enhances the arc spectrum in addition to causing the spark lines to appear. If the spectra of the gas between the electrodes are required no condenser is used. Under such circumstances, so long as the discharge current is small, only a few faint metal lines appear. If, however, a condenser is placed across the gap, the spectra of the metal electrodes become brighter and the gaseous spectra are partially masked. The explanation of these spectral phenomena will appear when the details of such discharges are considered later.

Spark, Glow, and Arc at Atmospheric Pressure.

A simple circuit which exhibits all types of discharge at atmospheric pressure is shown in fig. 4. The variable con-

Fig. 4.

denser C, shunted by a spark-gap is connected to a direct-current high-voltage supply through the variable resistance R. In the experiment performed by the writer the spark-gap electrodes were copper spheres 3 cm. in diameter, and the supply voltage was about 1600. R could be varied from 2 to 0·1 megohms, and C in steps from 2 to less than 0·0001 microfarads. A microscope was focussed on the gap. The type of discharge obtained depends on the values of R and C.

I. *Capacity Discharges.*—With C of the order of a microfarad, and the gap adjusted so that sparks would pass at 1500 volts (gap about 0·05 mm. in length), regular discontinuous discharges were obtained, the time between each depending upon the value of R. With $C = 2\mu F$, and $R = 2$ megohms, about 13 seconds elapsed between each discharge.

The time was reduced to 1 second, when R was equal to 0·2 megohms. In fact, as a simple analysis of the circuit shows, the time *t* between two successive discharges is given by the equation $t = ACR$, where A is a constant depending upon the length and nature of the air-gap. Each discharge of this type is bright, and, of course, carries a large current. The latter is oscillatory, being due to the discharge of the condenser, and typical in every way of the engineer's spark. It may be noted that the spectrum of the radiation emitted from such slow flashes is a mixture of copper and air lines, but by far the greater part of the light is due to the band spectrum of nitrogen.

If C is gradually decreased the flashes become more and more frequent, until, when $C = 0·001 \mu F$ and $R = 0·2$ megohms, the circuit emits an audible note of frequency about 200/sec. At the same time the spectrum of the radiation emitted undergoes a change. The copper lines become more prominent relative to the air ; when C is less than $0·001 \mu F$, the discharge is distinctly green in colour, indicating the presence of intense copper radiation.

II. *The Glow Discharge.*—If the condenser capacity is still further reduced, a time comes when the intermittent discharges, each of an oscillatory nature, cease abruptly, and an entirely different *régime* begins. The discharge is now continuous and unidirectional ; it is, indeed, a typical glow. The negative electrode is partly covered by a blue disk— the cathode glow, the area of which appears to vary directly with the current. Immediately beyond this is the Faraday dark space, while beyond that again is the red positive column, occasionally faintly striated and ending in a bright anodic spot. These details can, of course, only be seen under the microscope ; if higher potentials are used in the hope that the glow may be lengthened, convection currents of air in the gap bend the positive column so far upwards that the glow is extinguished.

This glow discharge at atmospheric pressure has been noted and partly investigated on numerous occasions. It has been observed in researches on the arc [4], but it was discovered and has been further analysed during researches on the mechanism of the gaseous discharge [5]. The writer cannot find that it is any way different from the typical low-pressure glow either with regard to its appearance and spectrum or with regard to the ionization phenomena involved. The band spectrum of nitrogen is responsible for almost all the light emitted, but, as the current is increased, the green

copper lines begin to be prominent. If the resistance R is continuously decreased (C being approximately zero), the glow degenerates into the " true arc," and the copper spectrum completely gains the ascendancy.

Thus by varying C and R it is possible, with the simple apparatus described to demonstrate all the phenomena usually entitled " arc," " spark," and " glow." A consideration of the mechanism of each in this simple case is helpful in formulating exact definitions.

Characteristics of the " Spark."—The discharge which usually goes by this name is obviously to be associated with the discharge of a condenser. All sparks, in other words, are capacity effects. Sparks may be obtained at any gas pressure, and indeed all the effects mentioned above in connexion with air at atmospheric pressure are obtainable at pressures as low as a tenth of a millimetre of mercury. It is, however, more difficult to obtain regular sparking of a small condenser at low pressures. This is to be attributed to the greater mobility of the ions. Even in the case of the " uncondensed " discharge of an induction coil, the capacity of the secondary is sufficient to produce the first spark. Indeed, if the resistance in the experiment described is made sufficiently high, the capacity of the gap itself is sufficient to prohibit the formation of the unidirectional glow. There can be no hesitancy, therefore, about associating the discharge commonly called a spark with the discharge of a capacity. Yet, even if the analysis given has succeeded in properly classifying this discharge, it has not made the common nomenclature more palatable. The condenser discharge is a *mixed* one; it contains at least two ionizing factors, which can hardly be associated in a fundamental definition. As has been observed, rapidly recurring " sparks " cause a large rise in temperature of the electrodes, so that metal vapour is liberated, thus introducing an " arc " element into the discharge. Although this is not present to the same extent in slow flashes, the tendency exists, and in condensed induction coil discharges the metal vapour plays an important part. The writer is therefore of the opinion that the terms to denote typical discharges should be redefined in terms of the knowledge we now possess of the processes at work.

Suggestions as to Rationalisation.

It is suggested that the nomenclature of the investigators of the gaseous discharge should be universally adopted. The following definitions would result :—

Spark.—The initial unstable stage in any discharge between cold electrodes.

The spark thus defined is associated with the sparking potential which may be measured, but the spark itself is a condition rather than an observable phenomenon.

Arc.—A discharge in which the current is carried by the metal of the electrodes as well as the gas between them.

This is an observable state. The definition takes no account of special techniques for the production of gaseous arcs by means of externally stimulated thermionic emission.

Glow.—A discharge between cold electrodes, when the current is entirely carried by gaseous ions.

Again this is an observable state so long as the energy given to the gap is controlled by external resistances.

To exemplify the connexions between these discharges, consider the following hypothetical experiment. A direct-current potential difference is applied across an air-gap in parallel with which there is no capacity, and in series with which there is no resistance. What will occur?

As soon as the potential difference is equal to the "static sparking potential" for the given gap, a small capacity discharge will take place. This in its initial stage is a spark, but, owing to the shape of the glow characteristic (fig. 3), it becomes a glow almost immediately. Simultaneously the capacity oscillations die out. The glow is then carrying a current of a few milliamperes. If the electrodes are of such a nature that a high temperature develops at the points where the discharge is occurring (low heat conductivity), and if the boiling-point of the cathode is lower than the temperature reached (which will usually be the case), some of the metal is vaporized. This increases the current, since the ionizing potential of the metal is lower than that of the gas. Hence a higher temperature is developed. The process is cumulative, and in a very short time the discharge takes the form of an arc. Since this amounts to short-circuiting the gap, the current is only limited by the power available.

In general, electric discharges are mixed, containing both of the components, arc and glow. Of this nature is the induction coil discharge, whether condensed or uncondensed. A consideration of the power available in each case explains the types of spectra which are obtained.

References.

(1) E. Taylor Jones, ' The Theory of the Induction Coil," p. 147, fig. 61.
(2) E. Taylor Jones, *op. cit.* p. 150, fig. 64.
(3) Taylor and Sayce, Phil. Mag. 1. p. 918 (1925) ; Penning, *Phys. Zeits.* xxvii. p. 187 (1926); Taylor, Phil. Mag. iii. p. 368, p. 753 (1926).
(4) H. Simon, *Phys. Zeits.* viii. ᴠ 471 (1907) ; Grotrain, *Ann. d. Phys.* xlvii. p. 141 (1915); Stark, *Ann. d. Phys.* xii. p. 692 (1903); Burstyn, *Electrotech. Zeits* p. 503 (1920) ; Chrisler, *Astrophys. J.* liv. p. 273 (1921) ; Slepian, *Frank. Inst. J.* cci. p. 79 (1926).
(5) Toepler, *Wied. Ann.* lxiii. p. 109 (1897), lxvi. p. 671 (1898); Kauffmann, *Ann. d. Phys.* ii. p. 158 (1900); Aubertin, *Le Radium,* ix. p. 186 (1912); Melçion, *Comptes Rendus,* clxxxix. p. 112 (1929).

September 1931.

LXXVII. *Wave Equations of an Electron in a real form.* By D. MEKSYN, *Ph.D., Mathematical Department, Edinburgh University* *.

§1. *Introduction and Summary.*

AS it is known the wave equations of an electron are imaginary expressions ; so are their solutions. It seems as if imaginary quantities are inherent in the wave mechanics.

In the present paper an attempt is made to present the wave equations and their solutions in a real form.

In a recent publication † I have derived Dirac's equations in a five-dimensional invariant form, and these equations, slightly modified for the case of an external electromagnetic field, may be presented in a real five-dimensional form.

It is proved that in the case when Dirac's equations have imaginary periodic solutions of the form $\psi e^{\frac{2\pi i}{h}Wt}$ our equations have a solution of the form

$$\lambda \cos \frac{2\pi}{h}(mcx_5 - Wt) + \mu \sin \frac{2\pi}{h}(mcx_5 - Wt), \quad . \quad (1)$$

where λ and μ are real functions.

Evaluating the energy tensor we obtain the characteristic difference of energies at transitions—namely, we get the following expression :

$$A \cos \frac{2\pi}{h}(W_1 - W_2)t + B \sin \frac{2\pi}{h}(W_1 - W_2)t, \quad . \quad (2)$$

* Communicated by the Author.
† Phil. Mag. [7] ix. p. 568 (1930).

where **A** and **B** are functions of the space variables; the five-dimensional term mcx_5 drops out from the energy tensor.

The real equations solve the difficulty mentioned by Dirac [*], namely, that the same relativity wave equations are valid for particles of opposite charges ; this is due to the imaginary terms in these equations.

As our equations are real, this difficulty does not arise in our case ; the equations and their solutions are different for positive and negative particles.

It seems that the five-dimensional space represents a natural system of reference for the wave equations.

§2. *Equations for Free Motion.*

The equations are derived from the Hamiltonian Principle (Phil. Mag. *ibid.*). The field is described by an anti-symmetric tensor of the second rank in five dimensions. The tensor has ten components, four of which are complex, and two scalar functions are introduced as a result of the variational problem, in all sixteen equations.

The equations, thus obtained, are analogous to Maxwell's, the latter being merely a four-dimensional projection of the former. They are

$$\frac{\partial F_{\alpha\beta}}{\partial x_\beta} + \frac{\partial \mu}{\partial x_\alpha} = 0, \qquad \alpha, \beta = 1, 2, 3, 4, 5 \quad . \quad (3$$

and

$$\left. \begin{array}{r} \dfrac{\partial F_{\alpha\beta}}{\partial x_\gamma} + \dfrac{\partial F_{\beta\gamma}}{\partial x_\alpha} + \dfrac{\partial F_{\gamma\alpha}}{\partial x_\beta} + \dfrac{\partial G_{\delta 5}}{\partial x_5} + \dfrac{\partial \lambda}{\partial x_\delta} = 0, \\[2mm] \dfrac{\partial G_{5i}}{\partial x_i} + \dfrac{\partial \lambda}{\partial x_5} = 0, \end{array} \right\} \quad . \quad (4)$$

$$\alpha, \beta, \gamma, \delta = 1\text{---}4, \qquad i = 1\text{---}5.$$

The expressions (3) and (4) comprise ten equations, and the six remaining are

$$\frac{\partial F_{\alpha\beta}}{\partial x_5} = \frac{\partial F_{\alpha 5}}{\partial x_\beta} - \frac{\partial F_{\beta 5}}{\partial x_\alpha} + \frac{\partial G_{\delta 5}}{\partial x_\gamma} - \frac{\partial G_{\gamma 5}}{\partial x_\delta}, \quad . \quad . \quad (5)$$

$$\alpha, \beta, \gamma, \delta = 1\text{---}4.$$

In order to make these equations real we assume that the following components are purely imaginary :—

$$F_{12}, \quad F_{31}, \quad F_{12}, \quad \mu, \quad F_{15}, \quad F_{25}, \quad F_{35}, \quad G_{45}, \quad x_4 = ict.$$

---

[*] Proc. Roy. Soc. A, cxvii. p. 610 (1928).

If we substitute $iF_{12},\ldots$ in (3), (4), (5) instead of $F_{12}\ldots$ we obtain sixteen real equations. They can, however, be combined into eight real equations. It appears that for our purpose eight functions suffice.

We denote

$$
\left.
\begin{aligned}
&F_{14}+F_{15}=\phi_1, \quad F_{24}+F_{25}=\phi_2,\\
&\qquad F_{34}+F_{35}=\phi_3, \quad \lambda+G_{45}=-\phi_4,\\
&F_{23}-G_{15}=\phi_5, \quad F_{31}-G_{25}=\phi_6,\\
&\qquad F_{12}-G_{35}=\phi_7, \quad \mu+F_{45}=\phi_8,
\end{aligned}
\right\} \quad . \quad (6)
$$

and combining in two's the equations (3), (4), and (5) we easily obtain

$$
\left.
\begin{aligned}
&\left(-\frac{\partial}{c\partial t}+\frac{\partial}{\partial x_5}\right)\phi_1+\frac{\partial\phi_7}{\partial x_2}-\frac{\partial\phi_6}{\partial x_3}+\frac{\partial\phi_8}{\partial x_1}=0,\\
&\left(-\frac{\partial}{c\partial t}+\frac{\partial}{\partial x_5}\right)\phi_2-\frac{\partial\phi_7}{\partial x_1}+\frac{\partial\phi_5}{\partial x_3}+\frac{\partial\phi_8}{\partial x_2}=0,\\
&\left(-\frac{\partial}{c\partial t}+\frac{\partial}{\partial x_5}\right)\phi_3+\frac{\partial\phi_6}{\partial x_1}-\frac{\partial\phi_5}{\partial x_2}+\frac{\partial\phi_8}{\partial x_3}=0,\\
&\left(-\frac{\partial}{c\partial t}+\frac{\partial}{\partial x_5}\right)\phi_4-\frac{\partial\phi_5}{\partial x_1}-\frac{\partial\phi_6}{\partial x_2}-\frac{\partial\phi_7}{\partial x_3}=0,\\
&\left(\frac{\partial}{c\partial t}+\frac{\partial}{\partial x_5}\right)\phi_5+\frac{\partial\phi_3}{\partial x_2}-\frac{\partial\phi_2}{\partial x_3}+\frac{\partial\phi_4}{\partial x_1}=0,\\
&\left(\frac{\partial}{c\partial t}+\frac{\partial}{\partial x_5}\right)\phi_6-\frac{\partial\phi_3}{\partial x_1}+\frac{\partial\phi_1}{\partial x_3}+\frac{\partial\phi_4}{\partial x_2}=0,\\
&\left(\frac{\partial}{c\partial t}+\frac{\partial}{\partial x_5}\right)\phi_7+\frac{\partial\phi_2}{\partial x_1}-\frac{\partial\phi_1}{\partial x_2}+\frac{\partial\phi_4}{\partial x_3}=0,\\
&\left(\frac{\partial}{c\partial t}+\frac{\partial}{\partial x_5}\right)\phi_8-\frac{\partial\phi_1}{\partial x_1}-\frac{\partial\phi_2}{\partial x_2}-\frac{\partial\phi_3}{\partial x_3}=0,
\end{aligned}
\right\} \quad . \quad (7)
$$

These equations can be reduced to Darwin's [*].

§3. *Equations for the Case of an External Electromagnetic Field.*

We now consider the case of an external electromagnetic field. For a free electron the equation of momenta is

$$
\frac{E^2}{c^2}-p_1{}^2-p_2{}^2-p_3{}^2=m^2c^2. \quad \ldots \quad (8)
$$

We assume that $mc=p_5$ is the momentum associated with the fifth dimension.

[*] Proc. Roy. Soc. A, cxviii. p. 658.

The wave function becomes accordingly

$$\psi \sim e^{\frac{2\pi i}{h}(p_1 x_1 + p_2 x_2 + p_3 x_3 + p_5 x_5 - E t)}, \quad \ldots \quad (9)$$

where E is positive.

Suppose now that we have an external electromagnetic field. In that case we know that instead of $\frac{\partial}{c\partial t}$ and $\frac{\partial}{\partial x_r}$ we have to substitute in our equations the expressions

$$\frac{\partial}{c\partial t} - \frac{2\pi i}{h}\frac{e}{c}\mathrm{V} \quad \text{and} \quad \frac{\partial}{\partial x_r} + \frac{2\pi i}{h}\frac{e}{c}\mathrm{A}_r.$$

We substitute, however, instead of $\frac{\partial}{c\partial t}$ and $\frac{\partial}{\partial x_r}$, the following forms (for the case of an electron) :

$$\frac{\partial}{c\partial t} - \frac{e\mathrm{V}}{mc^2}\frac{\partial}{\partial x_5}, \quad \frac{\partial}{\partial x_r} + \frac{e\mathrm{A}_r}{mc^2}\frac{\partial}{\partial x_5}, \quad r = 1, 2, 3 \ldots \quad (10)$$

The equations (7) remain real ; the wave functions enter all terms through their differential coefficients of the first order. We can combine the eight equations (7) into Dirac's four equations. We shall have then to solve them by imaginary quantities.

§4. *The Law of Conservation.*

Multiplying (7) by ϕ_1, ϕ_2... and combining the eight equations we easily find

$$\left.\begin{array}{l} \rho = -\dfrac{1}{c}\left[\dfrac{\phi_1^2 + \phi_2^2 + \ldots \phi_4^2 + \phi_5^2 + \ldots \phi_8^2}{2}\right], \\[2mm] j_1 = [\phi_1\phi_8 - \phi_2\phi_7 + \phi_3\phi_8 - \phi_4\phi_5], \\[2mm] j_2 = [\phi_1\phi_7 - \phi_3\phi_5 + \phi_2\phi_8 - \phi_4\phi_6], \\[2mm] j_3 = [\phi_2\phi_5 - \phi_1\phi_6 + \phi_3\phi_8 - \phi_4\phi_7], \\[2mm] j_5 = \dfrac{e\mathrm{V}}{mc^2}\rho + \dfrac{e}{mc^2}[\mathrm{A}_1 j_1 + \mathrm{A}_2 j_2 + \mathrm{A}_3 j_3] + \mathrm{H}, \end{array}\right\} \quad . \quad (11)$$

where

$$\mathrm{H} = \left[\frac{\phi_1^2 + . + \phi_4^2 - \phi_5^2 - . - \phi_8^2}{2}\right]. \quad . . \quad (12)$$

The law of " conservation " becomes

$$\frac{\partial j_1}{\partial x_1} + \frac{\partial j_2}{\partial x_2} + \frac{\partial j_3}{\partial x_3} + \frac{\partial \rho}{\partial t} + \frac{\partial j_5}{\partial x_5} = 0. \quad . . \quad (13)$$

In order that conservation shall take place it is necessary that the last term in (13) shall vanish, or

$$\frac{\partial j_5}{\partial x_5} = 0,$$

or, what comes to the same thing, that the current densities ρ, j_1, j_2, j_3 shall be independent of x_5.

The fifth component in (11) is rather complicated. For the case of a free electron, if ρ is equal to the energy E, the current is equal to p_1, p_2, p_3 and $j_5 = mc$, where $p_1 \ldots$ are the momenta of a moving electron, and m is the invariant mass ; thus in this case the fifth component has a simple physical interpretation.

§5. *Comparison with Dirac's Equations.*

We find now the connexion between the functions ϕ and Dirac's ψ.

Dirac's equations are

$$\left.\begin{array}{l}(p_0 + mc)\psi_1 + (p_1 - ip_2)\psi_4 + p_3\psi_3 = 0, \\ (p_0 + mc)\psi_2 + (p_1 + ip_2)\psi_3 - p_3\psi_4 = 0, \\ (p_0 - mc)\psi_3 + (p_1 - ip_2)\psi_2 + p_3\psi_1 = 0, \\ (p_0 - mc)\psi_4 + (p_2 + ip_2)\psi \;\; - p_3\psi_2 = 0, \end{array}\right\} \quad . \;\; (14)$$

where

$$p_0 = -\frac{h}{2\pi i c \partial t} \frac{\partial}{} + \frac{e}{c} V ; \quad p_1 = \frac{h}{2\pi i \partial x_1} \frac{\partial}{} + \frac{e}{c} A_1. \quad . \;\; (15)$$

Multiplying the first equation (7) by i, and subtracting from the second, we find that the obtained expression is equivalent to the second equation in (14) (in our expressions $\frac{\partial}{\partial x_5}$ appears instead of mc). Performing similar transformations with the remaining equations (7), and comparing the obtained results with (14), we arrive at the following connexion between the functions ϕ and ψ :—

$$\left.\begin{array}{ll}\psi_1 = \phi_4 - i\phi_3, & \psi_2 = \phi_2 - i\phi_1, \\ \psi_3 = -\phi_7 - i\phi_8, & \psi_4 = -\phi_5 - i\phi_6\end{array}\right\} \quad . \;\; . \;\; (16)$$

§6. *Solution of the Equations.*

We shall now prove that in all cases, when Dirac's equations have imaginary periodic solutions, the real equations have real periodic solutions.

We consider the general case of an external electromagnetic field, and assume that the periodic solutions depend upon time in the following way :—

$$\phi \sim \frac{\sin \alpha}{\cos \alpha}, \qquad \alpha = \frac{2\pi}{h}(mcx_5 - Wt). \quad . \quad . \quad (17)$$

A glance at the equations (7) and (10) shows that in the general case they cannot be satisfied by a simple sine or cosine solution, but must be a combination of both.

We assume accordingly for the ϕ's the following expressions :—

$$
\begin{aligned}
\phi_1 &= -\lambda_2 \sin \alpha - \mu_2 \cos \alpha, & \phi_5 &= -\lambda_4 \cos \alpha + \mu_4 \sin \alpha, \\
\phi_2 &= \lambda_2 \cos \alpha - \mu_2 \sin \alpha, & \phi_6 &= -\lambda_4 \sin \alpha - \mu_4 \cos \alpha, \\
\phi_3 &= -\lambda_1 \sin \alpha - \mu_1 \cos \alpha, & \phi_7 &= -\lambda_3 \cos \alpha + \mu_3 \sin \alpha, \\
\phi_4 &= \lambda_1 \cos \alpha - \mu_1 \sin \alpha, & \phi_8 &= -\lambda_3 \sin \alpha - \mu_3 \cos \alpha,
\end{aligned}
$$

$$. \quad . \quad . \quad (18)$$

Inserting these values of ϕ in (7), and equating to zero separately the cofactors of $\sin \alpha$ and $\cos \alpha$, we obtain sixteen equations for the eight functions λ and μ ; there are, however, only eight different equations, and they can be combined into four, which are found to be Dirac's equations.

Thus we obtain the following connexion between Dirac's functions ψ and the λ and μ :

$$\psi_k = \lambda + i\mu_k, \qquad k = 1-4, \quad . \quad . \quad . \quad (19)$$

or the λ's and μ's are the real and imaginary parts of the ψ's.

§7. *The Energy Tensor.*

We evaluate now the energy tensor, and show that we obtain the characteristic difference of energies at transitions. This is reached in wave mechanics by making use of imaginary quantities.

Let us consider only two terms in the expression ρ in (11), as the other terms give similar results.

For the case of transitions the terms $\phi_1^2 + \phi_2^2$ in ρ become

$$\phi_1 \phi_1^1 + \phi_2 \phi_2^1, \quad . \quad . \quad . \quad . \quad . \quad (20)$$

where ϕ and ϕ^1 belong to different states.

Inserting in (20) the values of the ϕ's from (18) we easily obtain

$$\phi_1\phi_1{}^1 + \phi_2\phi_2{}^1 = (\lambda_2\lambda_2{}^1 + \mu_2\mu_2{}^1)\cos\,(\alpha - \alpha^1)$$
$$+ (\lambda_2\mu_2{}^1 - \mu_2\lambda_2{}^1)\sin\,(\alpha - \alpha^1)$$

$$\alpha^1 = \frac{2\pi}{h}\,(mcx_5 - W^1 t),\quad \ldots\ldots \quad (21)$$

and hence

$$\alpha - \alpha^1 = \frac{2\pi}{h}\,(W^1 - W)t.\quad \ldots\ldots \quad (22)$$

This is the correct expression for the energies of transitions. As we see, the five-dimensional term mcx_5 drops out from the energy tensor.

It can be easily shown that our energy tensor is identical with Dirac's

§8. *The Hydrogen Atom.*

We consider now the case of the hydrogen atom, in order to give an instance of a certain peculiarity inherent in these equations.

It is known that a law of conservation can be derived from the imaginary wave equations, and every solution of these equations satisfies the law of conservation.

Now the position appears to be somewhat different in the case of the real equations. A law of conservation follows also from these equations; it is, however, expressed in a five-dimensional form, which represents a conservation in the usual sense only if the fifth term vanishes.

We have therefore to discard all solutions which do not satisfy the condition

$$\frac{\partial j_5}{\partial x_5} = 0.\quad \ldots\ldots \quad (23)$$

Let us now show the bearing of these considerations upon the solution of the problem of the hydrogen atom.

In that case $A_1 = A_2 = A_3 = 0$, and a glance at the equations (7) shows that they can be satisfied by assuming

$$\left.\begin{array}{l} \phi_1,\ \phi_2,\ \phi_3,\ \phi_4 \sim \sin\dfrac{2\pi}{h}(mcx_5 - Wt), \\[2mm] \phi_5,\ \phi_6,\ \phi_7,\ \phi_8 \sim \cos\dfrac{2\pi}{h}(mcx_5 - Wt). \end{array}\right\}\quad . \quad (24)$$

Now, evaluating the energy tensor for this solution we obtain that

$$j_5 \sim \sin \frac{2\pi}{h} (mcx_5 - W_1 t) \cos \frac{2\pi}{h} (mcx_5 - W_2 t). \quad . \quad (25)$$

Thus the fifth dimension does not drop out ; we do not obtain the difference of energies at transitions.

As in this case, however, $\dfrac{\partial j_5}{\partial x_5} \neq 0$, we have to conclude that the solution (24) does not represent a possible physical state.

Let us now give briefly the correct solution for this case. Dirac's equations have been rigorously solved for the hydrogen atom by Prof. Darwin [*]. We make use of Darwin's results.

The functions ψ's have the following expressions (Darwin's equations 7.4) :—

$$\left. \begin{aligned} \psi_1 &= -i F_k R_{k+1}^u [\cos u\phi + i \sin u\phi], \\ \psi_2 &= -i F_k R_{k+1}^{u+1} [\cos (u+1)\phi + i \sin (u+1)\phi], \\ \psi_3 &= (k+u+1) G_k R_k^u [\cos u\phi + i \sin u\phi], \\ \psi_4 &= (-k+u) G_k R_k^{u+1} [\cos (u+1)\phi + i \sin (u+1)\phi], \end{aligned} \right\} \quad (26)$$

where F_k and G_k are certain functions of r, and

$$R_k^u = (k-u)! \sin^u \theta \left(\frac{d}{d \cdot \cos \theta} \right)^{k+u} \frac{(\cos^2 \theta - 1)^k}{2^k \cdot k!}.$$

From (26) and (19) we obtain the values of λ and μ, and inserting the obtained expressions of λ and μ in (18) we get the required solutions of our equations.

So, for instance,

$$\lambda_1 = F_k R_{k+1}^u \sin u\phi, \qquad \mu_1 = F_k R_{k+1}^u \cos u\phi \; ;$$

hence

$$\phi_3 = F_k R_{k+1}^u \cos \left[u\phi + \frac{2\pi}{h} (mcx_5 - Wt) \right],$$

$$\phi_4 = F_k R_{k+1}^u \sin \left[u\phi + \frac{2\pi}{h} (mcx_5 - Wt) \right].$$

§9. *The Wave Equations for Positive Particles.*

Two difficulties, as Dirac [†] has pointed out, are inherent in the relativity wave equations.

* Proc. Roy. Soc. A, cxviii. p. 658.
† Proc. Roy. Soc. A, cxvii. p. 610.

(a) They have twice as many solutions as appear to be necessary. The solutions can be schematically represented as

$$
\begin{aligned}
&(1)\ \psi e^{-\frac{2\pi i}{h}Wt}, \qquad \overline{\psi} e^{\frac{2\pi i}{h}Wt}, \\
&(2)\ \psi e^{\frac{2\pi i}{h}Wt}, \qquad \overline{\psi} e^{-\frac{2\pi i}{h}Wt},
\end{aligned}
\right\} \quad \cdot\ \cdot\ (27)
$$

where ψ stands for all four functions and $\overline{\psi}$ is the conjugate of ψ.

The second set of solutions is associated with negative kinetic energy.

The appearance of negative energy is inherent in any relativity theory. It appears also in the classical theory, but there the kinetic energy changes continuously, and, as it is initially positive, it cannot become negative.

In the quantum theory discontinuous transitions are possible, and it is therefore not easy to separate these two sets of solutions.

Schrödinger *, however, has recently suggested how to separate the positive and negative solutions.

(b) The relativity imaginary equations have another difficulty; they are valid both for electrons and protons. It can be shown that the conjugates of (14) are equivalent to the same equations where e is changed into $-e$.

Let us elucidate this point by considering the conjugate of the fourth equation (14). It is equal to

$$
\left(-\frac{h}{2\pi i c}\frac{\partial}{\partial t} - \frac{e}{c}V + mc\right)\overline{\psi}_4 + \left[\left(\frac{h}{2\pi i}\frac{\partial}{\partial x} - \frac{e}{c}A_1\right)\right.
$$
$$
\left. -i\left(\frac{h}{2\pi i}\frac{\partial}{\partial y} - \frac{e}{c}A_2\right)\right]\overline{\psi}_1 - \left(\frac{h}{2\pi i}\frac{\partial}{\partial z} - \frac{e}{c}A_3\right)\overline{\psi}_2 = 0. \quad (28)
$$

We now consider the first equation for a positive particle; we have to change e into $-e$, and we obtain

$$
\left(-\frac{h}{2\pi i c}\frac{\partial}{\partial t} - \frac{e}{c}V + mc\right)\psi_1^+ + \left[\left(\frac{h}{2\pi i}\frac{\partial}{\partial x} - \frac{e}{c}A_1\right)\right.
$$
$$
\left. -i\left(\frac{h}{2\pi i}\frac{\partial}{\partial y} - \frac{e}{c}A_2\right)\right]\psi_4^+ + \left(\frac{h}{2\pi i}\frac{\partial}{\partial z} - \frac{e}{c}A_3\right)\psi_3^+ = 0. \quad (29)
$$

Comparing (29) with (28) we find that

$$\psi_1^+,\ \psi_2^+,\ \psi_3^+,\ \psi_4^+$$

are equivalent to

$$\overline{\psi}_4,\ -\overline{\psi}_3,\ -\overline{\psi}_2,\ \overline{\psi}_1,$$

* *Berliner Berichte*, p. 63 (1931).

or the equations for the proton are equivalent to the conjugate equations for an electron.

(*c*) Let us now consider the case of the real equations. Instead of Dirac's four complex functions we have eight real ones, with the corresponding positive and negative solutions :—

$$\phi \sim \frac{\sin}{\cos} \left[\omega + \frac{2\pi}{h} (mcx_5 - Wt), \right] \Bigg\} \qquad . \quad . \quad (30)$$
$$\phi \sim \frac{\sin}{\cos} \left[\omega + \frac{2\pi}{h} (mcx_5 + Wt), \right] \Bigg\}$$

and

$$\phi \sim \frac{\sin}{\cos} \left[\omega - \frac{2\pi}{h} (mcx_5 - Wt), \right] \Bigg\} \qquad . \quad . \quad (31)$$
$$\phi \sim \frac{\sin}{\cos} \left[\omega - \frac{2\pi}{h} (mcx_5 + Wt), \right] \Bigg\}$$

where (30) relates to an electron and (31) to a proton ; ω is a function of the space variables. We see that not only the equations but also the solutions are different for electrons and protons.

Dirac [*] has suggested that the negative solutions of an electron could be associated with a proton.

As we see from (30) and (31) this interpretation of negative solutions cannot be justified in our case because the negative solutions of (30) have a different form from (31).

To pass from (30) to (31) we have to change the sign not of W, but of *m*; this, however, is equivalent in our equations to changing the sign of *e*.

§10. *On the Meaning of the Fifth Dimension.*

It is known that the idea of the fifth dimension was advanced by Kaluza in order to bring about the welding of gravitation and the electromagnetic field ; but this conception appears to be very useful in wave-mechanics ; the latter gives us a definite interpretation of the fifth coordinate.

An easy way of introducing the fifth dimension is to follow the same procedure as in the case of four dimensions.

As it is known the four-dimensional principle of relativity is based upon the law of constancy of velocity of light

---

* Proc. Roy. Soc. A, cxxvi. p. 360 (1930).

propagation. If c is the velocity of light, the transformation of coordinates has to leave invariant the expression

$$\frac{ds}{dt} = c, \quad \ldots \ldots \quad (32)$$

or

$$dx^2 + dy^2 + dz^2 - c^2 dt^2 = 0 ; \quad \ldots \ldots \quad (33)$$

this leads to Lorentz's transformations.

In the case of five dimensions we start from the fundamental equation of the quantum theory,

$$h\nu = E. \quad \ldots \ldots \ldots \quad (34)$$

As de Broglie has pointed out, the transformation of this equation for moving systems does not conform with the usual principle of relativity; this led him to the wave conception of an electron.

Let us give a metrical representation of the equation (34). We have

$$h\nu = \frac{m_0 c^2}{\sqrt{1 - \frac{v^2}{c^2}}} = \frac{m_0 c^2 dt}{\sqrt{dt^2 - \frac{dx^2 + dy^2 + dz^2}{c^2}}}. \quad . \quad (35)$$

Let

$$\frac{m_0 c^2}{h} = \nu_0 = \frac{1}{T_0}, \qquad \nu = \frac{1}{T} ; \quad \ldots \quad (36)$$

we find from (35)

$$c^2 dt^2 - dx^2 - dy^2 - dz^2 - dx_5^2 = 0, \quad \ldots \quad (37)$$

where

$$dx_5 = \frac{cT}{T_0} dt, \quad \ldots \ldots \quad (38)$$
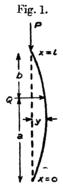
or Planck's frequency condition, applied to an electron in four dimensions, can be considered as a "wave" in a five-dimensional space. From (38) we see that the fifth coordinate describes the periodic phenomenon associated with energy. From (37) we obtain the law of transformation for the fifth coordinate ; it is invariant with respect to Lorentz's transformations.

I wish to express my thanks to Prof. Darwin for invaluable criticism of this paper and for many useful suggestions.

LXXVIII. *The Bending of Columns of Varying Cross-section.*—III. *By* J. A. WILCKEN, *B.Sc., Ph.D., Lecturer in Electrical Engineering at Armstrong College, Newcastle-upon-Tyne* *.

IN previous papers † the theory of tapering columns has been developed, as far as it concerns loads acting in a longitudinal sense, whether in the axis or eccentrically. Two types of columns have been discussed, specified as "straight tapering" or "bulging."

The case of a combined longitudinal and transverse load is important in all structures subject to wind pressure. In a transmission line for electric power any support may be loaded obliquely at times, due to wind effect on conductors and on the mast itself, and where the horizontal trajectory

Fig. 1.

of the line is curved the mast is always subject to a transverse pull.

The following investigation deals with some type of loading that may occur under these circumstances. We consider the transverse load represented by a single force Q, acting at a given point of the column, in addition to the usual axial thrust P.

(A)—*A column simply supported at both ends.* The equations of bending moments are, in the usual notation,

$$\mathrm{EI}\frac{d^2y}{dx^2} + Py + Qbx/l = 0 \text{ for } a > x > 0, \quad . \quad . \quad (63)$$

$$\mathrm{EI}\frac{d^2y}{dx^2} + Py + Qa(1-x/l) = 0 \text{ for } l > x > a, \quad . \quad (64)$$

* Communicated by the Author.
† Phil. Mag. iii. p. 418, *ibid.* p. 1065 (1927).

with the boundary conditions $y|^0 = y|^l = 0$, and subject to the conditions of continuity involving equality of deflexions and curvature at $x = a$

(i.) In case of a straight tapering column, specified by $P/EI = (\alpha + \beta x)^{-4}$, the equations integrate into

$$y = -\frac{Q}{P} bx/l + A(\alpha + \beta x) \sin(\chi_0 - \chi)$$

and

$$y = -\frac{Q}{P} a(1 - x/l) + B(\alpha + \beta x) \sin(\chi - \chi_1) \qquad (65)$$

respectively, where

$$\chi = (\alpha\beta + \beta^2 x)^{-1}, \quad \chi^0 = \chi_0, \quad \text{and} \quad \chi^l = \chi_1.$$

Writing also $\chi|^a = \chi'$, the conditions of continuity lead to

$$A \sin(\chi_0 - \chi') = B \sin(\chi' - \chi_1).$$

$$A \cos(\chi_0 - \chi') + B \cos(\chi' - \chi_1) = \frac{Q}{P}\, \alpha + \beta a);$$

$$\therefore \quad A = \frac{Q}{P}(\alpha + \beta a)\sin(\chi' - \chi_1)$$
$$\operatorname{cosec}(\chi_0 - \chi_1),$$

$$B = \frac{Q}{P}(\alpha + \beta a)\sin(\chi_0 - \chi')$$
$$\operatorname{cosec}(\chi_0 - \chi_1).$$

The quantity $\chi_0 - \chi_1 = l/\alpha(\alpha + \beta l)$, which for an axially loaded column of this type becomes equal to π for the "crippling load," we shall denote by λ, and write

$$\chi_0 - \chi = r\lambda,$$
$$\chi_0 - \chi' = s\lambda.$$

Defining, as before (*l.c.*), the taper-ratio ρ by

$$\alpha + \beta l = \rho\alpha,$$

and putting

$$\alpha + \beta x = \alpha\xi = \alpha\rho x/rl,$$
$$\alpha + \beta a = \alpha\xi' = \alpha\rho a/sl,$$

and substituting in (65), we find, after reduction,

$$y = \frac{Q}{P}(bx/l)\left\{ \frac{\sin(1-s)\lambda \sin r\lambda}{r(1-s)\lambda \sin\lambda} - 1 \right\} \text{ for } a > x > 0,$$

$$y = \frac{Q}{P}a(1 - x/l)\left\{ \frac{\sin s\lambda \sin(1-r)\lambda}{s(1-r)\lambda \sin\lambda} - 1 \right\} \text{ for } l > x > a, \qquad (66)$$

and the bending moments thus become

$$\left. \begin{aligned} \mathrm{M} &= \mathrm{Q}(bx/l)\frac{\sin(1-s)\lambda\sin r\lambda}{r(1-s)\lambda\sin\lambda} \text{ for } a > x > 0, \\ \mathrm{M} &= \mathrm{Q}a(1-x/l)\frac{\sin s\lambda\sin(1-r)\lambda}{s(1-r)\lambda\sin\lambda} \text{ for } l > x > a. \end{aligned} \right\} \quad (67)$$

When the column is uniform, *i.e.*, when $\rho=1$, we have $r=x/l$, $s=a/l$, $\xi=1$, and the bending moments become

$$\mathrm{M} = \mathrm{Q}l\frac{\sin(b\lambda/l)\sin(x\lambda/l)}{\lambda\sin\lambda} \text{ for } a > x > 0,$$

$$\mathrm{M} = \mathrm{Q}l\frac{\sin(a\lambda/l)\sin\{(l-x)\lambda/l\}}{\lambda\sin\lambda} \text{ for } l > x > a,$$

in agreement with the known formulæ.

(ii.) Considering the "bulging" type of column, specified by $\mathrm{P}/\mathrm{EI} = (\alpha+\beta x)^{-2}$, the solution to the fundamental equations (63) and (64) are written

$$y = -\frac{\mathrm{P}}{\mathrm{Q}}(bx/l)+\mathrm{A}(\alpha+\beta x)^{1/2}\sin(\chi_0-\chi),$$

and

$$y = -\frac{\mathrm{Q}}{\mathrm{P}}a(1-x/l)+\mathrm{B}(\alpha+\beta x)^{1/2}\sin(\chi-\chi_1),$$

respectively, where

$$\chi = \mu\log(\alpha+\beta x), \quad \mu=\sqrt{\beta^{-i}-\tfrac{1}{4}}.$$

Writing now

$$\chi_0-\chi_1 = -\mu\log\rho = \lambda,$$

where λ has the same meaning as above, and using the same notation as under (i.), we find, after reduction,

$$\left. \begin{aligned} y &= \frac{\mathrm{Q}}{\mathrm{P}}\{\alpha\sqrt{\xi\xi'}\sin(1-s)\lambda\sin r\lambda\cosec\lambda-bx/l\} \\ &\qquad\qquad\qquad\qquad\qquad\qquad \text{for } a > x > 0, \\ y &= \frac{\mathrm{Q}}{\mathrm{P}}\{\alpha\sqrt{\xi\xi'}\sin s\lambda\sin(1-r)\lambda\cosec\lambda-a(1-x/l)\} \\ &\qquad\qquad\qquad\qquad\qquad\qquad \text{for } l > x > a, \end{aligned} \right\}$$

$$\cdots \quad (68)$$

and so the bending moments become

$$\left. \begin{aligned} \mathrm{M} &= \mathrm{Q}\alpha\sqrt{\xi\xi'}\sin(1-s)\lambda\sin r\lambda\cosec\lambda \text{ for } a > x > 0, \\ \mathrm{M} &= \mathrm{Q}\alpha\sqrt{\xi\xi'}\sin s\lambda\sin(1-r)\lambda\cosec\lambda \text{ for } l > x > a. \end{aligned} \right\}$$

$$\cdots \quad (69)$$

The uniform column is to be considered a special case also of this type, as a simple calculation will show.

If the longitudinal thrust P does not act in direction of the axis, but at a distance f from it, there will be an additional deflexion as found above (*l. c.* p. 1066), namely,

$$y' = f \left\{ 1 - \xi \left(\cos r\lambda + \frac{1/\rho - \cos\lambda}{\sin\lambda} \sin r\lambda \right) \right\}$$

for the straight tapering column, and

$$y' = f \left\{ 1 - \sqrt{\bar{\xi}} \left(\cos r\lambda + \frac{\sqrt{1/\rho} - \cos\lambda}{\sin\lambda} \sin r\lambda \right) \right\}$$

for type (ii.); and, correspondingly, additional bending moments, due to the eccentricity of the load. The fact that these values are additively superposed on those due to the load Q is inherent in the linear character of the fundamental differential equations. An easy calculation based on the complete equations will bear out this statement.

As would be expected, the transverse load Q always causes a definite deflexion and a finite bending moment whether P is axial or not, and this bending moment is directly proportional to Q and depends in a more intricate manner on P through the quantity denoted λ, which may be written $\pi \sqrt{P/P_E}$, P_E being the Eulerian crippling load on an axially loaded column. If Q becomes vanishingly small, the bending moment decreases indefinitely unless at the same time $\lambda \to \pi$, *i.e.*, unless P approaches the crippling value.

(B)—*A column built in at one end and free at the other end.* The bending moments in the two portions of the column are given by the equations

$$\text{EI} \frac{d^2y}{dx^2} + \text{P}(y-h) + \text{Q}(x-a) = 0 \text{ for } a > x > 0, \left.\rule{0pt}{30pt}\right\} \quad .(70)$$
$$\text{EI} \frac{d^2y}{dx^2} + \text{P}(y-h) = 0 \text{ for } l > x > a,$$

with the boundary conditions $y^0 = 0 = \dfrac{dy}{dx}\Big|^0$, $y|^l = h$, and the conditions of continuity of deflexion and curvature at $x = a$.

(i.) If the column is of the type $(\alpha + \beta x)^{-4} = \text{P/EI}$, the solutions to the above equations are written

$$y = h + \frac{\text{Q}}{\text{P}}(a-x) + (\alpha + \beta x)(\text{A}_1 \cos\chi + \text{A}_2 \sin\chi)$$

and $\quad y = h + (\alpha + \beta x)(\text{B}_1 \cos\chi + \text{B}_2 \sin\chi)$ respectively.

The boundary conditions are equivalent to
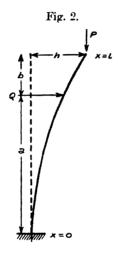
$$A_1 \cos \chi_0 + A_2 \sin \chi_0 = -\frac{1}{\alpha}(h + a\mathrm{Q}/\mathrm{P}),$$

$$A_1(\beta \cos \chi_0 + \frac{1}{\alpha}\sin \chi_0) + A_2(\beta \sin \chi_0 - \frac{1}{\alpha}\cos \chi_0) = \mathrm{Q}/\mathrm{P},$$

leading to

$$A_1 = -\frac{1}{\alpha}(h + a\mathrm{Q}/\mathrm{P})\cos \chi_0 + \{\beta h + (\alpha + \beta a)\mathrm{Q}/\mathrm{P}\}\sin \chi_0,$$

$$A_2 = -\frac{1}{\alpha}(h + a\mathrm{Q}/\mathrm{P})\sin \chi_0 - \{\beta h + (\alpha + \beta a)\mathrm{Q}/\mathrm{P}\}\cos \chi_0.$$

Fig. 2.

Substituting these values for the integration constants, we find, for the deflexion below Q,

$$y = h + (a - x)\mathrm{Q}/\mathrm{P} + (\alpha + \beta x)\left\{ -\frac{1}{\alpha}(h + a\mathrm{Q}/\mathrm{P})\cos(\chi_0 - \chi) \right.$$
$$\left. + [\beta h + (\alpha + \beta a)\mathrm{Q}/\mathrm{P}]\sin(\chi_0 - \chi) \right\}$$

and introducing the notation as defined above, and re-arranging,

$$y = h\left\{ 1 - \xi\left(\frac{1/\rho - 1}{\lambda}\sin r\lambda + \cos r\lambda\right)\right\}$$
$$+ \frac{\mathrm{Q}}{\mathrm{P}}\left\{ a - x + a\xi\left(\frac{1}{s\lambda}\sin r\lambda - \cos r\lambda\right)\right\} \quad \text{for } a > x > 0. \quad (71)$$

To determine the constants B_1 and B_2 we have the conditions

$$B_1 \cos\chi_1 + B_2 \sin\chi_1 = 0 \text{ for } x = l,$$

and

$$\left.\begin{array}{l}(A_1 - B_1)\cos\chi' + (A_2 - B_2)\sin\chi' = 0, \\ (A_1 - B_1)\sin\chi' - (A_2 - B_2)\cos\chi' = (\alpha + \beta a)Q/P,\end{array}\right\} \text{ at } x = a.$$

These give

$$B_1 = A_1 - (\alpha + \beta a)\frac{Q}{P}\sin\chi',$$

$$B_2 = A_2 + (\alpha + \beta a)\frac{Q}{P}\cos\chi',$$

whence the deflexion above Q becomes

$$y = h\left\{1 - \xi\left(\frac{1/\rho - 1}{\lambda}\sin r\lambda + \cos r\lambda\right)\right\}$$
$$+ a\xi\frac{Q}{P}\left\{\frac{1}{s\lambda}\left[\sin r\lambda - \sin(r-s)\lambda\right] - \cos r\lambda\right\} \text{ for } l > x > a.$$
$$\qquad \dots \quad (72)$$

The bending moments now are

$$M_1 = Ph\xi\left(\cos r\lambda + \frac{1/\rho - 1}{\lambda}\sin r\lambda\right) + Qa\xi\left(\cos r\lambda - \frac{1}{s\lambda}\sin r\lambda\right)$$
$$\text{for } a > x > 0,$$

and

$$M_2 = M_1 - Q\frac{a\xi}{s\lambda}\sin(r-s)\lambda \text{ for } l > x > a.$$
$$\qquad \dots \quad (73)$$

The deflexion at the top is obtained putting $\xi = \rho$ and $r = 1$ in the expression for $y |^{l > x > a}$,

$$y|^l = h = h\left\{1 - \rho\left(\frac{1/\rho - 1}{\lambda}\sin\lambda + \cos\lambda\right)\right\}$$
$$+ a\rho\frac{Q}{P}\left\{\frac{1}{s\lambda}(\sin\lambda - \sin\overline{1-s}\lambda) - \cos\lambda\right\}$$

leading to

$$h = a\frac{Q}{P}\frac{\frac{1}{s\lambda}\{\sin\lambda - \sin(1-s)\lambda\} - \cos\lambda}{\frac{1/\rho - 1}{\lambda}\sin\lambda + \cos\lambda}. \quad . \quad (74)$$

If the transverse load Q act at the top $a = l$ and $s = 1$, and we have

$$h = l\frac{Q}{P}\frac{1 - \lambda\cot\lambda}{1/\rho - 1 + \lambda\cot\lambda}. \quad \dots \quad (75)$$

These expressions become infinite for $\lambda \cot \lambda = 1 - 1/\rho$ unless at the same time Q becomes infinitely small. The meaning of this is that when the vertical load P approaches a certain value, such that $\lambda \cot \lambda \rightarrow 1 - 1/\rho$, an infinitely small transverse force is sufficient to cause deflexion. The limiting value of the vertical load is seen to agree with the "crippling load" previously defined (*l. c.* p. 424).

(ii.) For a column of the bulging type, as specified by $P/EI = (\alpha + \beta x)^{-2}$, the solutions to the equation (70) are written

$$y = h + (a - x)Q/P + \sqrt{\alpha + \beta x}(A_1 \cos \chi + A_2 \sin \chi)$$

and

$$y = h + \sqrt{\alpha + \beta x}(B_1 \cos \chi + B_2 \sin \chi)$$

respectively, with

$$\chi = \mu \log(\alpha + \beta x).$$

The conditions at $x = 0$ and $x = l$ lead to

$$A_1 \cos \chi_0 + A_2 \sin \chi_0 = -\frac{1}{\sqrt{\alpha}}(h + aQ/P),$$

$$A_1 \sin \chi_0 - A_2 \cos \chi_0 = -h/2\mu\sqrt{\alpha} - (Q/2\mu P)(2\sqrt{\alpha}/\beta + a/\sqrt{\alpha}),$$

from which we find

$$A_1 = -\frac{h}{\sqrt{\alpha}}\left(\cos \chi_0 + \frac{1}{2\mu} \sin \chi_0\right)$$

$$-\frac{Q}{P}\left\{\frac{a}{\sqrt{\alpha}}\left(\cos \chi_0 + \frac{1}{2\mu} \sin \chi_0\right) + \frac{\sqrt{\alpha}}{\mu\beta} \sin \chi_0\right\},$$

$$A_2 = -\frac{h}{\sqrt{\alpha}}\left(\sin \chi_0 - \frac{1}{2\mu} \cos \chi_0\right)$$

$$-\frac{Q}{P}\left\{\frac{a}{\sqrt{\alpha}}\left(\sin \chi_0 - \frac{1}{2\mu} \cos \chi_0\right) - \frac{\sqrt{\alpha}}{\mu\beta} \cos \chi_0\right\}.$$

Substituting above, we find for the deflexion below Q

$$y = h\left\{1 - \sqrt{\xi}\left(\cos r\lambda + \frac{1}{2\mu} \sin r\lambda\right)\right\}$$

$$+ \frac{Q}{P}\left\{a - x - \sqrt{\xi}\left[a\left(\cos r\lambda + \frac{1}{2\mu} \sin r\lambda\right)\right.\right.$$

$$\left.\left.+ \frac{l}{\mu(\rho - 1)} \sin r\lambda\right]\right\} \quad . \quad . \quad (76)$$

To determine the constants B_1 and B_2 we have

$$B_1 \cos \chi_1 + B_2 \sin \chi_1 = 0,$$

and the continuity conditions

$$(A_1 - B_1) \cos \chi' + (A_2 - B_2) \sin \chi' = 0,$$

$$(A_1 - B_1) \sin \chi' - (A_2 - B_2) \cos \chi' = \frac{Q}{P} \cdot \frac{\sqrt{\alpha + \beta a}}{\mu \beta},$$

and from these we find

$$B_1 = A_1 - \frac{Q}{P} \frac{\sqrt{\alpha + \beta a}}{\mu \beta} \sin \chi',$$

$$B_2 = A_2 + \frac{Q}{P} \frac{\sqrt{\alpha + \beta a}}{\mu \beta} \cos \chi'.$$

The deflexion above Q is thus expressed by

$$y = h \left\{ 1 - \sqrt{\xi} \left(\cos r\lambda + \frac{1}{2\mu} \sin r\lambda \right) \right\}$$

$$+ \frac{Q}{P} \sqrt{\xi} \left\{ \frac{l}{\mu(1-\rho)} (\sin r\lambda + \sqrt{\xi'} \sin (r-s)\lambda) \right.$$

$$\left. - a \left(\cos r\lambda + \frac{1}{2\mu} \sin r\lambda \right) \right\}. \quad (77)$$

The bending moments for the two portions of the column become

$$M_1 = Ph \sqrt{\xi} \left(\cos r\lambda + \frac{1}{2\mu} \sin r\lambda \right)$$

$$+ Q \sqrt{\xi} \left\{ a \left(\cos r\lambda + \frac{1}{2\mu} \sin r\lambda \right) - \frac{l}{\mu(1-\rho)} \sin r\lambda \right\}$$

$$\text{for } a > x > l, \quad \ldots \quad (78)$$

and $M_2 = M_1 - Q \sqrt{\xi} \frac{l\sqrt{\xi'}}{\mu(1-\rho)} \sin (r-s)\lambda$ for $l > x > a$.

The deflexion at the top is found as before,

$$h = \frac{Q}{P} \cdot \left\{ \frac{2l}{1-\rho} \cdot \frac{\sin \lambda + \sqrt{\xi'} \sin (1-s)\lambda}{\sin \lambda + 2\mu \cos \lambda} - a \right\}, \quad (79)$$

and if Q acts at the top this becomes

$$h = \frac{Q}{P} l \left\{ \frac{2}{(1-\rho)(1+2\mu \cot \lambda)} - 1 \right\}. \quad \ldots \quad (80)$$
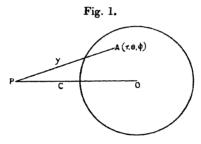
The two expressions for h show, as above, that if P approaches the crippling value, defined by $\cot \lambda \to -1/2\mu$ or $(\mu \log \rho) \cot (\mu \log \rho) \to \frac{1}{2} \log \rho$, an infinitely small transverse force will cause a finite bending moment.

LXXIX. *The Cohesive Force between Solid Surfaces and the Surface Energy of Solids.* *By* R. S. BRADLEY, *M.A.**

THE cohesion between quartz fibres and between equal glass spheres has been described by Tomlinson [1]. The cohesive force was measured by the bending of the fibres. In this paper an improved method is described for measuring the cohesive force between unequal spheres in geometrical contact, as it is difficult to get spheres exactly equal in radii, and the bearing of the measurements on the surface energy of solids is discussed.

1. *Theoretical.*— *The Cohesive Force between Two Spheres.*

The cohesive force between two spheres may be found on the assumption that two molecules of the solid, whose centres are a distance x apart, attract one another with a force

Fig. 1.

$\dfrac{\lambda}{x^n}$, where n is an integer. London and Eisenschitz [2] and Slater [3] have shown by wave mechanics that the predominant term in the attraction between molecules depends on the inverse seventh power of the distance at sufficient distances. London points out that, although this force is electrical in origin the attraction between two molecules is independent of the presence of a third, as with the gravitational force. This is exactly the type of force considered below. In particular surface molecules will attract with the same law as those in the interior.

The force between two spheres may be calculated rigorously as follows:—As a preliminary the potential of a single molecule, P in fig. 1, due to a solid sphere of centre O, will first be considered. The coordinates of any point A on the surface are r, θ, ϕ.

* Communicated by the Author.

Let there be q attracting molecules per unit volume of the solid sphere. The potential of a molecule at P due to a polar element of volume $r^2 \sin\theta . d\theta . d\phi . dr$ at A will be

$$- \frac{q\lambda r^2 \sin\theta \, d\theta \, d\phi \, dr}{(n-1).y^{n-1}},$$

where $PA = y$. Hence the potential at P due to a spherical shell is

$$- \frac{r^2 q\lambda \, dr}{(n-1)} \iint \frac{\sin\theta \, d\theta \, d\phi}{y^{n-1}}.$$

Since $y^2 = c^2 + r^2 - 2cr \cos\theta$, where $PO = c$, this becomes

$$- \frac{2\pi r q\lambda \, dr}{c(n-1)} \int_{c-r}^{c+r} \frac{dy}{y^{n-2}} = \frac{2\pi q\lambda \, dr}{c(n-1)(n-3)} \left[\frac{r}{(c+r)^{n-3}} - \frac{r}{(c-r)^{n-3}} \right].$$

On integrating with respect to r between the limits r and 0 we get the potential at P due to a solid sphere. This is

$$\frac{2\pi q\lambda}{c(n-1)(n-3)} \left[\frac{-1}{(n-5)(c+r)^{n-5}} + \frac{c}{(n-4)(c+r)^{n-4}} \right.$$
$$\left. + \frac{1}{(n-5)(c-r)^{n-5}} - \frac{c}{(n-4)(c-r)^{n-4}} \right].$$

Fig. 2.

We now consider the mutual potential of two solid spheres. In fig. 2 the potential of a molecule at P due to a solid sphere of centre O, radius r_1, is obtained from the last expression by putting $r = r_1$, $c = y_1$. Hence, as before, the mutual potential of a polar element of volume $r_2^2 \sin\theta \, d\theta \, d\phi \, dr_2$ at P and the sphere 1 is

$$\frac{2\pi q^2 \lambda r_2^2}{(n-1)(n-3)} \sin\theta \, d\theta \, d\phi \, dr_2 \left[- \frac{1}{(n-5)y_1(y_1+r_1)^{n-5}} \right.$$
$$+ \frac{1}{(n-4)(y_1+r_1)^{n-4}} + \frac{1}{(n-5)y_1(y_1-r_1)^{n-5}}$$
$$\left. - \frac{1}{(n-4)(y_1-r_1)^{n-4}} \right], \quad \cdots \cdots \quad (1)$$

where r_2 is the radius of the second sphere.

Since $y_1^2 = c_1^2 + r_2^2 - 2c_1 r_2 \cos \theta$, where $c_1 = O\,O'$, the mutual potential of a spherical shell of radius r_2 and the solid sphere 1, is

$$\frac{4\pi^2 q^2 \lambda r_2 dr_2}{(n-1)(n-3)c_1} \int_{c_1-r_2}^{c_1+r_2} y_1 . X . dy, \quad . \quad . \quad . \quad (2)$$

where X is the expression in square brackets in (1). The integral in (2) is easily evaluated to be

$$\frac{1}{(n-4)(n-5)} \left[\frac{1}{(n-6)(y_1+r_1)^{n-6}} + \frac{r_1}{(y_1+r_1)^{n-5}} \right.$$
$$\left. - \frac{1}{(n-6)(y_1-r_1)^{n-6}} + \frac{r_1}{(y_1-r_1)^{n-5}} \right]_{c_1-r_2}^{c_1+r_2} .$$

To obtain the mutual potential of the two solid spheres (2) is now integrated with r_2 as variable, between the limits r_2 and 0. This gives the result

$$\frac{4\pi^2 q^2 \lambda}{(n-1)(n-3)(n-4)(n-5)} \frac{Y}{c_1},$$

where Y is equal to

$$- \frac{1}{(n-6)(n-8)(c_1+r_1+r_2)^{n-8}} + \frac{(c_1+r_1)}{(n-6)(n-7)(c_1+r_1+r_2)^{n-7}}$$

$$+ \frac{1}{(n-6)(n-8)(c_1-r_1+r_2)^{n-8}} - \frac{(c_1-r_1)}{(n-6)(n-7)(c_1-r_1+r_2)^{n-7}}$$

$$- \frac{r_1}{(n-7)(c_1+r_1+r_2)^{n-7}} + \frac{r_1(c_1+r_1)}{(n-6)(c_1+r_1+r_2)^{n-6}}$$

$$- \frac{r_1}{(n-7)(c_1-r_1+r_2)^{n-7}} + \frac{r_1(c_1-r_1)}{(n-6)(c_1-r_1-r_2)^{n-6}}$$

$$- \frac{(c_1+r_1)}{(n-6)(n-7)(c_1+r_1-r_2)^{n-7}} + \frac{1}{(n-6)(n-8)(c_1+r_1-r_2)^{n-8}}$$

$$+ \frac{(c_1-r_1)}{(n-6)(n-7)(c_1-r_1-r_2)^{n-7}} - \frac{1}{(n-6)(n-8)(c_1-r_1-r_2)^{n-8}}$$

$$- \frac{r_1(c_1+r_1)}{(n-6)(c_1+r_1-r_1)^{n-6}} + \frac{r_1}{(n-7)(c_1+r_1-r_2)^{n-7}}$$

$$- \frac{r_1(c_1-r_1)}{(n-6)(c_1-r_1-r_2)^{n-6}} + \frac{r_1}{(n-7)(c_1-r_1-r_2)^{n-7}} \quad . \quad . \quad (3)$$

This is now differentiated with respect to c_1, and c_1 is put equal to r_1+r_2+d, where d is the nearest distance between

the centres of surface molecules of the spheres. Since the spheres are touching in the experiment, d is the molecular diameter; hence d may be neglected compared with c_1, r_1, or r_2. Therefore only those terms need be included which have $c_1 - r_1 - r_2$, i. e., d, in the denominator. Other terms are retained in (3) in order to show that the potential can be expressed in a finite form even if this condition is not complied with, and in order to avoid leaving out terms at an early stage in the calculation.

The force between the two spheres, when d is very small compared with r_1, r_2, and c_1, is therefore

$$\frac{4\pi^2 q^2 \lambda}{(n-1)(n-3)(n-4)(n-5)} Z,$$

where Z is given by

$$-\frac{1}{(n-6)} \frac{c_1 - r_1}{c_1 d^{n-6}} + \frac{r_1}{(n-6)(n-7) c_1^2 d^{n-7}} + \frac{1}{(n-6) c_1 d^{n-7}}$$

$$+ \frac{1}{(n-6)(n-8) c^2 d^{n-8}} + \frac{r_1(c_1 - r_1)}{c_1 d^{n-5}} - \frac{r_1^2}{(n-6) c_1^2 d^{n-6}}$$

$$- \frac{r_1}{c_1 d^{n-6}} - \frac{r_1}{(n-7) c_1^2 d^{n-7}}.$$

Here again only the fifth term is of any importance, as other terms are only approximately d^2, d^2, d^3 as large. Hence the attraction is

$$\frac{4\pi^2 q^2 \lambda}{(n-1)(n-3)(n-4)(n-5)} \frac{r_1 r_2}{r_1 + r_2} \frac{1}{d^{n-5}}. \quad \cdot \quad \cdot \quad (4)$$

The result (3) holds only when $n > 8$. As an inverse seventh power is likely from quantum mechanics, it is interesting to see what result is obtained in this case. Terms containing indices of the power $n - 6$ in Y remain the same, and, in addition, one must add

$$-(c_1 + r_1) \log \frac{c_1 + r_1 + r_2}{c + r_1} + (c_1 - r_1) \log \frac{c_1 + r_2 - r_1}{c_1 - r_1}$$

$$+ (c_1 + r_1) \log \frac{c_1 + r_1 - r_2}{c_1 + r_1} - (c_1 - r_1) \log \frac{c_1 - r_1 - r_2}{c_1 - r_1}.$$

On differentiating $\dfrac{Y}{c_1}$ as before with respect to c_1, the result (4) is again obtained, if c_1, r_1, r_2 are of the order 10^{-1} cm. and d is of the order 10^{-8} cm. The same result (4) is obtained if n is 8.

Expression 4 is symmetrical, as it should be in r_1 and r_2, and has the correct dimensions, since $\dfrac{\lambda}{d}$ is a force.

2. *The Surface Energy of the Solid.*

The measurement of the cohesive force between smooth surfaces provides a new method for finding the surface energy of solids. On the assumption already made for the law of force the total surface energy is [4]

$$\frac{\pi q^2 \lambda}{(n-1)(n-3)(n-4)(n-5)} \frac{1}{d^{n-5}}.$$

Let the diameters of the two spheres be d_1 and d_2. Then the cohesive force between them may be written in the form $A \dfrac{d_1 d_2}{d_1 + d_2}$, where A is a constant independent of the dimensions of the spheres in the region of dimensions considered. Then on the above analysis the surface energy of the solid is

$$\frac{A}{2\pi}.$$

This relation holds, moreover, if a repulsive term is included in the intermolecular force, which will then be of the form

$$\frac{\lambda}{x^n} \quad \frac{\mu}{x^m}$$
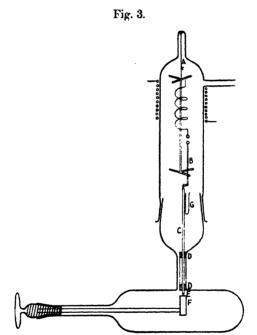
(probably more nearly representing the actual force). It thus appears that the total surface energy may be calculated without having to use accurately plane surfaces in order to measure the cohesion ; but owing to the assumptions involved the result can be regarded only as a first approximation. In view, however, of the small amount of experimental work on the surface energy of solids the author feels that the method is of interest. Previous calculations of the surface energy have involved solubility measurements. Antonoff's [5] method, which assumes that the surface tension of a solid equals that of a liquid which neither rises nor falls in a capillary tube of the solid has been criticized by Adam [6], who points out that what is measured is the work of adhesion of the liquid to the solid.

3. *The Apparatus.*

The essential part of the apparatus is shown in fig. 3. One of the spheres is supported by a quartz spiral spring, which is attached to a quartz frame hanging on a hook A. On sliding a glass tube constricted at one point round the spiral spring the base of the frame rests against the constriction, and the spring may be removed. The other sphere is

attached to the rod B, which is waxed, with vacuum wax, into the brass rod C.   C slides accurately through two guides D, D, fixed into a brass tube which is waxed to the surrounding glass tube on one side.   In this way a gap is left whereby the lower part of the apparatus may be evacuated. On the end of C is fixed a small wheel, which runs on the wheel of the cam F.   F is carried by a brass tube waxed to a stopper (made from a ground joint).   G is a tube carrying a small amount of radioactive deposit to discharge any electrification.   A heating coil may be slid over the two spheres. Apiezon grease was used.

Fig. 3.
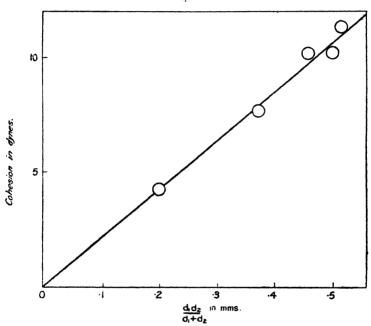
When a determination of the cohesive force is to be made the stopper is rotated slowly, so that the two spheres come into contact.   On rotating the stopper slowly in the reverse direction the upper sphere is pulled down until separation occurs.   The distance between two horizontal tangent planes to the spheres is read on the microscope, and gives a measure of the cohesive force between the two spheres in geometrical contact.   When the spheres are allowed to come together a slight flattening occurs at the region of contact, and on pulling the spheres apart by a force acting along their

line of centres this flattening will decrease until geometrical contact is reached just before separation.

The spring was calibrated by means of weights made from platinum wire.

4. *Results with Quartz Spheres.*

The upper quartz sphere was fused to the spiral spring, the lower to the quartz B. The spheres had thin necks, and

Fig. 4.

were then nearly spherical at the portions which came into contact. The spheres were heated to incandescence in an oxy-gas blow-pipe, the apparatus was assembled, and the cohesion measured. A large number of settings were made and the mean taken. A repetition of this procedure gave the same result to within a few per cent. The temperature was about 15° C.

The results are embodied in fig. 4, which gives the plot of the product of the diameter of the spheres divided by their sum against the cohesive force. A straight line is obtained, which, in agreement with theory, goes through the origin.

The apparatus was evacuated, with the heater on, by means of a mercury-vapour diffusion-pump. The same result was obtained to within the accuracy of the method.

From the straight line the constant A of section 2 is found to be 212. This corresponds to a surface energy of 33·8 ergs per sq. cm. It is unlikely that a surface film of water would withstand the baking-out adopted, so that the cohesive force is probably a true property of the surface. The fact that the same result was obtained in air as in a vacuum may be due to the squeezing out of adsorbed air molecules from quartz molecules which come nearly into contact, or the gas film may not be removed by baking-out. Consider two surface molecules, one on the surface of each sphere, and the line joining their centres parallel to the line of centres of the two quartz spheres. If the shortest distance between the surface of these surface molecules is Δ, then their centres lie on circles of radius $\left(\frac{d_1 d_2 \Delta}{d_1 + d_2}\right)^{\frac{1}{2}}$. If Δ corresponds to twice the diameter of an adsorbed molecule, say 5 Å.U., and $\frac{d_1 d_2}{d_1 + d_2}$ is ·5 × 10⁻¹ cm., this radius is 5 × 10⁻⁵ cm., so that only a small fraction of the surface of the quartz spheres need be desorbed of air molecules.

It is unlikely that the forces measured are due to electrification of the quartz. One would not expect the value of the force between the two spheres to be reproduced after heating the spheres again in the blow-pipe if the results were due to electrification; neither would one expect the force to remain constant with time in the presence of the discharging radioactive deposit. Before starting the work the author repeated Tomlinson's experiment with two fibres carrying quartz spheres. The fibres were drawn out from a quartz rod, which was waxed to a thick-walled glass capillary. The two glass capillaries were inserted through a rubber bung in a bottle, on the bottom of which was a cup containing a little radioactive salt. The glass tubes were bent towards one another until the quartz spheres touched. On bending the tubes away from one another the spheres remained in contact until the fibres had been bent to a certain amount, which did not appear to change for weeks.

The quartz spheres have cooled from the liquid by becoming increasingly more viscous. As there is presumably no violent discontinuity in this process, the surface of the quartz glass would be expected to be sufficiently smooth. The mean of a large number of determinations was taken in
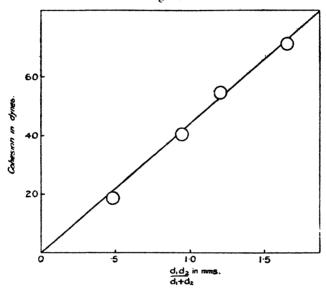
each case, so that neighbouring points could come into contact, and these means differed, as already stated, by only a few per cent.

5. *Results with Borate Spheres.*

The method is limited to glassy solids, as crystallization is bound to develop large cracks. Glass was considered unsuitable because of its uncertain composition ; sodium pyroborate, $Na_2B_4O_7$, was therefore tried. The tip of a platinum wire was fused to a small sphere in an oxy-gas

Fig. 5.

flame, and was dipped repeatedly into molten borax, which had been fused until free from bubbles. The blob of borax was manipulated in a small flame to form a sphere attached by a short thin neck to the platinum sphere. The borax did not then crack on cooling. One sphere was hung from a hook on the spiral spring, the platinum wire attached to the other was sealed into the rod B, now of glass.

Results for freshly fused spheres are shown in fig. 5. Here also a straight line is obtained, passing as it should through the origin. The constant A has the value 434, corresponding to a surface energy of 69 ergs per sq. cm. In this case the cohesion sinks in a vacuum to about a third. Very probably, therefore, a water film is responsible for the

cohesion in air, and the removal of this film probably leaves the surface in a rough condition, as one would expect the surface energy of a salt such as pyroborate to be greater than that of quartz. In accordance with this, while dry air had no effect, the cohesion rose on admitting water vapour to the spheres in a vacuum, but no reproducible result could be obtained.

My thanks are due to Mr. Tomlinson and to Professor Lennard-Jones for reading the manuscript in one stage of its preparation.

Summary.

An expression is obtained for the cohesive force between two unequal spheres in geometrical contact. From the constant in this expression the surface energy of the solid may be computed. Results are obtained in agreement with the theory. The surface energies of freshly fused surfaces of quartz and sodium pyroborate are 33·8 and 69 ergs per sq. cm. In the case of borate spheres, however, the cohesion is probably due to a surface film of water.

References.

(1) Tomlinson, Phil. Mag. vi. p. 695 (1928); x. p. 541 (1930).
(2) London and Eisenschitz, *Zeit. f. Physik.* lxx. p. 491 (1930); Loudon, *Zeit. f. Phys. Chem.* B, xi. p. 223 (1930).
(3) Slater, Phys. Rev. xxxvii. p. 682 (1931).
(4) Bradley, Phil. Mag. xi. p. 846 (1931).
(5) Antonoff. Phil. Mag. vii. p. 1258 (1926).
(6) Adam, Phil. Mag. vii. p. 863 (1927).

Department of Inorganic Chemistry,
  The University, Leeds.
    September 1931.

LXXX. *The Vibrations of Revolving Shafts.*
  By DAVID ROBERTSON, *D.Sc., M.I.E.E.*[*]

IN the Phil. Mag. for August 1931 (Suppl.), on pp. 297–311, there appears a paper by Dr. R. C. J. Howland bearing the above title.

The first portion of this paper is based on the inaccurate statements that the assumption of negligible gyrostatic effects gives "equations which are the same relative to axes rotating with the shaft as they would be with respect to fixed axes, except that a field of centrifugal force must be introduced.

[*] Communicated by the Author.

It also leads to the result that the motions in any two mutually perpendicular planes through the axis, and revolving with it, are sensibly independent."

These statements take no account of the Coriolis acceleration in the y-direction which is necessary to change the direction of the x-velocity as the axes of reference rotate, and to keep the point moving tangentially at the same rate as the reference plane as the distance from the centre of rotation alters because of the x-velocity ; and of the similar acceleration in the x-direction because of the y-velocity.

Let the coordinates of the moving point, referred to axes rotating at ω, be x, y ; and to fixed axes which coincide with the rotating axes at zero time be x', y'. Then, if the rotation is from x to y, we have

$$x' = x \cos \omega t - y \sin \omega t,$$

$$\dot{x}' = (\dot{x} \cos \omega t - \dot{y} \sin \omega t) - \omega(x \sin \omega t + y \cos \omega t),$$

$$\ddot{x}' = (\ddot{x} \cos \omega t - \ddot{y} \sin \omega t) - 2\omega(\dot{x} \sin \omega t + \dot{y} \cos \omega t)$$
$$- \omega^2(x \cos \omega t - y \sin \omega t),$$

with similar expressions for the y-coordinates.

The first two terms of the right-hand side of the last equation give the component in the fixed x-direction of the acceleration relative to the rotating axes ; the second pair gives that of the Coriolis acceleration, and the last pair that of the centripetal acceleration.

From the above equations it is evident that neither of the statements quoted above from Dr. Howland's paper is correct, and that the conclusions which he draws from them are consequently invalid.

Using stroboscopic vision it is quite easy to demonstrate experimentally that the frequency of vibration of a shaft does not vary with the speed of rotation as required by Dr. Howland's equation (5), but remains sensibly the same as when there is no rotation, so long as the speed is insufficient to produce appreciable gyrostatic effects.

The stroboscopic shutter may be attached to a small motor whose speed is kept constant at that value which makes the vibrating, but not revolving, shaft appear to stand still with a bent form which gradually straightens as the vibration dies away. With a single slot shutter this speed will be found identical with the critical speed of the shaft.

If whilst rotating at any speed the shaft be set into vibration by a blow, its stroboscopic appearance will be the same as when it was not rotating, except for the whirl due

to any want of balance, thus showing that the frequency has
not been altered by the rotation.

Near the critical speed the whirl due to unbalance may be
too large to permit the vibration to be distinguished from it;
but the proof can be extended to this range by attaching the
shutter to the motor driving the shaft instead of to a separate
motor.

The stroboscope then eliminates, so far as vision is con-
cerned, all periodic motions of the rotation frequency, includ-
ing the rotation itself, and the other vibrations are seen with
their frequency apparently reduced by an amount equal to
the speed of the shaft.   Within about 200 r.p.m. of the
critical speed the apparent frequency of the vibrations set
up by a blow can be timed, and their actual frequency deter-
mined by allowing for the speed of the shaft.   It will again
be found to be the same as the critical speed.

In essentials Howland's fallacy is identical with that of
Chree * and of the others who followed him in predicting a
critical speed at $\Omega/\sqrt{2}$.

This fallacy has been repeatedly exposed, among others
by Rodgers on pp. 129–130 of the 1922 paper which
Dr. Howland mentions.

There are at least four papers which give measurements of
the magnitude of elastic hysteresis, or internal friction, in
steel, and one point upon which they do agree is that the
forces concerned are *quite independent of the velocity of strain*†.

Thus the assumption that these forces are proportional to
the velocity of strain, upon which most of the remainder of
Dr. Howland's paper is founded, is contrary to the known
facts.

His reference to Filon and Jessop's paper misleads the
reader into supposing that these writers have put forward
this assumption as one which fairly represents the facts for
all materials, whereas they state quite the contrary.   After
mentioning that they tried it for *one* material, they pro-
ceed :—"A thorough examination of a number of curves,

* "The Whirling and Transverse Vibrations of Rotating Shafts," Proc.
Phys. Soc. 1903–05, xix. pp. 114-156 (11/3/04); and Phil. Mag. ser. 6,
vii. pp. 504–542 (May 1904).

† Hopkinson and Williams, "The Elastic Hysteresis of Steel," Proc.
Roy. Soc. A, lxxxvii. pp. 502–511 (13/12/1912); Rowett, "Elastic
Hysteresis in Steel," *ibid.* A, lxxxix. pp. 528–543 (2/3/1914); Kimball,
"Measurement of Internal Friction in a Revolving Deflected Shaft,"
Gen. Elec. Rev. xxviii. pp. 554–558 (Aug. 1925); Kimball and Lovell,
"Internal Friction in Solids," Mech. Engineering, xlix. pp. 440–442 (May
1927), and Phys. Rev. l. pp. 948–959 (Dec. 1927); Canfield, "Internal
Friction in Metals," Phys. Rev. xxxii. pp. 520–530 (Sept. 1928).

however, showed large and systematic divergences from this law, and it was definitely discarded " (p. 168).

Although Kimball is now of the opinion that some of the phenomena observed by Newkirk and himself were due to another cause discovered later, and although his quantitative theory may be disregarded as based on assumptions (the same as Dr. Howland's) which he himself found to be false when he made measurements of elastic hysteresis, his main conclusion that elastic hysteresis and cramping fits may, and often do, cause whirling in a shaft running above its critical speed is most certainly correct. The present writer has watched the phenomenon too often to admit the slightest doubt of its existence.

Dr. Howland is again in error when he states that a permanent external force is necessary to bring hysteresis into play ; all that is required is that there should be a bend in the shaft which does not rotate at the same speed as the shaft itself, so that the material is subject to an alternating strain.

Any accidental disturbance of the shaft from its position of equilibrium under the action of the main whirling forces will produce a transient whirl *which rotates at the critical speed.* When the shaft speed is higher than this the elastic hysteresis gives a driving force maintaining this whirl, and if this force exceeds the friction opposing the transient whirl that transient will grow until the shaft strikes the stops.

In his paper on "Shaft Whipping "* Newkirk explains how he measured the actual rotation of the whirl by means of an oscillograph, and states that he always found it equal to the critical speed and in the direction of rotation of the shaft.

Feb. 24th, 1932.

LXXXI. *On Oberbeck's Vortices.*

To the Editors of the Philosophical Magazine.

Gentlemen,—

I SHALL be obliged if you will kindly publish the following reply to the comments on section 7 of our paper † " On Oberbeck's Vortices " made by Messrs. Rutherford and Caldwell in the December 1931 issue of the ' Philosophical Magazine,' pp. 1190–1191.

* Gen. Elec. Rev. xxvii. pp. 169–178 (March 1924).
† Phil. Mag. xi. pp. 1057–1081 (May 1931).

The method adopted by us in this section is admittedly approximate. The rigorous hydrodynamical equations are too complicated, and it is impossible to obtain a solution. We had therefore necessarily to simplify the equations by making suitable assumptions. The problem is to determine the motion of a jet of water forcing its way through still water. There is a discontinuity of motion at the boundary between the "jet" and the "still water." All the equations written in section 7 refer to the "jet" and not to "still water." Initially no element of fluid in the jet has rotation. It is the interaction of "still water" and the "jet" that introduces rotation in the latter. Had there been no "still water" the jet would have merely traced a parabolic trajectory, and would not have developed into "spiral vortices." We therefore made the assumption that the forces producing rotation in the jet are due to an extraneous agency, namely, the "still water," and should therefore be included in the force terms (X, Y). It was further assumed that the rotation

$$\zeta = \frac{\partial u}{\partial y} - \frac{\partial v}{\partial x}.$$

which was initially zero for each element of fluid in the jet, continued to remain so throughout the motion. This step was supported by equation (9); because this equation shows that the rotation ζ involved in the "inertia terms" and the rotation λ in the "force terms" enter into the hydrodynamical equations in the same way. Unless therefore one of them be assumed to be zero, we would be taking account of the "rotation" twice in our equations. As in this case the rotation is produced by an extraneous agency the assumption $\zeta = 0$ would appear to be the most logical one. The comment that equation (10) "will certainly not be fulfilled for a fluid with friction" is tantamount to that "stream line" motion is impossible in a fluid with friction, and would thus appear to be absurd.

At any instant the velocities at the different points on a transverse section of the jet may be regarded as more or less constant. The internal viscosity of the fluid within the jet is negligible. The viscous forces, however, come into play at the boundary between the "still water" and the "jet." The viscous resistances introduced by "still water" to the motion of the jet are plainly extraneous forces. We therefore make the simple assumption, as is usually done, that such forces are proportional to the velocity at any point

of the jet. There is nothing in this assumption which goes against the rigorous equations of hydrodynamics. For incompressible fluid the rigorous equations are

$$\frac{Du}{Dt} = X - \frac{1}{\rho}\frac{\partial p}{\partial x} + \nu\nabla^2 u, \qquad \frac{Dv}{Dt} = Y - \frac{1}{\rho}\frac{\partial p}{\partial y} + \nu\nabla^2 v.$$

It is known * that the term $\nu\nabla^2 u$, due to viscosity, gives a variation of u " following the same law as that of temperature in thermal conduction or of density in the theory of diffusion. This variation is, in fact, proportional to the (positive or negative) excess of the mean value of u through a small sphere of given radius surrounding the point (x, y, z) over its value at that point." It is clear that if we draw a small sphere having its centre at any point of the boundary between "still water" and "jet" then at its centre $u=0$ and within the portion of the sphere in the jet $u=u$. Therefore we can take the viscosity term $\nu\nabla^2 u$ to be equal to $-\nu\kappa^2 u$, κ being a constant, or simply $-\mu u$. Within the limit of approximation involved in this deduction equation (6) would appear to be quite correct. If a narrow stream of water in any transverse section of which the velocity is more or less uniform has to force its way through another fluid which is stationary it must experience viscous resistances approximately in the manner of equation (6).

There is no assumption involved in equations (11) ; they are merely steps leading to a solution of the dynamical equations as formulated under (9). The fact that

$$\tan\theta = \frac{v}{u} = \frac{V}{U}$$

is independent of t is in no way inconsistent with our photographs. It has to be remembered that the dynamical equations (9) refer to axes having an arbitrary origin but when substitutions of the kind (11) are made in them the axes have the "pole" of the equiangular spiral as the origin. This is clear from the subsequent solution, and particularly from the expressions for velocity given in (29). Since the pole is moving the direction of flow at any point fixed in space certainly changes with time, but at a point fixed relatively to axes passing through the pole, the x-axis being parallel to the axis of the jet, the direction of flow measured with reference to these axes does not change with time. This is what the expressions for velocity given in (29) mean, and is in agreement with our observations.

* Lamb's 'Hydrodynamics,' fourth edition, p. 573.

In solving the equations we did assume that λ is uniform throughout the moving liquid, but stated that the solutions so obtained would be applicable over those regions where " this condition is strictly satisfied." The solution obtained on this assumption shows that the trajectory of the jet is a pair of equiangular spirals. If observations also show that the trajectory is a pair of equiangular spirals, then obviously λ is more or less uniform over the region covered by each of the spirals.

It is seen from equations (15) that $\nabla^2 L = 0$ and $\nabla^2 M = 0$. The equation of continuity gives $\nabla^2 \phi = 0$. Therefore from the second equation of (14) we get $\nabla^2 \psi = 0$. Since L, M, ϕ, ψ are all harmonic functions, we see that the second equation of (14), namely,

$$M = (\mu - \alpha)\psi + \lambda\phi,$$

can be satisfied only if

> (1) M is a constant, and ϕ and ψ are proportional to the *same* harmonic function,
>
> or, (2) M, ϕ, ψ are all proportional to the same harmonic function.

Whether we choose (1) or (2) the result comes out to be of the same form as given in (16). There is therefore no loss of generality if we take the solutions of equations (15) in the form

$$L = f(t) \quad \text{and} \quad M = \text{constant}.$$

The omission of the arbitrary constant in (16) is of no consequence. It is omitted because it does not affect any of the subsequent steps.

In (13) we express (U, V) in the form

$$U = \frac{\partial \phi}{\partial x} + \frac{\partial \psi}{\partial y}, \quad V = \frac{\partial \phi}{\partial y} - \frac{\partial \psi}{\partial x}.$$

It is definitely known that when the components of velocity are expressed in this form ϕ is not the " velocity potential " nor is ψ the " stream function." $U dx + V dy$ is not a perfect differential, even if ϕ is proportional to ψ as is given in (16), and therefore no velocity potential can exist. Equation (21), just like (16), is merely a functional relationship between ϕ and ψ. This equation does not make ϕ a " velocity potential " or ψ a " stream function." According to analytical geometry the curves

$$\psi - \frac{\lambda}{\mu - \alpha} \phi = \text{constant}$$

must intersect the curves

$$\phi = \text{constant}$$

at a constant angle. The orthogonality of the functions ϕ and ψ as expressed in (21) does not affect this angle of intersection in any way. The angle ϵ in equation (24) cannot be equal to $\frac{\pi}{2}$ unless $\mu = \alpha$. Equation (28) does not therefore become $r = \text{constant}$. The jet must therefore have the form of double equiangular spirals at any instant.

The mathematical theory is undoubtedly approximate, the more so because the motion in any section through the axis of the jet has been regarded as two-dimensional ; but it will I hope be clear from what has been written above that it has none of the defects stated by Messrs. Rutherford and Caldwell. The agreement between the results deduced from it and the experiments is so close in all the essential details that it is certainly not fair to ascribe it to mere coincidence.

<table>
<tr><td>The Observatory,
Bombay.
January 3, 1932.</td><td>I am, Gentlemen,
Yours faithfully,
S. K. BANERJI.</td></tr>
</table>

LXXXII. *Notices respecting New Books.*

Monographs on Biochemistry : The Glycosides. By Dr. E. F. ARMSTRONG, F.R.S., and K. F. ARMSTRONG. (London : Longmans, Green & Co., 1931. Price 12s. 6d. net.)

THIS work is based on a section of the well-known monograph 'The Simple Carbohydrates and the Glucosides,' written several years ago by the senior author. It affords a valuable account of our present knowledge of the chemistry of the " glucosides," and embodies much of the very latest work in this field. This is specially the case in Chapter III., which deals with the soluble plant pigments and contains a useful summary of various aspects of the researches of Robinson and his school, including the synthesis of anthocyanins and work on the position of the sugar molecule.

The term " Glycosides " does not meet with approval from all chemists, although it serves as a general name for the compounds yielding sugars (mannose, rhamnose, galactose, as well as glucose) and hydroxylic compounds on hydrolysis. Glucosides, therefore, form a special division of the class of glycosides. Still less euphonious and contrary to usual chemical nomenclature is the term " aglucone," suggested by Japanese workers for the non-sugar portion of the glycoside molecule. This may be an alcohol, a

phenol, an isothiocyanate, or a cyanohydrin, but rarely, if ever, a simple ketone, which is what the term would naturally imply.

The opening chapter pays homage to the pyranose and furanose formulæ for the sugars, but the older and now discarded term γ-sugar is occasionally met with.

In connexion with the cyanophoric or cyanogenetic glycosides (both terms are used) details are given of the many different factors, *e. g.*, temperature, humidity, stage of development, and cultivation (as distinct from "wild" growth), which affect the amount of hydrocyanic acid produced by the plant. This is obviously of economic and toxicological importance. Acetone cyanohydrin occurs combined with glucose as linamarin or phaseolunatin in young flax-plants and the seeds of the rubber-tree. It has been suggested that this acetone is the precursor of isoprene, from which not only rubber but most ingredients of essential oils may be derived. The importance of acetone in biochemistry is undoubted; it occurs also in the diabetic animal as a product of the bacterial decomposition of carbohydrate, and arises from aliphatic acids by the action of moulds.

The recent work of Baker and Robinson on the isoflavone glucosides also finds a place in Chapter III. This class of compound has only recently been recognized among natural products. Attention is drawn to the interesting formation of malonic acid on hydrolysis of the anthocyanin monardein occurring in golden balm. The malonic acid is attached through the sugar portion of the molecule. The work of Raistrick and his collaborators on mould fermentation is mentioned in Chapter I. ; reference might be made here, however, to Raistrick's isolation from cultures of *Penicillium luteum* of luteic acid, which also gives glucose and malonic acid on hydrolysis. Other micro-organisms can also produce malonic acid.

Reference is also made to the recent observation that certain anthocyanins yield *p*-hydroxycinnamic acid and *p*-hydroxybenzoic acid on hydrolysis. It may be mentioned that *p*-methoxycinnamic acid is also obtained on hydrolysis of yangonin, another γ-pyrone derivative of plant origin.

The last two chapters deal with the function of glycosides and the utilization of carbohydrates in plants. They will be valuable to those who propose to investigate changes occurring during the storage and ripening of fruits.

An excellent bibliography, which has come to be regarded as a feature of this series of monographs, greatly enhances the usefulness of this valuable work.

The Nature of Physical Theory: a Study in Theory of Knowledge. By VICTOR F. LENZEN, Ph.D. [Pp. 295 + xii.] (New York: John Wiley & Sons, Inc.; London: Chapman & Hall, Ltd., 1931. Price 21s. net.)

THIS book is an attempt to expound systematically how physical theory has developed by successive definition and approximation. The process of development is envisaged as follows:—There is an

abstraction of concepts from experience, a discovery and expression of laws in terms of the concepts, a redefinition of the original concepts to a higher order of approximation with increasing precision in the definition of conditions, a redefinition of new concepts in terms of the laws, and finally a reinterpretation of the original concepts in terms of the new.

After an examination of the basic concepts—space, time, body, quantity, etc.—the author proceeds to a survey of the methods, principles, and systems of physical theory. In this section, which covers some three quarters of the book, there is given, within the limits which brevity imposes, an eminently clear and readable account of theoretical physics. The treatment of the geometrical conception of nature is particularly attractive.

To the earnest student of physics as well as to the experimenter, who are only too often unable to see the wood for the trees, such a survey should provide a valuable bird's-eye view.

The analysis of the fundamental concepts with which the book opens, and the discussion of methodological principles with which it concludes, though stimulating and refreshingly free from philosophic jargon, would gain in force and clarity by some ruthless pruning of repetitions.

A useful list of references is appended to most of the chapters, an adequate index is provided, and the typography is excellent.

Theoretical Physics. By W. WILSON, F.R.S.—Vol. I. *Mechanics and Heat* (NEWTON-CARNOT). [Pp. 332, 80 diagrams. Boards.] (London : Methuen & Co., 1931. Price 21s. net.)

THIS volume is the first of three which purpose to present an account of the theoretical side of Physics particularly intended for teachers and students.

In this first volume Mechanics and Heat are presented, with appropriate introductory chapters on Euclidean and Vector Analysis, the theorems of Gauss, Green, and Stokes, followed by useful chapters on Dynamics, Hydrodynamics, and Electricity. Chapters on Kinetic Theory, Thermodynamics, and, of course, Statistical Mechanics complete the volume.

It is made clear in the preface that the author aims at treating the subject on broad historical lines, with the result that the first volume is necessarily "entirely classical"; moreover, the mathematical treatment is kept within the limits set by a reasonable mathematical equipment. Special mathematical methods, where employed, are given special explanatory attention.

The book is likely to be of considerable value to the earnest student of Physics at the University. The title is perhaps a shade misleading, in that the subject of Heat, as dealt with in this volume, is confined within the region of Thermodynamics and Kinetic Theory; but this is a small matter of criticism in view of the generally good character of the book.

It is well printed, and the considerable mathematical reproduction is very pleasing.

LXXXIII. *Proceedings of Learned Societies.*

GEOLOGICAL SOCIETY.

February 10th, 1932.—Prof. E. J. Garwood, M.A., Sc.D.,
F.R.S., President, in the Chair.

Prof. S. JAMES SHAND, D.Sc., Ph.D., F.G.S., delivered a
lecture on ' The Reaction between Granitic Magma and
Limestone at Palabora, Transvaal.'

The Lecturer said that the Palabora granite is intrusive
among ancient schists which include bodies of crystalline
limestone. The hill Lulu Kop is a mass of metamorphosed
dolomitic limestone isolated in the granite. Between granite
and limestone there is a belt of flat ground, up to 2 miles wide,
within which all the rocks exposed are rich in diopside and
apatite ; they vary from shonkinite to pyroxenite and massive
apatite. Between these rocks and the granite there is a narrow
belt of diopside-arfvedsonite-syenite. The evidence indicates
extensive reaction between granitic magma and limestone,
producing syenite and shonkinite, and it is suggested that the
pyroxenite was formed by the sinking of diopside crystals from
the contaminated magma. As assimilation of limestone
went on, soda seems to have been progressively expelled from
the magma, for in the shonkinite the only felspar is a highly
potassic microcline. No nepheline is found at the present
level, but there is a possibility that the expelled soda may have
formed nepheline-rocks at higher levels, now removed by
erosion.

The following communication was read :—

' The Lavas of Mauritius.' By Prof. S. James Shand.
D.Sc., Ph.D., F.G.S.

The lavas of Mauritius are mainly basalts, some rich in
olivine and others almost or quite free from it. No felspathoids
have been detected, but some of the rocks are of the ' pacificite '
type, having nepheline in the norm. Soda-trachyte was
found at two localities, and must be regarded as a differentiate
of the basaltic magma. This rock, too, holds normative
nepheline and is not far from a true phonolite. The problem
of deriving phonolite from a basaltic magma is briefly discussed.

FIG. 5.

FIG. 6.

FIG. 7.
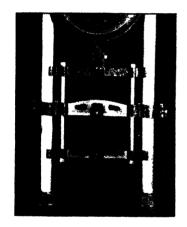
FIG. 8.

FIG. 9.

FIG. 10.

FIG. 16.
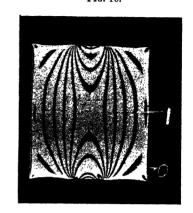
FIG. 17.
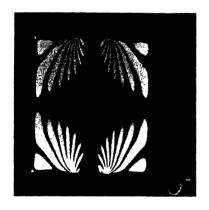
FIG. 18.
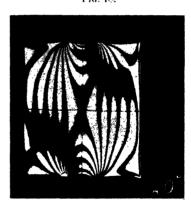
FIG. 19.
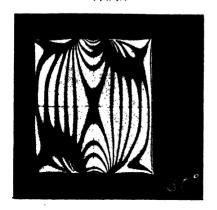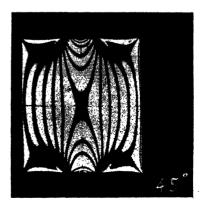
FIG. 20.

LXXXIV. *Collisional Friction on Electrons moving in Gases. By* E. C. Childs, *B.Sc., Ph.D.**

IT is customary to include in the equation of motion of an electron moving in a gas under the influence of electric fields a term representing a force of frictional type, *i. e.*, a resistance to the motion proportional to velocity. The equation of motion may then be written

$$m\frac{d^2x}{dt^2} + g\frac{dx}{dt} = e\mathrm{E}_x, \quad . \quad . \quad . \quad . \quad (1)$$

where the electron of mass m and charge e moves in the direction, say x, of the field E_x. This simple expression implies no motion excepting that produced by the field. This is justifiable provided that the velocity acquired, due to the field, between collisions is small compared with the random velocity due to thermal agitation. The coefficient g is the frictional term referred to, and it can be shown † that it is given by

$$g = \frac{m}{\tau}. \quad . \quad . \quad . \quad . \quad . \quad (2)$$

In this expression τ is the average time elapsing between two consecutive collisions, and the value is deduced on the

* Communicated by Prof. E. V. Appleton, F.R.S.
† See, for example, Townsend, 'Electricity in Gases,' p. 84.

assumption that directed momentum is completely destroyed at each impact. A more rigorous treatment gives [*]

$$g = \frac{m}{0.75\tau}.$$

This is only valid for conditions such that the free paths are distributed according to an exponential law, *i. e.*, they are determined by the laws of chance. This implies that the mean free path must be much smaller than the dimensions of the vessel containing the gases and the electrons. When these dimensions set an effective limit to the lengths of the free paths, the value of g increases, and in particular when all free paths have the same length, *i. e.*, the separation of the walls of the vessel when the gas is at very low pressure, g becomes equal to $\frac{2m}{\tau}$. In the present work only the first-mentioned conditions are considered.

The frictional forces play an important part in the refraction of wireless waves at the ionized layers in the upper atmosphere, for they are the cause of components of current in phase with the alternating electric fields, and hence determine the absorption. If this is sufficient, the circular polarization of downcoming waves is accounted for [†].

It was considered that experimental confirmation of the value of the frictional force calculated on a kinetic theory basis would be of value, particularly as doubts had been expressed [‡] as to the ability of an unmodified kinetic theory to yield correctly the mean free path of an electron, even to the right order. Briefly, Ponte and Rocard have shown, by applying the reasoning of Sutherland [§] and Wellisch [||] to electrons, that the electronic mean free path is not $4\sqrt{2}$ times that of the molecules of the gas in which the electron moves, but is only about one twenty-fourth of this, *i. e.*, τ is only about $\frac{1}{160}$ of the commonly accepted value. This is due to the polarization of homopolar molecules or rotation of permanent dipoles by the approaching electron. The field thus set up draws in the electron, possibly to make a collision which otherwise would not occur. The authors then proceed to show that the phenomenon of "skip-distance" indicates that this result is quite incompatible with the

---

[*] Loeb, ' Kinetic Theory of Gases,' p. 448.
[†] Appleton and Ratcliffe, Proc. Roy. Soc. A, cxvii. p. 576 (1928).
[‡] ' L'Onde Electrique,' viii. p. 179 (1929).
[§] Phil. Mag. (5) xxxvi. p. 507 (1893).
[||] Phil. Trans. A, ccix. p. 249 (1909).

experimental results of Appleton [*] and his co-workers, which yield a Heaviside layer height of only some 90–100 km. In fact this height is an over- rather than an under-estimation, since in the present state of knowledge of the charge distribution of the layer it is impossible to allow for reduction of group velocity suffered by the wireless waves.

The property of ionized gas upon which attention was focussed in the present work was its electrical conductivity when high-frequency alternating electric fields were impressed upon it. A knowledge of this, together with the electron concentration, suffices to determine g [†], for

$$\sigma = \frac{Ne^2g}{m^2p^2 + g^2}, \quad \ldots \ldots \quad (3)$$

where σ is the conductivity of ionized gas containing N carriers per c.c., each of mass m and charge e, when the field frequency is $\frac{p}{2\pi}$. As we have seen, it is necessary that the mean free path of the electrons should be but a small fraction of the dimensions of the apparatus, this condition necessitating high pressure or, what is the same thing, large g. When this condition is satisfied, g is large compared with mp for all ordinary values of p. (3) then reduces to the simple form

$$\sigma = \frac{Ne^2}{g}. \quad \ldots \ldots \ldots \quad (4)$$

Determination of N *and* $\frac{m}{\tau}$.

In order to compare the experimental value of g with the theoretical value of $\frac{m}{\tau}$, it is necessary to know the average velocity of the electrons or, what is actually measured, the electron temperature to which the Maxwellian velocity distribution corresponds. In this work, then, full use was made of Langmuir's probe-current analysis method [‡], for it is capable of yielding information both on the electron concentration and on the electron temperature.

The method consists of observation of the current to a probe electrode, inserted in the discharge in the region

---

[*] Proc. Roy. Soc. A, cxxvi. p. 542 (1930) and preceding papers.
[†] Appleton and Childs, Phil. Mag. (7) x. p. 974 (1930).
[‡] Gen. Elec. Rev. xxvii. p. 449 (1924).

to be investigated, when the potential with respect to some fixed point, usually the anode, is varied. The probe is conveniently a short length of fine wire, in the present case of tungsten of diameter 0·07 mm. sheathed in glass except for a protruding length of 7 mm. A curve of total current against voltage is plotted, and from the strongly negative region information is obtained which enables the total current to be corrected for positive ion contribution. The logarithm of the electron current, i_-, is then plotted against voltage, and the curve is found to be a straight line over part of the range, of slope

$$S = \frac{d(\log_e i_-)}{dV} = \frac{e}{KT}, \quad \cdots \quad (5)$$

K being Boltzmann's constant and T the absolute temperature of the electrons. This expression is only valid for current carried by retarded electrons. At space potential the semi-log curve departs from linearity, and at this point the electron current is given by

$$i_- = ANe\sqrt{\frac{KT}{2\pi m}}, \quad \cdots \quad (6)$$

A being the probe area and N the electron concentration in the discharge. N can be calculated from (6) and (5) while $\bar{v}$, the average velocity of the electrons, can be obtained from (5) for

$$\bar{v} = \sqrt{\frac{8}{\pi} \cdot \frac{KT}{m}}. \quad \cdots \quad (7)$$

A typical semi-log curve is shown in fig. 1. N may also be found from the accelerated electron current, but it was found that such currents were accompanied by distorted discharges, the results being meaningless.
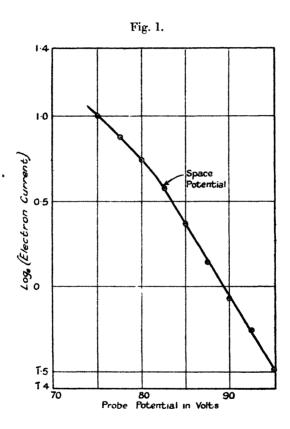
The value of τ is, of course, easily obtained from (7), for

$$\tau = \frac{\lambda_e}{\bar{v}}, \quad \cdots \quad (8)$$

λ_e, the electronic mean free path, being obtained from tables.

Determination of σ.

As we have seen, once N is known it is only necessary to find the electrical conductivity, σ, in order to ascertain the value of g. Many methods were tried before σ was satisfactorily evaluated. In all of them the device of

substitution of resistances of known value for the leak-resistance of the ionized gas was resorted to. In one method the ionized gas, produced by a direct-current discharge between cold electrodes in a cylindrical tube containing air at low pressure, constituted the core of a screened solenoid. Eddy currents in the core had the effect of reducing the effective self-inductance of the coil. In

Fig. 1.

other cases the ionized gas was placed in the field between two parallel condenser plates, forming the whole or part of the dielectric. The difficulty in this case is that, if positive ion sheaths form, results are not capable of numerical interpretation, while if the sheaths are removed by maintaining the condenser plates at space potential, the damping is so excessive that the triode oscillator supplying the high-frequency field ceases to function. Some of the effects of sheath formation had been observed in earlier work on the

dielectric constant of ionized gas *. Some anomalous results showing the inconsistencies produced by sheath formation, will be given.

Two condenser plates were fixed externally to a discharge-tube so mounted that it could easily be removed from the field between the plates and an exactly similar tube containing a mixture of xylol and alcohol substituted. The condenser plates were connected to the ends of a Lecher wire system, which was excited by a triode oscillator oscillating at a frequency of about 3×10^8 cycles per sec. The amplitude of the potential difference between the plates was indicated by a crystal detector circuit, and the damping produced was used as a measure of the resistance in parallel with the condenser. It was assumed that the mixture of xylol and alcohol producing the same damping as the ionized gas possessed the same electrical conductivity. It may be mentioned that the high frequency was used in an endeavour to penetrate the sheaths which formed on the glass walls. Measurement of the conductivity of the liquids at low frequencies presented no difficulties.

It was found that the experimental value of g was very much larger than the calculated value, but decreased as the ionization increased in intensity. For example, with a tube current of 6 m.a. $\dfrac{g_{\text{obs.}}}{g_{\text{calc.}}} = 136$, while at 10 m.a. $\dfrac{g_{\text{obs.}}}{g_{\text{calc.}}} = 45$, gas-pressure remaining constant. This result is not remarkable when it is remembered that the probe experiments give the electron concentration in the main discharge, while positive ion sheaths have a considerably lower concentration. Consequently they have a considerably lower conductivity, to which the positive ions, in which the sheaths are rich, make but little contribution by reason of their considerable relative mass. The overall conductivity, which is the quantity measured by substitution of similar bodies of liquids, is therefore much lower than that of a similar body of main discharge containing the measured number of electrons per c.c. Reference to equation (4) shows that this error produces an excessive value of g. Moreover, as the electron concentration is increased, the sheaths become thinner in consequence of space-charge laws †, so that the discharge becomes more and more nearly uniform over the whole cross-section of the tube. The overall conductivity

---

* Appleton and Childs, *loc. cit.*

† Child, Phys. Rev. xxxii. p. 492 (1911); Langmuir, Phys. Rev. ii. p. 450 (1913).

is therefore more nearly equal to that of the core of uniform discharge, and g tends towards the calculated value. Tonks *, working with mercury vapour, recognizes the sheath effect, but neglects it in obtaining a resistance value of the right calculated order. This is probably due to the great mass of the positive mercury ions, for the positive ion current determines sheath thickness, and the space-charge equation shows that, other things being equal, a heavy carrier requires a shorter distance between source and collector.

It was clear from these results that the sheaths must be removed, and this was impossible while they formed on the walls of the tube. Hence, in the next tube built provision was made for the introduction of the condenser plates inside the tube. They were of Eureka, 1 cm. by 1·5 cm. each, and were spot-welded to short Eureka wire helices. The plates were introduced into the 3 cm. diameter tube from one end, and the stiff wire leads, which also were the sole supports, were pushed down capillary side arms and into the wire helices. The latter were slightly too small, so that the leads could only be pushed in by turning against the direction of winding, thus insuring reasonably good contact and rigid support.
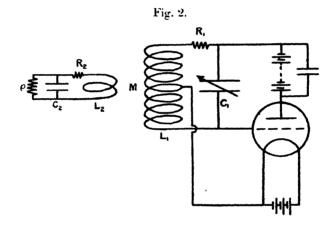
These plates were maintained at space potential, and therefore the previous method of comparison with known resistances, *i. e.*, observation of damping of the circuit containing the condenser, was useless, for reasons which have been stated. In order to maintain oscillations it was necessary to couple the oscillator to the condenser *via* a step-down transformer, and the method of comparison used was the observation of change of effective inductance of the primary coil of this transformer. The latter was connected, together with a variable condenser, to a triode to form a source of maintained oscillations, as in fig. 2.

The oscillation frequency was about 10^6 cycles/sec. As is well known, closing of the secondary circuit through resistance produces a decrease of effective self inductance of the primary, this in turn causing an increase in frequency of the oscillations. This change was so small in practice as to be observed only by change of pitch of the heterodyne note produced by the oscillator of fig. 2 and another of slightly different and fixed frequency. This change of pitch was the means of comparing the conductivity of the ionized gas (the leak-resistance ρ of fig. 2) with known liquid conductivities, an audio-frequency oscillator being used

* Tonks, Phys. Rev. xxxvii. p. 1458 (1931).

to measure change of pitch. It is necessary to develop the simple air-cored transformer theory for cases, such as that under consideration, where the reactance of the condenser in the secondary circuit is of the same order as the leak resistance at the frequencies used, and where the primary circuit is tuned.

We will first consider the resonant frequency of the circuit. This is not exactly equal to the natural frequency, but is approximately the same as the frequency of *maintained* oscillations. In fig. 2, C_2 and ρ represent the ionization condenser and its leak (either due to ionized gas or connected resistance) respectively. It is connected to L_2, a coil of one or two turns of resistance R_2. The latter is coupled by

Fig. 2.

mutual inductance M to the primary coil, of inductance L_1, and resistance R_1, which is tuned by the condenser C_1. Consider an alternating E.M.F. of form $E_0 \exp(jpt)$ injected into the primary circuit. Then the primary and secondary currents, i_1 and i_2, may be obtained as follows.

Let the vector resistances of the primary and secondary circuits be written, respectively,

$$\left. \begin{array}{l} Z_1 = a + jb, \\ Z_2 = c + jd, \end{array} \right\} \quad \cdots \cdots \cdots (9)$$

where j represents $(-1)^{\frac{1}{2}}$. Then we have, as the expression of Kirchhoff's laws,

$$\left. \begin{array}{l} i_1(a+jb) + jpMi_2 = E_0 \exp(jpt) = E, \\ i_2(c+jd) + jpMi_1 = 0. \end{array} \right\} \quad \cdots (10)$$

Solving for the primary current we find

$$_0i_1 = \frac{E_0}{\sqrt{\left(a + \frac{cp^2M}{c^2+d^2}\right)^2 + \left(b - \frac{dp^2M^2}{c^2+d^2}\right)^2}}. \qquad . \quad (11)$$

In this expression $_0i_1$ is the current amplitude. Reference to fig. 2 shows that

$$\left.\begin{aligned}
a &= R_1, \\
b &= pL_1 - \frac{1}{pC_1}, \\
c &= R_2 + \frac{\rho}{1 + p^2C_2^2\rho^2}, \\
d &= pL_2 - \frac{pC_2^2\rho^2}{1 + p^2C_2^2\rho^2}.
\end{aligned}\right\} \quad . \quad . \quad . \quad . \quad (12)$$

If the circuit is tuned to resonance by variation of L_1 or C_1, then b is the only variable, and resonance occurs when

$$b = \frac{dp^2M^2}{c^2+d^2}$$

i.e., $$pL_1 - \frac{1}{pC_1} = \frac{dp^2M^2}{c^2+d^2} \quad . \quad . \quad . \quad . \quad (13)$$

The resonant frequency therefore depends on both C_2 and ρ, and the dependence may more clearly be seen by substitution of circuit constants. C_2 is of the order of 0·1 cm., ρ lies between 10,000 and 100,000 ohms, and therefore $p^2C_2^2\rho^2$ is quite negligible compared with unity. R_2 is negligible compared with ρ, being at most a few ohms at radio frequency, therefore,

$$\left.\begin{aligned}
c &\doteqdot \rho, \\
d &\doteqdot p(L_2 - C_2^2\rho^2),
\end{aligned}\right\} \quad . \quad . \quad . \quad . \quad (14)$$

and d is much smaller than c. Hence (13) may be approximately rewritten

$$pL_1 - \frac{1}{pC_1} = \frac{dp^2M^2}{c^2} . \quad . \quad . \quad . \quad (15)$$

Hence, when ρ decreases then c decreases and d increases, while when C_2 decreases c remains constant and d increases.
Therefore, when either or both of C_2 and ρ decrease

we see from (15) that $pL_1 - \dfrac{1}{pC_1}$ must increase if the resonant frequency is to remain unaltered, *i. e.*, the value of the tuning capacity, C_1, must be increased. Alternatively, if C_1 remains constant the resonant frequency increases, and this, as already described, was the method of carrying out the experiment. More laborious substitution, without approximations, yields the same conclusions.

Conversely, increase of C_2 or ρ, or both, leads to a decrease of resonance or natural frequency. C_2 and ρ always vary together and in the same direction, for the dielectric constant of ionized gas is known to be reduced by increasing ionization *. In this connexion it is interesting to note yet further experimental evidence confirming the necessity for sheath removal. When the condenser plates were left free to assume their own potential, sheaths formed, which increased the effective value of C_2 beyond the un-ionized value *, and kept ρ large (resistance of positive ion sheaths). In this case the oscillation frequency was found to decrease, as expected.

Since reduction of ρ is accompanied by reduction of C_2, and both result in increase of oscillation frequency, it is clearly necessary, in order to measure conductivity, to be able either to separate the effects or to be able to assign to each its proper proportion of the total frequency change. If k is the dielectric constant of ionized gas,

$$\left.\begin{array}{l} k = 1 - \dfrac{4\pi N e^2 m}{g^2}, \\[2mm] \sigma = \dfrac{N e^2}{g}, \end{array}\right\} \quad \cdot \quad \cdot \quad \cdot \quad \cdot \quad \cdot \quad \cdot \quad (16)$$

so that the larger g is the more nearly is change of C_2 negligible compared with change of ρ. Substitution in (13) showed that if g is of the order of 10^{-17}, change of ρ is almost solely responsible for change of frequency, while with g equal to 10^{-18} the effect of change of ρ outweighed that of change of C_2 by about three to two. It was proposed to determine g approximately by neglecting consideration of change of C_2, and by successive approximation to arrive at a final value. The method, however, was found to be insufficiently sensitive to make this process worth while. The results, however, showed that the observed value of g was of the same order as the theoretical value.

* Appleton and Childs, *loc. cit.*

Experimental Results.—I.

Air-pressure . . . . $= 1$ mm. Hg.
Mean free path of electrons (calc.*). $= 3\cdot6 \times 10^{-2}$ cm.

Tube current.	Electron speed, v.	Electron concentration, N.	Conductivity, σ.	$g(\text{obs.}) = \dfrac{Ne^2}{\sigma}$.	$g(\text{calc.})$ $= \dfrac{m}{\tau}$.
6 m.a.	6·6 volts $= 1\cdot4 \times 10^8$ cm./sec.	$9\cdot5 \times 10^7$/c.c.	$2\cdot2 \times 10^{-14}$ e.m.u.	$0\cdot96 \times 10^{-18}$ dyn./cm./sec.	$3\cdot5 \times 10^{-18}$
10 m.a.	4 volts $= 1\cdot1 \times 10^8$ cm./sec.	$2\cdot5 \times 10^8$/c.c.	4×10^{-14} e.m.u.	$1\cdot4 \times 10^{-18}$ dyn./cm./sec.	$2\cdot75 \times 10^{-18}$

Efforts were directed towards increase of sensitivity by
(*a*) increasing frequency change, and (*b*) decrease of
local noise from the H.T. generator producing the discharge,
but experience showed that progress did not lie in this
direction. It may be remarked that the gas conductivity
was compared, not with liquids of the same shape and
known conductivity, but with known resistances of sputtered
type. These all possessed self-capacity comparable with
that of the ionization condenser, but different resistances
possessed sensibly the same capacity. A 3-megohm leak
was therefore connected in parallel with the ionization
condenser during the discharge experiments, and was
replaced by leaks of lower resistance when comparison
was being sought. In this way the self-capacities of the
resistances were eliminated. It was proposed to correct for
edge-effects by a single experiment with a liquid of known
conductivity in the tube. This would, of course, spoil the
tube for further work, and neither this nor the successive
approximation mentioned was carried out, the accuracy
of measurement of σ not warranting the labour. Attention
was then turned to another method.
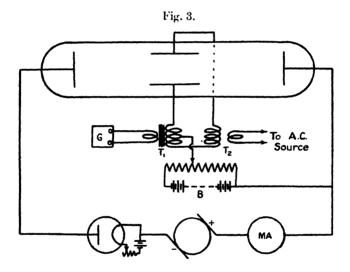
Final Determination of σ.

It is not difficult to see that in order to minimize the
effect of change of capacity on the impedance of the
ionization-condenser circuit the reactance of the condenser

* Mean free path of molecules from Bloch, 'Kinetic Theory of
Gases.'

should be very large compared with the equivalent paralle resistance. This implies the use of quite low frequencies, and at once rules out the heterodyne method. The method finally adopted was the comparison of the current passed by the ionization condenser with that passed by various high resistances of sputtered type. The discharge-tube of the previous experiment was retained and the circuit is shown in fig. 3, which is self-explanatory.

Alternating E.M.F.'s of small amplitude were injected into the circuit by the transformer T_2. Large amplitudes were necessarily avoided, since the potential of the condenser plates must never depart sensibly from space-potential,

Fig. 3.

to which they were adjusted by means of the battery B and its potential divider. When the discharge was struck, in general the potential divider was out of adjustment, and sheaths formed These were visible as relatively non-luminous regions surrounding the condenser plates. Small alternating currents flowed in the condenser circuit and were detected by the measuring instrument G coupled by the step-down transformer T_1. G was at first the most sensitive vacuo-junction obtainable (6 mv. for 2 m.a. heater current), but this was abandoned, partly because of lack of sensitivity, but mainly because of violent self-oscillation of the discharge at certain conditions of pressure and tube current. A tuned detector was plainly indicated. A 300 cycle/sec. moving-coil vibration galvanometer was kindly

Friction on Electrons moving in Gases. 885

lent by Messrs. H. Tinsley and Co., Ltd.; this instrument
had, of course, greatly superior sensitivity. With this
galvanometer the method was immediately successful. The
300 cycles per sec. alternating current in the circuit was
detected without a trace of the tube oscillations, at some
other frequency, creeping in.

The experimental procedure was as follows. The galvano-
meter was first tuned to resonance with the frequency
of the source, and a reading without discharge taken.
This was not zero, owing to a little mutual inductance
between the coils of the oscillator and the secondary winding
of the transformer T_1, although the offending units were
separated as far as was convenient and suitably orientated.
The discharge was then struck, the gas-pressure having
first been adjusted to a suitable value and measured by
a McLeod gauge.

On striking the discharge, the galvanometer spot opened
out slightly, and sheaths were in general observed. The
condenser-plate potential was gradually altered so that
the sheaths decreased in thickness; at the same time
the galvanometer spot was seen to widen slowly. As the
condenser plates approached space-potential, the spot rapidly
widened, and the reading was taken when the sheaths just
disappeared. Owing to the length of the plates (1 cm.) and
the potential fall along the positive glow in which they were
placed, they were not at space-potential over the whole area
at any one instant. The error introduced, however, was
slight, the galvanometer deflexion when the sheath over the
edge nearer the cathode disappeared being not appreciably
different from that when the whole sheath was too thin
to be observable. In fact, the effect of the potential fall
would not have been noticed had it not been observed that
glow due to ionization by collision set in over the cathode
edge of the condenser plate and spread as the potential was
made more and more positive with respect to space-potential.

These observations having been made for various values
of tube current, a series of Langmuir probe experiments
were carried out as already described. The discharge was
then stopped and various high resistances of known value
were connected in parallel with the ionization condenser.
From the curve obtained by plotting conductance against
vibration galvanometer deflexion, the conductance of the
ionized gas was read off. Finally, the edge correction for
the condenser was ascertained by filling the tube with
alcohol of known conductivity and measuring the con-
ductance of the condenser under these conditions. In this

way the factor for converting conductance of the ionization condenser into conductivity of the medium between the plates was found to be 0·57.

Experimental Results.—II.

Air-pressure . . . . $= 1$ mm. Hg.
Mean free path of electrons (calc.). $= 3·6 \times 10^{-2}$ cm.

Tube current.	Electron concentration, N.	Electron velocity, v.	Conductivity, σ.	$g \text{ (obs.)} = \dfrac{Ne^2}{\sigma}$.	$g \text{ (calc.)} = \dfrac{m}{\tau}$.
5 m.a.	$9·6 \times 10^7$/c.c.	$1·3 \times 10^8$ cm./sec.	1×10^{-14} e.m.u.	$2·5 \times 10^{-18}$	$3·2 \times 10^{-18}$
10 m.a.	$2·4 \times 10^8$/c.c.	$1·5 \times 10^8$ cm./sec.	$1·9 \times 10^{-14}$ e.m.u.	$3·1 \times 10^{-18}$	$3·8 \times 10^{-18}$
15 m.a.	$3·6 \times 10^8$/c.c.	$1·7 \times 10^8$ cm./sec.	$3·7 \times 10^{-14}$ e.m.u.	$2·5 \times 10^{-18}$	$4·3 \times 10^{-18}$

These results show that the frictional coefficient of electrons moving in air is not very different from the value calculated from kinetic theory, and is at least of the same order. Hence any calculation of the behaviour of the Heaviside layer based on this assumption is not appreciably incorrect.

Discussion.

It is, perhaps, not surprising that the deductions of Ponte and Rocard * have not been confirmed by experiment. It has been known for some years that the shortening of mean free path due to attraction, while true of molecular ions, cannot be applied to electrons. Methods devised by Ramsauer † and his co-workers and by Jones ‡ for the measurement of electronic mean free paths have demonstrated that these, while departing from simple kinetic theory values, are not of the order of one-hundredth of the latter. Even in the case of the inert gases, which depart most from expected behaviour, the shortening is not large,

---

* *Loc. cit.*
† Ramsauer, *Phys. Zeit.* xxix. p. 823 (1928); Ramsauer and Kollath, *Ann. der Phys.* (5) iii. p. 535 (1928): iv. p. 91 (1930).
‡ Jones, *Phys. Rev.* (2) xxxii. p. 459 (1928).

and takes place over only a small range of velocities. In the case of nitrogen, which gas undoubtedly predominated in the present experiments, no marked peculiarities were observed by Ramsauer. It is true that the conditions of the experiments in the cases cited were quite different from those of the present work and from conditions prevailing in the Heaviside layer. In the former case well-defined beams of electrons having velocities comprised within a narrow range were used, while in the latter instances the electron velocities are distributed according to the Maxwell law. This case has also been considered by Langmuir and Jones*, who find no more than 10 per cent. discrepancy between observed and kinetic theory values of electronic mean free path, although in this work the electron speeds were somewhat higher than those prevailing in the present investigation.

The assumption of Ponte and Rocard that the molecular polarization is correctly calculable from dielectric constant data is probably at the root of the discrepancy between their theory and experiment. These data are available only for steady electric fields or alternating fields of long time period compared with the time in which a molecule is in the field of an electron travelling with a few volts of energy. The electron velocity was taken into account in determining whether a given polarized molecule would attract the polarizing electron to make a collision, but it was not realized that in dealing with very short time intervals the electric moment is itself a function of the velocity of the electron, and is smaller the faster the approaching electron. In the case of permanent dipoles, the rotation into the direction of the electron is, on account of the moment of inertia, a function of electron velocity. There is some experimental evidence in support of this conjecture, for Ramsauer, working with very slow electrons (less than 1 volt) finds a tendency for some gas-molecules to present very large target areas, *i. e.*, the electronic mean free paths are very short. At normal temperatures, however, there are comparatively few electrons with such velocities.

* Phys. Rev. (2) xxxi. p. 357 (1928).

LXXXV. *Theory of Heat Conduction and Convection from a Low Hot Vertical Plate. By* W. S. KIMBALL *and* W. J. KING, *Michigan State College, East Lansing, Mich., and General Electric Company, Schenectady, N.Y.**

THIS paper is a mathematical theory of heat conduction and convection from a low hot vertical plate in air. Heat transfer by radiation is not considered. It is hoped that exhaustive treatment of this simplest case will open the way for adequate theory of heat transfer from more complicated structures. It is assumed that heat transfer takes place by pure conduction through gas in stream line motion. This assumption restricts the applicability of this theory to low vertical plates not more than about 2 feet high. For experiment shows † that above this limiting height turbulence sets in and the state of affairs is quite different from that described here.

Outstanding recent contributions to the subject are the Langmuir Film Theory ‡ and Rice's § development of it by dimensional analysis. The gist of the film theory is that heat transfer laws etc. are exactly what they would be in case of pure conduction across a stationary film of gas having uniform (in the vertical plate case) thickness determined by the measurable physical constants that apply. The Langmuir Theory deals with resultant effects, and does not purport to include the details of the mechanism of heat transfer across this film; and the associated idea of pure conduction across the included stationary gas is a useful but hypothetical physical picture quite distinct from the actual physical details.

The present treatment, on the other hand, is a detailed analysis based on the actual gas temperature and velocities inside an actual film having for outer boundary an isothermal surface at temperature halfway between the hot surface and the ambient air, and which approaches the equivalent Langmuir film of uniform thickness asymptotically as the height increases.

The experimental basis used to check it is very recent (within three years), and thorough work by E. Schmidt ‖, of
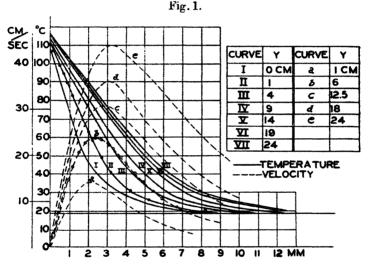
Danzig, Germany, and Nusselt and Jurges *, of Dresden, Germany. Schmidt's measurements are given in fig. 1, from which the isotherms of fig. 2 have been plotted. Although Nusselt and Jurges did not measure the velocities directly, their results are in qualitative agreement with those of Schmidt. In fig. 4 the mean temperature opposite the height (H) of the plate is calculated from the measured temperature field by means of the equation

$$t_m = \frac{1}{H} \int_0^H t \, dy.$$

Fig. 1.

CURVE	Y	CURVE	Y
I	0 CM	a	I CM
II	I	b	6
III	4	c	12.5
IV	9	d	18
V	14	e	24
VI	19		
VII	24		

—— TEMPERATURE
----- VELOCITY

Temperature and velocity fields in the air over a heated vertical plate 25 cm. high (from Schmidt).

The mean velocity curve is calculated from a relationship between temperature and velocity, which they derived from theoretical considerations.

In the following analysis the mode of treatment is novel in that it involves, besides the simplified hydrodynamic equations, two approximate empirical laws.
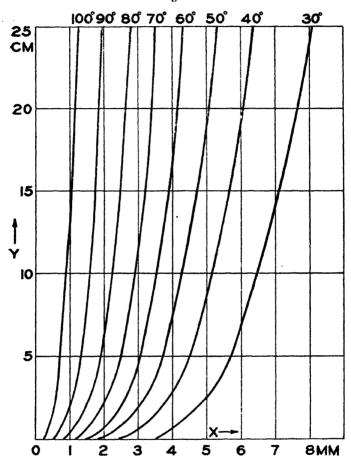
Law I.—The locus of the maxima of the velocity curves is an isothermal surface whose temperature

$$T_m = \frac{T_1 + T_0}{2}$$

* W. Nusselt and W. Jurges, *Zeits. des V. D. I.* lxxii. p. 597 (1928).

is halfway between that of the hot plate and the ambient air.

Fig. 2.
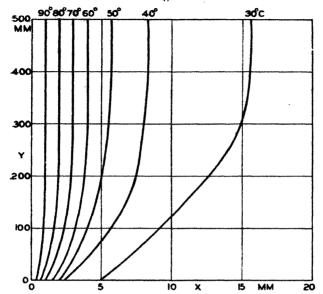
Isotherms in the temperature field over the plate.

It is a striking *experimental* fact (apparently) that this isothermal T_m, halfway between T_1 and T_0, has on it the maxima of all the velocity curves.
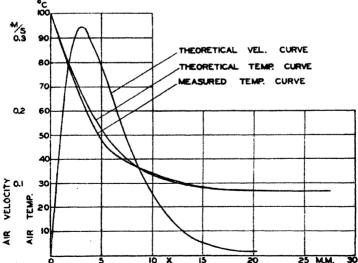
Within this surface the temperature gradient, like that for pure conduction, is constant (for each value of the height

Fig. 3.

Isotherms for a plate 50 cm. high (from Nusselt and Jurges).

Fig. 4.

THEORETICAL VEL. CURVE

THEORETICAL TEMP. CURVE

MEASURED TEMP. CURVE

Mean temperature and velocity curves for the 50 cm. plate
(from Nusselt and Jurges).

3 M 2

y), *i. e.*, $T = T_1 - ax(1 + be^{-xy})$ is the empirical expression for temperature inside the surface, where a, b, and α are constants, two of them determined below. Hence the surface is taken as the boundary of the " film " (a modification of the Langmuir film since the present one is of variable thickness).

Law II.—Half the heat is convected up away inside this film and half outside.

The equations for the isothermal surfaces within the film are given by solving the above temperature expression

$$x = \frac{T_1 - T}{a(1 + be^{-\alpha y})}.$$

The equation for the film boundary is the special case of the above, where $T = \dfrac{T_1 + T_0}{2}$:

$$x_m = \frac{T_1 - T_0}{2a(1 + be^{-\alpha y})} \quad . \quad . \quad . \quad . \quad (1)$$

The empirical temperature expression

$$T = T_1 - ax(1 + be^{-\alpha y})$$

satisfies a differential equation,

$$-K\left(\frac{d^2T}{dx^2} + \frac{d^2T}{dy^2}\right) = \frac{cdT}{dy}, \quad . \quad . \quad . \quad (2)$$

which differs from the classical heat equation for the case in hand *only* in that $c = \alpha K$ (where K is the conductivity coefficient), being approximately constant, instead of $c = \dfrac{3}{2} knv$

the convection energy flux density per degree which varies from zero at the hot plate to a maximum at the film boundary. It is not yet determined why the classical heat theory, which seems to be applied correctly, does not fit the experimental facts as represented by the above empirical expression for temperature. If we take $K = 27 . 10^2$ for the conductivity coefficient in c.g.s. units (see below, p. 901), and the experimental value of α as between ·3 and ·08 (see experimental check at the end), then $c = \alpha K$ is a constant between 200 and 1000 c.g.s. units in magnitude ; on the other hand, the value of c called for by the classical theory, $c = \dfrac{3}{2} nkv = \dfrac{3pv}{2T}$, ranges from zero at the hot plate to about $28 . 10^4$ c.g.s. units at the film boundary, where $v = 44$ cm./sec. (using $T = 340$ at the

latter place, see table of constants, p. 901). The experimental value of c is seen to be a fair average (as regards order of magnitude) between the extremes of zero and $28 \cdot 10^4$ of the classical heat equation ; but the fact that it is constant rather than variable can scarcely be accounted for by turbulence, since the following analysis is based on stream-line conditions and affords excellent experimental checks. Rather this constancy of $c = \alpha K$ seems to indicate the need for some modification of the classical theory as applied to heat transfer within the film.

The fundamental equations of hydrodynamics are simplified by neglecting *within* the film inertia effects, second order velocity effects. and horizontal velocities, and using the gas law. One force equation is then left :—

$$-\eta \frac{\partial^2 v}{\partial x^2} = n_0 mg - nmg = mg(n_0 - n). \quad . \quad . \quad (3)$$

The right member is the buoyancy (molecular mass times the acceleration of gravity is multiplied by the difference in molecular concentration at temperature T and at ambient temperature T_0). The left member is the viscous drag (coefficient of viscosity multiplied by the second derivative of the velocity) *.

THEOREM I.—*The rate of doing work per unit volume by the buoyancy is proportional to the rate of heat transfer through unit area.*

If we use the gas law $p = nk\mathrm{T}$ (p is the pressure, n the molecular concentration, k Boltzmann's constant, and T the absolute temperature) the above equation can be written

$$-\eta \frac{\partial^2 v}{\partial x^2} = mg(n_0 - n) = \frac{mgp}{k\mathrm{T}_0} \frac{\mathrm{T} - \mathrm{T}_0}{\mathrm{T}}. \quad . \quad . \quad (3)$$

If v is the velocity of the convection currents the rate of doing work by the buoyancy force is the product of v by the above force equation :

$$\frac{mgp}{k\mathrm{T}_0} \left(\frac{\mathrm{T} - \mathrm{T}_0}{\mathrm{T}} \right) v = \text{rate of work per unit volume by the buoyancy} \quad . \quad . \quad (4)$$

Compare this rate with the rate of heat convection through unit area. This comprises the excess of molecular energy of a molecule where T is the temperature over the molecular

* Lehigh Page, ' Introduction to Theoretical Physics,' p. 230.

energy for the ambient temperature $\frac{3}{2}k(\mathrm{T}-\mathrm{T}_0)$ multiplied by nv, the concentration times the velocity of flow :
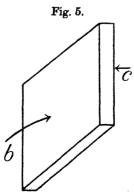
$$\frac{3}{2}k\,(\mathrm{T}-\mathrm{T}_0)\,nv=\frac{3}{2}\,p\,\frac{(\mathrm{T}-\mathrm{T}_0)v}{\mathrm{T}}\;.\;\;.\;\;.\;\;.\;\;(5)$$

This is seen to be proportional to the rate per unit volume of doing work by the buoyant forces, and about a million times larger $\left(\text{proportionality factor is }\dfrac{mg}{\frac{3}{2}k\mathrm{T}_0}\right)$.

It is noteworthy that the buoyant forces are the *sole* forces that push the gas upwards in convection currents, being opposed by viscous drag and inertia effects (gravity is included in the buoyancy). If the inertia effects are negligible, then, according to (3) and Theorem I., the rate of doing work against viscosity is proportional to the rate of heat transfer. This is in accord with the famous proportionality of Osborne Reynolds between fluid friction and heat transfer, which is thus where (3) and (5) apply put on an exact basis. This proportionality, however, between viscous drag and heat transfer is seen not to hold where inertia effects prevent the validity of (3). On the other hand, the rate of doing work by the buoyancy (4) is always proportional to the rate of heat transfer (5) wherever the gas law and stream line conditions prevail.

THEOREM II.—*The viscous forces operating in gas in a steady state form a mechanical couple, and hence their sum is always zero. Viscosity's sole mechanical effect is that of a couple : it passes on the reactions from place to place within the gas or to the walls of the container, together with a corresponding torque.*

Consider a vertical slice of unit cross-section and thickness dx :

Fig. 5.

$$-\eta \frac{dv}{dx_b} = \text{viscous drag down at the left.}$$
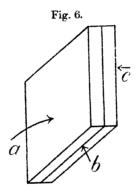
$$\eta \frac{dv}{dx_c} = \text{viscous drag up at the right.}$$

$$\eta \left(\frac{dv}{dx_c} - \frac{dv}{dx_b} \right) = \frac{d}{dx} \eta \left(\frac{dv}{dx} \right) dx = \eta \frac{d^2v}{dx^2} dx$$

is the excess force down at the left over that up at the right, being the resultant downward drag that balances the buoyancy, $mg(n-n)dx$, of the slice according to (3). If $\frac{d^2y}{dx^2}$ were zero, the viscous drag would have no effect on balancing buoyancy *within* the gas.

Now consider two similar slices together, each of thickness dx and unit area :

Fig. 6.

$$-\eta \frac{dv}{dx_a} = \text{viscous drag down at left of first slice.}$$

$$\eta \frac{dv}{dx_b} = \text{viscous drag up at right of first slice.}$$

$$-\eta \frac{dv}{dx_b} = \text{viscous drag down at left of second slice.}$$

$$\eta \frac{dv}{dx_c} = \text{viscous drag up at right of second slice.}$$

Evidently the resultant effect of the viscous drag between the slices on surface b is zero, due to action and reaction. Likewise other slices may be considered on each side of those depicted, and the total effect is solely to pass along the reactions to the hot plate at the left of the film. The

summation of these effects between the hot plate and film boundary gives

$$-\int_0^{x_m} \eta \frac{d^2v}{dx^2}\, dx = \eta \frac{dv}{dx_1} = mg\, \overline{(n_0 - n)}\, x_m. \quad . \quad . \quad (6)$$

Here the integral vanishes at the upper limit, where the slope of the velocity curves is zero, and the right member is readily understood to be the total buoyancy (for unit cross-section) between hot plate and film boundary, and $\overline{n_0 - n}$ is the mean value of the concentration difference. The middle term is the viscous upward pull per unit area on the hot plate, being equal in magnitude and direction to the total buoyancy. Thus the buoyancy is not really balanced by viscosity, but its effect is merely transferred from within the gas to the wall of the hot plate where the equivalent mechanical upward thrust operates without diminution. Viewed as a couple $\eta\left(\dfrac{dv}{dx_1}\right)$ is the upward viscous force (positive) at the hot plate, and

$$\int_0^{x_m} \eta \frac{d^2v}{dx^2}\, dx$$

is the sum of the downward reactions (negative) throughout the gas, being equal and opposite to the former; and besides this there is, of course, the corresponding torque.

Consider now the effect of viscosity outside the film. At the point of inflexion of the velocity curve the second derivative is zero and since the buoyancy is obviously different from zero we see that equation (3) does not apply, and we must add an inertia term:

$$mg\, (n_0 - n) = -\eta \frac{d^2v}{dx^2} + mnv \frac{dv}{dx} \quad . \quad . \quad . \quad (7)$$

Assuming this to be the vertical force equation, integrate between film boundary x_m and the point of inflexion x_f:

$$mg\, \overline{(n_0 - n)}\, (x_f - x_m) = -\eta \frac{dv}{dx_f} + mnv \overline{\frac{dv}{dx}}(x_f - x_m) \, . \quad (8)$$

The left member is the total buoyancy per unit cross-section and the right member is the balancing downward pull of

viscosity plus inertia working together in the same direction. Now integrate (7) between the limits infinity and x_f:

$$mg\overline{(n_0 - n)}(\infty - x_f) = \eta \overline{\frac{dv}{dx_f}} + mnv\overline{\frac{dv}{dx}}(\infty - x_f) ; \qquad (9)$$

$$\text{or} \quad mg(n_0 - n)(\infty - x_f) - \eta \frac{dv}{dx_f} = mnv\overline{\frac{dv}{dx}}(\infty - x_f). \quad . \quad (10)$$

Between these limits $\frac{d^2v}{dx^2}$ is positive, and so the viscous drag per unit volume is up rather than down. That is to say, viscosity is pulling up over this interval and is helping the buoyancy to react against the now large inertia term. Thus each term in the left member of (10) is now positive $\left(\frac{dv}{dx_f} \text{ is minus}\right)$ and represents upward force, whereas the right member corresponds to the downward inertia reaction. Now add equations (8) and (9), cancelling out viscosity :

$$mg(n_0 - n)(x_f - x_m) + mg\overline{(n_0 - n)}(\infty - x_f) = mnv\overline{\frac{dv}{dx}}(x_f - x_m)$$

$$+ mnv\overline{\frac{dv}{dx}}(\infty - x_f). \quad (11)$$

The left member is the total buoyancy between film boundary and infinity and the right is the total balancing inertia, and the equation shows by cancellation of vertical viscous forces how viscosity contributes nothing, according to Theorem II., towards balancing buoyancy except torque. Its sole effect is to pass on the extra buoyancy of (8), where the gas is hot, to help pull up the cold gas where (9) and (10) apply. Viewed as a mechanical couple the downward viscous forces represented by the viscous term of (8) are equal and opposite to the upward viscous forces beyond the point of inflexion x_f represented by the viscous term of (9), the former being balanced by buoyancy and the latter by inertia. Although this theorem is illustrated by differential equations referring to a special case, the reasoning is general and can probably be extended to other cases, and hence the theorem may be one of general application.

Corollary —The total buoyancy is always balanced by inertia effects plus a downward pull by the walls of the container equal and opposite to the viscous drag on them.

Application of the Laws.

The integration of the force equation, expanding in series and using second order terms, and using Law I. to determine the constant of integration $\left(\dfrac{dv}{dx}=0 \text{ when } x=x_m \text{ according to (1)}\right)$, gives

$$v = B(x^3 - Cx^2 + Dx) \quad \left\{ \begin{array}{l} \text{where } B = \dfrac{pmga(1+be^{-\alpha y})}{6k\eta T_1{}^2}, \\[2mm] \text{and } C = \dfrac{6T_1}{T_0} x_m, \\[2mm] \text{and } D = x_m{}^2 \dfrac{12T_1}{T_0}\left(\dfrac{1-T_0}{4T_1}\right). \end{array} \right. \quad (12)$$

The maximum value of v for changes in x is (substitute (1))

$$v_m = \frac{pmg(T_1 - T_0)^3}{12k\eta T_0 T_1 a^2(1+be^{-\alpha y})^2} \quad \cdot \quad \cdot \quad \cdot \quad (13)$$

$$\left(\text{taking } \tfrac{1}{2} - \frac{T_0}{6T_1} = \tfrac{1}{3}, \text{ for } T_0 = 293, \ T_1 = 383 \right).$$

The heat conduction per unit area at the hot plate is

$$q = -K \frac{\partial T}{\partial x} = Ka(1 + be^{-\alpha y}).$$

$q = h(T_1 - T_0)$ where K is the conductivity coefficient, h the heat transfer coefficient, and a, b, and α are constants; a and α are expressed below in terms of physical constants, whereas b is purely experimental as yet.

The total heat convected away (per unit plate width) is then

$$\overset{\text{L=height of plate.}}{Q = \int_0^L q\,dy = K\int_0^L a(1+be^{-\alpha y})dy.}$$

$$Q = Ka(L + \tfrac{b}{\alpha}(1-e^{-\alpha L})).$$

We take, according to Law II.,

$$KaL = Ka\frac{b}{\alpha}(1 - e^{-\alpha L}), \quad \cdot \quad \cdot \quad \cdot \quad \cdot \quad (14)$$

since KaL is the heat transferred to beyond the film, and $Ka\dfrac{b}{\alpha}(1-e^{-\alpha L})$ is the excess supply of heat at lower part due

to larger temperature gradient down there, being convected up through the film. The theoretical justification for (14) is tied up with the theoretical incompleteness of (2), involving convection up through the film. Equation (14), like (2), is thus to be taken as an experimental fact, checked below by theory and experiment. We may, however, interpret the equivalence of KaL and $\frac{Q}{2}$ (which is (14)) by reliance on the Langmuir film concept, that actual rates of heat transfer, heat transfer coefficients, etc. are exactly what they would be if the heat were transported away from a hot body by pure conduction across a film of practically stationary gas, and of thickness determined by the conditions of the problem. For our hot plate we have thus

$$Q = KL \frac{(T_1 - T_0)}{d} \quad . \quad . \quad . \quad . \quad . \quad (15)$$

And since Q, K, L and the temperatures are actual measureable physical quantities, the film thickness d, so determined by them, is a very real and useful concept, being for the case in hand the space interval that would correspond to the entire temperature drop between hot plate and ambient air, so as to give $\frac{T_1 - T_0}{d} = \frac{dT}{dx}$, the right magnitude needed to take care of Q according to the above equation. The physical picture of the hypothetical state of affairs within the (very actual) film thickness d is that of pure conduction, *i. e.*, $\frac{dT}{dx}$ is constant hence $\frac{d^2T}{dx^2} = 0$, and hence no loss of heat occurs *en route* in process of transmission of heat by conduction from hot plate to film boundary. Hence the left member of (15) represents (according to the hypothetical physical picture) heat transferred across the film to the gas *beyond* it and disposed of there. The fact that only part of Q is actually transported to the region beyond and outside the film does not impair, of course, the usefulness of the hypothetical physical picture, with its associated actual value of d, the film thickness determined by (15).

Now divide (15) by 2, retaining this hypothetical physical picture of pure conduction across a film of thickness d:

$$\frac{Q}{2} = \frac{KL}{d} \left(\frac{T_1 - T_0}{2} \right). \quad . \quad . \quad . \quad (16)$$

This shows that if half the total temperature drop took place

between hot plate and Langmuir film boundary $x = d$, then in case of pure conduction half the total heat would be transported beyond the film. Conversely, if we have $\frac{Q}{2}$ units of heat transported by pure conduction beyond a plane $x = $ const., where the temperature drop from the hot plate is half the total temperature drop, then that surface is the Langmuir film boundary $x = d$. Now this latter situation just fits the case in hand, for experiment shows by Law II. that $\frac{Q}{2}$ units of heat are carried off outside a plane surface $x = \dfrac{T_1 - T_0}{2a}$ (our film thickness at the top), which, when substituted for d in (16), gives KaL for (16)'s right member, being the heat transported by pure conduction beyond $x = d$, having half the total temperature drop.

Thus $x = d = \dfrac{T_1 - T_0}{2a}$ is the Langmuir film boundary as checked below by both theory and experiment. Thus heat transferred to the gas from the hot plate has a dual aspect:
(*a*) KaL (the right member of (16)) represents pure conduction beyond the Langmuir film $x = \dfrac{T_1 - T_0}{2a}$, whereas

(*b*) $Ka\dfrac{b}{\alpha}(1 - e^{-aL})$ is convected up away within this plane surface $x = \dfrac{T_1 - T_0}{2a}$. Therefore

$$Q = 2KaL \text{ is the total input of heat}$$

Half the output is, by Law II.,

$$\frac{3}{2}\int_0^{x_m} k(T - T_0)\, nv\, dx = \frac{1}{28}\frac{p^2 mg(T_1 - T_0)^5}{k\eta T_0 T_1^2 a^3 (1 + be^{-aL})^3} = \frac{Q}{2} \text{ at } y = L ;$$

$$\therefore \quad KaL = \frac{1}{28}\frac{p^2 mg(T_1 - T_0)^5}{k\eta T_0 T_1^2 a^3 (1 + be^{-aL})^3}.$$

Solving for $a = \left(\dfrac{p^2 mg(T_1 - T_0)}{28\, k\eta T_0 T_1^2(1 + be^{-aL})^3 KL}\right)^{1/4} (T_1 - T_0).$

$$\cdots \quad (17)$$

Therefore

$$Q = 2KaL = \left(\frac{16\, p^2 mg(T_1 - T_0)\, (KL)^3}{28\, k\eta T_0 T_1^2(1 + be^{-aL})^3}\right)^{1/4} (T_1 - T_0).$$

This checks the 5/4 power law for variation of heat transferred with temperature difference $(T_1 - T_0)$.

Since $q = Ka\,(1 + be^{-ay}) = h\,(T_1 - T_0)$, we have for the heat transfer coefficient

$$h = \frac{Ka}{T_1 - T_0}(1 + be^{-ay}) = K^{3/4}$$

$$\left(\frac{p^2 mg(T_1 - T_0)}{28k\eta T_0 T_1{}^2(1 + be^{-aL})^3 L}\right)^{1/4}(1 + be^{-ay}),$$

which seems to check known data.

Using the above value of a gives for the maximum convection velocity at the top of the plate, where $y = L$,

$$v_m = \frac{5}{12}\sqrt{\frac{mg(T_1 - T_0)KL}{k\eta T_0(1 + be^{-aL})}}, \quad \cdots \quad (18)$$

which checks the experimental data of Schmidt. If we use the above value of a in the first derivative of v given by (12), taking $x = 0$, we get the slope of the velocity curves at the hot plate :

$$\frac{dv}{dx_1} = \cdot 93\left(\frac{mg(T_1 - T_0)(1 + be^{-aL})}{k\eta T_0}\right)^{3/4}\sqrt{\frac{p}{T_1}}\frac{(KL)^{1/4}}{(1 + be^{-ay})} \quad (19)$$

(here $1 - \dfrac{T_0}{4T_1} = \cdot 87$).

Note that this velocity slope at the hot plate, and hence the vertical viscous drag per unit area there, varies, among other factors, as the three-quarters power of the temperature difference between the hot plate and ambient air.

Equations (18) and (19) may be used as a check on the validity of equation (3) as applied to the case in hand, from which they are derived by integration. Using c.g.s. units, we have for the case of air at atmospheric pressure

$p = 1 \cdot 013 \cdot 10^6,$ $k = 1 \cdot 37 \cdot 10^{-16},$ $\eta = 2 \cdot 00 \cdot 10^{-4},$

$m = 46 \cdot 5 \cdot 10^{-24},$ $T_1 = 383,$ $T_0 = 293,$

$g = 980,$ $K = 2272\sqrt{\dfrac{383}{273}} = 2720,$ $a = 91,$

$T_1 - T_0 = 90$, and taking $b = 2$; $(1 + be^{-b}) = 1 \cdot 278$ (see below). Substituting these constants in (18) gives for v_m, the maximum convection velocity at the top of the plate, a value of about 46 cm./sec. This is almost too good a check on the 44 cm./sec. shown in Schmidt's graph. For $b = 5$, v_m comes to the value 51 cm./sec. It will readily be understood that neglect of inertia forces in equation (3) within the film

accounts for the slightly increased values of v_m, as we shall show in more detail below, and the fact that v_m is so close to 44 cm./sec. is an excellent check on the present theory.

Now substitute these constants in (19), or, perhaps easier in the first derivative of (12), taking $a = 91$, and obtain for the slope of the velocity curve at the top of the hot plate a value of about 450 cm./sec./cm. We may compare this with the average slope of the velocity curve within the film obtained roughly by dividing 44 cm./sec. by the thickness of the film ·33 cm., *i.e.*, 133 cm./sec./cm. It will be seen by examination of Schmidt's graphs that they indicate to the extent justified by the data that the slope at the hot plate is for the upper curve three or four times the average slope 133, being hence not so far from the 450 given by the present theory. Since the present theoretical values of v_m, $\dfrac{dv}{dx_1}$ and $\dfrac{dv}{dx}$ average, agree relative to each other as well as in order of magnitude with the corresponding experimental quantities obtained from Schmidt's graphs, we infer that the shape of the theoretical curves matches the shape of the experimental curves, and that the differential equation (3) from which the former spring is thoroughly justified. Incidentally it is to be noted that $\dfrac{dv}{dx_1} = 450$ when multiplied by the coefficient of viscosity gives the viscous drag per unit area at the hot plate. Hence the experimental and theoretical values of this force check one another. Using the above value of η gives this force as about ·09 dynes per sq. cm.

More detailed checks are obtained by substituting the above physical constants in equation (3) in the form

$$\eta \frac{d^2 v}{dx^2} = \frac{pmg}{kT_1^2}\left(a(1 + be^{-\alpha y})x - \frac{T_1}{T_0}(T_1 - T_0)\right) = mg(n - n_0), \quad (3)$$

which was integrated to get (12). Taking $x = 0$ gives the buoyancy per unit volume at the hot plate, *i. e.*, $\eta \dfrac{d^2 v}{dx_1^2} = ·27$ dynes/c.c., and since *there* the convection velocity is zero and hence the inertia is zero, this is exactly equal to the viscous drag per unit volume there. To get the buoyancy per unit volume at the film boundary, where $x = x_m$, we substitute (1) in (3) above, and taking $\left(1 - \dfrac{T_0}{2T_1}\right) = \dfrac{17}{27}$ and using the

previous physical constants, we get $\eta \dfrac{d^2v}{d r_m^2} = \cdot 17$ dynes per c.c.

The average of $\cdot 22$ for these buoyancies when multiplied by $(\cdot 4+)$, the film thickness, is seen to give approximately the above $\cdot 09$, the viscous upward drag at the hot plate according to Theorem II., which is thus checked numerically.

We may compare the buoyancy per unit volume at the film boundary with the inertia at the same place. Here obviously, from the graphs, this latter is greater than it is nearer the hot plate. Since a steady state prevails, time does not appear explicitly in the inertia terms, and they are all negligible for the case under consideration, except perhaps the type

$$I_m = nmv \frac{dv}{dy} = \frac{pmv}{kT_m}\frac{dv}{dy}, \quad \cdot \quad \cdot \quad \cdot \quad \cdot \quad (20)$$

where the subscript m is used to indicate that the temperature refers to the film boundary. Taking $T_m = 350$, and from the graph $v = 44$ and $\dfrac{dv}{dy} = \dfrac{4}{3}$, and using the above physical constants, gives $I_m = \cdot 059$ dynes per c.c. This *largest* value of the inertia reaction is seen to be about one-third of $\cdot 17$, the *smallest* buoyancy term which is at the same place, which we have set by (3) equal to the viscosity. This shows that the inertia term, though small at the top of the plate, is not negligible, and indicates why our maximum velocity of 46 to 51 cm./sec. exceeded the experimental one of 44 cm./sec. If the inertia reactions were balancing one-third the buoyancy *everywhere* between hot plate and film boundary the viscosity would have only 2/3 of the buoyancy left to balance, so that the buoyancy member of (3) would need to be multiplied by 2/3 to give correct results. Since, however, the buoyancy member of (3) needs only to be multiplied by about 11/12 to check the experimental v_m (11/12 of 48 equals 44), it appears that only 1/12 of the total buoyancy forces between hot plate and film boundary is balanced by the corresponding inertia reactions. These numerical conclusions refer of course to the top of the plate which supplied the data, and thoroughly justify the use of (3) in this region.

These considerations show how the method of successive approximations may be used if a more accurate expression for v than (12) is needed, *i. e.*, integrate (7) instead of (3), substituting (12) and its derivative in the inertia term corresponding to (20). Furthermore, we may check the

applicability of (7) *beyond* the film at the point of inflexion, where $\dfrac{d^2v}{dx^2} = 0$, and hence the viscous drag per c.c. is zero, and the buoyancy must balance the inertia. If we eliminate the n's by means of $p = nkT = n_0 kT_0$, and factor out $\dfrac{mp}{kT}$ from both sides of (7) (without the viscosity term), there remains

$$g\,\frac{(T - T_0)}{T_0} = v\,\frac{dv}{dy}.$$

Now refer to Schmidt's graphs and take $v = 25$ and $T - T_0 = 15$ at the point of inflexion of the upper velocity curve. Substituting above gives $\dfrac{15g}{T_0} = 49 = 25\,\dfrac{dv}{dy}$, which requires $\dfrac{dv}{dy}$ to be about 2, a value which checks the graph fairly well.

Using the above a in the expression x_m for film thickness gives

$$x_m = \frac{T_1 - T_0}{2a(1 + be^{-\alpha y})} = \left(\frac{28\,k\eta T_0 T_1^2 (1 + be^{-aL})^3 KL}{16\,p^2\,mg(T_1 - T_0)}\right)^{1/4} \frac{1}{(1 + be^{-\alpha y})}.$$

This checks the data for variation of film thickness with temperature difference (inversely as the quarter power).

We may express Q in terms of the film thickness x_m (see equation (1)) at the top of the plate where $y = L$:

$$Q = 2KaL = \frac{KL(T_1 - T_0)}{x_m(1 + be^{-aL}}\,,$$

which may be written

$$Q = \frac{KL(T_1 - T_0)}{d}\,,$$

where $d = x_m(1 + be^{-aL}) =$ thickness of the equivalent Langmuir film, *i.e.*, the equivalent film of constant thickness. This shows that $2a = \dfrac{T_1 - T_0}{d}$. Therefore, a is one-half the temperature gradient of the equivalent Langmuir film.

The above results check the numerical experimental data.

$$a = \frac{106}{(1 + be^{-b})}$$

$= 91$ if $b = 2$ and $= 102$ if $b = 5$ (using the approximation

$b = aL$, which is (14) when the exponential term is neglected).
Referring to Schmidt's paper,

$$T_1 = 383,$$
$$T_0 = 293,$$
$$T_1 - T_0 = 90:$$

$$\therefore \quad x_m = \frac{T_1 - T_0}{2a(1 + be^{-ay})},$$

taking $b = 2$;

$$\therefore \quad x_m = \frac{45}{91(1 + 2e^{-.08y})},$$
$$x_m = .165 \text{ at } y = 0,$$
$$= .38 \text{ at } y = L,$$
$$= .49 \text{ at } y = \infty \ ;$$

this latter is the thickness of the equivalent Langmuir film.
Taking $b = 5$,

$$x_m = \frac{45}{102(1 + 5e^{-2y})},$$
$$x_m = .077 \text{ at } y = 0,$$
$$x_m = .44 \text{ at } y = L = 25,$$
$$x_m = .44 \text{ at } y = \infty,$$

thickness of the equivalent Langmuir film.

The Theory checks

    I. The numerical values of a.

    II. The 5/4 power law $Q \propto (T_1 - T_0)^{1/4}$.

    III. The maximum velocity is independent of pressure and proportional to $(T_1 - T_0)^{1/2}$.

    IV. Film thickness varies inversely as fourth root of temperature difference

$$x_m \propto \frac{1}{(T_1 - T_0)^{1/4}} \ .$$

    V. Heat transfer coefficients are proportional to the square root of the pressure

$$h \propto \sqrt{p}.$$

    VI. The thickness of the equivalent Langmuir film (uniform thickness) is

$$d = \frac{T_1 - T_0}{2a} = \left(\frac{28 \cdot k\eta T_0 T_1^2 (1 + be^{-b})^3 KL}{16 p^2 mg (T_1 - T_0)} \right)^{1/4}$$

= between .40 and .50 cms. (depending on choice of b).

VII. Law II. is checked by graphical integration to the extent justified by the data and method.

Taking the upper temperature and velocity curves shown in Schmidt's graph as applicable to the top of the plate where $y = L$, the mean values for each square shown in the graph are tabulated :—

	No. of Square.	Absolute Temp. $T=t+273$.	Temp. Diff. $T-T_0 = t-18.5$.	Veloc. v.	Temp. Ratio. $\frac{T-T_0}{T}$.	Product. $\frac{T-T_0}{T}v$.	Sum. $\left(\frac{T-T_0}{T}\right)v$.
	1	383	91·5	12	·239	2·86	
	2	370	78·5	30	·212	6·35	
	3	356	64·5	42	·181	7·60	$=18.25.$
1/5 interval	4	348	56·5	44·5	·162	1·44	
4/5 interval	4	343	51·5	44	·150	5·28	
	5	331	39·5	40	·119	4·75	
	6	321	29·5	36	·092	3·32	
	7	312	20·5	31	·066	2·04	
	8	305	13·5	27	·0445	1·20	
	9	302	10·5	23	·0348	·80	$=18.45.$
	10	299	7·5	18	·0250	·45	
	11	297	5·5	16	·0185	·296	
	12	296	4·5	13	·0152	·198	
		295	3·5	10	·0117	·117	

The sums in the right-hand column, when multiplied by $\frac{3}{2}p$, as per equation (5), give the energy flux inside and outside the film respectively, and are seen to be approximately equal.

Note.—Since the above paper was written the results of some new experimental and theoretical work on Free Convection have been published by Schmidt and Beckmann[*].

Their new temperature and velocity curves are quite similar to those of fig. 1.

The writers are much indebted to Dr. H. Poritsky, of the General Electric Company, Schenectady, N.Y., for valuable constructive criticism.

[*] E. Schmidt and W. Beckmann, *Tech. Mech. und Thermo.* i. no. 10, p. 341, and no. 11, p. 391 (1930).

LXXXVI. *A Preliminary Report on the Anomalous Variation of the Electrical Conductivity of Quartz with Temperature. By* SADAKICHI SHIMIZU, *Physical Institute of Tohoku Imperial University, Sendai* [*].

§ 1. *Introduction.*

THE variation of the electrical conductivity of dielectrics with temperature has been studied by many experimenters. Curie [†] has measured the conductivity of quartz plates, cut parallel and perpendicular to their optical axes with the temperature in a range from 7° C. to 300° C., and deduced the formula $\sigma = at^{-n}$, where σ is the conductivity, t the temperature, and a and n the constants.

Tegetmeier and Warburge [‡] have measured the electrical conductivity with a temperature up to 300° C., and reported that the axial conductivity has an electrolytic character.

Exner [§] has measured the conductivity of quartz in a temperature range 100–150° C.

Ambronn [‖] has measured the current through the quartz plate with a temperature from 166° C.–466° C., and reduced the expression of the resistivity to

$$R = A e^{\frac{B}{T-C}},$$

where A, B, C are constants and T the absolute temperature, and has given numerical values also, *i.e.*, the constant C is equal to $224 \cdot 9 \pm 2 \cdot 3$, and B lies between 1413–1586, and A has different values depending on the direction of the current with respect to the optical axis.

Joffé [¶] has measured the variation of the electric conductivity for quartz, calcite, ammonium alum, and copper-sulphate, and has found the following formula :

$$\log \sigma = \frac{A}{T} + B, \quad \ldots \ldots \quad (1)$$

where A is the nearly constant for these crystals. Assuming

the variation of the conductivity with the temperature as due to the dissociation of ions, he gets the expression of A as a function of the gitter constants of these crystals.

Doelter * has measured the resistivity of quartz in the range of the temperature 500° C.–1400° C., using the Wheatstone bridge, but no satisfactory result is obtained, especially in the temperature range 600° C.–900° C.

Recently many experimenters have made a study of the electric conductivity in relation to the temperature effect of some dielectric crystals as a part of the general investigation of conduction mechanisms; for example, N. Ussataja and B. Hochberg † have measured the electrical conductivities of dielectric crystals with temperature, such as $NaNO_3$ from 20° C. to 360° C., CaF_2 from 200° C. to 500° C., NaCl and mica from 100° C. to 500° C., and deduced the following formulæ :

$$\log \sigma = \frac{A}{T} + B \text{ for } 550° \text{C.–}600° \text{C.,} \quad . \quad . \quad . \quad (1')$$

$$\log \sigma = A_1 T + B_1 \text{ above } 650° \text{C.,} \quad . \quad . \quad . \quad (2)$$

where A, A_1, and B, B_1 are constants.

V. Seelen ‡ has measured the conduction current of rock-salt with a temperature from 15° C. to 500° C., and found that the expression of conductivity can be expressed by equation (1).

B. Hochberg and A. Walther § have measured also the variation of conductivity of rock-salt with a temperature from 25° C.–800° C., and concluded that above a temperature 550° C. the Cl ions become the carriers of the electric charge.

W. Seith ‖ has examined the conductivities of $PbCl_2$ and PbI_2, and deduced the following expressions :

$$\sigma = A e^{-\frac{Q}{RT}} \text{ for } PbCl_2, \quad . \quad . \quad . \quad . \quad . \quad . \quad (3)$$

$$\sigma = A_1 e^{-\frac{Q_1}{RT}} + A_2 e^{-\frac{Q_2}{RT}} \text{ for } PbI_2, \quad . \quad . \quad (4)$$

---

* Doelter, *Sitzungs. Kals. Wiss. Wien. Math. Nat. Kl.* cxvii. 1, pp. 845–874 (1908) ; cxix. 1, pp. 49, 11 (1910).
† N. Ussataja and B. Hochberg, *ZS. f. Phys.* xlvi. p. 88 (1927).
‡ V. Seelen, *ZS. f. Phys.* xxix. p. 125 (1924).
§ B. Hochberg and A. Walther, *ZS. f. Phys.* lxiv. p. 39 (1930).
‖ W. Seith, *ZS. f. Phys.* lvi. p. 802 (1929).

where A, A_1, A_2, and Q, Q_1, Q_2 are constants, and conclude that in the case of $PbCl_2$ its anion may be the carrier of the electric charge, and in the case of PbI_2 both ions were taken into account in considering the electrolytic conduction, and the latter case is verified theoretically by Smekal [*].

B. Hochberg and A. Walther [†] have also verified the fact that the conductivity for $NaNO_3$, SiO_2, Ag-halogenides satisfy the expression (3) for $PbCl_2$, and Na, K-halogenides satisfy expression (4) for PbI_2. On the other hand, Königsbergers and Reichenheim [‡] have studied the conduction in dielectries, as the conduction is performed by electrons instead of ions, and deduced the following formula :

$$\sigma = AT^2 e^{-\frac{B}{T}}; \quad \ldots \ldots \quad (5)$$

and also H. Saegusa [§] deduced theoretically the following expression, assuming that the electric conduction in a dielectric is performed by electrons:

$$\sigma = ATe^{-\frac{\phi}{kT}}\{1 - BT^2 e^{-\frac{\phi}{kT}} - CTe^{-\frac{\phi}{kT}}\}, \quad . \quad (6)$$

where
$$A = \frac{lce^2}{4k}A', \qquad B = 2\rho^2 A', \qquad C = \frac{2\rho e^2}{k}A',$$

k = Boltzmann constant, $\qquad \phi$ = work function,

l = mean free path, $\qquad$ A, A', B, C = constants.

ρ = density,

From the above mentioned results we cannot find any discontinuous variation of electrical conductivity of dielectrics with respect to temperature, and especially for the $\alpha - \beta$ transformation temperature of quartz. In the present investigation, we have studied the variation of electrical conductivity of quartz with temperature in a somewhat wider range than those of the above-mentioned physicists, and have considered especially whether any discontinuous variation of conductivity occurs or not at the transformation temperature.
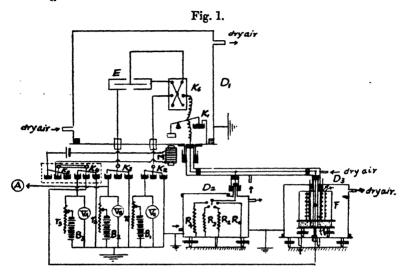
* A. Smekal, *ZS. f. Phys.* lviii. p. 322 (1929).
† B. Hochberg and A. Walther, *l. c* (9).
‡ Königsbergers and Reichenheim, *Phys. ZS.* vii. p. 570 (1906); viii. p. 833 (1907).
§ H. Saegusa, 'Sci. Report of the Tohoku Imperial University,' I. vol. xv. no. 6, p. 795 (1926).

§ 2. *Apparatus and the Methods of the Experiments.*

The main part of the apparatus of the experiment is shown in fig. 1.

Fig. 1.

The symbols in the figure are as follows :—

E, Dolezalek quadrant electrometer.

K_1, K_2, K_3, K_4, K_5, K_6, keys.

M, electromagnet to cut the circuit from the earth.

V_A, precision voltmeter for measuring the applied voltage.

V_B, precision millivoltmeter for measuring the potential of one pair of the quadrants.

V_C, precision voltmeter for measuring the needle potential or the quadrant potential.

r_1, r_2, r_3, resistances to reduce the battery voltage.

R_0, R_2, R_3, R_4, standard resistances for producing the potential fall of the current from the specimen to the earth.

F, electric furnace including the specimen.
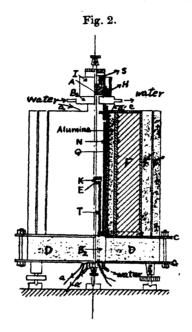
D_1, D_2, D_3, metallic boxes enclosing the apparatus.

As is seen from this figure, the leading wire from the specimen to the electrometer is enclosed entirely with metallic boxes to prevent any external influences.   The dry air which passes through the pure sulphuric acid and P_2O_5 is forced into the metallic boxes D_1, D_2, D_3, and P_2O_5 and

H_2SO_4 are placed in the spare spaces of the boxes, and the equilibrium state is kept with a vapour pressure of P_2O_5.

The variation of the zero point of the electrometer which comes from the geometrical irregularities of the needle due to the temperature difference from day to night is prevented

Fig. 2.

The symbols in the figure are as follows :—

A, supporter of the leading wire made of ambroid.

B_1, B_2, water-cooling tubes made of copper.

C, concentric copper cylinder to prevent external influences.

D, fireproof brick to prevent the dissipation of heat inside the furnace.

E, nickel electrodes supporting the specimen.

H, mercury, which serves for the electrical coupling.

I, iron case.

K, quartz test specimen.

N, concentric cylinder made of nickel to keep the temperature of its interior uniform.

S, spring.

T, thermo-junction made of Pt and Pt-rhodium.

by maintaining constant temperature outside of the box D_1 by using a thermostat made of wood and nichrome wire. The constancy of the temperature is such that its variations is about 1 degree within 10 hours. K_4 is made of ambroid and ebonite with particular precautions, and its insulation is maintained as well as the other supports of the circuit ; thus the leakage of the charge from this switch is prevented as much as is possible. When the accumulating charge is small we connect the specimen with one pair of quadrants, and when it is large we connect the specimen with the needle of the electrometer. In the latter case interaction between the applied potential and the measuring charge is prevented completely.

To get rid of the induction effect due to the measuring potential of the specimen a special switch is used, *i. e.*, the switches K_4, K_5 are coupled together, and it consists of the mercury column and the spring; by operating K_4, K_5 instantaneously after the measuring potential is given to the specimen, the electrometer side is momentarily earthed and then disconnected from the earth.

When the battery which serves for the magnet M varies its potential the force which moves the switch K_1 also varies, so that we take care especially concerning the battery potential.

When the temperature increases we measure the potential difference of standard resistances R_0, R_1, . . . R_4 due to the current from the specimen to the earth passing through them, using a dial switch made of ambroid and ebonite with special precautions.

The electric furnace heating the specimen is shown in fig. 2.

The electrodes and the guard ring of the specimen are platinized by spluttering, under the same conditions. After spluttering both sides of the specimen are earthed more than 200 days, and the effect of previously applied potential of spluttering was removed completely. The leading wire is a very thin nickel wire, because small conducting area prevents the effect of the heat. Since the mixed phases of α and β quartzes exist at 573° C., and therefore the temperature gradient in the specimen produces a twin, especially during cooling, we diminish the electrode mass, and spend a sufficiently long time to reach the equilibrium state. The earth of the guard ring is composed of three nickel springs, and one part of a thermo-junction is also used for the earthing. The electrodes are made of nickel, which are

supported by a silica tube, and the silica tube is also
supported by the ambroid column A. The specimen is

Fig. 3.
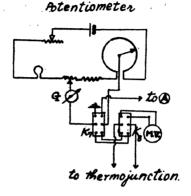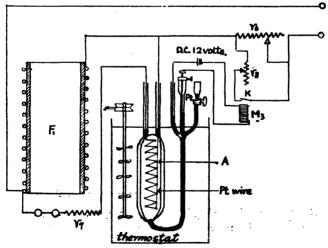
Fig. 4.
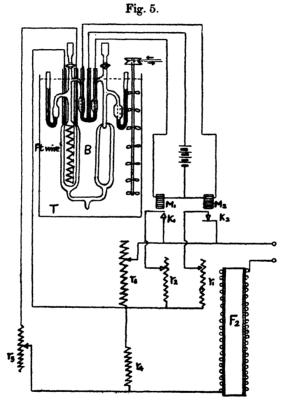
A, toluene regulator; F_1, outer furnace; K, key; M_3, magnet;
r_6, r_7, r_8, suitable resistances.

directly in contact with the electrodes by the spring S, and
by this device any piezo-electric effect produced by the
mechanical expansion due to temperature increase is avoided.
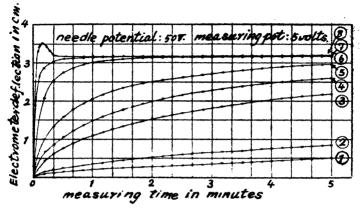
To avoid the heating of the insulators for the conducting wires from the specimen to the electrometer, and also from the battery to the specimen, the copper rings B_1, B_2 are used, and cooling water is forced to flow through the insides of these rings, and the upper part I of the ring B_1 is covered with an enamelled iron tube, and the insulator of the leading wire is protected from the moisture and also the spring S is

Fig. 5.

B, toluene regulator ; F_2, inner furnace ; r_1, r_2, r_3, r_4, r_5, suitable resistances ; K_1, K_2, keys; M_1, M_2, magnets ; T, thermostat.

protected from rust. To obtain a uniform temperature and to protect from any external effect a concentric cylinder N made of nickel is inserted around the specimen. To keep any required temperature constant we use an electric furnace with double layers, *i. e.*, the inner layer is a quartz tube furnace and the outer layer is a porcelain tube furnace,
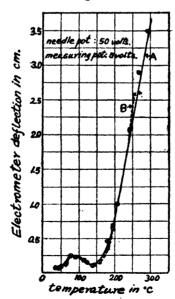
Fig. 6.
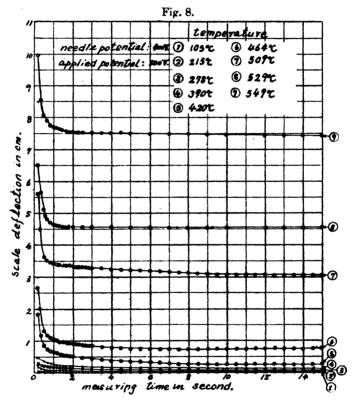
Temperature.

(1)	136° C.	(5)	208·0° C.
(2)	151·5° C.	(6)	240·0° C.
(3)	178·0° C.	(7)	267·0° C.
(4)	195·0° C.	(8)	297·0° C.

Fig. 7.

as is shown in fig. 2, and any fine adjustment of temperature is made by the inner layer. F', F'' are asbestos wool layers which are separated from each other and from F by the concentric copper cylinder C. These protective layers increase the heat capacity of the apparatus and prevent the dissipation of heat. D is the fireproof brick, and the coolers B_1, B_2 make the temperature gradient in the furnace symmetrical.

Fig. 8.
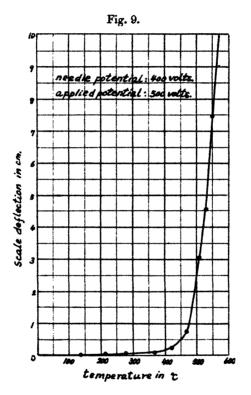
For measuring the temperature of the furnace accurately a thermo-junction made of Pt–Pt rhodium and a millivoltmeter are used, and this millivoltmeter is calibrated by the potentiometer. Sometimes we used the potentiometer to measure the potential difference of the thermo-junction accurately. The main connexion is shown in fig. 3. G is the galvanometer of Leeds and Northrup (current sensibility 10^{-9} amp.), MV the millivoltmeter, and K_7, K_8

reversing switches. To avoid the variation of voltage due to the temperature difference at contact points of mercury and keys petroleum is used.

Fig. 4 shows the device to maintain the constant temperature of the outer furnace. Fig. 5 is the arrangement of the fine adjustment of temperature in the interior furnace. The relay B in fig. 5 was first made by T. Watase *, and we

Fig. 9.
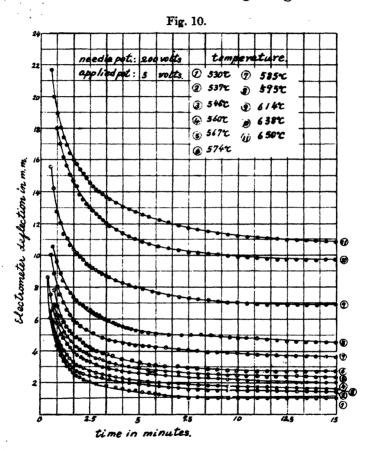
modified his apparatus, *i. e.*, the part which contains toluene was made of double bottoms and their internal parts silvered. The heat produced by the variation of the terminal potential of furnace is maintained during a few minutes; after that an equilibrium state with the surrounding temperature of thermostat is obtained. Fig. 4 is the simple case of fig. 5, and these relays are put into the thermostat. The temperature of the thermostat is adjusted approximately by a gas-

---

* T. Watase, *Kinzoku no Kenkyu*, vol. v. no. 12, p. 1 (1928).

regulator, and, moreover, a small adjustment is made by the electric regulator, and its constancy is such that the variation of the temperature is within $\dfrac{7}{1000}$ ° C.

The observation of the accumulating charge is made in

Fig. 10.

quite a similar way to that of the former paper *, *i. e.*, the variation of electrometer deflexion with the time is observed, and then the resistance is calculated from the formula
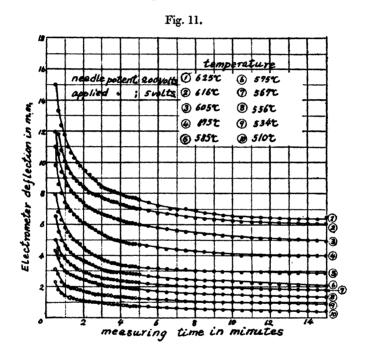
$$R = \frac{V}{\left(\dfrac{dQ}{dt}\right)_{t=0}}.$$

* H. Saegusa and S. Shimizu, Phil. Mag. ix. p. 474 (1930).

For high temperatures, since the accumulating charge becomes rather large, the potential difference due to conduction through the standard resistances is measured, and the apparent resistivity of the specimen is calculated by Ohm's law.

§ 3. *Results of Experiments.*
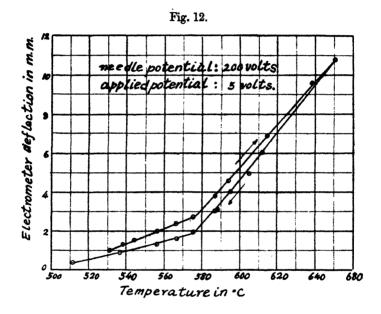
(1) The variation with the temperature of the electrical conductivity of a quartz plate perpendicular to axis.

Fig. 11.

The thickness of the specimen is 0·294 mm., and the electrode area of spluttering is 0·603 sq. cm.   Fig. 6 shows the relation between the electrometer deflexion and the time for various temperatures, when the applied potential is 5 volts. Fig. 7 shows the variation of the electrometer deflexion at 10 seconds from the start with the temperature.   This shows the variation of the conductivity with the temperature, and curves A, B are measured under the same conditions, and these values coincide with each other.   As is seen from this figure the deflexion increases at first slowly, then decreases

a little, and from about 150° C. increases rapidly with the temperature. This phenomenon is probably due to the leakage of the charge through the surface, so that the results given below are measured by the potential difference due to the conduction through a standard resistance. Fig. 8 shows the variation of the potential difference between the ends of the standard resistance, with the measuring time for various temperatures. As is seen from this figure the potential difference decreases at first rapidly and then tends to a stationary value. This shows that the current through the

Fig. 12.
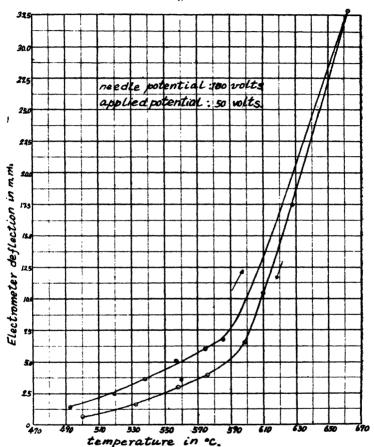
specimen decreases as the opposing potential due to the polarization increases, and tends to a stationary value as the opposing potential tends to a saturation value and the current becomes conduction alone. Fig. 9 shows the relation between the temperature and the stationary value of the potential difference. As is seen from this figure the conductivity increases with the temperature, and from about 400° C. it increases abruptly.

(2) Variation of the conductivity at the transformation temperature.

Fig. 10 is the result of the observation for the measuring potential of 5 volts and the needle potential, 200

volts for the increasing temperatures; the temperatures are given in the figures. Fig. 11 is the same relation for decreasing temperatures. To study the variation of conductivity about the transformation point accurately we use

Fig. 13.
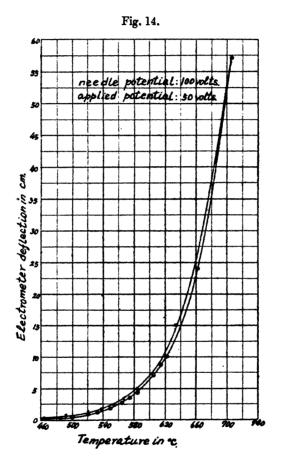
the standard resistance 800,000 ohms as an auxiliary, and observe the deflexion of the electrometer carefully with temperatures from about 500° to 600° C., the increase and decrease of temperature being made as slowly as possible, *i. e.*, the time interval is about 15 hours. Fig. 12 shows the relation between the stationary value of electrometer deflexion and the temperature taken from figs. 10 and 11. As is seen from

this figure the electrometer deflexion (*i. e.*, the conductivity) increases linearly with the temperature, and at 573° C. it increases abruptly and transforms to another linear relation. The arrow indicates the increasing and decreasing temperature. Thus the conductivity for a decreasing temperature is a little smaller than that for an increasing one.

Fig. 14.

(3) Change of the variation of conductivity at the transformation point due to the effects of electrode's oxidation.

We used nickel plates as the supporting electrodes of the specimen; hence the electrodes are oxidized at the high temperature. The oxidation of the electrodes affects apparently the conductivity of the specimen. Fig. 13 is the result of

a measurement after maintaining at the temperature about 500° C. during 40 hours. As is seen from this figure the conductivity gradually increases up to about 580° C., then increases rapidly with the temperature. Then the same specimen is kept still further for about 40 hours at the temperature of 500° C., and the observation is made. Fig. 14 is the result thus obtained. As is seen from this

Fig. 15.
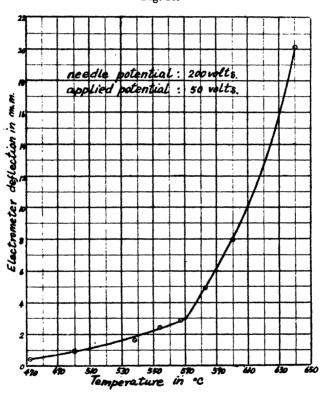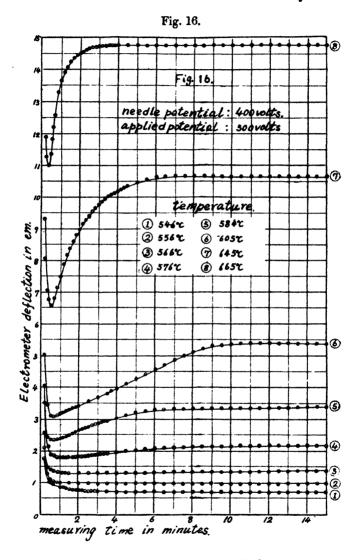
figure the relation between the conductivity and the temperature at 573° C. becomes a continuous curve. Next we polish the electrode surfaces and make a good contact with a platinized quartz plate, and a similar measurement is again made. In this case the increase of conductivity at the transformation point becomes somewhat sharp, as is shown in fig. 15. Thus we may conclude that the oxidation of the
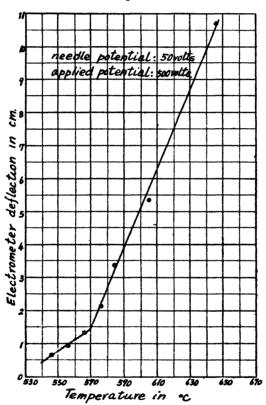
electrode modifies the abrupt increase of conductivity at the transformation point. As is seen from the above results it is a remarkable fact that the electric conductivity increases

Fig. 16.

Fig. 16.

needle potential : 400 volts.
applied potential : 500 volts

temperature.

① 546℃		⑤ 584℃	
② 556℃		⑥ 605℃	
③ 566℃		⑦ 645℃	
④ 576℃		⑧ 665℃	

Electrometer deflection in cm.

measuring time in minutes.

abruptly at the transformation point, and the transformation point is sharply defined by the conductivity, and the oxidation of the electrode modifies the transformation point. Many experimenters who have examined the conductivity of quartz platinized or silvered the specimen, but electrode metals were

very different; *e.g.*, R. Ambronn * used silvered copper
electrodes, Exner † used liquid electrodes, Tegetmeier and
Warburg ‡ used platinum electrodes, and Doelter § also used
the platinum electrodes. In order to get definite values
we must use the same electrode metal and be careful
concerning its oxidation.

Fig. 17.
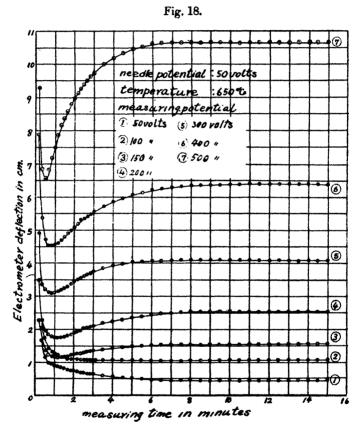
(4) Conductivity for a large measuring potential.

Next we measured the conductivity for a large measuring
potential above the limiting potential. Fig. 16 shows the
result for a measuring potential of 500 volts. As seen from
this figure the conductivity varies as that of the semi-
conductors. Fig. 17 shows the variation of the stationary

* *Loc. cit.* † *Loc. cit.*
‡ *Loc. cit.* § *Loc. cit.*
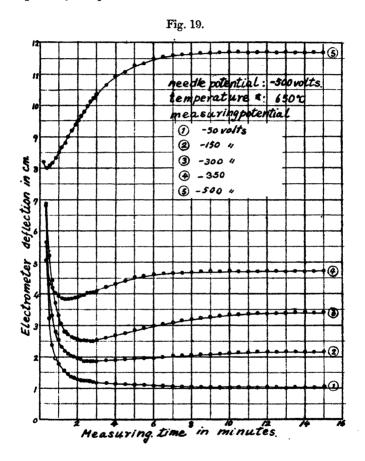
value of potential difference with the temperature. In this case also the conductivity increases discontinuously at the temperature $573°C$. To study the initial decrease of potential difference as in fig. 16 we measured it with various measuring potentials for the case when the temperature is $650°C$. These experimental results are given in figs. 18 and 19 ; the former is for positive potential and the latter for negative

Fig. 18.

potential. As is seen from these figures the initial decrease appears for large measuring potentials; thus we state that dielectrics for a large measuring potential at high temperature become as if they were semi-conductors. Fig 20 shows the relation between the stationary value of conductivity and the measuring potentials obtained from figs. 18 and 19, *i. e.*, the A curve is for the positive potential and the B curve for the negative potential. The A curve shows a sharp part
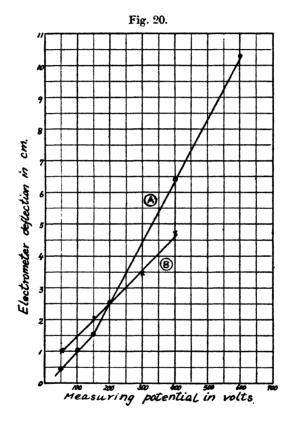
above the limiting potential for dielectric hysteresis, but the B curve does not; moreover these two values are very different. On these different characters we should like to state no definite conclusion for the present.

(5) Variation with temperature of electrical conductivity of quartz plate parallel to axis.

Fig. 19.

We studied this problem with a quartz plate cut parallel to its optical axis. The specimens used in the experiment are two plates, one of them 0·477 mm. in thickness and the other 0·480 mm. thick, and these plates are taken from the same parent crystal, and for convenience we call the former the A specimen and the latter the B specimen. For the

parallel plate the conductivity is comparatively smaller than that of the perpendicular specimen, so that we used the accumulation-charge method in this case. Fig. 21 shows the relation between the electrometer deflexion and the temperature, when the needle and the applied potential are both 50 volts, where A, B curves are for A, B specimen respectively, and these values are nearly equal. Fig. 22 shows the

Fig. 20.
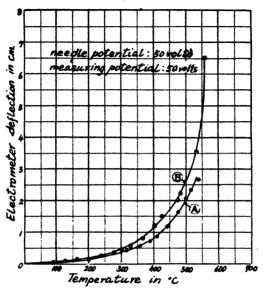
result when the needle potential is 50 volts and the applied potential is 5 volts. As is seen from this figure the variation of conductivity at the temperature 573° C. shows the discontinuous change as in the case of quartz plate cut perpendicular to its optical axis, but the variations are somewhat different.
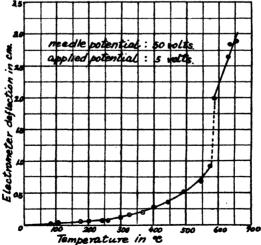
Fig. 23 shows the relation between the electrometer deflexion and the temperature, when the needle potential is 50 volts and the applied potential is 8·11 volts; this potential

is equivalent to 5 volts for the perpendicular specimen of a thickness of 0·294 mm. In this case the discontinuous

Fig. 21.

Fig. 22.

change at the temperature 573° C. is remarkably large compared with the case of fig. 22.

Fig. 23.
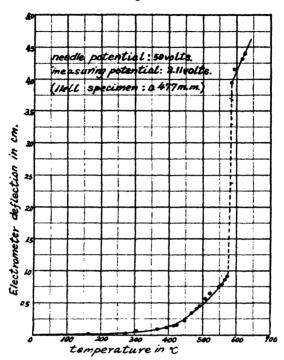
Fig. 24.
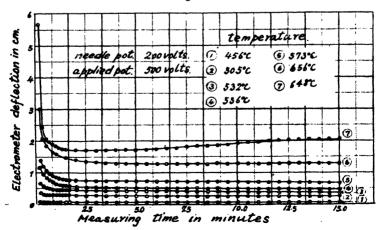
Fig. 25.
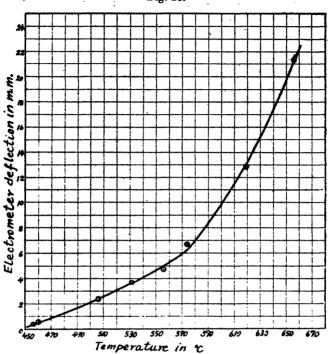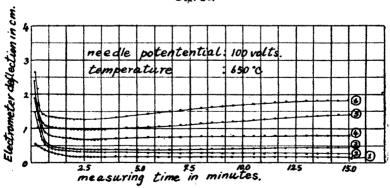
Fig. 26.

Measuring potential.

(1) 100 volts.	(4) 400 volts.
(2) 200 „	(5) 600 „
(3) 300 „	(6) 700 ,

Next we measured the conductivity by the potential fall method as in the case of the quartz perpendicular plate. The standard resistance used in this experiment is the same as in the former case. Fig. 24 shows the relation between the potential difference and the time for various temperatures, when the measuring potential is 500 volts and the needle potential is 200 volts ; and fig. 25 shows the stationary value of the potential difference and the temperature. As is

Fig. 27.

applied potential in volts
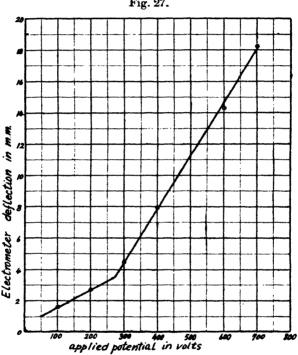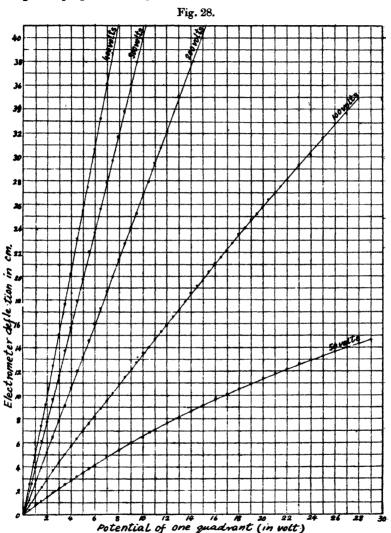
seen from the figure the variation of conductivity at the temperature 573° C. is quite of the same character as in the case of the quartz perpendicular plate, but in comparing with the case in fig. 23 there are remarkable differences. Nevertheless there exists no difference in both results, because in the former the initial value of conductivity is taken, but in the latter the stationary value.

Next we measured the conductivity for various applied potentials under a constant temperature. This result is shown in fig. 26. Fig. 27 was obtained from fig. 26, and shows the relation between the conductivity and the applied

potential. In this case the variation of conductivity also has a sharp point about its limit potential, as in the case of the quartz perpendicular plate.

Fig. 28.

Lastly, in order to compare absolute magnitudes on the curves, the relation between the potential of one quadrant and the electrometer deflexion at each needle potential is shown in fig. 28.

§ 4. *Concluding Remarks.*

1. The variation of electrical conductivity of quartz plates, one cut perpendicular the other parallel to their optical axes, with temperature for various measuring potentials, is carefully measured with various precautions, and we learn that the conductivity increases greatly with the temperature, and at the transformation point increases abruptly or discontinuously. It is a well-known fact that the refractive index, expansion coefficient, and other physical properties discontinuously change at the transformation point ; in the present experiment it is found that the electrical conductivity shows also a similar behaviour at the transformation point.

2. As the result of our accurate measurement the conductivity increases gently up to 573° C., then abruptly increases with the temperature above 573° C., and the transformation point is markedly defined by the measurement of conductivity.

3. At high temperatures above the transformation point the electrical conductivity increases also with the measuring potential, and at the limiting potential the curve transforms to another form ; thus the conductivity shows the anomalous change at the limiting potential.

4. The oxidation of the electrode-metal affects seriously the conductivity, *i.e*, it makes a sharp variation at the transformation point smooth.

In conclusion, I am greatly indebted to Prof. H. Saegusa, under whose kind guidance the present experiment has been carried out.

September 1931.

LXXXVII. *Decay of Torsional Oscillation of an Iron Wire ·Effect of Variation of Period. By* F. W. ALEXANDER, *B.Sc., Research Student, University College, Dundee* *.

IT has been shown by Prof. Peddie (Phil. Mag. 1894) that the law of torsional oscillation of wires can be extremely accurately represented in many cases by the formula

$$y^n(x+a) = b,$$

where n, a, and b are constants for any one experiment, y the range of oscillation, and x the number of oscillations

---

* Communicated by Prof. W. Peddie, D.Sc., F.R.S.E.

which have taken place since torsion was first applied and
the wire left to itself so that the oscillations gradually
diminished. The present investigation was undertaken to
find out the variation in the constant n when the period
of oscillation, *i. e.*, the moment of inertia of the system, was
varied, the length of the wire, the load on the wire, and the
torsion applied being constant.

The apparatus used consisted of a stout wooden arm,
rigidly fixed to the wall, holding the hollow brass socket of
a torsion head, which consisted of a brass cone with
a central pin-vice. The angle through which the head
could be turned was limited by two projecting screws. The
lower end of the wire was fixed symmetrically by a similar
pin-vice to the oscillator, which consisted of a long horizontal
hollow cylinder, with two solid lead cylinders of the same
diameter, capable of sliding within it, fixed symmetrically
at each side by two screws projecting through a long slot in
the cylinder. The moment of inertia of the system could
be varied by fixing the lead cylinders at any distance along
the hollow cylinder. Attached to the cylinder with the pin-
vice as centre was a thin metal circular ring, carrying
a graduated scale. The maximum angular rotations about
the wire were observed by means of a reading telescope.

In each experiment, with the lead cylinders clamped at
a measured distance from the ends of the cylinder, torsion
oscillations were started by turning the torsion head in and
out five times between the limits fixed by the projecting
screws, each turn being timed so as to amplify the swing.
The system was then left to itself, and readings were taken
through the telescope of the maximum amplitude of oscilla-
tion, first on one side and then on the other. By subtracting
these two readings the amplitude of the complete oscillation
could be found. A curve was then plotted with scale
readings as ordinates and the number of swings as abscissæ ;
the latter have already been shown to be almost isochronous
(Phil. Mag. 1894).

The method adopted for finding n was that given by
Prof. Peddie (Trans. R. S. E. 1896). Using the formula
given above we obtain

$$n \log y + \log (x + a) = \log b.$$

If $\log (x + a)$ be plotted against $\log y$, the points lie on
a straight line which intersects the axis along which $\log y$
is measured at an angle whose tangent is n if the proper
value of a is chosen. If a wrong value of a is used the
points will not lie on a straight line. If a is too large the

curve is convex towards the origin and concave if a is too small.

The moment of inertia of the system was found by observing the periodic time of torsional oscillations of small amplitude. The two similar brass disks of known dimensions and mass were placed symmetrically on each side of the circular ring, and the periodic time was again found as before. From these two periodic times and the calculated moment of inertia of the disks about the wire the moment of inertia of the system was found.

An iron wire thinly coated with copper, 55·45 cm. in length between the two pin-vices, was used. A series of

TABLE I.

No.	Date.	Distance of Pb cylinders from ends.	Time of oscillation.	Moment of inertia.	Value of n.	Average. value of n.
		cm.	sec.			
4......	25/4/29	6	9·9 ⎫	288,000	·647 ⎫	·657
5......	26/4/29	6	9·9 ⎬		·668 ⎭	
6......	14/10/29	8	8·5 ⎫	192,000	·629 ⎫	·645
7......	15/10/29	8	8·5 ⎬		·650 ⎭	
8......	21/10/29	10·6	7·26	129,000	·621	·621
9......	24/10/29	0	14·65 ⎫	627,000	·671 ⎫	·662
10......	29/10/29	0	14·65 ⎬		·654 ⎭	
11......	4/11/29	2·5	12·68 ⎫	434,000	·623 ⎫	·630
12......	5/11/29	2·5	12·68 ⎬		·647 ⎭	
13......	14/11/29	5	10·63		·633	·633
14......	21/11/29	6·5	10 ⎫	252,000	·592 ⎫	·579
15......	22/11/29	6·5	10 ⎬		·602 ⎭	
16......	7/1/30	0	14·46 ⎫	627,000	·602 ⎫	·609
17......	9/1/30	0	14·64 ⎬		·617 ⎭	
18......	20/1/30	7	9·63 ⎫	240,000	·546 ⎫	·549
19......	21/1/30	7	9·63 ⎬		·553 ⎭	

experiments spread over a considerable period of time was carried out, with as many different periods of oscillation as possible, care being taken to avoid torsional frequencies which were in too close agreement with the natural pendulum frequencies. This precaution was necessary because the energy of torsional oscillations was apt to be transformed into energy of pendular oscillations which destroyed the accuracy of the readings. Thus, the lead cylinders could only be placed at certain positions, found by trial and error, along the hollow cylinder. Table I. gives the results.

The value of the constant a varied between 30 and 50. As the maximum value of y was not large, only one value of n was found for each experiment.

It will first of all be noticed from Table I. that, if an experiment was repeated on the following day, the determination gave a higher value of n (*vide* nos. 4 and 5 ; 11 and 12, etc.), but if an interval of a week or more intervened the second gave a lower value of n (*vide* nos. 9 and 10). Nos. 9 and 10, carried out on 24th and 29th Oct., 1929, with the maximum moment of inertia, gave an average value of n equal to ·662 ; but nos. 16 and 17 gave the value ·609 for the same moment of inertia repeated on 7th and 9th January, 1930. From the above values of n no law between the period of oscillation or moment of inertia and n is apparent, any connexion being masked by the decrease of n with time. The physical condition of the

TABLE II.

No.	Date.	Distance of Pb cylinders from ends.	Time of oscillation.	Value of n.	Average value of n.
		cm.	sec.		
20	11/3/30	3·5	12·17	·586	·577
21	11/3/30	3·5	12.17	·571	
22	11/3/30	5	10·6	·574	·573
23	12/3/30	5	10·6	·573	
24	12/3/30	8	8·5	·558	·561
25	12/3/30	8	8·5	·563	
26	13/3/30	9	7·9	·564	·564
27	13/3/30	9	7·9	·564	
28	13/3/30	1·5	13·45	·575	·575
29	14/3/30	1·5	13·45	·575	
30	14/3/30	0	14·63	·572	·572
31	14/3/30	0	14·63	·572	

wire must have gradually altered as a result of the torsional strain to which it was subjected as time passed.

It was next decided to carry out another series of experiments, taking precautions to keep the wire in as nearly as possible the same physical state. The wire at the beginning of each day's work was fatigued slightly by being set in torsional oscillations which were allowed to decay. Then as many sets of readings as possible were taken in one day, the whole series being done in the consecutive days of one week. The plotting of the graphs and the calculations were carried out later. Table II. gives the results.

It is evident that, within the limits of experimental error, there is no variation in the value of n as the period of oscillation is altered by change of the moment of inertia, the period being varied between 7·9 sec. and 14·63 sec. The moment of inertia was not calculated for this series.

It has been shown (Phil. Mag. 1894) that large torsional oscillations of a wire cause the rupture of molecular groups in the wire, thus resulting in a loss of potential energy. But theory indicates that the value of n is increased if more groups break down under given conditions. Thence it would appear from the constancy of n that on the average the same number of molecular groups are broken up irrespective of the period of oscillation, *i. e.*, irrespective of the *speed* of deformation of the groups within the observed range.

In conclusion, I wish to thank Prof. W. Peddie and Dr. J. Forest for their guidance and helpful advice throughout this investigation.

LXXXVIII. *On certain Variations in the Optical Constants of Copper.* By H. LOWERY, *Ph.D., F.Inst.P., Head of the Department of Pure and Applied Physics, and* R. L. MOORE, *M.Sc. Tech., Technological Research Scholar, College of Technology, University of Manchester* *.

I. GENERAL DISCUSSION.

ON the initiation of a research aiming at the determination of relationships (if any) between the optical properties of a series of alloys and their crystalline constitution, it soon became evident, in view of the disparity between the results of previous observers, that a general survey of the methods, technique, and apparatus for the determination of the optical constants of metals was desirable.

Numerous workers (*e. g.*, Jamin [1], Quincke [2], Drude [3], Minor [4], Meier [5], Tool [6], Tate [7], and many others) given data from which the refractive index, absorption, and reflexion coefficients of a metal may be deduced, and their methods of measurement have usually been based on either the transmission or reflexion of light. In illustration of the manner in which transmission methods have been used, reference may be made to the work of Kundt [8], Pflüger [9], Shea [10], and du Bois and Rubens [11]. These observers determined the refractive index of various metals by sending light through a very thin prism of the substance under investigation and measuring the deviation of the

beam. The technique of methods involving light transmission is extremely difficult, and the collected results show considerable variations among themselves. Drude [12], after having made a very careful survey of the various methods of determining the optical constants of metals, came to the conclusion that *reflexion* methods are likely to prove more satisfactory than *transmission* methods for the study of the optical properties of metals, mainly on account of the ultra-refined technique and consequent practical difficulties incidental to the latter.

Leaving on one side the direct method, in which the reflecting power of a metal is measured by determining the proportion of the incident light reflected, using, say, a bolometer (*e.g.*, Hagen and Rubens [13], and Coblentz [14]), reflexion methods usually consist in determining the form of the ellipse of vibration in a beam of light reflected from the polished surface of a metal. The standard method since the work of Drude is to reflect a beam of light polarized at an azimuth of 45° to the incident plane, and then to determine the phase change (Δ) between the reflected components in and perpendicular to the incident plane. To complete the data specifying the ellipse of vibration of the reflected light, the azimuth (ψ) of the reflected light after restoration to plane polarization is measured. Various devices have been used for the purpose; thus, Haughton [15] and others have used Jamin's modification of Babinet's compensator. Drude [3] has employed the Soleil modification of the same compensator, and his example has been followed by many more recent workers. Tool [6] has evolved a very accurate half-shade analyzing system, and Minor [4], Meier [5], Weld [16], and others have used a photographic method due to Voigt [17].

These methods enable the two quantities Δ and ψ to be measured for any metal surface, from the values of which the three optical constants, viz., the refractive index (n), absorption coefficient (k), and reflexion coefficient (R) may be deduced.

The truth of the formulæ from which the optical constants are deduced is proved by a general rather than exact agreement between the results of polarimetric measurements and those of transmission methods. Tate [7] has determined the reflecting coefficients of several metals by direct measurement and also polarimetrically, using the *same surface*, and has found an almost exact agreement between the two sets of measurements. Thus it seems reasonable to suppose that the values of n, k, and R, derived from polari-

metric measurements, are at least the correct values for the
particular surface under consideration. Drude [12] has also
shown that the errors of measurement are least when
observations are made at an angle of incidence for which
Δ is approximately 90°; but despite very elaborate pre-
cautions and a wealth of experimental skill the polarimetric
observations of various observers show serious discrepancies.
These variations have been noticed by most observers since
the time of Biot, and Wheeler [18] has illustrated the extent
of the divergencies in a striking manner by graphing the
results of several investigators for silver, copper, gold,
nickel, and cobalt. It is generally recognized that it is
almost impossible to reproduce a polished surface giving the
same constants even by the most careful repetition of the
conditions of polishing.

The results of Drude, Minor [4], and Tool [6] indicate
that these variations are due to

    (*a*) impurities picked up in polishing ;

    (*b*) an incomplete polish ;

    (*c*) films produced on the test surface.

Drude investigated this latter effect theoretically [12], and
showed that a film of impurity tends to lower the value
of Δ considerably and increase the value of 2ψ very slightly.
From this it is concluded that the "standard" or "best"
condition for a surface is such as to produce a maximum
value of Δ for the particular angle of incidence used.
Unfortunately the attainment of standard conditions is by
no means as easily obtained as this. Wheeler [18] says that
"there seems to be at least, tacitly, a general assumption
that since Drude's specification of the 'normal' condition
for a reflecting surface, it only requires sufficient care in the
preparation of the metallic mirror in order to get consistent
results ; and that consequently our knowledge of the optical
constants is nearly as precise as that of the methods of
measurement used. It is safe to say, however, that no one
who has had much experience in this line of work has
held such an opinion for long. In fact, experience teaches
that it is well nigh impossible to exactly reproduce (even by
the same observer) the same condition of the reflecting
surface in different samples of the identical material, or
even in the same sample at different times. Thus we
cannot regard the experimental values of the optical constants
as anything but rather rough approximations to the specific
values characteristic of the substances."

With such acknowledged discrepancies it would seem desirable to investigate more closely the various factors which contribute to the general non-agreement of the various observations. It seems fairly certain that impregnation of the surface with impurity during the polishing processes is one of the root causes, but little work has been done with a view to arriving at a complete statement of all the factors affecting the results. Beilby [19] has developed a theory of polish which seems to throw some light on the question. According to Beilby, polishing, as distinct from grinding, consists in the flowing of a film of metal until all the ridges and crevices produced by previous grinding are filled up. Evidence has been put forward to show that this film is amorphous. The work of G. P. Thomson [20] on electron diffraction by polished surfaces probably means that a polished surface is structureless to a depth of several atoms at least. Ignoring for a moment the question whether this layer is truly amorphous or not, it is well known that its chemical and mechanical properties are different from those of the unstrained crystalline metal. Any kind of cold work tends to increase the electrical resistance of a metal, and from these facts it appears that actual polishing may produce a surface which is not truly characteristic of the metal. It has, in fact, been suggested by Tool that this is the case. The work of Weld, Sieg, and others on small single metal crystals has shown quite definitely that the optical constants vary according to the direction of the axis of the crystal ; so metallic reflexion is evidently dependent in some way on the arrangement of atoms as well as on any inherent properties of the atoms themselves. It remains to see whether this flowed metal is of sufficient depth to cause any appreciable change in the constants. Beilby [21] was able by polishing and etching to prepare *transparent* films which he estimated to be between 10 and 20 $\mu\mu$ thick. Such films Beilby considered to be very thin, and he mentions that it is possible to vary the thickness of the film very considerably. His work suggests that polishing may produce either amorphous films or layers of distorted crystals with a minimum thickness of 10 to 20 $\mu\mu$.

If we now consider the depth of metal which is concerned in optical reflexion we can estimate the extent to which variations in the thickness of the film could possibly affect optical measurements. Hagen and Rubens [13] have measured the amount of light reflected at normal incidence from gold films of varying thickness, and from their results it

is clear that the amount of light reflected reaches a maximum for red light when the thickness is about 80 $\mu\mu$. The absorption coefficient (k) for copper is about half that of gold, so we can safely say that the maximum depth of metal concerned in reflexion from copper is something between 150 and 200 $\mu\mu$. This, then, suggests the possibility of variations in the optical properties of the metal due to the formation of poor conducting layers of metal of thickness greater than 10 to 20 $\mu\mu$. As quite opaque layers can easily be produced, 10 to 20 $\mu\mu$ will probably be a low limit for the thickness of this layer.

As far as we are able to discover, Margenau [22] is the only observer who has made an attempt to vary the degree of polish in order to find any relationship between the amount of surface disturbance and the optical constants. He carried out direct measurements on the reflecting power of silver in the ultra-violet, and came to the conclusion that a light polish increased the reflecting power of a metal. This is presumably what would happen if a light polish left the greater portion of the metal concerned with reflexion in its normal high-conducting state, and a heavy polish produced a poorer conducting layer of much greater depth. Sieg [23] has made direct measurements of the reflecting power of small single crystals of selenium, and has obtained, as might be expected, different reflecting powers according as the long axis of the crystal was parallel or perpendicular to the electric vector of the incident beam. He points out that it might be expected that the results for a polished plate would be the mean of his extreme values. Comparing his results with those of Foersterling and Freedericksz [24] and Pfund [25] for polished cast plates, he shows that this is not so and that the values of the reflexion coefficient of these other observers are *below* the mean value—in fact, for part of the spectrum below the recognized minimum value. He suggests that this difference may be caused by the preferred orientation of crystals to a cast plate of selenium; but it is clear from Sieg's work that, using small crystals, the reflecting coefficient is at least not *increased* by polishing.

On the other hand, Drude's [26] result for a natural crystal of lead sulphide (probably a much larger crystal) shows that the reflexion coefficient is increased by polishing, and Tate [7], on some work on electro-deposited *unpolished* gold and copper surfaces found absorption and reflexion coefficients considerably smaller, and the refractive index higher, than those of Tool.

With these apparently contradictory results it would seem desirable to estimate the extent and direction of changes in the optical constants with varying degrees of heaviness of polish. The first part of the present work is an attempt to discover some relationship between the state of strain of a surface and the optical constants using a polarimetric method, and the second part attempts to assess the rate at which atmospheric deterioration takes place. In both cases copper was the metal examined.

II. EXPERIMENTAL.

1, *The Method of Production of Varying Degrees of Polish.*

It has been pointed out that several causes for the variations of optical constants are already known and agreed upon by all observers, and that it is almost impossible to control the chief factors successfully. Thus, with several factors acting it may be in the same or opposite directions, a search for a further factor is attended by serious difficulties. The three main factors which it was desired to keep constant throughout all changes of degree of polish were

(*a*) the purity of the surface ;

(*b*) the completeness of the polish ;

(*c*) the state of a film of foreign matter (if any) between the metal surface and the air.

(*a*) According to Drude [12] the test for a surface which is perfectly free from impurities is that Δ shall be a maximum. In this case the variations which the experimentally changed conditions may produce will possibly involve changes in Δ. This at once introduces an element of uncertainty which can only be eliminated by a reproduction of the results several times.

(*b*) Drude's [12] criterion for perfection of polish is that the scratches in the surface should not give values of 2ψ for perpendicular and parallel positions differing by much more than about a degree, and that all the scratches should be in the same direction. Such conditions were again difficult to maintain, but a fairly large mirror was used, and the surface explored by a microscope until an area of about 6×6 mm. was found, which would satisfy these conditions. The rest of the mirror was then covered with black paper.

(c) The transition layer it was hoped would be very small, and an attempt was made to keep it constant by making the final processes of polishing always the same.

2. *The Production of the Test Surfaces.*

Two specimens of copper were used, obtained from quite different sources. Specimen A was prepared in a high-frequency induction furnace, in air, from electrolytic copper surrounded with plenty of carbon. The metal was only just allowed to melt and the furnace switched off. By this means a casting fairly free from blow-holes was produced.

Specimen B was a piece of cold-drawn high-conductivity copper rod obtained from the Broughton Copper Company, Manchester. It was entirely free from all blow-holes, and enabled very perfect mirrors to be produced. The impurity in both specimens was chiefly oxide in small inclusions at the crystal boundaries.

3. *The Unstrained Surface.*

The metal was planed up quite smooth on a shaping machine and then ground on a series of emery papers of increasing fineness placed on a glass plate. The final paper was a French *oooo* paper. After this, since the processes had probably cold-worked the metal, it was annealed in the induction furnace under a pressure of 4 cm. of hydrogen. The surface was very clean, and it was only necessary to grind very lightly on the *oooo* paper before polishing.

To produce a mirror with a thin cold-worked layer some polishing process must be used which produces a polish with as little surface flow as possible. Alumina polishing satisfies these conditions by its abrasive as well as polishing properties. Polishing was done on a wheel covered with "Selvyt" polishing cloth impregnated with alumina mixed in a fine paste. The specimen was held down quite lightly, and as soon as the scratches had been removed it was washed and dried. Great trouble was experienced in preventing the alumina from scratching the surface beyond repair, and only about one-third of the polishes were of value. The specimen was now etched lightly (until small etching pits appeared all over the surface) in order to remove the flowed layer, and repolished for a very short time as lightly as possible. The reason for this is that the amount of cold work involved in polishing a light etch is considerably less than that necessary to remove scratches from an emery polish. The mirror was now washed with soap and water, then with

alcohol and carbon tetrachloride solution, in order to remove all traces of grease.

4. *Heavily Polished Specimens.*

The initial grinding process was in this case the same. The metal was not annealed, but was burnished by rubbing gently with a polished steel tool, using a rocking motion, after the manner of Drude. After this the metal was taken on to a piece of cloth and polished lightly with alumina. It was not, of course, a vigorous polish, but the metal was allowed to come into contact with the alumina, so that variations attributed to any impregnation of the surface might be prevented. The specimen was then washed in the usual manner.

5. *Apparatus and Calibration.*

The main part of the apparatus consisted of a Fuess No. 1 A Spectrometer-Goniometer *, a very complete description of which is given in Tutton's ' Crystallography,' p. 453 (1911).

The instrument consists of two arms capable of rotation through 360° about a massive centre pillar, after the manner of an ordinary spectrometer. By means of microscopes with micrometer eye-pieces the positions of the arms could be read to 10″. The collimating arm was fitted with an adjustable slit and a Glan-Thompson nicol mounted on a vertical circle reading to minutes. The other arm carried a similar nicol and an attachment for a Jamin modification of Babinet's compensator. This arm could be fitted with either a telescope eye-piece for adjusting the position of the arm or a microscope eye-piece focussing on the compensator.

6. *Preliminary Adjustment.*

Since it was necessary to set the polarizing nicol at an angle of 45° to the incident plane, the scales of both nicols were calibrated with respect to the axis of the instrument. A small piece of plane glass was mounted on a levelling table and adjusted so as to be parallel to the axis of the instrument by making observations of the slit image with the telescope eye-piece. The polarizing nicol was set so as to polarize light as nearly as possible in the incident plane, and readings of the analyzing nicol for extinction were made on

* This instrument was formerly in the possession of Professor A. E. H. Tutton, F.R.S.

either side of the circle. Since the plane of polarization was originally practically in the incident plane, the reflected light near the polarizing angle was almost completely polarized in this plane, and thus the setting of the analyzing nicol necessary to polarize light exactly perpendicular to the axis of the instrument could be found. The polarizing nicol circle was calibrated against the analyzer by crossing them several times. By this means the position of both circles with respect to the main axis could be found.

Using a monochromatic illuminator, the yellow mercury line (5770 Å) was focussed on to the slit of the goniometer and the compensator calibrated by making settings on the -2π, 0, and $+2\pi$ fringes. Owing to a small amount of parallax, caused by imperfect alignment of the nicol, all settings of the compensator were made with the analyzing nicol in a fixed position. The calibration was repeated, and in all 440 settings were made, each of the two calibrations giving the same result to one part in 3000. The mirror was mounted in a black metal cup, which could be adjusted by means of a rocking table to be parallel to the axis of the instrument and also to be capable of rotation about a normal to its surface. Observations were confined to an angle of incidence which made Δ approximately 90°. Δ was calculated by measuring the shift of the fringes.

The angle 2ψ was determined by setting the analyzing nicol for maximum blackness of the fringes with the polarizing nicol in each of the four positions at 45° to the incident plane. Considerable trouble was experienced in making these readings, but the setting became more critical when the intermediate light was cut down by interposing a small slit near the compensator. This allowed a single fringe to be viewed against a dark background.

7. *Check Experiments.*

There is little risk of error in measurements of Δ, but 2ψ may be altered by internal reflexions at the various transparent surfaces. This latter error was shown to be small by making a series of settings of the analyzing nicol with the polarizing nicol at two positions 90° apart, the arms of the goniometer being in the end-on position. As a further check on the whole method the constants for mercury were measured for sodium light. This was done chiefly on account of the fact that the question of polish does not affect the mercury constants, and also because Wheeler[27] has made an exact study of the mercury constants for sodium

light. His method was followed in detail and need not be described here. Our results (the mean of two separate determinations) are compared with those of other observers in Table I., those for Wheeler being calculated from his values for Δ and 2ψ.

It is seen that our results are consistent with those of other observers, the variation, as optical constants of metals go, being small. From the results of these checks it was assumed that the experimental technique was quite trustworthy.

<div align="center">

TABLE I.

Optical Constants of Mercury. λ 5893.

</div>

Observer.	*n.*	*k.*	R.
Drude	1·73	4·96	0·784
Meier	1·624	4·406	0·753
Wheeler	1·56	5·07	0·806
H. L. & R. L. M. ...	1·604	4·803	0·767

<div align="center">

8. *The Optical Constants of Copper.*

</div>

Specimen A was used as a check in case B, which was the specimen upon which most of the experiments were conducted, should owing to any cause give unreliable results. Specimen A was given a light polish ; specimen B was given two separate light polishes, a moderate burnish and a heavy burnish. The heaviness of the burnish was very roughly estimated by the amount of time taken to produce the surface, and checked by determining the time the metal had to be etched to produce a recognizable structure when examined under a microscope. By this means an attempt was made to gain some idea of the relative magnitude of the flowed layer. The results are shown in Table II.

It will be noticed that the value of Δ seems to bear no very clear relationship to the degree of cold working of the surface. This is probably because its value is very greatly affected by surface films and traces of impurity, so that if any change occurs it is completely masked by fluctuations due to these other causes. The changes in 2ψ due to films and impurity are much smaller, and it is in this constant (2ψ) that we find large changes in value. This latter

TABLE II.

Optical Constants of Copper at $\lambda = 5770$ Å.

Expt. no.	Treatment and notes.	Etching time.	Angle of incidence.	Δ.	2ψ.	2ψ₁ -2ψ₂.	n.	k.	R.
	Specimen A.								
1.........	Light polish.	—	70°	90° 24'	78° 37'	1° 3'	0·500	2·87	0·737
	Specimen B.								
2...... ...	Light polish.	—	71° 30'	94° 56'	80° 26'	1° 59'	0·539	2·88	0·793
3.........	Ditto. (Slight scratches in direction perpendicular to main scratches.)	4 secs.	70°	89° 33'	80° 7'	0° 45'	0·480	2·29	0·746
4.........	Light burnish.	25 secs.	70°	94° 2'	79° 2	0° 10'	0·506	2·53	0·791
5.........	Heavy burnish.	Several minutes.	70°	87° 57'	77° 14'	1° 32'	0·600	1·25	0·687

constant appears to possess a higher value (by a degree or so) after a light polish than after a heavy burnish. In the third result 2ψ was probably a little smaller owing to slight scratching perpendicular to the main direction. Increasing heaviness of polish seems to lower the value of 2ψ and cause definite variations in the values of n, k, and R.
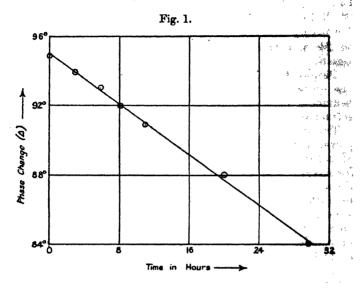
Despite the erratic fluctuations in the value of Δ there are quite definite decreases in k and R with increasing heaviness of polish and an increase in the value of the refractive index.
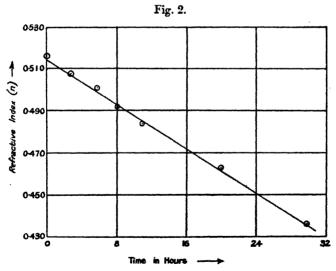
The evidence seems to point to an increase in the reflecting power as the surface was subjected to less vigorous method of polishing, and this result agrees with that of Margenau for silver. The divergence from Drude's and Tate's suggestions may only be apparent. Their surfaces were produced in quite different ways, but the weight of evidence does seem to point to the fact that a variation in the amount of cold work may be one of the causes in producing the discrepancies between the results of various observers on the optical constants of metals. It would also seem desirable in view of this to determine the optical constants of a metal after polishing as lightly as possible (consistent with a perfect surface) and not burnishing, as has been done by many workers.

9. *The Variation of the Optical Constants due to Atmospheric Deterioration.*

It was noticed in carrying out some experiments that a comparatively short exposure to air reduced the value of Δ very considerably. Since in measuring the dispersion curve the mirror would have to be kept in the atmosphere for some considerable time, a series of observations extending over two days was taken, with a view to testing the reliability of dispersion measurements (Table III.). Observations of Δ were the mean of eighty readings. The number of readings for 2ψ were reduced to forty on account of the eye-strain involved. This accounts for the somewhat erratic changes in this constant. In calculating the final values of n and k a mean value is taken for 2ψ, as the changes, although suggesting a slight increase, were not sufficiently in excess of the experimental error. Curves are given showing the fall in the value of Δ, n, and k with time (figs. 1, 2, and 3). It will be seen that the refractive index changes rapidly, but k is much less affected by variations in

the value of Δ. On account of the sharp fall of Δ and its effect upon n it is suggested that in measuring the optical

Fig. 1.

Fig. 2.

constants for several wave-lengths it would be advisable to measure all the values of Δ prior to measuring 2ψ.

Using this condition, measurements could be made with

the mirror remaining in air for several hours, and the points on the dispersion curve obtained consistent to within 1 or 2 per cent.

Fig. 3.
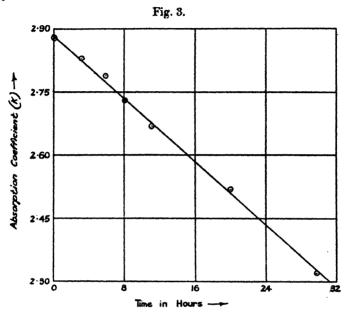
TABLE III.

Variation of the Optical Constants of Copper with Time.

Time.	Angle of incidence.	Δ.	2ψ.	Mean. 2ψ.	n.	k.
0 hrs.	71° 30'	94° 56'	80° 26'	80° 50'	0·516	2·88
2 hrs. 55 mins.	,,	93° 54'	80° 28'		0·508	2·83
5 ,, 55 ,,	,,	93° 8'	81° 3'		0·501	2·79
8 ,, 5 ,,	,,	91° 59'	81° 5'		0·492	2·73
11 ., 5 ,,	,,	90° 57'	80° 30'		0·484	2·67
20 ,, 0 ,,	,,	88° 0'	80° 31'		0·463	2·52
29 ., 40 ,,	,,	84° 2'	81° 36'		0·436	2·32

III. SUMMARY.

A brief survey of the methods of determining the optical constants of metals is given, and the discrepancies between

the results of various observers using polarimetric methods are discussed.

It is suggested that the Beilby theory of polish may offer an explanation of these divergencies, and to test this the optical constants of a piece of copper are measured for $\lambda = 5770$ Å, using varying degrees of surface strain. It seems evident from the results that a heavy polish increases the refractive index and decreases the absorption and reflexion coefficients. This agrees with Margenau's results for silver, but there seems to be an apparent deviation from Drude's and Tate's results. Some experiments were carried out on the rate of deterioration of a copper mirror, and from the results the most satisfactory condition for measurement of the dispersion curve (when the specimen must remain in the air for some time) is deduced.

IV. BIBLIOGRAPHY.

(1) See Beer, Pogg. *Ann.* xcii. p. 417 (1854).
(2) Quincke, Pogg. *Ann.* Jubelband, p. 336 (1874).
(3) Drude, Wied. *Ann.* xxxvi. p. 532 (1889); xxxix. p. 481 (1890); lxiv. p. 159 (1898).
(4) Minor, *Ann. d. Phys.* (4) x. p. 581 (1903).
(5) Meier, *Ann. d. Phys.* (4) xxxi. p. 1017 (1910).
(6) Tool, Phys. Rev. xxxi. p. 1 (1910).
(7) Tate, Phys. Rev. xxxiv. p. 321 (1912).
(8) Kundt, Wied. *Ann.* xxxiv. p. 477 (1888); xxxvi. p. 824 (1889).
(9) Pflüger, Wied. *Ann.* lviii. p. 493 (1896).
(10) Shea, Wied. *Ann.* xlvii. p. 177 (1892).
(11) du Bois and Rubens, Wied. *Ann.* xli. p. 507 (1890).
(12) Drude, Wied. *Ann.* xxxix. p. 481 (1890).
(13) Hagen and Rubens *Ann. d. Phys.* (4) viii. p. 1 (1902).
(14) Coblentz, Bur. Stds. ii. p. 472 (1906); vii. p. 198 (1911); Journ. Frank. Inst. clxx. p. 169 (1910).
(15) Haughton, Phil. Trans. Roy. Soc. p. 81 (1803).
(16) Weld, Phys. Rev. xi. p. 249 (1918).
   Van Dyke, Journ. Opt. Soc. Amer. vi. p. 917 (1922).
   Sieg, Journ. Opt. Soc. Amer. vii. p. 147 (1923).
   Graber, Phys. Rev. xxvi. p. 380 (1925).
(17) Voigt, *Phys. Zeitschr.* ii. p. 303 (1901).
(18) Wheeler, Amer. Journ. Science, xxxv. p. 493 (1913).
(19) Beilby, 'Aggregation and Flow of Solids' (1921).
(20) Thomson, Proc. Roy. Soc. A, cxxviii. p. 649 (1930).
(21) Beilby, Proc. Roy. Soc. A, lxxxix. p. 593 (1914).
(22) Margenau, Phys. Rev. xxxiii. p. 639 (1929).
(23) Sieg, Journ. Opt. Soc. Amer. vi. p. 459 (1922).
(24) Foersterling and Freedericksz, *Ann. d. Phys.* xliii. p. 1227 (1914).
(25) Pfund, *Phys. Zeit.* x. p. 340 (1909).
(26) Drude, *Ann. d. Phys.* xxxvi. p. 532 (1889).
(27) Wheeler, Phil. Mag. xxii. p. 229 (1911).
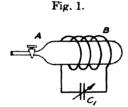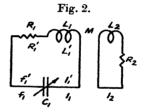
LXXXIX.—*Measurement of Current in Electrodeless Discharges by means of Frequency Variations* *. By J. TYKOCINSKI-TYKOCINER, *Research Professor of Electrical Engineering, University of Illinois* †.

FOR quantitative investigations of electrodeless ring discharges the knowledge of current densities involved in this type of discharges is required. As no method is known which would serve this purpose an attempt was made to apply the principle of mutual reaction between two coupled circuits for the measurement of such currents.

At first we will assume with J. J. Thomson that the phenomenon is due solely to electromagnetic induction. The rarefied gas in a tube or bulb A (fig. 1) inserted in the high-frequency field of a solenoid B becomes ionized, and may be regarded as carrying the secondary current of

Fig. 1.   Fig. 2.

Excitation circuit of   Equivalent circuit of
discharge-tube.   discharge-tube excitation.

a transformer whose primary current is oscillating in the windings of the excitation solenoid B. We should therefore expect that the ring discharge will react on the primary circuit, increasing its resistance and decreasing its inductance. Let the excitation be produced by continuous oscillations of constant amplitude (fig. 2), and let the current, resistance, inductance, and frequency of the primary circuit, when no discharge is taking place in the tube, be denoted by I_1, R_1, L_1, and f_1 respectively. All of these magnitudes change when the discharge sets in, and acquire then the values I_1', R_1', L_1', and f_1', while the corresponding values for the discharge itself are I_2, R_2, L_2, and $f_2 = f_1' = \omega_2/2\pi$.

---

* Paper read before the Am. Phys. Soc. Nov. 28, 1931. See Abstract in Phys. Rev. xxxvii. p. 100 (1930).
† Communicated by the Author.

The relation between these magnitudes is given by the expressions

$$\Delta R_1 = R_1' - R_1 = \left(\frac{\omega_2 M}{Z_2}\right)^2 R_2$$

$$-\Delta L_1 = L_1 - L_1' = \left(\frac{\omega_2 M}{Z_2}\right)^2 L_2,$$

$$(\omega_2/\omega_1)^2 = L_1/L_2,$$

and

$$Z_2^2 = L_2^2\omega_2^2 + R_2^2,$$

which lead to the following formula for the increase of frequency caused by the reaction of the ring discharge upon the primary circuit, namely :—

$$\Delta f = \frac{2\pi^2 f_2^3 M^2}{(2\pi f_2 L_2)^2 + R_2^2} \frac{L_2}{L_1}. \quad \dots \quad (1)$$

Considering that

$$I_2 = I_1\omega_2 M/z_2,$$

and that from (1)

$$(\omega_2 M/z_2)^2 = 2\Delta f L_1/f_2 L_2,$$

we obtain for the secondary current

$$I_2 = I_1 \sqrt{2\Delta f L_1/f L_2}, \quad \dots \quad (2)$$

an expression in which all parts with the exception of L_2 can be measured.

By inserting in (1) the coupling coefficient $K^2 = M^2/L_1 L_2$ we obtain the relation

$$\Delta f = \frac{1}{2} \frac{f_2 K^2}{1 + \dfrac{R_2^2}{(2\pi f_2)^2 L_2^2}},$$

which may be used for the determination of the angle ϕ of phase difference between the electromotive force E_2 and the current I_2,

$$\cot\phi = R_2/2\pi f_2 L_2 = \left(\frac{K^2 f_2}{2\Delta f} - 1\right)^{\frac{1}{2}}. \quad \dots \quad (3)$$

In deriving the above relations no attempt was made to consider the influence of the axial and radial distribution of the high-frequency currents in the tube. What was aimed at first of all was solely an approximate expression for checking the proposed method of current measurement, and also for verifying on the basis of J. J. Thomson's theory the picture usually drawn showing how currents are induced
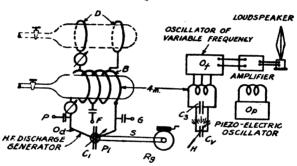
within gases. A concise mathematical treatment of the problem, including the calculation of L_2, will be given in a following paper by J. Kunz.

The experimental arrangement for a precise determination of frequency variations Δf, due to discharges induced in a rarefied gas, is shown in fig. 3.

The high-frequency discharge generator O_d consisted of two 75 Watt Ux-852 radiotron tubes, whose plate, filament, and grid were connected through blocking condensers to the solenoid B at the points P, F, and G respectively. This solenoid, together with the condenser C_1, formed the primary excitation circuit. The solenoid B, 12·5 cm. in diameter and 12·5 cm. long, was made of twelve turns of nickel-plated copper strip 0·4 by 0·15 cm. thick. The variable air

Fig. 3.
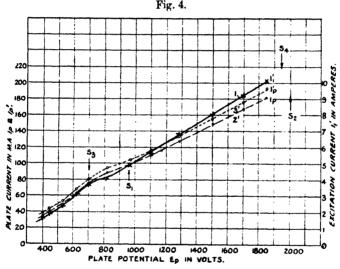
Arrangement of apparatus for the measurement of
frequency variations.

condenser C_1 could be varied from 50 to 220 micro microfarads by means of a Vernier dial supplied with a pulley, Pl. The latter was driven by means of a string S and reduction gear Rg, so that at a distance of 4 m. the frequency could be adjusted to correspond to that of a piezoelectric oscillator O_p, which served as a standard of fixed frequency f_1. Coupled with the piezoelectric oscillator was another thermionic oscillator O_t, whose condenser C_3 could be varied over a large range of frequencies, while a Vernier condenser C_v in parallel connexion and supplied with a long handle H made possible finer adjustments for tuning O_t into resonance either with O_p or with O_d. Resonance was determined by the audible beat method. For this purpose the oscillator O_t was coupled with an amplifier and loud-speaker, or a head

telephone receiver was inserted directly in the plate circuit
of O_t. All measurements were made at $f_1 = 3173$ k.c.

Two discharge-tubes made of pyrex glass and primed with
electrolytically produced H_2 at a pressure of about 0·1 mm.
Hg were used in the course of experiments. Both tubes
had a length of 25 cm., while the diameters were 3 cm. and
6 cm. respectively. Any one of the tubes could be placed
either inside the solenoid B, where the electromagnetic
field predominated, or inside the rings D, where chiefly
the electrostatic field was acting. By changing the two
positions of the discharge-tube the influence of the character

Fig. 4.
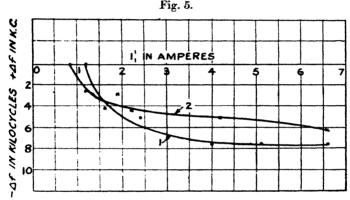
Relation between plate current, excitation current, and
plate potential.

of the field could be studied. The intensity of the excitation
could be varied by changing the plate potential at the
75 watt thermionic tubes. A storage battery of 2000 volts
was used for this purpose.

In fig. 4 curve 1 represents the relation between the plate
potential E_p and the oscillating current in the solenoid B
before the discharge-tube is inserted. This current decreases
slightly whenever the tube is inserted, which indicates that
the discharge current reacts on the primary current. The
reaction may be more distinctly traced by comparing the
values of plate current I_p for the tube outside the solenoid
(curve 2) with values I_p' when the tube is inserted (curve 3).

The procedure of the Δf measurement as function of the primary current is as follows :—The frequency of the oscillator O_d is set to correspond to the fundamental or to one of the harmonic frequencies of the piezoelectric oscillator O_p. Also the oscillator O_t is tuned into resonance with the same frequency. Then the discharge-tube is inserted in the solenoid B, and the plate potential adjusted below the point at which a discharge takes place. The frequency increase which is caused by the effect of the glass walls on the capacity of the circuit is next determined. When the condenser C_1 is re-set, so that again zero beats indicate resonance, the potential E_p is increased until a visible discharge sets in. The loud-speaker makes it audible by a sudden change in the pitch of the note. The capacity

Fig. 5.

Frequency variations with discharge-tube inside excitation solenoid.

of the Vernier condenser C_v of the oscillator O_t is then readjusted until the loud-speaker becomes silent, indicating again resonance. With the value ΔC_v thus determined the frequency variation Δf produced by the discharge is then computed from the relation $\Delta f = \Delta C_v f / 2c$.

By gradually increasing E_p the plate potential, the primary current I_1', as also the secondary current I_2 induced in the discharge-tube, is increased. Consequently, if the theory holds, we should expect frequency increments which become larger with increasing values of E_p and I_1'.

Measurements were made with the tube 6 cm. in diameter as well as with the tube 3 cm. in diameter. In both cases the effect of an induced discharge was to decrease the frequency of the oscillator. In fig. 5 the values of Δf are

shown plotted against the primary current I_1'. Curve 1 represents values obtained with the small tube in a solenoid 7·5 cm. in diameter. Curve 2 shows values for the larger tube when inserted in a solenoid 12·5 cm. in diameter. Effects similar in character though smaller in magnitude were obtained when plane spirally wound coils were used instead of solenoids. Evidently the results of measurements do not support the theory, and are contrary to the calculations based on the simple assumption of electromagnetic induction.
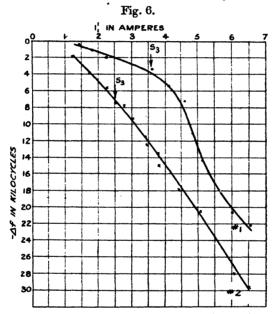
The hypothesis may be made that in all cases investigated the electrostatic field inside the excitation coils causes a decrease of frequency. When the electrostatic field is strong as compared with the electromagnetic induction the trajectories of the electrons which move in the discharge-tube become complex and differ greatly from circular motions. Therefore the assumptions of the theory of electro-magnetic induction cannot be applied for such general cases.

It was for the purpose of testing the above hypothesis that the solenoid in fig. 3 was supplied with two rings, D, supported by two metal strips 12 cm. long. The experi-mental procedure, as described, was repeated for the discharge-tube placed between the rings D, which served as outside electrodes for a purely electrostatic excitation. The curve in fig. 6 represents the value of frequency variation as function of primary current obtained for the same two tubes subjected to such an excitation. Again, the variations were found to be decrements of frequency, but their absolute values increasing at a much larger rate than in the case (fig. 5) when the tube was placed inside the solenoid B. In order to account for such a striking increase of the rate of change of Δf we must consider that in the portion of the tube inside the solenoid the gas is subjected to both the electrostatic and to the electromagnetic fields, which force the electrons to move in complex spirals. If, however, the tube is placed between the rings D the electrostatic field forces the electrons to move predominantly in lines parallel to the axis of the tube.

It appears as if two effects would combine inside the excitation solenoid, of which one produces a decrease the other an increase of frequency; indeed, it is possible to separate the frequency variations due to circular currents from those variations which are caused by the combined action of axial and circular currents in the tube. For this purpose it is necessary to establish between the rings D an electrostatic field which will be equal in intensity and distribution to that which exists inside the solenoid.

It may be assumed, on the basis of observations made in the course of many experiments, that it is always an axial field which by preliminary ionization causes the discharge to set in. If the magnitude of the potential which starts the discharge in each of the positions of the tube be made equal the electrostatic field in both cases may be regarded as similar.

In carrying out this method of separation the ring electrodes D were chosen of such a diameter (7·5 cm.) that the solenoid current I^1, necessary for the discharge to just set

Fig. 6.

Frequency variations with discharge-tube outside excitation solenoid.

in, becomes of equal intensity for both positions of the tube. By slightly displacing the rings along the axis small differences in the starting primary current I may be eliminated. Slight discrepancies of the electrostatic field distribution inside the solenoid, as compared with the field between two rings separated by a distance slightly greater than the length of the solenoid, may be disregarded.

Under these conditions the electrostatic field which produces axial currents in the tube remains approximately the same for both positions. It does not matter for the magnitude of the axial current component whether the tube

is placed between the rings D or inside the solenoid B. In the latter case, however, a circular current component is produced additionally which influences the frequency variations. By subtracting the frequency variations in case of axial currents from those variations which are caused by the combined action of electrostatic and electromagnetic fields the two components can be separated and their relative values determined.

The result of such measurements on the larger tube (diameter 6 cm.) is represented by the curves *a*, *b*, and *c* in fig. 7. Hydrogen electrolytically produced from $Ba(OH)_2$ at a pressure of 0·1 mm. Hg was subjected first to the combined action of electromagnetic and electrostatic fields inside the solenoid B. Curve *a* shows the decrement of frequency (Δf_a) as function of primary current I_1. Then the same tube was inserted between the rings D. Curve *b* (Δf_b) shows the values of frequency decrements due solely to axial currents produced by the electrostatic field. The difference $\Delta f_c = -\Delta f_a - (-\Delta f_b)$, as shown by the curve *c*, gives the increase of frequency due to circular currents induced by the high-frequency electromagnetic field of the solenoid.

For the curve *c* an expression was empirically obtained
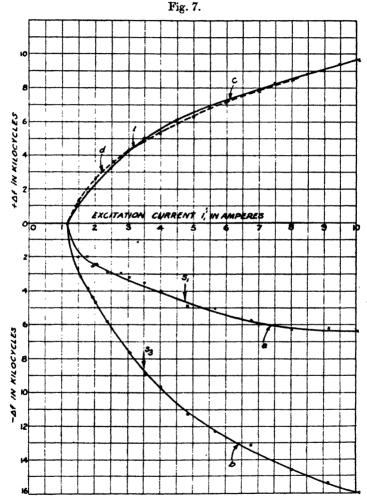
$$\Delta f = k \sqrt{I_1' - i}, \quad \ldots \ldots \quad (4)$$

where $k = 3320$ and $i = 1·4$ amperes, *i. e.*, the value of the excitation current at which a discharge sets in. Both k and i are functions of frequency and pressure.

The maximum deviation of the experimental results (full line curve *c*) from the above expression (dotted curve *d*) is 9 per cent. In this connexion the character of the discharge as evidenced by its appearance may be significant. The discharge sets in at an excitation current of 1·4 ampere as a pinkish-grey uniform glow, whose luminosity increases with the intensity of excitation. At a certain critical value of the current I_1' striations become visible. First they are of an unstable character, indefinite in number, and moving to and fro along the axis of the tube. By a slight increase of the current the striæ become stable. They appear then in pairs six to eight in number. Increasing the excitation current decreases the number of pairs of striæ. They continue to disappear one by one until at another critical value of the excitation current a uniform glow is again established, but of a more intense luminosity than that of the first stage. The striæ appear when the tube is excited by the combined action of electromagnetic and electrostatic induction inside

the solenoid. They also appear when the tube is exposed to the action of electrostatic field alone between the external rings D (fig. 3). However, in case of the complex form of excitation the striæ start and disappear at larger currents than in the case of the simple electrostatic excitation.

Fig. 7.

Separation of frequency variations due to circular currents.

The values of the excitation current at which stable striæ appear are marked in figs. 4, 6, and 7 by arrows S_1, while S_2 in fig. 4 indicates the current at which the latest pair of striæ disappears. Thus S_1 to S_2 includes the range of

current values connected with formation of stable striæ when the tube is placed inside the solenoid. Similarly S_3 to S_4 includes the range of stable striæ formation for the tube placed between external ring electrodes.

The deviations of the curve *d* from *c* may be correlated with the appearance of striæ at currents different in magnitude for each of the two types of excitation ; indeed, the deviation is maximum at $I_1' = 4 \cdot 75$ amperes near the region marked S_1, and diminishes towards increasing as well as towards decreasing values of I_1'. The intersection of the curves *c* and *d* at *e* coincides with the zone S_3.

Further measurements have shown that the decrease of frequency due to the axial current component increases with the length of the solenoid and with the frequency of the oscillator which excites the discharge tube. An explanation may be offered on the basis of our hypothesis. With increased frequency of the oscillator the distribution of current and potential in a coil approaches that of a standing wave. Potential antinodes are being built up at both ends of the solenoid. The larger its length the more these potential antinodes concentrate at the ends of the solenoid. The end windings act then like ring electrodes which project electrostatic lines of force through the cross-section of the solenoid.
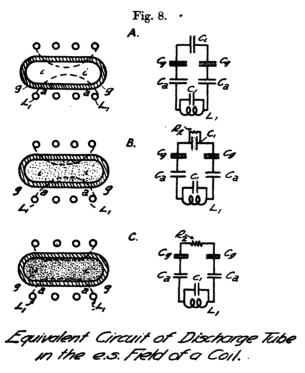
The question may be asked, how does the electrostatic field produce an increase of frequency? Fig. 8 serves to illustrate the influence electrostatic fields exert on the frequency of the oscillator.

Electrostatic lines of force in passing from one end of the coil L_1 to the other end penetrate three media, of which each possesses a different dielectric constant. The lines pass first through air, then through glass, then through ionized gas, and at last again through glass and air. A corresponding equivalent circuit A may be represented by a branch of condensers connected parallel to the condenser C_1 of the excitation circuit. This branch consists of a pair of condensers C_g, which represent the effect of glass walls of the tube, a pair of air condensers C_a, and a single condenser C_i to indicate the rôle of the ionized gas inside the discharge-tube.

The effect of the latter is composed of three parts ; one is comparatively small and consists in the change of capacitance produced by the dielectric constant as function of ionization. The other part consists in the increased conductivity, which is equivalent to the decrease of a resistance R_i shunted across the condenser C_i, as shown in the equivalent

circuit B. The third part of the effect is due to the redistribution of the electrostatic field with increased conductivity of the ionized gas. With increasing current inside the tube. more of the electric flux concentrates in the glass, so that the capacity C_g increases. Gradually the gas conductivity becomes so large that the condenser C_i may be regarded as shorted and the equivalent circuit changed from B to C. The resultant capacitance of the branch C_a, C_g, R_2, C_g, C_a

Fig. 8. ·

Equivalent Circuit of Discharge Tube in the e.s. Field of a Coil.

thus increases and causes a corresponding decrease of the frequency of the oscillating circuit.

The results of the investigation may be summarized as follows :—

1. By measuring frequency variations evidence was obtained for the existence of two current components, axial and circular, in discharges produced by high-frequency excitation of H_2 in a tube inserted inside a solenoid.

2. The axial component produces a decrease of frequency which may be determined by inserting the discharge-tube

within two external electrodes connected to the terminals of the solenoid.

3. The circular component produces an increase of frequency. The effect of circular currents can be separated from the effect of axial currents.

4. The intensity of the circular current and the phase difference between this current and the induced electromotive force can be determined from the magnitudes of frequency variations.

5. As a consequence of the experiments it became evident that the theory of induction as given by J. J. Thomson may be applied only to special cases when the induced currents are large enough to produce a conductivity in the gas sufficient to shield the electrostatic field of the excitation coil.

Following our investigation Prof. Chas. T. Knipp checked our results by qualitative experiments in which luminous effects due to the two current components were made visible by a method of shadows *. Not only do his experiments confirm the existence of circular and axial currents, but they visualize also the effect of simultaneous action of both currents in accordance with our theory.

In the following paper Prof. J. Kunz gives a theoretical investigation which led to more general expressions for the current in the discharge tube as function of the primary excitation current and of frequency variations. References of other authors who investigated electrostatic effects in electrodeless discharges are included in that paper.

Acknowledgment is due to the students (M. McGregor, R. L. Gougler, W. A. Laning, Jr., and D. E. Chapman) who at different times assisted in the experiments and measurements.

XC. *Theory of Electromagnetic and Electrostatic Induction in Electrodeless Discharges.* By JAKOB KUNZ, *Professor in the University of Illinois* †.

SIR J. J. THOMSON ‡ has given a theory of the electrodeless ring discharge based on the assumption that the luminous current is caused by the electric force

due to electromagnetic induction. The formulæ of J. J. Thomson enable us to calculate the circular current in the discharge, a current, that appeared to be the only one produced in an experiment, which has not yet been measured. We therefore intended at first to measure this current by some indirect method. We shall see that the current can be determined by measuring the e.m.f. around the circuit and the change of the frequency in the primary circuit. Accepting the notations of Sir J. J. Thomson, we find the magnetic force in the discharge-tube given by

$$H = H_0 \sin \omega t \, \frac{J_0(jnr)}{J_0(jnR)},$$

the components of the current densities by

$$4\pi i_y = \frac{\partial H}{\partial z} = H_0 \frac{\sin \omega t}{J_0(jnR)} \frac{\partial J_0(jnr)}{\partial r} \cdot \frac{z}{r},$$

$$4\pi i_z = -\frac{\partial H}{\partial y} = -H_0 \frac{\sin \omega t}{J_0(jnR)} \frac{\partial J_0(jnr)}{\partial r} \cdot \frac{y}{r},$$

and the resultant density by

$$4\pi i = H_0 \frac{\sin \omega t}{J_0(jnR)} \frac{\partial J_0(jnr)}{\partial r} \cdot \frac{jn}{jn}.$$

The total induced current i_t per unit length measured along the axis is given by

$$4\pi i_t = 4\pi \int_0^R i \, dr = \frac{H_0 \sin \omega t}{J_0(jnR)} \int \frac{\partial J_0(jnr)}{\partial r} \cdot dr,$$

$$i_t = \frac{H_0}{4\pi} \sin \omega t \, \frac{J_0(jnR) - J_0(jno)}{J_0(jnR)} = I \sin \omega t.$$

The magnetic flux ϕ through the tube is given by $\phi = \int H 2\pi r \, dr$, and the e.m.f. around a circle of radius r by

$$E.m.f._r = \int_0^r 2\pi r \, dr \frac{\partial H}{\partial t}$$

$$= 2\pi \omega \frac{H_0 \cos \omega t}{J_0(jnR)} \int_0^r J_0(jnr) \, r \, dr$$

$$= 2\pi \omega H_0 \cos \omega t \, \frac{r J_1(jnr)}{jn J_0(jnR)}.$$

The e.m.f. around the circle of radius R is equal to

$$E.m.f._R = 2\pi \omega H_0 \cos \omega t \, \frac{R}{n} \text{ (when } Rn \text{ is large)}$$

$$= \dot{E}_a \cos \omega t.$$

This e.m.f.$_R$ can be measured directly, its amplitude

$$E_a = 2\pi\omega H_0 \frac{R}{n}.$$

If we measure E_a, ω, H_0, and R we can determine n. Knowing n, we can determine σ by means of $n^2 = j4\pi\omega\sigma$ or

$$n = \sqrt{j}\sqrt{4\pi\omega\sigma},$$

$$n = \frac{1+j}{\sqrt{2}}\sqrt{4\pi\omega\sigma},$$

and the real part of it is

$$n_{\text{real}} = \sqrt{2\pi\omega\sigma},$$

while ϕ_R is equal to

$$\phi_R = 2\pi H_0 \sin\omega t \int_0^R \frac{J_0(jnr)dr}{J_0(jnR)}$$

$$= 2\pi H_0 \frac{\sin\omega t}{J_0(jnR)} R J_1(jnR) = \phi_1 + \phi_2, \quad . \quad (1)$$

equal to the resultant flux through the tube. ϕ_1 is the flux due to the primary current i_1 through the coil, ϕ_2 due to the induced current $i_2 = i_t.l$ in the discharge.

$$\phi_1 = H_0\pi R^2 \sin\omega t,$$

$$\phi_2 = \pi R^2 H_0 \sin\omega t \left\{ \frac{2}{R}\frac{J_0(jnR)}{J_0(jnR)jn} - 1 \right\} = L_2 i_t l. \quad (2)$$

L_2 is the coefficient of self-induction of the current $i_2 = i_t.l$. Substituting i_t of a previous equation in equation (2), we find

$$L_2 = 4\pi^2 R^2 \frac{\dfrac{2}{R}\cdot\dfrac{J_1(jnR)}{jn} - J_0(jnR)}{J_0(jnR) - J_0(jno)};$$

as we know σ and n, we can evaluate the Bessel functions and calculate L_2. We consider the oscillating circuit of fig. 1. The potential difference between the condenser plates shall be p, the primary current i_1, the number of turns per unit length N, the coefficient of self-induction of the system L, the resistance R_e and the coefficient of mutual inductance between the primary and the secondary currents M. The generalized Ohm's law gives the equation

$$p = i_1 R_e + L\frac{di_1}{dt} + M\frac{di_2}{dt}. \quad . \quad . \quad . \quad (3)$$

Moreover,

$$H = H_0 \sin \omega t = 4\pi N J_1 \sin \omega t.$$

$$i_1 = I_1 \sin \omega t = -\frac{dq}{dt} = -C \frac{dp}{dt};$$

hence

$$\frac{H_0}{4\pi} = N I_1, \quad i_2 = i \, l$$

$$= l N I_1 \sin \omega t \frac{J_0(jnR) - J_0(jno)}{J_0(jnR)} ;$$

As i_2 is opposite to i_1, we write

$$i_2 = -l N i_1 \frac{J_0(jnR) - J_0(jno)}{J_0(jnR)} .$$

With these substitutions we obtain from (3)

$$\frac{d^2p}{dt^2} \left[LC - MCN \frac{J_0(jnR) - J_0(jnr)}{J_0(jnR)} \right] + R_e C \frac{dp}{dt} + p = 0.$$

Neglecting the second term, we may write the solution in the form $p = P \cdot e^{j\omega t}$, where ω_2^2 is equal to

$$\omega_2^2 = \frac{1}{LC - MNC \left[\dfrac{J_0(jnR) - J_0(jno)}{J_0(jnR)} \right]} ,$$

while

$$\omega_1^2 = \frac{1}{LC} ;$$

hence

$$\omega_2^2 = \omega_1^2 \cdot \frac{1}{1 - \dfrac{MN}{L} \left[\dfrac{J_0(jnR) - J_0(jno)}{J_0(jnR)} \right]} , \quad . \quad . \quad (4)$$

or approximately

$$\omega_2^2 = \omega_1^2 \left[1 + \frac{MN}{L} \left(\frac{J_0(jnR) - J_0(jno)}{J_0(jnR)} \right) \right]. \quad . \quad (5)$$

Neglecting the resistance again, we obtain from (3)

$$p = L \frac{di_1}{dt} + M \frac{di_2}{dt},$$

or after the given substitutions

$$p = L I_1 \omega \cos \omega t - \omega M l N I_1 \cos \omega t \, f(\omega, \sigma, R),$$

where $f(\omega, \sigma, R) = \dfrac{J_0(jnR) - J_0(jno)}{J_0(jnR)}$,

a function which approaches 1 with increasing frequencies.

$$p = I_1 \omega \cos \omega t [L - MlNf(\omega, \sigma, R)] = P \cos \omega t ;$$

hence the amplitude P of the potential difference is equal to

$$P = I_1 \omega [L - MlNf(\omega, \sigma, R)]. \quad . \quad . \quad . \quad (6)$$

If we measure I_1, the current, then we know P by this equation. From (5) we obtain

$$\frac{\omega_2^2}{\omega_1^2} - 1 = \frac{(\omega_2 - \omega_1)(\omega_2 + \omega_1)}{\omega_1^2} = \frac{\Delta\omega \cdot 2}{\omega_1} = \frac{MN}{L} f(\omega, \sigma, R), \quad (7)$$

or ω_1, which is more nearly equal to ω, is given by

$$\omega_1 \simeq \omega \simeq \frac{2\Delta\omega L}{MNf(\omega, \sigma, R)} .$$

Substituting this in (6), we obtain

$$P = I_1 \frac{2\Delta\omega L}{M . Nf(\omega, \sigma, R)} (L - MNf(\omega, \sigma, R),$$

or

$$P = I_1 2\Delta\omega L \left[\frac{L}{MNf(\omega, \sigma, R)} - l \right] \quad . \quad . \quad . \quad (8)$$

This formula shows how $\Delta\omega$ changes with P, the amplitude of the potential difference. Moreover, we obtain from (7)

$$\Delta\omega = \frac{\omega_1}{2} \frac{MN}{L} f(\omega, \sigma, R), \quad . \quad . \quad . \quad (9)$$

from which we can calculate $f(\omega, \sigma, R)$ and σ, the conductivity itself; but the specific resistance is $= \dfrac{1}{\sigma}$, and the total (ring) resistance of the tube is equal to

$$R_e = \frac{2\pi R/2}{\sigma R l} = \frac{\pi}{\sigma l},$$

or the resistance per unit length $= R_{e_1} = \dfrac{\pi}{\sigma}$. The total induced ring current

$$i_2 = i_l l = lN I_1 \sin \omega t f(\omega, \sigma, R),$$

or by means of (9)

$$i_2 = lN I_1 \sin \omega t \frac{2\Delta\omega L}{\omega_1 MN} = I_2 \sin \omega t, \quad . \quad . \quad (10)$$

where the amplitude I_2 is equal to

$$I_2 = lI_1 \frac{2\Delta\omega L}{\omega_1 M}. \quad \ldots \ldots \quad (11)$$

In this way the ring current can be determined. By (5) the frequency of the primary circuit ω_2, when ionization is produced in the tube, is larger than ω_1, the frequency without luminous discharge. The same statement holds when the luminous ring in the gas is replaced by a wire or by a ring filled with an electrolyte. This result is intuitively evident, because the effective self-induction L of the primary is decreased when a current in a neighbouring circuit is induced in a direction opposite to the primary current.

In order to estimate the order of magnitude of $\Delta\omega$ given by (9) we calculate at first $f(\omega, \sigma, R)$, assuming the following values:

$$R_e = \frac{1 \cdot 6}{\sigma} = 500 \cdot 10^9, = 3 \cdot 10^{-12} \text{ e.m. unit.}$$

$$f(\sigma, \omega, R) = \frac{J_0(jnR) - J_0(jno)}{J_0(jnR)},$$

$$J_0(jx) = 1 + \frac{\left(\frac{1}{2}x\right)^2}{1!^2} + \frac{\left(\frac{1}{2}x\right)^4}{2!^2} + \ldots,$$

$$J_0(jnR) = 1 + \frac{1}{4}n^2R^2 + \frac{1}{2^6}n^4R^4 + \ldots,$$

$$J_0(jno) = 1,$$

$$f(\omega, \sigma, R) = \frac{\frac{1}{4}n^2R^2 + \frac{1}{2^6}n^4R^4 + \ldots}{1 + \frac{1}{4}n^2R^2 + \ldots},$$

but

$$n^2 = j4\pi\omega\sigma;$$

hence

$$f(\omega, \sigma, R) = \frac{\frac{1}{4}4\pi\omega\sigma jR^2}{1 + \frac{1}{4}4\pi\omega\sigma jR^2}.$$

Assuming

$$\omega = 2 \cdot 10^7, \quad \sigma = 3 \cdot 2 \cdot 10^{-12}, \quad R = 2,$$

the real part of $f(\omega, \sigma, R)$ becomes approximately $= 8 . 10^{-4}$.

$$\Delta\omega = \frac{\omega_1}{2}\frac{MN}{L}f(\sigma.\omega, R).$$

As an example we assume

$$\omega_1 = 2.10^7, \quad M = 2.10^{-6} \text{ henry}, \quad L = 2.10^{-5} \text{ henry},$$

$$N = 4, \quad f(\omega, \sigma, R) = 8.10^{-4},$$

and find

$$\Delta\omega = 3\cdot2.10^3.$$

In the preceding paper, J. T. Tykociner found that in all cases ω_2 was smaller than ω_1. This result shows that our theory can only explain a part of the phenomenon, and that the greater part in the change of ω is due to another cause.

It has been suggested by O. Lehmann [*], E. Lecher, A. Steiner [†], and more recently by J. S. Townsend [‡], that the electrostatic forces between the ends of the coil are stronger than the electric forces due to electromagnetic induction, and K. A. MacKinnon [§] came to the conclusion that the glow discharge in the electrodeless tube is largely electrostatic, while the ring discharge, investigated by Sir J. J. Thomson is of electromagnetic origin. In addition, C. J. Brasefield [‖] has shown that the luminous discharge ceased when the glass tube was shielded by a set of wires parallel to the axis of the tube joined at each end by a ring with a small gap in it. If in this way the tube is shielded and the current in the primary coil is strong enough, it should be possible to obtain a pure electromagnetic ring discharge.

We proceed to find out how the ionization due to electrostatic forces leads to a decrease of the frequency. In fig. 1 the potential difference $p_1 - p_2$ is equal to

$$p_1 - p_2 = \frac{d}{dt}(H\pi R^2 N l) = \pi R^2 N l \frac{dH}{dt},$$

and the axial electric force

$$E_{es} = \frac{p_1 - p_2}{l} = \pi R^2 N \frac{dH}{dt},$$

if we assume a uniform magnetic field H in the coil. In a

[*] Wied. *Ann.* xlvii. p. 427 (1892).
[†] *Wiener Ber.* cxiii. *a*, p. 403 (1904).
[‡] Phil. Mag. v. p. 178 (1928).
[§] Phil. Mag. viii. p. 605 (1929).
[‖] Phys. Rev. xxxiv. p. 1627 (1929).

conducting circle of radius R_1 in the tube, the e.m.f. induced is equal to $\pi R_1^2 \dfrac{dH}{dt}$, and the circular electric force

$$E_m = \frac{\pi R_1^2}{2\pi R_1}\frac{dH}{dt} = \frac{R_1}{2}\frac{dH}{dt} \, ;$$

hence
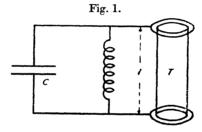
$$\frac{E_{es}}{E_m} = 2\pi N \frac{R^2}{R_1} .$$

In the tube T with external electrodes we consider electrons moving under the influence of an alternating electric field,

$$E = E_0 \cos(\omega t + \phi).$$

The differential equation of motion of the electrons is as follows :

$$m\frac{d^2x}{dt^2} = eE_0 \cos(\omega t + \phi),$$

Fig. 1.

and the conductivity is equal to

$$\sigma = \frac{e^2}{c}\frac{l}{m}\frac{nN_e}{\omega^2 + n^2} \text{ e.m.u.,}$$

where N_e is the number of ions per unit volume, n the number of collisions of one ion per unit time, ω the frequency per 2π seconds, e the charge, and m the mass of the ion. If we assume uniform ionization in the discharge-tube of radius R and length l, then the resistance will be

$$R_i = \frac{l}{\pi R^2}\frac{1}{\sigma} = \frac{l}{\pi R^2}\frac{c^2 m(\omega^2 + n^2)}{e^2 nN_e} \, ;$$

the axial current in the tube will be

$$i = \frac{p_1 - p_2 - p_g}{R_i} = \frac{\left(\pi R^2 N l \dfrac{dH}{dt} - p_g\right)}{lc^2 m(\omega^2 + n^2)}\pi R^2 e^2 nN_e.$$

p_g is due to the loss of the electric force through the glass

3 R 2

walls. The electric field in the glass tube, however, is far from being uniform. If the electric force E between two successive windings in the middle of the coil is strong enough, we might get a pure electrostatic ring discharge in the beginning. And if in general the electrostatic force E_{es} is stronger than the electromagnetic force E_m, we may expect at first an electrostatic discharge, followed by an electromagnetic induction, which cannot fail to appear, when there is sufficient ionization, as long as the electromagnetic laws hold.

If there is no ionization in the tube, the frequency ω_1 of the discharge in the system of fig. 2 will be given by

$$\omega_1{}^2 = \frac{1}{LC} - \left(\frac{R_1}{2L}\right)^2 ;$$

if, however, there is a resistance R_i in the tube, the frequency will change, and there is another effect which we have to consider: the capacity of the glass tube will be changed by the motion of the electrons in it. Indeed, if the electric force in the tube is given by

$$E = E_0 \cos \omega t,$$

then

$$m \frac{d^2x}{dt^2} = E_0 e \cos \omega t$$

is the differential equation of motion of the electron; hence

$$\frac{dx}{dt} = \frac{E_0 e}{m\omega} \sin \omega t.$$

If there are N_e electrons per cm.³, then the density of the convection current is equal to

$$i_c = N_e e \frac{dx}{dt} = \frac{N_e e^2 E_0}{m\omega} \sin \omega t,$$

and the displacement current

$$i_d = \frac{k_0}{4\pi} \frac{\partial E}{\partial t} ;$$

hence the resultant current

$$i = i_d + i_c = \left(\frac{k_0}{4\pi} - \frac{N_e e^2}{m\omega^2}\right) \frac{\partial E}{\partial t} = \frac{k}{4\pi} \frac{\partial E}{\partial t},$$

or the dielectric constant of the tube with the moving ions is equal to

$$k = k_0 - \frac{4\pi N_e e^2}{m\omega^2},$$

or the capacity of the condenser is decreased by ionization

It can be shown by means of Maxwell's equations that

$$\sigma = \frac{kn}{4\pi}.$$
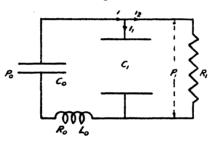
If we take the collisions of the electrons into account, we should expect the following relation:

$$k = k_0 - 4\pi N_e \frac{e^2}{m} \frac{l}{\omega^2 + n^2}.$$

This relation has indeed been given by P. O. Pederson and others.

We shall now consider the oscillations in the system represented by fig. 2. The condenser C_1 is the glass tube with the ionization, *i.e.*, a leaking condenser, or a condenser of capacity C_1 with a parallel resistance R_1, R_0 and L_0, are

Fig. 2.

very small resistance and self-induction respectively. We obtain the following equations:

$$i = i_1 + i_2 ; \quad i = -\frac{dq_0}{dt} = -C_0 \frac{dp_0}{dt}. \quad . \quad . \quad (1)$$

$$i_1 = -\frac{dg_1}{dt} = -C_1 \frac{dp_1}{dt} ; \quad i_2 = \frac{p_1}{R_1}. \quad . \quad . \quad (2)$$

$$p_0 = iR_0 + L_0 \frac{di}{dt} + i_2 R_1. \quad . \quad . \quad . \quad . \quad (3)$$

$$\frac{dp_0}{dt} = \frac{di}{dt} R_0 + L_0 \frac{d^2 i}{dt^2} + \frac{di_2}{dt} R_1. \quad . \quad . \quad . \quad (4)$$

$$-\frac{i}{C_0} = \frac{di}{dt} R_0 + L_e \frac{d^2 i}{dt^2} + R_1 \frac{di}{dt} - R_1 \frac{di_1}{dt}. \quad . \quad . \quad (5)$$

But $i_2 R_1 = p_1$; hence from (2) and (3)

$$i_1 = -C_1 \frac{dp_1}{dt} = -C_1 \left[\frac{dp_0}{dt} - R_0 \frac{di}{dt} - L_0 \frac{d^2 i}{dt^2} \right], \quad . \quad (6)$$

or, by means of (1),

$$i_1 = \frac{C_1 i}{C_0} + C_1 R_0 \frac{di}{dt} + L_0 C_1 \frac{d^2 i}{dt^2}. \quad \cdots \quad (7)$$

Differentiating i_1, and substituting it in (5) we obtain

$$R_1 C_1 L_0 \frac{d^3 i}{dt^3} + \frac{d^2 i}{dt^2} [R_1 R_0 C_1 - L_0] - \frac{di}{dt}(R_0 + R_1) - \frac{i}{C_0} = 0. \quad (8)$$

In a first approximation we shall neglect the first term and write *

$$\frac{d^2 i}{dt^2} + \frac{di}{dt}\frac{R_1 + R_0}{L_0 - R_1 R_0 C_1} + \frac{i}{C_0(L_0 - R_1 R_0 C_1)} = 0,$$

which gives the frequency

$$\omega_e = \sqrt{\frac{1}{C_0(L_0 - R_1 R_0 C_1)} - \frac{1}{4}\left(\frac{R_1 + R_0}{L_0 - R_1 R_0 C}\right)^2}.$$

The capacity C_1 is small compared with C_0, the resistance R_1 is larger than R_0, and L_0 is a small quantity; the frequency ω_e will therefore be small compared with the frequency

$$\omega = \sqrt{\frac{1}{L C_0} - \left(\frac{R}{2L}\right)^2}$$

of the original system.

In a beautiful experiment with two concentric spheres, Sir J. J. Thomson has shown that when the inner bulb was exhausted it glowed under the action of a discharge; when, now, the outer bulb was exhausted, the ring discharge appeared in the outer bulb and disappeared in the inner one; but as the outer bulb was completely evacuated it ceased to glow, while the inner bulb became luminous again. The extinction of the inner glow is explained by Sir J. J. Thomson as caused by a magnetic screening effect. Indeed, if the current in the ring discharge of the outer sphere is sufficiently strong, its magnetic field, opposite in direction to the field of the exciting coil, may become so strong as to wipe out the magnetic field in the centre. We have repeated this experiment with an electrostatic field alone, and have found results similar to those of Sir J. J. Thomson. The double sphere was placed either between two condenser plates or between two closed and separated loops of wire, parallel to each other over the outer sphere. The inner sphere, properly evacuated, began to glow at first, in the

---

* A complete solution will be given later.

measure, as the vacuum increased, the outer glow appeared, and finally the inner sphere became luminous again. The distribution of light, however, is different in the two experiments. In the magnetic field the discharge appears mostly in the form of a ring, and quite intense ; in the electrostatic field the discharge is a more or less uniform, comparatively weak glow. There is, however, a tendency for two luminous rings to form parallel to the two circular wires. Again, when the outer tube is luminous, the exciting electrostatic field is screened from the inner bulb as the lines of force pass through the outer discharge.

The conditions for the initial discharge under the electrostatic action have been given by Dr. J. Thomson in this Magazine (vol. x. p. 280 (1930)).

Summary.

The electrodeless discharge has been investigated in two parts. In the first part the effect of the magnetic field has been studied on the basis of the theory of Sir J. J. Thomson. It has been shown that the frequency increased by the magnetic ring discharge. The induced ring current and other quantities have been deduced. In the second part the electrostatic effect has been treated. Expressions have been given for the conductivity and the coefficient of self-induction of the glass bulb containing the ionization. The frequency of this discharge has been determined. An experiment analogous to one by Sir J. J. Thomson has been described, showing the effect of electric forces on the glow discharge in a double sphere.

XCI.—*The Effect of Spatial Induction on the Discrimination of Differences in Brightness.* By JAMES F. SHEARER, *M.A., B.Sc., Head of the Department of Mathematics and Physics in the Technical College, Coatbridge* *.

§ 1. IF I is the brightness of a surface and ΔI its least perceptible increment Dr. Houstoun † showed, from the results of König and Brodhun, that when $I/\Delta I$ was graphed as a function of log I it formed a Gaussian probability curve,

and in a recent paper *, in conjunction with Dr. Houstoun, I made a further experimental study of the subject. In that paper we gave results obtained by two different methods. In one of these the observer looked into the eyepiece of a telescope and saw two rectangles touching each other. He altered the relative intensity of these by rotating a polarizer. In the other method the observer saw two faces of a rhomb bounded by a sharp line of separation which was brought close up to a circular aperture in a plate ; and the relative intensity was altered by means of neutral wedges. The first of these methods proved to be the more accurate, but from the nature of the method the rectangles appeared on a dark ground, *i. e.*, we were restricted to a dark surround. With the second apparatus we were not so restricted, and this paper describes an investigation made with it of the effect of illuminating the surround.

In the apparatus then (*cf.* fig. 1 of former paper) the eye of the observer looked down vertically through an aperture of 2 mm. diameter, which was fitted with a magnifying lens, at the circular aperture in the plate, bisected by the edge of the rhomb and situated about 12 cm. below the magnifying lens. The latter was chosen so that the edge of the rhomb was exactly in focus, while the circular aperture in the plate was of 1 cm. diameter. Thus the eye saw a half shadow field the intensities of which could be altered by moving two wedges. One 220 volt Pearl Osram lamp was used to illuminate both halves of the field, and it was connected in series with a resistance and a milliammeter. By over-running it to 250 volts and reducing the current till the limit of visibility was reached a range of brightness of from 1 to 10^7 was at my disposal. The brightness of the field was determined in absolute measure in the manner described in the previous investigation.

In the first test a piece of cardboard, with a diamond-shaped hole in it, was fixed with its plane at 45° to the vertical and so that the hole was directly above the edge of the rhomb. The cardboard was illuminated by an 8 c.p. carbon lamp which could be moved along a horizontal bench, and the brightness varied through a large range. With this arrangement the eye of the observer saw a diamond-shaped half shadow field divided along its shorter diagonal. This diagonal subtended about $2\frac{1}{2}°$ at the eye, and the diamond appeared in the middle of a rectangular luminous surround which subtended 22°×15°. Outside of this the field was

* *Ibid.* x. p. 433 (1930).

dark. The least perceptible increase in brightness was then determined for various illuminations of the surround ; and the following table gives some results obtained through a Wratten red standard tricolour filter :—

TABLE I.

Log of brightness of test object in " illumination units "
= 3·5

Log of brightness of surround in illumination units.	I/ΔI.
1·85	27·5
0·44	26·5
1·04	46·1
1·65	50·9
2·60	19·9

The illumination unit here used is one-tenth of a photon. The results show that under the conditions of the experiment the power of the eye to discriminate intensity rose to a maximum, and then diminished as the brightness of the surround increased further.

An isolated series of experiments like this is, however, of little value. We know that if the surround is dark I/ΔI is a probability curve when graphed against log I. We wish to know whether it preserves the same shape when the surround is light, and if so whether it shifts, widens, or increases in intensity. Only when we know the change that occurs over the whole range of brightness can we draw theoretical deductions about the nature of the processes involved. I decided therefore to measure I/ΔI for red light over the whole range. The conditions thus had to suffer a double variation : (i.) I_0, the brightness of the surround, had to vary ; (ii.) I, the intensity of the test object, had also to vary.

The cardboard was removed from the 1 cm. aperture and replaced by a brass plate in which a circular hole of ⅛ inch diameter had been accurately drilled. The angle subtended by the diameter of the test field was thus limited to 1·75°, while the area of the brass plate to be used as the surround was limited by inserting a short vertical tube immediately below A. The diameter of the surround then subtended 25°.

Before each set of readings was taken the surface of the brass plate was freshly coated with a deposit of magnesium oxide by holding it in the smoke of burning magnesium ribbon. It was decided to work with four brightness levels of the surround, one of these being darkness. The others were obtained by means of three lamps, fixed in clamps at the side, and operated by switches convenient to the hand of the observer. They were measured by bringing the test field up to the same brightness and looking up the current through the Pearl Osram in the calibration chart. The observer was, of course, screened from the direct rays of the lamps and saw nothing whatever but test field and surround.

The procedure adopted was as follows :—After I had been in the dark room for five minutes I set the current through the Pearl Osram to give the lowest intensity desired and kept the surround dark. Then I set the sliding wedges till one-half of the object was just darker than the other, read the wedge-scale with the aid of a 2-volt lamp, set the wedges so that the other half of the object was now the darker, read the scale again, and noted down the readings. Then I set the current to the next higher value, and repeated as above until the maximum current was reached. Next I switched on one of the lamps at the side to get the second level of surround, and repeated for all the current values again until the lowest was reached. Thereupon I switched on the second side-lamp and reascended through the same current values, and, lastly, switched on the third lamp and descended through all the values again. To avoid undue fatigue only nine different intensities of the test field were used, but even this meant 72 settings at one sitting.

The next set was taken the following day at the same time, but, though the surrounds were taken in the same order, the first reading of all was taken at the highest intensity, *i. e.*, the order was descending, ascending, descending, and ascending. The third set was taken with the currents rising and falling as in the first, but the order in which the surrounds were taken was reversed ; and so on, the object being not to favour any one surround in any way, either in always being taken first or always being taken with the currents increasing. Altogether ten sets were made. After the last set was completed the brightness levels of the surrounds were verified, and they were found to have almost their initial values.

It will be noticed that I read the scales myself and also entered up the readings between the settings. This is better than employing an assistant, because it brings the eye into the same condition of adaptation before each reading.

The following table shows the results obtained (the intensities are expressed in illumination units):—

TABLE II.
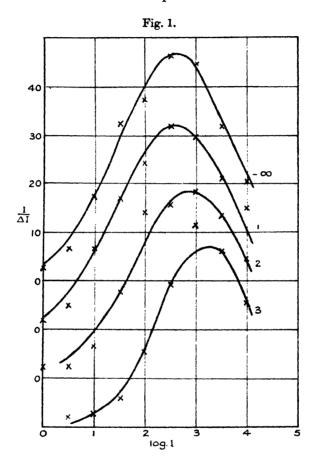
Log I_0	$-\infty$.	1.	2.	3.
Log I.	I/ΔI.	1/ΔI.	I/ΔI.	I/ΔI.
0·0	2·59	2·00	1·95	—
·5	6·56	4·90	2·38	1·96
1·0	17·54	16·69	6·48	2·44
·5	32·26	26·67	17·61	5·83
2·0	37·31	34·25	34·05	15·40
·5	46·30	41·84	35·65	28·99
3·0	44·64	39·59	38·17	41·36
·5	31·65	30·86	33·51	36·05
4·0	20·16	24·92	24·67	25·55

The results are graphed in fig. 1, the smooth curves being exponential curves adjusted by trial and error to fit the observations. In the interests of clearness each curve is displaced one square below its predecessor.

It will be noticed that the smooth curves fit the observations well; but as the level of the surround is raised they are displaced towards the right and at the same time the maximum ordinate diminishes slightly. There is no appreciable change in the shape, *i. e.*, the standard deviation remains unaltered. It will be remembered that the curve represents a distribution of percipient elements with different thresholds; consequently, as the level of the surround is raised the level of the thresholds is raised generally, and simultaneously some of the elements with thresholds below the level of the surround are put out of action. Further than this it would not at present be safe to go ; the data are hardly sufficient to establish a formula.

Let us now return to the results recorded in Table I. If we look at abscissa 3·5 in the table we find I/ΔI increasing slightly as log I_0 changes from — ∞ to 3, whereas according to the preliminary investigation it should increase to a maximum at 1·65 and then suffer a marked diminution. The difference must be ascribed to the difference in the size of the test object, which extended beyond the foveal region in the preliminary experiment.

§ 2. The most extensive previous study of the effect of the surround is that of E. M. Lowry*. His surround consisted of a hemispherical bowl 1 metre in diameter, coated inside with matt white paint, which could be illuminated up to 600 millilamberts. The comparison surfaces were aerial

Fig. 1.

images of the faces of an illuminated alabaster prism which were formed in an aperture in the centre of the hemispherical surface. His tables are reproduced below, his Fechner fraction being converted into our form $I/\Delta I$. It will be noted that the angle subtended by the object was 50′ except in one case, so foveal vision was generally ensured, and that four

* J. Opt. Soc. Amer. xviii. p. 29 (1929); Phot. Ind. xxvii. p. 878 (1929).

different values of surround brightness were employed, viz., 0·0005, 10·7, 53, and 100 millilamberts. Sometimes he used one eye and sometimes two for the observations, as one of the objects of his investigation was a comparison of monocular and binocular vision. In the table I is measured in millilamberts.

His results are in accordance with mine. Some of the sets are irregular, each point resting apparently on a single

TABLE III.—Contrast Sensibility.

0·0005 ml. (50′ test field).				0·0005 ml. (2° 30′ field).	
Monocular.		Binocular.		Binocular.	
Log I.	I/ΔI.	Log I.	I/ΔI.	Log I.	I/ΔI.
$\bar{3}$·85	1·82	$\bar{3}$·10	1·16	$\bar{4}$·92	1·44
$\bar{3}$·93	1·93	$\bar{3}$·37	1·50	$\bar{3}$·34	3·14
$\bar{2}$·02	2·65	$\bar{3}$·61	1·97	$\bar{3}$·91	5·08
$\bar{2}$·81	6·71	$\bar{2}$·00	3·10	$\bar{2}$·22	6·02
$\bar{2}$·86	4·31	$\bar{2}$·35	4·83	$\bar{2}$·48	10·00
$\bar{1}$·53	7·81	$\bar{2}$·81	8·00	$\bar{2}$·71	12·82
$\bar{1}$·97	12.50	$\bar{1}$·25	11·49	$\bar{1}$·38	9·52
0·66	10·64	$\bar{1}$·73	15·38	0·02	20·83
1·88	9·52	0·44	18·18	0·52	47·62
2·18	10·10	1·17	18·87	1·10	125·00
2·44	8·93	1·80	17·24	1·66	52·63
2·78	9·71	2·46	14·29	1·90	83·33
				2·31	41·67
				2·77	28·57
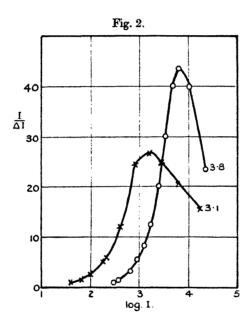
observation; but if we consider the last four sets, which are averages, the set at 10·7 ml. is represented by the crosses in fig. 2 and the set at 100 ml. by the circles. The two sets at 53 ml. do not differ appreciably from the set at 100 ml. In the diagram I is given in illumination units, the data of Reeves on pupil aperture being used to make the change. The relative heights of the two curves has probably little value, as they were not made under the same conditions, but the shift and change in width are undoubtedly genuine. The maximum moves from 3·3 to 3·8 on the scale of abscissæ when log I_0 goes up from 3·1 to 3·8. According to my

TABLE IV.—Contrast Sensibility.

10·7 ml.				53 ml.						100 ml.	
Monocular.		Binocular.		Binocular. Av. 3 obs.		Monocular. Av. 4 runs, 2 obs.		Binocular. Av. 5 runs, 4 obs.		Binocular. Av. 3 runs.	
Log I.	I/ΔI.	Log I.	I/ΔI.	Log I.	I/ΔI.	Log I.	I/ΔI.	Log I.	I/ΔI.	Log I.	I/ΔI.
2̄·97	1·36	2̄·85	1·41	2̄·99	1·00	0·45	1·00	0·08	1·00	0·24	1·00
1̄·30	2·23	1̄·17	2·70	1̄·20	1·43	0·67	2·50	0·17	1·24	0·36	1·34
1̄·68	4·27	1̄·64	6·80	1̄·52	2·50	0·80	3·85	0·39	2·00	0·62	3·05
0·08	9·71	0·00	12·35	1̄·88	5·00	1·00	8·47	0·80	5·00	0·81	5·26
0·53	14·29	0·52	20·83	0·00	5·59	1·20	13·70	0·92	8·67	0·99	8·33
1·87	14·29	1·85	66·67	0·40	12·05	1·40	23·26	1·09	10·00	1·20	12·50
2·17	15·63	2·15	35·71	0·80	24·39	1·60	34·48	1·20	12·50	1·40	20·00
2·43	19·23	2·42	27·03	1·20	26·32	1·80	38·46	1·38	20·00	1·60	30·30
2·77	20·00	2·76	37·04	1·60	24·39			1·60	33·30	1·80	40·00
				2·00	20·41					2·00	43·48
				2·60	15·63					2·40	40·00
										2·73	23·26

results the maximum changed from 2·6 to 3·2 when log I₀
rose from 1 to 3. It is impossible to state how much of the
difference is due to difference in the observers and how much
to difference in the conditions under which the measurements
were made.

§ 3. After concluding the experiments described in § 1 of
this paper it was decided to investigate what effect was
produced on the discriminating power of one eye when the
other eye was stimulated with the same colour. Accordingly
the apparatus was modified as follows:—To the left of the

Fig. 2.

aperture and at the same height was fixed a similar aperture,
at a distance equal to the interocular distance of the observer.
Through the one aperture the right eye looked at the same
half shadow field as before, but now the surround was always
kept dark ; and through the other aperture the left eye
looked at a bright circular patch of the same angular sub-
tense as the surrounds used in § 1. The illumination of the
patch was produced by a lamp in series with a resistance, in
conjunction with a system of mirrors. By means of various
screens fitting closely to the head and nose it was ensured
that each eye was acted on only by its appropriate stimulus.

By varying the resistance in the circuit of the second lamp
currents were determined which gave brightnesses of 0, 10,

100, and 1000 illumination units, these values being chosen because they were identical with the surround values used in § 1.

The manner of making the test was much the same as before. With the left eye looking at the dark surround the right eye was taken through the same ascending values of intensity as previously, two settings of the wedges being made and noted at each value. Then the current through the second lamp was altered to the predetermined value, so that the left eye now looked at a circular patch of intensity 10 units, and, with this kept fixed, the intensities of the test object were reduced through the range, two settings of

TABLE V.

Patch values.	— ∞ .	1.	2.	3.
Log I.	I/ΔI.	I/ΔI.	I/ΔI.	I/ ΔI.
0·0	2·34	1·78	—	—
·5	3·61	3·08	3·27	3·85
1·0	10·83	9·53	8·03	7·13
·5	17·25	15·40	14·32	17·43
2·0	21·44	20·48	21·87	24·25
·5	23·13	26·23	26·56	27·69
3·0	29·84	26·13	27·23	29·73
·5	29·92	22·64	25·05	29·06
4·0	21·01	20·29	23·68	22·24

the wedges again being made at each point. Next with the circular patch at a brightness of 100 units settings were made for the right eye with the brightness of the test object increasing, and, finally, the brightness of the patch was changed to 1000 units and the test object diminished in intensity through the usual values. All the above readings were taken at one sitting and formed one set. Seven subsequent sets were made with the brightness of the patch and of the test object taken in different orders, and the following table shows the final results. Again the intensities I are in illumination units and the brightness of the patch is expressed in the same units as the values in column 1.

When these results are plotted it is found that *one* error curve can be drawn to fit quite well the values in all the four columns. Thus it seems clear that excitation of the left eye had no appreciable effect on the discriminating power of the right eye. There is certainly no such shift of the curves as has been shown to exist when the brightness of the surround is altered.

During the experiment it was found that sometimes the patch viewed by the left eye disappeared or fluctuated in and out, but naturally when the setting of the wedge was being made I took care that the patch was visible. The fluctuation could be overcome by an effort of will.

In 1930 S. W. Kravkov * investigated the influence of the state of illumination of one eye upon acuity determinations made with the other. The test object consisted of either two white rectangles on a black ground or two black rectangles on a white ground. The separation of these rectangles was variable, and they were viewed by the right eye in an optical arrangement which diminished their size through an artificial pupil. The left eye was either closed or viewed simultaneously a sheet of milk-glass which was illuminated by a 40-watt lamp. It was found that illumination of the left eye increased the acuity of the right eye in the case of black objects on a white ground, but diminished it in the case of white objects on a black ground, that the effect was independent of colour and passed away gradually in three or four minutes if the left eye was closed ; also when the peripheral acuity of one half of the one eye was investigated, the illumination of the opposite half of the other eye had no effect.

It is natural to expect that the power of discriminating differences of brightness should vary in the same way as the acuity, and it is consequently difficult to bring Kravkov's work into line with my own.

In one of the papers of the series † of which this forms the concluding number Dr. Houstoun put forward a quantum explanation of the Purkinje effect. That explanation has now been withdrawn ; it would make the colour of a spectral line change slightly with its intensity, and the electromotive force it requires is too large to be possible.

* Archiv f. Ophthalm. cxxiv. p. 76 (1930).
† Phil. Mag. x. p. 431 (1930).

XCII. *The Dielectric Constant and Power Factor of some Solid Dielectrics at Radio Frequencies.* *By* W. Anderson, *B.Sc., Physics Department, The College of Technology, Manchester*.*

Abstract.

The variation of the dielectric constant and power factor with frequency between 150 kilocycles and 1500 kilocycles of some solid dielectrics is investigated.

Introduction.

ALTHOUGH a knowledge of the dielectric constant and power factor of solid dielectrics is of considerable technical and theoretical importance, there appears to be a lack of information published on the subject, and such data as there are by different authors do not seem to be in very close agreement. For example, the B.E.S.A. specification [1] for ebonite specifies a power factor at 800 cycles for Grade I. of not greater than 0·006, and for Grade II. not greater than ·008, Moullin [2] gives "about 0·0125," Warren [3] 0·01 to 0·33, and Griffiths [4] gives 0·025 as an approximate value at radio frequencies for the power-loss factor (the product of the dielectric constant and power factor) for best ebonite, and this makes the power factor about 0·008 if the dielectric constant is taken as 3. It has, therefore, seemed desirable to make some further tests on ebonite and other solids, and these are described below.

Preliminary.

The term power factor (herein denoted by $\cos \phi$) as applied to a dielectric means the power factor of a condenser in which that substance is the dielectric, a definition which requires that the power factor of a condenser depends only on the nature of the dielectric and not on the shape of the condenser.

A parallel plate condenser of plate-area A and plate-distance t has a capacity $C = KA/4\pi t$, K denoting the constant of the dielectric.

If the dielectric has a specific resistance ρ, the resistance of the condenser is $R = \rho t/A$. At the frequency $f = \omega/2\pi$ the impedance of the condenser is Z with $1/Z = 1/R + j\omega C$.

* Communicated by H. Lowery, Ph.D., F.Inst.P.

So
$$\cos\phi = \frac{1}{R}\frac{1}{\left[\left(\frac{1}{R}\right)^2 + \omega^2 C^2\right]^{\frac{1}{2}}} \doteqdot \frac{1}{R\omega C}$$

since $1/R$ is small compared with ωC.
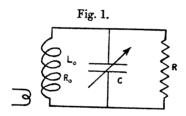
That is,
$$\cos\phi = \frac{1}{R\omega C} = \frac{1}{\dfrac{\omega\rho t}{A}\cdot\dfrac{KA}{4\pi t}} = \frac{4\pi}{\omega K\rho}$$

and is independent of A and t.

When an e.m.f. $e = E\sin\omega t$ is applied to such a condenser the mean power absorbed in the condenser is

$$\frac{1}{2}\frac{E^2}{R} = \tfrac{1}{2}E^2\omega C\cos\phi = \tfrac{1}{2}E^2\frac{\omega A}{4\pi t}K\cos\phi,$$

and so far as the properties of the dielectric are concerned it is proportional to $K\cos\phi$, for which reason $K\cos\phi$ is called the power-loss factor.

Fig. 1.

The chemist or physicist is interested in K and ρ and the engineer in $K\cos\phi = 4\pi/\omega\rho$.

K and ρ depend in general on ω and also on the temperature.

Theory.

Fig. 1 shows an inductance L_0 of resistance R_0 in series with a condenser C and resistance R in parallel. If an e.m.f. $e = E\sin\omega t$ is injected into L_0 the current through L_0 is $i = e/(R_0 + j\omega L_0 + Z)$ and the e.m.f. across Z is $e_1 = Zi = Ze/(R_0 + j\omega L_0 + Z)$, Z denoting the impedance of C and R in parallel.

That is
$$\frac{e_1}{e} = \frac{1}{1 + (R_0 + j\omega L_0)/Z}$$

$$= \frac{1}{1 + \left(R_0 + j\omega L_0\right)\left(\dfrac{1}{R} + j\omega C\right)}$$
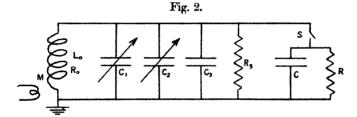
$$= \cfrac{1}{\left(1 + \dfrac{R_0}{R} - \omega^2 L_0 C\right) + j\left(\dfrac{\omega L_0}{R} + \omega C R_0\right)}.$$

The amplitude E_1 of e_1 is therefore

$$\left(\frac{E_1}{E}\right)^2 = \cfrac{1}{\left(1 + \dfrac{R_0}{R} - \omega^2 L_0 C\right)^2 + \left(\dfrac{\omega L_0}{R} + \omega C R_0\right)^2}$$

$$= \cfrac{1}{(R_0^2 + \omega^2 L_0^2)\left\{\left[\omega C - \dfrac{\omega L_0}{R_0^2 + \omega^2 L_0^2}\right]^2 + B^2\right\}}$$

with

$$B = \frac{R_0}{R_0^2 + \omega^2 L_0^2} + \frac{1}{R}.$$

If E and ω are kept constant and C is varied the maximum

Fig. 2.

value of $E_1 = E_{1\text{max.}}$ occurs when $C = L_0/(R_0^2 + \omega^2 L_0^2) = C_0$, say, and is

$$\left(\frac{E_{1\text{max.}}}{E}\right)^2 = \frac{1}{(R_0^2 + \omega^2 L_0^2) B^2}.$$

For a value of $C = C_0 + \delta C$, E_1 is

$$\left(\frac{E_1}{E}\right)^2 = \frac{1}{(R_0^2 + \omega^2 L_0^2)[(\omega \delta C)^2 + B^2]}.$$

Therefore

$$\frac{(\omega \delta C)^2 + B^2}{B^2} = \left(\frac{E_{1\text{max.}}}{E_1}\right)^2 = m^2 \text{ say,}$$

and

$$\pm \frac{\omega \delta C}{\sqrt{m^2 - 1}} = B = \frac{R_0}{R_0^2 + \omega^2 L_0^2} + \frac{1}{R} \quad \cdot \cdot \cdot \quad (1)$$

Experiment.

A diagram of the arrangement employed is shown in fig. 2 in which

L_0 is an inductance suitably chosen for each value of ω.

C_1 is a variable condenser of maximum capacity $=1000 \, \mu\mu$ F.

C_2 is a variable condenser of capacity $=0\cdot6 \, \mu\mu$ F per angular degree.

C_3 and R_3 represent the effective capacity and parallel resistance of the valve voltmeter.

C and R are the capacity and parallel resistance of the condenser whose dielectric is the material under test. The condenser plates are of brass, circular, and 6 inches in diameter.

S is a switch.

M is a mutual inductance between the test circuit and a valve oscillator.

The deflexion of the galvanometer in the anode circuit [of the valve voltmeter is proportional to the square of the applied e.m.f.

The oscillator having been set to a known frequency, C_1 and C_2 are adjusted for resonance and M is adjusted for a suitable maximum deflexion of the galvanometer which is noted. C_2 is varied upwards and downwards to reduce the galvanometer deflexion to half this maximum value, and these two readings of C_2 are noted. If δC_2 is the difference in C_2 in these two settings, then from (1)

$$\frac{R_0}{R_0{}^2 + \omega^2 L_0{}^2} + \frac{1}{R_3} = \frac{\omega \delta C_2}{2} \quad \dots \quad (2)$$

since we have made $m^2 = 2$, and the δC_2 in (2) is twice the δC in (1). S is now closed and the procedure repeated.

If $\delta C_2{}'$ is the new value of δC_2

$$\frac{R_0}{R_0{}^2 + \omega^2 L_0{}^2} + \frac{1}{R_3} + \frac{1}{R} = \frac{\omega \delta C'}{2} \quad \dots \quad (3)$$

From (2) and (3)

$$\frac{1}{R} = \frac{\omega}{2}(\delta C'_2 - \delta C_2). \quad \dots \dots \quad (4)$$

This gives R, and the only assumption made about the losses in C_1 and C_2 is that they are independent of the settings.

The value of C is obtained from the difference of the readings of C_1 and C_2 with S open and closed. The power factor is then

$$\cos \phi = \frac{1}{\omega CR} = \frac{1}{2}\frac{\delta C_2{}' - \delta C_2}{C},$$

and K is obtained from

$$\frac{10}{9}\frac{KA}{4\pi t} = C \text{ (expressed in } \mu\mu \text{ F)},$$

A and t being in cm.^{2} and cm.

The oscillator was calibrated by means of a heterodyne wave-meter, and the condenser C_1 had been calibrated at the National Physical Laboratory.

The effect of the reaction of the test circuit on the frequency of the oscillator is discussed by Moullin [5]. To test this effect experiments were made at 150 kc. and 1500 kc. in which the magnitude of the oscillator current was varied by adjusting the H.T. volts, and M varied to get the same e.m.f. across C_1. The normal oscillator current was never less than 20 milliamps., and it was found that decreasing this to 6 milliamps. did not produce any observable difference in δC_2, from which it is concluded that the effect of frequency drift is negligible here.

The accuracy with which the condenser C_1 can be set controls the accuracy obtained in the determination of K and is here about 1 per cent. A vernier on C_1 would make possible an accuracy of 0·1 per cent.

Since the power factor

$$\cos \phi = \frac{1}{2} \frac{\delta C_2' - \delta C_2}{C},$$

it is seen that the accuracy obtainable for $\cos \phi$ depends mainly on the accuracy in $\delta C_2' - \delta C_2$, which in these experiments is determined to about $\pm 0·1 \mu\mu$ F.

So if $\cos \phi = 0·005$ and $C = 200 \mu\mu$ F., $\delta C_2' - \delta C_2 = 2C \cos \phi = 2\mu\mu$ F, and thus an error of 0·1 $\mu\mu$ F in $\delta C_2' - \delta C_2$ involves an error of 5 per cent. in $\cos \phi$. The error is correspondingly less at higher values of $\cos \phi$.

The experimental observations were reduced by plotting the observed values of C and $\delta C_2' - \delta C_2$ against the frequency and drawing smooth graphs through the mean positions. From the smoothed values of C and $\delta C_2' - \delta C_2$, K and $\cos \phi$ were calculated.

Results.

In all twelve samples were tested. In nine of these K and $\cos \phi$ only vary slightly, if at all, in the range explored. The values at the limits of frequency employed are given in the table.

In the remaining three samples the variations in K and cos ϕ are not great, but they are not linear with the frequency and so the relations are shown in the graphs fig. 3.

Curves I. and II. show respectively the dieletric constant and power factor for millboard. Curves III. and IV. show the same quantities for india-rubber, while Curves V. and VI. relate to a specimen of ebonite obtained from a wireless dealer.

TABLE.

	K.		Cos ϕ.	
	150 kc.	1500 kc.	150 kc.	1500 kc.
(1) Glass (mirror)...............	6·3	6·3	·0060	·0060
(2) Porcelain (unglazed)	4·7	4·7	·0066	·0066
(3) Ebonite	2·9	2·9	·0077	·0077
(4) Ebonite	3·1	3·1	·011	·011
(5) Keramot	4·0	3·9	·011	·009
(6) Paxolin (Grade " T ")	4·2	4·2	·026	·026
(7) Paxolin (Grade " P ")	4·3	4·3	·034	·034
(8) Bakelite (Grade EXE 549)	4·7	4·7	·038	·038
(9) Paxolin	5·5	5·1	·044	·049

(3) is an ebonite marked B.E.S.A. 234/1925. This specification requires a power factor of not greater than 0·006 at 800 cycles.

(4) is an ebonite supplied by a manufacturer to the specification " best, quality."

(5) is a loaded ebonite made by Messrs. Siemens Bros., Ltd., Woolwich, London, S.E. 18.

(6) and (7) are samples supplied by Messrs. The Micanite and Insulators Co., Ltd., Walthamstow, London, E. 17.

(8) is a sample of bakelite laminated sheet supplied by Messrs. Bakelite, Ltd., 68 Victoria Street, London, S.W. 1.

(9) is a specimen from a wireless dealer.
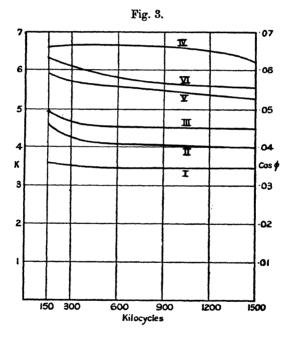
According to the theory of Debye ([6]), as applied to polar liquids, K and cotangent ϕ are given by

$$K = \frac{K_1 + K_0 x^2}{1 + x^2}, \quad \cot \phi = \frac{(K_1 - K_0)x}{K_1 + K_0 x^2},$$

where

$$K_1 = \text{the value of K at } \omega = 0,$$
$$K_0 = \text{the value of K at } \omega = \infty,$$
$$\omega = 2\pi \times \text{frequency},$$
$$x = \frac{K_1 + 2}{K_0 + 2} \omega\tau = a\omega,$$
$$\tau = \text{``relaxation-time,''}$$

and this is in fair qualitative agreement with experiment. Debye [7] also finds that the observations of Errera on ice may be fairly represented by a formula of the same type.

Fig. 3.

An attempt has therefore been made to see if our results for the materials referred to in fig. 3 can be expressed in this way, but without success.

If $$\frac{(K_1 - K_0)x}{K_1 + K_0 x^2} = \cot\phi \doteq \cos\phi, \text{ and } \frac{K_1 + K_0 x^2}{1 + x^2} = K,$$

then $$\frac{(K_1 - K_0)a\omega}{1 + a^2\omega^2} = K\cos\phi = K\frac{\delta C_2' - \delta C_2}{2C} = \frac{\delta C_2' - \delta C_2}{2C'},$$

where $$C' = \frac{A}{4\pi t} \cdot \frac{10}{9} \mu\mu \, F.$$

is the geometric capacity of the condenser. That is

$$(K_1 - K_0)2C'a \frac{\omega}{\delta C_2' - \delta C_2} = 1 + a^2\omega^2,$$

and if $\dfrac{\omega}{\delta C_2' - \delta C_2}$ is plotted against ω^2 the graph should be a straight line, a relation which is not found to hold.

References.

(1) British Engineering Standards Association Specification, No. 234 (1931).

(2) E. B. Moullin, 'Radio Frequency Measurements,' p. 315 (Griffin & Co., 2nd ed. (1931)).

(3) H. Warren, 'Electrical Insulating Materials,' p. 218 (Ernest Benn, Ltd. (1931)).

(4) W. H. F. Griffiths, 'Wireless World,' April 1930, p. 441.

(5) *Loc. cit.* pp. 278-281.

(6) P. Debye, 'Polar Molecules' (Chemical Catalog Co. (1929)).

(7) *Loc. cit.* pp. 102-108.

XCIII. *Light Absorption, the Raman Effect, and the Motions of Electrons in Gases. By* V. A. BAILEY, *M.A., D.Phil.(Oxon), F.Inst.P., Associate Professor of Physics, The University of Sydney* [*].

1. IN a communication on the motions of electrons in gases which was published [†] in 1921, the last section contained a discussion of the consistency of our observations with some of the conceptions of the Quantum Theory on the exchanges of energy between electrons and molecules at collisions which were then current.

Since that time the quantum theory has become radically changed, so it is of interest to reconsider its relation to those experimental conclusions of ten years ago.
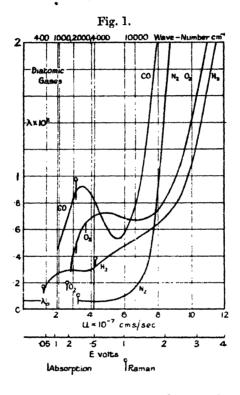
In order to make the examination wider we shall also consider the results obtained for electronic collisions in some other gases which have been obtained since 1921 by the same or similar methods.

It will be found that the new quantum theory is in closer agreement with the experimental results than was the old.

---

[*] Communicated by the Author.
[†] J. S. Townsend and V. A. Bailey, Phil. Mag. (Dec. 1921).

2. The experiments on electrons in gases by means of Townsend's methods (and those developed in Sydney [*]) determine the values of the mean energy of agitation E (in volts) and the velocity W in the direction of the electric force of the electrons for different values of the ratio Z/p, where Z is the intensity of the uniform electric field and p is the pressure of the gas in which the electrons move.

Fig. 1.

The mean kinetic energy of an electron is $mu^2/2$, where u is the mean velocity of agitation. This energy may be expressed in volts E by the relation $mu^2/2 = \epsilon E/300$, e being the charge on the electron in electrostatic units.
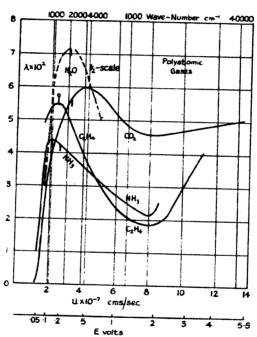
The mean free path L may be calculated from the results of the experiments, also the values of the quantity $\Delta E/E$, where ΔE is the mean energy lost by an electron of energy E at a collision with a molecule [†].

* V. A. Bailey and W. E. Duncanson, Phil. Mag. (July 1930).
† *Vide* J. S. Townsend, 'Motion of Electrons in Gases,' 1925 (Clarendon Press).

We are here mainly concerned with the fraction $\lambda = \Delta E/E$, so in respect to the result for L the reader may be referred to a recent comprehensive account by Brose and Saayman*.
. The variation of λ as a function of the mean energy of an electron at a collision was shown in the earlier publications by means of tables of the quantity $f = \frac{1}{2}(1+e)$, where e is the coefficient of restitution of the molecule.

Fig. 2.

It is more convenient for our purpose to represent these results by means of curves, as in figs. 1 and 2.

The abscissæ are the values of the velocity of agitation $u . 10^{-7}$ (in cm./sec.), and the ordinates are the values of λ † expressed in "per cent." For our purpose scales are

* H. L. Brose and E. H. Saayman, *Ann. d. Physik*, Bd. 5, p. 797 (1930).

† The values for H_2 have been corrected for the effect of the energy of agitation of the molecules on the energy lost by the electrons at collisions. This correction is negligible for the other gases considered.

also given for the potential E and for the wave-number equivalent to the frequency ν, where ν is derived from E by means of Einstein's relation, $h\nu = Ee$, in which h is Planck's constant. The values of E are given in volts in the figures.

3. In a recent communication * it was pointed out that these curves show that a correspondence exists between the relative magnitudes of the fraction λ and the absorption of light of frequency ν for the same kind of molecule.

Accordingly, for each kind of molecule a short vertical mark is drawn on its λ-curve for the value of λ corresponding to the centre of its *strongest* fundamental absorption band, wherever the data make this possible.

It is evident from figs. 1 and 2, that for each of the molecules CO, CO_2, N_2O, NH_3†, C_2H_4, the maximum of the curve corresponds approximately to the frequency of that radiation in the infra-red region which is absorbed most strongly by the molecule.

The experiments on N_2O are still in progress in Sydney ‡, so the curve representing it is necessarily provisional. With all the other gases the λ-curves had been determined without any suspicion that they might thus be related to the light-absorbing properties of the gases.

The agreement is therefore somewhat remarkable, especially as no attempt had been made to determine the positions of the maxima with the greatest possible precision.

The published data about infra-red absorption in O_2 are somewhat conflicting; *e. g.*, Coblentz § found very weak bands at 3·1 and 4·7 μ, Burmeister ‖ found none, and more recently Snow ¶ mentions a very weak one at 6·5 μ. Coblentz's results are indicated on the curve for O_2.

The results obtained for the gases HCl, NO, H_2O, and C_5H_{12} are not given here, since the values of λ for these gases have not been determined accurately. The experimental errors are due to the great rate of attachment of electrons to form negative ions, and new investigations

---

* V. A. Bailey and W. E. Duncanson, *loc. cit.*

† Data for CO and C_2H_4 from Coblentz, Phys. Rev. xx. p. 273 (1905).
    „ CO_2 from G. Hertz, *Verh. d. D. Phys. Ges.* 1911, p. 617.
    „ N_2O „ E. v. Bahr, *idem*, 1913, p. 710.
    „ NH_3 „ Coblentz, *loc. cit.*; and Schierkolk, *Z. f. Phys.* xxix. p. 277 (1924).

‡ Skinker and White's observations are not sufficiently extensive for application here.

§ W. W. Coblentz, Phys. Rev. xx. p. 273 (1905).

‖ W. Burmeister, *Ver. d. Deut. Phys. Ges.* 1913, p. 589.

¶ C. P. Snow, Phil. Mag. (Sept. 1929).

are being made with a view to obtaining a higher accuracy. There is a lack of absorption data for C_5H_{12} vapour, but the data for liquid C_5H_{12} show a good agreement with the maximum of the λ curve for the gas.

4. The gases H_2 and N_2, which are known to be almost completely transparent to infra-red radiation, show no definite maxima.

For the latter, Snow found a very weak absorption band at 4·3 $μ$, which corresponds to the end of the λ-curve, where a slight rise exists. This suggests that more extended observations of λ in N_2 for the low velocities might reveal a maximum.

All the diatomic gases show a very rapid increase of λ with u for the larger velocities, which may indicate that maxima are being approached in the region corresponding to ultra-violet radiation. The fact that the velocities of the electrons are distributed about a mean value u would tend to produce a rise in the curve for values of u distinctly lower than that corresponding to a strong light-absorption band (or notable ionization by collision), but this is not sufficient to account for the parts of the curve for H_2 and N_2 corresponding to values of u less than 5×10^7.

It is therefore necessary to postulate some other kinds of energy transference from a slow electron to a molecule of H_2 or N_2 in order to account for the fact that λ is several times larger than it would be for perfectly elastic collisions.

5. Another phenomenon which in recent years has required other than light-absorption transference of energy for its full explanation is that known as the Smekal-Raman effect in the scattering of light.

It is therefore of interest to examine whether any connexion exists between the λ-curves of N_2 and H_2 and the frequency differences $Δν$ between the fundamental Raman lines and the unaltered Rayleigh lines. The values of u given by $\frac{1}{2}mu^2 = hΔν$ are indicated by short vertical lines with circles attached (to distinguish them from the absorption lines) ; the values of $Δν$ are those found by Rasetti [*].

With H_2 the Raman lines correspond remarkably with the parts of the λ-curve which are beginning to rise. This is made clearer by indicating with a horizontal line on the diagram the value $λ_0$ for perfectly elastic collisions between electrons and molecules.

* F. Rasetti, Phys. Rev. xxxiv. p. 367 (1929) Proc. Nat. Acad. Sci. Wash. xv. (1929).

With N_2 this correspondence is perhaps masked by the presence of the weak absorption band found by Snow close to the Raman line, but the λ-curve is definitely beginning to rise at about the velocity 5×10^7.

Unfortunately, the Raman line for O_2 lies a little outside the λ-curve, but it may also possibly contribute to the rise of the curve in its neighbourhood.

In CO the Raman and absorption lines coincide, in C_2H_4 the strongest are not very different, and in both gases they lie close to the maxima of the λ-curves. It is interesting to note that in C_2H_4 the Raman effect was found by Rasetti to be exceptionally intense.

With N_2O, CO_2, and NH_3 the strong absorption bands mask any effect which may correspond to a Raman line.

It is probable then, that with polyatomic molecules, the energy transferred from a slow electron to a molecule has a relation to the energy transferred from radiation to a molecule, whether in the process of absorption or of scattering.

In the current theories these processes are referred to changes in the energy of rotation or vibration of the molecule. Accordingly we may refer the larger energy losses of electrons in H_2 to a rotational change when $u = 1\cdot25 \times 10^7$ and a vibrational additional change when $u = 4\cdot28 \times 10^7$.

It is well known that the intensity of the Raman lines increases with the frequency of the exciting light. Something analogous may happen in regard to the probability of certain transferences of energy from the electron to the molecule as u increases, and the rapid rise of the λ-curves in the region of velocities $8-10 . 10^7$ may be in part due to this.

6. If the conclusions about the relation between λ-curves and absorption are correct, it is possible to predict something about the curves for certain gases in which the motions of electrons have not yet been investigated. For example, since, according to Burmeister *, Cl_2 and Br_2 are transparent to radiations of wave-length greater than 1μ, we may expect low values of λ for velocities less than $6\cdot6 \times 10^7$. The fact that these gases are coloured makes it probable that large values of λ will be found for velocities between 7×10^7 and 12×10^7.

Experiments with these gases are projected in order to examine these points.

* *Loc. cit.*

It would also be interesting to compare the λ-curves for C_2H_4 and HCN, since Burmeister finds a great similarity between the light-absorbing properties of these two gases.

7. For many years Franck and Hertz and their followers have expounded views which are in strong disagreement with many of the experimental conclusions of Townsend and his collaborators.

For example, they have stated that the lowest electronic energies which correspond to large losses at collisions with the molecules of hydrogen and oxygen are 11 and 9 volts respectively, and that with lower energies the losses are essentially due to an "electron affinity" which also causes negative ions to be formed in these gases *.

But in 1926 Franck's † opinion of his original experiments and his arguments on the energy losses of slow electrons in H_2 and O_2 is that they are inconclusive. He is evidently aware of the results for these and other gases obtained by us since 1921, for in the same book he and Jordan say ‡: "In a very indirect way Townsend and Bailey have calculated the effective cross-sections from their experiments on the lateral diffusion of electrons in an electric field. The results agree only in part with those already mentioned. Theory and experiment are not suitable for discussion in the scheme of this book."

Among the methods mentioned in their book is that used by Franck and Hertz § in 1913, and so it is interesting to recall that in that year they confidently asserted "In agreement with Lenard, it is found that the free paths of electrons, with velocities between 10 and 2 volts, is very near to the free path calculated by means of the kinetic theory of gases." This fact, then, may be taken as one reason why Franck and Jordan do not consider our experiments "suitable for discussion."

From the first experiments ‖ made by Townsend's method with air at low pressures and small electric forces, it was shown that electrons move long distances in the gas and

* *E. g.* J. Franck und G. Hertz, *Verh. d. Deut. Phys. Ges.* 1913, p. 922.
† J. Franck und P. Jordan, *Handbuch d. Physik,* Bd. xxii. p. 721 (1926).
‡ Translated from the German.
§ J. Franck und G. Hertz, *Verh. d. Deut. Phys. Ges.* 1913, p. 389.
‖ J. S. Townsend and H. T. Tizard, Proc. Roy. Soc. A, vol. lxxxviii. p. 336 (1913).

collide with large numbers of molecules of oxygen without becoming attached to the molecules and forming ions.

8. Our experiments of 1921* also showed plainly that, even at pressures of several mm. of Hg, the electronic streams in hydrogen (with energies less than 6 volts) contained no appreciable number of negative ions, and Brose's later experiments on oxygen indicated that notable energy losses occurred without negative ions being evident. Franck and Hertz † and their supporters have maintained that all electrons on reaching a critical potential lose all their energy in a collision with a molecule of a gas, so that when electrons move under electric forces in gases at a few millimetres pressure the critical potential is an upper limit to the energy that the electron may acquire.

The conception that, in general, only a fraction of the collisions with a given energy E result in a definite process is originally due to Townsend, a fact which is recognized by L. Bloch, who stated in his book ‡ :

"Par contre, on doit à Townsend diverses constations experimentals qui montre la nécessité de faire intervenir dans le calcul des courants d'ionization un *facteur de probabilité* different de 1.

"Il n'en demeure pas moins qu'un resultat intéressant, tout à fait acceptable pour les theorie des quanta, ressort des observations de Townsend ; La Dynamique des chocs entre électrons et atoms fait intervenir des facteurs de probabilité specifiques . . . ."

This conception is referred to by Franck § and Jordan under the name "Ausbeute," but in discussing it they make no reference to Townsend.

It is of interest to note that Townsend's conception is now incorporated in the new quantum theories of Dirac, Heisenberg, and Schrödinger.

The same conception must also be borne in mind in interpreting the curves giving λ in terms of E. It is only in a small proportion of the collisions with velocities greater than a critical value that electrons lose energy in amounts greater than the average small loss λE.

---

* J. S. Townsend and V. A. Bailey, *loc. cit.*

† *E.g.*, J. Franck and G. Hertz, *Verh. d. Deut. Phys. Ges.* 1913, p. 932.

‡ 'Ionization et Resonance des Gas et des Vapeurs,' 1925.

§ *Handbuch d. Physik*, Bd. xxiii. p. 721 (1926).

XCIV. *Transient Phenomena at the Breaking of an Inductive Circuit. By* J. A. WILCKEN, *B.Sc., Ph.D., Lecturer in Electrical Engineering at Armstrong College, Newcastle-upon-Tyne* *.

WHEN an inductive circuit on direct current supply is broken the stored electromagnetic energy becomes free and is dissipated as heat in the switch, usually giving rise to an arc between the separating switch-jaws. As long as the arc is burning the current persists, and so a further amount of energy is drawn from the supply until the arc is extinguished. In an alternating current system the problem is essentially different, since the electromagnetic energy is not permanently stored, but oscillating between the source and the circuit and vanishing in the integral over a whole number of periods, as long as the current wave-form is symmetrical.

The decay of direct current, with the concomitant rise in potential at the switch, and the bearing of these phenomena on commutation, have been thoroughly discussed, notably by Arnold and La Cour †.

The question regarding the energy, however, seems to have received less consideration than it merits, in view of its importance in connexion with switch design; in the present paper, attention is mainly directed towards the energy dissipated in the switch, as dependent on the constants of the circuit and the speed of breaking.

We consider a direct current circuit of constant inductance L, and assume the total resistance to increase from R, the resistance of the circuit proper, to infinity, during the period 0 to T. The function $\frac{RT}{(T-t)}$ satisfies this condition for $T > t \geq 0$, and may be taken to represent the actual value of the resistance, when the increase is due to a gradually diminishing contact area or pressure at the switch; the contact resistance alone is then

$$\frac{RT}{(T-t)} - R = \frac{Rt}{(T-t)}.$$

When an arc strikes between the switch-jaws the resistance increases as the arc becomes longer, but the exact manner in which this increase takes place is not known. We shall adopt the same expression, as a plausible approximation, also in this case.

---

* Communicated by the Author.
† 'Theorie der Wechselströme,' i. pp. 620–34 (Berlin, 1923).

It is convenient to take the period of breaking, T, as unit of time, and write simply $\dfrac{R}{(1-t)}$ for the total resistance.

The voltage equation is then

$$L\frac{di}{dt} + \frac{R}{1-t} = E, \quad \ldots \ldots (1)$$

valid for $1 \geq t \geq 0$, and the solution is written

$$i = (1-t)^{\frac{R}{L}} \left\{ \text{const.} + \frac{E}{L} \int (1-t)^{-\frac{R}{L}} dt \right\}. \quad . \quad (2)$$

Determining the integration constant by the initial condition $i/^0 = \dfrac{E}{R}$, and introducing the time constant $\dfrac{L}{R} = \tau$, or, measured in units of T, $\dfrac{\tau}{T} = \theta$, we find, after reduction,

$$i = \frac{E}{R} \cdot \frac{1-t}{1-\theta} \{ 1 - \theta (1-t)^{\frac{1}{\theta}-1} \}, \quad \ldots (3)$$

provided $\theta < 1$. The potential difference at the switch is given by

$$e_1 = \frac{R\,it}{1-t} = \frac{Et}{1-\theta} \{ 1 - \theta\,(1-t)^{\frac{1}{\theta}-1} \}, \quad . \quad (4)$$

and at the moment $t = 1$,

$$e_1/' = \frac{E}{1-\theta}. \quad \ldots \ldots (5)$$

If $\theta = 1$, the solution is written

$$i = \frac{E}{R}(1-t)\{1 - \log(1-t)\}, \quad \ldots (6)$$

to which corresponds a switch voltage

$$e_1 = Et\{1 - \log(1-t)\}. \quad \ldots \ldots (7)$$

The potential difference at the switch would thus become infinity towards the end of the period of breaking if that period is equal to the time constant of the circuit; the physical interpretation is, of course, that the circuit is not broken, but the arc remains until T has become greater than $\dfrac{L}{R}$.

The energy dissipated in the switch is given by $\displaystyle\int_0^1 e_1\,i\,dt$, but the general expression for this integral is too complicated
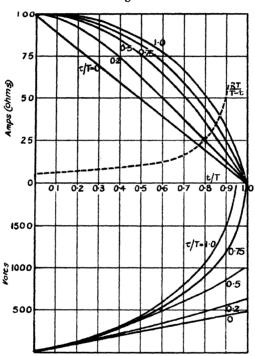
to admit of interpretation, except when the circuit is strictly non-inductive. In this case $\theta = 0$, and the current,

$$i = \frac{E(1-t)}{R},$$

decreases linearly, while the switch voltage is simply

$$e_1 = Et,$$

Fig. 1.

Current decrease and switch voltage rise on breaking inductive circuits.

and the energy
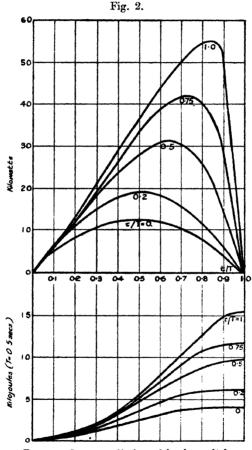
$$\int_0^1 e_1 i \, dt = \frac{E^2}{R} \int_0^1 t(1-t) dt = \frac{E^2}{6R}. \quad \cdot \quad \cdot \quad \cdot \quad (8)$$

To illustrate the behaviour of circuits with a finite inductance I have calculated the following tables, showing the variation of current, switch voltage, and power throughout the time of breaking for different values of the

3 T 2

$t/T =$	0	0·1	0·2	0·3	0·4	0·5	0·6	0·7	0·8	0·9	1·0	
(1) $r/T=0$.												
Current	100	90	80	70	60	50	40	30	20	10	0	amperes.
Switch volts	0	50	100	150	200	250	300	350	400	450	500	volts.
Power	0	4·50	8·00	10·50	12·00	12·50	12·00	10·50	8·00	4·50	0	kilowatts.
(2) $r/T=0·2$.												
Current	100	97·7	91·8	83·3	73·1	61·7	49·7	36·9	25·0	12·5	0	amperes.
Switch volts	0	54·2	114·7	178·5	243·7	308·5	372·8	430·5	500·0	562·5	625·0	volts.
Power	0	5·30	10·53	14·87	17·81	19·03	18·53	15·89	12·50	7·03	0	kilowatts.
(3) $r/T=0·5$.												
Current	100	99·0	96·0	91·0	84·0	75·0	61·0	51·0	36·0	19·0	0	amperes.
Switch volts	0	55·0	120·0	196·0	280·0	375·0	480·0	595·0	720·0	855·0	1000·0	volts.
Power	0	5·44	11·52	17·84	23·52	28·12	30·72	30·34	25·92	16·24	0	kilowatts.
(4) $r/T=0·75$.												
Current	100	99·2	97·0	93·2	88·1	80·9	71·6	59·7	44·9	26·0	0	amperes.
Switch volts	0	55·1	121·2	199·7	293·7	404·5	537·0	696·5	898·0	1170·0	2000·0	volts.
Power	0	5·47	11·76	18·61	25·87	32·72	38·45	41·58	40·32	30·42	0	kilowatts.
(5) $r/T=1$.												
Current	100	99·5	97·9	95·0	90·6	84·7	76·7	66·1	52·2	33·0	0	amperes.
Switch volts	0	55·3	122·4	203·6	302·0	423·5	575·2	771·2	1044·0	1485·0	∞	volts.
Power	0	5·50	11·98	19·34	27·36	35·87	44·12	50·97	54·50	51·20	—	kilowatts.

characteristic ratio $\dfrac{L}{RT} = \dfrac{\tau}{T}$. The tabulated figures may readily be interpreted in terms of actual inductances and time units; thus, for example, the values in table (2) $\tau/T = 0.2$, would correspond to a circuit of inductance

Fig. 2.

Power and energy dissipated in the switch.

0·25 henry, resistance 5 ohms, which is broken in $\frac{1}{4}$ second. The values are given in ordinary units for a 500-volt supply and a normal steady current of 100 amperes.

Fig. 1 shows the curves of current decrease and rise of potential for five different values of τ/T, and fig. 2 gives the

power dissipated at any moment and the total energy up to any moment released at the switch, assuming $T = 0.5$ second.

The danger in breaking an inductive circuit lies not only in the rise of potential, which may cause puncture of insulation, but also in the increase in power absorbed by the switch. The energy is not released at a uniform rate during the period of opening, but if the switch is opened quickly the power rises to a high maximum value towards the end of the period.

A switch opening a 500-volt circuit of inductance 0·25 henry and resistance 5 ohms in $\frac{1}{15}$ second must dissipate energy at the rate of 40 kilowatts towards the latter third of the time of breaking.

XCV. *A Simple Method for the Numerical Solution of Differential Equations. By* W. G. BICKLEY, *D.Sc., Imperial College of Science and Technology* *.

METHODS for the approximate integration of differential equations are of considerable value, especially in technical applications, both in cases where the formal solution is unobtainable, and also in cases where, though obtainable, the formal solution is of such form that the calculation of pairs of corresponding values of the variables is troublesome. Some years ago, a useful and comprehensive series of articles upon graphical methods of solving differential equations of the first order was contributed to the 'Mathematical Gazette' by Professor Brodetsky [1]. While these methods are of considerable value and interest, especially when it is merely the general trend of the solution that is sought, it will be conceded that if any considerable degree of accuracy is desired, recourse to numerical methods is inevitable. Of numerical methods, that of Runge-Kutta is ingenious, and has the advantage that it allows the use of a fairly large interval—at the expense of a number of separate computations for each interval, and by the use of a formula whose derivation is complicated and which is not easily remembered. The method generally regarded as the best is due to Adams [2], and depends upon an integration formula in finite differences. This method has undoubted merits, and for very elaborate work is probably the most accurate, since as many orders of differences can be used as

* Communicated by the Author.

prove to be necessary. However, all exponents of the method advise—for good and obvious reasons—that the interval should be chosen so that the third and higher differences are small. If these differences be neglected, the finite difference integration formula becomes equivalent to Simpson's Rule, and the purpose of the present article is to outline a method in which Simpson's Rule plays the primary role. The advantages claimed for the method are :—

(*a*) Simpson's Rule is a well-known integration formula, so that no acquaintance with the theory of finite differences is necessary before the method can be understood and used.

(*b*) The arithmetical operations are considerably simpler and shorter, and the amount of writing considerably less, than in the Adams method.

(*c*) The method is much better adapted to use with any calculating machine than the Adams, the arithmetical operations consisting (see below) of a multiplication by 4, an addition, and a multiplication by $h/3$ (h being the interval) —this last step is, usually, mental—as opposed to the use of coefficients $1/2$, $1/12$, $1/24$, $3/8$, $19/720$, etc.

The principle underlying the method is, of course, the same as in the Adams method. Given a differential equation

$$dy/dx = f(x, y) \quad . \quad . \quad . \quad . \quad . \quad (1)$$

and initial conditions, say $y = y_0$ when $x = x_0$, we have, by integration,

$$y - y_0 = \int_{x_0}^{x} f(x, y) \, dx,$$

and the unknown values of y corresponding to a set of values of x are found by the method of successive approximation, essentially due to Picard [3].

Suppose that a set of values of y corresponding to a set of equidistant values of x, x_0, $x_0 + h$, $x_0 + 2h$, ..., $x_0 + nh$, has been obtained, and the corresponding values of dy/dx calculated by (1) : thus

x_0	y_0	y_0'
$x_0 + h$	y_1	y_1'
$x_0 + 2h$	y_2	y_2'
$x_0 + (n-1)h$	y_{n-1}	y'_{n-1}
$x_0 + nh$	y_n	y_n' .

From the trend of these values, a fair approximation to the value of y'_{n+1} can be estimated, and an approximation to y_{n+1} then calculated by Simpson's Rule, for, by this rule,

$$y_{n+1} - y_{n-1} = h(y'_{n+1} + 4y'_n + y'_{n-1})/3.$$

This is now used to correct y'_{n+1}, and another of the above formula gives a second approximation to y_{n+1}. This cycle of operations is repeated until the limit is reached. It is known that, if the integration is carried out accurately, and if the sequence of approximations to y_{n+1} obtained does converge to a limit, then this limit is the accurate value of y_{n+1}. In practice, it is rarely necessary to go beyond the second approximation, since a little judgment, quickened by experience, will usually make the first approximation very close to the true value.

Two further points need mention, the choice of the interval, h, and the determination of a few sets of values to start the process.

The error of Simpson's Rule is of the order

$$h^5 f^{iv}(x, y)/90$$

per double interval, and so is less than

$$h^4(x - x_0) f^{iv}(x, y)/180$$

in the range $(x - x_0)$, f^{iv} being the greatest numerical value of f^{iv} in this range. We must therefore choose h, so that this error will not affect the last place of decimals we desire to retain.

At the beginning, it is necessary that y_1' (at least) be known *accurately*—for errors once introduced are liable to be cumulative in *any* numerical process of this kind. For this purpose the Taylor's series is usually advocated [4], and is in most cases satisfactory—if, of course, it exists. This may be obtained by evaluating successive differential coefficients by differentiating equation (1) and using the initial conditions, by substitution of a trial series and equating coefficients, or by Picard's iteration method. Which of these involves the least labour depends upon the equation and the initial conditions. Having obtained a few terms of the series, it may with advantage be used until the magnitude of the last term included shows that the accuracy is insufficient—or even beyond, as furnishing approximations to be corrected numerically.

We will now attempt to show the practical working of this method by means of a particular example. The equation we shall use is

$$dy/dx = x + y,$$

with the initial condition

$$y_0 = 1.$$

The formal solution of this equation is both known and calculable, but this is an advantage, as the accuracy of the numerical work can be definitely checked.

Here, we obtain from our equation,

$$f^{iv}(x, y) = 1 + x + y.$$

A rough graphical solution shows that, when $x = 1$, y lies between 3 and 4, so that if we propose to integrate as far as $x = 1$, the value of f^{iv} in our range will not exceed 6. The value of the interval, h, which will ensure the accuracy of four places of decimals must then satisfy the condition

$$6h^4/180 < 0.00005$$

or

$$h < 0.19 \ldots .$$

By taking $h = 0.2$, our purpose would probably be achieved, but it is better to take $h = 0.1$, and this we shall do.

The series solution is easily found to be

$$\bullet \quad y = 1 + x + x^2 + x^3/3 + x^4/12 \ldots .$$

Putting $x = 0, 0.1, 0.2, 0.3, 0.4 \ldots$, we find

x	0	0.1	0.2	0.3	0.4
1	1	1.0000	1.0000	1.0000	1.0000
x		.1000	.2000	.3000	.4000
x^2		.0100	.0400	.0900	.1600
$x^3/3$		.00033	.00267	.0090	.02133
$x^4/12$		.00000	.00013	.00067	.00213
y	1	1.1103	1.2428	1.3997	1.5835

in which the last figure when $x = 0.4$ is doubtful. We now tabulate, as in Table I., having material for the first four lines accurate, while the fifth is doubtful.

To correct this, we have

$$y(.4) - y(.2) = 0.1\,(1.4428 + 4 \times 1.6997 + 1.9835)/3$$
$$= 0.3408,$$

so that

$$y(.4) = 1.2428 + 0.3408 = 1.5836.$$

We enter the corrected values of $y(.4)$ and $y'(.4)$, but the correction does not affect δy.

We now need a trial value for $y'(.5)$. Noting the successive differences of $.21 \ldots, .23 \ldots, .25 \ldots, .28 \ldots$, we are led

to expect a difference of about ·32..., and so try $y'(\cdot 5)$ = 2·30 ...   Now, using Simpson, we have,

$$y(\cdot 5) - y(\cdot 3) = 0\cdot 1(1\cdot 6997 + 4 \times 1\cdot 9836 + 2\cdot 30...)/3$$
$$= 0\cdot 3978,$$

making $y(\cdot 5) = 1\cdot 3997 + 0\cdot 3978 = 1\cdot 7975,$

and $y'(\cdot 5) = 2\cdot 2975.$

TABLE I.

$$y' = x + y\ ;\ y_0 = 1.$$

$x.$	$y.$	$y'.$	$\delta y.$
0	1·0000	1·0000	
0·1	1·1103	1·2103	
0·2	1·2428	1·4428	
0·3	1·3997	1·6997	
0·4	1·5835	1·9835	·3408
	1·5836	1·9836	
0·5	—	2·30...	·3978
	1·7955	2·2795	·3977⟋
	1·7974	2 2974	
0·6	—	2·66...	·4611
	2·0447	2·6447	·4606
	2·0448	2·6448	
0·7	—	3·02...	·5298
	2·3272	3·0272	·5301
	2·3275	3·0275	
0·8	—	3·45...	·6068
	2·6510	3·4510	
0·9	—	3·92...	·6920
	3·0195	3·9195	
1·0	—	4·43...	·7853
	3·4363	4·4363	·7855
	3·4365	4·4365	

Using this corrected value, we then find 0·3977 instead of 0·3978, as the increment, and so 1·7974 is evidently the value of $y(\cdot 6)$.

For $y'(\cdot 6)$ a trial value is evidently 2·66...,—and so the process goes on.   In the table all trials are shown and the

final values are underlined. In practice, trial values would be entered in pencil, and final values in ink, giving one line to each value of x.

Anyone familiar with the use of a calculating machine will realize how simply the multiplication by 4 and the addition can be performed upon such a machine, and the division by 30 mentally, when there will be no writing other than that shown in the table.

As for the accuracy of the results, the solution of our equation, with the given initial condition, is

$$y = 2e^x - 1 - x,$$

so that, when $x = 1$,

$$y = 2e - 2 = 3\cdot43656\ldots$$

Our error is less than a unit in the fourth place of decimals ; what error there is is, in fact, more due to the " rounding off " than to Simpson's Rule, for if the value of $y(1)$ be found by applying this rule to the complete y' column, we find

$$y(1) = 3\cdot43658\ldots$$

It is, therefore, usually worth while to carry an extra figure throughout in order to minimize this type of error.

The method leaves nothing to be desired on the score of accuracy, at any rate in this example.

There is no difficulty in applying the same principles to equations of the second—or higher—order, and although the labour is greater, the proportionate saving over that involved in the Adams method is greater still. In the case of the most general equation of the second order,

$$y'' = f(x, y, y'),$$

we must estimate first approximations to both y and y' at each stage, and then correct them by numerical integration. A cycle now involves the calculation of y'' from the approximations to y and y', by means of the above differential equation, correcting y', and then y by Simpson, and it will be appreciated that any method which ensures that our first approximations are close, and thus reduces the number of cycles that are necessary at each stage, will be very desirable.

Such a method, based upon the first and second differences of y, which has worked very well in practice, will now be outlined. It may first be emphasized, however, that it demands very little acquaintance with finite differences to appreciate the fact that the regularity of these affords a check upon the accuracy of the work. In constructing the table

of differences for our purpose, the "horizontal" form is most convenient. This is defined by the scheme

$$y_0$$
$$y_1 \qquad \Delta y_2$$
$$y_2{}^2 \qquad \Delta y_2 \qquad \Delta^2 y_2$$

$$\overline{\quad y_n \qquad \Delta y_n \qquad \Delta^2 y_n \quad}$$

where the rule for the calculation of any difference is

$$\Delta^{m+1} y_n = \Delta^m y_n - \Delta^m y_{n-1}.$$

TABLE II.

$$y'' + y'/x + y = 0 \; ; \; y_0 = 1, \; y_0' = 0.$$

x.	y''.	$y'_n - y'_{n-2}$.	y'.	$y_n - y_{n-2}$.	y.	Δy.	$\Delta^2 y$.
0·0	− ·5000	—	·0000	—	1·0000	—	—
0·2	− ·4925	—	− ·0995	—	·9900	100	—
0·4	− ·4704	− ·1960	− ·1960	− ·0396	·9604	296	196
0·6	− ·4342	− ·1872	− ·2867	− ·0760	·9120	484	188
0·8	− ·3853	− ·1728	− ·3688	− ·1141	·8463	657	173
1·0	− ·3252	− ·1534	− ·4401	− ·1468	·7652	811	154
1·2	− ·2559	− ·1295	− ·4983	− ·1782	·6711	941	130
1·4	− ·1795	− ·1010	− ·5420	− ·1984	·5668	1043	102
1·6	− ·0992	− ·0715	− ·5698	− ·2157	·4554	1114	71
1·8	− ·0170	− ·0395	− ·5815	− ·2262	·3400	1154	40
2·0	+ ·0644	− ·0069	− ·5767	− ·2315	·2239	1161	7
2·2	·1423	+ ·0255	− ·5560	− ·2296	·1104	1135	−26
2·4	·2141	·0565	− ·5202	− ·2213	·0026	1078	−57

With this arrangement, we have the approximate formula

$$\Delta^2 y_n \doteqdot h^2 y''_{n-1},$$

so that the second difference of y in the next line can be calculated very closely from the value of y'' already known, in the line which has just been completed. Again, we have, approximately

$$y'_{n+1} - y'_{n-1} \doteqdot 2h y_n'',$$

and this enables us to forecast, with fair accuracy, the next value of y'. With the help of these two formulæ, it is possible to make the process comparatively speedy.

To illustrate, we give in Table II. the final values obtained in integrating Bessel's equation of zero order,

$$y'' + y'/x + y = 0,$$

subject to the conditions that, when $x=0$, $y=1$, and $y'=0$, by this method. An interval of 0·2 is used, and the calculations are carried far enough to enable an approximation to the first root to be obtained. In the light of the foregoing, the table should be self-explanatory, but the reader should compare the values in the column headed $\Delta^2 y$ with 0·04 (h^2) times those in the preceding line of the column headed y'', and he will see how little adjustment the values of y have needed.

Applying Newton's method to the last line gives, as an approximation to the root,

$$x = 2·405\,(0) \ldots$$

as compared with the accurate value

$$x = 2·404\,(8) \ldots.$$

By comparison with a table of Bessel functions, it will also be seen that y and y' are each correct to four places of decimals, at each stage.

It may further be noted that the differences show up an error sooner, and with more insistence, than they do in the Adams method. To see this, imagine that an error of amount α creeps into y_n', by inaccuracy of addition or otherwise. The effect upon y_n is then $h\alpha/3$, but that on y_{n+1} is $4h\alpha/3$ (together with "second order" effects). There will also be, in the case of a second order equation, an error of α in y'_{n+2}, and thus an error of amount $2h\alpha/3$ in y_{n+2}. In consequence of the inequalities of these errors in the y's, the second differences will at once commence, and will continue, to oscillate about a mean which approximates to $h^2 y''$, so that the presence (and amount) of error will be immediately visible. In the Adams method, the error once introduced remains, apart from "second order" effects, constant, so that only a few differences are affected. This may easily pass unnoticed, since the oscillations soon die out.

Finally, although the equations used by way of illustration have been linear, the method is equally applicable to non-linear equations. It has been used, for instance, to obtain solutions of equations of the form $d^2y/dx^2 = \alpha \sin y - x \cos y$.

References.

(1) Math. Gazette, ix. and x. (1918-20).
(2) 'Theories of Capillary Action,' Cambridge, 1883. See also
Whittaker and Robinson,' Calculus of Observations,' or J.B.Scarborough,
'Numerical Mathematical Analysis.'
(3) *Journ. de Math.* (4) vi. pp. 197–210 (1890) ; *Traite d'Analyse*, ii.
p. 337 (1905).
(4) E. B. Moulton, in his article in the Smithsonian ' Mathematical
Formulæ and Tables of Elliptic Functions,' advocates a process of trial
and error, which seems cumbersome, and uses Simpson's Rule as a check
upon the early values, but abandons it later.

XCVI. *Rates of Condensation and Evaporation in intensively
dried Systems. The Effect of Intensive Drying on the
Accommodation Coefficient of Liquid and Solid Surfaces for
Molecules of their own Vapours. By* F. J. WILKINS,
*M.Sc., Ph.D.**

SINCE the early classical investigation of Baker of the
influence of intensive drying on the physical proper-
ties of substances much research work has been carried
out, and extraordinarily diverse and contradicatory results
have been obtained. In spite of the controversial nature of
many of the experimental data one important difference
between dried and undried systems appears to be well
established (see, *e. g.*, J. W. Smith, Phil. Mag. viii. p. 380
(1929). This is the slowness with which intensively dried
systems return to a condition of equilibrium after having
been displaced from it. A particular case of this phenomenon
is the decrease observed in the rate of evaporation and
condensation during the progress of drying. In the following
pages it is proposed to discuss this topic and show that one
must conclude that intensive drying decreases the accommo-
dation coefficient of liquid and solid surfaces for molecules of
their own vapours.

Rodebush and Michalek (J. A. C. S. li. p. 748 (1929) ;
Proc. Nat. Acad. xiv. p. 131 (1928)) have shown that the
intensive drying of ammonium chloride, while leaving the
vapour pressure and density unchanged, causes a marked
decrease in the rate of condensation and evaporation. For
example, a distillation of ammonium chloride from a hot to a
cold bulb was complete for the undried salt in ten minutes ;
the same distillation for the dried salt took several hours.

* Communicated by Prof. F. G. Donnan, C.B.E., M.A., LL.D., Ph.D.,
D.Sc., F.R.S.

The decrease in the rate of evaporation due to drying was also noticed in experiments designed to measure the vapour density by the Knudsen effusion method. J. W. Smith (*loc. cit.*) points out that the results of A. Smith and Menzies (*Z. Phys. Chem.* lxxvi. p. 713 (1911)) on the vapour pressure of dry calomel reveal the same effect. They found that dry calomel had no vapour pressure at temperatures at which ordinary calomel had a measurable vapour pressure. He suggests that since the experiments only lasted for times of the order of a quarter of an hour the dry calomel had not vaporized to any extent. Both Smith, and Rodebush and Michalek attribute many of the anomalous vapour density measurements of intensively dried substances to the slowness with which they vaporize.

Similar experimental evidence has been obtained by J. W. Smith for liquid systems. He has demonstrated that drying decreases the rates of distillation of nitrogen peroxide (J. C. S. cxxvii. p. 869 (1927)), and ethyl bromide (*ibid.* cxxxi. p. 2573 (1931)) considerably. The most detailed measurements were made with ethyl bromide. In this case it was shown that as drying proceeded the rate of distillation gradually decreased (the rate of decrease with time of drying being greatest in the initial stages), until, after twenty-six weeks' drying, the rate of distillation became almost constant, the final rate being half the initial. Moreover, during drying no change took place in the vapour pressure of the ethyl bromide. It was concluded that intensive drying did not alter the equilibrium of the liquid phase.

The above experimental results may be extended quite readily, for it can be shown that they indicate a decrease in the accommodation coefficient as drying proceeds. The results of Rodebush and Michalek will be discussed first.

1. *The Rates of Vaporization and Condensation of Ammonium Chloride.*

The distillation experiment already referred to was carried out under conditions such that the temperature of the cold bulb was so low that the vapour pressure of the condensed ammonium chloride was probably too small to cause any appreciable back diffusion into the hot bulb. The rate of distillation, therefore, corresponds with the rate of vaporization. Let V be the rate of vaporization from unit area of the solid surface at a given temperature, and P the vapour pressure at the same temperature. Then if α is the accommodation coefficient, the rate of condensation on to unit area

from the vapour when it is in equilibrium with the solid is $k\alpha P$, where k is a constant given by the Herz-Knudsen equation as equal to $43{\cdot}07.10^{-7}$ $\sqrt{M/T}$. $M =$ mol. wt., $T =$ abs. temp. Therefore

$$V = k\alpha P.$$

Now experiment shows that V decreases with drying, while the vapour pressure and density are unchanged. Therefore k and P are unchanged by drying, and the decrease in V must be accompanied by a decrease in α : *i. e.*, intensive drying causes a decrease in the accommodation coefficient of ammonium chloride vapour at an ammonium chloride surface. α appears to be decreased by a factor of about ten.

2. *The Rate of Distillation of Ethyl Bromide.*

In these experiments the receiver was kept at a temperature of $0°$ C., where the ethyl bromide has a considerable vapour pressure. Let V, k, α, and P have the same meaning as before, and let p be the vapour pressure of ethyl bromide in the still at a distance from the surface of the liquid equal to a mean free path of a molecule in the vapour phase. Then, D, the rate of distillation when a steady state has been established, is equal to the difference between the rates of vaporization and condensation at the ethyl bromide surface. The molecules striking the surface come from a distance into the vapour phase of a mean free path, and the rate of condensation is then

$$k\alpha p.$$

Therefore,
$$D = V - k\alpha p. \quad \ldots \quad \ldots \quad (1)$$

Further, since P is the vapour pressure,
$$V = k\alpha P \quad \ldots \quad \ldots \quad \ldots \quad (2)$$

and consequently,
$$D = k\alpha(P - p).$$

Now P is unaltered by drying; further, since p is a function for given experimental conditions only of P and the vapour pressure in the receiver, it also is unaltered by drying. The experimentally observed decrease in D must therefore be due to a decrease in either k or α separately or together. It is quite inconceivable that k should be decreased by drying, for that would imply (*vide supra*) a decrease in the molecular weight of the vapour. We must therefore conclude that intensive drying causes a decrease in the accommodation

coefficient of ethyl bromide molecules at an ethyl bromide surface. Since D is proportional to α, and since D is decreased to $\frac{1}{2}$ by drying, α must be decreased by a half.

A second conclusion which may be drawn is that the rate of vaporization is also decreased by intensive drying. This follows immediately from the equation for equilibrium

$$V = ka\mathrm{P},$$

since both k and P are unaltered by drying. These results are, therefore, in accord with those of Rodebush and Michalek, since the rates of vaporization and condensation of both solid ammonium chloride and liquid ethyl bromide are decreased by intensive drying.

One of the features of these experiments which distinguishes them sharply from many others on intensive drying is that the effects become observable after comparatively short periods of drying. This perhaps demonstrates most effectively how sensitive rates of condensation and evaporation are to traces of water, for the *total* amount of water removed was not sufficient to cause a measurable change of vapour pressure.

Discussion.

Relevant experimental determinations of α.—The number of determinations of the accommodation coefficients of solids for condensing gas molecules is not large. Only in one or two instances have estimates been made of the accommodation coefficient of a solid for its own vapour. Volmer and Estermann (*Zeits. f. Physik*, vii. p. 1 (1921)) state that near the melting-point α for mercury against mercury is slightly less than unity and increases as the temperature is lowered. Langmuir (Phys. Rev. ii. p. 329 (1913)) in his work on the vapour pressure of high melting metals suggests that α is unity.

Only in two investigations has the influence of impurities on the accommodation coefficient been studied. Roberts (Proc. Roy. Soc. A, cxxix. p. 146 (1930)) has measured the accommodation coefficients of helium on wires of nickel and tungsten. He finds that α for a freshly outgassed wire is in both cases less than α for a wire which has been allowed to remain in the apparatus and readsorb any residual impurities. These results are in agreement with those deduced above for ammonium chloride, since intensive drying may be considered as a process of removing impurities of a certain type. Johnson (Proc. Roy. Soc. A, cxxviii. pp. 432, 444 (1930)) has shown that if α is 0·26 for hydrogen at a glass surface

containing a monomolecular layer of adsorbed water-vapour, then washing with hydrogen *in vacuo* increases α to 0·305. The value of α for a glass surface covered with a layer of hydrogen atoms is 0·295. These figures are completely opposite in type to those of Roberts, and those deduced in this paper, for the removal of the adsorbed water *increases* α.

No measurements of the influence of impurities on α for a liquid/gas interface have been made. Knudsen (*Ann. d. Physik*, xlvii. p. 697 (1915)) finds α for mercury at a liquid mercury surface to be within 1 per cent. of unity. Similarly Alty and Nicoll (Canadian J. Research, iv. p. 547 (1931)) find α for carbon tetrachloride and benzene against their own vapours to be nearly unity. None of these liquids had been dried.

Theoretical treatment of α.—It is a well-known fact that α is increased by increasing the roughness of the surface. This is usually interpreted to mean that incident molecules tend to become entrapped in the irregularities and therefore make more than one collision before they leave the surface. If this were the explanation of the decrease in α due to intensive drying one would have to assume that drying tended to make surfaces smoother. For solids this is unlikely and for liquids it is quite impossible.

An extensive theoretical treatment of α has been given by Baule (*Ann. d. Physik*, xliv. p. 145 (1914)), who assumes that the collisions between incident molecules and the surface atoms are perfectly elastic. He shows that

$$\alpha = (1 - \beta \eth),$$

where

$$\beta = \frac{M^2 + m^2}{(M + m)^2},$$

M is the mass of the solid atom and m is the mass of the condensing atom ; $\eth$ is the fraction of the incident molecules which make only one collision with the surface. The remainder $(1 - \eth)$ make sufficient collisions to come into thermal equilibrium with the surface. Johnson (*loc. cit.*) finds that his results satisfy Baule's equation. He assumes that the "impurities" present on his glass surfaces, water and hydrogen atoms, load the surface vibrators. Using the same method for ammonium chloride and putting $\eth$ equal to unity, we obtain the greatest possible effect which the weighting of ammonium or chloride ions with water could have on α. In this way for the dry ammonium ion α is 0·37, while for the ammonium ion weighted with water α is 0·48. The

corresponding figures for the chlorine ion are 0·48 and 0·50 respectively. The observed experimental decrease is of the order of ten times this.

Roberts (*loc. cit.*) also finds that Baule's equation does not correspond with his experimental figures. He concludes that there is an important amount of specular reflexion of the type studied by Stern and his co-workers. This specular reflexion is a direct consequence of the wave-structure of matter, the solid surface acting as a diffraction grating. The condition for reflexion (see Fraser, 'Molecular Rays,' p. 82, *et seq.*), is that $h \sin \theta \sim \lambda$ where θ is the glancing angle, h the average height of the inequalities on the surface, and λ the wave-length of the material particle as given by the de Broglie equation. Impurities will tend to distort the grating and thus spoil the lattice. Consequently the amount of specular reflexion is decreased and α is increased, as his experiments show. Since he used helium the amount of specular reflexion may be considered to be perhaps important, but as θ for ammonium chloride is less than $2°$ the specular reflexion must be very slight. Roberts's theory, therefore, cannot apply to the cases discussed here.

The accommodation coefficient has been treated theoretically by Langmuir (Phys. Rev. viii. p. 149 (1916)). He suggests that Baule's analysis can have no general validity, as it fails to take into account the attractive forces which exist between molecules and surfaces. The part of his theory which is of importance for this investigation is that he shows that the surface field, which is effective in the condensation process, must be considered as that due not only to the atom at which condensation is occurring, but also to those which surround it. The effects discussed is this paper seem to indicate that a polar impurity such as water may influence surface fields over distances of several molecular diameters. (The transference of polar influences over comparatively great distances has been advocated by de Boer—see, *e. g.*, de Boer and Zwikker, *Zeits. Phys. Chem.* B. iii. p. 407 (1929), and Topley, J. S. C. I. (1931).) Whether Langmuir's theory is able to account for the results quantitatively it is not possible at present to determine. An analogous problem, the reflexion of electrons at a surface has been treated by Nordheim (*Zeits. f. Physik*, xlvi. p. 833 (1928)) using the new quantum mechanics.

The influence of intensive drying on the rate of evaporation has been discussed by J. W. Smith (*loc. cit.*). It is interesting to note that all changes in the rate of evaporation are exactly balanced by changes in the accommodation

coefficient, since the vapour pressure remains unchanged (*cf.* equation 2).

Summary.

It is shown that the experiments of Michalek and Rodebush which indicate that intensive drying decreases the rate of evaporation and condensation without changing the vapour pressure, prove that intensive drying decreases the accommodation coefficient of ammonium chloride for its own vapour. J. W. Smith found that drying decreased the rate of distillation of ethyl bromide without altering its vapour pressure, and it is shown that a similar conclusion can be drawn. These conclusions are discussed theoretically.

The Sir William Ramsay Laboratories
of Physical and Inorganic Chemistry,
University College, London.

XCVII. *Precision Measurements of the Crystal Parameters of some of the Elements.* By Prof. E. A. OWEN, *M.A., D.Sc.,* and JOHN IBALL, *M.Sc., University College of North Wales, Bangor* [*].

[Plates XVII. & XVIII.]

IN the course of an investigation on the accurate determination of the crystal parameters of certain alloys and the effect of different methods of heat treatment on these alloys, we had occasion to measure the crystal parameters of a few of the elements to a high degree of accuracy. The parameters of most of the elements contained in published tables [†] are given to the third significant figure, but for the work in hand it was desired to know the parameters, if possible, to the fourth figure. As the few elements which were initially examined yielded consistent results to this accuracy, it was decided to extend the measurements to include as many of the elements having

cubic structure as were immediately obtainable. The results of the measurements are collected together in this paper, which is confined entirely to elements possessing cubic symmetry. It may conveniently be divided into two sections, namely : (1) the examination of the elements aluminium, copper, and silver by a precision method using radiations of different wave-lengths ; (2) the examination of a number of other elements by the same precision method employing only copper radiation.

Method of Measurement.

The X-ray camera employed for the measurements was similar to that used by Gayler and Preston [*] in an investigation on the age-hardening of aluminium alloys. It consists of a cylindrical drum in the circumference of which is a narrow slit. A divergent beam of X-rays from the slit falls on a specimen of the material under examination, which is mounted on a curved plate covering a short arc diametrically opposite to the slit. After reflexion the rays fall on a photographic film extending over half the circumference of the drum and arranged symmetrically about the slit. With this arrangement the rays come to a sharp focus on the film and lines are observed in symmetrical positions on either side of the slit. From a knowledge of the distance (s) between corresponding lines and the radius (r) of the drum, the angle of reflexion (θ) can be calculated from the relation $s/8r = (\pi/2 - \theta)$. Combining this with Bragg's law of reflexion, the distance between the planes giving the reflexion is given by the relation $d = \lambda/2 \cdot \sec s/8r$, where λ is the wave-length of the radiation employed. Since $d = a \cdot f(hkl)$ for cubic crystals, where a is the lattice parameter and h, k, and l, the Miller indices of the reflecting plane, then $\delta a/a = \tan s/8r \cdot \delta(s/8r) = (s/8r)^2 \delta s/s$, where $s/8r$ is small. The percentage error in measuring s is therefore multiplied by the square of a small quantity, so that the percentage error in the value of the parameter is exceedingly small.

It will be seen from the photographs that when the reflecting angle θ is large the lines lose in definition, making it more difficult to measure the distance between them with a high degree of accuracy. High accuracy of measurement is, however, not necessary at large angles of reflexion. For instance, the angle of reflexion of the Kα-radiation of copper from the (422) planes of rhodium is about 83°. Now $\delta\theta = \delta s/8r$, so that if $r = 50$ mm. and the error in measuring

s is as much as ± 0.3 mm., then $\delta\theta = 3/2000$ and $\delta a/a = 0.02$ per cent.

The camera was carefully constructed, and certain modifications were introduced to increase the accuracy of the determinations. The drum had to be perfectly rigid, so that it remained undistorted when subjected to strains such as those set up by the weight of the lead shield covering the photographic film. The final form of camera adopted was made in the following manner :—

Two cast iron disks about 4 inches in diameter and $\frac{3}{8}$ inch thick were turned in the lathe to form two annular rings about $\frac{3}{4}$ inch wide. The outside of the rings was carefully turned, so that a true surface at right angles to the plane of the rings was obtained and the rings were both of exactly the same diameter. In a brass sheet $\frac{1}{16}$ of an inch thick and $1\frac{3}{4}$ of an inch wide were cut suitable slots to be covered by the photographic film and by the material to be examined. The sheet was bent into a circle in the rolling machine, so as to fit over the two circular rings already prepared, and was fixed to the rings with about a dozen countersunk screws. Constructed thus the camera was extremely rigid. After the screws had been inserted, the camera was put in a lathe and the outer surface made cylindrical by turning off a thin layer of the metal. Thus there could be no possibility of irregularities on the brass surface or of distortion in the camera ; and the diameter of the camera could be accurately determined. Several methods were employed to measure the diameter, all of which agreed well with each other, giving for the diameter a mean value of 102.92 mm.

Further precautions had to be taken to obtain the correct radius for the calculation of the crystal parameters. The film was wrapped in black paper and held firmly and uniformly against the circumference of the camera. With this arrangement the film was displaced from the true circumference. Also, since the gelatine of the film was coated with emulsion on both sides, there were two images formed, which were not exactly coincident. The lines were measured from the middle of one to the middle of the corresponding line on the opposite side of the centre of the film. This procedure gave the correct distance between the lines if the images had been formed at the position occupied by the middle of the gelatine between the two emulsions. Hence a correction had to be applied both for the thickness of the black paper and for the position of the images on the surface emulsions of the film. The thickness of the film before development was 0.23 mm., so that the

middle of the gelatine was 0·12 mm. radially from the outer surface of the black paper which was 0·08 mm. thick, and thus was situated on a circle of radius 51·66 mm. The formula from which the results are calculated is derived on the assumption that the reflecting material and the film are on the circumference of the same circle, so that the reflecting material must also lie on the circumference of a circle of radius 51·66 mm. This was arranged by fixing to the camera, around the slot where the reflecting material was placed, a sheet of aluminium which had been carefully rolled down to a thickness of 0·20 mm.

Several slit systems were tried; the arrangement which yielded spectral lines showing the best definition, consisted of a short brass rod through which was drilled a small round hole about 1 mm. in diameter. The rod was covered on the inner face with a thin lead disk, in which was pierced a smaller hole with a needle-point. The rod could be adjusted to any desired position in a tube fixed to the circumference of the camera. Several photographs of aluminium were taken with the slit in different positions and the rod finally fixed in the position which gave lines showing the best definition.

The film was held in position by an elastic band, which also held the reflecting powder in position. Underneath the elastic band and just covering the film was a light steel spring, which acted as a screen and also served to press the film tightly against the camera. Over the elastic band was a lead screen, held in position by two buttons fixed to the camera. The whole camera was mounted on a stout piece of brass, by means of which it was held firmly in a suitable stand.

The film on development contracts. This contraction was very small, but was allowed for by recording on each film, near its ends, two fiducial marks, the exact distance between which was known and assuming a linear contraction along the film. The travelling microscopes were also calibrated against standard lengths and were correct along the scale to within 0·05 mm., an accuracy much higher than was required for the measurement of the film.

The installation consisted of a modified Shearer tube operated on a Schall transformer at a voltage of about 40,000 volts and 10 ma. The exposures varied between two and four hours.

To obtain well-defined spectral lines at these large angles of reflexion, it was necessary, with most of the elements examined, to pay particular attention to the heat treatment.

The metals were annealed *in vacuo* for many hours at appropriate temperatures, varying with different materials, and then quenched in cold water.

Single-coated photographic films were experimented with, but no better definition was obtained whilst the exposures had to be prolonged. A second precision camera having effective radius 69·63 mm. was constructed to serve as a check on the first. Both cameras were used in the investigation.

TABLE I.—Aluminium.

Target.	Arc (mm.).	λ.	Reflecting planes.	Parameter.
				Å.
Chromium.	197·9	$K\alpha_1$	(311)	4·0415
	195·1	$K\alpha_2$		4·0415
	113·1	$K\alpha_1$	(222)	4·0408
	108·4	$K\alpha_2$		4·0409
Cobalt.	152·3	$K\alpha_1$	(331)	4·0411
	147·7	$K\alpha_2$		4·0408
	109·9	$K\beta$	(422)	4·0403
	86·2	$K\alpha_1$	(420)	4·0403
	77·5	$K\alpha_2$		4·0398
	152·2	$K\alpha_1$	(331)	4·0408
	147·9	$K\alpha_2$		4·0408
	110·1	$K\beta$	(422)	4·0405
	86·2	$K\alpha_1$	(420)	4·0403
	77·8	$K\alpha_2$		4·0401
Copper.	207·1	$K\alpha_1$	(422)	4·0419
	203·3	$K\alpha_2$		4·0417
	84·4	$K\alpha_1$	{ 511	4·0406
	74·6	$K\alpha_2$	333 }	4·0406
Iron.	184·9	$K\beta$	(331)	4·0411
	165·7	$K\alpha_1$	(400)	4·0414
	161·7	$K\alpha_2$		4·0411
	136·5	$K\beta$	(420)	4·0407
Nickel.	152·8	$K\beta$	{ 511	4·0404
			333 }	

Results.

The three elements aluminium, copper, and silver were investigated with radiation from anticathodes of chromium, cobalt, copper, iron, and nickel.

(1) *Aluminium.*—Table I. contains the results of the measurements made on aluminium.

It will be observed that the values of the parameter vary between 4·0419 and 4·0398 and that they diminish in each case with increase of glancing angle. A further examina-

tion was carried out with this element, using very thin
sheets of thickness not exceeding 0·02 mm. backed by
copper. The results obtained with one of these sheets,
using a copper target, are given in Table II.

The value of the parameter is now constant for each of the
four lines recorded on the film. Thus the variation in
the value of the parameter observed in Table I. was probably
due mainly to the penetration of the X-rays in the material.

TABLE II.

Arc (s) in mm.	λ.	Reflecting planes.	Parameter.
			Å.
206·54	Kα₁ ⎫	(422)	4·0406
203·02	Kα₂ ⎭		4·0407
84·37	Kα₁ ⎫	{ 511 ⎫	4·0406
74·55	Kα₂ ⎭	{ 333 ⎭	4·0404

TABLE III.—Copper.

Target.	Arc (mm.).	λ.	Reflecting planes.	Parameter.
				Å.
Chromium.	165·4	Kβ	(311)	3·6081
Cobalt.	119·8	Kβ	(331)	3·6075
	79·5	Kα₁ ⎫	(400)	3·6073
	70·3	Kα₂ ⎭		3·6071
Copper.	211·6	Kα₁ ⎫	(331)	3·6079
	208·0	Kα₂ ⎭		3·6078
	171·6	Kα₁ ⎫	(420)	3·6076
	167·1	Kα₂ ⎭		3·6074
Iron.	213·4	Kα₁ ⎫	(222)	3·6080
	210·5	Kα₂ ⎭		3·6078
Nickel.	212·9	Kβ	(420)	3·6074

This effect, as will be seen below, was not so pronounced
in metals of higher atomic weight, such as silver and copper.
When the values of the parameter recorded in Table I. are
plotted against length of arc (s), the values tend to a constant
for small values of s, this constant value being about
4·0405 Å. This agrees with the value 4·0406 Å. obtained
from the independent photographs taken with thin aluminium
foil 0·02 mm. thick.

(2) *Copper and Silver.*—Tables III. and IV. contain the
results obtained with copper and silver.

There is good agreement between the values of the parameter obtained with the different targets ; the wave-lengths of the Kα-doublet and the Kβ-radiation of the materials of the targets were taken from the ' International Critical Tables '*.

The mean values of the parameters of these three elements are therefore :—

Aluminium	....	$4·0406 \pm 0·0003$ Å.
Copper	....	$3·6076 \pm 0·0003$ Å.
Silver	....	$4·0773 \pm 0·0003$ Å.

TABLE IV.—Silver.

Target.	Arc (mm.).	λ.	Reflecting planes.	Parameter.
				A.
Cobalt.	169·2	$K\alpha_1$	(331)	4·0775
	165·3	$K\alpha_2$		4·0776
	132·7	Kβ	(422)	4·0771
	113·8	$K\alpha_1$	(420)	4·0770
	107·9	$K\alpha_2$		4·0771
Copper.	215·8	$K\alpha_2$	(422)	4·0776
	150·3	Kβ	(440)	4·0771
	112·5	$K\alpha_1$	(511)	4·0771
	105·4	$K\alpha_2$	(333)	4·0774
Iron.	198·8	Kβ	(331)	4·0776
	180·8	$K\alpha_1$	(400)	4·0771
	177·3	$K\alpha_2$		4·0767
	155·5	Kβ	(420)	4·0778
Nickel.	60·8	$K\alpha_1$	(422)	4·0770
	47·5	$K\alpha_2$		4·0769

Specimens of the spectra are reproduced in fig. 1 (Pl. XVII.) and were all taken with the larger camera, radius 69·63 mm.

Aluminium in foil and in powder form was annealed at different temperatures (250° C. and 500° C.). No difference was found in the parameter of the material due to the differences in temperature of annealing or to the form of the material.

(3) The parameters of the elements gold, iridium, lead, molybdenum, nickel, palladium, rhodium, tantalum, and tungsten were mainly measured with the smaller precision camera having an effective radius of 51·66 mm.

* Int. Crit. Tables, vol. vi. p. 36.

Radiation from a copper target only was employed in these measurements. The metals had to be annealed *in vacuo* and quenched as previously; in some cases considerable difficulty was experienced in obtaining lines well enough defined to give accurate results.

TABLE V.

Element.	Atomic number.	Arc (mm.).	λ.	Reflecting planes.	Parameter. Å.	Mean parameter.	Distance of closest approach of atoms.
Gold (f.c.).	79	80·4 75·0	$K a_1$ $K a_2$	$\begin{Bmatrix} 511 \\ 333 \end{Bmatrix}$	4·0711 4·0712	4·071$_1$	2·879
Iridium (f.c.).	77	141·3	$K\beta$	$\begin{Bmatrix} 511 \\ 333 \end{Bmatrix}$	3·8312	3·831$_4$	2·709
		76·7 71·0	$K a_1$ $K a_2$	(422)	3·8316 3·8314		
Lead (f.c.).	82	151·3	$K a_1$	(600)	4·9392	4·939$_3$	3·493
		148·5	$K a_2$	(422)	4·9391		
		73·4	$K a_1$	(620)	4·9392		
		67·6	$K a_2$		4·9398		
Molybdenum (b.c.).	42	145·7	$K\beta$	(330)	3·1403	3·140$_3$	2·720
		84·6 79·5	$K a_1$ $K a_2$	(400)	3·1402 3·1404		
Nickel (f.c.).	28	127·8 124·5	$K a_1$ $K a_2$	(331)	3·5775 3·5773	3·517$_9$	2·487
		88·8 83·9	$K a_1$ $K a_2$	(420)	3·5785 3·5784		
Palladium (f.c.).	46	102·8 98·6	$K a_1$ $K a_2$	(422)	3·8848 3·8853	3·885$_0$	2·747
Rhodium (f.c.).	45	51·7 42·5	$K a_1$ $K a_2$	(422)	3·7955 3·7953	3·795$_4$	2·684
Tantalum (b.c.).	73	71·9 65·9	$K a_1$ $K a_2$	(330)	3·3113 3·3116	3·311$_4$	2·868
Tungsten (b.c.).	74	152·5	$K\beta$	(330)	3·1600	3·159$_2$	2·736
		95·7 90·9	$K a_1$ $K a_2$	(400)	3·1591 3·1588		
		75·3	$K\beta$	(420)	3·1588		

Table V. shows the results obtained.

These parameters may be taken to be accurate to within ± 0.001 Å. The photographs were all taken at a mean temperature of 16·5° C. Specimens of the spectra obtained are reproduced in fig. 2 (Pl. XVIII.).

The results of the measurements of the lattice parameters of all the elements so far investigated are collected in Table VI., which includes also the atomic weights and the crystal densities, calculated from the mass of the hydrogen atom $(1{\cdot}663 \times 10^{-24}$ gm.), and the atomic weights, taken from the 36th Annual Report of the Committee on Atomic Weights published in the 'Journal of the American Chemical Society,' March 1930. The experimental values of the densities taken from the 'International Critical Tables,'

TABLE VI.

Group.	Element.	Lattice parameter (Å.).	Distance of closest approach of atoms (Å.).	Degree of purity.	Atomic weight.	Calculated crystal density at mean temp. 16·5 °C. (gm. per c.c.).	Experimental density (from Int. Crit. Tables, vol. ii.) (gm. per c.c.).
		$\pm 0{\cdot}0003$		Per cent.			
I.	*Ag (f c.).	$4{\cdot}077_3$	2·883	99·9	107·880	$10{\cdot}50_6$	10·50 at 0°C.
	Al (f.c.).	$4{\cdot}040_6$	2·857	99·6	26·97	$2{\cdot}69_4$	2·703 at 20
	*Cu (f.c.).	$3{\cdot}607_6$	2·551	99·9	63·57	$8{\cdot}93_7$	8·94 at 20
		$\pm 0{\cdot}001$					
II.	*Au (f.c.).	$4{\cdot}071_1$	2·879	99·9	197·2	$19{\cdot}29_1$	19·30 at 0
	*Ir (f.c.).	$3{\cdot}831_4$	2·709	99·5	193·1	$22{\cdot}66_1$	22·4 at 0
	*Mo (b.c.).	$3{\cdot}140_3$	2·720	99·5	96·0	$10{\cdot}23_1$	10·2 —
	*Ni (f.c.).	$3{\cdot}517_9$	2·487	99·9	58·69	$8{\cdot}89_3$	8·90 —
	*Pb (f.c.).	$4{\cdot}939_3$	3·493	99·9	207·22	$11{\cdot}35_6$	11·347 at 16·34
	*Pd (f.c.).	$3{\cdot}885_0$	2·747	99·5	106·7	$12{\cdot}01_1$	12·1 at 0
	Rh (f c.).	$3{\cdot}795_4$	2·684	99·5	102·91	$12{\cdot}42_3$	12·5 at 0
	*Ta (b.c.).	$3{\cdot}311_4$	2 868	99·8	181·5	$16{\cdot}49_7$	16·6 —
	*W (b.c.).	$3{\cdot}159_2$	2·736	99·9	184·0	$19{\cdot}25_9$	19·3 —

vol. ii. p. 456, are included for comparison in the last column of the Table.

The elements marked with asterisks in Table VI. were supplied by Messrs. Johnson Matthey of Hatton Garden. We are indebted to the firm for supplying us with the information included in Column 5 of the Table as to the degree of purity of these elements. The aluminium was obtained from a single crystal of the material. The figure given in each case for the degree of purity denotes the minimum, and not the maximum purity of the material.

Bangor, October 1931.

XCVIII. *An X-Ray Investigation of the Bismuth-Antimony Alloys. By* E. G. Bowen, *M.Sc., and* W. Morris Jones, *M.A., M.Sc., F.Inst.P.* (*Physics Department, University College, Swansea*) *.

BISMUTH and antimony are chemically related elements having similar face-centred rhombohedral crystal structures. In common with certain other related metals having similar structures (Cu and Au, for example, having face-centred cubic structures), bismuth and antimony might be expected to be completely soluble in one another.

However, no definite evidence for the existence of such an unbroken range of solid solution was obtained in the earlier metallurgical examinations of the system, while conflicting data were obtained by different observers of the electrical conductivities, thermo-electric powers, and magnetic properties of the alloys. From a consideration of all the existing data, Guertler † concluded that there was solid solution of bismuth in antimony up to 70 per cent. of bismuth, but no solution of antimony in bismuth. Alloys containing more than 70 per cent. of bismuth were considered to be a mixture of two constituents—a mixture of bismuth and the solid solution of bismuth in antimony.

More recent work by Cook ‡ indicates that the rate of diffusion of antimony into bismuth is extremely small, and that by adopting a special method of preparation, alloys of every composition can be rendered homogeneous. As a result of his investigations, Cook gives the thermal diagram reproduced in fig. 1.

As with earlier workers, Cook found that microphotographs of both slowly and quickly-cooled alloys showed a mixture of two constituents, and annealing for a considerable period at a temperature just below the melting-point of bismuth did not cause the two constituents to combine. Annealing the specimens at this temperature did not allow the constituent rich in antimony to go into solution in the bismuth. But, by maintaining them at a temperature *above* the melting-point of bismuth, the bismuth constituent was kept molten, and the remaining solid constituent, containing both antimony and bismuth, was able to go completely into solution. After being subjected to this treatment, alloys which had previously been a mixture of constituents were

* Communicated by the Authors.
† Guertler, 'Metallographie,' i.
‡ Cook, Journ. Inst. Metals, xxviii. p. 421 (1922).
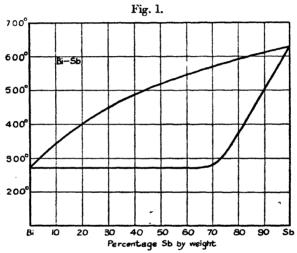
found to be completely homogeneous.. The failure of previous workers to obtain homogeneous alloys over the whole range of compositions was thus due to a method of preparation which made no allowance for the extremely slow rate of diffusion of antimony into bismuth.

The present investigation was undertaken with the object of determining, by X-ray methods, whether the alloys are rendered homogeneous by the method of preparation adopted by Cook, and, if so, to find the relation between the lattice constants and the composition of the alloys.

Fig. 1.

The equilibrium diagram due to Cook.

Preparation of the Alloys.

For the purposes of the present investigation, a series of nine alloys having composition intervals of 10 per cent. were prepared and transferred immediately to a furnace standing at 280° C.—at a temperature 10° above the melting-point of bismuth. They were maintained at this temperature for 400 hours and allowed to cool gradually to room temperature over a further period of 200 hours. The alloys were allowed to cool at this very slow rate in order that the marked expansion on solidification should not set up internal strains in the specimens.

Method of Experiment.

The crystal structures of the alloys were examined by the X-ray powder method. Details of the apparatus used and

Table of Results of X-ray Investigations of the Bismuth-Antimony Alloys.
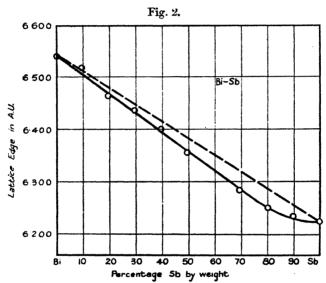
Plane.	Intensity.	Pure Bi.		10 per cent. Sb.		20 per cent. Sb.		30 per cent. Sb.		40 per cent. Sb.		50 per cent. Sb.		60 per cent. Sb.		70 per cent. Sb.		80 per cent. Sb.		90 per cent. Sb.		Pure Sb.	
		d/n.	$a_0/2$.	d/n.	$a_0/2$.	d/n.	$a_0/2$.	d/n.	$a_0/2$.	d/n.	$a_0/2$.	d/n.	$a_0/2$.	d/n.	$a_0/2$.	d/n.	$a_0/2$.	d/n.	$a_0/2$.	d/n.	$a_0/2$.	d/n.	$a_0/2$.
100 (2)	St.	3·260	3·266	3·247	3·253	3·228	3·234	3·215	3·221	3·201	3·207	3·172	3·178	3·146	3·152	3·136	3·142	3·120	3·126	3·114	3·120	3·107	3·113
110 (2)	M.	2·359	3·273	2·349	3·259	2·329	3·230	2·324	3·223	2·312	3·207	2·290	3·176	2·286	3·169	2·263	3·138	2·250	3·119	2·248	3·116	2·246	3·113
¯110 (2)	M.	2·260	3·266	2·255	3·280	2·241	3·242	2·228	3·224	2·214	3·203	2·192	3·169	2·183	3·158	2·169	3·138	2·155	3·118	2·154	3·118	2·145	3·105
111 (2)	W.	1·859	3·269	1·852	3·257	1·844	3·244	1·832	3·229	1·820	3·201	1·802	3·171	1·795	3·158	1·775	3·138	1·769	3·113	1·768	3·112	1·766	3·109
100 (4)	W.	1·634	3·270	1·627	3·259	1·614	3·234	1·607	3·220	1·597	3·201	1·587	3·180	1·580	·166	1·567	3·140	1·560	3·126	1·554	3·124	1·552	3·110
331	V.W.	1·549	3·271	1·546	3·285	1·539	3·229	1·528	3·225	1·522	3·212	1·509	3·184	1·504	3·171	1·490	3·142	1·482	3·125	1·479	3·118	1·475	3·110
210 (2)	M.	1·484	3·270	1·480	3·260	1·465	3·227	1·461	3·218	1·453	3·200	1·446	3·184	1·438	3·166	1·429	3·146	1·419	3·125	1·416	3·117	1·411	3·106
¯210 (2)	M.	1·436	3·269	1·432	3·261	1·414	3·230	1·410	3·211	1·402	3·192	1·394	3·175	1·388	3·162	1·380	3·144	1·368	3·118	1·368	3·118	1·364	3·109
211 (2)	V.W.	1·381	3·272	1·379	3·267	1·368	3·239	1·360	3·220	1·350	3·196	1·347	3·188	1·337	3·163	1·331	3·148	1·325	3·137	1·317	3·113	1·315	3·109
¯211 (2)	M.	1·323	3·268	1·321	3·264	1·308	3·232	1·301	3·215	1·296	3·202	1·285	3·175	1·279	3·161	1·271	3·141	1·263	3·122	1·262	3·120	1·259	3·112
¯211 (2)	W.	1·306	3·269	1·302	3·259	1·290	3·231	1·282	3·211	1·276	3·193	1·266	3·172	1·268	3·152	—	—	—	—	1·241	3·111	1·241	3·111
110 (4)	V.W.	1·180	3·275	1·176	3·264	—	—	—	—	—	—	1·148	3·184	1·139	3·158	—	—	1·082	3·131	—	—	1·122	3·110
¯110 (4)	W.	1·131	3·269	1·128	3·262	—	—	—	—	—	—	1·102	3·184	1·096	3·171	— ··		1·082	3·131	—	—	1·076	3·115
100 (6)	W.	1·090	3·276	1·084	3·258	—	—	—	—	—	—	1·057	3·177	1·050	3·156	—	—	1·041	3·129	—	—	1·034	3·108
Lattice dimensions in A.U.		a_0=6·340, α=87° 34'.		a_0=6·520, α=87° 33'.		a_0=6·466, α=87° 32'.		a_0=6·438, α=87° 31'.		a_0=6·403, α=87° 30'.		a_0=6·356, α=87° 29'.		a_0=0·323, α=87° 28'.		a_0=6·283, α=87° 27'.		a_0=6·249, α=87° 26'.		a_0=6·234, α=87° 25'.		a_0=6·220, α=87° 24'.	

Explanation of the Table.—The first column gives the Miller indices of reflecting planes, and the second the intensity of the lines on the films. Subsequent columns contain in turn the plane spacings (d/n) and the half-lattice edge ($a_0/2$) deduced from each line on a film. For any one alloy the lattice edge is the mean of the values determined from all the lines on a film of that alloy. In every case the plane spacings correspond to a face-centred rhombohedral structure.

of the precautions observed to ensure accuracy have been described in previous papers[*]. Adopting the procedure outlined there, the accuracy of measurement in the present investigation can be estimated as within 1 in 1000.

Results.

The complete results for all nine alloys and for bismuth and antimony are given in the Table. The first column gives the Miller indices of reflecting planes, and the second the intensity of the lines on the films. Subsequent columns contain in turn the plane spacings, deduced from measurements on films of each alloy. In every case the plane

Fig. 2.

The variation of lattice edge with composition of the bismuth-antimony alloys.

spacings correspond to a face-centred rhombohedral structure and from each observation of plane spacing is calculated a value of the lattice edge for this structure. The mean value of the lattice edge determined from all the lines on a film is taken as the lattice constant for that alloy.

The lattice constants of the pure metals are :—

Bismuth ...... $a_0 = 6\cdot540$ A.U., $\alpha = 87° 34'$,
Antimony ...... $a_0 = 6\cdot220$ A.U., $\alpha = 87° 24'$,

---

[*] Morris Jones and Evans, Phil. Mag. iv. p.1302 (1927). Grime and Morris Jones, Phil. Mag. vii. p. 1113 (1929).

the angles of the rhomb differing by only 10'. If in the alloys the variation of angle with composition is linear, the change of angle from one alloy to the next would be a change of but 1', while the accuracy of measurement is only sufficient to detect a change of 4' to 5'. In the calculation of the lattice edge for each alloy it has therefore been necessary to assume that the change of angle with composition is linear. A small deviation of 2' to 3' from linearity would make no difference to the calculated lattice edge, while a deviation greater than 5' would have been evident. The results in this instance are consistent with a linear change of angle with composition.

The change of lattice edge with composition is plotted in fig. 2. The curve is almost linear ; there is slight curvature only at the antimony end for alloys containing up to 25 per cent. of bismuth. This emphasises that on the introduction of the larger bismuth atom there is at first only a slight expansion of the antimony lattice, while at the bismuth end, introduction of the smaller antimony atom into the lattice of pure bismuth causes an immediate contraction of the lattice. The curve illustrates an effect which is generally exhibited in solid solutions of extended range:—the contraction of a lattice due to the introduction of smaller atoms generally takes place as anticipated, but expansion against the forces in the lattice on substitution of larger atoms does not occur so readily.

Prolonged exposure of alloys rich in bismuth gave films showing no trace of a mixture of constituents as suspected by Guertler. The regularity of the curve of the lattice edge plotted against composition is additional evidence that there is no region over which there is a mixture of constituents.

Summary.

Alloys of bismuth and antimony prepared and annealed in the usual way are a mixture of two constituents, but Cook (Jour. Inst. Metals, xxviii. p. 421, 1922) showed that they can be rendered homogeneous by maintaining them at a temperature above the melting-point of bismuth for a considerable time and allowing to cool very slowly. This is verified in the present investigation by an X-ray study of the crystal structures of a series of such alloys. Measurements of the lattice constants of the alloys show that the change of lattice edge with composition is almost linear over the whole range of compositions.

XCIX. *Operational Calculus.*—Part I. *The Definition of an Operational Representation of a Function and some Properties of the Operator derived from this Definition.* By H. V. LOWRY [*].

SUMMARY.

THE first part of this paper contains a discussion of some fundamental points in the theory of operational calculus. In particular, it is shown that there are good reasons for preferring the definition of an operational representation of a function by Bromwich's contour integral along a contour from $-\infty -0i$ to $-\infty +0i$ to the definition by Carson's integral.

Some fundamental properties of an operational representation $f(p)$ of a function $h(x)$ are derived from this definition of $f(p)$, the most important of which are the following :—

$$h(0) = \operatorname{Res}_\infty \left\{ \frac{f(p)}{p} \right\}, \quad \ldots \ldots \quad (16)$$

$$h(0) = \operatorname{Res}_0 \left\{ \frac{f(p)}{p} \right\}, \quad \ldots \ldots \quad (20)$$

where $\operatorname{Res}_n\{\phi(p)\}$ denotes the value of the integral

$$\frac{1}{2\pi i} \int_{-\pi}^{\pi} \phi(p_n + re^{i\theta}) ire^{i\theta} d\theta,$$

which is the residue of $\phi(p)$ at $p = p_n$ when $\phi(p)$ has a simple pole at this point :

$$\frac{f(p)}{p} = \int_0^x h(x)\, dx + \operatorname{Res}_\infty \left\{ \frac{f(p)}{p^2} \right\} \quad \ldots \quad (23)$$

$$= \int_0^x h(x)\, dx + \operatorname{Res}_0 \left\{ \frac{f(p)}{p^2} \right\} \quad \ldots \quad (24)$$

$$-p \int_a^p \frac{f(p)}{p}\, dp = \frac{h(x)}{x} \ldots \ldots \quad (26)$$

$$\int_0^\infty \frac{h(x)}{x}\, dx = (\operatorname{Res}_0 - \operatorname{Res}_\infty) \left[\frac{1}{p} \int_a^p \frac{f(p)}{p}\, dp \right]. \quad (32)$$

$$\int_0^\infty x^r h(x)\, dx = (\operatorname{Res}_0 - \operatorname{Res}_\infty) \left[\frac{1}{p}(-D)^r \frac{f(p)}{p} \right], \quad (34)$$

where r is a positive integer and $D = \dfrac{d}{dp}$.

[*] Communicated by the Author.

If $h(x)$ has no singularities except at $x=0$, and when $x \to 0$,

$$h(x) \to A x^m,$$

and if

$$f(p) \doteqdot h(x),$$

then, if m is not an integer,

$$\frac{2\pi i}{1-e^{i2\pi m}} p\, h(p\, e^{i\pi}) \doteqdot \frac{f(x)}{x}, \quad . \quad . \quad . \quad (37)$$

but if m is an integer,

$$-p \log p \,.\, h(-p) \doteqdot \frac{f(x)}{x} \quad . \quad . \quad . \quad . \quad (38)$$

Some of the above results are true only if certain conditions are satisfied. The numbers against the equations are those which they have in the paper.

---

1. *The Definition of the Operational Representation of a given Function.*

IN the various books and papers on the operational calculus, the operational representation $f(p)$ of a function $h(x)$ is usually defined by Carson's equation

$$f(a) = a \int_0^\infty e^{-ax} h(x)\, dx. \quad . \quad . \quad . \quad (1)$$

Bromwich showed that

$$h(x) = \frac{1}{2\pi i} \int_L e^{px} \frac{f(p)}{p}\, dp, \quad . \quad . \quad . \quad (2)$$

in which $R(x) > 0$ and L is a contour from $c - i\infty$ to $c + i\infty$, $c > 0$, which passes to the right of all the singularities of $f(p)$, is a solution of Carson's equation considered as an integral equation for $h(x)$.

If $\dfrac{f(p)}{p} \to 0$ as $|p| \to \infty$, then

$$h(x) = \frac{1}{2\pi i} \int_L e^{px} \frac{f(p)}{p}\, dp = \frac{1}{2\pi i} \int_C e^{px} \frac{f(p)}{p}\, dp, \quad . \quad (3)$$

where C is a contour from $-\infty - 0i$ to $-\infty + 0i$ which encloses all the singularities of $f(p)$.

It appears more reasonable to say that "*f*(*p*) *is an operational representation of h(x) if it is any solution of the integral equation*"

$$h(x) = \frac{1}{2\pi i}\int_C e^{px}\frac{f(p)}{p}\,dp. \quad . \quad . \quad . \quad . \quad (4)$$

Although this does not define a unique $f(p)$, we can often find a value of $f(p)$ which satisfies it by expansion in series and similar methods when $h(x)$ is a function which makes Carson's integral divergent. Briefly the chief points in favour of the definition by means of equation (4), compared with the definition by Carson's equation (1), are

A. It enables us to find operational representations of functions like $\log x$, $J_0(x)/x$, $Y_n(x)$ etc., which make Carson's integral divergent. On this point many writers are rather misleading, for after starting with Carson's definition of $f(p)$ they find, by series and otherwise, operational representations of functions which make Carson's integral divergent. In practically all cases these operators are correct when the definition (4) is used.

B. It enables us to find functions which are given by operators which make (2) divergent.

C. In equation (4) x can have any value, real or complex.

D. $$p\,f(p) = \frac{d\,h(x)}{dx}, \quad . \quad . \quad . \quad . \quad (5)$$

in all cases, whereas with Carson's definition this is true only if $h(0)=0$.

The disadvantages of the definition by equation (4) are :

E. It does not define a unique $f(p)$ for any given $h(x)$.

F. $$\frac{1}{p}f(p) = \int_0^x h(x)\,dx. \quad . \quad . \quad . \quad . \quad (6)$$

only under certain conditions, although with Carson's definition (6) is true whenever $f(p)$ is defined.

Neither of these disadvantages is a very real one. Actually it is sometimes very convenient that several different operators should give the same function of x ; as for instance that

$$\frac{p}{p^2+1}, \quad -\frac{p^3}{p^2+1}, \quad \frac{p}{p^2+1}+pe^p,$$

should all be operational representations of sin x.

Further we shall see that when equation (6) is not true, then $\frac{1}{p}f(p)$ is the operational representation of

$$\int_{\infty}^{x} h(x)\,dx,$$

so that with our definition of $f(p)$ the operator $\frac{1}{p}f(p)$ is of more general scope than it is with Carson's definition of $f(p)$.

In what follows we shall therefore take the definition of $f(p)$ given above in italics as the basis of our work, and following Dr. B. v. d. Pol [*] we shall write :

$$f(p) \doteqdot h(x), \quad \ldots \ldots \quad (7)$$

or occasionally

$$f(p)\,.\,1 = h(x).$$

From the definition (4) it is easily shown that

$$f\left(\frac{h}{a}\right) \doteqdot h(a\,x), \quad \ldots \ldots \quad (8)$$

$$p\,f(p) \doteqdot \frac{d\,h(x)}{dx}, \quad \ldots \ldots \quad (9)$$

$$\frac{p}{p+a}f(p) \doteqdot e^{-ax}\,h(x), \quad \ldots \ldots \quad (10)$$

$$e^{\lambda p}f(p) \doteqdot h(x+\lambda), \quad \text{for all } x \text{ and } \lambda.$$
$$\ldots \quad (11)$$

These relations are similar to those given by Carson and summarized by Dr. B. v. d. Pol in the second section of his paper on the "Operational Solution of Differential Equations," but there are slight differences as, for instance, that equation (11) is true here for all values of x and λ, and not for $x > \lambda$ only.

It should, however, be noted that, if n is *not integral*,

$$p^{-n} \doteqdot \frac{x^n}{\Pi(n)}, \quad \text{only if } \mathrm{R}(x) > 0, \quad (12)$$

because when $\mathrm{R}(x) < 0$ the integral in the definition (4) is divergent.

---

* Dr. B. v. d. Pol, "On the Operational Solution of Differential Equations," Phil. Mag. viii. p. 861.

The Function $H(x)$.

If $\dfrac{f(p)}{p} \to 0$ as $|v| \to \infty$ and x is real, then

$$\frac{1}{2\pi i}\int_L e^{px}\frac{f(p)}{p}\,dp \begin{aligned} &= h(x), \quad x>0, \\ &= 0, \quad\ \ x<0. \end{aligned}\Bigg\} \quad . \quad (13)$$

Following Bromwich and Jeffreys we shall write

$$H(x) = \frac{1}{2\pi i}\int_L \frac{e^{px}}{p}\,dp \begin{aligned} &= 1, \quad x>0, \\ &= 0, \quad x<0, \end{aligned}\Bigg\} \quad . \quad (14)$$

and write

$$f(p)\,H(x) = \frac{1}{2\pi i}\int_L e^{px}\,\frac{f(p)}{p}\,dp\,;$$

then by (13),

$$f(p)\,H(x) \doteqdot f(p)\,.\,1 \doteqdot h(x), \quad x>0, \atop \doteqdot 0 \qquad\qquad , \quad x<0, \Bigg\} \quad . \quad (15)$$

When $\dfrac{f(p)}{p} \to 0$ as $|p| \to \infty$ it is very often useful to change over from $f(p).1.$ to $f(p)\,H(x)$; for example, when $f(p)$ can be expanded in a series on L but cannot be expanded in a similar series on C. It should be noted that (13), (14), (15), are true only when *x is real*.

The object of the first part of this paper is to consider various properties of $f(p)$ which follow from the definition (4). Many of these properties are not true if $f(p)$ is defined by Carson's integral.

2. *The Values of* $h(0)$ *and* $h(\infty)$ *under Particular Circumstances.*

Putting $x = 0$ in equation (4) we get

$$h(0) = \frac{1}{2\pi i}\int_C \frac{f(p)}{p}\,dp.$$

Now C can be taken to be an infinitely large circle Γ from $-\infty - 0i$ to $-\infty + 0i$, and hence :

$$h(0) = \frac{1}{2\pi i}\int_\Gamma \frac{f(p)}{p}\,dp$$

$$= \mathrm{Res}_\infty\left\{\frac{f(p)}{p}\right\}, \quad \text{say.} \quad . \quad (16)$$

If $\dfrac{f(p)}{p}$ has a simple pole at $p=\infty$, then $\operatorname{Res}_\infty\left\{\dfrac{f(p)}{p}\right\}$ is the residue of $\dfrac{f(p)}{p}$ at infinity; also if $\dfrac{f(p)}{p}\to 0$ as $|p|\to\infty$,

then,

$$\operatorname{Res}_\infty\left\{\frac{f(p)}{p}\right\}=0,$$

but when $\dfrac{f(p)}{p}$ does not satisfy either of these conditions, then we cannot say anything in general about $\operatorname{Res}_\infty$.

$h(\infty)$.

Suppose $\dfrac{f(p)}{p}$ has singularities $p_1,\ p_2,\ \dots\ p_n$ and that C is deformed into loops from $-\infty$ round the points $p_1,\ p_2,\ \dots p_n$. The loop C_n may be considered to be made up of straight lines from $-\infty$ to p_n parallel to the real axis, and a small circle round p_n. Then,

$$\frac{1}{2\pi i}\int_{C_n} e^{px}\frac{f(p)}{p}\,dp$$

$$=\frac{e^{p_n x}}{2\pi i}\int_0^\infty e^{-rx}\frac{f(p_n+re^{-i\pi})-f(p_n+re^{i\pi})}{p_n-r}\,dr$$

(from the straight lines)

$$+\frac{e^{p_n x}}{2\pi i}\int_{-\pi}^{\pi}\frac{f(p_n+re^{i\theta})}{p_n+re^{i\theta}}\,i\,re^{i\theta}\,d\theta\ \ \dots\ \dots\ (17)$$

(from the circle).

Now let $p_n=\alpha_n+i\beta_n$ where α_n is *negative or zero*, and let $R(x)>0$, then

$$\left|\frac{e^{p_n x}}{2\pi i}\int_0^\infty e^{-rx}\frac{f(p_n+re^{-i\pi})-f(p_n+re^{i\pi})}{p_n-r}\,dr\right|$$

$$<\frac{e^{\alpha_n x}}{2\pi}\int_0^\infty e^{-rx}\,\mathrm{M}\,dr,$$

$$=\frac{\mathrm{M}\,e^{\alpha_n x}}{2\pi x},\ \dots\ \dots\ \dots\ \dots\ (18)$$

where M is the maximum value of

$$\left|\frac{f(p_n+re^{-i\pi})-f(p_n+re^{i\pi})}{p_n-r}\right|.$$

between $r=0$ and ∞. M is finite if $f(p)$ has not got another singularity with the same imaginary part as p_n, and when this is so, we can obtain a similar result by deforming C_n so that it passes round the other singularity by small semicircles. From equation (18) it follows that, when $x \rightarrow + \infty$, the first term in equation (17) approaches zero. Further,

$$\frac{1}{2\pi i} \int_{-\pi}^{+\pi} \frac{f(p_n + re^{i\theta})}{p_n + re^{i\theta}} \, i\, re^{i\theta} \, d\theta = \text{Res}_n \left\{ \frac{f(p)}{p} \right\} , \quad . \quad (19)$$

where

$$\text{Res}_n \left\{ \frac{f(p)}{p} \right\} = 0, \quad \text{if } f(p) \rightarrow 0, \text{ as } p \rightarrow p_n$$

$$= \text{residue of } \frac{f(p)}{p} \text{ at } p = p_n,$$

if $\frac{f(p)}{p}$ has a simple pole at $p = p_n$.

Hence, we find that

$$h(\infty) = \lim_{x \rightarrow +\infty} \sum \frac{1}{2\pi i} \int_{C_n} e^{px} \frac{f(p)}{p} \, dp$$

$$= \lim_{x \rightarrow +\infty} \sum e^{p_n x} \text{Res}_n \left\{ \frac{f(p)}{p} \right\}$$

$$= \text{Res}_0 \left\{ \frac{f(p)}{p} \right\} , \qquad \begin{array}{l} \text{if } \alpha_n > 0, \text{ except, of} \\ \text{course, at } p=0, \end{array}$$

or $\qquad = \text{Res}_0 \left\{ \frac{f(p)}{p} \right\} , \qquad \begin{array}{l} \text{if } \alpha_n = 0 \text{ and the value} \\ \text{of } \text{Res}_n \left\{ \dfrac{f(p)}{p} \right\} \\ \text{is zero at every} \\ \text{other singularity} \\ p_n. \quad . \quad . \quad (20) \end{array}$

If $\alpha_n = 0$ and $\text{Res}_n \left\{ \dfrac{f(p)}{p} \right\} \neq 0$, then when x is a very large real number,

$$h(x) \sim \sum e^{i\beta_n x} \text{Res}_n \left\{ \frac{f(p)}{p} \right\} .$$

3. *The Functions given by the Operator* $\dfrac{f(p)}{p}$.

Since

$$\frac{d}{dx} \left[\frac{1}{2\pi i} \int_C e^{px} \frac{f(p)}{p^2} \, dp \right] = \frac{1}{2\pi i} \int_C e^{px} \frac{f(p)}{p} \, dp$$

$$= h(x) ;$$

it follows that

$$\int^x h(x)\,dx = \frac{1}{2\pi i}\int_C e^{px}\frac{f(p)}{p^2}\,dp + A.$$

Therefore, when $x\to 0$, we find by equation (16) that

$$\int_0^x h(x)\,dx = \frac{1}{2\pi i}\int_C e^{px}\frac{f(p)}{p^2}\,dp - \operatorname{Res}_\infty\left\{\frac{f(p)}{p^2}\right\}, \quad (21)$$

and making $x\to\infty$ we get by equation (20)

$$\int_\infty^x h(x)\,dx = \frac{1}{2\pi i}\int_C e^{px}\frac{f(p)}{p^2}\,dp - \operatorname{Res}_0\left\{\frac{f(p)}{p^2}\right\}, \quad (22)$$

provided the conditions imposed in (20) are satisfied.

In operational form (21) and (22) become

$$\frac{f(p)}{p} \doteq \int_0^x h(x)\,dx + \operatorname{Res}_\infty\left\{\frac{f(p)}{p^2}\right\} \quad . \quad . \quad . \quad (23)$$

$$\frac{f(p)}{p} \doteq \int_\infty^x h(x)\,dx + \operatorname{Res}_0\left\{\frac{f(p)}{p^2}\right\} \quad . \quad . \quad . \quad (24)$$

Subtracting we get

$$\int_0^\infty h(x)\,dx = \operatorname{Res}_0\left\{\frac{f(p)}{p^2}\right\} - \operatorname{Res}_\infty\left\{\frac{f(p)}{p^2}\right\}. \quad (25)$$

As examples of (23) and (24) we find from the operator

$$e^{-ax}\sin x \doteq \frac{p}{(p+a)^2+1},$$

$$\int_0^x e^{-ax}\sin x\,dx \doteq \frac{1}{(p+a)^2+1} - \operatorname{Res}_\infty\left[\frac{1}{p\{(p+a)^2+1\}}\right]$$

$$= \frac{1}{(p+a)^2+1},$$

but

$$\int_\infty^x e^{-ax}\sin x\,dx \doteq \frac{1}{(p+a)^2+1} - \operatorname{Res}_0\left[\frac{1}{p\{(p+a)^2+1\}}\right]$$

$$= \frac{1}{(p+a)^2+1} - \frac{1}{a^2+1}.$$

These include by subtraction

$$\int_0^\infty e^{-ax}\sin x\,dx = \frac{1}{a^2+1},$$

which is a particular case of Carson's integral.

4. *The Operator for* $\dfrac{h(x)}{x}$.

From equation (4).

$$
\begin{aligned}
\frac{h(x)}{x} &= \frac{1}{2\pi i}\int \frac{e^{px}}{p}\left\{\frac{f(p)}{p}\right\}dp \\[2mm]
&= \left[\frac{1}{2\pi i}\left\{\int^p \frac{f(p)}{p}\,dp\right\}\frac{e^{px}}{x}\right]_{\mathrm{C}} \\[2mm]
&\quad - \frac{1}{2\pi i}\int_{\mathrm{C}}\frac{e^{px}}{p}\left\{p\int^p \frac{f(p)}{p}\,dp\right\}dp \\[2mm]
&= -\frac{1}{2\pi i}\int_{\mathrm{C}}\frac{e^{px}}{p}\left\{p\int^p \frac{f(p)}{p}\,dp\right\}dp,
\end{aligned}
$$

provided $R(x) > 0$.

Hence

$$
-p\int_a^p \frac{f(p)}{p}\,dp \doteqdot \frac{h(x)}{x}, \quad R(x) > 0, \quad (26)
$$

where a is any constant.

From equation (26) it follows that

$$
-\int_a^p \frac{f(p)}{p}\,dp \doteqdot \int_0^x \frac{h(x)}{x}\,dx - \operatorname{Res}_\infty\left\{\frac{1}{p}\int_a^p \frac{f(p)}{p}\,dp\right\} \quad (27)
$$

$$
\doteqdot \int_\infty^x \frac{h(x)}{x}\,dx - \operatorname{Res}_0\left\{\frac{1}{p}\int_a^p \frac{f(p)}{p}\,dp\right\}. \quad (28)
$$

It is best to choose $a = \infty$ in (27) and $a = 0$ in (28) because $\operatorname{Res}_\infty$ and Res_0 are then usually zero (but this is not necessarily always so). We shall therefore write

$$
-\int_\infty^p \frac{f(p)}{p}\,dp \doteqdot \int_0^x \frac{h(x)}{x}\,dx - \operatorname{Res}_\infty\left\{\frac{1}{p}\int_\infty^p \frac{f(p)}{p}\,dp\right\}, \quad (29)
$$

and

$$
-\int_0^p \frac{f(p)}{p}\,dp \doteqdot \int_\infty^x \frac{h(x)}{x}\,dx - \operatorname{Res}_0\left\{\frac{1}{p}\int_0^p \frac{f(p)}{p}\,dp\right\}. \quad (30)
$$

Subtracting these equations

$$
\int_0^\infty \frac{f(p)}{p}\,dp = \int_0^\infty \frac{h(x)}{x}\,dx
$$
$$
+ \operatorname{Res}_0\left\{\frac{1}{p}\int_\infty^p \frac{f(p)}{p}\,dp\right\} - \operatorname{Res}_\infty\left\{\frac{1}{p}\int_0^p \frac{f(p)}{p}\,dp\right\},
$$
$$
\cdots \quad (31)
$$

but a more convenient result is got by subtracting (27) and (28) ; this gives

$$\int_0^\infty \frac{h(x)}{x}\,dx = (\mathrm{Res}_0 - \mathrm{Res}_\infty)\left\{\frac{1}{p}\int_a^p \frac{f(p)}{p}\,dp\right\}. \quad (32)$$

Equations (29), (30), and (31) are more exact forms of those given by Dr. B. v. d. Pol. Equation (32) is, I think, new. As an example of it consider the integral

$$\int_0^\infty \frac{e^{-cx} - J_0(bx)}{x}\,dx.$$

Since

$$e^{-cx} - J_0(bx) \doteqdot \frac{p}{p+c} - \frac{p}{\sqrt{p^2+b^2}},$$

$$\frac{1}{p}\int_a^p \frac{f(p)}{p}\,dp = \frac{1}{p}\{\log(p+c) - \log(p+\sqrt{p^2+b^2}) - C\},$$

where C is a constant.

Hence

$$(\mathrm{Res}_0 - \mathrm{Res}_\infty)\left\{\frac{1}{p}\int_a^p \frac{f(p)}{p}\,dp\right\}$$

$$= \log c - \log b + \log 2 = \log\left(\frac{2c}{b}\right).$$

Other integrals of this type can be evaluated in a similar way.

5. *The Operator for $x^r h(x)$ and the Value of* $\int_0^\infty x^r h(x)$, *when r is a Positive Integer.*

From the definition (4)

$$x\,h(x) = \frac{1}{2\pi i}\int_C x\,e^{px}\frac{f(p)}{p}\,dp$$

$$= \frac{1}{2\pi i}\left\{e^{px}\frac{f(p)}{p}\right\}_C - \frac{1}{2\pi i}\int_C e^{px} D\left\{\frac{f(p)}{p}\right\}\,dp,$$

where $D = \dfrac{d}{dp}$.

Hence, if $R(x) > 0$,

$$x\,h(x) = -\frac{1}{2\pi i}\int_C e^{px} D\left\{\frac{f(p)}{p}\right\}\,dp$$

$$\doteqdot -p\,D\left\{\frac{f(p)}{p}\right\},$$

and so by induction

$$x^r h(x) \doteqdot p(-D)^r \left\{ \frac{f(p)}{p} \right\} \quad . \quad . \quad . \quad . \quad (33)$$

Therefore by equation (25) we get

$$\int_0^\infty x^r h(x)\,dx = (\text{Res}_0 - \text{Res}_\infty) \left[\frac{1}{p}(-D)^r \left\{ \frac{f(p)}{p} \right\} \right]. \quad (34)$$

6. *Carson's Integral.*

Since

$$e^{-ax} h(x) = e^{-ax} f(p)$$

$$\doteqdot f(p+a) \frac{p}{p+a},$$

we find, by equation (25), that

$$\int_0^\infty e^{-ax} h(x)\,dx = (\text{Res}_0 - \text{Res}_\infty) \left\{ \frac{f(p+a)}{p(p+a)} \right\}.$$

If $\dfrac{f(p)}{p} \to 0$ as $|p| \to \infty$, then $\text{Res}_\infty = 0$, and if $a > \alpha_n$ at every singularity of $\dfrac{f(p)}{p}$, then every singularity of $\dfrac{f(p+a)}{p(p+a)}$ except $p=0$, lies to the left of the imaginary axis, and this function has therefore a simple pole at $p=0$. Hence

$$\text{Res}_0 \left\{ \frac{f(p+a)}{p(p+a)} \right\} = \frac{f(a)}{a},$$

and therefore

$$\int_0^\infty e^{-ax} h(x)\,dx = \frac{f(a)}{a}, \quad . \quad . \quad . \quad (35)$$

provided

(A) $\dfrac{f(p)}{p} \to 0$ as $|p| \to \infty$,

(B) $a > \alpha_n$ at every singularity of $f(p)$.

From this result we conclude that there is only one value of $f(p)$ which makes

$$f(p) \doteqdot h(x) \quad \text{and} \quad \frac{f(p)}{p} \to a \text{ as } |p| \to \infty.$$

We may, for instance, find a value of $f(p)$ which makes

$$f(p) \doteqdot h(x),$$

but does not make $\dfrac{f(p)}{p} \to 0$ as $|p| \to \infty$. This operational representation of $h(x)$ cannot therefore be used in Carson's integral, but there must be another operator $F(p)$ which gives $h(x)$ and also satisfies the required conditions. This means, of course, that

$$f(p) - F(p) \doteq 0.$$

As an example, consider the function $J_n(x)$:

$$\frac{p}{\sqrt{p^2+1}}(\sqrt{p^2+1}-p)^n \doteq J_n(x),$$

and $\dfrac{f(p)}{p} \to 0$, as $|p| \to \infty$ if $n > -\frac{1}{2}$, so

$$\int_0^\infty e^{-ax} J_n(x)\, dx = \frac{1}{\sqrt{a^2+1}}(\sqrt{a^2+1}-a)^n, \quad n > \tfrac{1}{2}.$$

But, if n is a negative integer, then we can find another operator for $J_n(x)$ which satisfies the condition $\dfrac{f(p)}{p} \to 0$ as $|p| \to \infty$, for then

$$J_n(x) = (-1)^n J_{-n}(x)$$
$$\doteq \frac{(-1)^n p}{\sqrt{p^2+1}}(\sqrt{p^2+1}-p)^{-n},$$

and therefore

$$\int_0^\infty e^{-ax} J_n(x)\, dx = \frac{(-1)^n}{\sqrt{a^2+1}}(\sqrt{a^2+1}-a)^{-n},$$

where n is a negative integer. It is easily verified that in this case the difference between the two operators for $J_n(x)$, namely,

$$\frac{p}{\sqrt{p^2+1}}(\sqrt{p^2+1}-p)^n \quad \text{and} \quad \frac{p}{\sqrt{p^2+1}}(\sqrt{p^2+1}-p)^{-n},$$

is a polynomial in p and is therefore an operational representation of zero.

6. *An Inversion Formula.*

Suppose the function $h(x)$ has no singularities except at $x = 0$, and that when $x \to 0$

$$h(x) \to A\, x^n, \qquad n > -1.$$

Then

$$\int_C e^{ap} h(pe^{-i\pi}) \, dp$$

$$= -\int_\infty^0 e^{-ax} h(x) \, dx - \int_0^\infty e^{-ax} h(xe^{2\pi i}) \, dx$$

$$+ \lim_{r \to 0} \int_{-\pi}^\pi h\{re^{i(\theta+\pi)}\} \, i \, re^{i\theta} \, d\theta$$

$$= \int_0^\infty e^{-ax} h(x)(1 - e^{i \, 2\pi m}) \, dx$$

$$= (1 - e^{i \, 2\pi m}) \left\{ \frac{f(a)}{a} \right\}, \quad \ldots \ldots \quad (36)$$

by equation (35), provided $f(p)$ satisfies the required conditions.

Equation (36) shows that

$$\frac{2\pi i}{1 - e^{i \, 2\pi m}} p \, h(pe^{i\pi}) \doteq \frac{f(x)}{x}. \quad \ldots \quad (37)$$

If $h(x)$ has no singularity at $x = 0$, then the left-hand side has to be replaced by

$$\lim_{m \to 0} \frac{2\pi i \, p \, h(pe^{i\pi})}{1 - e^{i \, 2\pi m}} = -p \log p \, h(-p),$$

and so

$$-p \log p \, h(-p) \doteq \frac{f(x)}{x}. \quad \ldots \quad (38)$$

The formulæ which contain Legendre and Bessel functions as function and operator respectively, form a good example of this inversion. Thus

$$p^{\frac{1}{2}} I_{-n-\frac{1}{2}}(p) \doteq \cos x\pi \sqrt{\frac{2}{\pi}} P_n(x), \quad \ldots \quad (39)$$

and $P_n(x)$ has no singularities except at $x = 0$. Hence, by equation (37),

$$\frac{2\pi i}{1 - e^{i \, 2\pi m}} \cos n\pi \sqrt{\frac{2}{\pi}} p \, P_n(pe^{i\pi}) \doteq x^{-\frac{1}{2}} I_{-n-\frac{1}{2}}(x).$$

The left-hand side simplifies to

$$-\sqrt{2\pi} \cos n\pi \cdot p \, P_n(p),$$

and so

$$-\sqrt{2\pi} \cos n\pi \cdot p \, P_n(p) \doteq x^{-\frac{1}{2}} I_{-n-\frac{1}{2}}(x). \quad \ldots \quad (40)$$

If in this equation we change n into $-n-1$, we get

$$\sqrt{\frac{2}{\pi}}\, p\, Q_n(p) = x^{-\frac{1}{2}} I_{n-\frac{1}{2}}(x), \quad \ldots \quad (41)$$

since

$$Q_n(p) = \pi \cot n\pi\, P_{-n-\frac{1}{2}}(p).$$

Equations (39) and (41) are those numbered (45) and (63 *a*) in Dr. B. v. d. Pol's paper, except that (39) has here been generalized so as to be true for all values of n instead of for integral values only.

As another example, from the equation

$$\frac{2^n}{\sqrt{\pi}}\, \Pi(n-\tfrac{1}{2})\, \frac{p}{(p^2+1)^{n+\frac{1}{2}}} \doteqdot x^n\, J_n(x),$$

we get by equation (37)

$$\frac{2^n \Pi(n-\tfrac{1}{2})}{\sqrt{\pi}}\, \frac{1}{(x^2+1)^{n+\frac{1}{2}}} \doteqdot \frac{2\pi i}{1 - e^{i4\pi n}}\, \{p^{n+1} J_n(p)\, e^{i2\pi n}\}$$

$$= \frac{2\pi i}{e^{-i2\pi n} - e^{i2\pi n}}\, p^{n+1} J_n(p)$$

$$= \frac{-\pi}{\sin 2\pi n}\, p^{n+1} J_n(p),$$

which becomes

$$-\pi \frac{1}{2}\left[J_n(p) \log p + \frac{d J_n(p)}{dn} \right] p^{n+1},$$

where n is an integer.

7. *The Solution of Differential Equations.*

The solution of differential equations with constant coefficients by using operators has been dealt with in detail by Jeffreys, Pol, and others, but the method used by Pol to solve linear differential equations with variable coefficients can be considerably shortened by using equation (33), which is

$$x^r h(x) \doteqdot p(-D)^r \left\{ \frac{f(p)}{p} \right\}, \qquad R(x) > 0.$$

The method which follows was suggested by the author in a paper in the 'Journal' of the Manchester College of Technology in 1927. It is in effect thus. Substitute for y

$$y = h(x) \doteqdot f(p),$$

and then apply equation (33) until no x is left in the equation. The resulting differential equation is one to find $f(p)$. Thus the equation

$$x\frac{d^2y}{dx^2}+(1-n)\frac{dy}{dx}y=0, \quad . \quad . \quad . \quad . \quad (42)$$

becomes

$$x\,p^2f+(1-n)pf+f\doteqdot0.$$

By equation (33) this can be written

$$-p\,\mathrm{D}(\,pf)+(1-n)pf+f\doteqdot0,$$

whence

$$-p^2\frac{df}{dp}+(1-np)f\doteqdot0. \quad . \quad . \quad . \quad (43)$$

This is satisfied if

$$p^2\frac{df}{dp}+(1-np)f=\mathrm{A}\,p^r,$$

where r is any positive integer.

The general solution of this equation is

$$f(p)=\mathrm{C}\,p^{-n}e^{-\frac{1}{p}}+\mathrm{A}\,p^{-n}e^{-\frac{1}{p}}\int p^{n+r-2}e^{\frac{1}{p}}\,dp. \quad . \quad (44)$$

The first term is the operational representation of $\mathrm{C}\,x^{\frac{1}{2}n}\mathrm{J}_n(2\sqrt{x})$, which is one solution of (42), and the second term is the operational representation of another solution of equation (42). We can take r to be any number we please, but we naturally take the simplest, namely, $r=1$; this makes the second term of (44) become

$$\mathrm{A}\,p^{-n}e^{-\frac{1}{p}}\int p^{n-1}\Big(1+\frac{1}{p}+\frac{1}{2\,!\,p^2}+\ ...\Big)dp$$

$$=\mathrm{A}\,e^{-\frac{1}{p}}\Big(\frac{1}{n}+\frac{1}{n-1\,.\,p}+\frac{1}{n-2\,.\,2\,!\,p^2}+\ ...\Big)$$

$$=\mathrm{A}\Big(\frac{1}{n}-\frac{1}{n(n-1)p}+\frac{1}{n(n-1)\,(n-2)p^2}+\ ...\Big)$$

$$\doteqdot\mathrm{A}\Big(\frac{x}{n}-\frac{x^2}{n(n-1)\,.\,2\,!}+\frac{x^3}{n(n-1)\,(n-2)\,.\,3\,!}\ ...\Big). \quad (45)$$

It is easily verified that this is a solution of equation (42). Equation (43) is satisfied if we take

$$-p^2\frac{df}{dp}+(1-np)f$$

equal to any operator which is an operational representation of zero; each operator of this kind will give us a value of $f(p)$ leading to a solution of (42) which may be a combination of $x^{\frac{1}{2}} J_n(2\sqrt{x})$ and (45).

In the same way we can find the operational solution of the differential equation

$$x\frac{d^2y}{dx^2} + (1-n)\frac{dy}{dx} + y = \Pi(n + \tfrac{1}{2})\frac{(x)^{n+\frac{1}{2}}}{\sqrt{\pi}}, \quad . \quad (46)$$

which is satisfied by $x^{\frac{1}{2}n} S_n(2\sqrt{x})$, where $S_n(x)$ is Struve's function

$$S_n(x) = \sum_{r=1}^{\infty} \frac{(-1)^r(\tfrac{1}{2}x)^{n+2r+1}}{\Pi(n+r+\tfrac{1}{2})\Pi(r+\tfrac{1}{2})}.$$

In just the same way as above we find that equation (46) transforms into

$$p^2\frac{df}{dp} + (1-np)f = \frac{p^{-\frac{1}{2}-n}}{\sqrt{\pi}},$$

of which the solution is

$$f = p^{-n}e^{-\frac{1}{p}}\int_a^p \frac{u^{-\frac{1}{2}}e^{\frac{1}{u}}}{\sqrt{\pi}}\,du,$$

where, in order to get Struve's function, the constant a has to be chosen so that when x is small

$$f(p) \doteqdot \frac{x^{\frac{1}{2}n+\frac{1}{2}}}{\Pi(n+\tfrac{1}{2})} \quad \text{nearly.}$$

This is so if we take

$$f(p) = p^{-n}e^{-\frac{1}{p}}\int_{\infty}^p \frac{u^{-\frac{1}{2}}e^{\frac{1}{u}}}{\sqrt{\pi}}\,du$$

$$= p^{-n}e^{-\frac{1}{p}}\int_0^{\sqrt{p}} \frac{2e^{-u^2}\,du}{i\sqrt{\pi}}$$

$$= \frac{p^{-n}e^{-\frac{1}{p}}}{i}\ \mathrm{erf}\ \frac{i}{\sqrt{p}}.$$

C. *Electromagnetic Waves and Pulses.*
By W. E. Sumpner, D.Sc., M.I.E.E.*

CONTENTS.

1. The Independence of Waves.

ONE of the oldest views about light, traceable as far back as the time of Huygens, is that light waves cross each other's path, or travel together, without interfering with each other in any way. Each wave behaves as if others do not exist. This assumption does not seem to have been ever questioned or discussed. Experimental evidence in its favour appears overwhelming. The accuracy of a message conveyed by a light ray, and imprinted on it by a far distant star, is never doubted by the spectrum analyst, or by the mathematician who founds upon it a theory about some remote universe. During recent years further evidence has been given by broadcasting. No receiving-set, however good, could possibly reproduce perfectly the programme of any one of a number of stations broadcasting simultaneously if any interference occurred between electromagnetic waves.

The bearing of this assumption upon the application of Maxwell's electromagnetic theory does not appear to have received any attention. A little consideration of the matter seems to show that the independence principle facilitates the use of Maxwell's theory, although it imposes some restraint. It calls for some reconsideration of such principles as superposition, interference, and reversibility in connexion with light, and also of the exact meaning to be attached to the Poynting flux of energy.

All seems to turn upon the meaning of the superposition of two vector fluxes E_1 and E_2 of the same kind. Any located physical entity which is *completely* represented by a vector E must be neutralized by the addition at the same place of a similar entity represented by the vector equal and opposite to E. But a physical entity may have some property represented by E and another property represented by the square of E. If now we superpose two such entities represented by vectors E_1 and E_2, the first property will

---

* Communicated by the Author.

be represented by $E_1 + E_2$, while the second property will be represented by $E_1^2 + E_2^2$, not by $(E_1 + E_2)^2$. If E_1 and E_2 are equal and opposite, the first resultant *property* will vanish, but not so the second.

In a wave of light if the electric flux density is E, the energy per unit volume is proportional to E^2. If two beams of light are directed along the same ray, the fluxes being E_1 and E_2, the energies add, the sum being $E_1^2 + E_2^2$, but the fluxes do not combine to a single flux $E_1 + E_2$, since, if they did so, the energy would be $(E_1 + E_2)^2$, where $E_1 + E_2$ is a vector whose tensor may have any value between the sum or difference of the tensors of E_1 and E_2. The energies are necessarily positive, but E_1 and E_2 may be of opposite sign.

In standard treatises on light nothing is said to suggest any conflict between the principle of the independence of waves and that of the interference of light. In some books the two principles are asserted in the same paragraph. Although it is not explicitly stated, the writer of the treatise appears to have in mind some such idea as follows :—The interference of light is a special case of the action of electromagnetic waves on matter. The effect may be optical, as in vision, or illumination ; or chemical, as in photography ; or a heat effect, as with a bolometer plate. In all cases matter intervenes. Two waves of vector strengths E_1 and E_2 have energies given by $E_1^2 + E_2^2$; yet the effect on matter may be assumed to be that due to an energy transfer-force represented by the vector sum $E_1 + E_2$, which will vanish if these two vectors are equal and opposite. The waves do not destroy each other any more than two batteries destroy each other if of equal and opposite electromotive forces and applied to the same circuit. The batteries simply neutralize each other's tendency to produce the electric current which forms the flux corresponding with the electromotive force. If $E_1 + E_2$ is not zero the flux, or rate of yield of the medium, is in general proportional to the transfer-force $E_1 + E_2$, so that the rate of transfer of energy is proportional to $(E_1 + E_2)^2$; but the energy in the wave available for transfer is not measured by $(E_1 + E_2)^2$, but by $E_1^2 + E_2^2$.

When parallel monochromatic light is passed through a grating ruled, say, with 100 lines, the waves sent along the ray corresponding with the first diffraction image of the slit contain 100 equal fluxes E. The energy is $100\,E^2$, not $(100\,E)^2$. Along the path of interference there are also 100 equal fluxes ; but while 50 of these are $+E$, the other 50 are $-E$. The energy, as before, is

$$100\,E^2 = 50\,E^2 + 50\,(-E)^2.$$

In the first case the effect on matter is determined by the transfer-force 100 E, and the rate of transfer of energy is given by (100 E)². In the second case the effect on matter is zero. Such a view seems to contain nothing in conflict with experimental results, while it quite harmonizes the principles of independence and interference. It leads to the conclusion that the wave along the path of interference has the same energy as that along the path of reinforcement. This is not recognized as a fact, but in view of the assumption made about the action on matter it does not appear to conflict with any known experiment. Unless some arrangement of matter can be devised capable of acting in regard to light fluxes in a way similar to that of a thermionic valve in regard to the alternating electromotive forces involved in wireless telegraphy it does not seem possible that such a conclusion can experimentally be either established or disproved. The assumption about the influence of waves on matter, so far as light is concerned, is essentially what is actually made in order to explain the phenomenon of interference.

The assumption of the non-interference of radiation is made essentially in the theory of every electrical experiment, since such theory always ignores all other simultaneous electrical experiments. There is no scientific difference between two cases, one of which consists of a single experiment with two independent energy sources, and another which involves two experiments each with an independent energy source. If two separate experiments influence each other the cause is always traceable to the intervention of matter which absorbs part of the energy impinging upon it and redistributes it in other forms of radiation in addition to giving rise to reflected waves. Such phenomena are secondary and involve no direct action of waves on each other. The magnetization of light discovered by Faraday was stated by him to be a secondary effect due to the intervention of matter. The effects found by Kerr and Zeeman are other instances.

2. THE POYNTING FLUX.

In Poynting's proof * of the flux of energy there is the tacit assumption that only one energy system is involved. No one supposes that the formula applies, or was ever

* "Transfer of Energy in the Electromagnetic Field," Phil. Trans. 1884, pp. 343–361, or Coll. Papers, art. 10. A year later a second paper on a similar subject appears in Phil. Trans. 1885, pp. 277–306, Coll. Papers, art. 11.

intended to apply, to two cases, A and B, in which the system B is made to differ from that of A merely by superposing on A the magnetic field due to a permanent magnet brought up to a fixed position in A. The magnet brings an energy system with it, but does not alter the flux of energy, though it certainly alters the Poynting formula, since, if the magnetic fluxes can be combined vectorially, these fluxes are all changed, while the electric fluxes are not altered. The case taken by Poynting was of such a general character that it is possible to interpret it in many ways. He assumes that the energy per unit volume is given by one magnetic flux in conjunction with one electric flux. This is not the case in the system B, even if true of system A. Poynting dealt with two fluxes whose energies were not necessarily equal and whose directions were not necessarily perpendicular to each other. He did not consider whether a single energy system could be represented by such fluxes.

In order to bring out the points involved we give Heaviside's brief proof of Poynting's theorem, simplified by eliminating all matter and all electric or magnetic charges from the region investigated, and also by using Heaviside's compact vector methods in conjunction with his form of Maxwell's equations.

The physical quantities concerned form four pairs, electric and magnetic, which we distinguish by suffixes e and m, as follows :—

$$
\begin{array}{lll}
\text{Force intensity} & \mathbf{H}_e & \mathbf{H}_m, \\
\text{Flux density} & \mathbf{B}_e & \mathbf{B}_m, \\
\text{Inductivity} & e & m, \\
\text{Energy density} & \mathrm{T}_e & \mathrm{T}_m.
\end{array}
$$

The Maxwell equations also form four pairs :—

Law 1 $\qquad \mathbf{B}_e = e\mathbf{H}_e \; ; \; \mathbf{B}_m = m\mathbf{H}_m,$

Law 2 $\qquad \mathrm{div.}\,\mathbf{B}_e = 0 \; ; \; \mathrm{div.}\,\mathbf{B}_m = 0,$

Law 3 $\qquad \mathrm{T}_e = \tfrac{1}{2}\overline{\mathbf{H}_e\mathbf{B}_e} \; ; \; \mathrm{T}_m = \tfrac{1}{2}\overline{\mathbf{H}_m\mathbf{B}_m},$

Law 4_e $\qquad \dot{\mathbf{B}}_e = \mathrm{curl}\,\mathbf{H}_m \equiv [\nabla \mathbf{H}_m],$

$\qquad\qquad\qquad -\dot{\mathbf{B}}_m = \mathrm{curl}\,\mathbf{H}_e \equiv [\nabla \mathbf{H}_e].$

We use Heaviside's units and his vector notation. A vector product is shown by square brackets and a scalar product by a superposed bar. The unit vectors parallel to the axes are i, j, k, with $i = [jk]$, $j = [ki]$, and $k = [ij]$. The Hamiltonian differentiator is ∇, with components $\nabla_1, \nabla_2, \nabla_3$. A vector is printed in heavy type and its tensor in corresponding

lighter type, the components of the latter being distinguished by suffixes 1, 2, 3.

Now, if **P** is the Poynting flux, or the vector flux of energy per unit area perpendicular to **P**, the rate of loss of energy per unit volume is

$$\text{div. } \mathbf{P} \equiv \overline{\nabla \mathbf{P}}.$$

If the region is free from matter, and also free from electric and magnetic charges, we have

$$\overline{\nabla \mathbf{P}} = -\frac{d}{dt}\left(\frac{1}{2e}\mathbf{B}_e{}^2 + \frac{1}{2m}\mathbf{B}_m{}^2\right) = -\frac{1}{e}\overline{\mathbf{B}_e\dot{\mathbf{B}}_e} - \frac{1}{m}\overline{\mathbf{B}_m\dot{\mathbf{B}}_m}$$

$$= -\overline{\mathbf{H}_e[\nabla \mathbf{H}_m]} + \overline{\mathbf{H}_m[\nabla \mathbf{H}_e]}$$

$$= -\begin{vmatrix} \mathbf{E}_1 & \mathbf{E}_2 & \mathbf{E}_3 \\ \nabla_1 & \nabla_2 & \nabla_3 \\ \mathbf{M}_1 & \mathbf{M}_2 & \mathbf{M}_3 \end{vmatrix} + \begin{vmatrix} \mathbf{M}_1 & \mathbf{M}_2 & \mathbf{M}_3 \\ \nabla_1 & \nabla_2 & \nabla_3 \\ \mathbf{E}_1 & \mathbf{E}_2 & \mathbf{E}_3 \end{vmatrix}$$

$$= \begin{vmatrix} \nabla_1 & \nabla_2 & \nabla_3 \\ \mathbf{E}_1 & \mathbf{E}_2 & \mathbf{E}_3 \\ \mathbf{M}_1 & \mathbf{M}_2 & \mathbf{M}_3 \end{vmatrix} = \overline{\nabla[\mathbf{H}_e\mathbf{H}_m]},$$

where

$$\mathbf{H}_e \equiv i\mathbf{E}_1 + j\mathbf{E}_2 + k\mathbf{E}_3,$$

$$\mathbf{H}_m \equiv i\mathbf{M}_1 + j\mathbf{M}_2 + k\mathbf{M}_3,$$

and where in working out the determinants it is supposed that the factors of any product are taken in the order of the rows from top to bottom.

We thus have

$$\overline{\nabla \mathbf{P}} = \overline{\nabla[\mathbf{H}_e\mathbf{H}_m]},$$

which means

$$\mathbf{P} = [\mathbf{H}_e\mathbf{H}_m] + \mathbf{T},$$

where **T** is any circuital flux for which $\overline{\nabla \mathbf{T}} = 0$, and is the flux pointed out by J. J. Thomson shortly after Poynting had given his formula for the energy flux as usually stated.

Now, if we look back to laws 1, 3, and 4 and to the above proof, it will be seen that if we superpose a number of energy systems,

$$\mathbf{H}_{e1}, \mathbf{H}_{m1}; \mathbf{H}_{e2}, \mathbf{H}_{m2}; \text{ etc.,}$$

the energy associated with the system

$$\mathbf{H}_e = \Sigma\mathbf{H}_{er}, \quad \mathbf{H}_m = \Sigma\mathbf{H}_{mr},$$

will not correspond either in distribution or in amount with the superposed energies of the single systems. The Poynting flux will hold for each energy system alone. If we add the systems and regard them as independent we have

$$\mathbf{P} = \sum_r [\mathbf{H}_{er}\mathbf{H}_{mr}] + \mathbf{T}',$$

but this is not the same as

$$\mathbf{P} = [\mathbf{H}_e\mathbf{H}_m] + \mathbf{T} ;$$

the first formula represents the energy system

$$\sum_r \tfrac{1}{2}(e\mathbf{H}_{er}{}^2 + m\mathbf{H}_{mr}{}^2),$$

while the second represents the energy system

$$\tfrac{1}{2}(e\mathbf{H}_e{}^2 + m\mathbf{H}_m{}^2).$$

In Poynting's proof the second formula is assumed to hold, but we must use the first if there are two or more energy systems denoting independent disturbances. These systems must be treated as if each had a separate existence.

Oliver Heaviside discovered the energy flux independently of Poynting, but published it later. He put it in what he stated to be an *extended* form [*],

$$\mathbf{W} = [(\mathbf{E}-\mathbf{e})(\mathbf{H}-\mathbf{h})].$$

It may perhaps be more correctly described as a *restricted* form, since it appears to assume that only one disturbance

---

[*] Poynting's Phil. Trans. paper dates from Jan. 1884. Heaviside's article on " Electromagnetic Induction and its Propagation " dates from Jan. 1885. The above formula for W dates from Feb. 1885 (see El. Papers, i. p. 450). It is repeated and developed in Heaviside's Phil. Trans. paper on the " Electromagnetic Field," read June 1891, published 1892. This last paper is admitted to be obscure. To the professional mathematician the analysis itself can present no difficulty, but the basic assumptions underlying it are numerous, and are so abstract and so little recognized that no one seems to understand exactly what Heaviside means by the various forces and fluxes to which he refers, and in terms of which he expresses the behaviour of matter. In this paper a great deal of attention is given to " the proper form of the Poynting flux," pp. 440–455, after " a full and rigorous examination of all the fluxes of energy concerned." Heaviside appears to be quite clear about the need, when applying Maxwell's equations, to deal only with those forces or fluxes which correspond with the impressed forces whose action is directly under investigation. He realized that this is necessary if the energy relationships are to be correctly dealt with. He subtracted from the

can be considered at a time.. Using the above notation, we can put

$$\mathbf{E} = \mathbf{H}_{e1} + \mathbf{H}_{e2} + \mathbf{H}_{e3} + \dots ,$$
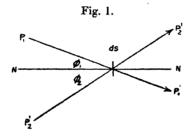
$$\mathbf{H} = \mathbf{H}_{m1} + \mathbf{H}_{m2} + \mathbf{H}_{m3} + \dots ,$$

$$\mathbf{e} = \qquad \mathbf{H}_{e2} + \mathbf{H}_{e3} + \dots ,$$

$$\mathbf{h} = \qquad \mathbf{H}_{m2} + \mathbf{H}_{m3} + \dots ,$$

$$\mathbf{W}_1 = \mathbf{P}_1 = [\mathbf{H}_{e1}\mathbf{H}_{m1}] = [(\mathbf{E}-\mathbf{e})(\mathbf{H}-\mathbf{h})].$$

Heaviside's formula is the same as Poynting's except that it appears to insist upon the independence of disturbances. It is a mistake to add the various electric (or magnetic) fluxes to form a single flux system. The Poynting energy

Fig. 1.

fluxes, separately calculated, may for some purposes be added, yet never amalgamate to form a single flux.

The rate of outflow of energy through an element *ds* of a surface whose normal NN′ makes angles ϕ_1 and ϕ_2 with two

---

total "force of the flux" any extraneous, intrinsic, or motional force, in order to get the "force of the field" with which he was directly concerned. This really amounted to applying the principle of the independence of disturbances, by using Maxwell's equations in connexion with each disturbance apart from the rest.

His remarks on Maxwell's general stress, pp. 468-9, are clear and emphatic. He distinguishes between intrinsic and induced magnetization. "Maxwell's magnetization is the sum of the two without reservation or distinction. But to unite them is against the whole behaviour of induced and intrinsic magnetization in the electromagnetic scheme of Maxwell, as I interpret it." One "keeps up a field of force," the other is "kept up by the field." "In the circuital law" they therefore "behave differently." "It is the resultant magnetization of the whole assembly that is in question, and there is a great difference between its nature according as it disappears on removal of an external cause or is intrinsic. The complete amalgamation of the two in Maxwell's formula must certainly, I think, be regarded as a false step."

Poynting fluxes $\mathbf{P}_1$, $\mathbf{P}_2$, directed along P_1P_1' and P_2P_2' respectively, is

$$\mathbf{P}_1(ds \cos \phi_1) + \mathbf{P}_2(ds \cos \phi_2),$$

or $ds(\mathbf{P}_1 \cos \phi_1 + \mathbf{P}_2 \cos \phi_2),$

and this is the same as if there were a single Poynting flux,

$$\mathbf{P} = \mathbf{P}_1 \cos \phi_1 + \mathbf{P}_2 \cos \phi_2,$$

directed along NN' the normal to ds, but the vector $\mathbf{P}$ does not represent the physical facts, since the energy flux $\mathbf{P}_1 \cos \phi_1$ goes along P_1P_1', while the flux $\mathbf{P}_2 \cos \phi_2$ goes along P_2P_2'. None of it goes along the normal NN'.

3. Waves and Pulses.

Poynting, in his two papers on Maxwell's theory, 1884 and 1885, gave a number of examples illustrating the application of the Poynting flux. They, however, all involved matter and referred to states of steady flow of energy. A steady state involves fluxes which at any point are constant in time; but if the flux be regarded as a surface density of lines or tubes the individual lines are not necessarily fixed in space, since they may move sideways provided that the number threading any closed circuit remains constant in time. For present purposes we have to consider the fluxes involved in radiation. In order to do this we shall use and develop an illustration first suggested by Poynting in the 1884 paper (Coll. Papers, pp. 190–192).

The pair of circuital laws 4_c can be put in the physical or local-action form 4_r. The three laws we require then become

Law 1 ...... $\mathbf{B}_e = e\mathbf{H}_e$; $\mathbf{B}_m = m\mathbf{H}_m,$

Law 3 ...... $T_e = \frac{1}{2}\mathbf{H}_e\mathbf{B}_e$; $T_m = \frac{1}{2}\mathbf{H}_m\mathbf{B}_m,$

Law 4_v...... $\mathbf{H}_e = [\mathbf{B}_m\mathbf{v}_m]$; $\mathbf{H}_m = [\mathbf{v}_e\mathbf{B}_e],$

where $\mathbf{v}_m$ is the velocity with which the flux $\mathbf{B}_m$ crosses the direction of the force $\mathbf{H}_e$, and where $\mathbf{v}_e$ is the velocity with which the flux $\mathbf{B}_e$ crosses the direction of the force $\mathbf{H}_m$. The first of the local-action laws, 4_v, is a direct result of Faraday's discovery in 1831; the second was one which Faraday tried hard [*] to establish experimentally. No direct

---

[*] 'Experimental Researches,' 1658, etc. "I have long sought and still seek for an effect or condition which shall be to static electricity what magnetic force is to current electricity; for as the lines of discharge are associated with a certain transverse effect, so it appeared to me impossible but that the lines of tension or of inductive action, which of necessity precede that discharge, should also have their correspondent transverse condition or effect."

experimental evidence has yet been found for it, but it is deducible mathematically from the remote-action law of the magnetic circuit in exactly the same way as the first local-action law is derived from the remote-action law stating the electromotive force induced in a closed electric circuit. Heaviside * pointed out how extraordinary it was that Maxwell overlooked this deduction.

Now, suppose that in a region free from matter and from electric or magnetic charges we have a disturbance denoted by $\mathbf{H}_e$, $\mathbf{H}_m$, $\mathbf{B}_e$, and $\mathbf{B}_m$. We have not to consider any action at a distance, or even another disturbance in the neighbourhood. Maxwell's laws must therefore apply directly to the disturbance under consideration.

From laws 1 and 4, used numerically it follows that, if *either* $\mathbf{v}_m$ *or* $\mathbf{v}_e$ is zero, all four quantities $\mathbf{H}$, $\mathbf{B}$ vanish. Whatever the disturbance or its cause the disturbance must thus be in motion.

Let us assume it possible for the disturbance to move like a wave, so that, except for the motion, it remains unchanged as it progresses, and let us find what conditions are imposed by the above laws.

It follows from the assumption made that we must have

$$\mathbf{v}_m = \mathbf{v}_e = \mathbf{v}.$$

From laws 1 and 4, used numerically, we get

$$v^2 em = 1,$$

or the velocity must be fixed in amount. The same two laws used vectorially show that $\mathbf{H}_e$ and $\mathbf{H}_m$ are perpendicular to each other and also to the velocity v.

If we use the value found for v in laws 1 and 3 we get numerically

$$\tfrac{1}{2}\mathbf{H}_e\mathbf{B}_e = \tfrac{1}{2}\mathbf{H}_m\mathbf{B}_m = \frac{1}{2v}\mathbf{H}_e\mathbf{H}_m.$$

Thus the electric and magnetic energies per unit volume must be equal, and there must be a fixed ratio between the two forces (or fluxes)

$$\sqrt{e}\,\mathbf{H}_e = \sqrt{m}\,\mathbf{H}_m \quad \text{and} \quad \frac{\mathbf{B}_e}{\sqrt{e}} = \frac{\mathbf{B}_m}{\sqrt{m}}.$$

The total energy per unit volume is $\mathbf{H}_e\mathbf{H}_m/v$, and it is moving with velocity v in a direction perpendicular to both $\mathbf{H}_e$ and $\mathbf{H}_m$. The rate at which energy is flowing across a unit area

* 'Electromagnetic Theory,' i. pp. 68–69 (1893).

perpendicular to **v** and containing the directions of **H,** and **H**$_m$ is thus the product H H$_m$. It is represented vectorially by the Poynting flux

$$\mathbf{P} = [\mathbf{H}_e\mathbf{H}_m].$$

Poynting did not follow up his illustration (Coll. Papers, p. 191) far enough to arrive at the Poynting flux, of which he had just given a full mathematical proof (pp. 178–181) ; but in his 1885 paper, after modifying Maxwell's equations and dealing with the electromagnetic field, he says (p. 217) :—

" But it is, perhaps, worth noting that if we suppose that the electric intensity is produced by the motion of magnetic induction, and that the magnetic intensity is produced by the motion of electric induction, each carrying its energy with it, the right quantity of energy crosses the unit area."

Now why the word perhaps? The significance of this result, which does not appear to have been noticed, is that unless the pulse carries all its energy with it the right quantity of energy does *not* cross the unit area, while if it does carry all its energy with it its fluxes must remain unchanged in magnitude, and no energy can be left behind the moving pulse. There can be no disturbance left in its track, since such disturbance would need energy, and there is no source of such energy.

In the above argument it has been assumed that it is possible for the disturbance to move forward unchanged. This may be admitted provided that no claim be made that the illustration yields a proof of the Poynting flux. We can, however, use the established value of the Poynting flux in conjunction with the known relationships of the fluxes in an electromagnetic wave to justify the assumption made, and thus to establish the important property of a pulse of light. Such a pulse, of duration τ, and depth $v\tau$, takes a time τ to pass any point in its path, and during that interval the corresponding energy flux has just the value needed to prove that the pulse energy per unit volume is passing on unchanged with a velocity v. The energy flux at the point is zero until the pulse reaches the point, and is also zero after the pulse has passed on. A wave of light consists of a sequence of pulses each of which behaves just as if the other pulses were absent, and as if it were quite unaffected by other waves through which it passes. This basic fact explains the result which is always assumed that the light pulses from a star convey to the spectrum analyst a correct reproduction of

the messages * given to them long ago by the star ; neither frequency nor wave-length seems to have anything to do with the process.

The examples used by Poynting in the 1884 and 1885 papers to illustrate his flux were all cases of steady flow. The only difference between such cases and those of light waves is that the stream of pulses exhibits, in regard both to magnitude and to polarization, constancy in the first case and variability in the second. If we take an energy tube bounded by four level surfaces, two of these being electric at potentials V_1 and V_2, and the other two magnetic at potentials Ω_1 and Ω_2, and if $d\eta$ and $d\mu$ be elements of the normals to the V and Ω surfaces respectively, we have

$$H_e = \frac{dV}{d\eta} \quad \text{and} \quad H_m = \frac{d\Omega}{d\mu},$$

and each will be perpendicular to the corresponding level surface. The Poynting flux, which is perpendicular to both, is along the energy tube, and its amount for the element of cross-area $d\eta\,d\mu$ is $dV\,.\,d\Omega$, the integral of which across any energy tube is $(V_2-V_1)(\Omega_2-\Omega_1)$. Thus, even in a state of steady energy flow, the lines B_e and B_m are always moving, and the pulses are travelling with all their energy just as in a wave of light.

The above seems to suggest a simple way of regarding the action on the medium of an optical source. This source must exert on the medium some transfer force F producing a yield ϕ whose rate $\dot\phi$ is such that at any moment $F\dot\phi$ is the power transferred to the medium, while $F\phi$ has the nature of energy. We may know nothing about F and ϕ, yet we can always put

$$\dot\phi = \eta F + G,$$

---

* It is not perhaps recognized that Heaviside's problem of high-speed electrical signalling was that of finding the conditions under which an electromagnetic pulse imparted to a transmitting line would afterwards behave like a pulse of light in space in spite of the interference of the matter of the transmitting line. This matter must absorb energy from the pulse and weaken the signal, but if conditions can be so arranged that the electric and magnetic energies are absorbed at equal rates the equality of the two energies will be preserved, and the effect will be only like what occurs in a light wave due to spherical spreading. No reflexions will occur to influence the effect on matter of succeeding pulses. Each pulse will go on independently and will be reduced in the same proportion, so that the whole wave, or sequence of pulses, will preserve its wave form as it progresses, and will deliver a perfect signal to the receiving station, however complex the wave form may be.

where the equation forms the definition of G, and where we can still choose η, such that for a particular interval τ_1 we have

$$\int_0^{\tau_1} F\dot{\phi}\, dt = \eta \int_0^{\tau_1} F^2\, dt,$$

so that

$$\int_0^{\tau_1} FG\, dt = 0.$$

Thus FG represents a flow of energy oscillating between the source and the medium whose integral value is zero for the interval τ_1, while ηF^2 represents a flow of energy which is permanently radiated from the source. Now, though η must depend on the action of the source during the special interval τ_1, it does not seem unreasonable to assume that we can regard it as constant for an appreciable time, and thus independent of a small interval τ_1. On the average FG is zero. If we multiply the equation through by F and take means for a time τ we have

$$\text{av. } F\dot{\phi} = \eta \text{ av. } F^2 + \text{av. } F.G.$$

The first term on the right is the rate at which unreturning energy is radiated during the time τ, while the second represents energy which is oscillating and which must thus remain within a bounded distance measured from the source. Maxwell's theory indicates that the energy
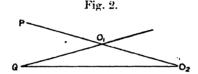
$$\eta\tau \text{ av. } F^2 \quad \text{or} \quad \eta \int_0^\tau F^2\, dt$$

travels at a constant speed v, and at any subsequent time t is contained between two spheres of radii vt and $v(t-\tau)$. This holds however small τ may be. Thus, if the source is impulsive and exerts the transfer force F only for an infinitesimal interval of time, the corresponding radiated energy remains within an expanding spherical shell of constant thickness $v\tau$ and of expanding radius vt. This is quite in accordance with the properties of a pulse of light and with the assumption of the independence of pulses and of waves.

There seems to be no necessary relation between successive pulses in either amplitude, energy, or plane of polarization. The successive amplitudes may follow some periodic law conferring properties of frequency and wave-length, but such law is due to the source. The pulse itself can be looked upon as an independent entity, which, except for weakening due to spherical spreading, remains constant as it progresses. It is

not a wave, but the ordinate of a wave, and one whose properties cannot be represented by a simple number, since polarization as well as magnitude have to be taken into account.

Moreover, the pulse is not necessarily single. It may involve a great number of fluxes, each having its own polarization, magnitude, and associated law of sequence. Suppose P and Q are two points on a star emitting light received by a spectrum analyst at O_1 or O_2. If PO_1 is of the order of a light year (10^{18} cm.), the surfaces of two spheres through and near O_1, with centres at P and Q on the star, are essentially the same. A light pulse at O_1 will contain fluxes from both P and Q. These do not combine into one or even travel together, since the one travels along PO_1O_2 and the other travels along QO_1, while the pulses from Q received at two points O_1 and O_2 have travelled by different paths. Now the star contains myriads of sources

Fig. 2.

such as P and Q, and each source may itself be complex, so that a light pulse at O_1 contains myriads of independent fluxes. This presents no theoretical difficulty if the independence of fluxes is assumed, but if the fluxes are supposed to combine into one, serious difficulties arise in connexion with the amount and distribution of the energy involved.

The general result strongly suggests that the fluxes of energy behave as if associated with some physical entity which preserves its individuality as the pulse progresses through space. Each pulse seems to consist of groups of Faraday tubes, and it is to these tubes that in all probability the individuality is due.

In space free from matter and from charges we have the relations given by law 2,

$$\overline{\nabla \mathbf{B}_e} = \mathrm{div}.\, \mathbf{B}_e = 0 \; ; \quad \overline{\nabla \mathbf{B}_m} = \mathrm{div}.\, \mathbf{B}_m = 0.$$

Now, if each flux **B** is regarded as the density of lines per unit cross area, these relations suggest that the fluxes have individuality. They express the fact that each line has the unending characteristic associated with an ordinary line. The line goes unceasingly on, never stops at a point, never

separates into two lines, and never amalgamates with another, though it may form a closed loop. Such a line if it enters a closed region must also leave that region, and the zero divergence relation necessarily follows.

The physical aspect of Faraday tubes received much attention from Poynting *. The subject has been most fully developed by J. J. Thomson in the first chapter of 'Recent Researches' (1893), where the tubes are treated as "real physical quantities having definite sizes and shapes." The tubes "are all of the same strength." "The phenomena of electrolysis show that 'this strength' is a natural unit." It is assumed that "fractional parts of this unit do not exist." The tubes, in accordance with Faraday's views, may stretch across a vacuum. They may be open or closed, and in the latter case may be of infinitesimal size. They can "neither be created nor destroyed," so that "a change in the number passing through any fixed area must be due to the motion or deformation of the tubes."

Attention is concentrated on electrostatic tubes, since "molecular structure has an exceedingly close connexion with" them, "much closer than we have any reason to believe it has with tubes of magnetic induction." The ether is assumed to contain "multitudes of tubes" of the closed type.
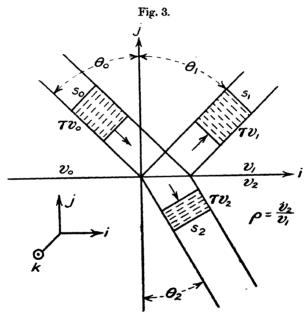
The phenomena of the magnetic field follow from the motion of the electrostatic tubes, and both Poynting and J. J. Thomson appear to regard the electrostatic tube as the primary conception ; but there is so much symmetry and such an intimate connexion between the properties of electric and magnetic tubes, as shown by Maxwell's equations, that it seems as if these equations can be regarded as defining the properties of a physical concept involving both sets of tubes. Some of the above ideas about the electric tubes seem equally applicable to the magnetic ones. When an electric current produces a flux of magnetic lines through its coil these lines must presumably come from the opening out of "closed" magnetic tubes, and when the current falls to zero these lines must presumably return to the closed state.

Some conception, such as that of J. J. Thomson, seems needed to explain the physical nature of a pulse, and to turn Maxwell's theory into a physical, as distinct from a mathematical, theory of light. The properties of pulses suggest that light is to be regarded as corpuscular rather than undu-

* See his 1884 and 1885 papers, and also his paper on "Molecular Electricity," Coll. Papers, pp. 269-298.

latory. What seems wanted is the definition of some physical entity possessing at one and the same time two vector properties, the vectors being at right angles to each other and representing equal amounts of electric and magnetic energy. I have not succeeded in finding a satisfactory definition of such a quantity, but as a contribution to the subject it is proposed to show that an isolated pulse of light, when incident on the surface bounding two different non-absorbing media, splits up into two such pulses, one being reflected and the other transmitted, in accordance with the ordinary

Fig. 3.

laws of light, and with energy relations given by the usual formulæ. The surface conditions assumed in all theories of reflexion raise questions about the physical nature of the fluxes involved.

4. THE REFLEXION AND REFRACTION OF PULSES.

Let the plane of incidence ij be that of the paper, and let the positive direction $\odot$ of the normal k to this plane be upwards, so that

$$i = [jk], \quad j = [ki], \quad k = [ij].$$

Let suffixes 0, 1, 2 distinguish corresponding quantities

referring to the incident, reflected, and transmitted rays. Let ik be the plane separating two media of inductivities e_1, m_1 and e_2, m_2. Consider an incident pulse of duration τ within a beam of square section, the sides being unity perpendicular to the paper and also $1 = s_0$ in the plane of the paper. Let θ_0, θ_1, and θ_2 be the angles between the rays and the axis of j. If the pulse after incidence splits up into a reflected and a transmitted pulse, the depths of the pulses are $v_0\tau$, $v_1\tau$, $v_2\tau$, where v_0, v_1, and v_2 are the velocities, while $s_0 v_0\tau$, $s_1 v_1\tau$, $s_2 v_2\tau$ are the sections in the plane of the paper and also the pulse volumes. We assume equal magnetic inductivities $m_0 = m_1 = m_2$. Define a quantity ρ as

$$\rho = \frac{v_2}{v_1} = \sqrt{\frac{e_1 m_1}{e_2 m_2}} = \sqrt{\frac{e_1}{e_2}} = \sqrt{\frac{1}{k}} = \frac{1}{\mu},$$

where k is the specific inductive capacity and μ the index of refraction of the second medium as compared with that of the first.

It will be seen that the pulses exhibit the following ratios (assuming $\theta_0 = \theta_1$) :—

Depths.......... ..... $v_0\tau : v_1\tau : v_2\tau = 1 : 1 : \rho$,

Cross-sections... $s_0 : s_1 : s_2 = 1 : 1 : \sigma$,

Volumes .... $s_0 v_0 : s_1 v_1 : s_2 v_2 = 1 : 1 : \rho\sigma$,

where $e_1 = \rho^2 e_2$, and where σ has to be defined.

Our first assumption in regard to the pulses is that the ordinary laws of reflexion and refraction hold,

$$\left. \begin{array}{ll} \theta_0 = \theta_1 = \phi, & \theta_2 = \theta, \\ \sin\theta = \rho\sin\phi, & \cos\theta = \sigma\cos\phi. \end{array} \right\} \quad . \quad . \quad . \quad (1)$$

The last equation defines σ, since

$$s_0 : s_1 : s_2 = \cos\theta_0 : \cos\theta_1 : \cos\theta_2.$$

If the electric *flux* is denoted by **E** and the magnetic *flux* is denoted by **M**, we have for equality of electric and magnetic energy per unit volume

$$\frac{E_0^2}{e_0} = \frac{M_0^2}{m_0}, \qquad \frac{E_1^2}{e_1} = \frac{M_1^2}{m_1}, \qquad \frac{E_2^2}{e_2} = \frac{M_2^2}{m_2}, \quad . \quad . \quad (2)$$

and for unaltered total energy, electric or magnetic,

$$
\left.
\begin{aligned}
\frac{E_0^2}{e_0} &= \frac{E_1^2}{e_1} + \rho\sigma \frac{E_2^2}{e_2}, \\
\frac{M_0^2}{m_0} &= \frac{M_1^2}{m_1} + \rho\sigma \frac{M_2^2}{m_2}.
\end{aligned}
\right\} \quad \cdots \cdots \quad (3)
$$

The relations (3) only give one additional condition if the three relations (2) hold.

In addition, it is necessary to meet the exacting set of conditions needed to ensure, assuming the fluxes **E, M** in a pulse are perpendicular to each other and also to the ray, that :—

> The Poynting flux for each pulse must have the correct magnitude, and must be directed along the corresponding ray in the right sense. . . . (4)

The conditions (1)–(4) are numerous, but so also are the adjustable constants needed to define the vectors. It turns out on trial that the above conditions are consistent with a solution, but are not quite sufficient to determine a single-valued one.

We have not yet considered the boundary conditions to be met at the surface separating the two media. In all theories of light these are stated to be :—

> The sum of the surface components of the *forces* must be equal on the two sides of the surface.
>
> The sum of the normal components of the *fluxes* must be equal on the two sides of the surface.

These two conditions must hold both for electric and for magnetic quantities. Hence these additional conditions are four in number, and we may conveniently refer to them as the four surface conditions.

The physical meaning of these conditions is not clear in the present case. We are dealing with pulses whose properties are defined by electromagnetic equations having no reference to matter or to charges either electric or magnetic. The conditions in question are based on consideration of mechanical forces on such charges, and depend in general on the properties of matter. It turns out that in order to determine a single valued solution it is not necessary to assume all four surface conditions if conditions (1)–(4) are imposed. We reserve for the present further comment on these surface conditions.

The plane of polarization of the incident ray has yet to be defined. We shall consider two cases:

1. **E** perpendicular to the plane of incidence.
2. **M** „ „ „ „

E *perpendicular to the Plane of Incidence.*

For this case we shall assume, in addition to conditions (1)-(4), the two *electric* surface conditions, but not the *magnetic* ones. We thus have

$$\frac{\mathbf{E}_0}{e_0} + \frac{\mathbf{E}_1}{e_1} = \frac{\mathbf{E}_2}{e_2},$$

or $\qquad \mathbf{E}_0 + \mathbf{E}_1 = \rho^2 \mathbf{E}_2.$

There can be no component perpendicular to the surface, and each of the three fluxes **E** must be perpendicular to one of the rays. These fluxes are thus parallel, but not necessarily all of the same sign. Using the tensors algebraically we must have

$$E_0 + E_1 = \rho^2 E_2. \quad \ldots \quad (5_e)$$

Now from (3) we have

$$E_0{}^2 = E_1{}^2 + \rho^3 \sigma E_2{}^2,$$

and from this and (5_e) we have

$$E_0 - E_1 = \rho \sigma E_2. \quad \ldots \quad (6_e)$$

From (5_e) and (6_e) we thus have E_1 and E_2 in terms of E_0.

The problem now becomes a straightforward example in vectors, the details of which may be omitted. The solution is

$$\left.\begin{array}{ll} \mathbf{E}_0 = E_0 k, & \mathbf{M}_0 = -M_0(i \cos\phi + j \sin\phi), \\[4pt] \mathbf{E}_1 = \alpha E_0 k, & \mathbf{M}_1 = \alpha M_0(i \cos\phi - j \sin\phi), \\[4pt] \mathbf{E}_2 = \beta E_0 k, & \mathbf{M}_2 = -\rho\beta M_0(i \cos\theta + j \sin\theta), \end{array}\right\}$$

where E_0 and M_0 are each positive quantities related by

$$E_0{}^2/e_0 = M_0{}^2/m_0,$$

and where

$$\sin\theta = \rho \sin\phi, \quad \cos\theta = \sigma \cos\phi,$$

$$\alpha = \frac{\rho - \sigma}{\rho + \sigma}, \quad \beta = \frac{2}{\rho(\rho + \sigma)}.$$

$$\left.\vphantom{\begin{array}{l}a\\b\\c\\d\\e\\f\\g\end{array}}\right\} \quad . \quad (7_e)$$

The solution (7_e) will be found to meet completely all the conditions (1)-(4). It will also be found that the two

magnetic surface conditions are satisfied. One of these requires a relationship between the i components of the quantities **M**, and the other a relationship between the j components of those quantities. Each relationship is satisfied, and this shows that if we had assumed the four surface conditions together with conditions (2)–(4), we could have arrived at a solution consistent with the ordinary laws of reflexion and refraction without assuming these laws, as is done by condition 1. It is easy by using a modification of Huygen's construction to see a physical reason for the laws of reflexion and refraction, but the physical meaning of the surface conditions is not clear. It is these surface conditions which in all theories of light seem to determine the ratio of the fluxes in the reflected and refracted rays. They seem to replace Newton's theory of fits in the corpuscular theory.

M *perpendicular to the Plane of Incidence.*

In this case we assume the two *magnetic* surface conditions, but not the *electric* ones. We thus have

$$\frac{\mathbf{M}_0}{m_0} + \frac{\mathbf{M}_1}{m_1} = \frac{\mathbf{M}_2}{m_2},$$

or, using tensors algebraically as before, it follows that

$$\mathbf{M}_0 + \mathbf{M}_1 = \mathbf{M}_2 ; \quad \ldots \ldots (5_m)$$

from (3) we have

$$\mathbf{M}_0{}^2 - \mathbf{M}_1{}^2 = \rho\sigma \mathbf{M}_2{}^2,$$

and with the aid of (5_m) we get

$$\mathbf{M}_0 - \mathbf{M}_1 = \rho\sigma \mathbf{M}_2. \quad \ldots \ldots (6_m)$$

(5_m) and (6_m) give $\mathbf{M}_1$ and $\mathbf{M}_2$ in terms of $\mathbf{M}_0$, and, as before, we have a determinate vector problem. The solution is

$$\left.\begin{aligned}
&\mathbf{E}_0 = \mathrm{E}_0(i\cos\phi + j\sin\phi), && \mathbf{M}_0 = \mathrm{M}_0 k, \\
&\mathbf{E}_1 = \alpha' \mathrm{E}_0(i\cos\phi - j\sin\phi), && \mathbf{M}_1 = -\alpha' \mathrm{M}_0 k, \\
&\mathbf{E}_2 = \beta' \mathrm{E}_0(i\cos\theta + j\sin\theta), && \mathbf{M}_2 = \rho\beta' \mathrm{M}_0 k,
\end{aligned}\right.$$

where E_0 and M_0 are essentially positive quantities connected by

$$\mathrm{E}_0{}^2/e_0 = \mathrm{M}_0{}^2/m_0,$$

and where

$$\alpha' = \frac{\rho\sigma - 1}{\rho\sigma + 1}, \quad \beta' = \frac{2}{\rho(\rho\sigma + 1)},$$

$$\sin\theta = \rho\sin\phi, \quad \cos\theta = \sigma\cos\phi.$$

$$\left.\right\} \quad . \quad (7_m)$$

This solution will be found completely to satisfy (1)-(4) and also the two *electric* surface conditions.
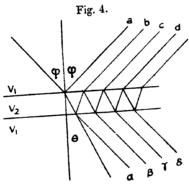
The reflecting and refracting coefficients will follow from (3) in accordance with (7_e) or (7_m), whichever is appropriate to the case considered.

If r_{12} is the proportion of the pulse energy reflected in the first medium at the surface of the second, and if t_{12} is the corresponding ratio for the transmitted energy, we have

for case (7_e), $\quad r_{12} = \left(\dfrac{\rho - \sigma}{\rho + \sigma}\right)^2, \quad t_{12} = \dfrac{4\rho\sigma}{(\rho + \sigma)^2}; \quad . \quad . \quad (8_e)$

for case (7_m), $\quad r_{12} = \left(\dfrac{\rho\sigma - 1}{\rho\sigma + 1}\right)^2, \quad t_{12} = \dfrac{4\rho\sigma}{(\rho\sigma + 1)^2} . . \quad . \quad (8_m)$

If we substitute for ρ and σ their values as given above in terms of ϕ and θ, the angles of incidence and refraction,

Fig. 4.

these formulæ will be found the same as those given by Fresnel's theory of light. The same formulæ were obtained on Maxwell's theory for the first time by G. F. Fitzgerald [*], and later on by other workers.

It will be seen from (8_e) and (8_m) that if ρ and σ are each inverted, the values of r and t are unchanged. In any case of multiple reflexions at the surfaces of a parallel plate of a transparent medium whose velocity v_2 differs from v_1, that of the incident beam, it will be seen from the figure that the

[*] G. F. Fitzgerald, Phil. Trans. pt. ii. 1880, p. 691, received Oct. 26, 1878; Shuster and Nicholson, 'Optics,' 3rd ed. 1923, pp. 238-241; Drude, 'Optics,' Eng. trans. 1902, p. 282; Wood, 'Physical Optics,' 1905, p. 294. In all cases the problem treated is that of a wave or train of pulses. An isolated constant pulse is not considered. The four surface conditions are always assumed. In spite of the great difference between the two theories of Fresnel and Maxwell, the reflecting coefficient is given by the same formula in all cases.

values of ϕ and θ are interchanged at successive transmissions, so that the values of ρ and σ are inverted. Hence

$$r_{12} = r_{21} = r, \qquad t_{12} = t_{21} = t.$$

The energies of the reflected rays a, b, c, ... will be r, rt^2, r^3t^2, ..., while those of the transmitted rays a, β, γ, ... will be t^2, t^2r^2, t^2r^4, ..., expressed in each case in terms of the incident pulse energy.

The sums of these series will be found to be

$$R = \frac{2r}{1+r}, \qquad T = \frac{1-r}{1+r},$$

giving

for case (8_e), $R = \dfrac{(\rho-\sigma)^2}{\rho^2+\sigma^2}$, $T = \dfrac{2\rho\sigma}{\rho^2+\sigma^2}$;   . . . ($9_e$)

for case (8_m), $R = \dfrac{(\rho\sigma-1)^2}{\rho^2\sigma^2+1}$, $T = \dfrac{2\rho\sigma}{\rho^2\sigma^2+1}$ . . . . (9_m)

ρ and σ cannot be equal except for identical media. If one exceeds unity the other must be less. The product $\rho\sigma$ can be unity, in which case Brewster's law holds. For normal incidence σ is unity, and the formulæ for the e and m cases become the same.

$$\left.\begin{array}{l} R = \dfrac{(\rho-1)^2}{\rho^2+1} = 1 - \dfrac{2\sqrt{k}}{k+1} = 1 - \dfrac{2\mu}{\mu^2+1}, \\[2mm] T = \dfrac{2\rho}{\rho^2+1} = \dfrac{2\sqrt{k}}{k+1} = \dfrac{2\mu}{\mu^2+1}, \end{array}\right\} \quad . \quad (10)$$

where k is the specific inductive capacity and μ is the index of refraction. These last formulæ, allowing for the fact that they refer to multiple reflexions, are the same as those given by Fresnel's theory. They are, however, obtained for a single pulse, not for a complete wave. Multiple reflexion involves a sequence of pulses. These are quite separate if the time taken to traverse the plate is greater than the duration of the pulse, otherwise they overlap. In all cases they are successive, not simultaneous. For ordinary light we can assume the radiant energy is halved between pulses of types (9_e) and (9_m), and hence a mean must be taken between the two values given for R or for T.

5. The Physical Nature of Pulses.

For present purposes the primary interest of the result is that an isolated pulse behaves, when reflected or refracted,

just like a complete wave. A search for the physical meaning of the fluxes must, however, raise the question of the physical meaning of the surface conditions assumed in all theories of the reflexion of light. Fresnel's theory is entirely mechanical. Maxwell's theory does not appear to involve anything mechanical or anything about electric or magnetic charges. The surface conditions, whatever the theory, seem to be the main factor in determining the ratio of the reflected light. If the first medium e_1, m_1 represents the ether, experimental evidence shows that the second medium e_2, m_2 must contain matter. In reflexion, according to Maxwell's theory, the behaviour of matter is assumed to be summarized in the properties e_2, m_2, and in the surface conditions ; but the physical meaning of the latter has yet to be found.

The laws of reflexion and refraction follow from simple time considerations if it can be assumed that any flux in a wave front remains in that wave front. This will be evident from Huygen's construction. It also seems natural to expect that the normal components of the *fluxes* must add up to the same total on each side of the surface, though it is not at all clear, in view of the apparent individuality of fluxes, whether any flux can be split physically into two components. But what is the meaning of the surface components of the *forces* having the same total on each side of the surface? An explanation often given amounts to asserting that, unless the equality holds, a Maxwell demon can manipulate an electron so as to get work out of the system. But such a result would not conflict with the principle of the conservation of energy, since this merely asserts that in any energy transfer the energy gained in one form is lost in another. The absence of experimental evidence of such a transfer is no proof that the law of equality of surface forces must hold. The second law of thermodynamics is assumed to hold in the kinetic theory of gases, even though a sorting demon can in theory upset it.

The present investigation has merely followed up the principle of the independence of waves, the assumption of which is a very old one in connexion with light. It is not apparent that any new assumption has been made, but in order to reconcile the phenomena of interference with the independence principle it has been suggested that a compound ray of light may exist in what may be called a neutralized state, such that the ray has no observable effect on matter, although it conveys electromagnetic energy. This state occurs when the vector sum of the fluxes E is zero, a

condition necessarily involving the same relation between the corresponding fluxes M.

It is not easy to suggest how experimental evidence in support of such a view can be found, and until such evidence is forthcoming the view will be looked upon as speculative. On the other hand, it can scarcely be claimed that the reflecting and refracting coefficients given by Fresnel's formulæ have as yet been thoroughly confirmed[*], or that the surface conditions assumed are as yet completely established.

In the theory given above of the reflexion of an isolated pulse the ideas of frequency and phase do not arise, but it is clear that reversals of the direction of a flux do occur. If we take the case of normal reflexion, at the surface of a transparent and very thin film of a medium 2, of a ray incident in a medium 1, the **E** flux is reversed for one of the reflected rays but not for the other, so that the dark spot in Newton's ring experiment is accounted for by the neutralization of the compound reflected ray, although the energy of each component ray must remain positive. If we consider the case of multiple reflexions nearly normal to a plate of glass, we have, from (7$_e$) and (8$_e$), with $\phi = \theta = 0$, $\sigma = 1$,

$$\mathbf{E}_0 = \mathrm{E}_0 k, \qquad \mathbf{M}_0 = -\mathrm{M}_0 i,$$

$$\mathbf{E}_1 = \alpha \mathrm{E}_0 k, \qquad \mathbf{M}_1 = \alpha \mathrm{M}_0 i,$$

$$\mathbf{E}_2 = \beta \mathrm{E}_0 k, \qquad \mathbf{M}_2 = -\rho \beta \mathrm{M}_0 i,$$

with

$$\alpha = \frac{\rho - 1}{\rho + 1}, \qquad \beta = \frac{2}{\rho(\rho + 1)},$$

$$r_{12} = \alpha^2, \qquad t_{12} = 1 - \alpha^2.$$

With glass ρ is less than unity for the first reflexion (see fig. 4), but for all internal reflexions it is greater than unity, since ρ is inverted. Thus the electric fluxes in the rays $a, b, c, \ldots$ are respectively $-, +, +, \ldots$, as compared with that of the incident ray. The opposite signs hold for the magnetic fluxes. Thus, while the formula (9$_e$) holds for the reflected energy, this energy may not all be in a state to affect matter, owing to partial neutralization of the ray. This
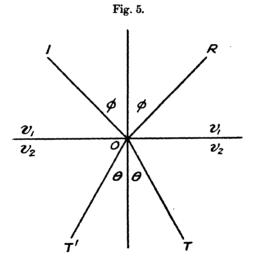
---

[*] Lord Rayleigh [Proc. R. S. xli. pp. 275-294 (1886), or Sci. Papers, no. 138] has measured the intensity of the light reflected at "nearly perpendicular incidences." His work, as is always the case, is impressive on account of its care and skill. It also suggests that in order to confirm the surface conditions experimentally much more care and skill are needed than have probably yet been given to the matter.

effect cannot occur in the transmitted rays, since it will be seen that, whatever the sign of α, the ratios $\mathbf{E}_0 : \mathbf{E}_2$ and $\mathbf{M}_0 : \mathbf{M}_2$ are each positive.

It seemed desirable, in connexion with the present subject, to examine the "principle of reversibility" in regard to light. This was done, with the surprising result that the principle [*] does not appear to hold with light on the theory of Maxwell as extended by Poynting's theorem. According to this principle, if a ray of light IO is split up into a reflected ray OR and a refracted ray OT, and if these latter rays are each reversed without loss of energy, the original ray of

Fig. 5.

light is reproduced with direction reversed ; but each of the reversed rays must cause a ray along OT' having energy necessarily positive, so that the compound ray sent back

---

[*] See Schuster and Nicholson, 'Optics,' 3rd ed., 1923, p. 45. The principle is based on an investigation originally due to Stokes, and is stated as follows :—" If at any time all velocities in a dynamical system are reversed and there is no dissipation of energy, the whole previous motion is reversed. Any configuration of the system which existed at a time t before reversal took place will therefore again exist at a time t after reversal." A ray of light can be reversed by reversing one only of its fluxes. If both fluxes are reversed the ray proceeds as before. A pulse of light does not appear to be a mechanical system at all. The assumption on which the principle of reversibility is based, that all velocities are reversed, does not seem to hold when a ray of light is reversed or reflected back perfectly along its original direction.

along OI cannot have the original energy. If we look at the energy coefficients (8_e) or (8_m), we have, in either case,

for energy along OI, $\qquad r_{12} \times r_{12} + t_{12} \times t_{21}$,

,, ,, ,, OT', $\qquad r_{12} \times t_{12} + t_{12} \times r_{21}$,

where $\qquad r_{12} = r_{21} = r, \quad t_{12} = t_{21} = t, \quad r + t = 1$:

the first amount is $r^2 + t^2$ and the second $2rt$. Each quantity is positive, and the sum of the two is unity. The same conclusion holds good for the reversal of the compound rays of fig. 4, as will be evident from the values of R and T given by (9_e) or (9_m).

Though the energy ratios r and t are necessarily positive, it will be found that of the two reflecting coefficients r_{12} and r_{21} one reverses the flux while the other does not. The two pulses sent along OT' have fluxes reversed, and form a neutralized ray. The two pulses sent back along OI have fluxes in the same direction.

One result which comes out is that a single energy system, represented by the incident ray IO, is turned after incidence into two energy systems, OR and OT; and that *each* of these, if reversed so as to be incident again on the bounding surface, splits up into two energy systems also, so that four energy systems result.

Our investigation points to the conclusion that an isolated pulse of light behaves in a way quite independent of the action of other pulses, and also that a pulse may itself be complex and consist of a number of distinct pulses which behave independently of each other. This in turn suggests that a single pulse may consist of a group of distinct physical entities associated in some way represented by the polarization. If such an entity exists a suitable name for it would be a *radion*. This being the object to aim at, an attempt to formulate it may be made as follows:—

For any electromagnetic pulse let

$$\lambda u = \frac{\mathbf{E}}{\sqrt{e}} = \frac{\mathbf{M}}{\sqrt{m}},$$

then $\lambda^2 u^2$ is the energy per unit volume, where λ is a number and u^2 is a unit of the nature of energy per unit volume.

This number λ represents each flux density $\mathbf{E}$, $\mathbf{M}$, in terms of units $u\sqrt{e}$ and $u\sqrt{m}$ respectively, and we may think of λ as a flux density in what we may call *lynes* per unit area in each case. Each force intensity $\mathbf{E}/e$ and $\mathbf{M}/m$ is also represented by λ in units which are $u/\sqrt{e}$ and $u/\sqrt{m}$

respectively. The Poynting flux density $[\mathbf{EM}]/em$ is represented by

$$\lambda^2 u^2/\sqrt{em} = v\lambda^2 u^2.$$

Thus in suitable units the number λ, which we can call the *energy number* of the pulse, represents each flux density, and also each force intensity; while in other units the number λ^2 represents the energy per unit volume, and also the Poynting flux per unit area.

Now consider a pulse of unit depth within a rectangular beam of dimensions a and b drawn in the direction of $\mathbf{E}$ and $\mathbf{M}$ respectively. The number of electric *lynes* will be λb and that of magnetic *lynes* will be λa. We can conceive these lynes as partitions perpendicular to the direction of the corresponding flux and containing the velocity direction v. These partitions will have *crossings* in $\lambda a \times \lambda b = ab\lambda^2$ lines parallel to v. The number of these *crossings* will thus be λ^2 per unit area of wave front and also per unit volume of the pulse. In the wave front the crossings will be the points in which the lynes representing the flux densities cross, but we can consider them also as lengths parallel to v within the pulse.

If d is the depth of a pulse and s its sectional area the energy is measured by $\lambda^2 sd$, and the number of crossings considered as points in the wave front is $\lambda^2 s$. The crossing considered as a line in the direction of v will be of length d, and if we consider it to consist of *radions* of fixed length put end to end the number of these radions will be measured by $\lambda^2 sd$, so that each radion will be associated with

(i.) a fixed amount of energy, (ii.) a fixed length measured along v, and (iii.) a state of polarization defined by two vectors at right angles to each other and to v, and representing the directions of $\mathbf{E}$ and $\mathbf{M}$.

The number of radions per unit of volume will be proportional to λ^2, and will measure the energy of the pulse per unit volume. If we suppose these radions are radiating in straight lines from the source, all at constant speed v, the number per second which cross unit area of wave front will measure the Poynting flux density. We have only to suppose that each radion moves through space with its velocity and state of polarization unaffected by any other radion to account for the constant properties of the wave front due originally to the action of the source. If we consider the lynes as partitions perpendicular to the wave front, it will be seen that lynes are really level surfaces of equal potential,

magnetic or electric. If we take a pulse of depth equal to the length of a radion, the lynes divide the pulse into cells the number of which is equal to the number of crossings or to the number of radions in the pulse. These cells compare with the unit cells of Maxwell, except that instead of representing a stationary state they denote a state moving with speed v, the number of radions crossing unit area of the wave front per second being the Poynting flux density. It is tempting to imagine that the closed tube concept of J. J. Thomson may represent a closed electric induction tube linked with a closed magnetic one ; that a radion consists of such a tube opened out both electrically and magnetically so as to form a right-angled cross representing the polarization of the radion, the energy needed to do this being fixed in amount and being returnable if the cross closes up again ; that the unit cell of Maxwell, if electric, may contain such a tube opened out only electrically, and, if magnetic, may contain such a tube opened out only magnetically ; that the unit cells of Maxwell, being fixed, and each containing half a unit of energy, may contain a stationary polarized entity which could be called a semiradion; and that the energy tubes of a beam of light formed by the lynes contain radions moving in polarized formation at speed v.

It is certainly safer, however, to regard the radion as a purely mathematical concept, in accordance with the energy known to be in a wave of light, and associating this energy with a twofold polarization and also with a velocity harmonizing with Maxwell's equations.

Dec. 5, 1931.

CI. *Notices respecting New Books.*

The Mathematical Papers of Sir William Rowan Hamilton.— Vol. I. *Geometrical Optics.* Edited for the Royal Irish Academy by A. W. Conway and J. L. Synge. Cunningham Memoir No. XIII. (Cambridge University Press, 1930. Price 50s. net.)

WHEN the scientific progress of the nineteenth century comes to be summed up in so far as it relates to mechanics and physics, the Englishman Faraday, the Scotsman Maxwell, and the Irishman Hamilton will be found to represent the three main pillars upon which the structure of modern mechanics and physics rests.

The introduction of the Characteristic Function into the treatment of Optics, and the application of its underlying idea to the study of the equations of dynamics, was an historical event comparable with the formulation of the classical laws of motion, or of the law of gravitation. Dynamics has, since the introduction of the Hamiltonian equations, been an entirely different subject, even from the subject as it left the hands of Lagrange. One has only to think of the transformation theory, integral invariants, and Hamilton's principle, with their extensive ramifications into all branches of modern physics, to realize the significance of Hamilton's great work.

As happens so often in the exact sciences, Hamilton's greatest achievement was the result of ideas which he developed as a very young man. He was born at Dublin in August 1805. At the age of seventeen, before he entered Trinity College, Dublin, as an undergraduate, he had already written and communicated to the President of the Royal Irish Academy a paper on Caustics, which contained the germ of his conception of optical propagation. The paper on Caustics was read to the Academy in December 1824, although it was not published until 1827, under the title of "The Theory of Systems of Rays," and in an entirely recast and enlarged form. This paper contains a reference to the extension of the method to dynamics, so that we can claim that, at the age of twenty-one, Hamilton had developed his characteristic function, and had realized that it could be applied to dynamics. In October 1830 Hamilton published, in a supplement to this paper, his discovery of Conical Refraction. This gained him the Cunningham Medal from the Royal Irish Academy and the Royal Medal of the Royal Society when he was still under thirty.

The present volume is the first of four volumes, which will contain the mathematical papers of Hamilton. It is issued under the auspices of the Royal Irish Academy, with the financial help of Trinity College, Dublin, University College, Dublin, and the Royal Society. The editors, Professor A. W. Conway and Professor J. L. Synge, have done their work remarkably well, and the four volumes, when issued, will constitute an indispensable part of any scientific library.

The present and first volume is entitled 'Geometrical Optics.' It consists of three parts:—Part I. gives the "Major Papers," namely, the "Theory of Systems of Rays," and three "Supplements," all published in the 'Transactions of the Royal Irish Academy,' between 1827 and 1837, and occupying nearly three hundred pages of the present volume.

Part II. is entitled "Minor Papers," published in the 'Reports of the British Association,' the 'Philosophical Magazine,' and the 'Dublin University Review.' The most interesting is the paper entitled "On a General Method of Expressing the Paths of Light, and of the Planets, by the Coefficients of a Characteristic Function," published in the 'Dublin University Review' in 1833. This gives a valuable historical review of Geometrical Optics, and

the theory of the Characteristic Function, with an indication of its application to dynamics.

While Parts I. and II. are reprints of Hamilton's published papers on Optics, Part III. consists of unpublished manuscripts. The volume of unpublished material that Hamilton left behind him at his death in 1865 was such that there are more than two hundred of his notebooks containing his meditations and the details of his researches, both successful and unsuccessful, deposited in the library of Trinity College, Dublin.

The first paper in Part III. is Hamilton's original "On Caustics" paper, submitted to the Academy in 1824. There is also included an interesting account of coma and astigmatism in the case of a symmetrical optical instrument corrected for spherical aberration. The really important work now published for the first time is one " read " to the Royal Irish Academy in 1824, but never completed. It is called "On the Improvement of the Double Achromatic Object Glass," with special application to the correction of spherical aberration and coma in an infinitely thin system.

There is an Appendix by the editors that elucidates many historical and mathematical points. Specially interesting are Notes 14 and 20. The first sets out briefly the relation of Hamilton's optical methods to dynamics, and the second shows how Schrödinger developed his Wave Mechanics from Hamilton's ideas.

This volume of Hamilton's Mathematical Papers is the first contribution to the most fitting memorial to Ireland's greatest mathematician. It is printed and produced in the characteristically efficient manner that one associates with the mathematical productions of the Cambridge University Press.

Alcoholic Fermentation. By ARTHUR HARDEN, Ph.D., D.Sc., LL.D., F.R.S. Fourth and New Edition, 1932. (London: Longmans, Green & Co. Price 15*s.* net.)

THE last edition of Professor Harden's well-known work was published in 1923 and comprised 157 pages of text and 31 pages of Bibliography. In the present volume the subject-matter has been extended to 198 and the Bibliography to 38 pages. The publication of this work almost coincides with the retirement of the author from the Headship of the Chemistry Department at the Lister Institute, and it is fortunate that Professor Harden has so soon found opportunity to summarize the present position of the branch of biochemistry which he has done so much to advance. The number of publications, both from his own and other laboratories, devoted to some aspect of the study of the hexose-phosphates is an enduring monument to the epoch-making observation of Harden and Young on the influence of phosphates on the fermentation of sugar by yeast-juice, which was communicated to the Chemical Society on June 1st, 1905. Although the

importance of this discovery was at once recognized, it would have been difficult to foresee at that time the wide-reaching biochemical significance to which it has since attained.

An illuminating aspect of modern work in biochemistry is the frequency with which a mechanism established for one type of metabolic change is later found to bear closely on some biochemical process which at first appears unconnected.

The author (on p. 17) writes :—" The mechanism for the decomposition of the sugar molecule is not confined to the yeast-cell, for it has been found that the same processes are involved in the conversion of carbohydrate into lactic acid in muscle, and in the decomposition of carbohydrates by bacteria, moulds, and the higher plants." And again (on p. 75) : " Phosphate plays an essential part in the decomposition of carbohydrates both in the yeast-cell and in the animal organism." The high degree of specialization which, however, characterizes many biochemical processes is illustrated by recent work on the part played by pyrophosphoric acid in the chemical changes occurring in yeast and in muscle.

The use of the enzyme known as bone phosphatase is mentioned on several occasions. The value of this book to the general biochemist would have been, if possible, enhanced by a short account of the work of Robinson which led to the detection of this enzyme and to the determination of the part it plays in ossification in animals. This most valuable outcome of Harden and Young's work could hardly have been foreseen at the time of their first communication in 1905.

In the last edition the views of Neuberg on the mechanism of alcoholic fermentation and the results obtained on addition of foreign substances (" traps ") to the fermenting medium were fully described. His striking experiments were, however, somewhat lacking in completeness, since methylglyoxal had at that time never been isolated from fermenting solutions, while the recognition of pyruvic acid rested on experiments the interpretation of which was in dispute. Further evidence of the participation of both methylglyoxal and pyruvic acid in alcoholic fermentation has now been obtained by Neuberg. The fermentation of magnesium hexose phosphate by sterile dried yeast preparations in which the activity of the co-enzyme has been impaired by treatment with toluene, bromo-benzene, ether, etc. can be partially arrested at either the methylglyoxal or pyruvic acid-glycerol stages, and these intermediate compounds isolated as crystalline derivatives. Glycerol and pyruvic acid have now been obtained from glucose by living yeast also. This work is summarized in the new edition and forms an interesting extension of another fundamental research of Harden and Young—that on the co-enzyme of yeast-juice.

One of the most important advances recorded in the new edition is the recognition of the hexose diphosphate of yeast fermentation as a 1 : 6-diphosphate of fructofuranose. A hexosemonophosphate also formed in the alcoholic fermentation of sugar is probably a

6-phosphoric ester of an aldopyranose. Chapter III. contains a valuable summary of this and other work on the constitution of the various hexose-phosphates. Recent studies of the effect of sodium fluoride, iodoacetic and bromoacetic acids on fermentation, and on formation of lactic acid by muscle, which appear to open up a wide field of work, are also summarized.

The Atomic and Molecular Forces of Chemical and Physical Interaction in Liquids and Gases, and their Effects. By R. D. KLEEMAN, B.Sc., B.A., D.Sc. [Pp. vi+133.] (London : Taylor & Francis. Price 10s. 6d. net.)

THE extensive researches of Dr. Kleeman in this subject are well known from his many contributions to scientific journals. In this book he has attempted to weld together his results into a connected whole. The problem is attacked from a classical thermodynamic standpoint. Functional properties of the law of force between atoms and molecules in gases and liquids are obtained, and are used to deduce relationships for and between various properties, such as latent heat, specific heat, viscosity, surface energy, coefficient of expansion, critical quantities, etc.

In view of the complexity of the problems considerable freedom must admittedly be allowed in assumption and approximation. While Dr. Kleeman makes ample use of this freedom, the experimental evidence he adduces in support of the relationships deduced shows that, even if they are regarded as more or less empirical, they are bound to have at least a pragmatic importance for the physical chemist.

The striking way in which it is shown how the sum of the square roots of the atomic weights of the atoms in a molecule is related to so many physical properties cannot fail to excite interest and to give food for thought to the theoretical physicist.

The arrangement of the book makes the absence of an index more than usually inconvenient.

The Combination of Observations. By DAVID BRUNT, M.A., B.Sc. Second Edition. [Pp. 239.] (Cambridge University Press, 1931.)

THIS is a useful text-book dealing in the main with the method of Least Squares, but it contains also a few other statistical problems. The first part deals with the method of Least Squares : it contains a chapter on Errors of Observation, the Gaussian Error Law, the case of one and more than one Unknown, the Weight of Observations, the problem of the Most Probable Values of the Unknown, the case of Conditioned Observations and the Rejection of Observations. The other chapters deal with alternatives to the Normal Error Law (method of moments, Pearson's types and Charlier's formula), Correlation (including the Theory of Contingency and of Partial Correlation), Harmonic Analysis (Fourier Series), and Periodogram Analysis.

CII. *Proceedings of Learned Societies.*

GEOLOGICAL SOCIETY.

February 24th, 1932.—Sir Thomas Henry Holland, K.C.S.I.,
K.C.I.E., F.R.S., President, in the Chair.

THE following communication was read :—

' The Geology of the N'Changa District, Northern Rhodesia.
By Gerald Christopher Arden Jackson, D.Sc. M.A.Sc. D.I.C.
F.G.S. (Read, in the absence of the Author, by Prof. C. G.
Cullis, D.Sc. F.G.S.)

The paper treated of the general geology, petrology, corre-
lation, and structure of the N'Changa district, Northern
Rhodesia.
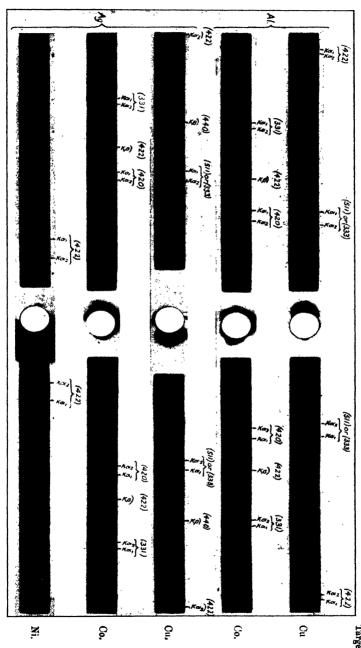
The area, which forms part of the original Rhodesian Congo-
Border Concession, covers approximately 800 square miles,
and lies immediately to the south of the Belgian Congo border.
It is a wooded peneplain, underlain by four principal series
of ancient metamorphosed and unfossiliferous sediments :
namely, Basement Schists, Muva Series, Bwana M'Kubwa
Series, and Kundelungu Series. Into these have been intruded
batholiths and stocks of grey and red granites and ada-
mellites, and sill-like masses of scapolitized and uralitized
gabbros and norites. The Basement Schists and Muva Series
have, in addition, been invaded by large granitic intrusions
of pre-Bwana M'Kubwa age : namely, the Muliashi porphyritic
granite-gneiss, and possibly the M'Kushi granite-gneiss.

The complex ranges from the Archæan to possibly the Lower
Palæozoic in age. The shaly and arkosic members of the
Lower Bwana M'Kubwa Series and its equivalents contain
the enormous replacement copper deposits occurring in
Northern Rhodesia. The copper mineralization is attributed
to late-stage pneumatolytic action which accompanied the
intrusion of the younger grey and red ' granites'. Details of
the ores and related economic problems of the N'Changa
mineralized zone are treated by the Author in a separate paper.
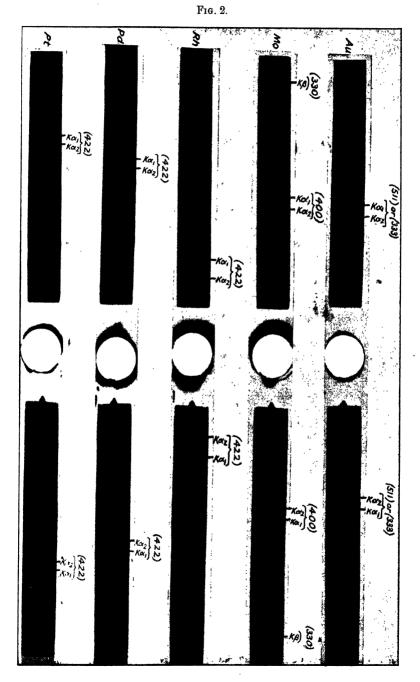
Petrological descriptions were given of all the principal rock
types, and their distribution and correlation were discussed.
Many interesting rocks were described, including a suite of
gabbros and norites exhibiting progressive stages of auto-
scapolitization.

FIG. 1.

Fig. 2.

CIII. *On the Variation of the Resistance of Thermionic Valves at High Frequencies.* By S. K. MITRA, *D.Sc., Khaira Professor of Physics, and* BHABANI CHARAN SIL, *M.Sc., Khaira Research Scholar in Physics, Calcutta University* *.

1. INTRODUCTION.

THE influence of electrons and ions in changing the dielectric constant and conductivity of a gas has of late received a good deal of attention on account of its bearing on the mode of propagation of radio waves in the ionized upper atmosphere †. The nature of the influence can be most easily understood by considering the behaviour of an electron situated between the plates of a unit condenser in vacuum ‡. An alternating voltage applied to the plates sets the electron in motion, and the current produced thereby lags a quarter period behind the applied voltage. The effect of such an electron in motion can be shown to be equivalent to that of a self inductance of value $L = \dfrac{m}{e^2}$, shunted across the unit condenser. This effective self

———

* Communicated by the Authors.

† Eccles, Proc. Roy. Soc. A, lxxxvii. p. 79 (1912); Salpeter, *Phys. Zeit.* xiv. s. 20 (1913); Larmor, Phil. Mag. (6) xlviii. p. 1025 (1924); Elias, *Jahrb. f. drahtl. Tel.* Band xxvii. (1926); Lassen, *Jahrb. f. drahtl. Tel.* Band xxviii. (Nov. 1926).

‡ P. O. Pedersen, 'Propagation of Radio Waves,' published by Denmarks Naturvidenskabelige Samfund, p. 87 (1927).

inductance in its turn may be regarded as equivalent to a reduction in the dielectric constant of the medium by an amount $\Delta\xi = \dfrac{4\pi e^2}{\omega^2 m}$ (e, ω, m having their usual significance). It should be noted that since the electron is moving in free space devoid of matter, it does not on the whole cause any dissipation of energy. During part of the cycle it absorbs energy from the field and is set in motion, and during another part it gives energy back to the field and is brought to rest. The resistance of the medium thus remains infinite, as it had been previous to the introduction of the electron. If, instead of a single electron, there are N electrons, the expression for the dielectric constant is correspondingly modified. It is interesting to note that even in the case of a swarm of N electrons there is no loss * of electrical energy due to collision among the electrons themselves, and consequently the resistance of the medium might still be regarded as infinite.

Conditions are changed, however, if the electrons move in a gas atmosphere and collide with the molecules. In this case the molecules of the gas-filled space absorb energy from the electrons and the resistance of the space is brought down from infinity to some finite value. The expressions for the dielectric constant and the conductivity in this case are modified as follows † :

$$\Delta\xi = -N\frac{4\pi e^2}{m}\cdot\frac{1}{\omega^2+v^2} = -K \text{ (say)}. \quad . \quad . \quad (1)$$

$$\sigma = -\frac{v}{4\pi c^2}\cdot K, \quad . \quad . \quad . \quad . \quad . \quad . \quad (2)$$

where v is ʃthe number of collisions per second between electrons and gas molecules.

During recent years a large number of investigations have been carried out to measure the dielectric constant at various frequencies, either of an ionized gas in which both electrons and gas molecules are present ‡, or of a pure

---

* Pedersen, Proc. Inst. Rad. Eng. xvii. p. 1762 (Oct. 1929).

† Pedersen, 'Propagation of Radio Waves,' p. 91. See also Benner, *Annalen der Phys.* (3) vii. p. 993 (1929).

‡ Bergmann & Düring, *Ann. der Phys.* ser. v. vol. i. no. 48 (May 1929); Appleton & Childs, Phil. Mag. (10) lxvii. p. 969 (Dec. 1930); Jonescu & Mihul, *Compt. Rendus*, cxci. (Dec. 1930). See, however, H. Gutton & J. Clement, *Compt. Rendus*, clxxxiv. (Feb. 1927); criticism thereto by Pedersen, *loc. cit.* p. 93, Bergmann & Düring, *loc. cit.*, and reply by H. Gutton, *L'onde Électrique*, vii. (Jan. 1928) and *Annales de Physique*, xiii. (Jan. 1930).

electronic atmosphere as may be found in a highly evacuated triode value *. Results show that a change in the dielectric constant is produced in the same sense as indicated by the above theory when extraneous causes are eliminated. Comparatively little work seems to have been done on the measurement of the conductivity, especially its variation with frequency. The purpose of the present paper is to investigate, both theoretically and experimentally, the change produced in the conductivity of a space containing free electrons and bounded by two electrodes (as is usually found in a thermionic valve) when a high-frequency E.M.F. is applied across the electrodes.

From what has been said before it might appear that in the high vacuum of a triode valve, where the collisions between electrons and the remnant gas molecules are few and far between, the only effect of high frequency will be to produce an oscillatory motion of the electrons resulting in a slight reduction in the capacity due to the inertial effect. Since there is no collision there is no dissipation of energy, and, consequently, there is no change of resistance. But it must not be lost sight of, that though the electrons do not collide with any gas molecules, they do collide with the electrodes where they give up both their kinetic energy and their charges. In this respect the resistance of a triode valve differs from an ordinary resistance. When a current flows through an ordinary resistive medium the dissipation of energy occurs in the medium itself, the electrodes merely acting as current leads ; but in a thermionic valve, on account of the scarcity of gas molecules, the dissipation of energy occurs not in the interelectrode space but rather in the electrodes themselves, which not only lead the current in and out, but also dissipate the kinetic energy of the electrons converting it to heat. In fact, the dissipation of energy depends entirely upon the number of electrons reaching the plate and on their kinetic energy, the latter being independent of the paths by which the electrons might have travelled up to the plate.

We will show in the present paper that if we assume the electrons in the interelectrode space to be endowed with

---

* Benham, Phil. Mag. (7) xi. p. 457 (Feb. 1931, Suppl.) ; Hartshorn (Proc. Phys. Soc. xli. p. 113) seems to have obtained a variation of interelectrode capacity in the opposite sense to that of the Eccles-Larmor theory. This result, as well as a similar one obtained by Ballantine (Journ. Frank. Inst. ccvi. no. 2, p. 159 (Aug. 1928)), can be explained as due to neglecting the inertial effect of the electrons. *Cf.* Benham, *loc. cit.* p. 473 ; also Wireless Eng. and Exp. Wireless, viii. p. 489 (Sept. 1931).

a Maxwellian distribution of velocity, then the number of electrons reaching the plate per unit time under the action of an applied E.M.F. will depend not only on the magnitude of the E.M.F. but also on its duration, specially when it is so small as to be comparable with the time of flight of the electrons from one electrode to another. As the duration of the pulse is diminished, or in other words, as its frequency is increased, the number of electrons reaching per unit time will diminish and the resistance will increase [*].

That the number of electrons striking the plate will depend upon the frequency is also seen from the fact that the amplitude of the electron moving under the action of an alternating field is given by $\dfrac{e\mathbf{F}_m}{\omega^2 m}$ ($\mathbf{F}_m$ is the peak value of the applied alternating field). As the frequency is raised the amplitude is diminished, and the electrons have less chance of reaching the plates, which form as it were the boundary of the space containing the electrons. It will also be shown that this hypothesis is fully borne out by experimental result. It should be noted that the sense of the change of resistance with frequency is the same as that given by equation (2) for the case of an ionized gas. A rise in frequency is accompanied by a rise in resistance. This must be so because the mechanism of the loss of energy is the same in both cases. In the one the gas molecules on either side of the oscillating electron form the boundary, and in the other these are replaced by the walls of the electrodes which restrict the amplitude of the electrons.

2. Theory of the Variation of Resistance with Frequency.

Consider an electron situated midway between the plates of a parallel plate condenser. Under the action of the high-frequency E.M.F. the electron will oscillate about its mean position provided the peak value of the high-frequency E.M.F. is not sufficiently high to drive it to one of the

---

[*] In the paper already referred to, and also in Expt. Wireless, viii. pp. 415–16 (Aug. 1931), Hartshorn shows that the resistance of the thermionic valve at very high frequencies should be *smaller* than that at very low frequencies by about 11 per cent. The results obtained by us show that at very high frequencies the resistance *increases* with the rise of frequency. The considerations on which Hartshorn's results are based are altogether different from ours. Moreover, we have found an *increase* in resistance of more than 100 per cent. in going from 10^7 to 6×10^7 cycles, as against Hartshorn's *decrease* of only 11 per cent. in oing from very *low* to very high frequencies.

condenser plates. As mentioned in the introduction, the presence of this oscillating electron will, on the average, cause no dissipation of energy in the condenser. During one part of the cycle it will absorb energy and will be set in motion, and during another part this energy will be given back to the electric field between the plates.

Let us now consider what will happen if the electron is driven to one of the plates. The electron gives up its charge as well as its kinetic energy to the plate. The former gives us the conduction current and the latter is spent in heating the condenser plates. We are now justified in conceiving the space between the plates as having a finite conductivity or resistance, and the latter is measured in the usual way by dividing the applied voltage by the quantity of electricity carried to the plate per unit time under the action of the voltage.

Now suppose that the space between the condenser plates contains a source of electrons which replenishes the electrons lost by absorption in the plate. Let us further suppose that the electrons are endowed with a Maxwellian distribution of velocity.

If an alternating voltage is applied between the two plates of the condenser, the electrons coming out of the source will oscillate within the space between the plates. When one of the plates becomes positive during a half cycle, the electrons which were moving towards that plate are caught by the electric field and carried to the plate. If the frequency of alternation is not high, some of those which were at rest, and even some of those which were moving in the opposite direction to the field, will also reach the plate and give up their charges to it.

Now let t be the time during which the positive half of the impressed high-frequency E.M.F. (supposed to be constant during the interval) acts, and let n be the number of electrons reaching the plate during this time. Then the conductivity is evidently given by $\frac{ne}{tV_a}$, where V_a is the potential difference between the plates. A little consideration will show that the quantity $\frac{n}{t}$ is not constant, as is usually supposed, but that it depends on t. This is particularly so when the time-period $2t$ of the high frequency impressed E.M.F. becomes comparable with the time taken by the electron to reach the plate. The following will make the point clear :—

Take the case of an electron at a distance s from one of

the condenser plates and moving with a velocity v_0 along s towards it. Let the velocity v_0 be such that the electron, if left to itself, will fail to reach the plate during the time t. If, however, a field is applied between the plates, then it is possible that, under the influence of this field, the electron will be able to strike the plate and give up its charge to the latter. It is, therefore, possible to find a critical velocity v_0, with which the electron must be moving initially in order that the applied field of frequency $\frac{1}{2t}$ is just able to carry the electron to the plate at the end of the interval t. It is evident that all the electrons which have been moving with a velocity greater than this critical velocity v_0 at the instant when the field began to act will also reach the plate within the time t. The number of electrons reaching the plate will thus depend not only on the time t but also on the total number of electrons lying within the velocity range v_0 to ∞. In fact, this latter is a measure of the conductivity of the space between the condenser plates for the particular frequency to which the critical velocity v_0 corresponds.
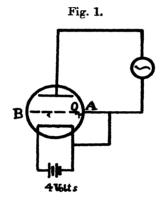
The problem of finding out the conductivity for a particular frequency $f = \frac{1}{T}$ (where T is the time period of alternation) is thus reduced to finding out (a) the critical initial velocity v_0, such that an electron moving initially with this velocity is just able to reach the plate at the end of the period $\frac{T}{2}$, during which the impressed E.M F. acts in one direction, and (b) calculating the number n of electrons moving in the velocity range v_0 to ∞. The conductivity for the particular frequency $\frac{1}{T}$ is then proportional to n.

3. CALCULATION OF THE CHANGE OF RESISTANCE WITH FREQUENCY.

As it was inconvenient to obtain a parallel plate condenser with a source of electrons between its plates, the condenser actually employed for the measurement was a cylindrical one formed by the grid and the plate of a triode valve. The source of the electrons, namely, the filament being along the axis of the cylindrical condenser was outside the condenser space. But the electrons emitted from the filament had sufficient thermic velocity to reach the plate-grid condenser space through the mesh of the grid. The conductivity

of this space as modified by the presence of the electrons was measured for various frequencies by the distuning method to be described later. The grid was normally connected to the negative of the heating battery, and the high-frequency E.M.F. for measuring the resistance was applied between the grid and the plate (fig. 1). We will therefore proceed to calculate, on the basis of the theory outlined in the preceding section, the variation of the resistance of this space with frequency due to the presence of electrons with a Maxwellian velocity distribution.

It will be observed that in order to reach the plate the electrons have to move in two distinct fields of force : (*a*) the field between the filament and the grid-cylinder; and (*b*) that

Fig. 1.

4 Volts
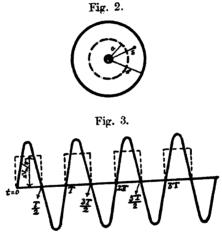
between the grid-cylinder and the plate when the impressed E.M.F. was acting. By " grid-cylinder " we mean the imaginary cylindrical surface on which the grid wire is coiled in the form of a helix. The potential of the grid-cylinder is not in general the same as the potential of the grid wire. Its potential V_0 is a function of μ, the amplification factor of the valve, of V_a the anode potential, and of V_g the grid potential, and is given by the formula

$$V_0 = \frac{\mu V_g + V_a}{\mu + 1}. \quad \cdots \cdots (3)$$

3 (1). *Some Simplifying Assumptions.*

In order to carry out the above calculations and arrive at a formula giving the proportionate number of electrons which will reach the plate corresponding to a particular

time-interval t, we will make a number of simplifying assumptions as described below :—

(a) The high-frequency voltage used in the measurement varied sinusoidally, as shown by the full line curve, fig. 3. We will, however, assume that the time-voltage curve is as shown by the dotted line. In other words, we assume that in the positive half-cycle the voltage suddenly rises from zero value to the value $\dfrac{2V_m}{\pi}$ at $t=0$, T, 2T, etc., maintains that value during the intervals $t=0$ to $t=\dfrac{T}{2}$, $t=T$ to $t=\dfrac{3T}{2}$, etc., and then suddenly drops to zero value again at $t=\dfrac{T}{2}$, $\dfrac{3T}{2}$, etc.

Fig. 2.

Fig. 3.

V_m being the peak value of the high-frequency voltage, $\dfrac{2V_m}{\pi}$ is obviously the mean value during one half-cycle.

We are not concerned with what happens during the negative half-cycle, because no current flows during this period and nothing is contributed towards the conductivity.

In the actual experiment the value of $\dfrac{2V_m}{\pi}$ was ·21 volt.

(b) In calculating the time taken by the electron to reach the plate under the influence of the impressed plate-grid voltage, we will assume that the source of electrons is the grid-cylinder and that the electrons reaching the plate are all drawn from this region. Thus if V_x is the potential at

a point distant x from the end A of the grid-cylinder (fig. 1) then the concentration in the neighbourhood of x is in accordance with Boltzmann's law $N e^{-\frac{\varepsilon V_x}{KT}}$, where N is the electronic concentration near A. Thus the contribution to the plate current from any portion of the cylinder varies exponentially with the potential at that point.

(c) Since there is a drop of 4 volts along the filament due to its resistance, it follows that the voltage of the grid-wire is not constant throughout its length with respect to the portion of the filament immediately in front of it, i. e., the portion of the filament near the foot of the perpendicular dropped from the point under consideration (of the grid-wire) on to the filament. The voltage varies between zero at A to −4 volt at B (fig. 1). The voltage along the length of the plate also varies in a like manner. During the positive half-cycle it varies between ·21 at A to −4+·21 at B, and during the negative half-cycle between −·21 at A to −(·21+4) at B. Due to the joint influence of the plate voltage and the grid voltage, the voltage along the grid-cylinder varies between ·035 volt at A to −3·3 volt at B during the positive half-cycle, and between −·035 at A to −3·37 at B during the negative half-cycle (see equation (3)). The mean voltage drop along the grid-cylinder thus varies between 0 at A to −3·335 volt at B.

(d) During the positive half-cycle the voltage of the grid-cylinder has a value ·035 volt at A and −3·3 volt at B, the variation along the length being linear. It is easy to calculate that at the point O (fig. 1), distance ·02 cm. from A, the voltage of the grid-cylinder with respect to the portion of the filament "in front of it" is zero. (The total length of the grid-cylinder is 2 cm.) We divide the grid-cylinder into two portions, P and Q. Portion P from the end A to 0 is taken to be approximately at the same potential as that of the point A, namely, ·035 volt, and portion Q from the point O to the end B is everywhere lower than the potential of the filament, being zero at O and −3·3 volt at B. On the assumption (b) that the electrons drawn to the plate all come from the neighbourhood of the grid-cylinder and that the contribution from any portion is proportional to the concentration there, we can find out the comparative contributions to the plate current by the two portions P and Q of the grid-cylinder. The contribution by the portion P is proportional to ·02N, since N is the concentration near A

and it has been assumed to be constant over the small length ·02 cm., A to O. The contribution by the portion Q is given by $N \int_{0}^{1\cdot 98} \epsilon^{-\frac{eV_x}{KT}} dx$, where V_x is the potential at a distance x from O. The expression when evaluated gives for the value of the contribution by the portion Q as proportional to ·021 N approximately. It is thus seen that although the portion P is only one-hundredth part in length of the portion Q, yet the contribution from the former is nearly the same as that from the latter.

(*e*) The electrons which reach the anode might be divided into three groups in accordance with the nature of the paths they follow :—

(i.) Electrons which start from the grid-cylinder and move outward towards the anode in a radial direction.

(ii.) Electrons which start from the grid-cylinder and move inward towards the filament in a radial direction. Of these, those which start from the region Q of the grid-cylinder move in an accelerating field and have no chance of returning back to the grid-cylinder. But those which start inward from region P are moving in a retarding field and consequently may turn back if the retarding field produced during the positive half-cycle of the impressed E.M.F. is sufficiently strong. Such electrons thus repass through the grid-cylinder and reach the plate by the action of the impressed field between the grid and the anode.

(iii) The electrons which move inwards but, instead of travelling in a radial direction, leave the grid-cylinder obliquely, get past the filament, and return after describing an orbit round the filament.

3 (2). *Calculation of the Time of Flight of the Electrons.*

We will now proceed to calculate the time taken by electrons of classes (i.) and (ii.) to reach the anode for various initial velocities. It has not been found possible to calculate with any degree of approximation the time of passage for class (iii.), and the contribution to the conductivity of this group of electrons has been neglected. To this reason might be attributed the discrepancy between the calculated and the observed values of the conductivity which has been found for the case of large time-intervals (low frequencies).

(a) *Time of flight for an electron of class* (i.) *from grid to anode.*—Let the electron be at a distance S from the centre of the filament (fig. 2). If an electric field is applied between the grid and the plate, the plate being at a higher potential, the force on the electron will vary inversely as its distance S from the centre of the filament. Since the force is in a direction away from the filament, the equation of motion of the electron may be written as

$$\frac{d^2 S}{dt^2} = \frac{K}{S}.$$

If F_m is the peak value of the impressed high-frequency oscillations between grid and plate, then, in accordance with assumption (3·1 a)

$$K = \frac{2 F_m}{\pi m}.$$

Integrating the equation, we have

$$\frac{1}{2}\left(\frac{dS}{dt}\right)^2 = K \log S + C.$$

Let the initial velocity of the electron be v_0, *i. e.*,

$$\frac{dS}{dt} = v_0, \text{ when } S = a.$$

Then

$$C = \tfrac{1}{2} v_0^2 - K \log a,$$
$$= K \log P, \text{ say}$$

where

$$P = \epsilon^{\left(\frac{1}{2K} v_0^2 - \log a\right)}.$$

Thus

$$\frac{dS}{dt} = \sqrt{2K \log PS}.$$

∴

$$t = \frac{1}{\sqrt{2K}} \int_a^b \frac{dS}{\sqrt{\log PS}}.$$

Put $\log PS = y$.

Then

$$t = \frac{1}{\sqrt{2K}\, \epsilon^{\left(\frac{1}{2K} v_0^2 - \log a\right)}} \int_{\frac{1}{2K} v_0^2}^{\frac{1}{2K} v_0^2 + \log \frac{b}{a}} y^{-\frac{1}{2}} \epsilon^y \, dy$$

$$= \frac{1}{\sqrt{2K} \, \epsilon^{\left(\frac{1}{2K}v_0{}^2 - \log a\right)}} \left[\int_0^{\frac{1}{2K}v_0{}^2 + \log \frac{b}{a}} y^{-\frac{1}{2}} \epsilon^y \, dy - \int_0^{\frac{1}{2K}v_0{}^2} y^{-\frac{1}{2}} \epsilon^y \, dy \right].$$

The integrals are of the form $\int x^{-\frac{1}{2}} \epsilon^x \, dx$, and for obtaining numerical results the following series expansion may be used :

$$\int x^{-\frac{1}{2}} \epsilon^x \, dx = \frac{\epsilon^x}{x^{\frac{1}{2}}} \left[1 + \frac{1}{2x} + \frac{3}{(2x)^2} + \frac{3 \cdot 5}{(2x)^3} + \ldots \right],$$

also

$$= \frac{\epsilon^x}{x^{\frac{1}{2}}} \left[2x - \frac{(2x)^2}{3} + \frac{(2x)^3}{3 \cdot 5} - \ldots \right].$$

From these equations the values of t are found for different values of v_0.

(b) *Time of flight of the electrons of class* (ii.), *grid to filament and back to anode.*—As mentioned previously, electrons moving inward radially from the grid-cylinder towards the filament may also reach the plate under the influence of the positive field developed between the grid-cylinder and the filament due to the impressed E.M.F. between the former and the plate. The process is as follows :—An electron starting inward with velocity v_0 from the region P (see assumption 3·1 d) of the grid-cylinder is caught up in a retarding field between the grid-cylinder and the filament, and its velocity is reduced to zero in time t_1 after it has travelled a certain distance "d." It then moves back towards the grid-cylinder and reaches the same after another lapse of time t_1. Thenceforward it moves in the accelerating field between the grid-cylinder and the plate and reaches the latter after a further lapse of time t_2. The total time taken by the electron to reach the plate is thus equal to $t = t_1 + t_1 + t_2$. t_2 can be calculated as in the previous case. In order to calculate t_1 the equation in case (a) has to be slightly modified. As before, we have

$$\frac{1}{2} \left(\frac{dS}{dt} \right)^2 = K \log S + C.$$

Let the velocity be reduced to zero when the electron has traversed inward a distance d in time t_1·

Then $\dfrac{dS}{dt} = 0$, when $S = d$.

Thus $$C = -K \log d,$$

and $$\frac{1}{2}\left(\frac{dS}{dt}\right)^2 = K \log \frac{S}{d}.$$

When $S = a$, *i. e.*, when the electron reaches the grid-cylinder its velocity v_0 is given by

$$\tfrac{1}{2}v_0^2 = K \log \frac{a}{d},$$

v_0 is obviously also the initial negative velocity of the electron at the moment when the field is applied.

To find the time t_1 taken by the electron to move from $S = d$ to $S = a$, we have

$$\frac{dS}{dt} = \sqrt{2K \log \frac{S}{d}}.$$

$$\therefore \qquad t_1 = \frac{1}{\sqrt{2K}} \int_d^a \frac{dS}{\sqrt{\log \frac{S}{d}}}.$$

Changing the variable by putting

$$y = \log \frac{S}{d},$$

we have $$t_1 = \frac{d}{\sqrt{2K}} \int_0^{\log \frac{a}{d}} y^{-\frac{1}{2}} \epsilon^y \, dy.$$

We can now employ the series expansion as in the previous case and deduce the numerical value of t_1, for various values of d and corresponding values of v_0. The actual time taken by an electron of class (ii.) to reach the plate is thus equal to $t = t_1 + t_1 + t_2$.

3 (3). *Calculation of the Conductivity.*

The value of v_0 thus obtained gives for the two cases the critical velocity with which the electrons must leave the grid-cylinder in order to reach the plate in the time t under the influence of the impressed E.M.F. V_m. As indicated before it is obvious that all electrons starting with velocity greater than v_0 will also reach the plate within the scheduled time t. The total number of electrons n reaching the plate will therefore be the time-interval t multiplied by the
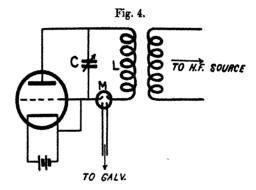
number of electrons lying within the velocity range v_0 to ∞, and is therefore given by

$$ t\mathrm{N}\sqrt{\frac{m}{2\pi \mathrm{KT}}}\int_{v_0}^{\infty} \epsilon^{-\frac{mv_0^2}{2\mathrm{KT}}}\,dv_0. $$

The conductivity of the grid-plate space for the high frequency impressed E.M.F. of periodicity $\mathrm{T}=2t$ is thus proportional to n

$$ = \frac{t\mathrm{N}}{2t}\sqrt{\frac{m}{2\pi \mathrm{KT}}}\int_{v_0}^{\infty} \epsilon^{-\frac{mv_0^2}{2\mathrm{KT}}}\,dv_0 $$

$$ = \frac{\mathrm{N}}{2}\sqrt{\frac{m}{2\pi \mathrm{KT}}}\int_{v_0}^{\cdot} \epsilon^{-\frac{mv_0^2}{2\mathrm{KT}}}\,dv_0. $$

All the quantities in the expression are known except N.

Fig. 4.

TO H.F. SOURCE

TO GALV.

Hence the fraction $\dfrac{n}{\mathrm{N}}$ of the total number of electrons N reaching the plate for a particular velocity v_0 corresponding to a frequency $f=\dfrac{1}{2t}$ can be calculated. The conductivity of the grid-plate space is evidently proportional to this number.

4. EXPERIMENT AND RESULT.

As mentioned previously, the resistance of the grid-plate space was found by the distuning method. The experimental arrangement is shown diagrammatically in fig. 4. The resistance of the oscillatory circuit associated with the valve, consisting of the condenser C in parallel with the

condenser formed by the grid-plate capacity, and the thermo-junction M in series with the inductance L is first determined with the filament of the valve cold. This resistance R_1 includes the total loss resistance in the circuit such as losses in the condenser, in the valve legs, high-frequency resistance of the coil, the resistance of the thermo-junction, etc. The resistance is again measured (R_2) with the filament lighted. The resistance R_2 consists of the previous resistance R_1, together with the equivalent series resistance r due to the conductivity acquired by the plate-grid space owing to the presence of the electrons. The difference $R_2 - R_1$, which gives the equivalent series resistance, is related to the con-ductivity $\frac{1}{r'}$ of the grid-plate space by the relation

$$r = \frac{1}{r'} \cdot \frac{1}{\omega^2 C^2}.$$

If a condenser is shunted by an ordinary non-inductive resistance of value r', then the value as determined by the above method for various frequencies is found to be sensibly constant. But, for the shunt-resistance formed by the grid-plate space of a glowing valve, this resistance is not constant, but varies in accordance with the formulæ derived in the previous section.

The distuning method of measuring resistance of an oscillatory circuit * consists, as is well known, in noting the value of the current, first, while it is in resonance with the impressed high-frequency oscillations, and again, while the reactance of the circuit has been varied by slightly distuning the circuit.

The formula employed in the calculation was

$$R = \frac{153\lambda_m(C_2 - C_1)}{C_0^2},$$

where R is the total resistance of the circuit, λ_m is the resonant wave-length of the circuit, C_0 the capacity for resonance condition, and C_2 and C_1 are the altered values of the capacity, respectively greater and less than C_0, to bring the resonant current to ·71 of its original maximum value.

Table I. shows the proportionate number of electrons reaching the plate for different frequencies, *i. e.*, the pro-portionate conductivity of the plate-grid space for different

---

* E. B. Moullin, ' Radio Frequency Measurements,' 2nd ed. p. 276 (1931). (Charles Griffin & Co.)

wave-lengths of the high-frequency oscillating field. Table II. shows the values of the resistance of the plate-grid space, obtained experimentally for different wave-lengths.

Curve A (fig. 5) shows the relation between wave-length and the resistance, obtained by calculation. Curve B shows

TABLE I.

Frequency.	n Conductivity $\overline{N}$ × const.	Wave-length (λ) (metres).	$\frac{1}{n}$ Resistance $\overline{N}$ × const.
6·8 × 10⁷	1·683 × 10⁻⁸	4·41	·594 × 10⁸
5·3 × 10⁷	1·994 × 10⁻⁸	5·06	·501 × 10⁸
4·21 × 10⁷	2·43 × 10⁻⁸	7·11	·411 × 10⁸
3·77 × 10⁷	2·636 × 10⁻⁵	7·95	·379 × 10⁵
3·2 × 10⁷	3·135 × 10⁻⁸	9·37	·318 × 10⁸
2·8 × 10⁷	3·484 × 10⁻⁸	10·71	·287 × 10⁸
1·026 × 10⁷	2·116 × 10⁻⁸	29·2	·236 × 10⁸
8·65 × 10⁶	2·214 × 10⁻⁸	34·6	·225 × 10⁸
8·3 × 10⁶	2·36 × 10⁻⁸	36·1	·220 × 10⁸

TABLE II.

Frequency.	Wave-length (λ) (metres).	Resistance (megohm).
6 × 10⁷	5	·61
3·2 × 10⁷	9·37	·361
2·3 × 10⁷	13	·31
1·75 × 10⁷	17·1	·280
1·2 × 10⁷	25	·255
1 × 10⁷	30	·251

the same relation obtained by actual measurement. In order to compare the two curves, the values of the resistance obtained experimentally were multiplied by a suitable constant. It will be seen that the two curves drawn to the same scale agree with each other very satisfactorily.

As a check on the measurements, the resistance of a noninductive grid-leak of approximately the same value as that

of the plate-grid space was measured simultaneously for the two extreme frequencies. The results (Table III.) show that the high-frequency resistance increases but slightly.

It may be remarked here that calculations show that for time-intervals greater than those corresponding to 36 metres,

Fig. 5.
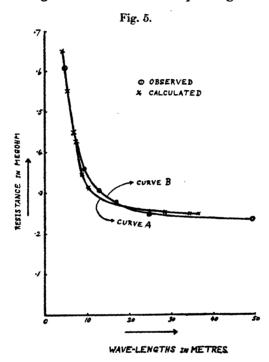
TABLE III.

Frequency.	Wave-length (λ) (metres).	Resistance (megohm).
5.3×10^7	5·6	·226
8.1×10^6	37	·220

the number of electrons reaching the plate under the action of the applied E.M.F. is equal to N. As a consequence the resistance should remain unaltered for all wave-lengths greater than 36 metres. Measurements show, however, that the resistance does increase, though to a smaller extent, for

wave-lengths greater than 36 metres. This is probably due to the fact that we have not been able to take into account the electrons of class (iii.) for which we have not found it possible to calculate the time of flight.

5. CONCLUSION.

Experiments have been made to determine the variation of conductivity of the plate-grid space of a triode valve within the frequency range 10^7 to 6×10^7 cycles per sec. The results show that in going from the lower to the higher frequency, the conductivity decreases by more than 100 per cent. A theory of the variation of resistance has been developed on the following lines :—

It is assumed that the electrons within the plate-grid space have a Maxwellian distribution of velocity. An alternating field applied between the plate and the grid produces in the electrons an oscillatory motion, which is superimposed on their original Maxwellian velocity. The chance of an electron reaching the plate and thereby contributing towards the conductivity of the plate-grid space thus depends both on the time during which the impressed E.M.F. acts in the direction grid to plate and also on the electron's initial thermic velocity of Maxwellian type. It is possible to find a critical velocity v_0 with which the electron must be moving initially in order that the applied field acting for a small interval of time t is just able to carry the electron to the plate. All the electrons which had been moving with a velocity greater than v_0 will also reach the plate within this time t, which is half the time-period T of the applied high frequency E.M.F. The number of electrons reaching the plate per unit time (*i.e.*, the conductivity) for a particular frequency f can thus be found by calculating the critical velocity v_0 corresponding to the time-interval $\frac{1}{2f}$, and determining the number of electrons lying in the velocity range v_0 to ∞. Values of the conductivity calculated on the above hypothesis agree well with the values found experimentally.

Wireless Laboratory,
University College of Science,
Calcutta.
October 13, 1931.

CIV. *The Damping of Pendulums immersed in a Viscous Fluid. By* E. TYLER, *DSc., F.Inst.P., Senior Lecturer, Physics Department, College of Technology, Leicester* *.

INTRODUCTION.

IN an earlier paper †, entitled "The Free Damping of an Aerofoil Pendulum immersed in a Fluid," it has been shown that for an object of aerofoil section attached to the lower end of a vertical reed and free to vibrate with part of it submerged in a stationary fluid, the damping experienced is mainly influenced by the area of projection of the immersed part, when in the undisturbed position, upon a vertical plane perpendicular to that in which the vibrations take place. When such a pendulum is immersed in a steady stream of fluid and free to vibrate at right angles to the flow, provided the speed is sufficient to produce the disengagement of alternate vortices in its wake, as a consequence of such eddy formation, it will be acted upon by periodic forces tending to make it vibrate across the stream. Such a phenomenon was shown in effect by Rayleigh ‡, using a cylindrical pendulum in water, and Riabouchinsky § has subsequently confirmed the condition for maintained vibrations of a pendulum in a current of air, namely, resonance when its natural period coincides with that of the production of pairs of vortices.

This phenomena provides a method for measuring the frequency of vortex formation at varying Reynolds numbers, which many experimenters ‖ have employed.

An attempt to evaluate the strength of the impulses given to a cylinder in water by the shedding of alternate vortices has recently been made by Thom ¶, who, by measuring the amplitude of maintained vibration of the cylinder, together with the corresponding fluid speed, has computed the cross-force in terms of the drag coefficient, the fluid speed, and

---

* Communicated by the Author.

† Tyler, Phil. Mag. xi. (Suppl.) Feb. 1931.

‡ Phil. Mag. xxix. p. 433 (1915).

§ L'Aerophile, 1st Jan. 1911; also Internat. Air Congress, London, 1923. p. 282.

‖ Kruger and Lauth, *Ann. d. Phys.* xliv. p. 801 (1914); Richardson, Proc. Phys. Soc. xxxvi. (1924); Tyler, Phil. Mag., June 1931; Dupin, *Comp. Rend.* cxci. no. 12 (Sept. 1930); Dupin and Crausse, *Comp. Rend.* cxcii. no. 12 (March 1931); Dupin and Teissie-Solier, *Comp. Rend.* cxcii. April 27, 1931; Crausse and Baubiac, *Comp. Rend.* no. 24, June 15th, 1931; also *loc. cit.* no. 22, June 1st, 1931.

¶ Aero. Res. Comm., Rep. and Mem. no. 1373, Dec. 1930; Phil. Mag., Aug. 1931.
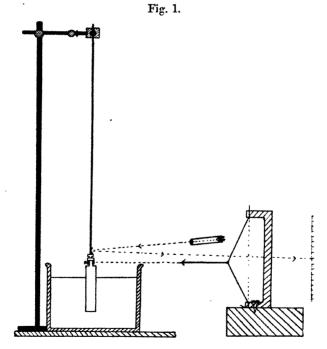
the maximum velocity attained by the cylinder in an alternation. In view of this resonance criterion, it is to be expected that the free vibrations of any pendulum with damping may vary considerably with and without flow, and it is with this primary object that the following investigation appertaining to cylinders and inclined plates in different liquids has been attempted.

The problem was attacked from two directions, namely :—

1. Immersion of cylinders and plates in different liquids at varying depths, and examination of the free damping of the pendulum motion without flow.
2. Repetition of 1, with cylinders in a stream of water at different speeds of flow.

Fig. 1.

EXPERIMENTAL ARRANGEMENT.

The arrangement of suspending the models was similar to that used for the aerofoil pendulum, in which a long steel vertical blade was clamped at its upper end and carried a small metal clamp at its lower, into which was mounted either the cylinder or plate under test (see fig. 1). Rotation

of the clamp in a horizontal plane enabled the plate attached to it to be set at any required angle with the plane of vibration, and the attachment of a mirror to the lower end of the reed permitted, with the aid of a lamp and scale, the pendulum motion to be followed clearly. Throughout the whole work the distance of the lamp and scale was kept fixed with respect to the mirror, namely, 100 cm.

In the first investigation using the cylinders (wood or ebonite), each in turn was immersed vertically to a fixed depth in the given liquid contained in a large circular tank mounted on an adjustable table, and then displaced about 5° from its position of rest.

When the amplitude of vibration had reached a suitable value for observation on the scale, successive amplitudes of swings on the same side of the zero were observed at intervals of two vibrations, until the motion had become practically damped out. The same amplitude was reached each time before observations were made at successive intervals. A similar process was effected repeating with a brass plate in water inclined at varying angles to the plane of vibration and at different depths of immersion.

In the second investigation a water-channel ($150 \times 17 \times 25$ cm.) of the return-flow type was employed, actuated at one end by a motor-driven paddle. The immersed cylinder was set vibrating with and without flow, and the corresponding decay curves obtained in the same way as before, the speed of flow being evaluated by timing the movement of dust particles over the water surface. An electrically heated nickel wire of diameter ·002″, carrying a current of 1 amp., and forming one arm of a Wheatstone bridge, served also in this respect, the wire being previously calibrated on a whirling arm.

The possibility of the walls of the channel influencing the vibrations must not be overlooked, and to test this point, results using the same cylinder both in the large tank and water-channel were compared for equal immersion depths with no flow. In both methods good consistency was obtained, leaving little doubt for any serious discrepancy due to channel-wall interference. The drag influence due to the bottom of the channel was also found negligible with the depths used.
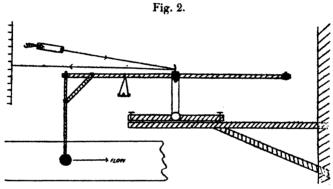
MEASUREMENT OF DRAG COEFFICIENTS.

As it was desirous of knowing these coefficients for the cylinders, an ordinary laboratory balance with extended

arms was employed (see fig. 2), provision being made for mounting the cylinders horizontally and at right angles to the stream, each cylinder being in complete immersion.

Computation of the drag forces was effected by adjusting weights in the small scale pan provided on one arm of the balance. A small correction had to be applied to allow for the drag on the suspension-rod, this being known from previous calibration without the attachment of the cylinder.

In order to measure the linear displacement of the cylinders, two fine pointers were attached, one at the bottom and one half-way up the middle of each cylinder, and their displacements from the vertical determined for various scale-reading deflexions.

Fig. 2.

The differences in the observations of both pointers was so small as to justify the assumption made in the theory, namely, the cylinder as a whole moves with the average displacement of the mid-point at its middle section.

Furthermore, the desirability of measuring the restoring force per unit displacement at the lower end of the blade, or at the middle section and mid-point of the cylinder, necessitated the use of some form of balance capable of operating horizontally and at the same time sensitive to small forces. Fig. 1 shows such an arrangement used.
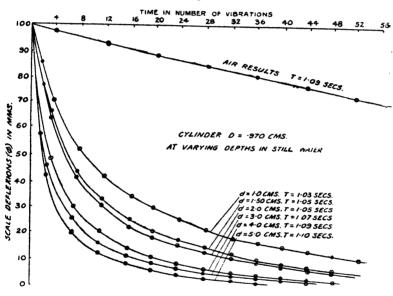
The horizontal displacement of the middle point of a stretched piece of rubber fixed vertically between two clamps, and connected either to the mid-point of the cylinder by a piece of thread or to the lower end of the blade sufficed to yield values of the restoring forces, in terms of the displacements, after calibration had been effected with the rubber-cord in the horizontal position and

weights added to a small scale pan hanging vertically from its mid-point.

RESULTS WITHOUT FLOW.

Fig. 3 exhibits a typical set of decay curves for a cylinder of diameter ·970 cm. immersed in water without flow at different depths, and fig. 4 results for a plate at constant depth, also without flow, but at varying angles of inclination to the plane of vibration.

Fig. 3.

The corresponding log (amplitude) time graphs are shown in figs. 5 & 6, from which it will be observed the vibrations are of two distinct types: (1) with large amplitudes of swing the logarithmic decrement of the damping is not constant, and may be referred as turbulent damping, and (2) with smaller amplitudes there is constancy of the logarithmic decrement, corresponding to the linear parts of the graphs ; this we shall regard as streamline damping.

Analogous effects have been observed by Hoare*, Brindley, and Emmerson, for spherical pendulums suspended by fine wires in a viscous medium.

* Phil. Mag., Aug. 1931.

Fig. 4.

RESULTS IN AIR & STILL WATER AT CONSTANT DEPTH d = 1·50 CMS.
PLATE b = 1·17 CMS

Fig. 5.

CYLINDER D = ·970 CMS.
AT VARYING DEPTHS IN STILL WATER

Fig. 6.

PLATE b = 1.17 CMS
d = 1.50 CMS IN STILL WATER AT
CONSTANT DEPTH d = 1.50 CMS

Fig. 7.

CYLINDERS IN STILL WATER
AT DIFFERENT DEPTHS OF IMMERSION.
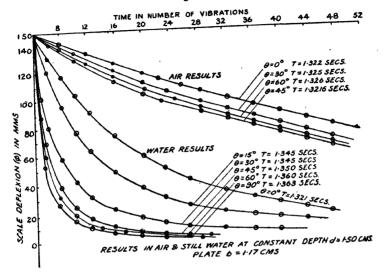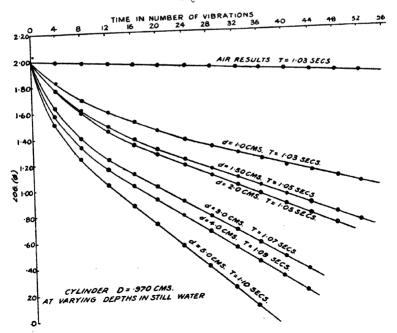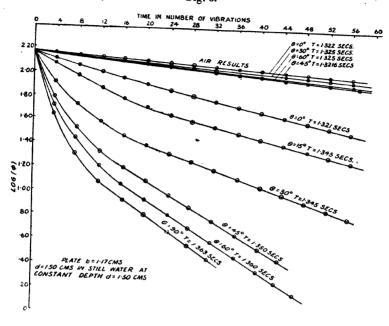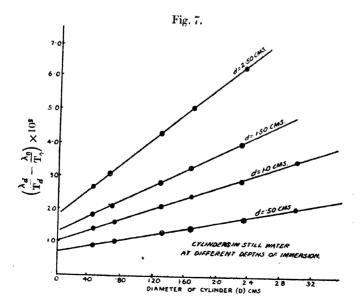
A summary of results for cylinders and plates of different diameters immersed in water are included in figs. 7, 8, 9, & 10

Fig. 8.
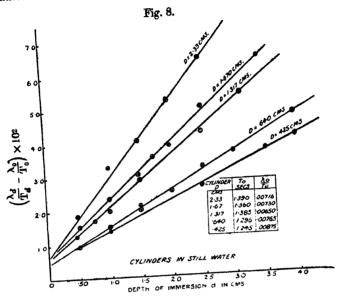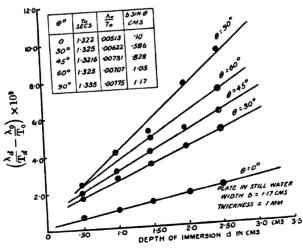
Fig. 9.

and Table I., the logarithmic decrements being deduced in each case from the linear parts of the graphs similar in character to those in fig. 5.
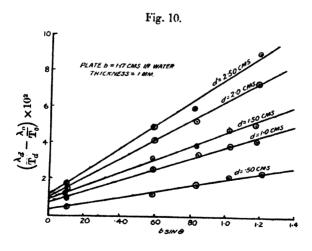
In order to test the influence on the free damping with respect to a change in viscosity and density of the fluid solutions of treacle, aniline, alcohol, and paraffin were used with

TABLE I.

Plate $b = 1\cdot17$ cm. Thickness 1 mm.
Depth immersed in water $= 1\cdot50$ cm. (d).

Angle of inclination. θ°.	Period, T_d sec.	$\frac{\lambda_0}{T_0}$.	$\frac{\lambda_d}{T_d}$.	$\left(\frac{\lambda_d}{T_d} - \frac{\lambda_0}{T_0}\right)$.	$b\sin\theta$.
0	1·321	·00513	·01635	·01122	·10
15	1·345	·00560	·01845	·01285	·302
30	1·345	·00622	·02850	·02228	·586
45	1·350	·00731	·04890	·04159	·825
60	1·360	·00707	·05180	·04473	1·05
90	1·357	·00750	·0570	·0495	1·10

Fig. 10.

a cylinder of diam. $= 1\cdot317$ cm. and period about $1\cdot300$ sec., and the data incorporated in figs. 11 & 12 and Table II. demonstrate the marked effect those properties have on the logarithmic decrement. Further reference is made later.

Fig. 11.
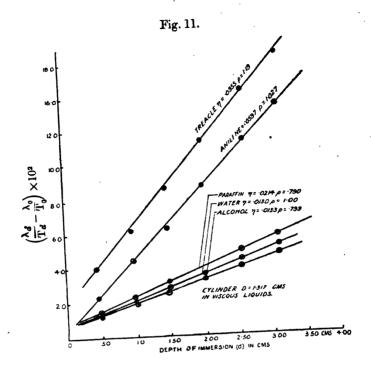
Fig. 12.
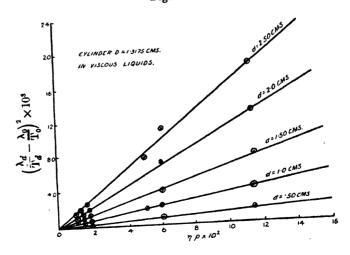
TABLE II.

Cylinder $D = 1.317$ cm. in different liquids at rest.

Liquid.	$d.$ cm.	Period, T_d sec.	$\dfrac{\lambda_0}{T_0}.$	$\dfrac{\lambda_d}{T_d}.$	$\left(\dfrac{\lambda_d}{T_d} - \dfrac{\lambda_0}{T_0}\right)^2 \times 10^4.$
Aniline. $\eta = .0517$ gm./cm./sec. $\rho = 1.027$ gm./c.c.	0	1.385	.0063	.0063	0
	.50	1.385		.0310	6.10
	1.00	1.400		.0520	20.90
	1.50	1.417		.0635	33.40
	2.00	1.442		.0988	85.50
	2.50	1.460		.1120	111.5
Alcohol. $\eta = .0135$ gm./cm./sec. $\rho = .799$ gm./c.c.	0	1.385	.0063	.0063	0
	.50	1.383		.0203	1.96
	1.00	1.400		.0259	3.86
	1.50	1.410		.0340	7.70
	2.00	1.422		.0399	11.28
	2.50	1.425		.0451	15.00
Paraffin. $\eta = .0214$ gm./cm./sec. $\rho = .790$ gm./c.c.	0	1.380	.0061	.0061	0
	.50	1.400		.0210	2.22
	1.0	1.410		.0320	6.70
	1.50	1.425		.0376	9.90
	2.00	1.430		.0429	13.52
	2.50	1.430		.0524	21.50
Treacle. $\eta = .0955$ gm./cm./sec. $\rho = 1.19$ gm./c.c.	0	1.375	.0061	.0061	0
	.50	1.395		.0505	19.75
	1.00	1.402		.0681	38.50
	1.50	1.450		.0915	73.0
	2.00	1.485		.1208	131.5
	2.50	1.486		.1421	185.0
Water. $\eta = .013$ gm./cm./sec. $\rho = 1.0$ gm./c.c.	0	1.385	.0065	.0065	0
	.50	1.397		.0225	2.55
	1.00	1.405		.0274	4.36
	1.50	1.410		.0366	9.05
	2.00	1.430		.0450	14.85
	2.50	1.450		.0485	17.62
	3.00	1.460		.0505	19.40

RESULTS WITH FLOW.

Two effects were examined:

(1) Maintaining steady flow at resonant condition, free damping curves for cylinders were obtained at different depths of immersion and also different periods in water.

(2) At a constant depth for a cylinder, free damping curves at varying speeds of flow.

Fig. 13.

CYLINDER D = ·970 CMS AT VARIOUS DEPTHS WITH & WITHOUT FLOW IN WATER AT RESONANCE
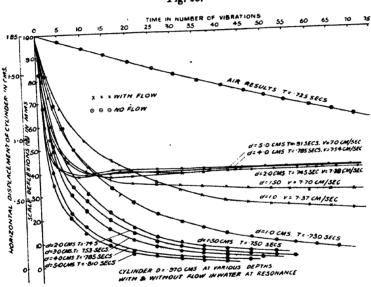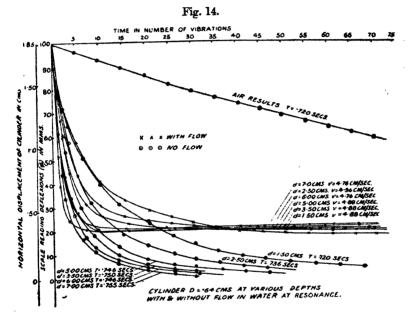
With regard to the influence of flow on the free damping under these conditions, this is clearly exhibited in figs. 13, 14, 15, & 16, which contain results for cylinders D=·970, ·64, and 1·317 cm. respectively. Figs. 17 & 18 show the effect of variation of the speed of flow on the damping at constant depth of immersion.

It is of interest to notice the quicker response to maintained vibrations at resonance speed for increased depth of immersion, which is to be expected from hydrodynamical conditions of the forces in operation on the cylinder by the detachment of a single vortex, despite the greater damping and increase of resistance produced by the fluid.

Typical maintained vibration responses at various speeds of flow for cylinders of diameter D ·970 cm. and 1·317 cm. are shown in figs. 19 & 20, similar in character to the results obtained by Thom, and it will be observed the resonance response is more critical with the cylinder of shorter period (fig. 20).

The phenomenon of beats could be easily recognized, and this effect indirectly served as a means of indicating when resonance speeds had been reached, namely, non-existence

Fig. 14.

CYLINDER D = ·64 CMS AT VARIOUS DEPTHS WITH & WITHOUT FLOW IN WATER AT RESONANCE.

of beats, but an increasing amplitude of swing to a steady maintained value.

THEORY AND DISCUSSION OF RESULTS.

Case 1.—Free streamline damping of cylinders and plates immersed in a stationary fluid at varying depths.

The equation of motion of a short cylinder or plate attached to the lower end of a long vertical vibrating reed in air, and executing damped harmonic motion, may be be written as

$$\mathrm{M}\frac{d^2x}{dt^2} + k_0\frac{dx}{dt} + \mu x = 0, \quad \cdots \cdots (1)$$
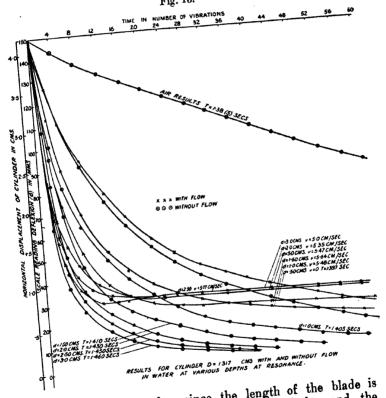
where $M =$ the effective mass of the vibrating system supposed concentrated at the lower end of the blade ;

$x =$ the mean linear displacement of the mid-point of the cylinder from the vertical position, this being assumed the same for the whole

Fig. 15.

RESULTS FOR CYLINDER D = 1317 CMS WITH AND WITHOUT FLOW IN WATER AT VARIOUS DEPTHS AT RESONANCE.

cylinder, since the length of the blade is much longer than the cylinder and the displacement is small ;
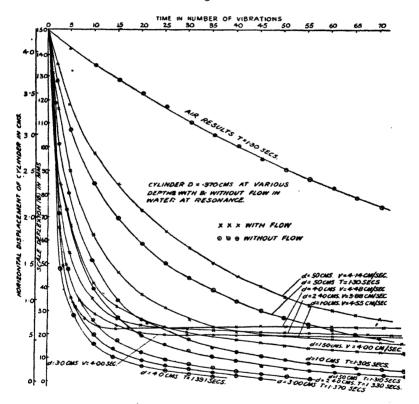
$k_0 \dfrac{dx}{dt} =$ the frictional damping force experienced by the cylinder or blade ;

$u.x =$ the restoring force exerted by the blade and cylinder dependent upon the effective mass of the system and the elasticity of the blade.

When a cylinder of diameter D cm. is immersed in a stationary fluid to a depth d cm., allowing for the frictional damping of the fluid and neglecting the buoyancy effect, since it is small, the equation of motion now becomes

$$M\frac{d^2x}{dt^2} + (k_d + k_r) \cdot \frac{dx}{dt} + \mu x = 0, \quad \ldots \quad (2)$$

Fig. 16.

where $k_d\dfrac{dx}{dt}$ = the frictional damping force exerted by the fluid on the cylinder, and

$k_r\dfrac{dx}{dt}$ = the frictional damping force exerted on the blade and the remainder of the cylinder not immersed.

Fig. 17.

RESULTS FOR CYLINDER D = 1·317 CMS IN WATER AT VARIOUS SPEEDS
CONSTANT DEPTH d = 3·0 CMS

Fig 18.

RESULTS FOR CYLINDER D = ·970 CMS. IN WATER
DEPTH d = 4·0 CMS. AT VARIOUS SPEEDS
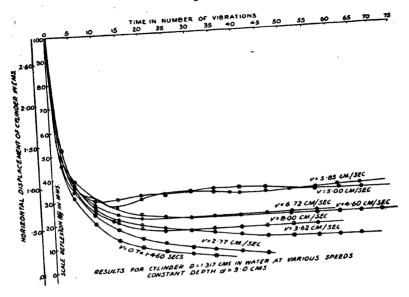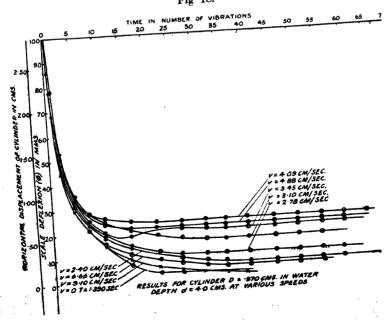
The solution of equation (2) is

$$x = x_0 e^{-\frac{k_d + k_r}{2M} \cdot t} \cdot \cos\left[\sqrt{\frac{\mu}{M} - \left(\frac{k_d + k_r}{2M}\right)^2} \cdot t + \phi\right],$$

Fig. 19.

C.M.S.
D=1·670 d=3·0 CMS. T=1·50 SECS.
D=1·317 d=3·0 CMS. T=1·460 SECS.
D=·970 d=4·0 CMS. T=1·390 SECS.

MAINTAINED RESPONSE
FOR DIFFERENT CYLINDERS
IN WATER

HORIZONTAL DISPLACEMENT OF CYLINDER IN CMS
MAINTAINED SCALE DEFLEXION (θ_s) (IN MMS.)
SPEED OF FLOW (V)

Fig. 20.

C.M.S.
d=1·50 T= ·750 SEC.
d=5·0 T= ·81 SEC.
d=3·0 T= ·753 SEC.

CYLINDER D=·970 CMS.

HORIZONTAL DISPLACEMENT OF CYLINDER IN CMS
MAINTAINED SCALE DEFLEXION (θ_s) IN MMS
SPEED OF FLOW (V).

x_0 and ϕ being constants dependent upon the initial conditions. The maximum value of x after m complete vibrations from the start is given as

$$x_m = x_0 e^{-\frac{k_d + k_r}{2M} \cdot mT_d}, \quad \cdots \cdots \quad (3)$$

4 C 2

where T_d=the period of the system for depth of immersion d cm., and the successive amplitudes of swing are x_0, x_1, x_2, x_3, etc. Also

$$\log_e \frac{x_0}{x_m} = 2m.\lambda_d,$$

which, connecting with equation (3), gives

$$\lambda_d = \frac{1}{4} \frac{(k_d + k_r)}{M}.T_d. \quad \ldots \ldots \quad (4)$$

Putting λ_0=the log dec. of the system for zero depth of immersion, and T_0 as the period, $k_d = 0$ and k_r becomes k_0.

$$\therefore \qquad \lambda_0 = \frac{1}{4}.\frac{k_0 T_0}{M}, \quad \ldots \ldots \quad (5)$$

whence from equations (4) and (5),

$$\frac{\lambda_d}{T_d} - \frac{\lambda_0}{T_0} = \frac{1}{4M}(k_d + k_r - k_0) \eqsim \frac{1}{4}\frac{k_d}{M},$$

since $(k_r - k_0)$ is generally small compared with k_d.

Assuming, now, for a given fluid that k_d varies linearly with respect to the effective area of the immersed part of the cylinder projected on to a vertical plane perpendicular to the plane of vibration, suggestive from the previous results of the aerofoil pendulum, hence for a cylinder of diameter D cm. immersed to a depth d cm., we may put

$$k_d = A + B.(D.d),$$

giving

$$\left(\frac{\lambda_d}{T_d} - \frac{\lambda_0}{T_0}\right)_{\text{cylinder}} = A_1 + B_1.(D.d),$$

A, A_1, B, B_1 being constants for the fluid, depending on the nature of the fluid in respect of density and viscosity.

In the case of a plate of width b cm., inclined at $\theta°$ to the plane of vibration and immersed d cm., we must replace $D.d$ by $bd \sin \theta$, whence

$$\left(\frac{\lambda_d}{T_d} - \frac{\lambda_0}{T_0}\right)_{\text{plate}} = A_2 + B_2(bd \sin \theta).$$

In order to account for the effect of the viscosity η and the density ρ of the fluid, since there is a linear relationship between $\left(\frac{\lambda_d}{T_d} - \frac{\lambda_0}{T_0}\right)^2$ and $\eta\rho$ (see fig. 12), we may include

these quantities as follows to express the experimental results, viz.,

$$\left(\frac{\lambda_d}{T_d} - \frac{\lambda_0}{T_0}\right)_{\text{cylinder}} = A_3 + B_3 (D.d)\sqrt{\eta\rho} \quad . \quad . \quad . \quad (6)$$

and

$$\left(\frac{\lambda_d}{T_d} - \frac{\lambda_0}{T_0}\right)_{\text{plate}} = A_4 + B_4 b.\sin\theta \sqrt{\eta\rho} ; \quad . \quad . \quad . \quad (7)$$

alternately we obtain

$$\left(\frac{\lambda_{d_1}}{T_{d_1}} - \frac{\lambda_{d_2}}{T_{d_2}}\right)_{\text{cylinder}} = B_3 . D(d_1 - d_2)\sqrt{\eta\rho} \quad . \quad . \quad . \quad (8)$$

and

$$\left(\frac{\lambda^{d_1}}{T_{d_1}} - \frac{\lambda_{d_2}}{T_{d_2}}\right)_{\text{plate}} = B_4 . b . \sin\theta(d_1 - d_2)\sqrt{\eta\rho}, \quad . \quad (9)$$

where λ_{d_1} and λ_{d_2} = the log decs. for depths of immersion d_1 and d_2 cm. and periods T_{d_1} and T_{d_2} respectively.

Equations (6), (7), (8), and (9) are therefore representative of the behaviour of cylinders and plates, and their validity is borne out by the data contained in figs. 11 and 12, which exhibit linear relationships between the varying quantities.

Case II.—Free streamline damping of cylindrical pendulums in a stream of fluid under the influence of vortices.

It is known * that the detachment of alternate vortices behind a cylinder in a fluid stream begins in the neighbourhood of $\dfrac{VD}{\nu} = 48$. The existence of such eddies brings into operation periodic cross-forces as a result of alternating circulation about the cylinder, the sign of the force being the same as that of the vortex in formation.

Generally the net circulation round the cylinder is less than that in a single detached vortex. A knowledge of the circulation round the cylinder enables the magnitude of the cross-force to be calculated under the experimental conditions of maintained vibrations, or, *vice versa,* knowing the factors controlling maintained vibration, the circulation round the cylinder may be deduced.

Assuming K = the circulation in a single detached vortex, then γK is the circulation round the cylinder where $\gamma < 1$. When the cylinder of diameter D cm. is immersed to a depth d cm. in a fluid of density ρ and speed V cm./sec., the cross-force will be $\gamma K \rho dV$.

* Tyler, Journ. Scientific Inst. vii. no. 11 (Nov. 1930).

As a tentative suggestion, assuming the cross-force is periodic and simple harmonic to a first approximation, we write

$$F = F_0 \cos pt,$$

where $F = \gamma K \rho d V$, and the vortex frequency $N = \dfrac{p}{2\pi}$, then the equation of motion of the system becomes

$$M \frac{d^2 x}{dt^2} + (k_d + k_r) \frac{dx}{dt} + \mu x = F_0 \cos pt,$$

a solution of the particular integral being

$$x = \frac{F_0 \sin \epsilon}{p(k_d + k_r)} \cos (pt - \epsilon),$$

where

$$\tan \epsilon = \frac{p}{M} \cdot \frac{k_d + k_r}{\dfrac{\mu}{M} - p^2},$$

and the general solution is

$$x = \frac{F_0 \sin \epsilon}{p(k_d + k_r)} \cos (pt - \epsilon) + x_0 e^{-\frac{k_d + k_r}{2M} \cdot t} \cos \left[\sqrt{\frac{\mu}{M} - \frac{1}{4} \left(\frac{k_d + k_r}{M} \right)^2} \cdot t + \phi \right]$$

In the steady state, when the amplitude of the free vibration is small with respect to that of the forced vibration, we get

$$x_s = \frac{F_0 \sin \epsilon}{p(k_d + k_r)} \cos (pt - \epsilon)$$

or

$$x_s = \frac{F_0}{M \left\{ \left(\dfrac{\mu}{M} - p^2 \right) - p^2 \left(\dfrac{k_d + k_r}{M} \right)^2 \cdot \right\}^{\frac{1}{2}}} \cos (pt - \epsilon).$$

At resonance $\dfrac{\mu}{M} = p^2$, giving maximum displacement

$$[x]_m = \frac{F_0}{p(k_d + k_r)} \quad \cdot \quad \cdot \quad \cdot \quad \cdot \quad \cdot \quad (10)$$

Now since $\lambda_d = \dfrac{(k_d + k_r)}{4M} T_d$ and $p = 2\pi N$,

we derive the relation

$$[x]_m \frac{\lambda_d}{T_d} = \frac{F_0}{8\pi MN} = \frac{\gamma K \rho d V}{8\pi MN} \quad \cdot \quad \cdot \quad \cdot \quad (11)$$

It is impossible to determine M directly, but its value may be expressed in terms of the free period of the system without damping T_0, together with μ, the restoring force per unit displacement; thus

$$M = \frac{\mu T_0{}^2}{4\pi^2},$$

because k_0 is small compared with μ.

Substituting in equation (11) gives

$$[x]_m \frac{\lambda_d}{T_d} \mu T_0{}^2 = \frac{\pi}{2} \cdot \frac{\gamma K \rho d V}{N}.$$

Finally, in order to account for the effect of viscosity of the fluid at low Reynolds numbers $\frac{VD}{\nu}$, it is sufficient to substitute for $\frac{V}{N}$ from the expression

$$\frac{ND}{V} = A'\phi\left(\frac{\nu}{VD}\right) = a\left(1 + b\frac{\nu}{VD}\right),$$

in which A', a, b are constants and $\nu = \frac{\eta}{\rho}$.

Experimentally $\frac{ND}{V} = \cdot198\left(1 - 19\cdot7\frac{\nu}{VD}\right)$, neglecting the higher powers of $\frac{\nu}{VD}$.

Hence $[x]_m \frac{\lambda_d}{T_d} \mu T_0{}^2 = 2\cdot52\,\pi\gamma K\rho dD\left(1 + 19\cdot7\frac{\nu}{VD}\right)$, (12)

from which γK may be evaluated. Such values are included in Tables III., IV., and V.

This expression also enables one to compute comparatively the circulation around a given cylinder under maintained vibration at different periods for constant depth, since it follows that

$$\frac{[x]_{m_1} \dfrac{\lambda_{d_1}}{T_{d_1}} \mu_1 [T_0]_1{}^2}{[x]_{m_2} \dfrac{\lambda_{d_2}}{T_{d_2}} \mu_2 [T_0]_2{}^2}$$

$$= \frac{K_1\left(1 + 19\cdot7\dfrac{\nu}{V_1 D}\right)}{K_2\left(1 + 19\cdot7\dfrac{\nu}{V_2 D}\right)} \doteq \frac{V_1\left(1 + 19\cdot7\dfrac{\nu}{V_1 D}\right)}{V_2\left(1 + 19\cdot7\dfrac{\nu}{V_2 D}\right)},$$

Table III.
Cylinder D = ·64 cm.

$d.$ cm.	$T_d.$ sec.	$\dfrac{\lambda_d}{T_d}$ No flow.	$[x]_m.$ cm.	$\mu.$ gm.	V cm./sec.	$[x]_m \cdot \dfrac{\lambda_d}{T_d} \mu T_0^2$	$V \rho d D^2 \left(1+19\cdot7 \dfrac{\nu}{\sqrt{D}}\right)$	$\gamma K.$ cm.²/sec.
0	·720	·0120						
1·50	·720	·0523	·310	3·06	4·88	·0264	3·22	3·16
2·50	·736	·0750	·319	2·92	4·96	·0440	5·46	3·22
3·50	·750	·0870	·360	3·71	4·88	·0505	7·61	2·60
5·00	·746	·1150	·375	3·03	4·88	·0675	10·73	2·45
7·00	·755	·1460	·390	2·92	4·76	·0866	14·65	2·25
0	1·00	·0063						
1·0	1·005	·0251	·320	1·63	3·57	·0130	1·60	2·30
2·0	1·020	·0377	·340	1·65	3·78	·0210	3·39	1·86
3·0	1·020	·0469	·330	1·67	3·87	·0258	5·19	1·53
4·0	1·035	·0645	·340	1·65	3·45	·0361	6·25	1·60
5·0	1·035	·0773	·340	1·65	3·92	·0434	8·75	1·57
6·0	1·051	·0843	·340	1·65	3·61	·0472	9·55	1·39
0	1·280	·0083	—			—		
1·50	1·300	·0310	·250	1·28	2·73	·0162	1·89	1·86
2·50	1·300	·0372	·250	1·28	2·85	·0195	3·28	1·35
4·00	1·350	·0510	·250	1·28	2·67	·0267	4·95	1·15
5·50	1·350	·0690	·250	1·28	2·85	·0361	7·19	1·14
7·00	1·360	·0739	·250	1·28	2·74	·0387	8·85	·95

TABLE IV.

Cylinder D = ·970 cm.

d. cm.	T_d. sec.	$\frac{\lambda_d}{T_d}$ No flow.	$[x]_m$. cm.	μ. gm.	V. cm./sec.	$[x]_m \cdot \frac{\lambda_d}{T_d} \mu T_0^2$.	$V \rho d D^2 \left(1 + 19\cdot7 \frac{\nu}{\sqrt{VD}}\right)$.	γK. cm.²/sec.
0	·725	·0093						
1·0	·730	·0492	·350	3·14	7·37	·0284	7·14	2·75
1·5	·750	·0665	·540	3·07	7·70	·0680	11·17	4·80
2·0	·745	·0760	·650	3·10	7·28	·0805	14·07	5·00
3·0	·753	·0885	·715	3·10	7·70	·1030	22·35	4·27
4·0	·785	·1140	·715	3·10	7·54	·1330	29·25	4·13
5·0	·810	·1332	·715	3·19	7·00	·1600	33·90	4·00
0	1·03	·0057						
1·0	1·03	·0268	·430	1·86	5·00	·0228	4·92	2·19
1·50	1·05	·0397	·630	1·90	5·26	·0503	7·72	(4·14)
2·00	1·05	·0423	·680	1·88	5·10	·0673	10·02	3·52
3·00	1·07	·0602	·685	1·90	5·04	·0830	14·82	3·89
4·00	1·09	·0656	·680	1·88	5·00	·0890	19·62	2·78
5·00	1·10	·0857	·680	1·88	5·29	·1160	16·00	2·84
0	1·300	·0075						
·50	1·300	·0170						
1·00	1·305	·0251	·450	1·33	4·55	·0264	4·50	2·41
2·50	1·330	·0354	·590	1·32	3·88	·0465	9·27	2·25
3·00	1·370	·0450	·610	1·34	4·00	·0562	11·85	2·26
4·00	1·391	·0538	·650	1·29	4·30	·0761	16·98	2·30

TABLE V.

Cylinder D = 1·317 cm.

d. cm.	T_d. sec.	$\frac{\lambda_d}{T_d}$ No flow.	$[x]_m$. cm.	μ. gm.	V. cm./sec.	$[x]_m \frac{\lambda_d}{T_d} . \mu T_0{}^2$	$V\rho dD^2\left(1+19\cdot7\frac{\nu}{\sqrt{D}}\right)$	γK. cm.²/sec.
0	1·385	·0061	·460	1·56	5·48	·0878	9·80	3·67
1·0	1·405	·0274	·610	1·54	5·64	·0660	15·30	4·44
1·50	1·410	·0366	·800	1·55	5·35	·1070	19·20	5·41
2·00	1·430	·0450	·850	1·53	5·77	·1210	25·90	4·89
2·50	1·450	·0485	·850	1·53	5·00	·1260	26·90	4·20
3·0	1·400	·0505				—	—	—
0	1·720	·0062	—	—	—	—	—	4·55
1·50	1·795	·0218	·70	1·057	4·33	·0880	11·73	(3·28)
2·00	1·825	·0316	(·62)	1·110	4·05	(·0652)	14·70	3·90
3·00	1·830	·0488	·75	1·095	4·00	·1180	21·60	4·24
4·00	1·900	·0550	·765	1·150	4·00	·170	29·00	3·79
5·00	1·930	·0765	·765	1·150	4·06	·190	35·30	

the suffixes denoting the respective values of each quantity for periods T_{d_1} and T_{d_2}, K_1 and K_2 being the circulations for speeds of flow V_1 and V_2 cm./sec., and the free periods without damping are $[T_0]_1$ and $[T_0]_2$ respectively.

TABLE VI.

Cylinder $D = \cdot 970$ cm.

	$d=5\cdot0$ cm.	$d=4\cdot0$ cm.	$d=4\cdot0$ cm.	$d=3\cdot0$ cm.
$[x]_{m_1}\dfrac{\lambda d_1}{T_{d_1}}\cdot\mu_1(T_0)_1{}^2$ (α)	$\cdot160$	$\cdot089$	$\cdot133$	$\cdot103$
$[x]_{m_2}\dfrac{\lambda d_2}{T_{d_2}}\cdot\mu_2(T_0)_2{}^2$ (β)	$\cdot116$	$\cdot076$	$\cdot089$	$\cdot083$
V_1 cm./sec.	$7\cdot00$	$5\cdot00$	$7\cdot54$	$7\cdot70$
V_2 cm./sec.	$5\cdot29$	$4\cdot30$	$5\cdot00$	$5\cdot04$
$\dfrac{K_1}{K_2}=\dfrac{\alpha}{\beta}$	$1\cdot38$	$1\cdot17$	$1\cdot66$	$1\cdot24$
$\dfrac{V_1}{V_2}$	$1\cdot32$	$1\cdot16$	$1\cdot51$	$1\cdot54$

Cylinder $D = \cdot64$ cm.

	$d=5\cdot0$ cm.	$d=4\cdot0$ cm.	$d=3\cdot0$ cm.	$d=2\cdot50$ cm.
$[x]_{m_1}\dfrac{\lambda d_1}{T_{d_1}}\cdot\mu_1(T_0)_1{}^2$ (α)	$\cdot0635$	$\cdot0361$	$\cdot0400$	$\cdot0240$
$[x]_{m_2}\dfrac{\lambda d_2}{T_{d_2}}\cdot\mu_2(T_0)_2{}^2$ (β)	$\cdot0434$	$\cdot0267$	$\cdot0258$	$\cdot0195$
V_1 cm./sec.	$4\cdot88$	$3\cdot45$	$4\cdot96$	$3\cdot80$
V_2 ,,	$3\cdot92$	$2\cdot67$	$3\cdot87$	$2\cdot85$
$\dfrac{K_1}{K_2}=\dfrac{\alpha}{\beta}$	$1\cdot46$	$1\cdot35$	$1\cdot54$	$1\cdot23$
$\dfrac{V_1}{V_2}$	$1\cdot25$	$1\cdot30$	$1\cdot28$	$1\cdot33$

To test the validity of this ratio equality, comparison values obtained are incorporated in Table VI., from which it will be observed good agreement is revealed.

We may furthermore express $[x]_m$ in terms of the maximum velocity v_m of the cylinder in an alternation, for putting

$$v_m = \frac{2\pi}{T_d}[x]_m,$$

we derive the simple relation

$$\frac{v_{m_1}\lambda_{d_1}\mu_1[T_0]_1{}^2}{v_{m_2}\lambda_{d_2}\mu_2[T_0]_2{}^2} \doteq \frac{V_1}{V_2},$$

or, generally omitting the suffixes,

$$\frac{v_m}{V} \cdot \lambda_d\mu T_0{}^2 = \text{a constant for a given } d D.$$

Deduction of γ.

By dimensional consideration, the maximum value of the cross-force given to any cylinder by each eddy should be of the form $\phi(R)\rho d D V^2$, where $R = $ Reynolds's number, and, in the case of simple harmonic considered, F_0 is therefore $\phi(R)\rho d D V^2$.

Now from the previous theory $F_0 = \gamma K \rho d V$; therefore, following Karman's assumption that in the formation of detached vortices, a surface of discontinuity is first formed which then breaks up into discrete vortices in which $K = V l$ (l being the longitudinal spacing of successive vortices in the same row), and accepting the approximate experimental conditions, namely, $l = b D$ generally (b is a constant), we get

$$F_0 = \gamma b \rho d D V^2,$$

and a comparison of both expressions of F_0 gives

$$\phi(R) = \gamma b.$$

It is now necessary to express $\phi(R)$ in terms of the drag coefficient K_d, and this can be done by adopting a similar treatment to that used by Thom. The total fluid force exerted on the cylinder is

$$F = K_d \rho d D q^2,$$

q being the resultant velocity of the cylinder relative to the fluid.

The component of this force acting across the stream is $\frac{Fv}{q}$ or $K_d \rho d D q v$, and is a maximum when $v = v_m$, whereupon putting

$$q = (V^2 + v_m{}^2)^{\frac{1}{2}}$$

as an approximation, the maximum component of the cross-force is

$$K_a \rho d D V v_m \left(1 + \frac{v_m^2}{V^2}\right)^{\frac{1}{2}}.$$

Equating this expression to that formerly given leads to the relation,

$$\phi(R) = K_d \frac{v_m}{V} \left(1 + \frac{v_m^2}{V^2}\right)^{\frac{1}{2}},$$

TABLE VII.

$$\gamma = \frac{K_d}{b} \cdot \frac{2\pi}{T_d} \cdot \frac{[x]_m}{V} \left\{ 1 + \left(\frac{2\pi}{T_d} \cdot \frac{[x]_m}{V}\right)^2 \right\}^{\frac{1}{2}}.$$

Cylinder D. cm.	Period T_d. sec.	V. cm./sec.	$[x]_m$. cm.	K_d.	$\frac{VD}{\nu}$.	γ.	$\phi(R) = \gamma b$.
·970	·785	7·54	·715	·520	640	·115	·495
,,	1·09	5·00	·680	·530	425	·122	·525
,,	1·391	4·30	·650	·600	364	·114	·490
·64	1·360	2·74	·250	·680	175	·0715	·307
,,	1·035	3·45	·340	·675	193	·110	·474
,,	·755	4·76	·390	·650	217	·123	·530
1·317	1·460	5·00	·350	·535	575	·116	·498
,,	1·930	4·06	·765	·600	468	·101	·435
1·670	1·550	6·78	1·21	·525	1130	·110	·474

Average value of γ from graph on fig. 21 = ·136.

and since $\phi(R) = \gamma b$,

$$\therefore \quad \gamma = \frac{K_d}{b} \frac{v_m}{V} \left(1 + \frac{v_m^2}{V^2}\right)^{\frac{1}{2}}.$$

Finally, substituting for v_m in terms of $[x]_m$ for the purpose of experimental evaluation,

$$\gamma = \frac{K_d}{b} \cdot \frac{2\pi}{T_d} \cdot \frac{[x]_m}{V} \left\{ 1 + \left(\frac{2\pi}{T_d} \frac{[x]_m}{V}\right)^2 \right\}^{\frac{1}{2}}.$$

This equation thus enables γ to be deduced in terms of quantities which can be measured experimentally.

A summary of such values is included in Table VII. for the greatest depths of immersions of the cylinders, since it is

Dr. E. Tyler *on the Damping of*

reasonable to take these values in order that the theory for a vortex of infinite length, previously assumed, should apply.

Alternately we may obtain γ by substituting Karman's value for K in equation (12), thus giving

$$[x]_m \frac{\lambda_d}{T_d} \mu T_0{}^2 = 2\cdot 52\pi\gamma b V\rho dD^2 \left(1+19\cdot 7\,\frac{v}{VD}\right).$$

Verification of such an equality is established by plotting

$$[x]_m \frac{\lambda_d}{T_d}\mu T_0{}^2 \quad \text{against} \quad V\rho dD^2 \left(1+19\cdot7\,\frac{v}{VD}\right),$$

as in fig. 21, where it will be observed that, apart from experimental errors, the average results fall on a straight
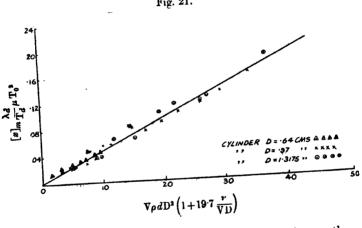
Fig. 21.

line. From a knowledge of the slope of this graph, together with $b=4\cdot30$ (a value deduced elsewhere)[*], the average value of γ is $\cdot13$, which compares favourably with values given in Table VII. obtained by using the former expression. Moreover, since $\phi(R)=\gamma b$, we can evaluate this coefficient of eddy force, and such values are also included in Table VII., which agree fairly well with Thom's[†] results.

It is evident that the net circulation around the cylinder producing the cross-force is considerably less than that in a

[*] Karman and Rubach, *Phys. Zeits.* xiii. p. 49 (1912); Walton, Scientific Proc. Roy. Dublin Soc. xviii. no. 47 (Jan. 1928); Fage, Roy. Aero Soc. Journ. Jan. 1928; Tyler, Phil. Mag., June 1930 and April 1931.

[†] Thom, R. & M. no. 1373, Dec. 1930.

single detached vortex, and Thom concludes from his results, the side-force is an attribute of the circulation about the cylinder of the same sign as the vortex in formation. This vortex either causes a circulation about the cylinder, or the previously formed vortex on the opposite side of the street, by its withdrawal from the neighbourhood of the cylinder, leaves behind a circulation of the opposite sign.

With either explanation, each vortex must produce sufficient circulation to destroy that left by its predecessor, and then establish sufficient required for the cross-force.

The relative phase detachment of a vortex with respect to a swinging pendulum in water has been examined photographically by Richardson [*], and evidence supports the condition that a vortex grows on one side while the pendulum is moving to that side, and is disengaged just after the pendulum begins to swing back.

SUMMARY.

The free damping of short cylinders and plates attached to the lower end of a vertical reed, and immersed in (*a*) various liquids at rest, and (*b*) in a stream of water is examined.

In the former case, with a fluid of density ρ and viscosity η, for a cylinder of diameter D cm., under streamline damping,

$$\left(\frac{\lambda_{d_1}}{T_{d_1}} - \frac{\lambda_{d_2}}{T_{d_2}}\right) = \text{a constant.} \, D(d_1 - d_2)\sqrt{\eta\rho},$$

where λ_{d_1} and λ_{d_2} are the log decs. of the damping for depths of immersion d_1 and d_2 cm., and T_{d_1} and T_{d_2} the periods of vibration. With a plate of width b cm., inclined at θ degrees to the plane of vibration,

$$\left(\frac{\lambda_{d_1}}{T_{d_1}} - \frac{\lambda_{d_2}}{T_{d_2}}\right) = \text{a constant.} \, b \sin\theta(d_1 - d_2\sqrt{\eta\rho}.$$

In the latter case, observation of the amplitude of maintained vibration of the cylinders under the influence of the alternate eddies formed at resonance with the system is made, and this, together with a knowledge of

(1) the log dec. of the system without flow at the same depth of immersion,
(2) the restoring force and free period of the system without damping, and
(3) the speed of the fluid,

---

* Richardson, Roy. Aero. Soc. Journ. March 1927 (proof copy)

enables the net circulation around the cylinders responsible
for the cross-force to be determined, the assumption being
made that Karman's theory of discontinuity at the surface of
a cylinder holds good, in which case the fluid breaks up into
discrete eddies.

The drag coefficients for the cylinders are also deduced,
and these, together with the fluid speeds and amplitudes of
maintained vibration, also permit computation of the cross-
forces and circulation around the cylinders. Good agreement
is exhibited in both cases, where it is found the net circula-
tion around the cylinders is about ·13 of that in a single
detached eddy.

CV. *The Graphic Computation of Solar Altitude.*
By A. F. DUFTON, *M.A., D.I.C.* *

1. IN the *Meteorologische Zeitschrift* for August † Dr. Karl
Schütte describes a simple graphic method of com-
puting the altitude of the sun. By means of an intersection
diagram, comprising a network of three systems of straight
lines, he obtains the solution of the equation

$$\sin h = \cos \delta \cos \phi \cos t + \sin \delta \sin \phi, \quad \cdot \quad \cdot \quad (1)$$

which, for latitude ϕ, expresses the altitude h in terms of
the declination δ and the hour angle t.
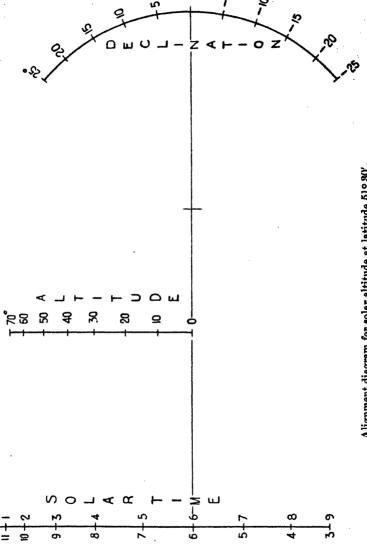
The advantage of an intersection diagram is that it is
usually simpler to construct than an alignment diagram.
An alignment diagram, however, is generally more convenient
to use, as there is no tracing back along a line to read its
graduation and interpolation by eye is only necessary upon
simple scales.

2. Equation (1) can be expressed in the form

$$\begin{vmatrix} 1 & 0 & -\sin h \\ 0 & 1 & -\cos t \\ 1-\cos \phi \cos \delta & -\sin \phi \sin \delta \end{vmatrix} = 0,$$

* Communicated by R. E. Stradling, Esq., Director of Building
Research.
† *Meteorologische Zeitsch.* xlviii. (8) p. 314 (1931).

Alignment diagram for solar altitude at latitude 51° 30′.

The figure shows the diagram for the latitude of London (51° 30′ N.). The time-scale is conveniently figured in hours.

which is the condition that the three points,

$$u \qquad -\sin h \qquad =0,$$
$$v \qquad -\cos t \qquad =0,$$

and
$$u - v \cos \phi \cos \delta - \sin \phi \sin \delta = 0,$$

expressed in parallel coordinates, u and v, are collinear. Transferred to cartesian coordinates, by comparison with

$$u(1 - x/a) + v\, x/a - y/b = 0,$$

the first two points are

$$x = 0, \qquad y = b \sin h$$

and $\qquad x = a, \qquad y = b \cos t$

and define two parallel straight scales, while the third point is given by

$$\frac{1 - x/a}{1} = \frac{x/a}{-\cos \phi \cos \delta} = \frac{y/b}{\sin \phi \sin \delta}, \qquad . \quad . \quad (2)$$

the locus being the conic

$$\left(\frac{x}{a \cos \phi}\right)^2 + \left(\frac{y}{b \sin \phi}\right)^2 = \left(\frac{a - x}{a}\right)^2,$$

which reduces to the circle

$$(x - b \cos \phi)^2 + y^2 = b^2,$$

if a be made equal to $-b \sin \phi \tan \phi$.

3. An alignment diagram, therefore, may be set out by choosing a suitable unit b for the scales of h and t and drawing them at a distance apart equal to $b \sin \phi \tan \phi$. The δ scale is a circle of radius b with its centre at a distance $b \cos \phi$ from the h scale. The scale of δ is readily projected, since, from (2),

$$y/x = -(b/a) \tan \delta \tan \phi$$
$$= \tan \delta / \sin \phi.$$

CVI. *Entropy, Strain, and the Pauli Exclusion Principle.* By W. S. KIMBALL *and* G. BERRY [*].

1. *Newtonian Forces in Momentum Space.*

UNTIL 1931 [†] physics seems to have neglected the fact that Newtonian forces are operating in velocity and momentum space in addition to and distinct from their operation in ordinary space. It was then pointed out that the equations that determine the classical Maxwell-Boltzmann distribution law are actual equilibrium equations between stress and strain in velocity and momentum space, and that the changes that automatically take place in the *absence* of such equilibrium (as postulated by the Second Law of Thermodynamics) are hence to be explained, interpreted, and accounted for as due to operation of stresses and strains in velocity and momentum space. To be sure, this "explanation" of the Second Law of Thermodynamics would be more complete if formulas had been supplied which gave the actual rates of change in one or more particular illustrations of the Second Law, indicating in each case the controlling part played by the stress and strain in momentum space. In anticipation of this hoped-for result we may note already how forces may act in momentum space.

First, we may be absolutely clear that it is actual Newtonian forces that are operating in momentum space. Imagine a perfect gas of elastic spheres with n molecules per c.c. in a container of constant volume, and disregard gravity. Then for a given temperature the pressure is given by $p = nk\mathrm{T}$. Consider now what happens when heat is added very slowly to this gas. Since the volume is constant and heat is added slowly we may think of each small element of volume as being undisturbed as to the number of molecules it contains, and the gas density hence remains constant and equal to n during the increase of temperature. Each molecular position of equilibrium is occupied, after heating the gas, by a molecule with more energy of agitation than previously. The essential point to be emphasized is that this cannot have been brought about without the operation of Newtonian forces (assuming that it is Newton's laws that determine the molecular behaviour). A molecule at a place x in gas, where u_0 is its root mean square agitation velocity,

---

cannot emerge later at the same place x with a different u for its agitation velocity without a time rate of change of momentum, involving Newtonian forces. Suppose heat is supplied to it from opposite sides at an equal rate, so that the assumed equilibrium can be maintained. Let the change in momentum in the x direction at the ends of its free path be as indicated in the following table :—

TABLE I.

The x-component of Momentum Changes per Average Molecule.

Impact number.	Momentum change upon even numbered impact.	Momentum between Impacts.	Momentum change upon odd numbered impact.	Impact number.
		$u_0.$		
2	$2u_0+3\epsilon=2u_1+\epsilon$	$-u_1=-(u_0+\epsilon)$	$-(2u_0+\epsilon)=-(2u_0+\epsilon)$	1
		$u_2=(u_1+\epsilon)$		
4	$2u_0+7\epsilon=2u_3+\epsilon$	$-u_3=-(u_2+\epsilon)$	$-(2u_2+\epsilon)=-(2u_0+5\epsilon)$	3
		$u_4=u_3+\epsilon$	$-(2u_4+\epsilon)=-(2u_0+9\epsilon)$	5
6	$2u_0+11\epsilon=2u_5+\epsilon$	$-u_5=-(u_4+\epsilon)$		
		$u_6=u_5+\epsilon$	$-(2u_6+\epsilon)=-(2u_0+13\epsilon)$	7
8	$2u_0+15\epsilon=2u_7+\epsilon$	$-u_7=-(u_6+\epsilon)$		
		$u_8=u_7+\epsilon$	$-2u_8=-(2u_0+16\epsilon)$	9
10	$2u_0+16\epsilon=2u_8$	$-u_8=-(u_0+8\epsilon)$		

The table represents a very simple transition from the state where u_0 is the momentum of the agitation velocity component to a final state where it is $u_8=u_0+8\epsilon$, with the assumption that the latter state of the molecule is reached by eight impacts, each of which adds ϵ to the last previous momentum magnitude. Thus it will be observed that impacts number 9 and 10 do not change the momentum magnitude, but correspond to the steady state where this momentum is $u_8=u_0+8\epsilon$.

Now the force in ordinary space, due to the change of the vector momentum component of this molecule, is evidently zero, since the odd numbered impacts and even numbered ones have momentum changes of opposite sign, and hence cancel each other ; and corresponding to this we have the familiar fact of Pascal's Law that the hydrostatic pressure is exerted equally in all directions, and hence the vector sum of the forces involved is zero.

In actual detail it will be seen that after the eighth impact, when a steady state is reached, the total negative momentum change (due to the odd numbered impacts) *exceeds* by 8ϵ the

total positive momentum change (from even numbered impacts), or *vice versa,* according as the molecule has had an odd or even number of impacts. Since the time average of this effect is zero, it represents zero resultant force in ordinary space. Thus no resultant force is exerted or work done in ordinary space, corresponding to the transition represented by Table I., when viewed from the long time, large scale point of view.

On the other hand, there is a time rate of change of momentum (and consequent force) involved, whose effect is manifested by the increased momentum between impacts. Since this Newtonian force does no work in ordinary space *except* to increase agitation velocity, it is conveniently referred to as operating only in momentum or velocity space.

Conversely, any change of molecular position in momentum space necessarily involves the operation of forces that may do no resultant work in ordinary space, and hence are to be thought of as operating only in momentum or velocity space.

2. *The Geometrical Expression for Weight.*

Boltzmann's famous relation between the entropy, S, of a gas and W, the probability of its state, is given by

$$S = k \log W + C. \qquad (1)$$

Here k is Boltzmann's constant and C is a constant depending on the zero from which entropy is to be measured. The probability W of the gaseous state is calculated rigorously in statistical mechanics by counting the "complexions" or possible arrangements of molecules in phase space. The product of the number of complexions each raised to a suitable power measures the probability, being a physical quantity called (for the sake of definiteness) the weight. This weight represents the W of equation (1) and forms the basis of entropy calculations in statistical mechanics.

There has recently been developed [*] a "geometrical weight method," based on a physical concept called the "range" or volume occupied per molecule in phase space. The geometrical weight method has been extended [†] to include the new statistical mechanics of Einstein, Bose, Fermi, and Dirac. Problems usually handled by the classical statistical mechanics all seem within the scope of this new

---

[*] W. S. Kimball, "Entropy and Probability," J. Phys. Chem. xxxiii. p. 1558 (1929).
[†] S. Chandrasekhar, Phil. Mag. ix. p. 621 (1930).

method. One important advantage is that Stirling's approximations and associated difficulties * do not enter at all into this direct geometrical treatment (since factorials never enter). Another advantage is the geometrical picture of weight † which the method affords. This contrasts favourably with counting complexions to find the measure of thermodynamic probability. It is the contention of this and previous papers that the great successes of the statistical method (herein purposely set aside) have been overestimated, and that all of its successes and more in the thermodynamic field can be taken care of by the present mechanical stress and geometrical weight and strain theory.

The most noteworthy achievement of this geometrical weight method is the new explanation which it suggests of the Second Law of Thermodynamics. By using this method it has been shown ‡ that the equilibrium equations which (by the Lagrange method of conditional maxima and minima) determine a state of maximum entropy and probability are equilibrium equations between stress and strain. Entropy then appears as k times the total strain Y :

$$S = k \log W + C = kY. \quad \ldots \ldots \quad (2)$$

This suggests that the Second Law of Thermodynamics may be accounted for as being due to the operation of these internal forces or stresses in velocity or momentum as well as ordinary space. The equilibrium state of maximum entropy is thus interpreted as really the state of maximum strain brought about by these forces.

Accordingly, the known equilibrium § equations that lead to the Maxwell-Boltzmann distribution law may be put in the form :

$$-W \frac{f'}{f} du_i = -\lambda m u_i du_i = W \frac{dr_i}{r_i}, \quad \ldots \quad (3)$$

wherein the λ is an undetermined constant and the f is the Maxwell-Boltzmann distribution function. The r's in the right member are the ranges‖ or intervals between successsive

* J. Rice, ' Statistical Mechanics for Students,' p. 282.
† Kimball, *loc. cit.* sec. 8.
‡ W. S. Kimball, " Entropy, Elastic Strain, and the Second Law of Thermodynamics," J. Phys. Chem. xxxv. p. 611 (1931), sec. 5.
§ R. C. Tolman, ' Statistical Mechanics,' chap. 4.
‖ Kimball, *loc. cit.* sec. 8.

molecules in velocity or momentum space, and the u's are the x components of velocity for each molecule :

$$r_i = u_{i+1} - u_i = \frac{1}{f(u_i)} \cdot \ldots \ldots \quad (4)$$

When λ is given its value $-W/kT$ in terms of the absolute temperature T, determined from the distribution function in the usual way [*], equations (3) take the form of equilibrium equations between stress and strain [†] acting in velocity or momentum space :

$$kT = \frac{mu_1 \, du_1}{dr_1/r_1} = \frac{mu_2 \, du_2}{dr_2/r_2} = \ldots = \frac{mu_i \, du_i}{dr_i/r_i} \cdot \ldots \quad (5)$$

In the present paper we extend the geometrical weight method to include real gases in which the volume is restricted according to Van der Waals's equation and the energy according to the Pauli exclusion principle [‡]. We find that the isothermal bulk modulus for gases obeying these restrictions is the same as that of the classical perfect gas provided molecular attractions are neglected. This holds true both for momentum space and ordinary space. Also the state of maximum entropy or weight for a given internal energy again corresponds to a state of equilibrium between stress and strain acting in momentum space as well as ordinary space, just as was the case for perfect gas. The entropy again appears as k times the total strain in phase space. The velocity distribution function which these equations represent is the same Fermi-Dirac distribution law that is usually derived by the new statistics, and which Chandrasekhar has shown [§] can be derived by the geometrical weight method.

Perhaps the most important result of the present investigation is the contribution it makes towards a mechanical interpretation of the Pauli exclusion principle. We show that forces acting in momentum space exclude particles from occupied cells with the same vigour that they are excluded from occupied positions in ordinary space, as represented by Van der Waals's constant b. Thus Pauli's exclusion principle is explained, generally speaking, as due to the same mechanical tendency as the Second Law of Thermodynamics. Each is a physical aspect of intrinsic processes arising from

[*] L. B. Loeb, 'Kinetic Theory of Gases,' chap. 4.

[†] W. S. Kimball, " Entropy, Elastic Strain, and the Second Law of Thermodynamics," J. Phys. Chem. xxxv. p. 611 (1931), sec. 5.

[‡] Rice, *loc. cit.* p. 277.

[§] Chandrasekhar, *loc. cit.*

objections* which groups of particles have toward compression in phase space. The corrections introduced by the Pauli exclusion principle show the degree of objection which particles feel when compression tends to put additional ones in an occupied phase volume. The mechanical vigour of the objections is the same in momentum space as in ordinary space as measured by the gas law and Van der Waals's equation.

3. *The Bulk Modulus and the Stress-strain Relations for Real Gases in Ordinary Space.*

From the gas law we calculate the isothermal bulk modulus by differentiation at constant temperature :

$$p = -\frac{dp}{dV/V} = nkT. \quad \ldots \quad (6)$$

Here p is the pressure, V the volume, and n is the number of molecules per c.c. Multiplying both members of equation (5) by n gives the modulus for stress and strain in momentum space :

$$p = \frac{n\, mu\, du}{dr/r} = nkT. \quad \ldots \quad (7)$$

Comparison of (6) and (7) shows the striking fact † that the isothermal bulk modulus p is the same for changes in momentum space as for changes in ordinary space in case of perfect gas.

For real gases obeying Van der Waals's equation

$$\left(p + \frac{a}{V^2}\right)(V - b) = RT$$

the isothermal bulk modulus calculated as above takes a modified form :

$$p' = p + \frac{a}{V^2} = -\frac{dp'}{dV/(V-b)}. \quad \ldots \quad (8)$$

If we consider only repulsive forces due to impact the potential energy term a/V^2 due to molecular attractions drops out, and Van der Waals's equation simplifies to

$$p(V - b) = RT.$$

---

* Kimball, *loc. cit.*
† Kimball, *loc. cit.* p. 620.

This simplified form gives, instead of (8),

$$p = -\frac{dp}{dV/(V-b)} = \frac{dp}{\dfrac{dF}{F}\Big/\Big(1-\dfrac{F}{B}\Big)} \quad \cdots \quad (9)$$

for the isothermal bulk modulus. In the right member of (9) we let $V = N/F$ and $b/N = 1/B$ for the sake of later comparisons (see (14)). Equation (9) shows that if molecular attractions are neglected, and account taken only of molecular size, the modulus of elasticity p is the same as for gases obeying the gas law. Hence the incorporation of what might be called the " Van der Waals exclusion principle " has no effect on the modulus of elasticity.

4. *Entropy, Strain, and Weight for Real Gases in Ordinary Space.*

If we use the gas law, and restrict attention to isothermal changes, the First Law of Thermodynamics gives the relation between the entropy change and the work term :

$$dS = \frac{dQ}{T} = \frac{p\,dV}{T} = R\frac{dV}{V} \quad \cdots \quad (10)$$

The right member shows the relation between entropy and strain.

If we consider real gases represented by Van der Waals's equation, and again restrict attention to isothermal changes, the work term will be modified :

$$dS = \frac{dQ}{T} = \Big(p + \frac{a}{V^2}\Big)\frac{dV}{T} = R\frac{dV}{(V-b)}. \quad \cdots \quad (11)$$

Here again the entropy appears as the sum of the strains multiplied by Boltzmann's constant k :

$$S = R\Sigma \frac{dV}{V-b} = R \log (V-b) + C = kY. \quad \cdots \quad (12)$$

It has been shown * for perfect gas in which molecules are mere points how the range in ordinary space, $1/n$, the volume occupied per molecule is related to the weight that measures the thermodynamic probability for one out of N molecules. The N is the number of molecules in a gram molecule, the amount of gas considered

$$W = N(1/n) = V. \quad \cdots \quad (13)$$

For real gases, following the idea of Van der Waals's equation and his constant b, we see that the range, instead

* Kimball, *loc. cit.* p. 1567.

of being $1/n$, will be restricted by the effective volume attributed to each molecule by whatever method is used in calculating b. Thus

$$r = \frac{1}{n} - b_1 = \frac{1}{n} - \frac{b}{N} = \frac{1}{F} - \frac{1}{B} \quad \cdots \quad (14)$$

is the range or volume which each particle has to itself, being the previous range reduced by b_1, the effective volume displaced by its physical size. In the right member we let F, a constant distribution function, represent the number of particles per unit volume in ordinary space, just as f represents the number per unit volume in momentum space. Also $B = 1/b_1$ is evidently the number of particles that could be packed into a unit volume in case there is no free motion. Hence the weight per molecule when N are equally likely to be included in the range r is

$$W = Nr = \frac{N}{n} - Nb_1 = V - b = \frac{N}{F}\left(1 - \frac{F}{B}\right) \cdots \quad (15)$$

For N molecules the weight is

$$W = (V - b)^N = \left(\frac{N}{F}\right)^N \left(1 - \frac{F}{B}\right)^N, \quad \cdots \quad (16)$$

which, when substituted in Boltzmann's equation, gives

$$dS = Nk \frac{dV}{V - b}, \quad \cdots \cdots \quad (17)$$

and $\quad S = k \log W + C = Nk \log (V - b) + C = kY. \quad (18)$

Equations (17) and (18) check equations (11) and (12), and the entropy strain equation (2) shown * to hold for gases obeying the gas law. Here b and B represent the fact that only one particle at a time can occupy a volume displaced by its physical dimensions. We might refer to this as the Van der Waals exclusion principle by analogy with or perhaps a part of the Pauli exclusion principle, which excludes extra particles from an occupied cell in phase space.

5. *Entropy, Strain, and Weight for Real Gases in Velocity and Momentum Space.*

As in the classical statistics the number of particles in a unit volume of velocity or momentum space is also represented by a distribution function

$$\frac{dN}{d\omega} = f(u, v, w) = n_i = \frac{1}{v}, \quad \cdots \quad (19)$$

* Kimball, *loc. cit.*

where $d\omega = du\, dv\, dw$ is the volume element in the space and u, v, and w are the velocity components. The volume occupied by a molecule at this place in velocity space is given by the reciprocal of this number as indicated. Where the gas law applies this volume equals the range $(r_i = v_i)$ that leads[*] to the classical distribution law. It has to be multiplied by N to give the weight per molecule, and the product for N molecules gives the total weight W, being related to entropy and the Maxwell-Boltzmann distribution law in the same familiar way[†] that the statistical expression for weight is related to them.

For real gases we restrict the range given by (19) according to the Pauli exclusion principle:

$$r_i = \frac{1}{n_i} - a_1 = \frac{1}{f_i} - \frac{1}{A} = v_i - a_1 = \frac{1}{g_i}. \quad . \quad . \quad (20)$$

This is the free empty range left to a particle at that place in velocity or momentum space after deducting a_1, the minimum range it can occupy. Here $A = \frac{1}{a_1}$ is evidently the number of such minimum ranges or cells in unit volume of momentum space, being the usual symbol[‡] used to represent the Pauli exclusion principle. Equation (20) is seen to be identical with (14), except that it applies to velocity or momentum space instead of ordinary space, and suggests possible physical relationship between the Pauli exclusion principle and the Van der Waals exclusion principle.

A causal relationship between these two has already been considered[§] and then dismissed[||] by Ehrenfest. The present treatment purports to show that both are aspects of the *modus operandi* of elastic *forces* in a restricted phase space. Meanwhile we note the striking parallelism between $a_1 = 1/A$ and $b_1 = b/N = 1/B$, the latter being the volume in ordinary space that a particle must occupy to the exclusion of other particles by virtue of its very physical existence.

Having obtained the expression for range, we multiply this by N to give the weight per molecule which measures the probability that any one out of N molecules may occupy this particular range:

$$w_i = N r_i = \frac{N}{f_i}\left(1 - \frac{f_i}{A}\right) = \frac{N}{g_i}; \quad . \quad . \quad . \quad (21)$$

---

[*] Kimball, *loc. cit.*
[†] Kimball, *loc. cit.*
[‡] Chandrasekhar, *loc. cit.*
[§] Ehrenfest, 'Nature,' cxix. p. 196 (1927).
[||] Ehrenfest, 'Nature,' cxix. p. 602 (1927).

and for N molecules the weight is

$$W = N^N(r_1 r_2 \dots r_N) = N^N \left(\dots \frac{1 - \frac{f_i}{A}}{f_i} \right) = \frac{N^N}{g_1 g_2 \dots g_N}, \quad (22)$$

where the g's defined by (20) are the reciprocals of the ranges. Substitution in Boltzmann's equation gives the entropy,

$$S = k \left(\sum_1^N \log r_i \right) + C = k \sum_1^N \int \frac{dr_i}{r_i} = kY = Nk \log r + C. \quad (23)$$

Equations (21) and (22) have been given by Chandrasekhar[*]. They are here shown in terms of the free range (20). It is significant that the weight is still N^N times the product of the free ranges reserved to the particles in momentum space, and the entropy (23) is the sum of the corresponding strains exactly as it was in the case of gas obeying the gas law.

Although the argument of this section refers to velocity or momentum space, it may be generalized [†] to include phase space (action space), and leads to formulæ of the same form as (21), (22), and (23).

6. *The Equilibrium Equations for Stress and Strain in the Fermi-Dirac Statistics.*

To find the maximum value of W subject to a constant energy E we use the method of Lagrange. The function ϕ is formed by adding E times an undetermined constant λ to W, $\phi = W + \lambda E$. Take the N partial derivatives of the now N independent u's, and set each derivative equal to zero :

$$\frac{\partial \phi}{\partial u_i} = \frac{\partial W}{\partial u_i} + \lambda \frac{\partial E}{\partial u_i} = -W \frac{d}{du_i} \log g_i + \lambda m u_i = 0, \quad (24)$$

or, in view of (20),

$$W \frac{dr_i}{r_i} + \lambda m u_i \, du_i = 0, \quad \dots \quad (25)$$

where the partial derivatives are taken with respect to the x components of the molecular velocities. Equations (25) show that there is a constant ratio, namely,

$$-\frac{W}{\lambda} = \frac{m u_1 \, du_1}{dr_1/r_1} = \frac{m u_2 \, du_2}{dr_2/r_2} = \dots = -\frac{m u \, du}{\frac{df}{f} \left/ \left(1 - \frac{f}{A} \right) \right.}, \quad (26)$$

between energy change per molecule (between successive

---

[*] Chandrasekhar, *loc. cit.*
[†] Chanrdasekhar, *loc. cit.*

molecules) and the corresponding strain, just as was shown *
to be the case for the Maxwell-Boltzmann distribution. This
ratio actually is the elastic modulus per molecule corre-
sponding to the operation of stresses and strains in momentum
space, since it has all the characteristics of such a physical
constant as shown in detail for the perfect gas case †.

The distribution function corresponding to (24), (25), or
(26) takes the form

$$f(u) = \frac{1}{ce^{-\frac{\lambda m u^2}{2W}} + \frac{1}{A}}, \quad \dots \dots (27)$$

which is the Fermi-Dirac distribution law, thus derived by
the geometrical weight method as already shown by
Chandrasekhar ‡. It is well known § that the constant λ is
required by thermodynamics to be $- W/kT$. Substitute this
in (26) above, and obtain

$$kT = \frac{mu\,du}{dr/r} = \frac{mu\,du}{\dfrac{df}{f}\Big/\Big(1 - \dfrac{f}{A}\Big)}. \quad \dots (28)$$

Multiplying both members of (28) by n gives

$$p = nkT = \frac{n\,mu\,du}{dr/r} = -\frac{n\,mu\,du}{\dfrac{df}{f}\Big/\Big(1 - \dfrac{f}{A}\Big)}. \quad \dots (29)$$

These formulæ are like (6) and (7), and show that in the
case of the Fermi-Dirac statistics, as well as the classical law,
the elastic modulus per molecule is kT. For a unit volume
it is equal to the simple pressure formula ($p = nkT$). Like-
wise the elastic modulus appearing in (29) is the same as
that in (9), which refers to real gases in ordinary space.
Now (9) represents real gases in which the Van der Waals
constant b restricts the volume, and no intermolecular
attractions are considered. Thus there appears a striking
parallelism (as represented by (28) and (29) on the one hand,
and (9) on the other) between the behaviour of molecules in
velocity space and ordinary space. In both types of space
molecules "object" to being crowded together with the same
vigour (same modulus of elasticity) whether their range is
curtailed by the Pauli exclusion principle or the Van der
Waals exclusion principle. Furthermore, this resistance to

* Kimball, *loc. cit.* p. 617.
† Kimball, *loc. cit.* p. 617.
‡ Chandrasekhar, *loc. cit.*
§ Rice, *loc. cit.* p. 274.

compression is the same in each case as for the simple theory in which the exclusion principles are neglected *.

7. *Intermolecular Attractive Forces.*

On the other hand, the elastic modulus given by equation (8) is not the same as in the other cases, since here intermolecular attractions are considered. It is recognized † in connexion with the new statistics that the Fermi-Dirac distribution law, with the negative correction term $\left(\dfrac{f}{A}\right)$ appearing in (21) and (22), corresponds experimentally to the case of an extra repulsion between particles, and is well verified by a gas of electrons or protons. Where attractive forces exist, as with neutral molecules, the Bose-Einstein statistics ought to hold. If we were to introduce attractive forces into the equilibrium equations like (24) and (25) it seems likely that they would correspond to the new statistical expressions for weight like (21) and (22), except with a positive correction term $\left(+\dfrac{f}{A}\right)$. Such a change ‡ would give the Bose-Einstein statistics, which can thus probably be fitted into the stress-strain entropy theory. The present treatment, however, considers only the repulsions corresponding to the Pauli exclusion principle.

8. *Experimental Verification; Mechanical Interpretation of the Pauli Exclusion Principle.*

The most important verification of the stress-strain equilibrium equations, and the allied entropy-strain equations (2), (18), and (23), is that they suggest a natural and obvious explanation § of the Second Law of Thermodynamics. On the other hand, the ergodic hypothesis has proved quite unsatisfactory ‖ to most physicists.

The present viewpoint is also very suggestive in connexion with the Pauli exclusion principle. Not only is there a striking analogy between the equilibrium equation (9) for ordinary space and (28) and (29) for momentum space, but the modulus of elasticity is the same for the two cases, indicating the operation of the same mechanical causes in the two realms. Even the exclusion of occupied regions in the

---

* Kimball, *loc. cit.*

† P. Ehrenfest and J. R. Oppenheimer, Phys. Rev. xxxiii. p. 333 (1931).

‡ Chandrasekhar, *loc. cit.*

§ Kimball, *loc. cit.* sec. 7, p. 621.

‖ Tolman, *loc. cit.* p. 39.

two cases introduces the correction terms $\left(\dfrac{b}{N} = \dfrac{1}{B}\right)$ for Van der Waals's equation and 1/A for the Pauli exclusion principle in an exactly analogous way. This indicates that their mechanical effect in these force equations is seemingly of the same type.

The operation of the Pauli exclusion principle is thus interpreted as an aspect of the same fundamental process as the Second Law of Thermodynamics. Each is a mechanical aspect of the operation of forces acting in momentum or phase space. The Pauli principle is a kind of measure of the force that excludes particles from occupied cells, and the correction term represents the degree of " objection " which particles feel towards forces tending to put them into already occupied phase positions.

It is significant that the two places where the statistical method seemingly fails to give satisfaction, namely, (*a*) the Second Law of Thermodynamics, and (*b*) the Pauli exclusion principle, are both partly taken care of and interpreted by the present mechanical stress-strain theory. Furthermore, these two fundamental and far-reaching principles are both interpreted as aspects of the same general process, *i. e.*, the operation of stress-strain relations in momentum space.

The dual aspects of light and electricity, as mechanical and corpuscular on the one hand and wave phenomena on the other, are familiar. The present and previous * papers show that certain phenomena also of thermodynamics and statistical mechanics fit nicely when incorporated into the theory of elasticity, and thus can be given a mechanical interpretation as well as one based on probability.

In conclusion, it is to be emphasized that this paper, like the previous one †, does not " extend the meanings of force and strain " ‡, but merely points out that classical Newtonian force and classical zero dimensional strain are actually functioning in momentum space, and that the way they act helps to account for the Second Law of Thermodynamics and the Pauli exclusion principle.

Our thanks are due to Prof. G. E. Uhlenbeck, of Ann Arbor, and Prof. H. A. Kramers, of Utrecht, for very valuable criticism.

Michigan State College,
East Lansing, Michigan.

---

* Kimball, *loc. cit.*
† Kimball, *loc. cit.*
‡ ' Science Abstracts,' 2744 (August 1931).

CVII. *Operational Calculus.*—Part II.* *The Values of certain Integrals and the Relationships between various Polynomials and Series obtained by Operational Methods.* By H. V. LOWRY, *Lecturer in Mathematics in the Manchester College of Technology* †.

SUMMARY.

In this part operational methods are used

(a) to find the values of certain integrals ;

(b) to establish the relationships between Bernouilli polynomials and some other polynomials of a similar type ;

(c) to sum some series of Bessel functions of the type

$$\sum_{r=1}^{\infty} r^{-\frac{1}{2}} J_n(2\sqrt{rx}) ;$$

(d) to sum series of Bessel functions of the Schlömilch type, such as

$$\sum_{m=1}^{\infty} J_n(mx), \quad \sum_{m=1}^{\infty} J_n(mx)/m ;$$

(e) to sum series of the type

$$\sum_{m=1}^{\infty} J_n(mx) \cos my,$$

which we may call Bessel-Fourier series ;

(f) to sum series of Struve functions corresponding to the series of types (d) and (e).

Of the formulæ proved, those of most interest are :

$$\int_0^x P_m(\cos u) \sin^{m-1}(x-u)du = \frac{\sin^m x}{m}, \quad . \quad . \quad (8)$$

$$\int_0^x \sin^{2n} u \sin^{2n+1}(x-u)du$$
$$= \frac{2n! \; 2n+1! \; 2^{4n-1} \sin^{4n}(\frac{1}{2}x) \cos\frac{1}{2}x}{4n-1!}, \quad . \quad (9)$$

$$_2\psi_n(x) = {_1}\psi_n(x+\tfrac{1}{2}), \quad . \quad . \quad . \quad . \quad (45)$$

$$2^n \cdot {_3}\psi_n(x) = {_2}\psi_{n+1}(\tfrac{1}{2}x) - {_1}\psi_{n+1}(\tfrac{1}{2}x), \quad . \quad . \quad (46)$$

$$_4\psi_n(x) = {_3}\psi_n(x-\tfrac{1}{2}), \quad . \quad . \quad . \quad . \quad (47)$$

---

* For Part I. see Phil. Mag. pp. 1033–1048 (May 1932).
† Communicated by the Author.

where the ψ's are polynomials associated with Bernouilli polynomials.

$$x^{-\frac{1}{2}n} \sum_{r=1}^{\infty} r^{-\frac{1}{2}n} J_n(2\sqrt{rx})$$

$$= \frac{x^{n-1}}{\Pi(n-1)} - \frac{x^n}{2\Pi(n)} - \sum_{r=1}^{\infty} \frac{(-1)^r B_r x^{n+2r-1}}{2r!\,\Pi(n+2r-1)}. \quad . \quad (51)$$

$$\sum_{r=1}^{\infty} \frac{1}{(\sqrt{a^2+r}+a)^n}$$

$$\sim \frac{1}{2^{n-2}a^{n-2}} - \frac{1}{2^{n+1}a^n} - \sum_{r=1}^{\infty} \frac{(-1)^r B_r \Pi(n+4r-1)}{2r!\,\Pi(n+2r-1)2^{n+2r}a^{n+4r-1}}.$$

$$. \quad . \quad . \quad (58)$$

$$x^n 2^{-n+1} \sum_{m=1}^{\infty} m^{-n} J_n(mx)$$

$$= -\frac{x^{2n}}{\Pi(n)2^{2n}} + \frac{\sqrt{\pi}}{\Pi(n-\frac{1}{2})2^{2n-1}}$$

$$\left[x^{2n-1} + 2 \sum_{k=1}^{r} \{x^2-(2k\pi)^2\}^{m-\frac{1}{2}} \right].$$

$$2r\pi < x < 2(r+1)\pi. \quad . \quad . \quad . \quad . \quad . \quad (64)$$

$$2 \sum_{m=1}^{\infty} m^{-n} J_n(mx) \cos ny = -\frac{x^n}{\Pi(n)2^n}, \quad \begin{matrix} 0 < x < y, \\ 0 < y < \pi. \end{matrix} \quad (72)$$

$$2x^{\frac{1}{2}} \sum_{m=1}^{\infty} m^{-n-1} S_n(2m\sqrt{x})$$

$$= -\frac{x^{n+\frac{1}{2}}}{\Pi(n+\frac{1}{2})} + \pi \left[\frac{x^n}{\Pi(n)} + 2 \sum_{k=1}^{r} \frac{x^n}{\Pi(n)} \right.$$

$$\left. - \frac{x^n}{\Pi(n-\frac{1}{2})} \int_x^{\infty} \frac{y(x-\frac{1}{4}y^2)^{n-\frac{1}{2}}}{4x^{n-1}} dx \right],$$

$$r^2\pi^2 < x < (r+1)^2\pi^2. \quad . \quad . \quad . \quad . \quad (83)$$

$$2x^{\frac{1}{2}n} \sum_{n=1}^{\infty} n^{-n-1} S_n(2m\sqrt{x}) \cos my = -\frac{2x^{n+\frac{1}{2}}}{\sqrt{\pi}\Pi(n+\frac{1}{2})},$$

$$\begin{matrix} 0 < x < y, \\ 0 < y < \pi. \end{matrix} \quad . \quad . \quad (86)$$

In the last two equations $S_m(x)$ is Struve's function of order m. In equations (72) and (86) above the results are given for $0 < x < y$, but in the text formulæ are given for the sums for all values of x.

1. *The Operator for* $\sin^m x$ *and some Integrals obtained from it.*

SINCE

$$\frac{p}{p^2+1} \doteqdot \sin x,$$

$$\sin^2 x \doteqdot \frac{e^{ix}-e^{-ix}}{2i}\frac{p}{p^2+1}$$

$$= \frac{1}{2i}\left\{\frac{p-i}{p(p-2i)}\left(\frac{p}{p-i}\right) - \frac{p+1}{p(p+2i)}\left(\frac{p}{p+i}\right)\right\}$$

$$= \frac{1}{2i}\left(\frac{1}{p-2i} - \frac{1}{p+2i}\right)$$

$$= \frac{2}{p^2+2^2}.$$

Similarly,

$$\sin^3 x \doteqdot \frac{3!\,p}{(p^2+1^2)(p^2+3^2)},$$

and so, by induction,

$$\sin^{2n} x \doteqdot \frac{2n!}{(p^2+2^2(p^2+4^2)\ldots\{p^2+(2n)^2\}}, \quad \cdot \quad (1)$$

and

$$\sin^{2n+1} x \doteqdot \frac{2n+1!\,p}{(p^2+1^2)(p^2+3^2)\ldots\{p^2+(2n+1)^2\}}. \quad (2)$$

Now, since

$$P_{2n}(\cos x) \doteqdot \frac{(p^2+1^2)(p^2+3^2)\ldots\{p^2+(2n-1)^2\}}{(p^2+2^2)(p^2+4^2)\ldots\{p^2+(2n)^2\}}, \quad (3)$$

and

$$P_{2n+1}(\cos x) \doteqdot \frac{(p^2+0^2)(p^2+2^2)\ldots\{p^2+(2n)^2\}}{(p^2+1^2)(p^2+3^2)\ldots\{p^2+(2n+1)^2\}}, \quad (4)$$

we find, by substitution in Borel's integral,

$$\frac{1}{p}f_1(p)f_2(p) \doteqdot \int_0^x h_1(u)h_2(x-u)du, \quad \cdot \quad (5)$$

---

* "The Operational Solution of Linear Equations," by Dr. B. v. d. Pol, Phil. Mag. viii. p. 888 (1929).

that

$$\int_0^x P_{2n}(\cos u) \sin^{2n-1}(x-u)du$$

$$\doteqdot \frac{2n-1\,!}{(p^2+2^2)(p^2+4^2)\dots\{p^2+(2n)^2\}}$$

$$= \frac{\sin^{2n} x}{2n}, \quad \cdot \quad \cdot \quad \cdot \quad \cdot \quad \cdot \quad \cdot \quad \cdot \quad (6)$$

and

$$\int_0^x P_{2n+1}(\cos u) \sin^{2n}(x-u)du$$

$$\doteqdot \frac{2n\,!\,p}{(p^2+1^2)(p^2+3^2)\dots\{p^2+(2n-1)^2\}}$$

$$= \frac{\sin^{2n+1} x}{2n+1}. \quad \cdot \quad \cdot \quad \cdot \quad \cdot \quad \cdot \quad \cdot \quad (7)$$

(6) and (7) are both included in

$$\int_0^x P_m(\cos u) \sin^{m-1}(x-u)du = \frac{\sin^m(x)}{m}. \quad \cdot \quad (8)$$

Iu the same way, from (1) and (2) we get

$$\int_0^x \sin^{2n} u \sin^{2n+1}(x-u)du$$

$$\doteqdot \frac{2n\,!\,2n+1\,!\,p}{(p^2+1^2)(p^2+2^2)\dots\{p^2+(2n)^2\}}$$

$$= \frac{2n\,!\,2n+1\,!\,2^{4n}}{4n\,!}\,p\,.\,\sin^{4n}(\tfrac{1}{2}x)$$

$$= \frac{2n\,!\,2n+1\,!\,2^{4n-1}\sin^{4n}(\tfrac{1}{2}x)\cos(\tfrac{1}{2}x)}{4n-1\,!}. \quad \cdot \quad (9)$$

2. *Properties of Bernouilli Polynomials and the Relationships of these Polynomials to certain other Polynomials.*

From (1) we find that

$$\tfrac{1}{2}\operatorname{cosech}\tfrac{1}{2}p\pi \doteqdot \lim_{n\to\infty} \frac{(n\,!)^2\,2^{2n}}{\pi p(p^2+2^2)\dots\{p^2-(2n)^2\}}$$

$$\doteqdot \lim_{n\to\infty} \frac{(n\,!)^2\,2^{2n}}{\pi\,.\,2n\,!}\int_0^x \sin^{2n} x\,dx.$$

4 E 2

From this limit it is easily shown that, if x is real,

$$\tfrac{1}{2}\operatorname{cosech}\tfrac{1}{2}p\pi \doteqdot r, \quad (r-\tfrac{1}{2})\pi < x < (r+\tfrac{1}{2})\pi *; . \quad (10)$$

so

$$\tfrac{1}{2}\operatorname{cosech}\tfrac{1}{2}p \doteqdot r, \quad (r-\tfrac{1}{2}) < x < (r+\tfrac{1}{2}). \quad . \quad (11)$$

From this operator we easily find that

$$\frac{1}{e^{p}-1} = \tfrac{1}{2}e^{\frac{1}{2}p}\operatorname{cosech}\tfrac{1}{2}p \doteqdot r, \quad r < x < r+1 ; \ . \ . \ . \ (12)$$

$$\frac{e^{p}}{e^{p}-1} = \tfrac{1}{2}(1 + \operatorname{coth}\tfrac{1}{2}p) \doteqdot r, \quad r-1 < x < r ; \quad . \ . \ (13)$$

$$\frac{1}{e^{p}+1} = \frac{e^{p}}{e^{2p}-1} - \frac{1}{e^{2p}-1} \doteqdot \begin{array}{l} 0, \quad 2r < x < 2r+1, \\ 1, \ 2r+1 < x < 2r+2 ; \end{array} \quad (14)$$

and

$$\tfrac{1}{2}\operatorname{sech}\tfrac{1}{2}p = \frac{e^{\frac{1}{2}p}}{e^{p}+1} \doteqdot \begin{array}{l} 0, \quad 2r-\tfrac{1}{2} < x < 2r+\tfrac{1}{2}, \\ 1, \quad 2r+\tfrac{1}{2} < x < 2r+\tfrac{3}{2}. \end{array} \quad . \ . \ . \ (15)$$

Heaviside, followed by other writers, found the functions given by these operators by expanding the operators in powers of e^{-p}. In order to be able to do this we must have

$$| e^{-p} | < 1 \quad \text{that is,} \quad \mathrm{R}(p) > 0,$$

and so we have to operate on $\mathrm{H}(x)$ instead of on 1. This means that, with the operator $\dfrac{1}{e^{p}-1}$ for example, we get

$$\frac{1}{e^{p}-1}\,\mathrm{H}(x) \doteqdot 0, \quad x < 0,$$

$$\doteqdot r, \quad r < x < r+1 ; \ (r \geqq 0).$$

Equation (12) is more general than this because it is true for all real values of x.

Similarly, equations (13), (14), (15) are more general than the corresponding equations obtained by expanding in series and operating on $\mathrm{H}(x)$.

Now from equations (11) to (15) we find by successive integration from 0 to x that, when n is a positive integer,

$$\tfrac{1}{2}p^{-n}\operatorname{cosech}\tfrac{1}{2}p \doteqdot \frac{1}{n!}\{(x-\tfrac{1}{2})^{n}+(x-\tfrac{3}{2})^{n}+ \ldots +(x-r+\tfrac{1}{2})^{n}\},$$

$$r-\tfrac{1}{2} < x < r+\tfrac{1}{2} ; \ . \ . \ . \ (16)$$

---

* See a paper by the author on " Approximation Curves for a Fourier Series," Phil. Mag. x. p. 695 (1930).

$$\frac{p^{-n}}{e^p-1} \doteqdot \frac{1}{n!}\{(x-1)^n+(x-2)^n+ \ldots +(x-r)^n\},$$

$$r < x < r+1; \quad \ldots \quad (17)$$

$$\frac{p^{-n}}{e^p+1} \doteqdot \frac{1}{n!}\{(x-1)^n-(x-2)^n+ \ldots +(-1)^{r-1}(x-r)^n\},$$

$$r < x < r+1; \quad \ldots \quad (18)$$

$$\tfrac{1}{2}p^{-n} \operatorname{sech} \tfrac{1}{2}p \doteqdot \frac{1}{n!}\{(x-\tfrac{1}{2})^n+(x-\tfrac{3}{2})^n+ \ldots +(x-r+\tfrac{1}{2})^n\},$$

$$r-\tfrac{1}{2} < x < r+\tfrac{1}{2}. \quad \ldots \quad (19)$$

From the expansion

$$\frac{1}{e^p-1} = \frac{1}{p} - \frac{1}{2} + \frac{B_1 p}{2!} - \frac{B_2 p^3}{4!} + \ldots$$

we find, by partial fractions, that, when m is a positive integer,

$$\frac{p^{-2m}}{e^p-1} = \frac{1}{p^{2m+1}} - \frac{1}{2p^{2m}} + \frac{B_1}{2!\,p^{2m-1}} - \ldots + \frac{(-1)^{m-1}B_m}{2m!\,p}$$

$$+ \sum_{k=-\infty}^{\infty} \frac{1}{(2k\pi i)^{2m}(p-2k\pi i)}$$

$$\doteqdot {}_1\psi_{2m+1}(x) + 2(-1)^m \sum_{k=1}^{\infty} \frac{\sin 2k\pi x}{(2k\pi)^{2m+1}}, \quad \ldots \quad (20)$$

where

$${}_1\psi_{2m+1}(x) = \frac{x^{2m+1}}{2m+1!} - \frac{x^{2m}}{2.2m!} + \frac{B_1 x^{2m-1}}{2!\,2m-1!} - \frac{B_2 x^{2m-3}}{4!\,2m-3!}$$

$$+ \ldots + \frac{(-1)^{m-1}B_m x}{2m!}. \quad \ldots \quad (21)$$

By differentiating equation (20) we get

$$\frac{p^{-2m+1}}{e^p-1} \doteqdot {}_1\psi_{2m}(x) + 2(-1)^m \sum_{k=1}^{\infty} \frac{\cos 2k\pi x}{(2k\pi)^{2m}}, \quad \cdot \quad (22)$$

where

$${}_1\psi_{2m}(x) = \frac{d\{{}_1\psi_{2m+1}(x)\}}{dx}$$

$$= \frac{x^{2m}}{2m!} - \frac{x^{2m-1}}{2.2m-1!} + \ldots + \frac{(-1)^{m-1}B_m}{2m!}. \quad \cdot \quad (23)$$

Both (20) and (22) are included in

$$\frac{p^{-n+1}}{e^p-1} \doteqdot {}_1\psi_n(x) + 2 \sum_{k=1}^{\infty} \frac{\cos \pi(2kx - \tfrac{1}{2}n)}{(2k\pi)^n}, \quad \cdot \quad (24)$$

where

$$_1\psi_n(x) = \frac{x^n}{n!} - \frac{x^{n-1}}{2 \cdot n-1!} + \frac{B_1 x^{n-2}}{2! \, n-2!} - \frac{B_2 x^{n-4}}{4! \, n-4!} + \dots, \quad (25)$$

the polynomial ending in a term in x or a constant.

From equations (17) and (24) it follows that

$$_1\psi_n(x) + 2 \sum_{k=1}^{\infty} \frac{\cos \pi(2kx - \frac{1}{2}n)}{(2k\pi)^n}$$

$$= \frac{1}{n-1!}\{(x-1)^{n-1} + \dots + (x-r)^{n-1}\},$$

$$r < x < r+1. \quad . \quad . \quad (26)$$

The polynomial $_1\psi_n(x)$ is closely related to the Bernouilli polynomial of the nth order $\phi_n(x)$, in fact

$$2m! \, _1\psi_{2m}(x) = \phi_{2m}(x) + (-1)^{m-1} B_m, \quad . \quad . \quad (27)$$

$$2m+1! \, _1\psi_{2m+1}(x) = \phi_{2m+1}(x), \quad . \quad . \quad . \quad . \quad . \quad (28)$$

but it appears to be more natural to use $_1\psi_n(x)$ here, because by using it in preference to $\phi_n(x)$ we can express the relationship between the polynomial and the Fourier series by the one equation (25) instead of the two which are necessary when Bernouilli polynomials are used.

In the same way, starting from the series

$$\tfrac{1}{2} \operatorname{cosech} \tfrac{1}{2}p = \frac{1}{p} - \frac{B_1(2^2-2)p}{2! \, 2^2} + \dots,$$

we find, by partial fractions, that

$$\tfrac{1}{2}p^{-n+1} \operatorname{cosech} \tfrac{1}{2}p \doteqdot {}_2\psi_n(x) + 2 \sum_{k=1}^{\infty} \frac{(-1)^k \cos \pi(2kx - \frac{1}{2}n)}{(2k\pi)^n},$$

$$. \quad . \quad . \quad (29)$$

where

$$_2\psi_n(x) = \frac{x^n}{n!} - \frac{B_1(2^2-2)x^{n-2}}{2! \, n-2! \, 2^2} + \dots, \quad . \quad . \quad (30)$$

the polynomial ending with a term in x or a constant.

By comparing (29) with (16) we get

$$_2\psi_n(x) + 2 \sum_{k=1}^{\infty} \frac{(-1)^k \cos \pi(2kx - \frac{1}{2}n)}{(2k\pi)^n}$$

$$= \frac{1}{n-1!}\{(x-\tfrac{1}{2})^{n-1} + \dots + (x-r+\tfrac{1}{2})^{n-1}\},$$

$$r-\tfrac{1}{2} < x < r+\tfrac{1}{2}. \quad . \quad . \quad (31)$$

Starting with the series

$$\frac{1}{e^p+1} = \frac{1}{2} - \frac{B_1(2^2-1)p}{2!} + \frac{B_2(2^4-1)p^3}{4!} \dots, \quad (32)$$

and

$$\tfrac{1}{2}\operatorname{sech}\tfrac{1}{2}p = \frac{1}{2}\left\{1 - \frac{E_1 p^2}{2!\,2^2} + \frac{E_2 p^4}{4!\,2^4} - \dots\right\}, \quad (33)$$

where $E_1, E_2, \dots$ **are Euler's numbers, we find that**

$$\frac{p^{-n}}{e^p+1} = {}_3\psi_n(x) - 2\sum_{k=1}^{\infty}\frac{\sin \pi\{(2k-1)x - \tfrac{1}{2}n\}}{\{(2k-1)\pi\}^{n+1}}, \quad (34)$$

and

$$\tfrac{1}{2}p^{-n}\operatorname{sech}\tfrac{1}{2}p \doteq {}_4\psi_n(x) + 2\sum_{k=1}^{\infty}\frac{(-1)^k \cos \pi\{(2k-1)x - \tfrac{1}{2}n\}}{\{(2k-1)\pi\}^{n+1}}.$$

$$\dots \quad (35)$$

In these equations, ${}_3\psi_n(x)$ and ${}_4\psi_n(a)$ are the polynomials

$${}_3\psi_n(x) = \frac{x^n}{2\cdot n!} - \frac{B_1(2^2-1)x^{n-1}}{2!\,n-1!} + \frac{B_2(2^4-1)x^{n-3}}{4!\,n-3!} - \dots,$$

$$\dots \quad (36)$$

$${}_4\psi^n(x) = \frac{1}{2}\left\{\frac{x^n}{n!} - \frac{E_1 x^{n-2}}{2!\,n-2!\,2^2} + \frac{E_2 x^{n-4}}{4!\,n-4!\,2^4} - \dots\right\}, \quad (37)$$

both polynomials ending with a term in x or a constant.

By comparing equations (34) and (35) with (18) and (19) we get

$${}_3\psi_n(x) - 2\sum_{k=1}^{\infty}\frac{\sin \pi\{(2k-1)x - \tfrac{1}{2}\}}{\{(2k-1)\pi\}^{n+1}}$$

$$= \frac{1}{n!}\{(x-1)^n - (x-2)^n + \dots\}, \quad r < x < r+1, \quad (38)$$

and

$${}_4\psi_n(x) + 2\sum_{k=1}^{\infty}\frac{(-1)^k \cos \pi\{(2k-1)x - \tfrac{1}{2}n\}}{\{(2k-1)\pi\}^{n+1}}$$

$$= \frac{1}{n!}\{(x-\tfrac{1}{2})^n - (x-\tfrac{3}{2})^n + \dots\}, \quad r-\tfrac{1}{2} < x < r+\tfrac{1}{2}.$$

$$\dots \quad (39)$$

From equations (26), (30), (38), and (39) we can find various relationships between the polynomials ${}_1\psi_n(x)$,

$_2\psi_n(x)$, $_3\psi_n(x)$, and $_4\psi_n(x)$.   Replacing x by $x+1$ in each equation, we get immediately

$$_1\psi_n(x+1) - {}_1\psi_n(x) = \frac{x^{n-1}}{n!}, \quad \ldots \ldots \quad (40)$$

$$_2\psi_n(x+1) - {}_2\psi_n(x) = \frac{(x+\frac{1}{2})^{n-1}}{n-1!}, \quad \ldots \quad (41)$$

$$_3\psi_n(x+1) - {}_3\psi^n(x) = \frac{x^n}{n!}, \quad \ldots \ldots \quad (42)$$

$$_4\psi_n(x+1) - {}_4\psi_n(x) = \frac{(x+\frac{1}{2})^n}{n!} \quad \ldots \ldots \quad (43)$$

Now if we put $x+\frac{1}{2}$ for x in equation (26), it becomes

$$_1\psi_n(x+\tfrac{1}{2}) + 2 \sum_{k=1}^{\infty} \frac{(-1)^k \cos \pi(2kx - \frac{1}{2}n)}{(2k\pi)^n}$$

$$= \frac{1}{n-1!}\{(x-\tfrac{1}{2})^{n-1} + (x-\tfrac{3}{2})^{n-1} + \ldots + (x-r+\tfrac{1}{2})^{n-1}\},$$

$$r - \tfrac{1}{2} < x < r + \tfrac{1}{2}. \quad \ldots \quad (44)$$

This equation, with equation (31), shows that

$$_2\psi_n(x) = {}_1\psi_n(x+\tfrac{1}{2}). \quad \ldots \ldots \quad (45)$$

In the same way, from equations (38) and (39)

$$_4\psi_n(x) = {}_3\psi_n(x+\tfrac{1}{2}). \quad \ldots \ldots \quad (46)$$

Further, from equations (26), (31), and (38) we find that

$$2^n {}_3\psi_n(x) = {}_2\psi_{n+1}(\tfrac{1}{2}x) - {}_1\psi_{n+1}(\tfrac{1}{2}x); \quad \ldots \quad (47)$$

alternatively this last equation can be deduced directly from the polynomials by comparing coefficients of the several powers of x.

Equations (45), (46), and (47) suffice to express each of the polynomials $_2\psi_n(x)$, $_3\psi_n(x)$, $_4\psi_n(x)$ in terms of $_1\psi_n(x)$, and hence in terms of Bernouilli polynomials. (45) gives the expansion of Bernouilli polynomials in powers of $x - \frac{1}{2}$, for by putting $x - \frac{1}{2}$ instead of x we get

$$_1\psi_n(x) = {}_2\psi_n(x-\tfrac{1}{2}).$$

This is the general formula of which the cases $n = 1$ to $n = 6$ are given in Bromwich's 'Infinite Series,' p. 300.

3. *Series of Bessel Functions and Allied Series.*

Since

$$\frac{1}{e^{1/p}-1} = p - \tfrac{1}{2} + \frac{B_1}{2!\,p} - \frac{B_2}{4!\,p^3} + \dots,$$

$$\frac{p^{-n}}{e^{1/p}-1} = \frac{1}{p^{n-1}} - \frac{1}{2p^n} + \frac{B_1}{2!\,p^{n+1}} - \frac{B_2}{4!\,p^{n+3}} + \dots$$

$$\doteqdot \frac{x^{n-1}}{\Pi(n-1)} - \frac{x^n}{2\Pi(n)} + \frac{B_1 x^{n+1}}{2!\,\Pi(n+1)} - \frac{B_2 x^{n+2}}{4!\,\Pi(n+3)} + \dots$$

$$\qquad\qquad\qquad\qquad \dots \quad (49)$$

Also expanding the operator in powers of $e^{-1/p}$, which is legitimate in the contour L but not in the contour C, we get

$$\frac{p^{-n}}{e^{1/p}-1}\,\mathrm{H}(x) = (p^{-n}e^{-1/p} + p^{-n}e^{-2/p} + \dots)\mathrm{H}(x)$$

$$\doteqdot x^{\frac{1}{2}n}\sum_{r=1}^{\infty} r^{-\frac{1}{2}n}J_n(2\sqrt{rx}), \quad x \text{ real} > 0, \quad . \quad . \quad (50)$$

the series on the right-hand side being convergent when $n > \tfrac{1}{2}$.

Therefore from (49) and (50) we get

$$x^{\frac{1}{2}n}\sum_{r=1}^{\infty} r^{-\frac{1}{2}n}J_n(\sqrt{rx})$$

$$= \frac{x^{n-1}}{\Pi(n-1)} - \frac{x^n}{2\Pi(n)} - \sum_{r=1}^{\infty}\frac{(-1)^r B_r x^{n+2r-1}}{2r!\,\Pi(n+2r-1)},$$

$$x \text{ real and} > 0, \; n > \tfrac{1}{2}. \quad . \quad . \quad (51)$$

In the same way, by expanding each of the operators

$$\frac{p^{-n}e^{1/p}}{e^{2/p}-1}, \quad \frac{p^{-n}}{e^{1/p}+1}, \quad \frac{p^{-n}e^{1/p}}{e^{2/p}+1}$$

in two different ways, we find that

$$x^{\frac{1}{2}n}\sum_{r=1}^{\infty}(2r-1)^{-\frac{1}{2}n}J_n\{2\sqrt{(2r-1)x}\}$$

$$= \frac{x^{n-1}}{2\Pi(n-1)} + \sum_{r=1}^{\infty}\frac{(-1)^r B_r(2^{2r}-2)x^{n+2r-1}}{2r!\,\Pi(n+2r-1)}, \quad . \quad (52)$$

$$x^{\frac{1}{2}n} \sum_{r=1}^{\infty} (-1)^{r+1} r^{-\frac{1}{2}n} J_n(2\sqrt{rx})$$

$$= \frac{x^n}{2\Pi(n)} - \sum_{r=1}^{\infty} \frac{(-1)^r B_r(2^{2r}-2) x^{n+2r-1}}{2r! \, \Pi(n+2r-1)}, \qquad . \quad (53)$$

$$x^{\frac{1}{2}n} \sum_{r=1}^{\infty} (-1)^{r+1} (2r-1)^{-\frac{1}{2}n} J_n\{2\sqrt{(2r-1)x}\}$$

$$= \frac{x^n}{\Pi(n)} + \sum_{r=1}^{\infty} \frac{(-1)^r E_r x^{n+2r}}{2r! \, \Pi(n+2r)}, \quad . \quad . \quad . \quad . \quad (54)$$

(52), (53), and (54) being true, when x is real and > 0 and $n > \frac{1}{2}$.

If we write $x^2/4$ for x in equation (51) it becomes

$$\frac{x^n}{2^n} \sum_{r=1}^{\infty} r^{-\frac{1}{2}n} J_n(rx)$$

$$= \frac{x^{2n-2}}{2^{2n-2}\Pi(n-1)} - \frac{a^{2n}}{2^{2n+1}\Pi(n)}$$

$$- \sum_{r=1}^{\infty} \frac{(-1)^r B_r x^{2n+4r-2}}{2^{2n+4r-2} 2r! \, \Pi(n+2r-1)} . \quad . \quad (55)$$

Now apply Carson's integral to this equation, remembering that

$$\frac{2^n \Pi(n-\frac{1}{2})}{\sqrt{\pi}} \frac{p}{(p^2+r)^{n+\frac{1}{2}}} \doteqdot r^{-\frac{1}{2}n} x^n J_n(\sqrt{r}.x) ;$$

this gives

$$\frac{\Pi(n-\frac{1}{2})}{\sqrt{\pi}} \sum_{r=1}^{\infty} \frac{1}{(a^2+r)^{n+\frac{1}{2}}}$$

$$= \frac{\Pi(2n-2)}{\Pi(n-1) 2^{2n-2} a^{2n-1}} - \frac{\Pi(2n)}{\Pi(n) 2^{2n+1} a^{2n}}$$

$$- \sum_{r=1}^{\infty} \frac{(-1)^r B_r \Pi(2n+4r-2)}{2r! \, \Pi(n+2r-1) 2^{2n+4r-2} a^{2n+4r-1}} .$$

$$. \quad . \quad . \quad (56)$$

The right-hand side of this equation is not convergent, but it is easy to show that Carson's integral of the sum of the terms after the rth in equation (55) is less than the integral of the rth term, so that the right-hand side of (56) is an asymptotic series. If we write $a^2 = b$ in equation (56) and apply Euler's summation formula to the left-hand side we get equation (56) exactly, thus verifying that this equation is correct.

Further, if we divide equation (55) by x^n, and apply Carson's integral again, using the operator

$$\frac{p}{\sqrt{p^2+r}}(\sqrt{p^2+r}-p)^n \doteq r^{\frac12 n}J_n(\sqrt{r}.x),$$

we find that

$$\sum_{r=1}^{\infty}\frac{(\sqrt{a^2+r}-a)^n}{r^n\sqrt{a^2+r}} \sim \frac{\Pi(n-2)}{\Pi(n-1)2^{n-2}a^{n-1}} - \frac{\Pi(n)}{\Pi(n)2^{n+1}a^{n+1}}$$
$$- \sum_{r=1}^{\infty}\frac{(-1)^r B_r\Pi(n+4-2)}{2r!\,\Pi(n+2r-1)2^{n+4r}a^{n+4r-1}}, \quad (57)$$

in which the left-hand side is convergent when $n > 1$. It does not appear that this asymptotic series can be deduced immediately from Euler's summation formula.

Since

$$\frac{d}{da}(\sqrt{a^2+r}-a)^n = -\frac{(\sqrt{a^2+r}-a)^n}{\sqrt{a^2+r}},$$

it follows that, if we integrate (57) from a to ∞, we get

$$\sum_{r=1}^{\infty}\frac{(\sqrt{a^2+r}-a)^n}{r^n} \sim \frac{1}{2^{n-2}a^{n-2}} - \frac{1}{2^{n+1}a^n}$$
$$- \sum_{r=1}^{\infty}\frac{(-1)^r B_r\Pi(n+4r-1)}{2r!\,\Pi(n+2r-1)2^{n+2r}a^{n+4r-2}}, \quad (58)$$

the left-hand side being convergent if $n > 2$.

4. *Bessel Function Series of the Schlömilch Type.*
Since

$$\pi\sqrt{p}\coth\pi\sqrt{p} = 1+2\sum_{m=1}^{\infty}\frac{p}{p^2+m^2},$$
$$\pi\sqrt{p}\left\{1+2\sum_{m=1}^{\infty}e^{-2m\sqrt{p}}\right\} = 1+2\sum_{m=1}^{\infty}\frac{p}{p^2+m^2}. \quad (59)$$

Hence, if we operate on 1 we get

$$\sqrt{\pi/x}\left\{1+2\sum_{m=1}^{\infty}e^{-m^2\pi^2/x}\right\} = 1+2\sum_{m=1}^{\infty}e^{-m^2x}, \quad (60)$$

the sides being convergent only if $R(x) > 0$. (60) is a relationship found by Jacobi*.

* Whittaker and Watson, 'Modern Analysis,' 2nd ed. p. 124, Ex. 18.

Writing $x = 1/p$ in (60), we find that

$$\sqrt{\pi p}\left\{1 + 2\sum_{m=1}^{\infty} e^{-m^2\pi^2 p}\right\} H(x) = \left\{1 + 2\sum_{m=1}^{\infty} e^{-m^2/p}\right\} H(x).$$

$$\ldots \quad (61)$$

If x is real the right-hand side of this equation is

$$\doteqdot 1 + 2\sum_{m=1}^{\infty} J_0(2m\sqrt{x}).$$

and the left-hand side is

$$\doteqdot \frac{1}{\sqrt{x}}, \qquad\qquad 0 < x < \pi^2,$$

and

$$\doteqdot \frac{1}{\sqrt{x}} + \frac{2}{\sqrt{x^2 - \pi^2}} + \ldots + \frac{2}{\sqrt{x^2 - r^2\pi^2}},$$

$$r^2\pi^2 < x < (r+1)^2\pi^2;$$

so

$$1 + 2\sum_{m=1}^{\infty} J_0(2m\sqrt{x})$$

$$= \frac{1}{\sqrt{x}} + 2\sum_{k=1}^{r} \frac{1}{\sqrt{x^2 - k^2\pi^2}}, \quad r^2\pi^2 < x < (r+1)^2\pi^2. \quad (62)$$

If we put $2\sqrt{x} = X$, equation (62) becomes

$$1 + 2\sum_{m=1}^{\infty} J_0(mX) = \frac{2}{X} + 4\sum_{k=1}^{r} \frac{1}{\sqrt{X^2 - 2^2 k^2 \pi^2}},$$

$$2r\pi < X < 2(r+1)\pi. \quad \ldots \quad (63)$$

This equation is a particular case of the type given by Schlömilch; but if we multiply equation (61) by p^{-n}, and proceed in the same way as above, we get a series of Bessel functions of the nth order, and so generalize equation (63). The final equation, after putting $2\sqrt{x} = X$, is

$$\frac{X^{2n}}{2^{2n}\Pi(n)} + \frac{X^n}{2^{n-1}}\sum_{m=1}^{\infty} m^{-n} J_n(mX)$$

$$= \frac{\sqrt{\pi}}{2^{2n-1}\Pi(n-\frac{1}{2})}\left\{X^{2n-1}\sum_{k=1}^{r}(X^2 - 2^2 k^2\pi^2)^{n-\frac{1}{2}}\right\},$$

$$2r\pi < X < 2(r+1)\pi. \quad \ldots \quad (64)$$

5. *Bessel-Fourier Series of the Schlömilch Type.*

Since

$$2 \sum_{m=1}^{\infty} \frac{p^2 q^2}{(p^2+m^2)(q^2+m^2)}$$

$$= 2 \sum_{m=1}^{\infty} \frac{p^2 q^2}{q^2-p^2} \left(\frac{1}{p^2+m^2} - \frac{1}{q^2+m^2} \right)$$

$$= \frac{q^2}{q^2-p^2} \{ \pi p \coth \pi p - 1 \} - \frac{p^2}{q^2-p^2} \{ \pi q \coth \pi q - 1 \}$$

$$= -1 + \pi \left\{ \frac{pq}{p+q} + \frac{2pq^2}{q^2-p^2} \sum_{k=1}^{\infty} e^{-2k\pi p} \right.$$

$$\left. - \frac{2qp^2}{q^2-p^2} \sum_{k=1}^{\infty} e^{-2k\pi q} \right\}, \quad \ldots \quad (65)$$

where $R(q) > 0$, if we write $\sqrt{p}$ for p we get

$$2 \sum_{m=1}^{\infty} \frac{pq^2}{(p+m^2)(q^2+m^2)}$$

$$= -1 + \pi \left\{ \frac{\sqrt{p}\, q}{\sqrt{p}+q} + \frac{2\sqrt{p}\, q^2}{q^2-p} \sum_{k=1}^{\infty} e^{-2k\pi \sqrt{p}} \right.$$

$$\left. - \frac{2qp}{q^2-p} \sum_{k=1}^{\infty} e^{-2k\pi q} \right\}, \quad R(q) > 0. \quad (66)$$

Now in (66) let p and q stand for x and y operators; then, operating first with q on $H(y)$ (since $R(q) > 0$), we get

$$2 \sum_{m=1}^{\infty} \frac{p}{p^2+m^2} \cos my$$

$$= -1 + \pi \left\{ \sqrt{p}\, e^{-\sqrt{p}\, y} + \sqrt{p}(e^{\sqrt{p}\, y} + e^{-\sqrt{p}\, y}) \sum_{k=1}^{\infty} e^{-2k\pi \sqrt{p}} \right.$$

$$\left. - \sqrt{p} \sum_{k=1}^{\infty} e^{\sqrt{p}(y-2k\pi)} - e^{-\sqrt{p}(y-2k\pi)} \right\}, \quad (67)$$

in which y is real and $2r\pi < y < 2(r+1)\pi$.

Since there is no restriction on p, we can operate with this equation on 1, using the contour C. This gives, after reduction,

$$2 \sum_{m=1}^{\infty} e^{-m^2 x} \cos my$$

$$= -1 + \sqrt{\frac{\pi}{x}} \sum_{k=-\infty}^{k=+\infty} e^{-(y-2k\pi)^2/4x}, \quad \ldots \quad (68)$$

which is a series found by Jacobi. Both sides of the equation are convergent only if $R(x) > 0$. This means that, if we change x to $1/p$ in (68), we must operate on $H(x)$. Carrying out this substitution we find that

$$2 \sum_{m=1}^{\infty} J_0(2m\sqrt{x}) \cos my$$
$$\doteq -1 + \left\{ \sum_{k=-\infty}^{k=+\infty} e^{-\frac{1}{4}(y-2k\pi)^2 p} \right\} (x^{-\frac{1}{2}}). \quad \cdots \quad (69)$$

When $0 < y < \pi$, equation (69) becomes

$$2 \sum_{m=1}^{\infty} J_0(2m\sqrt{x}) \cos ny$$
$$= -1, \qquad\qquad\qquad 0 < y < y^2/4,$$
$$= -1 + (x-y^2/4)^{-\frac{1}{2}}, \quad y^2/4 < x < (2\pi-y)^2/4,$$
$$= -1 + (x-y^2/4)^{-\frac{1}{2}} + \{x-(2\pi-y)^2/4\}^{-\frac{1}{2}},$$
$$(2\pi-y)^2/4 < x < (2\pi+y)^2/4, \quad \cdots \quad (70)$$

and so on.

Hence, if we write $2\sqrt{x} = X$, we get

$$2 \sum_{m=1}^{\infty} J_0(mX) \cos my$$
$$= -1, \qquad\qquad\qquad 0 < X < y,$$
$$= -1 + 2(X^2 - y^2)^{-\frac{1}{2}}, \quad y < X < 2\pi - y,$$
$$= -1 + 2(X^2 - y^2)^{-\frac{1}{2}} + 2\{X^2 - (2\pi-y)^2\}^{-\frac{1}{2}},$$
$$2\pi - y < X < 2\pi + y, \quad \cdots \quad (71)$$

etc., where X is real and > 0, and $0 < y < \pi$.

In the same way if, after putting $x = 1/p$, we multiply equation (68) by p^{-n} and then operate on $H(x)$, we find that

$$2 \sum_{m=1}^{\infty} m^{-n} J_n(mX) \cos my$$
$$= -\frac{X^n}{2^n \Pi(n)}, \qquad\qquad 0 < X < y$$
$$= -\frac{X^n}{2^n \Pi(n)} + \frac{\sqrt{\pi}}{2^{n-1} \Pi(n-\frac{1}{2})} (X^2 - y^2)^{n-\frac{1}{2}},$$
$$y < X < 2\pi - y, \quad \cdots \quad (72)$$

etc.

From equations (63), (64), and (73) it is easy to derive other identities containing Bessel functions. Thus from equation (63), by using the identity

$$\frac{J_0(rX)}{r^3} = \int_0^X \frac{1}{X}\Big|_0^X \times \frac{dJ_0(rX)}{dX}dX,$$

we get

$$2\sum_{r=1}^{\infty}\frac{J_0(rX)}{r^3} = 2X - \frac{X^2}{4}, \qquad\qquad 0 < X < 2\pi$$

$$= 2X - \frac{X^2}{4} + \frac{1}{4}(X^2 - 4\pi^2)^{\frac{1}{2}} - 8\pi\cos^{-1}\Big(\frac{2\pi}{X}\Big),$$

$$2\pi < X < 4\pi. \quad . \quad . \quad (73)$$

Also, by integrating equation (71) from 0 to y, we get

$$2\sum_{r=1}^{\infty}\frac{J_0(rX)\sin ry}{r}$$

$$= -y, \qquad\qquad 0 < X < y$$

$$= -y + 2\sin^{-1}\frac{y}{X}, \qquad y < X < 2\pi - y$$

$$= -y + 2\sin^{-1}\frac{y}{X} - 2\sin^{-1}\frac{2\pi-y}{X} + 2\sin^{-1}\frac{2\pi}{X},$$

$$2\pi - y < X < 2\pi + y, \quad . \quad . \quad (74)$$

etc.

From (74), by another integration,

$$2\sum_{r=1}^{\infty}\frac{J_0(rX)\cos ry}{r^2} - 2\sum_{r=1}^{\infty}\frac{J_0(rX)}{r^2}$$

$$= \frac{y^2}{2}, \qquad\qquad 0 < X < y,$$

$$= \frac{y^2}{2} - 2y\sin^{-1}\frac{y}{X} - 2(X^2 - y^2)^{\frac{1}{2}} + 2X,$$

$$y < X < 2\pi - y, \quad . \quad . \quad (75)$$

etc.

By combining equations (75) and (73) we find that

$$2\sum_{r=1}^{\infty}\frac{J_0(rX)\cos ry}{r^2}$$

$$= \frac{y^2}{2} + 2X - \frac{X^2}{4}, \qquad\qquad 0 < X < y,$$

$$= \frac{y^2}{2} + 2y\sin^{-1}\frac{y}{X} - 2(X^2 - y^2)^{\frac{1}{2}} + 4X - \frac{X^2}{4},$$

$$y < X < 2\pi - y; \quad . \quad . \quad (76)$$

in forming these equations it should be noticed that the interval $2\pi - y$ to $2\pi + y$ in equation (76) overlaps two intervals in equation (73).

6. *Series containing Struve's Functions.*

All the work in Section 5 can be repeated with Struve's functions $S_n(x)$, where $S_n(x)$ is defined by

$$S_n(x) = \sum_{k=0}^{\infty} \frac{(-1)^k (\tfrac{1}{2}x)^{n+2k+1}}{\Pi(n+k+\tfrac{1}{2})\,\Pi(k+\tfrac{1}{2})}.$$

We proceed as follows. From equation (59)

$$\frac{1}{\sqrt{p}} + 2\sum_{m=1}^{\infty} \frac{\sqrt{p}}{p+m^2} = \pi\left\{ 1 + 2\sum_{m=1}^{\infty} e^{-2m\pi\sqrt{p}} \right\}. \qquad (77)$$

Operating with this equation on 1 we get

$$2\sqrt{\frac{x}{\pi}} + 2\sum_{m=1}^{\infty} e^{-m^2 x}\frac{\mathrm{erf}(-mi\sqrt{x})}{mi}$$

$$= \pi + 2\pi\sum_{m=1}^{\infty}\left\{ 1 - \mathrm{erf}\left(\frac{m\pi}{\sqrt{x}}\right) \right\}, \qquad (78)$$

because

$$\frac{\sqrt{p}}{p+m^2} = \frac{1}{\sqrt{p}}\frac{p}{p+n^2} = \frac{1}{\sqrt{p}}e^{-n^2 x}$$

$$= e^{-n^2 x}\frac{1}{\sqrt{p-n^2}}$$

$$\doteqdot \frac{e^{-n^2 x}}{\sqrt{\pi}}\left\{ \frac{x^{\frac{1}{2}}}{\tfrac{1}{2}} + \frac{n^2 x^{\frac{3}{2}}}{\tfrac{3}{2}} + \frac{n^4 x^{\frac{5}{2}}}{\tfrac{5}{2}\cdot 2!} + \ldots \right\}$$

$$= \frac{e^{-n^2 x}}{\sqrt{\pi}}\int_0^x x^{-\frac{1}{2}}e^{-n^2 x}\,dx$$

$$= \frac{e^{-n^2 x}}{\sqrt{\pi}}\int_0^{ni\sqrt{x}} \frac{2e^{-u^2}}{ni}\,du$$

$$= \frac{e^{-n^2 x}\,\mathrm{erf}(ni\sqrt{x})}{ni}, \qquad\qquad (79)$$

where

$$\mathrm{erf}\,t = \frac{2}{\sqrt{\pi}}\int_0^t e^{-u^2}\,du.$$

Putting $x = 1/p$ in equation (78), and multiplying by p^{-n}, we get

$$\left[\frac{2}{p^{n+\frac{1}{2}}} + 2\sum_{m=1}^{\infty} \frac{p^{-n} e^{-m^2/p} \operatorname{erf}(mi/\sqrt{p})}{ni}\right] H(x)$$

$$= \pi p^{-n}\left[1 + 2\sum_{m=1}^{\infty}\{1 - \operatorname{erf}(m\pi\sqrt{p})\}\right] H(x). \quad (80)$$

Now

$$\left\{\frac{p^{-n} e^{-m^2/p} \operatorname{erf}(ni/\sqrt{p})}{ni}\right\} H(x)$$

$$\doteqdot \frac{2}{\sqrt{\pi}}\left\{\frac{x^{n+\frac{1}{2}}}{\Pi(n+\frac{1}{2})} + \cdots\right.$$

$$\left. + \frac{(-1)^r \Pi(\frac{1}{2}) x^{n+r+\frac{1}{2}} m^{2r}}{\Pi(n+r+\frac{1}{2})\Pi(r+\frac{1}{2})} + \cdots\right\} = \frac{x^{\frac{1}{2}n} S_n(2m\sqrt{x})}{m^{n+1}}.$$

$$\cdots \quad (81)$$

(81) is true if x is real and positive. If x is negative it can be shown by Jordan's Lemma that its value is zero. Further

$$\left[p^{-n}\{1 - \operatorname{erf}(m\pi\sqrt{p})\}\rfloor H(x)\right.$$

$$= \left[p^{-n} - m\pi p^{-n+\frac{1}{2}} + \frac{m^3\pi^3}{3} p^{-n+\frac{3}{2}} - \cdots\right] H(x)$$

$$= x^n\left[\frac{1}{\Pi(n)} - \frac{1}{\Pi(n-\frac{1}{2})}\left\{\frac{m\pi}{\sqrt{x}} - \frac{(m-\frac{1}{2})}{3}\left(\frac{m\pi}{\sqrt{x}}\right)^3 + \cdots\right\}\right]$$

$$= \frac{x^n}{\Pi(n)} - \frac{x^n}{\Pi(n-\frac{1}{2})}\int_x^{\infty} \frac{m\pi(x-m^2\pi^2)^{n-\frac{1}{2}}}{2x^{n+1}} dx. \quad \cdots \quad (82)$$

Clearly this equation is true only if $x > m^2\pi^2$, so that the infinite series is convergent. When $x < m^2\pi^2$

$$p^{-n}\{1 - \operatorname{erf}(m\pi\sqrt{p})\} H(x)$$

$$= p^{-n}\left\{1 - \frac{2}{\sqrt{\pi}}\int_0^{m\pi\sqrt{p}} e^{-u^2} du\right\} H(x)$$

$$= \left[\frac{2p^{-n}}{\sqrt{\pi}}\int_{m\pi\sqrt{p}}^{\infty} e^{-u^2} du\right] H(x)$$

$$= \left[\frac{p^{-n} e^{-m^2\pi^2 p}}{\sqrt{\pi}}\int_0^{\infty} \frac{e^{-\lambda} d\lambda}{\sqrt{\lambda + m^2\pi^2 p}}\right] H(x)$$

$$= e^{-m^2\pi^2 p} f(p) \cdot H(x),$$

where $f(p)$ is such that $\left|\dfrac{f(p)}{p}\right| \to 0$, as $|p| \to \infty$, when

$m > -3/2$.

This result shows that

$$p^{-n}\{1 - \operatorname{erf}(m\pi\sqrt{p})\}\mathrm{H}(x)$$

$$= \frac{1}{2\pi i}\int_{\mathrm{L}} e^{p(x-m^2\pi^2)}\frac{f(p)}{p}\,dp,$$

which can be shown by Jordan's Lemma to be zero if $x < m^2\pi^2$. Thus we have shown that when $x < m^2\pi^2$ the right-hand side of equation (82) is zero.

Using equations (81) and (82), equation (82) becomes

$$\frac{x^{n+\frac{1}{2}}}{\Pi(n+\frac{1}{2})} + 2x^{\frac{1}{2}n}\sum_{m=1}^{\infty}\frac{\mathrm{S}_n(2m\sqrt{x})}{m^{n+1}}$$

$$= \pi\left[\frac{x^n}{\Pi(n)} + 2\sum_{k=1}^{r}\left\{\frac{x^n}{\Pi(n)} - \frac{x^n}{\Pi(n-\frac{1}{2})}\right.\right.$$

$$\left.\left.\int_{x}^{\infty}\frac{k\pi(x-k^2\pi^2)^{n-\frac{1}{2}}}{2x^{n+2}}\,dx\right\}\right],$$

$$r^2\pi^2 < x < (r+1)^2\pi^2. \quad \cdots \quad (83)$$

In the particular case $n=0$ equation (83) takes the form

$$2\sqrt{\frac{x}{\pi}} + 2\sqrt{x}\sum_{m=1}^{\infty}\frac{\mathrm{S}_0(2m\sqrt{x})}{m}$$

$$= \pi\left[1 + 2\sum_{k=1}^{r}\left\{1 - \frac{1}{\sqrt{\pi}}\int_{x}^{\infty}\frac{k\pi(x-k^2\pi^2)^{-\frac{1}{2}}}{2x}\,dx\right\}\right]$$

$$= \pi\left[1 + 2\sum_{k=1}^{r}\left\{1 - \frac{1}{\sqrt{\pi}}\sin^{-1}\left(\frac{k\pi}{\sqrt{x}}\right)\right\}\right],$$

$$r^2\pi^2 < x < (r+1)^2\pi^2. \quad \cdots \quad (84)$$

If $2\sqrt{x} = \mathrm{X}$, (84) becomes

$$2\sum_{m=1}^{\infty}\frac{\mathrm{S}_0(m\mathrm{X})}{m}$$

$$= -\frac{2}{\sqrt{\pi}} + \frac{\pi}{\mathrm{X}}\left[1 + 2\sum_{k=1}^{r}\left\{1 - \frac{1}{\sqrt{\pi}}\sin^{-1}\left(\frac{2k\pi}{\mathrm{X}}\right)\right\}\right],$$

$$2r\pi < \mathrm{X} < 2(r+1)\pi. \quad \cdots \quad (85)$$

In the same way we can find Struve-Fourier series

corresponding to the Bessel-Fourier series in equation (70). In particular, if $0 < y < \pi$,

$$2x^{\frac{1}{2}n} \sum_{m=1}^{\infty} \frac{S_n(2m\sqrt{x})\cos my}{m^{n+1}}$$

$$= - \frac{2x^{n+\frac{1}{2}}}{\sqrt{\pi}\,\Pi(n+\frac{1}{2})}, \qquad 0 < x < y,$$

$$= - \frac{2x^{n+\frac{1}{2}}}{\sqrt{\pi}\,\Pi(n+\frac{1}{2})} + \frac{\pi x^n}{\Pi(n)}$$

$$\left\{ 1 - \frac{\Pi(n-\frac{1}{2})}{\Pi(n)} \int_x^\infty \frac{y\left(x - \frac{y^2}{4}\right)^{n-\frac{1}{2}}}{\frac{1}{4}x^{n+1}}\,dx \right\},$$

$$y < x < 2\pi - y \quad . \quad . \quad . \quad (86)$$

CVIII. *The Hume-Rothery Relationship between the Ionization Potentials of the Elements and their Atomic Number. By* H. YAGODA, *B.Sc. (Chem.Eng.), Sc.M., Sea Gate, New York, U.S.A.*[*]

HUME-ROTHERY has demonstrated that the interatomic distance between the atoms in a crystal (d) is connected with the atomic number of the element (Z), and the total quantum number of its outermost shell of electrons (n) by the simple relationship [1] :—

$$\frac{d}{n} = \left(\frac{1}{\alpha Z}\right)^x \quad . \quad . \quad . \quad . \quad . \quad (1)$$

In this equation α and x are constants for the members of any one subgroup of the periodic table, provided that the coordination number of the atoms remains constant. The values of x vary slightly from group to group, but can be considered as approximating the fraction 1/3 for the initial groups of the periodic system. From this primary relationship, Hume-Rothery has deduced that n^2V is, approximately, a linear function of $Z^{2/3}$, where V represents the ionization potential of the atom [2]. On further analysis of this connexion between n^2V and $Z^{2/3}$, I have found that only in the case of the neutral alkali atoms is a variation with $Z^{2/3}$ warranted, and that, in general, a functional relationship of the form

$$\log n^2V = a \log Z + b \quad . \quad . \quad . \quad . \quad (2)$$
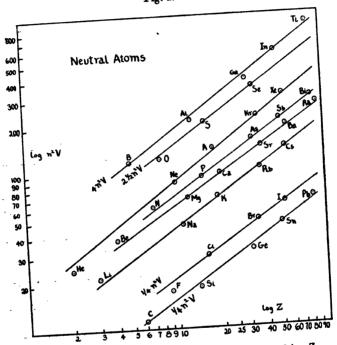
represents the ionization potentials of the atoms with greater accuracy.

The lines in figures 1 and 2 are the loci of the equations of form (2) shown in Tables I.–VIII. In order to avoid the crowding together of the lines in the figures, multiples of n^2V were plotted for several of the groups. Whenever the available data on the ionization potentials permitted, the

Fig. 1.

Graph showing the relationship between $\log n^2V$ and $\log Z$
for the neutral atoms.

coefficients of the equations were evaluated by averaging the coordinates of only the inner elements of each group. The properties of the elements belonging to the initial and seventh periods have, therefore, not influenced the magnitude of the coefficients in the equation for the group. For many elements, the ionization potentials cannot be calculated from spectroscopic data, as their spectra have not been analyzed into terms. However, several rough estimates of this

constant are given in the literature. Evidently these estimates cannot be employed for testing the precision of the Hume-Rothery relationship, but by assuming the validity of the $Z^{2/3}$ variation of n^2V, then the probable value of the ionization potential can be selected from the several estimates available, by interpolating the group equation. This has *been done for the neutral atoms of the 6th, 7th, and 8th groups, and also for all the singly ionized atoms studied, excepting the noble gases and the alkaline earths. The

Fig. 2.

Graph showing the relationship between log n^2V and log Z for the singly ionized atoms.

points on the graphs, therefore, represent either the ionization potential directly available from the spectrum of the atom, or else the particular value, of the several described in the literature, which agrees best with the present theorem. The ionization potentials represented in Tables I.–VIII. were obtained chiefly from the International Critical Tables[3] and the Landolt-Börnstein "Tabellen"[4]. The data for the singly ionized atoms were invariably taken from the latter work. In the few cases where the published estimates are

very discordant, the particular value chosen will be indicated subsequently.

It can be seen from fig. 1, in which log n^2V has been plotted against log Z, that the respective lines for the eight

TABLE I.

Ionization Potentials of the Noble Gases.

I. Log $n^2V = 0.7200$ log $Z + 1.2303$.
II. Log $n^2V = 0.7671$ log $Z + 1.4404$.

Element.	Z.	n.	Neutral atom.		Singly ionized atom.	
			Obs.	Calc. I.	Obs.	Calc. II.
Helium	2	1	24·48	28·0	54·16	46·9
Neon	10	2	21·5	22·3	40·77	40·3
Argon...........	18	3	15·69	15·1	27·82	28·1
Krypton.........	36	4	13·94	14·0	26·4	26·7
Xenon...........	54	5	12·08	12·0	(24)	23·6
Radon...........	86	6	—	11·6	—	23·3

TABLE II.

Ionization Potentials of the Alkalies.

I. Log $n^2V = 0.6664$ log $Z + 0.9783$.
II. Log $n^2V = 0.7438$ log $Z + 1.5041$.

Element.	Z.	n.	Neutral atom.		n.	Singly ionized atom.	
			Obs.	Calc. I.		Obs.	Calc. II.
Lithium	3	2	5·37	4·94	1	75·28	72·3
Sodium	11	3	5·12	5·23	2	47·5	—
Potassium	19	4	4·32	4·22	3	31·7	—
Rubidium	37	5	4·16	4·19	4	(16)	29·3
Cæsium	55	6	3·88	3·82	5	—	25·2
Eka-cæsium......	87	7	—	3·81	6	—	24·4

periodic groups are roughly parallel to each other ; meaning that n^2V is a linear function of Z^a, where the exponent a has approximately the same value throughout the periodic system. From the equations (I.) of each table it can be seen that the values of a averages close to 2/3, but that the departure from this fractional value is often quite marked,

and that only in the case of the alkalies has the coefficient of log Z a magnitude (0·6664) which can be accurately represented by the fraction 2/3. In the 4th group the coefficient is also close to 2/3, viz., 0·6669, but the equation was fitted only to carbon and tin, and so does not represent an average value for the group.

TABLE III.

Ionization Potentials of the Alkaline Earths.

I. Log $n^2V = 0·6316$ log $Z + 1·1605$.
II. Log $n^2V = 0·6188$ log $Z + 1·4667$.

Element.	Z.	n.	Neutral atom.		Singly ionized atom.	
			Obs.	Calc. I.	Obs.	Calc. II.
Beryllium	4	2	9·28	8·69	18·14	17·3
Magnesium	12	3	7·61	7·72	14·97	15·1
Calcium	20	4	6·09	6·02	11·82	11·7
Strontium	38	5	5·67	5·78	10·98	11·1
Barium	56	6	5·19	5·09	9·95	9·79
Radium	88	7	(5·4)	5·01	10·23	9·53

TABLE IV.

Ionization Potentials of 3rd Group Atoms.

I. Log $n^2V = 0·6413$ log $Z + 1·0745$.
II. Log $n^2V = 0·6870$ log $Z + 1·4620$.

Element.	Z.	n.	Neutral atom.		Singly ionized atom.	
			Obs.	Calc. I.	Obs.	Calc. II.
Boron	5	2	8·33	—	23·98	21·9
Aluminium	13	3	5·96	6·84	18·75	—
Gallium	31	4	5·97	6·72	18·9	19·2
Indium	49	5	5·76	—	(16·8)	—
Thallium	81	6	6·08	5·49	20·30	16·5

Figures 1 and 2 also show that in nearly all cases the first member of each group exhibits definite departures from the linear relationship. This anomalous behaviour of the elements of the first period is characteristic of most of the group relationships in the periodic system. It also appears, judging from the ionization potential of the radium atom

(Table III.), that another deviation from the linear relationship occurs in the seventh period. Here the exceptional character of the radium atom (apart from its nuclear instability) is quite apparent. For the ionization potentials of all the alkaline earth atoms diminish progressively as the group is descended from beryllium to barium, but the

TABLE V.

Ionization Potentials of 4th Group Atoms.

I. Log $n^2V = 0\cdot6669$ log $Z + 1\cdot1323$.
II. Log $n^2V = 0\cdot7134$ log $Z + 1\cdot3480$.

Element.	Z.	$n.$	Neutral atom.		Singly ionized atom.	
			Obs.	Calc. I.	Obs.	Calc. II.
Carbon............	6	2	11·22	—	24·28	20·0
Silicon	14	3	8·12	8·77	16·27	—
Germanium......	32	4	7·85	8·56	15·6	16·4
Tin	50	5	7·37	—	14·52	—
Lead...............	82	6	7·38	7·13	14·97	14·3

TABLE VI.

Ionization Potentials of 5th Group Atoms.

I. Log $n^2V = 0\cdot6577$ log $Z + 1\cdot1994$.

Element.	Z.	$n.$	Neutral atom.		Singly ionized atom.	
			Obs.	Calc. I.	Obs.	Calc. II.
Nitrogen	7	2	14·48	14·2	29·47	—
Phosphorus ...	15	3	10·3	10·5	19·81	—
Arsenic	33	4	9·96	9·81	—	—
Antimony	51	5	8·35	8·38	—	—
Bismuth	83	6	8·0	8·00	29·5	—

ionization potential of the radium atom is greater than that of barium. This is also characteristic of certain elements of the 6th period, as lead and thallium, which are the last members of their respective groups. Comparison of the calculated with the observed values of the ionization potential shows that though, in these cases, the equations do not predict a reversal in the order of progression of the constant,

the calculated values are very close to that of the homologous element directly above it.

The ionization potential of the neutral arsenic atom is given as 9·4 volts in the 'International Critical Tables,' and 9·96 volts in the Landolt-Börnstein "Tabellen." The value of

TABLE VII.

Ionization Potentials of the 6th Group Atoms.

I. Log $n^2V = 0.6518$ log $Z + 1.1836$.

Element.	Z.	n.	Neutral atom.		Singly ionized atom.	
			Obs.	Calc. I.	Obs.	Calc. II.
Oxygen............	8	2	13·56	14·8	34·93	—
Sulphur	16	3	10·31	—	23·30	—
Selenium	34	4	(9·5)	—	—	—
Tellurium	52	5	—	8·0$_2$	—	—
Polonium.........	84	6	—	7·6	—	—

TABLE VIII.

Ionization Potentials of the 7th Group Atoms.

I. Log $n^2V = 0.7121$ log $Z + 1.1904$.

Element.	Z.	n.	Neutral atom.		Singly ionized atom.	
			Obs.	Calc. I.	Obs.	Calc. II.
Fluorine	9	2	17·4	18·5	34·5	—
Chlorine	17	3	12·96	—	22·5	—
Bromine	35	4	12·2	—	—	—
Iodine	53	5	10	10·5	—	—
Eka-iodine	85	6	—	10	—	—

9·96 volts is in better agreement with the equation for the 5th group atoms than the former. Again, it appears that the value of 8·0 volts assigned to bismuth in the 'International Critical Tables' is a closer approximation to the ionization potential than the value of 7·25 volts ascribed to the element in the "Tabellen." In the halogen family, the value of 10 volts given in the 'International Critical Tables' as the constant for iodine is in better agreement with the

line passing through chlorine and bromine than the estimate of 8 volts found in the other compendium.

The equations permit an estimation of the ionization potentials of several heavy elements. For the neutral atoms these estimates are : 11·6 volts for radon, 3·81 volts for eka-cæsium, 8·0 volts for tellurium, 7·6 volts for polonium, and 10 volts for eka-iodine. The ionization potential of the singly ionized radium atom is 10·23 volts, the value calculated from Equation II. (Table III.) is only 9·53 volts ; if this behaviour is typical of all the atoms occurring in the 7th period, then the estimates for radon and eka-cæsium are probably too low. K. T. Bainbridge [5] has estimated the ionization potential of eka-cæsium from the alkali and alkaline earth isoelectronic levels, and ascribes to the constant a value of 4·05± 0·05 volts. The following equations express the ionization potentials of the heavy alkali and alkaline earth metals somewhat better than the equations given in Tables II. and III.

Alkalies .... $n^2V = 9·836\ Z^{2/3} - 2·58.$

Alkaline Earths... $n^2V = 12·60\ Z^{2/3} + 2·38.$

By extrapolation, the second equation leads to a value of 5·13 volts for the neutral radium atom, which is only a small improvement on the value calculated in Table III., since the observed ionization potential is 5·4 volts. Extrapolation of the equation for the alkalies gives 3·89 volts as the ionization potential of eka-cæsium. This value just exceeds that of cæsium, but it is well to note that a purely empirical formula, based on the normal trend of the ionization potentials in the alkali group, would yield a value much lower than that of cæsium.

In the case of the singly ionized atoms the variation of n^2V with $Z^{2/3}$ is not as uniform as for the neutral atoms. Only in the cases of the noble gases and the alkaline earths are sufficient data available for the evaluation of the coefficients on averaged points. The slopes of the lines representing these families are 0·7671 and 0·6188 respectively ; these figures can be interpreted as approaching the fraction 2/3 only in a very approximate way. In the alkali group the ionization potentials of only lithium, sodium, and potassium are definitely known. An estimate of 16 volts is given in the "Tabellen" for the second ionization potential of rubidium. This value deviates considerably from the family line ; the number found by extrapolation is 29 volts, which probably represents the true value, as the same equation predicts the ionization potential of lithium with only a small

error. A recent analysis of the spectra of rubidium [6] and cæsium [7] by Laporte, Miller, and Sawyer reveals that the ionization potential of the singly ionized atoms are 27·3 and 23·4 volts respectively.

Summary.

From considerations of the interatomic distance between atoms in crystals, Hume-Rothery has deduced that n^2V is approximately a linear function of $Z^{2/3}$. The present analysis shows that for the neutral atoms the theorem is essentially correct, but that a better correlation of the properties of the members of a specific group is given by the relationship : $\log n^2V = a \log Z + b$, where the coefficient a approaches the fraction 2/3 in the several periodic groups. For singly ionized atoms the latter relationship is also valid, but the values of a exhibit more marked deviations from the theoretical limit than in the case of the neutral atoms.

References.

(1) W. Hume-Rothery, Phil. Mag. [7] x. p. 217 (1930).
(2) *Ibid.* [7] xi. p. 670 (1931) ; [7] xiii. p. 196 (1932).
(3) 'International Critical Tables,' v. p. 392 (1929) ; vi. p. 70 (1929), 1st ed., N.Y.
(4) Landolt-Börnstein, 'Physikalisch-Chemische Tabellen,' 5th ed., ii. table 152 f, Berlin (1931).
(5) K. T. Bainbridge, Phys. Rev. xxxiv. p. 752 (1929).
(6) O. Laporte, G. R. Miller, and R. A. Sawyer, Phys. Rev. xxxviii. p. 843 (1931).
(7) *Ibid.* xxxix. p. 458 (1932).

CIX. *The Photoelectric Properties of Films of Beryllium, Aluminium, Magnesium, and Thallium. By* H. DE LASZLO, *Sir William Ramsay Laboratories of Physical and Inorganic Chemistry, University College, London, and Massachusetts Institute of Technology, Cambridge, Mass.**

SUMMARY.

OPAQUE films formed by the evaporation of the above metals in high vacuum on to a previously degassed surface were examined with respect to their photoelectric properties in monochromatic light. Measurements were made between λ 5000 and 2400 Å., and the photoelectric response in coulombs

* Communicated by Prof. F. G. Donnan, C.B.E., M.A., F.R.S.

por erg as well as in electrons per quantum was plotted against the wave-length. Magnesium was found to be a suitable surface to use in the construction of photoelectric cells for measurement in the ultra-violet.

OBJECT OF INVESTIGATION.

THE work here described was part of a programme for measuring accurately the photoelectric response (in absolute units) versus wave-length (both visible and ultra-violet) of a number of commercial photocells. The results obtained with these cells, although of interest industrially, were not suitable for scientific publication, owing to the fact that no two cells were reproducible. This was due to the presence of gas, and hence the sensitivity of the metal surface was variable.

Since much time had been expended in devising suitably accurate methods of measurement, we decided to determine the photoelectric properties of a number of elements, chiefly with the object of using such cells in lieu of thermopiles for energy measurements in the ultra-violet in conjunction with quantitative photochemical work, and for use in automatically measuring the variation in concentration of substances in the state of vapour or solution which absorb strongly in the ultra-violet and not in the visible.

Aluminium and magnesium have already been examined [1], but the results showed that there was a constant change in the photoelectric sensitivity, owing to gas being present. Nor could this have been avoided with the technique then available. We have sought to eliminate the factors of error present in the above investigation, and have obtained reproducible results for Be, Al, Mg, and Th.
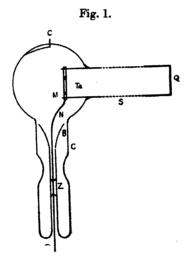
EXPERIMENTAL.

1. *Preparation of the Metal Films.*

In determining the photoelectric efficiency of a metal, it is of primary importance that all the incident light should be absorbed by the metal itself. This condition is best realized if the metal to be examined be deposited on the inner surface of a sphere, leaving only a small opening in the sphere for the radiation to enter by. Since the amount of energy available in the form of monochromatic radiation is usually very small the photoelectric currents are correspondingly small. For this reason it is essential that there should be a

very high leakage resistance between anode and cathode.
In order to measure the true photoelectric effect the whole
operation of forming the film is conducted in the highest
available vacuum so as to avoid occluded films of gas. After
many attempts, a cell of the type shown (fig. 1) was developed
for these measurements.

The metals examined were the purest type available.
Small pieces of metal (M) were spot-welded on to a 2 mm.
wide ring of degassed tantalum (Ta), which in its turn was
supported by a nickel wire (N) and sealed with tungsten
through the pyrex stem (Z). The Ta had been previously
degassed by heating for a few minutes at 1000° C. and was.

Fig. 1.

then allowed to cool to room temperature in a high vacuum.
This procedure removed any occluded gases. The metals to
be examined had previously been distilled in high vacuum.
The bulb of the cell was made of pyrex, and a quartz window
(Q) was sealed into the bulb with the aid of a graded seal (S).
On heating Ta with a high-frequency current applied
externally the metals present on the ring volatilized and
deposited on to the walls of the bulb. Owing to a continu-
ation of the window tube through the ring, none of the
metal was able to reach the quartz window. A short piece
of platinum strip attached to a piece of tungsten wire (C)
was melted on to the inner surface of the bulb in order to
provide electrical contact with the film. The upper part of
the anode stem was slightly belled out (B), while the outer

part of the stem was contracted below (B). In this way no metal could be deposited below the seal (Z). The leakage resistance of the cells used was of the order of 10^{-13} amps. Before heating Ta the entire cell was baked out at 400° C. for several hours while attached to a 3-stage quartz Volmer mercury pump. A liquid air-trap was provided between the seal and the pump. In this way we hoped to remove occluded gases that might be present on the interior of the bulb. When the experiment was ended the stem was cracked off at (C), a new charged Ta ring was welded on to the nickel, the interior cleaned with hot nitric and chromic acids, and the stem re-sealed on to the bulb. Sufficient metal was evaporated to render the film opaque.

2. *Method of measuring small Photoelectric Currents.*

The Wheatstone Bridge valve method of measuring small currents developed by Wynne-Williams [2] was tried, but found to be insufficiently sensitive owing to the small currents available. In the end a modified Rosenberg [3] method was evolved. This method consists of measuring the drop of potential through a high resistance, R, in which the photocell current flows. As long as this drop does not exceed 1 or 2 volts, the impedance of the resistance is negligible compared to that of the photocell. Resistances of the order of 10^8 to 10^{11} ohms were necessary, and after trying a number of types, that described by Gyemant [4] was found to be the most satisfactory. These resistances consisted of glass tubes 4 ins. in length and ½ in. in diameter, with a platinum wire sealed into either end, filled with a mixture of pure benzol containing 0·7 per cent. of picric acid by weight. Pure ethyl alcohol is added in sufficient quantity to give the desired resistance.
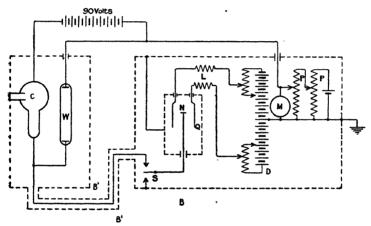
These resistances were calibrated against a 200,000 ohm standard with the aid of a sensitive galvanometer, and had the following values: $3·56 \times 10^7 \,\Omega$, $1·46 \times 10^9 \,\Omega$, $1·50 \times 10^{11} \,\Omega$. They showed a very low temperature coefficient, the variation being less than 0·2 of 1 per cent. over the range 15–20° C.

The circuit used is shown in fig. 2 and is self-evident. Any current flowing in the circuit causes a drop of potential in the resistor W. This charges and deflects the needle, N, of a Lindemann electrometer [5], which is returned to zero with the aid of a potentiometer, P. The balancing voltage, V, across P, is read by means of a precision millivoltmeter, M. Knowing V and resistance W, the current can be calculated.

The entire circuit, including electrometer and microscope for reading the same, was most carefully shielded by placing in an iron box, B, from which only the eyepiece of the latter protruded.

The photocell and high resistance were mounted in a separate metal box, B, the lead from the cell anode to the electrometer being carefully insulated with a quartz tube and shielded with metal braid. The box and contents were mounted on a rider which could slide along an optical bench placed at right angles to the exit beam of the monochromator. Currents greater than 10^{-13} amperes could be measured with precision, and 10^{-14} could be detected.

Fig. 2.

C, photoelectric cell; W, high resistance; S, earthing switch; Q, electrometer quadrants charged to about 30 volts; N, electrometer needle; L, Grid leaks 1-2 megohms; P, potentiometers about 2000 ohms; D, 90-volt battery.

3. *Source of Light.*

In order to reach a high degree of accuracy in our measurements it was necessary to have a strong source of monochromatic ultra-violet radiation. If this were weak, although a reading might be obtained with the photocell, yet the radiation energy would not be sufficient to give good readings with a thermopile.

The constricted mercury arc, as developed by Forbes[6], was found to be suitable when run at 1 ampere and 100 volts. The discharge took place in a quartz capillary 2 mm. I.D. and about 25 mm. long. This was placed very close to the

slit of the monochromator. To keep the arc steady a large inductance (several hundred Henries) was placed in series with it, and a controlled blast of air was directed on to the capillary. After burning for about 10 hours the quartz devitrifies to some extent and a yellow coating forms in the

TABLE.
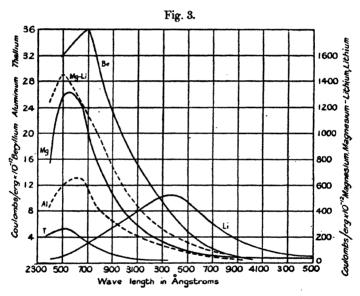
	Beryllium.		Aluminium.		Magnesium.		Thallium.	
A.	coul. ergs $\times 10^{-13}$.	electron quantum	coul. ergs $\times 10^{-13}$.	electron quantum	coul. ergs $\times 10^{-12}$.	electron quantum	coul. ergs $\times 10^{-13}$.	electron quantum
5791	—	—	—	—	—	—	—	—
5461	—	—	—	—	—	—	—	—
4347	·8	·0000021	—	—	21·6	·00061	—	—
4039	3·9	·000012	—	—	—	—	—	—
3655	24·3	·000084	·8	·000027	57·7	·0020	—	—
3341	91·5	·00034	2·4	·000088	—	—	—	—
3130	148	·00056	3·8	·00015	252·0	·010	2·4	·0000096
3022	182	·00075	4·9	·00020	—	—	6·3	·000026
2967	201	·00083	5·6	·00023	427·0	·018	10·1	·000042
2893	—	—	6·5	·00028	540·0	·023	—	—
2806	290	·0013	7·8	·00034	738·0	·033	21·7	·000093
2699	359	·0016	12·0 ⎫	·00053	—	—	30·8	·00014
2653	—	—	⎭		1200·0	·056	38·9	·00018
2536	331	·0016	12·7	·00062	1330·0	·065	52·8	·00026
2483	319	·0016	11·9	·00060	1260·0	·063	52·8	·00026
2399	—	—	0	0	792·0	·041	44·0	·00023

interior; the latter could be removed with hydrofluoric acid, but owing to the former, the capillary must be renewed from time to time. The monochromator was of the constant deviation type in which a triple quartz [7] prism was caused to rotate in a novel way that has already been described elsewhere [8]. The lenses were quartz-fluorite achromatic

triplets, 30 mm.[9], and were free from any visible fluorescence.

4. _Radiation Energy Measurement._

The radiant energy incident on the photocell was always measured in absolute units before and after each photoelectric observation. This was done by pushing a thermopile mounted on a rider along the same optical bench on which the photocell was mounted. Thus either the cell or the pile would be placed quickly and accurately in the path of the light. A photographic shutter was mounted in front of the exit lens of the monochromator. The thermopile consisted

Fig. 3.

of 17 elements of copper and bismuth and had a silver target which measured $20 \times 2\frac{1}{2}$ mm. It was calibrated against a standard lamp (Bureau of Standards, Washington, D.C.), and its sensitivity was found to be

$$\frac{\text{energy}}{\text{mm. deflexion}} = \frac{0.39 \times 10^{-6} \text{ watts}}{\text{mm.}}.$$

MEASUREMENTS.

Our results are tabulated in the Table. We have included values for what might be called the true photoelectric efficiency [10] of the surface in question at each wave-length, _i. e._, electrons emitted per quantum of incident energy. The

figures show how inefficient the whole process is. On fig. 3 we give curves of photoelectric efficiency versus wave-length. The curve for a commercial quartz-lithium cell is shown as well as for that obtained for an 80–20 per cent. Mg-Li alloy. The two latter are given for comparative purposes, as one set of measurements only were made for their determination. The results are accurate to at least ± 5 per cent.

CONCLUSION.

Be and Al would not be of great use in cell construction, owing to their low efficiency and to the fact that their spectral sensitivity is covered by that of the more efficient magnesium.

Th, although very insensitive, might be of use for certain purposes. It is responsive to the ultra-violet only, and cuts off sharply at 3400 Å.

Magnesium appears to be a very suitable material to use in the construction of ultra-violet photocells. Its efficiency between 2800 Å. and 2400 Å. is exceptionally high, and it would be of practical use as far down as 4000 Å. Such cells would be simple to construct owing to the ease with which Mg can be distilled in high vacuum.

The curve of the Mg-Li alloys shows that there is every possibility of constructing cells having any desired spectral sensitivity distribution. Thus alloys of Mg with any varying proportions of one or more of the alkali metals might be tried.

In conclusion, I should like to thank Mr. Poitras and Mr. St. Louis for their able assistance in the experimental part of this work.

REFERENCES.

(1) Pohl and Pringsheim, *Verh. d. D. Phys. Ges.* x. p. 548 (1912).
(2) Wynne-Williams, Phil. Mag. vi. p. 324 (1928).
(3) Rosenberg, *Z. f. Phys.* vii. p. 18 (1921).
(4) Gyemant, *Wiss. V. d. Siemens Konzern*, p. 58 (1928).
(5) Lindemann and Keeley, Phil. Mag. xlvii. p. 577 (1924).
(6) Forbes and Harrison, J. Opt. Soc. Am. xi. p. 99 (1925).
(7) Bernhard Halle, *Nachf. Berlin-Steglitz*,
(8) de Laszlo, J. Sci. Ins. vii. p. 292 (1930).
(9) Optique Scientifique,' 65 Rue Halle, Paris.
(10) de Laszlo, "Photoelectric Cells and their Application," Phys. and Opt. Soc. Discussion, p. 221 (1930).

CX. *Discharges maintained by Electrical Oscillations in Solenoids. By* G. D. YARNOLD, *B.A., Merton College, Oxford* *.

(1) IT is well known that the electric force inside a solenoid, which forms part of an oscillating circuit, consists of two distinct parts: a force due to the difference in potential E between the ends of the solenoid, and a force proportional to the rate of change of the magnetic field. The force due to the potential difference E may be referred to as the "electrostatic force," and the force due to the change of the magnetic field as the "electromagnetic force." The relative magnitudes of these two forces will obviously depend upon the dimensions of the solenoid. A simple calculation shows, however, that in solenoids of the dimensions of those generally used for exciting high-frequency discharges in gases, the electrostatic force is much greater than the electromagnetic force. Thus, in a solenoid of radius 5 cm., with turns 1 cm. apart, the electrostatic force is about thirty times as large as the electromagnetic force †.

High-frequency currents are obtained in rarefied gases when the tube containing the gas is placed inside the solenoid. The currents may be excited either by damped oscillations obtained with condenser discharges, or by continuous oscillations maintained by valves.

An account of the earlier experiments on electrodeless discharges, which were made with damped oscillations, is given by Mierdel in the *Physikalische Zeitschrift* ‡.

Many early investigators supposed that the electrodeless discharges excited by the high-frequency currents in a solenoid are due to the electromagnetic force. This view was held by Hittorf, who first obtained electrodeless discharges in 1884.

Lecher, however, showed that when the electrostatic force is reduced by means of a screen consisting of strips of tinfoil, inserted between the solenoid and the bulb containing the gas, it is impossible to obtain a discharge. He was thus led to the conclusion that the electrodeless discharges excited by the currents in the solenoid are due to the electrostatic force.

In these early experiments with damped oscillations, it was difficult to make any measurements either of the potential

---

* Communicated by Prof. J. S. Townsend, F.R.S.
† J. S. Townsend and R. H. Donaldson, Phil Mag. v. p. 178 (1928).
‡ G. Mierdel, *Phys. Zeit.* xxv. p. 240 (May 1924).

difference E between the ends of the solenoid, or of the current flowing in the solenoid.

More recently, however, Townsend and Donaldson, using continuous oscillations, have made accurate measurements of the potential differences necessary to excite electrodeless discharges under various conditions, and have come to the same conclusions as Lecher.

In the last two or three years, other physicists * have also made experiments with continuous oscillations, and have sought to explain the results of their experiments on the hypothesis that the discharge is of electromagnetic origin.

As their arguments do not appear to be conclusive, it was considered desirable to make further experiments in order to find the relative importance of the electrostatic and electromagnetic forces. For this purpose, I have made two different investigations with continuous oscillations, both of which give very definite results.

Fig. 1.

(2) In the first of these investigations, I have observed a discharge in an electrostatic field and compared the results with those obtained in the field inside a solenoid.

The apparatus used is shown in fig. 1. The solenoid AB was 10 cm. long and had thirteen turns of wire of 19 cm. diameter. For simplicity, four turns are shown in the figure. It was loosely coupled with a continuous wave generator and was tuned by the condenser S. The strength of the oscillations induced in the solenoid was varied by adjusting this condenser. The potential difference E between the ends of the solenoid was measured by means of the thermo-milliammeter H in series with two condensers of equal capacity C, in the same way as in the experiments of Townsend and Donaldson.

The experiments recorded here were all made with oscillations of wave-length 97 metres; and the potential

---

* K. A. MacKinnon, Phil. Mag. xiii. p. 605 (Nov. 1929) ; C. T. Knipp, Phys. Rev. xxxvii. p. 756 (March 1931) ; H. Smith, W. A. Lynch, N. Hilbery, Phys. Rev. xxxvii. p. 1091 (May 1931) ; F. Esclangon, *Comptes Rendus*, cxcii. p. 1213 (May 1931).

differences given are the root mean square values expressed in volts.

The method of obtaining the same electrostatic field as that inside the solenoid, but without the accompanying electromagnetic field, was similar to that used by Esclangon. Alternate turns of the solenoid were connected to seven equally-spaced coaxial wire rings of the same diameter as the turns of the solenoid, and forming a cage CD of the same length as the solenoid. Each ring was at the same potential as the point on the solenoid to which it was connected, and therefore the electrostatic force inside the cage was approximately the same as that in the solenoid.

The discharges were produced in a bulb of 12 cm. diameter, containing neon at a pressure of about 1 mm.

(3) It was found that there is no discharge in the gas until the potential difference between the ends of the solenoid reaches a certain value E_1, at which the discharge starts

TABLE I.

	Solenoid.	Cage.
E_1	245	260
E_2	118	125

suddenly. If the potential is increased, the current in the gas increases, and if the potential is decreased, the current decreases. There is a certain minimum potential E_2, however, below which it is impossible to maintain even a small current in the gas,

When the bulb is held inside the cage the same phenomena are observed. The values found for E_1 and E_2 when the bulb was in the solenoid and when it was in the cage are shown in Table I.

The fact that the potentials E_1 and E_2 obtained with the bulb in the solenoid are nearly the same as those obtained with the bulb in the cage shows that the electromagnetic force is unimportant in starting or maintaining the discharge.

(4) In the second investigation the electrostatic force inside the solenoid was reduced by means of screens placed inside the solenoid, as in Lecher's experiments.

Four screens were made consisting of strips of tinfoil 5 mm. wide pasted on the inside of paper cylinders, in a

direction parallel to the axis. The lengths and distances apart of the strips in the four screens were as follows :—

I. Strips 30 cm. long and 5 mm. apart.

II.   „   30 cm.   „   „   1 mm.   „

III.   „   15 cm.   „   „   5 mm.   „

IV.   „   15 cm.   „   „   1 mm.   „

When a screen was inserted in a solenoid it was found that there is no discharge in a bulb placed inside the screen when the potential difference between the ends of the solenoid is equal to the potential E_1 given in Table I. The discharge does not start until the potential is raised to a value F_1 much larger than E_1. In the same way, the minimum potential F_2 which will maintain a discharge in the gas is much larger than E_2. The values found for F_1 and F_2, when screen III. is used, are shown in Table II., with the values of E_1 and E_2 for comparison.

TABLE II.

F_1	2500	E_1	245
F_2	860	E_2	118

It is seen from the table that when this screen is used the potential F_1, which is necessary to start a discharge, is over ten times as great as the potential E_1, which is necessary when no screen is used ; while to maintain a discharge the potential F_2 must be over seven times as great as the potential E_2.

With any of the screens except No. III. a potential difference of 2700 volts between the ends of the solenoid is insufficient to start a discharge in the bulb.

So long as the potential difference between the ends of the solenoid is as high as 2000 volts, however, it is possible to start the discharge by holding the bulb outside the screen, and then to transfer the bulb to its central position inside the screen, without stopping the discharge. In this way the minimum potential F_2, which will maintain a discharge when the bulb is inside the screen, can be found for each of the other three screens. The values obtained for F_2 with the different screens are shown in Table III.

(5) These results, and those given in Table II., show that when the electrostatic force inside the solenoid is reduced by means of one of the screens, then the potential difference

which must be applied between the ends of the solenoid in order to start a discharge, or to maintain a small current, is very much larger (in some cases more than twelve times larger) than the potential necessary when no screen is used.

In the first investigation it is shown that the potential which is required to start a discharge when the bulb is inside the cage, where there is no electromagnetic force, is practically the same as that required when the bulb is inside the solenoid.

Both investigations show that the discharge obtained when the bulb is inside the solenoid is due almost entirely to the electrostatic force.

The question arises whether the discharges obtained with the screens are maintained by the electromagnetic force, or by an electrostatic force due to incomplete screening.

Referring again to the results shown in Table III., it is seen that the potential F_2, which is required to maintain a small current in the gas, is not constant, but depends on the

TABLE III.

Screen.	I.	II.	III.	IV.
F_2	1160	1250	860	960

screen used. The value found for F_2 is lower with screen III. than with any other screen ; and, similarly, the value of F_2 is higher with screen II. than with any other screen. From its construction we should expect screen II. to be the most effective, and screen III. the least effective.

The fact that the potential F_2, necessary to maintain a small discharge, varies from screen to screen shows that the discharge obtained when the bulb is inside a screen is due, at any rate partly, to an electrostatic force arising from incomplete screening.

(6) That the discharge is also due partly to the electromagnetic force in this case is shown by measuring the potential G_2, which will maintain a discharge when the bulb is inside the cage, and a screen is inserted in the cage. Any discharge obtained under these conditions will be due entirely to the electrostatic force arising from incomplete screening.

In all cases it was found that the potential G_2 is greater than F_2 for the same screen. With screens I. and II. it is impossible to maintain a discharge, even though the potential

difference between the ends of the cage is as high as 2700 volts, and with no screen is it possible to start a discharge. The values found for G_2, with the values of F_2 for comparison, are shown in Table IV.

The difference between the potentials G_2 shown in Table IV. and the corresponding potentials F_2 can only be due to the electromagnetic force, which exists in the solenoid but not in the cage ; while the fact that it is possible to maintain a discharge when a screen is used inside the cage is further evidence that the screening is not perfect, and that the discharges obtained when the screens are used inside the solenoid are due partly to an electrostatic force.

(7) As has been mentioned already, we should expect from the theory of the electric field that the electromagnetic force inside the solenoid used in these experiments would be much less than the electrostatic force. In order to compare these

TABLE IV.

Screen.	I.	II.	III.	IV.
G_2	Over 2700	Over 2700	1180	1500
F_2	1160	1250	860	960

forces experimentally, measurements have been made of the electromotive force e induced in a circular loop of wire held in a central position inside the solenoid, with its plane perpendicular to the axis. The electromagnetic force in the bulb is then found by dividing the electromotive force e by the circumference of the loop.
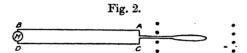
If a short length of high-resistance wire, to which is soldered a thermo-couple, is included in the loop, it is possible to measure the current flowing in the loop, and so to calculate the electromotive force e. For, if L and R are the inductance and resistance respectively of the loop, then the current i is given by

$$i = \frac{e}{\sqrt{L^2 p^2 + R^2}},$$

where i^2 and e^2 are the mean squares of the current and the electromotive force and p is the angular frequency of the oscillations. In these experiments Lp was much larger than R, so that the electromotive force is given by

$$e = i \cdot L \cdot p.$$

It was found that the current flowing in a loop of wire of about 9 cm. diameter is so large as considerably to reduce the potential difference between the ends of the solenoid, when the latter is kept tuned to resonance with the oscillator. Accordingly, the currents in the loop were reduced by adding extra inductance in the form of two parallel straight wires, AB and CD, placed outside the solenoid in such a position that there was no electromotive force induced in them by the currents in the solenoid. This arrangement is shown in fig. 2, where the dots represent a section of the solenoid. The connexions between the two parallel wires and the loop passed between two turns of the solenoid, and a thermo-milliammeter H was included in the circuit between B and D.

Fig. 2.

The values thus found for the electromotive force *e* induced in a circular loop of 9 cm. diameter are given in volts in Table V., the potential difference between the ends of the solenoid being adjusted to the values of F_2 given in Table III.

It is seen that when the potential difference between the ends of the solenoid is just sufficient to maintain a discharge,

TABLE V.

Screen.	I.	II.	III.	IV.
e	20	22	15	16
F_2	1160	1250	860	960

the electromagnetic force inside the screen at 4·5 cm. from the axis $(e/9\pi)$ is in no case as great as 1 volt per cm. In the case when no screen is used the electromotive force *e* is 1·6 volts and the electromagnetic force is less than 0·1 volt per cm., whereas the potential difference E_2 between the ends of the solenoid is 118 volts. The maximum value of the electrostatic force is therefore about 12 volts per cm. (since the length of the solenoid is 10 cm.). Even supposing that the electrostatic force at 4·5 cm. from the axis is half this, namely, 6 volts per cm., it is seen that the electrostatic force is at least sixty times as large as the electromagnetic force when there is no screen.

(8) From the foregoing evidence we must conclude that the force inside a solenoid which is sufficient to start a discharge, or to maintain a small current in the gas, is mainly electrostatic. This conclusion is borne out by the experiments of Lecher and of Townsend and Donaldson, to which reference has already been made.

The force at any point in the gas when the discharge is taking place, however, is not the same as the force at the same point when the bulb is removed, owing to the modification * of the field by the charges in the gas.

It has been found that in the uniform luminous columns of high-frequency discharges in wide tubes the force in the gas is independent of the current. Similarly, in discharges in bulbs placed inside a solenoid the electrostatic force in the gas does not exceed the force required to maintain a very small current. When the potential E between the ends of the solenoid is increased to values much greater than the potential required to maintain a small current, a large current is obtained in the gas, but there is no corresponding increase in the electrostatic force in the gas. The increase in the current in the solenoid required to increase the potential E is accompanied by a proportional increase in the electro-magnetic force. Thus in experiments where large currents are maintained in the gas the electromagnetic force may become comparable with the electrostatic force. This would account for the difference observed by Esclangon between the intensity of the light emitted by discharges in bulbs placed inside a solenoid and the intensity of the light from discharges in bulbs placed in a field where there was no electromagnetic force.

In conclusion, I should like to thank Professor Townsend for his helpful advice and criticism throughout this work.

CXI. *Similitude and the Heatflow through a Granulated Material. By* O. A. Saunders, *M.A., M.Sc. (Fuel Research Division, Department of Scientific and Industrial Research)* †.

MR. J. H. AWBERY'S "Note on Heatflow through a Granulated Material" ‡ is an interesting example of the use of the principle of similitude in heat problems. His

* J. S. Townsend, Phil. Mag. xiii. p. 745 (April 1932).
† Communicated by the Author.
‡ Phil. Mag. xii. p. 1152 (December 1931).

conclusions are, in fact, particular cases of the more general result given below, which follows immediately from the principle.

§ 1.

Consider the heat-flow by conduction in any heterogeneous body, with given surface temperatures. The principle of similitude can only be applied to similar systems, *i. e.,* to systems of fixed shape but differing in size. Further, in the present example, the distribution of the impressed surface temperatures must be fixed, while the absolute values are varied ; also the distribution of the thermal conductivity within the body (if not uniform) must be fixed while the absolute values are varied. If these conditions are fulfilled, the principle of similitude shows that the effective thermal conductivity, measured between any corresponding pairs of points, is independent of the size and surface temperatures and is proportional to the conductivity at any specified point.

These results follow directly from the principle, since the size l, surface temperature θ, and conductivity k, which have dimensions L, θ, and $\mathrm{MLT}^{-3}\theta^{-1}$ respectively, cannot be arranged to form a dimensionless group ; the systems are therefore similar whatever the values of l, θ, and k. The effective conductivity k', measured between any pair of corresponding points, can be arranged with l, θ, k in the dimensionless group k'/k only ; hence k' is independent of l, θ, and proportional to k. It is assumed that the conductivity k is independent of the temperature.

The cases considered by Mr. Awbery of similar solids in contact, with the intervening spaces either conducting or non-conducting, are particular examples of the above result, as also is Prof. Lees's case of a material made in check-board fashion with the black and white squares of different conductivities, the heat-flow being in the plane of the board. It also follows that, in Mr. Awbery's case, provided the ratio of the conductivity of the solids to that of the material filling the intervening spaces is constant, the effective conductivity is proportional to the conductivity of the solids.

The general result is applicable to any shapes or conductivity distributions, and to any distribution of impressed surface temperatures.

§ 2. *Surface Heat Transfer.*

Another case of some interest is that of a system of perfectly conducting bodies, between which heat is transferred either directly from surface to surface or between each surface and an intervening medium, the heat transfer per

unit surface area being proportional to the temperature difference and independent of the distance apart of the surfaces. In this case the principle of similitude shows that, for similar systems, the effective conductivity is independent of θ and proportional to αl, where α is the surface heat transfer coefficient This result is evident from the fact that l, θ, α cannot be arranged in a dimensionless group, while the dependent variable k' can only be grouped with them in the arrangement $k'/\alpha l$.

§ 3. *Application to a Granulated Material.*

§ (1) shows that if the heat transfer across the air spaces in a granulated materal were by conduction alone, the effective conductivity would be independent of the linear size of the grains, for geometrically similar grain structures. The effective conductivity would not be proportional to the conductivity of the grain material unless the ratio of the conductivity of the air to that of the grains were constant. Mr. Awbery has since pointed out, in correspondence with me on the subject, that since the conductivity of air is very small in comparison with that of most solids, it can often effectively be taken as zero. In this case the effective conductivity would be proportional to that of the solid material. These conditions are approached for very small air spaces, in which convection is restricted, while radiation is of decreasing importance compared with conduction, especially at low temperatures.

On the other hand, if the heat transfer across the spaces were independent of their distance apart, and if the grains were perfect conductors, § (2) shows that the effective conductivity would be directly proportional to the grain size. The larger the air spaces, especially at higher temperatures, and the higher the conductivity of the grains, the more nearly are these conditions approached.

Practical cases must fall somewhere between these two extremes.

CXII. *Note on the Electrocapillary Effect of Capillary-active Organic Molecules. By* A. W. DAVIS, *B.Sc., Mardon Research Scholar, Washington Singer Laboratories, University College, Exeter* [*].

THE electrocapillary curve of a solution of a capillary-active electrolyte is approximately parabolic. If to such a solution be added a capillary-active non-electrolyte,

e. g., one of the alcohols, and the electrocapillary curve of the
mixed solution be obtained, the second (modified) curve is
found to be depressed in the region of the maximum, but on
either side of the maximum ordinate the curves merge into
one another and finally coincide—the modified curve appears
to be a truncated replica of the primary curve. Gouy *
discovered this effect of non-electrolytes, and it has since been
studied by Frumkin†, Butler ‡, Ockrent §, and Wightman ‖.
The depression of the interfacial tension has been shown to
be due to adsorption and orientation of the inorganic mole-
cules in the mercury-solution interface ¶. If, however, the
electrolyte in the primary solution yields an active ion on
dissociation, then one branch of the electrocapillary curve is
shifted over its entire length, and the maximum with it,
e.g., with KI the active I-ion depresses both the left-hand
branch of the curve and the maximum, the right-hand branch
coinciding with that of such an inactive solution as KCl.
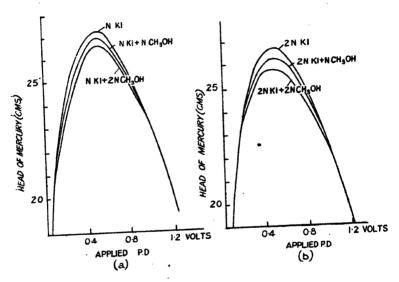
In the present work the effect of this active ion upon the
adsorption of active organic molecules in a mixed solution
was investigated. Normal and twice-normal solutions of
KI were prepared, and their electrocapillary curves obtained.
Then to each solution was added sufficient CH_3OH to give a
normal and twice-normal solution of the latter substance,
and the electrocapillary curves of the four mixed solutions
so formed were obtained. Measurements were made with
the aid of an ordinary Lippmann electrometer. The fine
capillary tubes were drawn out from pieces of ·5 mm. bore
thick-walled capillary tubing, and were attached to the
vertical tube of the electrometer by means of a short piece
of pressure tubing. Readings were taken at room-tempera-
ture which varied from 15° to 17° C. The methyl alcohol
used was pure and free from acetone, and the solutions were
saturated with mercurous iodide, the large electrode being
covered with a thin layer of HgI to eliminate polarization
at its surface. The potentials were applied by means of a
resistance-box potentiometer and an accumulator, the
accumulator being frequently standardized by balancing
against a Weston standard cell.

The resulting curves for the mixed solutions were superim-
posed on those of the corresponding KI solutions (see figure),

* *Ann. Chim. Phys.* viii. p. 291 (1906).
† *Zeits. Physik.* xxxv. p. 291 (1926).
‡ Proc. Roy. Soc. cxxii. p. 399 (1929).
§ Journ. Phys. Chem. xxxiv. p. 2297 (1930).
‖ *Ibid.* xxxv. p. 3293 (1931).
¶ Frumkin, 'Colloid Symposium Annual,' vii. (1929).

and the former were found to be of the "truncated" type of Gouy, that is, of a similar type to those obtained for solutions of capillary-inactive electrolytes when modified by the presence of surface-active organic molecules. In the region of the maximum the molecules of alcohol cause a depression of the interfacial tension both for the KI and KCl solutions, the depression being due to the adsorption and orientation of the organic molecules in the interfacial phase separating the solution and the mercury. With applied potential differences higher than that corresponding to the maximum, the interfacial tension depression decreases as the

negative potential across the interface increases until, with a certain applied potential difference depending on the relative concentration of the two substances in solution, the primary and modified curves merge into one another, the falling branches of the curves then coinciding with that due to the potassium ion alone. With applied potential differences less than that corresponding to the maximum, the effect is slightly different, since on this positive side of the electrocapillary curve both the active ions and the active molecules have a tendency to be adsorbed at the interface, but again the curves finally coincide. Thus, as the interfacial potential difference increases positively, *i.e.*, as we move away to the left of the maximum ordinate, the effect of the

active organic molecules decreases, and that of the ions increases relatively, until the CH_8OH molecules adsorbed at the interfacial phase, when the interfacial tension is near its maximum value, are replaced entirely by the active I-ions, and the curves follow the same path as for the pure KI solution. The alcohol thus causes a depression of the interfacial tension at the maximum of the electrocapillary curve, but the total depression with the mixed solutions is much less than the sum of the depressions caused by the I-ions and the CH_3OH molecules acting separately, *i.e.*, the depression produced by the alcohol in the KI solution is much less than that which it causes in a corresponding KCl solution; in the neighbourhood of the maximum, the iodide ions affect the values of the interfacial tension, so that the modified curves begin to follow more and more closely those of the corresponding KI solution until they become identical.

Thus the modifying effects of the active organic molecules are similar whether the primary solute is an active electrolyte or an inactive one, except that the active ions determine the form of that branch of the curve corresponding to their normal adsorption. This is in accordance with the results of Butler and Wightman [*] on the effect of capillary-active electrolytes on the adsorption curves of solutions containing surface-active substances, and with those of Butler and Ockrent [†] on the adsorption curves of mixtures of surface-active salts and non-ionized molecules. The latter workers found that the effect of the mixture is greater than that of either component alone, but much less than the sum of their separate effects.

An attempt was made to repeat Smith's work [‡] on the electrocapillary curves of aqueous solutions of capillary-active and inactive solutes, using alcohol as the solvent instead of water. Gouy [§] found that when he used a Lippman electrometer in such alcoholic solutions the capillary jet soon developed a "sticking" effect (which he termed "démouillage"); Newberry [‖] attempted to measure single potential differences in alcoholic solutions using such an electrometer, and he also found great difficulty in obtaining a fine capillary jet that would function, though he records ultimate success.

In the present work the tubes were drawn out as described

[*] *Loc. cit.*
[†] *Loc. cit.*
[‡] Phil. Trans. cxciii. p. 47 (1900).
[§] *Ann. Chim. Phys.* (7) xxix. p. 145 (1903).
[‖] Journ. Chem. Soc. p. 2553 (1914).

above, and great care was taken to keep them clean; but, using methyl alcohol and ethyl alcohol solutions, not one was found in which the small meniscus, between the mercury and the alcoholic solutions, retained its mobility for more than a few minutes. In aqueous solutions, the development of such a sticking effect can be checked by allowing the fine tubes to stand in distilled water; but although jets were left in pure alcohol for several days, the mercury meniscus still lost its mobility in a few minutes, so that only unreliable results were obtained. No successful attempt has been made to account for this effect; Gouy merely stated that alcohol developed a contact angle with glass, and abandoned further work with pure organic solvents.

CXIII. *The Dielectric Constant of Nitrogen up to 150 Atmospheres at* 25°, 75°, *and* 125° C. *By* A. *and* C. MICHELS, *Natuurkundig Laboratorium der Gemeente-Universiteit, Afd. Thermodynamica, Amsterdam**. (29th Communication of the Van der Waals Fund.)

THE dielectric constant of nitrogen at atmospheric pressure has been measured at several temperatures[1] and at pressures up to 226 atm. at room temperature[2], but no measurements have been made over a wide temperature range at higher pressures. The present paper gives the first results which have been obtained with an apparatus designed to measure the combined influence of pressure and temperature on the dielectric constant.

The dielectric constant was obtained from the change in capacity of a condenser containing the gas under investigation. This change in capacity was measured by the standard heterodyne beat method. One high-frequency circuit included the pressure condenser and a calibrated variable condenser, and the other was stabilised by means of piezo-electric quartz. The beat note from these circuits, after detection and amplification, was observed with a loud-speaker together with the note from a tuning-fork. The tuning-fork was kept in vibration in the ordinary way by means of a triode valve. During the measurements the variable condenser was set so that the audible beat between the heterodyne note and the tuning-fork disappeared. It was arranged that the capacity of the pressure and variable condensers could be compared with a normal set.

The pressure condenser consisted of two "precision" tubes insulated from each other with quartz and placed inside a steel vessel. The outer tube was connected to the latter and a lead from the inner tube brought through the steel wall with quartz insulation. As a result of this arrangement the condenser was subjected to hydrostatic· pressure, and the change of the zero-capacity due to the deformation of the materials could be calculated directly from the linear compressibility. The correction due to temperature changes could also be calculated from the expansion coefficient of the material. The steel pressure vessel was placed in a thermostat kept constant within 0·01°.

The zero-capacity of the condenser was calculated from the change in the capacity when the condenser was evacuated and filled with benzene. In order to avoid dismantling the apparatus the benzene was distilled into the evacuated condenser. The value for the dielectric constant of benzene (2·259 at 25°) was taken from the work of R. T. Lattey and O. Gatty [3]. The zero-capacity of the condenser was found to be 1443 cm.

Measurements were made with nitrogen guaranteed to contain less than 0·01 per cent. oxygen but not entirely free from inert gases. The pressure was measured with a spring manometer calibrated against a pressure balance. The experiments were carried out using a frequency of 508 kilocycles ($\lambda = 591$ metres). The results are given in Table I. and the accompanying figure.

TABLE I.
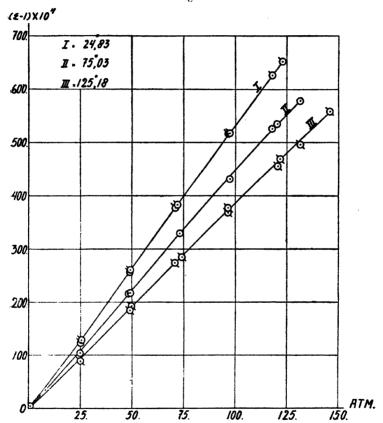
$P_{Atm.}$	$d_{Amagat.}$	$\epsilon.$	$\frac{\epsilon-1}{\epsilon+2} \cdot \frac{1}{d} \cdot 10^6.$
T = 24·83° C.			
0·97	0·89	1·0005	187
25·7	23·7	1·0130	182
49·6	45·7	1·0262	190
71·3	65·0	1·0379	192
96·9	88·4	1·0517	191
118·0	107·0	1·0628	192
123·4	111·7	1·0653	191
118·2	107·1	1·0627	191
97·3	88·8	1·0518	191
72·4	66·5	1·0384	190
49·1	45·2	1·0257	188
25·1	23·1	1·0125	180

TABLE I. (cont.).

P_Atm.	$d_{\text{Amagat.}}$	ϵ.	$\frac{\epsilon-1}{\epsilon+2} \cdot \frac{1}{d} \cdot 10^6$.
T = 75·03°C.			
0·97	0·76	1·0004	175
26·05	20·3	1·0114	186
48·6	37·8	1·0217	190
73·6	56·7	1·0330	192
97·8	74·7	1·0432	190
118·3	89·6	1·0526	193
131·8	99·2	1·0578	190
120·8	91·4	1·0536	192
97·8	74·7	1·0433	190
73·8	56·9	1·0330	191
49·3	38·3	1·0218	188
25·3	19·8	1·0106	179
T = 75·04° C.			
135·8	102·1	1·0597	191
120·3	91·0	1·0533	192
97·7	74·6	1·0435	191
73·3	56·5	1·0325	190
50·7	39·4	1·0225	189
26·0	20·3	1·0111	182
0·97	0·76	1·0004	175
23·1	18·1	1·0100	185
53·1	41·2	1·0236	189
75·1	56·4	1·0328	192
96·1	73·5	1·0424	190
117·5	89·0	1·0517	190
133·7	100·6	1·0586	190
T = 125·18° C.			
146·2	92·2	1·0558	193
122·0	79·8	1·0469	193
97·0	64·2	1·0377	193
71·2	47·6	1·0275	191
50·1	33·8	1·0192	188
25·7	17·5	1·0095	181
0·97	0·66	1·0003	176
25·4	17·2	1·0089	172
49·3	33·2	1·0185	184
74·8	50·0	1·0285	188
97·2	64·3	1·0369	189
121·0	79·2	1·0456	189
132·1	86·0	1·0496	189

From the experimental figures the value of the Clausius-Mosotti expression $\left(\dfrac{\epsilon-1}{\epsilon+2}\cdot\dfrac{1}{d}\right)$ was calculated. The values of the density at 25° and 75° were obtained from the critical summary of Bartlett's isotherm data given by Deming and

Fig. 1.

Shupe[4]. The values at 125° were obtained from the series expression of the nitrogen isotherms given by Holborn and Otto[5].

With the exception of the points at 1 and 25 atm. (where the small value of $(\epsilon-1)$ made the measurements less accurate) the value of the Clausius-Mosotti expression is seen to be independent of pressure and temperature. Using the

4 H 2

average value of the constant (191×10^{-6}) the value of the dielectric constant at 1 atm. and $0°$ was calculated to be 1·000573, which compares favourably with the figures given in the literature.

TABLE II.

Tangl[2]............	$\epsilon = 1·000581$
Bodareu[2]	1·000587
Zahn[1]	1·000581
Broxon[3]	1·000590
Our value........	1·000573

The work is being continued to higher pressures and a pressure balance used for measurement.

References.

(1) C. T. Zahn, Phys. Rev. xxiv. p. 400 (1924) ; xxvii. p. 455 (1926).
(2) K. Tangl, *Ann. der Physik*, xxvi. p. 59 (1908). E. Bodareu, *Atti Acad. Lincei*, xxii. (2) p. 480 (1913). J. W. Broxon, Phys. Rev. xxxviii. p. 2049 (1931).
(3) R. T. Lattey and O. Gatty, Phil. Mag. (7) vii. p. 985 (1929).
(4) E. Deming and Lola E. Shupe, Phys. Rev. xxxvii. p. 638 (1931).
(5) L. Holborn und J. Otto, *Zeit. f. Phys.* xxiii. p. 77 (1924) ; xxx. p. 320 (1924). Wien-Harms, *Handb. d. Exp. Phys.* viii. (2) pp. 167, 168.

CXIV. *On the Superconductivity of Alloys containing Gold and Silver.* By Prof. J. C. McLennan, *F.R.S.*, J. F. Allen, *M.A.**, *and* J. O. Wilhelm, *M.A.*†

IN two earlier papers[1] published by us on the appearance of superconductivity in alloys, particular attention was paid to the superconductive elements Pb, Sn, and Tl when alloyed with the non-superconductive members of the fifth group, namely, Bi, Sb, As, and P. It was pointed out at that time, that these alloys in general exhibited higher transition temperatures than did the pure superconductive metals alone.

The present publication is the third of the series, and deals with observations made on the alloy systems Ag–Sn, Au–Sn, and Au–Pb. Our attention was drawn to these groups by the work of de Haas and his associates. De Haas[2] found

* Student of the National Research Council of Canada.
† Communicated by the Authors.

that the components Ag$_3$Sn and AuSn were non-superconductive ; while in a previous investigation by us, the eutectics of Ag–Pb and Au–Pb were found to become superconducting at temperatures very close to the transition point of pure lead. It appeared, therefore, that the effect produced on the superconductivity by Au and Ag in Pb differed markedly from that produced in Sn.

This difference was considered worthy of our closer investigation. A comparison of the equilibrium diagrams of Ag–Sn, Au–Sn, Ag–Pb, and Au–Pb, as determined by Petrenko [3] and Vogel [4], showed that the system Ag–Pb possessed a simple two branch melting-point curve with one eutectic, whereas the other three systems exhibited more complex structures, forming compounds and containing several eutectics. The system Ag–Sn possesses the compound Ag$_3$Sn ; the Au–Sn system has AuSn, AuSn$_2$, and AuSn$_4$, while in the Au–Pb system Au$_2$Pb and AuPb$_2$ are present. An examination was made of all these compounds and of the various eutectics in the three systems.

The alloys were prepared in the usual manner, being melted together, strained through glass wool, and cast in pyrex glass tubes *in vacuo.* The casting took place in a thin section of the tube which had been drawn out to a length of about five centimetres. As a precaution against breakage, some of the alloys being crystalline and very brittle, the glass was cracked away only from the ends of the sample and the rod was thus left almost completely encased in the thin glass tube. To the ends of the sample were soldered current and potential leads of fine copper wire ; the potential drop along the rod was measured on a Cambridge Instrument Co. Vernier Potentiometer.

Description of the Alloys.

(1) *The Ag–Sn System.*

(a) Ag–Sn (Eutectic).
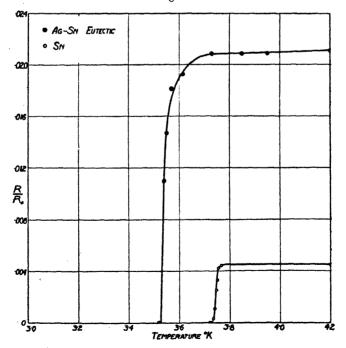
This alloy, which is the main eutectic of the system, contains 4 per cent. Ag by weight. According to Vogel, the eutectic constituents are Sn and Ag$_3$Sn. The measurements made on this sample are given in Table I. and shown graphically in fig. 1 in comparison with the superconducting curve for pure Sn. It will be seen that for this alloy the residual resistance above the transition point has increased about fivefold and that the superconducting point is about ·2° lower than that for pure Sn.

TABLE I.

Ag–Sn (Eutectic).

T° K.	R (microhms).	R/R₀.
300°	15200	1·113
273	13650	1·000
85	3290	0·2402
4·2	288	·0211
3·95	286	·02095
3·85	285	·02087
3·73	285	·02087
3·615	263	·01927
3·57	230	·01818
3·55	200	·01465
3·54	150	·01100
3·52	0	·0000

Fig. 1.

(b) Ag$_3$Sn–Sn (Eutectic).

In the equilibrium diagram, this alloy, which contains 50 per cent. Ag, is given as a minor eutectic. The constituents

Fig. 2.
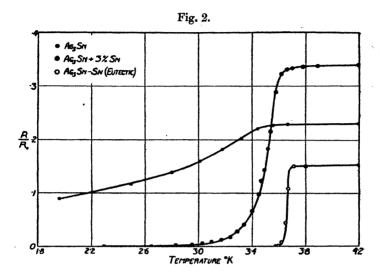
TABLE II.

Ag$_3$Sn–Sn (Eutectic).

T° K.	R (microhms).	R/R$_0$.
300	1900	1·071
273	1775	1·000
85	700	0·394
10	275	·155
4·2	270	·1521
3·8	267	·1504
3·71	267	·1504
3·67	193	·1087
3·65	79	·0445
3·62	13	·0073
3·60	2	·001113
3·57	0	·0000

of the alloy are Ag$_3$Sn and the eutectic (*a*) above. It is seen from fig. 2 and Table II. that the superconducting point for this alloy is very slightly higher than that for (*a*) above.

(c) Ag₃Sn.

This compound, which contains 73 per cent. Ag, has previously been examined by de Haas, van Aubel, and Voogd, who found it to be non-superconducting, although it did show a considerable drop in resistance below $3·6°$ K. Our measurements made on this alloy (fig. 2 and Table III.) agree very closely with those made by de Haas.

TABLE III.

Ag₃Sn.

T° K.	R (microhms).	R/R₀.
300	9740	1·080
273	9020	1·000
85	4050	0·449
8	2101	·2342
4·2	2060	·2285
3·67	2060	·2285
3·56	2049	·2272
3·44	1985	·2200
3·32	1826	·2024
3·18	1630	·1810
3·01	1434	·1588
2·80	1250	·1387
2·49	1050	·1163
1·96	800	·0888

(d) Ag₃Sn +3 per cent. Sn.

Due to a mishap in the preparation of a sample of Ag₃Sn, a small portion of the Ag was not dissolved in the melt. The resulting alloy therefore contained a slight excess of Sn. Nevertheless, measurements made on the alloy (Table IV. and fig. 2) are of interest, since they show the nature of the change from Ag₃Sn–Sn (Eutectic) to pure Ag₃Sn as the percentage of Ag increases. In the curve for (d) some of the features of the curves for both (b) and (c) are apparent. We have the very steep upper part of the transition curve which is similar to that for (b) ; we have also, as in the curve for (c), a slow final approach to superconductivity. In the case of (c), however, superconductivity disappears entirely.

(2) *The Au–Sn System.*

(e) AuSn$_4$–Sn (Eutectic).

The proportion of Au here is 9 per cent. by weight, and the alloy constitutes the main eutectic of the Au–Sn system.

TABLE IV.

Ag$_3$Sn + 3 per cent. Sn.

T° K.	R (microhms).	R/R$_0$.
300	4737	1·064
273	4450	1·000
85	2484	0·559
8·0	1515	·342
4·2	1500	·3373
3·9	1497	·3365
3·78	1494	·3360
3·70	1488	·3348
3·66	1470	·3330
3·62	1437	·3230
3·58	1287	·2895
3·54	960	·2155
3·52	816	·1833
3·49	630	·1415
3·47	540	·1212
3·45	429	·0965
3·40	294	·0662
3·34	189	·0425
3·29	120	·0270
3·24	84	·0189
3·17	63	·0142
3·10	45	·0101
3·03	33	·00742
2·95	21	·00472
2·86	15	·00338
2·83	10·5	·00236
2·65	6	·00135
2·30	0	·0000
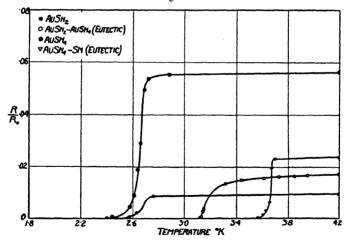
The data obtained (Table V. and fig. 3) show that this alloy has the highest superconducting temperature of the system, the point falling about ·2° below that for pure Sn.

TABLE V.

Au–Sn$_4$Sn (Eutectic).

T° K.	R (microhms).	R/R$_0$.
300	4830	1·0$\colon$8
273	4400	1·000
85	1210	0·275
7·0	103	·0234
4·2	102	·0232
3·7	101	·02295
3·68	85	·01933
3·66	27	·00614
3·63	15	·00341
3·61	8	·00182
3·57	0	·0000

Fig. 3.

(*f*) AuSn$_4$.

This compound contains 29 per cent. Au. The measurements are given in Table VI. and shown in fig. 3. The compound becomes superconducting at 2·4° K.

(*g*) AuSn$_2$–AuSn$_4$ (Eutectic).

The eutectic between these two compounds contains 40 per cent. Au, and the measurements (Table VII. and fig. 3) show

that it has a much higher superconducting point than that for $AuSn_4$; the transition occurs at $3\cdot125°$ K.

(*h*) $AuSn_2$.

This compound contains 45 per cent. Au. The measurements obtained are given in Table VIII. and shown graphically in fig. 3. The curve is very similar to that for $AuSn_4$. Superconductivity appears at $2\cdot48°$ K.

TABLE VI.

$AuSn_4$.

T° K.	R (microhms).	R/R_0.
300	11400	1·095
273	10350	1·000
85	4125	0·399
7·5	603	·0582
4·2	582	·0562
2·88	570	·0551
2·72	555	·0536
2·69	510	·04925
2·66	300	·02899
2·64	195	·01885
2·61	90	·0087
2·58	42	·00405
2·44	6	·000570
2·4	0	·0000

(*i*) AuSn.

De Haas and his associates have measured this alloy and announce that it is non-superconductive.

(*j*) AuSn–Au (Eutectic).

It was thought that perhaps this eutectic, which contains 80 per cent. Au, might become superconducting within the temperature range of our apparatus. The alloy, however, retained a comparatively high resistance down to 1·96 K., as shown in Table IX.

(3) *The Au–Pb System.*

(*k*) $AuPb_2$–Pb (Eutectic).

This alloy, containing 15 per cent. Au, is the main eutectic of the system Au–Pb. Measurements which we made on

this alloy were published some time ago as one of a group of lead alloys. The curve obtained has been reproduced in fig. 4

TABLE VII.

$AuSn_2$–$AuSn_4$ (Eutectic).

T° K.	R (microhms).	R/R_0.
300	14570	1·071
273	13600	1·000
85	4560	0·335
4·2	230	·0169
3·95	224	·01646
3·85	222	·01632
3·73	218	·01602
3·615	213	·01567
3·44	200	·01470
3·32	181	·01330
3·15	50	·00368
3·14	40	·00294
3·13	10	·000735
3·125	0	·0000

TABLE VIII.

$AuSn_2$.

T° K.	R (microhms).	R/R_0.
300	3230	1·133
273	2850	1·000
85	819	0·2875
11	37	·01296
4·2	26	·00913
2·76	24	·00843
2·63	6	·00210
2·57	2	·0007
2·48	0	·0000
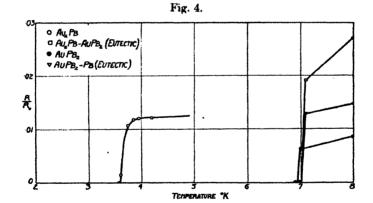
for the purpose of comparison with the present·results from other alloys of the system. This alloy becomes superconducting at 7·0° K.

(*l*) AuPb₂.

The gold-content of this compound is 33 per cent. Au by weight. Measurements made on it are shown graphically in fig. 4 from data in Table X. The superconducting point 6·9° K. is very little lower than that for the eutectic (*k*).

<div align="center">

TABLE IX.

AuSn–Au (Eutectic).

</div>

T° K.	R (microhms).	R/R₀.
300	8600	1·100
273	7820	1·000
85	2820	0·3605
4·2	1280	·1638
1·96	1280	·1638

<div align="center">Fig. 4.</div>

(*m*) Au₂Pb–AuPb₂ (Eutectic).

This eutectic contains 55 per cent. Au and becomes superconducting at the same temperature as eutectic (*k*), namely, 7·0° K. The data are given in Table XI. and shown in fig. 4.

(*n*) Au₂Pb.

This is a very crystalline compound with a rhombic structure, according to Vogel. The compound contains 65 per cent. Au and shows a transition temperature 3·59° K. (Table XII. and fig. 4), which is much lower than that for any of the other alloys in the AuPb system.

TABLE X.

AuPb$_2$.

T$^\circ$ K.	R (microhms).	R/R$_0$.
300	10470	1·085
273	9590	1·000
85	2990	0·3115
8·0	82	·00855
7·0	60	·00626
6·9	0	·0000

TABLE XI.

Au$_2$Pb–AuPb$_2$ (Eutectic).

T$^\circ$ K.	R (microhms).	R/R$_0$.
300	4070	1·102
273	3705	1·000
85	1160	0·3108
8·0	84	·0270
7·1	71	·01919
7·0	0	·0000

TABLE XII.

Au$_2$Pb.

T$^\circ$ K.	R (microhms).	R/R$_0$.
300	9800	1·090
273	9000	1·000
85	2600	0·291
4·2	110	·01222
3·95	108	·01200
3·85	106	·01177
3·73	104	·01056
3·615	13	·001445
3·59	0	·0000

Discussion.

In the foregoing results, we immediately notice two outstanding features. First, in alloys with the superconductive elements, that Au and Ag produce an effect on the transition temperature which is the opposite of that produced by Bi, Sb, and As. When we are observing alloys containing the latter metals, we find, usually, a pronounced elevation of

the superconducting point, while in alloys with Au and Ag we find an equally pronounced depression of the superconducting temperature. Second, that a binary alloy system composed of one superconductor and one non-superconductor does not necessarily have a unique transition temperature.

On closer examination of the system Ag–Sn, we see that the two eutectics became superconducting at temperatures slightly below that for pure tin, while the compound Ag_3Sn has almost entirely lost the property of superconductivity.

We are thus led directly to infer that eutectics are more " stable " as regards superconductivity than are compounds, or, more generally, than are proportions other than eutectics. The latter generalization is based on the case of $Ag_3Sn +$ 3 per cent. Sn, which, as has been stated before, occurs between Ag_3Sn and $Ag_3Sn–Sn$ (Eutectic). Here we see that the addition of 20 per cent. Ag to the $Ag_3Sn–Sn$ eutectic causes a lowering of the transition temperature by 1·3°, while the further addition of 3 per cent. Ag results in the complete disappearance of superconductivity. In dealing with this system, it is also interesting to note that Ag–Sn (Eutectic), containing only 4 per cent. Ag, has a slightly lower superconducting point than has $Ag_3Sn–Sn$ (Eutectic), which contains 50 per cent. Ag. Considering the rather large proportion of the non-superconductive Ag in the latter alloy, the result is somewhat unexpected.

The system Ag–Sn furnishes also a striking example of the variation of the residual resistance as the change in proportion takes place from pure tin, through the various alloys, to pure silver. This is shown in the following table :—

Alloy.	Residual resistance (R/R_0).
Pure Sn	·0045
Ag–Sn (Eut) 4 per cent. Ag	·021
$Ag_3Sn–Sn$ (Eut.) 50 per cent. Ag	·15
$Ag_3Sn + 3$ per cent. Sn (70 per cent. Ag).	·336
Ag_3Sn (73 per cent. Ag)	·228
Pure Ag	·006

In examining the system Au–Sn, we see the inference drawn from the Ag–Sn system (*i. e.*, that eutectics possess higher superconducting points than compounds) to be demonstrated more conclusively. The transition temperatures for the two compounds $AuSn_2$ and $AuSn_4$ are very close together, being 2·48° and 2·4° respectively. The eutectic $AuSn_2–AuSn_4$ shows a much higher transition temperature

than either of its component compounds, and the eutectic $AuSn_4$-Sn, which contains 91 per cent. Sn, shows a superconducting point very close to that for pure Sn. Soon after the gold-content increases past the $AuSn_2$ proportion, the superconductivity disappears, since it is absent both in the compound AuSn and in the eutectic AuSn-Au. In the system Au-Sn we notice the same unusual inversion of superconducting points that appeared in the Ag-Sn system, but in the case of Au-Sn, the inversion takes place between the compounds. Here we see that the compound $AuSn_2$ has a higher transition temperature than $AuSn_4$, which is the richer in tin.

Our primary inference concerning the greater superconductive stability of eutectics over compounds still holds in the case of the Au-Pb system. We have in this system two compounds, Au_2Pb and $AuPb_3$, and two eutectics. Both eutectics become superconducting at 7·0° K. (the transition temperature of lead is 7·2° K) and the compound $AuPb_3$, only slightly lower, at 6·9° K. Au_2Pb, on the other hand, appears to be totally different from the rest of the system, since its transition temperature is depressed 3·6° below that of lead. Besides differing so greatly from the others with regard to its superconducting point, this compound Au_2Pb differs also in certain other physical properties. For example, it is a very highly crystallized substance and can be quite easily pulverized, whereas the other alloys of the system are somewhat malleable. It seems, therefore, that the amount of gold must increase to over 60 per cent. of the alloy before the superconductivity is affected to any degree. This lack of effect on superconductivity in alloys with low gold-content is also clearly shown in the shape of the resistance curve immediately above the transition region of the temperature. The steeply sloping resistance curve in this temperature region is characteristic of pure lead.

In all the cases examined we have seen that superconductivity appears at higher temperatures in eutectic alloys than in compounds of the same metals. That is to say, more specifically, that in the case of a eutectic between compounds, the resulting superconductivity point is raised; but where the eutectic occurs between a compound and a pure superconductor, the resulting transition temperature lies somewhere between the superconducting points of the two components. The reason for this becomes a little clearer when we examine the differences in structure between compounds and eutectics. Compounds are microscopically homogeneous, whereas eutectics are not microscopically but only,

macroscopically homogeneous. Eutectics are composed usually of mixtures of crystals of the components of the alloy, the components being sometimes compounds, or, more usually, solid solutions of one metal in the other. De Haas[5] has shown that in multicrystal specimens of tin, super-conductivity begins to appear at a higher temperature than in single crystals. He has also found that tensional stresses on a sample of tin result in the onset of superconductivity at a higher temperature than normal. He therefore assumed that tensional stresses must exist between adjacent crystal faces of the multicrystal specimen and that superconductivity appears first in these places.

The present investigation bears out de Haas's theory : that is, between the crystal faces in the mixed structure of a eutectic there must exist forces of considerable magnitude which cause superconductivity to appear at temperatures other than would be expected. That these internal forces must be of greater magnitude in eutectics than in compounds or alloys of proportions other than eutectic, is essential from the nature of the eutectic. Since the eutectic is by definition the proportion with the lowest melting-point, it must therefore be, according to the theory of change of state, the proportion in which the greatest internal forces are present.

References.

(1) McLennan, Allen, and Wilhelm, Proc. Roy. Soc. Can. sect. iii. vol. xxiv. (1930).

(2) de Haas, van Aubel, and Voogd, Proc. K. Akad. Amst. xxxii. p. 218 (1929); xxxiii. p. 258 (1930).

(3) G. J. Petrenko, *Z.S. für Anorg. Chemie*, liii. p. 200 (1907).

(4) R. Vogel, *Z.S. für Anorg. Chemie*, xlv. p. 11 (1905); xlvi. p. 60 (1905).

CXV. *Notices respecting New Books.*

Foundations of Mathematics. By F. P. RAMSEY. (Kegan Paul. 1931. Price 15s.)

A VOLUME from the pen of one able in both the mathematical and philosophical fields is always of first-rate importance, and the posthumous collection of the writings of F. P. Ramsey is accordingly most welcome; for the realm of Mathematical Philosophy is one in which the mathematician is too often at a loss to appreciate philosophical difficulty, and the philosopher is at a loss to grasp the technical demands of the mathematician. Ramsey was one of the very few who suffer from neither deficiency, and he may well be said to have acquired a reputation both as a

philosophical thinker and as a mathematician. Although the subject-matter varies considerably as we proceed through his papers, yet there is a perceptible continuity of thought which runs through the volume, and gives a clear indication of the author's mode of thinking. At the same time the influence of Wittgenstein is very much in evidence, while a great deal of the work may be regarded as correction and adjustment of the work of Russell. In consequence a familiarity with the writings of these authors is desirable when reading almost any portion of Ramsey's work, and in places it is positively essential.

The first paper, from which the volume derives its name, is devoted to the criticism and development of the theory of Classes and Cardinals and of the Arithmetical Continuum, as set forth by Russell and Whitehead in their 'Principia Mathematica.' By means of a new discussion of "functions" and a new associated theory of types the difficulties which arise in connexion with the Russell theory of types are removed, and the Axiom of Reducibility is no longer necessary as an axiom. This paper is undoubtedly a valuable contribution to the theory of Mathematical Philosophy. It is followed by a more popularly constructed paper entitled "Mathematical Logic," consisting most pleasantly of a sketch of the ideas of Weyl, Brouwer, Hilbert, and Wittgenstein.

After a paper on a particular problem of formal logic there follow two papers entitled "Universals" and "Facts and Propositions." The former is a criticism of Russell's view that universals and particulars are essentially distinct; Russell's arguments in this connexion are shown to be inadequate, and it would seem that Ramsey held that the distinction was a fiction of words. The latter is a discussion of the nature of belief.

The last of the previously published papers included in this volume is called "Truth and Probability." It attempts to give an account of the principles underlying what is termed partial belief, and if it does not develop to any great extent, it at least has more contact with the probability judgments of human beings than the mathematical theory of probability, as set forth by Poincaré, for example. The volume concludes with a number of sketches of theories, as jotted down by the author and left in comparatively undeveloped states.

Throughout the volume it is of interest and importance to observe the way in which language and symbolism are presented as possible sources of apparent, but resolvable, difficulty. This may be regarded as following Wittgenstein, and it is certainly true that mathematicians have long been of this opinion in connexion with the difficulties of the theory of types, though their reasons for that opinion have been inadequate. But one wonders when Ramsey explains how he avoids certain confusions whether his words and sentences have one and only one meaning. Be that as it may, he has pointed out certain blemishes in other writers, he has smoothed out the difficulties of a profound theory—these are achievements in themselves.

Scientific Inference. By HAROLD JEFFREYS, M.A., D.Sc., F.R.S. [Pp. vii+247.] (Cambridge University Press, 1931. Price 10*s*. 6*d*.)

THE problem of scientific truth is one which is of fundamental importance, not only in its wider philosophical setting but also from a purely practical pragmatic standpoint. What is meant by the assertion that a scientific proposition is true? That is the main (though not the only) question that Dr. Jeffreys tries to answer in this book. The book will be disappointing to those who expect too much; they might hope to find justification for the choice of the simpler laws, where there are alternatives, and a sure foundation for the belief that it is possible to learn from experience. That hope is soon removed, for it is taken as a primitive postulate that it is possible to make inferences beyond the data known directly by sensation, and a high prior probability is attributed, as a necessary assumption, to simple laws. On that basis Dr. Jeffreys is able to show, by a most elegant application of the theory of probability, that the posterior probability of a possible simple law, after suitable tests have been made, may become extremely high. The views here developed had their beginnings some years ago in a series of papers in the ' Philosophical Magazine ' by the author and Dr. Dorothy Wrinch. It is a considerable step that certain aspects of scientific inference have in this way been treated virtually in a quantitative manner; and in so far as the treatment is successful the essential problem has been narrowed down to an examination of the assumed postulates which form the starting-point of the deductive argument.

Relevant to the theme are discussions of probability, sampling, quantitative laws, errors, and physical magnitudes. Chapters on mensuration, Newtonian dynamics, and light and relativity unified only the general point of view of the author, have a value rather as separate essays, being succinct outlines of a systematic treatment of these subjects, with frequent novel methods of presentation. There follows a discussion of miscellaneous topics, such as ultimate concepts, and an eclectic account of some other theories of scientific knowledge.

The book as a whole seems to suffer from a lack of artistic unity; but there is a compensation, in that the inevitably difficult matter in some sections is balanced by the pleasant manner of others. The book might perhaps more appropriately have been called "Essays on Scientific Inference and other Topics." As such, it should be welcomed by a wide circle of readers, whether their main interests are mathematical, scientific, or philosophical.

Cartesian Tensors. By H. JEFFREYS. (Cambridge University Press, 1931. Price 5*s*. net.)

PERHAPS one of the most useful consequences of the Theory of Relativity is the fact that mathematicians and physicists have become accustomed to tensors. If we add the Einstein summation convention, we have a powerful notation of extraordinary

compactness. Part, indeed, of the pleasure that one derives from the study of modern physical and mechanical developments is due to the elegance of the mathematical reasoning. Unfortunately, however, a rumour has been spread with remarkable persistence to the effect that tensors are very difficult to understand, whereas they are in reality no more difficult than most of the subjects that a good honours student at our universities can readily assimilate. Dr. Jeffreys has therefore done considerable service to mathematicians and physicists by the publication of his book on ʻCartesian Tensors.ʼ His object is to illustrate the use of tensor methods in Solid Geometry, Particle and Rigid Dynamics, Statics, Hydrostatics, Hydrodynamics, Elasticity, as well as the general theory of Electric and Magnetic Fields. Dr. Jeffreys does not claim to give a complete theory of these subjects. His aim is rather to illustrate the value of tensor notation and methods by reference to the fundamentals of these subjects. The results are in many cases interesting and striking, and there can be no doubt that a student who has received lectures on these matters based upon traditional methods will find Dr. Jeffreys's treatment very stimulating. Thus, the fact that Love's strain components do not constitute a tensor until some of them are halved, or that, in three dimensions, any vector can be associated with an anti-symmetrical tensor of the second order, shed much light upon the theory of continuous media.

The treatment of tensors in this book is necessarily incomplete. As the author restricts himself to rectangular Cartesian axes, the distinction between covariant and contravariant tensors disappears completely. This is perhaps a temporary advantage, but it means that the student can have only a very faint impression of the real beauty of tensor calculus. Would not the author have done better by showing how rectangular Cartesians lead to this simplification, by including some extension to other types of coordinates that are familiar to the student, and of even greater importance in many branches of physics and mechanics?

A particularly valuable feature of the book is the brief study of the substitution tensor, the alternating tensor, and isotropic tensors. The proof that there is no isotropic tensor of the first order other than zero, of the second order other than the substitution tensor, of the third order other than the alternating tensor, and also the form assumed by the general isotropic tensor of the fourth order are very instructive and illuminating. The treatment would probably have been even more instructive if isotropic tensors had been included in the first chapter of the book.

Dr. Jeffreys's latest production is a valuable addition to mathematical literature; yet it somehow leaves one with a haunting fear of the danger involved in the very simplifications of tensor methods that are characteristic of the book. Is it not dangerous to tell a student without some qualification that the gradient of a vector is a tensor of the second order?

INDEX TO VOL. XIII.

Boron fluoride, a search for the band spectra of, 501.

Bowen (E. G.) and Jones (W. Morris) on an X-ray investigation of the bismuth-antimony alloys, 1029.

Bradley (R. S.) on the cohesive force between solid surfaces and the surface energy of solids, 853.

Bramhall (E. H.) on Langmuir probe measurements in the normal copper arc, 682.

British carboniferous reticulate spiriferidæ, 583.

Brown (G. B.) on sensitive flames, 161.

Brown (R. C.) on the surface tensions of mixtures of normal propyl alcohol and benzene, 578.

Burch (F. P.) on potential dividers for cathode ray oscillographs, 760.

Cæsium vapour, an attempt to detect high photoelectric absorption at double the series limit, 300.

Capacity, effective, of the quadrant electrometer, 650.

Characteristic curves of the aluminium rectifying cell, 76.

Charge carried by atoms of radium D emitted by α-ray recoil from a source of radium C on a metallic surface and its relation with the surface forces, 1.

Childs (Dr. E. C.) on the collisional friction on electrons in gases, 873.

Circular disk, circular flow in, 674.

Clarke (T. E.) on the effect of surface changes on the photoelectric emission of silver and gold, 624.

Classical energy and the interpretation of Schrödinger's ψ function, 112.

Coagulation of homogeneous aerosols, the theory of, 523.

Cohesive force between solid surfaces and the surface energy of solids, 853.

Collisional friction on electrons moving in gases, 873.

END OF THE THIRTEENTH VOLUME.

'

INDIAN AGRICULTURAL RESEARCH
INSTITUTE LIBRARY, NEW DELHI.

Date of Issue	Date of Issue	Date of Issue